

# ADVANCED APPROACHES TO FATIGUE EVALUATION

(NASA-SP-309) ADVANCED APPROACHES TO  
FATIGUE EVALUATION (NASA) 1972 675 p CSDL  
20K

N72-29895  
thru  
N72-29917  
Unclas

H1/32 36358

Sixth ICAF symposium held at  
Miami Beach, Florida  
May 13-14, 1971



NATIONAL AERONAUTICS AND SPACE ADMINISTRATION



# ADVANCED APPROACHES TO FATIGUE EVALUATION

Sixth ICAF symposium held at  
Miami Beach, Florida  
May 13-14, 1971

*Prepared at NASA Langley Research Center*



*Scientific and Technical Information Office* 1972  
NATIONAL AERONAUTICS AND SPACE ADMINISTRATION  
*Washington, D.C.*

# ADVANCED APPROACHES TO FATIGUE EVALUATION

---

For sale by the National Technical Information Service  
Springfield, Virginia 22151 — Price \$9.00



## PREFACE

The Symposium on Advanced Approaches to Fatigue Evaluation held in Miami Beach, Florida, on May 13-14, 1971, was the sixth in a series sponsored by the International Committee on Aeronautical Fatigue (ICAF). The proceedings of the five earlier symposia were published as listed in the references to this preface.

The ICAF is an informal organization of experts on fatigue from 10 nations. Each nation is represented by a single representative, in most cases from the national aerospace research organization in his country. J. Branger of Eidg. Flugzeugwerk, Emmen, Switzerland, is Executive Secretary. The Committee was organized among five Western European nations in 1952 to promote a "fruitful and effective exchange of information on all aspects of aeronautical fatigue problems among the member nations." The Committee was gradually expanded until it reached its present size in 1965. Biennial meetings are organized and hosted by the members on a rotating basis.

The theme of the Symposium, "Advanced Approaches to Fatigue Evaluation," permitted discussion of many broad aspects of the fatigue problem in aeronautical structures.

The introductory lecture, "The Philosophy Which Underlies the Structural Tests of a Supersonic Transport Aircraft With Particular Attention to the Thermal Cycle," presented by E. L. Ripley of the United Kingdom who was especially invited as the Plantema Memorial Lecturer, follows a tradition established 4 years earlier at the Melbourne meeting of ICAF. The Memorial Lecture honors Dr. Frederick J. Plantema, the first Executive Secretary of ICAF. In his modest but effective manner, Dr. Plantema was the driving force for organizing and directing ICAF during its first 14 years.

This volume contains the complete text of each of the papers presented at the Symposium and three additional papers submitted later that were judged to be important adjuncts to these proceedings.

The editors sincerely appreciate the enthusiastic support of other ICAF members who solicited papers from their respective countries and acted as session chairmen at the meeting. They wish to express appreciation also to the authors who prepared and delivered papers for the Symposium. Finally, grateful acknowledgment is made to the National Aeronautics and Space Administration, whose financial and administrative support made the Symposium and the publication of these proceedings possible.

## REFERENCES

1. Plantema, F. J.; and Schijve, J., eds.: Full-Scale Fatigue Testing of Aircraft Structures. Pergamon Press, Inc., 1961.
2. Barrois, W.; and Ripley, E. L., eds.: Fatigue of Aircraft Structures. Macmillan Co., c.1963.
3. Schijve, J.; Heath-Smith, J. R.; and Welbourne, E. R., eds.: Symposium on Current Aeronautical Fatigue Problems. Pergamon Press, Inc., 1965.
4. Gassner, E.; and Schutz, W., eds.: Fatigue Design Procedures. Pergamon Press, Inc., c.1969.
5. Mann, J. Y.; and McMillan, I., eds.: Aircraft Fatigue - Design, Operational, and Economic Aspects. Programme of 5th ICAF Symposium (Melbourne, Australia), May 1967.



## CONTENTS

	Page
PREFACE . . . . .	iii

### THIRD FREDERICK J. PLANTEMA MEMORIAL LECTURE

1. THE PHILOSOPHY WHICH UNDERLIES THE STRUCTURAL TESTS OF A SUPERSONIC TRANSPORT AIRCRAFT WITH PARTICULAR ATTENTION TO THE THERMAL CYCLE . . . . .	✓ 96 1 ✓
by E. L. Ripley, Royal Aircraft Establishment, United Kingdom	

### SYMPOSIUM ON ADVANCED APPROACHES TO FATIGUE EVALUATION

2. FATIGUE EXPERIENCE FROM TESTS CARRIED OUT WITH FORGED BEAM AND FRAME STRUCTURES IN THE DEVELOPMENT OF THE SAAB AIR- CRAFT VIGGEN . . . . .	✓ 97 93 ✓
by S. E. Larsson, Saab-Scania Aktiebolag, Sweden	
3. THE BOEING 747 FATIGUE INTEGRITY PROGRAM . . . . .	✓ 98 127 ✓
by Max M. Spencer, The Boeing Company, United States	
4. FATIGUE AND FAIL-SAFE DESIGN FEATURES OF THE DC-10 AIRPLANE . . . . .	✓ 99 179 ✓
by M. Stone, McDonnell Douglas Corporation, United States	
5. THE PRACTICAL IMPLEMENTATION OF FATIGUE REQUIREMENTS TO MILITARY AIRCRAFT AND HELICOPTERS IN THE UNITED KINGDOM . . . . .	29800 213 ✓
by R. D. J. Maxwell, Royal Aircraft Establishment, United Kingdom	
6. A PROPOSED USAF FATIGUE EVALUATION PROGRAM BASED UPON RECENT SYSTEMS' EXPERIENCE . . . . .	✓ 01 231 ✓
by G. P. Haviland and G. F. Purkey, U.S. Air Force, United States	
7. FATIGUE TESTS WITH RANDOM FLIGHT-SIMULATION LOADING . . . . .	✓ 02 253 ✓
by J. Schijve, National Aerospace Laboratory, The Netherlands	
8. RELIABILITY ANALYSIS APPLIED TO STRUCTURAL TESTS . . . . .	✓ 03 275 ✓
by Patricia Diamond and A. O. Payne, Aeronautical Research Laboratories, Commonwealth of Australia	
9. FATIGUE OF COMPOSITES . . . . .	✓ 04 333 ✓
by Michael J. Salkind, Sikorsky Aircraft, United States	

10. FATIGUE DESIGN PROCEDURE FOR THE AMERICAN SST PROTOTYPE . . . . .	05	Page 365 ✓
by Ralph J. Doty, The Boeing Company, United States		
11. PRACTICAL ASPECTS OF DESIGNING FOR AND EVALUATING STRUCTURAL INTEGRITY . . . . .	04	405 ✓
by Marcel Peyrony and Daniel Chaumette, Avions Marcel Dassault, France		
12. ON THE CYCLIC STRESS-STRAIN BEHAVIOR AND LOW-CYCLE FATIGUE OF AEROSPACE MATERIALS . . . . .	01	425 ✓
by J. Burbach, Krupp Forschungsinstitut, Germany		
13. A PARAMETRIC APPROACH TO IRREGULAR FATIGUE PREDICTION . . . . .	68	429 ✓
by Dr. T. H. Erismann, Federal Laboratories for Testing Materials and Research, Switzerland		
14. FRACTURE CONTROL PROCEDURES FOR AIRCRAFT STRUCTURAL INTEGRITY . . . . .	09	437 ✓
by Howard A. Wood, U.S. Air Force, United States		
15. THE INFLUENCE OF MODIFICATIONS OF A FATIGUE LOADING HISTORY PROGRAM ON FATIGUE LIFETIME . . . . .	10	485 ✓
by J. Branger, Eidgenössisches Flugzeugwerk, Switzerland		
16. STATISTICAL ANALYSIS OF MISSION PROFILE PARAMETERS OF CIVIL TRANSPORT AIRPLANES . . . . .	11	541 ✓
by Otto Buxbaum, Laboratorium für Betriebsfestigkeit, Germany		
17. STATISTICAL LOAD DATA PROCESSING . . . . .	12	565 ✓
by G. M. van Dijk, National Aerospace Laboratory NLR, The Netherlands		
18. DETECTION OF STRUCTURAL DETERIORATION AND ASSOCIATED AIRLINE MAINTENANCE PROBLEMS . . . . .	13	599 ✓
by H. D. Henniker, British European Airways, and R. G. Mitchell, British Overseas Airways Corporation, United Kingdom		
19. FATIGUE FAILURE OF METAL COMPONENTS AS A FACTOR IN CIVIL AIRCRAFT ACCIDENTS . . . . .	A	611 ✓
by William L. Holshouser and Ruth D. Mayner, National Transportation Safety Board, United States		



## PAPERS SUBMITTED AFTER SYMPOSIUM

20. FATIGUE TESTS ON BIG STRUCTURE ASSEMBLIES  
OF CONCORDE AIRCRAFT . . . . . 15 ✓ 631 ✓  
by V. P. N'Guyen, Société Nationale Industrielle Aérospatiale,  
and J. P. Perrais, Centre d'Essais Aéronautiques, France
21. STRUCTURAL TESTING OF CONCORDE AIRCRAFT - FURTHER  
REPORT ON UNITED KINGDOM TESTS . . . . . ✓ 16 649 ✓  
by Norman Harpur, British Aircraft Corporation, United Kingdom
22. A COMPARISON OF RELIABILITY AND CONVENTIONAL ESTIMATION  
OF SAFE FATIGUE LIFE AND SAFE INSPECTION INTERVALS . . . . . ✓ 17 667 ✓  
by F. H. Hooke, Aeronautical Research Laboratories, Department  
of Supply, Commonwealth of Australia

N72-29896

THIRD FREDERICK J. PLANTEMA MEMORIAL LECTURE

THE PHILOSOPHY WHICH UNDERLIES THE STRUCTURAL TESTS OF  
A SUPERSONIC TRANSPORT AIRCRAFT WITH PARTICULAR  
ATTENTION TO THE THERMAL CYCLE

By E. L. Ripley  
Royal Aircraft Establishment  
Farnborough, Hampshire, United Kingdom



# CONTENTS

	Page
SUMMARY . . . . .	5
INTRODUCTION . . . . .	6
Background . . . . .	6
Structural-Load Environment . . . . .	7
Acknowledgements . . . . .	8
RESEARCH ON THERMAL-CYCLE EFFECTS . . . . .	8
Broad Pattern of Research . . . . .	8
Examples of Research . . . . .	10
Effect of repeated application of heat on fatigue life . . . . .	11
Effect of heat on nucleation and crack-propagation phases of fatigue life . . . . .	11
Acceleration of tests under combined thermal and mechanical cycles . . . . .	13
DESIGN DEVELOPMENT TESTS . . . . .	14
Large Component Specimens . . . . .	14
Centre Wing and Fuselage Specimen at C.E.A.T. . . . .	14
Forward-Fuselage Specimen at R.A.E. . . . .	15
CERTIFICATION TESTS . . . . .	17
Outline of Programme . . . . .	17
Major Static Test . . . . .	18
Major Fatigue Test . . . . .	19
Fail-Safe Tests . . . . .	21
THERMAL CYCLE IN MAJOR FATIGUE TEST . . . . .	22
Important Thermal Effects in Fatigue Test . . . . .	22
Accelerating the Test . . . . .	23
Accelerated Thermal Cycle . . . . .	25
Interpreting the Test . . . . .	28
HEATING AND COOLING FOR THE MAJOR FATIGUE TEST . . . . .	29
External Heating and Cooling . . . . .	29
Thermal duct . . . . .	29
External heating and cooling plant . . . . .	32
Internal Heating, Cooling, and Pressurisation . . . . .	35
Air circuits . . . . .	36
Fuel systems . . . . .	38
Background plant . . . . .	40
Safety Precautions . . . . .	41
Excess-air-pressure safeguards . . . . .	41

	Page
Antivacuum safeguards . . . . .	42
Fuel-level surveillance . . . . .	42
Explosive-hazard safeguard . . . . .	42
Fire detection and suppression . . . . .	42
Ammonia detection . . . . .	42
MECHANICAL-LOADING SYSTEM FOR MAJOR FATIGUE TEST . . . . .	42
Loads and Reactions . . . . .	42
Hydraulic System . . . . .	43
Loading Sequences . . . . .	44
Mechanical-Loading Letdown System . . . . .	46
Interactions With Multichannel Systems . . . . .	47
CONTROL AND MONITORING SYSTEMS FOR MAJOR FATIGUE TEST . . . . .	48
Basic Requirements . . . . .	48
Hardware and Its Operation . . . . .	49
Overall hardware configuration . . . . .	49
General operational principles . . . . .	50
Control of Air- and Fuel-Conditioning Plant . . . . .	52
External-air systems . . . . .	52
Internal-air systems . . . . .	52
Internal-fuel systems . . . . .	53
Jack Loading Computer . . . . .	53
Synthesis of net jack load . . . . .	53
Jack set-pointing system . . . . .	54
Droop nose . . . . .	54
Plant Monitoring . . . . .	55
General principles . . . . .	55
Types of checking and their frequency . . . . .	55
Types of output . . . . .	55
Data Logger . . . . .	56
Multiplexing configuration . . . . .	56
British standard interfaces . . . . .	57
Basic operational facilities . . . . .	57
Operation for Testing . . . . .	57
Startup and shutdown . . . . .	57
Data input and cross-checking . . . . .	58
Facilities for commissioning . . . . .	58

	Page
REFERENCES . . . . .	59
TABLES . . . . .	60
FIGURES . . . . .	62



THE PHILOSOPHY WHICH UNDERLIES THE STRUCTURAL TESTS OF  
A SUPERSONIC TRANSPORT AIRCRAFT WITH PARTICULAR  
ATTENTION TO THE THERMAL CYCLE

By E. L. Ripley  
Royal Aircraft Establishment  
Farnborough, Hampshire, United Kingdom

SUMMARY

The supersonic transport aircraft has brought a new challenge to the structural test engineer. Over the years he has developed skills in representing in the laboratory the conditions that occur in flight and in devising techniques to apply these to the structure. Supersonic flight has introduced important new features into the test programme, particularly for supersonic transport aircraft. Of these new features the most significant is probably the prolonged heating and then cooling of the structure during each flight. Much basic research has been necessary to understand the effects of such a thermal cycle on the structure, and novel engineering techniques have been developed to simulate the cycle in the test laboratory.

The information presented in this paper is based on data obtained from the Concorde. Much of this data also applies to other supersonic transport aircraft. The design and development of the Concorde is a joint effort of the British and French, and the structural test programme is shared, as are all the other activities. Vast numbers of small specimens have been tested to determine the behaviour of the materials used in the aircraft. Major components of the aircraft structure, totalling almost a complete aircraft, have been made and are being tested to help the constructors in each country in the design and development of the structure. Tests on two complete airframes will give information for the certification of the aircraft. A static test was conducted in France and a fatigue test in the United Kingdom. Fail-safe tests are being made to demonstrate the crack-propagation characteristics of the structure and its residual strength.

The paper describes these aspects of the structural test programme in some detail, dealing particularly with the problems associated with the thermal cycle. The biggest of these problems is the setting up of the fatigue test on the complete airframe; therefore, this is covered more extensively with a discussion about how the test time can be shortened and with a description of the practical aspects of the test.



## INTRODUCTION

### Background

In 1967 a paper entitled "Design Philosophy and Fatigue Testing of the Concorde" was presented at the Fifth Symposium of the International Committee on Aeronautical Fatigue (ICAF) at Melbourne, Australia. (See ref. 1.) Four years later, the basic subject of the structural testing of a supersonic transport aircraft is to be considered again by the ICAF, this time at the Sixth Symposium at Miami Beach, Florida, U.S.A. In the meantime, some updating of the subject was given in a paper to the Eleventh Anglo-American Conference at the Royal Aeronautical Society, London, in 1969 (ref. 2). The present paper brings the story up to date and in doing so incorporates an appreciable amount of the basic information from the other papers for completeness.

The state of the art in structural-strength testing is now well advanced, and the purpose of the present paper is to examine the way this state has to be further developed to meet the needs of the supersonic transport aircraft. The supersonic transport aircraft will be subjected to all the familiar patterns of ground and flight loads, and these patterns must be represented in the structural tests using the techniques which have been developed and proven over many years. What is new is the thermal cycle which produces prolonged heating and then cooling during each flight. The thermal cycle sets up thermal stresses which are in themselves another loading action. Prolonged time at elevated temperature introduces creep and overageing. Further consideration of interaction effects which the thermal cycle may have on the static and fatigue strengths of the aircraft is necessary.

The data presented in this paper were obtained from structural tests on the Concorde, and illustrations are given of what has been done on that aircraft. The principles underlying this work are believed to be equally applicable to other supersonic transport aircraft. The design and development of the Concorde (fig. 1) are a joint effort of the British and the French, and the structural test programme is shared, as are all the other activities. Throughout the programme the aim has been to employ wherever possible test techniques which have been well established and proven throughout the years. Much new research has, however, been necessary to understand the effects of the thermal cycle on the structure, and novel engineering techniques have been developed to simulate it in the test laboratory.

Vast numbers of small specimens have been tested to determine the behaviour of the materials used in the aircraft. Major components of the aircraft structure, totalling almost a complete aircraft, have been tested to help the constructors in each country in the design and development of the structure. Two complete airframes will be tested to give information for the certification of the aircraft. A static test will be made in France and a fatigue test in the United Kingdom. Fail-safe tests are being made to demonstrate



the crack-propagation characteristics of the structure and its residual strength. Drop, static, and fatigue tests are being made on the nose and main undercarriages. Acoustic fatigue tests are being made to investigate the effects on the structure of engine noise and various pressure-fluctuation effects in the airflow. Dynamic response in the structural loads is being measured on the structure in ground tests and in flight tests. The measurements and tests are most comprehensive, and the Concorde will certainly be one of the most thoroughly tested aircraft ever flown.

It is not possible in this paper to cover all these aspects in full detail, and preference is given to the strength-test programme with particular reference to the problems associated with the thermal cycle. The biggest problem has been the setting up of the fatigue test on the complete airframe, and some of the practical aspects of this are dealt with hereinafter.

Physical quantities used in this paper, their basic unit, and pertinent conversion factors are listed in table I.

### Structural-Load Environment

A typical flight profile of the Concorde is that after take-off the aircraft will climb subsonically to a suitable altitude and then, still climbing, accelerate to its cruising speed of about a Mach number  $M$  of 2.0. After the cruise phase has been completed, the aircraft will decelerate to subsonic speed at altitude and then descend to its destination. (See fig. 2.) In the initial climb at subsonic speeds, the external surfaces of the aircraft will cool a little and then heat up in the acceleration phase to a temperature of about  $100^{\circ}\text{C}$ , which will be maintained during cruise. (See fig. 3.) During deceleration and descent, the external structural temperature will drop to about  $-20^{\circ}\text{C}$  and rise again to ambient temperature on landing. (See fig. 4.)

The Concorde will be subjected to all the normal aircraft loads – taxiing loads, ground-air-ground cycle, gust and manoeuvre loads, cabin pressurisation, etc. Almost all of these will occur while the aircraft is on the ground or flying subsonically; that is, while the structure is at ambient temperature before the acceleration phase or is approaching ambient temperature after the deceleration phase. The exception is any turbulence which may be encountered while the aircraft is flying supersonically and the structure is hot.

One of the most important of the thermal effects is the thermal stress which develops because the temperature of the internal structure lags behind that of the surface structure as a result of the time it takes for heat to be conducted to it. Thus on the climb the external structure will be hotter than the internal structure, and this will set up thermal stresses due to the different amount of expansion. During the cruise the temperature of the internal structure will gradually approach that of the external structure and the

thermal stresses will decay. The reverse effect takes place during descent and recovery on the ground; thus, thermal stresses of opposite sign are produced. Such a stress situation has a significant effect on fatigue life. If the structure is deep, these stresses are about one-half the maximum stress permissible for the required life.

Two other thermal effects which need to be considered are overageing and creep. When a material is being manufactured, it is often subjected to heat treatment to "age" it in order to obtain its desired strength. If subsequently it is subjected to long periods at elevated temperature, it will "overage," and its strength will fall slightly. If the material is subjected to long periods at elevated temperature while under load, it will "creep" which means it will remain extended or deformed even after the load and temperature are removed. It is necessary to ensure that the amount of creep occurring is limited so that unacceptable deformation of the structure is prevented. An upper limit of 0.1-percent total plastic strain after 20 000 hours was chosen as a reasonable criterion, based mainly on structural experience in which a 0.1-percent tensile-proof condition has been used for design purposes for many years.

Thus the structure is subjected to the normal loading environment interspersed with periods at elevated temperature and a thermal-stress cycle each supersonic flight. This environment is further complicated by the presence of fuel tanks acting as heat sinks, with their changing levels of fuel during flight and with fuel transfer from tank to tank to preserve aircraft balance for subsonic and supersonic flight. The task of the designer and test engineer is indeed complex since he must understand and interpret all of these effects and their interactions.

#### Acknowledgements

The author gratefully acknowledges the able and willing assistance of his colleagues in the Royal Aircraft Establishment (R.A.E.), especially those in the Structures Department, who helped with all the many details necessary for the preparation of the paper and made valuable contributions to its content. Grateful acknowledgements are also made to the British Aircraft Corporation, Aerospatiale (S.N.I.A.S.), Centre d'Essais Aéronautique de Toulouse (C.E.A.T.), and Sulzer Brothers (London) Limited for their help with some of the illustrations.

### RESEARCH ON THERMAL-CYCLE EFFECTS

#### Broad Pattern of Research

One of the first engineering tasks was to evaluate a suitable material for the aircraft structure. Aluminium alloy was a desirable choice since its aircraft production capabilities were well understood and it would be able to withstand the thermal effects over almost



all the airframe. In a few areas where the temperatures were greater, such as near the engines, steel, titanium, or nickel alloys could be used. The task was therefore to choose a suitable aluminium alloy to give the best overall performance. Several were evaluated and the present Concorde material was evolved from an aluminium alloy which originally was developed to withstand the rigours of use in an aircraft engine. An important criterion in the choice of this material was its creep behaviour, which is superior to that of other aluminium alloys currently being used in subsonic aircraft. In parallel with the work on metallic materials, a similar programme was conducted on nonmetallic materials.

It is not possible within the scope of this paper to tell the story of all the research and development work. A tremendous amount of work has been done in both countries, is being continued, and will be continued right through the certification test programme to provide the necessary backup knowledge for planning and interpreting that programme.

Quite early, two things became apparent from the work on the Concorde aluminium alloy:

(1) Overall creep distortion was unlikely to be a hazard; that is, creep distortion at stresses to be used in the design would not reach the 0.1-percent limit set to avoid unacceptable distortion of the aircraft;

(2) Overageing had little effect on static strength; that is, the reduction in static strength due to prolonged time at elevated temperature was small and could easily be contained by a small factor in the allowable design stresses.

The next step was to see whether exposure to heat, with or without load, affected the fatigue performance of the material in structural configurations and to find out if stresses arising from temperature differences across the structure (thermal stresses) could be regarded simply as equivalent in effect to the same stresses arising from externally applied loads in accumulation of fatigue damage. Clearly at this stage in design, it would not have been practical to await results of tests in real time and temperature conditions; therefore, much of the early work was conducted under accelerated conditions on the basis of Fisher's parameter which gives a relationship of the form

$$\log \frac{t_1}{t_2} = C \frac{T_2 - T_1}{T_1 T_2}$$

where  $t_1$  and  $T_1$  are, respectively, the exposure time and absolute temperature in the real environment,  $t_2$  and  $T_2$  are the corresponding times and temperatures in accelerated conditions, and  $C$  is a constant (approximately  $8200^\circ \text{K}$  for the material concerned). On this basis the anticipated service environment was represented in much of the early work for Concorde by exposure times of 1000 hours at  $150^\circ \text{C}$ , which gives an



equivalence of 30 000 hours at 120° C or 400 000 hours at 100° C. At the same time as the accelerated test programmes were initiated, tests were begun using temperature and time exposures close to real service conditions; such tests span several years, and it is only recently that results have started to accrue.

In planning the research programmes, it was also borne in mind that both under the special conditions of the full-scale fatigue test and under the actual service environment, there would be considerable deviations at different points in the structure from the nominal stress and temperature conditions. To meet this situation, the general policy was to concentrate the more detailed investigations on the nominal conditions and to explore deviations to either side with a comparatively light coverage of test conditions. This approach would give sufficient information to enable correction factors to be derived under such deviating conditions, and these correction factors would be of vital importance in interpreting any failures occurring during the full-scale tests.

In the majority of the early programmes, attention was centred primarily on the effect of heat exposure on cycles (or "flights") to failure, but as the research and development programmes built up, increasing attention was paid to examining the effects of heat exposure on the crack-nucleation phase of damage growth and on the subsequent crack-propagation phase since there was no presupposed reason to assume that both phases of damage growth would be equally affected. This aspect had to be explored both under accelerated and real-time conditions so that, for example, crack-initiation times observed during the full-scale fatigue test could be interpreted in terms of true environment.

An enormous programme of work has been done and is continuing to obtain information on the foregoing problems; many types of specimens are being used, ranging from simple notched and riveted-joint coupon specimens to large structural components. Loading and environmental conditions have varied from simple sinusoids with a block of heat representing the total service exposure introduced at some point in the fatigue test to elaborate representations of a flight cycle of mechanical loads with appropriate heating and cooling conditions to induce representative thermal stresses.

All this work is giving an empirical understanding of the behaviour of the structure under the thermal environment. More fundamental work is also being done to try to understand the metallurgical phenomena involved.

### Examples of Research

It is beyond the scope of this paper to attempt full presentation of the results obtained so far, but some results are outlined subsequently. These serve to illustrate the kind of work that has been done and the nature of the answers that have been obtained. Three examples have been chosen. They show how this work has given understanding and

data for design, and also, particularly in the context of this paper, how this work provides essential information for planning and interpretation of the full-scale fatigue test.

Effect of repeated application of heat on fatigue life.- This first example shows the trends which have emerged from fatigue-heat interaction tests on Concorde material. The variation in the ratio of life with heat exposure to life cold with temperature during heat exposure and the creep stress is illustrated in figure 5. The results on which these trends are based were mainly obtained from tests in which periods of heat, with or without mean stress application, were applied periodically during the fatigue life; the mechanical loading patterns included a simple representation of the gust loading and the ground-air-ground cycles. It is considered unlikely that significant thermal stresses were induced in any of the specimen types. It should also be borne in mind that in grouping these data, results were put together from tests having considerable detail variations in loading patterns and numbers of heat interspersions during life. Nevertheless, the trends give a qualitative indication of behaviour, and the following conclusions may be drawn:

(1) Performance reduces as the temperature rises from 120° to 180° C.

(2) Performance is better with tensile creep stress than with zero creep stress, though the improvement is seen to be falling off for the riveted joints at the higher creep stresses.

(3) Performance appears to improve in moving from the simple notched specimen to the riveted-joint specimen and, again, to the relatively complex fabricated box; reasons why this may be so are discussed subsequently.

Effect of heat on nucleation and crack-propagation phases of fatigue life.- This example has been chosen to illustrate one of the more fundamental research studies. The work was undertaken to obtain an understanding of the modifying effects of heat on the growth of fatigue damage at different stages in the life of a specimen under test. In all the tests, fatigue cycling was carried out at room temperature under fluctuating tensile loading. After a mean (nominal) life to failure was established, a single application of heat was introduced at a certain percentage of nominal life; the fatigue cycling was stopped during this period, and the mean load was adjusted to give tensile, zero, or compressive creep. After cooling, the fatigue cycling was then resumed, and from consideration of the total fatigue life to failure, the damaging or beneficial effect of the heat exposure was assessed. In the majority of the tests, the heat exposure was 150° C for 1000 hours, but the work also included a small number of long-term tests in which the exposure was 120° C for 20 000 hours. The tests were carried out on notched, pinned-lug, and clamped-lug specimens. Some of the results for the notched and pinned-lug specimens are shown in figure 6. It is evident from the results of the tests on the notched specimen that



(1) Exposure to heat without load during the first half of the fatigue life has a detrimental effect on fatigue performance.

(2) This detrimental effect is to some extent alleviated by tensile creep, and conversely.

(3) Compressive creep increases the damaging effect of heat alone.

(4) Exposure to heat during the crack-propagation phase has a relatively small effect.

The foregoing test results, supported by examination of the fracture surfaces, have led to a general explanation of the effects of heat and creep on the growth of fatigue damage. The effect of heat alone is to speed up the development of fatigue damage nuclei and hence to reduce the crack-initiation period; a marked reduction in scatter in endurance has been noted after heat exposure, which is in keeping with this explanation. Until comparatively recently, the more rapid appearance of damage nuclei was explained in terms of the relaxing effect of the period of heat on beneficial residual compressive stresses which are often inadvertently introduced at the notch surfaces during manufacture. Recent metallurgical studies have shown that another, and perhaps more important, change takes place in the surface material at the notch during heating.

It has been found that machining leaves behind a work-affected zone some 50  $\mu\text{m}$  deep having a hardness approximately twice that of the interior material. In "as received" specimens, fatigue cracks, in fact, initiated below this zone. The heat exposure was found to reduce the surface hardness to that of the interior material, and cracks then developed from the surface. This phenomenon, combined with some relaxation of residual manufacturing stresses, is believed to explain the observed reduction in crack-initiation time; the biggest reductions, of course, were observed when heat preceded fatigue cycling. When load is applied during heating, plastic deformation of the material in the vicinity of the notch will be encouraged; that is, tensile loading will tend to induce compressive residual stresses at the notch so that after the heating period, the local mean stress will be reduced with consequent improvement in fatigue life relative to the heat-without-load condition. The reverse will be true with compressive load with heating.

It may be noted that results for the notched specimen under long exposure times at lower temperatures, 20 000 hours at 120<sup>0</sup> C, which have recently become available from tests for heat without load, confirm the appropriate pattern of behaviour. The results of tests on the pinned-lug specimens correspond to anticipated results, bearing in mind that the crack-initiation period is a much smaller percentage of the fatigue life in this type of specimen because fretting promotes early formation of surface cracks. As would therefore be anticipated, the effects of heat are considerably less in such specimens than in simple notched specimens. The general patterns of behaviour observed in the foregoing fundamental studies have been shown also to apply to the observed behaviour of more com-



plex specimens such as fabricated box beams containing riveted joints, cutouts, and so on. This basic understanding will be of great help in the full-scale fatigue test, both in indicating areas of structure where heat is likely to promote relatively early initiation of damage and in assessing the significance of failures that may develop.

Acceleration of tests under combined thermal and mechanical cycles.- The third type of investigation chosen to illustrate backup research and development work is concerned with the problem of accelerating the full-scale fatigue test, in which both thermal fatigue stresses and stresses arising from external loading actions contribute to the growth of fatigue damage. In order to keep the laboratory testing ahead of aircraft in service, the full-scale fatigue test must be accelerated to accumulate fatigue damage more rapidly than the real-time flight experience. This would present no problem if the loading actions were associated solely with externally applied mechanical loads because the frequency of application of such loads could easily be speeded up relative to real-time experience. It is the speeding up of the thermal-stress loading action that presents a problem since hot and cold soak times, for example, are controlled by the heat-transfer characteristics of the structure and cannot be hastened simply. This problem is discussed in more detail subsequently.

Some results of tests to give an assessment of one approach to this acceleration problem are shown in figure 7. The acceleration technique explored in this case was to conduct the accelerated test using a wider temperature range than used in the "real-time" test. The aim of this test was to attain the condition in which the increased range of the thermal-stress cycle would give twice the normal amount of fatigue damage in each test cycle. The accelerated test cycle included twice the number of mechanical loads experienced in one flight. Thus, each accelerated test cycle should give damage appropriate to two flights. The results given were obtained from tests on box beams (figs. 8 and 9) which were tested in four-point bending. The loading action applied resulted in mechanical and thermal stress conditions in the tension-compression surface of the specimen corresponding to those in certain areas of the pressure cabin to which gust loadings, cabin pressurisation, the ground-to-air cycle, and thermal-gradients contribute. It should be noted that in this exploratory work the severity of all the loadings was scaled up somewhat so that answers both in "real time" and accelerated conditions could be obtained in months rather than years. It will be seen from figure 7 that encouraging results were obtained. Damage rate, assessed on the basis of the time to first crack, was accelerated by a factor close to 2.

Though only two specimens were tested in each condition at this stage, the indications were that scatter was low, and therefore the results could be treated with considerable confidence. Low scatter has been found to be a characteristic of much of the background research and development work entailing heat application. This preliminary work

is being followed up in a major programme of tests on box beams of similar dimensions but of detail design representing much more closely the Concorde structure. The tests are being run in conditions corresponding closely to those envisaged both in service and in the full-scale test. In addition to providing information on acceleration conditions, analysis of the results also provides understanding of the equivalence of thermal and mechanical stresses in cumulative damage.

## DESIGN DEVELOPMENT TESTS

### Large Component Specimens

Quite early in the design of an aircraft, it is prudent to build representative sections of the structure to see how ideas work out in practice. This is particularly necessary for the supersonic transport aircraft with all the implications of the interaction of thermal and mechanical effects. Therefore, two sections of fuselage were built initially for the Concorde. Each had about a 15-foot length of representative structure. One was tested in France and the other in the United Kingdom (specimens 2.1 and 2.2 of fig. 10).

As the design took shape, actual components of the aircraft, such as parts of the wing and fuselage, have been made and are being tested to assist in design development. These specimens make almost a complete aircraft. (See fig. 10.) Again, these tests are being shared with the French. A wide range of tests are being done on these component specimens. They include the exploration of temperature and stress distributions under various design conditions, static tests to demonstrate the strength of the structure under extreme conditions, fatigue tests to show its behaviour under the recurring loads in service, and fail-safe tests to show that the structure is capable of withstanding safely damage or failures in service.

For this paper, two tests have been picked as examples of the work which has been covered on the large component specimens.

### Centre Wing and Fuselage Specimen at C.E.A.T.

Specimen 2.8B (figs. 10 and 11) is a large section of the centre wing and fuselage and contains the important cutouts for the main undercarriage. It is an early prototype standard and has completed its test programme at the Centre d'Essais Aéronautique de Toulouse (C.E.A.T.). It has been used to check the static strength of the aircraft and has given useful experience in preparation for the static test of the complete airframe, which is now being tested in the same laboratory.

The specimen weighed about 15 tons fully equipped and was approximately 35 feet long with a span of 44 feet. Kinetic heating effects were simulated by the use of 5000 radiant heaters, and cooling was simulated by ambient air and air cooled by liquid nitrogen



drawn over the specimen at low speed by extractor fans. (See fig. 12.) The specimen was equipped with 1500 strain-gauge points and 2000 thermocouples. The effect of fuel in the tanks was simulated by using Gilotherm, a fluid which has similar characteristics to kerosene but is noninflammable. The mechanical loading was done with hydraulic jacks.

One of the earliest tests was to measure the influence coefficients across the specimen. Thence followed a thorough investigation of the strain and temperature distribution throughout the structure under typical loading conditions. A number of design cases were taken to limit load. The residual strength of the structure was demonstrated by removing members and unbolting joints to simulate fatigue and other damage. Finally in this group of tests, the wing was taken to ultimate load in a flight case. To see how far cracks propagated, the simulated fuselage was pressurised and struck with a guillotine blade; the impact sites were such that the skin was cut between frames, or both the skin and a frame were cut.

#### Forward-Fuselage Specimen at R.A.E.

Specimen 2.4/2.5 (figs. 10 and 13) is the forward part of the fuselage and is being tested at the Royal Aircraft Establishment (R.A.E.). It is about 70 feet long and comprises the flight deck and forward part of the passenger cabin. The droop nose is included and also a dummy nose undercarriage. The specimen is made to preproduction standards. The rig provides facilities for static, fatigue, and fail-safe tests and gives experience for the fatigue test on the complete airframe which will use many of the same test techniques.

The specimen is cantilever mounted in the test frame at its aft end and is loaded by 19 hydraulic jacks. It weighs about 8 tons fully equipped. Kinetic heating and cooling effects are simulated by convective means. Hot air is blown over the specimen to heat it for the climb and cruise conditions, and cold air is blown over it to cool it for the descent and recovery conditions. The specimen is enclosed in a duct with about a 4-inch annular gap. The duct is articulated in sections on gimbals to allow for specimen movement. Normally, the specimen and duct are in a closed circuit in which the air can be heated by electrical resistance heaters in the airflow or cooled by the injection of liquid nitrogen. (See fig. 14.) The circuit can however be opened to allow the specimen to be cooled initially with ambient air which has sufficient cooling potential for the first part of the descent.

This method of convective heating and cooling was developed specially by the R.A.E. for the component specimen tests and will be used for the major fatigue test. It provides a very simple testing technique, and one which is inherently safe since rapid and dangerous temperature runaways are impossible. The principle used is that the heat-transfer conditions which are set up on the aircraft at high speed in the rarefied air at altitude can be reproduced in the laboratory by blowing the denser air at ground level at slower speeds



and heating or cooling it to the required temperature. In this test a specimen temperature range of  $150^{\circ}\text{C}$  to  $-35^{\circ}\text{C}$  can be achieved, and the maximum air speed required is about 170 ft/sec. Control therefore is extremely simple; all that is necessary is to regulate the air speed and the air temperature. Good representation along and around the specimen is obtained.

The cabin is pressurised and air-conditioned to represent the conditions in flight. Additional electrical heaters are provided in the cabin to simulate the heat input from the electronic equipment in the aircraft. The whole test is controlled by an interesting development of on-line computer control. Two KDF7 computers are used. The first controls the test, by giving the instructions for mechanical loading, temperature, airflow, and so forth, against the required test programme; the second monitors the test by reproducing the same programme and comparing the results achieved by the first computer. Two levels of discrepancy are identified. Those differences below the lower level are within the acceptable test tolerances and are ignored. Those between the lower and upper levels are printed out so that the test control staff is informed. Any discrepancies above the upper level automatically cause the test to stop. By this method the test programme can be agreed upon, internationally, before it is commenced. High reliability is achieved because of the built-in checking systems and because elaborate recording with subsequent analysis is avoided.

The specimen is fitted with about 1400 strain-gauge points and 500 thermocouples. The initial tests investigated the strain and temperature distributions throughout the structure under typical loading cases. As a quick check on its integrity, the cabin structure was pressurised 5000 times. The specimen was then rigged for a fatigue test under the full mechanical and thermal environment. The test was done on a flight-by-flight basis, but each test cycle was made slightly more severe and shorter than aircraft flight conditions in order to shorten the testing time for a given amount of fatigue damage. The problems associated with this are discussed more fully for the major fatigue test later in this paper.

These tests were interrupted to obtain early design development information on the fail-safe behaviour of machined skin panels. Soon the specimen is to be modified to bring it up to production standards, and then it will be used for the certification fail-safe tests on this part of the structure. In these tests, natural cracks or artificially induced cracks (or damage) will be propagated under the full environmental conditions for a given period, and then the specimen will be loaded to limit load to check its residual strength.

## CERTIFICATION TESTS

### Outline of Programme

When the aircraft has reached its production design standard, the aircraft must be shown to merit a Certificate of Airworthiness. Each country has its own certifying authority, in the United Kingdom it is the Air Registration Board, and each country must be satisfied that its particular regulations for this type of aircraft are met.

In the early days of the Concorde project, the French and British Governments agreed that the Concorde aircraft must qualify for both French and British Certificates of Airworthiness. The two airworthiness authorities therefore agreed jointly to produce new airworthiness requirements for supersonic transport aircraft which are now known as TSS standards. These contain the parts of the French and British national requirements which were applicable and such new requirements as were necessary to meet the special conditions arising for a supersonic transport aircraft. These TSS standards thus became the basis for the design of the Concorde.

The United States Federal Aviation Administration (FAA) has also produced a new document entitled "Tentative Airworthiness Standards for Supersonic Transports" (ref. 3). These standards have also been taken into account in the Concorde design and test programme.

Certification of the aircraft will be based partly on calculation, but most emphasis will be placed on the major acceptance tests. Thus static, fatigue, and fail-safe tests are to be done on the whole airframe. The tests in more detail are

- (1) The major static test on a complete airframe less the nacelles at C.E.A.T. (France)
- (2) The major fatigue test on a complete airframe less the nacelles at R.A.E. (U.K.)
- (3) Static and fatigue tests on the nacelles at the British Aircraft Corporation (U.K.)
- (4) Drop tests, static, and fatigue tests on the nose and main undercarriages at C.E.A.T. (France)
- (5) Fail-safe tests on component specimens in the country of manufacture

In planning the acceptance test programme, it was necessary to select appropriate airframes from the manufacturing sequence. The first two airframes to be made were used for the two prototypes, 001 and 002. The third airframe was chosen for the major static test so that the test results would be available in time for the certification of the aircraft. The airframe is to preproduction standard, and it was agreed that the test results would be reinterpreted to take account of any differences between preproduction and production aircraft. The next two airframes to be made are being used for the pre-production flight aircraft, 01 and 02. The sixth airframe was chosen for the major fatigue



test so that it should be closely representative of production standard and yet should be available sufficiently early for the test to have started before the certification of the aircraft.

The following paragraphs discuss the techniques and facilities used for the major static and major fatigue tests. Although the nacelle tests are not described in detail, the procedures used to reproduce air pressure loading and convective heating and cooling are similar to those used for the major fatigue test. Finally, some comment is given on the fail-safe test programme, as Concorde will probably be the first aircraft to satisfy the new FAA requirements for supersonic transport aircraft.

### Major Static Test

The purpose of the static test is to show that the structure is capable of withstanding extreme conditions which might arise in service and has an adequate margin of strength as laid down by the airworthiness authorities. A range of test cases has been selected to cover all the loading patterns which the aircraft will experience in service. The tests have been grouped so that those without heating are done first. Currently, the specimen is being rigged ready for the commencement of the hot tests.

The programme commenced with fuselage pressurisation tests and tests to check fuel-tank pressurisation and sealing. Then a number of tests were made to cover the take-off and landing conditions. Two flight cases at the beginning of the climb – the steady pullout case and the checked manoeuvre case – were also made. These tests were followed by a number of partial tests on local parts of the specimen covering various conditions arising from the nose undercarriage, tail bumper, engine loads, fin, flight controls, and the main undercarriage doors. In the next phase, the whole specimen will be subjected to the cases which are critical with the thermal cycle, such as a manoeuvre at the end of the climb, a pull-out at the end of the cruise, and gusts during the descent.

This large and comprehensive test is being made at C.E.A.T. in a test facility built for the Concorde tests. (See fig. 15.) The main test hall has a strong floor with under-floor ducts for cables, hydraulic pipes, and so forth. Portal frames provide support for the overhead and side loading. The loads are applied by hydraulic jacks, servocontrolled by Moog valves from a computer. Forty-eight separately controlled loading channels are available, and each can control more than one jack if required. Double-bridge load cells are used to control and monitor the loads.

The kinetic heating effect will be simulated by radiant heaters supplied by thyatron regulators controlled by the computer. One hundred and fifty channels are available, some of 200 kVA and some of 50 kVA capability. Air will be blown over the specimen at about 20 ft/sec during the heating phase, and increased to about 50 ft/sec in the cooling phase. Cooling will be obtained by the injection of liquid nitrogen into the airstream. The cabin



will be pressurised, air conditioned, and filled with polyurethane foam blocks to reduce the explosive risk.

The digital computer controls the sequencing of the whole test and also records the test data. Some 2000 strain gauges and 1500 thermocouples are installed on the specimen, and about 2000 selected inputs can be recorded and processed by the computer in real time. The transducer data are printed every 10 seconds to detect any transducers which may be outside of expected limits.

The load in each test case is built up in a series of steps in the usual way, and full use is made of the computer to examine strains and deflections at each step and to compare them with expected values. It is hoped by this means to be able to detect the onset of failure and to stop the test before catastrophic damage occurs. The inclusion of kinetic heating and cooling in the static tests produces problems of sequencing. For example, it would not be satisfactory to hold the specimen at a high load for a long period while the thermal cycle was applied. It would also be very time consuming to perform a thermal cycle for every load level in every case. Thus an optimum sequence is being worked out for conducting the tests. Care has been taken to install in the specimen strain gauges and thermocouples at corresponding points to those on the flight-test aircraft so that full comparison can be made of conditions measured in flight and reproduced in the test laboratory.

The test will be completed before certification of the aircraft. All the important static design conditions will have been covered, and the tests will demonstrate that the airframe is capable of withstanding extreme conditions which might arise in service.

### Major Fatigue Test

The purpose of the fatigue test is to subject the specimen to the whole structural load environment the aircraft would experience in service. The specimen is taken through a series of flight sequences in the laboratory and subjected to the environmental conditions it would encounter in typical flights. These conditions include the external loading actions, such as taxiing loads, take-off loads, gust loads, kinetic heating and cooling, and the internal loading actions, such as cabin pressurisation, air-conditioning, and fuel handling. These loading actions must be applied to the specimen flight after flight to build up in the specimens all the fatigue structural experience which the aircraft will accumulate in service.

By their very nature, fatigue tests must take a long time. However, for subsonic aircraft, it has always been possible to compress the loading actions so that a test cycle in the laboratory was considerably shorter than the flight it represented. The problem is very much more difficult for a supersonic transport aircraft, since the effects of the thermal cycle are time dependent. Nonetheless, it is essential to find a way to shorten the test time so that the tests may keep ahead of aircraft in service with an adequate

safety margin. The fatigue lives of nominally identical structures are often quite different. Consequently, the Concorde tests are designed so that the specimen will always have at least three times as much fatigue damage (or three times the equivalent loads and thermal cycles) as any aircraft in service. In order to do this, the test must be accelerated, that is, it must represent the aircraft conditions in a shorter time. The test will be run 24 hours per day, 7 days per week, but there will need to be pauses to inspect the specimen and to maintain it, for the essence of this test is to find the fatigue damage while it is still very small so that early preventive measures can be applied to the aircraft in service.

In this part of the paper, broad details only are given of the test techniques and procedures. These are amplified considerably and the practical problems discussed subsequently. The test is being done in the structural test laboratories at R.A.E. (See figs. 16, 17, and 18.) Mechanical loading is being applied by hydraulic jacks. Convective heating and cooling is being used to simulate the external thermal conditions. Because of the need to shorten the time of the test, additional forced heating and cooling systems are needed for the internal structure and the fuel. All this requires a considerable amount of plant to provide the heat and the cold. The test itself and the plant are controlled by two process computers and one monitor computer with a data logging and display system.

Currently the construction of the specimen in the test frame is about complete, and the test rig is being installed. When all this has been completed, the assembly will be calibrated initially by running a number of flight cycles in real time and comparing the achieved strains and temperatures with those measured in corresponding positions in flight. The problem then of accelerating the test will be tackled by shortening the test cycle and by making each test cycle represent more than one flight. This acceleration will be taken in steps, working down from the real-time cycle to ensure that the accelerated test cycle is meaningful. The chosen aim is to do each test cycle in 60 minutes and to make it represent two supersonic flights. Interspersed in the pattern of hot test cycles will be some without the thermal cycle to represent the subsonic flights which are expected to total about 20 percent of the service experience. The use of computer control ensures overall flexibility in the test, and advantage will be taken of this to vary the test cycles as appropriate to represent flight in different degrees of turbulence, at different gross weights, and with different flight patterns.

The engineering tasks involved in this test are considerable. The specimen weighs about 40 tons and the fuel about twice this amount. This entire mass has to be heated and cooled through the appropriate temperature range of each test cycle. Two major plants are required, one for external heating and cooling and the other for internal heating and cooling with all the special forcing systems included. The duct over the specimen is itself a major piece of engineering design. Then there is the mechanical loading system which must be capable of applying a multiple range of loads in a relatively short time.



Finally, the overall control system for the test must itself have high integrity and be able to control and monitor all functions so that the test as a whole achieves high reliability with safety.

Special attention has been paid to the need for extreme reliability of all parts of the rig, and wherever possible, well proven designs and techniques have been used. The tests will be continued for many years over many thousands of cycles to represent the service life of the aircraft with adequate margins. It is imperative therefore that the rig should be trouble free so that the only interruptions in the testing programme are for inspection and repair of the specimen.

While the equipment for the test is impressive, the technical judgement which lies behind it is more significant. The test must be meaningful. It must be possible to interpret the failures and apply preventive measures to aircraft in service. Much is being learned now from the research and development programme to give the necessary basis for this technical judgement. It is planned that the test will start before certification of the aircraft. The test specimen will then keep well ahead of the aircraft in service and will give practical demonstration that the airframe is capable of withstanding the recurring loads which make up its service experience.

#### Fail-Safe Tests

The Anglo-French TSS standards (ref. 4) call for analysis and substantiating tests to demonstrate the fail-safe characteristics of the structure. The tests are to be taken to limit load in combination with appropriate temperature effects and normal cabin operating pressure, if applicable.

The American FAA standards (ref. 3) go a little further than this. They require that all primary structure shall be designed fail-safe and that it shall be shown that adequate residual strength is provided to ensure that any partial failure will be detected before a hazardous condition develops. This involves showing that the structure remains capable of supporting the expected repeated loading and temperature spectrum and critical design limit loads without catastrophic results during the period after any fatigue failure or partial failure has progressed to obvious proportions and prior to detection by inspection. The intention is to cover the situation in which cracks or accidental damage might occur immediately following an inspection and then remain undetected in service until the next inspection, during which period they might be subjected to limit load. Thus, in a fail-safe test, it is necessary to cut the structure to simulate damage or to grow a crack, then to subject it to fatigue loads under the full environmental conditions for the equivalent of an inspection period, during which the damage may propagate, and then to show that it will withstand limit load. The results of these tests are required for type certification.

This fail-safe testing involves quite a large test programme to cover all aspects of the structure. The tests too are complex and time consuming because fatigue testing under full environmental conditions is required. For Concorde, it is planned to do these tests on the major component specimens, supplemented where necessary by tests on smaller specimens to cover design changes made since these specimens were made. Thus results will be available for type certification. In addition, check tests will be made on the major fatigue test specimen towards the end of its programme. These check tests, of course, will be made after the initial Certificate of Airworthiness tests are completed, but it is not thought practical to mix fail-safe tests with the major fatigue test, as the applications of limit load to check residual strength, necessary for the fail-safe tests, could affect crack initiation in the fatigue test.

## THERMAL CYCLE IN MAJOR FATIGUE TEST

### Important Thermal Effects in Fatigue Test

Before going into the practical details of how this test is to be done for the Concorde, an examination of why a fatigue test is to be done at all and what the main parameters are which dictate its complexity is appropriate.

A fatigue test is a firm requirement of the British and French certifying authorities. They specifically state in the TSS standards (ref. 4) that "A full scale complete airframe fatigue test programme shall be carried out under representative loading, pressure, heating, and cooling conditions." There is good reason for this. Experience, over many years, has shown that the fatigue test can reveal unexpected weaknesses and enable corrective action to be taken early, thus preserving safety. In safe-life designs, the fatigue test can reveal failures which would not have been found by inspection until they had become catastrophic. In fail-safe designs, the fatigue test shows where to make the inspections and gives guidance on their frequency, based on the rate of crack propagation. It has even been known to show that some structures designed to be fail-safe had unexpected weaknesses with safe-life characteristics. Thus it is extremely desirable for a fail-safe structure to be fatigue tested for its full life with an adequate factor to cover the possibility of unexpected safe-life failures. As well as the safety aspect, the early knowledge of possible fatigue damage in service has important warranty considerations.

Having established that a fatigue test shall be done, there is no doubt that the best and most up-to-date methods of simulation of the mechanical loads must be used, and this is no real difficulty with modern servo-hydraulic loading systems and on-line computer control. The major question, which governs the complexity of the test, is the manner in which it is necessary to include the thermal effects in order to do a meaningful test. There are a number of significant thermal effects including



(1) The thermal stress loading cycle produced by the thermal cycle, that is, heating and cooling each flight

(2) Creep arising from prolonged time at temperature under load

(3) Overageing arising from prolonged time at temperature and giving a reduction of static strength

(4) The interaction of all these thermal effects on each other and on the fatigue behaviour of the structure under mechanical loads.

Of these, the first is of overriding importance in determining if or how the thermal effects should be included in the test. Also intermittent heating is probably important because of its interaction effect on fatigue behaviour under mechanical loads.

It was shown previously that the difference in internal and external structural temperatures arising from the supersonic climb to altitude produced a thermal stress, which died away as the structural temperature equalised during the cruise. The process was repeated during the descent, giving rise to a thermal stress of the opposite sign. These thermal stresses are likely to be characteristic of all supersonic transport aircraft having a long range and to be an important part of the fatigue-loading environment. For the Concorde they are of comparable magnitude to the direct stress. They cannot therefore be ignored in a fatigue test. They might be simulated by mechanical means, but although this may be feasible in simple specimens, it is not thought to be practicable in the complex structure of a complete airframe. By their very nature, thermal stresses arise from the differential expansion or contraction of adjacent structure and have a varying pattern throughout the structure depending upon the temperature differences set up with time. It therefore is regarded as essential that the thermal stresses should be obtained in the fatigue test by the application of the thermal cycles.

The other thermal effects then need to be fitted into the test cycle. Not all of these necessarily involve intermittent heating and cooling for adequate representation. But they should be included in the test somehow, and can be included more easily if the thermal cycle is applied in the test. More details about thermal effects are given in the following sections where the problem of accelerating the test is considered.

### Accelerating the Test

Concorde is being designed to have a service life of 45 000 hours. The maximum utilisation for any particular aircraft is expected to be between 3000 and 4000 hours per year. Now, as mentioned previously, the aim is to run the fatigue test so that the specimen will always have achieved at least three times the fatigue life of any aircraft in service. This factor of three allows for the scatter in fatigue performance between nominally

identical structures, and allows for the variation between the test specimen and service aircraft. Hence, as much as 12 000 hours of flying may need to be represented in a year.

However, there are only 8760 hours in a year, and even by testing 24 hours per day, 7 days a week, it is unlikely that more than 4000 hours of actual test running can be achieved as time must be allowed for inspection of the specimen, maintenance, and so forth. Thus, the test has to be accelerated by a factor of approximately three, and it would be prudent to achieve rather better than this to allow provision for long delays which would inevitably occur if a major failure took place in the test.

Normally, it is quite a simple matter to accelerate a fatigue test as the mechanical load effects are amenable to grouping and can be represented in a much shorter time in the test than in a flight. This grouping has become a well-established technique, although some workers have slight doubts whether it would not be better to include more dwell periods between loading than is currently done. It is much more difficult to accelerate a test cycle including thermal effects because most of these effects are time dependent. The present plan is to accelerate the hot test cycle in two ways:

- (1) By making each thermal cycle as fatigue damaging as two supersonic flights
- (2) By shortening the thermal cycle to as near 60 minutes as practicable.

In planning the fatigue test, it has been assumed that

- (1) The average length of a supersonic flight is 2.5 hours.
- (2) The average length of a subsonic flight is 1.0 hour.
- (3) On the average the ratio of supersonic flights to subsonic flights is 4 to 1.

The current plan is to run the fatigue test in a sequence of two hot test cycles and one cold test cycle. The hot test cycle will represent two supersonic flights and will contain one accelerated thermal cycle equivalent to two supersonic flights and two groups of mechanical loads each equivalent to one flight. The cold test cycle will contain all the mechanical loads equivalent to one flight. The aim is to do the hot cycle in 60 minutes and the cold cycle in 15 minutes. If this is achieved then the sequence of two hot cycles and one cold cycle will take 2.25 hours and represent four supersonic flights plus one subsonic flight taking 11 hours. Thus, the time has been compressed by a factor of almost five.

Within this broad format, the individual test cycles will take account of flights in different degrees of turbulence, at different gross weights, and for different flight patterns. No test, however complicated, can provide a perfect representation for all aircraft in service, and a means of interpretation is necessary to relate the test results to service as previously mentioned.

Shortening the hot cycle brings a number of tricky problems to fit all the mechanical loadings into the time available, especially as each of these cycles is to represent two



flights. Basically, the plan is to associate one set of mechanical loadings with their appropriate place in the test cycle and then to add another set towards the end of the cycle while the specimen is recovering temperature equilibrium ready for the next test cycle. (See fig. 19.) The alternative plan would have been to have put in one set of mechanical loadings, but at a higher level to take account of the acceleration. This plan was rejected however, mainly because of the possible unrepresentative effect on crack propagation.

The time available for mechanical loading thus becomes critical in the shortened cycle; and therefore, great care needs to be taken in choosing the levels of loads to be used, particularly within the taxi and gust load spectra. Especially, it is necessary to ensure that sufficient small loads are applied to reproduce the effects of fretting, even though these small loads take a disproportionate testing time compared with their direct contribution to the fatigue damage. The computer-controlled hydraulic servo-loading system gives great freedom of choice of loading levels, and full advantage can be taken of this to pick an optimum combination of frequencies and levels.

Another advantage arising from this flexibility is that random loading can be used if desired. Random loading, of course, more nearly represents what happens in service, and its use reduces the number of assumptions necessary in setting up the test programme. A possible disadvantage is that it might make it more difficult to trace the progress of failures on the fracture surfaces. Some work is currently in hand to investigate this in laboratory specimens and also the possibility of arranging the random loading to include marker loads which could be found on the subsequent fracture. Certainly, it is an advantage to be able to trace the progress of a fracture, but experience shows that this is often not possible except in simple loading cases and advantages of random loading may well outweigh the disadvantage which might arise in this particular aspect.

#### Accelerated Thermal Cycle

As previously mentioned the thermal cycle is to be accelerated by making it represent more than one flight and by shortening it. The most important part of the thermal cycle is the representation of the thermal stress, although the effects of creep and over-ageing and of their interactions are not to be ignored. The thermal stress arises from differential expansion due to the temperature difference between the skin and the internal structure. This stress is proportional to the temperature difference, and hence by increasing this difference a corresponding increase in thermal stress is obtained. This increase, in turn, is related to life through the appropriate S-N relationship, and an increase in temperature range can be chosen to give in one test cycle the fatigue damage from thermal stress approximately equivalent to that occurring in two supersonic flights.

For illustration, a simple example of a hypothetical piece of deep structure which follows certain assumed conditions will be considered. In particular, it is assumed that



the skin and the deep structure start the climb at the same temperature and that the deep structure has warmed up only negligibly by the time the skin temperature has reached its cruise value. This would then give the condition for maximum thermal stress. It is also assumed that similar conditions apply for the descent. The comparison then becomes

	Real time conditions	Test conditions
Thermal stress due to climb:		
Skin and deep structure temperature at start of climb, °C . . .	15	22
Skin temperature at end of climb, °C . . . . .	100	130
Deep structure temperature at end of climb, °C . . . . .	15	22
Skin temperature range, °C . . . . .	85	108
Increase in skin-temperature range over real-time conditions, percent . . . . .		27
Thermal-cycle time-compression factor . . . . .		≈2
Thermal stress due to descent:		
Skin and deep structure temperature at start of descent, °C . . . . .	100	130
Minimum skin temperature during descent, °C . . . . .	-20	-25
Deep structure temperature at same time, °C . . . . .	100	130
Skin temperature range, °C . . . . .	120	155
Increase in skin-temperature range over real-time conditions, percent . . . . .		29
Thermal-cycle time-compression factor . . . . .		≈2

The example is imprecise because clearly all the assumed conditions are not exactly met. Nonetheless, it illustrates that practical test conditions can be found which for deep structure will enable the thermal cycle to be accelerated by approximately two, that is, to represent two real flights. Clearly, a wide range of test conditions could be chosen to achieve this effect. The particular combination of a top temperature of 130° C, a bottom temperature of -25° C, and an ambient temperature of 22° C is a reasonable compromise on plant requirements, consistent with minimum effect on material properties of the specimen, particularly at elevated temperature. There are, of course, varying depths of deep structure throughout the aircraft. Because only one external temperature distribution can conveniently be prescribed for the whole aircraft, each portion of the structure will experience a different acceleration, depending upon its depth within the total structure.

A similar approach to accelerate the conditions for shallow structure is possible by increasing rates of heating and cooling, and a useful compromise is to cover the new tem-



perature range in the original time. Again the resulting acceleration pattern is not uniform throughout the structure.

The second part of the problem is what can be done to shorten the test cycle. It has already been said that the most important reason for including the thermal cycle is to represent the thermal stresses, and for these it is important to represent the climb and descent phases in approximately real time. Thus, the only hope for shortening the test cycle lies in shortening the cruise and recovery phases. There are however two important constraints, namely, that the structural temperatures must be correct at the start of the climb and at the start of the descent so that the conditions are right for the generation of the thermal stress. If these conditions can be achieved artificially, the cruise and recovery phases can be shortened. Incidentally, a shorter cruise at higher temperature is compatible with maintaining the correct creep and overageing damage rates.

In cruise, the important criterion is that the structure reaches the conditions at the end of the cruise phase before the descent phase is started. Shallow structure will follow quite closely the temperature of the skin. Deeper structure will lag behind because of the time it takes for the heat to be conducted to it. The amount of lag will vary considerably throughout the structure. Most of the structure will, however, have reached a stable temperature by the end of the cruise phase. The problem, therefore, of shortening the cruise phase is to identify the structure which will not have reached a stable temperature in the shortened time and to force heat it in the test so that it does. The forced heating can be started as soon as the peak thermal stress has been reached in the climb. This peak will be reached at the end of the climb for deep structure and earlier for shallow structure.

Similar arguments for forced cooling apply to the shortening of the recovery phase. Forced cooling can be started as soon as the peak thermal stress has been reached; the peak thermal stress occurs at or before the time at which the skin reaches its minimum temperature. The situation is complicated by the fact that the final ambient temperature is higher than the skin temperature and lower than the temperature of the bulk of internal structure. Therefore, the forcing potentials are less than those obtained at the end of the cruise. The forced heating and cooling is being done by circulating hot and cold air and hot and cold fuel and is an extremely complex process.

For Concorde the chosen aim is to do the complete test cycle in 60 minutes, made up approximately of take-off and climb, 11 minutes; cruise, 20 minutes; descent and landing, 9 minutes; and recovery, 20 minutes. Initially test cycles will be run in real time, and results compared with measurements in flight. These have become known as "witness tests." Tests under accelerated conditions will then be made with the cycle time gradually being reduced, but ensuring always that the shortened test cycle remains meaningful. A comparison of the proposed accelerated thermal cycle with the flight cycle is shown in figure 20.



## Interpreting the Test

The presence of the thermal cycle adds a number of difficulties in interpreting the test. For the fatigue test of a subsonic aircraft, numerous simplifying assumptions have to be made to set up the test, and means have to be devised to interpret the failures and to apply them to aircraft whose service history differs from the loading spectra used in the test. All this is still necessary for the supersonic transport aircraft. There is, however, the added complication of the thermal cycle and of the compromises which have been necessary to include it in the test.

It has already been shown that compression of test time, that is, increasing the thermal stress damage in each test cycle, produces a nonuniform thermal-cycle time-compression factor throughout the structure. Even though the nominal value of this compression factor is 2, it is necessary to be able to calculate the actual value at any place where a failure occurs or at other points of interest.

The principle of the accelerated cycle is to increase the magnitude of the thermal stress so that less cycles are applied and time can be saved; however, these increased thermal stresses have to be combined with the direct mechanical stresses. In fact, the thermal stress can be regarded as a shift of mean stress for the alternating mechanical stresses since it is a slowly varying stress from zero to a maximum in one direction, through zero to a maximum in the opposite direction, finally returning to zero again. In order not to raise the peak stresses to too high an unrepresentative value, it was decided to apply the mechanical loads (real level) twice during the test cycle to compensate for the acceleration of the thermal cycle. This is a complex situation. Increased thermal stresses are being combined with mechanical stresses at real-aircraft level. At any particular point in the structure, the proportions of thermal and mechanical stress damage may not be correct since the mechanical cycles are being applied overall on the assumption of a nominal value of thermal-cycle time-compression factor of 2 whereas the actual value at that point may be different.

It is important that under these special conditions the form of failure should not be altered, or if it is, the difference should be recognised. To this end, the box tests and other backup research tests are being made to explore modes of failure, times to failure, and crack-propagation rates under combinations of mechanical and thermal stress and under real and accelerated conditions.

Fortunately, shortening the thermal cycle in association with accelerating the rate of thermal-stress damage results in the application of higher temperatures in the cruise for shorter times. Thus, in part, some automatic compensation is given for the creep and overageing effects, but these need to be calculated in detail throughout the structure to determine how much the structural properties are being changed from each of these causes and comparison made with real aircraft conditions.



Therefore, the need to assess the cumulative damage under all of these conditions and relate it to aircraft conditions so that test damage can be interpreted is great. The process for correcting fatigue-test results for different service conditions is now well established for subsonic aircraft. Basically, this correction depends upon the application of Miner's law to critical parts of the structure. To this process must now be added the thermal stress and the interaction effects of the thermal cycle, creep, and overageing on the mechanical stress. Preliminary methods are being tried and verification sought from the research programme.

## HEATING AND COOLING FOR THE MAJOR FATIGUE TEST

### External Heating and Cooling

The purpose of external heating and cooling is to apply to the specimen the kinetic heating which the aircraft receives in the supersonic climb and cruise and the cooling which results from the descent at subsonic speeds. (See fig. 4.) The heating and the cooling is being done convectively with air, which is blown over the specimen at the required temperature and at suitable speeds so that the heat-transfer coefficients experienced in flight are reproduced in the test laboratory. The specimen is enclosed in a thermal duct which is divided into five sections, one over the fuselage and one over and under each of the two wings. There are five closed circuits linking these sections to the heating and cooling plant. Closed circuits are used so that the air can be recirculated and the heating and cooling potential conserved. Each circuit contains a fan to circulate the air and heat exchangers to heat and cool it.

Thermal duct. - Initially it was intended that the thermal duct should totally enclose the specimen. Later for reasons of expediency, it was decided not to heat and cool the wing tips and the upper part of the fin. The justification for not heating and cooling these areas is that the thermal stresses in them are low, and what effects there are can be assessed by reading across from areas of similar structure which are being subjected to the thermal cycle. The most important advantage is that this exclusion enables a rigid duct to be used since the specimen deflections can be contained within the duct spacing from the specimen. The duct can therefore be supported by rigging from the structure of the laboratory. Some flow-restriction problems arise because of the specimen deflections, but these are small compared with the problems that would have arisen from the design and construction of a flexible duct or a duct with flexible joints. Even so the design of the duct is still a major engineering task. This duct has to be easily removable so that the specimen can be inspected at frequent intervals. It has to be airtight when closed to avoid large losses of hot and cold air. It has to have a minimum of thermal mass so that it does not absorb heat and cold from the airstream in an unnecessarily



wasteful manner. It must, of course, be able to withstand the effects of the continuous repetition of the thermal cycle.

As mentioned, the overall aircraft duct is divided into five main sections which are effectively in parallel – one over the fuselage and one over and under each wing. The wing ducts are further subdivided; the upper-surface duct splits into four parallel branches to cater for spanwise variation of heat-transfer coefficient, and the lower-surface duct splits initially into four branches which merge into three in order to bypass the engine nacelle. The fuselage duct is an annulus up to the wing leading edge, where it splits into two branches, a horseshoe sectioned upper duct and an approximately rectangular sectioned lower duct. The two ducts continue along the fuselage and rejoin at the wing trailing edge. Near the fin leading edge, a divider takes some of the air from the upper duct and passes it over the lower portion of the fin before rejoining the fuselage circuit in the return trunking. The ducts are shown diagrammatically in figures 21 and 22.

For each wing, the upper- and lower-surface ducts join at the trailing edge to form a plenum chamber with a static pressure common to both ducts. The return trunking for the two circuits is connected to the plenum chamber, and a short distance from the chamber the lower-surface duct trunking is provided with a vent to the atmosphere. The vent dictates the position of atmospheric static pressure in the circuits and allows the circuits to breathe during temperature changes. To prevent an increasing concentration of airborne fuel simulant in the circuits due to small fuel leakages, the circuits are constantly purged through the vent by bleeding fresh air into the circuits at appropriate positions. There are three vents, one for each wing and one for the fuselage. Provision is made for the insertion of suitable gauges in the three outer ducts of each wing circuit forward of the leading edge to adjust the mass flows in the ducts, and vane dampers are fitted in all ducts at the trailing edge for fine adjustment. Similarly, for the fuselage circuit, vane dampers are fitted in the upper duct and small fin duct.

The duct depths are designed to give the required heat-transfer coefficients from the Dittus and Boelter equation

$$\text{Nusselt number} = 0.023(\text{Reynolds number})^{0.8}(\text{Prandtl number})^{0.4}$$

with the overriding condition that the deflected aircraft structure shall not foul the duct. Average duct depths are fuselage, 7 inches; wing upper, 8 inches; and wing lower, 16 inches. The depth of the wing ducts is adjustable over a 3-inch range so that the ducts can be tuned to give the right temperature response in the fore and aft direction. The fuselage ducts also are adjustable but only in a vertical direction.



The duct is mounted on a massive steel structure with chordwise beams and span-wise intercostals bridging the specimen. Much of the duct is made up of a large number of removable panels constructed of aluminium alloy. These fit onto the beams and intercostals of the supporting structure and react to the loading due to the duct internal pressure. The duct panels and the fixed duct structure are insulated from the airflow on their inner surface by insulation panels attached to them. The insulant is a semirigid slab of mineral wool completely enclosed in a seam-welded stainless steel skin 0.010 inch thick to form insulating panels 1.25 inches thick around the aircraft and 1.75 inches thick in the inlet and exhaust ducts. The insulation panels are sealed to prevent ingress of fuel simulant which can be present within the duct in liquid and vapour form due to leakage from the specimen.

Since the aircraft moves relative to the duct, the chordwise walls separating the ducts from each other are flexible and constructed to extend and compress like an accordion. (See fig. 23.) The upper surface walls are coincident with chordwise rows of wing-load application rods which are used to give the walls lateral stability. The lower surface walls have built-in lateral stability since there are fewer loading rods attached to the lower surface. Sliding seals are provided where the wing tips protrude from the duct. The structure carrying the seal is counterpoised and follows the wing movements.

The fin duct is the only portion of duct not fixed relative to the floor. It is attached to the fuselage duct by a flexible seal and is moved vertically in step with the fin movement by means of hydraulic jacks with a self-contained hydraulic supply and control unit. With both fin and duct moving together, the problem of passing fin lateral loading rods through the duct is eased considerably.

An essential requirement of the duct is that it shall be easily removable for inspection of the specimen. To this end the duct panels are fitted with quick release devices, and as far as possible, the loading rods are passed through the joints between the panels. Nonetheless, removing the panels is still a very large task since there are about 80 around the fuselage, 32 above the wings, and 60 below the wings. Those on the fuselage are mainly removable, and those on the wing are mainly hinged.

Another major problem for the duct is the passing through it of the service pipes carrying air and fuel substitute to provide the internal heating, cooling, and pressurisation. There are some 100 of these pipes ranging in diameter from 4 to 14 inches. Many of these pipes pass through the lower fuselage duct and have a masking effect on the fuselage structure. They also increase the pressure drop through the duct considerably. In some cases it has been possible to group the pipes together and to shroud them with an aerodynamic fairing to reduce the interference to the airstream. There is a difficulty of sealing these pipes to the duct to avoid leakage and yet to allow movement of the pipes with the specimen as it deflects in the duct. Some pipes are fitted with corrugated fabric fairings to accommodate the movement and reduce the pressure drop and air leakage. For



others, clearance holes are filled with a sliding-plate device, which shows a relatively smooth surface to the airstream.

The temperature of the air and its mass flow are varied throughout the test cycle to give as near as possible the correct heat-transfer coefficient to match the corresponding flight conditions. The temperature of the air is regulated by the flow of fluids to the heat exchangers and the mass flow by adjusting the speed of the circulating fans. The heat-transfer coefficients vary during the different phases of the flight and a compromise has to be achieved on the rig mainly because, once it has been set up, there is a fixed geometrical relationship between the duct and the specimen. The duct panels are individually adjustable on their supports so that duct depths can be altered locally, thereby enabling the duct to be tuned to give the best overall compromise along the length of the specimen for the chosen air temperature and mass flow. Some experience of this has already been gained on the forward fuselage specimen, as mentioned previously, and it is confidently expected that good temperature distributions along and around the specimen will be achieved.

External heating and cooling plant.- The primary heating and cooling plant consists basically of the following equipment:

- (1) Axial-flow fans to circulate the air
- (2) Heat exchangers to heat and cool the air
- (3) Boilers and refrigerators for producing the hot and cold fluids
- (4) Storage vessels for all the fluids
- (5) Multitudinous pumps, control valves, and piping to distribute the fluids.

A simplified flow diagram of the plant is shown in figure 24. The plant generates hot and cold fluids continuously, and these are stored in large vessels to be transferred to the heat exchangers as required.

Some idea of the magnitude of the task can be gained from the facts that the structural specimen itself weighs about 40 tons and the fuel substitute about twice this amount. These specimens have to be taken through the appropriate temperature ranges approximately once every hour. This thermal cycling is, however, only part of the work which the plant has to do; since in circulating the air, the thermal duct, return trunking, and associated equipment are all cycled through the appropriate temperature ranges. Even though these are insulated as carefully as possible, they add up to the equivalent of about five more specimens.

The axial-flow air-circulating fan in each of the five circuits is fitted with adjustable inlet guide vanes and downstream air-straightening vanes and delivers about 3200 ft<sup>3</sup>/sec of air. The fan drive is through a shaft connected to a 2000-hp variable-



speed motor situated outside the circuit. The inlet guide vanes are set to give the best fan efficiency for the particular circuit-flow conditions. The total airflow in all five circuits is about 1250 lb/sec. The maximum air velocity is about 150 ft/sec. The fans also provide a considerable input of heat to the air. This heat input assists during the heating phase but is an embarrassment during the cooling phase, requiring additional cooling capacity from the plant to compensate for it. It may even need to be compensated for in part during the cruise if the heat input from the fans proves to be greater than the heat losses of the circuits.

The heat-exchanger fluids are water and ammonia, which are each stored at two different temperatures: water at 180° C and 5° C and ammonia at -62° C and 35° C. There are two heat exchangers in each air circuit, one for water and the other for ammonia. The water heat exchanger, immediately downstream of the fan, heats or cools the air when supplied with water at 180° C or 5° C, respectively. The ammonia heat exchanger supplies the cooling necessary to produce below-zero air temperatures and is so constructed that air can either flow through or bypass the exchanger matrix elements. The eleven elements of the heat exchanger are mounted one above the other with ten intervening gaps. Hydraulically operated shutters over the element inlets and gaps are so arranged that when the element shutters are open, the gap shutters are closed, making the air go through the elements. With the element shutters closed and the gap shutters open, the heat exchanger is virtually bypassed. The ammonia heat exchanger is bypassed whenever the circuit contains hot air; this bypass reduces the loss of heat into the exchanger mass, and in addition, the heat-exchanger mass is kept at a constant temperature by flowing ammonia at 35° C through its elements.

It is extremely important that the air leaving the heat exchangers and entering the thermal duct shall be uniformly heated or cooled over its cross section. The fluid flow across the heat exchangers has been specially designed with this in mind. In addition, the fluid in the heat exchangers is constantly recirculated so that it is at a uniform temperature. Fluids from the bulk storage are fed into these circuits to give the required air temperature.

The sequence of heat exchanger actions during a thermal cycle is

(1) Climb: The temperature of the water circulating through the heat exchanger is increased progressively by the addition of hot water at 180° C. Warm ammonia at 35° C is circulated through the bypassed heat-exchanger elements.

(2) Cruise: The hot water is gradually decreased and is cut off if the heat input of the fan is greater than the heat losses of the circuit; if this occurs, chilled water at 5° C is fed to the heat exchanger.

(3) Descent: The chilled water supply is increased progressively until it is no longer able to maintain the required air-cooling rate. Before the chilled water reaches



its maximum supply rate, the shutters over the ammonia elements open and cold ammonia, at  $-62^{\circ}\text{C}$ , is fed into the ammonia heat exchanger. The chilled water continues to act as a precoolers until the air temperature entering the water heat exchanger drops below the chilled water temperature. At this stage, hot water is fed to the heat exchanger to prevent freezing.

(4) Recovery: The supply of ammonia at  $-62^{\circ}\text{C}$  is stopped and the air temperature increases to its datum. If the fan heat input is too large, chilled water will be pumped before the end of the cycle to keep the air at its datum temperature. At the end of the recovery phase, the ammonia element shutters are closed and the gaps opened to bypass the air.

The heating and cooling phases demand large amounts of energy in relatively short periods of time, and in order to spread the requirements of the plant over a complete cycle, the heat-exchanger fluids are generated continuously and stored.

The hot water is heated by two oil-fired boilers with a total output of  $36 \times 10^6$  Btu/hr. The water is heated to  $180^{\circ}\text{C}$ , and some 100 tons are stored in the insulated storage vessel. The upper part of the vessel serves as an expansion chamber and is filled with nitrogen at  $180\text{ lb/in}^2$  to enable water temperature to be attained and to prevent cavitation in the water system.

Chilled water at  $5^{\circ}\text{C}$  is provided by an ammonia refrigerating machine with a two-stage piston compressor, condenser, and evaporator. The plant has a cooling capacity of  $13.5 \times 10^6$  Btu/hr. About 300 tons of chilled water are stored in two insulated vessels under the same pressure as the hot water so that either can be fed to the water heat exchanger.

Ammonia liquid at  $-62^{\circ}\text{C}$  is generated by two identical multistage turbocompressors working in parallel and having a total capacity of  $14.3 \times 10^6$  Btu/hr. Each turbocompressor uses three stages of flash evaporation. About 145 tons of the cold ammonia is stored in two insulated vessels which are interconnected with expansion vessels containing ammonia at  $35^{\circ}\text{C}$ . These hold the system at the vapour pressure of ammonia at  $35^{\circ}\text{C}$ , which is approximately the same as the pressures used in the hot and chilled water systems. The expansion vessels also serve as storage for the supply of ammonia at  $35^{\circ}\text{C}$  for the heat exchangers while they are bypassed during the heating phase.

A considerable quantity of cooled water is also required throughout the plant. It is used for

- (1) The initial cooling of the chilled water supply
- (2) The condensers of both refrigeration plants
- (3) Maintaining the liquid ammonia below  $35^{\circ}\text{C}$  in any parts of the plant where this temperature could be exceeded



- (4) Cooling the fan-motor speed controls, which are electrolytic resistors
- (5) Cooling the fluid coupling of the turbocompressors to their electric motors
- (6) Cooling pump glands and other similar applications.

The water is cooled from  $27^{\circ}\text{C}$  to  $22^{\circ}\text{C}$  in a two-cell cooling tower, having a total cooling capacity of  $70 \times 10^6$  Btu/hr and a cooling water flow rate of almost  $0.8 \times 10^6$  gal/hr.

The circuit of the fans, heat exchangers, and thermal duct is completed by the return trunking. This is constructed as a double shell, the inner lining being fabricated from 25 SWG (0.02-inch) stainless steel sheet and having an internal diameter of 6.5 feet. The outer cladding is fabricated from 19 SWG (0.04-inch) aluminium sheet and is separated from the inner lining by a 2-inch thick layer of mineral-wool insulation. Sections of the trunking are joined together by stainless steel bellows and cascaded corners are used to assist the airflow. The assembled trunking is completely air and oil tight. The total lengths of the five circuits vary slightly; the shortest is 590 feet and the longest 680 feet.

All of the plant for the external heating and cooling of the specimen is contained in a plant house 240 feet  $\times$  130 feet  $\times$  50 feet high located at the forward end of the test frame. (See figs. 17 and 25.) Inside this building is also the control room for the external plant. This is a strong room protected against dangers which might arise from explosion in the specimen or plant. The plant is started and monitored from this control room and, in normal operation, is controlled automatically from the computers. However, individual items of the plant can be run from this room for commissioning and checking purposes, and if necessary, a thermal cycle of the whole plant can be run. The plant house is heavily insulated so that noise from the equipment does not seriously disturb work in the adjacent offices or destroy the tranquility of the surrounding townships in the quiet of the night.

#### Internal Heating, Cooling, and Pressurisation

As the name implies, the basic functions of the internal facility are to thermally condition the inside of the specimen and to pressurise the specimen. These are two methods by which these functions may be performed: heating, cooling, and pressurisation with circulated air and heating and cooling with circulated fuel substitute, which for safety reasons is used in place of aircraft fuel. In more detail, the tasks needed to be performed are

- (1) To represent the normal air conditioning and pressurisation of the fuselage

(2) To force heat and cool those areas of the structure which would not reach their required conditions in the shortened accelerated test cycle. This forced heating and cooling is done as appropriate with air or the fuel substitute. This is the major task of the internal plant.



(3) To heat, cool, and load by pressure that area of the underside of the wing normally covered by the nacelle. In the test the real nacelle is not fitted, and all loading actions are applied to the wing by a dummy nacelle.

(4) To correct the thermal condition arising in the wing tips because these are not completely covered by the external thermal duct. This discontinuity in the external heating and cooling could give rise to unrepresentative loading in the specimen, and to correct this, special treatment is given to the fuel tanks and other structure in this area.

(5) To pressurise certain of the fuel tanks to represent inertia loads arising on the fuel during parts of the test cycle.

The whole internal facility divides into three groups, air circuits, fuel systems, and a background plant which supplies the heating energy, cooling energy, and pressurisation air to the primary systems. The major part of the internal plant is housed in a specially designed plant house, measuring 150 feet  $\times$  90 feet  $\times$  50 feet high, erected on the starboard side of the test frame. (See fig. 17.) The plant house contains the control room for the internal plant, from which the equipment is started and monitored. The plant is normally controlled by computers, but it can, if necessary, be run from this control room for commissioning or checking. Because of the extremely high noise level expected from the installed plant, the building is of massive construction to provide the necessary sound absorption qualities to avoid disturbance of the neighbourhood.

The major components of the primary circuits and systems are connected to the specimen via a very complex and congested system of piping traversing between the plant house and the main test frame.

Air circuits.- The areas conditioned by the air circuits are shown in figure 26. These cover the fuselage air-conditioning and pressurisation, the areas to be force heated and cooled by air, and the nacelle-wing areas. Among the force conditioned areas are fuel tanks 9 and 10, which are emptied in flight before the supersonic phase commences and hence do not need to be filled with fuel substitute in the test. All these areas are grouped into 16 zones, some duplicated on port and starboard sides of the aircraft. Zones which have similar thermal and pressure requirements are further grouped together to give seven primary air circuits.

The air circuits are all basically similar; each consists of a Roots blower, one or more heat exchangers, a number of control valves, and connecting piping. A typical circuit circulates about 14 pounds of air per second at a temperature of 130° C in the heating phase and at 15° C during the cooling phase. The blowers are driven by electric motors averaging about 700 hp each. Roots type blowers were chosen as air-moving machinery because of considerable pressure drops involved in each of the air circuits. Centrifugal



fans would have been inadequate and centrifugal compressors were not economically competitive in the sizes required. A typical air circuit is shown in figure 27.

Each circuit is a closed loop, the air being circulated by means of the Roots blower through the conditioning system to the various zones of the specimen and then back to the suction side of the blower. The air is heated to the required temperature ( $130^{\circ}\text{C}$  in most circuits) by a heat exchanger fed with water at  $180^{\circ}\text{C}$  from the background plant. For the cooling phase, the air passes through two coolers; the first, using cooling-tower water at  $22^{\circ}\text{C}$ , cools the air to about  $35^{\circ}\text{C}$ , and the second, using chilled water at  $5^{\circ}\text{C}$ , further cools the air to about  $15^{\circ}\text{C}$ . Selector valves control the passage of the air to the appropriate heat exchangers.

The total mass flow to the specimen is controlled by regulating the valve in the blower bypass which bridges the delivery and return pipes across the blower. This flow is subdivided in the appropriate circuits by setting inlet trimming valves to apportion the flow to each individual zone.

A bypass is provided between the inlet and outlet pipes to each zone to enable temperature preconditioning of the delivery pipes between phases if required and thereby allow a choice of initial air temperature into the specimen. A valve in the bypass prevents flow when not required. The specimen inlet valve dictates whether flow is allowed through the specimen.

Some circuits where the zone is not airtight are vented to atmosphere at the specimen; the remaining circuits servicing airtight zones are vented from outlet pipes adjacent to the specimen. In all instances therefore the return pipes operate at a subatmospheric pressure except when a circuit is pressurised. Circuits 1, 3, and 6 are required to be pressurised during certain phases of the test cycle and are individually supplied with air at either 7 or 14 lb/in<sup>2</sup> from the background plant via an inlet valve which regulates the supply when an increase of pressure is required. A separate valve decreases the pressure on command by controlled venting to atmosphere. Safety valves are provided at each specimen inlet to safeguard against overpressurisation and also at each specimen outlet to prevent negative pressure occurring within the specimen.

Each circuit is fitted with an impingement liquid separator to remove any fuel substitute which may have leaked into it. This is to avoid fouling of the heat exchangers, which would reduce their efficiency. A mist detector is installed in each circuit to give adequate forewarning should the air-fuel substitute ratio become an explosive hazard. Fire detection and suppression systems are also provided.

The Roots blowers are constructed with close running tolerances on their rotors, and it is necessary to protect them from harmful temperature fluctuations. Thus, in five of the circuits, where the temperature of the air can reach  $130^{\circ}\text{C}$ , a heat exchanger is



installed at the blower inlet to precool the air returning to the blower. The air temperature in the other circuits does not exceed 60° C.

The blowers and heat exchangers are installed in the internal plant house on the starboard side of the specimen (fig. 17), and there is therefore a considerable length of piping to bring the air to and from the specimen. In a typical circuit, the distance from the heat exchangers to the specimen is about 150 feet, and considerable care has had to be taken to keep the thermal mass of the delivery pipes to a minimum to ensure the required air temperatures at the specimen. The pipes have a wall thickness of only 0.04 inch and are covered with 2-inch-thick insulation of low density. The pipes vary in diameter between 6 inches and 24 inches according to the circuit.

Attaching these pipes to the specimen is also a major problem because of specimen movement caused by the mechanical loading and thermal distortion. There are about 80 of these pipes, and most of them have had to be fitted with a sliding joint to provide the necessary flexibility. The problem for those carrying pressure is even more severe as the end loads from these could provide unacceptable spurious loads on the specimen. This problem has been overcome by the design of special balanced fittings.

Having brought the air to the specimen, there is still the mammoth task of distributing it to all the zones requiring conditioning. Essentially this is done by a gallery system with air-distribution points along its length. A typical one for the fuselage air-conditioning is shown diagrammatically in figure 28. A similar gallery system is used to collect the air and return it to the plant. All pipes are taken into and out of the structure through existing holes wherever possible so that the primary structure of the specimen is not affected.

Fuel systems.- The layout of the fuel tanks is shown in figure 29. As mentioned previously, tanks 9 and 10 are conditioned with air, but all of the remainder need to be filled with fluid in the test to represent the fuel. The choice of a suitable simulant for the fuel has been a very difficult task. The use of kerosene itself would have been too dangerous and its repeated use through the many thermal cycles and long periods at elevated temperature would have presented deterioration. The main features that have been looked for in a simulant are

- (1) A sufficiently high flash point to avoid fire and explosion risks
- (2) Acceptable heat-transfer characteristics so that representative thermal conditions can be achieved in the specimen tanks
- (3) Compatibility with the constructional materials of both specimen and plant
- (4) Slow appreciation of acidic level and general stability when thermally cycled or maintained for long periods at elevated temperature
- (5) Low cost.



The fuel simulant chosen, Shell 7305c, is a mineral oil with antioxidant additives. Extensive tests have been made to develop the fluid and to show that it meets the previously mentioned qualifications. In the following description of the plant and the installations in the specimen, the fluid is referred to simply as fuel.

In the aircraft itself, there are varying levels in the tanks as the fuel is used up. These varying levels could have been represented in the test, but it was decided to simplify the procedure by using a constant quantity of fuel in the tanks. By carefully choosing the quantity of fuel and its temperature programme during the test cycle, it has been possible to achieve a close representation of the critical thermal stresses in the tank structure. Most tanks are about 75 percent full with some 90 percent full. Great care has been taken with the filling system so that the specimen shall not be damaged. The large fuel-circulating pumps cannot be used for this task, and a special small pump (25 gal/min) has been provided for the purpose. It is under manual control monitored from the computer. Thus the quantity of fuel in each tank can be chosen before cycling starts. Since each tank is in its own closed circuit, the quantity of fluid in the tank remains constant, apart from leakage, which may occur as the specimen is tested. One of the functions of the monitoring computer is to check these quantities and initiate shut-down if they go outside acceptable limits.

Special provision is available to change the level of fluid in the tank during the test cycle in order to simulate flight usage for the special witness tests in real time in which measurements on the specimen are compared with flight measurements. Varying this level, of course, changes the weight of the specimen during the cycle and has implications on the hydraulic loading and control systems.

In total there are thirteen separate fuel systems, each one serving a single tank within the specimen. Ten of the systems are temperature conditioned. Each system includes a pump, one heat exchanger, and control valves; these components are sized to meet the requirements of each particular tank. Two of the remaining three systems provide for fuel circulation only, while for the last tank provision is made for filling and emptying only. (See fig. 29.)

A typical specimen tank contains about 1800 gallons of fuel and requires a pumping rate of 350 gal/min through pipes of 5-inch diameter against a system resistance of about 120 lb/in<sup>2</sup>. Each system is vented at the specimen tank, and the pump is located in the main test frame to prevent cavitation at the inlet. A typical temperature conditioned system is shown in figure 30.

During normal cycling operation, the fuel is pumped from the specimen tank through the single heat exchanger located in the plant house and then back to the specimen tank. The flow rate in the system is controlled by a closed-loop servocontrol operating on the throttling valve.



During the heating phase, the fuel is progressively heated until that in the specimen tanks reaches the required temperature (usually 90° C). The heating is obtained by feeding hot water at 120° C to the heat exchanger at a preselected rate. Similarly in the cooling phase, the fuel is cooled until that in the specimen tanks reaches the required temperature (usually 25° C). The cooling is obtained by feeding chilled water at 5° C to the heat exchanger at a preselected rate. Between these phases the fuel may continue to be circulated, if required, with the energy supply to the heat exchanger interrupted to prevent further unwanted temperature increase or decrease, which prevents temperature stratification within the tank due to heat transfer through the skin from the external heating and cooling system.

Considerable attention has been given to the design of an efficient distribution system inside each specimen tank with the objective of ensuring 100-percent mixing of the ingoing fuel with the bulk. Internal pipes extend to the extremities of each tank and the ingoing fuel is injected at a pressure of about 20 lb/in<sup>2</sup> through a large number of small holes drilled along the length of the internal supply pipes.

Plate heat exchangers are provided because of their considerably superior heat-transfer qualities at the existing low Reynolds numbers. They have the additional advantage of being easy to dismantle for inspection and cleaning. Each system includes a small pump to maintain the water flow required through the heat exchanger to provide stable flow and heat-transfer characteristics.

Specimen considerations dictate that the acidic level of the fuel should not exceed a very low level; to this end chemical filters are provided in each system. Each filter is located in a bypass fed by a metering pump through a separate heater to provide continuous filtering at 30 gal/hr. All pipes and components with large surface areas in contact with the fuel are manufactured from stainless steel to minimise fuel contamination.

The total quantity of fuel in the system is a little over 20 000 gallons, and a storage tank of 25 000 gallons is provided to hold the fuel when it is removed from the specimen for structural inspections. The tank is lined with epoxy resin to prevent contamination.

Background plant.— The background plant consists of the heating plant, refrigeration plant, cooling tower, and pressurisation plant. An oil-fired boiler of  $16 \times 10^6$  Btu/hr output is provided to meet the overall heating demands of the primary air and fuel systems, the demands of which are about equal. The boiler produces water at 180° C and operates at a pressure of 180 lb/in<sup>2</sup>. This water is used directly in the heat exchangers of the air circuits, but for the fuel systems the water is reduced to a lower temperature through a heat exchanger which produces water at 120° C.

Although the heating demands of the facility are cyclic with a maximum rate of demand of approximately three times the average, it was not considered economically



advantageous to reduce the size of the boiler and install a storage system for the hot water. The boiler output will meet the demand on line for most of the cycle, the remainder being supplied from some spare capacity existing in the external plant.

Refrigeration energy is provided by means of a four-stage turbocompressor of  $13 \times 10^6$  Btu/hr capacity using freon as a transfer agent. It is driven by a 1000-hp electric motor and produces chilled water at  $5^\circ\text{C}$  for cooling in the air and fuel systems. The chilled water is generated continuously and stored in an insulated vessel of 28 000 gallons capacity (about 125 tons).

A single-cell tower cools almost  $0.5 \times 10^6$  gallons of water per hour from  $27^\circ\text{C}$  to  $22^\circ\text{C}$ , thereby dissipating about  $40 \times 10^6$  Btu/hr. This tower provides the eventual heat sink for all the energy going into the facility.

A battery of six Roots blowers with a total output of 18 pounds of air per second and a total power of 1500 hp provides the air for pressurisation on line when required. The air is pressurised in two stages, from ambient to  $7\text{ lb/in}^2$  gage and then from 7 to  $14\text{ lb/in}^2$  gage. Between stages the air is cooled to  $10^\circ\text{C}$  in a cooler using chilled water and the precipitating droplets are removed in a separator; the dewpoint then corresponds to  $5^\circ\text{C}$  at ambient pressure.

### Safety Precautions

The safety of the specimen is, of course, a major consideration in any full-scale fatigue test; for the Concorde it is even more important because of the very long time of testing involved. If this specimen were lost after some years of testing, it would be impossible to catch up the programme and to achieve the desired aircraft safety requirement. The specimen must always be tested to at least three times the life of any aircraft in service. Extensive safeguards against a number of hazards arising from different sources are therefore essential.

Excess-air-pressure safeguards. - Pressure within the specimen is measured by a transducer in all discrete compartments connected to the air system, whether they are normally pressurised or not. Areas normally unpressurised are included since the power of the circulating pumps is such that a blockage in the circuits could produce a hazard to the specimen. Some 40 measurement points are fitted and are checked at all times by the monitoring computer, which informs the operator of significant deviations from the required values and in extreme cases initiates automatic shutdown.

A mechanical direct-operating safety valve is fitted on the inlet pipe to each zone. Similar valves are fitted on the pressurisation feed pipes of the circuits that are pressurised. In addition there is built into each compartment, including all the fuel tanks, a direct-operating pressure-relief valve.

Antivacuum safeguards.- Pressures measured in all compartments are checked by the monitoring computer to ensure that a malfunction of an air-conditioning system does not create a subatmospheric condition within the specimen. A mechanical direct-operating safety valve is fitted on the outlet pipe from each zone.

Fuel-level surveillance.- The fuel level in each fuel tank is measured by a transducer and checked against the expected level by the monitoring computer. An increasing level could ultimately result in excess pressure and a decreasing level would indicate that fuel simulant was escaping, thereby creating a potential explosive hazard.

Explosive-hazard safeguard.- By the very nature of the test, it is likely that at some stage fuel simulant will leak from the specimen and will enter the air circuits. If it does so, there is a danger that in the fast-moving airstream of changing temperature, it will form a potentially dangerous fuel mist. To meet this possibility, a mist detector is installed in each of the external and internal air circuits to give adequate forewarning before the mist becomes an explosive hazard.

Fire detection and suppression.- Infrared and smoke detectors are installed both inside the specimen and in the external thermal duct surrounding the specimen. The detectors are connected to a bulk-storage CO<sub>2</sub> suppression system which will automatically flood the external ducts and the specimen should a detector become activated. Extensive fire detection devices are also fitted in the test laboratory and plant houses.

Ammonia detection.- To safeguard against the possible corrosion of the specimen should ammonia leak from a heat exchanger into an external air circuit, an ammonia detector is installed in each circuit. Further detectors are located in the external plant house to give adequate warning to personnel.

## MECHANICAL-LOADING SYSTEM FOR MAJOR FATIGUE TEST

The mechanical loading is applied by a conventional linkage system from hydraulic jacks, servocontrolled from the computer system.

### Loads and Reactions

The test laboratory, approximately 200 feet  $\times$  100 feet  $\times$  40 feet high, is effectively a strong box, so that vertical and side loads can be reacted directly to the building. It was designed as a general purpose test frame. The floor is strongly reinforced with steel beams with frequent attachment points, and a series of overhead moveable bridges can be placed at convenient locations to react the up loads. For the Concorde these are supplemented by portal frames over the wing tips and fuselage nose.

The loads are applied to the specimen by conventional means. Swivel loading points are bolted to the upper and lower surfaces of the wing and to each side of the fin. Groups



of loading points are connected together by a "Christmas-tree" linkage to hydraulic jacks. Fuselage loads are applied to bulkheads or distributed to the floor beams by a system of loading beams inside the specimen. These are linked by rods to a number of hydraulic jacks outside the specimen. Dummy undercarriages and dummy nacelles are fitted to the specimen, and through these, undercarriage and engine loads can be applied.

For the ground tests the specimen rests on the dummy undercarriages and is loaded through the hydraulic jacks and linkages to give the correct overall distribution. For the flight tests the specimen is balanced in its linkage system, but a number of constraints at the undercarriages restrict its movement. All of these constraints are fitted with load measuring devices and record either balancing reactions or zero load as appropriate. Table II and figures 31 and 32 give more detail of the loading system.

### Hydraulic System

Each hydraulic jack is set in a simple load-control circuit, which is made up of a load cell, electrohydraulic servo valve, and control module, which holds the load under analogue control until a new set point is given it from the overall control system. All the loading jacks are controlled by a PDP8/I computer.

The jacks mainly act in tension, although some act in tension and compression. They have been sized so that they can apply proof loads to the specimen as required for fail-safe testing towards the close of the fatigue test. They are fitted with PTFE seals to keep the friction low enough to avoid stick-slip effects in the system when small loads are being applied.

The load cells have two measuring bridges. One output is fed back to the control computer and is used to set up the required load; the other is fed back to the PDP10 monitor computer, where it is compared with the requested load level. Small, but significant, deviations from the required load are printed out and larger deviations initiate shutdown. Fuller details of the monitoring procedures are given subsequently.

Moog electrohydraulic servovalves are used throughout the system. These valves are two stage. The first, a preamplifier stage, uses a torque motor to convert the electrical input signal to a hydraulic signal, which drives the second, or power, stage. The torque motor operates a flapper which pivots between two hydraulic nozzles forming two variable orifices. Fluid under pressure is supplied to these nozzles through two fixed orifices, and the pressures between the orifices and the nozzles are applied to the ends of the spring-centred second stage, or main, spool. The flow through the valve is proportional to the main spool displacement and, thus, to the input electrical signal for a known pressure drop across the valve. Where higher flows are required, two servovalves are operated in parallel or a much larger valve is used.

The jack load is controlled by a simple error-signal device, which compares the required signal with the measured signal from the load cell. The error signal is amplified and drives the electrohydraulic servovalve to correct the load and so reduce the error signal to zero. This load is then held until a new set point is input to the system.

Each hydraulic control module has a number of local safety devices which are additional to the overall surveillance exercised by the monitoring computer. These local devices limit the maximum load and travel available at the jack. A typical hydraulic module circuit for a single acting tension jack is shown in figure 33. The differential pressure switch (DPS) initiates a fail-safe shutdown if the differential pressure across the jacks exceeds that set on the switch; the differential pressure relief valve (DPRV) vents high-pressure oil from either side of the jack to the other if the differential pressure exceeds a preset limit, these valves act as a backup to the differential pressure switches and prevent excessive loads on the specimen. When any safety device is activated, the isolating valves (LV) isolate the jack from the servovalve and ensure controlled dumping through the dump valves (DV). In addition, limit switches are used to sense excessive deflection of the jack rods and these also initiate shutdown.

The hydraulic power is supplied by 20 variable delivery pumps. Each pump is driven by a 30-hp motor and delivers 14 gallons per minute at 3000 lb/in<sup>2</sup> pressure. The pumps are arranged in banks of 5, each bank controlled by its own master control valve. This arrangement permits the independent shutdown of a bank of pumps if necessary. The pumps are supplemented by a battery of 8-gallon accumulators to provide for any peak demands of fluid in excess of pump output and to absorb any line pressure surges. Hydraulic fluid for the system is contained in two 750-gallon reservoirs. The temperature of the fluid (OM33) is maintained at 38° C by a thermostatically controlled immersion heater in each reservoir. Fluid is distributed from the pumps to hydraulic control modules situated in the various loading areas by a complex system of piping, which is located in trunking to contain any leakage.

Considerable attention has been given to achieving a high degree of cleanliness in the fluid. This cleanliness is necessary because of the small clearances and orifice diameters within the servovalve. These are susceptible to the fine particles which can cause silting or erosion of the orifices and hence alter the performance of the servovalve and ultimately possibly result in failure of the valve. Filters are fitted at the pump inlet (0.005-inch rating), at the pump outlet (10-micron rating), and at the inlet to the servovalve (1.5-micron rating).

#### Loading Sequences

The weight of the specimen, fuel substitute, and rigging is carried by the loading jacks, and account has to be taken of this in determining the loads to be applied by the



computer. Prior to starting a test cycle, the whole system is set up to a "weightless" condition. Small pretension loads are included where needed to remove slackness from the linkage. Under these conditions, all the load cells at the reaction points should read zero.

The test cycle commences with the ground loads, including the following conditions

- (1) 1g standing on the ground
- (2) Engine runup
- (3) Taxying loads
- (4) Take-off.

The appropriate reaction-point loads are checked throughout to ensure that the required loading pattern is being applied.

The loading is then adjusted to the various phases of the flight including

- (1) 1g climb
- (2) Gusts during climb
- (3) Manoeuvre during climb
- (4) 1g cruise
- (5) Gusts during cruise (including lateral gusts)
- (6) 1g descent
- (7) Gusts during descent and stand off.

This is followed by the landing and final taxying conditions including

- (1) Landing (including nosewheel "abattée" conditions)
- (2) Braking
- (3) Reverse thrust
- (4) Taxying
- (5) 1g standing on the ground.

Throughout these sequences, the loading has to take account of changes in the aircraft weight as the fuel is used up and of changes in the air-load distribution in subsonic and supersonic flight, together with the fuel transfer necessary to compensate these changes. The programme includes flights with different gust severities (rough flights and smooth flights) and similarly takes account of rough and smooth airfields and different landing conditions to represent real-service conditions.

### Mechanical-Loading Letdown System

If for any reason a test cycle has to be aborted while the specimen is under load, it is necessary to have a safe system to return it to the no-load condition. For the Concorde this is done by a controlled letdown procedure. On receiving a failure signal, the monitor computer deenergises a shutdown relay which in turn deenergises the following equipment:

- (1) The pilot control valves on each jack module, which momentarily lock the specimen in position
- (2) The main solenoid valves in both pump rooms, which divert oil in supply lines to reservoir tanks
- (3) The air-operated solenoid valve, which in turn vents pressure from the diverter valves in the return lines thereby directing returning oil to the letdown tank instead of the reservoir tank
- (4) The main hydraulic and pilot pressure pumps, which stop oil flow
- (5) The electrohydraulic servovalves, setting them to open circuit
- (6) The dump valves on each jack module, which initiates the letdown of the applied loads to zero.

The basic design of the letdown system is to separate the hydraulic jack return lines into 5 discrete groups which are

- (1) Over-specimen vertical jacks
- (2) Under-specimen vertical jacks
- (3) Fuselage and fin lateral jacks
- (4) Engine-nacelle jacks
- (5) Undercarriage jacks.

These groups are chosen so that a balance between port and starboard will be maintained during letdown. All jacks in groups 1, 2, and 3 have collapsible linkage of length such that compression loads cannot be transmitted to the specimen. In groups 1, 2, 3, and 4 when the dump valves are deenergised, the annulus side of all jack pistons in each group is connected to a common return pipe through a preset restrictor to the letdown tank. The restrictor flow can be varied between 0.25 and 15 gallons per minute. This flow rate determines the rate of letdown. All the undercarriage jacks (group 5) are equal area double rod types, and during letdown, pressure is vented from one side of the piston to the other.



In general, loads are controlled by the specimen returning to its natural no-load position. Excessive pressure or load is prevented by the differential pressure relief valves fitted in the hydraulic control module for each jack.

### Interactions With Multichannel Systems

When a single loading channel is controlling the load being imparted to a structure, it is relatively easy to determine the characteristics of the complete system (including the structure) and to achieve optimum response from the system. In the case of a multichannel loading system used for the fatigue testing of a large structure, it is necessary to ensure that all the loading channels are kept in phase and apply the correct loads. Each loading point in a multichannel loading system has different mechanical parameters, such as stiffness and inertia. Such a system is a compound one, with many subsystems or channels so interconnected by the test structure that they influence each other. The degree of this influence or interaction is dependent both on the strength of the coupling between respective channels and on the mechanical parameters of each channel. For example, there would be little interaction between two channels with high inertias which were weakly coupled; this type of compound system would show characteristics similar to those of the individual channels. On the other hand, if the coupling were strong, the characteristics of the compound system would be very different from those of the individual systems acting alone.

The magnitude of spurious loads caused by interaction depends on a number of factors. It will depend, firstly, on the degree of coupling between the channels and on the magnitude of the mechanical parameters of each individual channel; secondly, on the speed of application of loads; and thirdly, on the response characteristics of the individual channels. In many instances, the effects of interaction are minimal and can be ignored. Sometimes, however, significant errors arise because of interaction, and then it must either be counteracted by test techniques or, if this is impossible, taken into account in the analysis of the results.

Since the magnitude of the interaction loads is dependent on the speed of application of the loading, it can be diminished by slowing the rate of loading. It can also be diminished by increasing the response of the affected channel. Both these methods have their limitations, the first because of the time scale of the test being conducted and the second because by increasing the response, the stability margin is decreased, and unwanted oscillations can result. These oscillations can cause problems as great as the one eradicated.

Clearly, these problems are intimately connected with the particular characteristics of the specimen and system involved. They are difficult to predict. They produce further problems in the commissioning of the system which frequently has to be done channel by channel on a separate rig. Great care must therefore be exercised in the interpretation

of the results from such rigs when applying them to real structure. Small multichannel tests are being done for the Concorde system using dummy specimens of representative stiffness.

## CONTROL AND MONITORING SYSTEMS FOR MAJOR FATIGUE TEST

### Basic Requirements

The requirements imposed upon the control and monitoring systems divide into three main categories: control of the test, monitoring, particularly concerning the safety of the specimen, and collection of data, mainly from the specimen itself. Beside these explicit requirements, there are others, such as the need to achieve high reliability and to have a configuration giving a good margin of operational flexibility.

The requirements for the control function are, of course, dictated by the task which has to be performed. Essentially, this is in two parts, control of the heating and cooling plant and control of the mechanical loading system. There are about 50 channels of plant requiring continuous control with nearly 160 switching channels. The continuous control channels involve a complex thermal plant, where nonlinearities and significant time delays abound, making this an ideal application for the potential power of direct digital control. The mechanical loading system has a capacity for 150 channels of which currently about 100 are being used to control the hydraulic jacks, which because of their speed of response would impose a formidable task to control in a direct digital mode. These channels are, therefore, controlled by force feedback on continuous data control loops which only require updating with voltages proportional to the demand loads.

Because of the large number of components in the overall plant and in the control system itself, there is a very real chance that the specimen might be damaged as a result of a system failure. Hence, very careful monitoring must take place of all the systems, and automatic action must be taken if system failure develops. The cumulative nature of the fatigue process makes it acceptable to shut down the test when any failure is detected, alleviating any need to take over control. The provision of a failure detection system must aim at reducing to a very low probability the chance of applying an incorrect condition to the test specimen, during its several tens of thousands of hours of testing.

Anything less than a completely independent monitoring system relies on the ability to predict all the possible forms of failure of a shared component. Since the difficulty of achieving this independence increases rapidly as the shared component becomes complex, the only prudent solution is the totally independent system. This totally independent system will have a finite probability of failure; therefore, the chance of applying an unacceptable condition to the specimen is directly related to the probability of both the control and monitoring systems failing within an interval which is sufficient to allow a runaway chan-



nel to deviate unacceptably. It can be shown that even with mean time between failures for the whole system of as low as a few tens of hours and checking rates of approximately once per second, the probability of dual failure is very low. Thus separate control and monitoring systems have been chosen to take care of the test environment. (See fig. 34.) Although the system is primarily designed to run as a complete entity, the control computers may be run individually on their respective systems. Equally, it is possible to use the surveillance of the monitoring computer when parts of the overall testing facility are being run on their own hardware control systems.

A special peripheral unit housed in the monitoring computer is responsible for providing the time base for all the computer systems and at the same time checking that they are running in close synchronism. It consists of two separate crystal clocks, one of which produces pulses at a rate of 1 hertz and the other at rates of 1000 hertz and 1 hertz. Basically, each processor is made to count the 1000-hertz pulses and check them against the 1-hertz pulses; the safety of the system is preserved by having the two sources of 1-hertz pulses.

The effect of the test on the specimen is measured through attached strain, temperature, and deflection transducers. In all, these number about 3500 and require to be scanned in less than 10 seconds. Facilities are needed to scan subsets of the total number of transducers and to perform various degrees of processing on the recorded data. A data logging system associated with the monitoring computer performs this task.

### Hardware and Its Operation

Overall hardware configuration.- The overall hardware configuration is shown in figure 35 and may be summarised as follows:

#### PDP10 monitoring computer:

- Size of computer word, 36 bits
- 32K of 1.6 microsecond core store
- 16K of 1 microsecond core store
- Two 512K fixed head disc stores
- Four DEC tape controllers
- 300 lines per minute line printer
- Digital XY plotter
- VB10 visual display
- VR12 slave display
- Two British standard digital data interfaces
- 240 channel analogue multiplexer
- 174 digital inputs
- Two 10-8 data link interfaces
- 1000 ch/sec paper tape reader

300 ch/sec paper tape reader  
150 ch/sec paper tape punch  
50 ch/sec paper tape punch  
Four KSR 35 teletypes  
One ASR 33 teletype

**K70 plant control computer (incorporating a PDP8/I computer):**

Size of computer word, 12 bits  
20K of 3 microsecond core store  
32K fixed head disc store  
48 channels of direct digital control input/output  
190 digital outputs  
63 digital inputs  
ASR 33 teletype  
Shared 1000 ch/sec paper tape reader }  
Shared 150 ch/sec paper tape punch } With loading computer  
8-10 data link interface

**PDP8/I loading computer:**

Size of computer word, 12 bits  
8K of 3 microsecond core store  
256K fixed head disc store  
Extended arithmetic unit (hardware multiplier)  
5 digital outputs  
2 digital inputs  
150 jack output cards giving  $\pm 5$  or  $+10$  volt output  
ASR 33 teletype  
Shared paper tape punch and reader  
8-10 data link interface.

General operational principles.- After the computers have been switched on and have had their programs loaded, they first have to be synchronised. They are each informed of the real time at which they will expect to see the first clock pulse from the special clock unit situated in the PDP10. When this unit is switched on the appropriate parts of the programmes count up time to give each computer a real-time base on which to operate its plant control and monitoring functions. All control information or instruction to the computers is input via one or more of the teletypes attached to the machines. The next stage of operation involves the input of the engineering data giving the magnitudes of the functions to be performed which have already been defined, in principle, by the application programs written to make the computers perform the dedicated tasks associated with the test.



The engineering data are prepared in advance, in duplicate, by two independent punch operators from the carefully checked manuscript information formulated around the structural demands of the test. These identical punched paper tapes are then input to the control and monitoring computers; load information only is put into the loading computer and process information into the K70 machine. The computers then transform the engineering data into special internal machine formats and check the data for consistency with respect to both the hardware and the software. In a later stage of the startup procedure, the data are cross-checked within the computer system using the data links which connect the control machines to the PDP10. By this means it is possible to be sure that the information has been input correctly. Once the data have been input and the expected configuration of the plant has been defined to the computers, the computers can accept the various parts of the plant for control. This step is necessary because on certain occasions only limited parts of the plant may be run, especially during commissioning.

As and when the plant engineers request startup of each major unit of the plant, which has direct control over the conditions at the specimen, these requests are ratified by the control and monitoring computers and relayed back to the plant initiating startup of that unit. If the various units are started up in the previously defined order, it should be possible to take the whole of the specified plant onto control with its associated checking through the monitoring computer. During or after this stage, all the control points may be instructed to move to their precycle conditions. The whole of the test rig can thus be made ready for cycling, which it will commence on receipt of an instruction defining the start time. The actual programme that is then followed is inherent in the data input to the computers and is executed entirely automatically unless terminated prematurely. Various instructions exist to enable an operator to override the automatic sequence previously defined; these allow premature termination of a cycling sequence or alteration of its contents or a return to static conditions at the end of the current cycle.

Throughout the test rig, inner and outer limits are set for the variables, and these are checked by the monitoring computer through independent transducers by comparing measured values with expected values. The inner limits are set such that small deviations which would not significantly affect the accuracy of the test or prejudice its safety are permitted. Outer limits are set at levels which would be prejudicial to the test and exceedance of these automatically causes shutdown. Any variation between these two limits is recorded on teletype for the immediate information of the operator and also on paper tape for subsequent analysis. By these means the control of the test is virtually automatic and follows a prescribed plan; the burden imposed on the operators is thereby greatly minimised. If current information is required about any of the controlled conditions, instructions are available to allow the operator to display these on the cathode-ray tube, giving all relevant data to allow an assessment of the operating status of the test rig. In a similar way, the data logger may be instructed to survey a prescribed set of

transducers and print the resulting information in an engineering format on one of the teletypes. For larger data-collection surveys, the transducers to be scanned may be defined on punched paper tape, together with the times when they are to take place. The logging will take place automatically at the prescribed times, and the results may be output for subsequent processing on another machine.

Selective shutdown is possible on a predefined basis. This avoids shutdown of the whole of the plant when one small area is subject to failure and is not potentially damaging to the specimen. Later, this shutdown part of the plant may be brought back onto control during an artificially imposed pause in the cycling.

### Control of Air- and Fuel-Conditioning Plant

External-air systems.- Two parameters in each of the five circuits of the external conditioning systems are controlled by the K70 process computer in a direct digital control mode. They are the air temperature and the circulating fan speed. The air temperature is controlled through a cascaded loop which involves feeding the heat-exchanger-fluid temperature back to the computer as well as the air temperature itself. A hybrid computer simulation showed that this technique should be sufficient to give the required accuracies throughout a fatigue cycle without having to change the control algorithm; accuracy is improved significantly if it is accepted that the measured value is delayed from the set point by approximately 4 seconds. If during commissioning it becomes obvious that there are significant errors, then as a first step, it is possible to programme time-varying control parameters. There is an added virtue in having a measure of the heat-exchanger-fluid temperature within the computer, since it assists restarting particularly if a test cycle has been aborted at high temperature. It then becomes necessary to pick up the specimen at its elevated temperature and to force it back to room temperature conditions without inducing large temperatures differences. This procedure requires the heat-exchanger temperature to be controlled at the current specimen temperature before the circulating fan for that duct is switched on.

The control of the speed of each circulating fan is based on measurements of the fan speed using a tachogenerator and is obtained by altering an electrolytic resistance in series with the rotor of the fan motor.

Internal-air systems.- There are seven circuits air-conditioning the internal structure of the specimen, each of which has one or more parameters under direct digital control using the K70 computer. These systems are all based on similar principles, but some circuits provide more facilities than others. One of the more complex ones controls two mass flows, one temperature, and eight pressures. Like the controlled parameters of the external circuit, the set points may be specified as a series of points varying with time which are then interpolated by the computer to derive the once-per-second



values required for control. By this means it is possible to make significant economies in the amounts of input data which have to be prepared by hand. This facility is further enhanced by the provision of editing software making it possible to alter small amounts of data through a typewriter keyboard directly connected to the computer.

Internal-fuel systems.- The temperature in twelve of the thirteen tanks is controlled continuously through regulation of a single parameter per tank, namely, the fuel circulation flow. In the ten circuits which are temperature conditioned, this continuous control is achieved by an open-loop technique where the appropriate hot or cold fluid is switched into the heat exchanger; no temperature feedback is used, the method relying on the repeatability of conditions.

### Jack Loading Computer

Synthesis of net jack load.- Because of the overall requirement to retain the maximum flexibility in the test system combined with economy of storage space in the computers, the net load on any jack is built up from its fundamental components. Broadly, there are two components consisting of a slowly varying or steady load due to aerodynamic lift in flight or weight of the aircraft on the ground and a second, more rapidly varying, component due to turbulent conditions and manoeuvres in flight or taxiing bumps on the ground. The second component may be further subdivided into a part which defines the magnitude of the gust or bump on the aircraft as a whole, for example, a gust of 10 ft/sec at a specified time or a bump of 0.1g at another time, and another part specifying the load in that particular jack due to a unit gust or bump; this latter part defines the load distribution between jacks which may vary for the different loading conditions. In algebraic terms this becomes

$$L = S + WG$$

where

L        the load on a particular jack

S        the steady component of load for that jack

G        the gust or bump magnitude for the aircraft as a whole

W        the distribution factor defining the load seen by the jack per unit gust or bump

By this means it is possible to build up a large repertoire of flights from a relatively small amount of data.

Test cycles are quantised into phases where either or both the steady load and set of weighting factors  $W$  are constant. Gusts and bumps are required to be applied in synchronism throughout the specimen and to a constant waveform. In certain circumstances the waveform is extended in duration to limit the acceleration forces on the test specimen.

Jack set-pointing system.- The jack computer provides set-point voltages for up to 150 jack control channels, the force feedback control loops being entirely external to the computer. A flow diagram of the system is given in figure 36 which shows the basic computer, a PDP8/I, driving through a standard Kent processor interface to a special jack-driver interface through to the analogue output cards. It produces  $\pm 5$ -volt or 0- to 10-volt signals for bidirectional and unidirectional jacks, respectively, the particular voltage being selected by a simple shorting link on each output card. As may be seen, the hardware makes use of load synthesis as detailed in the previous section. The isolation of the computer central processor from the electrohydraulic control channels occurs at the input of the jack-driver interface and is implemented through optical coupling; it achieves a high standard of isolation allowing the use of separate power grounds, thereby helping to protect the computer from noise likely to produce malfunction.

A sample-and-hold circuit accepts the current steady-load voltage and holds it for one-half second until the next update, thereby restricting steady-load changes to a maximum rate of twice per second for small increments. Step changes of more than the odd least significant bit (the steady load is set up to a resolution of 9 bits plus sign) are unacceptable to the jack control system, so a special procedure is adopted for substantial load changes. For these changes the steady load is updated at a rate of 20 times per second during the change giving a fine linear staircase type of output. To create the gust component, a constant amplitude waveform representing a half gust is input to the jack output card. This is again to a resolution of 9 bits plus sign updated at the rate of 1000 times per second. Half gusts may be only initiated at 1-second bounds when the steady load is updated and the software imposes a constraint that the component be zero for the first and last 25 milliseconds of the half-gust period. Normally, the half-gust duration is 2 seconds, but it may be requested up to 16 seconds with an overall restriction that it be symmetric about the quarter-gust point. The constant-amplitude gust is scaled by a third digital input to the jack card which is to a resolution of 9 bits plus sign to select whether the half gust be positive or negative going.

A single jack card is set up within 160 microseconds giving a maximum delay between channel 1 and channel 150 of 24 milliseconds for the steady-load component. The comparable delay on the gust component is less than 2 milliseconds.

Droop nose.- The droop nose is activated by two digital outputs from the jack computer, the first switching on the hydraulic pump to generate supply pressure and the second switching the control valve to stroke the droop jack.



## Plant Monitoring

General principles.- As mentioned previously, there is a need for a failure detection system; this system is provided by the PDP10 computer and its peripheral devices. Strictly, it is an independent system which together with the control computers is able to indicate a lack of consistency between control and monitoring. By software its use is extended into a discriminating recording facility, where it disregards information which is consistent with correct operation, and promotes shutdown when there are gross errors, but stores and subsequently outputs data values between these two extremes. This technique avoids the vast quantities of redundant information which would be created by a continuous, conventional recording system. To be successful, the system depends upon the levels of discrimination being set up with great care; information which is intended to be disregarded must not have a significant effect on the test result, and that which initiates shutdown must preserve the safety of the specimen and the meaningfulness of the test.

In most cases the parameter which is controlled by the control computer is also monitored by the PDP10, but within the internal plant there are several exceptions. These exceptions occur either because the control function may be open loop or because the parameter of direct interest is only implicitly related to that which is directly controlled. Typically, in the internal air circuits the air temperature near the energy source and mass flow are controlled, but it is considered sufficient to monitor the temperature much nearer the specimen together with the state of any air distribution valves in that circuit. Because the digital computer inputs associated with valve monitoring are considerably cheaper than the analogue inputs for, say, mass flow, considerable economies can be achieved. There are complementary savings in computer time and storage.

Types of checking and their frequency.- Apart from the load channels, all checking is carried out at the same frequency as the related control functions are updated, that is, once per second. Analogue parameters are checked against inner and outer, upper and lower limits. Valve positions, which are input on a pair of digital inputs, are checked for the correct state, for example, binary 10 for off, 01 for on, and 00 for the transient state, which is allowed a preset time.

Since the loading channels can deviate more rapidly to an unacceptable level, their checking is conducted at a considerably higher rate, directly related to the required bandwidth necessary in control to produce the planned gusting rates and accuracies. Outer limits are checked twenty times per second and inner limits once per second unless extended duration gusts are being executed; then inner limits are only checked at the quarter cycle points.

Types of output.- There are three basic types of output available from the monitoring computer:

- (1) Typed output on teleprinters
- (2) Paper tape output
- (3) Visual display output

The first two are produced automatically when a variable exceeds inner limits. The purpose of the typed output is to draw the attention of the test controller to the current test situation, namely, that one or more channels are deviating from their expected conditions, so that a close watch can be kept on any developments. If more than a prescribed number of printouts occur, shutdown takes place automatically. This limit would normally be set at the number which can be output in any one test cycle so that there is not a steady accumulation of results. If the deviation on a channel does not change, it does not repeat printout; thereby, the output capacity is preserved.

The paper-tape output provides a record of the exceedances of the inner limits in a form which can subsequently be fed to a computer for further analysis.

The third form of output is via the visual display which can give rapid access to any of the monitored variables at a request through a keyboard input message. Up to two variables may be displayed concurrently against a time axis; and a data table giving the current measured values and the expected values of the inner and outer limits may accompany them. It may also be used for the display of logged information if a user program is written to interface with the display servicing software.

### Data Logger

Multiplexing configuration.- In order to achieve consistent measurements from strain gauges attached to specimens operating in unfavourable conditions, it is necessary to avoid pressure-type electrical contacts within the normal bridge measuring system. Thus small groups of gauges are collected into terminal units in which the bridge is formed using all soldered joints. Any initial imbalance of the bridge is catered for by extending the range of the recording apparatus. The terminal units are sited as near to the group of gauges as possible to minimise the effects of leads in the arms of the bridge. Up to 16 of these terminal units are then collected via cables into a sampling unit where they may be successively sampled by reed switches and the resulting signal amplified and fed to the recording console. Each terminal unit may accommodate up to 10 gauges with a further two calibration points available. Similar units containing cold junction compensators are used for collecting thermocouple signals.

The main console can accept up to 30 sampling boxes which are sampled through a high-speed solid-state multiplexer into a successive approximation analogue-to-digital converter. This converts the measured signal into digital form with a resolution of 12 bits (1 in 4096) when it is then transferred to the PDP10 computer through one of its two British standard digital data interfaces.



British standard interfaces.- Two of these units are attached to the memory buss of the PDP10 computer; each is capable of handling 8-bit words at transfer rates of more than 100 kilohertz. One is used for transferring control information to the logger main console while the other collects the resulting data; a useful feature of this arrangement is that the interfaces may be directly linked for fault diagnosis. An extension to the interfaces, on the logger side of them, provides isolation of the logger from the computer processor through an opto-electronic link for the reasons stated previously.

Basic operational facilities.- A total scan of all points on all the sampling boxes can be made in 6 seconds. The sampling time on each point is about 30 milliseconds, which is achieved by sampling all the sampling boxes concurrently. This concurrent sampling allows ample time to filter off any electrical noise at frequencies equal to or higher than the frequency of ac line voltage by a combination of analogue and numerical techniques. By using this method, it is possible to have available in the computer a measure of this noise level on each channel during sampling giving a useful guide to the effectiveness of any measurements. The diagnostic capability of the measuring system is further extended by having computer controlled grounding alternatives of the strain-gauge bridges. By this means it is possible to assess the electrical leakage between the gauge and specimen (a common cause of errors in elevated temperature strain measurement).

Integration of the logger with the computer gives a high degree of software control over its scanning ability from both conversational and preprogrammed input. By using the latter facility, logging can be made synchronous with the process control and loading functions. Input may be in either logger-channel-number format or gauge-code format.

Various types of output are available, their extent only being limited by the ingenuity of the programmer and the spare core store. Conversational type input normally results in a processed output in engineering terms, rather than machine code. Further processing and analysis of results is possible when the machine is dedicated to this task, that is, when fatigue cycling is not functioning. Alternatively, the raw data may be output on any of the output media to be subsequently processed on another computer.

### Operation for Testing

Startup and shutdown.- The requirements of both startup and shutdown necessitate that the computer controlled plant be partitioned into blocks that can be independently started and stopped. Whereas the former state will be initiated by a plant engineer when he considers that the correct conditions have been satisfied, the latter action will normally be taken automatically by the computer or plant hardware. To satisfy these demands, each section of the controlled plant is coupled to its appropriate computer and the monitoring computer by an interlock loop which operates as shown by the following example.

Considering one of the external air circuits and assuming that the appropriate background conditioning plant is running and that the K70 and PDP10 computers are operating and loaded with their correct programs, the startup sequence commences with the plant engineer pushing a button to start the air-circulating fan. If the associated background plant is ready, a request will be sent to the PDP10 for permission to start. When the computer has checked to see if this is a legitimate request, it will start upper limit checking and also relay the request on to the K70 computer. The K70 computer, in turn, will check for legitimacy and initiate control action at the same time as sending a signal to the plant confirming the startup request. The fan should then start; this action will consolidate the engineer's request to start and therefore latch the interlock loop. Thereafter, if either the plant or the two computers fail to activate the interlock loop, it will open and hence produce shutdown of the controlled plant on that loop.

The following sections of plant have interlock lines to the computers:

- (1) Each of the external circulating fans
- (2) Each of the internal circuit circulating blowers
- (3) One from the set of pressure blowers
- (4) One from the electrohydraulic loading system
- (5) One from the droop nose system
- (6) Each of the thirteen fuel systems.

This partitioning of the plant allows batched shutdowns where, under certain circumstances, only part of the plant is shut down if the outer limits of a monitored variable are exceeded.

Data input and cross-checking.- Before a test is started, the input data for control and monitoring functions have to be input to the computers. These input data are oriented towards user formats and in engineering units; therefore, they have to be processed to compressed computer formats after initial input. Following this it is necessary to check that the data have been input correctly into the stores of the computers. To facilitate the operation, the same data are input to both the control computer and the monitoring computer and then cross-checked through the data link between them. At this point, the monitoring data in the control computer and the control data in the monitoring machine may be discarded.

As the load data are input in a derived form, as discussed previously, an additional function of the programme is to calculate all the jack loads and print them out for comparison with the original data.

Facilities for commissioning.- The configuration of two control computers was adopted to add flexibility for the commissioning stages of the project. Each control com-



puter can be operated independently of the other and of the monitoring computer. Thus, for example, parts of the plant or loading system can be commissioned independently. It would not be desirable however to operate on the specimen without the monitoring computer in use, as the fail-safe properties of the complete system would be absent.

In general, the software has been designed to allow almost all the quantitative data defining the conditions of a test cycle to be replaced very quickly. For example, the standard three-term control algorithms available to control the plant may have their parameters changed, via the K70 console, by push buttons. Special provisions have also been made on the loading computer for a conversational type programme to control loads on up to 10 jacks. With these facilities, it is considered that most of the special problems which may arise during commissioning can be accommodated.

#### REFERENCES

1. Mann, J. Y.; and McMillan, I., eds.: Aircraft Fatigue – Design, Operational, and Economic Aspects. Programme of 5th ICAF Symposium (Melbourne, Australia), May 1967.
2. Ripley, E. L.: Structural Tests for the Supersonic Transport Aircraft. Paper presented at 11th Anglo-American Aeronautical Conference (London), Sept. 1969.
3. Anon.: Tentative Airworthiness Standards for Supersonic Transports. Flight Standards Service, FAA, Nov. 1, 1965.
4. Anon.: TSS Standards. Air Registration Board (England) or Secrétariat Général à l'Aviation Civile (France), July 28, 1969.

TABLE I.- CONVERSION FACTORS

Physical quantity	Basic unit	Conversion factor (*)	SI unit	Supplementary unit
Length	inch	25.4	millimeter	
Weight	long ton	$\left\{ \begin{array}{l} 2240 \\ 1016.05 \end{array} \right.$	kilograms	pounds
Volume	gallon	$\left\{ \begin{array}{l} 4.546 \\ 4.546 \times 10^{-3} \end{array} \right.$	meters <sup>3</sup>	liters
Acceleration	g	$\left\{ \begin{array}{l} 32.174 \\ 9.806 \end{array} \right.$	m/sec <sup>2</sup>	ft/sec <sup>2</sup>
Pressure	lbf/in <sup>2</sup>	$\left\{ \begin{array}{l} 6.895 \\ 6.895 \times 10^{-4} \\ 7.03 \times 10^{-4} \end{array} \right.$	kN/m <sup>2</sup>	hectobar kgf/mm <sup>2</sup>
Power	$\left\{ \begin{array}{l} \text{hp} \\ \text{Btu/hr} \end{array} \right.$	$\left\{ \begin{array}{l} 746 \\ 0.293 \end{array} \right.$	watts watts	

\*Multiply value given in basic units by conversion factor to obtain equivalent values in SI and supplementary units.



TABLE II.- DETAILS OF LOADING SYSTEM

Structural component	Loading points to structure	Jacks
Wing vertical loads:		
Upper surface . . . . .	284	42
Lower surface . . . . .	60	14
Fuselage:		
Vertical loads:		
Up . . . . .	165	4
Down . . . . .	181	9
Side loads (forward fuselage):		
Port . . . . .	34	2
Starboard . . . . .	34	2
Fin side loads:		
Port . . . . .	32	3
Starboard . . . . .	32	3
Nacelles:		
Vertical loads:		
Port . . . . .	1	1
Starboard . . . . .	1	1
Thrust loads:		
Port . . . . .	2	2
Starboard . . . . .	2	2
Reverse-thrust loads:		
Port . . . . .	2	2
Starboard . . . . .	2	2
Nose undercarriage (at bottom of leg):		
Vertical loads . . . . .	1	Reaction point
Fore and aft loads . . . . .	1	1
Side loads . . . . .	1	1
Main undercarriage (port):		
Vertical loads at bottom of leg . . . . .	1	Reaction point
Fore and aft loads:		
Bottom of leg . . . . .	1	1
Top of leg . . . . .	1	Reaction point
Side loads:		
Bottom of leg . . . . .	1	1
Top of leg . . . . .	1	Reaction point
Main undercarriage (starboard):		
Vertical loads bottom of leg . . . . .	1	Reaction point
Fore and aft loads:		
Bottom of leg . . . . .	1	1
Top of leg . . . . .	1	Reaction point
Side loads at bottom of leg . . . . .	1	1

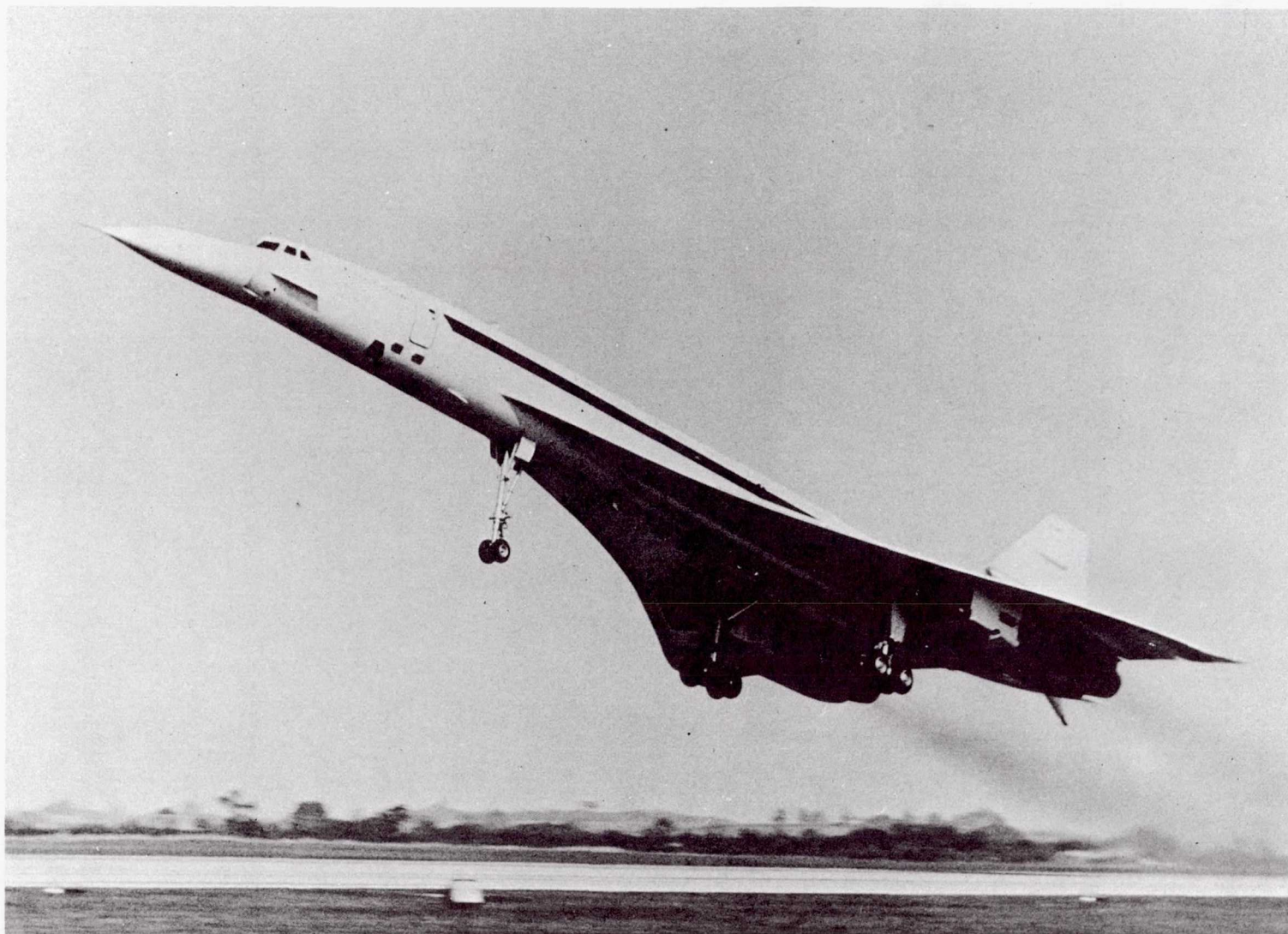


Figure 1.- Prototype Concorde aircraft 002.



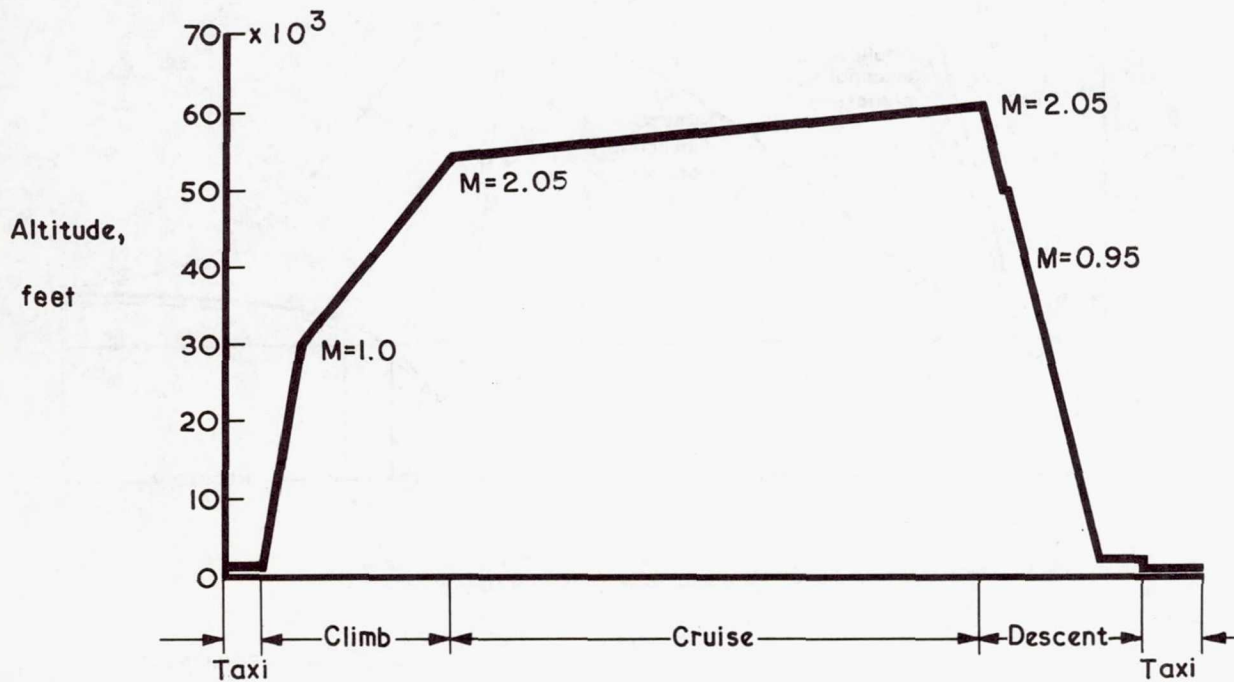


Figure 2.- Altitude and speed for a typical flight. M is Mach number.

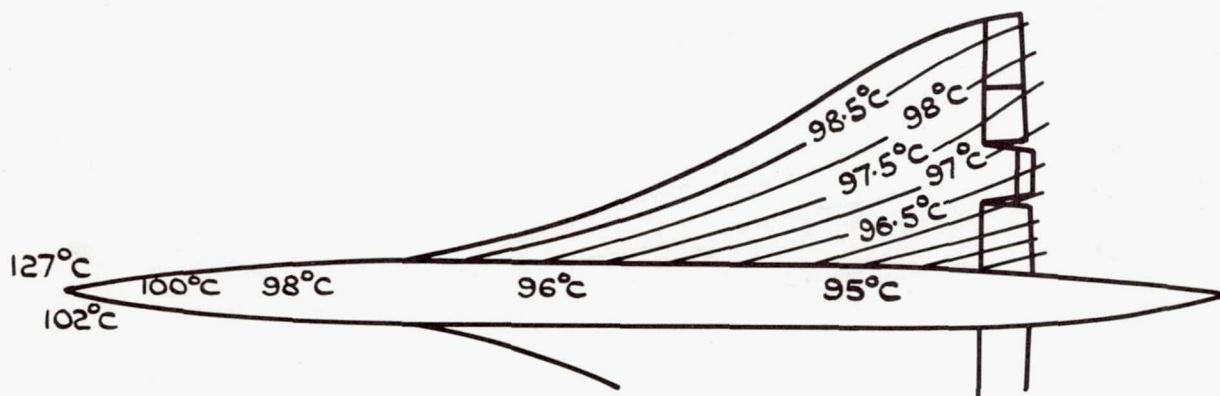


Figure 3.- External-structure temperature during cruise.

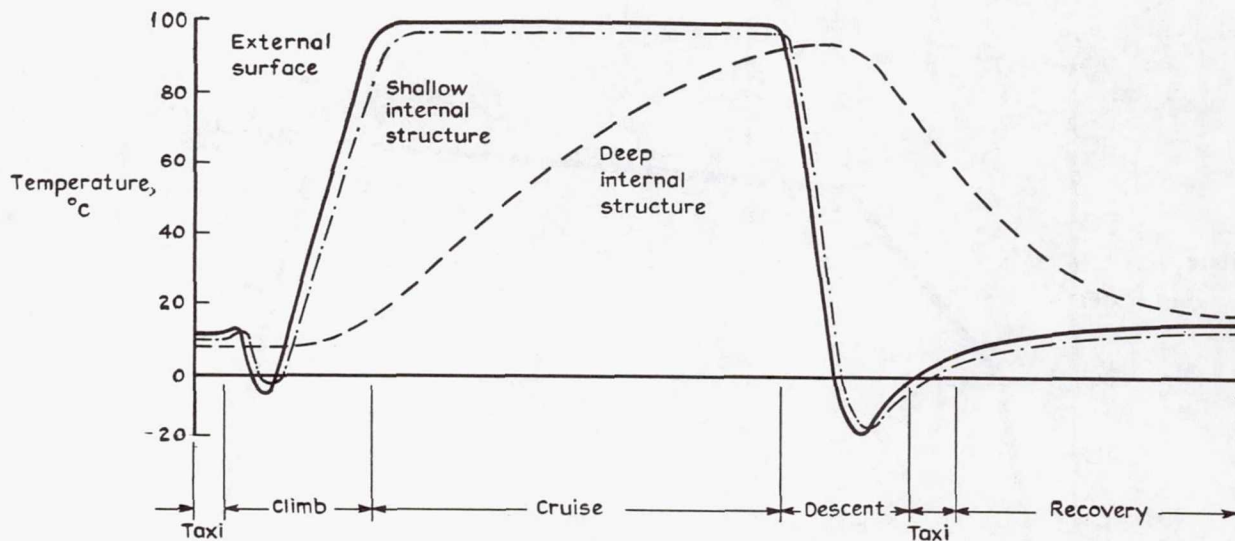


Figure 4.- Structural temperature for a typical flight.

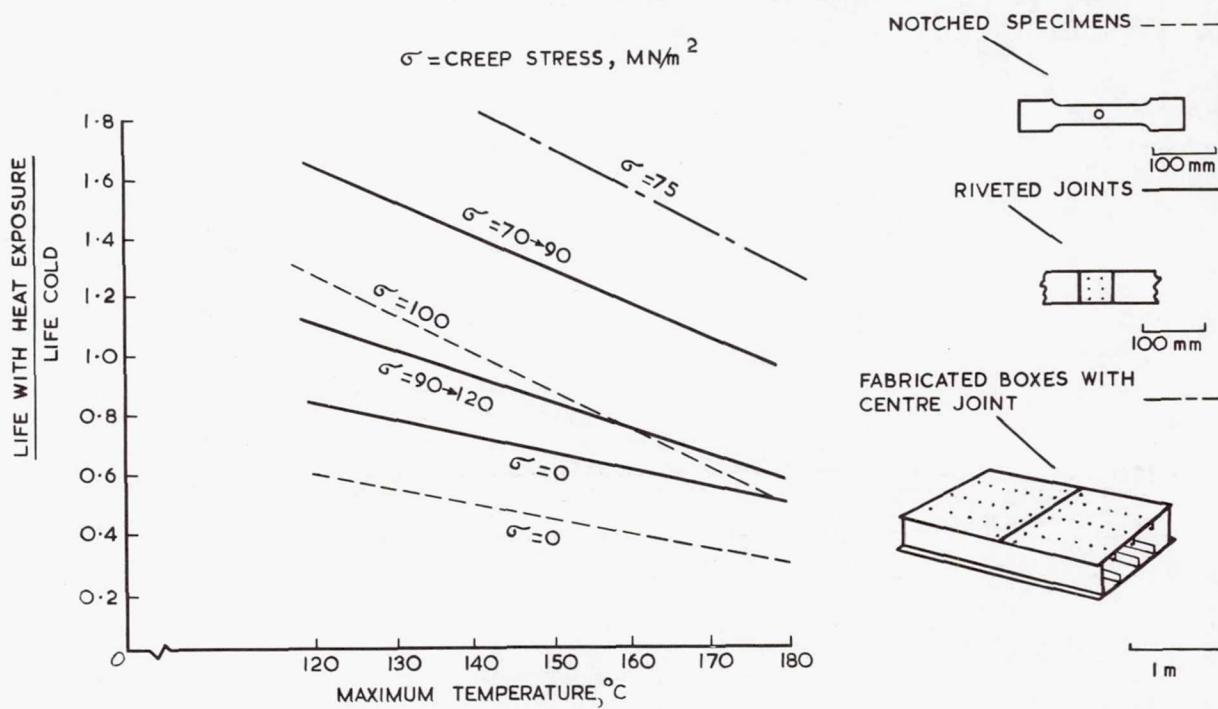
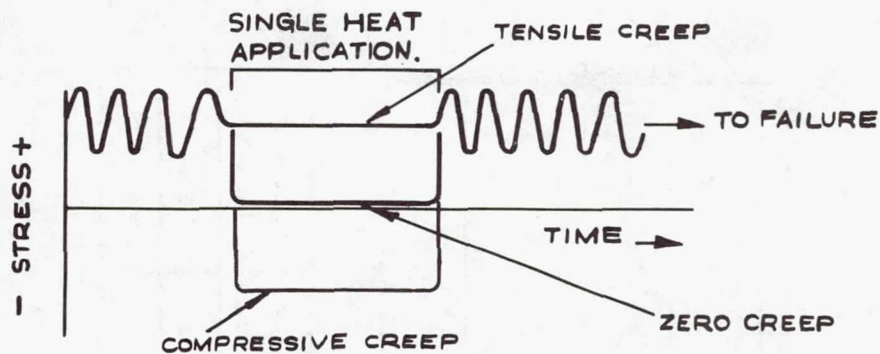
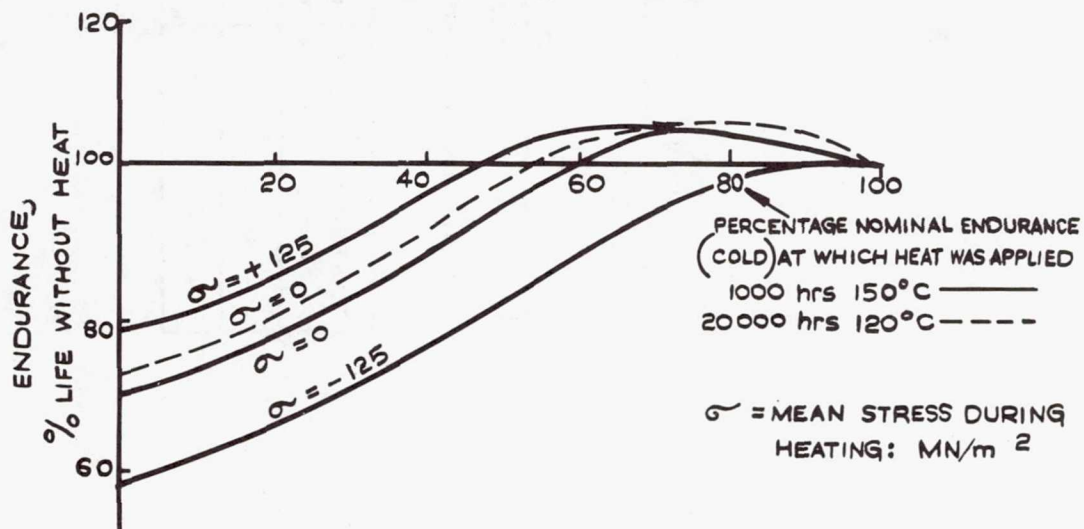


Figure 5.- General trends of influence of temperature and mean stress on life with intermittent heating.

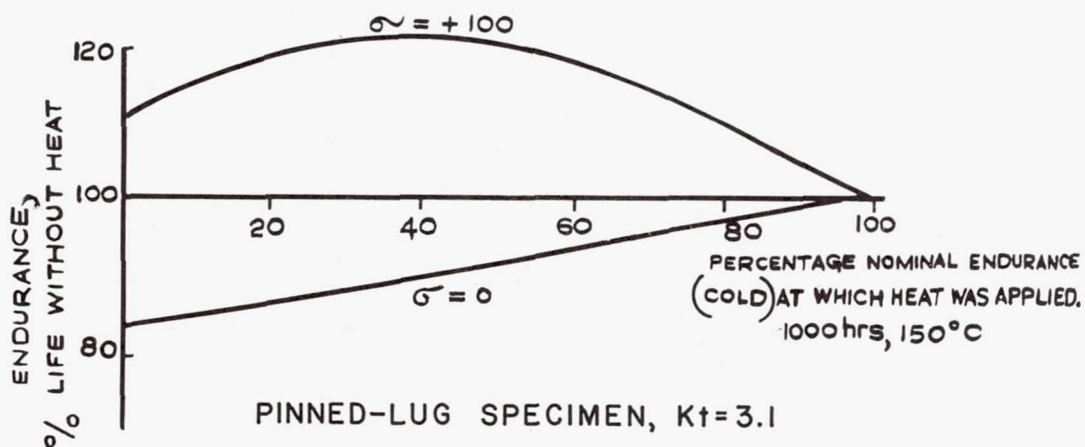




LOAD / TEMPERATURE ENVIRONMENT

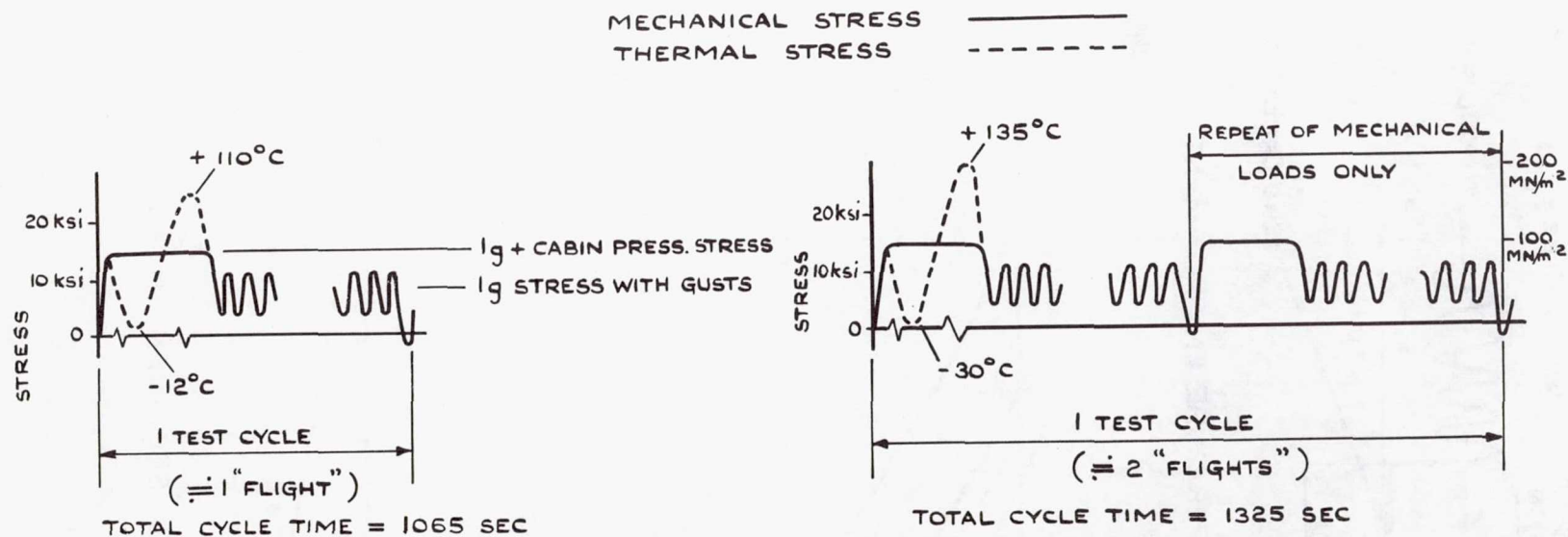


NOTCHED SPECIMEN,  $K_t = 3.4$



PINNED-LUG SPECIMEN,  $K_t = 3.1$

Figure 6.- Effect of heat exposure on fatigue.  $K_t$  is stress-concentration factor.



TEMPERATURE RANGE	TEST NUMBER	TEST CYCLES TO 1st CRACK	"FLIGHTS" TO 1st CRACK
$-12^{\circ}\text{C}$ $+110^{\circ}\text{C}$	1	7600	7600
	2	7200	7200

TEMPERATURE RANGE	TEST NUMBER	TEST CYCLES TO 1st CRACK	"FLIGHTS" TO 1st CRACK
$-30^{\circ}\text{C}$	3	3400	6800
$+135^{\circ}\text{C}$	4	3500	7000

Figure 7.- Real-time and accelerated tests on box-beam specimens.



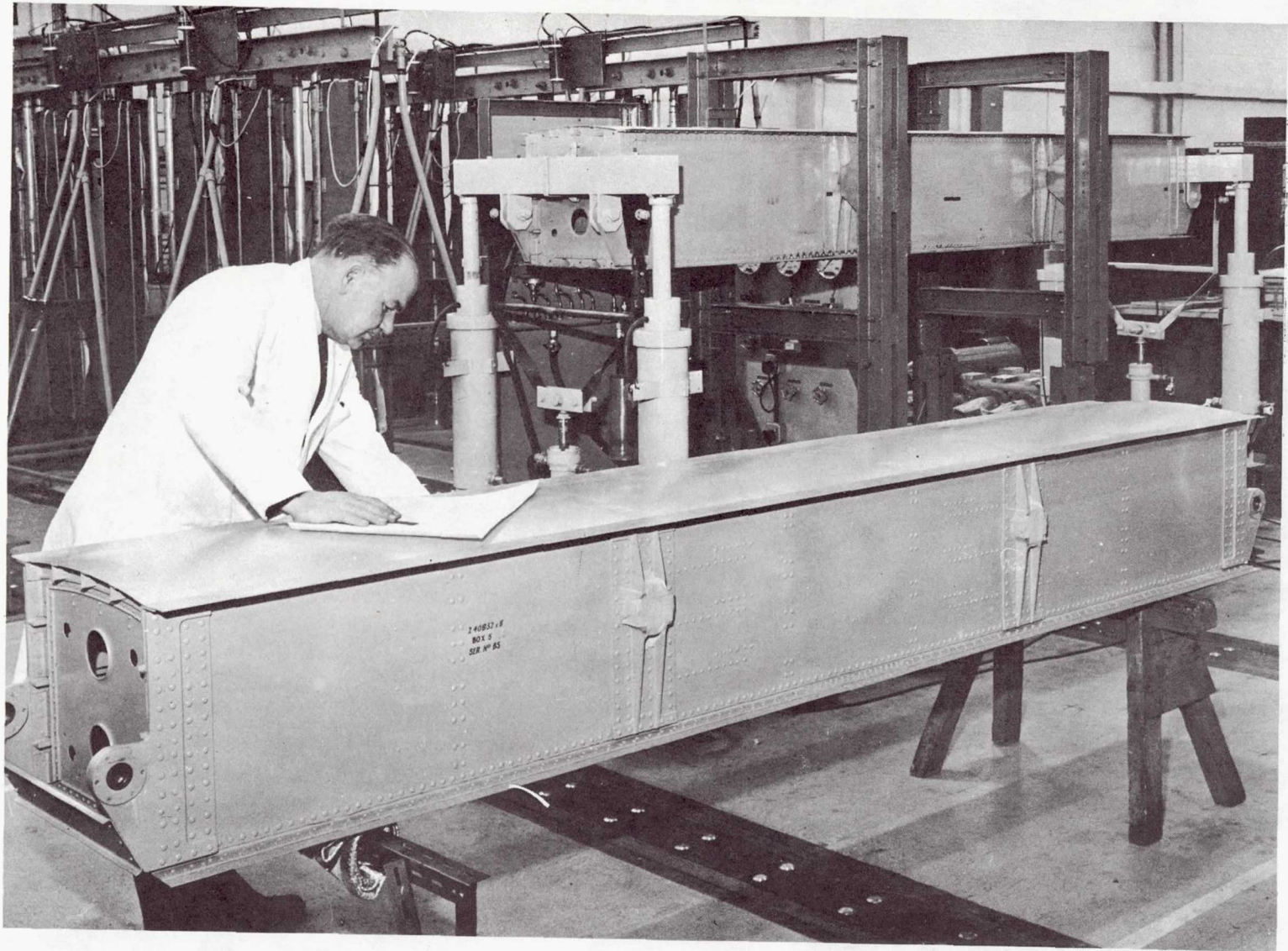


Figure 8.- Box-beam specimen for fatigue tests with thermal cycles.



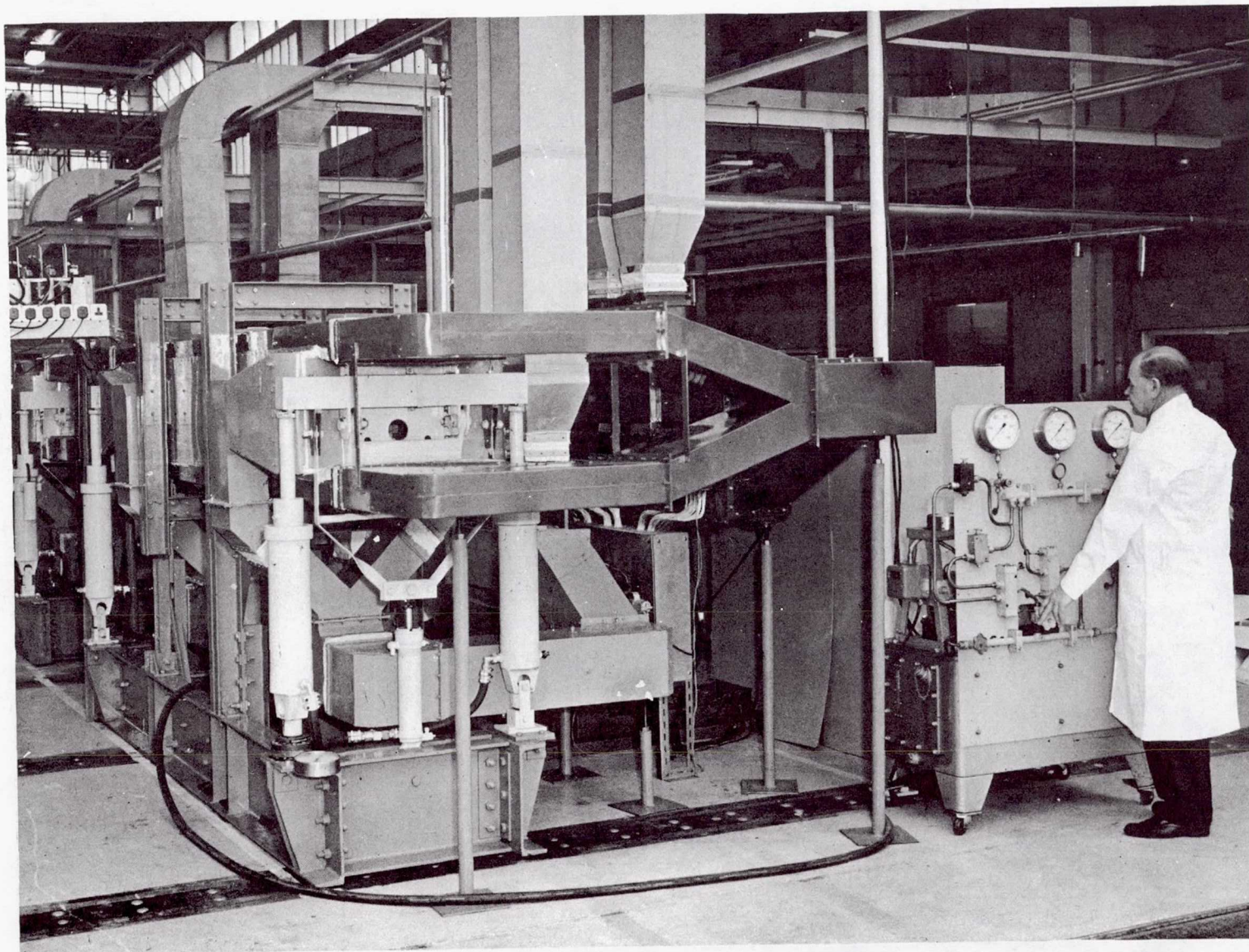


Figure 9.- Test rig for box-beam specimens at R.A.E.



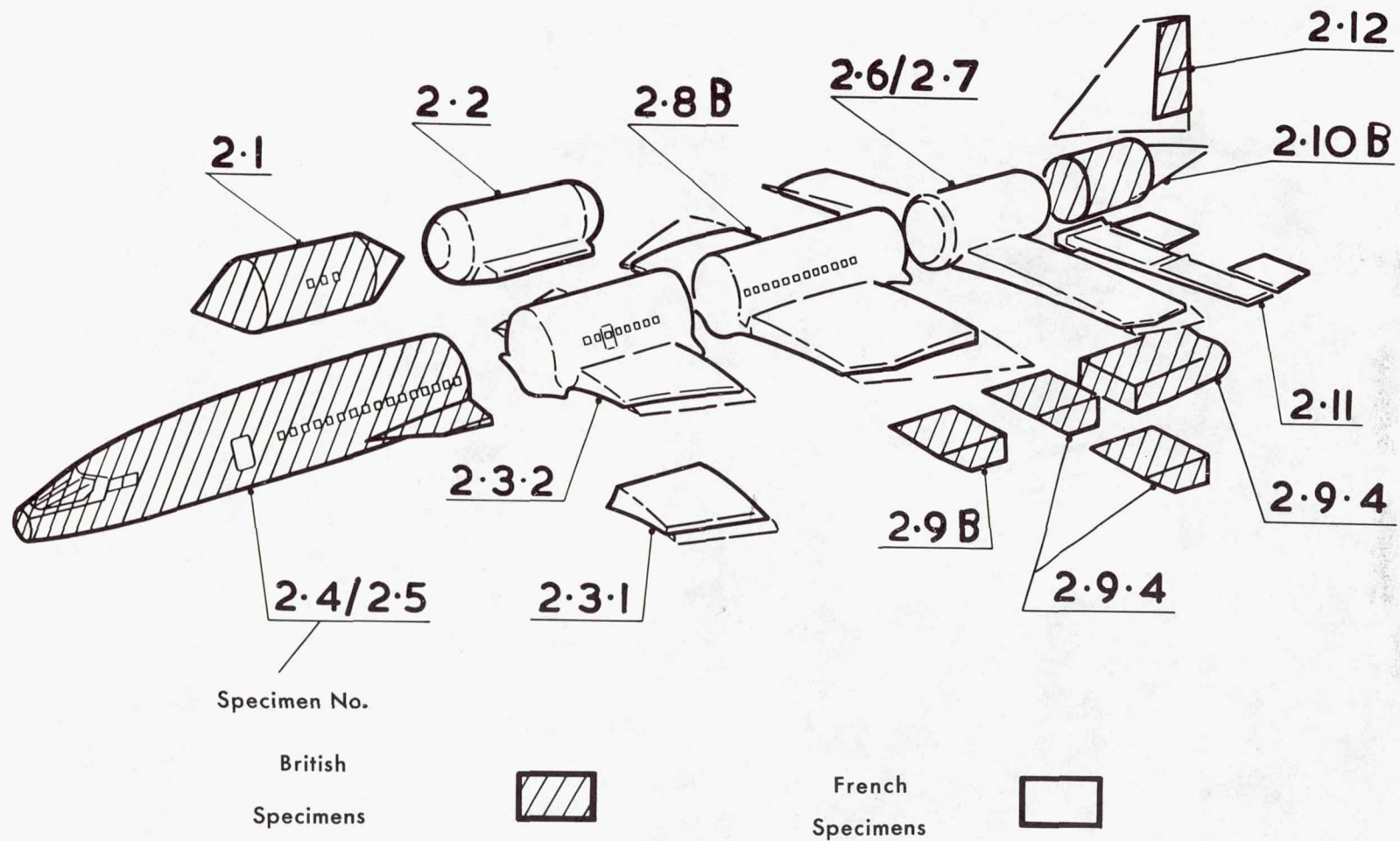


Figure 10.- Component test specimens.

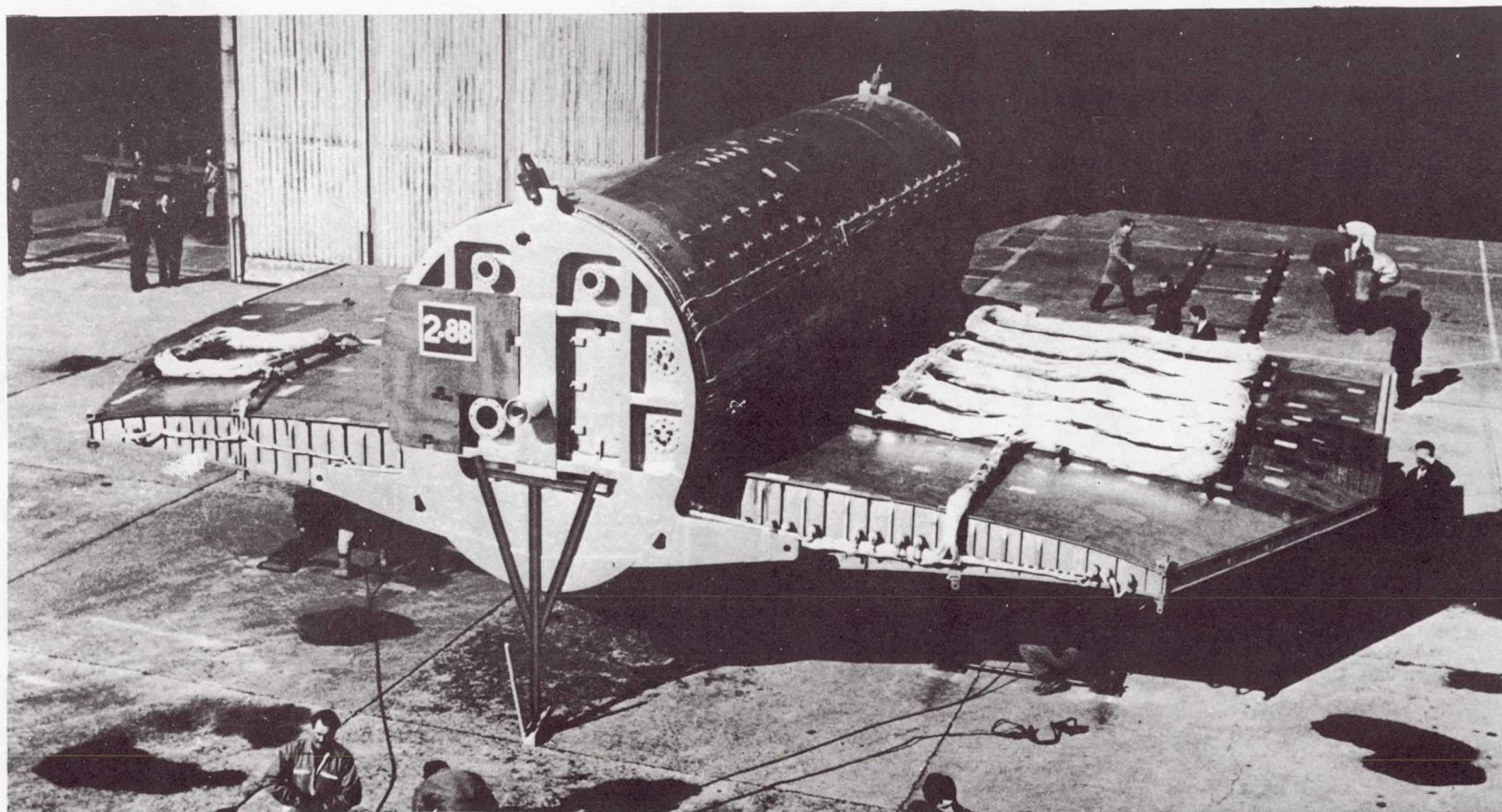


Figure 11.- Centre wing and fuselage specimen (2.8B).



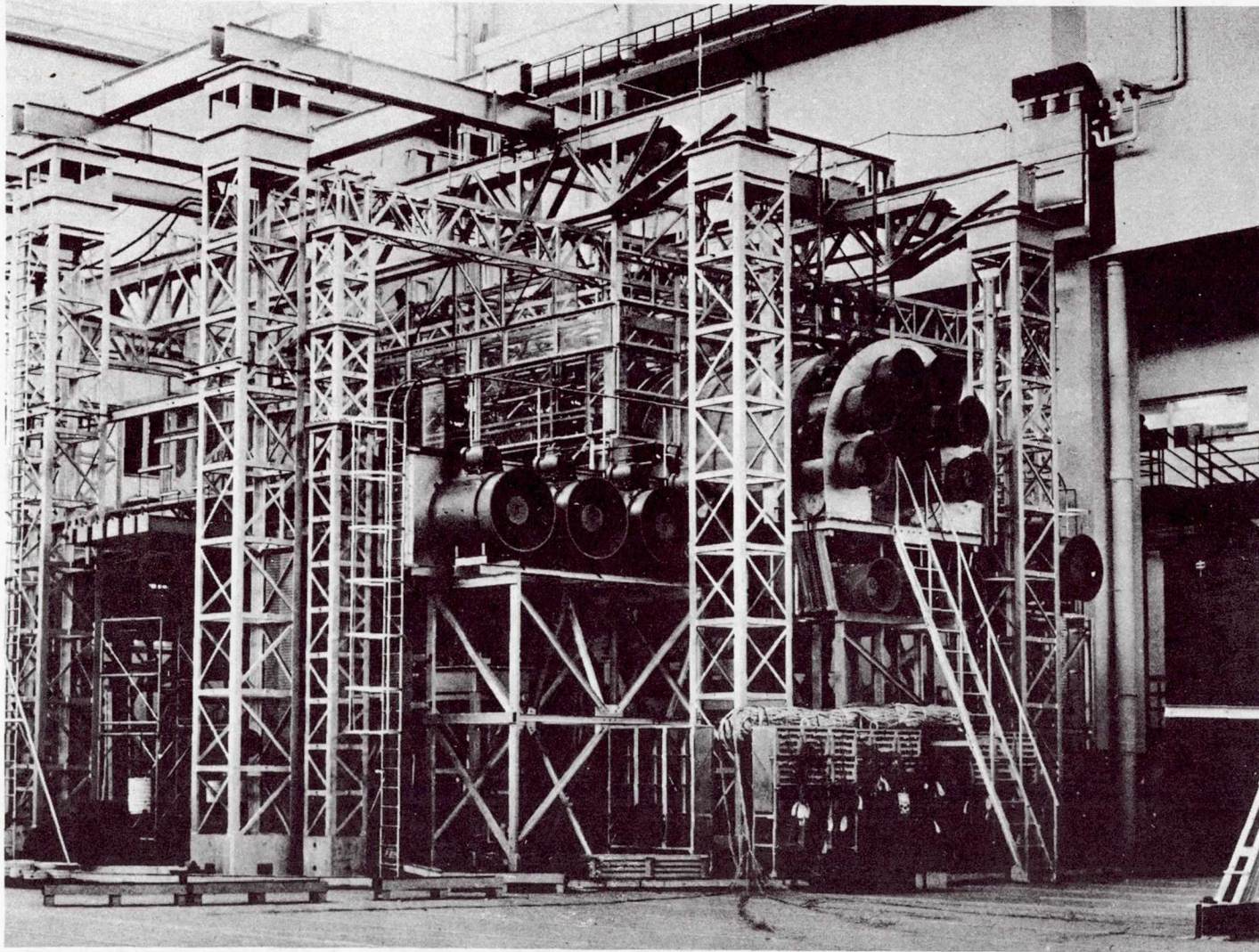


Figure 12.- Test rig for centre wing and fuselage specimen at C.E.A.T.



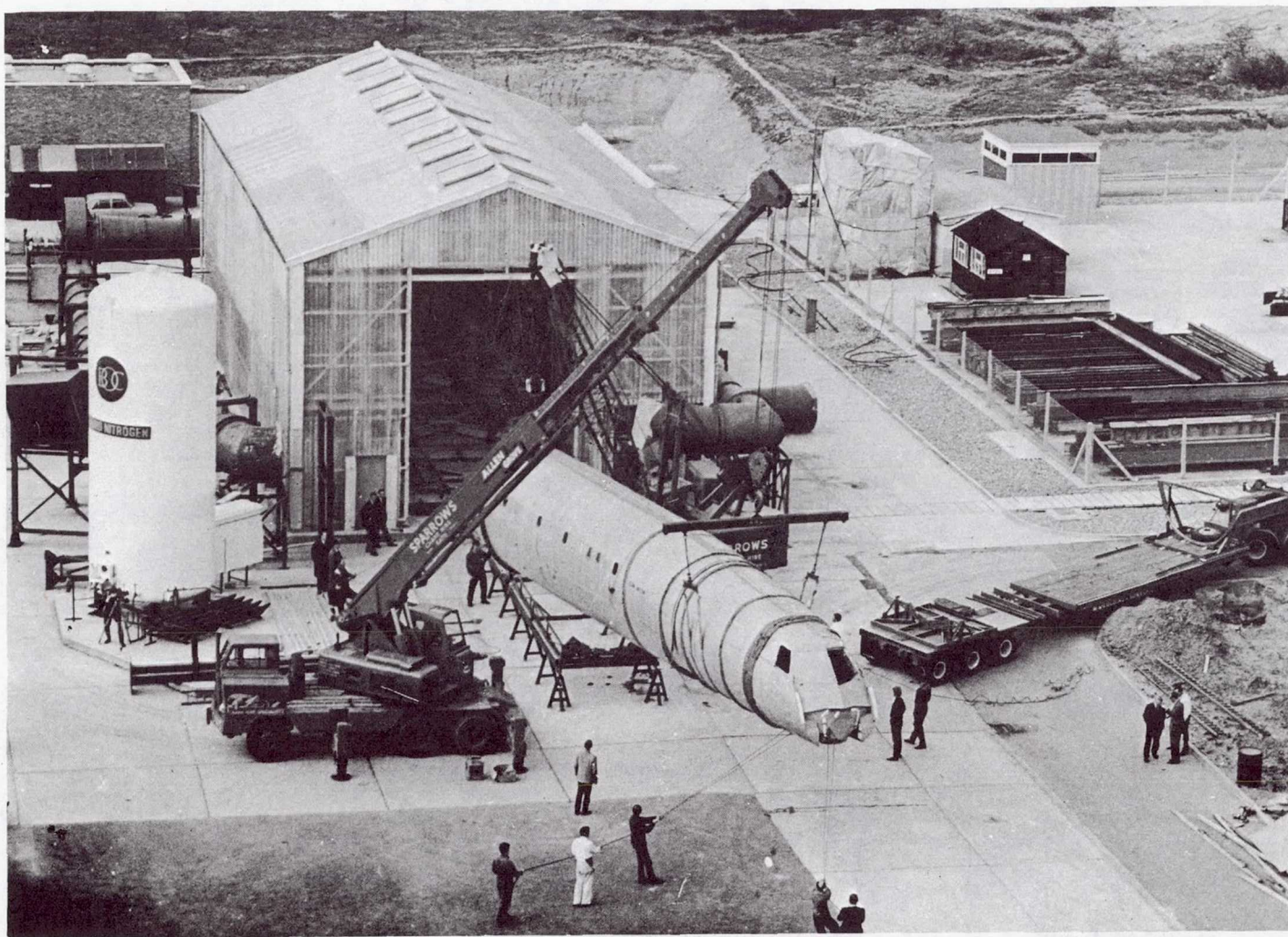


Figure 13.- Forward-fuselage specimen (2.4/2.5) and test rig at R.A.E.



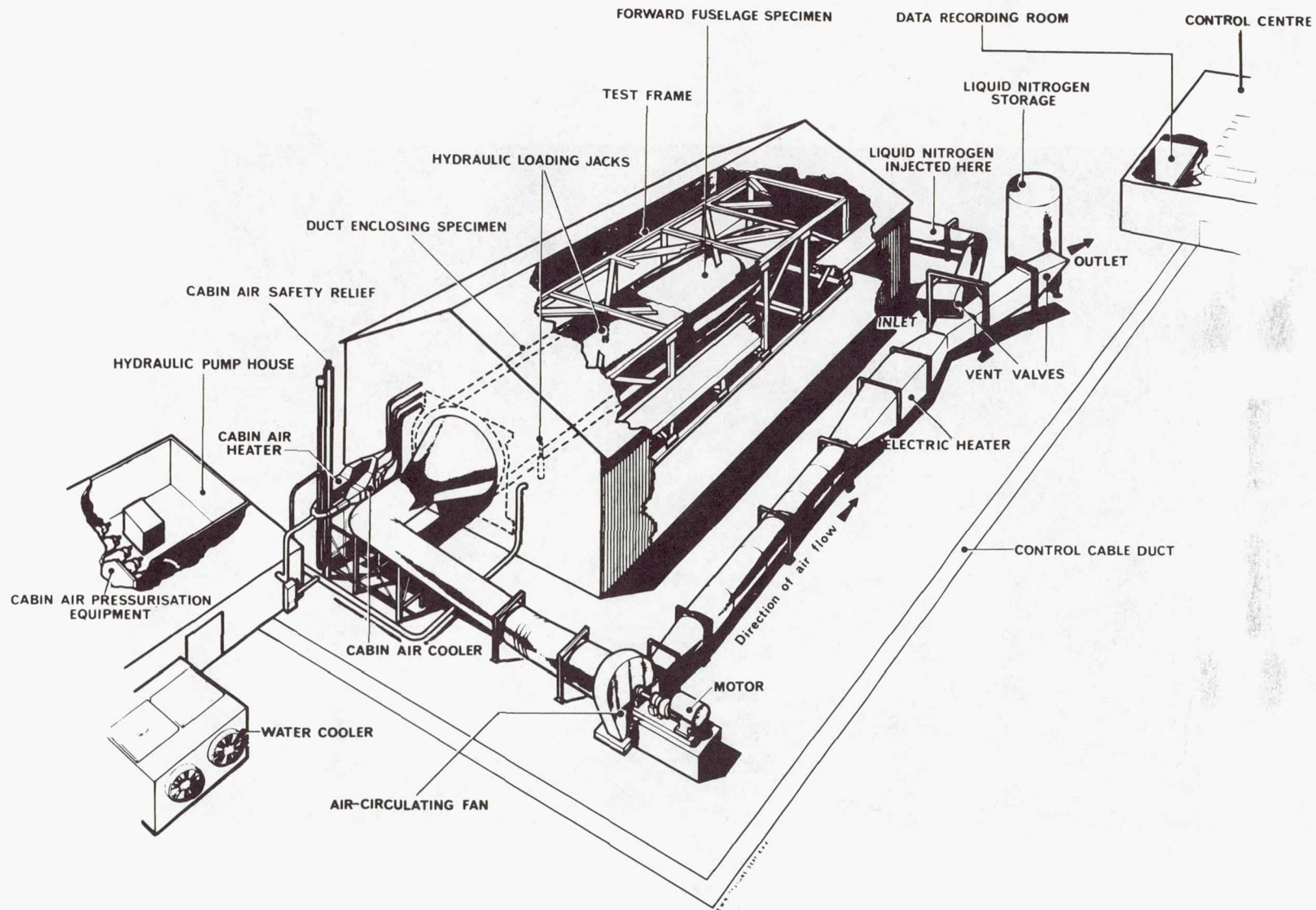


Figure 14.- Test rig for forward-fuselage specimen at R.A.E.

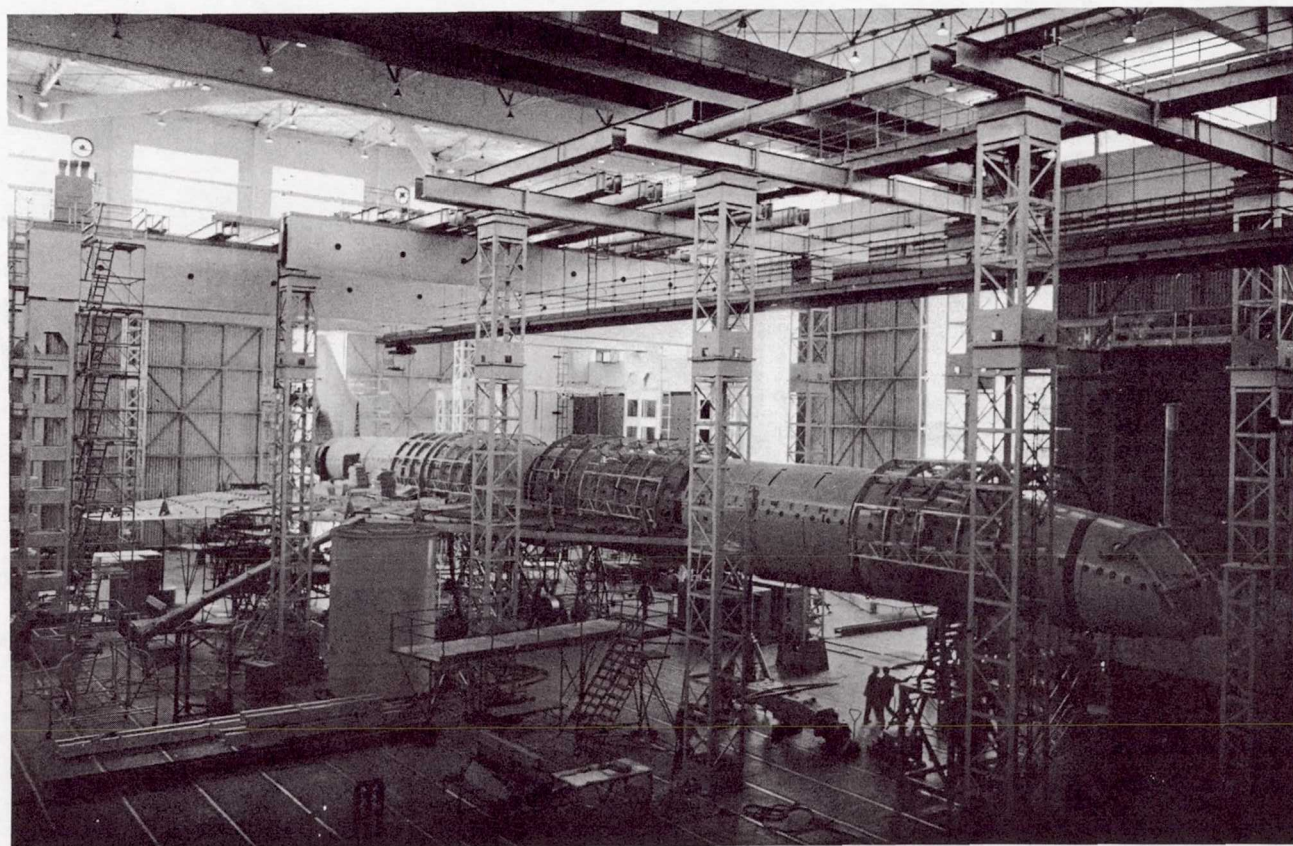


Figure 15.- Static-test specimen in test frame at C.E.A.T.



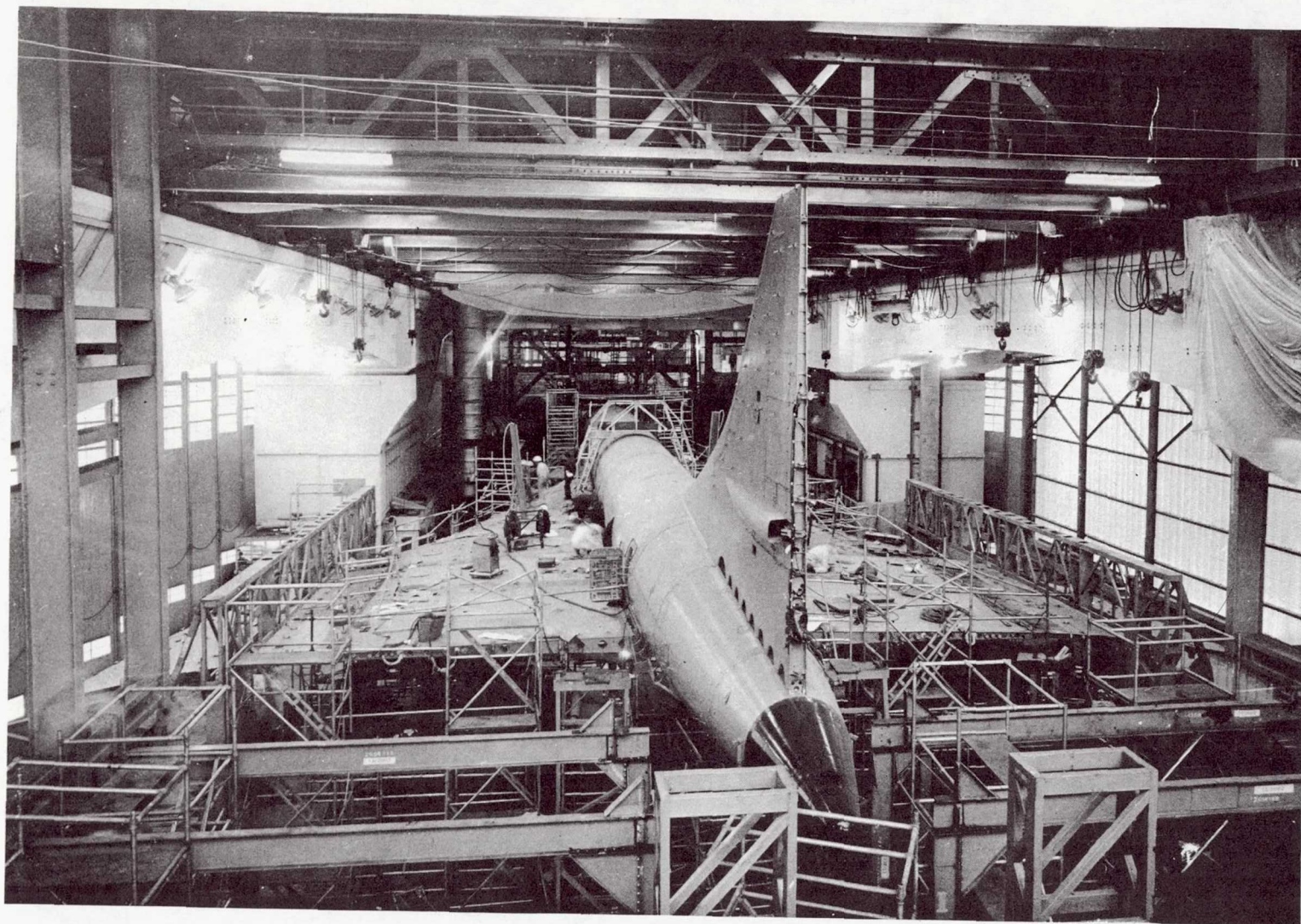


Figure 16.- Fatigue-test specimen in test frame at R.A.E.



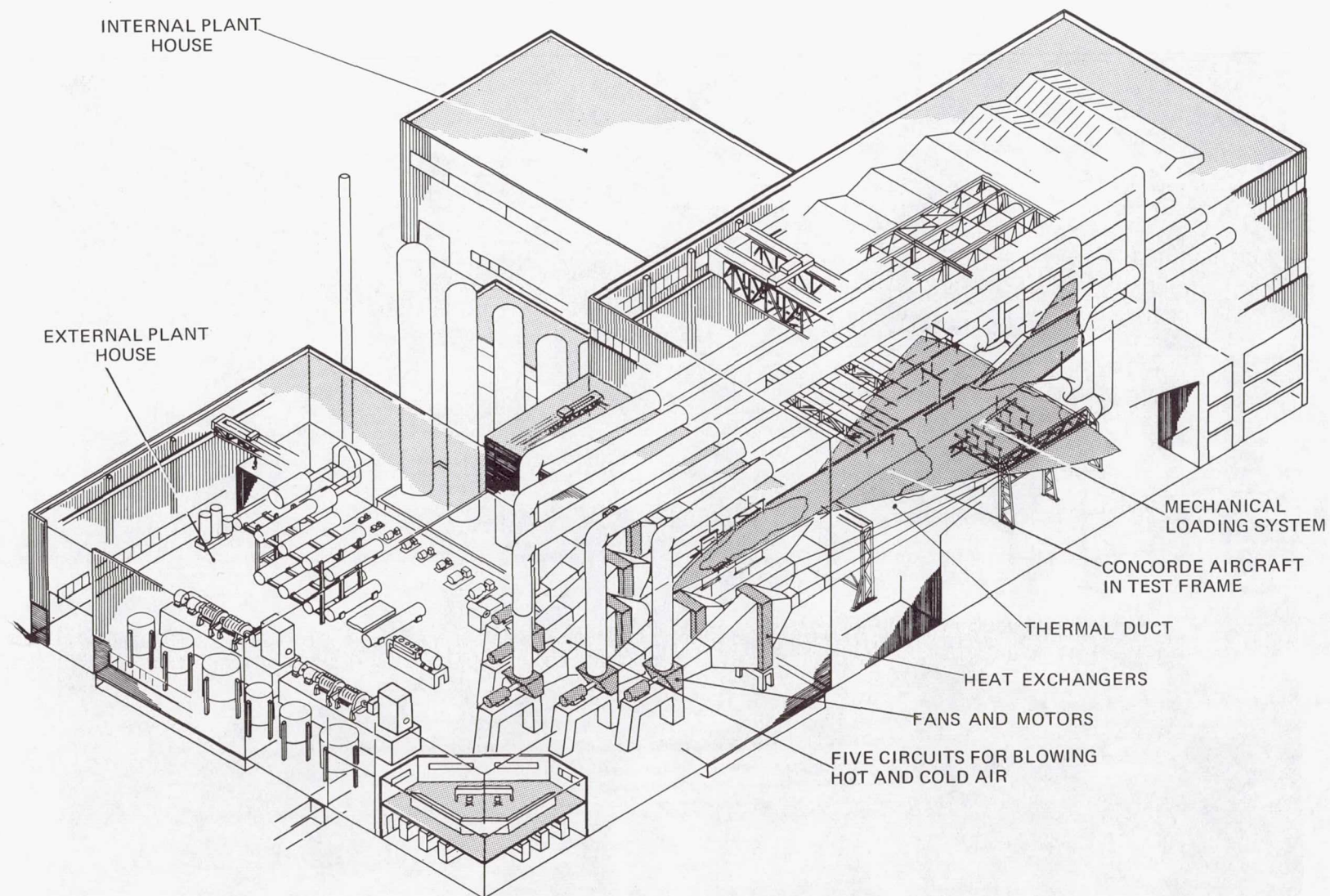


Figure 17.- Test rig for major fatigue test at R.A.E.



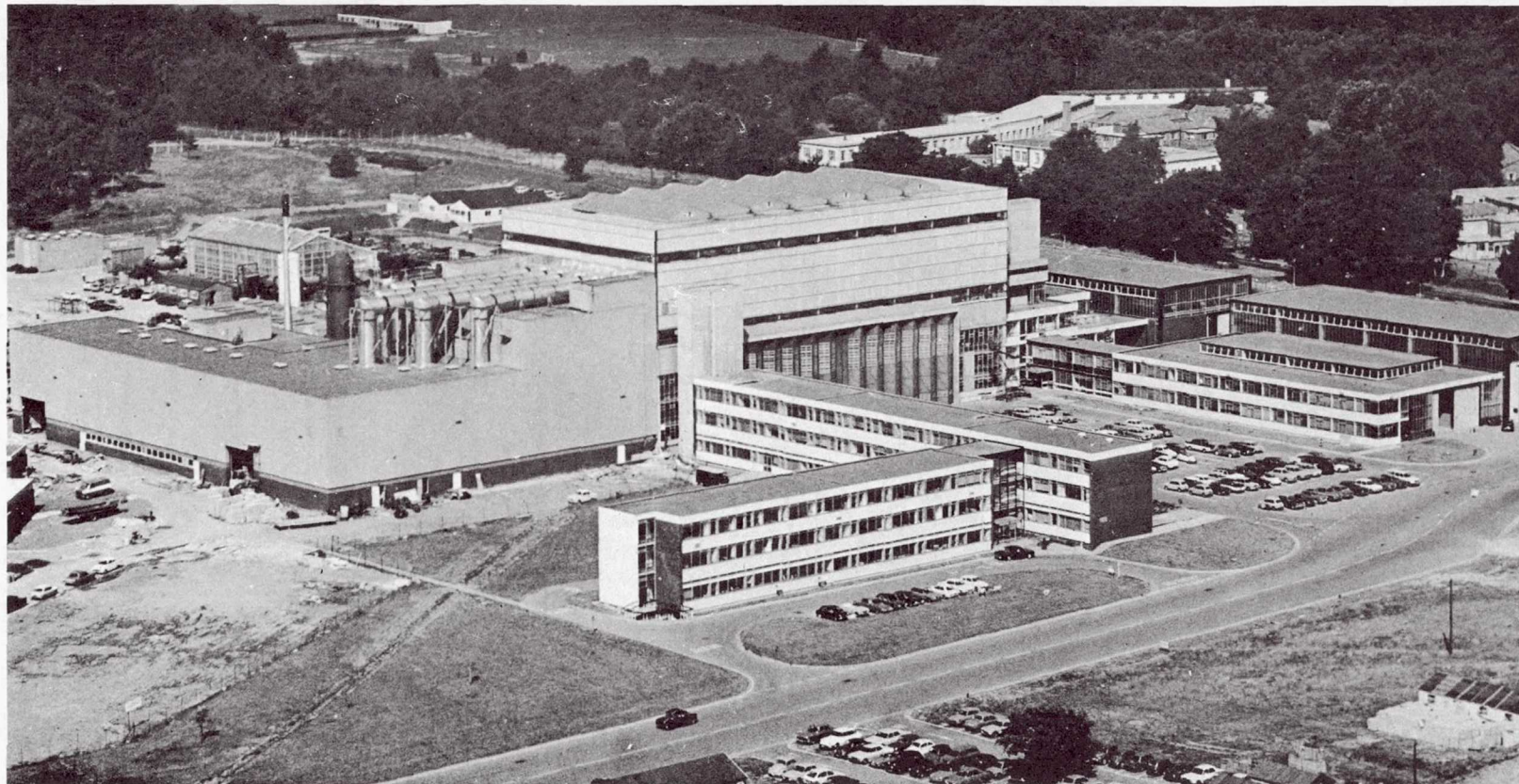


Figure 18.- Test facility at R.A.E.

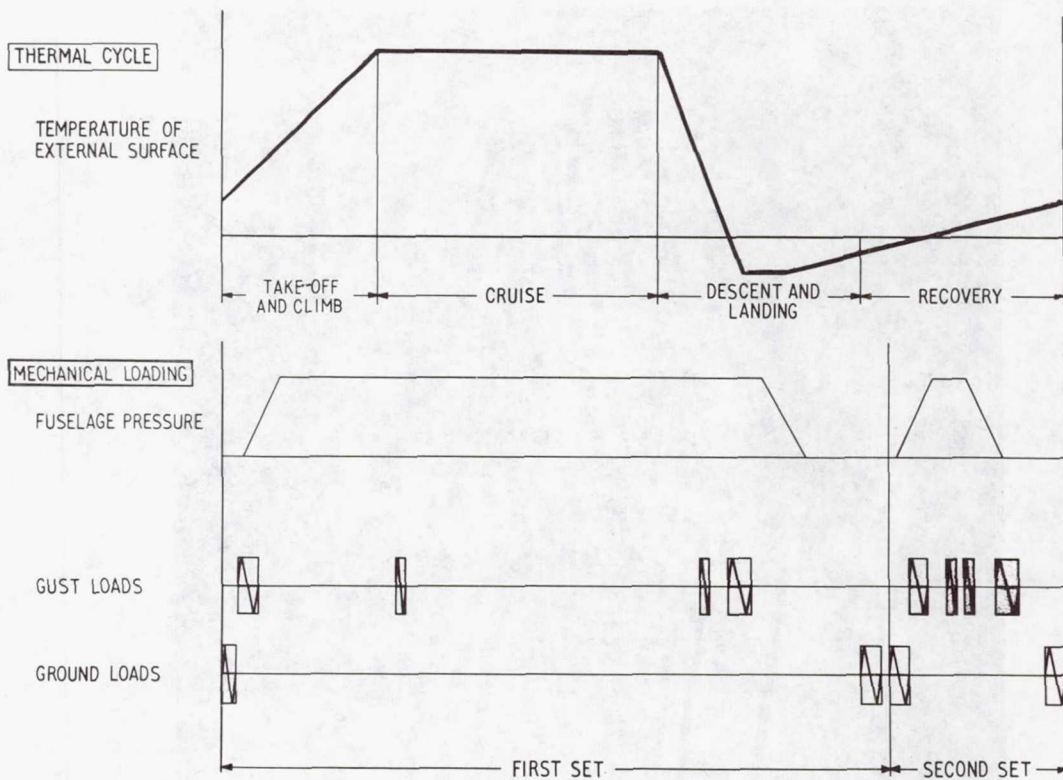


Figure 19.- Thermal cycle and mechanical loading in accelerated test cycle.

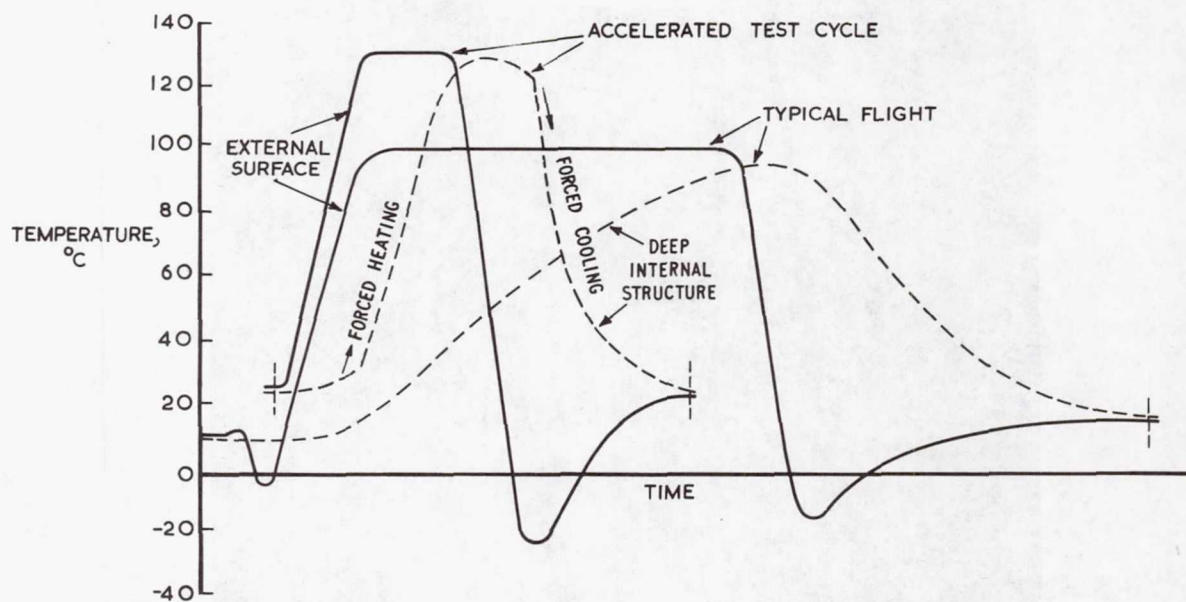


Figure 20.- Structural temperatures in accelerated test cycle and typical flight.



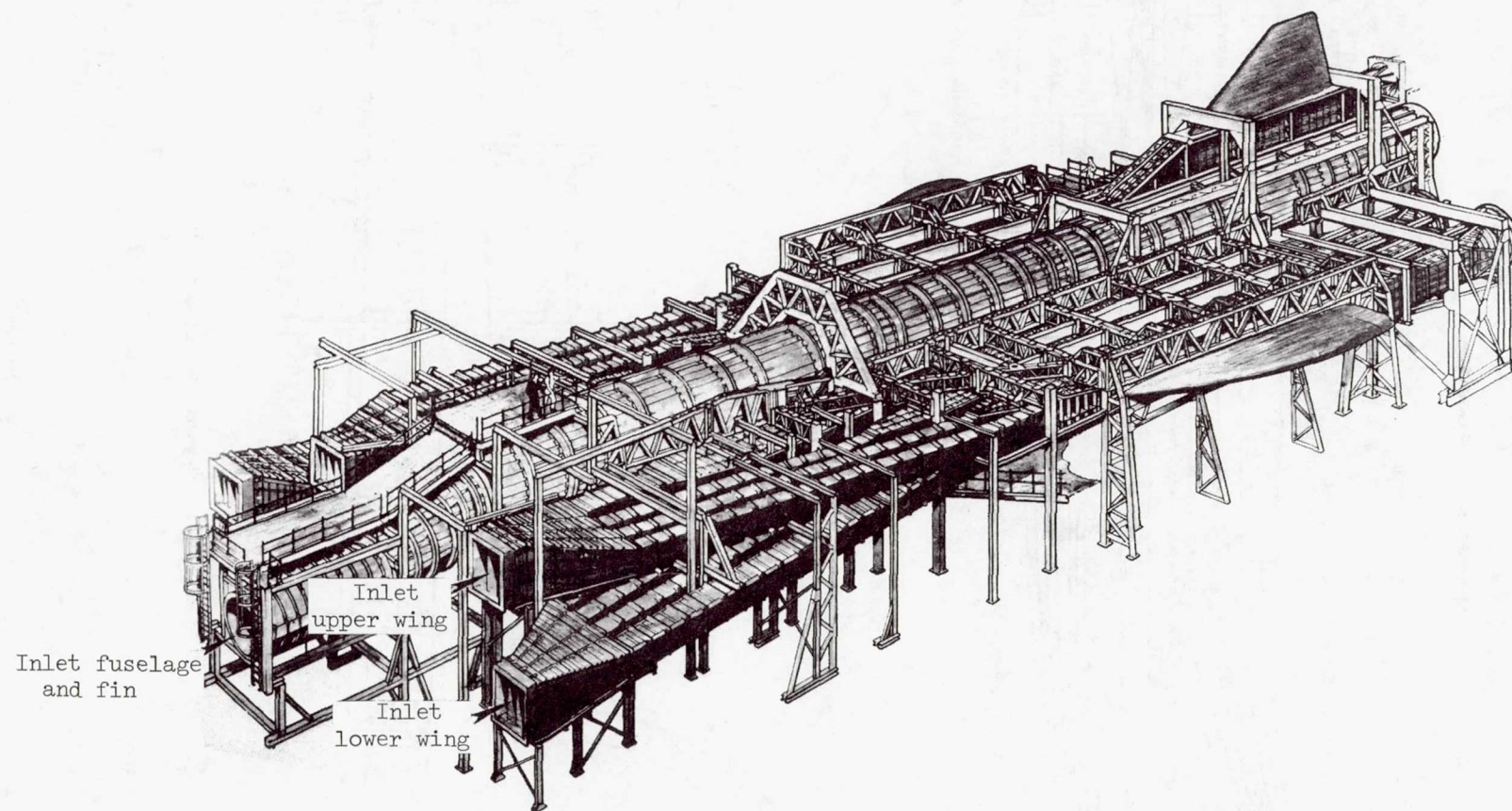


Figure 21.- Thermal duct surrounding specimen.

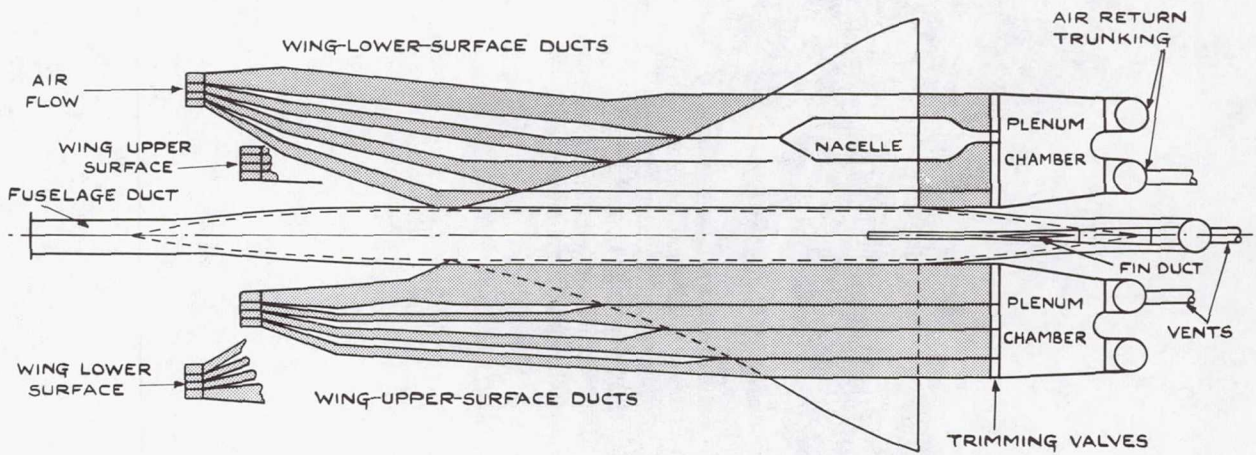


Figure 22.- Details of duct arrangement.

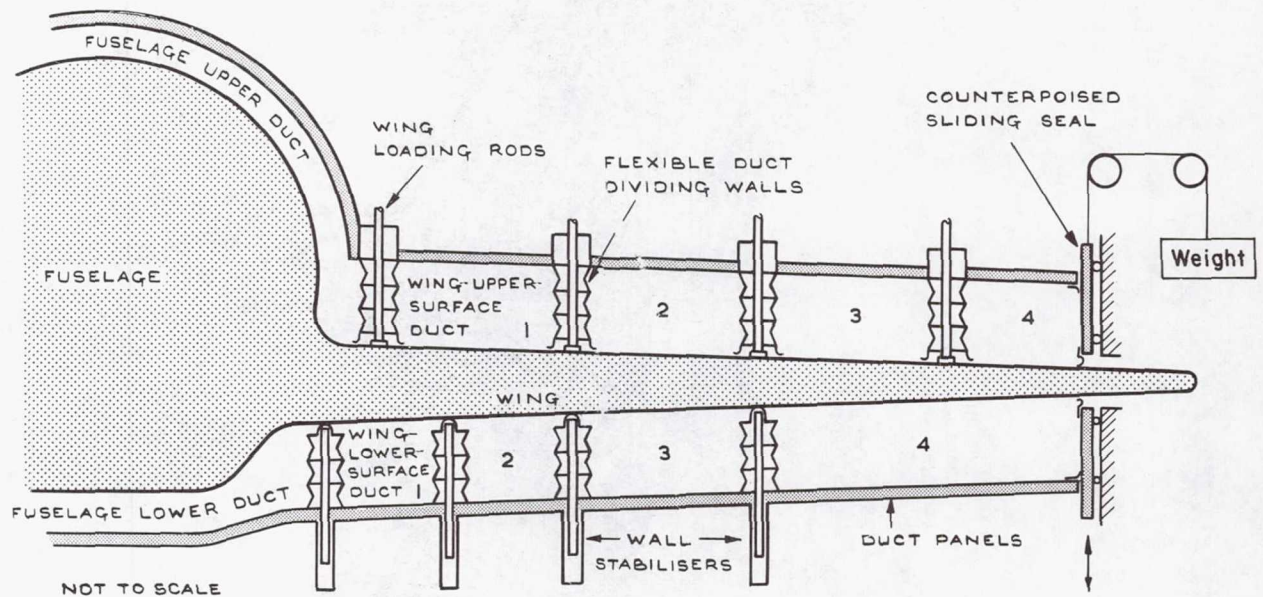


Figure 23.- Wing and fuselage duct dividers.



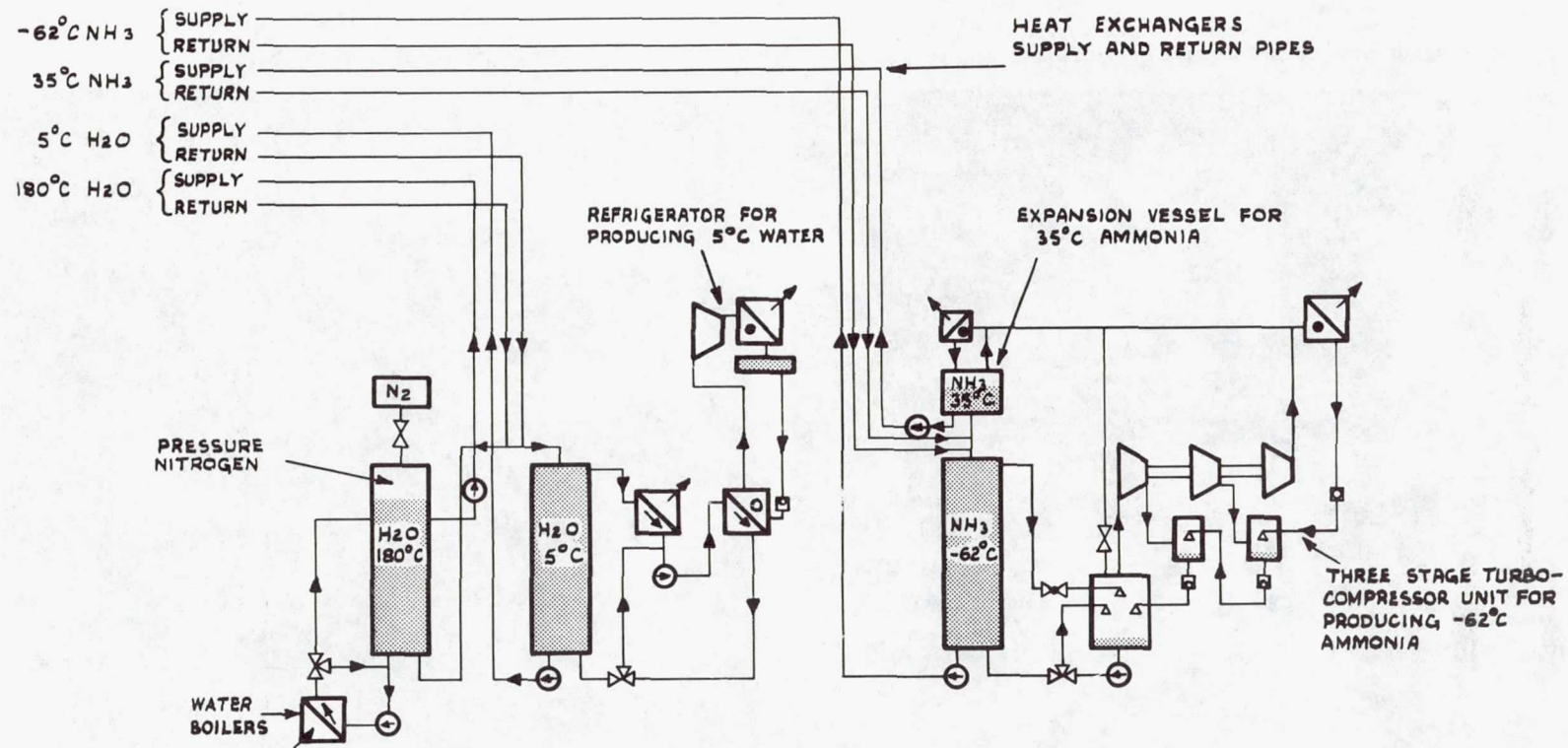
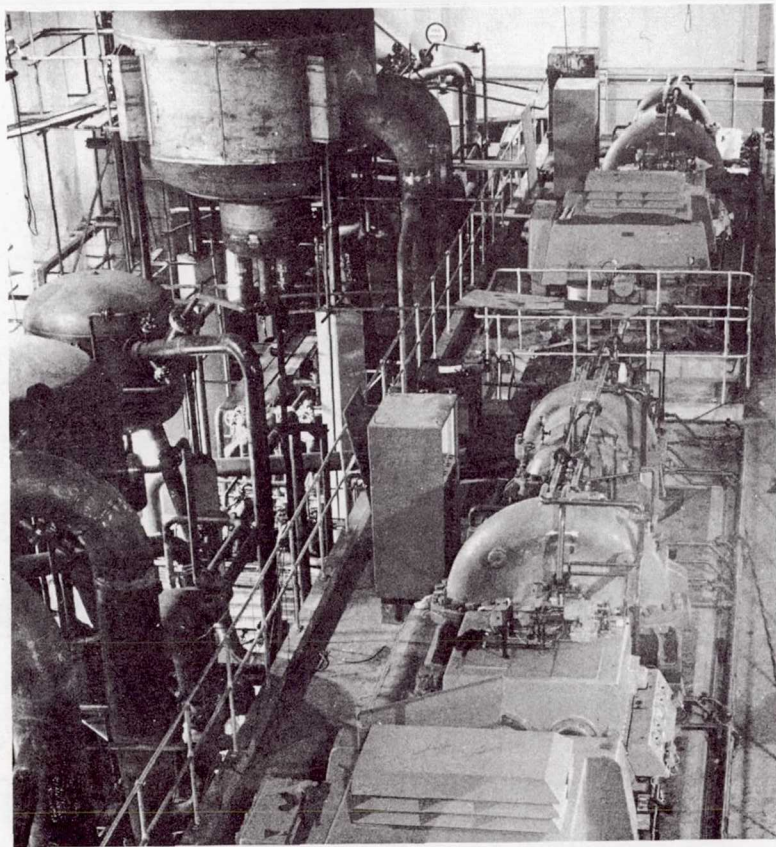
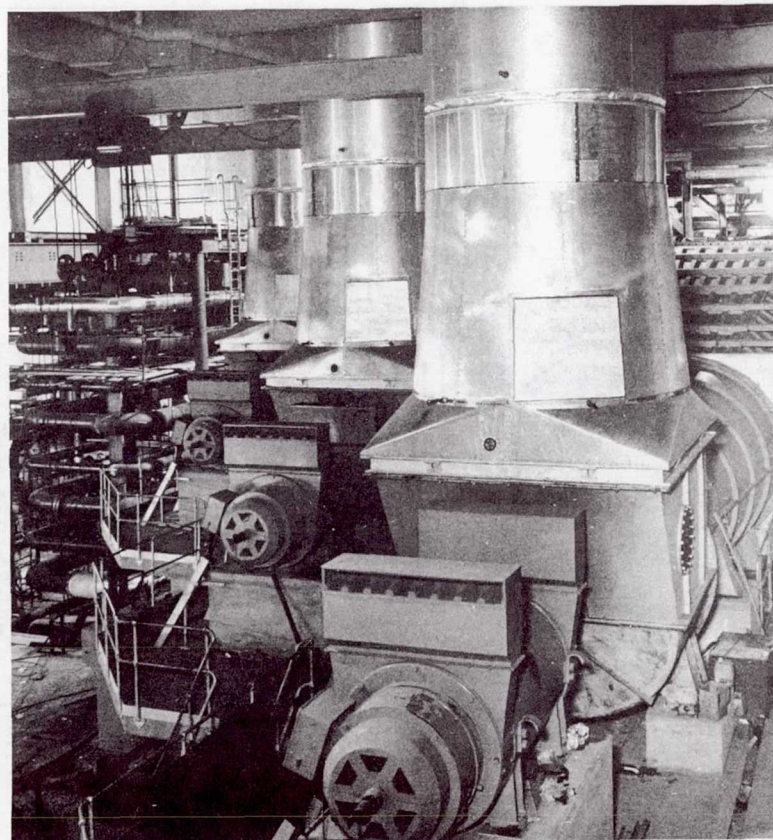


Figure 24.- Simplified flow diagram of external plant.



Ammonia refrigeration plant.



Three of the main air-circulating fans and motors.

Figure 25.- Views of external plant house.



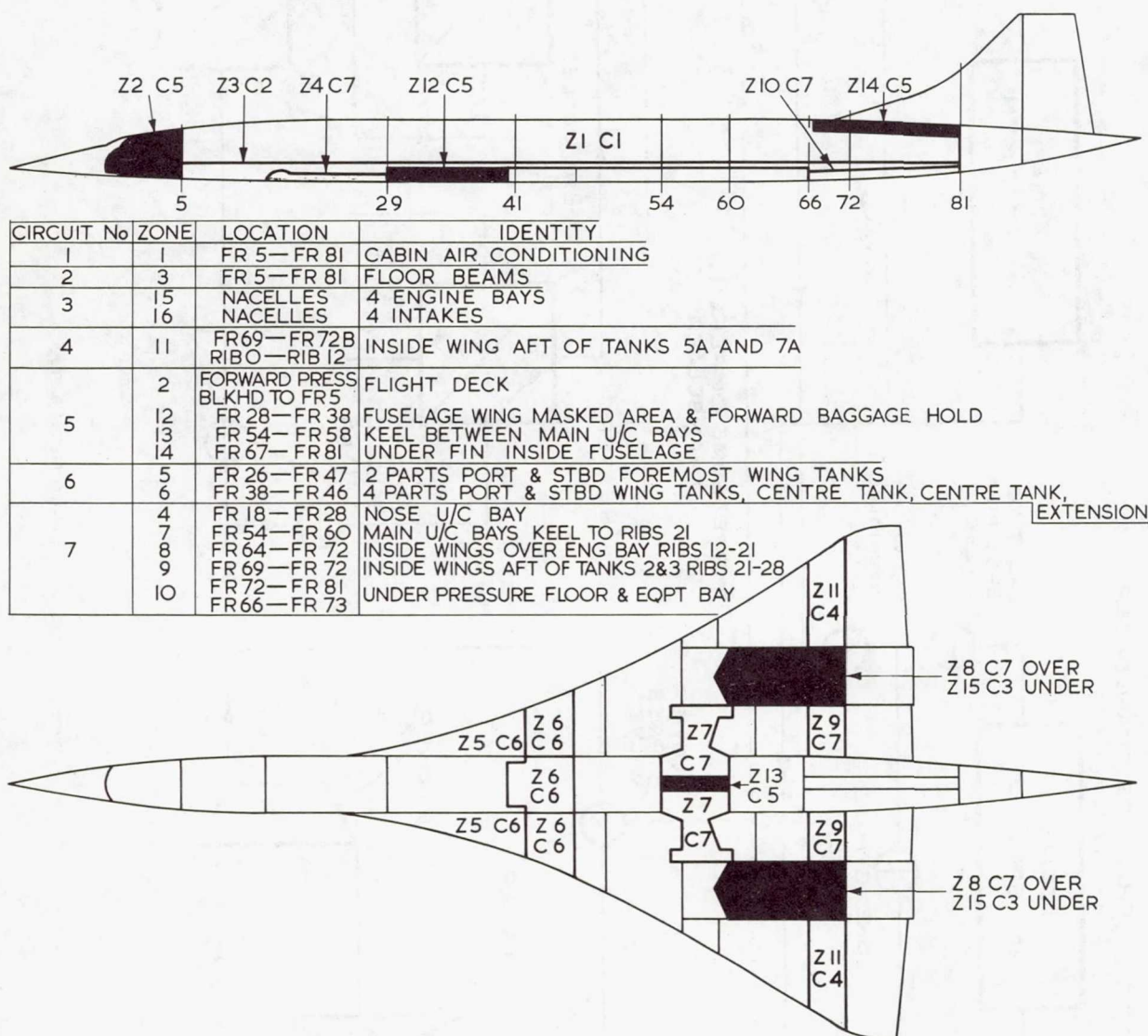


Figure 26.- Internal air-conditioning circuits.

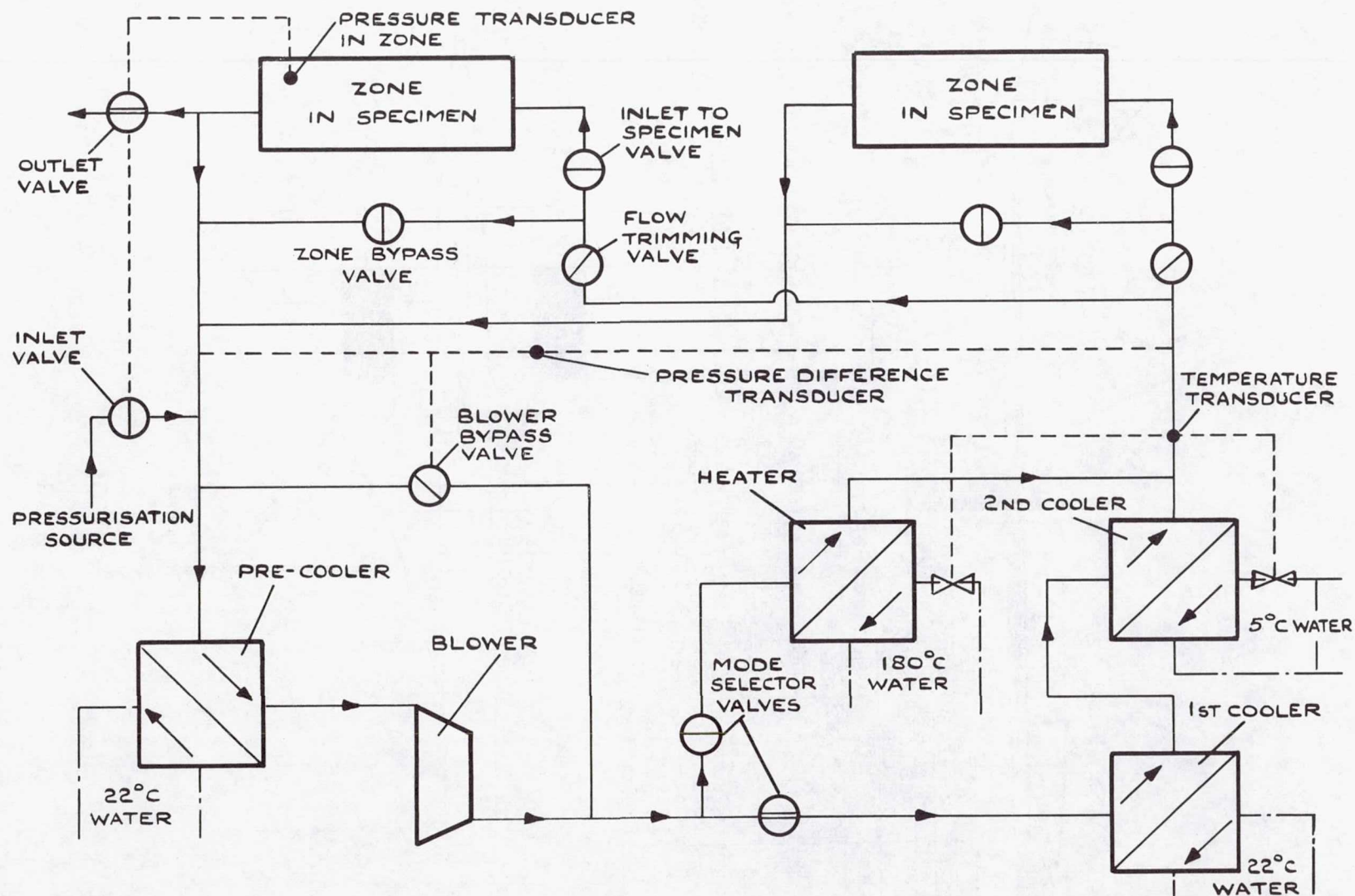


Figure 27.- Typical air circuit for internal plant.



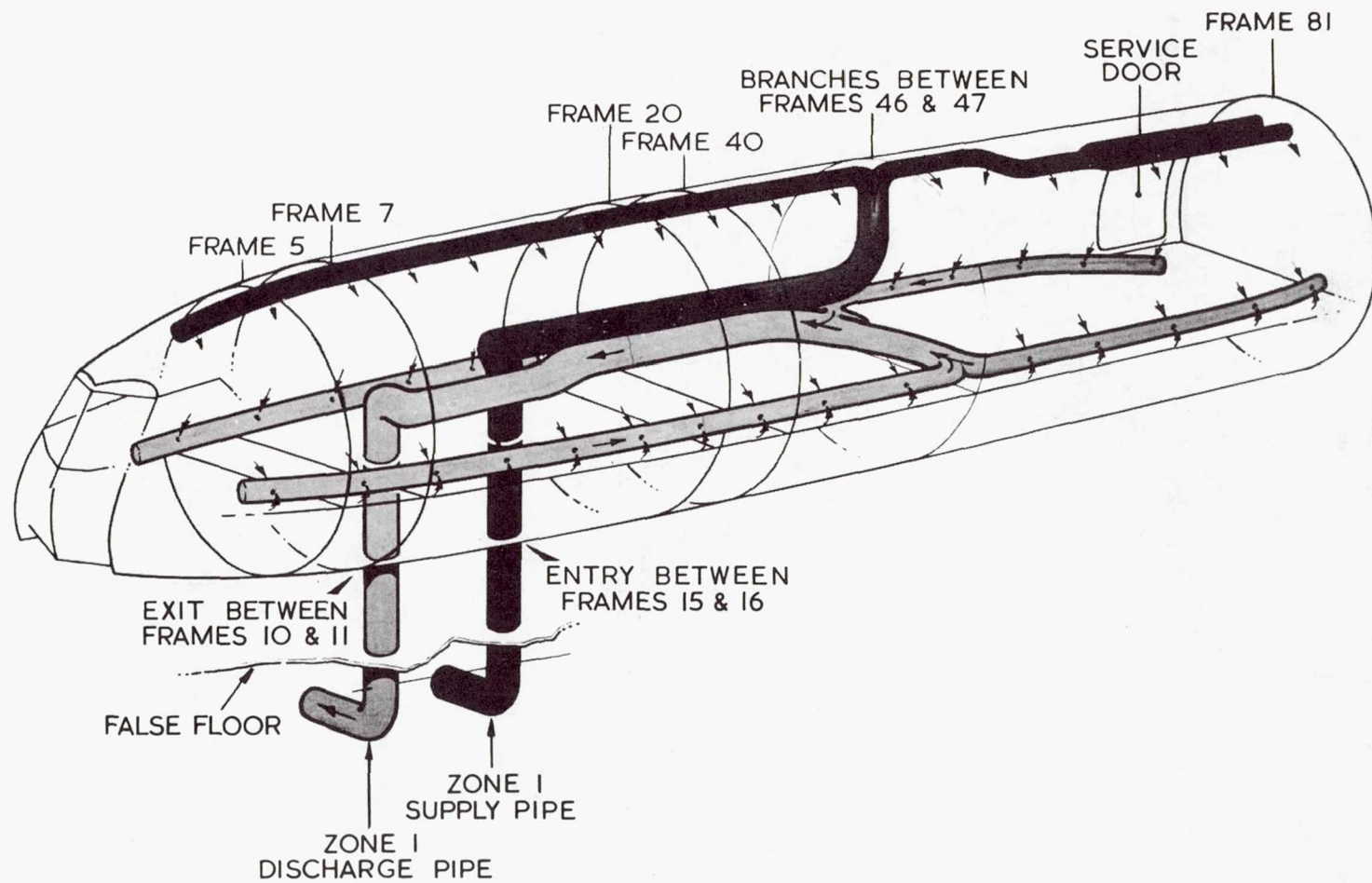


Figure 28.- Fuselage air-conditioning system.

- CONDITIONED WITH AIR ONLY
- FUEL SUBSTITUTE CIRCULATED AND CONDITIONED
- FUEL SUBSTITUTE CIRCULATED BUT NOT CONDITIONED
- FUEL SUBSTITUTE NOT CIRCULATED OR CONDITIONED

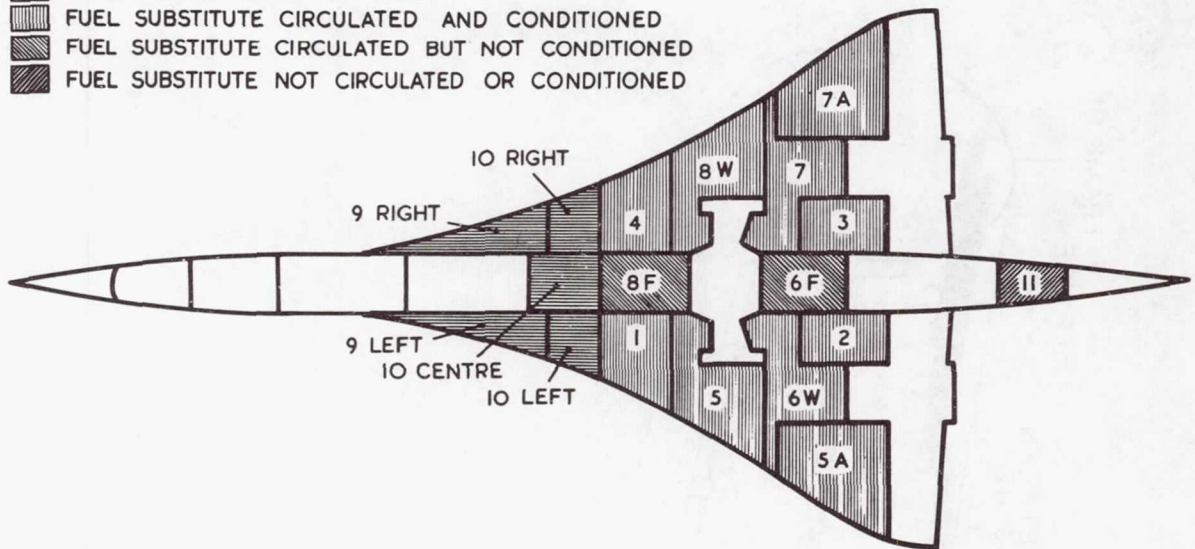


Figure 29.- Internal conditioning of fuel tanks.

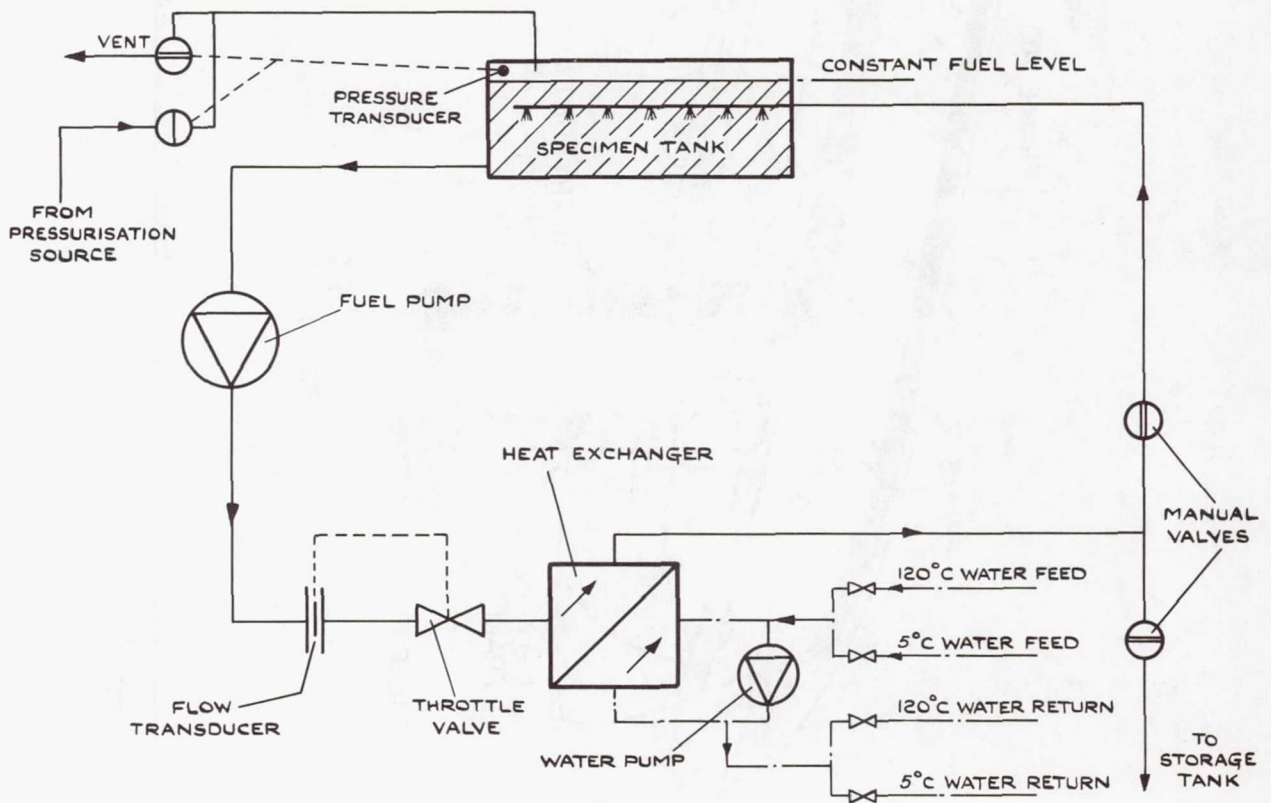


Figure 30.- Typical fuel system for internal plant.



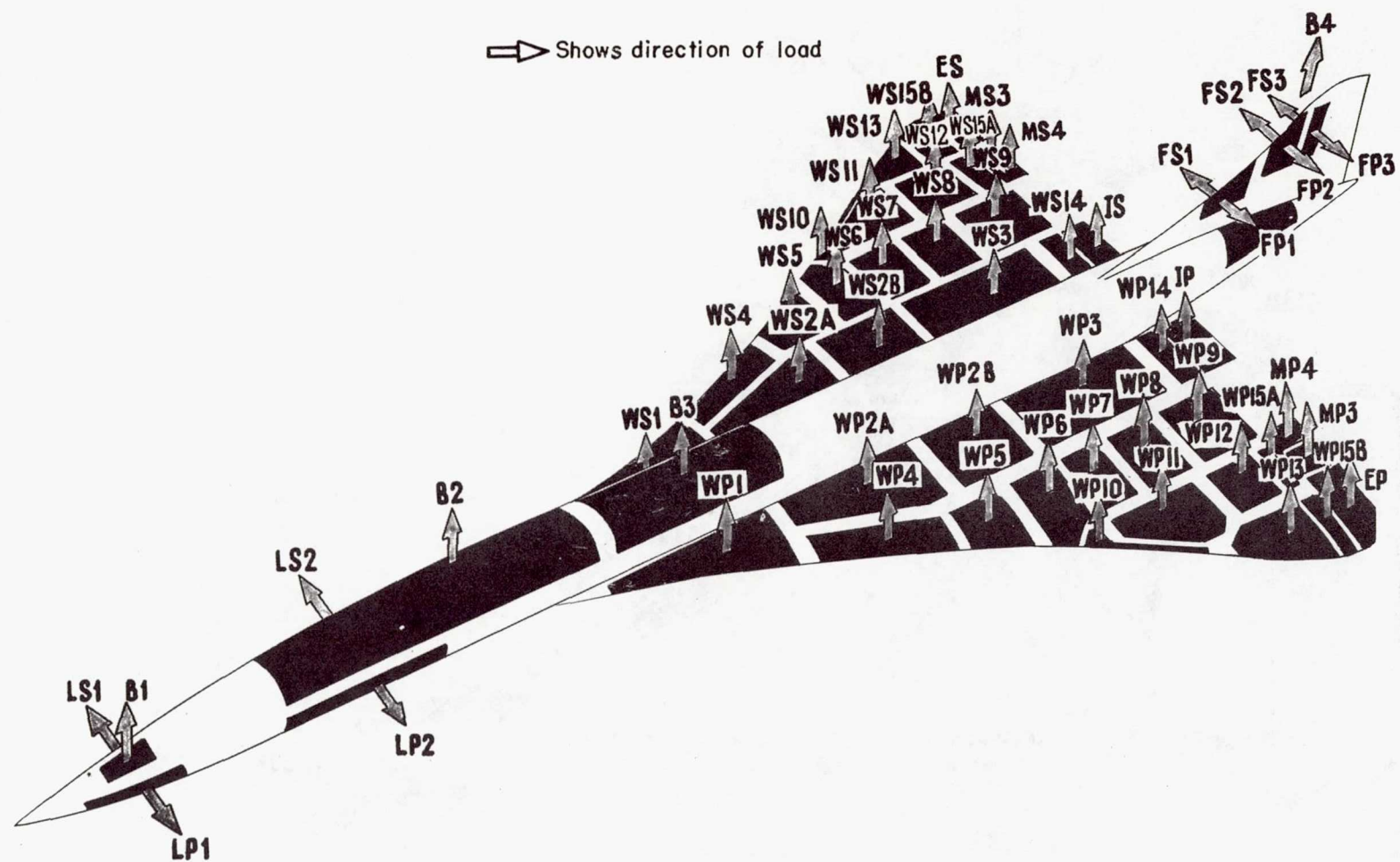


Figure 31.- Loading system, upper surface.

Figure 32.- Loading and reaction systems, lower surface.



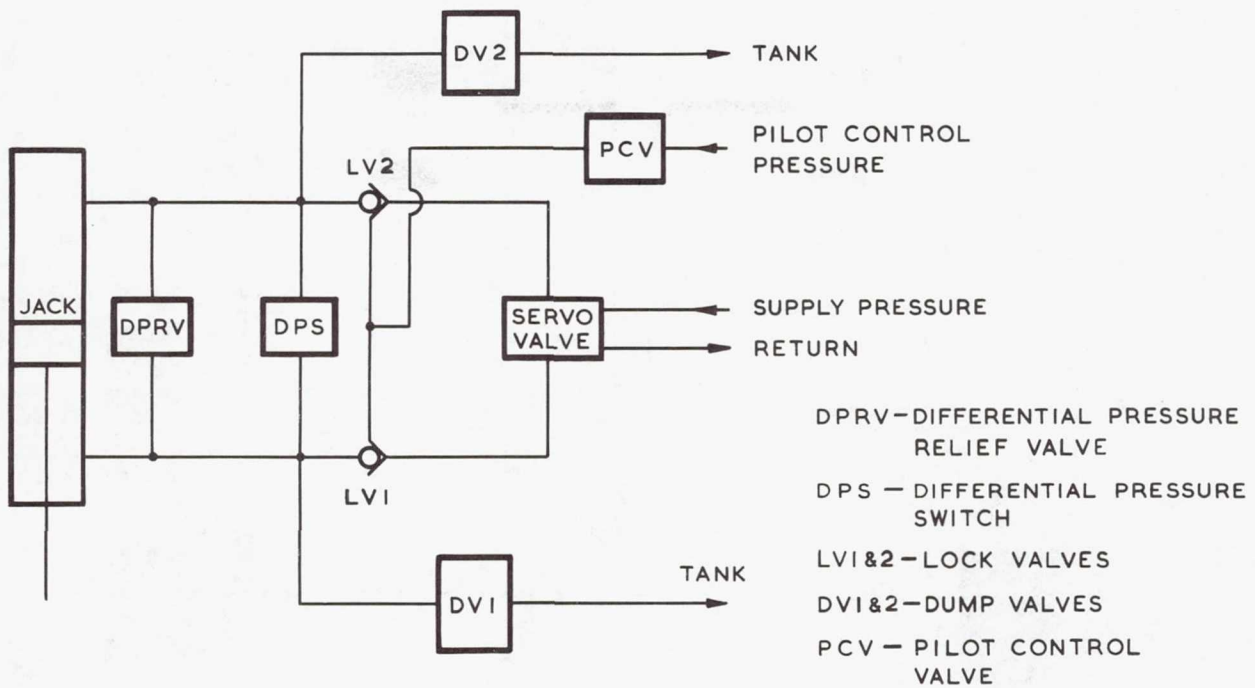


Figure 33.- Diagram of tension-jack-module circuit.

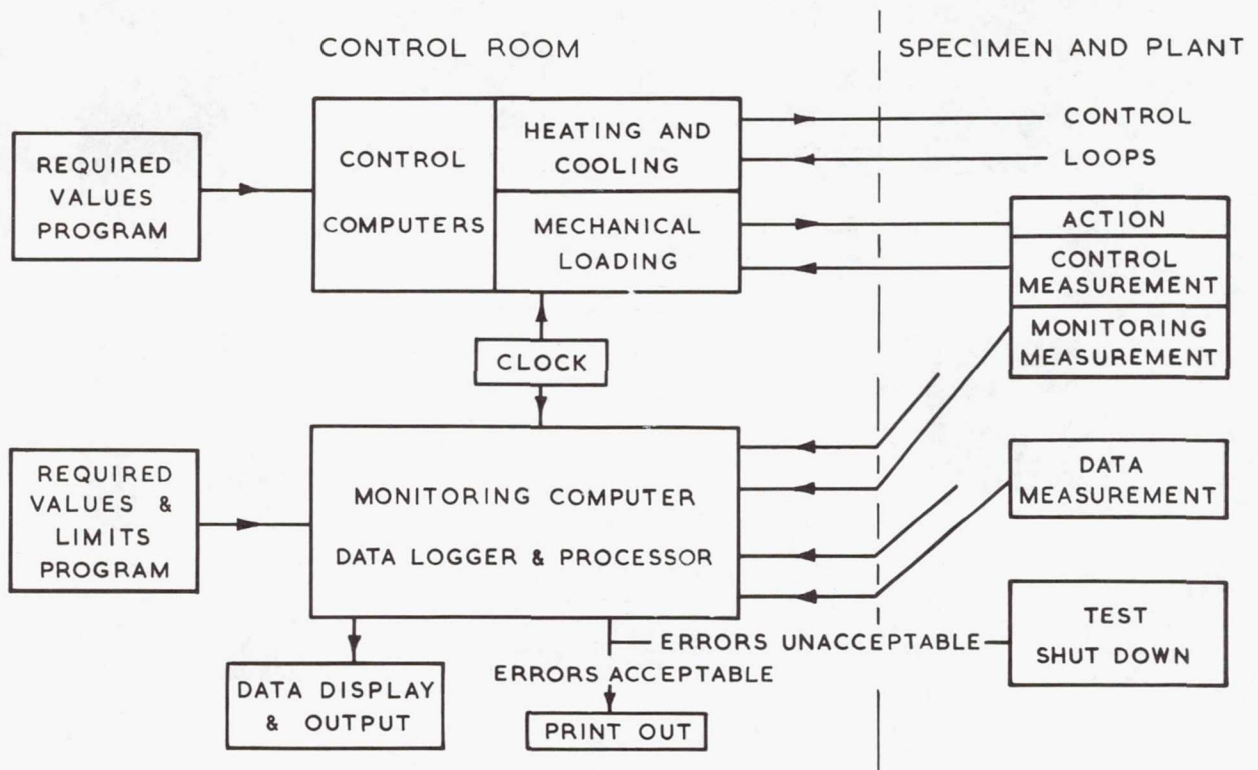


Figure 34.- Principles of control and monitoring system.

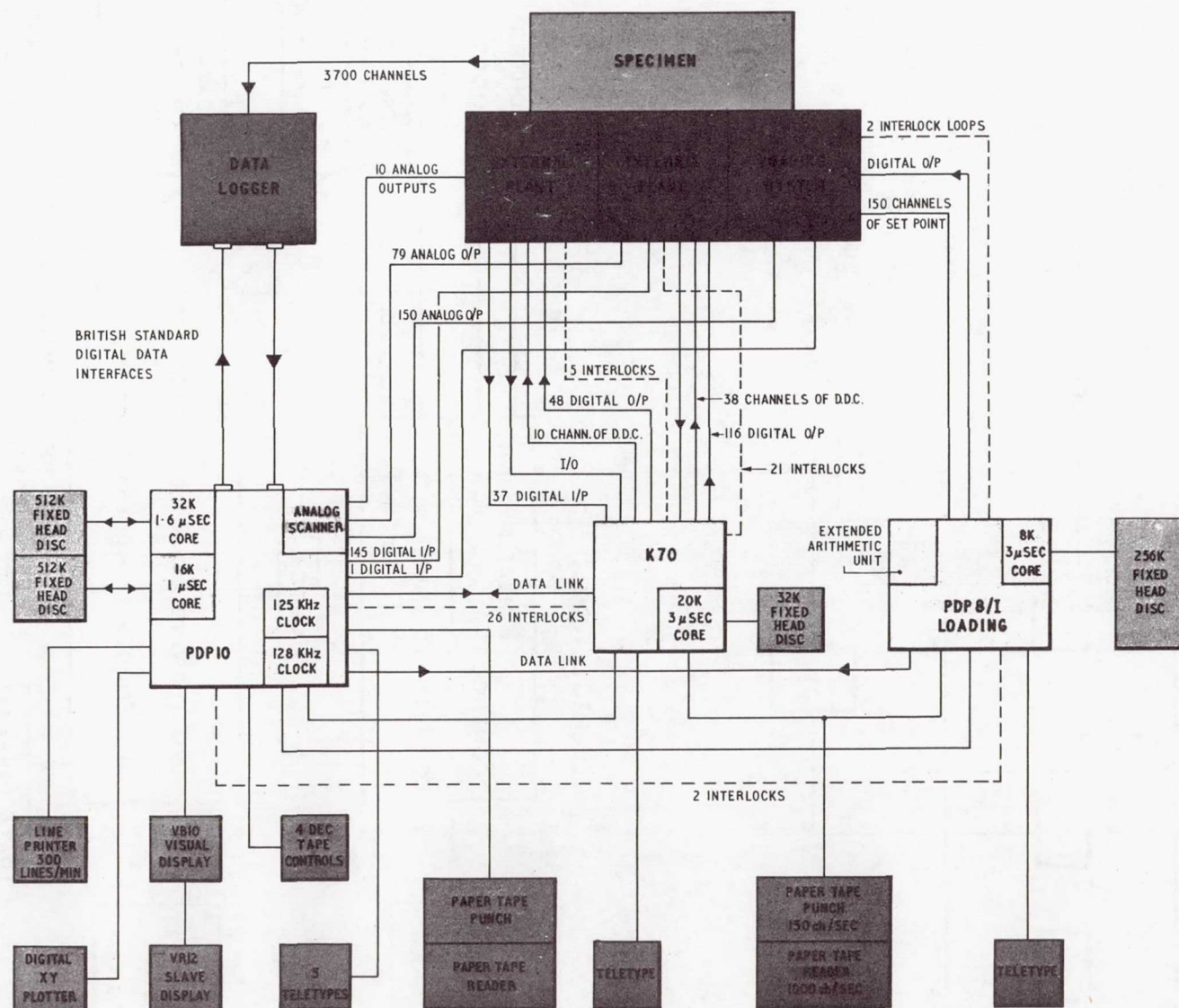


Figure 35.- Flow diagram of control and monitoring system.



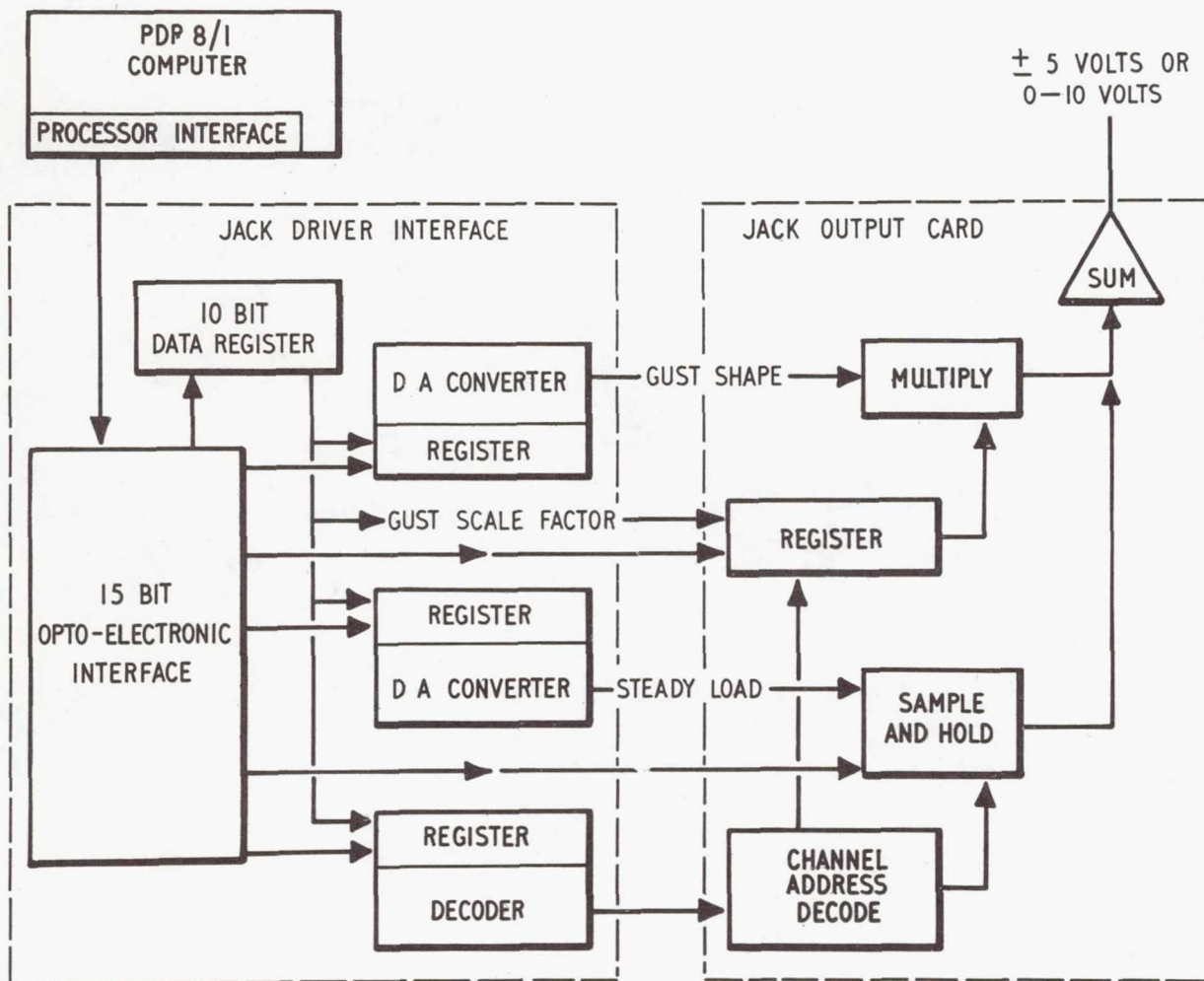


Figure 36.- Loading computer system.

FATIGUE EXPERIENCE FROM TESTS CARRIED OUT WITH FORGED  
BEAM AND FRAME STRUCTURES IN THE DEVELOPMENT  
OF THE SAAB AIRCRAFT VIGGEN

By S. E. Larsson  
Saab-Scania Aktiebolag  
Linköping, Sweden

SUMMARY

A part of the lower side of the main wing at the joint of the main spar with the fuselage frame was investigated. This wing beam area was simulated by a test specimen consisting of a spar boom of AZ 74 forging (7075 aluminum alloy modified with 0.3 percent Ag) and a portion of a honeycomb sandwich panel attached to the boom flange with steel bolts. The cross section was reduced to half scale. However, the flange thickness, the panel height, and the bolt size were full scale.

Further, left and right portions of the fuselage frame intended to carry over the bending moment of the main wing were tested. Each of these "frame halves" consisted of a forward and a rear forging (7079 aluminum alloy, overaged) connected by an outer and inner skin (Alclad 7075) creating a box beam. These test specimens were full scale and were constructed principally of ordinary aircraft components.

The test load spectrum was common to both types of specimens with regard to percentage levels. It consisted of maneuver and gust loads, touchdown loads, and loads due to ground roughness. A load history of 200 hours of flight with 15 000 load cycles was punched on a tape. The loads were randomized in groups according to the flight-by-flight principle. The highest positive load level was 90 percent of limit load and the largest negative load was -27 percent. A total of 20 load levels were used. Both types of specimens were provided with strain gages and had a nominal stress of about  $300 \text{ MN/m}^2$  in some local areas.

As a result of the tests, steps were taken to reduce the risk of fatigue damage in aircraft. Thus stress levels were lowered, radii were increased, and demands on surface finish were sharpened.

INTRODUCTION

In designing aircraft structures against fatigue, a practice that has been used for many years at Saab can be described as follows: Reasonably low stress levels are applied and structural elements and units are carefully shaped on the basis of



load-spectrum estimates, stress analysis, fatigue testing of small specimens, and fatigue calculations. By these means costly fatigue tests on complete aircraft structures have been avoided.

After thorough consideration, this practice was also applied to the Viggen aircraft. Later, however, conditions changed: An extended service life was desired, and the static full-scale test showed a somewhat more severe stress distribution than had been predicted — in the spar boom flanges of the main wing, for example. These new conditions necessitated some sort of fatigue testing in a late development stage. In considering time, cost, the desire for easy repeatable testing, and the possibility of introducing modifications, something intermediate to conventional full-scale testing and simple (small-specimen) testing was chosen.

Before proceeding with the description of current test specimens and testing, attention should be focused on the fact that several basic fatigue studies have been done at Saab for use in the design of aircraft structures. A study of fatigue strength of aluminum lugs (ref. 1), which was presented at the 4th ICAF Symposium in Munich in 1965, can be mentioned. Block-program fatigue of riveted joints and lugs has been studied in cooperation with The Aeronautical Research Institute of Sweden (FFA). These test results, correlated with experience from the literature, have been the basis for selecting values of  $\Sigma(n/N)$  for different conditions in designing. The stress engineer looks forward to data based on randomized load testing.

#### SYMBOLS AND UNITS

d	diameter, mm
f	life-reduction scatter factor
$K_{IC}$	plane-strain fracture toughness, $N/mm^{3/2}$
$K_t$	stress concentration factor
$l$	length of crack, mm
$l^*$	"total" length of crack (see fig. 20 for defining sketches), mm
N	number of cycles to failure at constant stress level
n	number of cycles applied at constant stress level

$P$	load, kN
$r$	notch radius, mm
$T$	time, h; equivalent flying time, h
$T_s$	service life, h
$t$	thickness of material, mm
$v$	crack propagation rate, $dl^*/dT$ , mm/h
$\delta$	depth of crack, mm
$\delta_5$	elongation, percent
$\rho$	root radius of milling step mark, mm
$\sigma$	normal stress, MN/m <sup>2</sup>
$\sigma_{\max}$	maximum value of stress, MN/m <sup>2</sup>
$\sigma_{\min}$	minimum value of stress, MN/m <sup>2</sup>
$\sigma_u$	material ultimate tensile strength, MN/m <sup>2</sup>
$\sigma_{0.2}$	0.2-percent-offset yield strength, MN/m <sup>2</sup>

Subscripts:

$y$	spanwise direction
$z$	vertical direction



Conversion factors for the units used in this report are given in the following table:

Physical quantity	SI unit (*)	Conversion factor (**)	Customary unit
Length	meter (m)	39.4	in.
Force	newton (N)	{ 0.225 0.102	lbf kp
Stress	MN/m <sup>2</sup>	{ 0.145 0.102	ksi kp/mm <sup>2</sup>

\*Prefixes to indicate multiples of units are as follows:

Prefix	Multiple
mega (M)	10 <sup>6</sup>
kilo (k)	10 <sup>3</sup>
milli (m)	10 <sup>-3</sup>

\*\* Multiply value given in SI units by conversion factor to obtain equivalent value in customary units.

## AIRCRAFT PARTS AND TEST SPECIMENS

In its present design the Saab Viggen is primarily an all-weather attack aircraft. Its configuration is unconventional, with one pair of front wings and one pair of main wings.

Figure 1 shows the location of the parts that have been the object of the investigation reported: the wing beam and the fuselage frame in the main-wing region. A rear view of the wing beam and fuselage frame assembly is shown in figure 2.

A part of the lower side of the main wing at the joint of the main spar with the fuselage frame was investigated. This wing beam area, indicated in figure 2, was simulated by test specimens A<sub>1</sub>, A<sub>2</sub>, and A<sub>3</sub>. Section I-I shows the aircraft design in this part, a honeycomb panel joined to the boom flange by steel bolts in two rows.

Left and right portions of the fuselage frame intended to carry over the bending moment of the main wing were also tested. These "frame halves" are denoted test specimens B<sub>1</sub> and B<sub>2</sub> in figure 2. Specimens B<sub>3</sub> and B<sub>4</sub>, used in a complementary test going on when this paper was prepared, are discussed in the appendix. Section II-II in figure 2 shows the wing joint with the attachment of the two-pronged beam lugs to the forward and rear frame forging and to the intermediate part, e. The purpose of the latter component is to get some load diffusion in a compact design. Part e is not included in the test speci-

men but its attachment forces are taken into account. The upper area of the frame, made up of separate forgings, was not represented in the test.

Figure 3 shows a test specimen of type A, consisting of a spar boom of forged AZ 74 (designation according to Otto Fuchs, Metallwerke, Germany, and equal to 7075 aluminum alloy modified with 0.3 percent Ag) and a portion of a honeycomb sandwich panel attached to the boom flange with steel bolts in one row. The cross section was reduced to half scale. However, the flange thickness, the panel height, and the bolt size were full scale. The first few bolt holes in the boom flange were thought to be the most critical points, but the tests showed the flange notch to be of equal importance.

The bolted joint was provided with a sealing compound in the attachment of the panel to the boom flange. The bolts (noninterference) were treated with dry  $\text{MoS}_2$ . From the beginning the boom was anodized in a chromic acid process over its entire length, but later on, highly stressed areas were modified. They were polished and chromated (in the aircraft they are also protected by a primer). The primary boom lug for axial loading of the test specimen and the transverse lugs for stabilizing it were not representative of the aircraft structure. The limit load was 711 kN and the outer force system was nonredundant.

Geometric differences between specimens  $A_1$ ,  $A_2$ , and  $A_3$  will be referred to in the reporting of fatigue test results. The test specimen booms were taken from three separate beam forgings in almost correct positions. Their strength properties are shown in the following table ( $y$  and  $z$  denote spanwise and vertical directions, respectively):

Specimen	$(\sigma_{0.2})_y$ , MN/m <sup>2</sup>	$(\sigma_u)_y$ , MN/m <sup>2</sup>	$(\sigma_{0.2})_z$ , MN/m <sup>2</sup>	$(\sigma_u)_z$ , MN/m <sup>2</sup>
$A_1$	496	551	427	491
$A_2$			432	507
$A_3$			427	497

The test specimens of type B are shown in figure 4. Each specimen consists of a forward and a rear forging of 7079 aluminum alloy, overaged, connected by an outer and an inner skin (Alclad 7075) creating a box beam. These test specimens were made up in full scale of essentially ordinary aircraft components.

The continuity of the outer skin is broken by a long opening in the joint area for the insert of the wing beam lugs. This is shown in section I-I and view II-II of figure 4. The inner skin has openings in the same area for the purpose of load transmission by the linkage system used in testing.



The skin was attached to the forgings mainly by countersunk aluminum screws developed for blind attachment of thick skins to extrusions and forgings. The threaded screw holes in the forgings were supposed to be critical points of the fatigue specimen. The countersunk holes in the inside Alclad sheet seemed also to be critical. Test specimens B<sub>1</sub> and B<sub>2</sub> did not include the intermediate forging (e in fig. 2). However, at the attachments a and d the test frames were clamped together with ordinary bolts and special distance elements. The frame forgings were anodized in a chromic acid process. The shear bolts in the principal lug joints (b and c) were mounted with sliced taper sleeves in bushings, which were prepared with bonded dry MoS<sub>2</sub>.

For the right "frame half" in figure 4, forces are indicated by arrows in proper scale. The applied jack force had a limit load value of 313 kN. The force system was chosen so that joint loads correct in value and direction would be simulated at b and c, and so that the bending moment would be representative in highly stressed parts of the frame assembly.

The basic material properties of the forgings of B<sub>1</sub> and B<sub>2</sub> have not yet been determined. General material properties for 7079, overaged, can be found in the section entitled "Materials and Small-Specimen Testing."

#### LOAD SPECTRUM AND TEST PERFORMANCE

The load spectrum used in testing is shown in figure 5. This total spectrum, which was used for both type A and type B specimens, includes maneuver and gust loads, touch-down loads, and loads due to ground roughness. Different kinds of loads were originally presented in separate load spectra, which made up the basis for computer randomization of loads in groups according to the flight-by-flight principle. Both the severeness level of the flights and the sequence of the individual loads of the same kind were randomized.

An example of load sequences in the randomized flight-by-flight program is shown in figure 6. A load history of 200 hours of flight with 15 000 load cycles was punched on a tape for the purpose of unlimited repetitions. The highest positive load level was 90 percent of limit load and the largest negative load was -27 percent. A total of 20 load levels were used.

A diagram of the test equipment is shown in figure 7. This system was based on a modified unit for numerically controlled milling machines, a hydraulic pump with variable flow governed by the stroke, hydraulic jacks with low-friction seals of Teflon, and pressure transmitters for controlling the oil pressure in the jacks. The mean value of the frequency was 0.5 cps.

The arrangement of test specimens is shown in figure 8. The two test groups A and B were loaded by separate jacks that were only hydraulically connected. They could

work either simultaneously or separately. The somewhat odd link and lever system at the left portion of the frames in figure 8 was made up in order to get a proper redistribution of the principal outer reaction force in this part.

The test specimens were provided with strain gages for calibration and monitoring of loads. Each test started with loading to 90 percent of limit load. This load level will also be applied once during the delivery control flight of every aircraft.

Crack searches with a fluorescent penetrant (Ardrox P1) and crack-length studies were performed especially on the A specimens while loaded to 40 percent of limit load. A search for new cracks was made every 600 h. Visual observations of crack length were made more frequently but irregularly.

### TEST RESULTS FROM SPECIMEN A (WING BEAM)

Table I presents a summary of test results from specimens A. The strain gages (01, 02, and 03) were applied to specimens A<sub>1</sub>, A<sub>2</sub>, and A<sub>3</sub> in the same areas. They are, however, shown only on A<sub>2</sub> in figure 10. From the location of the strain gages and the values in table I(a) the nominal stress at the flange notch and bolt hole 1 is estimated to have been 280 to 300 MN/m<sup>2</sup> at limit load, depending somewhat on definition.

Table I(b) shows equivalent flying hours (hours read on the punched tape) for observations of the state of cracks. Cracks 11 and 12 occurred in specimen A<sub>1</sub>, cracks 21, 22, and 23 in A<sub>2</sub>, and cracks 31 and 32 in A<sub>3</sub>.

It can be seen in table I(b) that cracks appeared in specimen A<sub>1</sub> after only 3400 h. These cracks, no. 11, are shown in figure 9. One crack started where a radius  $r = 3$  mm interacted with the principal notch radius  $r = 10$  mm. Another crack started from the opposite side in a rough edge of the notch. Many very small cracks were also found in the anodized surface of the flange notch area.

The specimen in this original shape was not quite representative of the aircraft structure, and it became less representative because the specimen was modified to remove the cracked material. However, the test was continued in order to study the area with bolt holes in the boom flange — that area which originally had been thought to be the most critical. For this case the cracked material was milled off, and the shape was modified to that marked with the dashed lines. Besides cracks in areas not considered significant, no new damage was found until crack 12 appeared in bolt hole 1 at about 21 000 h. The test was finished at 24 100 equivalent flight hours without a limiting failure.

Test specimens A<sub>2</sub> and A<sub>3</sub> were like the modified form of A<sub>1</sub>. They were polished and chromated in highly stressed boom portions.



Figure 10 shows specimen A<sub>2</sub> in a late stage with the cracks fully developed. Crack 21 was found after 8400 h, when it had a length of  $l = 1$  mm. Its slow propagation was studied and it was under control until the test was ended as a result of bolt failure in hole 1 at 15 200 h. The crack propagation history can be followed in figure 20 (which includes sketches defining  $l$  and  $\delta$ ). Figure 11 shows details of the cracked specimen A<sub>2</sub>.

Figure 12 shows fully developed cracks in specimen A<sub>3</sub>. The nature of crack 31 was about the same as that of crack 21 in figure 10. Crack 31 was found at 7700 h, when it had a length of  $l \approx 5$  mm. It propagated somewhat more rapidly than crack 21.

The most interesting crack in specimen A<sub>3</sub> was the crack designated 32. This crack was seen for the first time at 10 500 h (not seen at crack search 600 h earlier). When discovered it had a visible length of about 10 mm (about 12 mm was hidden under the panel). From this stage it propagated rapidly (a rate of about 0.02 mm/h) and then more slowly. The same tendency toward crack development from bolt hole 1 can be seen in figure 10. The new results, however, are the rapid propagation of crack 32 and the complicated interaction with crack 31.

Figure 13 shows the features of the locally developed fatigue fracture surfaces of the cracked area in specimen A<sub>3</sub>. The slightly concave boom-side surface of crack 32 is thought to be the result of "Stage I" crack growth according to reference 2. The 45° direction is pronounced, and no unusual material properties or defects have been found. The surfaces were rubbed and could not give adequate information. At the stage of figure 13, crack 32 shows a tendency to change over to a 90° fatigue fracture. Figure 13 also shows that crack 32 must have been present when crack 31 passed through its area. The less interesting surfaces are not numbered.

The fatigue test of A<sub>3</sub> was finished at 11 700 h by a boom fracture due to fatigue cracking from the root of a transverse lug, not significant for the aircraft structure. No damage to the panel could be found in the three specimens tested.

#### TEST RESULTS FROM SPECIMEN B (FUSELAGE FRAME)

Table II presents a summary of test results from specimens B. Strain gages F-01 and F-02 were located on the forward frame and strain gages R-01 to R-04 were located on the rear frame. (See fig. 17 and table II(a).) Table II(a) shows frame stresses of approximately 260 to 320 MN/m<sup>2</sup> at limit load.

Table II(b) shows equivalent flying hours for occurrence of cracks and ultimate failure. The letters S, F, and R in the crack designations refer to sheet, forward forging, and rear forging, respectively. Cracks 11 to 14 occurred in specimen B<sub>1</sub>, and cracks 21 to 23 occurred in specimen B<sub>2</sub>.

From table II(b) it can be seen that cracks appeared at screw holes in the inner sheet of the frame assembly after 4300 equivalent flying hours. Their propagation was observed, and in some cases they were stopped by the use of a blind rivet with  $d = 4.8$  mm or plug with  $d = 5$  mm (sheet thickness  $t = 3$  mm).

Ultimate failure of specimen B<sub>1</sub> occurred at 5300 h by fracture from an unexpected fatigue crack in web (1) of the rear forging, shown in figure 14. No crack search with fluorescent penetrant had been done in this area before failure. Afterward, however, four other cracks of about the same kind were indicated in three forgings of specimens B<sub>1</sub> and B<sub>2</sub>. The B<sub>2</sub> test was also ended. An inspection made clear that the surface finish of the web areas of the milled frame forgings was worse than specified.

Figure 14 shows test specimen B<sub>1</sub> with fatigue cracks and the location of failure indicated. Figure 15 shows the fractured area of specimen B<sub>1</sub> with a sketch of the fatigue fracture surface, which represented  $\approx 390$  mm<sup>2</sup>, or  $\approx 10$  percent of the whole area of the section. Figure 16 shows the surface shape of the fatigue crack that caused failure in B<sub>1</sub>. It is representative of a number of web areas in both B<sub>1</sub> and B<sub>2</sub>. The root radius  $\rho$  of the milling step marks was about 0.5 mm.

Figure 17 shows specimen B<sub>2</sub> with the location of cracks and strain gages indicated. Figure 18 shows the area with cracks in the inner sheet of the frame assembly. This area is not very representative of the aircraft because of the large unreinforced openings.

When the fatigue test was finished, specimen B<sub>2</sub> was provided with complementary strain gages for comparison with a simultaneous study of stress levels in a loaded complete fuselage. It was found that the fatigue test specimens had been loaded to stress levels about 20 percent too high in critical areas. The reasons were, in the first place, unavoidable differences between specimen and fuselage due to "skin load diffusion conditions," and in the second place, some lack of effectiveness of the frame forgings due to bad stabilization of the cross section in bending. A fourth to a half of the 20 percent difference was recovered in a modified set of specimens, B<sub>3</sub> and B<sub>4</sub>, with better stabilization provided by two ordinary bulkheads, reinforcement of the inner skin, and smaller openings for the linkage system. These specimens are discussed in the appendix.

## DISCUSSION

### Materials and Small-Specimen Testing

A decision was made to change from the earlier standard aluminum alloy (the over-aged 7079 with Saab-Scania designation 3624-5) to AZ 74 (Saab-Scania 3633-5) as material for some primary aircraft forgings. The reason was the better resistance to stress corrosion cracking of the latter alloy. This change was made gradually, and therefore both



alloys were used in this investigation. When forgings of AZ 74 were not available for test specimens, the 7079 (overaged) was used.

The composition of the alloys and the aging conditions prescribed by Saab-Scania standard specifications are as follows:

Alloy	Zn	Mg	Cu	Ag	Aging
AZ 74	6.0	2.5	0.9	0.3	120° C for 12 to 24 h and 170° C for 4 to 7 h
7079 (overaged)	4.3	3.3	0.6		160° C for 8 h

Some material properties from Saab-Scania specifications and mean values from tests of specimens from wing beam forgings are shown in the following table (values refer to large-size forgings):

Alloy	Longitudinal direction				Transverse direction				Source of values
	$\sigma_{0.2}$ , MN/m <sup>2</sup>	$\sigma_u$ , MN/m <sup>2</sup>	$\delta_5$ , %	$K_{IC}$ , N/mm <sup>3/2</sup>	$\sigma_{0.2}$ , MN/m <sup>2</sup>	$\sigma_u$ , MN/m <sup>2</sup>	$\delta_5$ , %	$K_{IC}$ , N/mm <sup>3/2</sup>	
AZ 74	390	470	7		380	450	4		Preliminary specification
	440	510	12	1090	410	490	10	850	Test series (mean values)
7079 (overaged)	430	500	6		410	480	3		Specification, $t \leq 150$ mm
	440	510	11	1010	440	500	10	780	Test series (mean values)

From the fatigue data in figure 19, which are for constant-amplitude tests, it can be seen that AZ 74 has about 10 percent higher fatigue strength than 7079 (overaged). These tests were carried out with small round specimens with diameter  $d = 8.5$  mm and notch radius  $r = 0.65$  mm.

Fatigue tests were also carried out with small specimens of various shapes in order to study other problems in connection with the main investigation. The aluminum blind-screw element used in specimens B (fuselage frame) was tested at constant amplitude in jointlike test pieces. Its fatigue behavior was good at stresses near limit stress but the behavior for long lives should be studied further (with regard to fretting, for example).

The "hard point effect" at bolt hole 1 in specimens A (wing beam) was simulated in a test series. A simple program of three-level tests was carried out on plain specimens "reinforced" by straps fastened to them with wing-panel attachment bolts. The intent was to find the effect of bolt fit in the boom flanges and ballizing of flange holes on the fatigue life. Ballizing was better than "easy" interference fit alone, which was better than the original small-clearance fit. However, differences were small and no change of design principle was made.

### Crack Propagation and Fractures

Propagation of the cracks in the AZ 74 boom flanges of specimens A<sub>2</sub> and A<sub>3</sub> (cracks 21 and 31) is shown in figure 20. Values of  $l^*$  (total visible crack length) were plotted against the number of equivalent flying hours  $T$ . The dashed lines make up a mean curve, visually estimated. This curve indicates that crack propagation, on the average, might be slow between  $T = 7000$  h and  $T = 11\ 000$  h. The mean crack propagation rate is  $v_1 = 0.0025$  mm/h in this time interval. (Environmental conditions, not considered in the tests, must also be accounted for when estimating the probable damage tolerance of the aircraft structure.)

The crack in specimen A<sub>3</sub> that caused the ultimate failure of the boom section at a nonrepresentative transverse lug had a fatigue-cracked area of  $\approx 650$  mm<sup>2</sup>, or  $\approx 25$  percent of the total boom cross section. The residual strength of this section, when it failed ultimately at 83.5 percent of limit load, and that of the cracked area in specimen B<sub>1</sub>, when it fractured at 90.1 percent of limit load, have been controlled with respect to fracture toughness behavior. Current combinations of stress levels, geometry, and  $K_{IC}$  values (from the table of material properties presented previously) could in both cases explain actual failures.

### Surface Conditions and Damage

Some problems with surface roughness and anodizing as detrimental factors in fatigue of wing beam specimen A<sub>1</sub> were reported. Fretting was found in the boom flange of specimens A in bolt holes and on the surface that makes contact with the panel. Mainly, however, the fatigue quality of the bolt-hole area of the flange was as good as wanted. The dry film lubricant and the sealing compound have certainly been positive factors.

The main surface problem with the frame specimens B<sub>1</sub> and B<sub>2</sub> was the milling step marks shown in figure 16. In highly stressed areas, these milling marks and other surface imperfections on parts of the aircraft were eliminated by surface-improving procedures followed by adequate corrosion protection.



The test of specimen A<sub>1</sub> and other recent tests indicated that serious fatigue problems are sometimes associated with anodizing on aluminum parts. Thorough studies of these problems are being made.

### Calculation Study

A recently developed computer method for fatigue calculations based on the linear cumulative damage theory was tested on specimens A and B and their fatigue-test results. The diagram in figure 21 shows calculated S-N curves for various  $K_t$  values based on the constant-amplitude fatigue data from figure 19, slightly reduced. The curves in figure 21 are for the specimen A material, AZ 74, the test load spectrum, and  $\Sigma(n/N) = 1$ . The nominal stress at limit load is plotted against calculated equivalent flying hours. The fatigue test result,  $\sigma = 290 \text{ MN/m}^2$  and  $T = 9000 \text{ h}$ , is plotted and found to correspond to  $K_t = 2.7$ . (The chosen time, 9000 h, corresponds to a 5-mm fatigue crack in the flange notch, according to the mean curve in figure 20. This time, however, is also supposed to be representative for the bolt-hole cracks.)

The value  $K_t = 2.7$  is larger than expected for the flange notch, but less than expected for the first and second bolt holes. This calculated result and the corresponding result for specimen B (overaged 7079 and rougher surface in the web case) are shown in the following table:

Specimen	Stress at limit load, $\sigma$ , $\text{MN/m}^2$	T, hr	$K_t$	Location of crack
A	290	9000	2.7	Flange notch and bolt holes
B	280	$\approx 5000$	2.4	Web (1)
	310	$> 5000$	$< 2.4$	Forging inner boom

It should be noted that in the case of residual tensile stresses from heat treatment and material removal by machining, the calculation result  $K_t = 2.4$  for the frame forging web will be changed. The fatigue failure corresponds to  $K_t = 2.0$  if a residual tensile stress of  $50 \text{ MN/mm}^2$  is assumed. Thus, residual tensile stresses in forgings may play a role not only in stress corrosion damage but also in fatigue life.

### Stress Concentrations

Problems caused by interacting stress concentrations frequently occur in connection with forging design. Interacting notch radii in critical areas have been observed in both specimens A and B.

In order to get a better collection of data as a basis for design and for making up some estimation rules, fatigue testing has been performed and is planned to progress with specimens of various shapes. Figure 22 shows two typical configurations, representing the problem of a hole in a radius (bolt hole in a part with variable cross section) and the problem of simultaneous area variation in perpendicular planes.

#### Reduction Factor on Life

When testing a small number of safe-life aircraft components with proper load history, a life-reduction scatter factor of  $f = 4$  is often applied to the mean test life. If specimen A, the wing-beam part of this investigation, is studied in this way, an overall service life under current test conditions can be determined. Specimen A<sub>1</sub>, which was not representative in the flange notch area, is neglected in spite of its information about fatigue life of the bolt-hole flange area. The mean value obtained from specimens A<sub>2</sub> and A<sub>3</sub> is

$$T = \frac{1}{2}(15\,200 + 11\,700) = 13\,450 \text{ h}$$

(In fact, the life of A<sub>3</sub> is based on a secondary-type failure.) Reduction with a factor  $f = 4$  gives an overall service life of

$$T_S = \frac{1}{4}(13\,450) = 3360 \text{ h}$$

The crack propagation rate is larger outdoors than indoors, as was observed by Schijve and De Rijk in tests on sheet specimens of 7075-T6 (ref. 3). This fact could be accounted for by using a higher reduction factor on the average time during which visible cracks exist; for example,  $f = 6$  on the time after  $T = 7000 \text{ h}$  (fig. 20):

$$T_S = \frac{1}{4}(7000) + \frac{1}{6}(13\,450 - 7000)$$

$$T_S = 1750 + 1075 = 2825 \text{ h}$$

Application of test results for wing-beam specimens of type A to the real wing-beam structure of aircraft must take into consideration differences in geometry, size, and so forth. The real aircraft structure has greater three-dimensional complexity than the specimens. Therefore stress levels can differ and new points may be critical. In proper design, however, constraints reduce secondary deformations, make section areas more effective, and usually lower the stresses.



The half-scale cross section tested had full-scale flange thickness, panel height, and bolt diameter. However, the two rows of bolts actually used for panel attachment were simulated with one row only, which must be conservative according to flange bending behavior. The testing of specimens B<sub>1</sub> and B<sub>2</sub> happened to be more conservative than was originally intended (higher stresses). Consequently the fatigue life became short and further study of it by use of such things as reduction factors is without meaning.

## CONCLUSIONS

The test method has turned out rather well and can be looked upon as an inexpensive and flexible alternative to conventional full-scale fatigue testing, for the purpose of structural development. However, specimens must be very carefully designed in order to represent actual load distribution on aircraft parts.

The fluorescent penetrant effectively indicated cracks at 40 percent of limit load, the inspection load used in this test.

The test results for type A (wing beam) specimens indicate an overall service life of 3360 hours if a scatter factor of 4 is applied on the mean total test life of two specimens. Many other factors, such as geometry, scale factor, and environment, could be taken into consideration.

The specimens of type B (fuselage frame) sustained a shorter total test life than the wing beam specimens. However, comparison with strain measurements on a complete fuselage showed the stress levels of the frame specimens to be too high. Further, the surface finish of the milled frame forgings happened to be worse than what is normally permitted. A new test with slightly modified specimens and load levels is going on with another two frame halves.

Attention has been focused on the problems of anodizing, surface roughness, interacting stress concentrations, and fretting.

As a result of the tests, steps were taken to reduce the risk of fatigue damage in aircraft. Thus, stress levels were lowered, radii were increased, and demands on surface finish were sharpened.

## APPENDIX

### WORK IN PROGRESS

A complementary fatigue test with "frame half" specimens B<sub>3</sub> and B<sub>4</sub>, indicated in figure 2, is in progress as this paper is being prepared. These specimens also have forgings of 7079 (overaged). They are, relative to B<sub>1</sub> and B<sub>2</sub>, constructed with better stabilization of the frame parts by two ordinary bulkheads, with reinforcement of the inner skin, and smaller openings for the linkage system. They are also polished in critical forging areas.

The test load spectrum has been slightly changed according to new conditions. Further, critical stresses are lowered 5 to 10 percent by a more favorable stress distribution in the modified specimen and 12 percent by a decrease of the jack load over the entire spectrum. Consequently, the total lowering is  $\approx 20$  percent. All these changes have been made in order to get a better load distribution with more correct stress levels for the proper simulation of aircraft structural fatigue conditions.



## ACKNOWLEDGMENTS

The author is indebted to Saab-Scania Aktiebolag for permission to prepare and publish this paper. Many persons involved in the reported investigations have kindly assisted with basic data for this paper. Invaluable assistance with the preparation of the manuscript has been given by Mr. E. Persson, senior stress engineer, fatigue branch, Saab-Scania.

## REFERENCES

1. Larsson, S. E.: The Development of a Calculation Method for the Fatigue Strength of Lugs and a Study of Test Results for Lugs of Aluminium. Fatigue Design Procedures, E. Gassner and W. Schütz, eds., Pergamon Press, Inc., c.1969, pp. 309-342.
2. Forsyth, P. J. E.: The Physical Basis of Metal Fatigue. Blackie & Son, Ltd. (London), 1969.
3. Schijve, J.; and De Rijk, P.: The Crack Propagation in Two Aluminium Alloys in an Indoor and an Outdoor Environment Under Random and Programmed Load Sequences. NLR-TR M.2156, Nat. Lucht- Ruimtevaartlab. (Amsterdam), Nov. 1965.

TABLE I.- SUMMARY OF TEST RESULTS FROM SPECIMENS A (THE WING BEAM)

## (a) Strain-gage results

Stress at limit load, $\sigma$ , MN/m <sup>2</sup> , for specimen -			Strain-gage no.	Strain-gage location (shown in fig. 10)
A <sub>1</sub>	A <sub>2</sub>	A <sub>3</sub>		
341	308	300	01	Beam at notch, 7 mm from edge, outer side
298	298	292	02	Beam at hole 1, 6 mm from step, mean value
269	286	271	03	Flange between holes 1 and 2, outer side

## (b) History of cracks

Figure no.	Crack no.	Equivalent flying hours for specimen -			Comments
		A <sub>1</sub>	A <sub>2</sub>	A <sub>3</sub>	
9	11	(3400)			Geometry and surface finish not representative. Cracks occurred at flange (principal notch radius $r = 10$ mm). Cracks were removed and shape of specimen was modified.
10 and 11	21		8 400 15 200		Modified shape and polishing. Small crack found, $l \approx 1$ mm. Crack increased to $l = t = 12$ mm, $\delta = 6.0$ to $11.5$ mm.
12 and 13	31			7 700 10 500 11 600	Modified shape and polishing. Small crack found, $l \approx 5$ mm. Several cracks joined in one, $l = t = 12$ mm, $\delta = 3$ to $4$ mm. Crack propagated to $\approx 45^\circ$ , $l = t$ , $\delta = 14$ to $16$ mm.
9	12	$\approx 21$ 000			Crack in flange in edge of bolt hole 1, $\delta = 2$ mm max., fretting.
10	22		15 200		Two cracks $\pm 45^\circ$ in flange at bolt hole 1, $l \approx 2$ mm $\approx 0.5t$ .
12 and 13	32			10 500 11 100	Crack out from flange at bolt hole 1, $\approx 10$ mm visible. Propagated $\approx 3.5$ mm, then nonpropagating.
10 and 11	23		15 200		Crack through $t$ in flange at bolt hole 2; crack through $\approx 0.5t$ in flange at bolt hole 9.
-----	---	24 100	15 200	11 700	Testing ended. No failure or secondary-type failure.



TABLE II. - SUMMARY OF TEST RESULTS FROM SPECIMEN B (THE FUSELAGE FRAME)

## (a) Strain-gage results

Stress at limit load, $\sigma$ , MN/m <sup>2</sup> , for specimen -		Strain-gage no.	Strain-gage location (shown in fig. 17)	
B <sub>1</sub>	B <sub>2</sub>			
---	*286	F-01	Sheet	} Section through upper wing-joint hole of forward frame
323	299	F-02	Boom	
---	*312	R-01	Sheet	} Section through upper wing-joint hole of rear frame
308	323	R-02	Boom	
---	277	R-03	Web (1)	} Principal stress on rear side $\approx 13$ mm from corner with radius of 15 mm
---	255	R-04	Web (2)	

\*Mean value over sheet thickness.

## (b) History of cracks

Figure no.	Crack no.	Equivalent flying hours for specimen -		Comments
		B <sub>1</sub>	B <sub>2</sub>	
18	S-11	4300 4800		Inner sheet of frame assembly; cracks from two screws, $l = 3$ to 5 mm visible. Cracks at three holes, $l = 4$ to 10 mm, stopped at two.
18	S-21		4300 4800	Inner sheet of frame assembly; cracks from one screw, $l = 1$ to 3 mm visible. Cracks from three screws, $l = 2$ to 5 mm visible.
14	F-12	5300		Forward forging, web (1); corner crack from milling step mark, $l \approx 30$ mm.
17	F-22		5300	Forward forging, web (1); corner crack from milling step mark, $l \approx 15$ mm.
17	F-23		5300	Forward forging, web (2); corner crack from milling step mark, $l \approx 10$ mm.
14 to 16	R-13	5300		Rear forging, web (1); failure due to crack, $l \approx 30$ mm, in corner.
14	R-14	5300		Rear forging, web (2); corner crack from milling step mark, $l = 19$ mm.

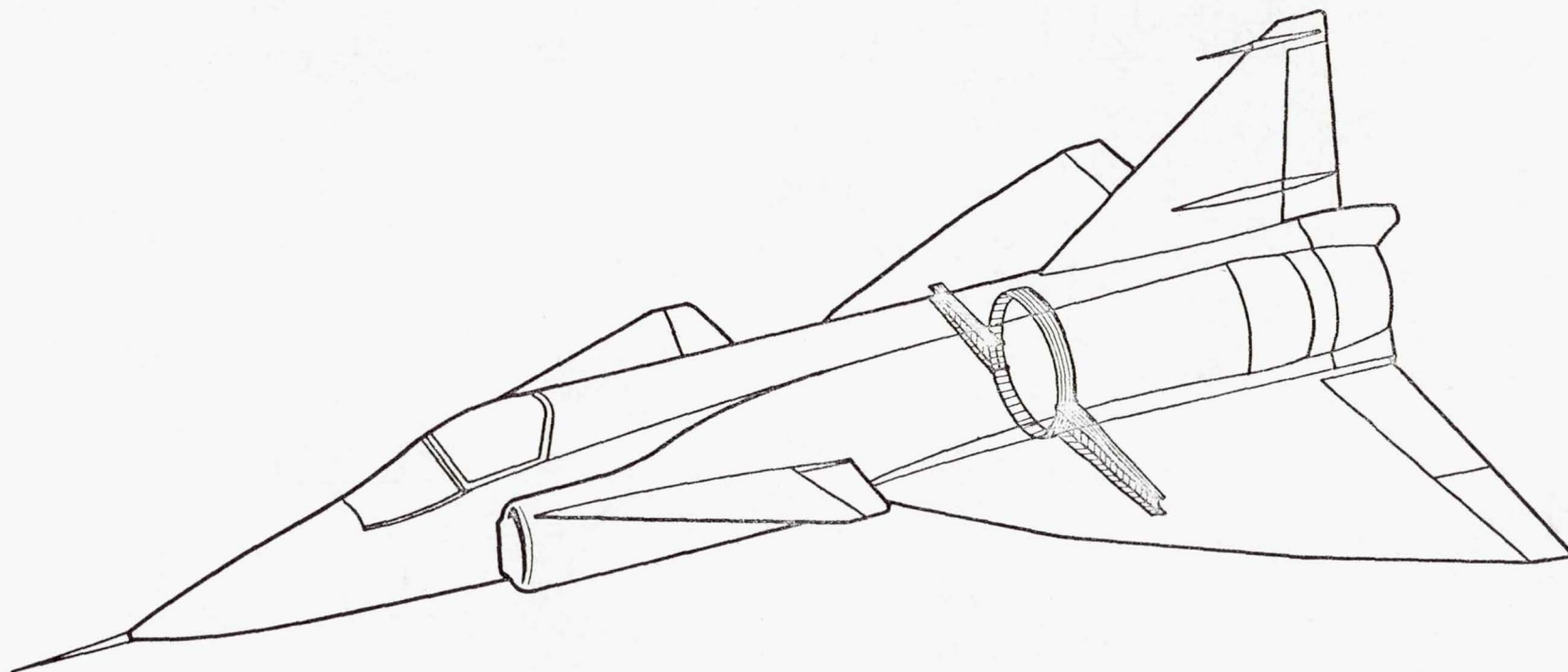


Figure 1.- Location of wing beam and fuselage frame in the Viggan aircraft.





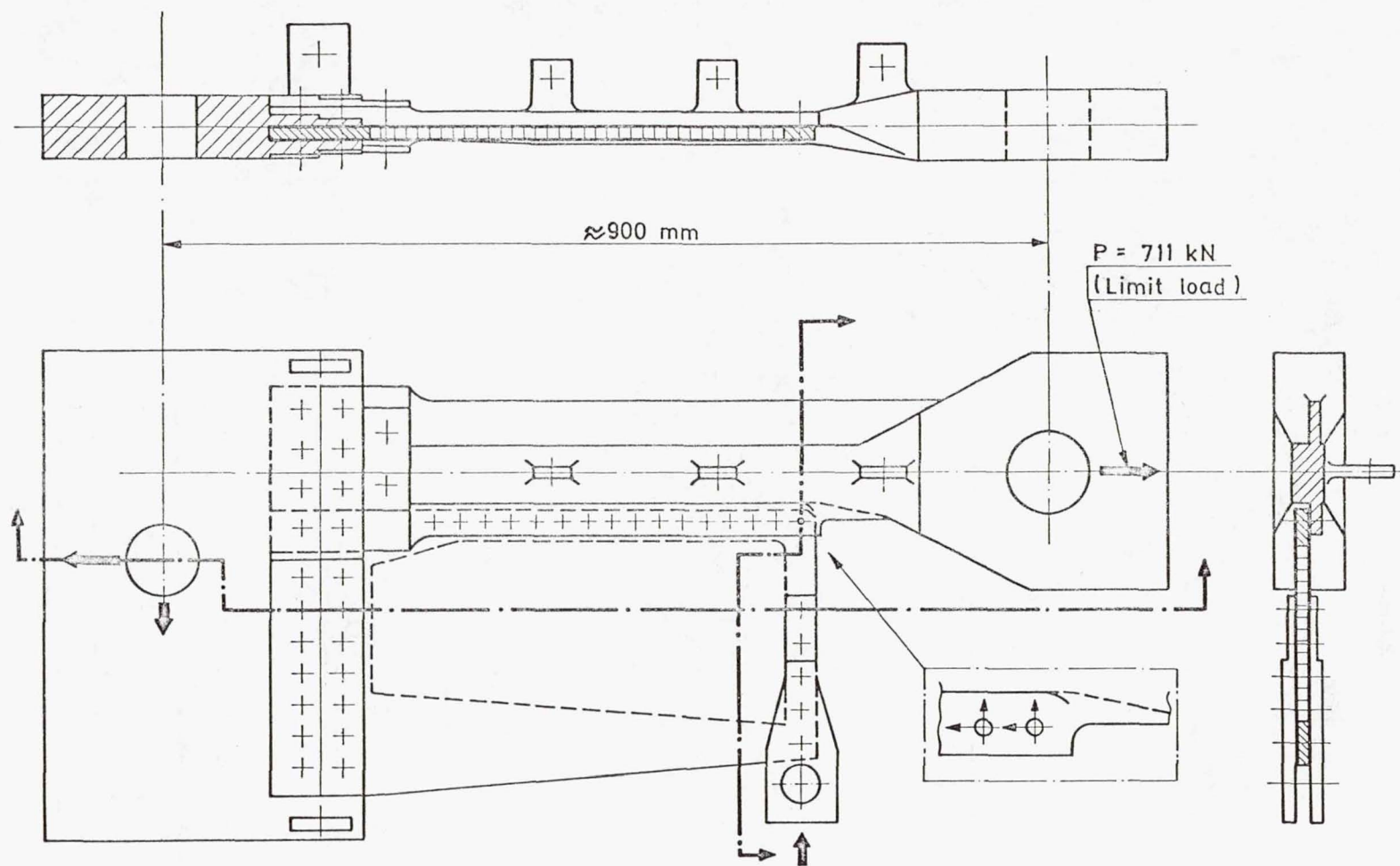


Figure 3.- Test specimen A with forces indicated by arrows.



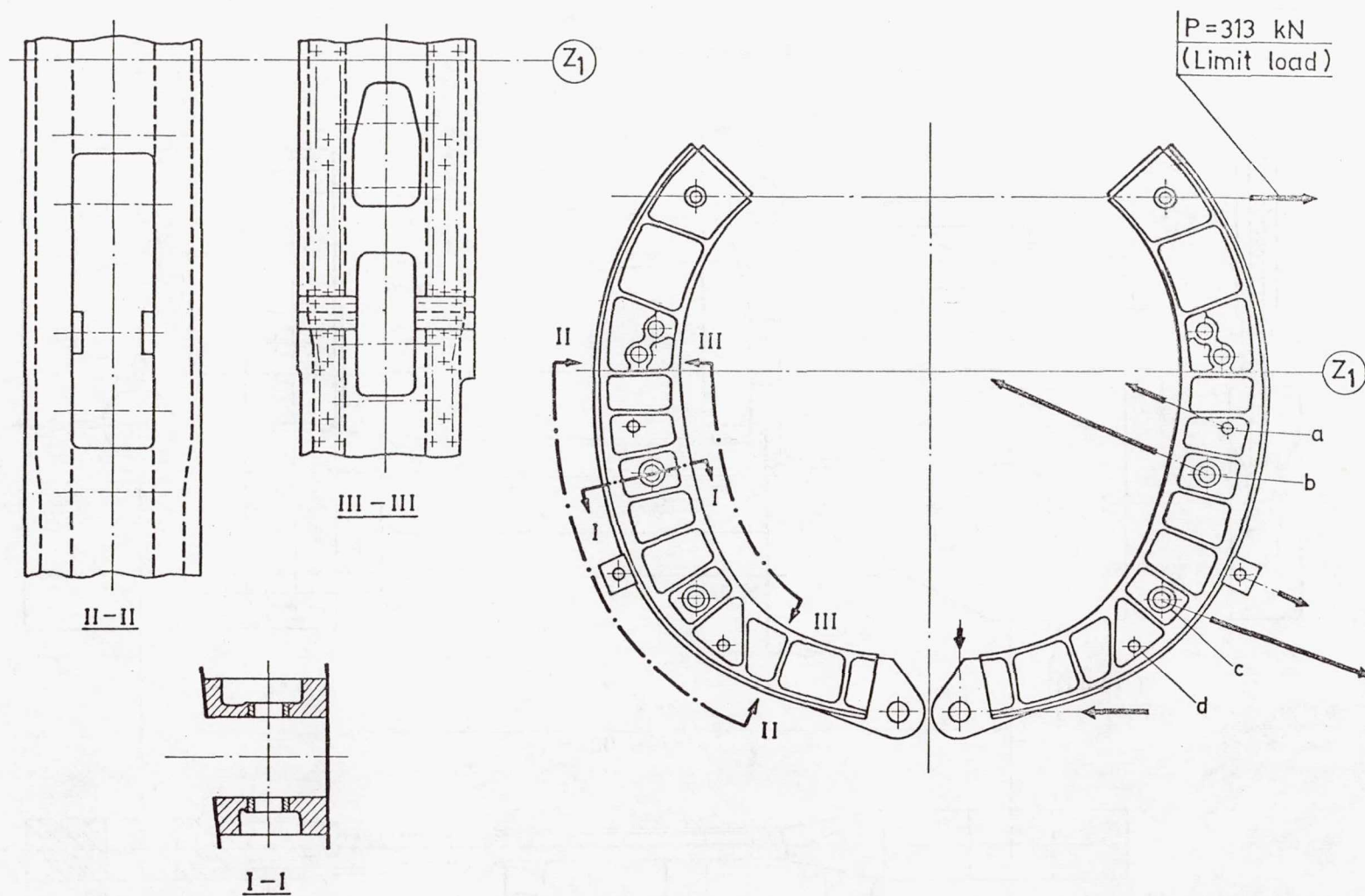


Figure 4.- Test specimen B with forces indicated by arrows.

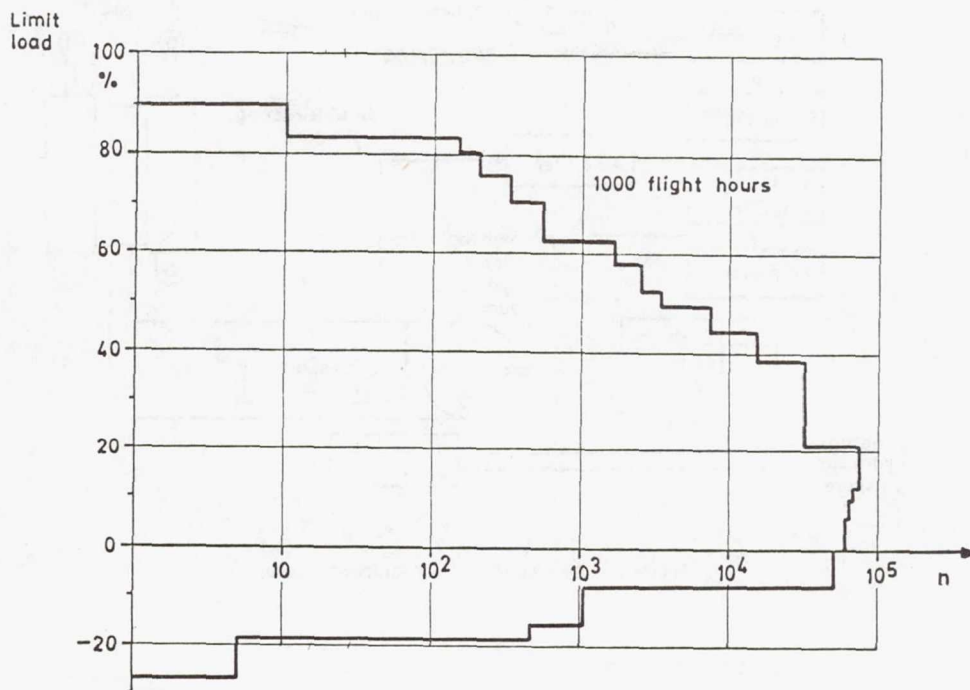


Figure 5.- The load spectrum used in testing.

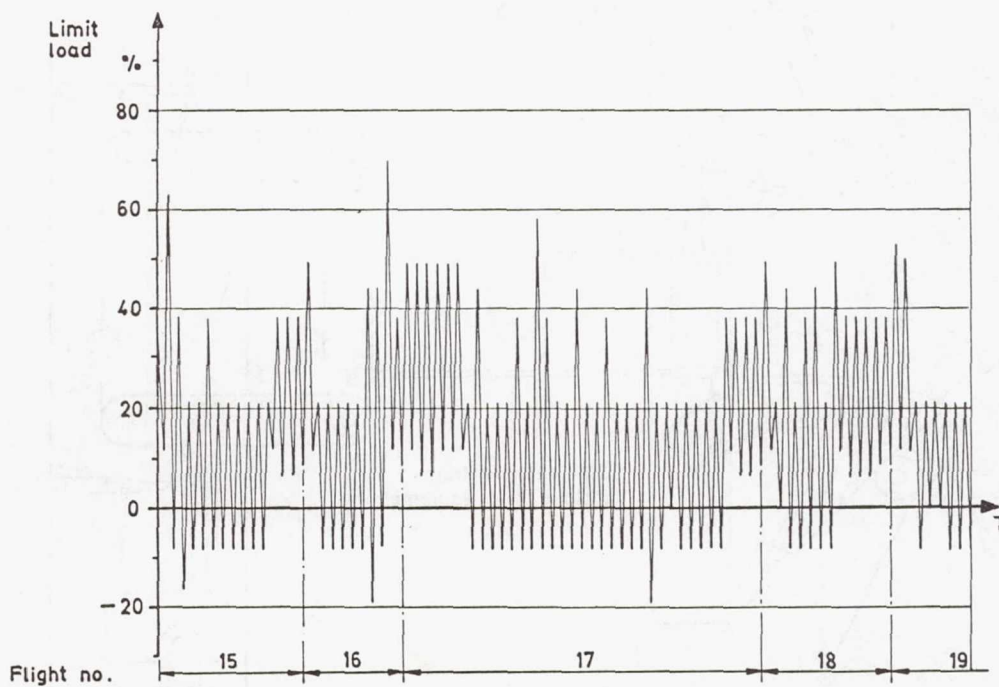


Figure 6.- Example of load sequences in the randomized flight-by-flight program.



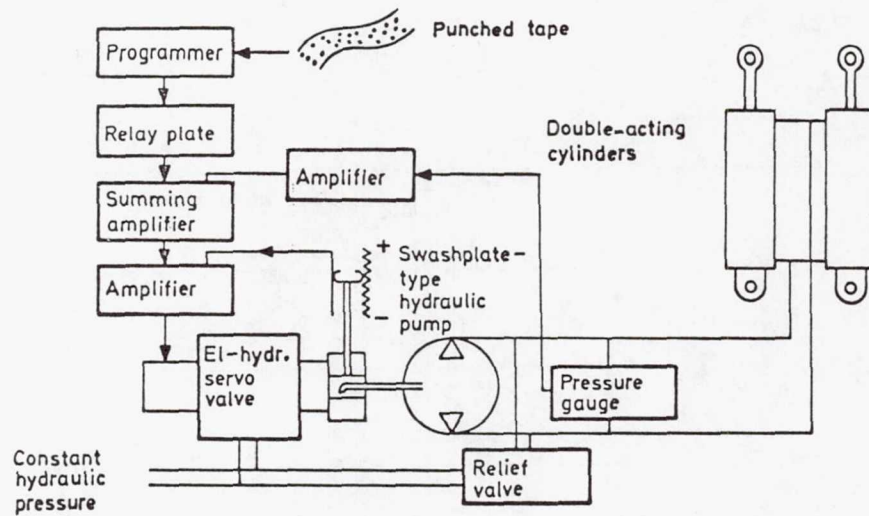


Figure 7.- Diagram of the test equipment system.

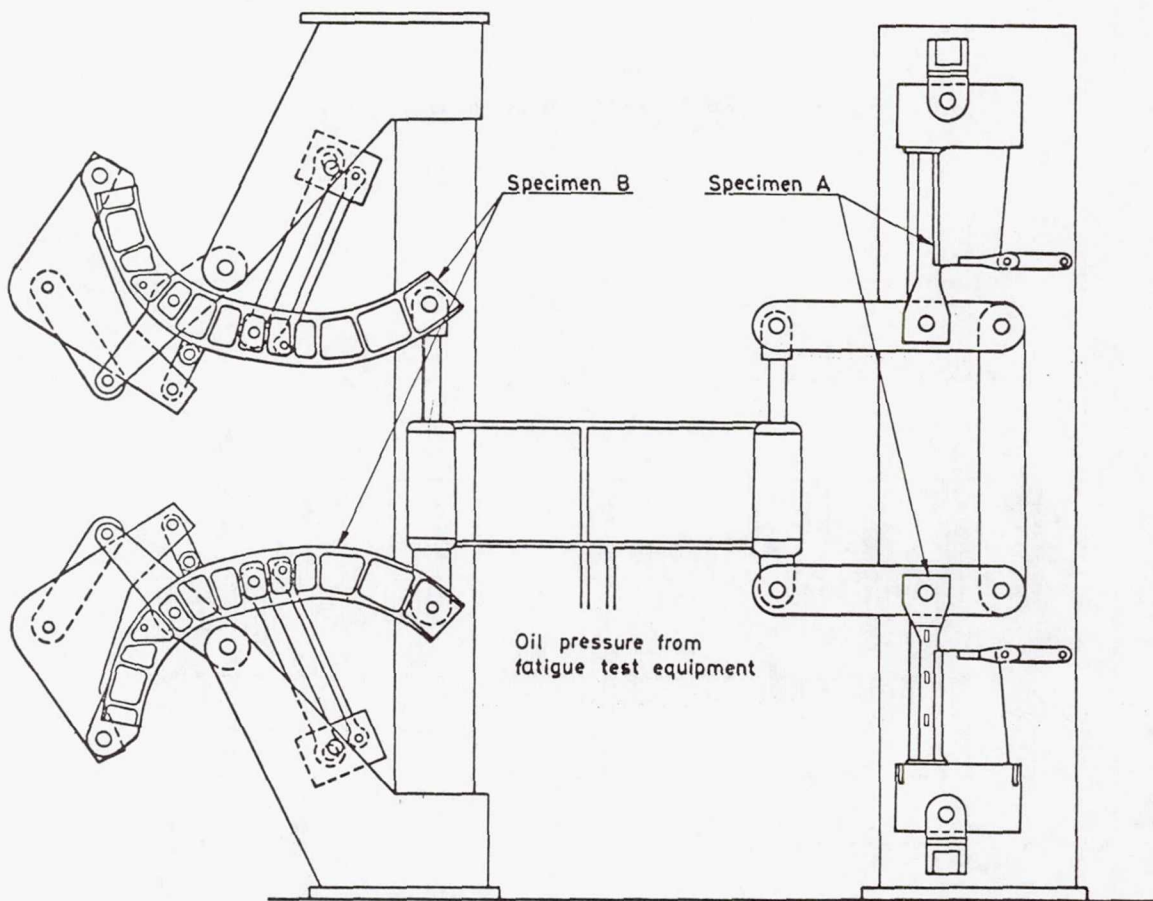


Figure 8.- Arrangement of test specimens.

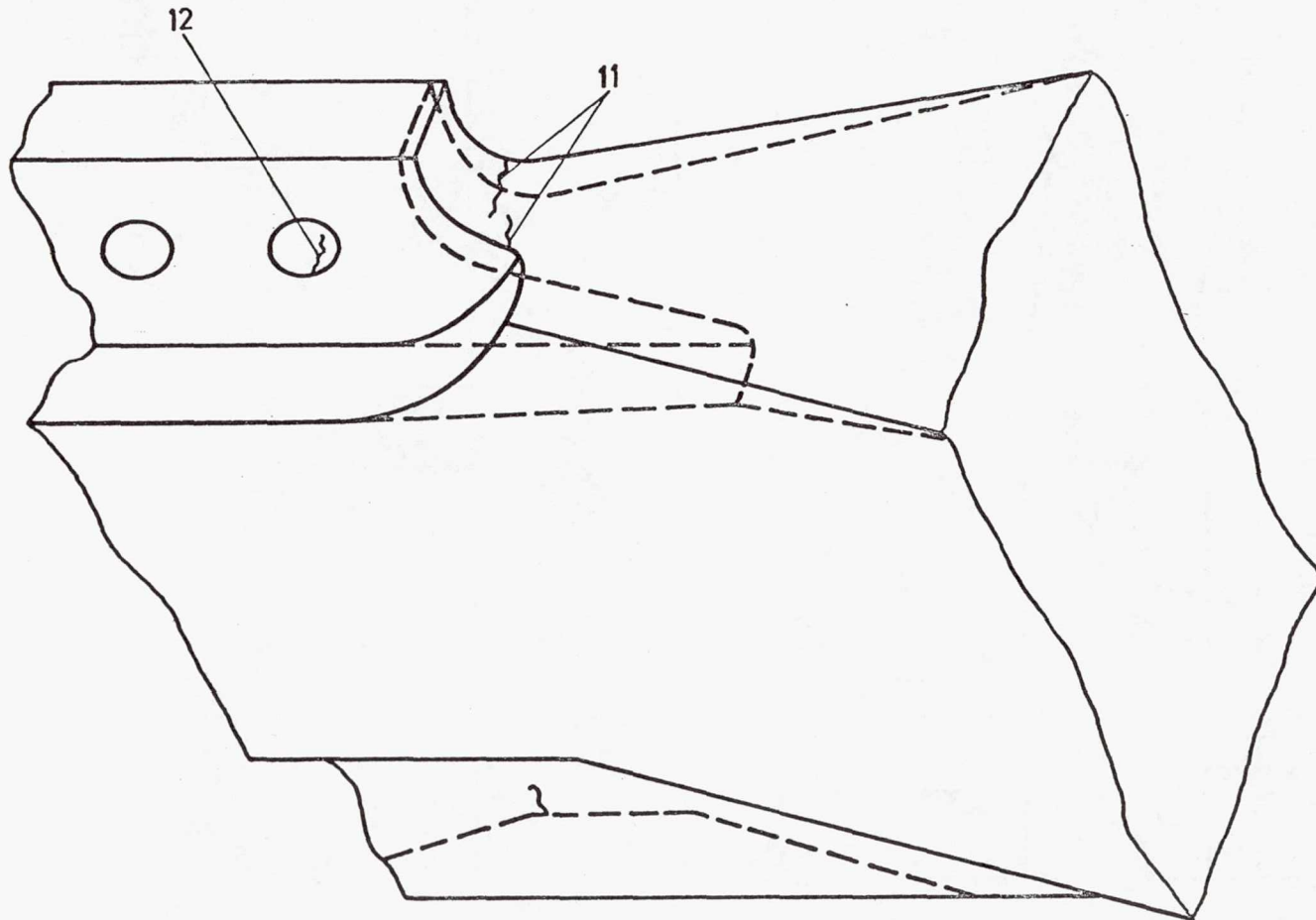


Figure 9.- Test specimen A<sub>1</sub> with cracks found. Solid lines indicate original specimen in which cracks 11 occurred. The cracked material was milled off and the shape of the specimen modified as shown by dashed lines before occurrence of crack 12.



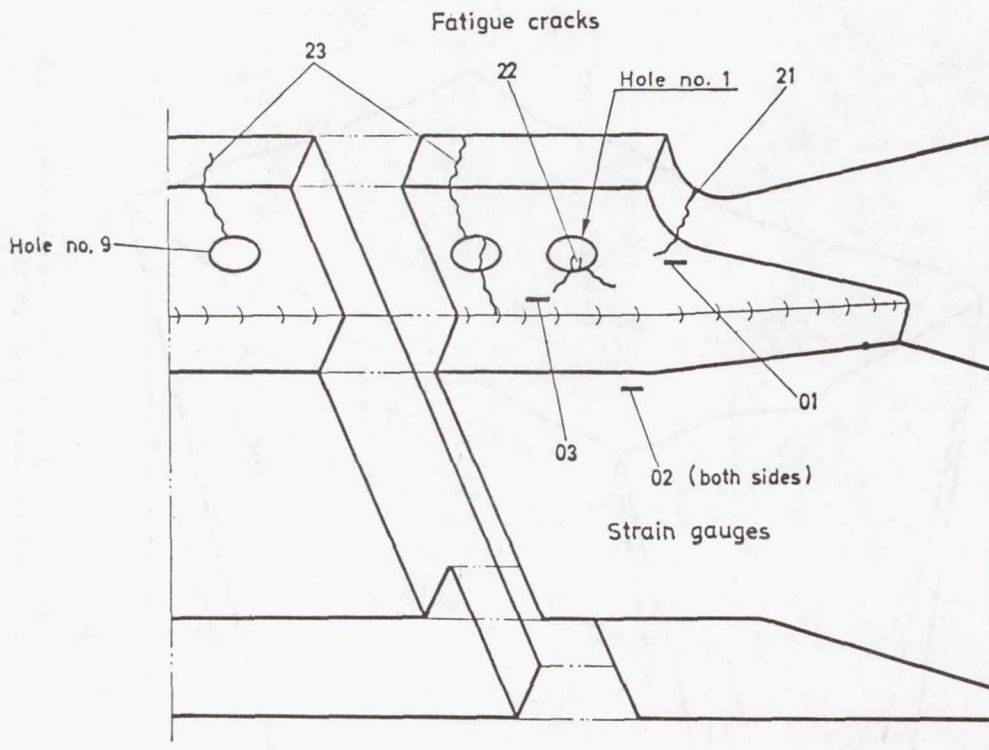


Figure 10.- Test specimen A<sub>2</sub> with cracks found.

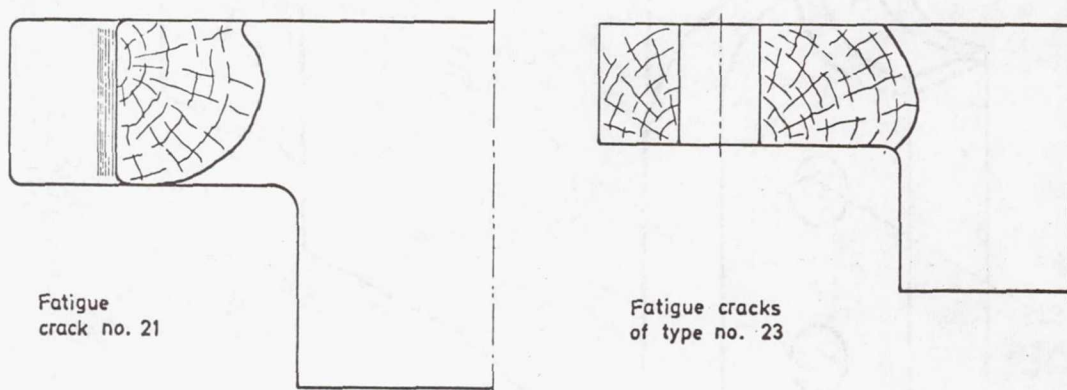


Figure 11.- Details of the cracked specimen A<sub>2</sub>.

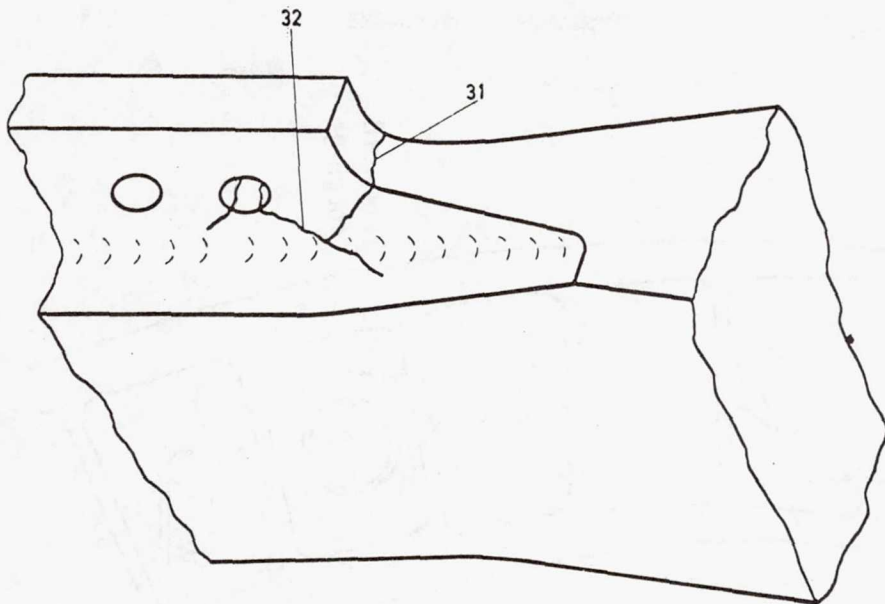


Figure 12.- Test specimen A<sub>3</sub> with cracks found.

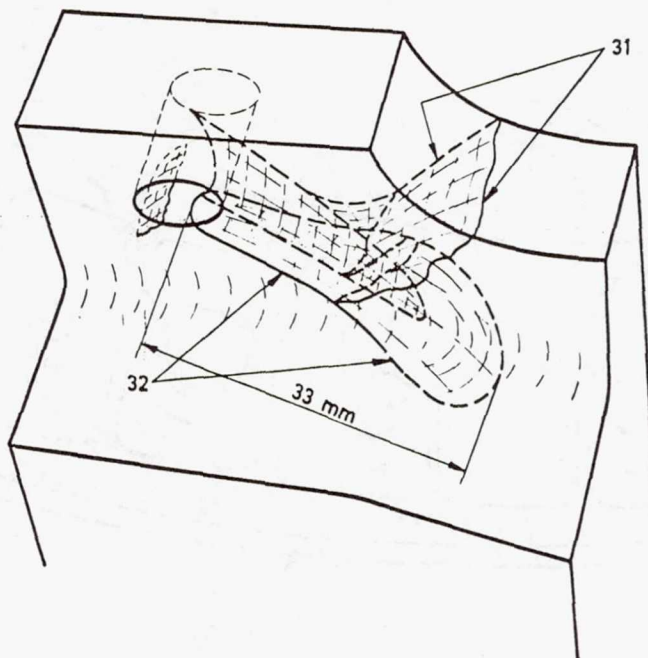


Figure 13.- Details of the cracked specimen A<sub>3</sub>.



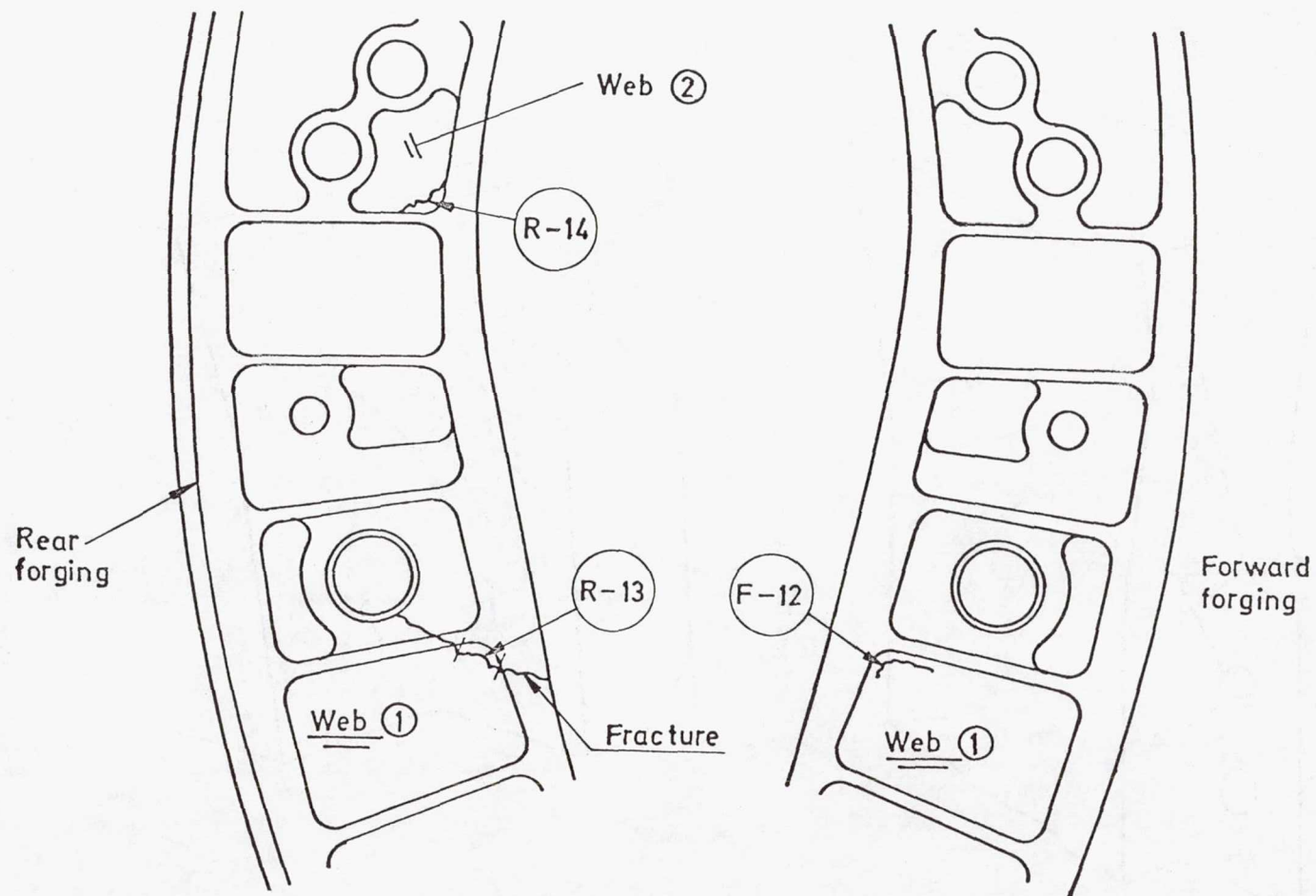


Figure 14.- Test specimen B<sub>1</sub> with fatigue cracks and the location of failure indicated.

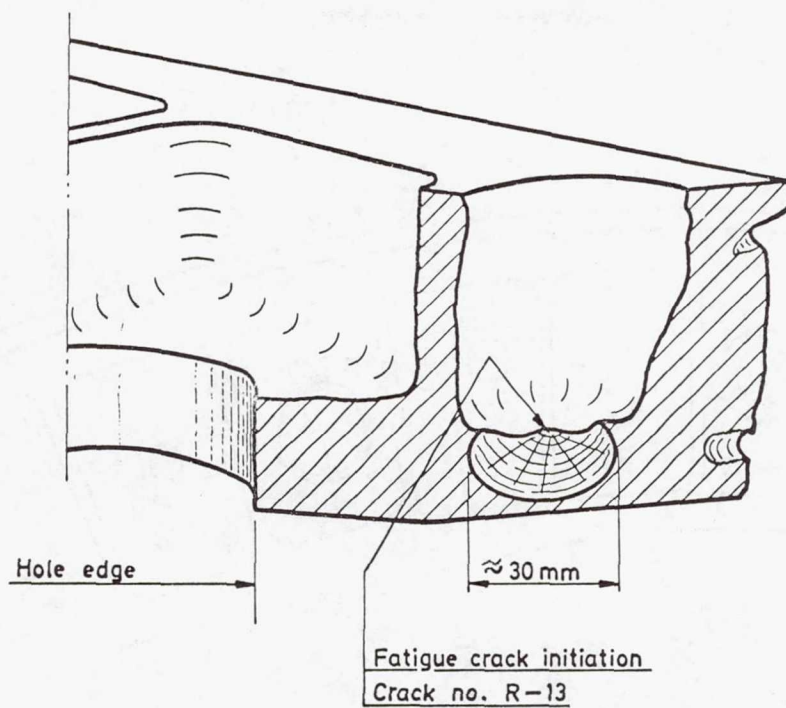


Figure 15.- Fractured area of specimen B<sub>1</sub>.

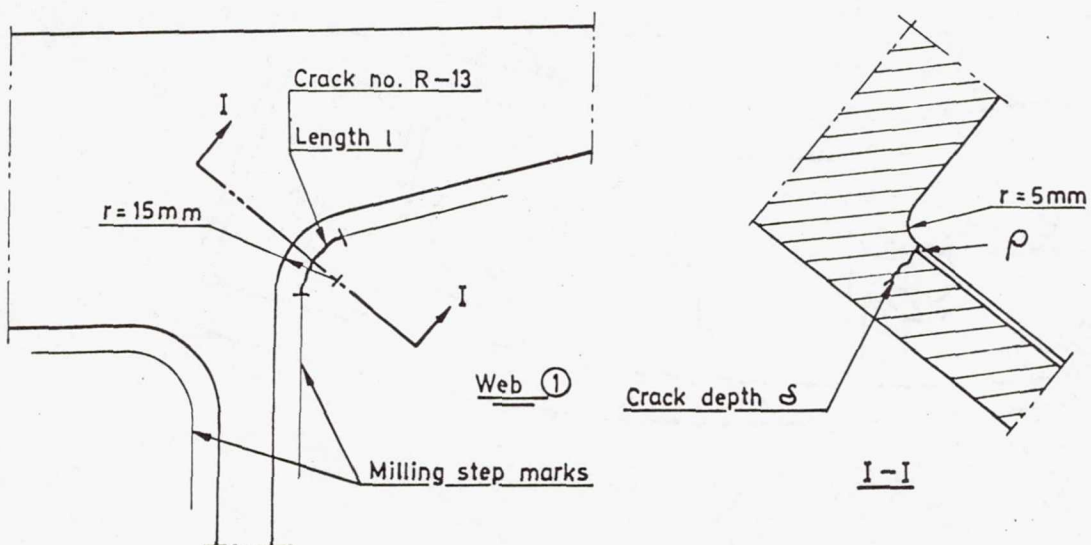


Figure 16.- The surface shape in a cracked area of specimen B<sub>1</sub>.



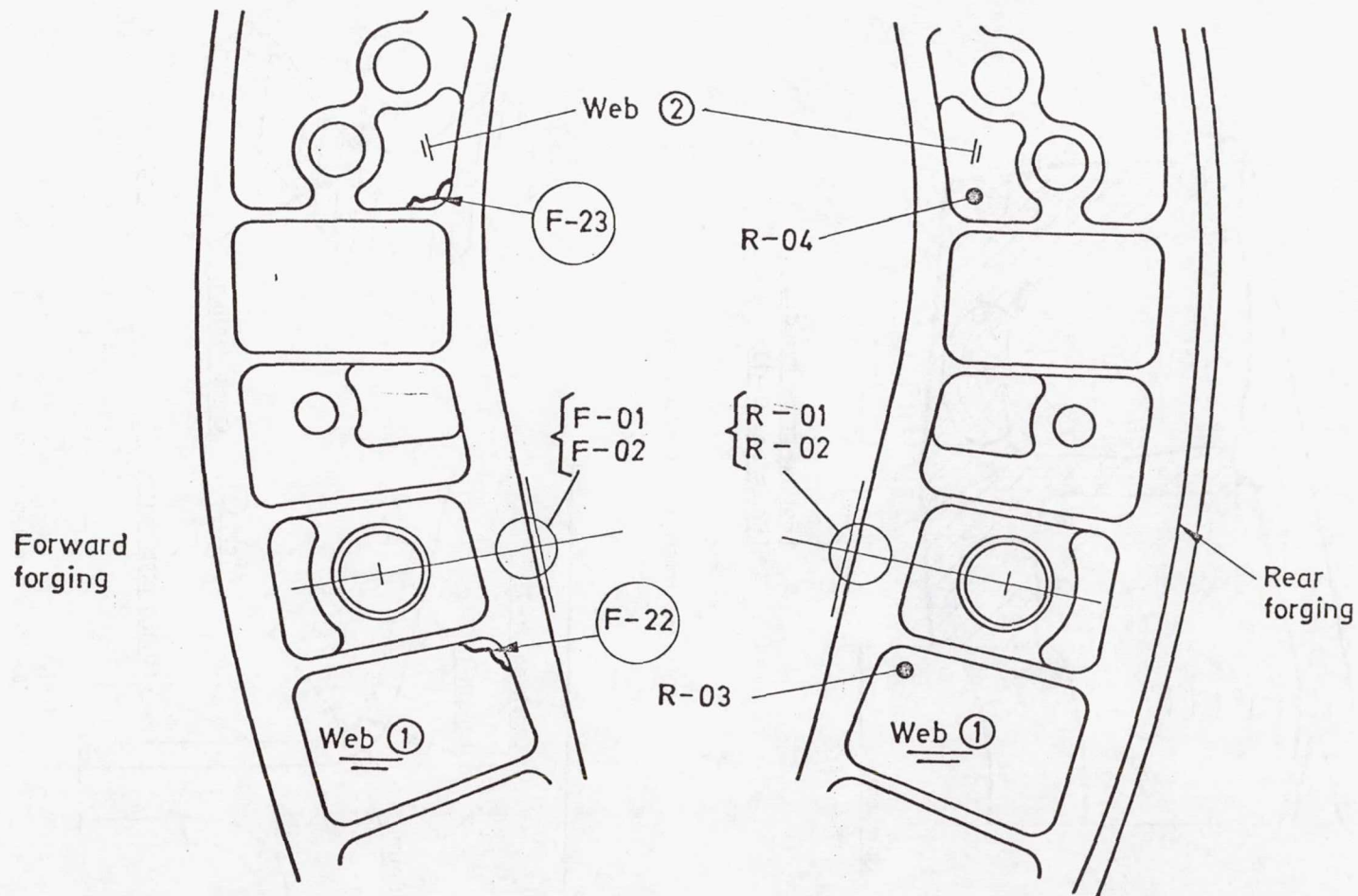


Figure 17.- Test specimen B<sub>2</sub> with cracks and location of strain gages indicated.

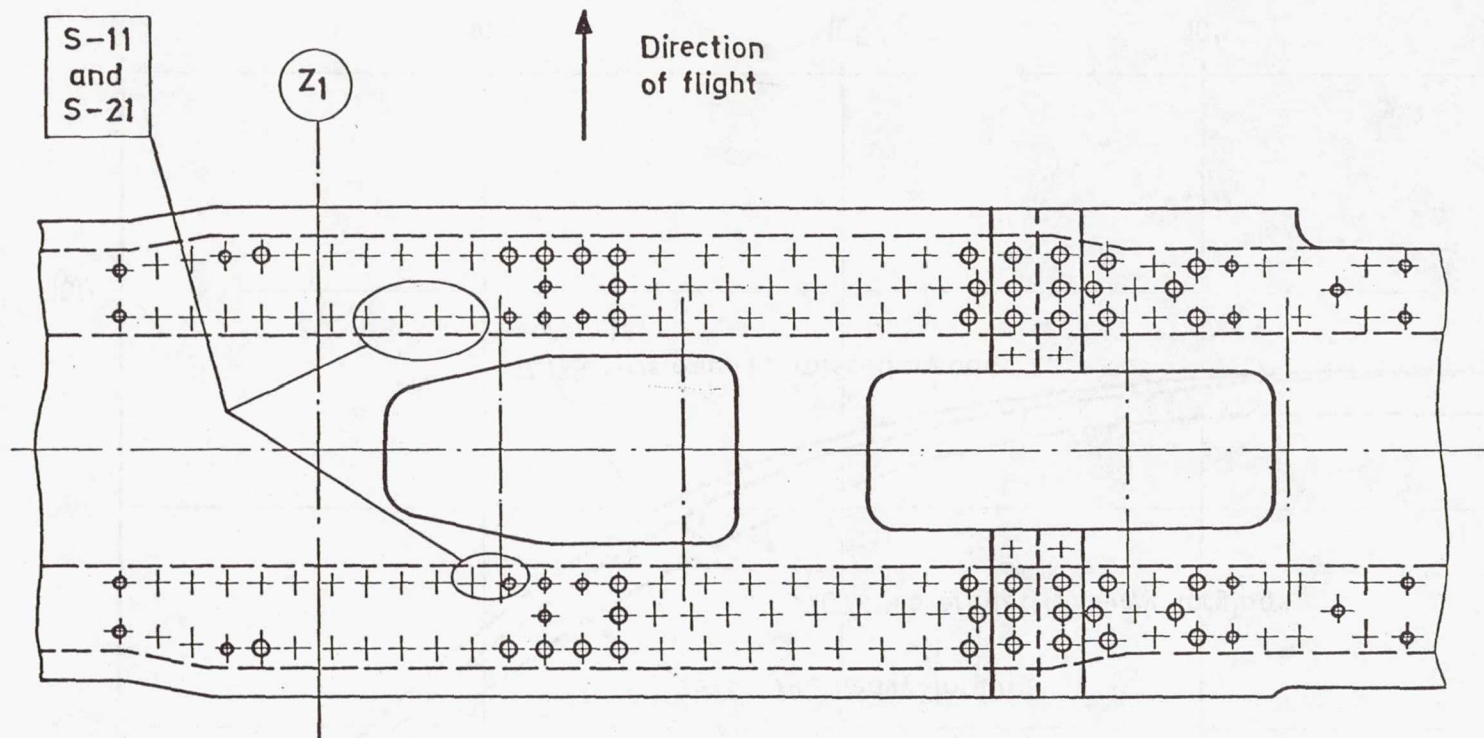


Figure 18.- Area with cracks in the inner sheet of the frame assembly. This figure represents both specimens B<sub>1</sub> and B<sub>2</sub>.



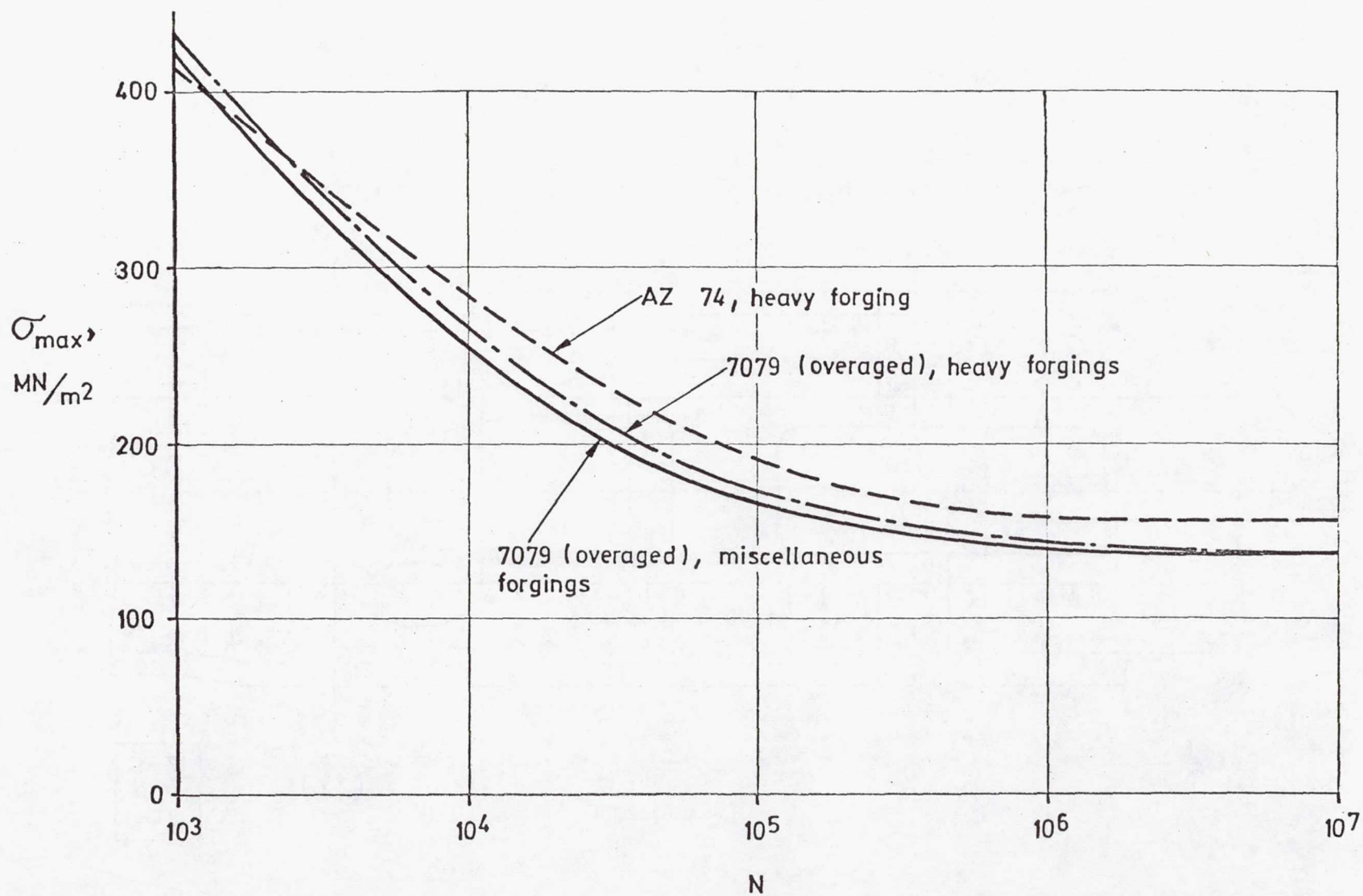


Figure 19.- Results of axial-load fatigue tests on notched round specimens.  $K_t = 2.5$ ;  $\sigma_{\min} = 0$ .

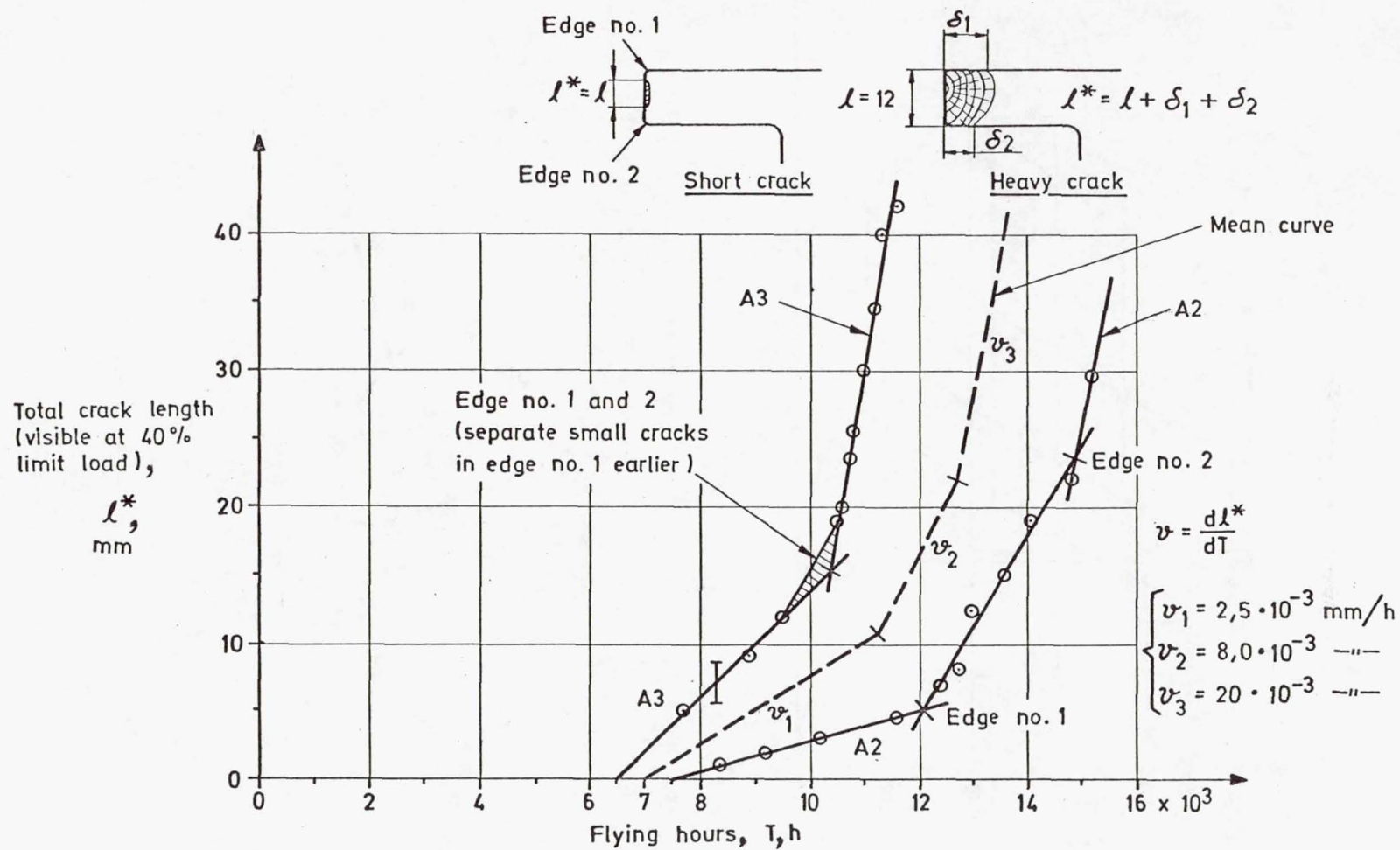


Figure 20.- Crack propagation at flange notch in specimens A2 and A3.



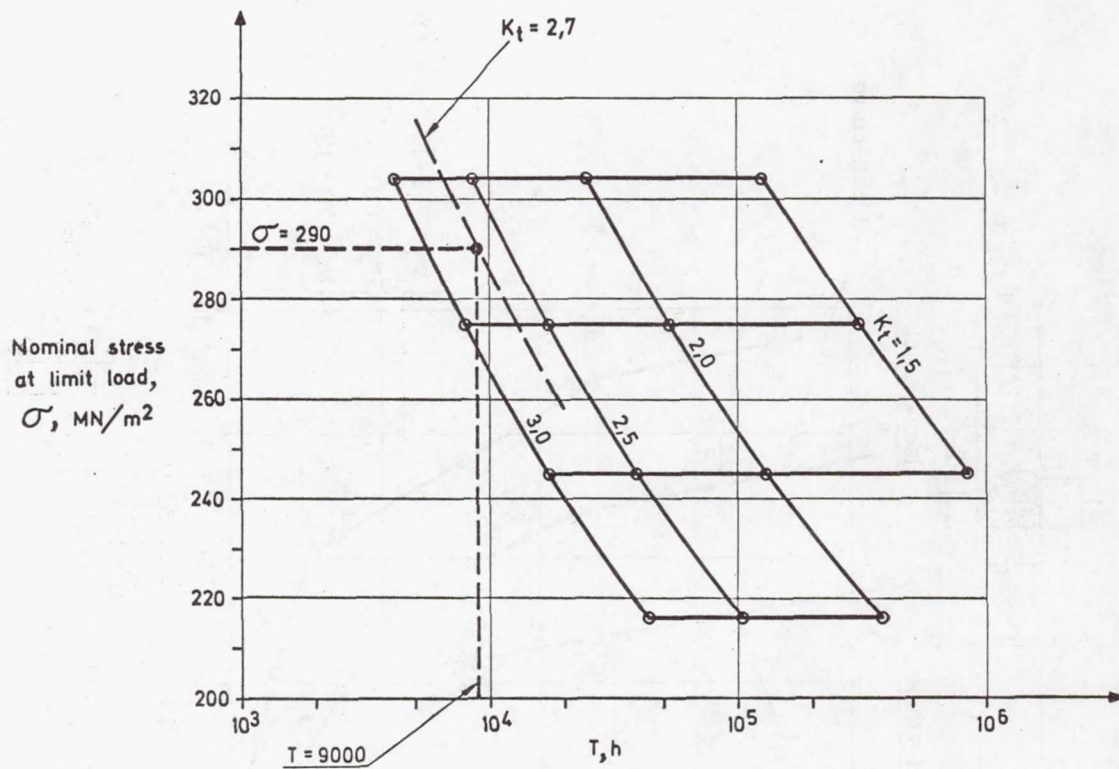


Figure 21.- Results of a cumulative damage calculation for specimen A material, AZ 74.

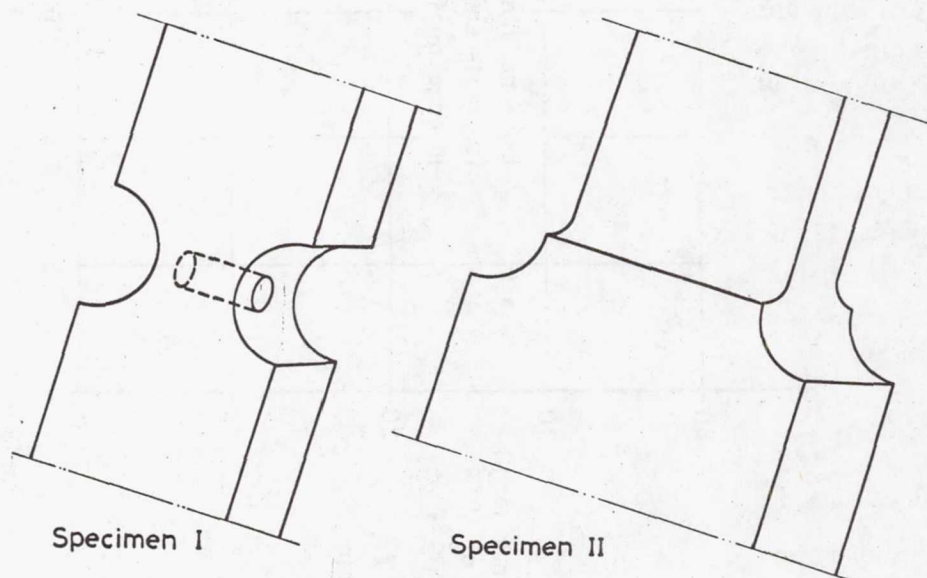


Figure 22.- Examples of interacting stress concentrations.

# THE BOEING 747 FATIGUE INTEGRITY PROGRAM

By Max M. Spencer  
The Boeing Company  
Everett, Washington, U.S.A.

1072-29898

## INTRODUCTION

The Boeing 747 is designed and certified as a fail-safe airplane. (See ref. 1.) The fatigue integrity program was established to insure economic operations and to provide foundation data for inspection and maintenance. Significant features of the 747 fatigue integrity program are

1. Fatigue analyses which are continually updated to reflect design changes, fatigue test results, and static and flight load survey measurements
2. Material selection and detail design by using initial fatigue analyses, service experience, and testing
3. Fatigue testing to check detail design quality and to verify the analyses, culminated by the test of a structurally complete airframe

These three features are interrelated during all program phases of conception, design, design check, production, and operation.

Desired fatigue reliability levels are established by using data from statistical studies on military as well as commercial fleets. Appropriate fatigue reliability factors (scatter factors) are considered in the fatigue life evaluations. Essential fatigue analysis factors are fatigue loading environment, load-stress relationships, fatigue performance data (S-N curves), and cumulative damage theory.

The 747 fatigue loading environments were established by using NASA, military, and Boeing data, in conjunction with aircraft aerodynamics and loads data, customer route structure analyses, and flight load surveys. Because of the airplane size and the complex landing-gear system, the 747 ground-handling and landing load spectra received special attention.

Fatigue stress analyses were performed with the aid of experimental as well as analytical procedures. Extensive application was made of the stress severity factor, developed at Boeing, for evaluating peak stresses in complex joints.

A frame of reference was established by families of structural fatigue performance curves (S-N curves) encompassing the range of materials and fatigue qualities anticipated for the 747 airplane design. Modifications to the endurance limit and the low-stress region of the curves were made by using service experience and structural



component and full-scale fatigue tests. These modifications were necessary to account for the inherent shortcoming of Miner's method for predicting fatigue life for spectrum-loaded structures by using constant-amplitude generated S-N curves.

Each family of fatigue performance curves was assigned a fatigue quality identified by a fatigue performance index (FPI). The FPI of structural details was estimated by a semiempirical relationship.

The most significant factors in attaining satisfactory fatigue quality are detail design and material selection. From previous airplane experience and initial fatigue analyses, material was selected which satisfied the static, fatigue, and fail-safe requirements. Careful consideration to detail design with respect to fatigue and fail safety was given to all primary structural components.

All major details on the airplane were analyzed by using the technique outlined above. These analyses were verified by extensive full-scale and component tests. Fatigue developmental and verification tests conducted specifically for the 747 airplane included

- Quonset-hut tests

- Wing, body, and nose landing-gear tests

- Outboard-flap functional and fatigue tests

- Full-scale horizontal-tail tests

- Fuselage crown stringer splice tests

- Side-of-body rib-component tests

- Numerous small-scale specimen tests concerning —

  - Shot peening

  - Fastener development

  - Cold working

  - Wing—side-of-body joint configuration

  - Window forging configurations

In addition, a full-scale airplane fatigue test is in progress. This test utilizes a flight-by-flight load spectrum including pressure cycles applied in a manner to represent the fatigue loading during a typical flight. The test objectives are to

1. Locate any fatigue-critical areas early in production
2. Provide test data for analytical service-life prediction

3. Help develop inspection and maintenance procedures
4. Evaluate fail-safe characteristics of major structural components and assemblies

The 747 fatigue integrity program provides a high degree of confidence in the ability of the structure to withstand service loads. Safe and economic operation is insured by the continual updating of analyses to reflect design changes and fatigue test results.

#### SYMBOLS

D	drag load
d	diameter, inches
$F_{MEAN}$	mean stress
g	acceleration due to gravity
$K_t$	stress concentration factor
$K_{t,b}$	bearing stress concentration factor
$K_{t,g}$	gross-area stress concentration factor
$\Delta P$	load transferred
$P - \Delta P$	bypass load
S	side load
T	torque
t	thickness, inches
V	vertical load
w	width, inches
$\alpha$	hole condition factor



$\beta$	hole filling factor
$\eta$	semispan station measured from root (see fig. 6)
$\theta$	bearing distribution factor
$\sigma$	stress

#### ABBREVIATIONS

AIRP, A/P	airplane
BS	body station
$\zeta$	center line
DMF	dynamic magnification factor
FLT	flight
FPI	fatigue performance index
FRF	fatigue reliability factor
FWD	forward
GAG	ground air ground
GRND	ground
IHL	intermittent high loads
INBD	inboard
LE	leading edge
MED	medium
ML	marker loads

OUTBD	outboard
SL	sea level
SSF	stress severity factor
TE	trailing edge
W/O	without
FS	forward spar
STA	station
UNSYM	unsymmetrical

## APPROACH

The service-life objective of current Boeing commercial airplanes is 20 years. In pursuing this objective on the 747, a program consisting of analysis, material selection and detail design, and testing has been followed. There is an obvious overlap and interdependence of these elements in design, development, and maintenance of aircraft. Delineation of specific subelements, such as analysis or testing, is done simply to affirm that many techniques may be used in designing for fatigue and to emphasize that several techniques have been applied in parallel as a check-and-balance approach on the 747.

### Analysis

Essential fatigue analysis factors include fatigue loading environment, load-stress relationships, fatigue performance data (S-N curves), and a cumulative damage theory. In defining expected aircraft fatigue loading, both usage (flight profiles) and environment (gust, maneuver, etc.) are required (table 1). Fatigue loadings were established by using military, NASA, and Boeing data for taxi, gust, maneuver, landing, and ground-handling environments. A peak-to-peak definition of the ground-air-ground cycle was used.

Extensive route structure analysis of expected 747-100 operation resulted in the flight length distribution illustrated in figure 1 and a 20-year usage goal of 60 000 hours for each airplane. To encompass the wide range of flight lengths from this study, the flight profiles shown in figure 2 were developed. The average flight length of the three simulated commercial flights is 3 hours, the average expected over a 20-year service



life. Four percent of the total 60 000 hours usage is expected to be consumed in training and is represented for analysis by 600 4-hour, zero-payload flights, also shown in figure 2.

Fuel consumption data are applied to all flight profiles to determine gross-weight variation within each flight. Each flight is subsequently divided into appropriate segments as shown in figure 3. Climb and descent portions of the flight are actually covered by numerous altitude segments to account for the very large variation in gust environment statistics with altitude. Flight mean loads, dynamic response to gust, and response to maneuver are determined from aeroelastic analysis for each flight segment.

Analytical techniques include engineering theory and finite-element methods; experimental techniques include photostress and strain gages. These analytical and experimental techniques are used to convert external airplane loads into the stresses required for fatigue analysis: 1g stress, stress response to gust, and stress response to maneuver. In addition to conventional stress analysis, the stress-severity-factor technique is used (ref. 2). This technique was developed primarily to evaluate load and stress distributions in multifastened joints. It is also used to locate fatigue-critical locations, establish fatigue performance estimates, and evaluate possible design improvements. The stress severity factor includes the effects of geometric stress concentration factor  $K_t$ , fastener load distribution, type of fastener, bearing stress distribution, hole surface condition, and residual stresses. The equation for the stress severity factor is

$$\begin{aligned} \text{SSF} &= \frac{\sigma_{\text{peak}}}{\sigma_{\text{ref}}} \\ &= \frac{1}{\sigma_{\text{ref}}} [\sigma_{\text{load transfer}} + \sigma_{\text{bypass}}] \alpha \beta \\ &= \frac{1}{\sigma_{\text{ref}}} \left[ \frac{\Delta P}{t_d} K_{t,b} \theta + \frac{P - \Delta P}{t_w} K_{t,g} \right] \alpha \beta \end{aligned}$$

Because of its ease of application and relatively good agreement in analyzing airplane structure (ref. 3), Miner's theory of cumulative damage is used. Two shortcomings of Miner's method have been observed in laboratory testing. One is the inability to account for damage from stress amplitudes below the constant-amplitude endurance limit; the other is the so-called sequence effect where in block-type loading, a substantial difference in life has been observed in some tests in which the order of application of high and low load blocks has been varied. The second shortcoming is somewhat academic for

evaluating flight structure since relatively few parts, if any, are subjected to two-step high-low or low-high block loads in service. The sequence effect is of course very real in simulated flight testing and is the primary reason that flight-by-flight testing is preferred.

To correct Miner's method to account for damage below the constant-amplitude endurance limit, two techniques are available. One is simply to translate (reduce) the S-N curve linearly on life at each alternating stress level (ref. 4). The other is to reshape (change the slope of) the S-N curve. The latter course has been followed in this work and is illustrated in figure 4. The level to which the S-N curves have been reduced at infinite life is the nonpropagating crack threshold stress. The shape and location of the upper portion of the S-N curve are essentially unaltered, which retains the advantage of fatigue quality determination from constant-amplitude testing. The resulting curves, which are then termed fatigue performance curves, are mathematically defined with a Stuessi type equation (ref. 5) and verified with fleet analysis and flight-by-flight spectrum tests.

In the early stages of airplane configuration development (prior to built-up structure tests), the fatigue quality of a given design may not be known with high confidence. To preclude having to rerun fatigue analysis whenever a slight change in detail geometry is made, as well as to provide a frame of reference for fleet analysis, a family of fatigue performance curves was developed for each of the materials used on the 747. The reference curve for each was that for basic structure (which is defined as skin-stringer construction having no significant load transfer between skin and stringer). The basic-structure curve was based on built-up structure fatigue performance data which were available for the material and type of construction in question. It should be noted that simple coupon ( $K_t$ ) data are not used to estimate life of aircraft structure directly (refs. 6 to 9). With the basic-structure curve as a reference, the remainder of the family of fatigue performance curves for each material was developed by using the variation of life with quality from past tests (refs. 10, 11, and 12).

The term used to identify fatigue quality is the fatigue performance index (FPI), and each of the many curves is identified with a fraction corresponding to the familiar  $1/K_t$  form. (Basic structure, for example, was initially identified as  $FPI = 1/2.5$ .) An example of curves used for analysis of a given detail is shown in figure 5. Fatigue analyses conducted in this manner are essentially parametric studies of life as a function of quality. A sufficient number of analyses are conducted to bracket the expected fatigue quality. Curves developed in this way, for fatigue performance indices of 0 to 1, and for each material, were mathematically defined and programed for computerized fatigue analysis.

Techniques for estimating fatigue quality involved stress-severity-factor analysis, previous airplane tests, or fleet data. The factors accounted for in the estimating tech-



nique are geometric stress concentration, load transfer, type of fastener (interference, design, and modulus of elasticity), bearing stress distribution, hole surface condition, residual stresses, and material. Constants were determined which provided the best fit of estimated life versus test- or fleet-demonstrated life from approximately 2000 assessments. The sequence of analysis, test, and fatigue performance estimation is discussed in the section entitled "Typical Results."

Figure 6 illustrates the scope of the fatigue analyses conducted on basic structures, and figure 7 illustrates typical details selected for analysis.

Fatigue reliability factors (scatter factors) accounting for fatigue performance variability, possible load environment variability, and the number of tests conducted on representative built-up structures are included in each basic structure or detail fatigue analysis. The magnitudes of the fatigue reliability factors varied from 2 to 4, with 4 being used in preliminary analysis when the least built-up structure data were available, and 2 being used when large numbers of representative built-up structure tests were completed.

#### Materials Selection and Detail Design

This facet of the 747 fatigue integrity program is intended to cover fatigue improvement activities which parallel the basic analysis. Fleet experience, for example, can play a major role in complementing preliminary fatigue analysis, that is, as a check and balance. Fleet experience with similar parts can augment conventional fatigue analysis, provide positive assessment of detail design quality, even derive new model fatigue performance providing usage, stress, and detail design are not substantially different.

During the design stage, guides for satisfactory fatigue design (or at least guides for identification of possible problems such as given in ref. 13) are of value. The best experience of course is fleet experience, and listings of previous industry airplane problems (cause and effect) were used as design background on the 747. These types of activities, together with preliminary fatigue analysis, resulted in numerous design improvements, a few of which are shown in figures 8, 9, and 10, and in the following materials section:

Wing lower surface - 2024 skin and stiffeners

Wing upper surface - 7075 skin and stiffeners

Body skin - primarily 2024

Body frames and stiffeners - 7075

Empennage - 7075

Landing gear – primarily 4340 steel heat-treated to yield an ultimate strength varying from 270 to 300 ksi

Forgings – 7075-T73 (stress corrosion is a prime consideration)

### Testing

Analysis and past experience are very important in establishing preliminary design geometries, materials, and allowable stress levels. The proof of fatigue quality, however, must come from test or flight experience. Since the objective of the fatigue integrity program is to minimize early flight fatigue experience (i.e., cracks), early testing is a key element (refs. 14 and 15). An extensive verification test program was conducted on representative sections of the entire airplane (figs. 11 to 17). All these test structures were constructed with the same finishes, fasteners, and geometries as were planned for production airplanes. Both constant-amplitude and flight-by-flight spectrum tests were run. In addition to the panel and pressurized fuselage test program summarized in figures 11 to 17, numerous small-scale development-type tests were conducted. Major-component tests, including landing gears, trailing-edge flaps, and horizontal stabilizer, are discussed in the section entitled "Tests of Major Components." The culmination of the 747 fatigue test program is the full-scale fatigue test, which is discussed subsequently.

### TYPICAL RESULTS

Typical of the analyses conducted on the airplane is that shown in figure 18. This particular analysis was conducted for three fatigue qualities and included a fatigue reliability factor (FRF) of 4.0. The analysis illustrates variation of life with spanwise and chordwise location as well as the approximate quality required to achieve the fatigue life goal of 60 000 hours.

Typical test quality determination is illustrated in figure 19, where fatigue quality is plotted against cycles to first crack. The quality associated with the number of cycles endured at the listed stress state is 0.361, or in  $1/K_t$  form,  $FPI = 1/2.77$ . This quality, incidentally, is very near the initial quality estimated for basic structure  $FPI = 0.4$  or  $1/2.5$  and is near the upper end of the qualities for which the analysis in figure 17 was conducted.

Application of test-determined quality and a revised fatigue reliability factor  $FRF = 2.95$  (which is appropriate after additional testing) results in the estimated fleet fatigue performance of stringer runouts shown in figure 20.

Additional examples of the type of data available from fatigue analyses are shown in figures 21, 22, and 23. Since several flights were included in the basic definition of usage,



parametric-type analyses illustrating the influence of flight length on fatigue life are available. These particular analyses have been useful in assessing fatigue life of 747 derivatives for different kinds of usage, especially short-range operation. Zones of life deficiencies and stress reductions or quality improvements required to achieve appropriate life goals for 1-hour average flight operation, for instance, are also fallouts of basic airplane analysis.

## TESTS OF MAJOR COMPONENTS

Major-component tests include: nose, wing, and body landing gears, horizontal stabilizer, and outboard trailing-edge flap. Photographs and descriptions of landing-gear test specimens are given in figure 24. In order to represent flight airplane structure, test specimens are production parts and jig structure is designed to simulate the flexibility of airplane support structure. These specimens are subjected to block-type loadings shown in figures 25, 26, and 27. Each block consists of loadings equivalent to 1000 flights, 5 percent of the one lifetime goal of 20 000 flights. The numerous environmental conditions included in analysis and test of each gear are also listed on the respective figures.

The outboard-flap test is illustrated in figure 28. The test consisted of stress surveys, functional testing in which the flap was raised and lowered 5000 times, and fatigue testing the outboard flap in the fully extended position. The inboard flap and leading-edge flaps are tested in the fatigue test on the full-scale airplane.

The horizontal stabilizer is tested separately from the full-scale airplane fatigue test primarily to avoid the complication of meshing with fin load systems (fig. 29). Since the stabilizer is mounted in a determinate manner on two hinges and a jackscrew, a fully representative load spectrum can be applied in both the full-scale test, through dummy stabilizer structure, and the separate test. An added advantage is that the stabilizer test can then be conducted at a faster rate. To allow for the fin-empennage airload interaction with the stabilizer, the vertical gust loads are applied in both separate and full-scale tests with a  $\pm 20$ -percent asymmetry. Derived spectrum loads are applied to the inboard and outboard elevators on the left side and through dummy elevators on the right side. Additional elevator loads representing take-off rotation and climb rotation are applied in the take-off phase, and loads representing spoiler trim and landing flare are applied in the landing phase.

## FATIGUE TEST OF FULL-SCALE AIRPLANE

### General Description of Specimen and Test Rig

The culmination of the test phase of the fatigue integrity program is the fatigue test of the full-scale airplane (fig. 30). The test specimen is a structurally complete airframe

of typical production configuration. Omitted are main and nose landing gears, trailing-edge flaps except left-hand inboard, leading-edge flaps except left-hand flap numbers 3, 7, and 12, ailerons, spoilers, engine pod, and the horizontal stabilizer, which is tested separately. Loads are applied through representative dummy structures for the major components omitted from the test.

Loads are applied to the airplane by using 86 hydraulic actuators, which are controlled by an automatic closed-loop electro-hydraulic servo system. The command or program signal is supplied to the servo systems by a digital programmer. This programmer and the data acquisition functions for the test are controlled by a Digital Equipment Corporation PDP-8 computer. The computer is also used to automate many of the operating functions of the test.

To prevent the test specimen from being loaded to levels that are outside defined tolerances, a lockup manifold is installed on each hydraulic actuator. When the lockup system is actuated, the actuator holds the load at the limit of present tolerances until problem correction. Stainless-steel safety links are included in all load systems attached to the airplane. These are designed to yield before local airplane structure is damaged by inadvertent overloading. There is also a two-way relief valve installed in each load system to limit actuator pressure and thereby prevent an overload.

#### Load Spectrum Derivation

The main purpose of the airplane fatigue test is to better determine the true structural fatigue performance by eliminating most of the assumptions which are necessary in the analysis. The specific objectives of the test are to locate as quickly as possible any fatigue-critical areas with a program accurately representing typical service loads, to provide test data for analytical service life predictions, to help develop inspection and maintenance procedures for the airlines, and to evaluate fail-safe characteristics of major structural parts. Criteria considered in developing the load spectrum are

- Flight-by-flight testing

- Average of mixture of flights used as base

- Match upper surface ground-air-ground stresses

- Match upper surface taxi damage

- Match lower surface flight segment damage distribution

- Match 1g stresses in 3-hour flight

- Equivalent gust and maneuver cycles

- One lateral cycle for one vertical cycle in flight segments



Lateral-load cycles quarter of a cycle out of phase with vertical-load cycles

Representative cabin pressurization and depressurization

Average flap utilization

Mean engine thrust in each flight segment

Equivalent landing-gear loads in ground-handling phase

Intermittent high loads and marker loads

To give the correct combination of spectrum loads, cabin pressure, and ground-air-ground cycle loads, the test is conducted on a flight-by-flight basis. An average flight based on the mixture of four analysis flights is used for deriving the test program. For convenience, damage in the average flight is factored by  $19\,800/20\,000 = 0.99$  to give 20 000 average flights in 60 000 hours of service. Therefore, each test spectrum represents 3 hours of flying in the mixture of flights.

From the derived gust, maneuver, and taxi damage in each flight segment, the required test cycles are found by using the appropriate stresses from the 3-hour flight (fig. 2).

Incremental stresses due to gust or maneuver and the relationship between gust speed and airplane acceleration differ for each component. Therefore, the damage due to gust and maneuvers is considered independently and is applied to each component with representative loads. Equivalent gust loads are factored by appropriate dynamic magnification factors.

On the basis of aircraft industry experience, both wing upper and wing lower surfaces are of fatigue concern. Therefore, a load program is derived which is representative for both surfaces. The wing upper surface GAG cycle (which is given by the cycle from the maximum once-per-flight tension stress on the ground, to the maximum once-per-flight compression stress in the air, to the maximum once-per-flight tension stress on the ground) damage is matched by a slightly modified GAG cycle for the 3-hour flight. This modification limits the maximum allowable tension stress in the taxi segment. To reduce the number of cycles, the mean stress in the taxi is reduced below the 1g level allowing a higher alternating stress. With this additional variable the required number of cycles, which was fixed at five, can be matched. Having fixed the upper surface GAG cycle stresses and matched the taxi damage, 97 percent of the total upper surface damage is matched.

For the wing lower surface, the GAG cycle gives approximately 30 percent of the total damage. The lower surface taxi damage corresponds to the cycles already determined for the upper surface. The small difference between the analysis and test taxi damage is corrected in the GAG cycle damage to give the correct total damage. The



lower surface GAG stresses are determined by the same method used for the upper surface. With a representative 1g stress in each flight segment, the maximum allowable alternating stress, and hence the maximum equivalent alternating cycle, is limited by the GAG cycle stresses. To achieve the best damage match at other locations, the maximum GAG stresses are fixed in the same flight segments as the analysis. Maximum upper surface tension and lower surface compression stresses occur in the taxi segments. The maximum upper surface compression stress occurs in the hold segment, and the maximum lower surface tension stress occurs during flaps-down climb. Gust and maneuver damage is matched in each segment by finding the minimum number of cycles based on the 1g and GAG stress limitations.

Figure 31 illustrates the vertical-load program derived for the wing. Fuselage vertical loads correspond to the gust, maneuver, and taxi loads derived similarly to those for the wing. Since it is impractical to load all the passenger and cargo floor, representative loads are applied in fore, mid, and aft body locations. The numerous other load spectra and the approximate phasing with vertical loads are shown in figure 32. For reference purposes, the average 3-hour flight is subdivided into eleven phases, shown by Roman numerals.

For the lateral-load program, the load magnitude is found by matching the damage in each segment with the same number of cycles as the vertical-load program. In the segments with an even number of cycles, half the cycles are applied with a gust load distribution and half with maneuver load distribution. The cycles in the other segments are arranged so that the total flight damage is half gust and half maneuver.

Additional discrete rudder loads which occur during take-off, flap extension, approach, and landing roll-out are applied during phase I for convenience. It is considered unlikely that the maximum lateral loads generally occur at the same time as the maximum vertical loads. Therefore, the lateral-load cycles are applied one-quarter of a cycle out of phase with the vertical-load cycles. This means the peak lateral load occurs with 1g vertical load and the maximum and minimum vertical loads occur with zero lateral load.

Cabin pressure differential varies from zero to 0.6 psi in phase IV, from 0.6 linearly to 9.0 psi in phase V, is constant at 9.0 psi in phases VI and VII, varies from 9.0 linearly to 0.6 psi in phase VIII, is constant at 0.6 psi in phase IX, and varies from 0.6 psi to zero in phase X.

Loads representing an average utilization are applied to the leading-edge (LE) and trailing-edge (TE) flaps. On the leading edge the loads are applied to flaps 3, 7, and 12 on the left-hand side. The remaining flap loads are applied through dummy flaps with representative loads on the support structure. Loads on trailing-edge flaps are applied to the inboard flap on the left side with the remaining loads applied to the tracks through



dummy flaps. Most of the damage to TE flaps occurs during approach with the flaps fully extended. Therefore, the test loads are applied with the flaps in the extended position. An equivalent load cycle is applied in phase III to represent the damage in the most critical track and carriage sections during take-off with flaps at  $15^{\circ}$ . In the analysis of the primary structure on the LE flaps, most of the damage occurs during take-off. The maximum flap load during take-off occurs with the flaps extended at the end of the take-off rotation. Therefore, the test loads are applied with the flaps in the extended position. An equivalent cycle is applied during the approach in phase X. When the LE flaps are retracted, the uplock load exceeds all the 1g, gust, and maneuver airloads. Therefore no loads are applied on the leading-edge flaps during the remaining flight stages. To represent the uplock stress which occurs during flight and the two cycles during ground handling, three equivalent load cycles are applied in phase I.

Mean fore and aft nacelle loads in the 3-hour flight are applied in each phase. Maximum gross thrust during take-off and reverse thrust during landing are applied in phases III and IX, respectively.

Landing-gear loads in an average flight are applied through dummy gears to the landing-gear support structure. The dummy gear has a representative relative stiffness to give a true load distribution. In phase I ground handling the vertical, fore and aft, and side loads are based on the same criteria used to derive the separate landing-gear test program. The main difference between the two tests is the block loading in the gear test, which has 1000 flights in each test spectrum and flight-by-flight loading in the airplane fatigue test. Vertical loads in phase II taxi correspond to the loads derived for the wing. Average spinup and springback loads are applied in phase XI landing.

The spectrum applied on the airplane fatigue test represents typical loads which occur in an average flight. In addition to these loads, the airframe is subjected to infrequent high loads during the 60 000-hour life of the airplane. These loads have a negligible effect on the cumulative fatigue damage but affect the damage rate and crack initiation and propagation. Therefore, to include this effect in the program, the loads which occur three times in 60 000 hours flying are applied. These loads are termed intermittent high loads (IHL).

Since any cabin pressure differential higher than the normal 9.0 psi is unlikely to occur, no intermittent high cabin pressure is applied.

In previous fatigue tests it has been difficult to establish crack initiation times, crack propagation rates, and crack life prior to rapid fracture in inaccessible areas, and for cracks which were not found until the test was completed. To help in establishing crack data, unique loads, termed marker loads (ML), are applied during the test. These marker loads are arranged in sequence with the intermittent high loads so that a definite test time can be determined from the striations (table 2).

In the test spectrum the cabin pressure is cycled from zero to 9.0 psi to zero once per flight. This gives a representative cycle for a typical flight. In the training flight the airplane climbs to a varying altitude three times. To represent these pressure cycles and concurrently provide a ML pattern for pressure-critical components, those additional pressure cycles from the training flights are applied.

The present status of the major-component and full-scale airplane fatigue tests is given in table 3. The differing test goals specified in this table are an outgrowth of the fatigue reliability factor criteria discussed in the section entitled "Approach." In general, critical details in landing-gear structure are single-detail-type items, for example, a fillet radius. For these types of tests, a larger statistical factor is required to achieve desired reliability levels in service.

In built-up structure tests such as the outboard flap, horizontal stabilizer, and full-scale airplane, several points usually are identically stressed and therefore constitute a larger sample and require lower statistical factors. All major components have been subjected to loads exceeding the planned requirements for the basic passenger airplane. Many of the tests have been continued beyond the original test goals in order to substantiate derivative airplane requirements. Pending identification of requirements more severe than those currently estimated, some tests have been suspended.

#### CONCLUDING REMARKS

The Boeing 747 fatigue integrity program provides a high degree of confidence in the ability of the structure to withstand service loads. Safe and economic operation is insured through fail-safe design augmented with a continually updated program reflecting past experience, analysis, and test-demonstrated fatigue performance.



## REFERENCES

1. Anon.: Airworthiness Standards: Transport Category Airplane. Federal Aviation Regulations - Part 25, Federal Aviation Agency, Nov. 1968.
2. Jarfall, L. E.: Optimum Design of Joints: The Severity Factor Concept. The Aero Research Institute of Sweden, May 1967.
3. Chrichlow, W. J.; Young, Louis; McCulloch, A. J.; and Melcon, M. A.: An Engineering Evaluation of Methods for the Prediction of Fatigue Life in Airframe Structures. Technical Report ASD-TR-61-434, Mar. 1962.
4. Smith, James M.: Extended Service Life Wing Design F-8 Crusader. Aerospace Structures Design Conference, Seattle, Washington, Aug. 1969.
5. Stuessi, F.: Theory and Test Results on the Fatigue of Metals. ASCE Proceedings, Vol. 85 (Jrle, Structural Div. #ST8), Paper #2222, pp. 65-90, Oct. 1959.
6. Hyler, W. S.; et al.: Fatigue Behavior of Aircraft Structural Beams. NACA TN 4137, Jan. 1958, p. 59.
7. Sines, G.; and Waisman, J. L., eds.: Metal Fatigue. McGraw-Hill, New York, 1959, pp. 319-320.
8. Harris, W. J.: Metallic Fatigue. Pergamon Press, 1961, p. 166.
9. Barrois, W.; and Ripley, E. L.: Symposium on Fatigue of Aircraft Structures. Pergamon Press, 1963, p. 88.
10. Grover, H. J.; Bishop, S. M.; and Jackson, L. R.: Fatigue Strength of Aircraft Materials-Axial-Load Fatigue Tests on Unnotched Sheet Specimens of 24S-T3 and 75S-T6 Aluminum Alloys and of SAE 4130 Steel. NACA TN 2324, Mar. 1951.
11. Grover, H. J.; Bishop, S. M.; and Jackson, L. R.: Fatigue Strengths of Aircraft Materials-Axial-Load Fatigue Tests on Notched Sheet Specimens of 24S-T3 and 75S-T6 Aluminum Alloys and of SAE 4130 Steel With Stress-Concentration Factors of 2.0 and 4.0. NACA TN 2389, June 1951.
12. Grover, H. J.; Bishop, S. M.; and Jackson, L. R.: Fatigue Strengths of Aircraft Materials-Axial-Load Fatigue Tests on Notched Sheet Specimens of 24S-T3 and 75S-T6 Aluminum Alloys and SAE 4130 Steel With Stress-Concentration Factor of 5.0. NACA TN 2390, June 1951.
13. Smith, C. R.: Tips on Fatigue. Navweps 00-25-559, 1963.
14. Ilg, W.: Factors in Evaluating Fatigue Life of Structural Parts. NASA TN D-725, Apr. 1961.

15. Schijve, J.: Cumulative Damage Problems in Aircraft Structures and Materials.  
The Aeronautical Journal of the Royal Aeronautical Society, vol. 74, no. 714,  
June 1970.



TABLE 1.- FATIGUE ANALYSIS DETAILS

- ENVIRONMENT
  - Gust
  - Ground Handling Loads
  - Landing Loads
  - Miscellaneous
- FLIGHT PROFILES
- FLIGHT SEGMENTATION
- STRESS DETERMINATION
- FATIGUE PERFORMANCE DATA
  - Built-Up Structure Panel Tests
  - Full-Scale Cyclic Tests
  - Fleet Service
- APPLY PRINCIPLES OF MINER'S METHOD TO  
PRODUCE CALCULATED FATIGUE PERFORMANCE

TABLE 2.- LOAD SEQUENCE OF MARKER LOADS AND INTERMITTENT HIGH LOADS

PROGRAM NUMBER	EQUIVALENT FLYING TIME	NUMBER OF ML CYCLES	NUMBER OF IHL CYCLES	TOTAL CYCLES
6,667	20,000 HR	2	1	3
13,333	40,000 HR	3	1	4
20,000	60,000 HR	4	1	5
26,667	80,000 HR	5	1	6
33,333	100,000 HR	3	1	4
40,000	120,000 HR	2	1	3

One Marker Load Is As Follows :



- FOR EACH MARKER LOAD CYCLE APPLY FIVE TYPE "A" ML CYCLES FOLLOWED BY ONE TYPE "B" ML CYCLE.

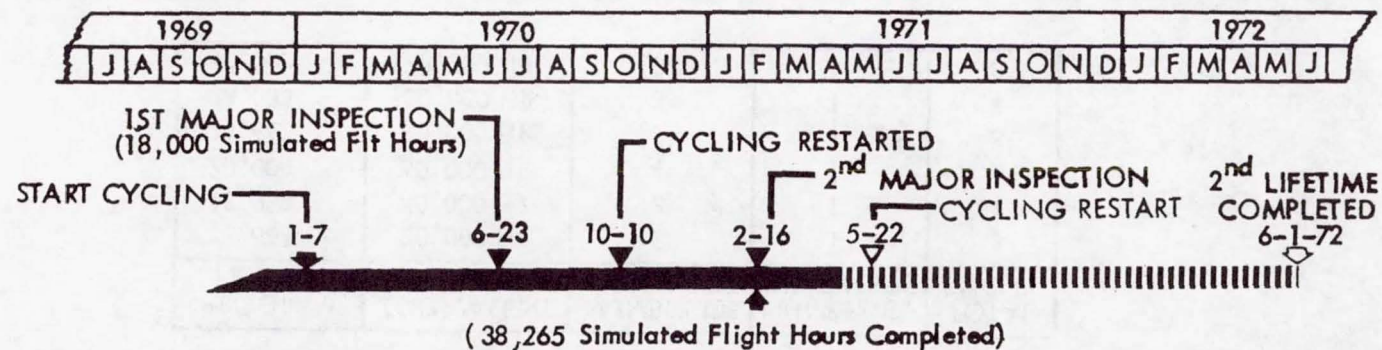
NOTE :

- MINIMUM LOAD IS ZERO UNLESS OTHERWISE STATED.
- THE ML'S AND IHL'S ARE TO BE APPLIED CONSECUTIVELY WITH THE TOTAL NUMBER OF ML'S APPLIED FIRST.
- THE ML AND IHL GUST CYCLES MUST INCLUDE THE APPROPRIATE DYNAMIC MAGNIFICATION FACTORS.



TABLE 3.- FATIGUE TEST STATUS

ITEM TESTED	TEST GOAL (LIFETIMES) <sup>①</sup>	BASIC A/P LIFETIMES COMPLETED	CURRENT STATUS
● LANDING GEAR			
● NOSE	4	4.6	SUSPENDED
● WING	4	5.5	SUSPENDED
● BODY	4	5.1	SUSPENDED
● HORIZONTAL STABILIZER	2	5.8	TEST IN PROGRESS
● OUTBOARD FLAP	2	2.2	SUSPENDED
● AIRFRAME CYCLING	2	0.64	STOPPED FOR INSPECTION



① 1 LIFETIME = 20 YEARS OF EXPECTED SERVICE  
(APPROX 20,000 FLIGHTS)

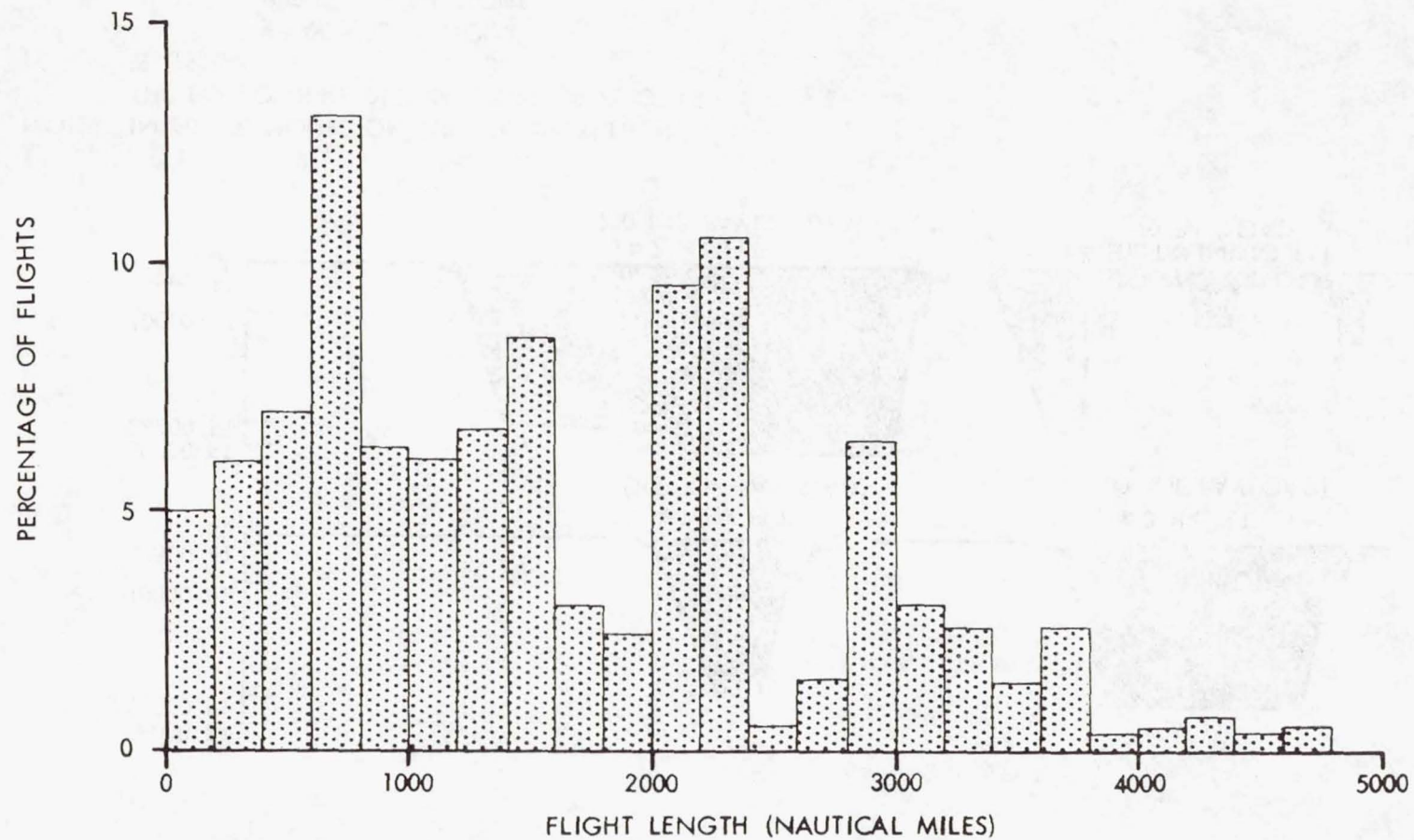
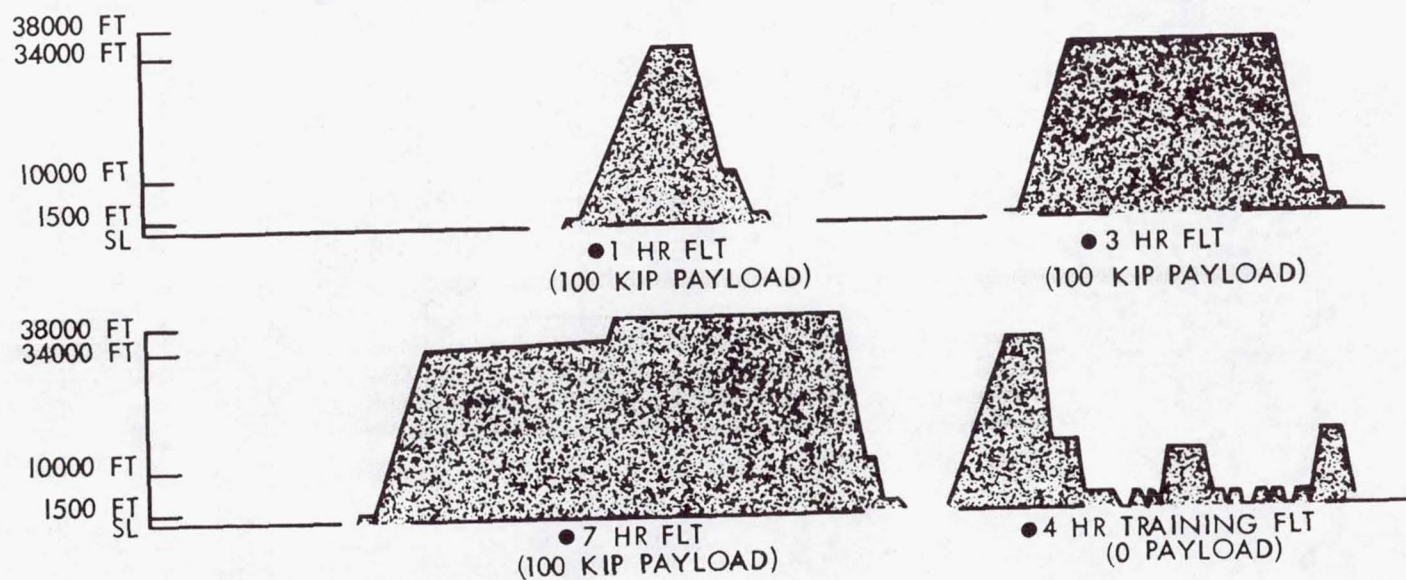


Figure 1.- Flight length distribution for Boeing 747-100 passenger airplane.





NOTE: IN 60,000 HOURS OF SERVICE OPERATION,  
THE FOLLOWING DISTRIBUTION OF FLIGHTS  
IS USED:

- 9600 - ONE HOUR
- 4800 - THREE HOUR
- 4800 - SEVEN HOUR
- 600 - TRAINING

Figure 2.- Flight profiles. Operating empty weight, 360 000 lb.

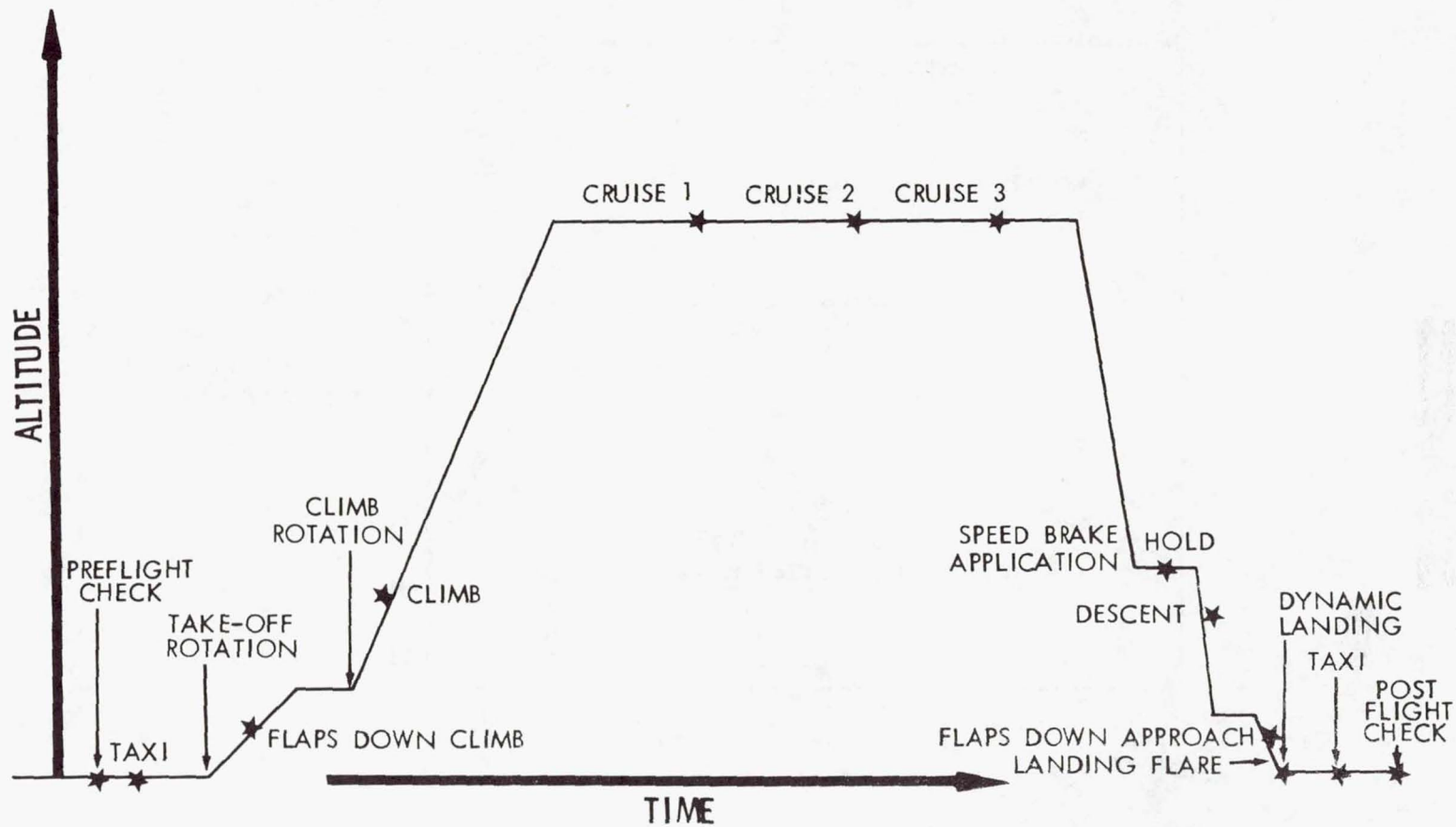


Figure 3.- Typical flight segmentation.



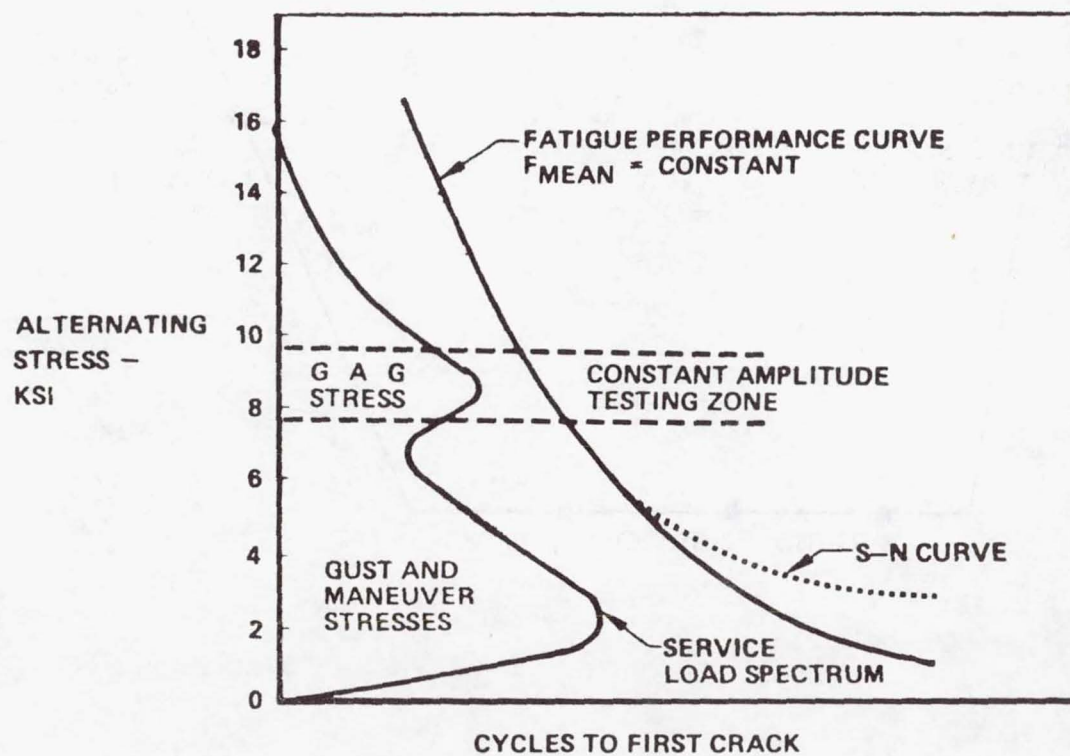


Figure 4.- Modified Miner's method.

**FATIGUE PERFORMANCE INDEX (FPI)**  
**DETERMINED BY ONE OF THE FOLLOWING:**

- **FPI = 1.0/ k SSF**
- **FLEET DATA**
- **TEST OF ACTUAL STRUCTURE**

**ALTERNATING  
 STRESS -  
 KSI**

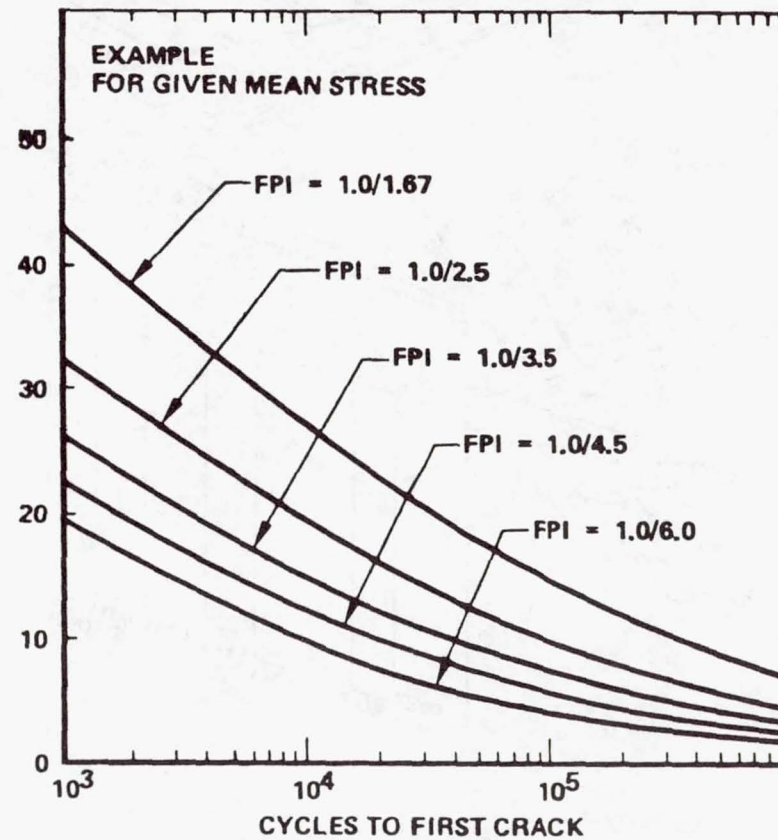


Figure 5.- Fatigue performance curves.



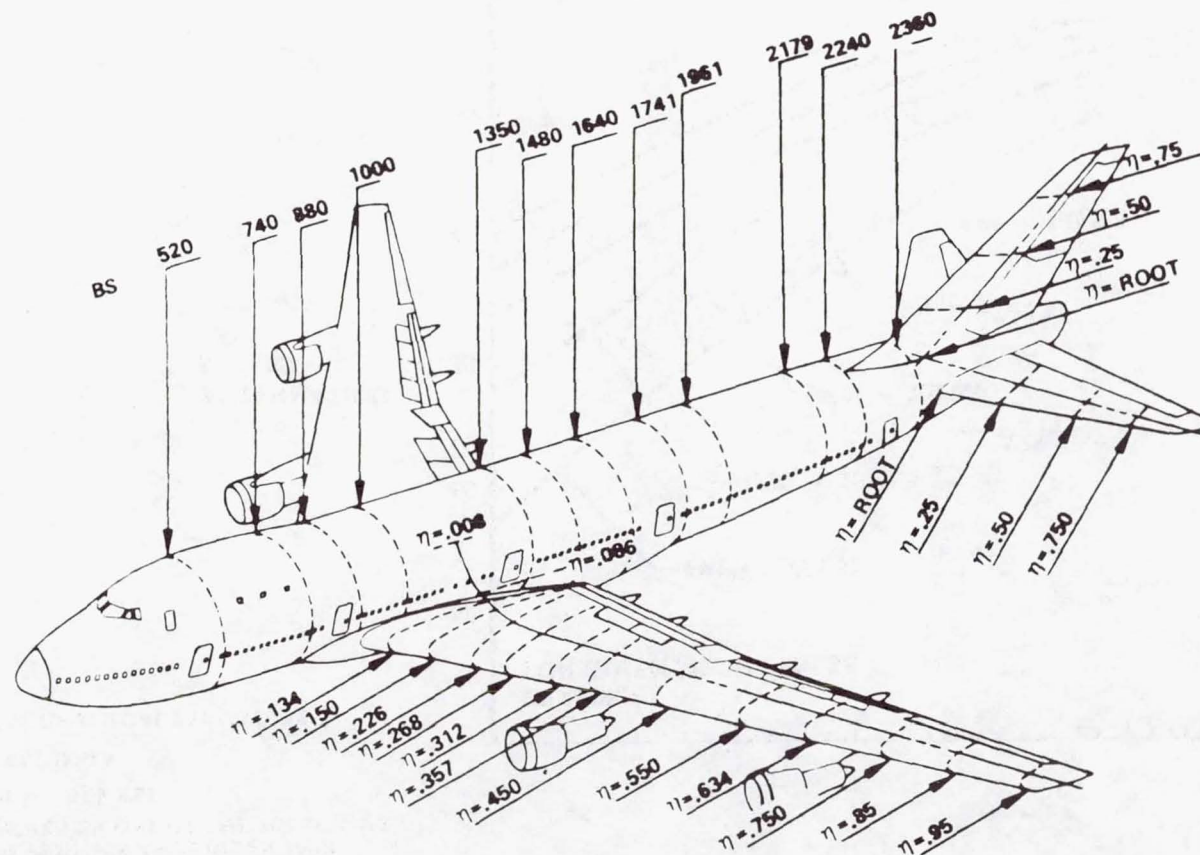
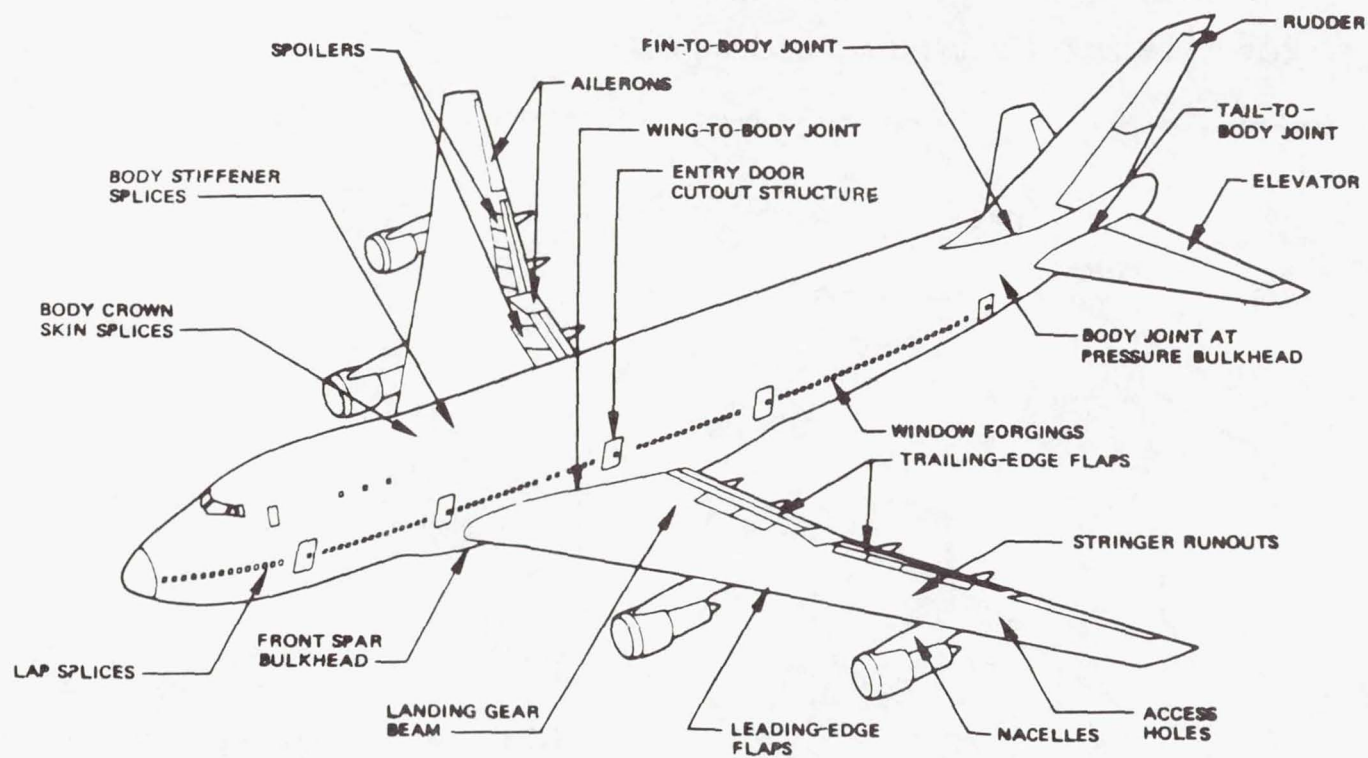


Figure 6.- Analysis locations on basic structure.



● ALSO DETAILS ON NOSE, WING,  
AND FUSELAGE LANDING GEARS

Figure 7.- Typical detail analysis locations.



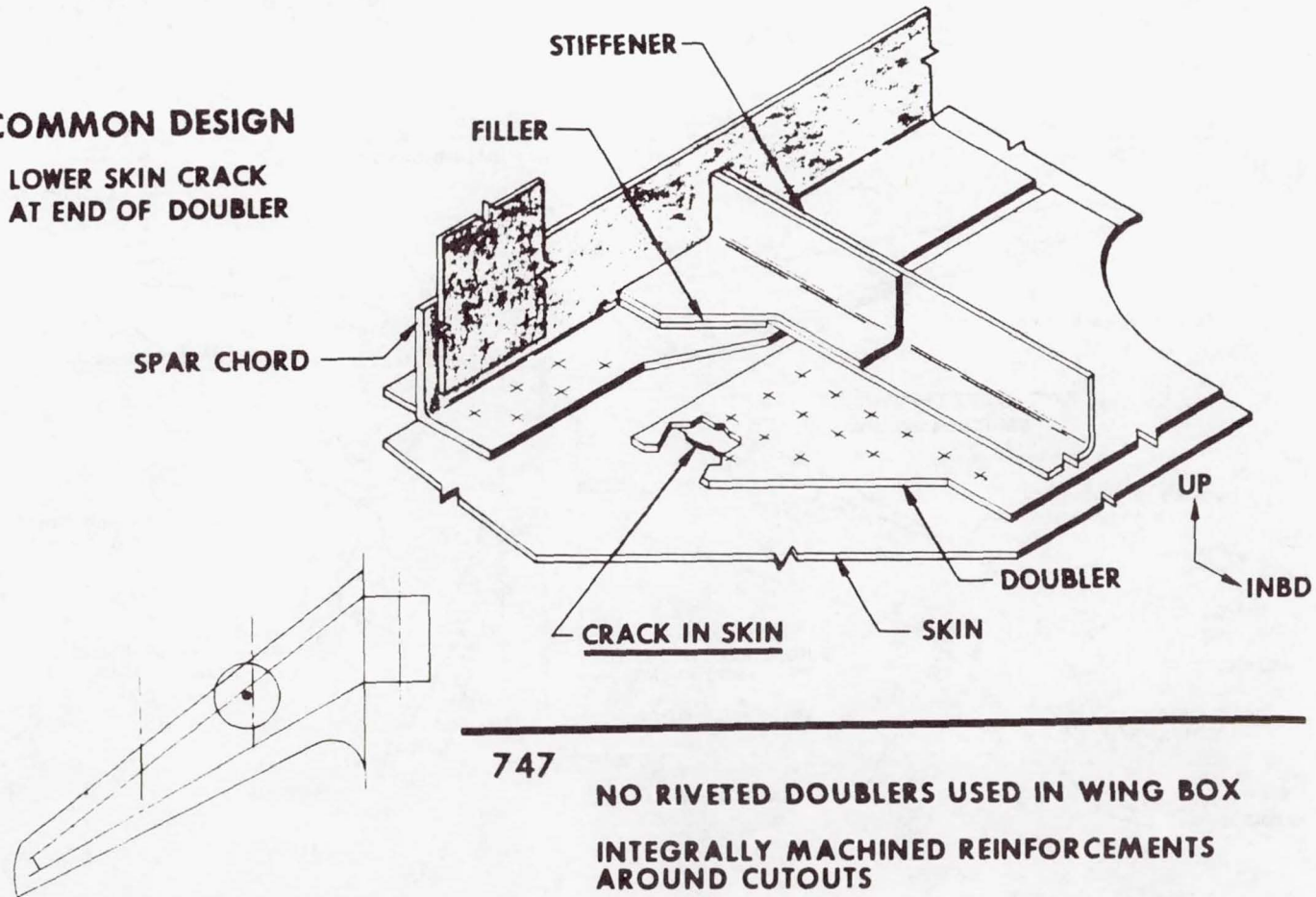
**COMMON DESIGN****LOWER SKIN CRACK  
AT END OF DOUBLER****747****NO RIVETED DOUBLERS USED IN WING BOX  
INTEGRALLY MACHINED REINFORCEMENTS  
AROUND CUTOUTS**

Figure 8.- Tension-critical design.

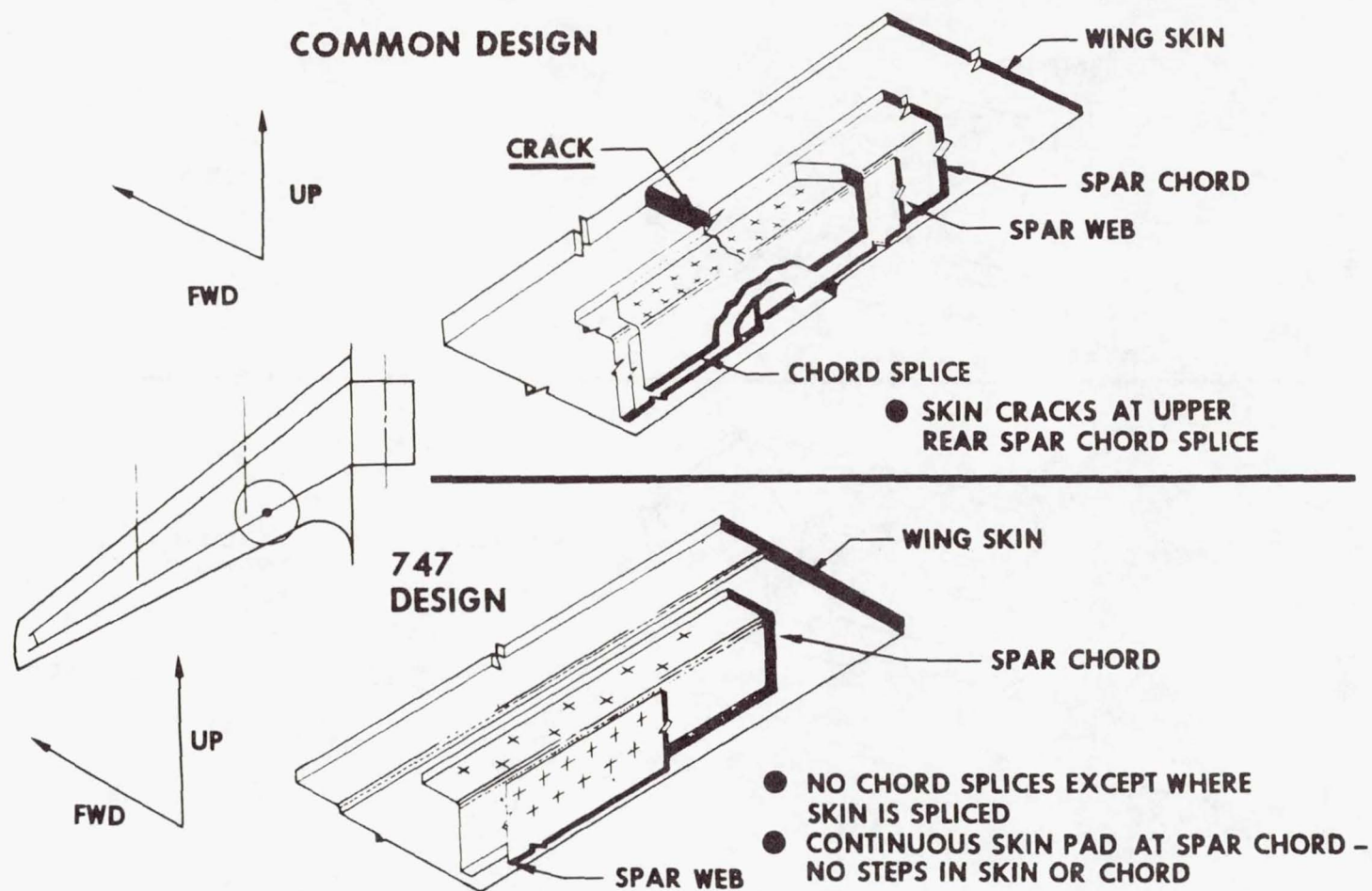
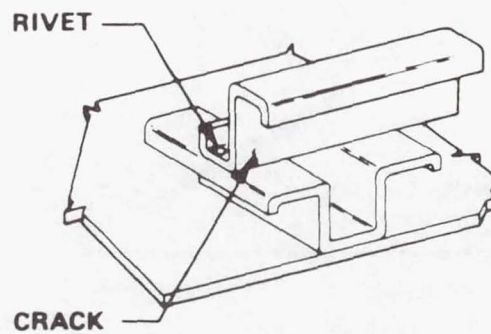


Figure 9.- Tension-critical design.



COMMON  
DESIGN



747  
DESIGN

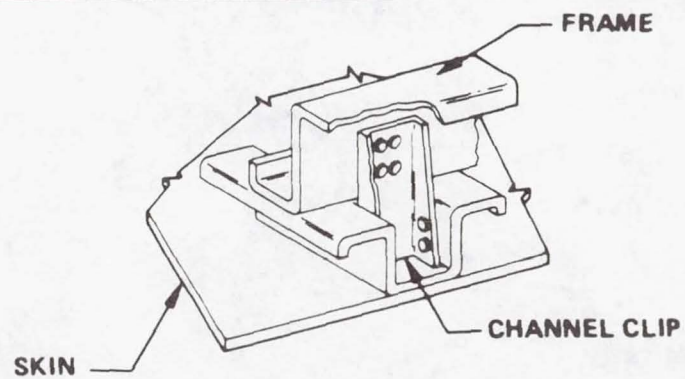


Figure 10.- Attachment of fuselage stiffener to frame.

PANEL DESCRIPTION	TEST STRESSES	NO. OF PANELS
1 ACCESS HOLE AND SPANWISE SPLICE	$10 \pm 9$ KSI & SPECTRUM	3
2 REAR SPAR STRINGER RUNOUT AND GEAR BEAM ATTACH AREA	$10 \pm 9$ KSI	2
3 NACELLE ATTACH AREA AT F 8	$10 \pm 9$ KSI	2
4 MIDSPAR RUNOUT AND NACELLE DRAG FITTING	$10 \pm 9$ KSI	2
5 JOINT AT SIDE OF BODY	$10 \pm 9$ KSI	2
6 FLAP DETAIL (FIBERGLASS) VC FLAP - FLEXURE CYCLING		5
7 FLAP DETAIL (AL HONEYCOMB) FLAP FAIRING SEGMENT - SONIC		
8 TRAILING-EDGE STRUCTURE AILERON SEGMENT - SONIC		
9 FUNCTIONAL FATIGUE AND FAIL-SAFE COMPLETE LE VARIABLE CAMBER FLAP AND COMPLETE OUTBOARD TE FLAP	SPECTRUM	1 FLAP

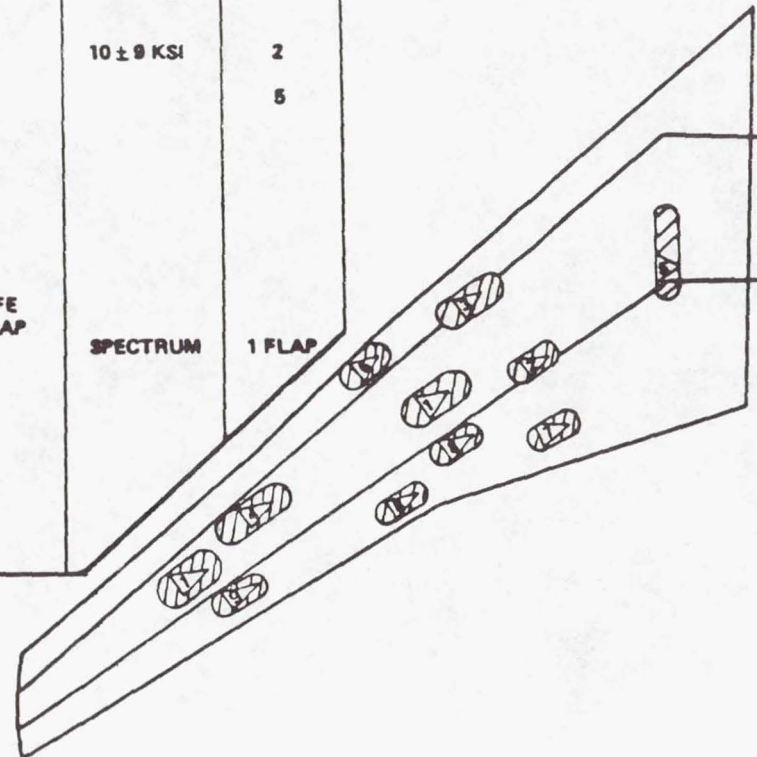


Figure 11.- Testing of wing lower surface.



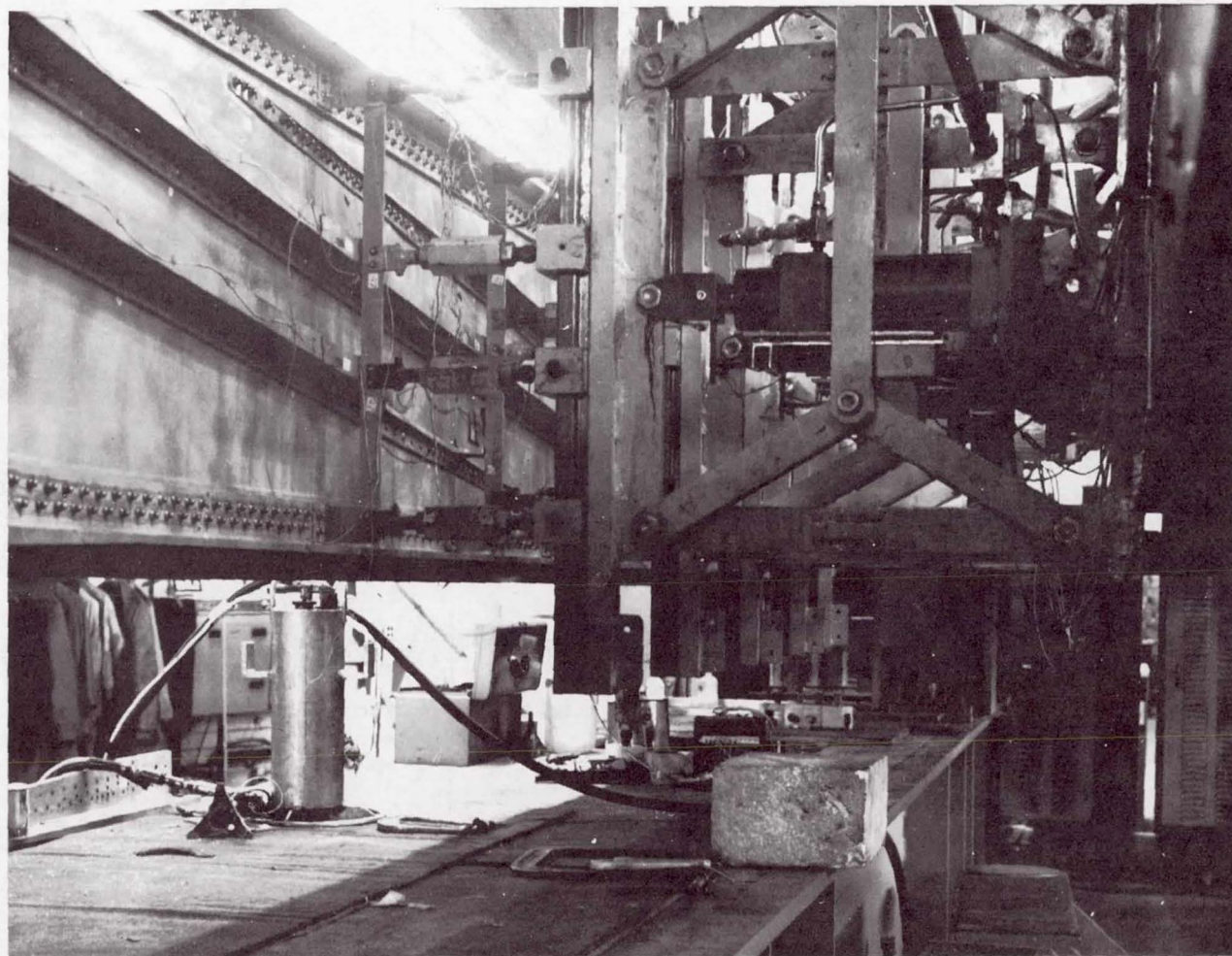


Figure 12.- Wing lower surface stringer runout.

PANEL DESCRIPTION		TEST STRESSES	NO. OF PANELS
1	BASIC SKIN-STRINGER (OUTBD)	$-5 \pm 18.5$ KSI	3
2	BASIC SKIN-STRINGER (INBD)		
3	JOINT AT SIDE OF BODY	$-5.5 \pm 14.5$	1
4	BASIC SKIN-STRINGER (CENTER)	$-5.5 \pm 14.5$	1

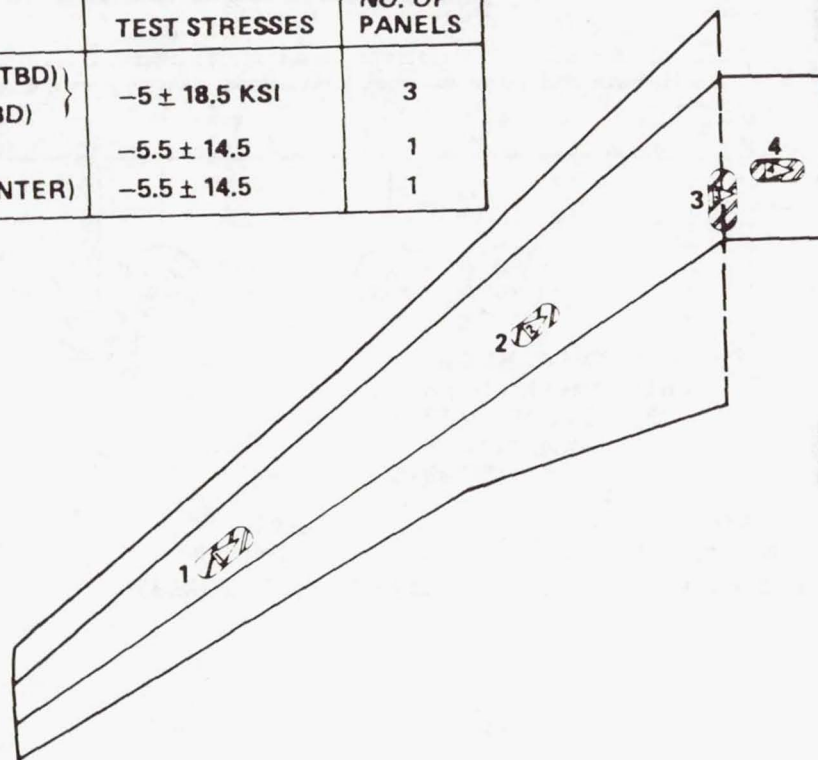


Figure 13.- Upper surface fatigue test panels.



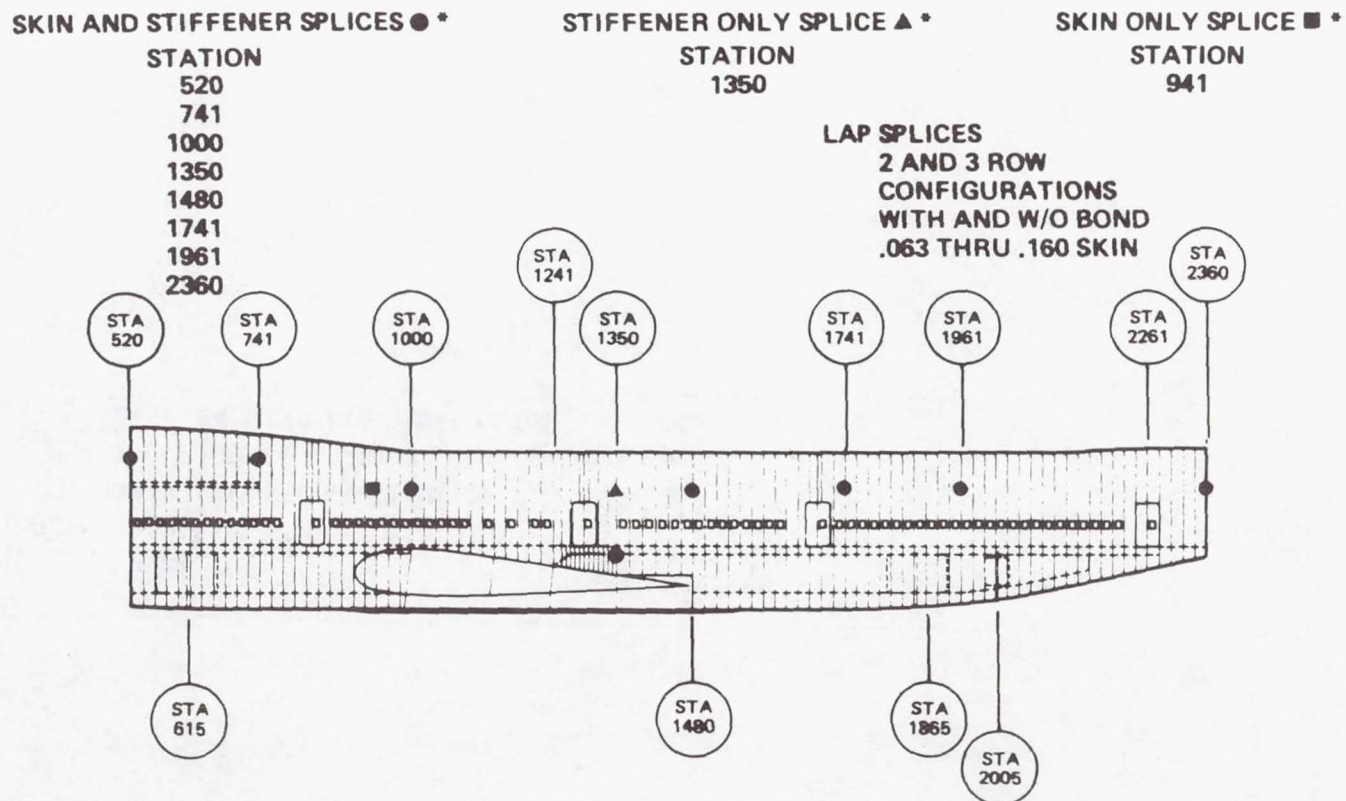
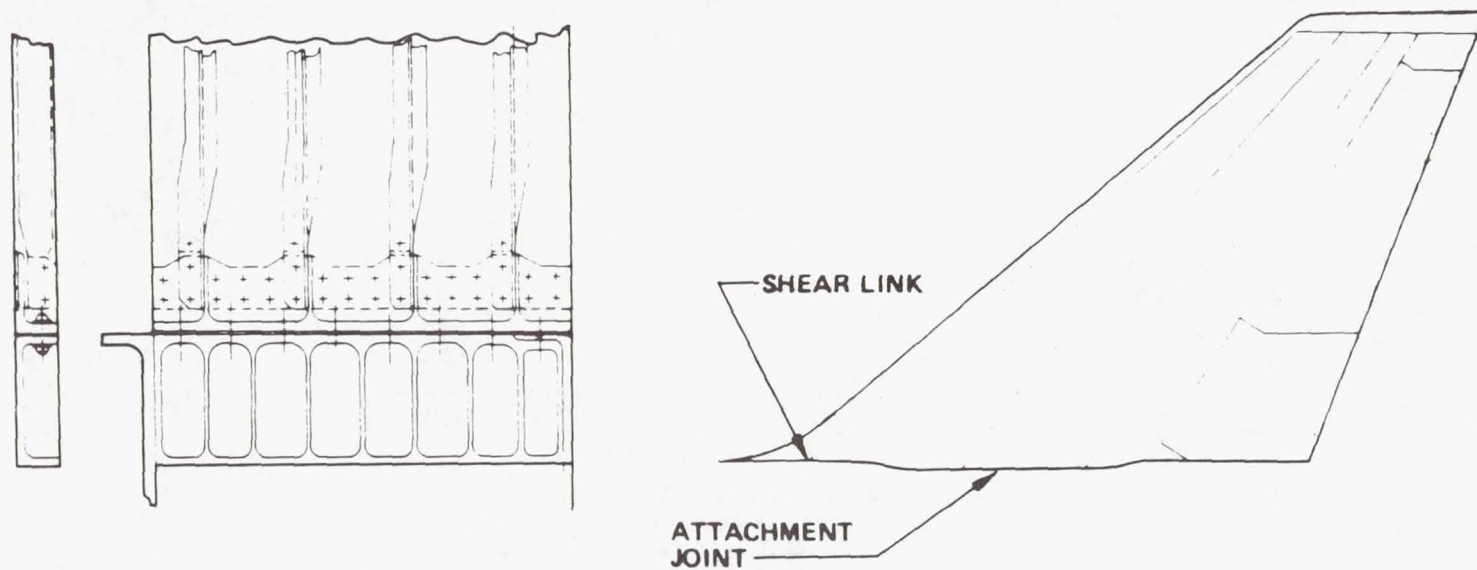


Figure 14.- Fuselage testing.



PANEL DESCRIPTION	TEST STRESSES	NO. OF PANELS
FIN TO BODY JOINT	$0 \pm 10$ KSI	3

Figure 15.- Vertical-tail testing.



PANEL DESCRIPTION	TEST STRESSES
1 BASIC STRUCTURE	$5 \pm 10$ KSI
2 CENTER SECTION JOINT	

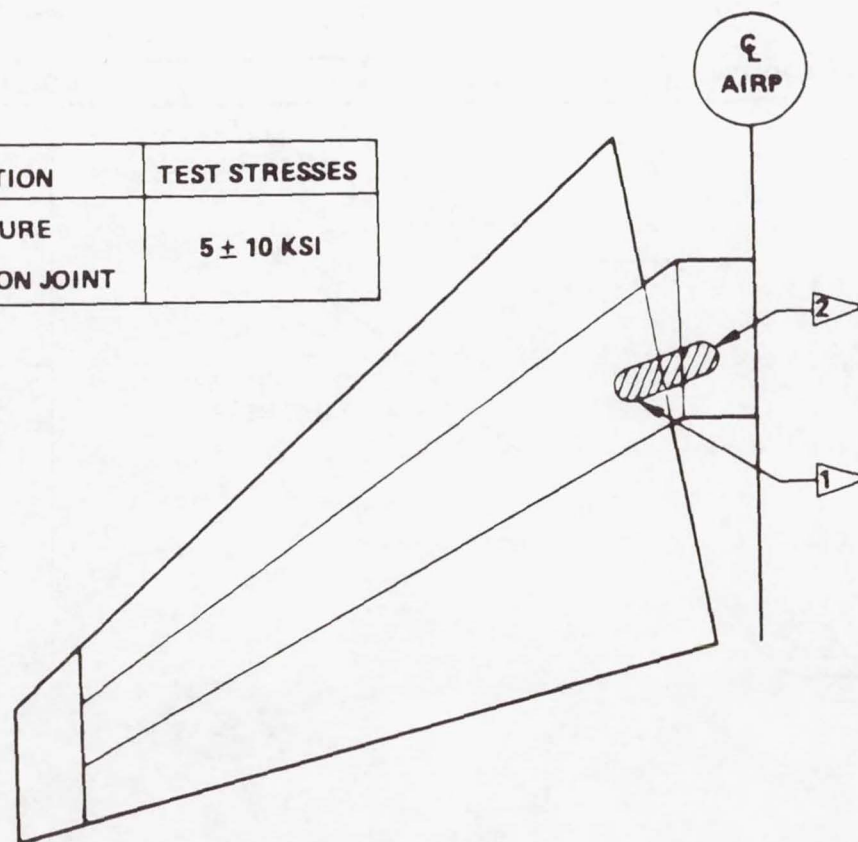


Figure 16.- Horizontal-tail testing (3 panels tested).

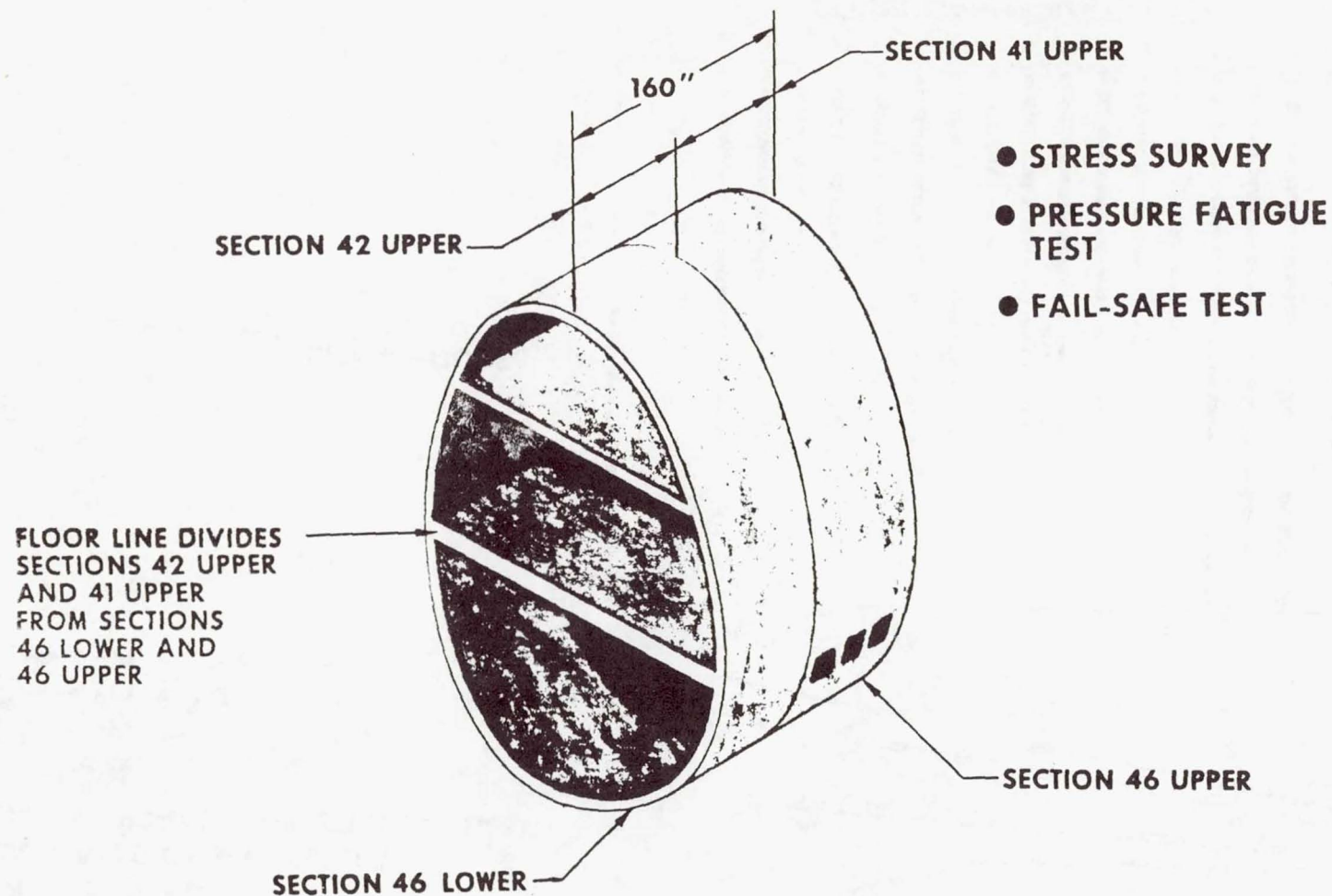


Figure 17.- Pressurized fuselage test.

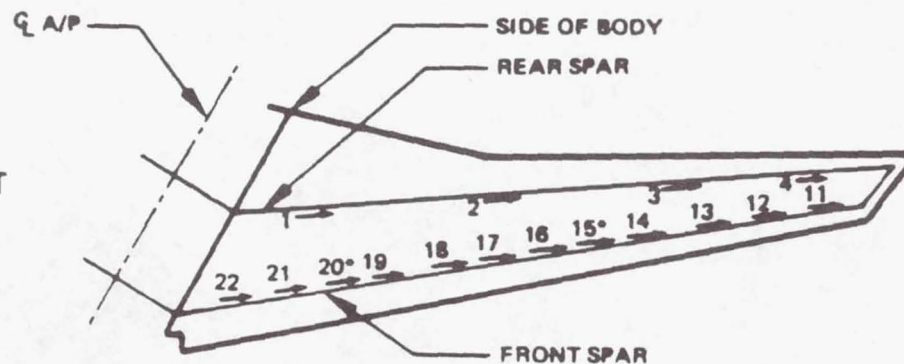


**NOTES:**

- (1) 2024-T3 MATERIAL
- (2) FRF = 4.0
- (3) BASED ON 3-HR FLIGHT
- (4) \*INDICATES SKIN SPLICE RUNOUT

**CODE**

- ..... FPI = 1/2.5
- FPI = 1/3.5
- FPI = 1/4.5



LIFE - HOURS

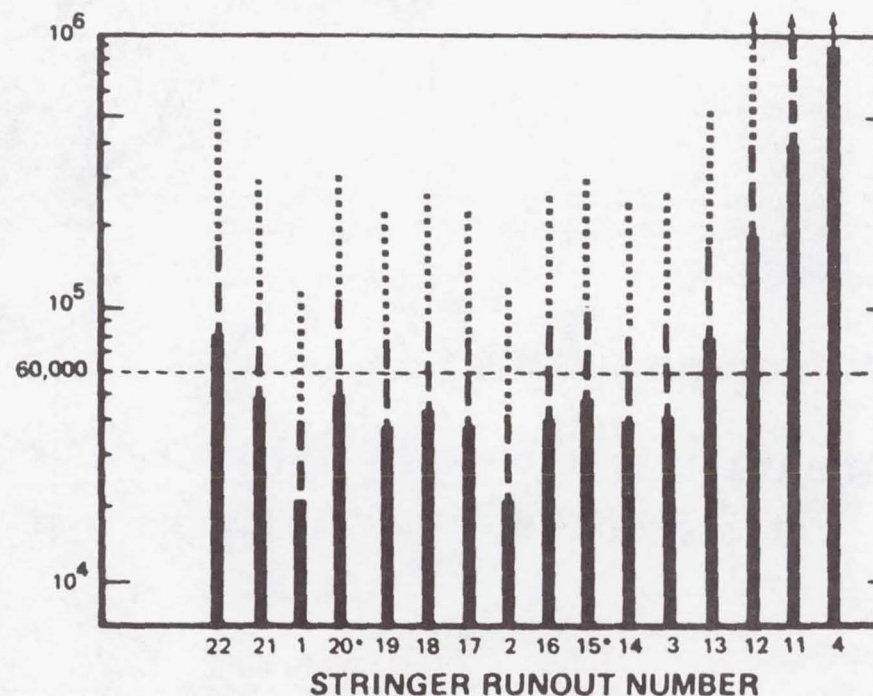


Figure 18.- Fatigue analysis example. Wing lower surface; stringer runouts.

● MATERIAL — 2024-T3

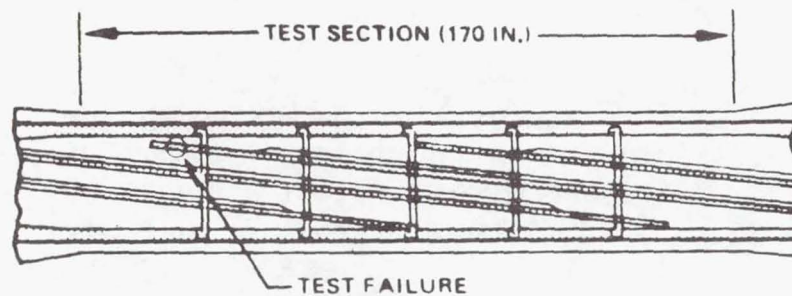
● TEST DATA

REFERENCES	TEST STRESS KSI	APPLICABLE TEST CYCLES
EWA 21-110012, PANEL NO. 2	$10 \pm 9$	327,200

● DEMONSTRATED FPI = .361 =  $1/2.77$

● FATIGUE PERFORMANCE RELIABILITY FACTOR (FRF)

$$\text{FRF} = 2.95$$



TEST DEMONSTRATED F.P.I.

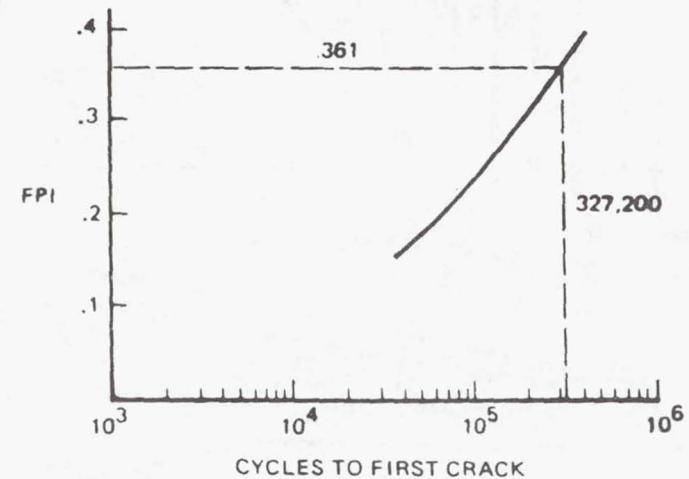
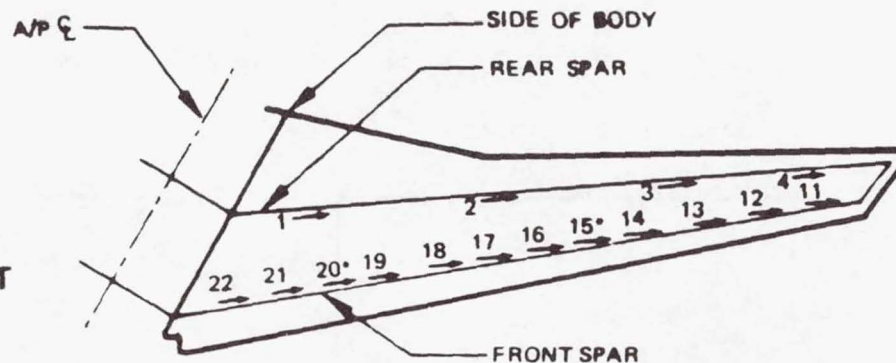


Figure 19.- Panel test data example. Wing lower surface; typical stringer runout.



**NOTES:**

- (1) 2024-T3 MATERIAL
- (2) FRF = 2.95
- (3) FPI = 1/2.77 FOR TYPICAL
- (4) FPI = 1/3.14 FOR SKIN SPLICE
- (5) \*INDICATES SKIN SPLICE RUNOUT
- (6) BASED ON 3-HOUR FLIGHT



LIFE - HOURS

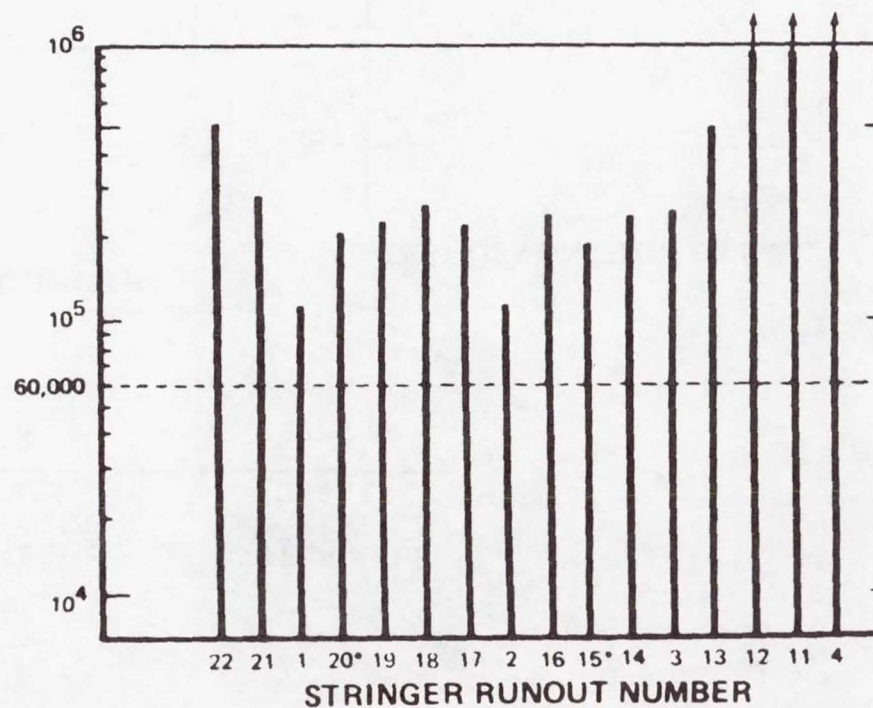


Figure 20.- Fatigue performance example. Wing lower surface; stringer runouts.

2024-T3 MATERIAL  
 FRF = 2.76  
 FPI = 1/2.9

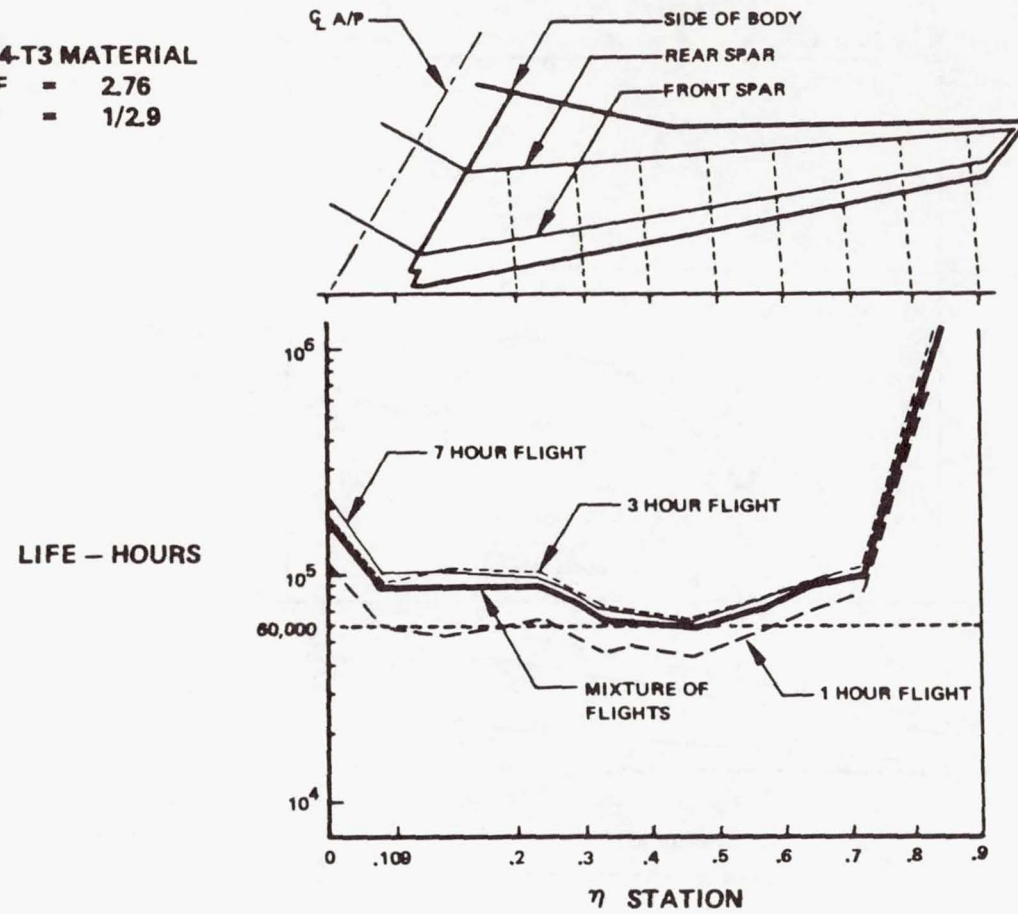


Figure 21.- Fatigue performance of wing lower surface on 747 basic passenger airplane.



7075-T6 MATERIAL  
 FRF = 2.22  
 FPI = 1/2.5

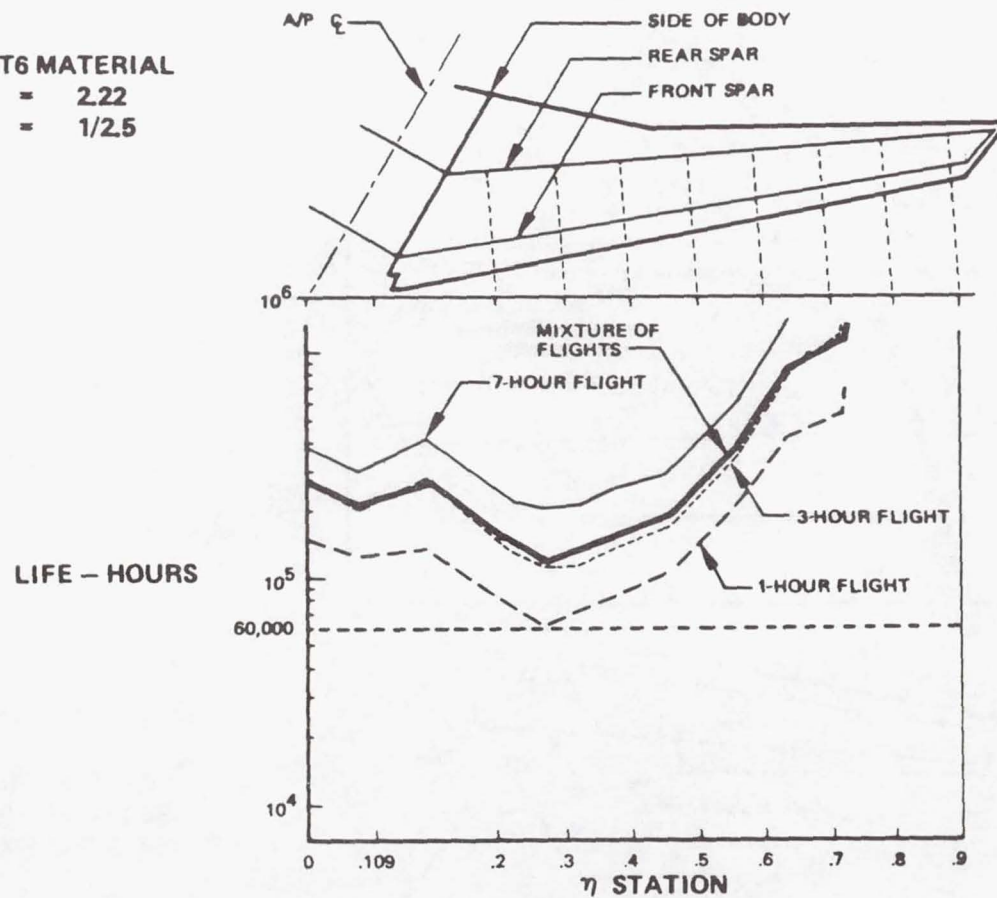


Figure 22.- Fatigue performance of wing upper surface on 747 basic passenger airplane.

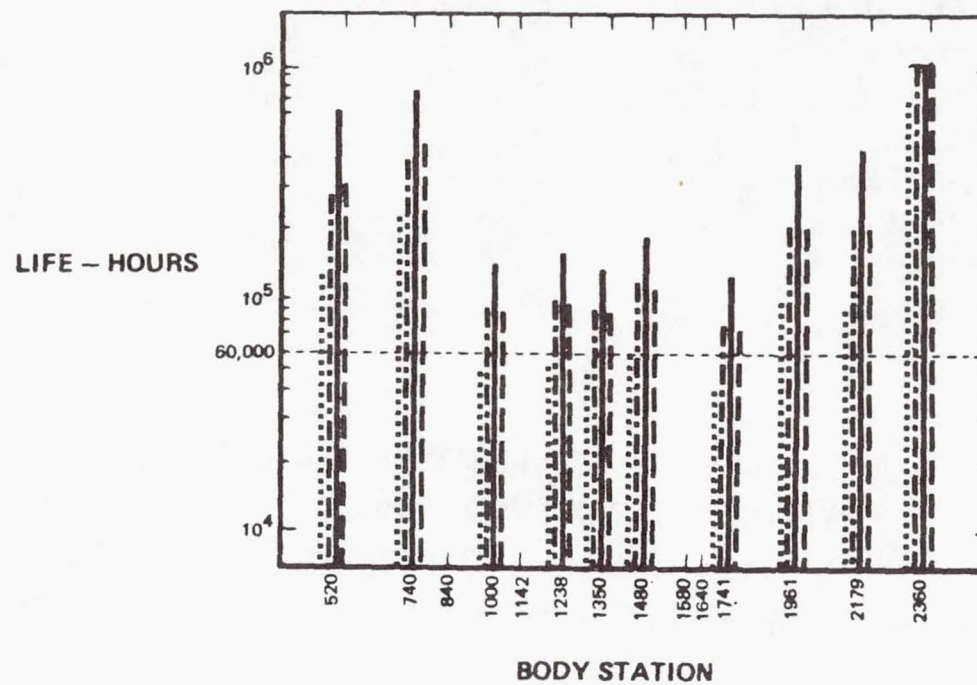
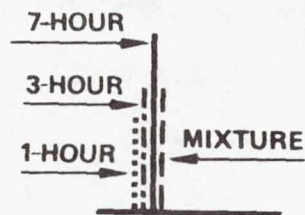
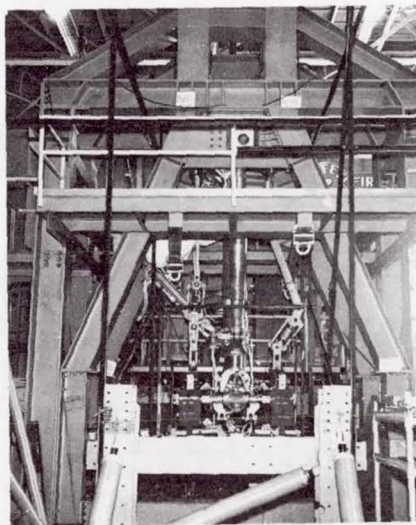


Figure 23.- Fatigue performance of fuselage crown stringer splices on 747 basic passenger airplane.

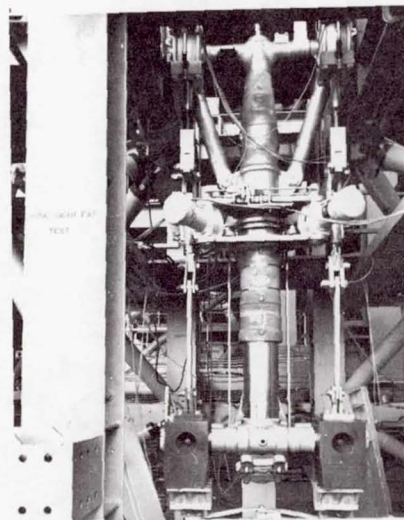


### DESCRIPTION

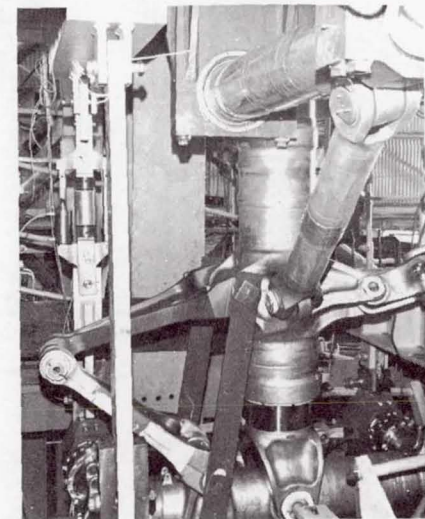
1. TEST SPECIMEN IS A PRODUCTION GEAR, EXCLUDING WHEELS, TIRES AND THREE BRAKES
2. JIG SIMULATES THE AIRPLANE SUPPORT STRUCTURE.
3. LOADS ARE APPLIED IN A MANNER TO SIMULATE ACTUAL GROUND LOADING.
4. TEST SCHEDULED FOR EQUIVALENT OF  $4 \times 60000 = 240000$  HOURS IN MIXTURE OF FLIGHTS.



WING GEAR



NOSE GEAR



BODY GEAR

Figure 24.- Landing-gear fatigue test.

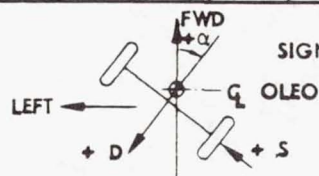
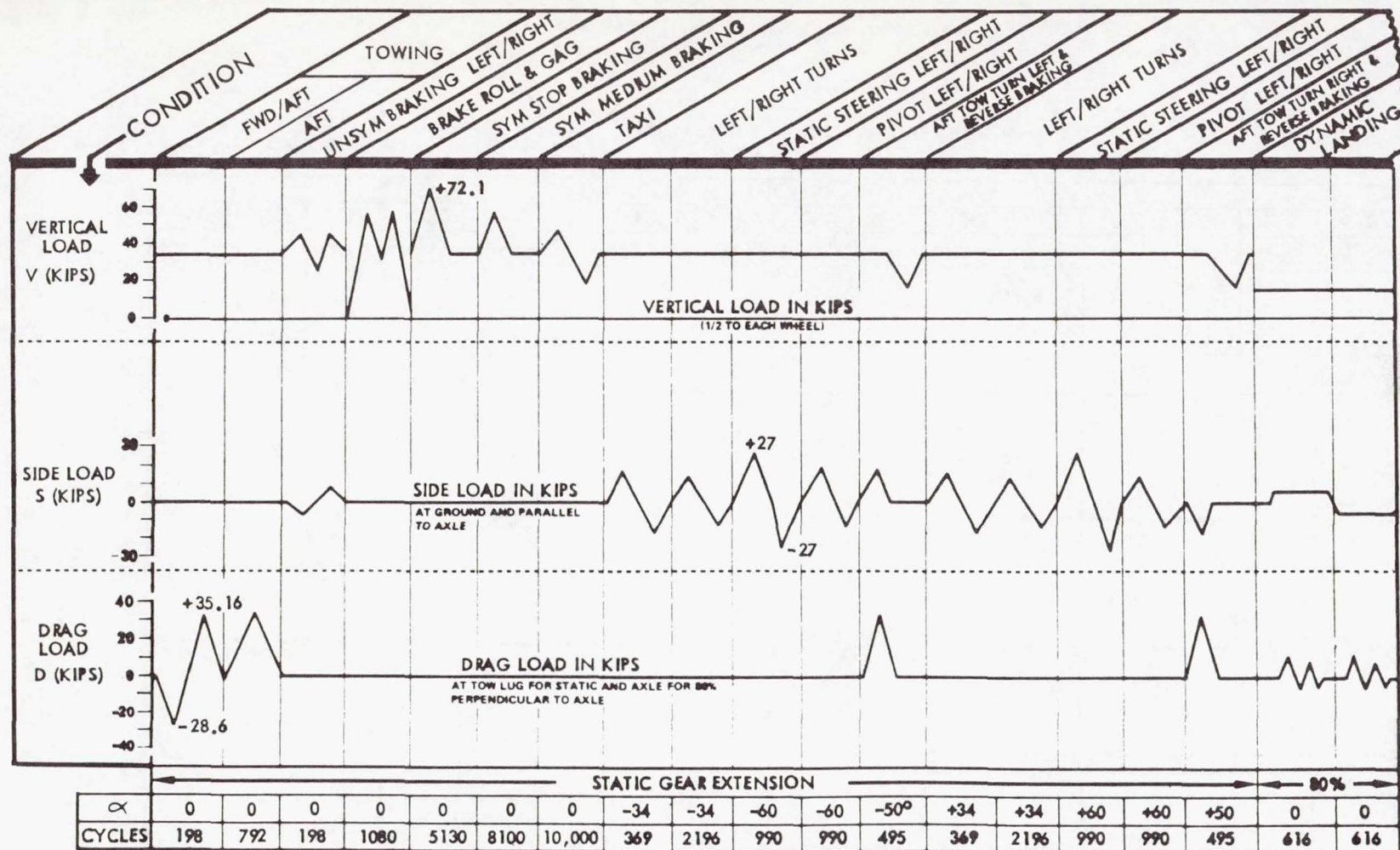


Figure 25.- 747 nose gear fatigue test. Loading block.



C.4

172

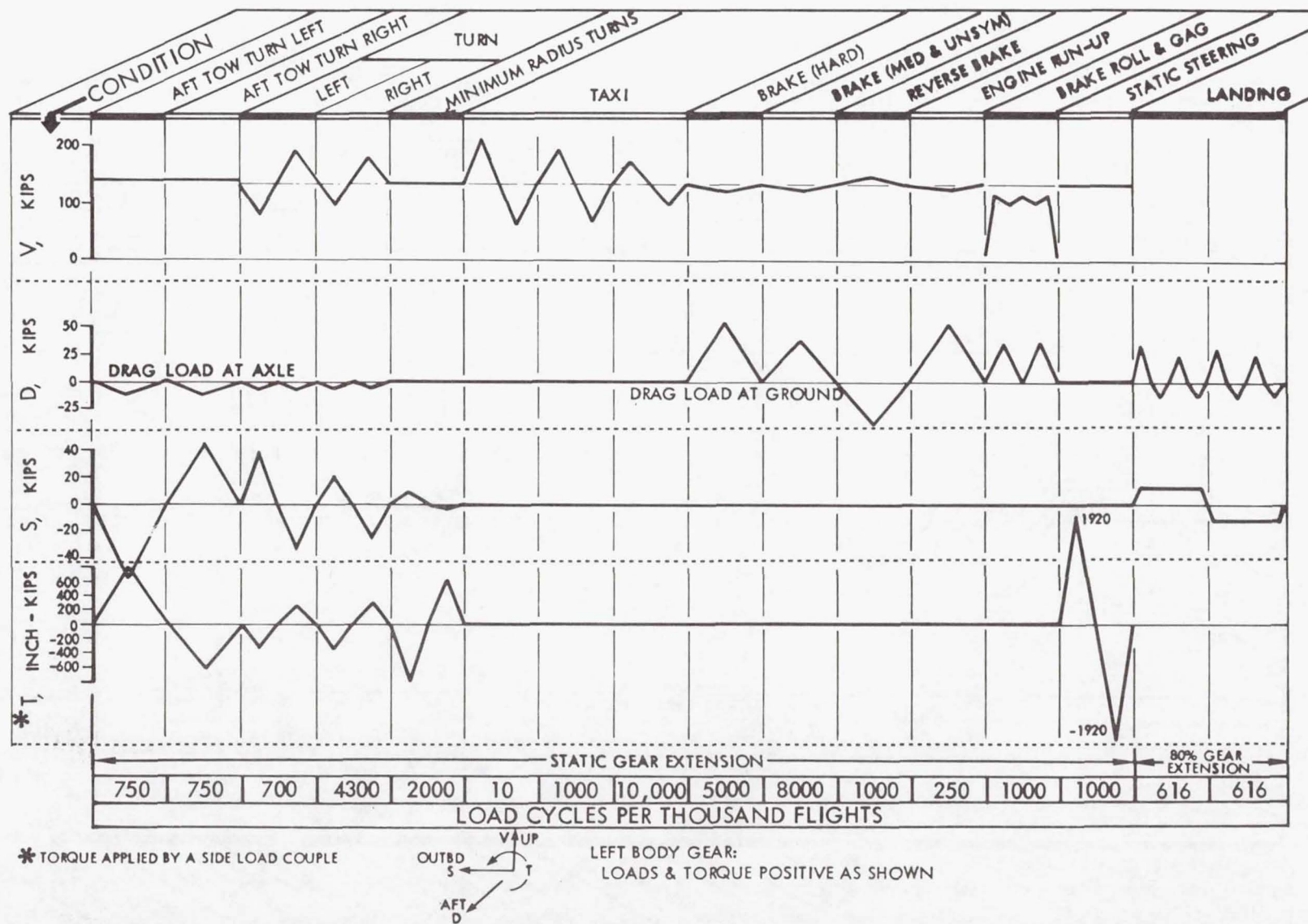


Figure 26.- 747 body gear fatigue test. Loading block.

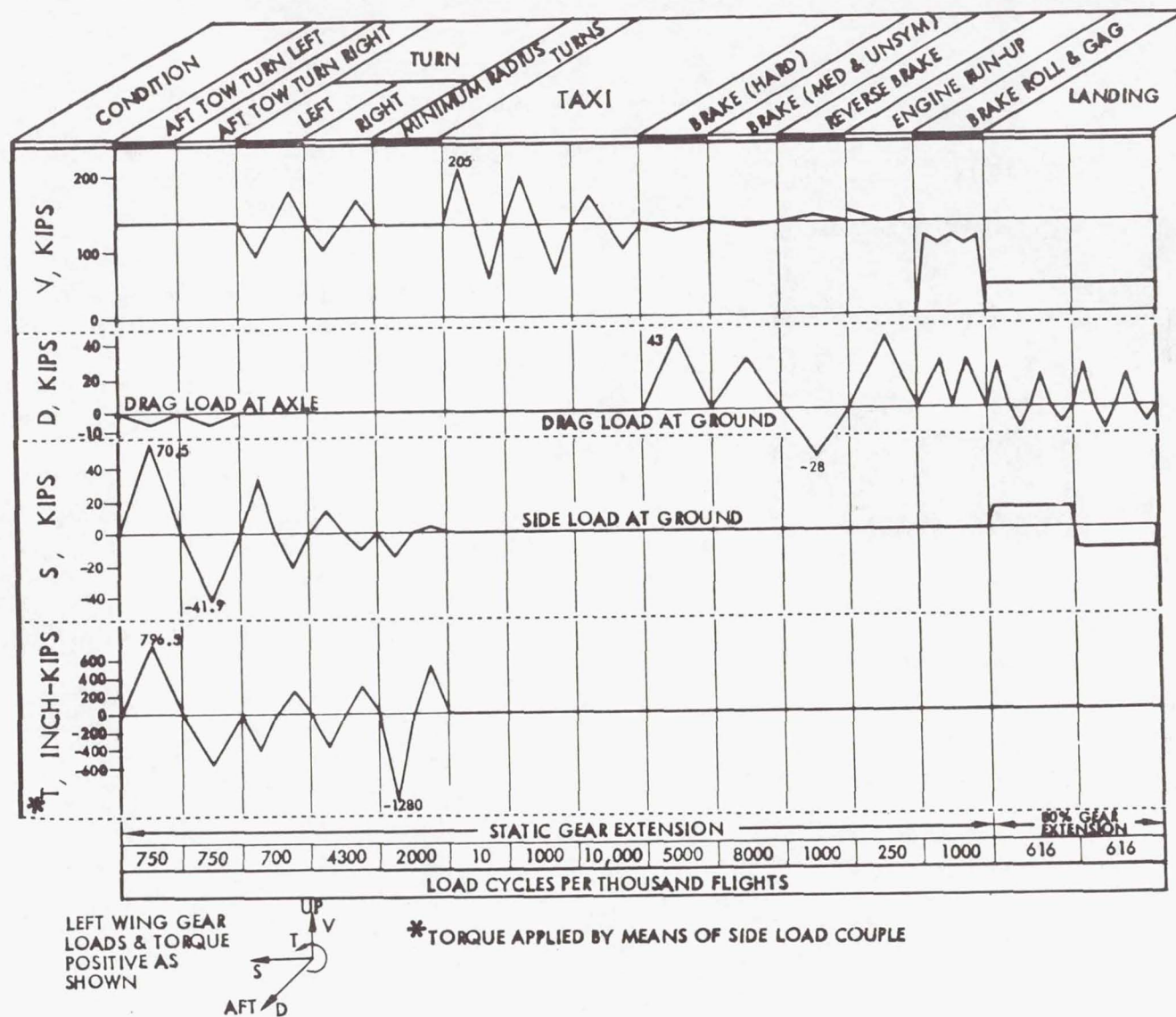
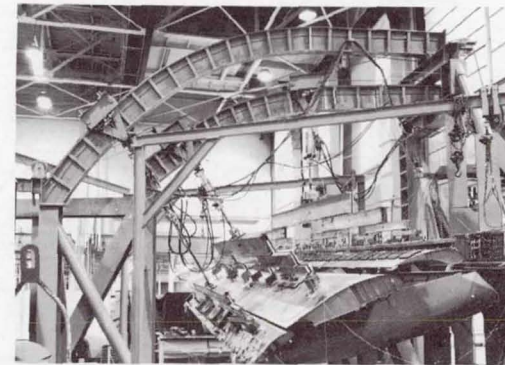


Figure 27.- 747 wing gear fatigue test. Loading block.

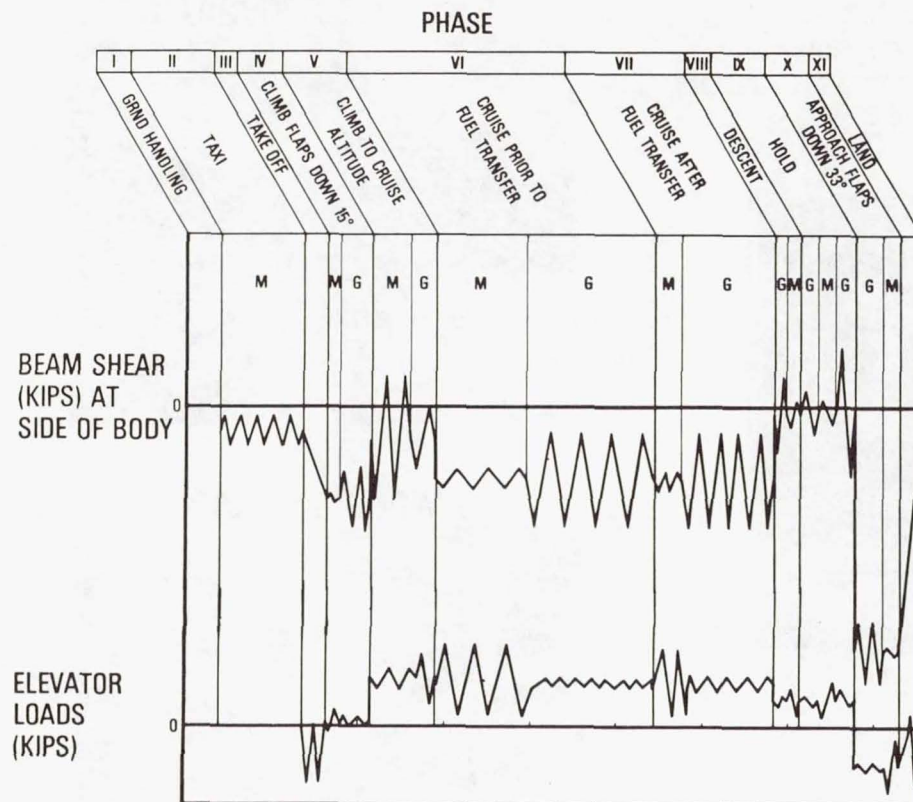


- TEST SPECIMEN CONSISTS OF COMPLETE PRODUCTION FLAP AND DRIVE SYSTEM
- TESTING INCLUDES STRESS SURVEY, SYSTEM CYCLIC TESTING, STRUCTURAL FATIGUE TESTING AND FAILSAFE TESTING
- SIMULATED AIRLOADS ARE APPLIED DIRECTLY TO THE FLAP SURFACES
- TEST IS SCHEDULED FOR EQUIVALENT OF 2 X 60,000 (120,000) HOURS IN MIXTURE OF FLIGHTS



OUTBOARD FLAP SYSTEM

Figure 28.- Tests of trailing-edge flap and flap drive system.



**STABILIZER TEST SET-UP**

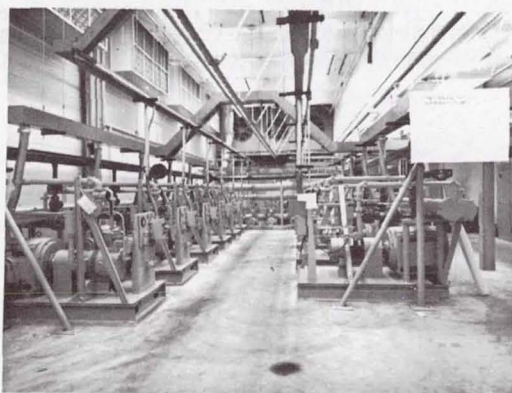
- NOTE:
- M = MANEUVER CYCLES
  - G = GUST CYCLES
  - TEST IS SCHEDULED FOR EQUIVALENT OF 2 X 120,000 (240,000) HOURS IN MIXTURE OF FLIGHTS

Figure 29.- Fatigue test of horizontal stabilizer.





CONTROL ROOM



HYDRAULICS ROOM



TEST SET-UP

NOTE: TEST IS SCHEDULED FOR 2 X 60,000 (120,000) HOURS IN MIXTURE OF FLIGHTS.

Figure 30.- Airplane fatigue test.





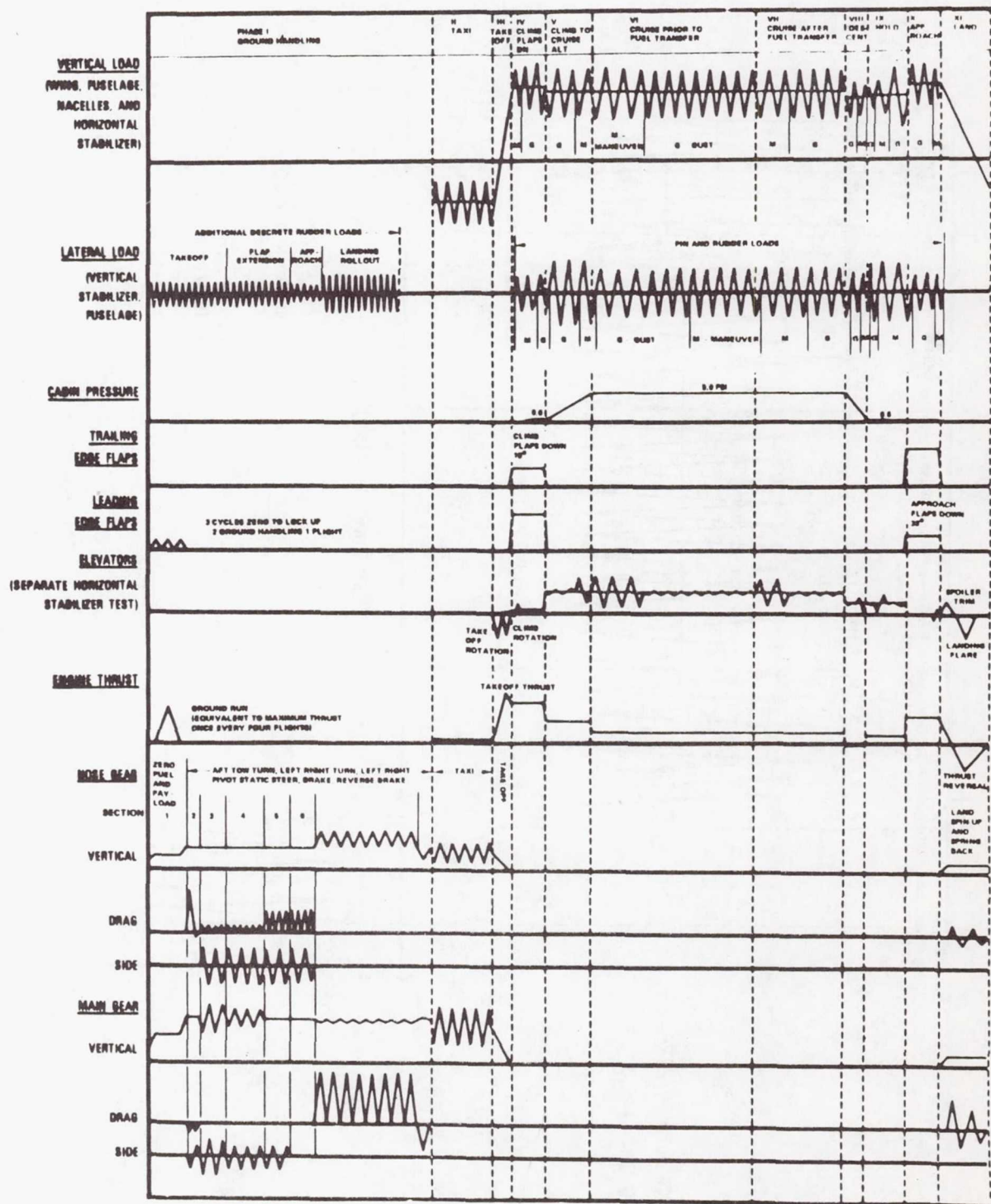


Figure 32.- 747 full-scale fatigue test.

# FATIGUE AND FAIL-SAFE DESIGN FEATURES OF THE DC-10 AIRPLANE

By M. Stone  
Douglas Aircraft Company  
McDonnell Douglas Corporation  
Long Beach, California, U.S.A.

N72-29899

## SUMMARY

The philosophy and methods used in the design of the DC-10 aircraft to assure structural reliability against cracks under repeated service loads are described in detail. The approach consists of three complementary parts: (1) the structure is designed to be fatigue resistant for a crack-free life of 60 000 flight hours; (2) inasmuch as small undetected cracks could develop from other sources, such as material flaws and manufacturing preloads, the structure also is designed to arrest and control cracks within a reasonable service-inspection interval; and (3) a meaningful service-inspection program has been defined on the basis of analysis and test experience from the design development program. This service-inspection program "closes the loop" to assure the structural integrity of the DC-10 airframe. Selected materials, fasteners, and structural arrangements are used to achieve these design features with minimum structural weight and with economy in manufacturing and maintenance. Extensive analyses and testing were performed to develop and verify the design.

The basic design considerations for fatigue-resistant structure are illustrated in terms of material selection, design loads spectra, methods for accurate stress and fatigue damage analysis, and proven concepts for efficient detail design. Special emphasis is given to the DC-10 development test program. The initial stage of this program was a series of screening tests of candidate materials, types of fasteners, stress coining, surface treatments, manufacturing processes, and so forth.

## INTRODUCTION

The structural design goals for the DC-10, shown in figure 1, were to produce an airplane that is superior to the DC-8 and DC-9 and that will be operated safely and economically for at least 20 years. Three complementary criteria were established to assure this goal:

(1) The structure has a crack-free life of 60 000 flight hours on the basis of design, analysis, and tests in excess of 120 000 flight hours.



(2) The structure is damage tolerant. Adequate residual strength is available after a crack has propagated, and the basic structural configuration provides for slow crack growth and arrestment before reaching critical lengths.

(3) An inspection program has been established on the basis of a fail-safe structure with adequate external detectability, as verified by component tests. In addition, the start of inspection and sampling intervals were based on fatigue, corrosion, and crack-propagation resistance of the structure.

## STRUCTURAL RELIABILITY

A distribution is shown in figure 2 to indicate the overwhelming influence of development testing and detail design on the structural reliability of the DC-10. These two items were accomplished during initial design stage; they allow true optimization of the DC-10 airframe by "placing the structural material where it is most effective" and thereby provide maximum-fatigue-life assurance. In any event, it is necessary to establish fatigue criteria, identify sensitive areas, establish fastener policies, and plan an early development testing program. Without these procedures, the structural design cannot be successful.

A new computer analysis system was used with a high degree of accuracy in predicting the actual working stress levels and deflections in the structural elements. Full-scale fatigue tests were used to reveal weak links and verify that proper analysis and detail testing were accomplished during the aircraft design.

## FATIGUE-SENSITIVE AREAS

Once the fatigue-sensitive areas are recognized, proper emphasis can be given to these problem areas to assure fatigue reliability. In the design of the DC-10 aircraft, these areas, as shown in figures 3 and 4, were given special attention during design, analysis, and testing.

The fatigue reliability of the wing box and fuselage pressure shell, splices, joints, and other discontinuities has been made equal to or better than that of the basic structural items 4, 9, and 10 of figure 3.

## ANALYSIS

### Evolution of FORMAT

In order to assure design static and fatigue strength, actual working stresses and deflections were predicted with the use of the FORTRAN Matrix Abstraction Technique

(FORMAT) developed by Douglas Aircraft Company over a period of 20 years (ref. 1). Improved computer methods and techniques, such as FORMAT, gave increased analysis capability and visibility over the original DC-8 airframe, as shown in figure 5.

The FORMAT system is fully automatic so, even during preliminary design, structural weight is minimized and fatigue characteristics are improved by placing the material where it is most effective (ref. 2).

### Deflections

Figure 6 shows the excellent correlation of deflections from FORMAT analysis with test results. The comparison shows deflections for limit-positive-load conditions for the wing, fuselage, and horizontal stabilizer. The test results were obtained from a successful static-load test completed on the second production aircraft in August 1970. The aircraft was fully instrumented with strain gages and deflection transducers by using a sophisticated 1000-channel data system.

### Stress Analysis

Figure 7 shows the stresses in the complicated root section of the wing subjected to limit positive-maneuver loads (from the front spar (F.S.) to the rear spar (R.S.)) and the equally sensitive fuselage section above the wing subjected to limit down-bending loads. The circles represent static test measurements, and the solid line indicates the stresses computed by FORMAT analysis. The dashed lines indicate the stresses computed by elementary beam theory which underestimates the stresses at the sensitive structural areas. The excellent accuracy of the detail stress analysis allows the calculation of reliable local stress levels and assures the fatigue quality of the DC-10 structure.

### Working Stresses

The working stress levels for the DC-10 wing have been carefully established on the basis of the working stresses used on earlier airplanes which, since, have had proven longevity (fig. 8). The working stress levels for the fuselage shell have increased mainly because of the wide-body cross section. This increase in stress has been accomplished with no loss in fatigue strength through improvement in detail design.

### Fatigue Quality Structure

The increase in working stress levels and the additional requirement for dependable long-life aircraft make it mandatory to increase the fatigue quality of all structural elements. The results of several thousand constant-amplitude component fatigue tests of structural elements of various configurations are summarized in figure 9. (R is the



maximum stress in any cycle divided by the minimum stress in the cycle.) It is noteworthy that the basic structure has considerable longevity as attested by the DC-3, DC-6, DC-7, and DC-8 airframe structure. As shown, the DC-6 and DC-7 joints were critical; the DC-8 joints were practically equivalent to the basic structure, and the DC-10 joints are equal to or better than the basic structure. The DC-10 structure incorporated the best structural details gained from knowledge of DC-8 structure and DC-10 development testing.

## DEVELOPMENT TESTS

The results of over 2000 fatigue development tests conducted on the DC-8 and DC-9 have been used in conjunction with an additional 1700 fatigue development DC-10 tests to substantiate crack-free, long-life structures. The fatigue development test program has been completed in time to permit the designer to incorporate the test findings into the design. The DC-10 program was planned to utilize small inexpensive specimens as well as large aircraft components.

### Specimen Development Testing

Double bow-tie wing specimens have been used to obtain reliable fatigue data in minimum time and at minimum expense. Results from specimens of this type have been found to correlate closely with results from more complex and expensive specimens composed of skin and stringers. These tests permit rapid evaluation of various attachment types, hole sizes, hole-preparation methods, material-thickness effects, claddings, and so forth, on the fatigue life of the basic structure. Bow-tie wing specimens cannot be used for all configurations; therefore, more typical simple wing slices were also used to evaluate fasteners. Over 300 specimens of these types were tested. The test results are shown in figure 10.

The simple longitudinal and transverse skin splices and the longeron-to-frame-connection fuselage fatigue development tests were separately conducted to evaluate and screen materials, fastener selection, surface treatment, and so forth. The results of the longitudinal and transverse tests are shown in figure 10.

### Component Development Testing

Structural-wing-component fatigue development tests were conducted on actual parts that are used in the final aircraft design. All the knowledge gained through the bow-tie and other specimen testing was incorporated in the structural components. Approximately 140 tests were conducted. These aircraft components (fig. 3) were tested and improved until at least 150 000 to 350 000 flight hours were attained. The results are shown in

figure 11 for constant-amplitude tests. After the final configurations were selected, flight-by-flight spectrum tests were conducted on major components to verify the minimum of 150 000 flight hours.

Six curved stiffened 168- by 104-inch panels, representing various areas of the fuselage, were tested under combined biaxial loads, pressure, and inertia loads. The design features gained on the previously described specimen development tests were incorporated into the design of these panels. The panels consisted of eight frames, 11 longerons, four-way splice (longitudinal and transverse) basic structure, and longeron-to-frame connections. Fatigue tests were performed on the curved panels. Both pressure and axial loads were cycled at constant load levels to simulate stresses higher than those which would produce fatigue damage equivalent to the full spectrum of loads experienced by the aircraft in flight (fig. 11). Additional fatigue tests were conducted on window-belt panels and pressure-bulkhead panels.

These specimens were tested in 1.5-million-pound fatigue test machines at the laboratory test facility. Four of these machines could each hold and test two specimens simultaneously. In this way, the tests were finished quickly so that the findings could be incorporated into the drawings early in the design.

#### DETAIL DESIGN

The basic design considerations for fatigue-resistant structure have been established for the DC-10 by paying strict attention to proven detail design concepts. Before fabrication, wooden models of all important structural fittings were made to review for notch concentrations and unexpected machine mismatch areas. Photo stress tests were also conducted on main fittings to determine the stress distributions and peak stress magnitudes in areas where stresses are difficult to predict. On the basis of DC-8 and DC-9 experience, coupled with the extensive DC-10 development test program, many fatigue design features were established, as shown in figures 12, 13, and 14.

The fatigue life of the DC-10 inboard sweep break skin-stringer joint (fig. 12) became greater than that of the adjoining basic structure after the components were properly tapered and material was added locally at the discontinuities. Interference-fit attachments were also used to increase fatigue life.

To attain maximum fatigue-resistant structure of basic leading-edge skin to spar-cap structure, a sacrificial doubler has been used to attach the interchangeable leading-edge section to the front-spar (F.S.) cap as shown in figure 13. This design allows the use of interference attachments in the heavier spar-cap flanges.

Figure 14 shows the fuselage detail design features. The use of properly stepped doublers around the fuselage door corners reduces stress concentrations. Adding a local



channel pad to the longeron reduces local bending between the longeron and frame connection. The scalloped longeron splice fitting and fingered doublers assure uniform load transfer and reduce the first attachment load.

### QUALIFICATION TESTING

The DC-10 is undergoing a flight-by-flight production-airplane fatigue test to 120 000 flight hours and 84 000 flights. The fourth production airplane is divided into three major sections, as shown in figure 15. The shaded test structures shown at the ends of each section represent steel drums that are a minimum of one fuselage diameter in length to assure that load is properly introduced into the aircraft structure. Special design aluminum transition sections modulate interaction effects between the steel drums and aircraft structure to preclude fatigue failures in that region. The division into three sections was based on the following factors:

- (1) There are fewer compromises in the load spectrum.
- (2) Noncritical loads can be eliminated and other critical loads added for each undivided section.
- (3) Sections can continue cycling while one section is down for inspection or repair.

The cycles are being applied to each individual section as shown in the following table:

Type of load	Number of cycles applied to -		
	Forward section	Wing-fuselage section	Aft section
Ground loads . . . . .	252 000	389 840	168 000
Flight loads . . . . .	383 040	913 332	753 648
Landing impact . . . . .	37 800	36 540	37 800
Ground-Air-Ground (G-A-G)* . . . . .	84 000	84 000	84 000
Fuselage pressurizations . . . . .	84 000	84 000	84 000
Total:	840 840	1 507 712	1 127 448

\*Inherently obtained because the load spectrum is applied on a flight-by-flight basis.

Testing experience has shown that proper loads can be applied more accurately to smaller components subjected to large concentrated loads. The main and nose landing gears and adjacent support structure, therefore, are tested separately so that every detailed area is subjected to the millions of cycles that occur in service (ref. 3).

## DAMAGE-TOLERANT STRUCTURE

The DC-10 primary structure is designed to be fail-safe, with the exception of the landing gear for which fail-safe design is not practical. The fail-safe criterion used in the DC-10 is more stringent than specification requirements; that is, the structure must support the fail-safe load soon after several components have failed.

### Identification of Sensitive Areas (Fuselage)

The radial loading due to cabin internal pressure can start a longitudinal skin crack in two locations:

- (1) At the skin line where the fingered doubler is attached to the skin of the longitudinal skin splice, shown in figure 16(a) (This type of fatigue crack results in a one-bay longitudinal skin crack.)
- (2) At the first attachment of shear clip frame to skin, shown in figure 16(b) (The fatigue crack of this type can propagate into a two-bay longitudinal crack.)

The combined pressure and axial loads can start a transverse skin crack where the longeron is attached to the frame. After failure of the longeron a skin crack can form which may propagate into two adjacent skin bays, shown in figure 16(c). Recognition of these facts led to the following damage-tolerant conditions selected for the fuselage shell structure shown in figure 16(d):

- (1) Two-bay longitudinal crack with center crack stoppers failed
- (2) Two-bay transverse crack with center longeron failed

The design selected contains titanium crack stoppers at each frame capable of arresting a two-bay longitudinal crack. The hat section longerons act as natural transverse crack stoppers.

### Stress Analysis (Fuselage Panels)

The equation for the fracture strength of stiffened thin panels containing a crack is

$$\sigma_R = \frac{K_C R_{ct}}{\sqrt{W \tan\left(\frac{\pi a}{W}\right)}}$$

where

$\sigma_R$       gross residual stress, psi

$K_C$       plane stress fracture toughness, psi  $\sqrt{\text{in.}}$



$$R_{ct} = \frac{\text{Crack-tip stress of unstiffened panel}}{\text{Crack-tip stress of stiffened panel}}$$

W	panel width, inches
a	half crack length, inches
$\sigma_s$	stiffener stress, psi
$\sigma$	gross applied stress, psi

Toughness  $K_{IC}$  is determined from tests on stiffened panels as shown in figure 17(a). The ratio  $R_{ct}$  is determined from analysis of unstiffened and stiffened panels having the same grid size by taking a ratio between the crack-tip stresses (ref. 4). The idealized structure and analysis are based on the FORTRAN Matrix Abstraction Technique (FORMAT) shown in figure 17(b).

#### Skin Fracture Criterion (Fuselage Panels)

Results of fuselage panel residual strength tests are shown that verify test and theory correlation. The shape of the curve is determined by analysis and the height by critical fracture toughness  $K_{IC}$ . (Note the point of fast fracture.) The curve plotted in figure 17(c) shows correlation with the analysis at critical crack length, crack arrest, and final failure.

The maximum allowable principal stress for a two-bay longitudinal crack is above the maximum operating principal stress for the DC-10 and provides an adequate margin of safety.

#### Stiffener Criteria (Fuselage Panels)

Stiffener strength must be adequate. In order to maintain the skin fracture strength, the stiffener must not fail. An example of frame (aluminum) stress and outer-crack-stopper (titanium) stress correlation is shown in figure 17(d).

#### Fail-Safe Testing (Fuselage Panels)

Extensive fail-safe testing has been completed. A comprehensive test program was initiated early in the DC-10 design to verify analytical methods and to evaluate various stiffener configurations and materials. Figure 18 illustrates some of the fail-safe development test specimens. Finally, six 118.5-inch-radius curved panels were tested to determine the residual strength. These tests showed that the fuselage shell structure

provides more than adequate fail-safe capability for the conservative two-bay selected damage-tolerance criteria.

### Stress Analysis and Testing (Wing Panels)

An important design consideration of the DC-10 wing structure is to sustain an initial failure of a member but allow for extension of the failure over a reasonable number of additional flight hours. This approach assures that an initial crack will not grow to critical proportion before it is detected during routine inspection intervals.

The damage-tolerance criterion, a two-bay crack with center stringer failed, has been incorporated into the design of the DC-10 wing box structure shown in figure 19. In addition, four separate skin panels are used on the wing lower surface to arrest further any crack propagation.

Figure 20 shows FORMAT analysis correlation with experimental results obtained from tests of large skin-stringer panels representing typical wing box construction. Stresses at adjacent stringers have been calculated as functions of crack length. The results have been verified by strain-gage test results.

### STRUCTURAL INSPECTION AND MAINTENANCE PROGRAM

The purpose of the structural inspection and maintenance program is to detect structural problems on aircraft before airworthiness is affected or expensive repairs become necessary. The importance of the structural inspection and maintenance program was recognized during initial DC-10 design stages. Goals were established to provide required structural airworthiness levels at minimum inspection and maintenance costs.

The main approach is to give full assurance that the aircraft structure will be relatively crack free for its intended service life of 60 000 flight hours and 42 000 flights. This high degree of structural reliability was achieved by designing, analyzing, and testing to (1) a fatigue life in excess of 120 000 flight hours and 84 000 flights to crack initiation and (2) a fail-safe life based on a two-bay crack length requirement.

### Fatigue Life

Item (1) – that is, a fatigue life in excess of 120 000 flight hours and 84 000 flights to crack initiation – incorporates various design features.

Working stress levels. – Accurate stress levels were predicted for structural sizing using FORMAT analysis. Stress levels are equivalent to those of the DC-8 and DC-9, which have excellent service experience.



Detail design. - Stress concentrations were minimized in joints, splices, and basic structure by the use of proper tapering and scalloping, stress coining, and interference-fit attachments (ref. 5). Preload stresses were minimized by providing flexible structure in design, shop fabrication assembly, and installation tolerance control. Detail design quality of the structure is equivalent to, or better than, DC-8 and DC-9 quality, as verified through component fatigue test results.

Corrosion and stress corrosion. - Corrosion was prevented through faying-surface sealing, priming, top coating epoxy paints, draining, using clad aluminum materials, and using high-strength fasteners installed wet with sealant or primer. Stress corrosion resistance was maximized by utilizing 7075-T73 material, which has a high corrosion threshold.

### Fail-Safe Life

Item (2) - a fail-safe life based on a two-bay crack length requirement - involves two main design considerations. The use of FORMAT analysis, verified by large panel component tests, enabled the structure to be designed for slow crack growth and crack arrestment.

Crack growth. - Slow crack growth is attained through the selection of 2024 aluminum with its high fracture toughness properties (low notch sensitivity) and by the use of low working stress levels (ref. 6).

Crack arrestment. - Cracks are arrested by the use of titanium straps at fuselage frames, additional spanwise splices, separately attached but closely spaced wing stringers, and stiffeners attached to the fuselage shell and bulkheads.

### Significant Structural Items

Because of the high probability of a long fatigue life, the inspection program will be started rather late in the service life. Also, because the structure is fail-safe, the inspections can be spaced somewhat farther apart than those on older types of aircraft (ref. 7).

The selection of the significant structural items to be inspected is based on the knowledge and experience with past programs and the manufacturer's assessment of the most fatigue- and corrosion-sensitive structure. It is necessary, therefore, to define the following two steps:

(1) External structural members are designed to crack before complex or hidden joints, doublers, frames, and so forth. This "controlled failure" approach was developed and confirmed by many component tests. For example, over 300 fuselage skin splice specimens were tested to assure skin external crack failures (fig. 21).

(2) Internal members, if cracked, are designed to eventually propagate the crack through to the external members so that the crack becomes externally detectable. The slow crack growth provides sufficient time to inspect and detect cracks before failure, and crack arrestment and the two-bay-crack residual strength of the design provide adequate fail-safe strength.

### Initial Inspection and Intervals

The inspection plan has been designed to detect crack initiation, early signs of corrosion, and manufacturing variabilities (preload). The statistical approach was used to obtain a feel for the effect of fatigue variability (ref. 8) and fracture roughness characteristics. The variabilities required the use of knowledge gained from the DC-8 and DC-9 successful service experience.

The plan of inspection for structural fatigue critical items is listed below:

(1) External items receive 100-percent inspection at periodic intervals.

(2) Internal items, with external detectability, receive 100-percent inspection externally at periodic intervals.

(3) Major load-carrying internal items, without external detectability, are inspected as frequently as the external items.

(4) Other load-carrying internal items, without external detectability, receive only sampling inspection.

The inspection and maintenance program for the DC-10 is designed to assure maximum vehicle airworthiness at minimum cost.

### CONCLUSIONS

To date, both the DC-8 and DC-9 fleets have been flown with only a few isolated fatigue failures in the primary structure; this fact is significant because high-time DC-8's have accumulated about 48 000 flight hours and 28 000 landings, and DC-9's have recorded 32 000 landings.

The DC-10 is a third-generation jetliner and, therefore, is expected to be superior to its predecessors because of the following factors:

(1) Crack-free life of 60 000 flight hours

(2) Slow crack growth and arrestment

(3) External detectability in main load-carrying structure

(4) Completed development testing during initial design



- (5) Detail design and fatigue procedures based on past experience
- (6) Working stress levels and deflections based on accurate design
- (7) Fatigue critical areas recognized in planning stage
- (8) Full-scale tests reveal weak links and check performance.

## REFERENCES

1. Picard, J.; and Morris, R. C.: FORMAT II - Second Version of Fortran Matrix Abstraction Technique. AFFDL-TR-66-207, Vols. I and III.
2. Warren, D. S.: Applications Experience With the FORMAT Computer Program. Douglas Paper 5095, presented to the Second Air Force Conference on Matrix Methods, Wright-Patterson Air Force Base, Ohio, Oct. 15-17, 1968.
3. Stone, M.: Fatigue and Fail-Safe Design of a New Jet Transport Airplane. Douglas Paper 3342, presented to the International Committee on Aeronautical Fatigue (ICAF) Symposium, Munich, Germany, June 16-18, 1965.
4. Swift, T.; and Wang, D. Y.: Damage Tolerant Design-Analysis Methods and Test Verification of Fuselage Structure. Presented to the Air Force Conference on Fatigue and Fracture of Aircraft Structures and Materials, Miami, Florida, Dec. 15-18, 1969.
5. Speakman, E. R.: Fatigue Life Improvement Through Stress Coining Methods. Douglas Paper 5516, presented at AIAA Meeting in Los Angeles, California, July 14-16, 1969.
6. Schijve, J.: National Aerospace Laboratory NLR, Amsterdam, Fatigue of Aircraft Structures, presented at the Twelfth Israel Annual Conference on Aviation and Aeronautics, Mar. 1970.
7. Eggwertz, S.; and Lindsjo, G.: Study of Inspection Intervals for Fail-Safe Structures. Report 120, Aeronautical Research Institute of Sweden, Stockholm, 1970.
8. Abelkis, P. R.: Fatigue Life Scatter Factors for Design and Analysis of Aircraft Structures. Douglas Paper 4807, 1968.

# STRUCTURAL DESIGN

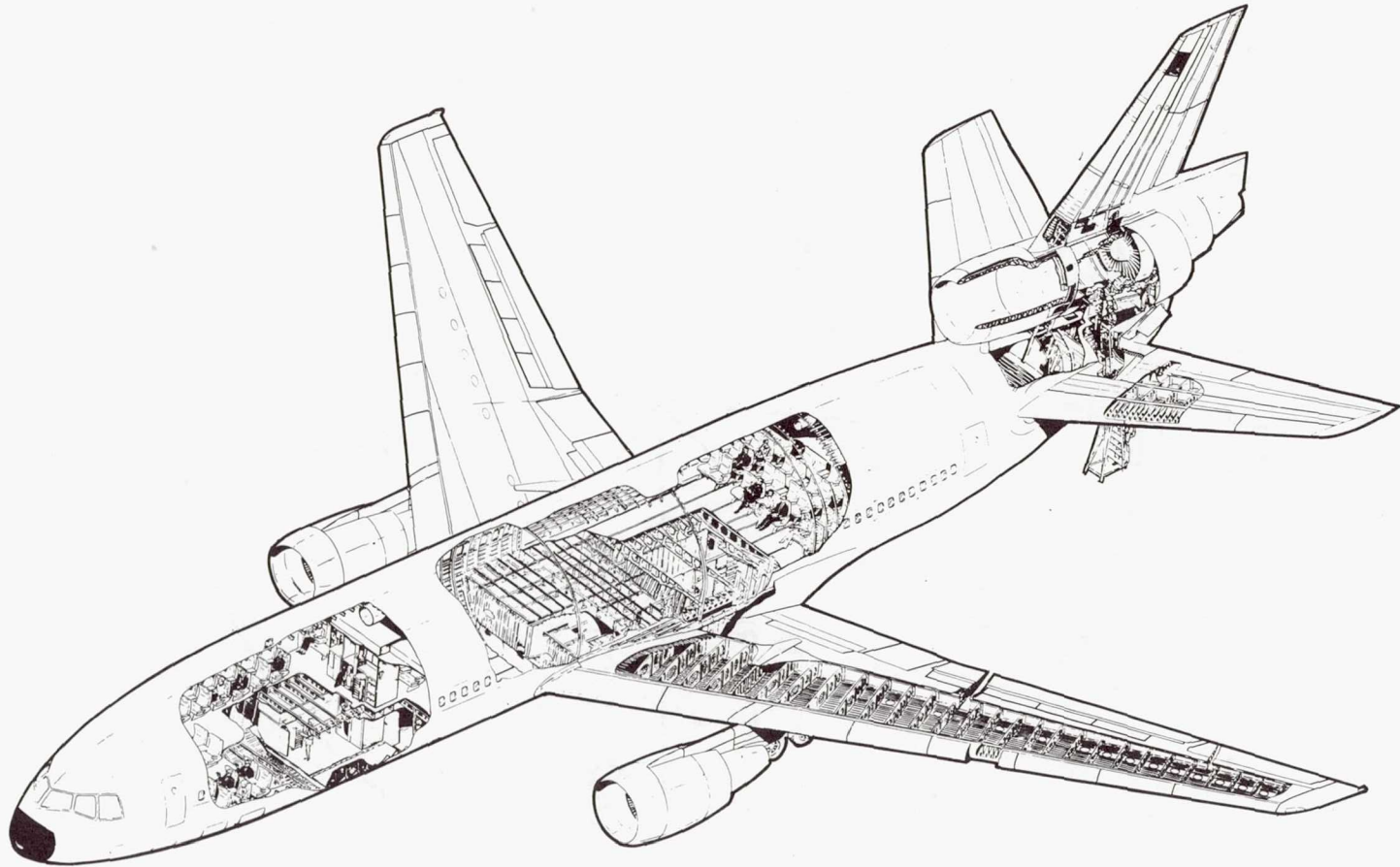


Figure 1



# STRUCTURAL RELIABILITY

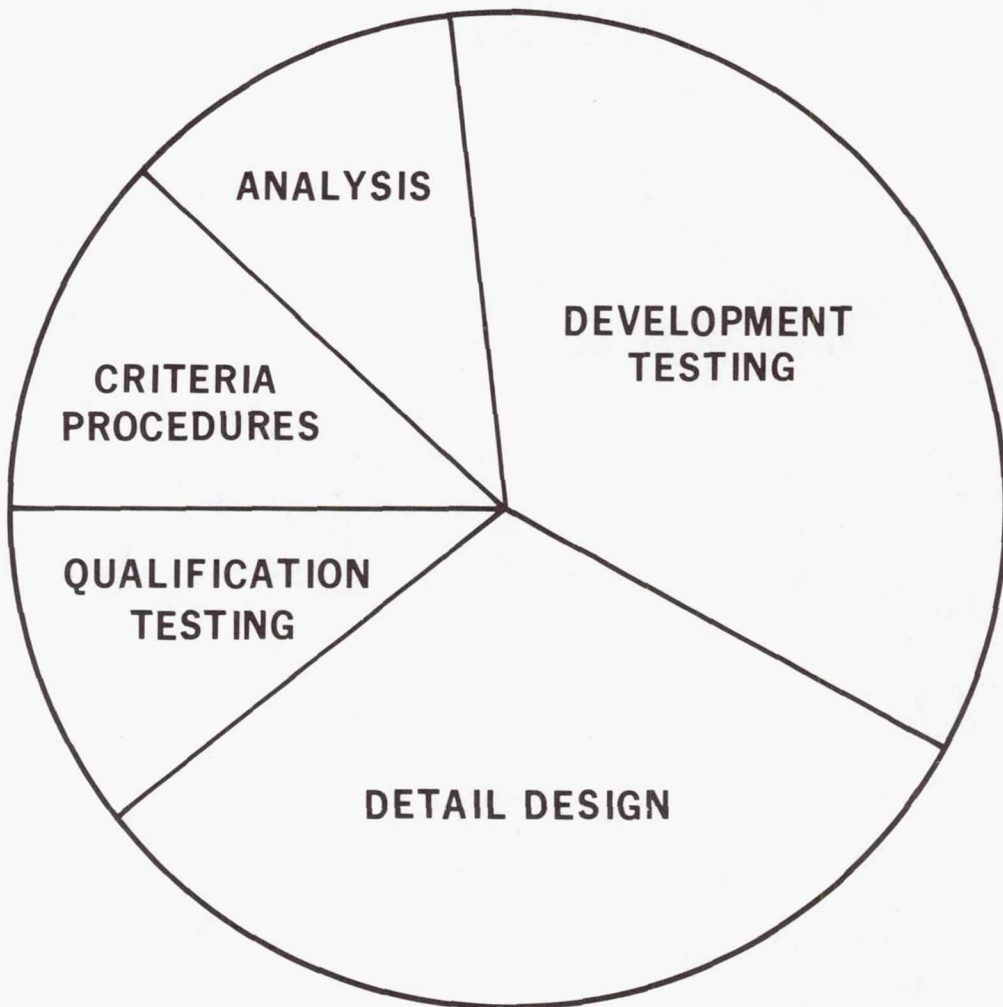


Figure 2

# WING FATIGUE-SENSITIVE AREAS

- 1 – FRONT SPAR SPLICE
- 2 – REAR SPAR SPLICE
- 3 – SWEEP BREAK JOINT
- 4 – INBOARD BASIC STRUCTURE
- 5 – FUEL PUMP ACCESS HOLE
- 6 – REAR SPAR SPLICE
- 7 – PYLON ATTACHMENTS
- 8 – FRONT SPAR CAP SPLICE
- 9 – AERO BREAK BASIC STRUCTURE
- 10 – OUTBOARD BASIC STRUCTURE
- 11 – STRINGER RUNOUT
- 12 – ACCESS DOOR PANEL
- 13 – FRONT SPAR BASIC STRUCTURE
- 14 – REAR SPAR BASIC STRUCTURE

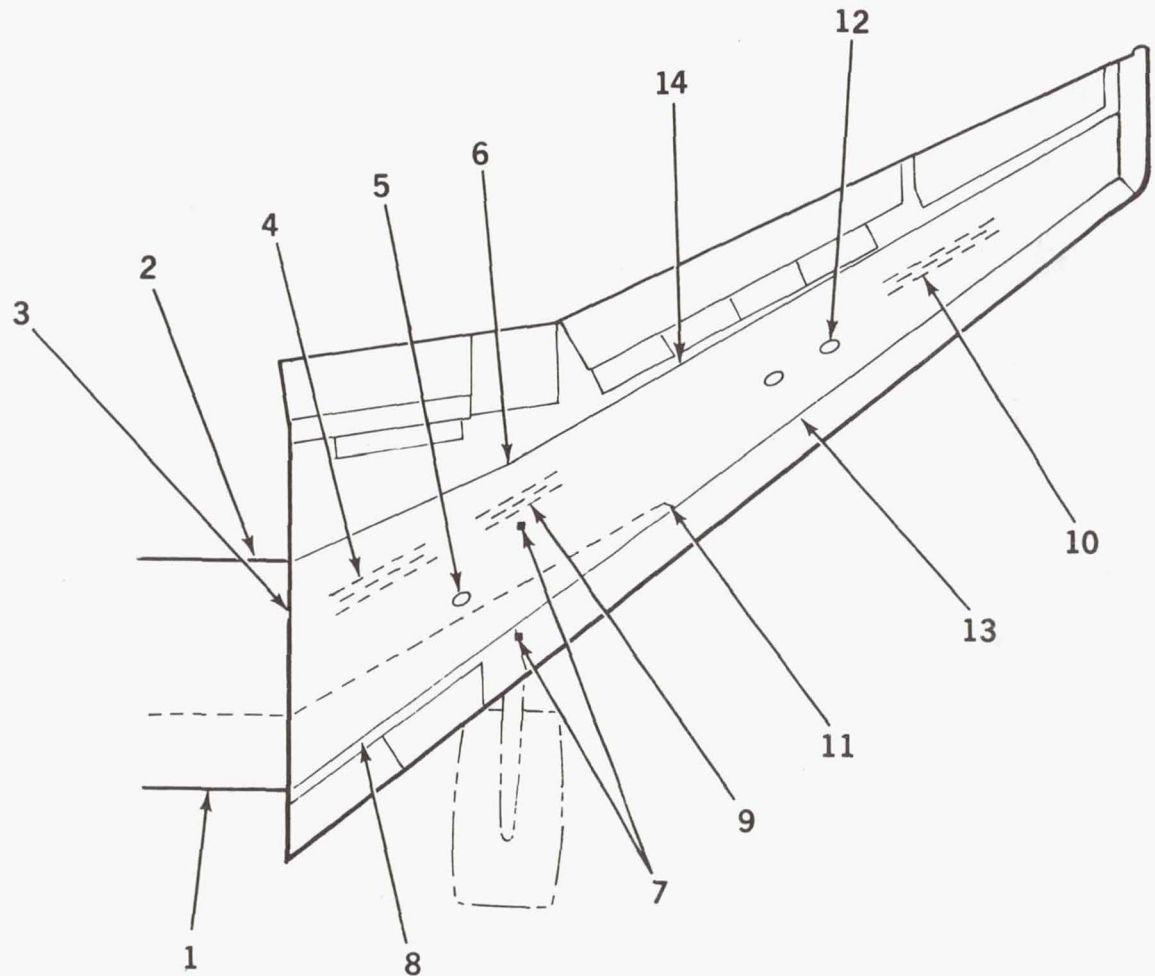


Figure 3



## FUSELAGE FATIGUE-SENSITIVE AREAS

- 1 – PRESSURE BULKHEADS
- 2 – EXIT DOOR AND JAMB STRUCTURE
- 3 – WINDOW BELT PANELS
- 4 – CARGO DOOR HINGES AND LATCHES
- 5 – LONGITUDINAL SPLICES
- 6 – FOUR WAY SPLICES
- 7 – LONGERON TO FRAME CONNECTIONS
- 8 – TRANSVERSE SPLICES
- 9 – WING TO FUSELAGE TITANIUM TEE
- 10 – WINDSHIELD POSTS

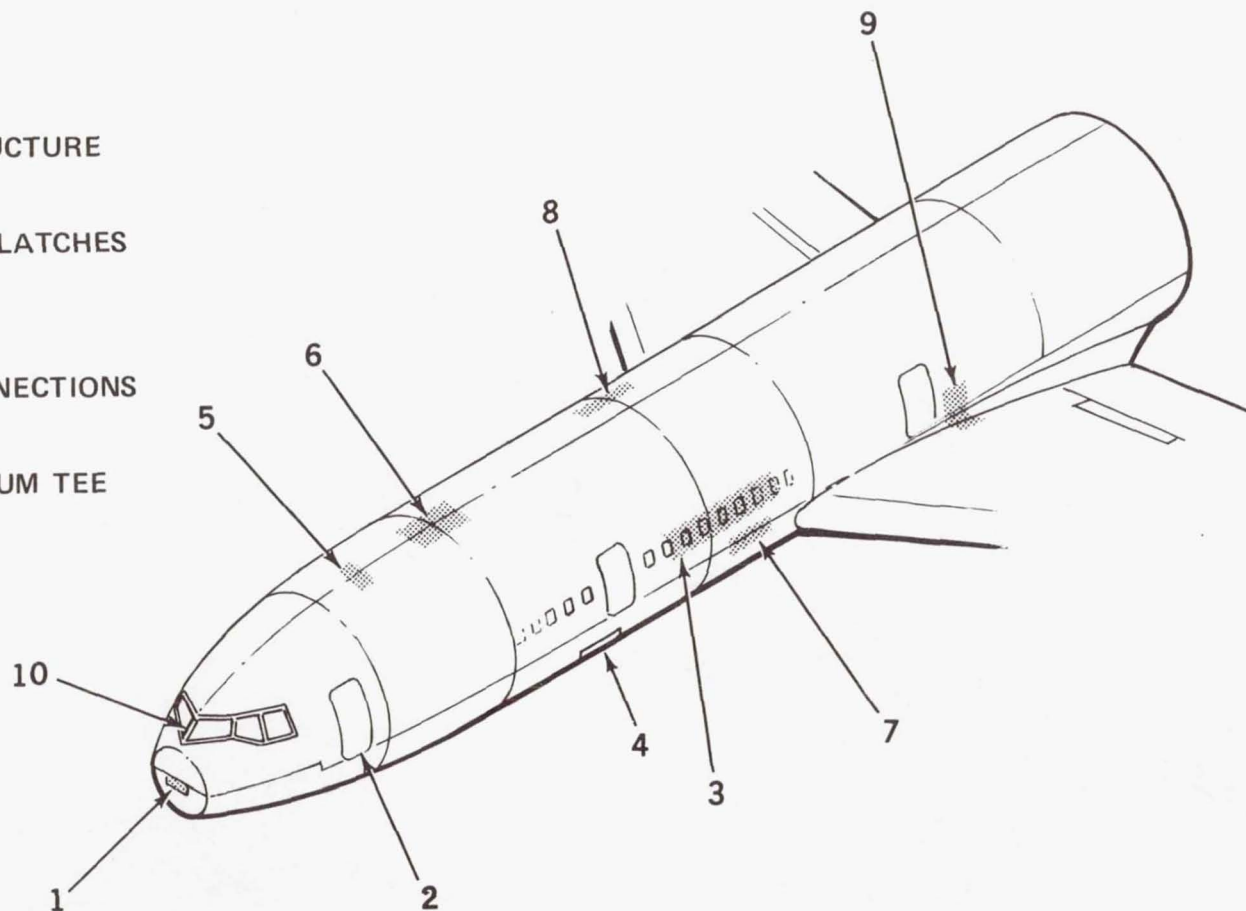


Figure 4

# EVOLUTION OF FORMAT

	<u>ADVANCE DESIGN ANALYSIS</u>	<u>DESIGN ANALYSIS</u>	<u>SUBSTANTIATION ANALYSIS</u>
<b>DC-8</b> (MAXWELL MOHR METHOD)	—	—	<b>20% OF AIRPLANE</b> (2000 FORCES)
<b>DC-8-60 SERIES AND DC-9</b> (REDUNDANT FORCE METHOD)	—	<b>10% OF AIRPLANE</b> (2000 FORCES)	<b>50% OF AIRPLANE</b> (20 000 FORCES)
<b>DC-10</b> (FORMAT)	<b>10% OF AIRPLANE</b> (6000 FORCES)	<b>70% OF AIRPLANE</b> (60 000 FORCES)	<b>90% OF AIRPLANE</b> (100 000 FORCES)

Figure 5



# DEFLECTIONS

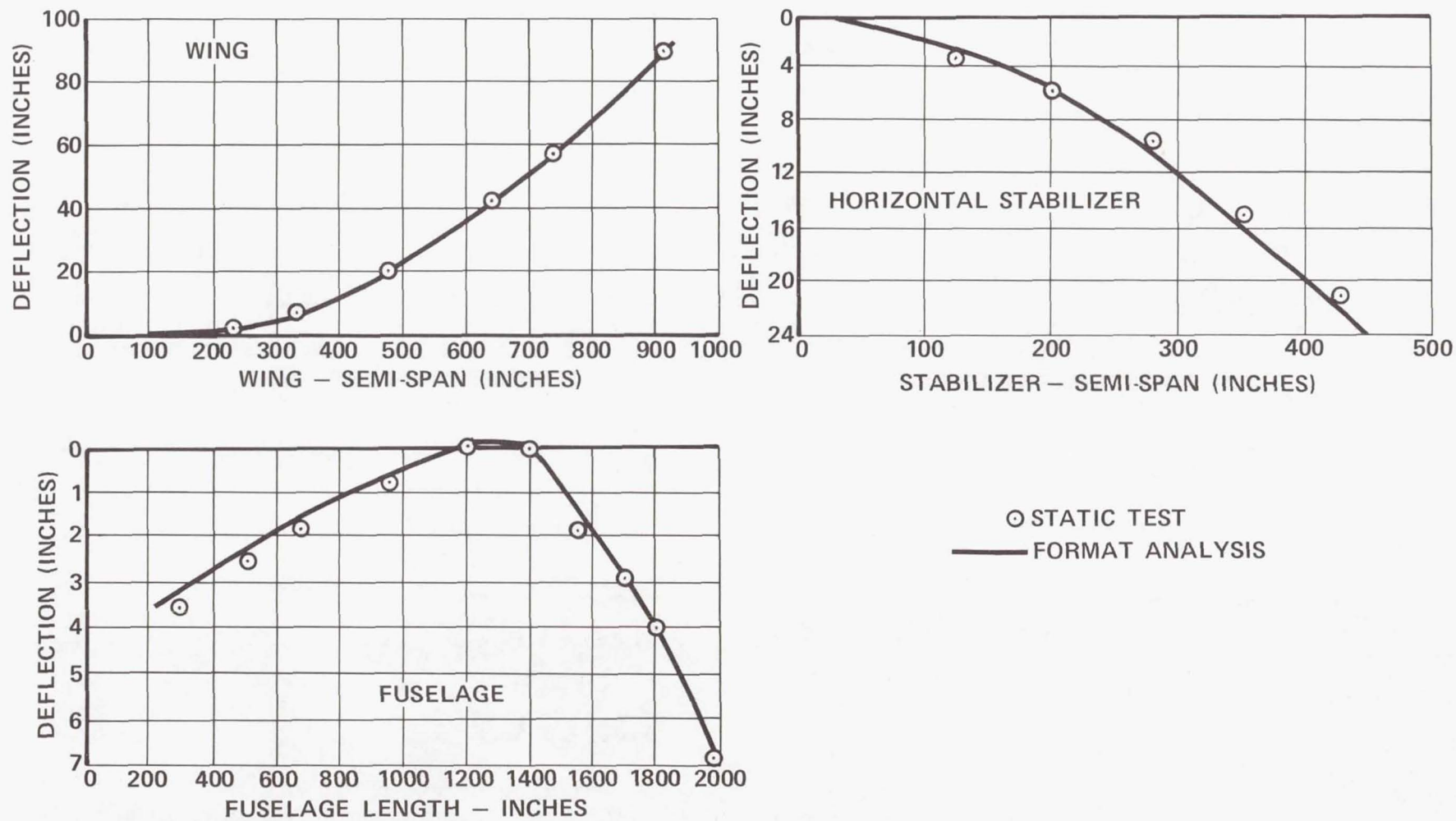


Figure 6

# STRESS ANALYSIS

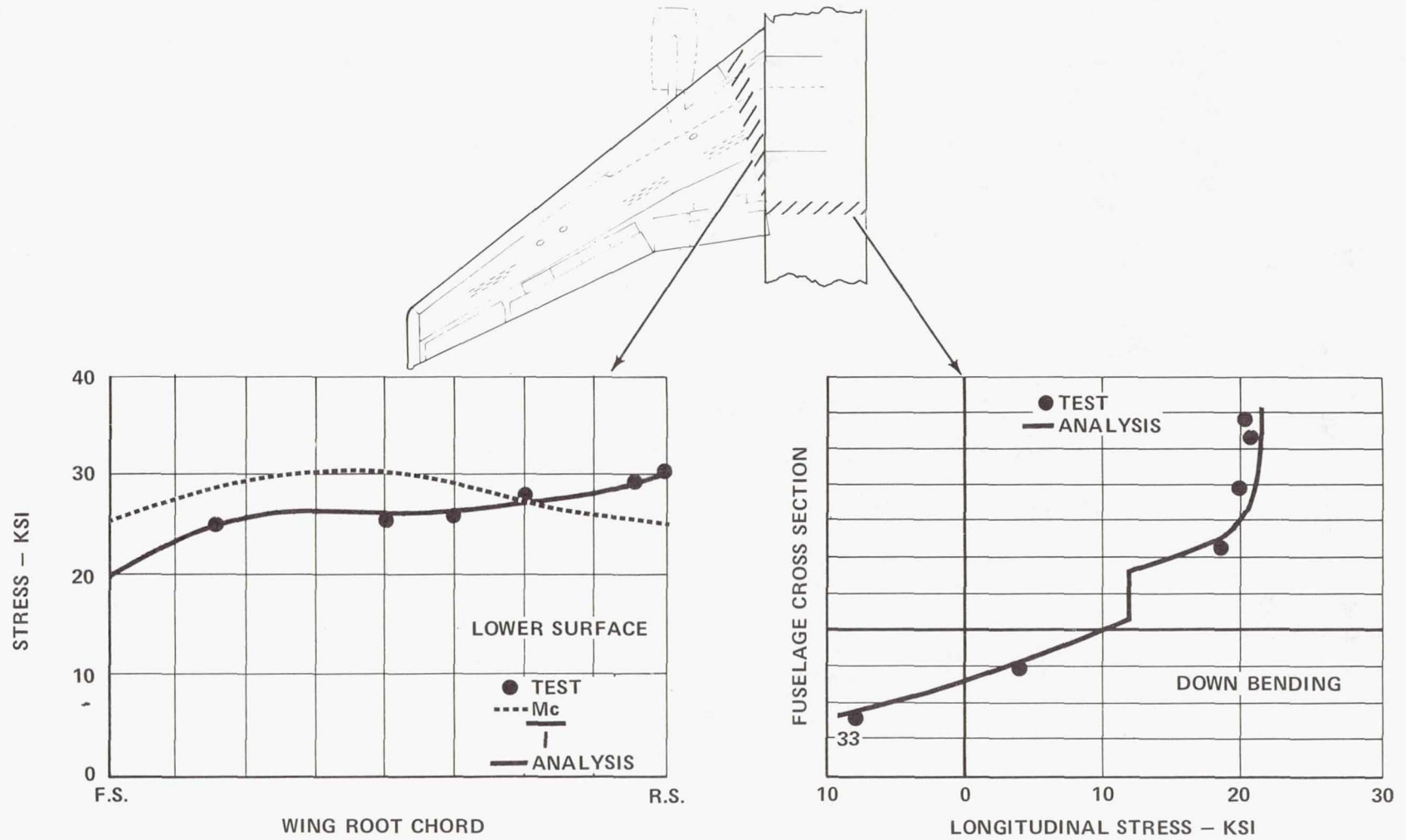


Figure 7



## WORKING STRESSES

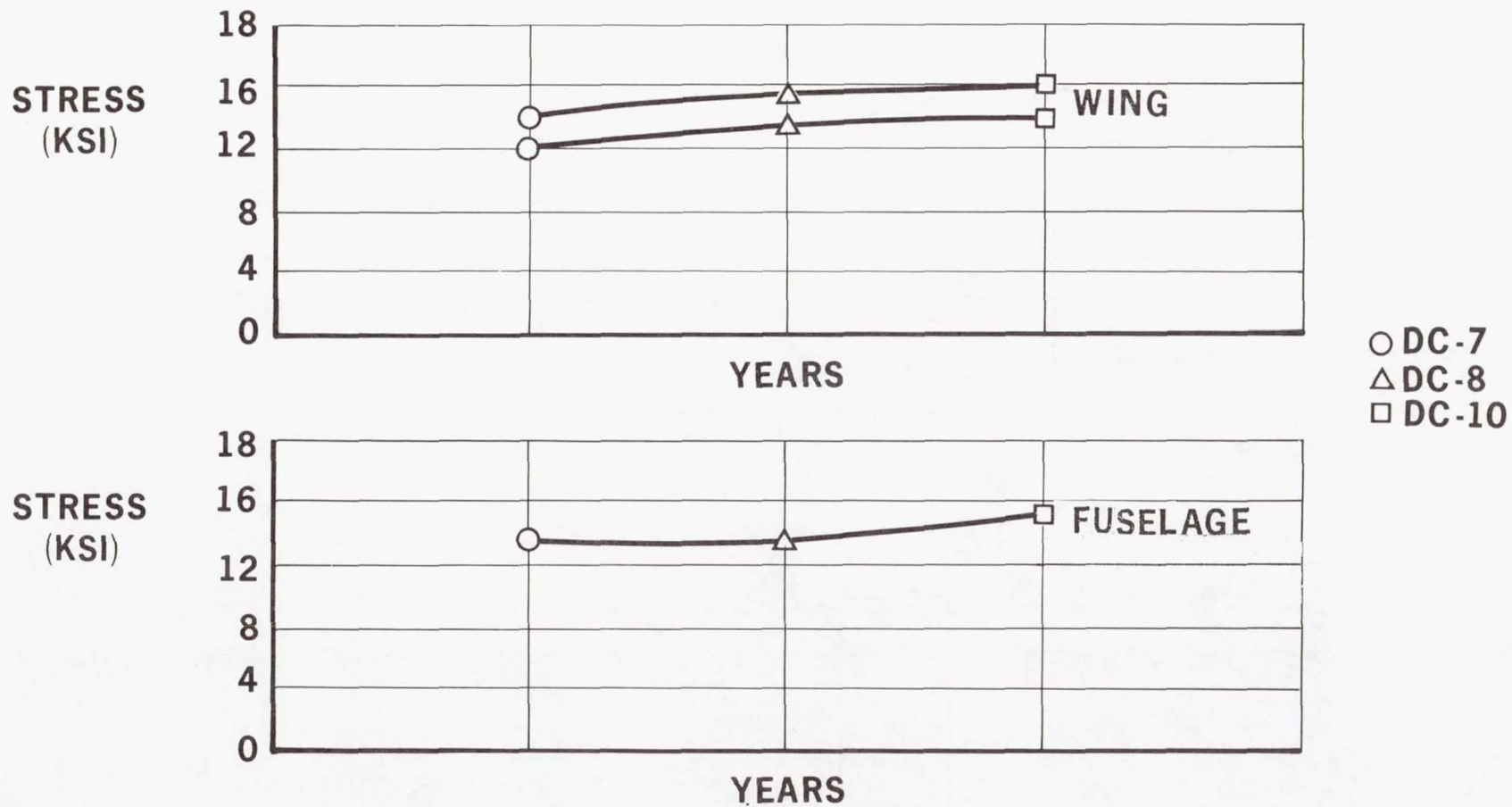


Figure 8

# FATIGUE QUALITY STRUCTURE

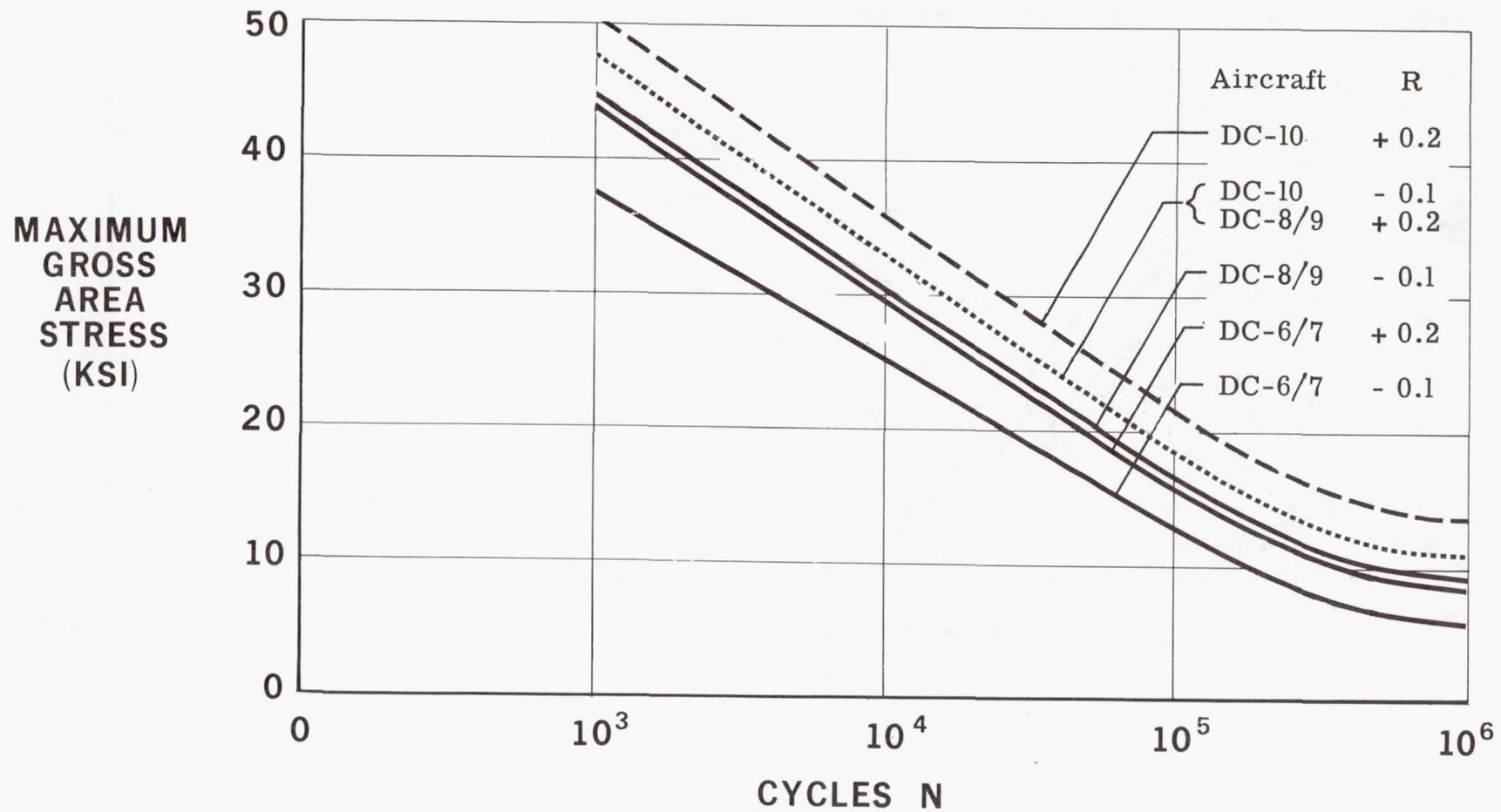


Figure 9



# SPECIMEN DEVELOPMENT TESTING

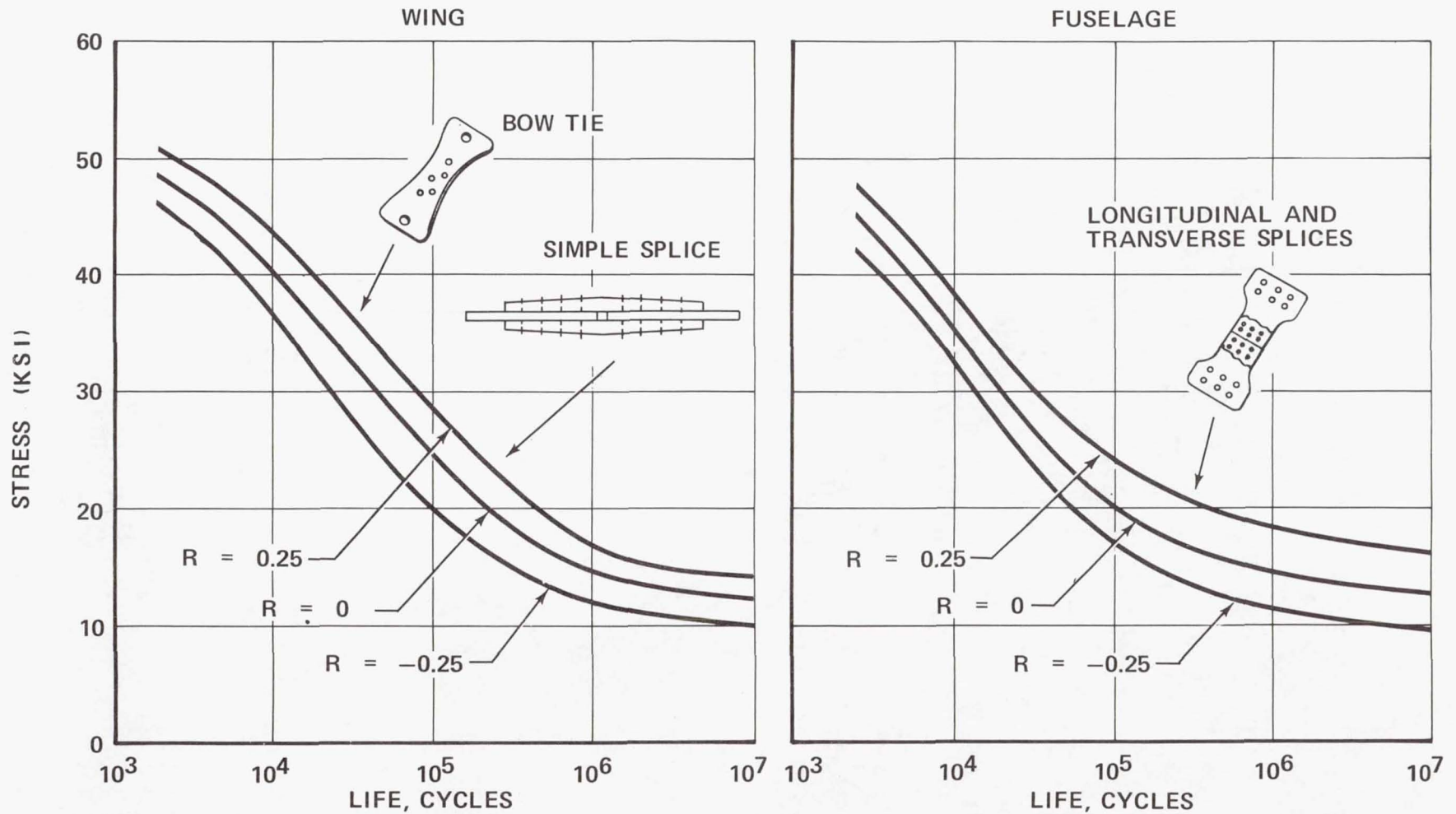


Figure 10

# COMPONENT DEVELOPMENT TESTS

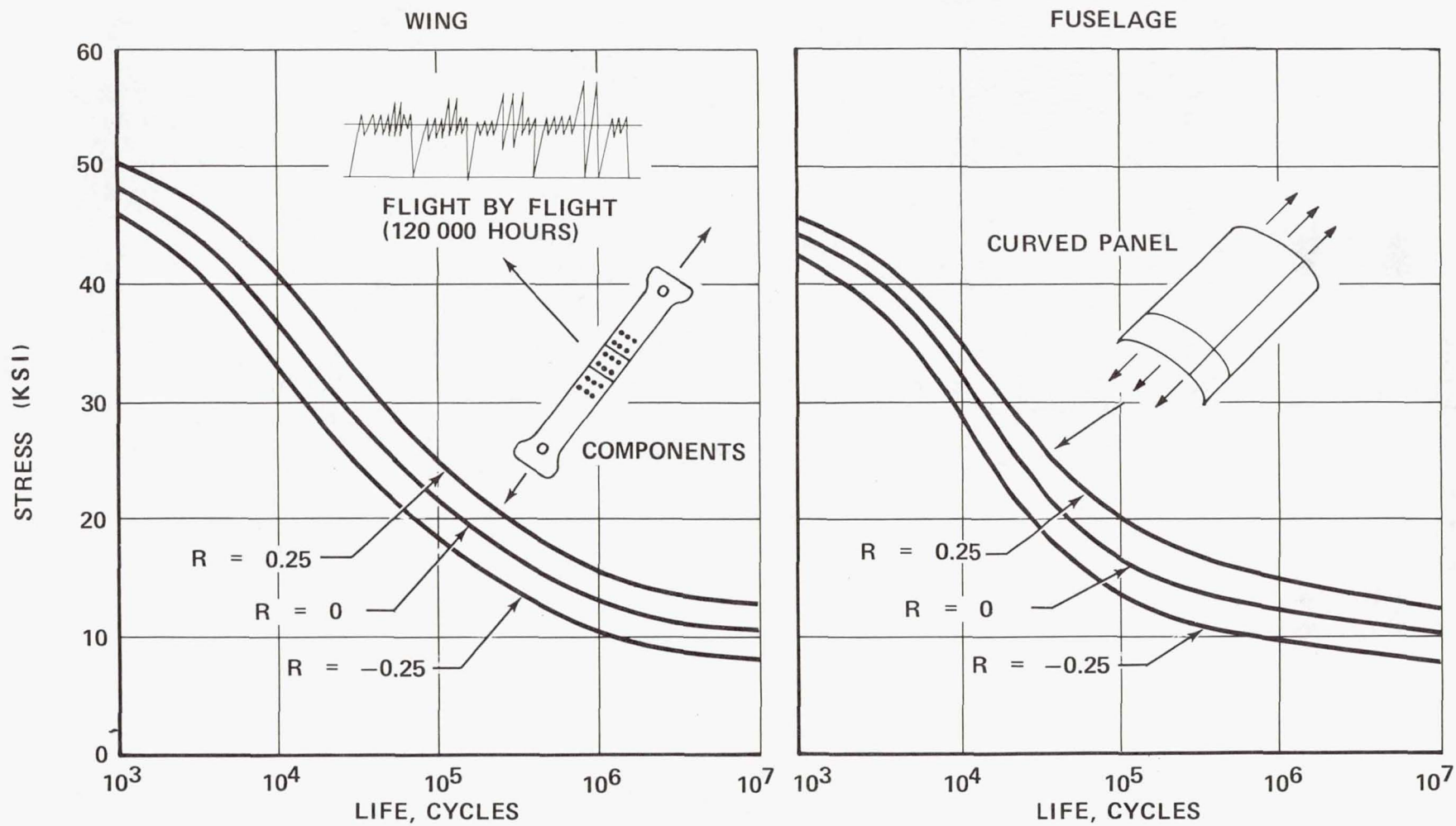


Figure 11



## WING DETAIL DESIGN

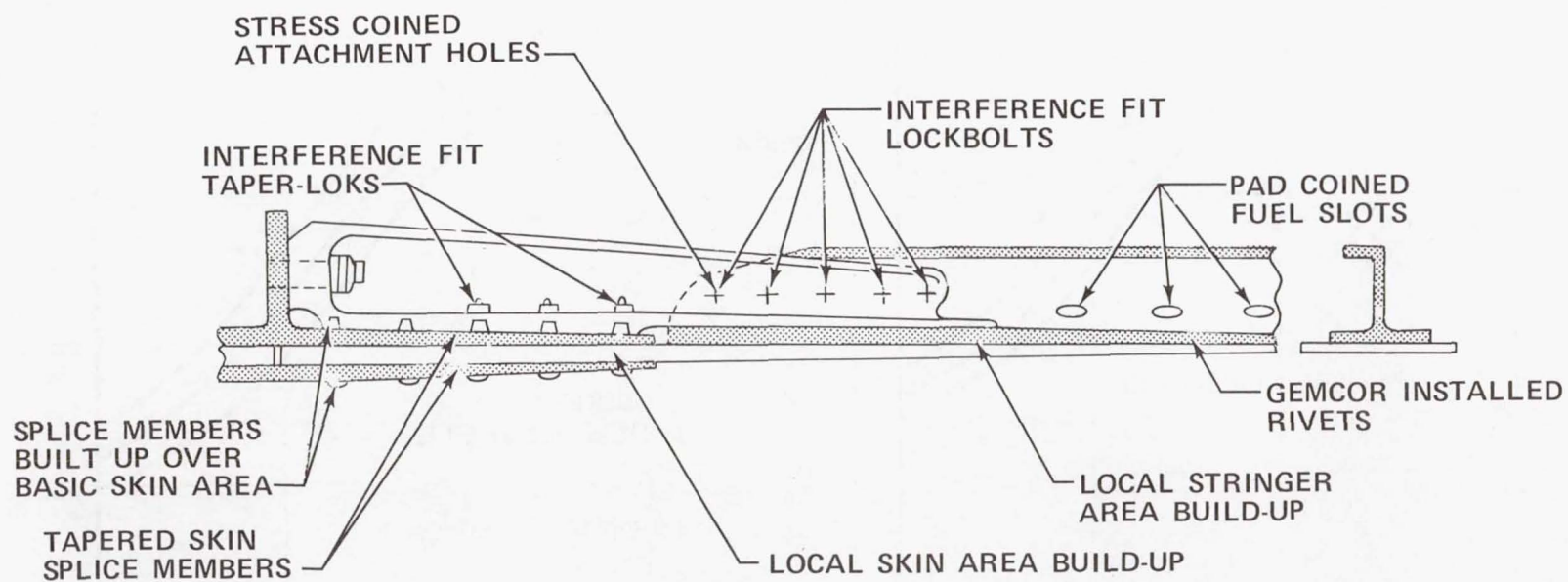


Figure 12

# SACRIFICIAL DOUBLER

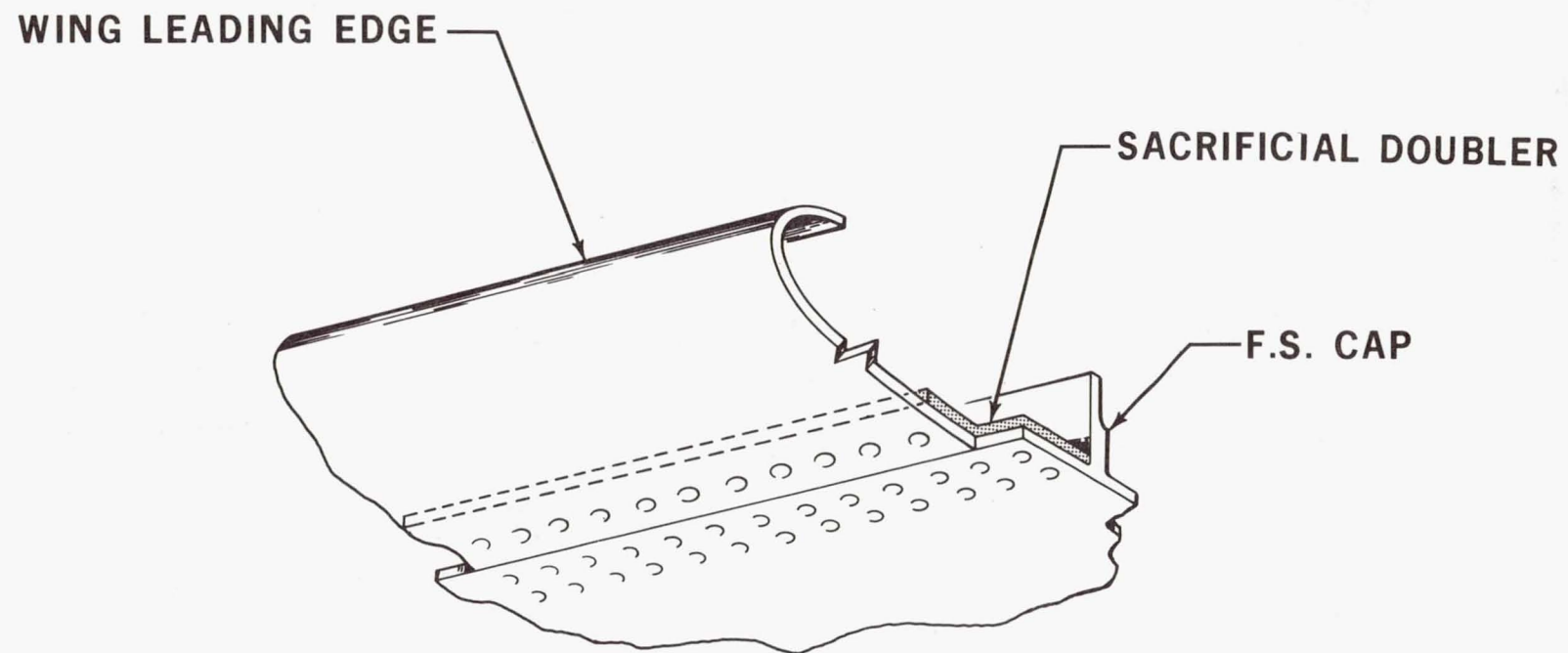


Figure 13



# FUSELAGE DETAIL DESIGN

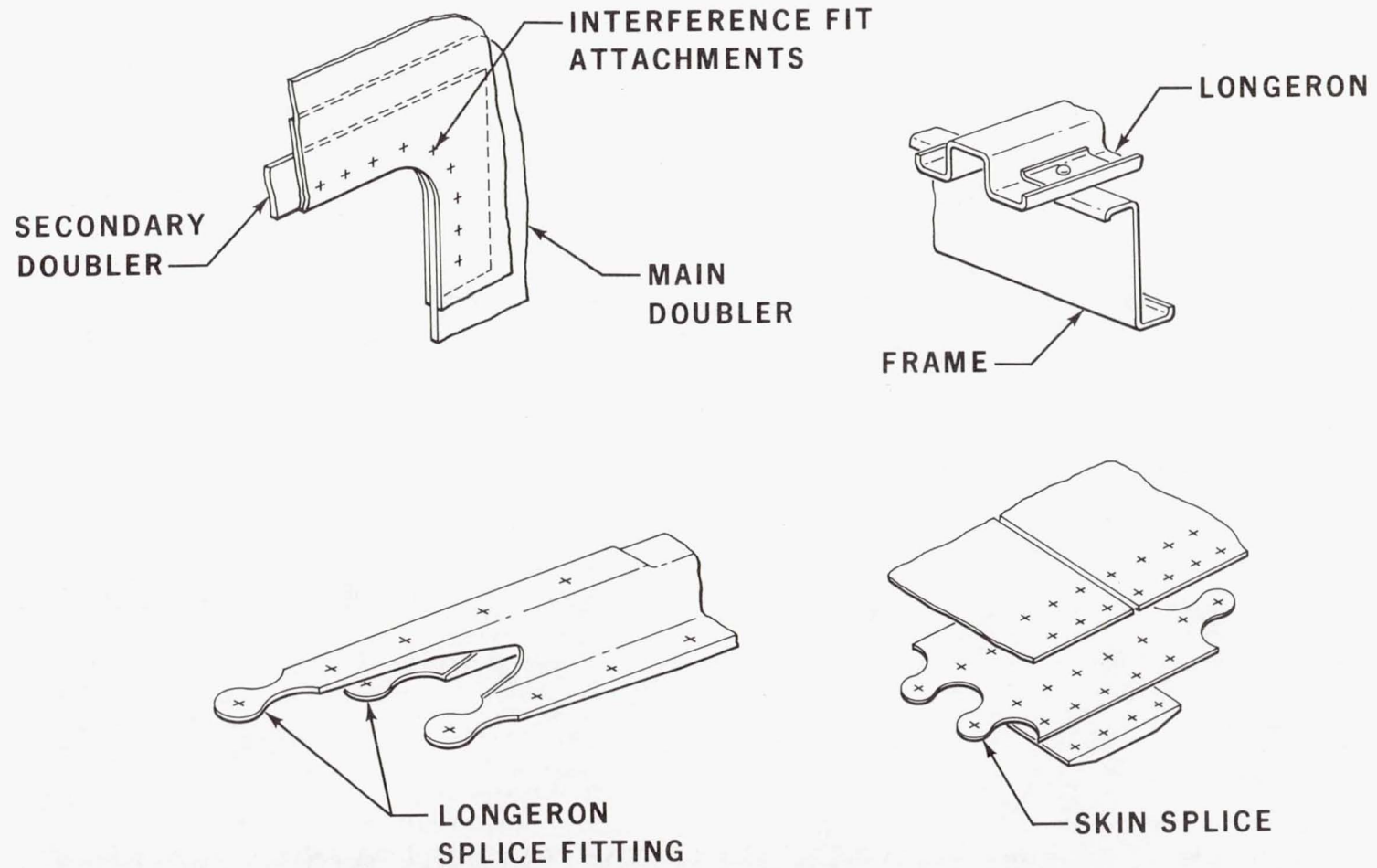


Figure 14

# MAJOR FATIGUE TESTS

LOADING BULKHEADS

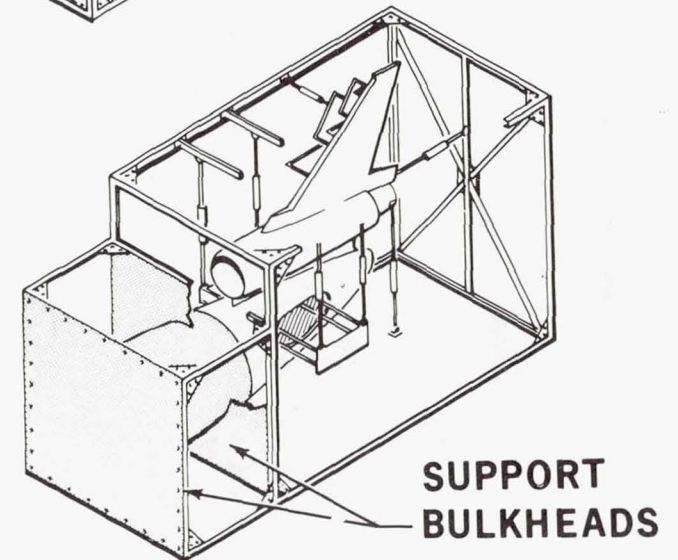
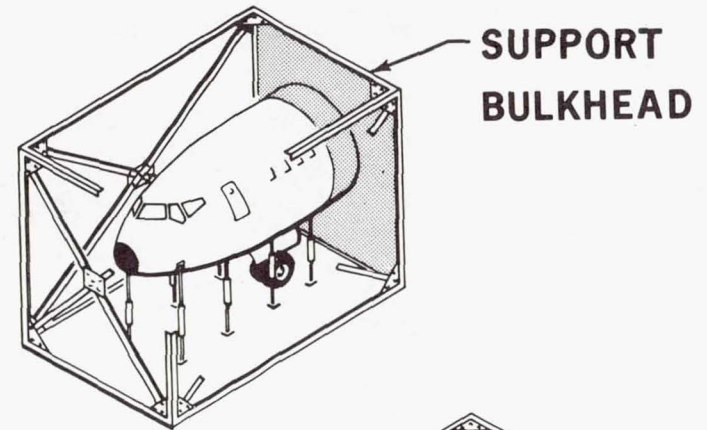
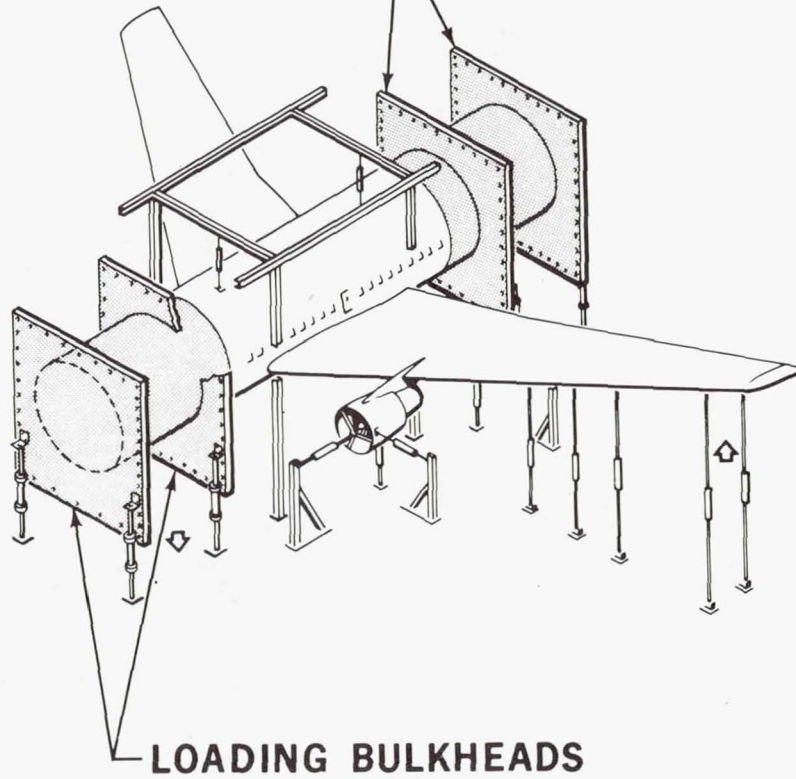


Figure 15



# FUSELAGE BASIC SHELL

## IDENTIFICATION OF SENSITIVE AREAS

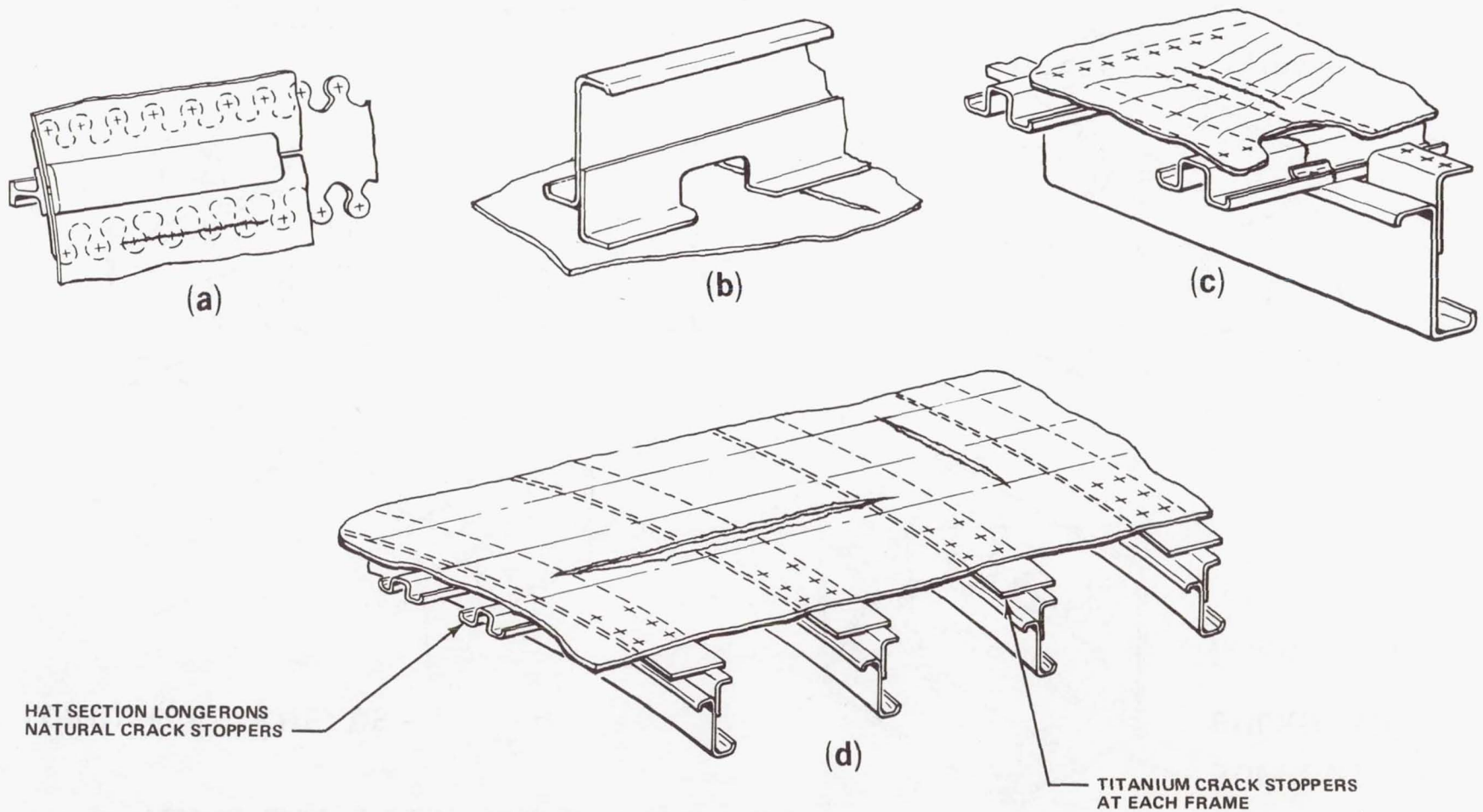


Figure 16

# STRESS ANALYSIS

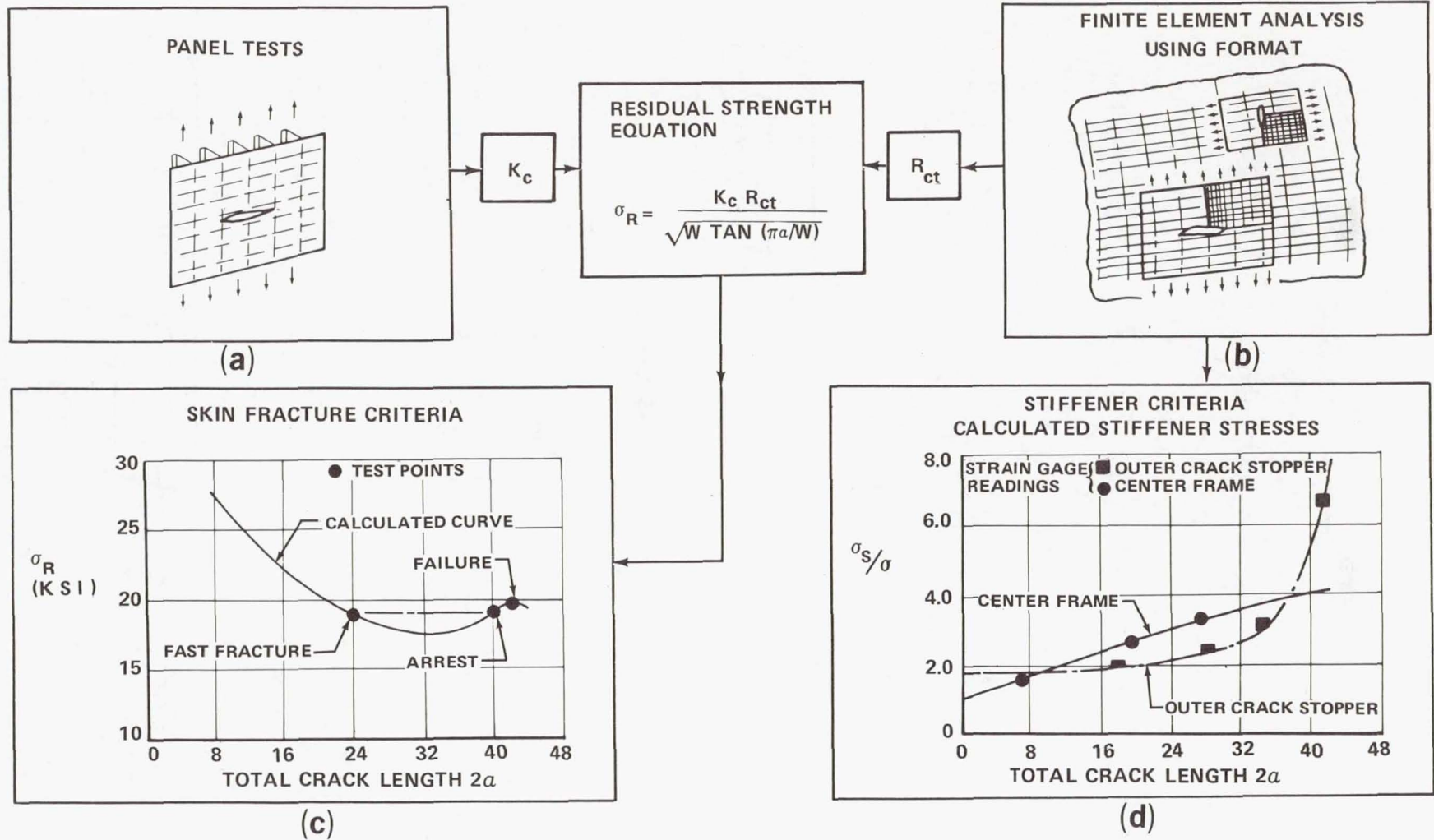


Figure 17



# FAIL-SAFE DEVELOPMENT TESTS

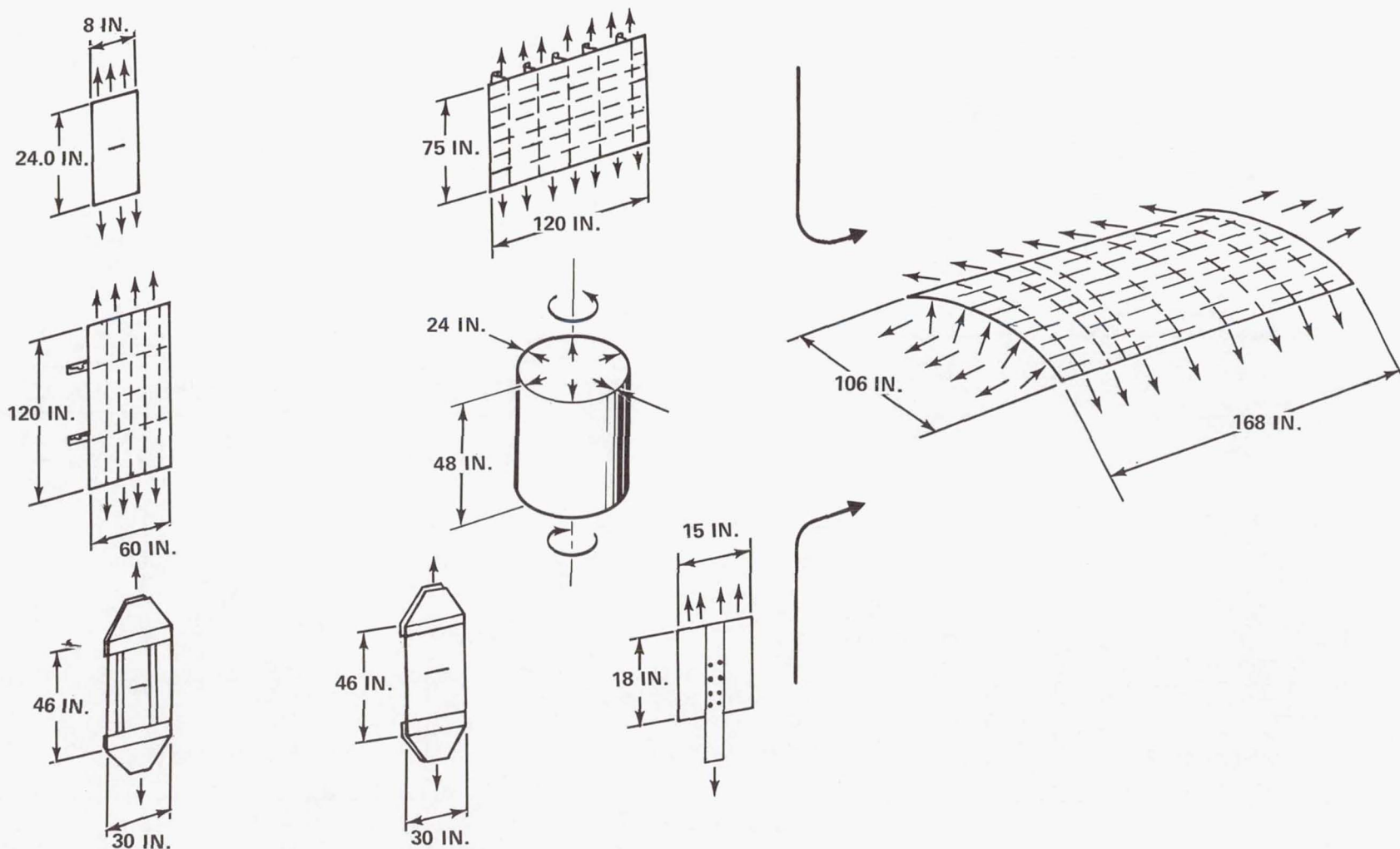
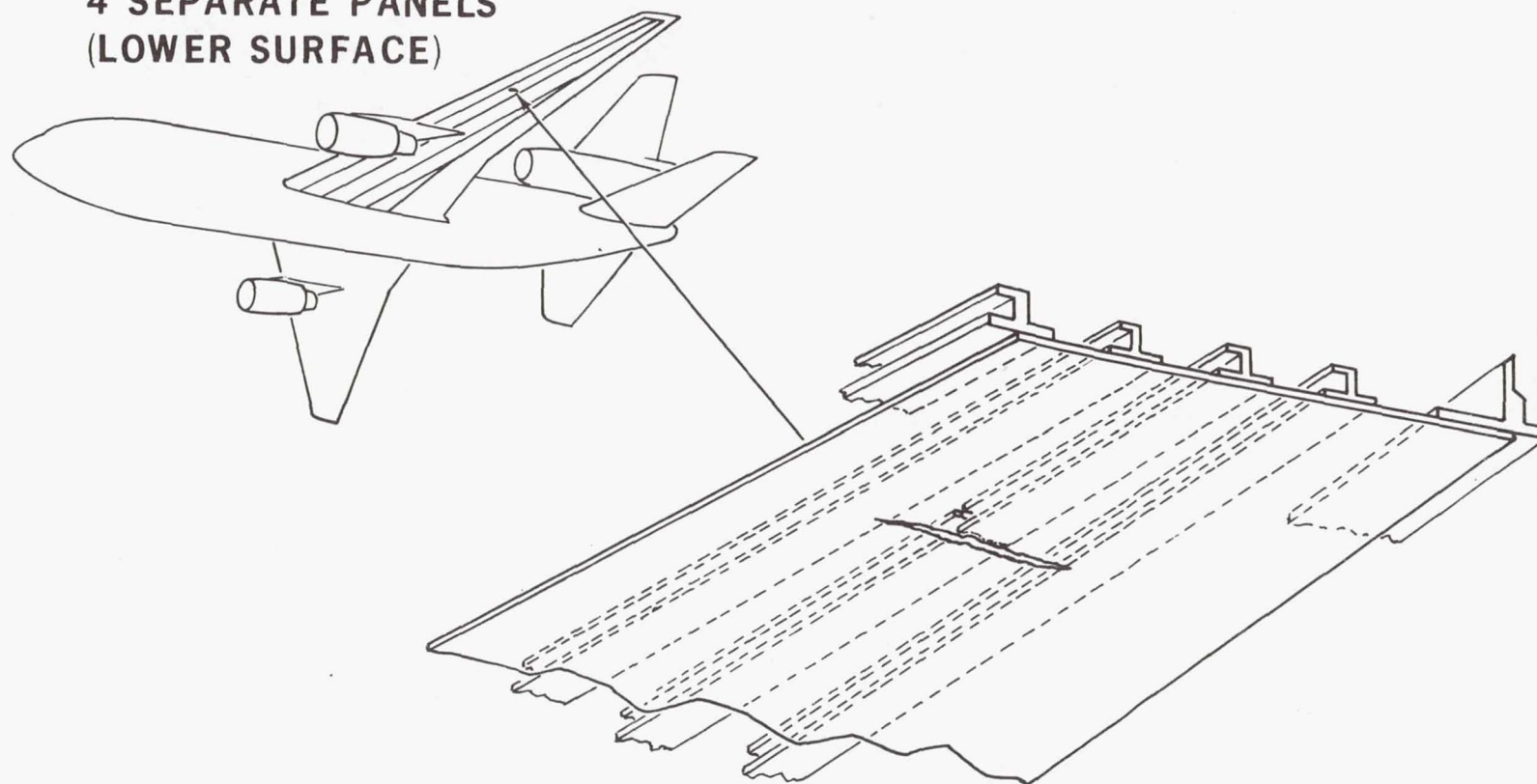


Figure 18

# WING BASIC PANELS

## IDENTIFICATION OF SENSITIVE AREAS

4 SEPARATE PANELS  
(LOWER SURFACE)



ARRESTMENT OF CRACK AT STRINGERS

Figure 19



# FULL-SCALE COMPONENT TESTS VERIFY DAMAGE-TOLERANCE CRITERIA AND ANALYSIS

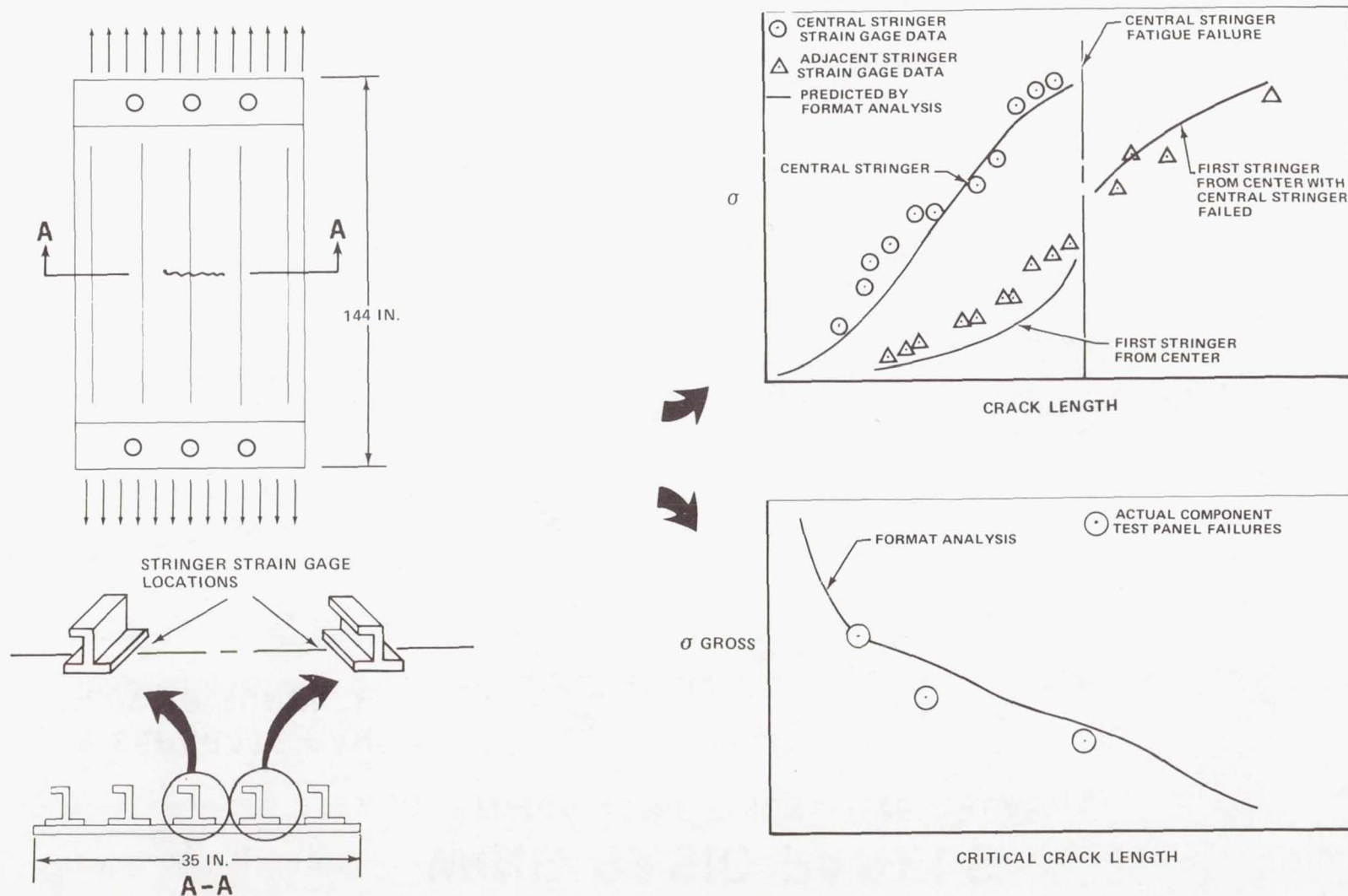


Figure 20

# FUSELAGE SKIN-CRACK DETECTABILITY

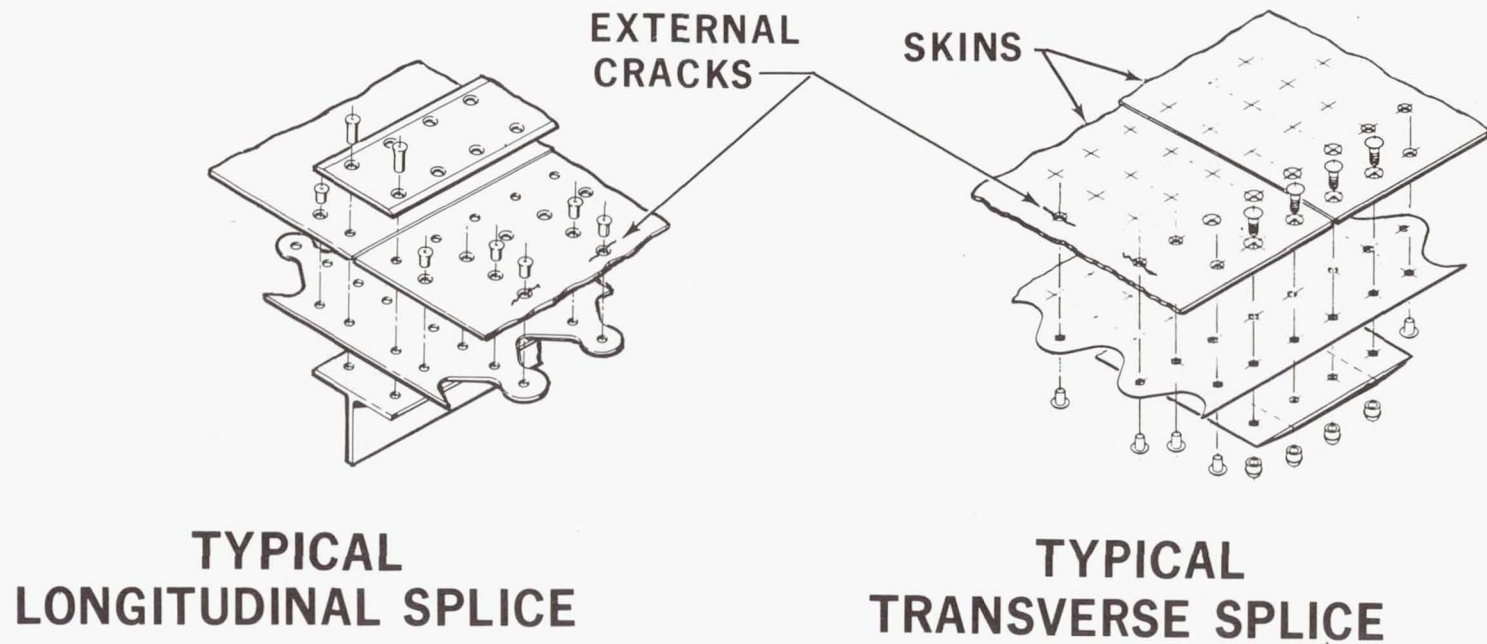


Figure 21



THE PRACTICAL IMPLEMENTATION OF FATIGUE  
REQUIREMENTS TO MILITARY AIRCRAFT AND HELICOPTERS  
IN THE UNITED KINGDOM

By R. D. J. Maxwell  
Royal Aircraft Establishment, Farnborough, Hampshire,  
United Kingdom

SUMMARY

The paper describes the methods adopted in the United Kingdom to ensure the structural integrity of military aeroplanes and helicopters from the fatigue point of view. It describes the procedure adopted from the writing of the specification to the monitoring of fatigue life in service, and outlines the requirements to be met and the way in which they are satisfied. It also indicates some of the outstanding problems that remain to be solved.

INTRODUCTION

The formal airworthiness requirements for the design of military aircraft and helicopter structures against fatigue are contained in the Ministry of Aviation Supply's publication AvP 970. This document lists a number of mandatory requirements together with advisory leaflets as to how these requirements may be satisfied. Although the mandatory parts, which are written in fairly general terms, are still valid, the advisory leaflets, written mainly in 1958-1959, are now a little out of date and do not always agree with current practice. The object of this paper is to describe the existing process of ensuring an acceptable fatigue performance including both the satisfaction of the mandatory requirements and the subsequent monitoring of that performance in service.

However, before starting the main part of the paper it is worth indicating how the Structures Department of the Royal Aircraft Establishment, which is part of the Ministry of Aviation Supply, is involved in the various phases of an aircraft's development and operational use. Its activities can be summarized as follows:

(a) Making critical comments on the initial specification from the Ministry of Defence, who is the customer, and the early brochures from the manufacturers. These comments are made through the Project team in the Ministry of Aviation Supply, which is the procurement authority.

(b) Interpreting the aircraft usage in terms of load spectra by discussions with the Ministry of Defence and the manufacturers.

(c) Agreeing with the manufacturers, as required by AvP 970, on the extent of fatigue testing to be done.

(d) Agreeing with the manufacturers after completion of fatigue testing on the service life to be promulgated to the Ministry of Defence through the Project team.

(e) Acting as technical adviser to the Project team in discussions on fatigue arising in service.

It is clear therefore that Structures Department has a hand in every phase of the aircraft's life.

### THE GENERAL PROBLEM

Throughout the sequence of operations, the general fatigue problem will be considered under three basic headings:

- (a) The determination of the loads/stress spectra experienced by various parts of the structure
- (b) The determination of the fatigue performance of various parts of the structure
- (c) The estimation and monitoring of the service life

In general, the procedure will be considered in two phases:

- (a) The design-development phase, that is, up to the aircraft's entrance into service
- (b) The production and service phase

Firstly, fixed-wing aircraft designed on safe-life principles will be considered; secondly, fixed-wing aircraft that are essentially fail-safe; thirdly, helicopters which are invariably designed safe-life; and lastly, fail-safe helicopters.

### WRITING THE AIRCRAFT SPECIFICATION

When the fatigue life specification is written, two important aspects need to be covered. Firstly, the role or combination of roles for which the specified life is required must be described in sufficient detail to enable load spectrum estimates to be made. This description is extremely important, as contractual compliance with the fatigue life requirements will be determined by tests under these load spectra. Thus, the requirement should indicate

- (a) The types of role in which the aircraft will be operated (that is, route flying, ground-attack, marine reconnaissance, etc.) and the proportion of time spent in each role



- (b) Flight profiles anticipated (heights, speeds)
- (c) Operating weights and stores to be carried
- (d) Numbers of landings
- (e) Numbers of pressurizations

Secondly, it must be made clear whether the required life is the minimum to be achieved in the stated mixture of roles or whether it is the average life to be achieved. This definition of the life determines whether the life is to be achieved under the most severe spectrum or under an average spectrum, estimated from the stated usage.

### DETERMINATION OF LOAD SPECTRA

At the beginning of the design-development phase, the load spectra for the aircraft are estimated for the specified utilisation. The estimates are obtained mainly from data collected from previous aircraft. Toward the end of this phase, the estimates may be modified by loads measured on prototype aircraft. The loads to be considered include those discussed in the following paragraphs.

#### Gust Loads

The gust loads are estimated from the flight profiles quoted in the aircraft specification by using mainly discrete gust data with rigid-body response giving centre-of-gravity accelerations. For larger aircraft some allowance is made for flexibility. The use of power spectral methods to estimate gust loads in terms of centre-of-gravity accelerations is under consideration. The same discrete gust data are used to estimate tailplane and fin loads. Fin load frequencies are arbitrarily multiplied by 3 to allow for Dutch roll type of response and to allow for some manoeuvre content.

#### Manoeuvre Loads

Manoeuvre loads again are obtained in the form of centre-of-gravity accelerations. They are compiled mainly from the load spectra collected from fatigue (load) meters (counting accelerometers) on previous aircraft flying similar roles with some allowance where necessary for different design limit values of centre-of-gravity acceleration. If new types of role are envisaged, manoeuvre loads must be estimated by consultation with the operators. Manoeuvre loads are mainly of significance for the wing and fuselage but may also be important for the tailplane. Attempts have been made on some aircraft to calculate the tailplane loads required to initiate the centre-of-gravity accelerations of the manoeuvre spectra. In general, such calculations suggest that peak loads of about twice the magnitude of the tail balancing loads for the manoeuvre under consideration are obtained.

## Ground-Air Cycle

Until recently this ground-air cycle, a once per flight cycle, which is mainly of importance for the wings has been considered to range from a lower limit given by the down load generated by a 1.2g acceleration while taxiing under maximum take-off load to an upper limit occurring in the 1g level flight condition. It is now considered that a more realistic allowance for the ground-air cycle is obtained for transport and heavy bomber aircraft if the upper limit of the cycle is taken as the 1g condition plus the positive load occurring once per flight. In addition, it is recognised that the once per flight down load for this class of aircraft is likely to be between 1.3g and 1.4g rather than 1.2g. The ground-air cycle is normally considered to be unimportant for fighter-attack aircraft where negative manoeuvres in flight give greater down loads than those experienced on the ground.

## Ground Loads

Estimates of ground loads are, of course, of primary importance for the fatigue-life assessment of the undercarriage, but the loads transmitted to the rest of the structure can also be important for the top surfaces of wings and fuselages of large aircraft. Many modern transports and heavy bombers have undercarriages on or near the fuselage. Consequently, the top surfaces of the large-span, fuel-filled wings are in tension on the ground. The alternating stresses generated by ground loads can therefore cause fatigue problems in the top wing surfaces. Similarly, bending loads in the long fuselages can produce fatigue-prone regions. In general, little data analogous to the gust and manoeuvre data exist. At present, methods of measurement and analysis of such loads on development aircraft are difficult and no operational recorders are available. Although power spectral methods of analysis are giving some indication of the vertical loads likely to be experienced, little has been done to calculate side loads, which may be extremely important for the undercarriage.

## Local and Acoustic Loads

Local loads include such loads as those due to flap and airbrake operations. Estimates of sound pressure levels for acoustic loads can be made once the engine type and configuration are known.

## CONVERSION OF LOAD SPECTRA TO STRESS SPECTRA

The structure is examined in detail and at all stations considered to contain possible fatigue problems, the local stresses corresponding to the various parts of the load spectrum are calculated. In general, rigid body conditions are used, but some allowance for



dynamic effects is made if it is thought that the stress levels will be significantly affected. In the later stages of the design-development phase, the stress calculations are supplemented by flight measurements on prototype aircraft. The importance of knowing the utilisation pattern in some detail again becomes apparent since the centre-of-gravity accelerations of the load spectrum must be associated with the correct weight and flight conditions to obtain the corresponding stresses. Hence, an estimate must be made of where in the flight the accelerations are most likely to occur.

## ASSESSMENT OF FATIGUE PERFORMANCE

The initial assessment of fatigue performance is by a calculation using Miner's hypothesis to evaluate the lives of those components for which the stress spectra have been determined together with S-N curves appropriate to the type of component and material considered. In general, manufacturers use their own S-N data based on tests on previous aircraft with components similar to those proposed for the new model. Where such curves are not available, either the basic material curves are used with some allowance for stress concentrations and other effects or some typical curve such as those in the Royal Aeronautical Society/Engineering Sciences Data Unit Data Sheets. In particular, the Heywood joint curve A, Data Sheet E.05.01 is regarded as a good starting point for calculations on aluminium alloy structures. Parts shown by the initial calculations to have marginally acceptable lives are tested under realistic load sequences of the required stress spectrum.

## ASSIGNMENT OF PROVISIONAL SERVICE LIFE

At this stage, the end of the design-development phase, there will be a number of prototype aircraft flying and production will be about to start. In order to provide some safeguard for early flying until the major fatigue test is completed, provisional fatigue lives are assessed on the basis of the calculations and test results available at this time. The life of the aircraft as a whole will be determined by the life of the most critical irreplaceable component. Within that life, other components may need replacing. In all cases lives will be calculated by using the average spectrum for the sortie, or mixture of sorties, required and either the standard S-N curves or the later component tests. These lives will then be the lives one would expect for average components, and must be divided by the following factors:

(1) By 2 to account for inaccuracies in calculation and component tests compared with full-scale (major) tests. This factor is based on a paper presented by Raithby to the I.C.A.F. in 1961 (ref. 1) which showed that lives based on component tests and calculations usually overestimated the lives subsequently achieved on the full-scale test.

(2) By a factor varying from  $3\frac{1}{3}$  to 5 depending upon the number of specimens tested. This factor is essentially to allow for scatter. In this context, since the standard S-N curves are usually based on a large number of results a scatter factor of  $3\frac{1}{3}$  is used. The greater uncertainty compared with results based on the component tests is usually allowed for by using what are thought to be conservative S-N data.

(3) By a factor of 1.5 to allow for variations in load spectrum from aircraft to aircraft flying the same role, when it is assumed that the calculated life is based on an average spectrum. This factor is not required if the provisional life is to be monitored for individual aircraft by the fatigue meter or some other method of recording individual variations of load spectrum. If it is decided to use the fatigue meter to monitor the provisional life, a formula will be derived as described subsequently, but unless the major fatigue test is likely to be delayed or the particular aircraft are going to fly consistently in a severe role, it is normal to wait for the results of the major fatigue test before developing the fatigue meter formula.

#### THE MAJOR OR FULL-SCALE TEST

It is now recognised that lives based on calculations or component tests are likely to be inaccurate. This condition exists partly because the loads on the particular components considered are difficult to assess accurately owing to the complex nature of the structure and partly because of the difficulty of predicting which are in fact the critical components. It has therefore become a matter of policy to carry out tests either on the complete structure or on the major components (complete wing, fuselage, fin, etc.). In the latter case, all parts of the structure must be covered.

The test specimen is normally an early production airframe to ensure that detail design and manufacturing standards are comparable with those of service aircraft. The load spectrum is again derived from the utilisation pattern in the specification. However, by this time some flight load measurements should have taken place on prototype aircraft so that more knowledge should be available, for example, on the dynamic response of the aircraft, and should lead to more realistic relationships between local stresses and centre-of-gravity accelerations.

Usually the loads are applied in realistic sequences by using many load levels. For transports and heavy bombers this procedure results in flight-by-flight loading so that ground-air cycles are interspersed with flight loads and in most cases, a ground load spectrum also is applied. In addition, on some of these aircraft, the manoeuvres and gust loads have been applied in a random order between the ground-air cycles. These realistic sequences are intended to ensure that the changing residual stress



patterns around the stress concentrations which are known to affect fatigue life, but which at this time are not taken into account in theoretical assessments, are reasonably accounted for on test. The random load sequence of gusts has another advantage over the more common block programme in that it is easier to use a large number of load levels because there is no fixed pattern for each flight and hence no need to choose intervals of load that result in finite numbers of each level per flight. This procedure enables a better representation of a continuous stress spectrum to be made than can be achieved with the usual block programme. The flight-by-flight representation is not always used on fighter-attack aircraft if the negative flight manoeuvres impose bigger down loads than those on the ground.

The test is normally carried on to the "factored" required life unless prior catastrophic failure occurs. If no such failure has taken place, a review is made and frequently the test is continued for another factored life or to failure to allow for any extension of life in service beyond that anticipated at the design stage.

#### INTERPRETATION OF MAJOR FATIGUE TEST

The failure or failures that have occurred under the known loading on test have to be related to the load spectra experienced in the various roles in service and safety factors applied to allow for scatter. For each failure, the following procedure is adopted:

(1) The S-N curve used to estimate the life of the failed item in the design-development phase is adjusted by factoring the stress scale until the calculation using the stress spectrum applied on the test gives the test life to failure.

(2) This adjusted S-N curve is then used to calculate the lives to be expected in the various service roles, using Miner's hypothesis and the anticipated spectra. The same curve is used to derive the coefficients of the fatigue meter formulae which are obtained by the method described by Phillips. (See ref. 2.) The use of these formulae is described subsequently.

(3) The lives for each role and the coefficients of the fatigue meter formulae are then divided by the factor to allow for scatter in performance. In general, only one specimen will have been tested so that according to the recommended factors in AvP 970 a value of 5 should be used, but in practice, a factor of  $3\frac{1}{3}$  has been used for all lives based on major tests. Although this procedure is difficult to justify theoretically, it was considered reasonable in view of the greater certainty obtained from this type of test. As there has been no regular shortfall in achieved service life that could be attributed to this cause, the practice has been allowed to stand. It should nevertheless be recognised that it is extremely difficult to obtain feedback of service data on which to base a reliable correlation analysis.

(4) The lives for each role are divided by a further factor of 1.5 to allow for variations of load spectrum experienced by individual aircraft flying the same role. This factor is not applied to the fatigue meter coefficients as the meter registers the individual variations.

It should be emphasized that the utilisation pattern originally laid down should represent as nearly as possible the anticipated usage in service because the fatigue test is based on this pattern and although estimates can be made for other patterns, as shown above, the accuracy of prediction is likely to fall when the new patterns deviate markedly from that used on test.

### FAIL-SAFE STRUCTURES

The procedure described is aimed primarily at preserving the safety of safe-life type structures which can fail without prior warning. A similar procedure is also necessary for fail-safe structures, which are defined as those in which fatigue cracks or component failures can be found before the strength falls to an unacceptable level. As the whole concept of fail-safe stands or falls by the ability to detect cracks early, the importance of ensuring that all cracks can be found cannot be overstressed. Hence, it is essential to obtain as much information as possible from the full-scale test on the probable location of cracks. Thus, the full-scale test is as important for fail-safe structures as for the safe-life type although the emphasis is different.

The test should first demonstrate that the structure really is fail-safe, that is, that at no time during the service life is there likely to be an undetectable major failure. The main dangers are design errors leading to an early unexpected catastrophic failure or the accumulation of many small failures late in the life which are insignificant and difficult to detect individually but which may suddenly join to give a catastrophic failure. The long riveted joints of pressure cabins are particularly vulnerable to this latter type of failure as the skin experiences similar stress cycles at all rivet locations. Hence, small cracks, which will almost certainly escape detection, are likely to form at about the same time along the rivet line, and these may suddenly join into one long, possibly catastrophic crack.

The second purpose of the test is to show which are the likely areas of cracking, when the cracks are likely to occur and how fast they will propagate. This information will enable inspections to be started early enough and to take place frequently enough to ensure safety. In addition, the actual inspection techniques can be developed on the complete built-up structure.

In order to show that no catastrophic failures will occur during the required life, a fail-safe structure is required to be tested to the same factors on life as a safe-life



structure. In order to demonstrate that cracks are fail-safe, a crack must be allowed to propagate on test for three inspection periods after it has reached the shortest length that can be found with certainty under the inspection method to be used. At the end of that time it must sustain 80 percent of the ultimate load.

The demonstration of the residual strength characteristics poses a practical problem. The 80 percent ultimate load cannot be applied at the end of the crack propagation phase if the test has not reached the factored required life because if it does not survive the application of the load, the specimen is lost or severely damaged and if it does survive, the rest of the test will be invalidated because of the unrepresentative residual stress pattern generated by this exceptionally high load. The usual technique is to run the crack for three inspection periods or until the crack is considered long enough just to sustain the test load. (In this case a shorter inspection period will be imposed in service.) The crack is then repaired with a patch and the test continued. At the conclusion of the test the patches are removed one at a time and the 80 percent ultimate load applied. This is clearly not entirely satisfactory but no completely satisfactory solution has been found. In some cases it may be possible to simulate the relevant cracks on the static test specimen if this is still available and apply the test load to that, but care must be exercised to ensure a crack tip that is typical of fatigue.

These requirements ensure safety but it is also necessary to ensure a reasonably economic aircraft. It is therefore a requirement that the first crack shall not appear on the weakest aircraft from a fatigue point of view before half the specified life has been achieved and that the amount of repair work shall not become uneconomic on the weakest aircraft before the whole specified life is achieved.

Hence it can be seen that the test requirements are similar for both fail-safe and safe-life aircraft. Therefore, although the designer is encouraged to design fail-safe (if he believes his design to be fail-safe he is at liberty to use lower factors in the design to allow for scatter than he would for safe-life design), the structure is judged on its performance in the test, such failures that occur being judged on their merits. Failures which can be considered fail-safe will require inspection in service starting at the factored life, followed by repair or replacement only if they occur, whereas safe-life failures require either modification of the failed item or retirement of the whole structure at the factored life.

### MONITORING IN SERVICE

The object of monitoring in service is to relate the load spectra experienced by individual aircraft to the failures that occur on the fatigue test. In order to assess the service load spectra, each aircraft is equipped with a fatigue (load) meter, which is a

counting accelerometer recording the number of times each of eight levels of centre-of-gravity acceleration is exceeded. The actual levels recorded depend upon the type of aircraft, there being a number of standard instruments, but usually there are five levels above 1g and three below. These instruments are read after every flight and the counts recorded together with information on the type of sortie, take-off and landing weight, stores carried, number of pressurizations and any other details considered relevant to the consumption of fatigue life.

There are then three main methods of using this information: the fatigue meter formula, role lives, and total number of occurrences of a particular event, each of which tells the operator to initiate some action. Each method relates a failure under the known test loading to the loads experienced in service with the appropriate factors. If the failure on test is safe-life, reaching the factored life means either that the item must be replaced or that the complete structure must be retired. If the failure is fail-safe, reaching the factored life means that inspection must start. These inspections continue at a frequency determined by the same methods; that is, the individual load spectra are related to the test loadings during the crack-propagation phase so that inspection periods may fluctuate in time depending upon usage. In practice, inspections are called for either at fixed time intervals to coincide with normal scheduled maintenance or when the monitoring system indicates an inspection to be due; it is usually possible to ensure that most inspections occur at scheduled maintenance periods.

Of the three methods of assessing the fatigue life, the fatigue meter formula is considered to be the most accurate and is used when the stress levels at the monitored stations can be related to centre-of-gravity accelerations. This usage usually covers wing stations and fuselage stations affected by longitudinal bending. The operator is supplied with a formula consisting of coefficients by which to multiply the counts recorded on each flight at each level of g, together with overall factors depending upon type of sortie, take-off and landing weight, stores carried, etc. He thus calculates flight by flight a steadily increasing number which is a measure of fatigue damage. When the number reaches a certain value, he initiates the appropriate action, either retirement or start of inspection. In the early days of fatigue meter formulae, one simple set of coefficients was used to monitor the one safe-life failure that determined the ultimate life of the structure. Today, with fail-safe structures it may be necessary to monitor a series of possible failures, inspections for which will start at different times. In addition, with the large variety and weight of stores that can be carried, it has become necessary to allow for relatively large variations in the relationship between stress at the station to be monitored and the centre-of-gravity acceleration recorded. Hence it is sometimes necessary to have a series of formulae and correction factors for one aircraft.



The second method of monitoring, role lives, is used to cover periods of flying in which the fatigue meter is unserviceable or to monitor parts for which the fatigue meter counts have no relevance but for which it is known that the load spectrum varies with the type of sortie, or role flown. In this method, the load spectra are first estimated for each type of flight (in the case of flying with an unserviceable meter these are obtained by analysis of other aircraft records on similar sorties). The factored lives are then calculated by using Miner's hypothesis and the adjusted S-N curve derived from the test. It should be noted that if average load spectra are used, the factor of 1.5 for variation within the same sortie must be included. Each hour's flying is then divided by the factored life in the role to give the fraction of damage done. When these fractions add up to 1, the appropriate action is taken. When used to cover periods of meter unserviceability, the operator is given a coefficient based on this fraction by which to multiply the number of hours flown in each role and this number can be added to the number obtained from the fatigue meter formulae.

The third method of monitoring is the simplest and can be used when the fatigue damage in a part is due entirely to one operation, say pressurization, when the life to "action" is given in terms of the numbers of occurrences of that operation. Again the time to action by the operator is based on the number of such cycles to failure in the fatigue test with the appropriate factor. In the case of pressurization, if the test is carried out by using maximum pressure differentials for every cycle and all pressurizations recorded in service are assumed to be to maximum differential, the factor used is  $3\frac{1}{3}$ .

One byproduct of the recording of fatigue meter readings after every flight together with the type of sortie flown is that the load spectra are analysed on a sortie basis and used in estimating load spectra for future aircraft.

In general, it is felt that although the fatigue meter has provided and is still providing an extremely valuable method of monitoring fatigue life in service, more elaborate methods are required to cope with the changes in the stress and centre-of-gravity acceleration relationship that now occur on most aircraft. Moreover, some monitoring system must be developed for areas such as the tailplane, fin and undercarriage for which methods of monitoring are still in the exploratory stage and for which there is little or no operational data on load spectra.

## THE GENERAL PROBLEM OF THE HELICOPTER

In general, the approach to the fatigue problem in the helicopter is based on the same concepts as those used for fixed-wing aircraft; that is, the load spectrum and fatigue performance for each component must be determined and its life estimated and monitored in service. In the helicopter, however, most of the critical items are

contained in the rotating parts and their controls and these parts are subjected to fluctuating loads even under steady flight conditions. Therefore, large numbers of cycles are accumulated in a short time, and there is a consequent shift of emphasis to the fatigue behaviour at the low stress end of the S-N curve. This shift of emphasis results in one of the main differences between fixed-wing aircraft and helicopter requirements; all the factors are on stress instead of on life as factors on life become meaningless when the S-N curve is nearly horizontal. The fact that stress cycles are generated even during steady flight has its impact on the estimation of load spectra. It is clear that in order to have any reasonable life at all, stress cycles in steady-flight conditions must be below the fatigue limit. Therefore, the life is determined principally by occasional excursions of the stress-cycle magnitude above the fatigue limit which are usually found to occur during a few transitory manoeuvres and short periods in a few flight conditions such as at high speed. Determination of load spectra becomes a process of defining these manoeuvres and flight conditions, estimating the frequency with which they will occur, and estimating the magnitudes and numbers of cycles occurring in each of the manoeuvres or flight conditions specified.

#### THE DESIGN-DEVELOPMENT PHASE FOR THE HELICOPTER

Essentially, the same information needs to be written into the customer's specification for the helicopter as for the fixed-wing aircraft, that is, life required, types of sortie to be flown, operating weights, and stores to be carried. However, the estimation of load spectra from this requirement is in terms of frequencies of occurrence of the various critical manoeuvres and flight conditions. Owing to the lack of measured operational data, these values have to be estimated from a consideration of how the helicopter is going to be used. However, with the present state of knowledge it is virtually impossible to calculate the stresses arising in the many components associated with the rotating parts and their controls during these critical manoeuvres and flight conditions. Consequently, at the design stage, the stresses calculated for steady cruise condition are multiplied by 1.5 and maintained below the fatigue limit of the factored S-N curve. Past experience has shown that this method provides a reasonable design starting point. The S-N curve used is either a relevant one from tests on similar components from a previous helicopter or a material curve with allowance for stress concentrations, etc. The factor at this stage is 2 on stress.

During development, the loads and stress spectra are steadily acquired by progressive flight measurement on an extensively strain gaged prototype helicopter. Simple manoeuvres are flown, and stresses are measured, related to the appropriate S-N data, and assessed for safety. The helicopter is then cleared for the next more complex manoeuvre. At the same time S-N data are built up by constant-amplitude tests on the more critical items.



## HELICOPTER FATIGUE SUBSTANTIATION

The final life substantiation is based on flight measurements of stress, S-N curves obtained either by constant-amplitude tests or programme-load tests factored to allow for scatter, and calculations using Miner's hypothesis.

In order to obtain the stress spectrum for each component, each of the manoeuvres or flight conditions considered likely to produce fatigue damaging cycles is flown at least three times. In those conditions where the three flights give widely different results, more measurements are made. In the first analysis only the maximum stress cycle is associated with each manoeuvre or flight condition and it is conservatively assumed that this cycle occurs at the typical frequency of the stress cycle in that component for as long as the manoeuvre exists. For those components and flight conditions where the subsequent fatigue analysis shows this analysis to give unacceptably low lives, a more elaborate analysis takes place which provides a spectrum of stress amplitudes to be associated with that flight condition. The total stress spectrum can then be obtained for each component by using the frequencies of occurrence of each manoeuvre or times spent in each flight condition estimated from the specification together with the measured stress amplitudes for these manoeuvres and conditions. To allow for variations in stress from helicopter to helicopter when flying the same manoeuvres, the measured stresses are usually multiplied by a factor of 1.2.

The S-N curve for each component is obtained in most cases by testing at least six specimens under constant-amplitude loading; normally three specimens are tested at each of two stress amplitudes. A curve of predetermined shape based on past experience is then drawn through the mean values of life obtained in each of the two groups and this curve is factored on stress values to allow for scatter. When six or more specimens have been tested, a factor of 1.6 is used for light-alloy components, and 1.4 steel and titanium. (The figure for titanium is provisional, being based on limited data.) Where less specimens have been tested, higher factors are used. It is considered that gear boxes show less scatter than other components; therefore, a factor of 1.4 is used if one gear box is tested and 1.3 if four or more specimens are tested. These factors are appreciably bigger than those quoted in AvP 970, but are based on the latest information on scatter and current practice.

The fatigue life is then determined by using Miner's hypothesis except that a value for  $\sum \frac{n}{N}$  of 0.75 is used. When the maximum stress amplitude in the whole stress spectrum is below the fatigue limit of the factored S-N curve for that component, the item is considered to have a virtually infinite life. The fatigue limit for light-alloy specimens is taken as that stress amplitude giving a life of  $10^9$  cycles and for low and medium strength steels, that giving  $5 \times 10^6$  cycles. Where testing of light-alloy

components has only been taken to  $5 \times 10^6$  cycles, a factor of 1.35 on stress is used to estimate the fatigue limit.

For components experiencing a complex load history, it is considered advisable to test under a mixed load level to simulate more nearly the actual conditions, although the loads will be increased to allow for scatter and to obtain failures in a reasonable time. (This procedure is in contrast to fixed-wing practice where tests are conducted under real loads for factored times.) The results are used to locate the mean S-N curve for the component in the same way as for fixed-wing aircraft; that is, a predetermined shape of S-N curve is factored in the stress direction until the cumulative damage calculation gives the mean life achieved on test under the known loads.

### MONITORING HELICOPTER LIFE

At present there are no monitoring instruments for the helicopter analogous to the fatigue meter for the fixed-wing aircraft. Therefore, all components are assigned safe lives in flying hours. Although the helicopter is used in many roles, there has been no attempt as yet to define different lives for each role or record times spent in each role. Consequently, lives have been assessed in whichever role is considered to be most severe for the component under consideration and those lives considered to be the retirement lives irrespective of the subsequent usage.

### FAIL-SAFE FOR THE HELICOPTER

It is clear from the previous two sections that in many ways there are greater difficulties in estimating safe lives for helicopters than for fixed-wing aircraft. The lives are very dependent upon a few transitory loads occurring during certain flight conditions and manoeuvres. The flight conditions themselves are not easy to define accurately and the magnitudes of the loads within those conditions are likely to vary considerably depending upon pilot technique and state of maintenance of the helicopter. Moreover, helicopters of the same type are used for a wide variety of jobs; hence, variations in life of similar components are liable to be very large. In addition, minor damage such as a small score can result in a drastic reduction in life as the large number of cycles of stress otherwise below the fatigue limit are thus raised to a level where they add to the damage. In the circumstances, designs to fail-safe principles are highly desirable from a safety point of view.

It is often thought that this concept with its implication of redundancy can only be obtained at the cost of extra weight. It has been found in fixed-wing aircraft that this is not necessarily the case and, in fact, once the principles of design detail have been



mastered, there may actually be a saving of weight in those areas of the structure designed by fatigue because lower factors to allow for scatter can be used in the design of fail-safe parts than could be used if those parts were safe-life. This condition occurs because it becomes no longer necessary to ensure that fatigue initiation probability approaches zero, the only criterion on frequency of fatigue failure being the economic ones of maintenance and repair costs. The fact that so many of the helicopter rotating parts are fatigue designed and the variations of loading from aircraft to aircraft are so great and yet there are so few fatigue failures in service suggests that there may be appreciable overdesign and therefore significant weight saving to be gained by fail-safe design as well as the added safety.

At present, there are no requirements for fail-safe for helicopters in AvP 970, but there should be no basic problem in writing such requirements in general terms. Indeed, the approach would be identical to that used for fixed-wing aircraft; namely, that any failure shall be found before the residual strength falls below an acceptable value. However, the real problem, once the principles of fail-safe as defined by the requirements are fully understood, is one of detail design and it is here that the main attack must be made if the advantages of fail-safe design are to be realised. In addition, since the early detection of failures or cracks is vital to fail-safe, it would be worth putting more effort into the development of inspection techniques. This effort may involve special systems for particular parts, such as the blade inspection method developed by Sikorsky in which the blade is inflated and cracks detected by loss of pressure. However, it must be remembered that helicopters frequently operate in relatively primitive conditions so that simple techniques are required.

## FUTURE WORK

The procedure described in this paper for coping with the problems of fatigue in aircraft structures which has evolved over the years has maintained an acceptable standard of safety. Nevertheless, every step in that process contains problems that could lead to inaccuracies. As the customer demands longer lives for his expensive aircraft, the need for better life estimation is of paramount importance, both for the safety of safe-life aircraft and the economy of fail-safe aircraft.

The areas in which effort is still needed can be considered in two main groups: those associated with defining the load-stress spectra and those concerned with the determination of fatigue performance. If the load-spectrum problems are considered first, wing loads and fuselage bending loads are reasonably served by the fatigue meter; this meter monitors loads on individual aircraft and provides operational data. However, with the wide variation in the stress and centre-of-gravity acceleration relationship

possible in modern aircraft because of the high rates of fuel usage, and the large range of stores carried, some more direct method of obtaining stress spectra is required. If such methods should be developed for operational use, they would be invaluable in monitoring fatigue life consumption of fins, tailplanes, undercarriages, and possibly even helicopter components, although in the latter case there is an additional practical problem of recording outputs through rotating machinery. In the event of monitoring by direct stress measurement being developed, it may be found that the process of feeding back to the design stage will be more difficult than that for current monitoring methods using counting accelerometers, bearing in mind that for both systems allowance must be made for the response characteristics of the aircraft on which the measurements were made before these measurements can be applied to the new aircraft. This procedure is already used to a large extent for response to turbulence, and the power spectral approach used in this connection is being applied to estimating undercarriage loads. However, more work needs to be done in relating the theoretical work in this field to measurements in flight and during ground operations.

The problems associated with fatigue performance will now be considered. The outstanding need is for a new cumulative damage hypothesis that takes sequence effects and fretting into account. With the greater understanding of the effects of residual stresses around stress concentrations, it is hoped that methods of accounting reliably for the former will not be too long delayed. In view of the increasing tendency to design fail-safe, there is a need for more work on methods of predicting crack propagation rates in complex structures under variable loading and the residual strengths of the cracked structures.

It is unlikely that even improved methods of estimating initiation time, crack propagation rates, and residual strengths will enable us to dispense with the major fatigue test. However, such improvements may help in the simplification and interpretation of this test. There are a number of questions in this connection that still require further attention. Firstly, to what extent can the time-consuming low-level stresses be omitted? Secondly, what should be the magnitude of the biggest load applied in test? What precisely is the effect of a load equal to or greater than proof load on the subsequent behaviour and can this effect be counteracted in any way? This consideration is important in solving the problem of proving the residual strength of a cracked structure.

To summarize, it is considered that work will be required in the following areas:

- (1) Theoretical work on dynamic response giving load and stress distributions
- (2) Development of flight measurement and analysis techniques to check and modify the theoretical assessments



(3) The development of operational monitoring devices measuring stress directly. These devices may be expensive and consequently limited to use on a few aircraft.

(4) The development of monitoring devices that can be used on every aircraft to measure parameters that can be related to the stresses measured on the more elaborate instruments. It is considered essential on military aircraft that some monitoring device is used on every aircraft as the variations in load spectra on aircraft in the same role can be very large.

(5) Development of new cumulative damage theories to account for sequence effects and fretting

(6) Development of methods of predicting crack-propagation rates in complex structures under variable loading

(7) Development of methods of predicting residual strengths of cracked structures

(8) Assessment of what stress levels should be included in fatigue tests under realistic loads

(9) The development of aircraft capable of sustained supersonic flight means that more work will be needed in the fields of estimating, measuring, and monitoring stresses due to thermal effects, and interpreting their influence on the fatigue problem.

## REFERENCES

1. Raithby, K. D.: A Comparison of Predicted and Achieved Lives of Aircraft Structures. Tech. Note No. Struct. 301, Brit. R.A.E., 1961. (Paper presented at I.C.A.F. Symposium on Fatigue (Paris), May 1961.)
2. Phillips, J.: Formulae for Use With the Fatigue Load Meter in the Assessment of Wing Fatigue Life. Tech. Note No. Struct. 279, Brit. R.A.E., 1960.

A PROPOSED USAF FATIGUE EVALUATION PROGRAM BASED  
UPON RECENT SYSTEMS' EXPERIENCEBy G. P. Haviland and G. F. Purkey  
Aeronautical Systems Division, U.S. Air Force  
United States

## SUMMARY

The United States Air Force has published a document entitled, "Aircraft Structural Integrity Program" (ASIP). One phase of the program is concerned with the fatigue life certification of all types of military aircraft. The document describes the criteria, analyses, and tests that are necessary in order to satisfy the USAF fatigue life requirement. The authors have noted that some recent and valid criticism has been directed toward the document, particularly the fatigue-life requirements contained in it. This paper proposes some changes based on surveys conducted in the United States and abroad as well as some recent systems' experience. The surveys covered both military and civilian organizations. The paper contains the fatigue certification case histories of selected military and commercial aircraft. The design development element tests, preproduction design verification tests, and full-scale fatigue tests of each are described. The paper concludes with a brief status report on the revisions to the MIL-A-008860 series specifications.

## INTRODUCTION

In 1965, Miller and Lowndes presented a paper before this group entitled "The U.S. Air Force Weapon Systems Fatigue Certification Program." (See ref. 1.) Their paper described the evolution of the USAF fatigue life requirements up to that time. One section of the paper listed the aircraft which were considered to be the first line systems of the USAF in 1965. These aircraft are as follows:

Fighters	Bombers	Trainers	Transport
F-89	B-47	T-37	C-130
F-100	B-52	T-38	C-133
F-101	B-66		KC-135
F-102			
F-104			
F-105			
F-106			



Of these only the following aircraft were committed to a fatigue evaluation program:

Fighters	Bombers	Trainers	Transport
F-101	B-47	T-37	C-130
F-104	B-52	T-38	C-133
F-105			KC-135
F-106			

Five years later, the first line systems of the USAF are as follows:

Fighters	Bombers	Trainers	Transport
F-100	B-52	T-37	C-130
F-105	FB-111	T-38	KC-135
F-106			C-5
F-4			
F-5			
F-111			
A-37			

Of these currently operational systems, every one except the F-4 has undergone the U.S. Air Force fatigue evaluation program. The F-4 was procured by the U.S. Navy and has not been required to conform to Air Force Aircraft Structural Integrity Program (ASIP). It is also acknowledged that the F-100 although not originally designed or tested under any formal program has required several life extensions. Each one has been approved after additional fatigue testing. It is interesting to note that all aircraft now in our inventory have undergone a fatigue evaluation program of some kind. This statement was not true 5 years ago. With this as an introduction, we wish to expand on the USAF's fatigue evaluation program and how it has changed over the last 5 years.

## HISTORY OF STRUCTURAL EVALUATION PROGRAM

### 1965 to 1968 Period

Figure 1 shows a typical structural evaluation program of the 1965 to 1968 time period. (Also see refs. 2 and 3.) At that time, ASIP required element and component tests, but the number and specimen sizes were left to the contractor's discretion. The static test, flight loads survey, and the first fatigue test were run concurrently. After initial operational capability (IOC) the program called for service-loads determination followed by a second fatigue specimen to be tested to the service-loads spectrum. At that

time, it appeared to be a good plan and the requirements formalizing the program were written as an ASD Technical Report 66-57 "Air Force Structural Integrity Program Requirements," dated January 1968 (ref. 4) and into various specifications and contracts. For those of you who are satisfied with your program now, please note that in 1968 we believed that this program was the best in the world. Events proved us to be wrong.

#### 1968 to Early 1970 Period

In September 1968 the Assistant Secretary of the Air Force for Research and Development, Dr. Flax, requested that a study be performed addressing problems associated with structural test program planning and with scheduling practices. (This study is referred to as the Flax study.) Briefly restated, the action items were

- (a) Examine current Air Force structural test procedures and policies for aircraft in development.
- (b) Assess structural test program scheduling problems.
- (c) Assess past and present structural testing to determine problems or deficiencies in established policies and procedures.
- (d) Provide recommendations to revise present Air Force structural test verification practices and policies, considering proper balance between program risks and costs.

The approach used in the Flax study was to prepare case histories of the then current systems and a number of typical earlier systems on which information was available. Included in the study were such data as original test schedules, the details of static and fatigue tests, actual start and completion of the tests, and the production rates. The case histories were carefully studied to establish trends and to identify problem areas. With these thoughts in mind, let us consider the actual structural program schedules of some of the Air Force aircraft that were used in the study.

The first aircraft is a large transport, the C-141. Figure 2 shows the schedule. The C-141 comes as close as any airplane to fulfilling the total ASIP requirements. It has a static test, structural flight tests, full-scale fatigue tests of two articles, and a life-history recorder program, the data from which are being used for the second fatigue test. Figure 2 refers to fatigue test articles A, B, C, D, and E which are shown pictorially in figure 3.

There were a large number of engineering changes generated by the C-141 fatigue test program. Most of them were incorporated in production but very late in time. You can see that there were essentially no component tests. We did a static test and a flight loads survey almost concurrently as called for by the 1968 ASIP schedule shown earlier, but the fatigue test was very late in starting. We had aircraft out in the operational fleet before we had one lifetime on the fatigue test specimen.



Using hindsight, if we had started the first fatigue test earlier, we would have been able to incorporate the changes into earlier production airframes. Instead, we were unable to get changes into production earlier than the 200th airframe and we only had 285 airframes in the production contract. The fatigue test article had been identified early enough (it was the seventh airframe), but the actual start of the testing slipped because of management considerations. The lesson learned here was an important one. If you have a production airframe, get started on the fatigue test as early as possible.

In order to understand more about how the commercial manufacturers design and build airframes, we will deviate from the Flax study and show you a comparison we made between the C-141 and, with the assistance of the Boeing Company, the Boeing 727. We found that Boeing uses a modified form of ASIP. Boeing does everything that ASIP requires, but not in as much depth or detail as we in the Air Force do. For example, a flight loads survey was conducted on the 727 because the FAA was interested in the T-tail. Otherwise, the survey would not have been flown. Our load survey on the C-141 was very comprehensive.

Let us consider the fatigue tests of the two aircraft. The preparation of the fatigue spectra for the C-141 was complicated by the large number of missions assigned to the aircraft. Low level penetration, air delivery of cargo and wartime training missions had to be included in the spectrum. Therefore, the C-141 required about twice the fatigue test segments needed for the 727. The Boeing 727 has essentially a single logistic mission at altitude.

The way we did our tests compared with the way Boeing performed their fatigue tests is also very interesting. A list of the fatigue test articles for the 727 and the 747 follow:

- 727 and 747 nose landing gear
- Main landing gear
- Airframe
  - Wing
  - Fuselage
  - Vertical tail
  - Horizontal tail
  - Control surfaces

The horizontal tail was a separate test specimen for the 747. You have already seen those for the C-141 fatigue test specimen in figure 3. We chose to break the airframe up into components so that a failure on one specimen will not cause an interruption to the others. This method is more expensive than the method used by Boeing but it is less risky.

Figure 4 is a direct comparison between the test schedules of the C-141 and the 727. The differences in magnitude of the scope of the tests are significant. Our static test took longer because of down time and a need to retest the wing after uncovering a different load distribution than expected during the flight loads survey. Our fatigue test also took longer because of the multimission requirement of the C-141. The major differences between Boeing tests and the USAF tests are as follows:

13 missions	C-141
1 mission	727
Boeing tests whole structure	
USAF test major components	
Boeing performs modest flight loads survey	
USAF performs full flight loads survey	

Now let us consider another Air Force aircraft test program, that for the F-5 (fig. 5). This program was successful for two reasons: First, the F-5 airframe was essentially the same as that of the T-38 and the Norair N-156 which had undergone an extensive structural evaluation program. Secondly, the items that were changed on the F-5 from the T-38 were tested as components during the design development testing phase of the program. The primary difference between the T-38 and the F-5 was, of course, that the T-38 was a trainer type aircraft designed for the training environment, whereas the F-5 was a fighter type with external stores and tip tanks, leading-edge flaps, and drag chute; the F-5 was also designed for the close ground support fighter environment. This type of redesign readily lends itself to verification of structural adequacy by utilizing small components or element testing. In the development of the F-5, if it had not had the T-38 as a predecessor, the component tests would have been required.

It should be noted that the service-loads—life-history phase was limited on the F-5 evaluation. It started late and was stopped much too early. If a continuous program had been accomplished, the loss of an F-5 at Williams Air Force Base in early 1970 might have been averted. At Williams AFB, training is conducted for Military Assistance Program (MAP) pilots. During this training a large number of 2g to 3g maneuvers are accomplished. The fatigue damage accumulated from this training is much greater than the average damage accumulation and a fatigue crack developed in the center wing lower skin that caused the loss of pilot and aircraft. This fatigue critical area had been detected in the full-scale fatigue test. Had an adequate service-loads or life-history program been in being, the damage accumulation should have been detected and an adequate inspection program could have anticipated the need for repair.

The timing of the full-scale fatigue test also could stand some improvement in that it could have started sooner. Again, the previous T-38 tests along with the F-5 develop-



ment tests minimized the impact of the later start and did allow the use of a truly production configuration for the full-scale fatigue test.

Out of the Flax study came some very significant recommendations:

- (a) Continue early static and fatigue tests
- (b) Emphasize component tests
- (c) Establish firm policy on structural integrity program

(d) Perform cost effectiveness studies during contract definition phase between developmental and production testing and between production build-up and structural retrofit. These recommendations were accepted and we revised our ASIP requirements document ASD TR 66-57 (ref. 5). It was published in May 1970 and many of you are familiar with it.

Now we want to discuss the present ASIP schedule, the one called for by the 1970 version of ASD TR 66-57. Before doing that, let us agree on some definitions of element tests, design-development tests, preproduction design verification tests, and full-scale tests. Element tests involve relatively small parts of the structure, joints, small panels, or stringer to frame splices. These are very small pieces but, as you know, extremely important to the structure. Design development and preproduction design verification tests consist of those tests of materials, structural elements, and structural components performed early in the design phase to provide a realistic basis for the design analysis and major structural ground tests. The design development tests are the most basic and earliest tests and are conducted to establish basic design concepts and configurations such as choice of materials, panel sizes, splices, fittings, etc. Preproduction design verification (PDV) tests are conducted after the design development tests, but prior to the full-scale static and fatigue tests. These tests of full-scale components (wing carry through, wing pivots, horizontal-tail support, etc.) are conducted to provide early design information wherever analytical methods may be inadequate to achieve a high degree of confidence in the strength and fatigue properties of the design. These tests are intended to reveal design "glitches" prior to the full-scale ground tests.

With these thoughts as background, let us consider our present ASIP schedule. It is representative of the program now being used on the F-15 and provided the original scheme for the B-1 (fig. 6). It requires that the contractor conduct early preproduction design verification component tests of major assemblies. It also requires two full-scale fatigue tests, the first as early as possible and concurrent with the static test and the flight loads survey. After IOC it requires a service-loads program to obtain the spectrum for the second fatigue test.

## 1970 to Present

Thus far we have traced the changes to the ASIP fatigue evaluation program from 1965 to 1970. Then we had some structural problems which focused national attention on the structural integrity of some of our systems, notably the F-111 and the C-5.

At the direction of Secretary of the Air Force, Seamans, a group of experts was formed to look into the problems we were having or might have in the future. There followed a year and a half of study, reappraisal, reviews, audits, and an overall reevaluation of ASIP and its requirements.

One phase of the structural integrity review involved a trip to Europe. The authors had an opportunity to visit some of you in your home countries of France, Holland, and England. We learned quite a bit from our discussions with you and have since been involved in various meetings and conferences on ASIP.

We had thought of ASIP as a logical, step-by-step program, which, if followed, would insure a structurally sound airplane. But we were mistaken, those of you in Europe seem to be able to design and build sound airframes without a formal structural integrity program such as ASIP. Moreover, we found that ASIP as applied to programs here in the U.S. sometimes worked and sometimes it did not. The primary variable seemed to be the contractor or perhaps the type of contract and not ASIP itself. Thus, our experience has shown that the structural quality of an airplane is a function of who designs it and how he designs and builds it. It has had little to do with the ASIP documentation. This may be an oversimplification of the situation we face in the Air Force today. We realize that our treatment so far has not addressed the basic question of "Do we really need an ASIP at all?" Even so, permit me to pursue a line of reasoning based on the following premises:

- (a) ASIP should be effective regardless of the contractor or the contract selected.
- (b) It is not.
- (c) Therefore, ASIP should be changed.

As a result of recent systems' experience, structural development cost restraints, and a review of international structural test practices, the Air Force is proposing a structural development test program that is different from that used before. The significant change is in the method of fatigue evaluation, as you will notice (fig. 7). The preproduction tests of major assemblies and the early fatigue tests now required seem to be duplicative efforts rather than what is desired. The preproduction tests should identify deficiencies that can be corrected in time for validation on the early full-scale fatigue test.

In the proposed program, design development and preproduction design verification (PDV) tests that are more extensive than those originally identified by the USAF in 1970



are envisioned. The very early component tests must now provide for complete structural evaluation (strength, fatigue, fracture) of the major critical areas of the primary structure. This is necessary (mandatory, even) inasmuch as these component tests are to be the main basis for determining adequacy of the design, proof of compliance, and even early life flight safety since the full-scale fatigue test will be delayed under this proposal. The PDV tests must be comprehensive. Note that this requirement is an intrinsic part of the proposed program.

The important scheduling of the full-scale static test and the flight loads measurement program retain their original timing. These tests are to coincide with the delivery of the first flight article and are to receive equal priority with other subsystem evaluation requirements.

The major change that we are proposing focuses on the full-scale fatigue test. Until now we have identified, in the initial system plans, a requirement for two full-scale fatigue tests, one strictly an early design evaluation test and the other a delayed test (approximately two or more years after initial operational capability) that utilized the results of the earlier design evaluation tests (static test, fatigue test, and flight loads survey). This late fatigue test was also intended to be delayed until completion of the service-loads recording program so that accurate service environment data would be available. However, even when faced with the real-world past experience that all first line military aircraft systems (especially fighters) eventually undergo more than one full-scale fatigue test, USAF management was unwilling to identify funds for two full-scale fatigue tests during initial program definition.

Recognizing this situation and the increased emphasis that we are placing on early component PDV testing and the desire to make the PDV tests effectively impact the design phase as well as the full-scale testing, we are proposing to identify a single fatigue test which will be conducted later than the first test and earlier than the second test previously required. This revised scheduling of the single full-scale fatigue test is necessary so that it will incorporate the findings of the PDV tests, static test, and the flight loads survey. In all probability, it will not be delayed a sufficient amount of time to use the results of the service-loads recording program.

Finally, we recognize, and everyone else should also, that additional laboratory tests (even flight tests) may be required as extensive service experience is accumulated. However, no attempt will be made to identify any additional test requirements in the original development process.

There are definite critical control points in our proposed program that must constantly be reviewed as new systems are developed. There are also some important questions that must be answered:

(1) Can the structures discipline effectively divert major airframe components from the ever present push to get a flight article as early as possible? Our proposed fatigue evaluation program has as its very foundation a comprehensive PDV test program that will require major structural components early enough to complete the tests before flight articles are produced. Can we win out against the competition and acquire these early components in time for the structural evaluation?

(2) The full-scale fatigue test can no longer be used as contractual proof that the design fatigue life requirements have been met. The test will now be based on results of earlier design and test information that cannot be accurately foreseen. Demonstration of structural fatigue quality assurance requirements must utilize the PDV tests.

(3) USAF management must be aware that major changes in the aircraft structure or mission may require further validation. Also, further validation may be required if the single fatigue test did not contain inputs that are representative of the service environment for the original design missions.

We have outlined the proposed changes that the U.S. Air Force is planning in the fatigue evaluation program for future systems. These changes are planned to be incorporated into a revision of both the technical report ASD TR 66-57, dated May 1970, and the appropriate Structures Military Specifications, commonly referred to as the 8860 series specifications.

## UPDATING OF SPECIFICATIONS

### MIL-A-8860 Specifications

To conclude our treatment of the proposed fatigue evaluation program, it may be useful to review our recent progress in updating the MIL-A-8860 specifications. As a result of the Seamans' study, it was suggested that our organization (Aeronautical Systems Division) have the prime responsibility for the documents. Previously, the responsibility rested with the Flight Dynamics Laboratory. We propose to cover some of the significant changes we are making in three selected specifications as well as in the ASD TR 66-57.

The revision of the technical report ASD TR 66-57 will convert the format of the report from an ASD TR to a MIL-STD-(USAF). In addition to the fatigue evaluation changes just discussed, it is planned to include in the revised MIL-STD new or increased emphasis on materials selection, fracture mechanics requirements, and damage tolerance design.

The addition of the requirements for materials selection are presently being written. The area of fracture mechanics principles is, of course, directly related to materials selection and some of the research work being accomplished in this area is the subject of



a paper by Howard A. Wood, of the Air Force Flight Dynamics Laboratory (paper no. 14 of this compilation).

In the area of damage tolerance design requirements, we have made some progress in updating our requirements. Since the new MIL-STD will only summarize the damage tolerance requirements that are contained in the MIL-A-8860 series specifications, our initial effort has been concentrated on revising these specifications. In an attempt to expedite the revision, the Air Force elected to revise and publish "USAF only" revisions. These limited coordinated (USAF only) military specifications have been prepared by using currently available technical information, but they have not been approved for promulgation as a fully coordinated (USAF, Navy, and Army) revision of military specifications. They are subject to modification. Pending their promulgation as fully coordinated military specifications, they may be used in procurement (USAF). The damage tolerance design requirements contained in these revised specifications are covered in the following sections.

#### Damage Tolerance Requirements for Inclusion in MIL-A-008860A (USAF)

The primary structure shall incorporate materials, stress levels, and structural configurations which will minimize the probability of loss of the aircraft due to propagation of undetected flaws, cracks, or other damage. Slow crack growth, alternate load-paths and systems, and other available principles shall be employed to achieve this capability. For this damage tolerance requirement, the primary structure is defined as including all structural elements the failure of which will

- (a) Cause uncontrollable motions of the aircraft within the speed limits for its structural design
- (b) Prevent an aircraft from achieving speeds sufficiently low to effect a safe landing
- (c) Reduce the ultimate factor of safety for flight design conditions from 1.5 to a value less than 1.0.

#### Damage Tolerance Requirements for Inclusion in MIL-A-008866A (USAF)

General requirements.- Safe-life design shall be employed as the primary means of satisfying the specified service life requirement established in appropriate contractual documents for each USAF aircraft system. In addition, damage tolerance concepts shall be applied as a design requirement for primary structure vital to the integrity of the vehicle or the safety of personnel. This latter requirement stems from the recognition that, despite concerted safe-life-insurance efforts through design, analyses, and tests, undetected flaws or damage can exist in critical structural components at some time during the life of the aircraft with attendant, serious consequences.

Safe life.- The fatigue critical areas of the airframe shall be identified through analyses and tests (developmental, preproduction component, and full-scale article). The structure shall be shown to withstand, without structural failure, the design repeated loads spectrum equal to the design fatigue-scatter factor times the service-loads spectrum. A service-loads spectrum is defined for one lifetime only and does not include a design fatigue-scatter factor. Modifications found necessary to satisfy this requirement shall be incorporated prior to aircraft delivery or by retrofit in fleet aircraft as agreed to by the procuring agency.

Design fatigue-scatter factor.- The design fatigue-scatter factor is a factor to provide protection against fatigue failure of those fleet airplanes that experience a service-loads spectrum more severe than the design service-loads spectrum and have fatigue-life capabilities less than those of laboratory test articles. The design fatigue-scatter factor shall be a minimum of 4.0 or as otherwise approved by the procuring activity.

Service-loads spectrum.- The service-loads spectrum is derived from a collection of loads spectra. Each loads spectrum in this collection shall define the expected (average) number of load cycles according to load magnitude for a given source of repeated loads. The loads spectrum for each significant source of repeated loads shall be based on a realistic interpretation of the design usage. The contractor shall include all significant sources of repeated loads. The sources of repeated loads may include, but not be limited to, ground handling and taxiing operations, landing operations, flight maneuvers, atmospheric turbulence, inflight refueling, autopilot, inputs, cabin pressurization, buffeting, terrain-following maneuvers, and the ground-air-ground cycle.

Damage tolerance.- The primary structure vital to the integrity of the vehicle or to the safety of personnel shall incorporate materials, stress levels, and structural configurations which minimize the probability of structural failure due to the propagation of undetected flaws, cracks, or other damage. The choice of damage-tolerant design concepts (fail safe, safe crack growth, or combinations thereof) for the design of specific critical structural components shall be as agreed between the procuring agency and the contractor. Analysis and supporting tests shall be conducted to evaluate the flaw growth and residual strength characteristics of the critical structural components.

Fail safe.- Primary structure that is designed fail safe shall be readily inspectable and meet the following requirements after failure of a principal structural element: (1) the remaining structure shall sustain without failure the maximum expected load or limit load, whichever is greater, (2) the airplane shall be controllable within the design speed limits, and (3) catastrophic failure of the remaining structure will not occur under repeated load conditions during the period to the next opportunity to detect the failure. Verification of the ability of the remaining structure to withstand the repeated loads shall be accomplished by determining the crack growth period from an initial flaw to failure of



a principal element, and then ensuring that the life (including the factor of four) of the remaining structure will equal or exceed the time interval established for the next inspection. Inspection intervals shall be as agreed to by the procuring agency, but, in general, these intervals shall be of reasonable duration commensurate with total system requirements. Readily inspectable structure is defined as that which can be inspected after removal of access panels, doors, etc. Removal of permanent type skins and fasteners is not included. The details of inspection shall be agreed upon by the procuring agency and the contractor.

Safe crack growth.- Critical primary structure that is not fail safe shall be designed so that initial flaws will not propagate to the critical crack length during the specified service life of the airplane. Through fracture data tests and analysis, the characteristics and dimensions of the smallest initial defect that could grow to critical size during the specified service life shall be determined. Once these initial flaw sizes have been identified, quality control procedures shall be developed so that parts containing initial flaws of these dimensions will not be accepted. In the event that the identified initial flaw sizes are smaller than the quality control detection capability, changes shall be made in the materials and/or stress levels so that larger initial flaws (compatible with quality control capability) can be tolerated.

#### Damage-Tolerance Test Requirements for Inclusion in MIL-A-008867A (USAF)

Fracture data tests.- Fracture data shall be generated during the design development test phase on all candidate materials for which no valid data base exists to support the analysis requirements. These tests shall include plane strain and plane stress tests to determine fracture toughness values as well as crack propagation tests to determine incremental crack extension rates. These data shall be used for comparative evaluation of proposed materials and designs. Fracture toughness values shall be determined in accordance with the procedures set forth in the current standards. Specifications shall be prepared to ensure that materials having minimum guaranteed fracture-toughness parameter ( $K_{1C}$ ) values are used in manufacture where test specimens having dimensions that satisfy ASTM requirements can be obtained. Continued sampling of final manufactured parts shall be accomplished throughout the production life to ensure consistency with the required strength and toughness levels.

Crack propagation tests shall be conducted on element specimens to determine the conventional cyclic crack growth rate and sustained load growth rate data. These tests shall include the evaluation of the effects of various atmospheric environments (such as temperature, humidity, fuel, salt, etc.). Spectrum tests of flawed specimens shall also be conducted when insufficient data exists or when proven analytical capability to predict spectrum effects is lacking.

Crack growth tests.- Crack growth tests of preproduction components shall be conducted as required to verify that the damage tolerance criteria have been met. These tests shall be accomplished by applying a spectrum of loads and environment that simulates operational usage which will determine the time to crack initiation and the time to failure of a single principal element. These tests shall utilize, wherever possible, the existing component structures fabricated for evaluation of the strength and fatigue properties as an "add-on" test effort. When necessary, additional component structures shall be fabricated.

The revised structural specifications are as follows:

Specification number	Short title
MIL-A-008860A (USAF)	General
MIL-A-008861A (USAF)	Flight loads
MIL-A-008862A (USAF)	Ground loads
MIL-A-008865A (USAF)	Miscellaneous loads
MIL-A-008866A (USAF)	Fatigue
MIL-A-008867A (USAF)	Ground tests
MIL-A-008869A (USAF)	Nuclear
MIL-A-008870A (USAF)	Flutter
MIL-A-8871A (USAF)	Flight test
MIL-A-8892A (USAF)	Vibration
MIL-A-8893A (USAF)	Sonic fatigue

These specifications listed are dated 31 March 1971 and are presently in printing; the estimated distribution date is July 1971. The MIL-A-008860A, 61A, 62A, 65A, 67A, 69A, and 70A are former ASG (joint) specifications which have been revised as USAF only specifications. MIL-A-008871A has always been a USAF only specification. MIL-A-8892 and MIL-A-8893 are new specifications which apply to USAF only.

The next two major efforts that are presently being accomplished are, revision of ASD TR 66-57 into a MIL-STD, and full coordination on the revised specification will result in ASG type specifications.

#### CONCLUDING REMARKS

We are proposing the elimination of one full-scale fatigue test article and replacing it with early full-scale component tests. The full-scale fatigue test is performed later than present requirements state but earlier than the previously required second fatigue test. To formalize this change in the fatigue evaluation program, we are revising the 8860 series of specifications and writing the USAF ASIP into a separate Military Standard.



The authors wish to express their appreciation to Mr. Troy King for his assistance in preparing this paper.

#### REFERENCES

1. Miller, W. B.; and Lowndes, H. B.: The U.S. Air Force Weapon Systems Fatigue Certification Program. Technical Paper, ASD, U.S. Air Force, June 1965.
2. Anon.: Detailed Requirements for Structural Fatigue Certification Programs. Tech. Memo. WCLS-TM-58-4, U.S. Air Force, June 27, 1968.
3. Anon.: Detailed Requirements and Status Air Force Structural Integrity Program. ASD TN 61-141, U.S. Air Force, Sept. 1961.
4. Anon.: Air Force Structural Integrity Program Requirements. ASD Tech. Rep. 66-57, U.S. Air Force, Jan. 1968.
5. Anon.: Air Force Aircraft Structural Integrity Program: Airplane Requirements. ASD Tech. Rep. 66-57, U.S. Air Force, May 1970.

# 1968 STRUCTURAL EVALUATION PROGRAM

## LIFE PHASES

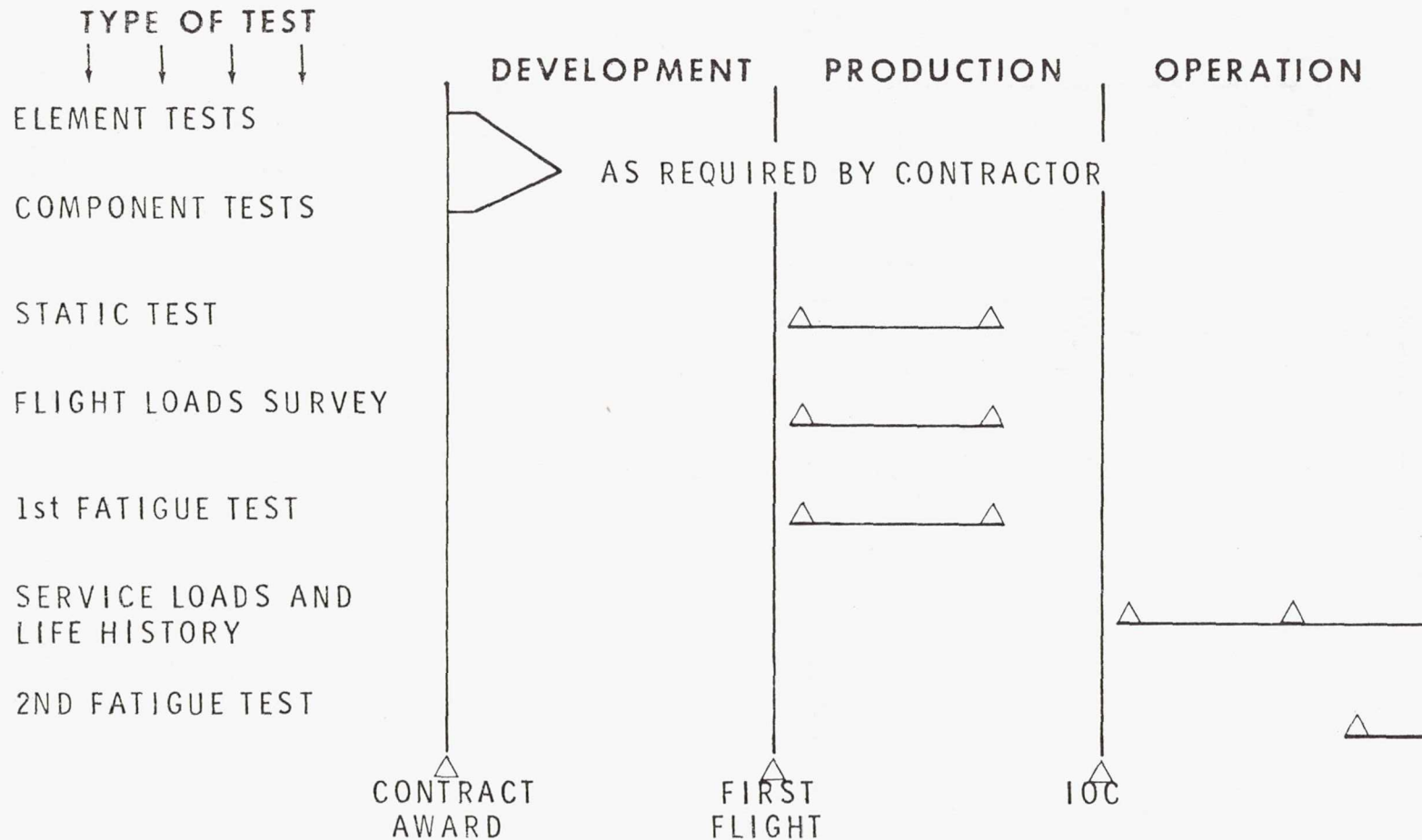


Figure 1



# C-141 STRUCTURAL EVALUATION PROGRAM

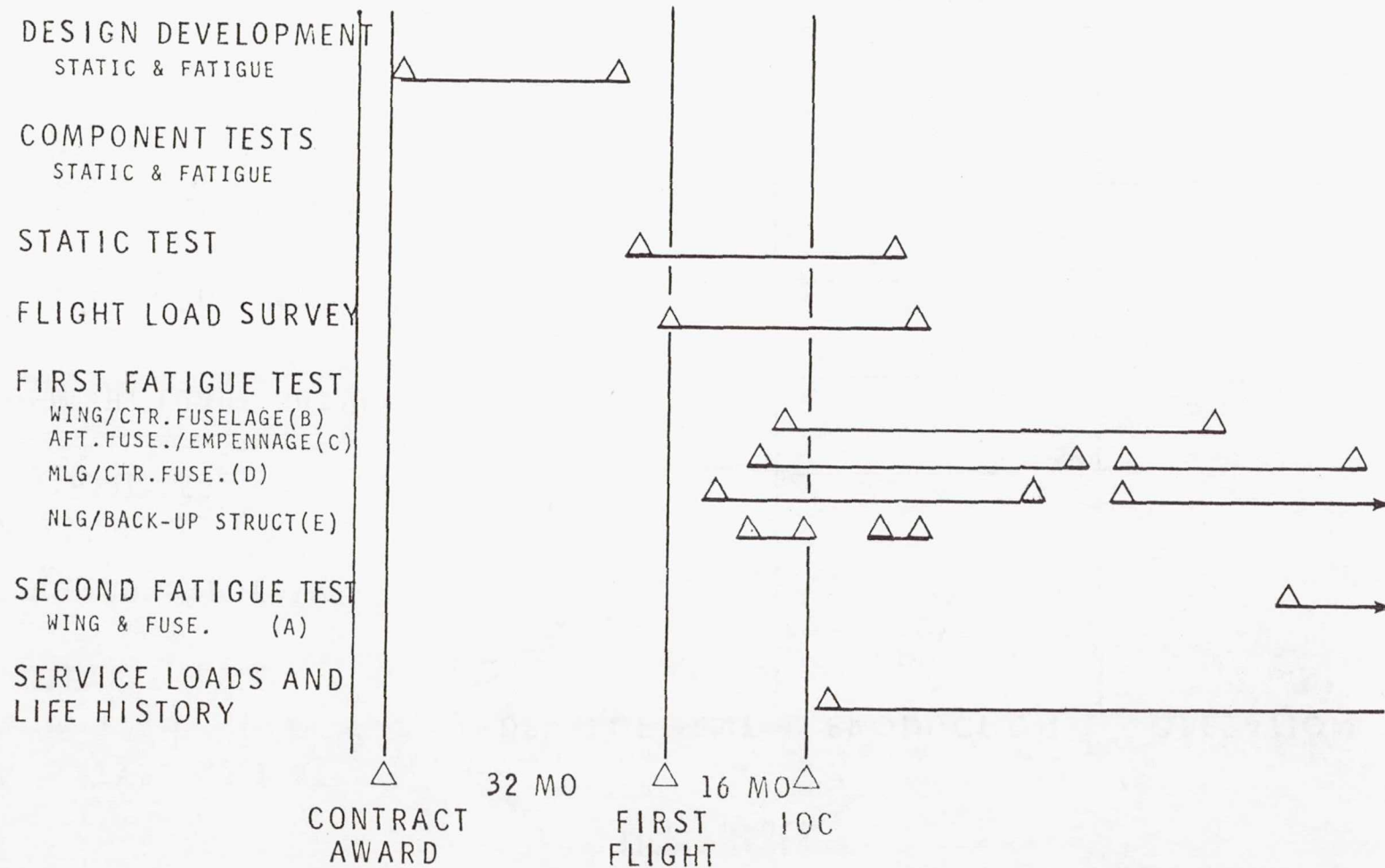


Figure 2

## FATIGUE TEST SPECIMEN

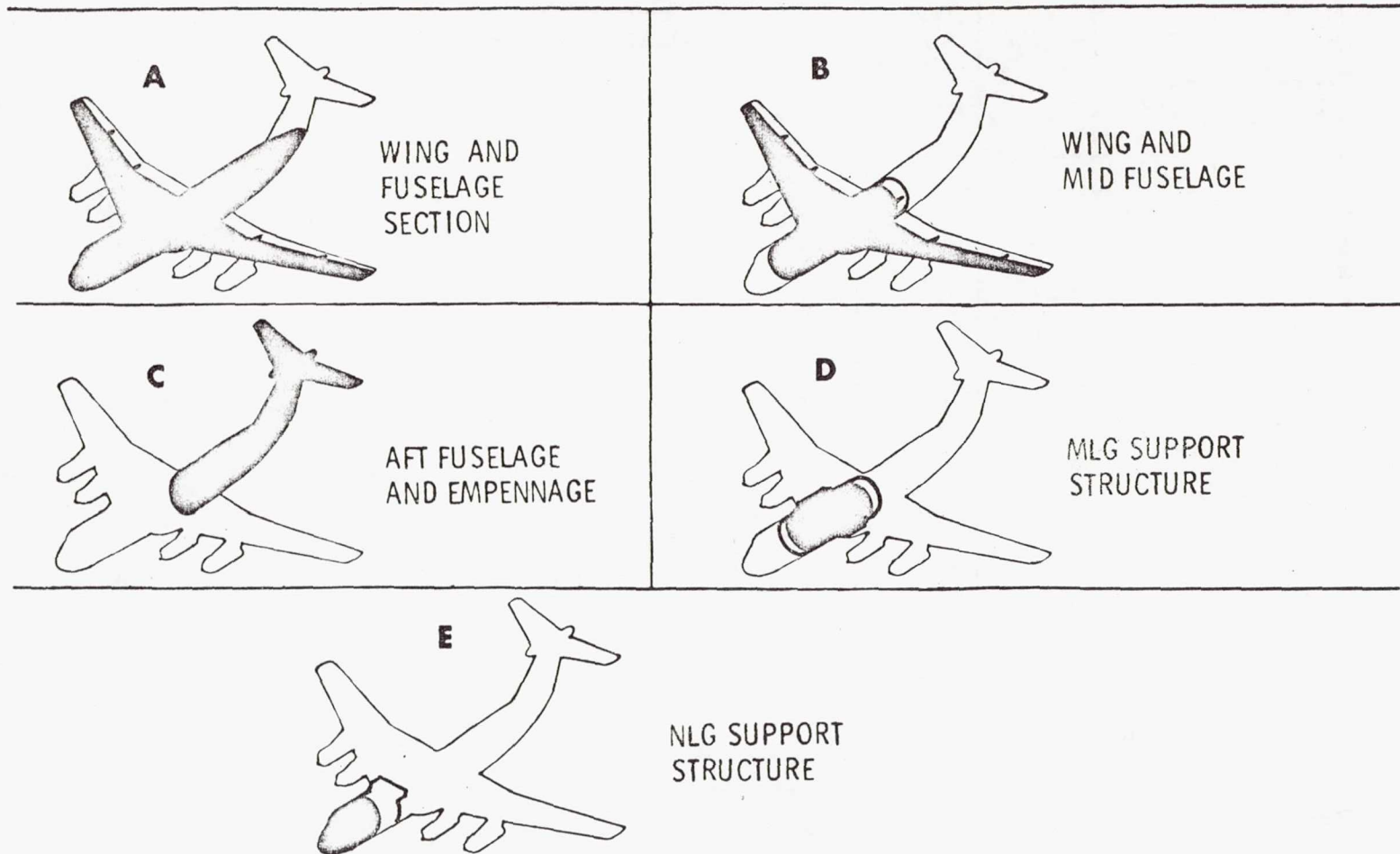


Figure 3



# COMPARISON OF TEST SCHEDULES

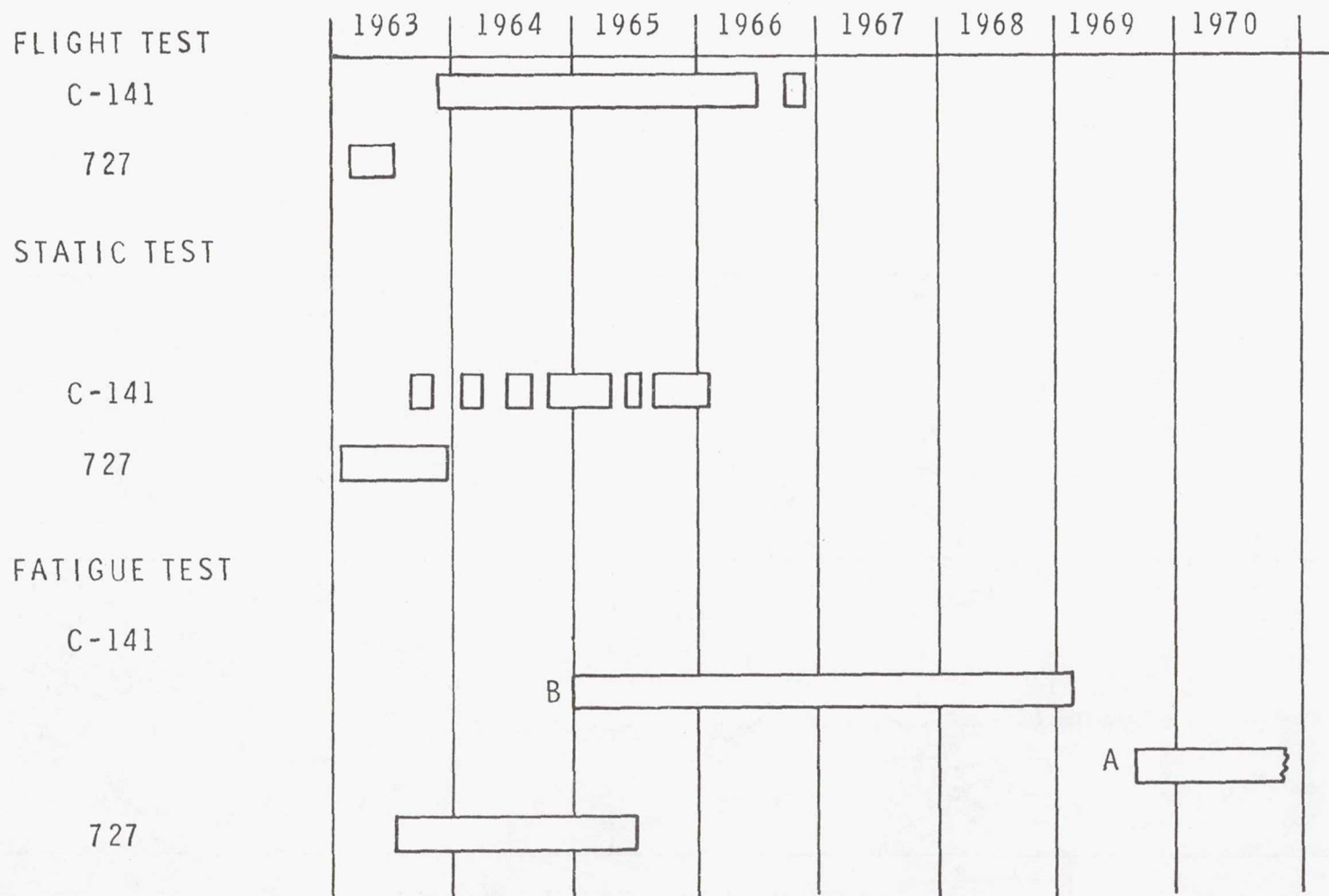


Figure 4

# F-5 STRUCTURAL EVALUATION PROGRAM

## DESIGN DEVELOPMENT

STATIC & FATIGUE

## COMPONENT TESTS

STATIC & FATIGUE

## STATIC TESTS

## FLIGHT LOAD SURVEY

## FATIGUE TESTS

F-5A FWD. FUSELAGE

F-5B FWD. FUSELAGE

## SERVICE LOADS AND LIFE HISTORY

NOTE: F-5 AIRFRAME IS ESSENTIALLY SAME AS ITS PREDESSORS, THE T-38 AND N-156

9 MO 19 MO 10C

CONTRACT AWARD FIRST FLIGHT

Figure 5



# 1969-1970 STRUCTURAL EVALUATION PROGRAM

## LIFE PHASES

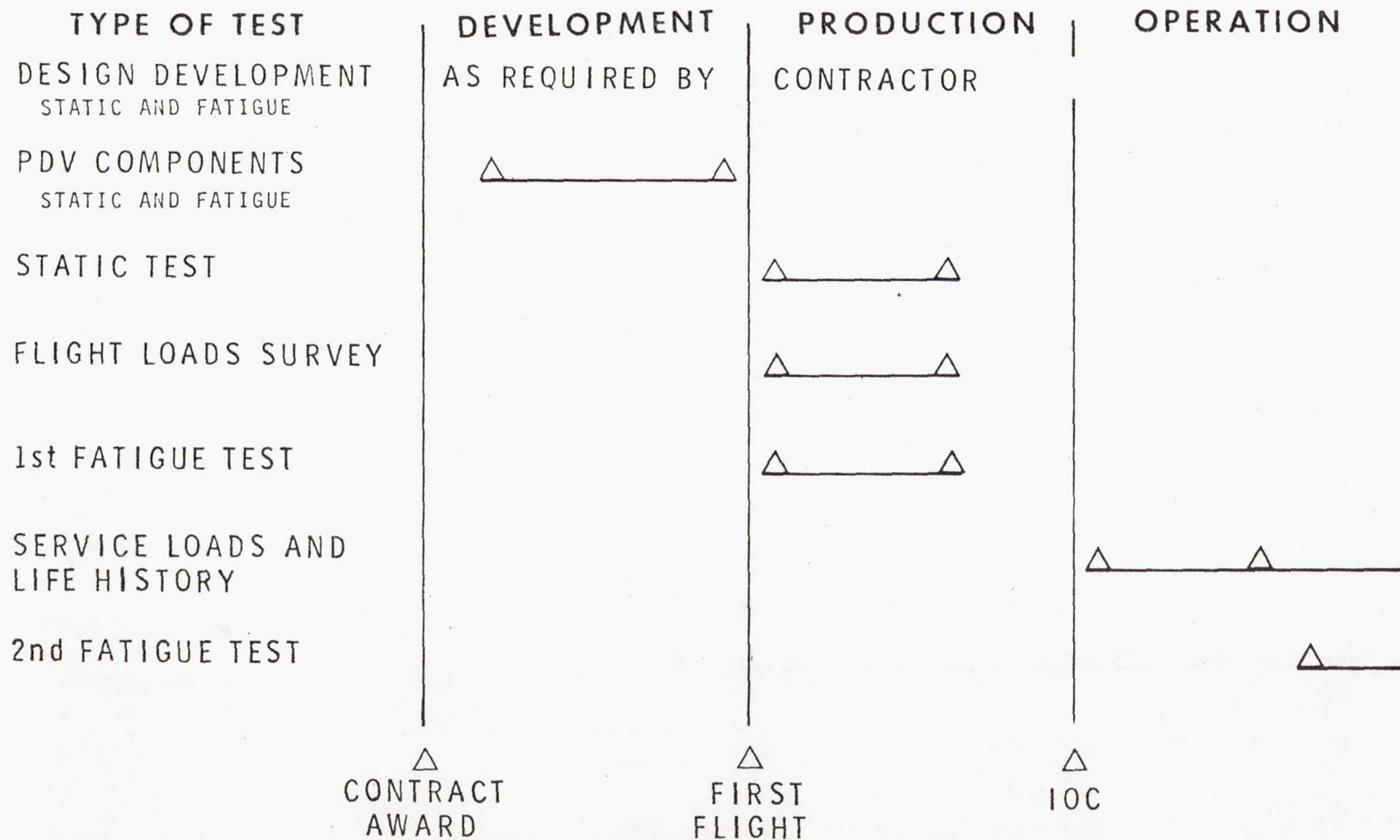


Figure 6

# PROPOSED STRUCTURAL EVALUATION PROGRAM LIFE PHASES

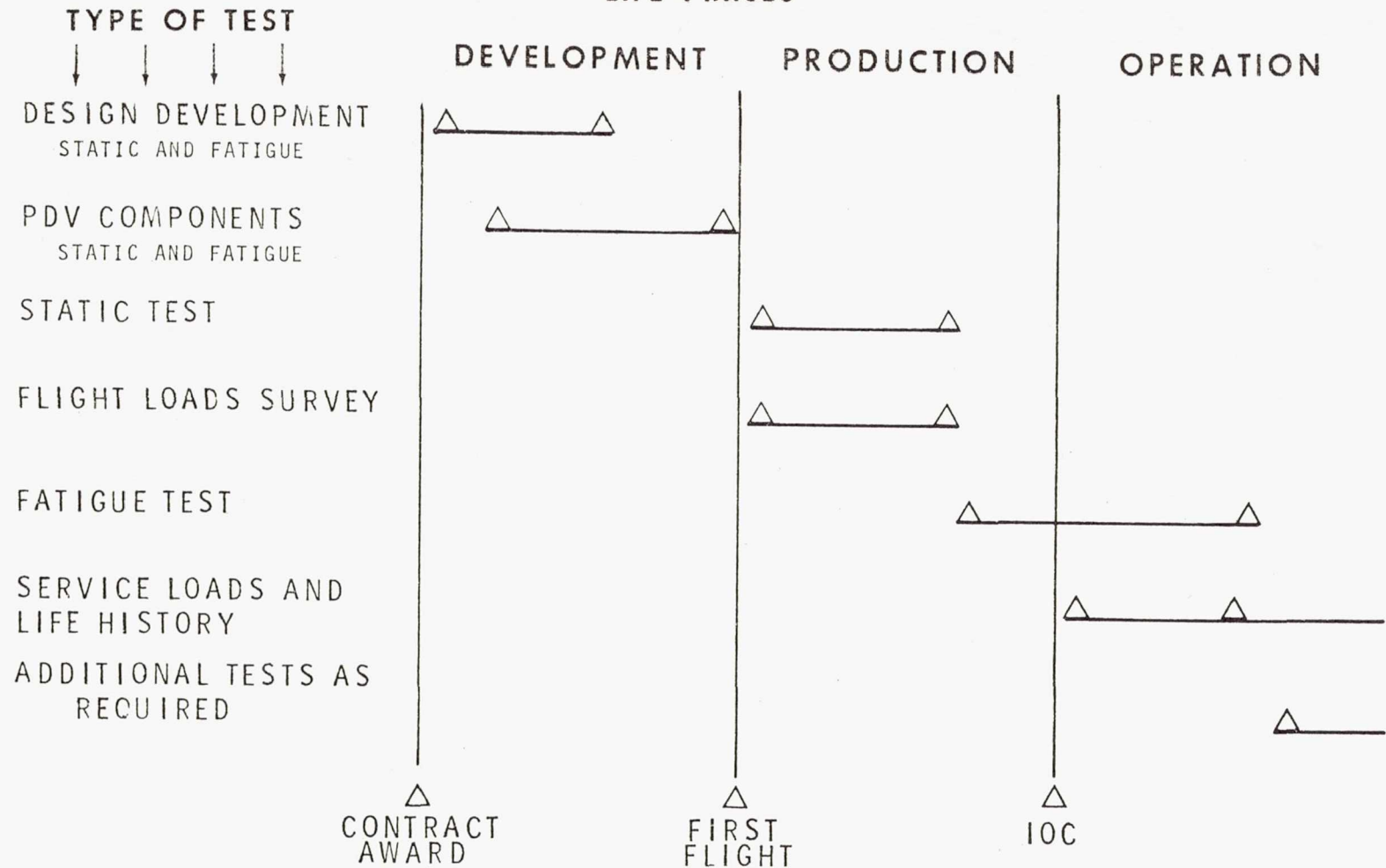


Figure 7



## FATIGUE TESTS WITH RANDOM FLIGHT-SIMULATION LOADING

By J. Schijve

National Aerospace Laboratory, Amsterdam, The Netherlands

## SUMMARY

Crack propagation was studied in a full-scale wing structure under different simulated flight conditions. Omission of low-amplitude gust cycles had a small effect on the crack rate. Truncation of the infrequently occurring high-amplitude gust cycles to a lower level had a noticeably accelerating effect on crack growth. The application of fail-safe load (100 percent limit load) effectively stopped subsequent crack growth under resumed flight-simulation loading.

In another flight-simulation test series on sheet specimens, the variables studied are the design stress level and the cyclic frequency of the random gust loading. In-flight mean stresses vary from 5.5 to 10.0 kg/mm<sup>2</sup>. The effect of the stress level is larger for the 2024 alloy than for the 7075 alloy. Three frequencies were employed: namely, 10 cps, 1 cps, and 0.1 cps. The frequency effect was small.

The advantages and limitations of flight-simulation tests are compared with those of alternative test procedures such as constant-amplitude tests, program tests, and random-load tests. Various testing purposes are considered. The variables of flight-simulation tests are listed and their effects are discussed.

A proposal is made for performing systematic flight-simulation tests in such a way that the compiled data may be used as a source of reference. The data could be used for estimating fatigue properties in the design stage of an aircraft and serve other purposes as well.

## INTRODUCTION

The fatigue loads in a flight-simulation test are supposed to be a valid representation of the loading conditions in service. In the present paper, an attempt is made to analyze the merits and the limitations of flight-simulation fatigue tests.

Recently at the National Aerospace Laboratory, extensive studies have been made regarding fatigue crack propagation under random flight-simulation loading in 2024-T3 and 7075-T6 aluminum alloys (refs. 1 to 3). Tests on crack propagation in a full-scale wing structure have just been completed and the results are summarized herein. Another program on the frequency effect under flight-simulation loading is halfway

finished. It also includes the effect of the design stress level. Preliminary data are given in a subsequent section.

A comparison is made between flight-simulation testing and alternative test procedures. The objectives of testing are obviously important for such a comparison. The variables of flight-simulation testing are listed and data on the significance of the variables are reviewed. The information is fairly limited as yet. Finally, a proposal is made for performing systematic flight-simulation tests in order to compile data that may be used as a source of reference.

## TWO RECENT NATIONAL AEROSPACE LABORATORY TEST PROGRAMS

### Crack Propagation in a Full-Scale Wing Structure Under Random Flight-Simulation Loading

The fatigue test and the fail-safe tests on the wing of the F-28 aircraft were successfully completed in April 1970. It was then decided to employ the test setup and the wing for a general crack propagation investigation. The aim of the investigation was to study the effects of

- (1) omitting low-amplitude gust cycles
- (2) truncating very-high-amplitude gust cycles to a lower level
- (3) increasing the stress level by 25 percent
- (4) preceding limit loads delaying subsequent crack growth.

The wing loads applied by 12 hydraulic cylinders included gust loads, ground-to-air cycles, flap loads, and undercarriage loads. The load sequence was a random flight simulation similar to the sequences applied in the certification tests on the wing and in tests on sheet specimens (refs. 1 to 3). A sample of a load record is given in figure 1, and the test setup is shown in figure 2. The gust load spectrum was approximated by a stepped function. (See fig. 3.)

Three test series (A, B, C) were carried out and data from the certification tests (series R) were also used for comparison. In the certification tests the low-amplitude cycles were not omitted. The omission of these cycles in test series A reduced testing time from 116 seconds to 46 seconds per flight; this implies a considerable time saving. The certification tests were completed by three fail-safe tests up to limit load, and this allowed observations on the effect of limit load application on subsequent crack growth during test series A, B, and C.

The numbers of simulated flights are indicated in figure 3. In each test series (A, B, C), groups of 2 to 4 artificial cracks were applied in the following elements: skin



between stringers, skin and stringer flange, stringer head (Z-stringer), and spar web. The cracks were applied at similar locations with approximately the same stress level in all test series. In the certification tests (series R), a large number of cracks were tested; however, for comparison with the present test series only a few cracks could be used in view of the similarity of location and stress level.

The complete results as given in reference 4 showed low scatter in each group of 2 to 4 similar cracks. A summary of the average results is presented herein. As an illustration, figure 4 shows average crack propagation curves for the skin when the stringer flange is also cracked. From similar curves, average crack rates were drawn and comparisons are made in this study.

Effect of omitting low-amplitude gust cycles.- The effect of omitting low-amplitude gust cycles from flight-simulation loading (comparison of results of test series A and R) is presented in the following table:

Cracked component	Material	Average effect on crack rate
Skin between stringers	2024-T3	Slightly slower
Skin at stringer	2024-T3	About equal
Stringer flange	7075-T6	1.5 times slower
Head of stringer	7075-T6	2 times faster
Spar web	7075-T6	1.5 times slower

The fourth result in the table (Head of stringer) is believed to be an erratic one which cannot be explained as yet. If this result is ignored, the table indicates a slightly slower or equal crack rate in the 2024-T3 skin material and a 1.5 times slower rate in the 7075-T6 material. These trends are in good agreement with previous tests employing similar load sequences (refs. 1 and 3) on 2024-T3 and 7075-T6 sheet specimens. In those tests, omitting gust cycles with the lowest amplitude implied that the average crack rates were about 1.2 times and 1.4 times slower for the 2024-T3 and 7075-T6 aluminum alloys, respectively.

Effect of truncating high-amplitude cycles.- The effect of truncating high-amplitude cycles is presented in figure 3 where it is seen that the three highest amplitudes were reduced to the next highest one. A summary of the results of truncating high-amplitude gust cycles of flight-simulation loading (comparison of results of test series B and A) is given in the following table:

Cracked component	Material	Average effect on crack rate
Skin between stringers	2024-T3	2.5 times faster
Skin at stringer	2024-T3	2 times faster
Stringer flange	7075-T6	2 times faster
Stringer head	2024-T3	4 times faster
Stringer head	7075-T6	2 times faster
Spar web	7075-T6	1.5 times faster

The last column of the table shows that truncation of the high-amplitude gust cycles to a lower level in all cases accelerated the crack growth. On the average the crack rate was about 2.3 times faster in test series B than in test series A. In reference 2 with flight-simulation tests on sheet specimens carried out at similar stress levels, the same truncation caused a 3 times faster crack rate. Although the factor is somewhat higher, it is still thought to be a fair agreement.

Effect of increasing the design stress level.- In test series C all loads applied were 25 percent higher than those in test series A. Obviously higher crack rates should then be expected which was confirmed by test series C. Unfortunately there was a fairly large variation between the accelerating effect of the various components. On the average the crack rate was 2.5 times faster in test series C. Sheet specimen data from reference 2 predicted a somewhat higher crack rate, whereas results in the following section of this paper predicted a lower crack rate.

Effect of fail-safe loads on subsequent crack propagation.- Several investigations (refs. 5 to 8) employing constant-amplitude loading have shown very long crack-growth delays if the test was interrupted for a high load. The wing test offered an opportunity to observe the effect of a high load on crack propagation under flight-simulation loading. Test series R was completed by applying limit load three times. Some 10 cracks that had shown a reasonable amount of crack growth during test series R were left unrepaired. Without exceptions, the limit load applications had a large delaying effect on the growth of these cracks. Some examples are shown in figure 5. The vertical bar in the graphs indicates the stable crack growth during the three fail-safe tests up to limit load. Several cracks came to a complete standstill with a tendency to resume crack growth during test series C (25 percent higher loads).

It was suggested now and then to apply periodically fail-safe loads in a full-scale test. The argument was that hidden cracks would then readily show up. Unfortunately, this might well be the best method to hide these cracks completely, since further growth will be drastically delayed.



## Effects of Frequency and Design Stress Level on Crack Propagation

### Under Random Flight-Simulation Loading

The test program is still in progress and preliminary results can be presented only. Tests are being carried out on 2024-T3 Alclad and 7075-T6 Alclad specimens. Specimen width is 160 mm and the thickness is 2 mm. The cracks are starting from a central saw-cut notch. Some specimens were precracked by constant-amplitude fatigue testing to a semicrack length  $l$  of 10 mm or of 20 mm. Others were given a saw cut to a semicrack length  $l$  of 8 mm and were tested without additional precracking.

The load sequences applied are the same as those applied to the wing, with one additional feature. In each flight each positive gust load was followed by a negative one and vice versa. However, the amplitude for each half-cycle was selected at random from the amplitudes to be applied in that flight.<sup>a</sup>

Truncation of the gust spectrum occurred at the same level as shown in figure 3 for test series B, whereas the low-amplitude cycles were not omitted. The first tests were started with the following values for the stress levels:

Mean stress in flight  $S_m = 7.0 \text{ kg/mm}^2$

Gust amplitudes  $S_a = 1.1, 2.2, 3.3, 4.4, 5.5, 6.6, 7.7 \text{ kg/mm}^2$

Minimum stress in GTAC  $S_{\min} = -3.4 \text{ kg/mm}^2$

Hence, the truncation level is  $S_a = 7.7 \text{ kg/mm}^2$ . The same values were applied in references 1 and 3.

Changing the design stress level implies that all stress levels should be multiplied by the same factor. With the mean stress in flight as the characteristic stress level, tests are carried out at  $S_m = 10.0, 8.5, 7.0, 5.5 \text{ kg/mm}^2$ . The gust amplitude and the minimum stress in the ground-to-air cycles are amplified accordingly. Test results are available for a loading frequency of 10 cps. (See fig. 6.<sup>b</sup>) It turns out that the effect of the stress level is different for the two alloys. At  $S_m = 5.5 \text{ kg/mm}^2$ , the 2024 alloy is still far superior to the 7075 alloy. At higher  $S_m$  values the difference is negligible. It is thought that this relatively good behavior of the 7075 alloy should be attributed to the fact that favorable residual stresses are better maintained in this alloy. It is noteworthy

---

<sup>a</sup> In the terminology of Naumann (ref. 9) the wing loading employed "random cycles" and the specimens were loaded by "random half-cycles, restrained."

<sup>b</sup> Since the stress histories were the same in all tests, except for the intensity of the stress, it was hoped to correlate the data for different stress levels by employing the stress intensity factor  $K$ . The results were disappointing and apparently similar  $K$  values do not imply similar crack rates in this case. This is attributed to different  $K$ -histories in the crack tip area and predominant interaction effects of stress cycles with different amplitudes. This issue will be discussed in more detail in the final report of this investigation.

that a trend such as that illustrated by figure 6 cannot be predicted from constant-amplitude data.

The effect of the load cycling frequency is studied by carrying out tests at 10 cps, 1 cps, and 0.1 cps. Available data have been compiled in the following table:

	2024-T3 aluminum alloy		7075-T6 aluminum alloy	
	24 to 60	40 to 60	24 to 60	40 to 60
Crack growth $2l$ , mm . . .	24 to 60	40 to 60	24 to 60	40 to 60
$S_m$ , kg/mm <sup>2</sup> . . . . .	10	8.5	10	8.5
Life in flights at –				
10 cps . . . . .	1105	1235	1382	1520
1 cps . . . . .	1262	1116	1265	1360
0.1 cps . . . . .	1234	1200		1350

As the table shows, the effect is not fully systematic but it is small, as might have been expected from constant-amplitude data (refs. 10 and 11). Of course one should be careful about generalizing the present data, especially if corrosive environments are present.

#### FLIGHT-SIMULATION TESTING

In this section of the paper, various aspects of flight-simulation testing are discussed and a proposal is made for a systematic compilation of flight-simulation fatigue test data.

##### Development of Several Fatigue Testing Procedures

In the past attempts were made to predict fatigue strength and fatigue life from simple fatigue data. Several complicating factors were early recognized and extensively studied. Examples are the presence of a mean stress as opposed to zero mean stress, the presence of notches as opposed to unnotched material, and the existence of large components as opposed to small laboratory specimens. Other factors, such as the effect of surface finish and fretting corrosion, led to an overwhelming number of empirical investigations. Qualitatively, understanding of all these influencing factors has highly increased. Nevertheless, it is still generally believed necessary to perform fatigue tests on the real components and preferably on a full-scale structure. For full-scale testing there are additional arguments, such as a realistic representation of eccentricities and load transmission in the structure and the indication of accidentally poor design features.

Testing a component or a full-scale structure implies that one wants to simulate the structural configuration as realistically as possible. In great contrast with these efforts, an unrealistic simulation of service load history was usually adopted in fatigue tests.



Since the accidents with the Comets in the early fifties, several new designs were subjected to a full-scale fatigue test. Usually this was a flight-simulation test, that is, with a flight-by-flight loading. However, the gust loading was highly simplified in many cases.

A simulation of a complex load time history was obviously impossible in the early days. In 1939 Gassner (ref. 12) published his first paper on program loading. He presented program loading as an improved method for estimating fatigue life although at that time Gassner had already realized that program loading was still afflicted with important deviations from load sequences in service. However, available testing equipment at that time could not do a better job.

Around 1960 random load fatigue tests started to draw much attention, partly because it became possible to carry out this type of testing. On the other hand, several types of fatigue loads in service had a random character. Moreover an elegant mathematical framework was available for dealing with random variables. Kirkby and Edwards (ref. 13) proposed to adopt narrow-band random loading in a way similar to that proposed by Gassner for program loading. This type of loading could still be applied in a resonance-type fatigue machine.

A real breakthrough was the introduction of the closed-loop electrohydraulic system with servovalves for monitoring the hydraulic load. An arbitrary load time history can be obtained from a similar electric signal. This system is now being used for relatively slow full-scale testing as well as fast testing of components or small specimens. The system has been developed to a high degree of reliability. Actually the impossibility of simulating a complex load time history has been eliminated. In other words, realistic load sequences can now be simulated in fatigue testing. It appears rather natural that a realistic simulation of a component or a structure should then be combined with a realistic simulation of service loading.

#### Purpose of Fatigue Testing

For a discussion on testing methods it is useful to keep in mind the variety of test purposes and test articles. A broad summary is given in the following table:

Test article	Testing method	Test purpose
Laboratory specimen	Constant-amplitude test	(a) Basic data for fatigue life estimates
Component	Program test	(b) Comparative design studies
Full-scale structure	Random-load test	(c) Direct life estimates
	Flight-simulation test	(d) Indication of fatigue critical elements, crack rates, and inspection methods

It is thought that testing purposes (c) and (d) require a realistic simulation of both the test article and the service load time history. Consequently, some type of flight-simulation loading is necessary. With respect to test purposes (a) and (b) different opinions may be held.

The utilization of constant-amplitude test data from laboratory specimens as basic data for life estimates is a complex problem. A cumulative damage rule has to be adopted – for instance, the Palmgren-Miner rule. Then, the differences between laboratory specimens and the actual structure have to be considered. The conclusion has to be that only very rough life estimates can be made in this way.

Gassner and Schütz (ref. 14) have proposed to use data from program tests as basic data for making life estimates. A similar proposal was made by Kirkby and Edwards (ref. 13) for random loading. There are some indications that life estimates may be improved in this way. However, discrepancies between the fatigue lives obtained in random tests and equivalent program tests (refs. 15 to 19) are not encouraging in this respect. Moreover, uncertainties about the damage rule and the relevance of the specimens remain. Actually flight-simulation fatigue test data could well be used for this purpose.

Test purpose (b) in the foregoing table is concerned with the comparison between different components, materials, and surface treatments for the same application in an aircraft structure. Many people still feel that constant-amplitude tests are a good means for this purpose. However, the possibility of intersecting (or nonparallel) S-N curves is making this doubtful. In figure 7, test results at stress level  $S_{a,1}$  would indicate design A to be superior to design B. However, at stress level  $S_{a,2}$  design B appears to be superior.

As an illustration of different answers to the same question, a recent investigation with constant-amplitude loading (ref. 3) indicated that the crack propagation in 7075-T6 was 4 times faster than the crack propagation in 2024-T3. However, under flight-simulation loading it was only twice as fast. The data of figure 6 are also illustrative in this respect.

The numerous test series with program loading carried out by Gassner and his coworkers (ref. 20) indicate that the risk of a misjudgment would be much smaller if program loading were adopted for comparative testing. This applies also to random loading (ref. 21). Nevertheless, if flight-simulation loading can be adopted, it apparently is the most preferable solution. Real problems should be tackled with realistic testing methods if possible. Recently Branger and Ronay (ref. 22) adopted random flight-simulation loading for exploring the fatigue behavior of a high-strength steel. Imig and Illg (ref. 23) adopted this method for studying the effect of temperature on the endurance of notched



titanium-alloy specimens. At the National Aerospace Laboratory (NLR) as part of an ad-hoc problem random flight-simulation loading was used to compare two alternative types of joints.

### Variables of Flight-Simulation Testing

A constant-amplitude loading is easily defined by its mean, amplitude, and cyclic frequency. For program loading, additional variables are (1) load spectrum, (2) amplitude sequence (the programming), and (3) the maximum and the minimum amplitude to be included in the test. For random tests, similar variables can be indicated. The sequence, however, has some random character rather than being programmed.

For a flight-simulation test, the situation is still more complex because different types of flight loads have to be simulated, such as gusts, maneuver loads, and ground-to-air cycles.

The main variables of flight-simulation loading, with some comments on their significance, are as follows:

#### (1) Load spectrum

Obviously the fatigue life depends on the type of load spectrum. For instance, there are large differences between the load spectra for civil and for military aircraft. Usually gusts are important for civil aircraft, whereas maneuver loads are less important. For military aircraft, the reverse is true. A realistic flight-simulation test requires the adoption of an appropriate load spectrum.

#### (2) Load sequence

If a flight-by-flight simulation is adopted, the fatigue loads superimposed on the ground-air-ground transitions can still be applied in various sequences. The effect of sequence was studied by several authors (refs. 1, 3, 9, 19, 23, and 24) and the general impression is that in a flight-by-flight loading the sequence of the loads in each flight is of secondary importance. Although this is a convenient observation, it still appears to be advisable to adopt a realistic sequence, which generally implies a random sequence.

#### (3) Design stress level

It is clear that an increase of the design stress level reduces fatigue life. This is illustrated for crack propagation by the curves in figure 6. Similar data were found by Branger (ref. 25) with a hole notched specimen of 7075 aluminum alloy and maneuver spectrum, by Branger and Ronay (ref. 22) with a hole notched specimen of chromium-nickel steel and maneuver spectrum, and by Imig and Illg (ref. 23) with an elliptical hole specimen of titanium alloy and supersonic transport load spectrum.

Curves giving the fatigue life as a function of the stress level applied in flight-simulation tests easily indicate the gain or loss of fatigue life if the design stress level is readjusted. Actually such curves have some similarity with Gassner's "endurance curves" (Betriebsfestigkeitskurven) and the curves of Kirkby and Edwards, who plotted the random-load fatigue life as a function of the root-mean-square stress level. However, curves pertaining to flight-simulation data give more relevant information.

#### (4) Maximum load allowed in the test (truncation level)

The wing test results presented in a previous section have confirmed earlier NLR data, which indicates that the truncation level has a predominant effect on crack propagation. It is expected that this effect is more applicable to a gust spectrum than to a maneuver spectrum in view of the different shapes of the spectra. Nevertheless, the assessment of the maximum load allowed in the test is a delicate issue. This problem was discussed in reference 26; these results led to the recommendation to truncate load amplitudes expected less than 10 times in the target life of the aircraft. This proposal was made in view of the favorable effect of higher loads and the uncertainty that all aircraft of a fleet will meet those loads.

At the same time, it would also be unrealistic to truncate at a much lower level since that may also lead to unrepresentative life indications. As a consequence, a realistic simulation is not compatible with a single loading pattern applied in all flights. Obviously different flights should be simulated. (See fig. 1, for an example.)

#### (5) Minimum amplitudes to be simulated

The results presented earlier for test series A have indicated that low-amplitude gust cycles may be slightly damaging in a flight simulation test. A similar indication was obtained by Naumann (ref. 9) when testing edge-notched 7075-T6 specimens. Remarkably enough Branger (ref. 25) found a small life reduction when omitting low-amplitude cycles from flight-simulation tests on 7075-T6 notched specimens (maneuver spectrum). Anyhow, if accurate data are required, low-amplitude cycles have to be included.

The situation is different for low-amplitude taxiing load cycles. If the mean stress during taxiing is in compression, it was found in NLR tests (refs. 1 and 3) and by Gassner and Jacoby (ref. 24) and Imig and Illg (ref. 23) that omitting the taxiing loads did not have a noticeable effect on the fatigue life. It is expected that this trend is applicable only if the mean stress of the taxiing loads is either small or negative.

#### (6) Loading frequency

Preliminary results presented in a previous section indicated a very small frequency effect if any. More data from flight-simulation tests were not available in the literature. It is expected that the frequency effect will be small for those materials that show a small frequency effect under constant-amplitude loading.



## Advantages and Limitations of Flight-Simulation Tests

The advantages of flight-simulation tests are clearly associated with the fact that the loading is a realistic simulation of the service load time history. For obtaining valid information on fatigue lives and crack propagation from testing components or a full-scale structure, a realistic flight-simulation test is a necessary condition.

For comparative fatigue tests on competing designs or materials, constant-amplitude tests, program tests, or random-load tests may be adopted. As explained previously, it is not certain whether the comparative result will also be valid under service loading. This uncertainty is eliminated by realistic flight-simulation loading.

With respect to estimating fatigue lives in the design stage, one could start from constant-amplitude data and calculate the fatigue life by employing a damage rule (Palmgren-Miner, for instance). This procedure implies a very large extrapolation with a doubtful extrapolation rule. By starting from relevant flight-simulation data, the extent of extrapolation and thus the uncertainty will be highly reduced. In the following section a proposal is made for compiling flight-simulation fatigue test data for this purpose.

A disadvantage is that flight-simulation testing requires a more expensive fatigue machine with more complex electrohydraulic systems. Actually the technical problems of this type of machine appear to be solved and the number of available machines is rapidly increasing. The closed-loop systems indeed allow a wide variation of testing procedures and it is sometimes surprising to see the limited utilization of the potentials of the machine in fatigue tests.

Another limitation which appears to be more serious is that the load spectrum in service will never be the same as the spectrum applied in the test. Although this is true, it is not a fair objection. If there are differences between assumed and actual load spectra, one might account for them by calculations or by testing. Unfortunately the Palmgren-Miner rule is unreliable for this purpose (ref. 3). It may even predict the wrong sign of life corrections. The only realistic approach is to rely on empirical trends as obtained in flight-simulation tests. The test program proposed in the following section may also be useful in this respect. For a particular aircraft, another solution is to conduct some comparative flight-simulation tests with the initial load spectrum and the actual service load spectrum. This could be done on components or relevant specimens. In this respect it was stimulating to see a good agreement between the crack propagation results of the wing and those of simple sheet specimens.

## A Proposal for Systematic Flight-Simulation Tests

In the foregoing sections, flight-simulation testing was recommended as being a more realistic approach to the problem of estimating fatigue properties. It was also

pointed out that a compilation of systematic data from such tests would be helpful. A proposal for a compilation was made in reference 27. A test program for this purpose should include flight-simulation tests with the following variables:

(1) Type of specimen

Representative riveted and bolted joints should be tested.

(2) Shape of load spectrum

Some typical shapes should be adopted, for instance, representing gust and maneuver spectra. If the effect of the load spectrum is known, one might interpolate for intermediate spectrum shapes.

(3) Design stress level

Some values should be adopted in order to study the effect of the stress level in a way similar to that of Gassner for program tests.

(4) Ground-to-air cycles

The number and the magnitude of ground-to-air cycles may be varied.

Such a program, which could well be extended, may be considered as an exploration of the effect of several variables on the life under flight-simulation loading. On the other hand, it may serve some practical purposes. Firstly, the data could indeed be used in the design stage for making life estimates. Secondly, this type of information could also be useful for correcting data from full-scale tests if the service load spectrum deviates from the test load spectrum. Thirdly, without actually having to design a standardized test one could use the data as a standard for comparison when checking the fatigue quality of new components. A handbook with results from systematic flight-simulation tests could be updated from time to time.

In fact, tests according to the foregoing program could be considered as collecting service experience in the laboratory. In general, the experience from fatigue failures in service does not become available in a suitable form because of insufficient data on load spectra, stress level, and structural configuration in most of the failures.

## SUMMARY OF RESULTS

Flight-simulation tests were made with a full-scale wing structure to study crack propagation under different loading conditions. The results are summarized as follows:

1. Omitting low-amplitude gust cycles from the flight-simulation test implied a considerable timesaving. However, it had a small but systematic effect on the crack propagation rate. The propagation rate was somewhat slower.

2. Truncation of infrequently occurring high-amplitude gust cycles to a lower level considerably accelerated crack growth.



3. Increasing the design stress level increased the crack propagation rate.

4. The application of fail-safe loads (100 percent limit load) caused a drastic delay of subsequent crack growth. Such loads increase the fatigue life.

5. Good agreement was found between wing test results and results from tests with simple sheet specimens. This illustrates that tests on laboratory specimens may indicate the effect of modifications of the load spectrum.

Flight-simulation tests were also made with 2024-T3 and 7075-T6 sheet specimens at loading frequencies of 0.1, 1, and 10 cps and at four design stress levels. Preliminary results are as follows:

6. The frequency effect was small and nonsystematic.

7. The design stress level had a considerable effect on the crack propagation rate which was different for the two alloys. The difference could not be predicted from constant-amplitude data.

A discussion was presented concerning the meaning of flight-simulation testing for various testing purposes. The variables of flight-simulation testing and their effects on the test results were discussed. The merits and the limitations of flight-simulation tests are summarized as follows:

8. As compared with constant-amplitude tests, program tests, and random-load tests, a flight-simulation test is a more realistic representation of service loading and gives more relevant information. For a full-scale test or a component test, a realistic flight-simulation loading is an essential requirement for estimating fatigue lives and crack propagation rates.

9. For comparison between competing designs, materials, or surface treatments, flight-simulation tests give more relevant indications than alternative testing methods.

10. If life estimates made in the design stage of an aircraft are based on flight-simulation test data, the extrapolation of the test results is smaller and, hence, more reliable than for alternative procedures employing data from constant-amplitude tests, program tests, or random load tests.

11. Since sufficient data from flight-simulation tests are not available as yet, a proposal has been made for a systematic compilation of such data. A handbook with this type of data would also be useful as a standard for comparison. Moreover, the data could be used for evaluating the significance of differences between the load spectrum of a test and the load spectrum in service. For this purpose, the Palmgren-Miner rule is unreliable.

## REFERENCES

1. Schijve, J.; Jacobs, F. A.; and Tromp, P. J.: Crack Propagation in Aluminium Alloy Sheet Materials Under Flight Simulation Loading. NLR TR 68117, 1968.
2. Schijve, J.; Jacobs, F. A.; and Tromp, P. J.: Crack Propagation in 2024-T3 Alclad Under Flight Simulation Loading. Effect of Truncating High Gust Loads. NLR TR 69050, June 1969.
3. Schijve, J.: Cumulative Damage Problems in Aircraft Structures and Materials. *Aeronaut. J.*, vol. 74, 1970, p. 517. (Also published as NLR MP 69005 and presented as 2nd Plantema Memorial Lecture, ICAF Symp. (Stockholm), 1969.)
4. Schijve, J.; and de Rijk, P.: Crack Propagation in a Full-Scale Wing Structure Under Random Flight-Simulation Loading. Prospective NLR TR.
5. Schijve, J.: Fatigue Crack Propagation in Light Alloy Sheet Material and Structures. *Advances in Aeronautical Sciences*, Vol. 3, Pergamon Press, 1961, p. 387. (Also published as NLR MP 195.)
6. Hudson, C. M.; and Hardrath, H. F.: Investigation of the Effects of Variable-Amplitude Loadings on Fatigue Crack Propagation Patterns. NASA TN D-1803, 1963.
7. Hudson, C. M.; and Raju, K. N.: Investigation of Fatigue-Crack Growth Under Simple Variable-Amplitude Loading. NASA TN D-5702, 1970.
8. McMillan, J. C.; and Hartzberg, R. W.: The Application of Electron Fractography to Fatigue Studies. *Electron Fractography*, Spec. Tech. Publ. 436, Amer. Soc. Testing Mater., 1968, p. 89.
9. Naumann, E. C.: Evaluation of the Influence of Load Randomization and of Ground-to-Air Cycles on Fatigue Life. NASA TN D-1584, 1964.
10. Schijve, J.: Significance of Fatigue Cracks in Micro-Range and Macro-Range. *Fatigue Crack Propagation*, Spec. Tech. Publ. 415, Amer. Soc. Testing Mater., 1967, p. 415. (Also published as NLR MP 243.)
11. Bradshaw, F. J.; and Wheeler, C.: The Effect of Environment on Fatigue Crack Propagation. Measurement on Aluminium Alloys at Different Frequencies. Tech. Rep. No. 68041, Brit. R.A.E., Feb. 1968.
12. Gassner, E.: Festigkeits-Versuche mit wiederholter Beanspruchung im Flugzeugbau. *Luftwissen*, Bd. 6, 1939, p. 61.
13. Kirkby, W. T.; and Edwards, P. R.: Variable Amplitude Loading Approach to Material Evaluation and Component Testing and Its Application to the Design Procedures. *Fatigue Design Procedures*, 4th ICAF Symposium, E. Gassner and W. Schütz, eds., Pergamon Press, 1969, p. 253.



14. Gassner, E.; and Schütz, W.: Assessment of Allowable Design Stresses and the Corresponding Fatigue Life. Fatigue Design Procedures, 4th ICAF Symposium, E. Gassner and W. Schütz, eds., Pergamon Press, 1969, p. 291.
15. Jacoby, G.: Comparison of Fatigue Lives Under Conventional Program Loading and Digital Random Loading. Effects of Environment and Complex Load History on Fatigue Life, Spec. Tech. Publ. 462, Amer. Soc. Testing Mater., 1970, p. 184.
16. Jacoby, G.: Beitrag zum Vergleich der Aussagefähigkeit von Programm – und Random-Versuchen. Z. Flugwiss., Jahrg. 18, 1970, p. 253.
17. Lipp, W.: Unterschiede in der Lebensdauerangabe nach Betriebsfestigkeitsversuchen gegenüber den Ergebnissen aus Fahrversuchen. LBF Ber. Nr. TB-80, 1968, p. 67.
18. Gassner, E.: Betriebsfestigkeit gekerbter Stahl- und Aluminiumstäbe unter betriebsähnlichen und betriebsgleichen Belastungsfolgen. Materialprüfung, Vol. 11, 1969, p. 373.
19. Schijve, J.; Jacobs, F. A.; and Tromp, P. J.: The Effect of Load Sequence on Fatigue Crack Propagation Under Random Loading and Program Loading. NLR TR 71014, Jan. 1971.
20. Schütz, W.: Über eine Beziehung zwischen der Lebensdauer bei konstanter und bei veränderlicher Beanspruchungsamplitude und ihre Anwendbarkeit auf die Bemessung von Flugzeugbauteilen. Z. Flugwiss., Jahrg. 15, 1967, p. 407.
21. Kirkby, W. T.; and Edwards, P. R.: Cumulative Fatigue Damage Studies of Pinned-Lug and Clamped-Lug Structural Elements in Aluminium Alloy. Tech. Rep. No. 69182, Brit. R.A.E., 1969.
22. Branger, J.; and Ronay, M.: Investigation of High Strength Steels Under History Program Fatigue. TR No. 56, Inst. for Study of Fatigue and Reliability, Columbia Univ., 1968.
23. Imig, L. A.; and Illg, W.: Fatigue of Notched Ti-8Al-1Mo-1V Titanium Alloy at Room Temperature and 550° F (560° K) With Flight-by-Flight Loading Representative of a Supersonic Transport. NASA TN D-5294, 1969.
24. Gassner, E.; and Jacoby, G.: Experimentelle und Rechnerische Lebensdauerbeurteilung von Bauteilen mit Start-Lande-Last-wechsel. Luftfahrttechnik-Raumfahrttechnik, Vol. 11, 1965, p. 138.
25. Branger, J.: A Review of Swiss Investigations on Aeronautical Fatigue During the Period June 1965 to July 1967. Minutes 10th Conf. ICAF, Melbourne.

26. Schijve, J.; Broek, D.; de Rijk, P.; Nederveen, A.; and Sevenhuysen, P. J.: Fatigue Tests With Random and Programmed Load Sequences With and Without Ground-to-Air Cycles. A Comparative Study on Full-Scale Wing Center Sections. NLR Rep. S.613, Dec. 1965. (Also published as AFFDL-TR-66-143, U.S. Air Force, Oct. 1966.)
27. Schijve, J.: Load Sequences for Fatigue Testing of Components and Full-Scale Aircraft Structures. Paper presented at Seventh Congress of the International Council of the Aeronautical Sciences (Rome), Sept. 1970. (Also published as NLR MP 70012.)



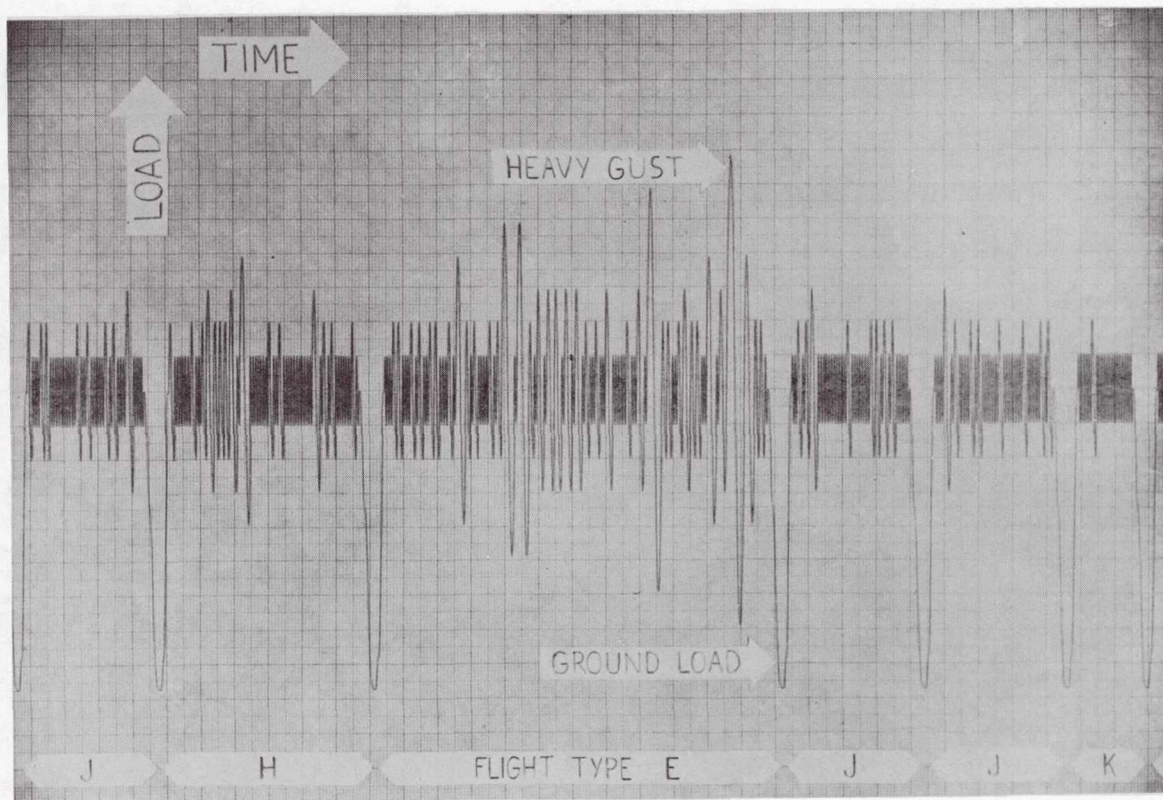


Figure 1.- Sample of a load record, illustrating the load sequence applied in the wing fatigue test. Ten different types of weather conditions are simulated; flight type E corresponds to fairly severe storm, whereas flight type K is good weather.

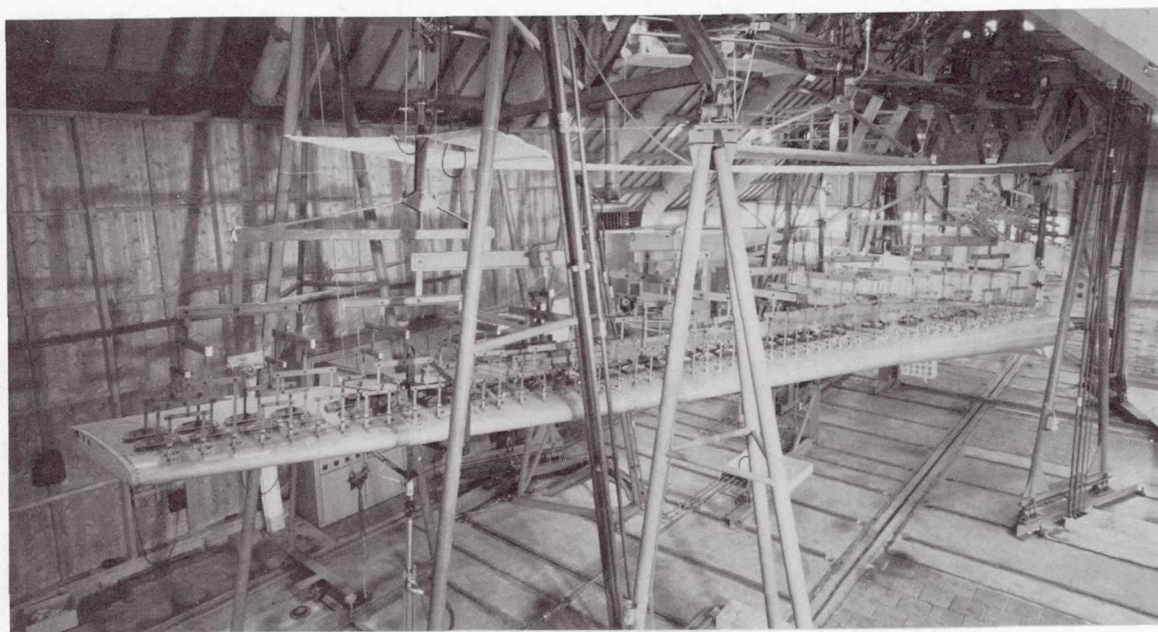
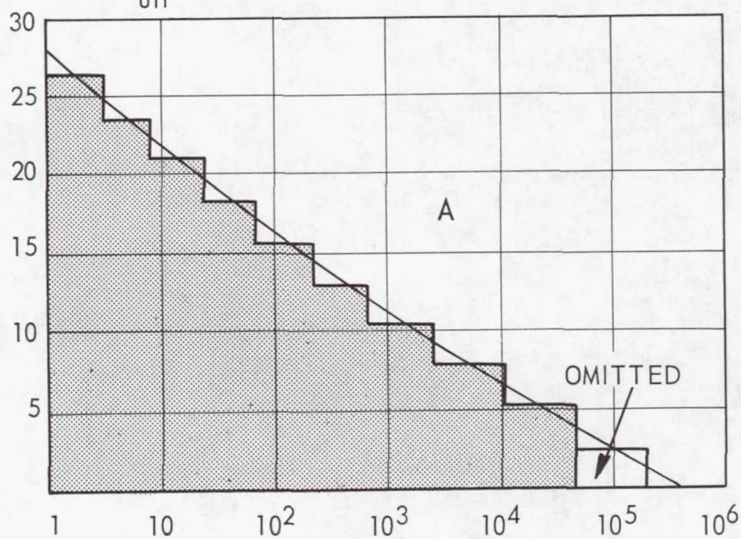


Figure 2.- Test setup with right wing and whiffle tree loading systems.

AMPLITUDE OF WING BENDING MOMENT,

$\% M_{ult}$



NUMBER OF EXCEEDINGS IN 5000 FLIGHTS

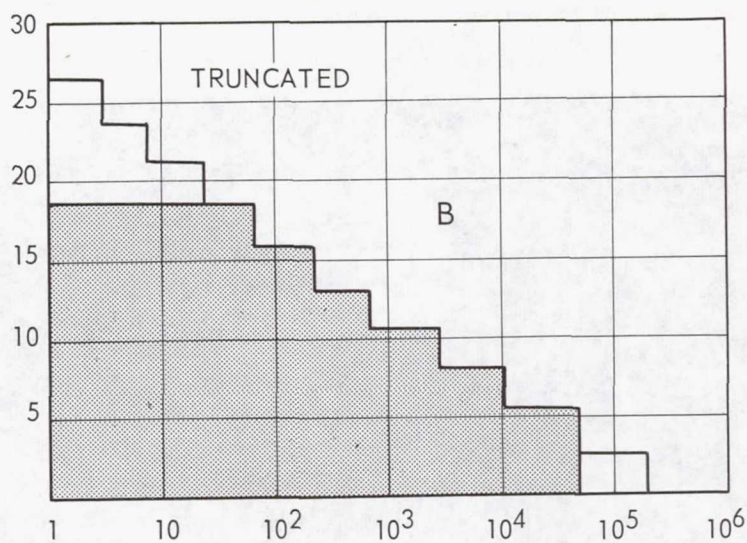
TEST SERIES

R

LOW-AMPLITUDE  
GUST CYCLES INCLUDED;  
47000 FLIGHTS

A

LOW-AMPLITUDE  
GUST CYCLES OMITTED;  
24000 FLIGHTS



B

HIGH-AMPLITUDE  
GUST CYCLES TRUNCATED;  
16000 FLIGHTS

C

SIMILAR TO A, BUT ALL  
LOAD LEVELS INCREASED  
25 %; 15000 FLIGHTS

Figure 3.- Gust load spectra in test series A, B, and C.



CRACK LENGTH, mm

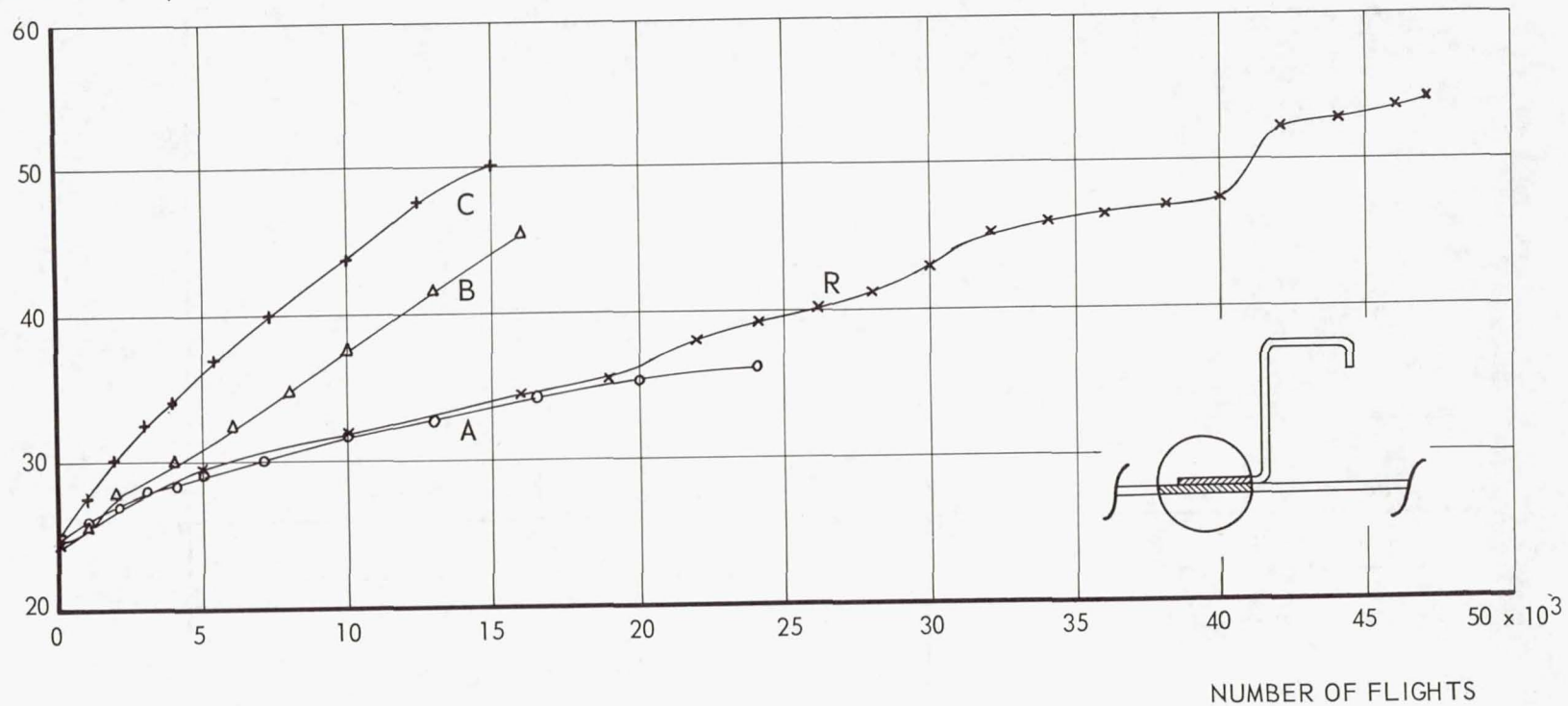


Figure 4.- Example of propagation curves for cracks in the skin. Comparison between the results of test series R, A, B, and C.

CRACK LENGTH, mm

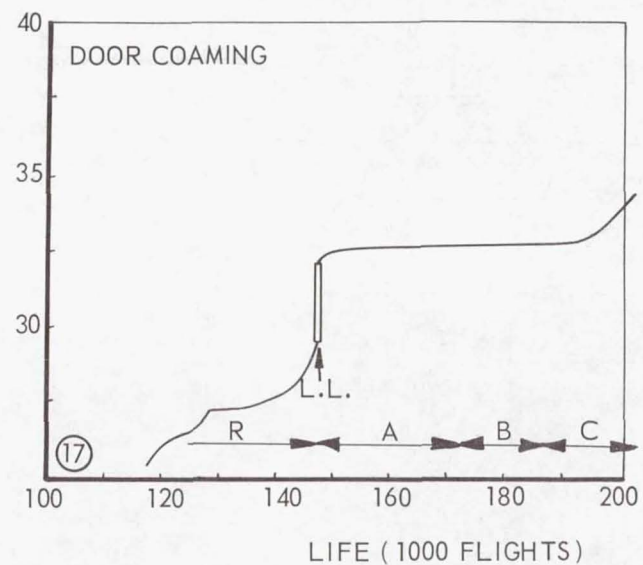
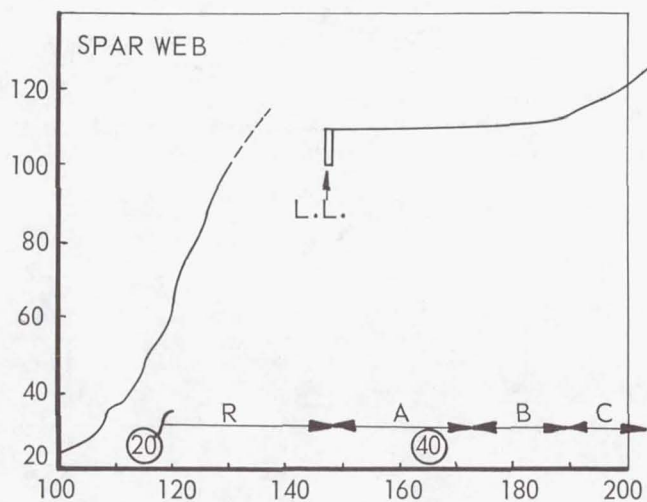
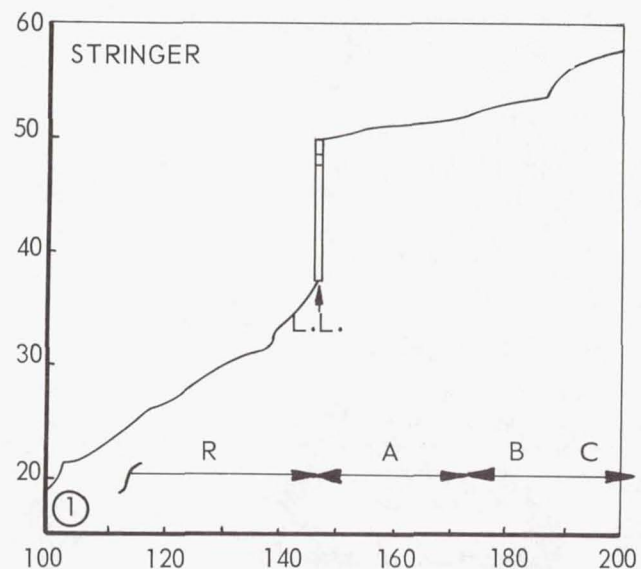
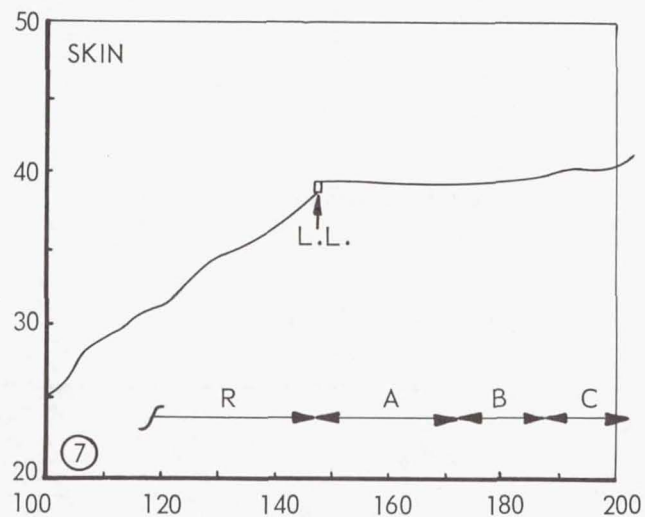


Figure 5.- The effect of limit load (L.L.) on crack propagation under flight-simulation loading.



MEAN STRESS IN FLIGHT,  
kg/mm<sup>2</sup>

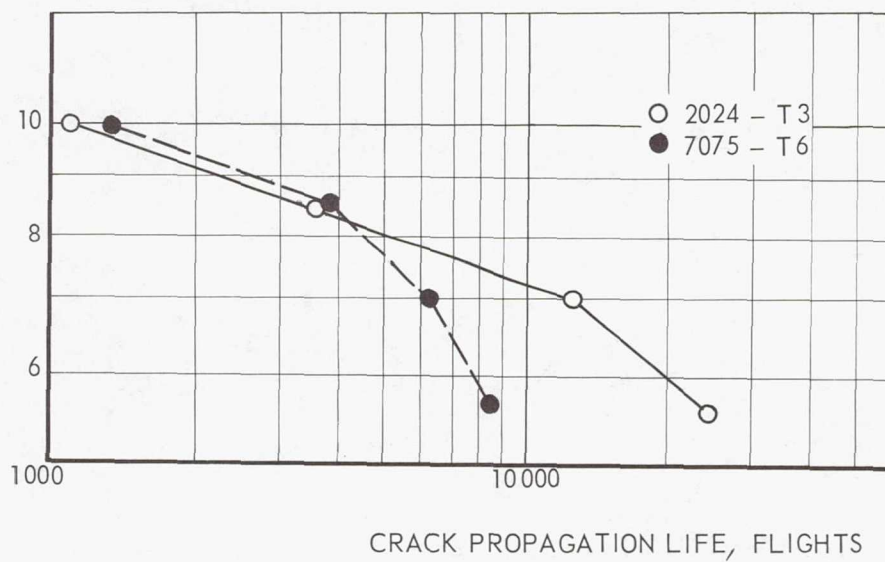


Figure 6.- Flight-simulation life for crack growth from  $2l = 24$  mm to  $2l = 60$  mm.

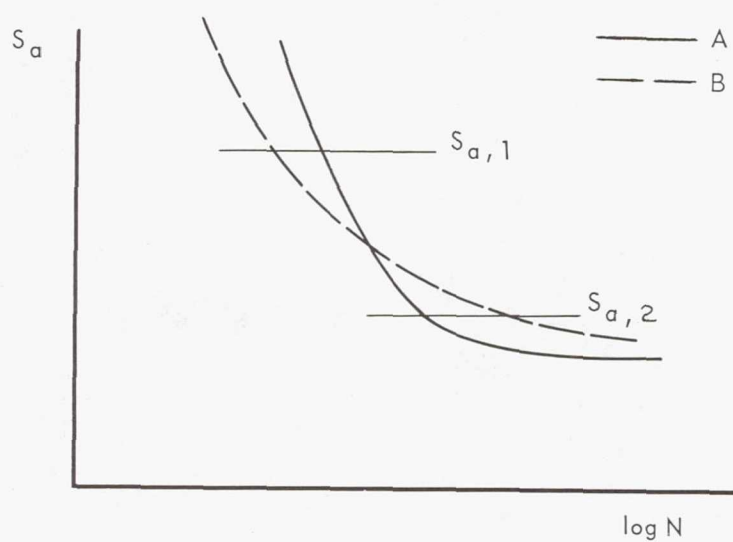


Figure 7.- Two intersecting S-N curves.

## RELIABILITY ANALYSIS APPLIED TO STRUCTURAL TESTS

By Patricia Diamond and A. O. Payne  
Aeronautical Research Laboratories  
Department of Supply  
Commonwealth of Australia

SUMMARY

Although full-scale fatigue testing is now widely adopted in modern aircraft design practice, the current fatigue-life assessment procedures do not utilise all of the test data that is obtained, and they only partly take account of the probability of failure of the structure during the period in which it is being progressively weakened by the fatigue crack.

The present paper is concerned with the application of reliability theory to predict, from structural fatigue test data, the risk of failure of a structure under service conditions because its load-carrying capability is progressively reduced by the extension of a fatigue crack.

The procedure is applicable to both safe-life and fail-safe structures and, for a prescribed safety level, it will enable an inspection procedure to be planned or, if inspection is not feasible, it will evaluate the life to replacement.

The theory has been further developed to cope with the case of structures with initial cracks, such as can occur in modern high-strength materials which are susceptible to the formation of small flaws during the production process.

The method has been applied to a structure of high-strength steel and the results are compared with those obtained by the current life estimation procedures. This has shown that the conventional methods can be unconservative in certain cases, depending on the characteristics of the structure and the design operating conditions.

The suitability of the probabilistic approach to the interpretation of the results from full-scale fatigue testing of aircraft structures is discussed and the assumptions involved are examined.

INTRODUCTION

In recent years the development of high-performance aircraft using new high-strength materials and more refined methods of stress analysis to satisfy the ultimate strength requirement has led to the fatigue performance of aircraft structures becoming a progressively more important factor.



Basic studies of the fatigue behaviour of complete structures, such as those described in references 1 and 2, have shown that a full-scale fatigue test of the structure under representative loading conditions is essential to identify the fatigue critical areas and accurately represent the complex stress conditions under fatigue loading.

Although full-scale fatigue testing is now widely adopted in aircraft design practice, this usually consists of applying to a single test specimen a loading sequence representing the service load history.

Complete failure under the test load sequence or the appearance of a crack of a particular length is defined as failure and the results are applied to determine a life under the service loading conditions.

However, such an arbitrary criterion of failure does not consider the increasing risk of static failure to which the structure is subjected as it is progressively weakened by the growing fatigue crack. The actual risk of failure could therefore differ considerably from that obtained by the currently used methods of life estimation.

Furthermore the difficulty of detecting very small cracks with current techniques, together with the susceptibility of the modern high-strength materials to the formation of flaws in production, may result in some probability of cracks existing in airframes prior to entering service.

This paper is concerned with applying reliability analysis to calculate the probability of survival as a function of life from the results of the full-scale fatigue test, including the case of structures which may be initially cracked.

### NOMENCLATURE

Footnotes for the nomenclature are found at the end of the list.

$a$	crack length (this may refer to crack length at surface, crack depth, or some other specified dimension of crack front)
$a_F$	crack length for complete collapse under mean load (or crack length at which slope of crack propagation curve becomes infinite)
$a_0$	length of the largest crack that will not be detected during production process
$a_D$	length of largest crack that will not be detected during in-service inspections

$a_c$	length of initial crack in any structure which is cracked at beginning of its service life
${}^{\dagger} F_t(t_1)$	probability of variate $t$ exceeding some particular value $t_1$
$h_l$	period of operation (or service life) to extend a crack to length $l$ in structure which contained initial crack of length $l_c$ , $h_l = n_l - n_c$
$l$	relative crack length $a/a_F$ ( $l$ is dimensionless and has same value whether "a" refers to crack length at surface or to crack depth)
$l_o, l_D, l_c$	relative crack lengths corresponding to $a_o$ , $a_D$ , $a_c$ , respectively
$\tilde{l}_N, \tilde{l}_n$	median values of distributions of $l$ at life $N$ and relative life $n$
$L(n)$	probability of survival to life $n$ (also called the survivorship function)
$L_F(n), L_S(n),$ $L_I(n), L_I^*(n),$ $L_{SL}(n), L_{S,\mu}(n)$	survivorship functions at relative life $n$ , corresponding to risk functions, $r_F(n)$ , $r_S(n)$ , $r_I(n)$ , $r_I^*(n)$ , $r_{SL}(n)$ , and $r_{S,\mu}(n)$ , respectively
$L_S(h)$	survivorship function at relative service life $h$ corresponding to risk function $r_S(h)$ for structures with initial crack
$N$	life of structure expressed as number of load applications or hours of operation
$N_i$	life to first formation of fatigue crack (also called life to initial failure)
$H$	service life of structure which was initially cracked expressed as number of load applications or hours of operation
$h$	relative service life of structure which was initially cracked, $H/N_i$
$N_l$	life to produce crack length $l$ in any structure
$\tilde{N}_i$	median of the distribution of $N_i$
$n$	relative life, $N/\tilde{N}_i$



$n_l$	relative life to crack length $l$ for any structure
$n_{l,z}$	life of structure which has life $z$ times median life at same crack length $l$
$n_F$	relative life to complete collapse of structure under mean load
$n_o, n_D, n_c$	relative lives to produce crack lengths of $l_o$ , $l_D$ , and $l_c$ , respectively
$\tilde{n}_l, \tilde{n}_F, \tilde{n}_o, \tilde{n}_D, \tilde{n}_c$	medians of distributions of $n_l$ , $n_F$ , $n_o$ , $n_D$ , and $n_c$ , respectively
$n_s$	relative life corresponding to particular life $N_s$
$\bar{N}_L$	estimated mean fatigue life obtained from structural fatigue test
$n_{I(1)}, n_{I(2)}, n_{I(m)}$	relative lives to 1st, 2d, and mth inspections carried out to detect fatigue cracks
$p_R, \mu_R$	probability density function of residual strength $R$ with mean value $\mu_R$
${}^{\dagger}p_x(x_1)$	probability density function of variate $x$ at particular value $x_1$
${}^{\dagger}P_x(x_1)$	probability distribution of variate $x$ at particular value $x_1$ , $P_x(x_1) = \Pr\{x \leq x_1\}$
$P(N)$	probability of failure up to life $N$
$R(l)$	static strength of structure containing fatigue crack of relative length $l$
$r(N)$	probability of failure in remaining fleet at $N$ th load application or risk of failure at life $N$
$r(n)$	risk of failure at relative life $n$ for unit change in $z$
$r(h)$	risk of failure after period of operation $h$ in population of structures which contain initial cracks for unit change in $z$

$r(h_S   l_0)$	risk of failure after a period of operation $h_S$ in population of structures all of which contain initial crack of length $l_0$
$r(h_S   p(l_c))$	risk of failure after period of operation $h_S$ in population of structures all of which contain initial cracks with probability distribution of initial crack lengths given by $p(l_c)$
$r_S(n_S)$	risk of static fracture due to fatigue at particular life $n_S$ , defined as failure at life $n_S$ from fatigue crack in structure which is still able to sustain applied service load exceeding mean load
$r_{S,\mu}(n_S)$	risk of static fracture due to fatigue at life $n_S$ , assuming no variability in residual static strength of structures all containing cracks of given length
$r_F(n_S)$	risk of fatigue fracture at life $n_S$ , defined as failure at life $n_S$ due to fatigue crack reaching such extent that structure is unable to sustain mean load
$r_{FT}(n_S)$	the total risk of fatigue failure at life $n_S$ , $r_{FT}(n_S) = r_S(n_S) + r_F(n_S)$
$r_{SL}(n)$	risk of failure at life $n$ as calculated by conventional safe-life procedure
${}^\dagger r_I(n_S; l_D, n_I)$	risk of fatigue failure at life $n_S$ in population of structures which have all been previously inspected at life $n_I$ with inspection procedure which detects crack lengths greater than $l_D$
${}^\dagger r_I^*(n_S; l_D, n_I)$	risk of fatigue failure at life $n_S$ when cracks of length exceeding $l_D$ are detected by inspection at $n_I$ and are then repaired and structures returned to service
${}^\dagger r_I^*(n_S; l_D, n_S)$	risk of fatigue failure at life $n_S$ with continuous inspection procedure by which cracks with length exceeding $l_D$ are detected and are then repaired and structures returned to service



$${}^{\dagger} r_I^*(h_S | p(l_C); l_D, h_S)$$

risk of fatigue failure after period of operation  $h_S$  in population of structures all initially cracked with distribution of initial crack lengths given by  $p(l_C)$  and continuously inspected to detect crack lengths exceeding  $l_D$ ; after cracks are detected they are repaired and structures returned to service

$${}^{\dagger} r_I^*(n_S; l_D, r_{\max})$$

risk of fatigue failure at life  $n_S$  with inspection procedure detecting crack lengths greater than  $l_D$  at inspection intervals designed to limit risk below some specified value  $r_{\max}$ ; after cracks are detected they are repaired and structures returned to service

$${}^{\dagger} r_I^*(h_S | p(l_C); l_D, r_{\max})$$

risk of fatigue failure after period of operation  $h_S$  in population of structures all initially cracked with distribution of initial crack lengths given by  $p(l_C)$  and inspected to detect crack lengths exceeding  $l_D$  at inspection intervals designed to limit risk below some specified value  $r_{\max}$ ; after cracks are detected they are repaired and structures returned to service

$${}^{\dagger} r_D^*(n_{I(m)}; l_D, n_{I(m-1)})$$

probability of detecting cracks by inspection at life  $n_{I(m)}$  in population of structures previously inspected at  $n_{I(m-1)}$  with an inspection procedure detecting crack lengths exceeding  $l_D$ ; after cracks are detected they are repaired and structures returned to service

$${}^{\dagger} r_D^*(h_{I(m)} | p(l_C); l_D, h_{I(m-1)})$$

probability of detecting cracks by inspection after period of operation  $h_{I(m)}$  in population of structures all initially cracked with distribution of initial crack lengths given by  $p(l_C)$  and previously inspected at  $h_{I(m-1)}$  to detect crack lengths exceeding  $l_D$ ; after cracks are detected they are repaired and structures returned to service

$S$  applied service load

$S_{Ult}$  ultimate design load

$S_m$	mean load on structure
$U$	gust velocity
$Y$	relative service load, $S/S_{Ult}$
$^{\dagger} \mu, \sigma^2$	general symbols for mean and variance of population; used with suffix to denote variate
$\mu_0$	mean strength (failing load) of uncracked structures
$\mu_R(l)$	mean strength of structures containing cracks of length $l$
$\tilde{l}_n$	median crack propagation curve for population of structures, $\tilde{l}_n = g(\tilde{n}_l)$
$\frac{\mu_R(l)}{\mu_0}$	mean residual strength expressed nondimensionally as function of crack length $l$ , $\frac{\mu_R(l)}{\mu_0} = \phi(l)$
$x(l)$	relative strength of any structure containing crack length $l$ , $x(l) = \frac{R(l)}{\mu_R(l)}$
$z$	comparative life or life factor of structure with life to crack length $l$ of $z$ times median life to same crack length, $z = \frac{N_{l,z}}{\tilde{N}_l}$ or $\frac{n_{l,z}}{\tilde{n}_l}$

---

<sup>†</sup>Where no confusion can arise subscript for variate may be omitted.

<sup>‡</sup>Actual dimension of detectable crack  $a_D$  may be specified instead of relative crack length  $l_D$ .



## INTERPRETATION OF FATIGUE TEST RESULTS

With the present practice of fatigue certification by full-scale testing, the data provided by the test specimen representing the median structure of the population includes

- (1) Location of the fatigue critical areas
- (2) The median crack propagation curve
- (3) The life to final failure under the test load sequence
- (4) Residual strength data from static failure of the cracked specimen under the test load sequence, which include the failing load and the extent of fatigue cracking

## CURRENT APPROACHES TO SAFETY IN FATIGUE

The current practice is to obtain from these results a mean fatigue life  $\bar{N}_L$  corresponding to failure at some arbitrarily selected point on the crack propagation curve.

For a safe-life structure,  $\bar{N}_L$  may be the life at which the specimen broke in the fatigue test or the life at which it would be estimated to fail under some specified load such as limit load. For a fail-safe structure,  $\bar{N}_L$  is often taken to be the test life at which the fatigue failure became readily detectable by the inspection procedures that would be used in service.

In order to allow for variability in fatigue performance for either structure, the estimated mean life  $\bar{N}_L$  is divided by a scatter factor to obtain a safe operating period for replacement or inspection of the structure. The scatter factor is obtained by using an assumed probability distribution of fatigue life with an acceptable probability of failure.

## DIFFICULTY WITH CURRENT METHODS

The difficulty with the previously discussed procedure is that although the safe life to replacement or inspection is based on failure at a given point on the crack growth curve, there is, in service, an increasing risk of failure as the fatigue crack extends and the structure may fail at any stage of the crack propagation.

This difficulty is well illustrated by the measurement of the collapse load of Mustang wings that were fatigue tested to destruction under a random load sequence (ref. 1). In figure 29 of reference 1, the relative frequency distribution is presented for the load at failure as determined by experiment. For the twelve structures tested the results indicate a wide range in the failing load from 30 percent to 60 percent of the ultimate load of the virgin structure. This means that for a given life the safety level in service may be significantly different from that indicated by the fatigue test result.

Clearly the effect will depend on the shape of the crack growth curve and on the service load spectrum; however to investigate the question further an example of an ultrahigh-strength steel welded structure has been taken. The crack propagation and residual strength curves of this structure are shown in figure 1 and indicate a reasonably typical safe-life construction in that once a fatigue crack has developed there is a very marked reduction in strength which leads rapidly to failure.

The probability of survival has been calculated for this structure by the conventional method, taking two rather extreme cases for the definition of failure as follows:

(1) Failure occurs at the limit load. This is a relatively high value of the load, being near the upper limit of loads at which failure would be expected in service.

$$\tilde{N}_L = \tilde{N}_{SL}$$

(2) Failure occurs at the mean load. This is the lowest load at which service failure can occur and it will give a lower limit to the definition of failing load.  $\tilde{N}_L = \tilde{N}_F$ .

The probabilities of survival corresponding to definitions (1) and (2),  $L_{SL}$  and  $L_F$ , have been evaluated for the two load spectra shown in figure 2 by a log normal distribution of fatigue life.

If  $N_l$  is the fatigue life to any crack length  $l$  and  $\tilde{N}_l$  is the median value, then

$$z = \frac{N_l}{\tilde{N}_l}$$

has a logarithmic normal distribution and

$$L_F(N) = \int_{N/\tilde{N}_F}^{\infty} p_z(z) dz \quad (1)$$

$$L_{SL}(N) = \int_{N/\tilde{N}_{SL}}^{\infty} p_z(z) dz \quad (2)$$

The results are plotted for the manoeuvre load spectrum and the gust load spectrum in figures 3 and 4, respectively. For both spectra,  $L_F$  is considerably more than  $L_{SL}$ ; this indicates that the point on the crack growth curve at which failure is defined will have a significant effect on the safety level.

#### RELIABILITY ANALYSIS OF FATIGUE FAILURE

Consider a more representative model of the fatigue process in which a structure progressively weakened by the fatigue crack may be broken by a service load at any stage



of the crack propagation. The structure may survive this risk and continue in service until the fatigue crack has reached the stage where the crack propagation curve is rising practically vertical. The residual strength of the structure then drops rapidly until it reaches the mean load when failure must ensue. This is essentially a case where failure occurs by the fatigue process alone and in this paper the failure is termed "fatigue fracture."

The risk of failure in this mode has been considered in the section "Interpretation of Fatigue Test Results" where the probability of survival  $L_F(N)$  at the life  $N$  has been derived in equation (1) as

$$L_F(N) = \int_{N/\tilde{N}_F}^{\infty} p_Z(z) dz$$

and the corresponding risk of failure is readily obtained as

$$r_F(N) = \frac{p_Z(N/\tilde{N}_F)}{\int_{N/\tilde{N}_F}^{\infty} p_Z(z) dz} \quad (3)$$

In addition to the risk due to fatigue fracture, there is the risk of failure due to chance occurrence of a service load on a structure weakened by fatigue cracking although the structure is still able to maintain the steady load. Current methods fail to take full account of this risk which is called herein the "risk of static fracture due to fatigue" and denoted as  $r_S(N)$ .

The total probability of fatigue failure at  $N$  is therefore given by

$$r_{FT}(N) = r_S(N) + r_F(N) \quad (4)$$

If it is desired to indicate a specified value of the service life,  $N_S$  may be used rather than  $N$ ; therefore, an alternative form of equation (4) is

$$r_{FT}(N_S) = r_S(N_S) + r_F(N_S)$$

#### RELIABILITY ANALYSIS WITH VARIABILITY IN FATIGUE STRENGTH

First consider the risk of static fracture due to fatigue in the simplified case where there is no variability in static strength but a characteristic distribution of fatigue life at

any given crack length. Next consider the probability of failure in the fleet at the Nth load cycle (i.e., the risk of failure at life N) of structures all containing cracks of the same crack length  $a$  which may be expressed nondimensionally in terms of the crack length  $a_F$  at which the structure would fail under the mean load; that is,  $l = a/a_F$ .

Let  $S_N$  denote the Nth service load and  $R(l)$  the residual strength of structures with crack length  $l$ .  $R(l)$  is a decreasing function of  $l$  and may be expressed nondimensionally in terms of the ultimate strength  $\mu_0$  of an uncracked structure as

$$\frac{R}{\mu_0} = \phi(l) \quad (5)$$

Hence

$$\begin{aligned} \Pr \left\{ \text{Failure at life } N \mid \text{crack length } l \right\} &= P_F(N/l) \\ &= \Pr \left\{ S_N \geq R(l) \right\} \\ &= \Pr \left\{ S_N \geq \mu_0 \phi(l) \right\} \\ &= F_S(\mu_0 \phi[l]) \end{aligned} \quad (6)$$

where  $F_S(s)$  is the probability of exceeding any service load  $s$ . The total probability of failure in the fleet at life  $N$  (i.e., the risk of failure at  $N$ ) is then obtained by summing over all crack lengths from  $l = 0$  to  $l = 1$

$$\begin{aligned} r_{S,\mu}(N) &= \int_0^1 p_F(N/l) p(l) dl \\ &= \int_0^1 F_S(\mu_0 \phi[l]) p(l) dl \end{aligned} \quad (7)$$

where  $r_{S,\mu}(N)$  denotes the risk of static fracture at the life  $N$  assuming that there is no variability in the static strength at a given crack length.

The probability density function  $p(l)$  of the crack length  $l$  at any given life  $N$  is not known but this difficulty is overcome by transposing the variate from crack length at a given life to life at a given crack length. This is done by using the model of the fatigue process shown in figure 5 in which it is assumed that for any structure the life  $N_l$  bears a constant ratio  $z$  to the median life  $\tilde{N}_l$  at the same crack length  $l$ ,

$$N_l = z \tilde{N}_l$$



or by expressing life nondimensionally in terms of the median life to initial failure  $\tilde{N}_i$

$$\frac{N_l}{\tilde{N}_i} = n_l = z \tilde{n}_l \quad (8)$$

where  $z$  is constant for any structure and is called the life factor. By considering the shaded element in figure 5 it can be seen that structures with crack lengths between  $l$  and  $l + dl$  at  $N$  have initial lives between  $n_i$  and  $n_i + dn_i$ . Hence

$$\begin{aligned} p(l) dl &= p(n_i) dn_i \\ &= p(z) dz \end{aligned}$$

since  $z = \frac{n_i}{\tilde{n}_i}$ . This expression neglects the effect on the probability density function of  $n_i$  of the very few structures that have failed between  $n_i$  and  $n_g$ .

If the equation of the median crack propagation curve

$$l = g(\tilde{n}_l) = g(n_l/z) \quad (9)$$

is used, equation (7) can now be transformed by changing the variable of crack length  $l$  to one of fatigue life represented by the life factor  $z$ . Taking  $z = n$  at  $l = 0$  and  $z = \frac{n}{\tilde{n}_F}$  at  $l = 1$ , equation (7) can now be written as

$$r_{S,\mu}(n) = \int_{n/\tilde{n}_F}^n F_S \left\{ \mu_0 \phi \left( g \left[ \frac{n}{z} \right] \right) \right\} p(z) dz \quad (10)$$

#### RELIABILITY ANALYSIS WITH VARIABILITY IN FATIGUE STRENGTH AND STATIC STRENGTH

In the preceding section it was assumed that there was no variability in the residual strength property, whereas, in general, at any crack length  $l$ , the residual strength  $R(l)$  will have a probability distribution about a mean value  $\mu_R(l)$ . If the dimensionless variate  $x(l) = \frac{R(l)}{\mu_R(l)}$  is assumed to have a characteristic distribution which applies for all values of crack length, then

$$R(l) = \mu_R(l) x(l)$$

and  $\mu_R(l)$  can be expressed as a decreasing function of  $l$  from equation (5) as

$$R(l) = \mu_0 \phi(l) x(l)$$

This is analogous to equation (6), and integrating over all crack lengths gives as before

$$r_S(n | x(l)) = \int_{n/\tilde{n}_F}^n F_S \left\{ x \mu_0 \phi \left( g \left[ \frac{n}{z} \right] \right) \right\} p(z) dz \quad (11)$$

To obtain the total risk of static fracture at  $n$ , integrate over all values of  $x(l)$  from 0 to  $\infty$  to get

$$r_S(n) = \int_0^\infty \int_{n/\tilde{n}_F}^n F_S \left\{ x \mu_0 \phi \left( g \left[ \frac{n}{z} \right] \right) \right\} p(z) p(x) dz dx \quad (12)$$

This equation is the general expression for the risk of static fracture by fatigue at life  $n$ . As stated earlier an alternative expression using  $n_S$  instead of  $n$  may be adopted where the risk at a specified value  $n_S$  of the service life is desired. This expression is

$$r_S(n_S) = \int_0^\infty \int_{n_S/\tilde{n}_F}^{n_S} F_S \left\{ x \mu_0 \phi \left( g \left[ \frac{n_S}{z} \right] \right) \right\} p(z) p(x) dz dx$$

#### PROBABILITY DISTRIBUTION OF THE LOAD AT FAILURE

It is of interest to consider the probability distribution of the load at failure since this indicates how the risk of failure is being affected by the changing residual strength of aircraft in the fleet.

The condition for investigation is the probability that at a given life  $n_S$  structures will fail with a residual strength less than some specified value  $R_0$ .

Requiring

$$R \leq R_0$$

or

$$x = \frac{R}{\mu_R} \leq \frac{R_0}{\mu_R}$$



then substituting

$$\mu_R = \mu_0 \phi(l)$$

$$x \leq \frac{R_0}{\mu_0 \phi(l)}$$

or

$$x \leq \frac{x_0}{\phi(l)}$$

where

$$x_0 = \frac{R_0}{\mu_0}$$

and transposing the variate from crack length  $l$  to the life factor  $z$  give

$$x \leq \frac{x_0}{\phi\left\{g\left[\frac{n_S}{z}\right]\right\}}$$

From equation (11)

$$\begin{aligned} & \Pr\left\{\text{Static fracture at } n_S \text{ with the collapse load } \leq R_0\right\} \\ &= r_S\left\{n_S \mid R \leq \mu_0 x_0\right\} \\ &= \int_{n_S/\tilde{n}_F}^{n_S} \int_{x=0}^{x=x_0/\phi\left\{g\left[\frac{n_S}{z}\right]\right\}} F_S\left\{x\mu_0\phi\left(g\left[\frac{n_S}{z}\right]\right)\right\} p(x) p(z) dx dz \end{aligned} \quad (13)$$

where

$$x_0 = \frac{R_0}{\mu_0}$$

Since the total probability of static fracture due to fatigue at  $n_S$  is given by  $r_S(n_S)$ , the required probability distribution for the load at failure at a specified life  $n_S$  is as follows:

$$\Pr \left\{ \text{Failing load} \leq \mu_0 x_0 \text{ at life } n_s \right\} = \int_{n_s/\tilde{n}_F}^{n_s} \int_0^{x_0} \frac{\phi \left\{ g \left[ \frac{n_s}{z} \right] \right\} F_S \left\{ x \mu_0 \phi \left( g \left[ \frac{n_s}{z} \right] \right) \right\} p(x) p(z) dx dz}{r_S(n_s)} \quad (14)$$

## APPLICATION OF THE METHOD

To illustrate the method of reliability analysis and to compare the results according to the various risk functions in equations (2), (1), (10), and (12), the risk of failure has been calculated for a nonredundant high-strength steel structure. Sample test data for the structure are shown in figure 1.

The crack propagation curve has been determined from the results of a representative full-scale fatigue test in which fractographic examination of the fracture surface of the critical failures has been used to determine the crack dimensions at various stages of the test life. Although the curve in figure 1 is based on the crack length at the surface of the material, use of the nondimensional relative crack length  $l = \frac{a}{a_F}$  enables it to represent also the crack depth or any other leading dimension of the crack front.

The residual strength curve  $\frac{\mu_R}{\mu_0} = \phi(l)$  has been estimated from the relationship  $l = \frac{A}{\left(\frac{\mu_R}{\mu_0}\right)^2}$  based on fracture mechanics theory, where  $A$  is a constant depending primarily on the fracture toughness of the material and the shape of the crack front.

The variability in residual strength about the mean value  $\mu_R$  was assumed to follow the three parameter Weibull distribution, and with representative data on small steel specimens (ref. 3), the following expression was obtained for the probability distribution of the relative residual strength  $x = \frac{R}{\mu_R}$ :

$$P_X(x) = \Pr \left\{ \frac{R}{\mu_R} \leq x \right\} = 1 - \exp - \left\{ \frac{x - 0.824}{1.017 - 0.824} \right\}^{2.55}$$

The crack length at failure under limit load, according to the relevant fatigue test data used, is approximately 0.08 in., giving a crack depth of 0.04 in. for a semicircular crack.

The distribution of fatigue life about the median value was assumed to be log normal with variance  $\sigma_{\log N}^2$  of 0.02.



Two service load spectra were assumed as shown in figure 2. Spectrum I is a spectrum of manoeuvre load derived from data on U.S. jet fighter operations in reference 4. A median life to initial failure of 2000 hours was assumed to correspond to the fatigue test result, and an ultimate load factor of 10 was assumed, which gives a mean load of 10 percent of the design ultimate.

Spectrum II was based on thunderstorm gust load data from reference 5 giving the probability of exceeding a gust load  $U$  as  $F_u(U) = e^{-0.197U}$ . Expressing load non-dimensionally as

$$Y = \frac{S}{S_{Ult}}$$

where  $S$  is the load due to a gust velocity  $U$  and  $S_{Ult}$  is the load corresponding to the ultimate design gust velocity of 99 fps with the mean load of the aircraft assumed to be 20 percent of the design ultimate, gives the following equation for the gust load spectrum:

$$F_S(Y) = e^{-24.4(Y-0.2)}$$

A life to initial failure of 20 000 hours was assumed as typical of this type of spectrum.

The four different risk functions of equations (1), (2), (10), and (12) have been evaluated by using numerical analysis techniques (ref. 6) for both spectra I and II. The corresponding probabilities of survival to life  $n$  have been calculated from the relationship  $L(n) = e^{-\int_0^n r(t) dt}$  and are plotted for spectrum I and spectrum II in figures 3 and 4, respectively.

These results show that conventional safe-life estimates as represented by  $L_{SL}$  ( $L_{SL}$  corresponds to static fracture of a fatigue cracked structure under limit load and is in accordance with current life estimation procedures) can be inaccurate since they fail to take proper account of the risk of static fracture of the structure weakened by the growing fatigue crack.

Comparison of  $L_S$  and  $L_{S,\mu}$  indicates that the variability in residual strength has a significant effect on the probability of survival (or failure). The probability of survival  $L_F$  refers to failure due to the fatigue fracture extending to the stage where the structure is not able to sustain the steady mean load. The risk from this type of failure is often small but as mentioned previously it must be included in the total risk.

## RISK OF FAILURE IN STRUCTURES INITIALLY CRACKED

With the high-strength materials of low ductility now being introduced into aircraft construction there is a difficulty of detecting very small cracks with current nondestructive inspection (NDI) techniques. This factor together with the susceptibility of these high-strength materials to the formation of flaws in the production process may result in a probability of cracks existing in a number of aircraft structures before they go into service.

### STRUCTURES WITH INITIAL CRACKS OF CONSTANT LENGTH

In the most adverse case, all structures are assumed to be cracked in the fatigue critical areas to a relative crack length  $l_0$  which corresponds to the maximum length of crack that will escape detection. According to this assumption all structures start their service life with a crack of length  $l_0$  present.

In the model of the fatigue process illustrated in figure 5, all the crack propagation curves can be regarded as radiating from a single point or pole P. If all structures are initially cracked to the same length  $l_0$ , this corresponds to shifting the pole to the point P' with coordinates  $(\tilde{n}_0, l_0)$  as shown in figure 6. Each structure now starts its service life  $h$  at the life  $n_0$  which would have produced a fatigue crack of length  $l_0$  in this particular structure. This infers that the initial crack or defect induces the same stress field as a fatigue crack of the same dimensions in the area being considered. It may be regarded as a fair assumption since under repeated loading the defect will rapidly initiate a fatigue crack which can be expected to give rise to a similar stress field as that which would result if the crack had been produced by fatigue alone.

Referring to figure 6 shows that for any structure which has a life factor  $z = n_l / \tilde{n}_l$ , the service life  $h_l$  to any crack length  $l$  is given by

$$h_l = n_l - n_0 = z\tilde{n}_l - z\tilde{n}_0 = z(\tilde{n}_l - \tilde{n}_0)$$

For the median values,

$$\tilde{h}_l = \tilde{n}_l - \tilde{n}_0$$

Hence

$$h_l = z\tilde{h}_l \tag{15}$$



Therefore, the same model of the crack propagation process applies as for structures without initial cracks except that the origin is shifted to  $(\tilde{n}_0, l_0)$ , the service life is given by  $h_s = (n_s - n_0) = z(\tilde{n}_s - \tilde{n}_0) = z\tilde{h}_s$ , and the equation of the median crack propagation curve is transformed to

$$l = g(\tilde{h}_l + \tilde{n}_0) = g\left(\frac{hl}{z} + \tilde{n}_0\right) \quad (16)$$

The risk of failure is therefore obtained in the same way as for structures initially uncracked, and by integrating over crack lengths from  $l = l_0$  to  $l = 1$ , the following equation is obtained from equation (7):

$$r_{s,\mu}(n | l_0) = \int_{l_0}^1 F_s \left\{ \mu_0 \phi(l) \right\} p(l) dl \quad (17)$$

Hence if the variable is changed from one of crack length to one of fatigue life at a given crack length as represented by the life factor  $z$ , the following equation is obtained from equations (17) and (16):

$$r_{s,\mu}(h_s | l_0) = \int_{h_s/(\tilde{n}_F - \tilde{n}_0)}^{\infty} F_s \left\{ \mu_0 \phi \left[ g\left(\frac{h_s}{z} + \tilde{n}_0\right) \right] \right\} p(z) dz \quad (18)$$

where  $r_{s,\mu}(h_s | l_0)$  denotes the risk of failure at a particular operating life  $h_s$  of structures having initial cracks of length  $l_0$  and having no variability in residual strength.

The corresponding expression when there is a probability distribution of residual strength  $x$  given by  $p(x)$  can be derived from equation (18) as

$$r_s(h_s | l_0) = \int_0^{\infty} \int_{h_s/(\tilde{n}_F - \tilde{n}_0)}^{\infty} F_s \left\{ x \mu_0 \phi \left[ g\left(\frac{h_s}{z} + \tilde{n}_0\right) \right] \right\} p(z) p(x) dz dx \quad (19)$$

where  $r_s(h_s | l_0)$  denotes the risk of failure at service life  $h_s$  for structures which are all cracked to a length  $l_0$  at the start of their service life.

The risk of failure by fatigue fracture for this case follows from the expression given in equation (3) and is

$$r_F(h_S | l_0) = \frac{p_Z\left(\frac{h_S}{\tilde{n}_F - \tilde{n}_0}\right)}{\int_{h_S/(\tilde{n}_F - \tilde{n}_0)}^{\infty} p_Z(z) dz} \quad (20)$$

The corresponding probabilities of survival can then be calculated as before.

## STRUCTURES WITH INITIAL CRACKS OF VARIOUS LENGTHS

In the general case the population of structures will contain cracks ranging from zero length up to the detectable length  $l_0$  and it can be assumed that there is a probability of a structure containing a crack of length  $l_c$  between 0 and  $l_0$  as given by the probability density function  $p(l_c)$ .

Consider the fraction of the population  $p(l_c) dl_c$  which has initial crack lengths between  $l_c$  and  $l_c + dl_c$ . The probability of failure at  $h_S$  for these structures is given by  $r(h_S | l_c)$  according to equation (19). Their contribution to the total risk of failure in the population at service life  $h_S$  is therefore,

$$\Delta r = r(h_S | l_c) p(l_c) dl_c \quad (21)$$

Since  $h_S$  is the same for all structures whatever their initial crack length  $l_c$ , the total risk of failure for all structures at service life  $h_S$  may be calculated by integrating equation (21) over all values of initial crack length from  $l_c = 0$  to  $l_c = l_0$ . Then

$$r_S(h_S | p(l_c)) = \int_{l_c=0}^{l_c=l_0} r(h_S | l_c) p(l_c) dl_c \quad (22)$$

As was done in the derivation of  $r_S(h_S | l_0)$  in equation (19), the variable of initial crack length  $l_c$  is expressed as the corresponding life  $\tilde{n}_c$  on the median crack propagation curve, with  $l_c = g(\tilde{n}_c)$  and

$$p(l_c) dl_c = p(\tilde{n}_c) d\tilde{n}_c$$

Then, since  $\tilde{n}_c = \tilde{n}_i$  when  $l_c = 0$  and  $\tilde{n}_c = \tilde{n}_0$  when  $l_c = l_0$ , the following equation is obtained from equation (22) by substituting  $r(h_S | l_c)$  from equation (19):

$$r_S(h_S | p(l_c)) = \int_{\tilde{n}_c=\tilde{n}_i}^{\tilde{n}_c=\tilde{n}_0} \int_{x=0}^{x=\infty} \int_{z=h_S/(\tilde{n}_F - \tilde{n}_c)}^{z=\infty} F_S\left\{x \mu_0 \phi\left[g\left(\frac{h_S}{z} + \tilde{n}_c\right)\right]\right\} p(z) p(x) p(\tilde{n}_c) dx dz d\tilde{n}_c \quad (23)$$



Similarly the risk of fatigue fracture can be derived from equation (20) as

$$r_F(h_S | p(l_c)) = \int_{\tilde{n}_c=1}^{\tilde{n}_c=\tilde{n}_0} \frac{\left[ p_Z \left\{ h_S / (\tilde{n}_F - \tilde{n}_c) \right\} p(\tilde{n}_c) d\tilde{n}_c \right]}{\int_{\tilde{n}_c=1}^{\tilde{n}_c=\tilde{n}_0} \int_{h_S / (\tilde{n}_F - \tilde{n}_c)}^{\infty} p_Z(z) p(\tilde{n}_c) dz d\tilde{n}_c} \quad (24)$$

### PROBABILITY DISTRIBUTION OF THE FAILING LOAD

The probability distribution of the failing load can be determined for the case of structures with initial cracks by a simple extension of the method developed in the section "Probability Distribution of the Load at Failure."

If one is interested in structures with residual strength  $R$  less than some specified value  $R_0$ , then as in the aforementioned section this corresponds to structures with

$$x \leq \frac{x_0}{(\mu_R / \mu_0)} \quad \left( x_0 = \frac{R_0}{\mu_0} \right) \quad (25)$$

Consider structures with initial cracks of length  $l_c$  corresponding to a life of  $\tilde{n}_c$  on the median crack propagation curve. Now from equation (16)

$$\frac{\mu_R}{\mu_0} = \phi(l) = \phi \left[ g \left( \frac{h_l}{z} + \tilde{n}_c \right) \right]$$

Hence substituting this equality into equation (25) gives the following equation:

$$x \leq \frac{x_0}{\phi \left[ g \left( \frac{h_l}{z} + \tilde{n}_c \right) \right]} \quad (26)$$

Thus, for structures with initial cracks of length  $l_c$  it follows from equation (19) that the probability of failure with residual strength  $\frac{R}{\mu_0}$  less than some given fraction  $x_0$  of the virgin strength is given by

$$r_S \left\{ h_S \mid \begin{matrix} l_c \\ R \leq \mu_0 x_0 \end{matrix} \right\} = \int_{h_S / (\tilde{n}_F - \tilde{n}_c)}^{\infty} \int_0^{x_0 / \phi \left[ g \left( \frac{h_S}{z} + \tilde{n}_c \right) \right]} F_S \left\{ x \mu_0 \phi \left[ g \left( \frac{h_S}{z} + \tilde{n}_c \right) \right] \right\} p(x) p(z) dx dz \quad (27)$$

The total risk of static fracture due to fatigue at  $h_S$  is given by  $r_S(h_S | l_c)$  and therefore it follows that

$$\Pr \left\{ \text{Failing load} \leq \mu_0 x_0 \text{ at life } h_s \right\} = \int_{h_s/(\tilde{n}_F - \tilde{n}_c)}^{\infty} \int_0^{x_0} \frac{\phi \left[ g \left( \frac{h_s}{z} + \tilde{n}_c \right) \right]}{r_s(h_s | l_c)} F_s \left\{ x \mu_0 \phi \left[ g \left( \frac{h_s}{z} + \tilde{n}_c \right) \right] \right\} p(x) p(z) dx dz \quad (28)$$

Where the population of structures have initial cracks with a probability distribution of crack length represented by  $p(l_c)$  it follows from equation (23) that the probability of failure with relative strength  $R/\mu_R$  less than  $x_0$  is given by an analogous expression to equation (27) as follows

$$r_s \left\{ h_s \mid \begin{matrix} p(l_c) \\ R \leq x_0 \mu_0 \end{matrix} \right\} = \int_{\tilde{n}_i}^{\tilde{n}_0} \int_{h_s/(\tilde{n}_F - \tilde{n}_c)}^{\infty} \int_0^{x_0} \frac{\phi \left[ g \left( \frac{h_s}{z} + \tilde{n}_c \right) \right]}{r_s(h_s | l_c)} F_s \left\{ x \mu_0 \phi \left[ g \left( \frac{h_s}{z} + \tilde{n}_c \right) \right] \right\} p(x) p(z) p(\tilde{n}_c) dx dz d\tilde{n}_c \quad (29)$$

If equation (29) is divided by  $r_s(h_s | p(l_c))$ , the total risk of static fracture due to fatigue at  $h_s$ , the probability that  $R \leq x_0 \mu_0$  at  $h_s$  is obtained as follows:

$$P_{x_0} \left\{ h_s \mid \begin{matrix} p(l_c) \\ x_0 \end{matrix} \right\} = \frac{\int_{\tilde{n}_i}^{\tilde{n}_0} \int_{h_s/(\tilde{n}_F - \tilde{n}_c)}^{\infty} \int_0^{x_0} \frac{\phi \left[ g \left( \frac{h_s}{z} + \tilde{n}_c \right) \right]}{r_s(h_s | l_c)} F_s \left\{ x \mu_0 \phi \left[ g \left( \frac{h_s}{z} + \tilde{n}_c \right) \right] \right\} p(x) p(z) p(\tilde{n}_c) dx dz d\tilde{n}_c}{r_s(h_s | p(l_c))} \quad (30)$$

## APPLICATION

The foregoing theory has been applied to calculate the risk of failure for the ultrahigh-strength steel structures considered previously for which the crack propagation and residual strength curves are shown in figure 1. The load spectrum used in the calculations was the manoeuvre load spectrum shown in figure 2 as spectrum I.

For the case of structures all initially cracked to the same extent, the relative crack length  $l_0$  has been taken as 0.075 from a consideration of the crack detection capability of the NDI techniques used in production.

For the case where it is assumed that there is a continuous probability distribution of initial crack size, an exponential distribution of initial crack length  $l_c$  has been adopted with the probability density function

$$p(l_c) = 26.2e^{-20.6l_c} \quad (0 \leq l_c \leq 0.075) \quad (31)$$



The exponential distribution has been adopted since it follows from the physically realistic assumption that the occurrence of a defect in a small element of the material follows a uniform probability law over the whole volume.

The detectable crack length  $l_D$  for in-service inspections has been taken as 0.15.

As stated in the section "Structures With Initial Cracks of Constant Length," the theory assumes that the initial defect produces the same stress field as a fatigue crack the same size as the defect. In applying fracture mechanics theory to deduce crack propagation and residual strength characteristics, the depth of the crack is the important parameter; whereas for crack detection, the length of the crack exposed at the surface is the controlling factor. However, with the nondimensional relative crack length

$$l = \frac{a}{a_F} \quad (32)$$

it is immaterial whether crack length or crack depth is taken since both yield the same value of  $l$ , provided the shape of the crack front does not change markedly as the crack propagates.

In establishing the detectable relative crack lengths  $l_O$  and  $l_D$ , it has been assumed that the crack length exposed at the surface which will be detected by the best available methods is 0.02 inch for production-line conditions and 0.04 inch for in-service inspections. Assuming a semicircular crack front, which is often characteristic of cracks originating at a surface, gives corresponding crack depths of 0.01 and 0.02 inch.

A value of  $a_F$  of 0.132 inch was obtained from typical crack propagation data by determining the crack depth at which the crack propagation curve becomes vertical since this is virtually equivalent to failure at mean load. The relative crack lengths  $l_O$  and  $l_D$  given previously were thus obtained from equation (32).

With these input data, the risk functions  $r_S^*(h | 0.01'')$  and  $r_S^*(h | p(l_c))$  for the two cases of constant initial crack depth of 0.075 and an exponential distribution of initial crack depths have been evaluated from equations (19) and (23) and are plotted in figures 7 and 9, respectively. The corresponding survivorship functions are plotted in figures 8 and 10. The probability distribution of the failing load at various service lives  $h_S$  has been calculated from equation (28) and the results are presented in figure 11.

It is apparent that the presence of initial cracks greatly increases the risk of failure at a given life. Also the risk of failure at the beginning of the service life is finite in this case as distinct from the case where all structures are without cracks initially. This arises because with all structures cracked initially every member of the fleet is exposed to the risk of static fracture from the outset.

## SAFETY BY INSPECTION

As inspection techniques become more highly developed, increasing applications are likely to be found in monitoring structural safety. However, inspections of a complex aircraft structure are both time consuming and costly, and the efficient planning of inspection intervals is becoming an essential requirement. The reliability approach by calculating the risk of failure as a function of life enables the effect of any inspection procedure to be investigated and suitable inspection intervals to be planned.

### CONTINUOUS INSPECTION

The optimum effect of inspection is, of course, obtained when every structure is inspected continuously. As soon as cracks reach the detectable length  $l_D$ , remedial action is taken and therefore the risk of fatigue fracture is eliminated.

The risk of failure is then equal to the risk of static fracture by fatigue which is determined by calculating the probability of failure for structures with crack lengths between  $l = 0$  and  $l = l_D$ .

If structures are repaired and replaced when cracks are detected, there is no reduction in size of the fleet and the risk of failure at any life  $n_S$  is obtained by integrating in equation (12) between the limits  $z = \frac{n_S}{\tilde{n}_D}$  to  $z = n_S$  since this corresponds to integrating over crack lengths between 0 and  $l_D$ . (See fig. 5.)

Hence the risk of failure for "continuous inspection with replacement" is given by

$$r_I^*(n_S; l_D, n_S) = \int_{n_S/\tilde{n}_D}^{n_S} \int_0^\infty F_S \left\{ x \mu_0 \phi \left( g \left[ \frac{n_S}{z} \right] \right) \right\} p(x) p(z) dx dz \quad (33)$$

The corresponding result for structures which are initially cracked is found in a similar manner from equation (20); that is,

$$r_I^*(h_S | p(l_c); l_D, h_S) = \int_{\tilde{n}_c = \tilde{n}_i}^{\tilde{n}_c = \tilde{n}_0} \int_0^\infty \int_{h_S/(\tilde{n}_D - \tilde{n}_c)}^\infty F_S \left\{ x \mu_0 \phi \left[ g \left( \frac{h_S}{z} + \tilde{n}_c \right) \right] \right\} p(z) p(x) p(\tilde{n}_c) dz dx d\tilde{n}_c \quad (34)$$

When cracked structures are not repaired but are taken out of service after detection, there is a continual depletion of the population since at life  $n_S$  all structures which have a life less than  $n_S$  at crack length  $l_D$  are eliminated by inspection; that is, the distribution of fatigue life  $p(z)$  is truncated at  $z = \frac{n_S}{\tilde{n}_D}$  and hence the proportion of the population remaining at life  $n_S$  is given by  $\int_{n_S/\tilde{n}_D}^\infty p(z) dz$ .



Therefore, for "inspection without replacement" the risk of failure at  $n_s$  (which is the probability of failure in the fleet remaining at  $n_s$ ) is derived from equation (33) as

$$r_I(n_s; l_D, n_s) = \frac{r_I^*(n_s; l_D, n_s)}{\int_{n_s/\tilde{n}_D}^{\infty} p(z) dz} \quad (35)$$

In a similar way the risk of failure for inspection without replacement in a population of structures which are initially cracked follows from equation (34) as

$$r_I(h_s | p(l_c); l_D, h_s) = \frac{r_I^*(h_s | p(l_c); l_D, h_s)}{\int_{\tilde{n}_c=\tilde{n}_i}^{\tilde{n}_c=\tilde{n}_0} \int_{h_s/(\tilde{n}_D-\tilde{n}_c)}^{\infty} p(z) p(\tilde{n}_c) dz d\tilde{n}_c} \quad (36)$$

### INSPECTION FOR LIMITED RISK

In practice, it is usually not economic or even feasible to inspect structures continuously but inspection is carried out at predetermined intervals. A method is proposed for the efficient planning of inspection intervals in which, when the risk of static fracture by fatigue reaches a prescribed upper limit, an inspection is carried out. The risk of failure is reduced at this stage to the same value as the risk of failure with continuous inspection, but it rises as the life continues until it again reaches the prescribed risk limit when a second inspection is carried out.

Repeated application of this process ensures that each inspection is equally effective in maintaining the risk of failure below a prescribed upper limit. The application of the procedure is shown in a subsequent section, and the expression for the risk function is presented in the appendix.

### CRACK DETECTION RATE

It is important to determine the probability of cracks being detected at each inspection since this gives the fraction of the fleet that can be expected to require repair and modification before continuing in service.

Reference to the model of the fatigue process in figure 5 shows that in the first inspection at life  $n_{I(1)}$  all structures with crack lengths between  $l = l_D$  and  $l = 1$  are eliminated. These correspond to structures which have values of  $z$  between  $z = \frac{n_{I(1)}}{\tilde{n}_D}$

and  $z = \frac{n_{I(1)}}{\tilde{n}_F}$ . Hence the fraction of the population in which cracks are expected to be revealed at the first inspection is given by

$$r_D^*(n_{I(1)}; l_D) = \int_{n_{I(1)}/\tilde{n}_F}^{n_{I(1)}/\tilde{n}_D} p(z) dz \quad (37)$$

Or in general for the  $m$ th inspection, the probability of cracks being detected in a structure is given by

$$r_D^*(n_{I(m)}; l_D, n_{I(m-1)}) = \int_{n_{I(m-1)}/\tilde{n}_D}^{n_{I(m)}/\tilde{n}_D} p(z) dz \quad (38)$$

where  $r_D^*(n_{I(m)}; l_D, n_{I(m-1)})$  denotes the probability of finding cracks at the  $m$ th inspection at life  $n_{I(m)}$  following the previous inspection at life  $n_{I(m-1)}$ . It is assumed that cracks with a length greater than  $l_D$  will be detected and that structures in which cracks have been detected will be repaired and returned to service.

For structures with initial crack lengths  $l = l_0$  it can be seen by reference to figure 6 that the probability of detecting cracks is

$$r_D^*(h_{I(m)} | l_0; l_D, h_{I(m-1)}) = \int_{h_{I(m-1)}/(\tilde{n}_D - \tilde{n}_0)}^{h_{I(m)}/(\tilde{n}_D - \tilde{n}_0)} p(z) dz \quad (39)$$

where, with a similar notation as for equation (38),  $r_D^*(h_{I(m)} | l_0; l_D, h_{I(m-1)})$  denotes the probability of detection at the  $m$ th inspection after a period of operation in service of  $h_{I(m)}$ , following a previous inspection at  $h_{I(m-1)}$ . It is again assumed that all cracks with a length exceeding  $l_D$  will be detected and  $\tilde{n}_D$  and  $\tilde{n}_0$  denote the lives on the median crack propagation curve corresponding to crack lengths of  $l_D$  and  $l_0$ .

If the population of structures has a continuous distribution  $p(l_c)$  of initial crack lengths between  $l_c = 0$  and  $l_c = l_0$  the probability of detection can be derived from equation (39) by integrating over the initial crack lengths from  $l_c = 0$  to  $l_c = l_0$ ,

$$r_D^*(h_{I(m)} | p(l_c); l_D, h_{I(m-1)}) = \int_0^{l_0} \int_{h_{I(m-1)}/(\tilde{n}_D - \tilde{n}_c)}^{h_{I(m)}/(\tilde{n}_D - \tilde{n}_c)} p(z) p(l_c) dz dl_c$$

or



$$r_D^*(h_{I(m)} | p(l_c); l_D, h_{I(m-1)}) = \int_{\tilde{n}_1}^{\tilde{n}_0} \int_{h_{I(m-1)} / (\tilde{n}_D - \tilde{n}_c)}^{h_{I(m)} / (\tilde{n}_D - \tilde{n}_c)} p(z) p(\tilde{n}_c) dz d\tilde{n}_c \quad (40)$$

expressing  $l_c$  in terms of the corresponding life  $\tilde{n}_c$  according to the median crack propagation curve, and integrating with  $\tilde{n}_c = n_1$  at  $l_c = 0$  and  $\tilde{n}_c = \tilde{n}_0$  at  $l_c = l_0$ .

## APPLICATION

The foregoing theory has been applied to demonstrate the effect of planned inspection procedures for the case of a high-strength steel structure under a manoeuvre load spectrum (spectrum I in fig. 2) which has been considered previously.

The risk function for fatigue failure with continuous inspection has been calculated by using numerical analysis procedures (ref. 6) for the three cases of structures without initial cracks, structures with initial cracks of constant length  $l_0$ , and structures with a distribution of initial crack sizes given by the probability density function  $p(l_c)$ . The risk functions for periodic inspection with limited risk have been calculated for the same three cases. The results have been plotted in figures 12, 7, and 9, respectively, and the corresponding survivorship functions are shown in figures 13, 8, and 10. The inspection intervals for inspection with limited risk for each of the three cases are shown in table I together with the expected detection rate at each inspection which has been calculated according to the procedure developed in the preceding section.

With periodic inspection, the risk function returns to the continuous inspection curve at each inspection. The continuous inspection curve therefore has a basic significance since it indicates the maximum extent to which the risk of failure can be reduced by inspection.

## DISCUSSION OF RESULTS

Consider the results of applying the foregoing theory to the case of the high-strength steel structure described previously with particular reference to the suitability of the fail-safe and safe-life procedures.

### RISK OF FATIGUE FAILURE

Reference to the risk functions  $r_{SL}$  and  $r_F$  in figure 14 illustrates the difficulty with the conventional approach. As the life extends, the difference in these two risks becomes considerable, although as was stated in the section "Interpretation of Fatigue

Test Results" they merely represent two rather extreme conditions in the application of the conventional safe-life approach.

In fact, the risks  $r_{SL}$  and  $r_F$  differ only in the point on the crack growth curve at which failure is taken to occur. This difference introduces a problem in the interpretation of the fatigue test result since the structure under a representative test load sequence may well fail at a rather different stage of the crack propagation curve as compared with the structures that happen to fail at a relatively short fatigue life in service.

This can be seen by reference to the curves of the probability distribution of the failing load in figure 15. These show that at lives typical of service operation ( $n = 1.0$  to  $1.25$ ), the expected value of the failing load, for the few structures that fail, is relatively high, being above the limit load, whereas at longer lives the expected value of the failing load is considerably reduced. Therefore the fatigue test specimen, representing the average structure, is likely to fail at loads considerably below those at which service failures will occur.

The basic difficulty is that neither  $r_{SL}$  nor  $r_F$  represents the true situation in that they do not take account of the fact that there is some probability of failure at all points along the crack propagation curve as the fatigue crack extends. This effect (the risk of static fracture) is taken account of by  $L_{S,\mu}(n)$  which, as can be seen in figures 3 and 4, gives an increased probability of failure for the example taken.

Another effect of considerable importance in considering static fracture due to fatigue is the variability in residual static strength of cracked structures since this may have a significant effect on the probability of failure (or survival) depending on the severity of the loading spectrum. This is shown by the comparison between  $L_{S,\mu}$  and  $L_S$  for the two load spectra as shown in figures 3 and 4. The probability of survival  $L_S$  calculates the increasing risk of failure as the fatigue crack extends in the same way as  $L_{S,\mu}$  but it also includes the effect of the variability in residual static strength.

The probability of survival  $L_S$  can be applied with equal validity to calculate the probability of survival for structures with initial cracks as outlined in the section "Risk of Failure in Structures Initially Cracked." This has been done for example of the high-strength steel structure taken previously and the results for two cases of initial cracking are shown in figures 8 and 10 where it will be noted that, for an equivalent probability of survival, the fatigue life is greatly reduced by the presence of initial cracks. The shortcomings of the conventional methods of life calculation are more marked in this case, since for all structures the whole of the service life involves the propagation of a fatigue crack with continual exposure to the progressively increasing risk of static fracture due to fatigue.



## PROBABILITY DISTRIBUTION OF THE FAILING LOAD

Curves showing the probability distribution of the collapse load for static fracture by fatigue for the high-tensile steel structure are shown at a series of lives in figure 15. In the early stages of the life when only small cracks are present the majority of the structures that fail do so from occurrence of a high load in excess of the design limit load. At longer lives, however, when a large percentage of the fleet has developed more extensive fatigue cracks, failure tends to take place by the occurrence of the much more frequent lower loads. The curves for the probability distribution of the failing load have a well defined "knee" which marks the transition from failures of structures with low static strength properties (according to the Weibull distribution of relative strength which has a lower limit at  $x = 0.82$ ) to structures with low fatigue strength and hence larger crack lengths at any given life.

With the corresponding curves in figure 11, for all structures with initial cracks of a 0.010-inch depth, this knee does not occur. In this case, at any particular life, all structures have substantial cracks and the extent of these is largely independent of the fatigue strength so that the probability distribution of static strength is the controlling factor for all values of failing load.

## THE EFFECT OF INSPECTION

The effect of inspection on the risk of failure and probability of survival for initially uncracked structures is shown in figures 12 and 13. Although it is not usually a feasible procedure in practice, continuous inspection has an important basic significance which warrants some consideration here.

The risk function for continuous inspection slowly approaches an upper limiting value when there is no repair and replacement of structures in which cracks are detected ("inspection without replacement"). This situation arises because as the initial cracks are propagated by fatigue to the detectable length these structures are eliminated by inspection and a stage is therefore reached where the increase in risk due to the extension of fatigue cracks is offset by the continual removal from service of structures with detectable cracks and high risk of failure.

In the more practical case where structures are repaired and returned to service after detection of cracks ("inspection with replacement") the risk function goes through a maximum value and then eventually approaches zero. The explanation of this behaviour appears to be that, as fatigue cracks extend, the number of cracked structures replaced by sound structures increases until a stage is reached where this counteracts and then

outweighs the increasing risk of static fracture by fatigue in the dwindling members of the original fleet.

With this model therefore the original fleet is eventually replaced by new structures which are taken to be free of any fatigue weakness and the risk of fatigue failure decreases to zero. If the service life were to be prolonged to this stage, however, other areas of the structure would become fatigue critical and their risk of failure would have to be considered.

In practice, cracked structures or components are often replaced by new members from the same population as the structures or components in the original fleet. This model of the fatigue process ("inspection with renewal") would show a behaviour intermediate between the two procedures considered above.

The risk functions for continuous inspection of structures with initial cracks are presented in figures 7 and 9 and these show a similar behaviour to that found with initially uncracked structures although for the case of a continuous distribution of initial crack size in figure 9 the peak of the "inspection with replacement" curve is much flatter because of the wider range of crack sizes that results.

Turning now to the practical case of periodic inspections designed to limit the risk of failure below a specified value  $r_{\max}$ , it can be seen from figures 12, 7, and 9 that in all cases the risk of failure fluctuates between the risk for continuous inspection and the specified maximum value  $r_{\max}$ .

For inspection with replacement it can be seen that because of the peak in the curve for the risk function with continuous inspection, the inspection intervals for limited risk at first decrease with each inspection and then increase.

This effect is clearly shown for the three cases considered by the inspection intervals given in table I which also lists the expected fraction of the fleet in which cracks will be detected at each inspection.

The curves showing the corresponding survivorship functions for inspection with limited risk are shown in figures 13, 8, and 10, and it is apparent that inspection for limited risk can give a comparable performance to the ideal case of continuous inspection. At the cost of decreasing the inspection intervals, the probability of survival can be increased by reducing the maximum allowable risk  $r_{\max}$ , although this must always exceed the maximum risk for continuous inspection for the inspection procedure with limited risk to be possible.



## APPLICATION

The reliability approach to structural design has received increasing attention in recent years and it is proposed here that the safety against fatigue of aircraft structures is one of the most important and promising fields of application.

### DEVELOPMENT OF THE RELIABILITY APPROACH TO FATIGUE

Early work on the probabilistic approach to fatigue of aircraft structures was mainly concerned with efforts to establish the fail-safe philosophy on a more quantitative basis by considering the probability of failure of the structure during the crack propagation stage.

One of the first papers on this subject was concerned with the fail-safe operation of transport aircraft (ref. 7), and a similar approach was used subsequently (refs. 8 and 9) in efforts to develop a proposal for ensuring the airworthiness of fail-safe structures.

In references 10 and 11 reliability analysis was applied to derive the probability of failure for a fail-safe structure by using a sophisticated model to represent the effect of multiple redundancies in the structure.

Probably influenced by the successful application of reliability techniques to electronic systems, the reliability approach to structural safety in general received increasing attention and several papers dealing with the basic development of the philosophy (refs. 12 to 15) also dealt at some length with its application to the fatigue of structures.

The reliability approach to structural design has received increasing attention more recently and papers (some relating to the aspect of fatigue) have been represented at a number of International Conferences (refs. 16 to 24).

However, a major difficulty in applying reliability theory to the fatigue of structures is the extensive amount of data required since this is not normally available. The present paper seeks to overcome this difficulty by presenting an approach which allows representative data to be used in conjunction with the full utilisation of the information which can be obtained from the full-scale tests now widely adopted in aircraft design practice.

### RELIABILITY ANALYSIS WITH FULL-SCALE TESTING

The method proposed in this paper calculates the probability of failure of a structure at each stage of the life with data obtained from full-scale tests on the actual structure in conjunction with other representative data. It therefore estimates the risk of failure in

the fleet, and hence the probability of failure (or survival) up to any required life, taking account of the flight loads to be encountered, the progressive reduction in strength due to the growing fatigue crack, and the variability in static and fatigue strength.

The inspection or replacement of structures in service can then be planned to achieve a prescribed safety level using basic data from the fatigue test without requiring any arbitrary decision as to the crack length that constitutes failure or as to whether a structure is "fail safe" or not.

#### Application of the Method

With the risk function having been calculated, the life  $n_I$  to reach the allowable risk  $r_{\max}(n_I)$  is determined as the life for inspection or replacement.

From the physical nature of the failure as revealed by the fatigue test and the risk function for continuous inspection with the detectable crack length, a judgement can be made whether to rely on inspection or on replacement.

If replacement is decided on all structures are replaced at  $n_I$  and the process can be repeated with the constant inspection interval  $n_I$  until the probability of survival has been reduced to the minimum allowable value.

If inspection is adopted the inspection intervals are calculated as described in the section "Inspection for Limited Risk" and the process is continued up to the life  $n_S$  at which the probability of survival has been reduced to the minimum allowable value. The fraction of defective structures that can be expected to be revealed at each inspection can be calculated from equation (39). Also the probability distribution of the failing load can be calculated and used to estimate the average value of the failing load at the life for any inspection, from which an indication of the average crack length can be obtained.

It is clear from figures 13 and 10 that the safe operating life can be greatly extended by this type of inspection procedure and therefore as the service life continues other fatigue-prone areas of the structure revealed in the fatigue test may need to be included in the analysis in the same way.

#### Basic Assumptions

The following basic assumptions are involved:

(a) The service load  $S$  is independent of the failing load of the structure  $R$ . This assumption infers that any increase in flexibility of the structure as a fatigue crack extends does not affect its response to the applied loads.

(b) There is no correlation between the residual strength of a cracked structure and its fatigue strength. This is supported by the fact that in a complex structure static



ultimate load failure usually occurs in a different area and by a different mechanism to fatigue failure.

(c) The relative residual strength  $x = \frac{R(l)}{\mu_R(l)}$  of structures cracked to some crack length  $l$  has a characteristic probability distribution which applies for any value of  $l$ . For the monolithic structure considered in the section on page 289, the fracture mechanics relationship  $R(l) = K\sqrt{\frac{2}{\pi l}}$  is assumed to apply. It can be shown from this that  $R(l)$  has the same probability distribution as the fracture toughness  $K$  and it is therefore the same for all crack lengths.

(d) The distribution of fatigue life  $N_{l,z}$  at a given crack length  $l$  has a log normal distribution. The log normal distribution is often used in making safe-life estimates and it has been supported as a good approximation by comprehensive surveys of fatigue test data (refs. 25 and 26).

(e) At all points on the crack propagation curve of any structure, the fatigue life  $N_{l,z}$  bears a constant ratio to the median life  $\tilde{N}_l$  at the same crack length  $\frac{N_{l,z}}{\tilde{N}_l} = z$ . It can be shown that this follows from the properties of the log normal distribution of fatigue life assumed in assumption (d).

(f) As structures fail by fatigue and are thus eliminated from the population there is no change in shape of the probability density functions of fatigue life  $z$ , relative strength  $x$ , or initial crack length  $l_c$ . In practice some distortion of these functions will occur but for the small probabilities of failure considered it is regarded as a reasonable assumption.

#### Input Data

The following data are required:

(a) The service load spectrum  $F_S(s)$  which can usually be estimated from the considerable body of flight load data available.

(b) The mean value of the ultimate failing load  $\mu_0$  which can usually be obtained from the results of static strength tests on the structure.

(c) The probability distribution of relative strength  $x = \frac{R(l)}{\mu_R(l)}$  which must be estimated from representative data (as was done for the case of the high-strength steel structure by using data from high-tensile steel specimens) and the results from component testing during the design stage.

(d) The median crack propagation curve for the structure  $\tilde{l}_n = g(\tilde{n}_l)$ ; it is proposed to rely on the crack propagation curve obtained in the full-scale fatigue test of the structure.

### CONCLUDING REMARKS

From a reliability analysis of the fatigue failure in aircraft structures under service loading conditions it is concluded that the current procedures for obtaining safety are not entirely adequate. These methods do not take full account of the probability of failure of the structure during the period in which it is being progressively weakened by the growing fatigue crack and they are therefore subject to inaccuracies which may be significant depending on the structural design parameters and the service conditions.

It is also concluded that a reliability approach to the safety in fatigue of aircraft structures must be considered, using the results available from the structural tests and design analysis in conjunction with other representative data.

Such an approach is quite feasible although an extensive body of data and a number of assumptions are involved which warrant some development and testing of the procedure in practice.

However, the reliability approach has major potential advantages by enabling the safety of both safe-life and fail-safe structures to be determined on a quantitative basis, including the planning of efficient inspection procedures and allowance for the possibility of initial flaws in the material where appropriate.

### ACKNOWLEDGEMENT

The authors wish to acknowledge the efforts of their colleagues in Structures Division of Aeronautical Research Laboratories who have assisted with the preparation of material for this paper.



## APPENDIX

### TABULATION OF RISKS OF FAILURE AND PROBABILITY OF CRACK DETECTION

For simplicity the risk functions in the body of the paper have been expressed in terms of the dimensionless variate  $z$  and they have been compared on a common basis in the various figures using the dimensionless variate  $N_S/\tilde{N}_1$ . However, in this appendix they are expressed in a form more suitable for practical application, the risk of failure per hour using the relation:

$$r(N_S) dN_S = r(z) dz$$

$$r(N_S) = r(z) \frac{dz}{dN_S}$$

where  $N_S$  is the service life in hours.

If the risk of failure were to be required in units other than hours – such as load applications, for example – the dimensional variable  $N_S$  (or for cracked structures  $H_S$ ) would have to be expressed in those units.

The footnotes for this appendix are included at the end of the appendix.

#### STRUCTURES WITH NO INITIAL CRACKS

##### No Inspection

Risk with safe-life analysis. – Risk of failure per hour at  $N_S$  hours, based on an estimated mean life  $\tilde{N}_L$  determined from a fatigue test as the life to some crack length  $L$  at which failure occurred, is given by

$$r_L(N_S) = \frac{\frac{1}{\tilde{N}_L} p_z\left(\frac{n_S}{\tilde{n}_L}\right)}{\int_{n_S/\tilde{n}_L}^{\infty} p_z(z) dz} \quad (A1)$$

where  $\tilde{N}_L$  is the estimated mean life to the crack length  $L$  expressed in hours.

Risk of fatigue fracture<sup>a</sup>. – Risk of failure per hour by fatigue fracture at a life of  $N_S$  hours can be given by

$$r_F(N_S) = \frac{\frac{1}{\tilde{N}_F} p_Z\left(\frac{n_S}{\tilde{n}_F}\right)}{\int_{n_S/\tilde{n}_F}^{\infty} p_Z(z) dz} \quad (A2)$$

where  $\tilde{N}_F$  is the median of the life in hours to complete collapse under the mean load.

Risk of static fracture due to fatigue. - Risk of failure per hour by static fracture due to fatigue at a life of  $N_S$  hours is given by

$$r_S(N_S) = \int_{x=0}^{x=\infty} \int_{z=n_S/\tilde{n}_F}^{z=n_S} F_S\left\{x\mu_0\phi\left(g\left[\frac{n_S}{z}\right]\right)\right\} p(z) p(x) dz dx \quad (A3)$$

where  $F_S(s)$  denotes here the probability of exceeding a service load  $s$  per hour of operation<sup>b</sup>.

Probability distribution of the failing load. -

$$\begin{aligned} & \Pr\left\{\text{At life } N_S \text{ hours that the loads causing}\right. \\ & \quad \left.\text{static fracture due to fatigue} \leq \mu_0 x_0\right\} \\ &= \int_{x=n_S/\tilde{n}_F}^{z=n_S} \int_{x=0}^{x=x_0} \frac{\phi\left\{g\left[\frac{n_S}{z}\right]\right\} F_S\left\{x\mu_0\phi\left(g\left[\frac{n_S}{z}\right]\right)\right\} p(x) p(z) dx dz}{r_S(N_S)} \end{aligned} \quad (A4)$$

where  $r_S(N_S)$  is given by equation (A3), and  $F_S(s)$  is taken as the probability of exceeding a service load  $s$  per hour of operation<sup>b</sup>.

Periodic Inspection at  $N_{I(1)}, N_{I(2)}, \dots, N_{I(m)}$  Hours

Risk of fatigue fracture with replacement<sup>c d</sup>. - Risk of failure per hour by fatigue fracture at a life of  $N_S$  hours with structures repaired and returned to service after cracks have been detected is given by

$$\begin{aligned} r_F^*(N_S; l_D, N_{I(m)}) &= \frac{1}{\tilde{N}_F} p_Z\left(\frac{n_S}{\tilde{n}_F}\right) & \left(N_S > N_{I(m)} \frac{\tilde{n}_F}{\tilde{n}_D}\right) \\ &= 0 & \text{(Otherwise)} \end{aligned}$$



where  $\tilde{N}_F$  is the median of the life in hours to complete collapse of structures under the mean load.

Note: For continuous inspection the risk of fatigue fracture is zero in this case.

Risk of static fracture due to fatigue with replacement <sup>c</sup>. - Risk of failure per hour by static fracture due to fatigue at a life of  $N_S$  hours with structures repaired and returned to service after cracks have been detected is given by

$$r_I^*(N_S; l_D, N_{I(m)}) = \int_{z=N_{I(m)}/\tilde{n}_D}^{z=N_S} \int_{x=0}^{x=\infty} F_S \left\{ x \mu_0 \phi \left( g \left[ \frac{n_S}{z} \right] \right) \right\} p(x) p(z) dx dz \quad (A5)$$

where  $F_S(s)$  denotes here the probability of exceeding a service load  $s$  per hour of operation<sup>b</sup>.

Note: For continuous inspection substitute  $N_S$  for  $N_{I(m)}$  and  $n_S$  for  $n_{I(m)}$ .

Probability of detecting cracked structures with replacement <sup>c</sup>. - Probability of detection at the  $m$ th inspection with structures repaired and returned to service after cracks have been detected is given by

$$\begin{aligned} r_D^*(N_{I(m)}; l_D, N_{I(m-1)}) &= \int_{n_{I(m-1)}/\tilde{n}_D}^{n_{I(m)}/\tilde{n}_D} p(z) dz - \Pr \left\{ \text{Fatigue fracture between } N_{I(m-1)} \text{ and } N_{I(m)} \right\} \\ &= \int_{n_{I(m-1)}/\tilde{n}_D}^{n_{I(m)}/\tilde{n}_D} p(z) dz \end{aligned}$$

Since it follows that where an inspection procedure is feasible, the probability of fatigue fracture is relatively insignificant compared to the probability of crack detection.

Note: For continuous inspection the probability of detection per hour at any life  $N_S$  hours is given by

$$r_D^*(N_S; l_D, N_S) = \frac{1}{\tilde{N}_D} p_Z \left( \frac{n_S}{\tilde{n}_D} \right)$$

where  $\tilde{N}_D$  is the median of the life in hours to the detectable crack length  $l_D$ .

Probability distribution of the failing load with replacement.-

$$\begin{aligned} & \Pr \left\{ \text{At life of } N_S \text{ hours following } m\text{th inspection, the loads} \right. \\ & \quad \left. \text{causing static fracture due to fatigue} \leq \mu_0 x_0 \right\} \\ &= \int_{z=n_{I(m)}/\tilde{n}_D}^{z=n_S} \int_{x=0}^{x=x_0} \frac{1}{\phi \left\{ g \left[ \frac{n_S}{z} \right] \right\}} \frac{F_S \left\{ x \mu_0 \phi \left( g \left[ \frac{n_S}{z} \right] \right) \right\} p(x) p(z) dx dz}{r_I^*(N_S; l_D, N_{I(m)})} \end{aligned} \quad (A6)$$

where  $r_I^*(N_S; l_D, N_{I(m)})$  is given by equation (A5), and  $F_S(s)$  is taken as the probability of exceeding a service load  $s$  per hour of operation<sup>b</sup>.

Note: For continuous inspection substitute  $N_S$  for  $N_{I(m)}$  and  $n_S$  for  $n_{I(m)}$ .

STRUCTURES WITH INITIAL CRACKS (PROBABILITY DENSITY  
OF CRACK LENGTHS  $p(l_c)$ )

No Inspection

Risk of fatigue fracture<sup>a</sup>. - Risk of failure per hour by fatigue fracture at a service life of  $H_S$  hours is given by

$$r_F(H_S | p(l_c)) = \frac{\int_{\tilde{n}_c=1}^{\tilde{n}_c=\tilde{n}_0} \frac{1}{\tilde{N}_F - \tilde{N}_c} p_z \left\{ \frac{h_S}{\tilde{n}_F - \tilde{n}_c} \right\} p(\tilde{n}_c) d\tilde{n}_c}{\int_{\tilde{n}_c=1}^{\tilde{n}_c=\tilde{n}_0} \int_{z=h_S/(\tilde{n}_F - \tilde{n}_c)}^{z=\infty} p(z) p(\tilde{n}_c) dz d\tilde{n}_c} \quad (A7)$$

where  $\tilde{N}_F$  is the median of the life in hours to complete collapse of initially uncracked structures under the mean load, and  $\tilde{N}_c$  is the median of the life in hours to produce a crack of length  $l_c$  for initially uncracked structures.

Risk of static fracture due to fatigue. - Risk of failure per hour by static fracture due to fatigue after a service life of  $H_S$  hours is given by

$$r_S(H_S | p(l_c)) = \int_{\tilde{n}_c=1}^{\tilde{n}_c=\tilde{n}_0} \int_{x=0}^{x=\infty} \int_{z=h_S/(\tilde{n}_F - \tilde{n}_c)}^{z=\infty} F_S \left\{ x \mu_0 \phi \left( g \left[ \frac{h}{z} + \tilde{n}_c \right] \right) \right\} p(z) p(x) p(\tilde{n}_c) dz dx d\tilde{n}_c \quad (A8)$$

where  $F_S(s)$  denotes here the probability of exceeding a service load  $s$  per hour of operation<sup>b</sup>.



Probability distribution of the failing load.-

$$\Pr \left\{ \text{At service life } H_s \text{ hours that the loads causing} \right. \\ \left. \text{static fracture due to fatigue } \leq \mu_0 x_0 \right\} \\ = \frac{\int_{\tilde{n}_c=1}^{\tilde{n}_c=\tilde{n}_0} \int_{z=h_s/(\tilde{n}_F-\tilde{n}_c)}^{z=\infty} \int_{x=0}^{x=x_0/\phi\left(\frac{h_s}{z}+\tilde{n}_c\right)} F_s\left\{x\mu_0\phi\left(\frac{h_s}{z}+\tilde{n}_c\right)\right\} p(x) p(z) p(\tilde{n}_c) dx dz d\tilde{n}_c}{r_s(H_s | p(l_c))} \quad (A9)$$

where  $r_s(H_s | p(l_c))$  is given by equation (A8), and  $F_s(s)$  is taken as the probability of exceeding a service load  $s$  per hour of operation<sup>b</sup>.

Periodic Inspection at  $H_{I(1)}, H_{I(2)}, \dots, H_{I(m)}$  Hours

Risk of fatigue fracture with replacement<sup>e d</sup>.- Risk of failure per hour by fatigue fracture after a service life of  $H_s$  hours with structures repaired and returned to service after cracks have been detected is given by

$$r_F^*(H_s | p(l_c); l_D, H_{I(m)}) = \int_{\tilde{n}_c=1}^{\tilde{n}_c=(h_s \tilde{n}_D - h_{I(m)} \tilde{n}_F) / (h_s - h_{I(m)})} \frac{1}{\tilde{n}_F - \tilde{n}_c} p_z\left(\frac{h_s}{\tilde{n}_F - \tilde{n}_c}\right) p(\tilde{n}_c) d\tilde{n}_c \quad \left(H_s > H_{I(m)} \frac{\tilde{n}_F - 1}{\tilde{n}_D - 1}\right) \\ = 0 \quad (\text{Otherwise})$$

where  $\tilde{n}_F$  is the median of the life in hours to complete collapse of uncracked structures under the mean load, and  $\tilde{n}_c$  is the median of the life in hours to produce a crack of length  $l_c$  for initially uncracked structures.

Risk of static fracture due to fatigue with replacement<sup>e</sup>.- Risk of failure per hour by static fracture due to fatigue after a service life of  $H_s$  hours with structures repaired and returned to service after cracks have been detected is given by

$$r_I^*(H_s | p(l_c); l_D, H_{I(m)}) = \int_{\tilde{n}_c=1}^{\tilde{n}_c=\tilde{n}_0} \int_{x=0}^{x=\infty} \int_{z=h_{I(m)}/(\tilde{n}_D-\tilde{n}_c)}^{z=\infty} F_s\left\{x\mu_0\phi\left(\frac{h_s}{z}+\tilde{n}_c\right)\right\} p(z) p(x) p(\tilde{n}_c) dz dx d\tilde{n}_c \quad (A10)$$

where  $F_s(s)$  denotes here the probability of exceeding a service load  $s$  per hour of operation<sup>b</sup>.

Note: For continuous inspection substitute  $H_s$  for  $H_{I(m)}$  and  $h_s$  for  $h_{I(m)}$ .

Probability of detecting cracked structures with replacement<sup>e</sup>.- Probability of detecting cracked structures at the  $m$ th inspection with structures repaired and returned to service after cracks have been detected is given by

$$r_D^*(H_{I(m)} | p(l_c); l_D, H_{I(m-1)}) = \int_{\tilde{n}_c=1}^{\tilde{n}_c=\tilde{n}_0} \int_{z=h_{I(m-1)}}^{z=h_{I(m)}} \frac{p(z) p(\tilde{n}_c)}{(\tilde{n}_D - \tilde{n}_c)} dz d\tilde{n}_c - \Pr \left\{ \text{Fatigue fracture between } H_{I(m-1)} \text{ and } H_{I(m)} \right\}$$

$$= \int_{\tilde{n}_c=1}^{\tilde{n}_c=\tilde{n}_0} \int_{z=h_{I(m-1)}}^{z=h_{I(m)}} \frac{p(z) p(\tilde{n}_c)}{(\tilde{n}_D - \tilde{n}_c)} dz d\tilde{n}_c$$

Since it follows that when an inspection procedure is feasible the probability of fatigue fracture is relatively insignificant compared to the probability of crack detection.

Note: For continuous inspection the probability of detection per hour at any service life  $H_S$  is given by

$$r_D^*(H_S | p(l_c); l_D, H_S) = \int_{\tilde{n}_c=1}^{\tilde{n}_c=\tilde{n}_0} \frac{1}{\tilde{N}_D - \tilde{N}_c} p_Z \left( \frac{h_S}{\tilde{N}_D - \tilde{n}_c} \right) p(\tilde{n}_c) d\tilde{n}_c$$

where  $\tilde{N}_D$  and  $\tilde{N}_c$  are the median values of the lives in hours to produce crack lengths of  $l_D$  and  $l_c$ , respectively, in initially uncracked structures.

#### Probability distribution of the failing load with replacement.

$$\Pr \left\{ \text{At a service life } H_S \text{ hours following the } m\text{th inspection} \right. \\ \left. \text{that the loads causing static fracture due to fatigue } \leq \mu_0 x_0 \right\}$$

$$= \frac{\int_{\tilde{n}_c=1}^{\tilde{n}_c=\tilde{n}_0} \int_{z=h_{I(m)}}^{z=\infty} \int_{x=0}^{x=x_0} \frac{\phi \left[ g \left( \frac{n_S}{z} + \tilde{n}_c \right) \right]}{(\tilde{n}_D - \tilde{n}_c)} F_S \left\{ x \mu_0 \phi \left( g \left[ \frac{n_S}{z} + \tilde{n}_c \right] \right) \right\} p(x) p(z) p(\tilde{n}_c) dx dz d\tilde{n}_c}{r_I^*(H_S | p(l_c); l_D, H_{I(m)})}$$

where  $r_I^*(H_S | p(l_c); l_D, H_{I(m)})$  is given by equation (A10), and  $F_S(s)$  is taken as the probability of exceeding a service load  $s$  per hour of operation<sup>b</sup>.

<sup>a</sup>The term in the denominator of this expression is a normalising factor resulting from the truncation of the  $z$  distribution by the removal from the population of the structures that fail by fatigue fracture. However, it is very close to unity for the probabilities of survival that are acceptable in practice.

<sup>b</sup>In the body of the paper where  $r_S(n_S)$  has been compared with other risk functions using the dimensionless variate  $N_S/\tilde{N}_i$ ,  $F_S(s)$  has been taken as the probability of exceeding a service load  $s$  in a time interval  $\tilde{N}_i$ .

<sup>c</sup>When there is no replacement of those structures in the fleet in which cracks have been detected, the corresponding probabilities and risk functions are obtained by dividing by the normalising factor  $\int_{n_{I(m)}}^{\infty} \frac{p(z)}{\tilde{n}_D} dz$ . For continuous inspection,  $n_{I(m)}$  is replaced by  $n_S$ .

<sup>d</sup>When an inspection procedure is applied, the effect on the risk function resulting from truncation of the  $z$  distribution, by elimination of structures that fail by fatigue fracture, is so small that it has been neglected here.

<sup>e</sup>When there is no replacement of those structures in the fleet in which cracks have been detected the corresponding probabilities and risk functions are obtained by dividing by the factor

$$\int_{\tilde{n}_c=1}^{\tilde{n}_c=\tilde{n}_0} \int_{z=h_{I(m)}}^{z=\infty} \frac{p(z) p(\tilde{n}_c)}{(\tilde{n}_D - \tilde{n}_c)} dz d\tilde{n}_c$$

For continuous inspection  $h_{I(m)}$  is replaced by  $h_S$ .



## REFERENCES

1. Payne, A. O.: Determination of the Fatigue Resistance of Aircraft Wings by Full Scale Testing. Proceedings of Symposium on Full-Scale Fatigue Testing of Aircraft Structures, F. J. Plantema and J. Schijve, eds., Pergamon Press, 1961, pp. 76-132.
2. Raithby, K. D.: A Comparison of Predicted and Achieved Fatigue Lives of Aircraft Structures. Proceedings of Symposium on Fatigue of Aircraft Structures, W. Barrois and E. L. Ripley, eds., Pergamon Press, 1963, pp. 249-261.
3. Lyman, Taylor, ed.: Metals Handbook. Vol. 1.- Properties and Selection of Metals. 8th ed., Amer. Soc. Metals, c.1961, pp. 87-94.
4. Mayer, John P.; and Hamer, Harold A.: Applications of Power Spectral Analysis Methods To Maneuver Loads Obtained on Jet Fighter Airplanes During Service Operations. NASA TN D-902, 1961.
5. Tolefson, H. B.: Summary of Derived Gust Velocities Obtained From Measurements Within Thunderstorms. NACA Rep. 1285, 1956. (Supersedes NACA TN 3538.)
6. Mallinson, G. D.; and Graham, A. D.: A Multiple Integration Technique for the Numerical Evaluation of Probability Integrals. S.M. Rep., Aeronaut. Res. Lab. (Melbourne). (To be published)
7. Shaw, R. R.: The Level of Safety Achieved by Periodic Inspection for Fatigue Cracks. J. Roy. Aeronaut. Soc., vol. 58, no. 526, Oct. 1954, pp. 720-723.
8. Ferrari, R. M.; Milligan, I. S.; Rice, M. R.; and Weston, N. R.: Some Considerations Relating to the Safety of Fail-Safe Wing Structures. Proceedings of Symposium on Full-Scale Fatigue Testing of Aircraft Structures, F. J. Plantema and J. Schijve, eds., Pergamon Press, 1961, pp. 413-526.
9. Lundberg, B. K. O.; and Eggwertz, S. (With appendix by L. vonSydow): A Statistical Method for Fail-Safe Design with Respect to Aircraft Fatigue. Proceedings of the Second Congress of the International Council of the Aeronautical Sciences, Pergamon Press, 1960.
10. Eggwertz, S.; and Lindsjo, G.: Analysis of the Probability of Collapse of a Fail-Safe Aircraft Structure Consisting of Parallel Elements. FFA Rep. HU-961, Aeronaut. Res. Inst. of Sweden, 1963.
11. Heller, R. A.; and Heller, A. S.: A Probabilistic Approach to Cumulative Fatigue Damage in Redundant Structures. Rep. No. 17 (Contract No. NONR 266-91), Inst. for Study of Fatigue and Reliability, Columbia Univ., 1965.

12. Freudenthal, A. M.: Safety and Probability of Structural Failure. Proc. Amer. Soc. Civil Eng., vol. 80, no. 468, Aug. 1954, pp. 468-1 - 468-46.
13. Freudenthal, A. M.; and Shinozuka, M.: Structural Safety Under Conditions of Ultimate Load Failure and Fatigue. WADD Tech. Rep. No. 61-177, U.S. Air Force, 1961.
14. Freudenthal, A. M.; and Payne, A. O.: The Structural Reliability of Airframes. AFML-TR-64-401, U.S. Air Force, 1964.
15. Pugsley, A.: The Safety of Structures. Edward Arnold Ltd. (London), 1966.
16. Freudenthal, A. M.: Reliability Analysis Based on Time to the First Failure. Aircraft Fatigue - Design, Operational, and Economic Aspects, Programme of 5th ICAF Symposium (Melbourne), J. Y. Mann and I. McMillan, eds., May 1967.
17. Black, H. C.: Safety Reliability and Airworthiness. Proceedings of International Conference on Structural Safety and Reliability, Smithsonian Institute, Apr. 1969.
18. Butler, J. P.: Reliability Analysis and Fatigue Performance Estimation of Transport Type Aircraft. Proceedings of International Conference on Structural Safety and Reliability, Smithsonian Institute, Apr. 1969.
19. Cornell, C. A.: Structural Safety Specifications Based on Second-Moment Reliability Analysis. Proceedings of IABSE Symposium on "Concepts of Safety and Methods of Design" (London), 1969.
20. Ang, A. H. S.: Critical Analysis of Reliability Principles Relative to Design. Paper presented at International Conference on Applications of Statistics and Probability to Soil and Structural Engineering (Hong Kong), Sept. 1971.
21. Payne, A. O.; and Grandage, J. M.: A Probabilistic Approach to Structural Design. Paper presented at International Conference on Applications of Statistics and Probability to Soil and Structural Engineering (Hong Kong), Sept. 1971.
22. Cornell, C. A.: The Future of Probabilistic Design. Paper presented at Australian Institution of Engineers Symposium on Reliability and Risk in Structural Design (Melbourne), 1971.
23. Payne, A. O.: Fully Probabilistic Design. Paper presented at Australian Institution of Engineers Symposium on Reliability and Risk in Structural Design (Melbourne), 1971.
24. Itagaki, H.; and Shinozuka, M.: Application of Monte Carlo Technique to Fatigue Failure Analysis under Random Loading. Technical Report No. 16 (NSF-GK3858 and 24925), Columbia Univ., July 1971. (Also presented at the Symposium on Probabilistic Aspects of Fatigue, 74th Annual Meeting of ASTM (Atlantic City), 1971.)



25. Impellizeri, L. F.: Development of a Scatter Factor Applicable to Aircraft Fatigue Life. Spec. Tech. Publ. No. 404, Amer. Soc. Testing Mater., 1966, pp. 136-156.
26. Ford, D. G.; Graff, D. G.; and Payne, A. O.: Some Statistical Aspects of Fatigue Life Variation. Proceedings of Symposium on Fatigue of Aircraft Structures, W. Barrois and E. L. Ripley, eds., Pergamon Press, 1963, pp. 179-208.

TABLE I  
INSPECTION INTERVALS AND DETECTION RATES WITH INSPECTION FOR LIMITED RISK

Inspection number, m	Uncracked structures, $a_c = 0.0$ , $r_{\max} = 0.025$			Structures with initial cracks, $a_c = a_o = 0.010$ in., $r_{\max} = 0.05$			Structures with distribution of initial cracks, $p(l_c) = 2.22e^{-20.61c}$ , $r_{\max} = 0.05$		
	$n_{I(m)}$	$N_{I(m)}$ , hr	$r_D(n_{I(m)})$	$n_{I(m)}$	$N_{I(m)}$ , hr	$r_D(n_{I(m)})$	$n_{I(m)}$	$N_{I(m)}$ , hr	$r_D(n_{I(m)})$
1	1.44	2880	0.0005	0.17	340	0.030	0.30	600	0.018
2	1.86	3520	.0055	.19	380	.032	.42	840	.055
3				.22	440	.076	.54	1080	.052
4				.23	460	.032	.67	1340	.057
5				.26	520	.111	.80	1600	.046
6				.29	580	.122			
7				.32	640	.120			
8				.39	780	.224			
9				.51	1020	.185			
10				.73	1460	.063			

- $\tilde{N}_i$  median of life to initial failure, 2000 hr  
 $N_{I(m)}$  life in hours to mth inspection  
 $n_{I(m)}$  relative life to mth inspection,  $N_{I(m)}/\tilde{N}_i$   
 $r_D(n_{I(m)})$  probability of detectable cracks at mth inspection  
 $a_o$  depth of smallest crack detectable during production  
 $a_c$  depth of initial crack in any structure  
 $l$  relative crack length (or depth),  $a/a_F$



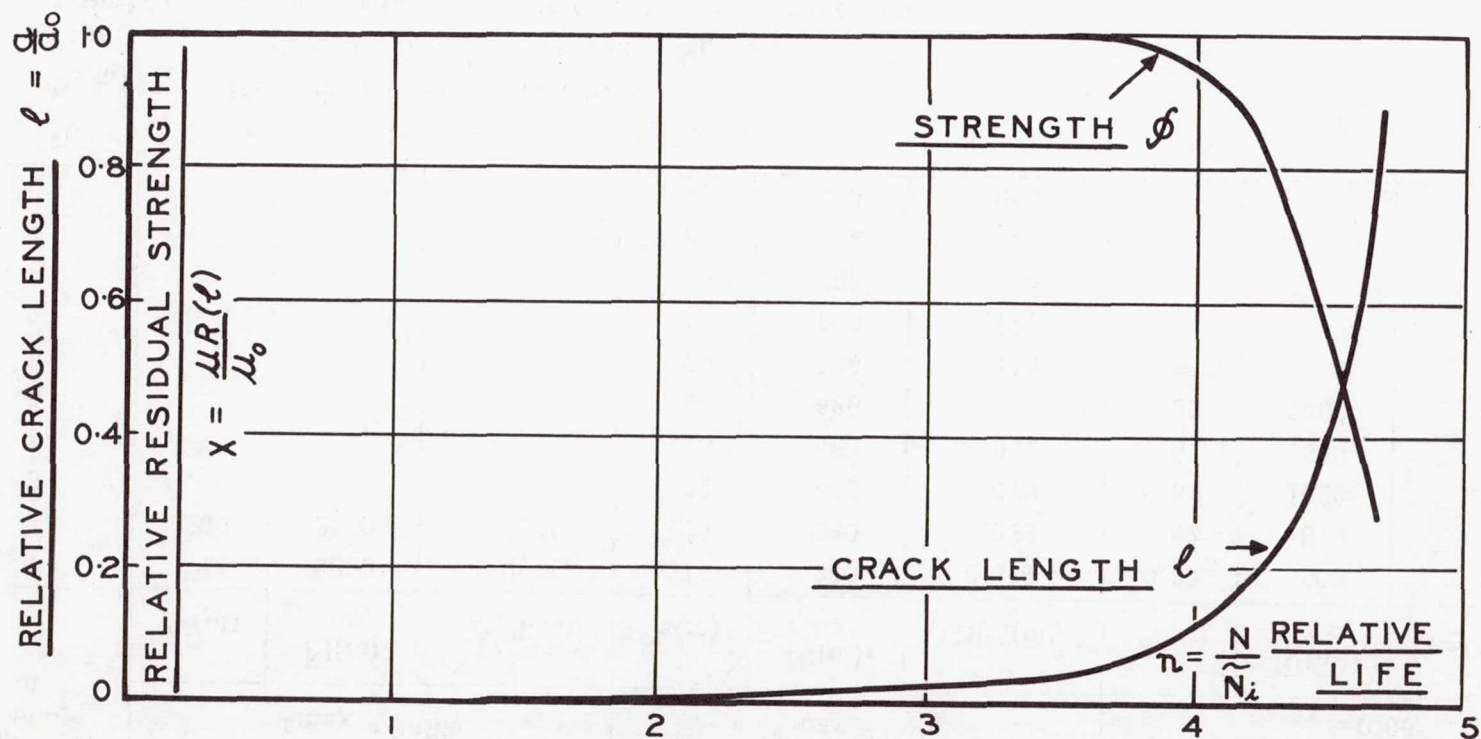


Figure 1.- Fatigue characteristics of high-tensile steel structure.

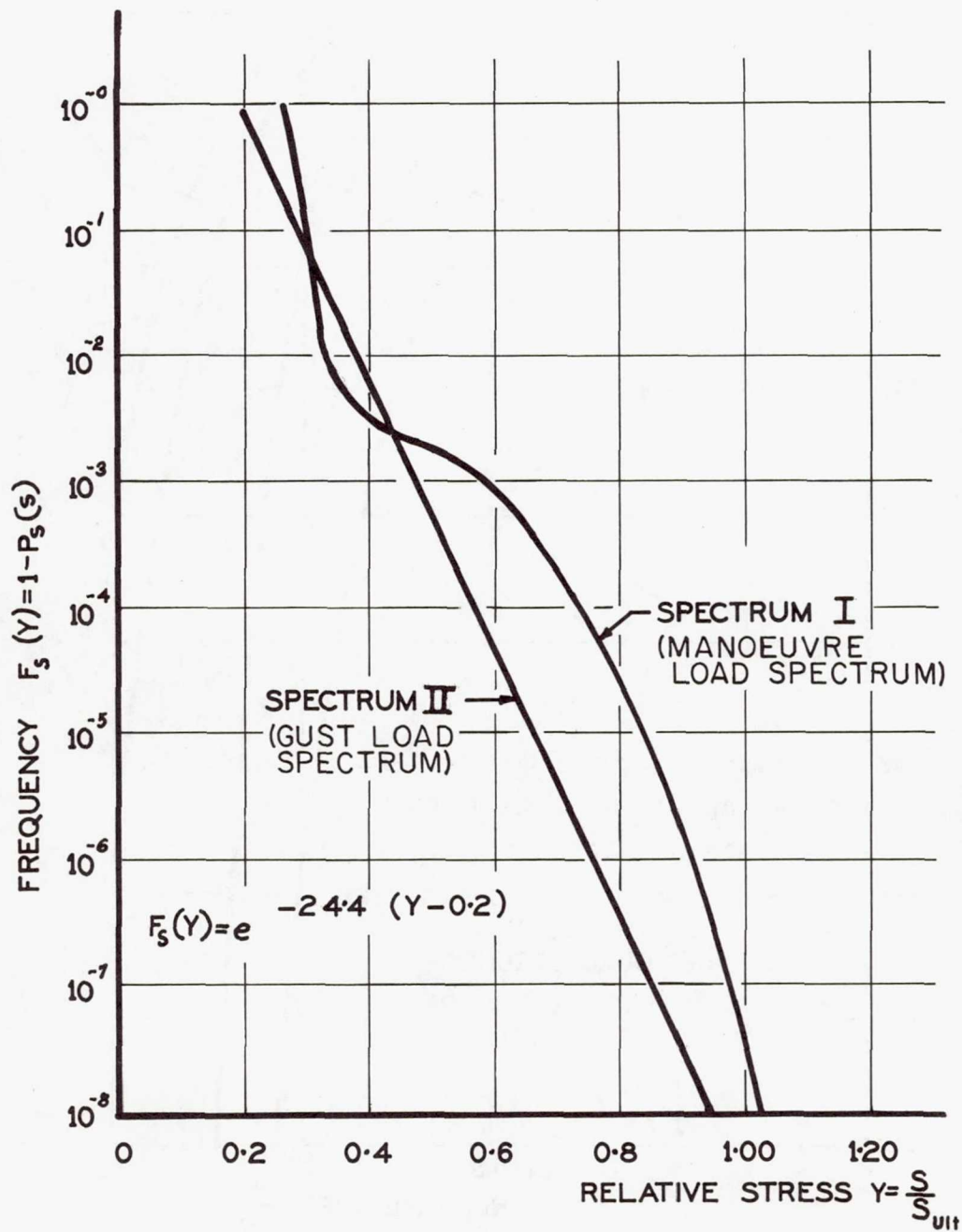


Figure 2.- Load spectra.



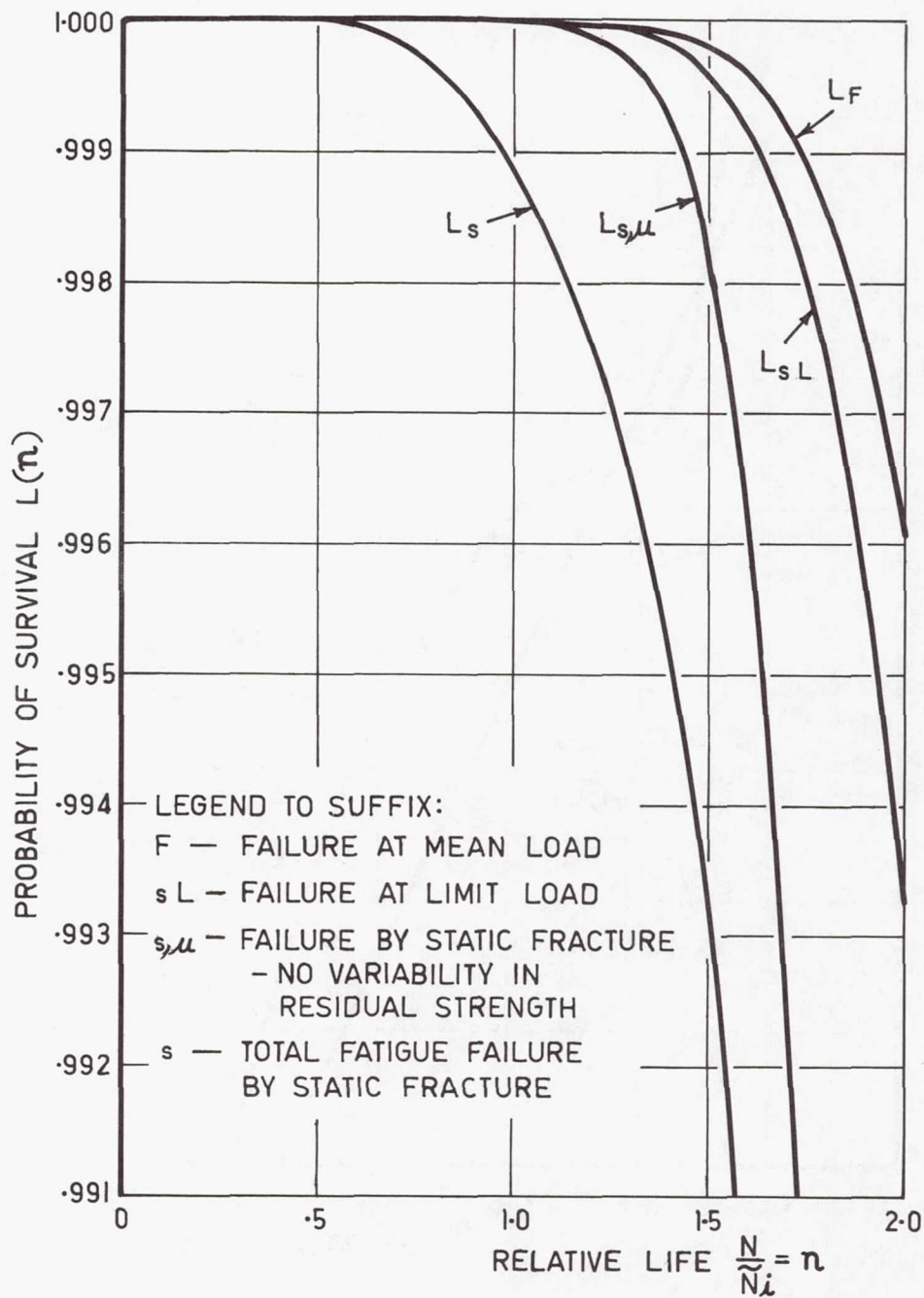


Figure 3.- Probability of survival for spectrum I.

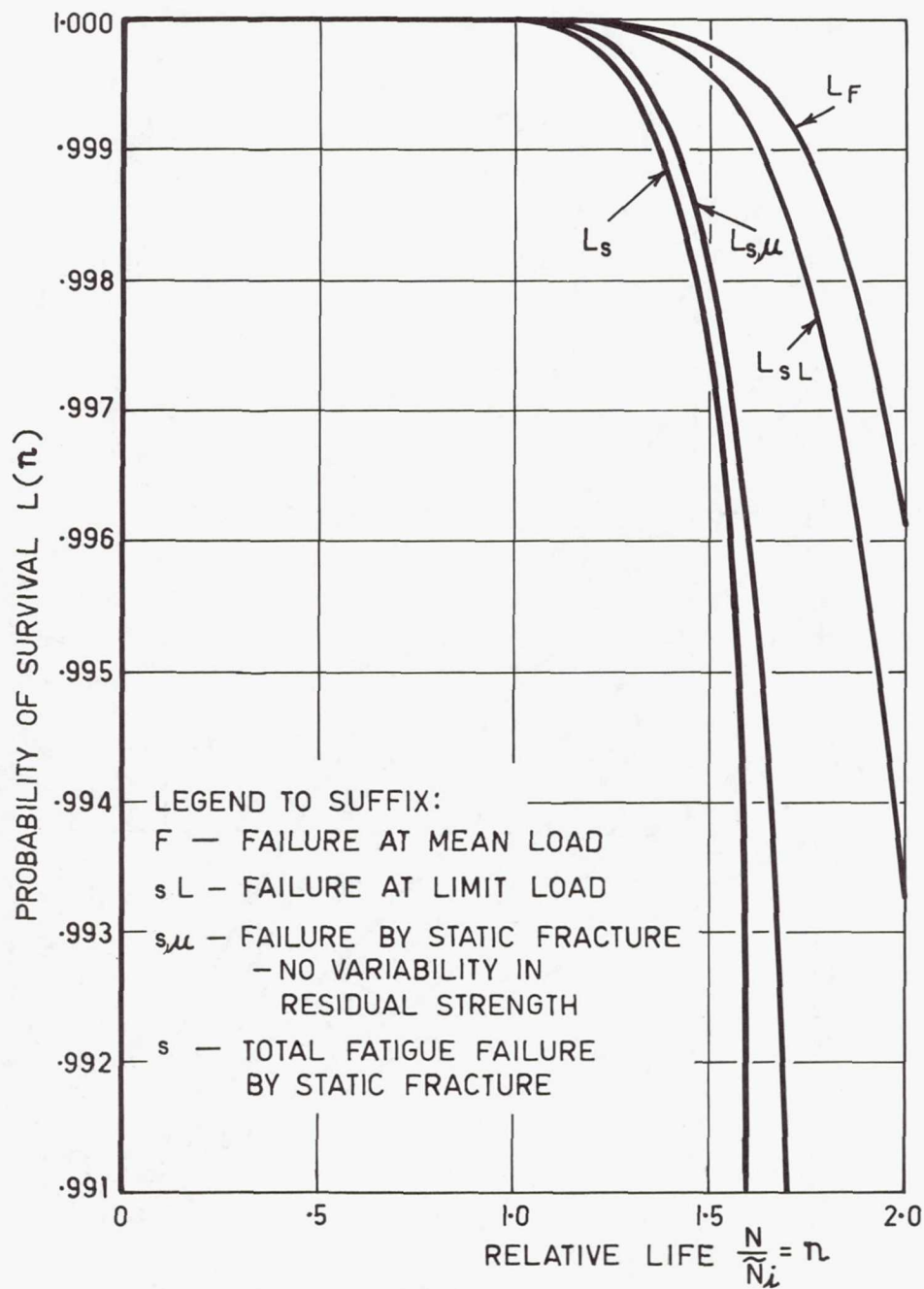


Figure 4.- Probability of survival for spectrum II.



Figure 5.- Calculation of risk of failure due to fatigue.

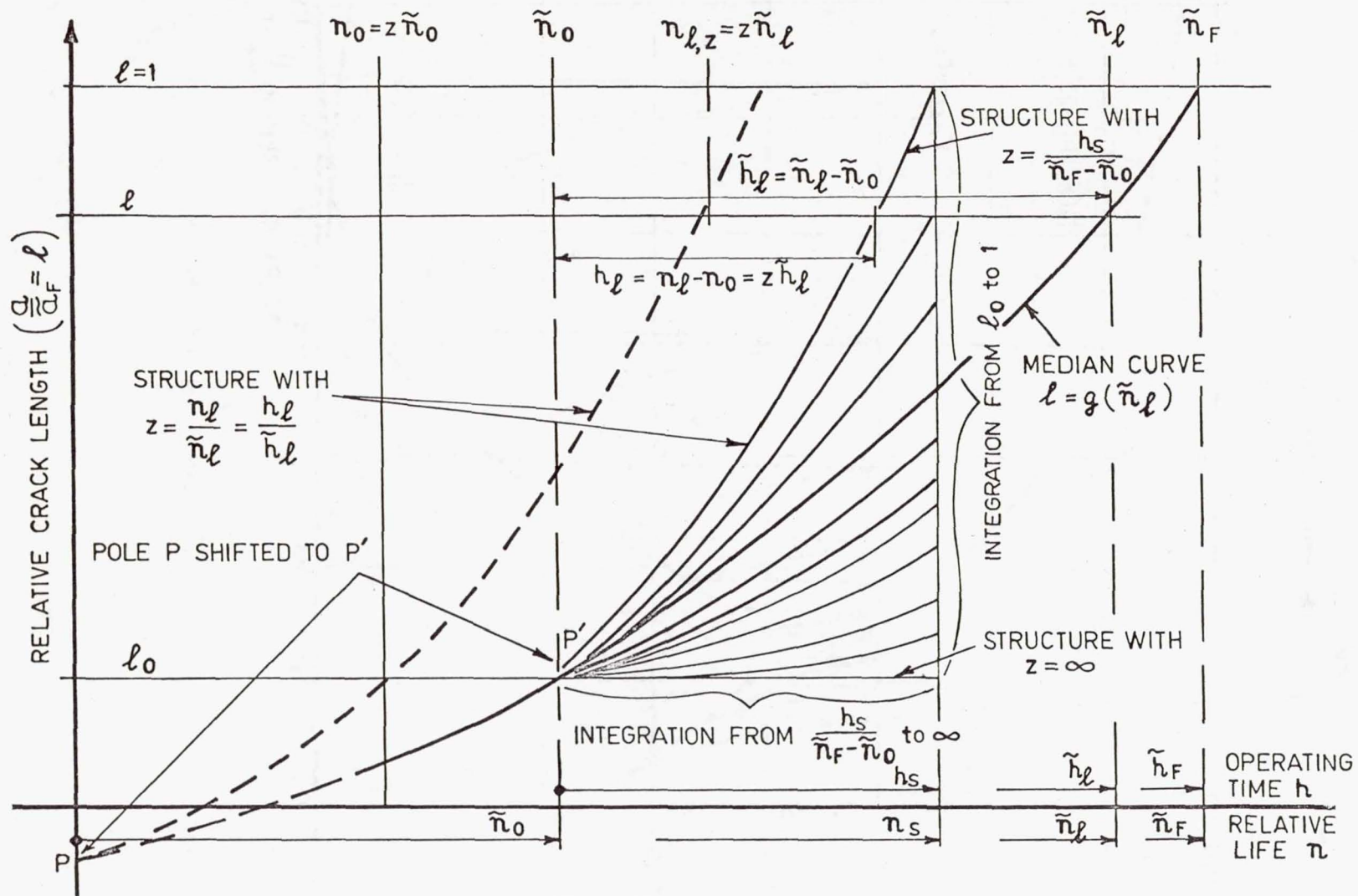


Figure 6.- Risk of fatigue failure in initially cracked structures.



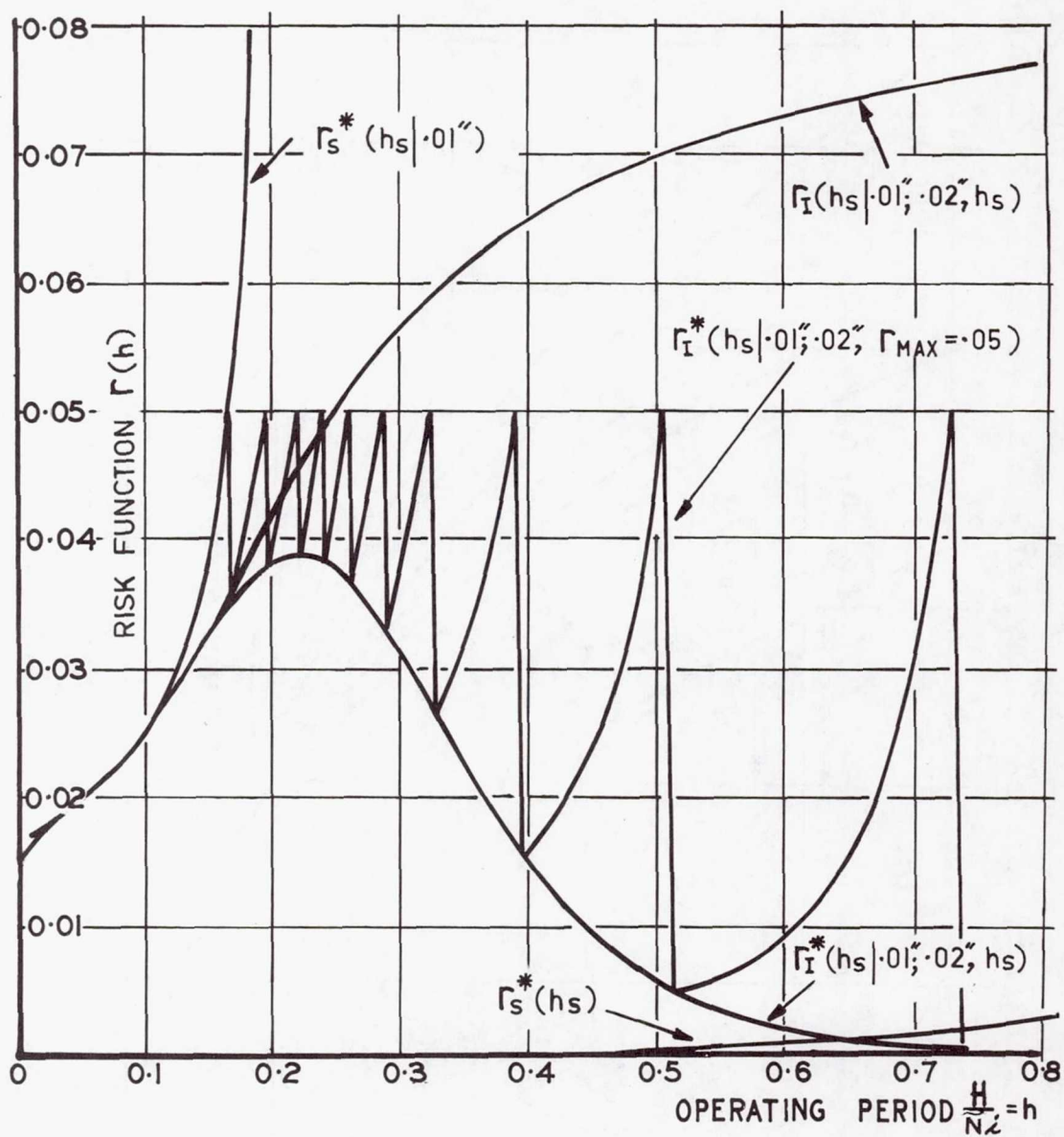


Figure 7.- Risk function for structures with initial crack depth  $a_0 = 0.01$  in. for various inspection procedures.

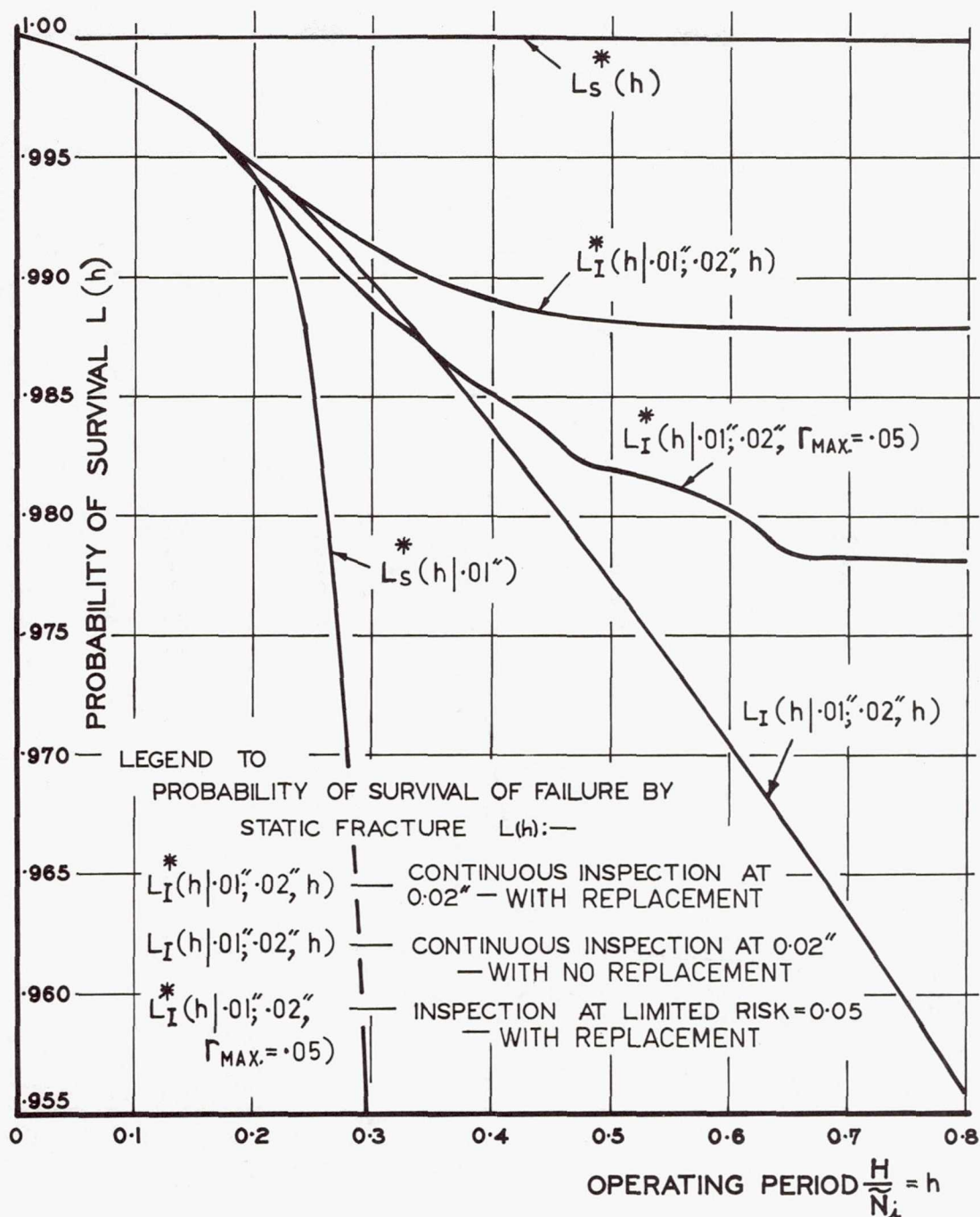


Figure 8.- Probability of survival of structures with initial crack depth  $a_0 = 0.01$  in. for various inspection procedures.



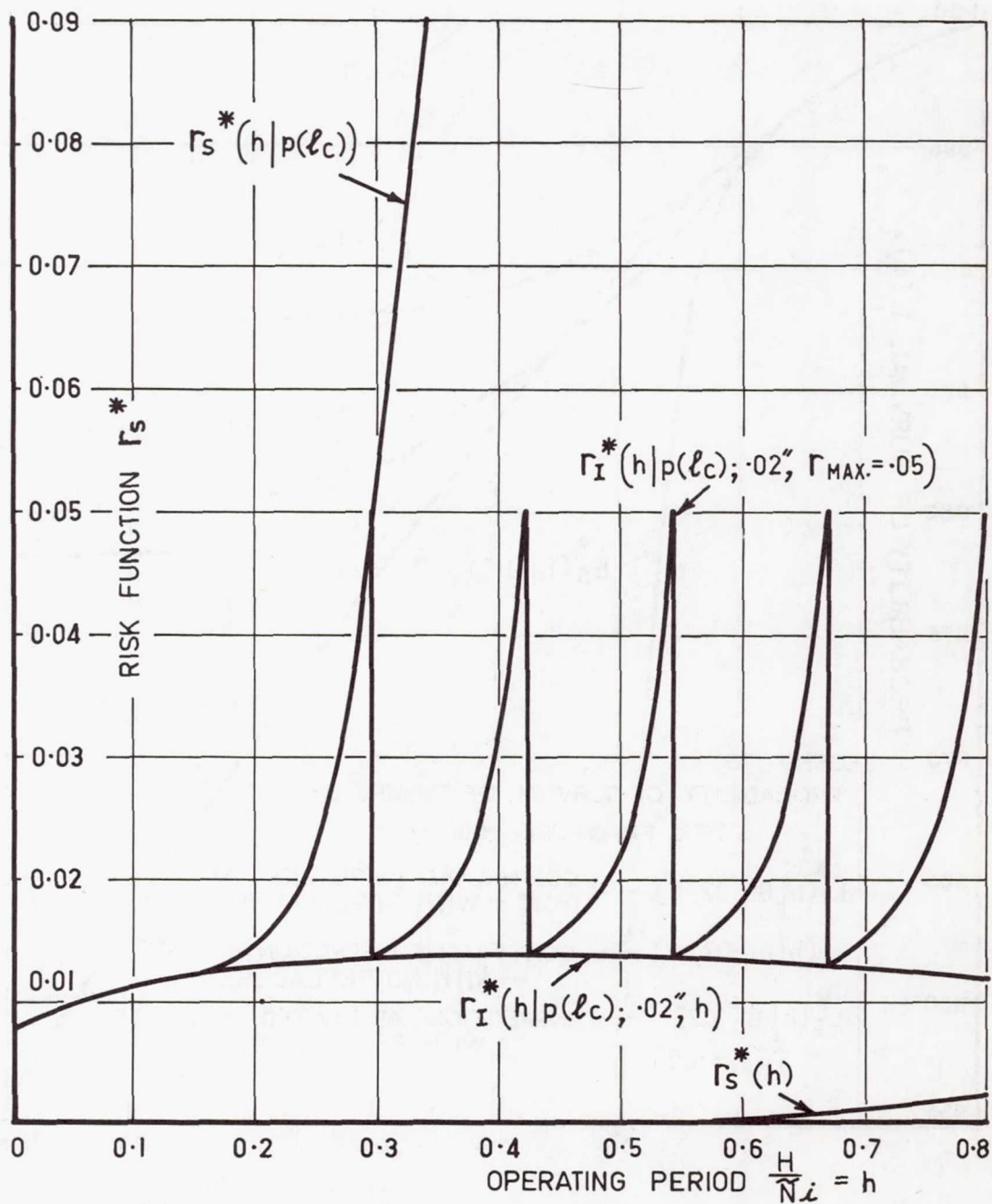


Figure 9.- Risk function for structures with variable initial crack depth  $l_c$  for various inspection procedures.

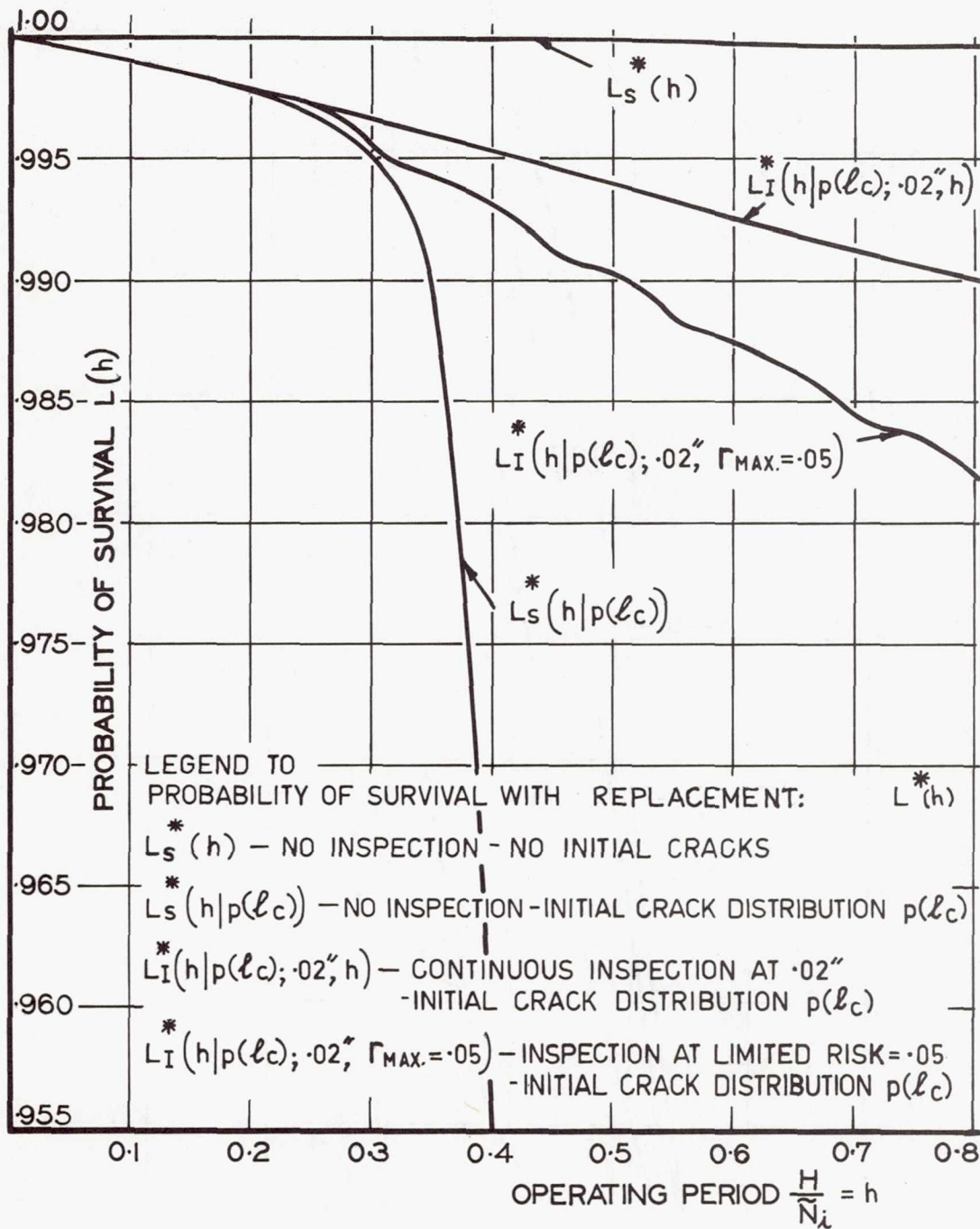


Figure 10.- Probability of survival of structures with variable initial crack depth  $l_c$  for various inspection procedures.



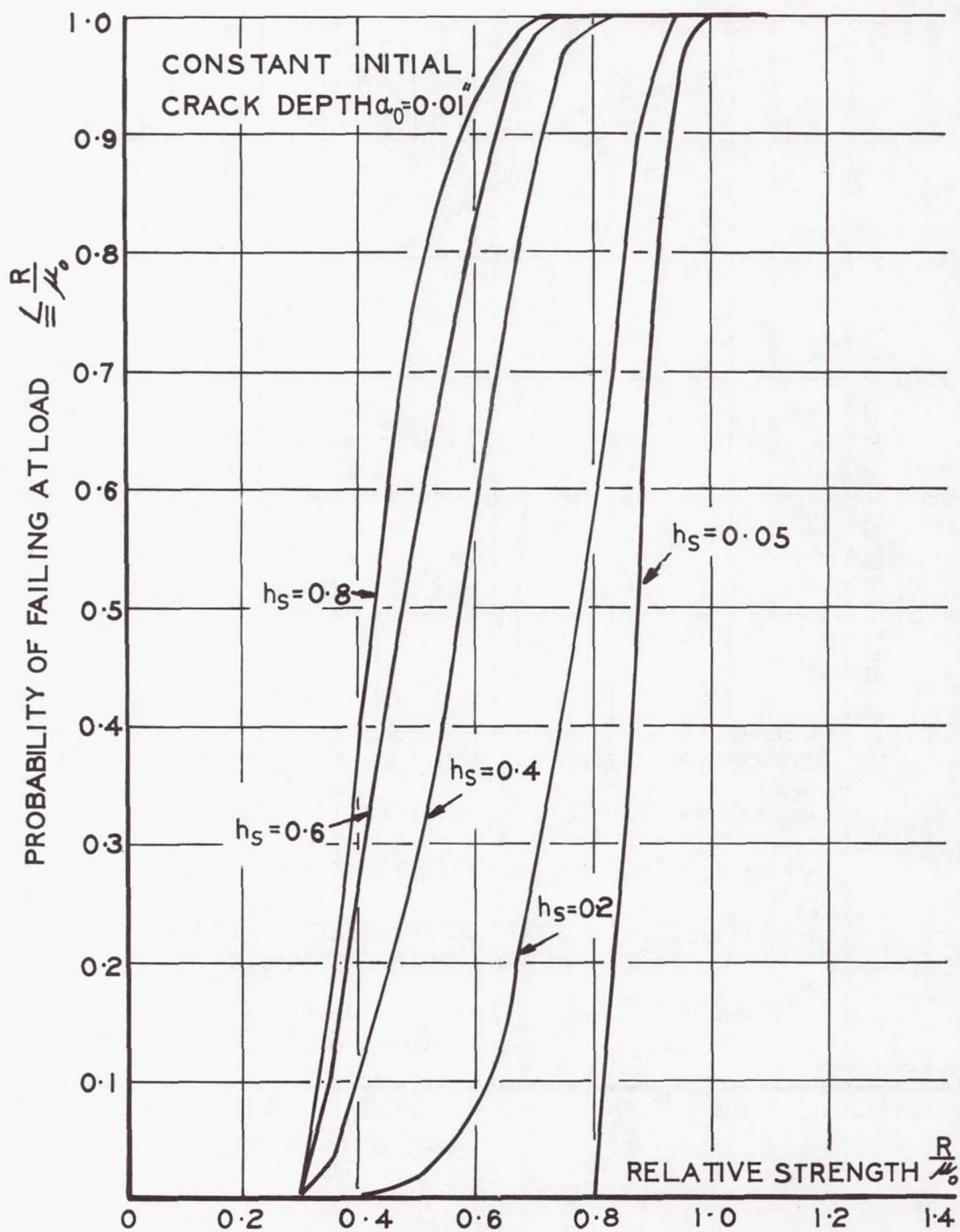


Figure 11.- Probability distribution of the failing load with spectrum I. Cracked structures.

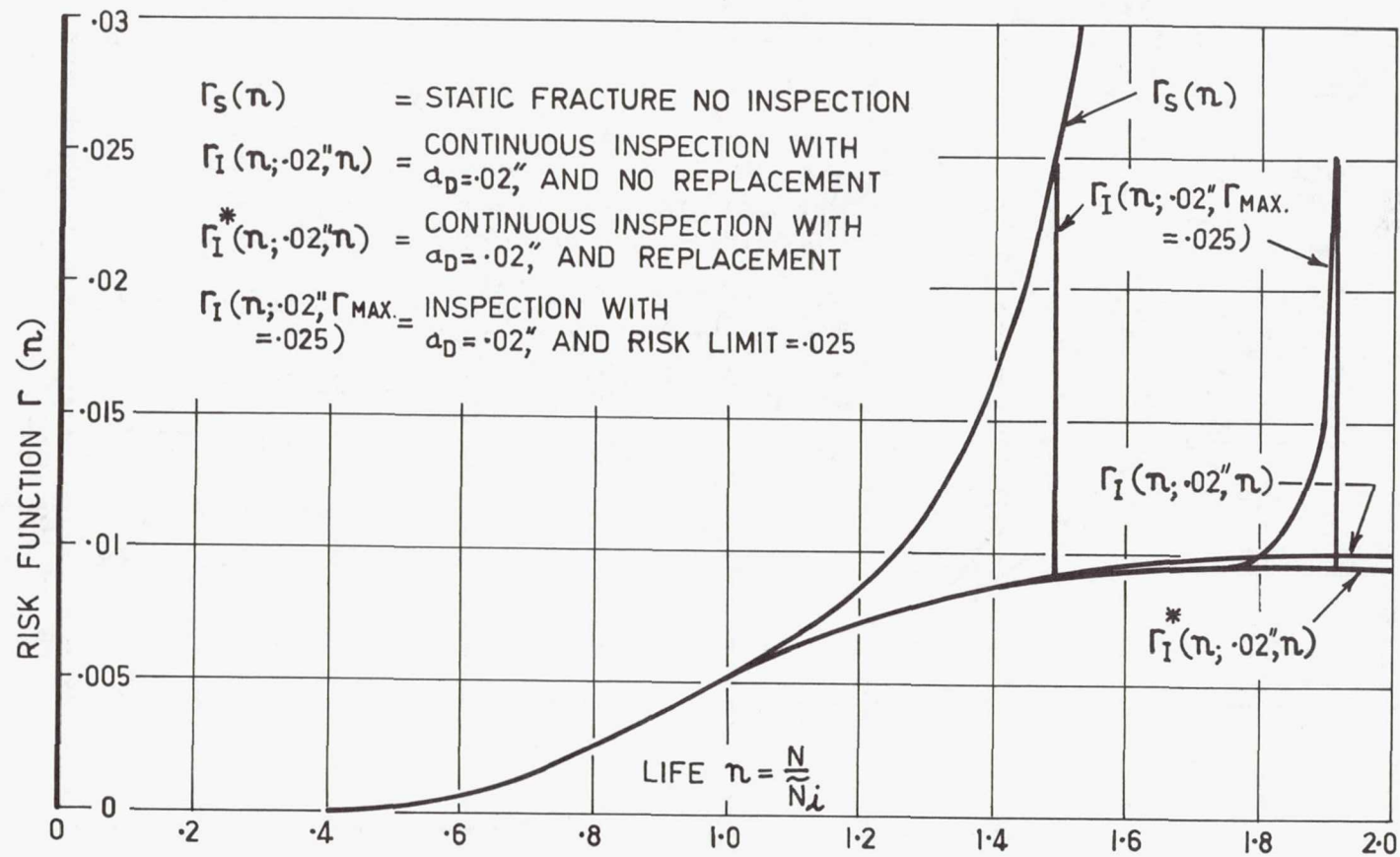


Figure 12.- Risk functions for structures without initial cracks for various inspection procedures.



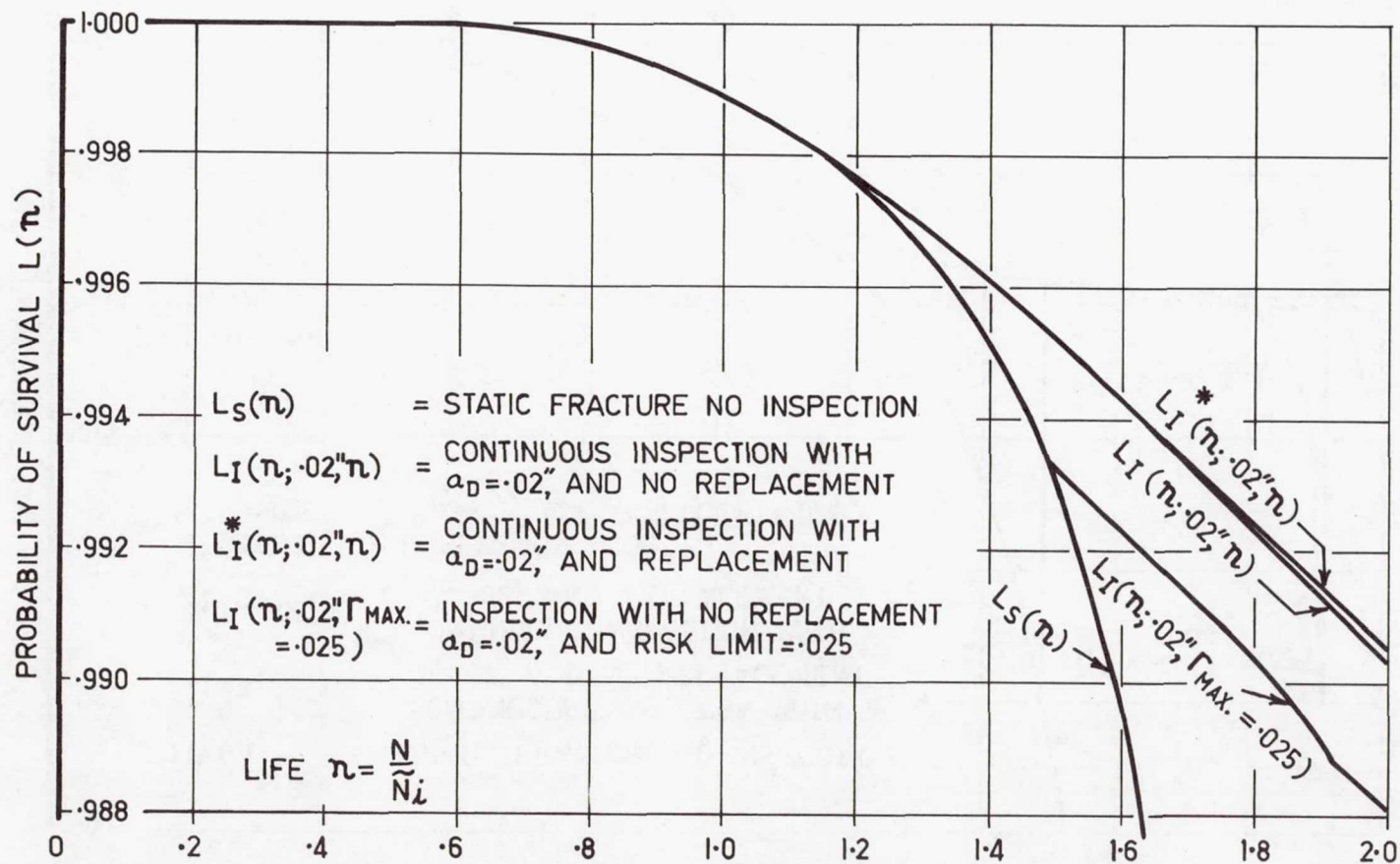


Figure 13.- Survivorship functions for structures without initial cracks for various inspection procedures.

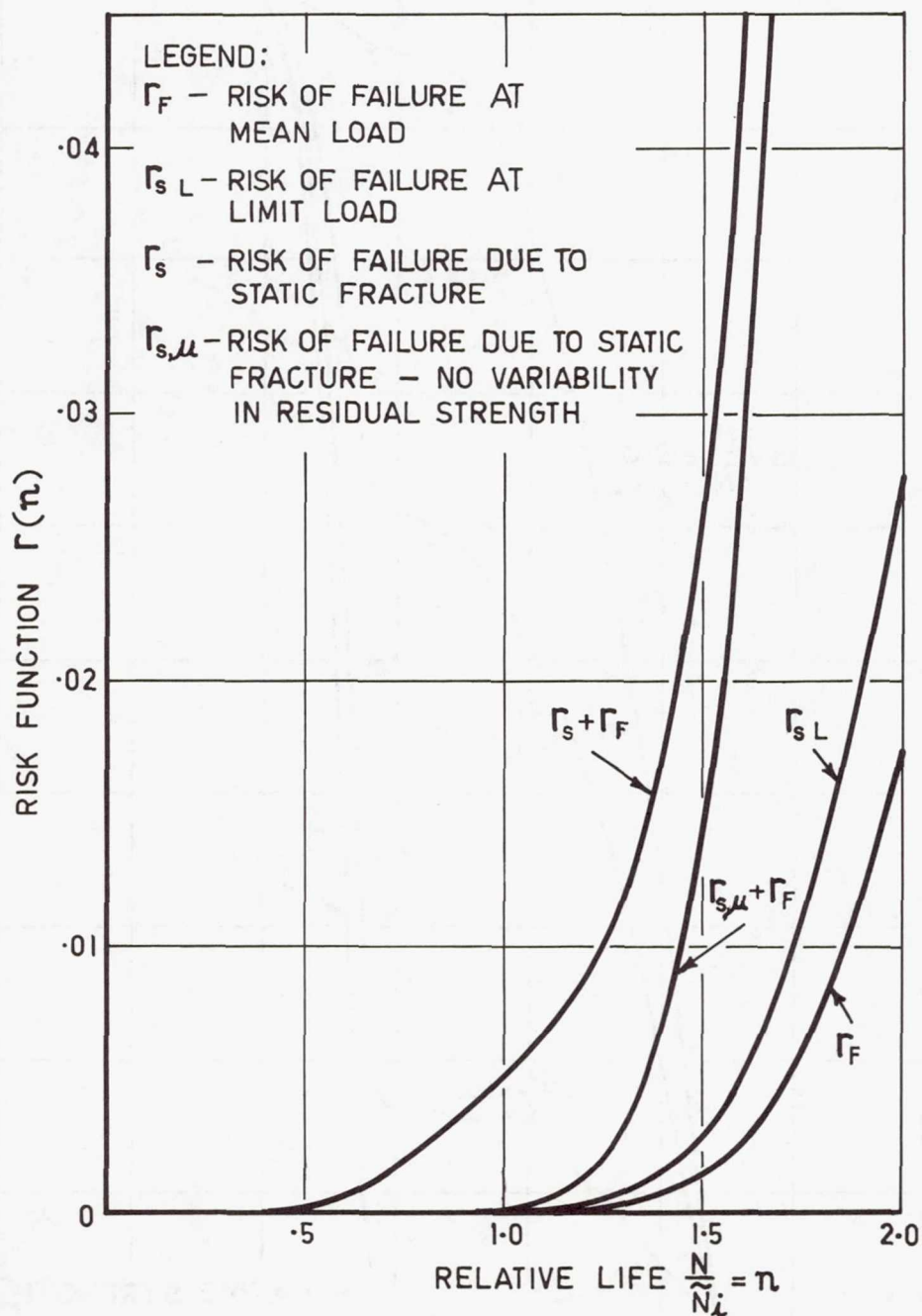


Figure 14.- Risk of failure for spectrum I.



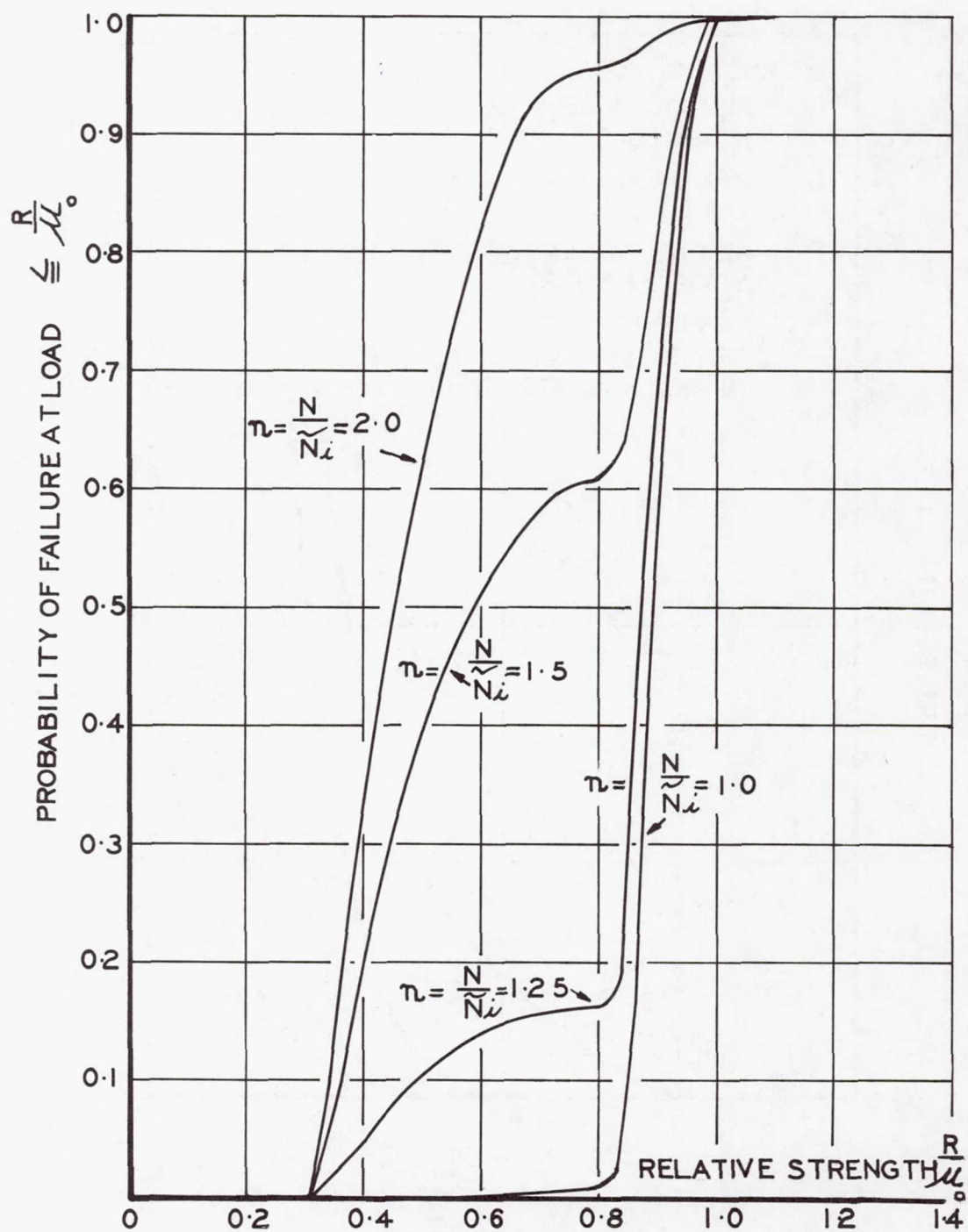


Figure 15.- Probability distribution of failing load with spectrum I. Uncracked structures.

## FATIGUE OF COMPOSITES\*

By Michael J. Salkind

Sikorsky Aircraft Division, United Aircraft Corporation, United States

## INTRODUCTION

During the past decade, the extensive development activity in composite structures has indicated the promise of substantial improvements in the performance of aerospace systems. This experience, however, has shown that composite materials are substantially different from our former materials of construction, and new concepts in analysis, design, fabrication, quality assurance, and even systems management will be necessary.

A major difference between composites and metals exists in their respective behavior in a fatigue environment. Whereas metals usually fail by crack initiation and growth in a manner which has come to be predictable through fracture mechanics analysis, composites exhibit several modes of damage including delamination, matrix crazing, fiber failure, void growth, matrix cracking, and composite cracking. A particular structure may exhibit any or all these damage modes, and it is difficult to predict, a priori, which mode will dominate and cause failure. The selection of fiber and matrix can produce predictable fiber or matrix-dominated failure in simple unidirectional specimens. (See refs. 1 to 4.) In real structures, however, the complex multidirectional loadings and complex reaction of nonsimple laminates precludes easy prediction of failure modes. Also, joints and attachments in composite structures generally result in failure modes which are peculiar to a particular design.

A characteristic of composite materials which differs substantially from metals is the relative difference between low- and high-cycle fatigue behavior. Whereas most metals behave according to the so-called Coffin-Manson relationship (refs. 5 to 7) in low-cycle fatigue, composites have been shown to be more sensitive to strain range (ref. 4). This sensitivity results in the high-cycle fatigue strength of composites being high with respect to static- and low-cycle fatigue strength. Many structures designed for fatigue experience a spectrum of high as well as low stresses, and whereas the more numerous low stresses may be the critical design factor for a metal structure, the same structure made from a composite material may well be critical in low-cycle fatigue.

A problem arises in the design of composite structures for fatigue loading because of the lack of an adequate definition of failure. A large part of the fatigue

---

\*Also published in ASTM STP 497.



data in the literature is based on time to fracture. For high-cycle fatigue, metals are generally structurally adequate to the point of crack initiation (and to some extent beyond that), which is usually a large part of the time to fracture. Although it is preferable to use fatigue data based on crack initiation, the error introduced by designing metal structures using fatigue data based on fracture is usually not significant. Using such an approximation for composites, however, could lead to disastrous results. Composites generally begin to exhibit changes in properties very early in the total life to fracture. Such changes in elastic properties could lead to structural failure long before the structure is in danger of fracturing. Rotating airfoils such as helicopter rotor blades or gas turbine blades are subject to aeroelastic instabilities if the fundamental frequency shifts because of early fatigue damage that causes stiffness changes. A composite spring whose spring constant changes beyond an acceptable value would be considered failed even though it was in no danger of fracturing. The same composite used for a tension cable application for which stiffness is not critical might have an acceptable fatigue life to failure several orders of magnitude higher than the stiffness critical spring under the same loading conditions. A further complication to this problem is the fact that composites are anisotropic, and for any number of cycles, the change in stiffness in one direction may be unrelated to the change in stiffness in a second direction.

The requirement for an adequate failure criterion, coupled with the challenge of providing adequate damage detection schemes for multiple damage modes, clearly indicates the requirement for a new approach to the design of fatigue-critical composite structures. This paper includes a review of the fatigue behavior of composite materials and structures and a proposed approach for design of fatigue-critical components.

## FATIGUE OF COMPOSITE MATERIALS

A large body of small specimen fatigue data has been generated over the past 10 years. These data are primarily for unidirectional laminates and, as mentioned previously, are based upon fracture as the definition of failure. Hence, much of it is of limited value for use in design. A survey of pertinent observations is included in this section.

### Fiber-Reinforced Polymers

The most widely used class of composite materials, glass-fiber-reinforced polymers, has been the subject of extensive fatigue testing (refs. 8 to 23). Although the data in references 8 to 23 are based upon fracture as the failure criterion, they give us an indication of the effect of significant variables, such as resin composition and content and fiber composition and orientation on fatigue. Boller (ref. 11) has evaluated a variety



of matrix systems and found epoxides to be superior in fatigue. His data, seen in figure 1, is more than 15 years old, and improved surface treatments and processing have since been developed; however, the relative ranking remains unchanged (ref. 19). As seen in figure 2, varying the resin content between 20 and 37 percent has a negligible effect on fatigue behavior for  $\pm 5^\circ$  glass-fiber composites. The effect of fiber orientation is rather complex. Although the tensile strength of unidirectional composites is a maximum at  $0^\circ$  to the fibers (ref. 24), in fatigue the unidirectional construction is not optimum, as can be seen in figure 3. The best explanation for this phenomenon is the fact that unidirectional material is subject to splitting and rapid crack propagation in the matrix parallel to the fibers. Fatigue data for  $\pm 5^\circ$ , 67%  $0^\circ$ /33%  $90^\circ$ , and Style 181 satin weave ( $0^\circ$ / $90^\circ$ ) are compared in figure 4. In general, nonwoven materials are superior to woven materials in fatigue. Note also the low notch sensitivity of these materials. A comparison of the behavior of S-glass and E-glass composites (ref. 15) is seen in figure 5. The higher modulus S-glass is consistently stronger in fatigue than E-glass. The effect of mean stress is seen in figure 6 for tension-compression and tension-tension behavior. There have also been some measurements of the compression-compression fatigue behavior in low-cycle fatigue (ref. 20). These data indicate that the effect of mean stress is similar to that for metals, that is, the Goodman diagram is approximately linear.

In recent years, the realization that fracture was not an adequate design criterion for failure has led to studies of failure mechanisms in fatigue which provide a foundation for design. Broutman (ref. 25) studied the mechanisms of failure in glass-fiber-reinforced polymers subjected to fatigue loading. He noted cracks originating at fiber-matrix debonds propagating through the matrix and being deflected by fibers. Recent studies (refs. 26 to 30) have quantitatively described the changes in elastic and strength properties associated with this type of damage. Smith and Owen (ref. 26) evaluated eleven different composite systems with modulus values ranging from  $0.5 \times 10^6$  to  $6.5 \times 10^6$  psi and found that the initial damage debonding occurred at 0.3% strain as seen in figure 7. Thus, the limiting factor in fatigue is not the fiber but the interface or the matrix. As described in the following section, studies with metal matrix composites confirm this behavior. The data seen in figure 8 for chopped-strand mat-reinforced polyester laminates confirm that initial damage occurs at stresses well below those required for fracture. The effect of such damage on structural capability will determine whether the part has failed. Based on the observation of a critical strain, Smith and Owen postulated a critical maximum stress independent of mean stress for any material. As seen in figure 9, this postulation was found to be incorrect (ref. 26).

Cessna et al. (ref. 27) performed constant-deflection flexural fatigue tests on glass-reinforced polypropylene and monitored the load decay (proportional to modulus decay) with cycles as seen in figure 10. They also monitored the temperature rise, as seen in



figure 10, due to viscoelastic energy dissipation, which is common for polymeric composites. (See refs. 31 to 37.) In addition to indicating progressive fatigue damage, the temperature rise also contributes to weakening the material and shortening its fatigue life. As seen in figure 11, by cooling their specimens to maintain isothermal conditions, Cessna et al. (ref. 27) were able to extend both the cycles to onset of stiffness change and the fracture life by an order of magnitude.

Broutman and Sahu (ref. 28) have related the changes in residual tensile strength and modulus to the development of cracks in  $0^0/90^0$  crossplied material as seen in figure 12. Although the decrease in residual strength and primary modulus is expected because of the increasing crack density, the initial increase in secondary modulus remains unexplained. A quantitative relationship between modulus change and crack density (fig. 13) has been developed on the same material. Fujii and Mizukawa (ref. 30) have also determined the change in elastic and strength properties with cycling for laminates consisting of several combinations of roving cloth, chopped mat, and woven cloth.

The higher modulus composite materials, graphite and boron, have exhibited higher fatigue strengths than glass-reinforced polymers, as seen in figure 14 (refs. 15, 38 to 41). This difference is primarily attributed to the higher modulus resulting in less strain in the matrix and interface at the same cyclic stress level. The phenomenon of low fatigue strength at zero mean stress for the high modulus composites as seen in figure 14 was first noted for boron-reinforced aluminum. It is thought to be the result of low transverse strength of unidirectional composites resulting in splitting under cyclic compressive loads. This behavior severely limits the use of unidirectional composites as discussed above.

A major variable which can affect the data obtained in a composite fatigue test is the specimen geometry. This variable is very much a function of the particular laminate orientation being tested, as interlaminar shear can be a primary controlling factor (refs. 42 and 43). Although this problem is negligible for a unidirectional material, it becomes a major factor in fatigue testing of  $\pm 45^0$  laminates. Figure 15 compares the axial tension-tension fatigue behavior (based on fracture) for  $\pm 45^0$  1002 E-glass composites for three different specimen configurations (ref. 43). The straight-sided specimen is flat, and each fiber terminates at the edge, thus, high interlaminar shear stresses are created. The x-type specimen has all fibers continuous from grip to grip; thus, interlaminar shear stresses at the edge are precluded. The latter type has the disadvantage of having a vanishingly small gage length and very uniformly loaded fibers, which are not representative of the types of loading experienced in most structures; thus, the resultant data are considered to be too optimistic for design. The tubular specimen has a uniformly loaded gage section and no fiber edges; thus, interlaminar shear is precluded. It is felt that such a specimen comes closest to yielding representative material properties

for design. Edges are usually handled as a separate factor in design. Although the difference between the straight-sided and tubular specimens is only 5% for glass, it is approximately 50% for boron, as can be seen in figure 16. The reason for this effect is that the interlaminar shear stresses are higher for high modulus materials.

### Fiber-Reinforced Metals

Although fiber-reinforced metals considerably lag reinforced polymers in terms of development and usage, some of the earliest and best fundamental studies of fatigue have been accomplished with metal matrix composites. Forsyth, George, and Ryder (ref. 1) demonstrated that the inclusion of steel wires in an aluminum-alloy sheet reduces the rate of crack propagation substantially (fig. 17), although the improvement in total fatigue life to fracture is small (fig. 18). Baker and Cratchley (refs. 2, 44 to 48) performed extensive studies of the fatigue behavior of silica- and steel-fiber-reinforced aluminum alloys. Although silica-reinforced aluminum did not show promise as a fatigue-resistant material, Baker and Cratchley made important observations concerning failure modes and anelastic behavior. They identified the crack-diverting capability of strong fibers (ref. 2) and made important observations concerning the stress-strain behavior and damping capability of composites as seen in figure 19 (ref. 44). In addition, Baker quantitatively defined the effect of fiber length on fatigue behavior (ref. 46) and evaluated the effects of fiber fatigue behavior and the interface (ref. 47).

Extensive studies have been made of the fatigue behavior of composites made by unidirectional solidification of eutectic alloys (refs. 4, 49 to 52). Because these composites have very regularly distributed fibers and well-bonded interfaces, they serve as excellent systems for studying the mechanical behavior of composites without the variable fabrication effects common to other composites. The Al-Al<sub>3</sub>Ni (10% reinforcing Al<sub>3</sub>Ni whiskers) and the Al-CuAl<sub>2</sub> (50% reinforcing CuAl<sub>2</sub> platelets) composite materials exhibit markedly different fatigue behavior as seen in figure 20. A comparison of the stress-strain behavior of the two materials showing fatigue failure at the same stress amplitude (ref. 49) reveals that Al-CuAl<sub>2</sub> appears to work-harden more rapidly with narrower hysteresis loops than Al-Al<sub>3</sub>Ni. It can be speculated that the wide CuAl<sub>2</sub> platelets are more effective at blocking plastic flow than the Al<sub>3</sub>Ni whiskers (which have a spacing at least an order of magnitude too large for optimum dispersion hardening). In addition, the greater volume fraction of CuAl<sub>2</sub> is more effective at blocking plastic flow in the matrix. If matrix strain is the controlling factor, then the behavior seen in figure 20 would be an expected consequence of the difference in stress-strain behavior.

The fatigue behavior of metals has been found to obey a simple empirical relationship (refs. 5 to 7, 53 and 54)



$$\Delta\epsilon_T = \underbrace{MN^z}_{\text{Plastic}} + \underbrace{\frac{G}{E}N^\gamma}_{\text{Elastic}} \quad (1)$$

where

$\Delta\epsilon_T$       total cyclic strain range

E            elastic modulus

N            number of cycles to failure

M, G, z,  $\gamma$       material constants

This relationship is depicted schematically in figure 21, and it is seen that the plastic component (first term of eq. (1)) dominates at low cycles (high strain amplitudes), and the elastic component dominates at high cycles. Although most metals exhibit values of  $z$  of -0.5 to -0.6 (refs. 53 and 54),  $\text{Al}_3\text{Ni}$  whisker-reinforced aluminum exhibits much lower values as seen in figure 22. It has been proposed (ref. 4) that the low-cycle fatigue behavior is not governed entirely by the plastic behavior of the aluminum ( $z = -0.5$ ) but also by the elastic behavior of the  $\text{Al}_3\text{Ni}$  ( $\gamma < -0.1$ ). This type of behavior would be expected for most composites having fibers which behave elastically in the stress range of use (glass, boron, graphite, highly cold-worked steel) and accounts for the relatively flat S-N (that is, stress  $S$  - number of cycles to failure  $N$ ) curves discussed in the Introduction.

As seen in figure 23, the flexural fatigue behavior of Al- $\text{Al}_3\text{Ni}$  is substantially higher than that for the matrix alone. The mode of failure is matrix cracking, the fibers serving to reduce matrix strain. Testing in a protective atmosphere such as argon results in higher fatigue strength as seen in figure 24, which further verifies the fact that failure is matrix dominated. Although the aluminum is susceptible to attack by moisture in the atmosphere, the  $\text{Al}_3\text{Ni}$  whiskers are not.

The fatigue behavior of boron-reinforced aluminum has been extensively studied (refs. 55 to 59). The very high modulus of the reinforcing fiber keeps the matrix strain low for any given stress level. This factor, coupled with the excellent fatigue resistance of boron fiber itself (ref. 60), provides extremely good fatigue resistance as seen in figure 25. The data by Young and Carlson (ref. 56) is particularly valuable as it records changes in deflection for torsion, tension, and combined-load fatigue testing.

Gates and Wood (ref. 61) performed detailed studies of the microstructural changes which accompanied the torsional fatigue testing of copper reinforced circumferentially by

tungsten or molybdenum wire. They noted that work hardening followed by crack initiation occurred in the matrix between fibers.

## FATIGUE OF COMPOSITE STRUCTURES

In order to define a design base for structures, it is necessary to determine the full-scale fatigue behavior of composite materials to identify the effects of size, manufacturing variation, and combined loads. A limited amount of experience now exists with full-scale components (refs. 62 and 63); however, much of it relates to specific geometries and constructions and few generalizations may be drawn. Two things which are clear from this experience is the fact that composite structures are very fatigue resistant in aerospace applications relative to metal structures, and joints and attachments remain a major design problem, especially in fatigue.

The most substantial body of structural fatigue data exists for helicopter rotor blades (refs. 62 and 63). Jarosch and Stepan (ref. 62) have done fatigue testing of root end and outboard sections of the BO-105 fiberglass/epoxy rotor blade. The blade construction, seen in figure 26, consists of a C-spar of unidirectional E-glass-reinforced epoxy wound around a pin fitting at the root end, a skin of woven-glass cloth/epoxy oriented at  $\pm 45^\circ$ , and a foam core. Measured values of the spar and skin elastic modulus in the spanwise direction were  $6.0 \times 10^6$  and  $2.6 \times 10^6$  psi, respectively. The root end was fatigue tested, as seen in figure 27, with equal flapping and lagging loads of  $1900 \pm 2600$  ft-lb and a steady centrifugal load of 24 000 lb. Fatigue lives varied to  $13 \times 10^6$  cycles. Failure generally occurred in the unidirectional roving at the root-end pin attachment and was accompanied by considerable heating due to interlaminar friction. Readily visible delamination and gradual changes in stiffness and damping also occurred. Outboard specimens were tested in flapping resonance at a fatigue strain level of  $\pm 0.8\%$ , which is ten times the maximum strain in flight. Typical fatigue lives were more than  $10^6$  cycles, and failure was preceded by obvious visible delaminations and accompanying changes in damping and stiffness.

Fatigue tests of boron/epoxy and glass/epoxy CH-47 rotor blades (ref. 63) have also indicated excellent fatigue resistance although failures occurred in the metal root-end fitting. Similarly, fatigue testing of the boron/epoxy F-111 horizontal tail resulted in failure associated with the attachment of the composite to the titanium root end. Spectrum testing of components of a boron/epoxy wing box has shown excellent fatigue resistance, as has sonic fatigue testing of a boron/epoxy C-5A slat component. Both of these items have exhibited failure in fittings of composite bonded to metal.



## COMPOSITE FATIGUE DESIGN CONSIDERATIONS

A successful design procedure for composite materials in fatigue applications will not be a simple extrapolation of procedures used for metals. Metal parts exhibit cracks when they begin to fail in fatigue, and the cracks generally propagate in a predictable manner to failure. Thus, the metal part may be inspected at specific intervals and removed from service prior to failure. Composites, on the other hand, do not fail in the same manner.

The difference between fatigue behavior of a composite and that of a metal structure is depicted schematically in figure 28. The primary mode of damage in a metal structure is cracking. Cracks propagate in a relatively well defined manner with respect to the applied stress, and the critical crack size and rate of crack propagation can be related to specimen data through analytical fracture mechanics. In this discussion, the critical damage size is defined as that amount of damage at which the composite will be no longer structurally adequate. In general, the crack initiation time (defined as the time to detectable cracking (inspection threshold)) occupies a large part of the fatigue life of a metal part (ref. 64). It should be noted that all structures have some initial damage in the form of microcracks, surface imperfections, inclusions, and other stress risers and that much of the so-called crack initiation time involves propagation of this damage to detectable size. With composite structures there is no single damage mode which dominates. Matrix cracking, delamination, debonding, voids, fiber fracture, and composite cracking can all occur separately and in combination, and the predominance of one or more is highly dependent on the laminate orientations and loading conditions. In addition, the unique joints and attachments used for composite structures often introduce modes of failure different from those typified by the laminate itself.

The composite damage propagates in a less regular manner and damage modes can change. (See fig. 28.) Present experience with composites, although limited, indicates that the rate of damage propagation in composites does not exhibit the two distinct regions of initiation and propagation. Although, as mentioned previously, the crack initiation range in metals is actually propagation, there is a significant quantitative difference in rate. This quantitative difference appears to be less apparent with composites. This observation is very subjective and apparently dependent upon the observer's definition of initiation. Some investigators have observed matrix crazing and other indications early in their tests but have reported short-time rapid propagation because they define the latter based upon their experience with metals as crack propagation. Indeed, composite cracking may occupy only a small part of the fatigue life at the very end, but we can certainly make use of all the earlier indications which are prevalent.

It is expected that composite materials will be more damage tolerant than metals. Again, this expectation is based upon limited experience and will depend upon the laminate orientation (unidirectional composites are subject to splitting) and loading conditions, but, in general, it can be argued that each fiber is a separate load path and that a composite is therefore highly redundant. Our present analytical fracture mechanics tool must be supplemented for use with composites before we have a better understanding of this behavior. Several investigators have indicated that, in general, composites exhibit good fracture toughness (refs. 65 to 67) and, unlike metals, increase fracture toughness with increasing strength. It is thus reasonable to predict the critical damage size in composites to be greater than that for metals (fig. 28), although the multiple failure modes make this value a band for composites. Similarly, the inspection threshold is depicted as a band in figure 28 because there are multiple failure modes and multiple inspection methods.

The problem then is to determine the critical mode or modes of failure and develop detection schemes in order to insure fail safety in critical components. One such procedure involves the determination of changes in the static or dynamic stiffness properties of the component. A change in the resonant frequency or damping behavior of a part is an indication of damage. Failure criteria can be developed from data such as those seen in figures 10 to 12 as substantial changes occur early enough in the fatigue life to allow safe detection and removal from service. This characteristic may provide excellent fail safety for rotor blades in that the aeroelastic behavior may degrade noticeably long before the part has sustained damage of critical size. Other detection schemes such as temperature rise measurements (fig. 10), embedded conducting wires, radiography, sonics, ultrasonics, holography, infrared inspection, dye penetrant, and visual inspection will probably be used separately or in conjunction with dynamic measurements.

As mentioned earlier, a major consideration for developing a valid design methodology is a definition of failure. A problem exists however, in that a single failure criterion may be inadequate for all applications. This situation is seen schematically in figure 29. The example considers two structures, a spring and a tension cable, and two candidate materials, a metal and a composite, for each application. The failure criterion for the spring is a specified loss in stiffness, whereas that for the cable is fracture. Since metal structures exhibit little change in stiffness until cracking is extensive, the metal spring and metal cable have approximately the same life, and a single criterion based on fracture is probably adequate for design. The composite material spring would lose sufficient stiffness to be considered failed at only a fraction of its fracture life, whereas, the tension cable made of the same material and subject to the same loading would have a much greater useful life. In order to provide for such design considerations, it will be desirable to record fatigue data as depicted schematically in figure 30.



## CONCLUDING REMARKS

Composite materials appear to offer excellent resistance to fatigue loading and, as such, will likely find use in dynamic components. A second factor which makes composites attractive for these applications is the opportunity for tailoring of the stiffness in different directions, thus the designer is given the capability of tuning dynamic components. As composites find wider application, it will be necessary to provide more precise definitions of failure and to couple these definitions with proper damage detection schemes. New, sophisticated damage detection methods will probably not be necessary; however, because of the multiple damage modes possible, it will be necessary to utilize multiple detection schemes. The apparent high damage tolerance of composites will allow somewhat relaxed inspection requirements and will provide for improved repairability procedures. At this writing, the cost of high modulus composites is still high and must be further reduced to allow wider usage.

## REFERENCES

1. Forsyth, P. J. E.; George, R. W.; and Ryder, D. A.: Some Preliminary Tests on Aluminum Alloy Sheets Reinforced With Strong Wires. *Appl. Mater. Res.*, vol. 3, no. 4, Oct. 1964, pp. 223-228.
2. Baker, A. A.; and Cratchley, D.: Metallographic Observations on the Behaviour of Silica Reinforced Aluminum Under Fatigue Loading. *Appl. Mater. Res.*, vol. 3, no. 4, Oct. 1964, pp. 215-222.
3. Morris, A. W. H.; and Steigerwald, E. A.: An Investigation of the Fatigue Behavior of Tungsten-Reinforced and Steel-Reinforced Silver Composites. *Trans. Met. Soc. AIME*, vol. 239, 1967, pp. 730-739.
4. Salkind, M. J.; and George, F. D.: Fatigue and Bonding of  $Al_3Ni$  Whisker Reinforced Aluminum. Rep. G910583.4 (Contract No. 0019-68-C-0016), United Aircraft Corp., July 31, 1968. (Available from DDC as AD 838 871.)
5. Tavernelli, J. F.; and Coffin, L. F., Jr.: A Compilation and Interpretation of Cyclic Strain Fatigue Tests on Metals. *Trans. Amer. Soc. Metals*, vol. LI, 1959, pp. 438-453.
6. Manson, S. S.: Behavior of Materials Under Conditions of Thermal Stress. NACA Rep. 1170, 1954. (Supersedes NACA TN 2933.)
7. Sachs, G.; Gerberich, W. W.; Weiss, V.; and Latorre, J. V.: Low-Cycle Fatigue of Pressure-Vessel Materials. *Proc. Amer. Soc. Testing Mater.*, vol. 60, 1960, pp. 512-529.
8. Boller, K. H.: Fatigue Tests of Glass-Fabric-Base Laminates Subjected to Axial Loading. Rep. 1823, Forest Prod. Lab., U.S. Dep. Agr., May 1952.
9. Stevens, G. H.; and Boller, K. H.: Effect of Type of Reinforcement on Fatigue Properties of Plastic Laminates. TR 59-27, U.S. Air Force, May 1959. (Available from DDC as AD 213 835.)
10. Kimball, Kenneth E.: Supplement to Fatigue Tests of Glass-Fabric-Base Laminates Subjected to Axial Loading - Effect of Notches. Rep. No. 1823-C, Forest Prod. Lab., U.S. Dep. Agr., Oct. 1958.
11. Boller, Kenneth H.: Resumé of Fatigue Characteristics of Reinforced Plastic Laminates Subjected to Axial Loading. ASD-TDR-63-768, U.S. Air Force, July 1963.
12. Boller, K. H.: Effect of Pre-Cyclic Stresses on Fatigue Life of RP Laminates. *Modern Plastics*, vol. 42, no. 8, Apr. 1965, pp. 162, 165-166, 168, 171, 173.



13. Boller, Kenneth H.: Effect of Tensile Mean Stresses on Fatigue Properties of Plastic Laminates Reinforced With Unwoven Glass Fibers. ML-TDR-69-86, U.S. Air Force, Mar. 1964. (Available from DDC as AD 605 412.)
14. Boller, Kenneth H.: Effect of Pre-Cyclic Stresses on Fatigue Life of Plastic Laminates Reinforced With Unwoven Fibers. ML-TDR-64-168, U.S. Air Force, Sept. 1964. (Available from DDC as AD 606 769.)
15. Boller, Kenneth H.: Fatigue Strength of Plastic Laminates Reinforced With Unwoven "S" Glass Fibers. AFML-TR-64-403, U.S. Air Force, Dec. 1964.
16. Boller, Kenneth H.: Fatigue Characteristics of Two New Plastic Laminates Reinforced With Unwoven "S" Glass Fibers Under Cyclic Axial or Shear Loading. AFML-TR-66-54, U.S. Air Force, Mar. 1966.
17. Boller, Kenneth H.: Effect of Notches on Fatigue Strength of Composite Materials. AFML-TR-69-6, U.S. Air Force, Apr. 1969. (Available from DDC as AD 853 045.)
18. Boller, K. H.: Fatigue Fundamentals for Composite Materials. Composite Materials: Testing and Design, Spec. Tech. Publ. No. 460, Amer. Soc. Testing Mater., c.1969, pp. 217-235.
19. Broutman, Lawrence J.: Fiber-Reinforced Plastics. Modern Composite Materials, Lawrence J. Broutman and Richard H. Krock, eds., Addison-Wesley Pub. Co., Inc., c.1967, pp. 337-411.
20. Cornish, R. H.; Nelson, H. R.; and Dally, J. W.: Compressive Fatigue and Stress Rupture Performance of Fiber Reinforced Plastics. Proceedings 19th Annual Technical and Management Conference, sec. 9-E, Soc. Plast. Ind., Inc., Feb. 1964.
21. Mettes, David G.; and Lockwood, Paul A.: The Mechanical Properties of Laminates Reinforced With High Performance Glass Fiber Fabric. Proceedings 21st Annual Technical and Management Conference, sec. 4-G, Soc. Plast. Ind., Inc., Feb. 1966.
22. Davis, J. W.; McCarthy, J. A.; and Schurb, J. N.: The Fatigue Resistance of Reinforced Plastics. Mater. Des. Eng., vol. 60, no. 7, Dec. 1964, pp. 87-91.
23. Cutler, Martin B.; and Pinckney, Robert L.: Static and Fatigue Test Properties for Woven and Nonwoven S-Glass Fibers. USAAVLABS Tech. Rep. 69-9, U.S. Army, Apr. 1969. (Available from DDC as AD 688 971.)
24. Kelly, A.; and Davies, G. J.: The Principles of the Fibre Reinforcement of Metals. Metallurgical Rev., vol. 10, no. 37, 1965, pp. 1-77.
25. Broutman, L. J.: Failure Mechanisms for Filament Reinforced Plastics. Modern Plastics, vol. 42, no. 8, Apr. 1965, pp. 143-145, 148, 150, 153, 214, 216.

26. Smith, T. R.; and Owen, M. J.: Fatigue Properties of RP-1. Modern Plastics, vol. 46, no. 4, Apr. 1969, pp. 124-125, 128-132.
27. Cessna, L. C.; Levens, J. A.; and Thomson, J. B.: Flexural Fatigue of Glass-Reinforced Thermoplastics. Proceedings 24th Annual Technical and Management Conference, sec. 1-C, Soc. Plast. Ind., Inc., Feb. 1969.
28. Broutman, L. J.; and Sahu, S.: Progressive Damage of a Glass Reinforced Plastic During Fatigue. Proceedings 24th Annual Technical and Management Conference, sec. 11-D, Soc. Plast. Ind., Inc., Feb. 1969.
29. Lavengood, R. E.; and Anderson, R. M.: Matrix Properties Controlling Torsional Fatigue Life of Fiber Reinforced Composites. Proceedings 24th Annual Technical and Management Conference, sec. 11-E, Soc. Plast. Ind., Inc., Feb. 1969.
30. Fujii, Taichi; and Mizukawa, Kiyoshi: The Effect of the Combination of Roving Glass Cloth and Mat Upon the Fatigue Strength of Reinforced Polyester Laminates. Proceedings 24th Annual Technical and Management Conference, sec. 14-D, Soc. Plast. Ind., Inc., Feb. 1969.
31. Hagerup, E.: Flexural Fatigue Testing of Polyesters. J. Appl. Polymer Sci., vol. 7, no. 3, May 1963, pp. 1093-1116.
32. Lazan, B. J.: Some Mechanical Properties of Plastics and Metals Under Sustained Vibrations. Trans. ASME, vol. 65, no. 2, Feb. 1943, pp. 87-104.
33. Lazan, B. J.; and Yorgiadis, A.: Behavior of Plastics Under Repeated Stress. Symposium on Plastics, Spec. Tech. Publ. No. 59, Amer. Soc. Testing Mater., Feb. 1944, pp. 66-94.
34. Boller, Kenneth H.: Fatigue Characteristics of RP Laminates Subjected to Axial Loading. Modern Plastics, vol. 41, no. 10, June 1964, pp. 145-150, 188.
35. Thompson, A. W.: Fatigue and Creep Properties of Reinforced Plastics. Plastics Inst.-Trans., vol. 30, no. 85, Feb. 1962, pp. 39-50.
36. Owen, M. J.: New Fatigue Testing Machine for Reinforced Plastics. Plastics Inst.-Trans., vol. 35, no. 115, Feb. 1967, pp. 353-357.
37. Dally, J. W.; and Broutman, L. J.: Frequency Effects on the Fatigue of Glass Reinforced Plastics. J. Compos. Mater., vol. 1, no. 4, Oct. 1967, pp. 424-442.
38. Shockey, P. D.; Anderson, J. D.; and Hofer, K. E.: Structural Airframe Application of Advanced Composite Materials. Vol. V - Mechanical Properties - Fatigue. AFML-TR-69-101, Vol. V, U.S. Air Force, Mar. 1970. (Available from DDC as AD 867 017.)



39. Hayes, R. D.: Flightworthy Graphite Fiber Reinforced Composite Aircraft Primary Structural Assemblies. Vols. 1 and 2. FML-TR-70-207-Vols. 1 & 2, U.S. Air Force, 1970. (Available from DDC as AD-877 234 and AD-877 235.)
40. Holmes, R. D.; and Wright, D. W.: Creep and Fatigue Characteristics of Graphite/Epoxy Composites. ASME Paper 70-DE-32, Amer. Soc. Mech. Eng., May 1970.
41. Owen, M. J.; and Morris, S.: An Assessment of the Potential of Carbon Fibre Reinforced Plastics as Fatigue Resistant Materials. Proceedings 25th Annual Technical and Management Conference, sec. 8-E, Soc. Plast. Ind., Inc., Feb. 1970.
42. Puppo, A. H.; and Evensen, H. A.: Interlaminar Shear in Laminated Composites Under Generalized Plane Stress. J. Compos. Mater., vol. 4, Apr. 1970, pp. 204-223.
43. Pipes, R. Byron; and Pagano, N. J.: Interlaminar Stresses in Composite Laminates Under Uniform Axial Extension. J. Compos. Mater., vol. 4, Oct. 1970, pp. 538-548.
44. Baker, A. A.; and Cratchley, D.: Stress-Strain Behaviour and Toughness of a Fibre-Reinforced Metal. Appl. Mater. Res., vol. 5, no. 2, Apr. 1966, pp. 92-103.
45. Baker, A. A.: The Effect of Fibre Volume Fraction and Interfacial Bond on the Fatigue of Aluminum Reinforced With Stainless Steel Wires. Appl. Mater. Res., vol. 5, no. 3, July 1966, pp. 143-153.
46. Baker, A. A.: The Effect of Fibre Diameter and Discontinuous Fibres on the Fatigue of a Fibre-Reinforced Metal. Appl. Mater. Res., vol. 5, no. 4, Oct. 1966, pp. 210-217.
47. Baker, A. A.; Mason, J. E.; and Cratchley, D.: High-Strain Fatigue Studies of a Composite Material. J. Mater. Sci., vol. 1, no. 3, Aug. 1966, pp. 229-237.
48. Baker, A. A.: The Fatigue of Fibre-Reinforced Aluminum. J. Mater. Sci., vol. 3, no. 4, July 1968, pp. 412-423.
49. Salkind, M. J.; George, F. D.; Lemkey, F. D.; and Bayles, B. J.: Investigation of the Creep, Fatigue, and Transverse Properties of  $Al_3Ni$  Whisker and  $CuAl_2$  Platelet Reinforced Aluminum. E910344-4 (Contract NOW-65-0384d), United Aircraft Corp., May 11, 1966. (Available from DDC as AD 633 241.)
50. Salkind, M. J.; Lemkey, F. D.; and George, F. D.: Whisker Composites by Eutectic Solidification. Whisker Technology, Albert P. Levitt, ed., Wiley-Interscience, c.1970, pp. 343-401.

51. Thompson, E. R.; George, F. D.; and Kraft, E. H.: Investigation To Develop a High Strength Eutectic Alloy With Controlled Microstructure. Rep. J910868-4 (Contract No. 0019-70-C-0052), United Aircraft Corp., July 31, 1970. (Available from DDC as AD 873 832.)
52. Hoover, W. R.; and Hertzberg, R. W.: The Fatigue Characteristics of Unidirectionally Solidified Al-Al<sub>3</sub>Ni Eutectic Alloy. Trans. Amer. Soc. Metals, vol. LXI, 1968, pp. 769-776.
53. Manson, S. Stanford; and Hirschberg, Marvin H.: Fatigue Behavior in Strain Cycling in the Low- and Intermediate-Cycle Range. Fatigue - An Interdisciplinary Approach, John J. Burke, Norman L. Reed, and Volker Weiss, eds., Syracuse Univ. Press, 1964, pp. 133-178.
54. Coffin, L. F.: A Study of the Effects of Cyclic Thermal Stresses on a Ductile Metal. Trans. ASME, vol. 76, no. 6, Aug. 1954, pp. 931-950.
55. Forest, J. D.; and Christian, J. L.: Development and Application of Aluminum-Boron Composite Material. AIAA Paper No. 68-975, Oct. 1968.
56. Young, J. R.; and Carlson, R. G.: Advanced Composite Material Structural Hardware Development & Testing Program. AFML-TR-70-140-Vol. I, U.S. Air Force, July 1970. (Available from DDC as AD 872 264.)
57. Shimizu, H.; and Dolowy, J. F., Jr.: Fatigue Testing and Thermal-Mechanical Treatment Effects on Aluminum-Boron Composites. Composite Materials: Testing and Design, Spec. Tech. Publ. No. 460, Amer. Soc. Testing Mater., c.1969, pp. 192-202.
58. Kreider, K. G.: Mechanical Testing of Metal Matrix Composites. Composite Materials: Testing and Design, Spec. Tech. Publ. No. 460, Amer. Soc. Testing Mater., c.1969, pp. 203-214.
59. Toth, I. J.: Creep and Fatigue Behavior of Unidirectional and Cross-Plied Composites. Composite Materials: Testing and Design, Spec. Tech. Publ. No. 460, Amer. Soc. Testing Mater., c.1969, pp. 236-253.
60. Salkind, M.; and Patarini, V.: Fatigue of Boron Filament. Trans. Met. Soc. AIME, vol. 239, 1967, pp. 1268-1270.
61. Gates, R. G.; and Wood, W. A.: Evaluating Potential Fatigue Performance of Composites (Cu/W and Cu/Mo) From Microstructural Behavior. Metal Matrix Composites, Spec. Tech. Publ. No. 438, Amer. Soc. Testing Mater., c.1968, pp. 218-228.



62. Jarosch, E.; and Stepan, A.: Fatigue Properties and Test Procedures of Glass Reinforced Plastic Rotor Blades. J. Amer. Helicopter Soc., vol. 15, no. 1, Jan. 1970, pp. 33-41.
63. Stratton, Warren: The Potential of Advanced Composites for V/STOL Propellers. Proceedings of the V/STOL Technology and Planning Conference, U.S. Air Force, Sept. 23-25, 1969.
64. Manson, S. S.: Fatigue: A Complex Subject – Some Simple Approximations. Exp. Mech., vol. 5, no. 7, July 1965, pp. 193-226.
65. Salkind, M. J.; and George, F. D.: The Charpy Impact Behavior of  $Al_3Ni$  Whisker-Reinforced Aluminum. Trans. Met. Soc. AIME, vol. 242, 1968, pp. 1237-1247.
66. Cooper, G. A.; and Kelly, A.: Tensile Properties of Fibre-Reinforced Metals: Fracture Mechanics. J. Mech. Phys. Solids, vol. 15, no. 4, July 1967, pp. 279-297.
67. Tetelman, A. S.: Fracture Processes in Fiber Composite Materials. Composite Materials: Testing and Design, Spec. Tech. Publ. No. 460, Amer. Soc. Testing Mater., c.1969, pp. 473-502.

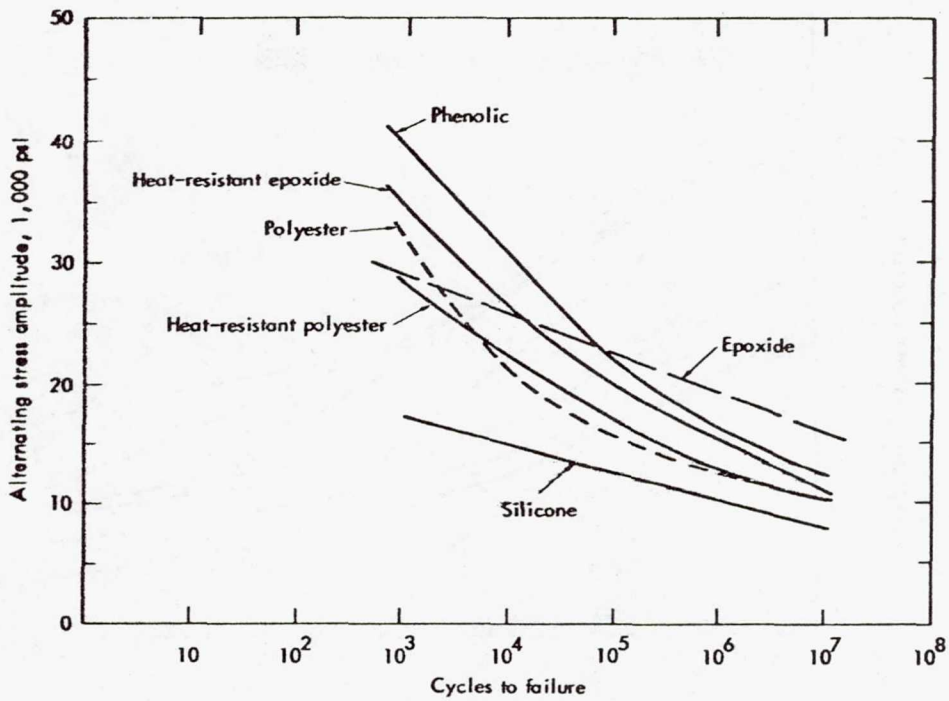


Figure 1.- Effect of matrix material on fatigue of glass fabric composites (from ref. 18).

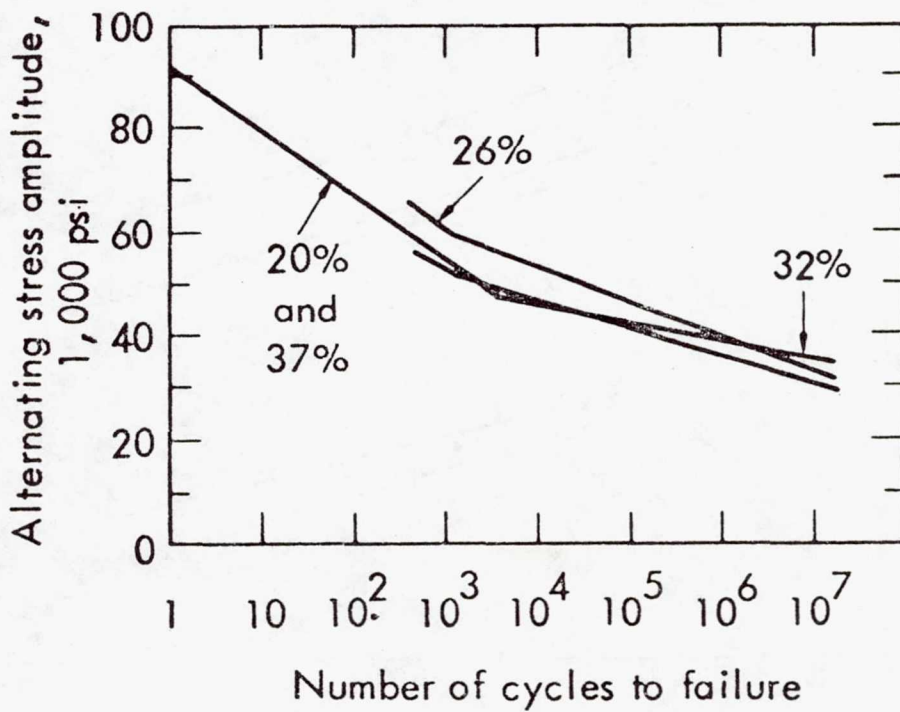


Figure 2.- Effect of matrix content on fatigue of  $\pm 50$  glass-fiber-reinforced epoxy (from ref. 13).



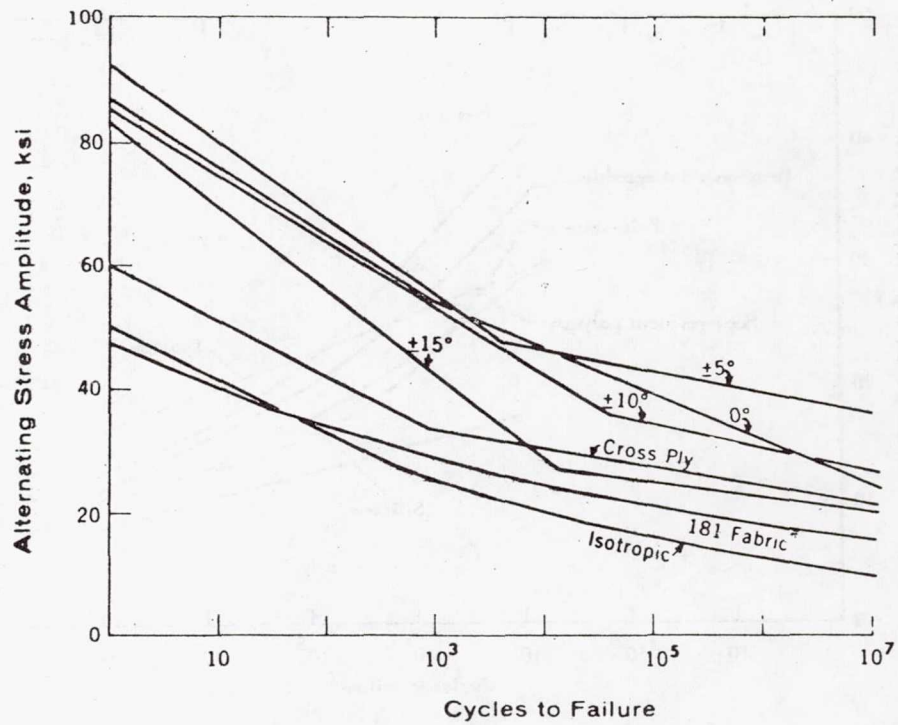


Figure 3.- Effect of fiber orientation (from ref. 18).

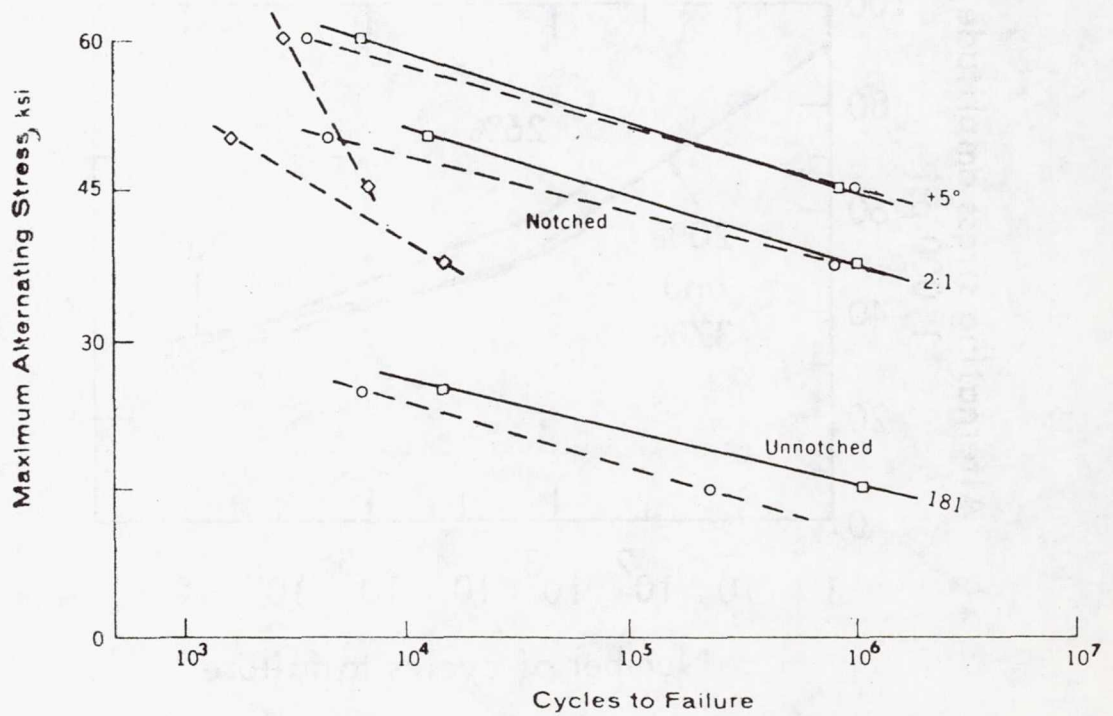


Figure 4.- Fatigue of woven and nonwoven materials (from ref. 18).

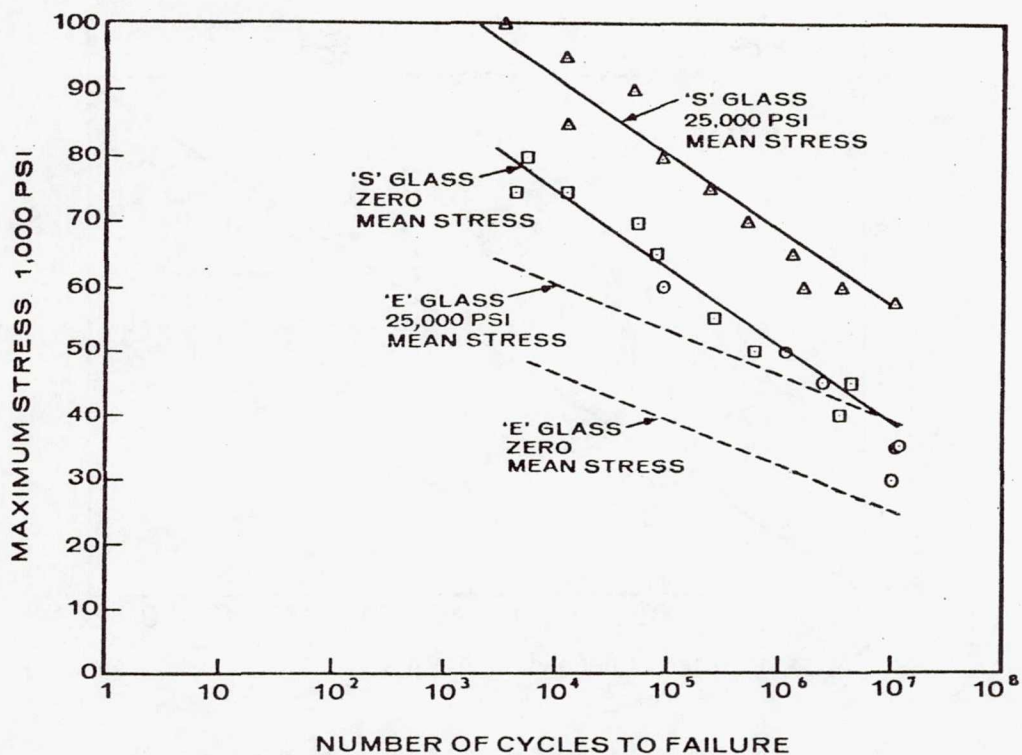


Figure 5.- Fatigue of E- and S-glass composites (from ref. 15).

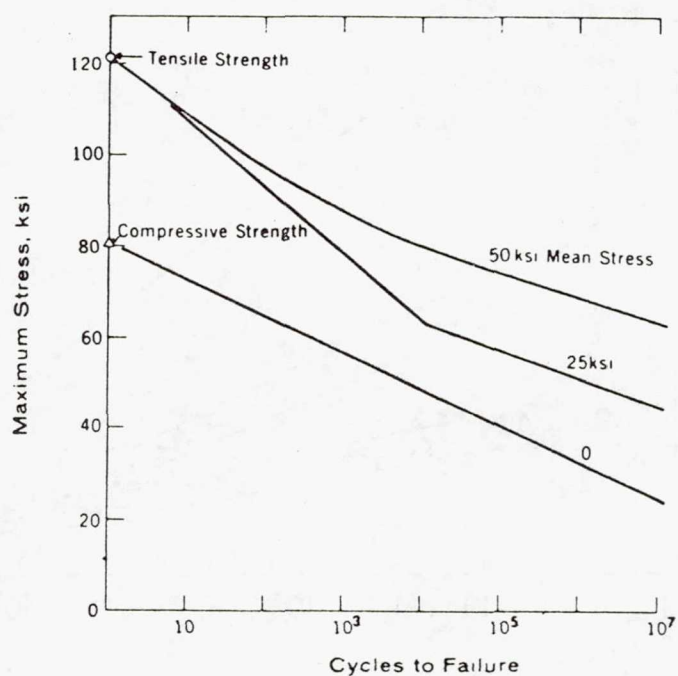


Figure 6.- Effect of mean stress level (from ref. 18).



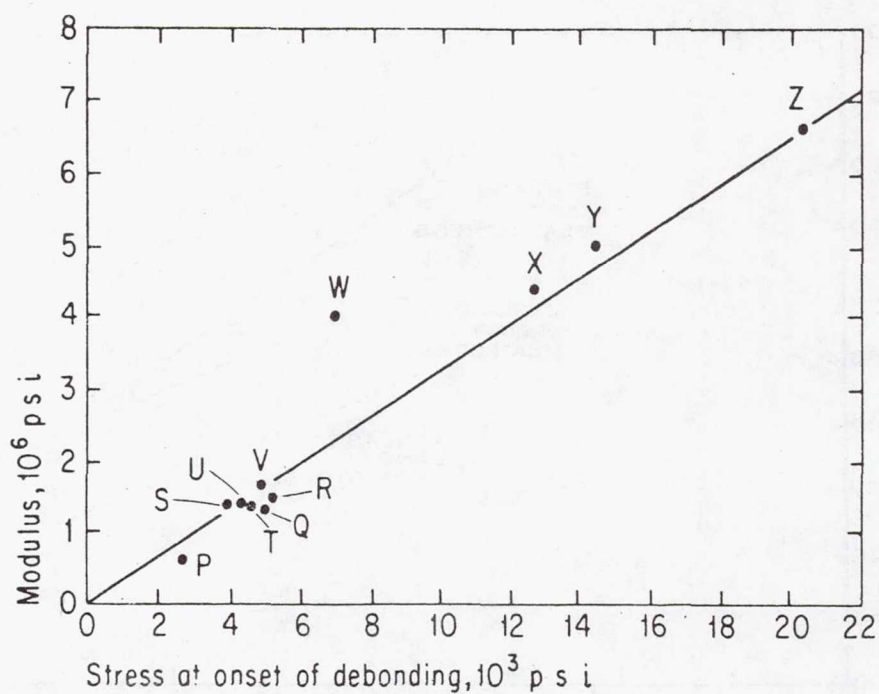


Figure 7.- Composite modulus as a function of stress at onset of debonding (from ref. 26).

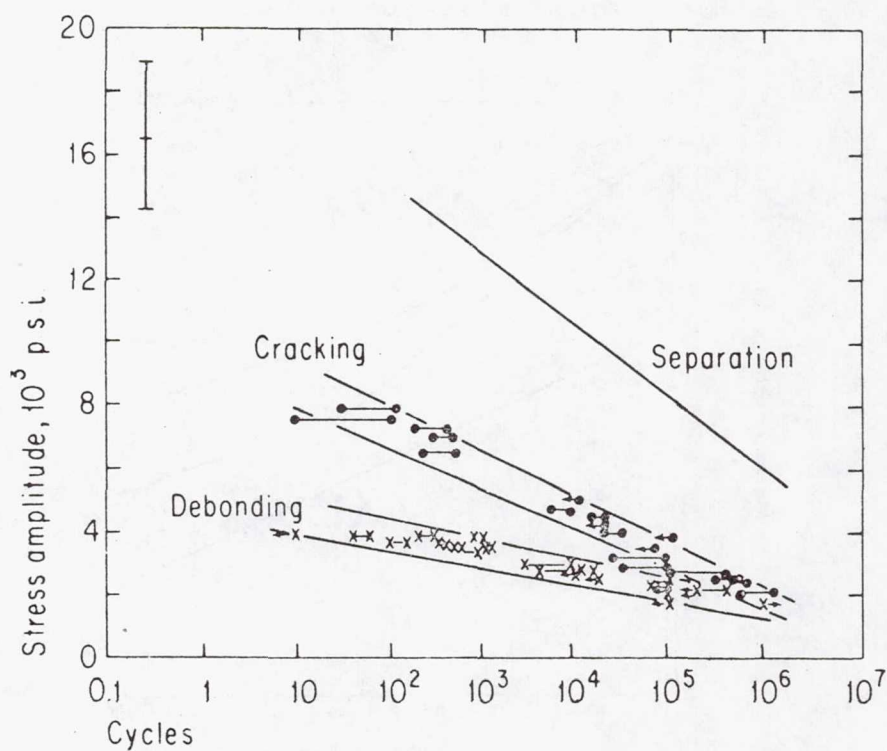


Figure 8.- Fatigue behavior of glass-mat-reinforced polyester (from ref. 26).

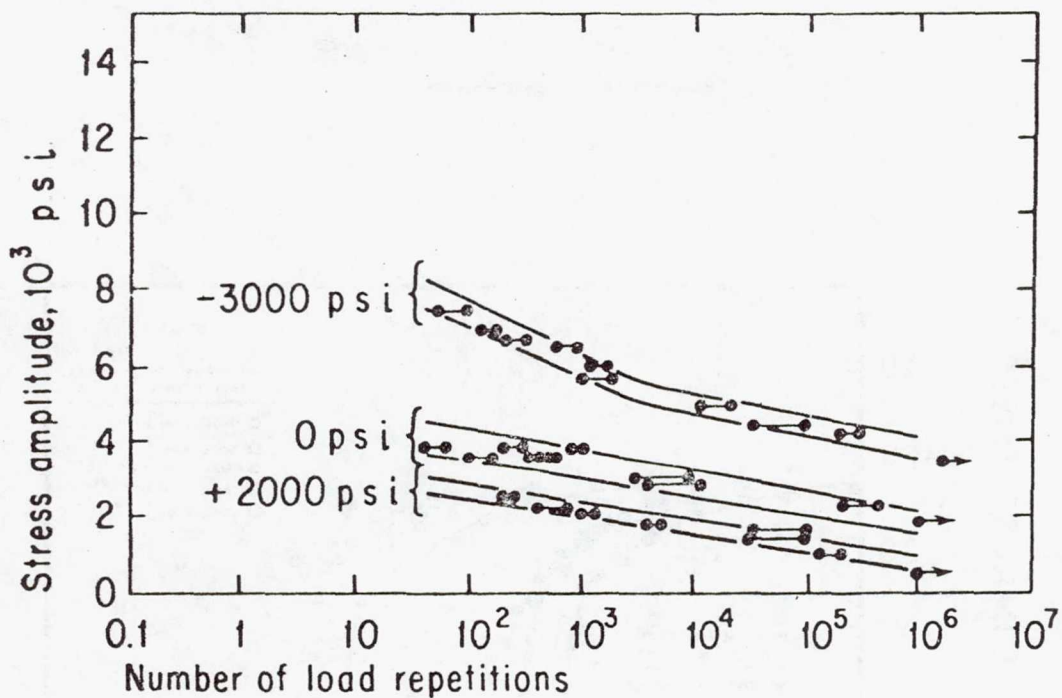


Figure 9.- Effect of mean stress on debonding of glass-mat-reinforced polyester (from ref. 26).

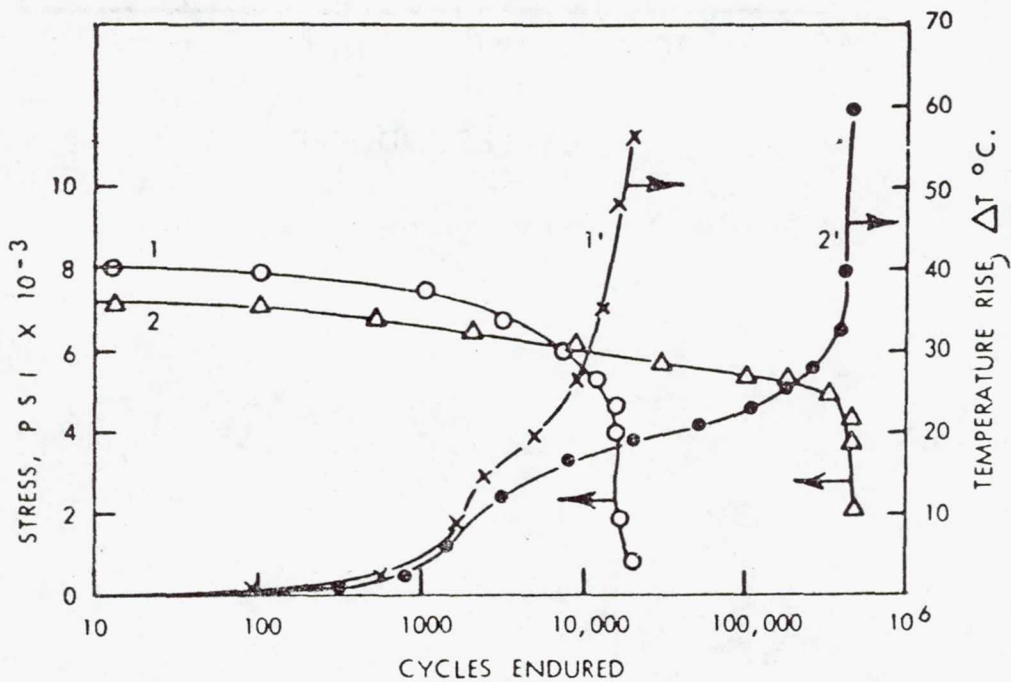


Figure 10.- Apparent stress and temperature rise in glass-reinforced polypropylene (from ref. 27).

C.7



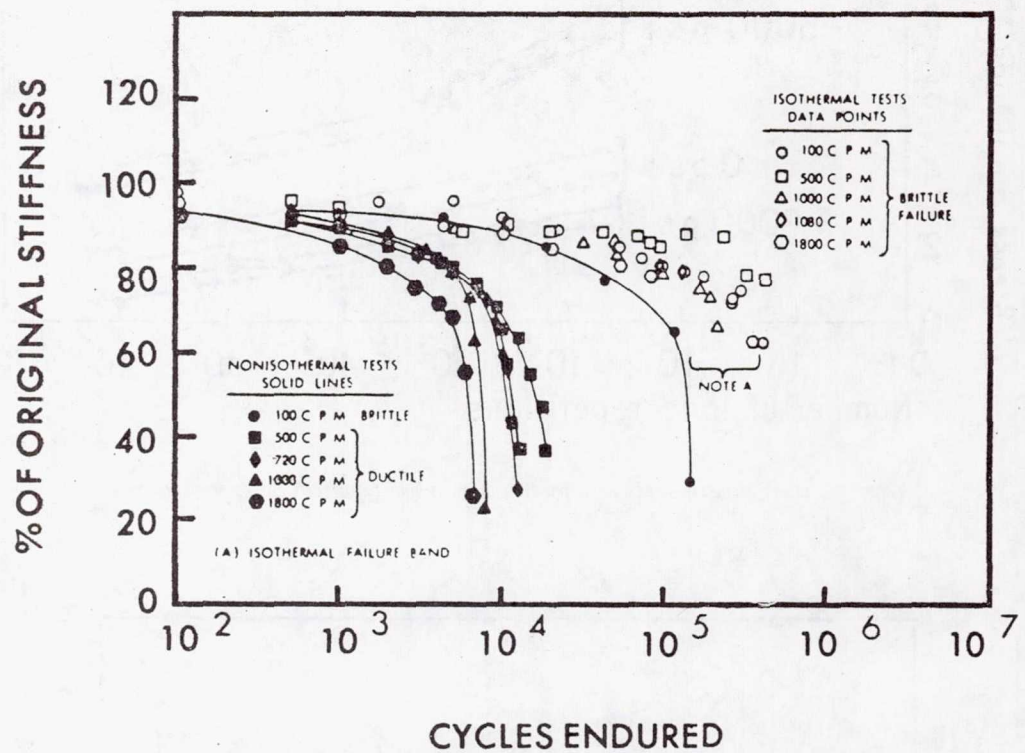


Figure 11.- Stiffness decay during fatigue of glass-reinforced polypropylene (from ref. 27).

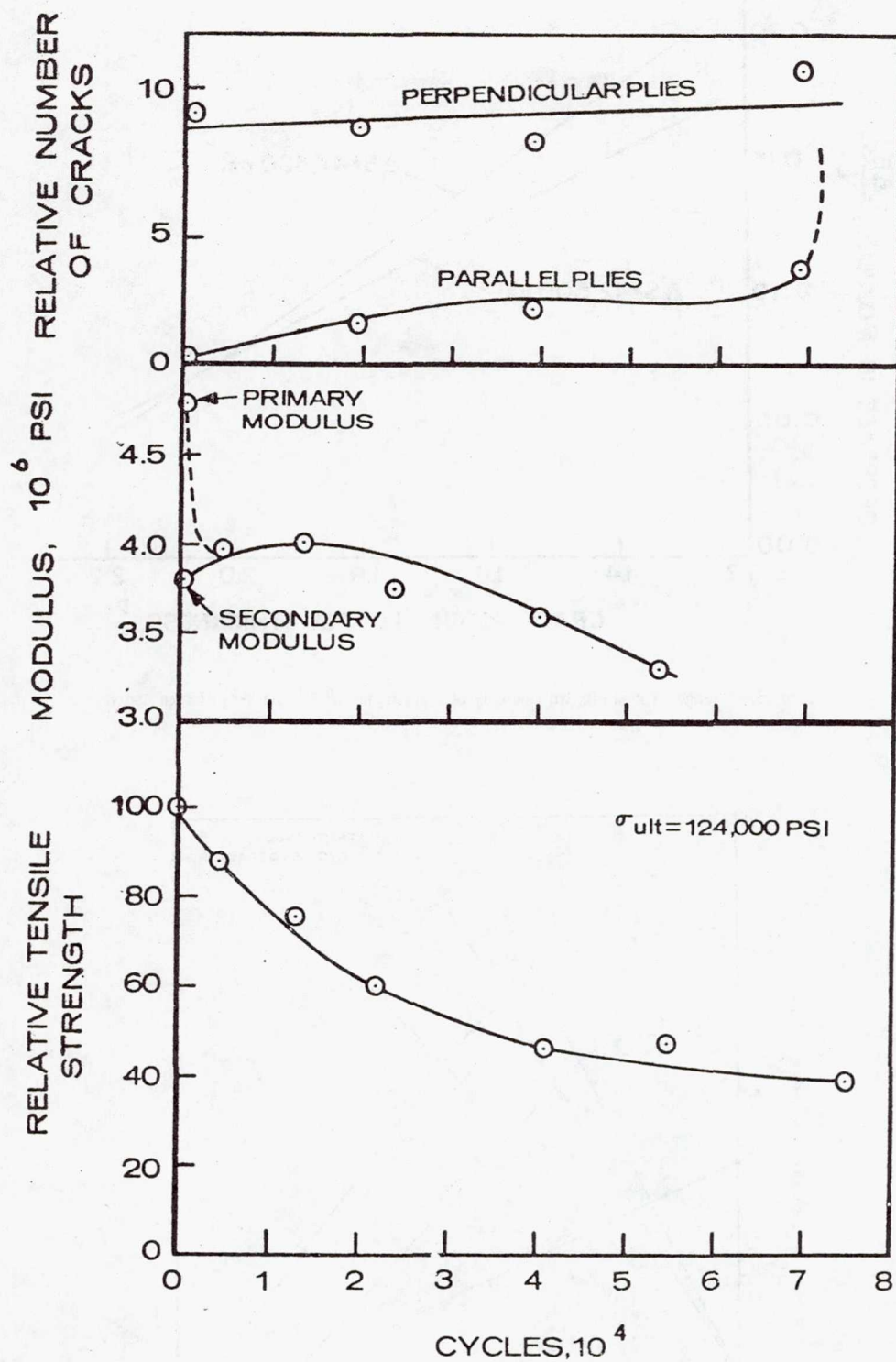


Figure 12.- Changes in strength, modulus, and cracking of  $0^\circ/90^\circ$  glass-reinforced epoxy (from ref. 28).



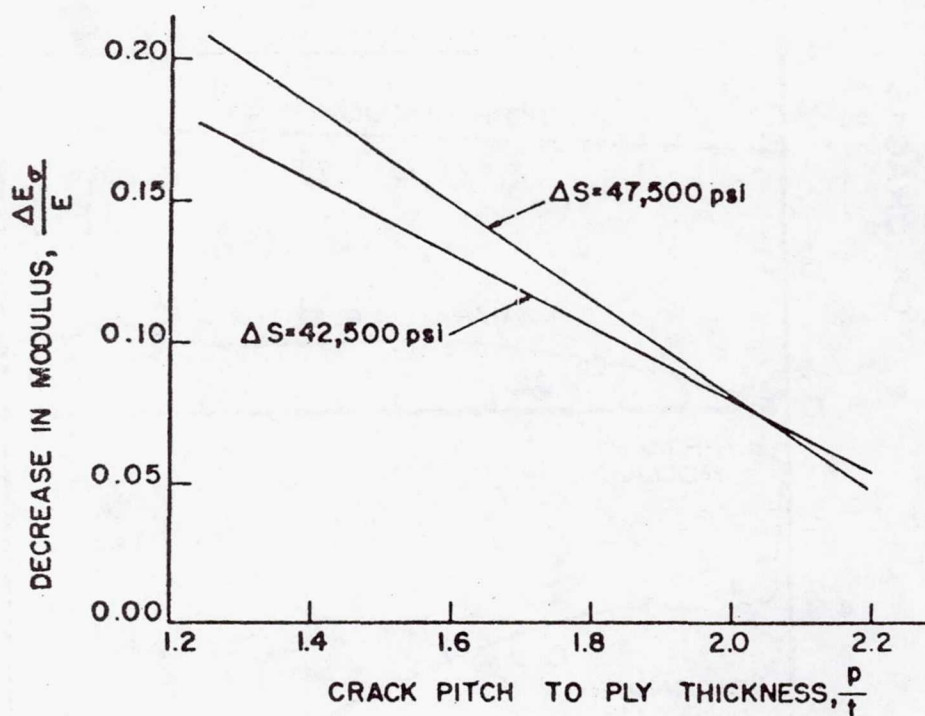


Figure 13.- Change in modulus with density of cracking for 0°/90° glass-reinforced epoxy.

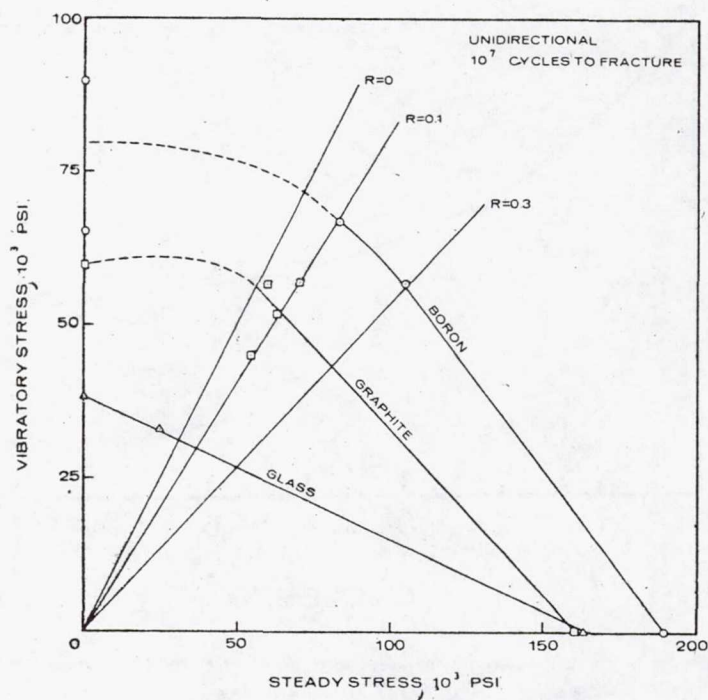


Figure 14.- Comparison of fatigue behavior of unidirectional boron, graphite, and glass-reinforced polymers.

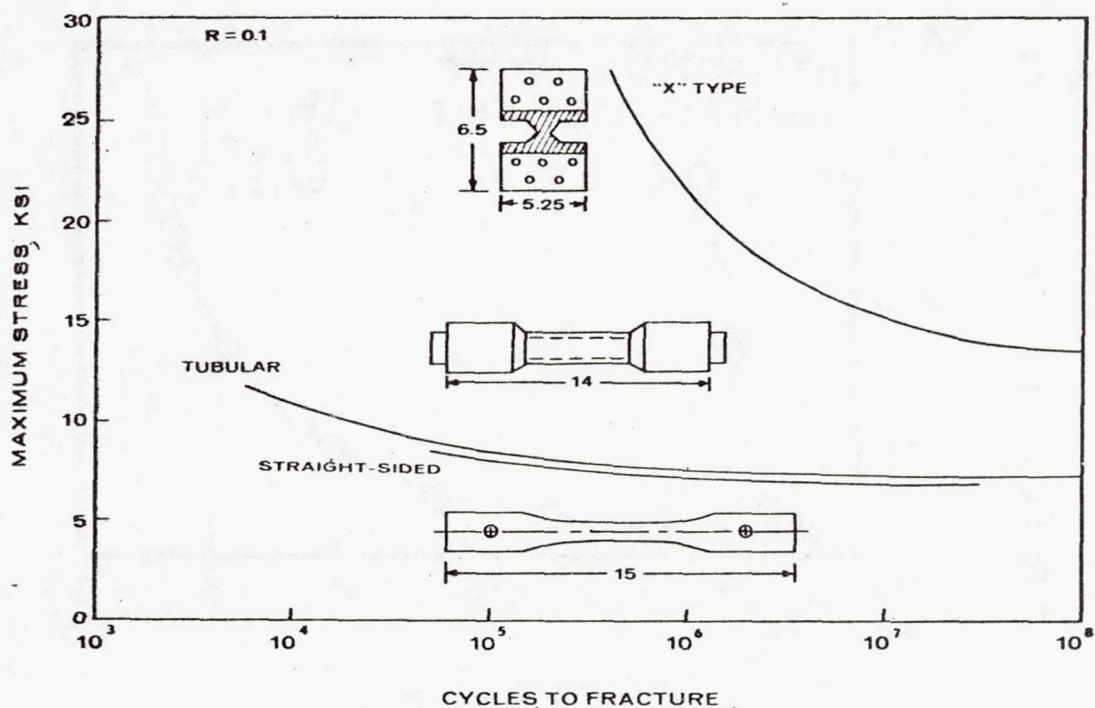


Figure 15.- Effect of specimen configuration on axial fatigue behavior of  $\pm 45^\circ$  1002 E-glass/epoxy.

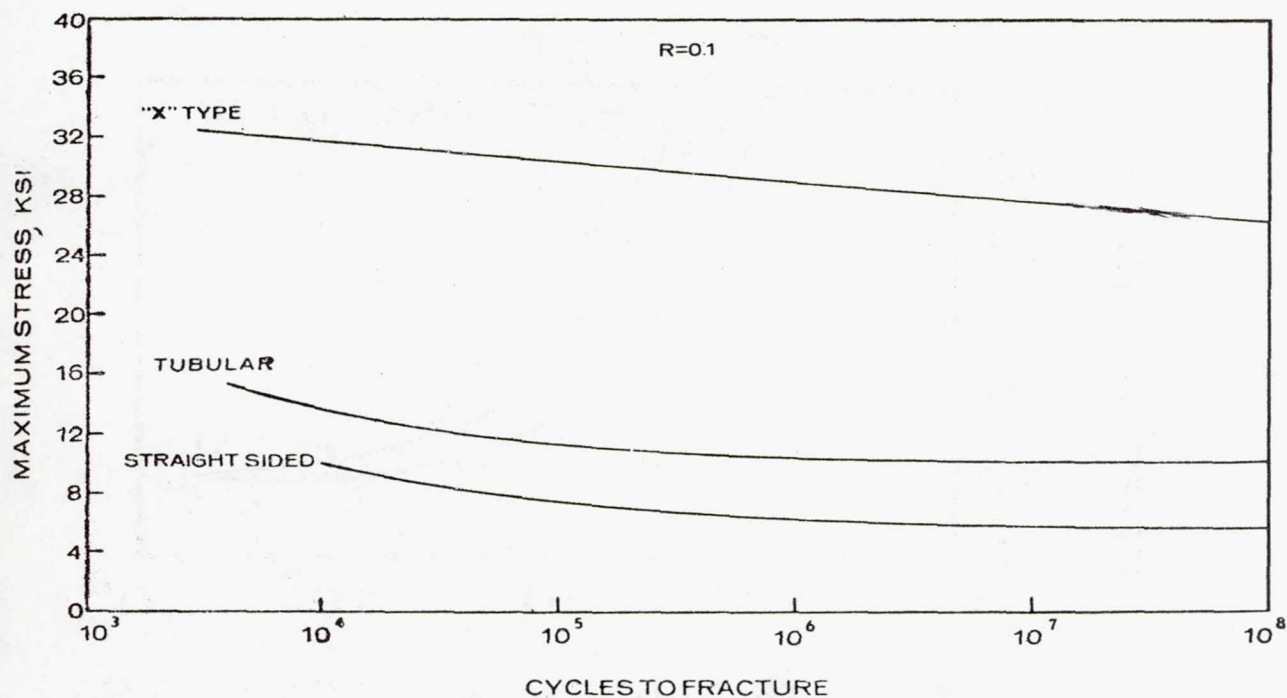


Figure 16.- Effect of specimen configuration on axial fatigue behavior of  $\pm 45^\circ$  boron/epoxy.



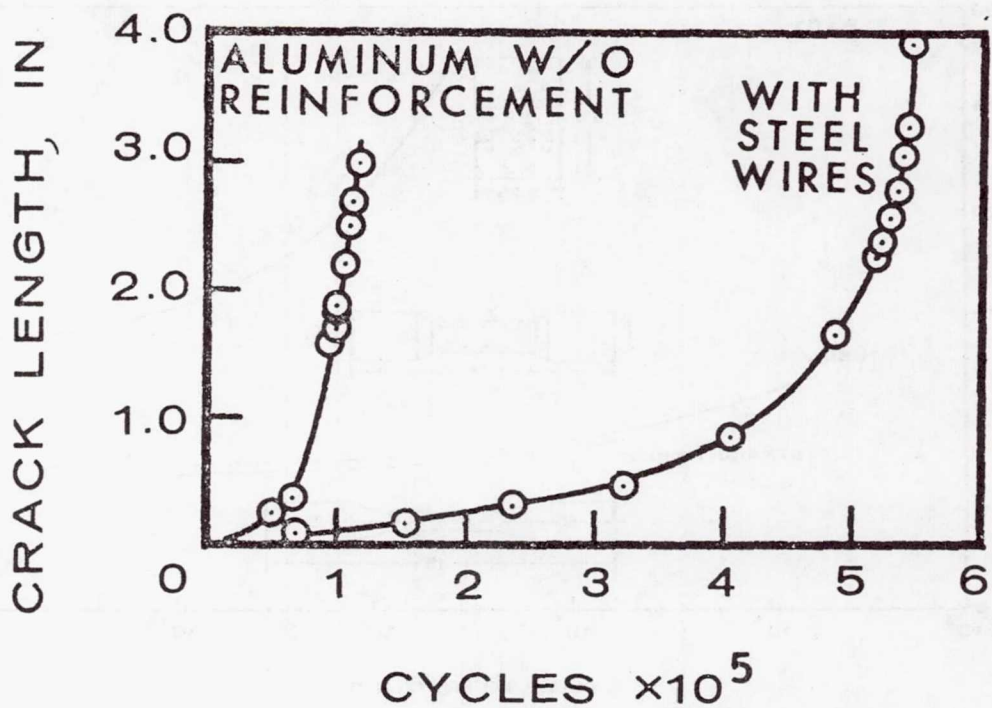


Figure 17.- Effect of steel wire mesh on the crack growth behavior of aluminum alloy sheet (from ref. 1).

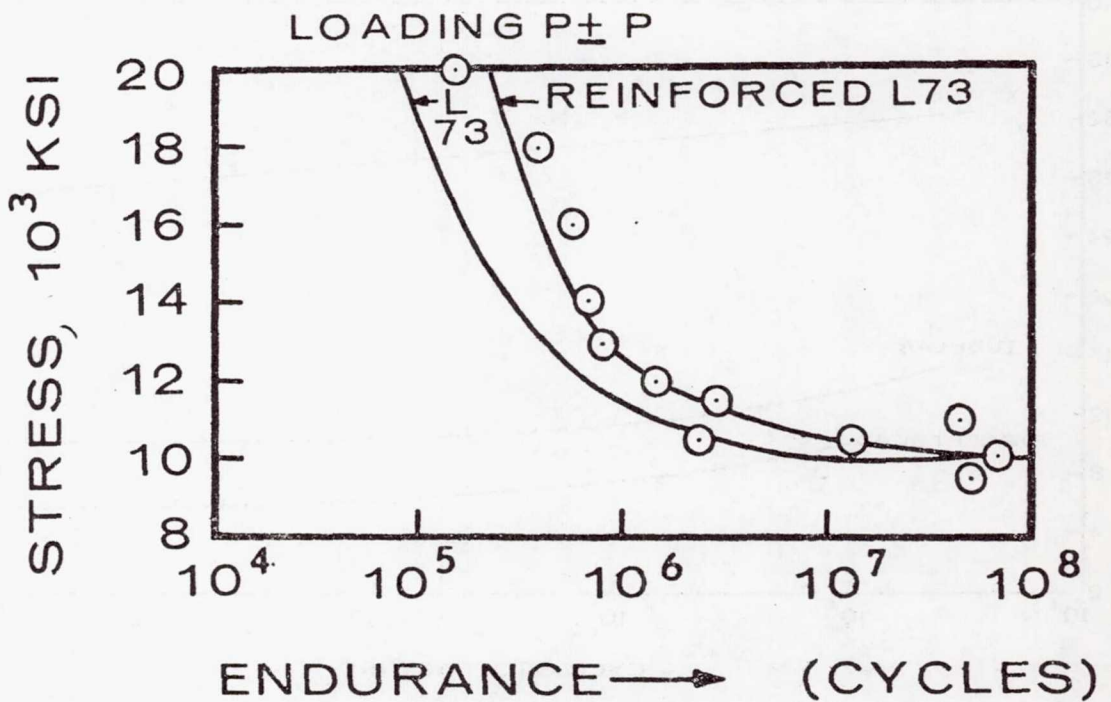


Figure 18.- Fatigue behavior of aluminum alloy with and without 13.5 volume percent steel wire (from ref. 1).

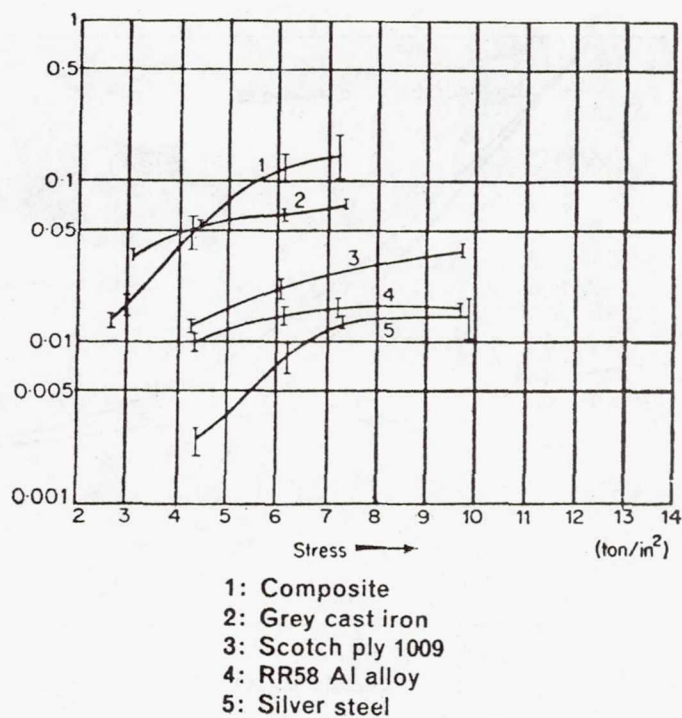


Figure 19.- Vibrational damping capacity ( $\delta$ ) as a function of stress for silica-reinforced aluminum compared with conventional engineering materials (from ref. 44).

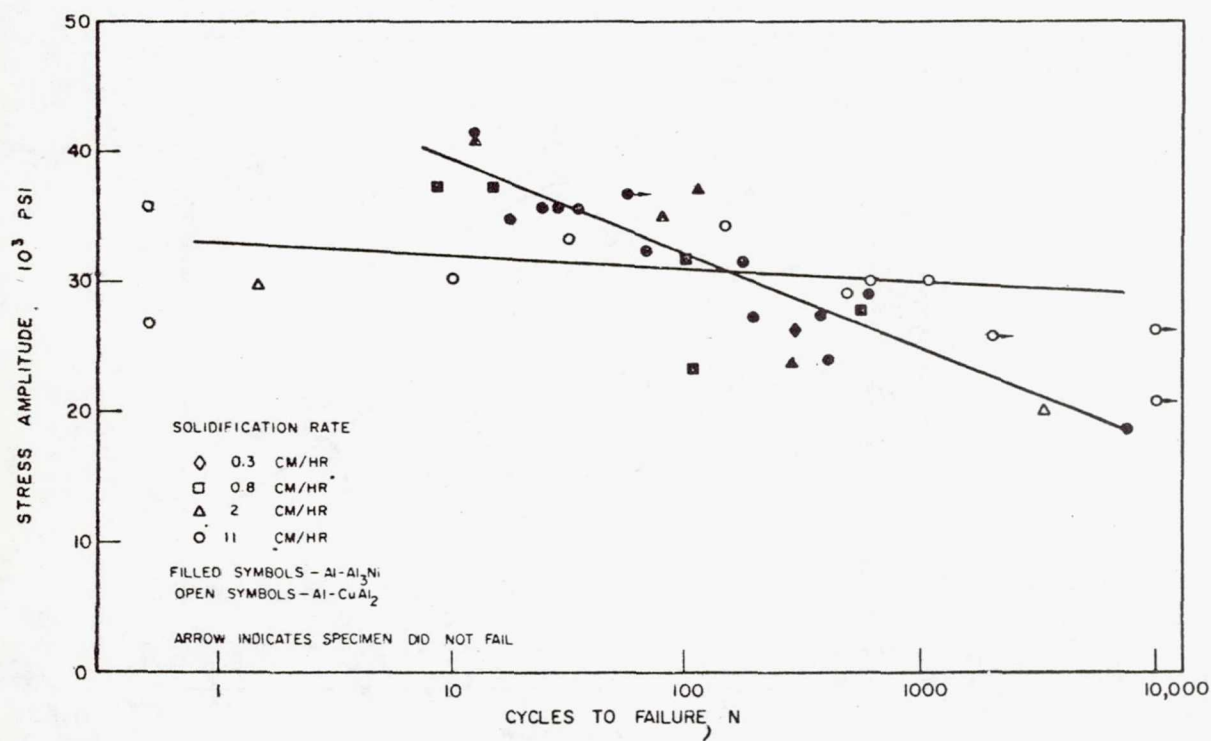


Figure 20.- Comparison of fatigue behavior of lamellar ( $\text{Al-CuAl}_2$ ) and fiber ( $\text{Al-Al}_3\text{Ni}$ ) composites (from ref. 49).



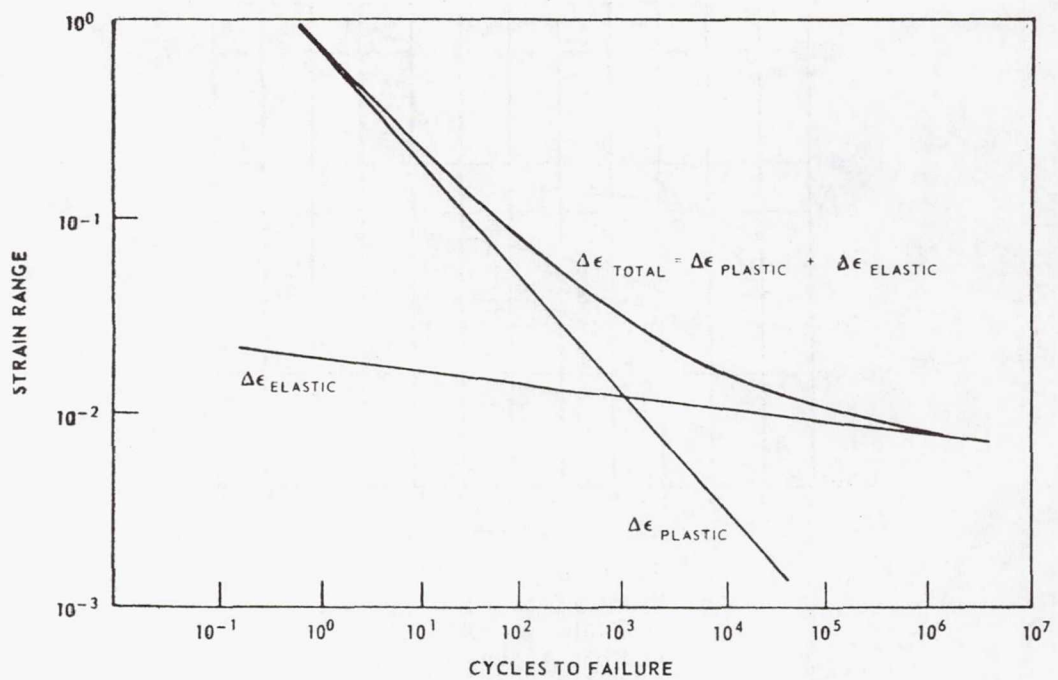


Figure 21.- Schematic behavior of metals in strain cycling (from ref. 57).

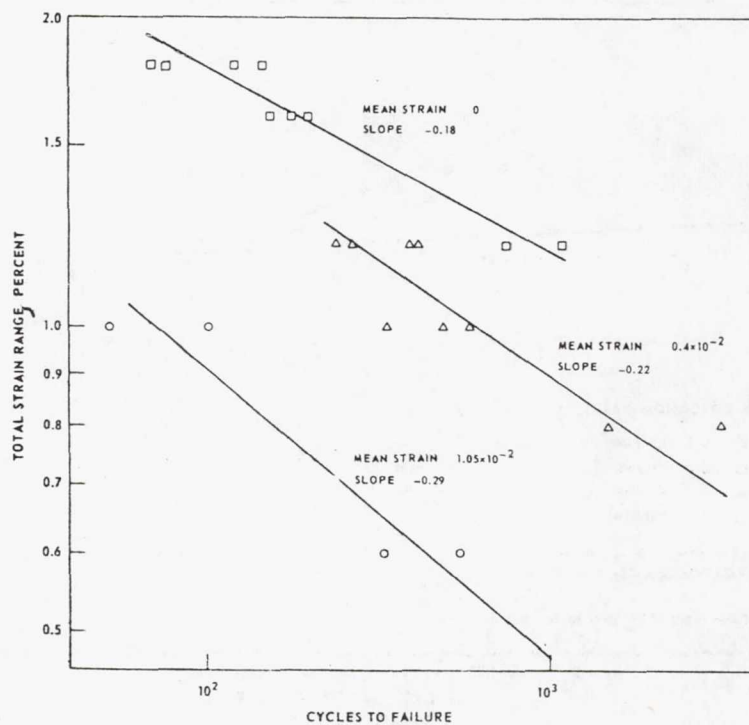


Figure 22.- Low-cycle axial fatigue of  $\text{Al}_3\text{Ni}$  whisker-reinforced aluminum (from ref. 4).

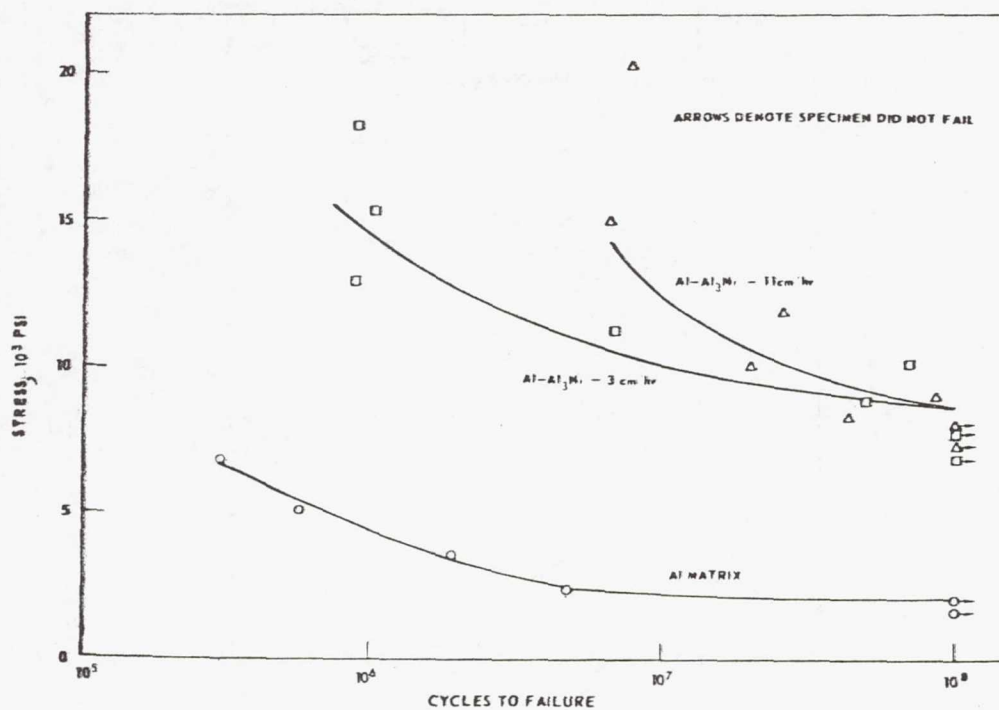


Figure 23.- Flexural fatigue behavior of Al-Al<sub>3</sub>Ni in air (from ref. 4).

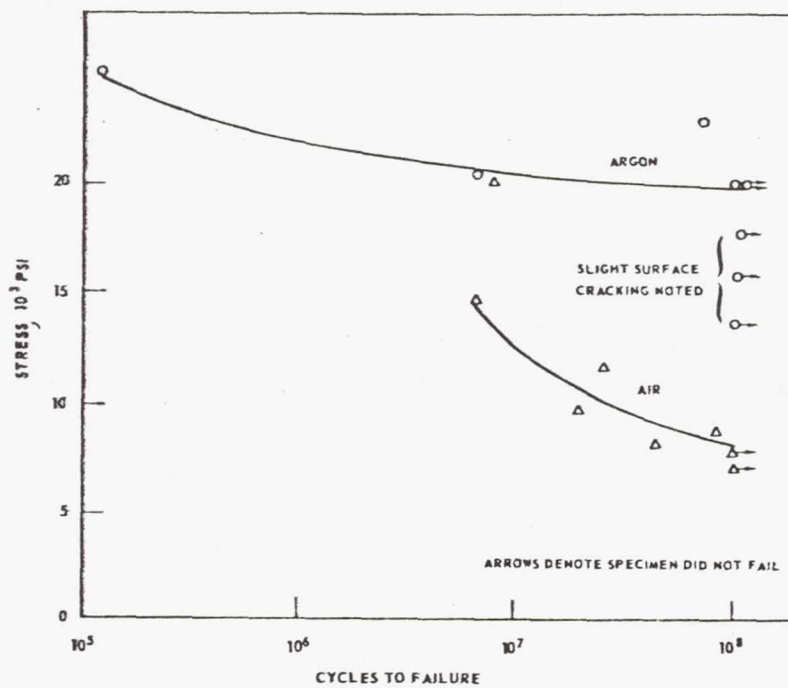


Figure 24.- Effect of environment on the flexural fatigue behavior of Al-Al<sub>3</sub>Ni (from ref. 4).



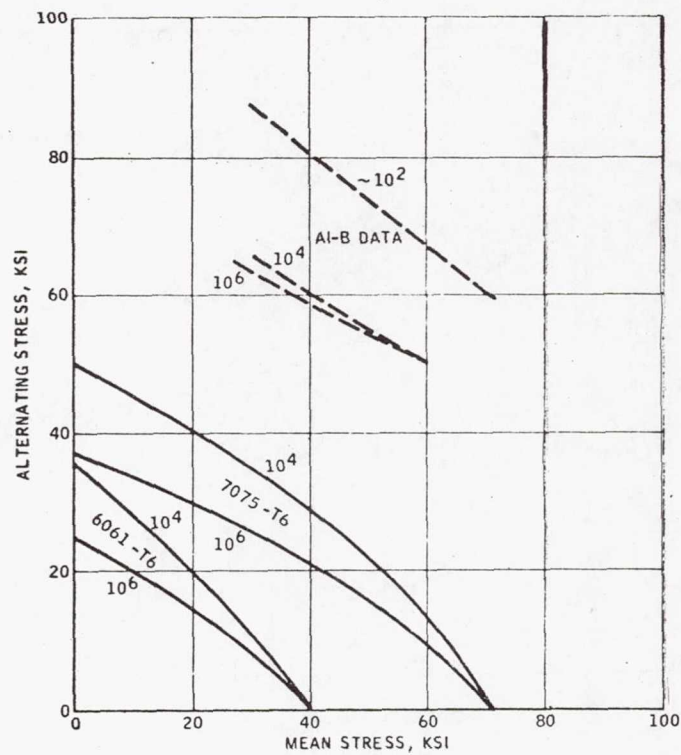


Figure 25.- Fatigue behavior of 40 volume percent boron-reinforced 6061 aluminum, compared with unreinforced aluminum alloys (from ref. 57).

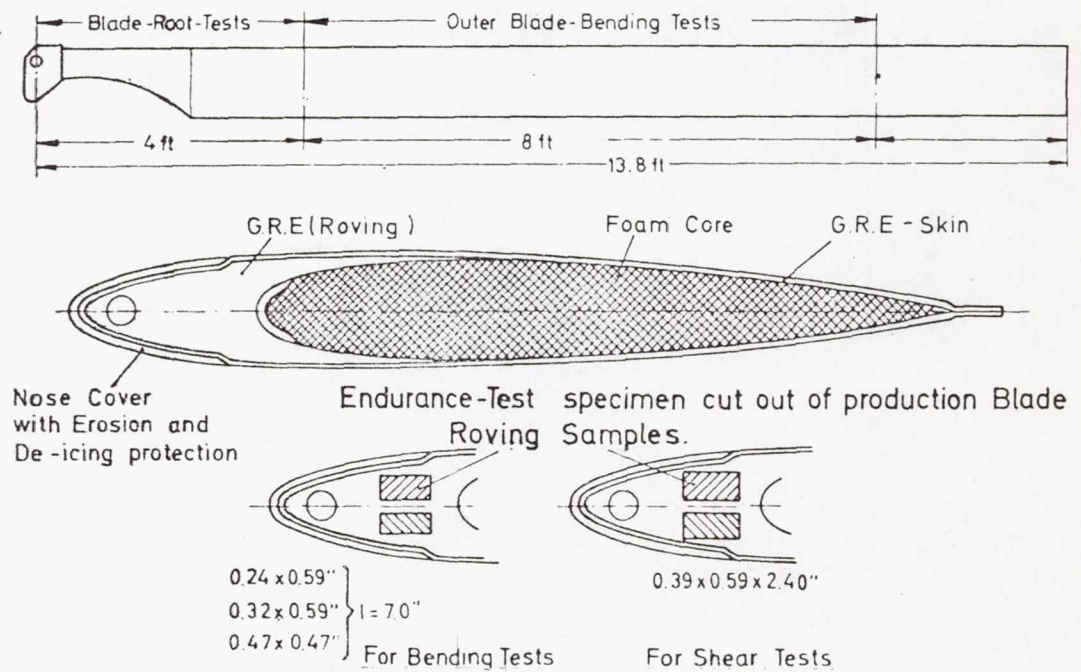
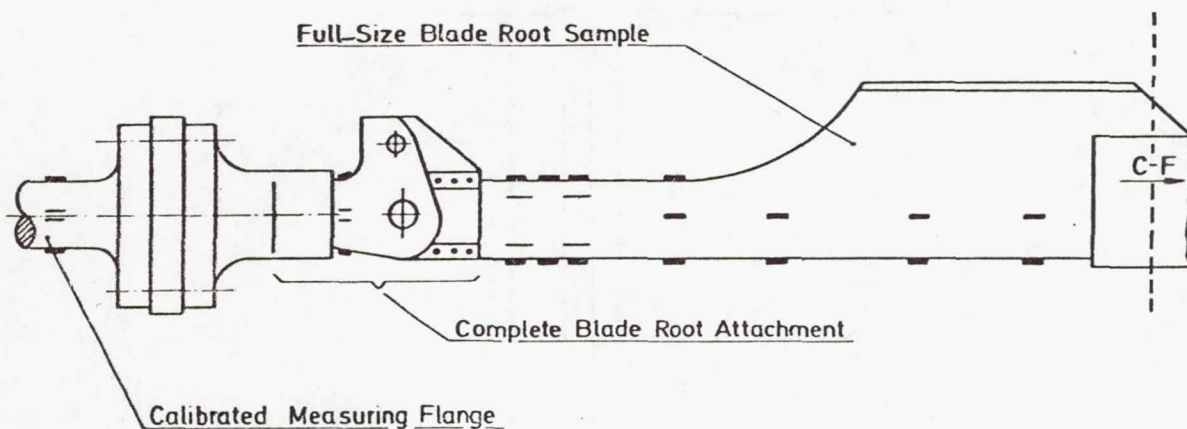


Figure 26.- Glass/epoxy BO-105 rotor blade (from ref. 62).



$$M_{\text{flap}} = M_{\text{lag}} \approx 1900 \div 2600 \text{ ft-lbs}$$

$$\text{Tension (C.F.)} \approx 12 \text{ t}$$

Figure 27.- Root-end fatigue test specimen of BO-105 rotor blade (from ref. 62).

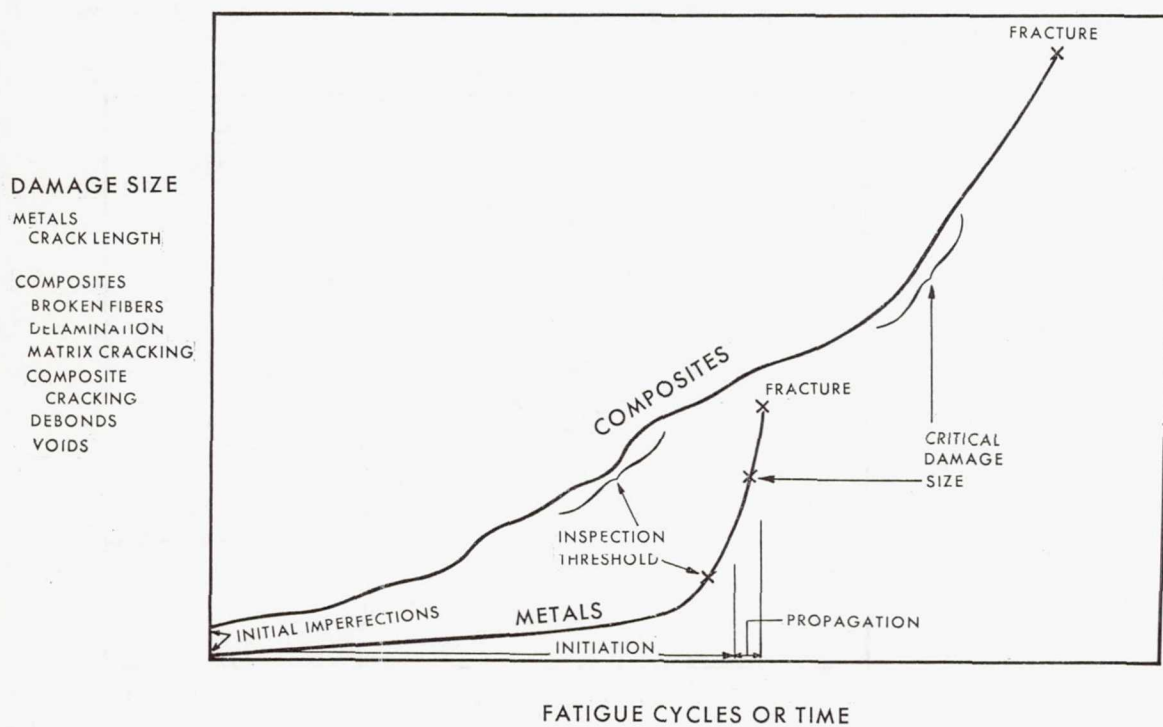


Figure 28.- Comparison of fatigue behavior in metals and composites.



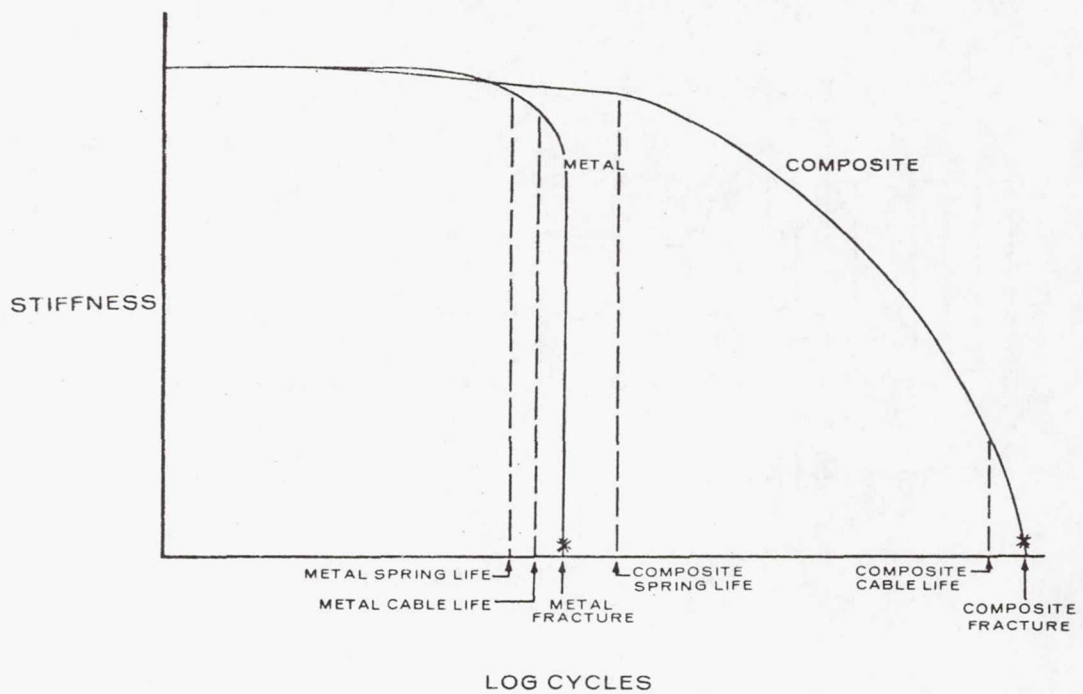


Figure 29.- Schematic fatigue behavior comparison of spring and tension cable made of metal or composite.

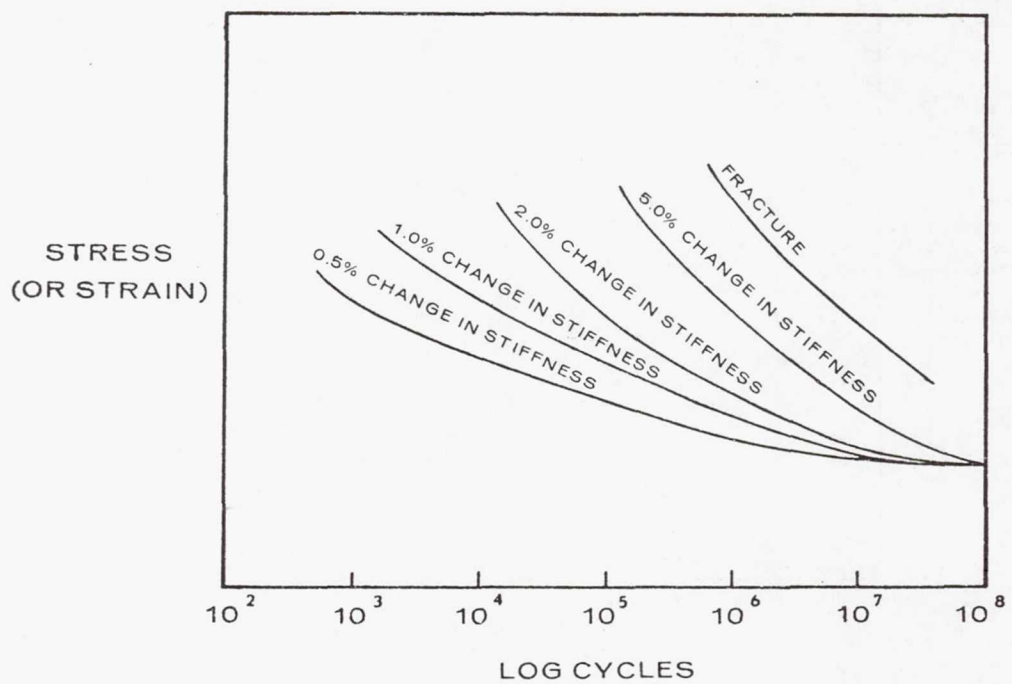


Figure 30.- Proposed method for reporting composite fatigue data.

# FATIGUE DESIGN PROCEDURE FOR THE AMERICAN SST PROTOTYPE

By Ralph J. Doty

The Boeing Company, Seattle, Washington, U.S.A.

## SUMMARY

For supersonic airline operations, significantly higher environmental temperature is the primary new factor affecting structural service life. Methods for incorporating the influence of temperature in detailed fatigue analyses are shown along with current test indications. Thermal effects investigated include real-time compared with short-time testing, long-time temperature exposure, and stress-temperature cycle phasing.

A method which allows designers and stress analyzers to check fatigue resistance of structural design details is the primary theme of this paper. A more communicative rating system is presented which defines the relative fatigue quality of the detail so that the analyst can define cyclic-load capability of the design detail by entering constant-life charts for varying detail quality. If necessary then, this system allows him to determine ways to improve the fatigue quality for better life or to determine the operating stresses which will provide the required service life.

A supersonic vehicle structure, which is subject to major airload center-of-pressure shifts as well as to the addition of thermal-gradient stresses to mechanical stresses, experiences a relatively large percentage of damage from ground-air-ground (GAG) cycles. In studying the 1g thermal-gradient history of a design detail, the analyst will produce a 1g stress history. Application of simple factors to this history allows determination of dynamically instantaneous maximum and minimum stresses statistically realized once per flight which represent the GAG cycle. The relationship of GAG damage to total damage on various parts of the vehicle is used to facilitate a quick fatigue-resistance check.

A quick fatigue-check method for designers and stress analysts benefits the design by making designers and stress analysts more cognizant of fatigue problems throughout the detail design phase of an aircraft development.

## THE PROTOTYPE TASK

At the 1967 ICAF meeting in Melbourne, Australia, the philosophy and scope of an integrated program of analysis, development testing, and verification testing for the American supersonic transport (SST) were presented. Since that time the program has developed to the point where the prototype configuration is being designed and fabricated. Figure 1 shows the SST in take-off and cruise configuration and figure 2 gives an idea of



the structural configuration. Attention to fatigue and fail-safe requirements in the detail design of the prototype will assure a structure representative of the 50 000 flight hour and 20-year service life design goal for a production SST.

If a total SST program schedule is reviewed, the significant location of the prototype job becomes apparent. Figure 3 presents the essential schedule elements. A 30- to 40-year time span is needed to include a 20-year operating period. The prototype design release, which is labeled NOW on figure, comes fairly early in the program after a company study period, a research and competition period, and a prototype design development period. Careful planning and implementation of investigation programs with extensive testing will provide the required structural confidence for the production design. For the prototype, fatigue resistance representative of production design must be engineered into the structure with a strictly fundamental analysis without a great depth of titanium structural component tests. This paper presents the basic tools used along with discussion of the significant factors affecting fatigue and how they are accounted for in the prototype design.

Good fatigue design is most effectively accomplished when both designers and design analysts understand and implement fatigue requirements in the drawing release process. Design analysts on the SST prototype are required to check their designs for production requirements specifying 50 000 flight hours of normal usage. The projected composite airplane usage includes 49 250 hours of revenue service used in 22 000 flights and 750 hours of training containing 1500 full-stop landings and 2600 touch-and-go landings. Application of these service life requirements in addition to other loads criteria truly makes the prototype design an exercise in production design.

The fatigue analysis procedure, made available to the design analyst in handbook form, allows him to determine the service life capability quickly. A rating system which gives the relative fatigue quality of a design detail so that the analyst can determine cyclic-load capability by entering constant-life charts for varying detail quality is presented. Consequently, he can determine whether to improve quality for known life improvement or to establish operating stress levels which will provide satisfactory service life. With a minimum of experience with different details, an engineering understanding of relative fatigue values is developed.

## THE SUPERSONIC TRANSPORT FATIGUE PROBLEM

In the transition from subsonic to supersonic transport operations, the major new parameter influencing structural fatigue resistance is elevated-temperature exposure. There are many other more subtle influences in this operational transition, but the thermal environment necessitates development of new tools for fatigue-performance evaluations.



Figure 4 shows schematically a comparison of equidistant subsonic and supersonic transport operations. The supersonic mission is clearly a high-speed high-altitude type of operation with a lower percent of time spent in cruise operation. High-altitude operation puts the SST in a less damaging gust environment during cruise. Also, because the SST must be designed for efficient high-speed supersonic cruise, the effects of relatively large center-of-pressure shifts between the subsonic and supersonic operation are apparent on this type of vehicle. When the relative parts of the damage resulting from gust, maneuver, taxi, take-off, landing, and ground-air-ground (GAG) operation are considered, it is apparent that a large part of fatigue damage will be due to the GAG cycle on critical parts of the primary wing and body structure. This conclusion is used to advantage in developing a simple fatigue-check procedure.

The subsonic operation produces no significant thermal environment but supersonic operation at Mach 2.7 subjects the airplane to a stagnation temperature of 500° F. Figure 5 shows the stabilized temperatures existing during cruise. Realizing that the mission requires climb and acceleration into and finally descent and deceleration from such a condition, the design analyst knows that fatigue analysis must account for many thermal effects. For convenience in the development of analytical procedures, the total thermal effect will be evaluated as thermal-gradient loading, long-time temperature exposure, and an interrelated cyclic exposure of stress and temperature.

After analysis of projected operational SST route structures, a mean mission was selected to establish representative fatigue damage for the SST prototype structural design. Figure 6 shows the details of this mission. The consequences of this operation on a structural detail are illustrated in figures 7 to 9. Figure 7 shows a typical 1g stress and external temperature history at a wing lower surface location. Figure 8 shows the thermal-gradient stress and temperature history as it will develop on two types of typical wing surface structures. Figure 9 shows a combined total stress and temperature history for the structural detail being analyzed. The design analyst studying the load and temperature effects on any structural detail will prepare these histories to understand his problem. These histories provide him with the initial tool leading into the fatigue-check procedure.

The first step in the analysis procedure is to define the stress level of a primary GAG cycle from the data obtained in producing figure 9. It is not the intent of this report to discuss in detail the criteria loadings for gust, maneuver, taxi, take-off, and landing. However, with a clear definition of a GAG cycle, a statistical factor can be determined to apply to the maximum and minimum stresses of figure 9 to establish dynamically instantaneous maximum and minimum stresses that are realized 1000 times in 1000 flights. These factors, indicated in figure 9, are used by the design analyst to establish the stress limits of a primary GAG cycle.



From the general aspect of fatigue analysis the analyst now has viewed the effects of the thermal cycle associated with supersonic flight and has established the GAG stresses for his design detail. It is now important to again realize that temperature is the primary new factor affecting fatigue and that the balance of the factors affecting fatigue are handled in the same manner as those on subsonic transports. Consideration of the primary factors affecting service life will point out how they are evaluated and how the effect of the thermal cycle is included in the analysis.

### FACTORS AFFECTING SERVICE LIFE

Based on broad scope categories, the primary factors influencing service life of an operational vehicle are

- (1) Selection of structural material
- (2) Type of design and fabrication
- (3) Service reliability
- (4) Operational environment

Each of these categories is handled in a particular manner to facilitate the application of a fatigue-check procedure at the point of drawing release.

All factors associated with the SST mission, service life, and vehicle production are considered in selecting the structural material. Annealed Ti-6Al-4V was selected as the primary structural material because good fracture and fatigue properties are combined with a good strength-weight ratio, particularly in the SST operating environment. High-strength steels, as applicable, augment the primary structural material. For analysis purposes, after the selection decision, the material is represented by S-N curves for varying quality of structure. In addition, when considering service reliability, the level of backup test and service knowledge for the material and type of detail application influence the selection of reliability factors.

Type of design and fabrication with its many facets is controlled in this procedure by establishing a detail fatigue rating (DFR) number. Effectively, the DFR of a design will direct the analyst to the correct quality of S-N data for determining the service life. Surface finish, fabrication techniques, geometric design details, fastener installations, and design assembly patterns are typical influencing factors determined by the type of design and fabrication. Based on test data and service experience, DFR values are determined with formulas or established in charts.

Service reliability must account for the variability of fleet statistics, loading environment, test representation, and structural material properties. In a well defined loading environment on a fail-safe design detail with good test and service background,

the analyst can consider going as low as 2.0 for a fatigue reliability factor (FRF) to be applied to specified life for analytical life requirements. As background data becomes minimum in the design of a good fail-safe structure, FRF values of 4 to 6 are required. In cases where fail-safe design is difficult or impossible, safe-life design must be developed with FRF values twice those that would be required for fail-safe design. For the analysis procedure, FRF values are specified in general terms and the design analyst consults with fatigue specialists if further refinement is necessary.

The operational environment is usually well defined at the current state of development of specifications and investigation studies. Gust, maneuver, taxi, take-off and landing criteria for the SST are very much like that required for subsonic vehicles with fairly well defined adjustments to account for SST operation. The airline operation effects are included by developing a pattern of missions to represent the total scope of SST operation. The means of including all these effects in determining service life are practically the same for subsonic and supersonic operation and have been developed from a history of subsonic transport operation. The new influence on service life not significantly present in subsonic operation, is the thermal cycle associated with a Mach 2.7 transport. The effects of this thermal cycle require special attention to assure a proper accounting in analytical procedures.

## ENGINEERING THE TEMPERATURE EFFECTS

Investigations of thermal cycle considerations required for Ti-6Al-4V structure in environments in the region of 500° F indicated that developing the following areas of influence will properly account for the thermal cycle: real-time and short-time test correlation, long-time temperature exposure, and phase-cycle relationship of temperature and stress. As indicated in figure 9, the mechanical stress and thermal-gradient stress are added directly when studying the history of stress with temperature on a design detail. Consideration of these factors shall provide the corrections necessary to account for thermal effects.

Temperature and time have always been two variables strongly related in establishing material properties. Some indication of real-time and short-time test correlation is shown in figure 10. Initial testing reported under this Department of Transportation contract began in 1963 and is continuing at this date. The program data shown here was designed to compare a 65-minute flight cycle with three accelerated tests. An accelerated load spectrum was run at 90° F constant temperature, 500° F constant temperature, and a 90° F to 500° F cyclic temperature. The accelerated tests on sheet and extrusion material both showed a deterioration in life at higher constant temperature and also showed deterioration at cyclic temperature, although not as great as at 500° F constant temperature. Real-time tests have completed in excess of 36 000 flight cycles, only one



sheet specimen out of a total of 12 sheet and extrusion specimens failing. These test results encourage further analyses with a hope that accelerated tests may correlate with real-time tests somewhere near a factor of one. Testing is continuing and other tests are underway to augment this data.

The effect of long-time temperature exposure was conveniently included in the basic S-N data by developing the data with specimens previously exposed to 500° F for 500 hours. This procedure is justified by data shown in figures 11 to 13. Figure 11 shows the ratio of exposed to unexposed cyclic maximum stresses and gives  $10^5$  cycles of life at a stress ratio  $R = 0.06$  for Ti-6Al-4V baseline specimens heat soaked for the indicated hours and then tested at room temperature. Figure 12 shows the same ratio for Ti-6Al-4V lap joints with varying fastener installations exposed to both load and temperature for 500 hours and 1000 hours. These data demonstrate a reduction in allowable stress for equivalent life with temperature exposure for 500 hours. Further exposure produces little change. Figure 13 shows results of similar more extensive testing conducted in Ti-8Al-1Mo-1V center-notched specimens exposed to both steady-state and cyclic load and temperature. In this case subsequent fatigue testing is at 500° F after the specified exposure. With varying exposure up to 20 000 hours cyclic and 30 000 hours steady state, all data, independent of how much exposure, falls into a reasonable scatter band. For analysis of the SST prototype, this type of data justified a convenient, 500° F, 500 hours (3 weeks) exposure before life testing. Thus, the effect of long-time temperature exposure is included in the S-N curves used for fatigue-check analysis.

In the accelerated test data of figure 10 with the same maximum temperature, there is an indication that fatigue life improved over that at constant temperature when temperature and stress were both cycled. From many sources the data of figure 14 establishes a life ratio curve for life at constant elevated temperature. A comparison in figure 15 of this curve with data from tests wherein temperatures were cycled in phase with stress, shows an improvement in fatigue life for the 0° phase difference stress-temperature cycle. Extending this basic idea through all phase-angle differences develops the life ratio factor  $\eta$  of figure 16 as a means to correct service life computations for variations of the phase angle between stress cycles and temperature cycles. The design analyst reviewing his temperature and stress history, in addition to determining GAG stress limits, must determine the maximum temperature and the significant phase-angle difference between his stress and temperature flight cycle.

In order to engineer temperature effects into a simplified fatigue-check procedure for prototype design, the following guidelines are offered:

- (1) Accelerated test procedures can be established to assure real-time and short-time test correlation near a factor of one.

(2) Long-term temperature exposure is accounted for by exposing test specimens for S-N data to 500° F for 500 hours and then testing at room temperature.

(3) The stress-temperature cycle phasing correction factor  $\eta$  of figure 16 will account for the balance of temperature effects.

#### TOTAL DAMAGE RELATED TO GAG DAMAGE

Since a method has been provided for the design analyst to define the primary GAG stress cycle, one key to establishing a quick fatigue-check procedure is to relate total damage to GAG damage on the elements of primary structure. By extensive use of computer programs to define internal load distribution and conduct fatigue analysis on discrete parts of typical primary structure, the ratio  $\delta$  of GAG fatigue damage to total fatigue damage can be determined. Typical plots of the GAG damage ratio developed for handbook use are shown for the wing lower surface in figure 17 and for the body sections in figure 18. It is now possible to set up a simple formula which determines a number of GAG cycles  $N_{GAG}$  which will produce equivalent total fatigue damage.

$$N_{GAG} = n_{GAG} \frac{(FRF)}{\eta \delta}$$

where

$N_{GAG}$  number of cycles to produce equivalent total fatigue damage

$n_{GAG}$  the number of flights in which the primary GAG cycle is determined for a 50 000 flight hour service life, or where a primary GAG cycle is not apparent, a number of primary load cycles in a 50 000 flight hour service life for which the damage ratio  $\delta$  is known or can be estimated

FRF fatigue reliability factor defined in handbook tables

$\eta$  ratio of fatigue life at stress-temperature cycle phasing to room-temperature fatigue life

$\delta$  ratio of GAG fatigue damage to total fatigue damage

Since  $N_{GAG}$ ,  $GAG \sigma_{MAX}$ , and  $GAG \sigma_{MIN}$  are known, it is now necessary to determine the proper quality level of S-N data which can be used to determine service life.



## RATING OF STRUCTURAL DETAILS

It has been common practice to rate structural details by determining apparent stress concentration factors  $K_T$  and using S-N curves with the same apparent stress concentration factor to determine fatigue life of that detail. Many textbook and handbook sources are available to determine apparent stress concentration factors. For communication to the design analyst, who likes to do his thinking with loads, load paths, and stresses,  $K_T$  gives some feel for fatigue quality but does not necessarily provide good communication. High values of apparent stress concentration  $K_T$  give low values of service life. The quantity  $K_T$  defines some local magnification of stresses that reduce life. Although for calculation purposes the detail fatigue ratings (DFR) defined in this report depend on values of  $K_T$ , DFR values are a more useful communication term with an engineering feel closer to the design analyst's pattern of thinking.

The DFR number found useful in this report is defined as the maximum cyclic stress  $\sigma_{MAX}$  in a constant-amplitude loading cycle at which the design detail will withstand  $10^5$  cycles at a stress ratio  $R$  of 0.06. This stress ratio is a convenient testing ratio and  $10^5$  cycles represents a reliability factor of 4 on 25 000 flights, which is near the fatigue life range of significance on the SST prototype. Figures 19 and 20 show ranges of value of the DFR number for various detail coupon tests and for various lap joint tests, respectively. If this DFR number is plotted against  $1/K_T$  for variations in a type of structural detail, it will develop, within test scatter, as a straight line, as shown in figure 21. Consequently, for the convenience of the design analysts, tables can be produced with governing constants specified for various design details. Somewhat more convenient, as more test data and experience develops, charts similar to figure 22 are prepared and added to the analysis handbook.

For communication purposes the DFR number communicates a stress number; the greater it is, the better the fatigue quality. A value of 65 ksi is high quality in Ti-6Al-4V structure and is achieved in basic skin-stringer structure with high-quality fastener installations. Low-quality values can go below 20 ksi in the low-quality joint installations.

The significance of the DFR number in specifying S-N data is illustrated in figures 23 and 24. Figure 23 is a set of S-N curves for a DFR of 30 ksi and figure 24 is for a DFR of 45 ksi. In each case this rating number establishes the relative quality of each set of curves by being the  $\sigma_{MAX}$  giving  $10^5$  cycles at  $R = 0.06$ . If on each plot the design analyst considers a design detail for which he has determined  $GAG \sigma_{MAX} = 50$  ksi and  $GAG \sigma_{MIN} = 20$  ksi, the service life variation is apparent. ( $\sigma_{MIN}$  is the minimum cyclic stress.) At DFR = 30 ksi, the fatigue life is about  $5 \times 10^4$  cycles; at DFR = 45 ksi, the fatigue life is about  $2 \times 10^5$  cycles. The higher quality provides four times the fatigue life.

## CONSTANT-LIFE CHECK CHARTS

After development of a family of S-N curves for a range of design quality, it is a simple procedure to prepare detail fatigue-check charts for a range of constant-life values. As shown for  $N = 10^5$  cycles in figure 25, this procedure allows a plot of the two variables,  $GAG \sigma_{MAX}$  and DFR, in a form most useful to the design analyst. These two variables plot as a family of lines for different values of stress ratio. With a family of these detail fatigue-check charts covering the range of cyclic interest, interpolation can be conducted for a design detail at any  $N_{GAG}$  to establish the required relationship of DFR and  $GAG \sigma_{MAX}$  at a known value of  $R$ .

The design analyst can enter the fatigue-check charts with either  $\sigma_{MAX}$  or DFR and determine important design trades. Entering the chart with a calculated cyclic  $\sigma_{MAX}$  might represent a case where a desired level of working stress is apparent from other design considerations. Figure 26 illustrates this case and points out the design terms established for the case where  $N = 200\ 000$  cycles. The ordinate value defines a minimum detail quality required for this  $\sigma_{MAX}$ . If DFR is actually higher or lower, the design analyst moves up or down the  $R$  value line to determine an appropriate allowable  $\sigma_{MAX}$ . Entering the chart with a trial DFR is illustrated in figure 27. In either case the design analyst can quickly determine the value of improving his design quality or of changing his cyclic stress level.

## FATIGUE ANALYSIS PROCEDURE

The fatigue-check procedure is made available to each design analyst on the SST prototype by a structural fatigue handbook. By management directive, a design has not been structurally reviewed unless it has been checked for its repeated load environment as well as for its strength and stiffness requirements. Unless a specific exception can be justified for prototype only, the prototype design details shall qualify for the specified production service life of 50 000 flight hours.

To illustrate the fatigue-check procedure, assume the design analyst is looking at a wing lower surface skin-stringer detail forward of the rear spar at buttock line (BL) 550. (See fig. 17.) He would like to use standard rivet installations in order to minimize assembly costs. The procedure would be

(1) Following through the segmented sections of the mean mission of figure 6, computations of internal load distribution and the gradient effects of the thermal cycle will produce a normal operating stress and temperature history similar to that of figure 9. From such data the primary GAG stress cycle is determined as

$$\sigma_{MAX} = 25 \text{ ksi } (R = -0.5)$$



Also from a plot similar to figure 9 it appears that the stress-temperature phase relationship is near  $90^\circ$  with a maximum temperature of  $430^\circ$  F.

(2) It is now necessary to determine the number of GAG cycles  $N_{\text{GAG}}$  that will produce equivalent total fatigue damage. By referring to figure 16, the stress-temperature cycle phasing correction is

$$\eta = 0.85$$

By referring to figure 17, the GAG damage ratio is

$$\delta = 0.80$$

From handbook tables and test data considerations, the fatigue reliability factor for this detail in Ti-6Al-4V is

$$\text{FRF} = 5.8$$

Conservatively, including full-stop landings in the number of required flights,

$$n_{\text{GAG}} = 23\,500 \text{ cycles}$$

Consequently,

$$N_{\text{GAG}} = n_{\text{GAG}} \frac{\text{FRF}}{\eta \delta} = 200\,000 \text{ cycles}$$

(3) With  $N_{\text{GAG}}$  and  $\sigma_{\text{MAX}}$  at  $R = -0.5$  known, the design analyst enters figure 26 and determines the minimum DFR required to provide 50 000 flight hours of service life; that is, a required DFR of 40 ksi.

(4) With the geometric, fabrication, and installation details, the design analyst must determine the actual DFR. From figure 22,

$$\text{Actual DFR of } 56 \text{ ksi} > \text{Required DFR of } 40 \text{ ksi}$$

Therefore the installation provides more than satisfactory service life. If surrounding installations are compatible, weight may be removed from the installation by increasing stress levels to match the actual DFR. The weight reduction is only possible if static strength and stiffness requirements will permit.

If testing or previous experience had not provided a chart of DFR values for this installation, the structural fatigue handbook would have provided the constants needed in figure 21 to calculate an actual DFR. By the use of this procedure the design analyst can develop an understanding of the stress or detail quality modifications necessary to qualify for service life.

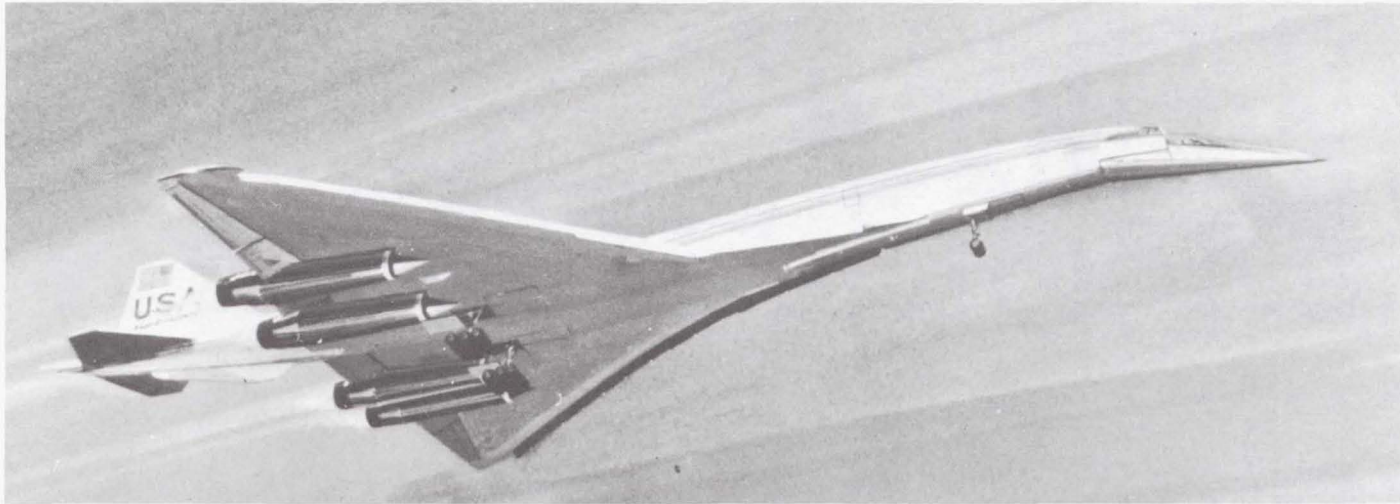
## CONCLUDING REMARKS

A fatigue-check procedure requiring minimum additional effort is proposed for use by design analysts who must review structure and "firm up" design details before drawing release. The concept presented here satisfies part of the need of having the designer of structural details cognizant of the good and bad points of design for service life.

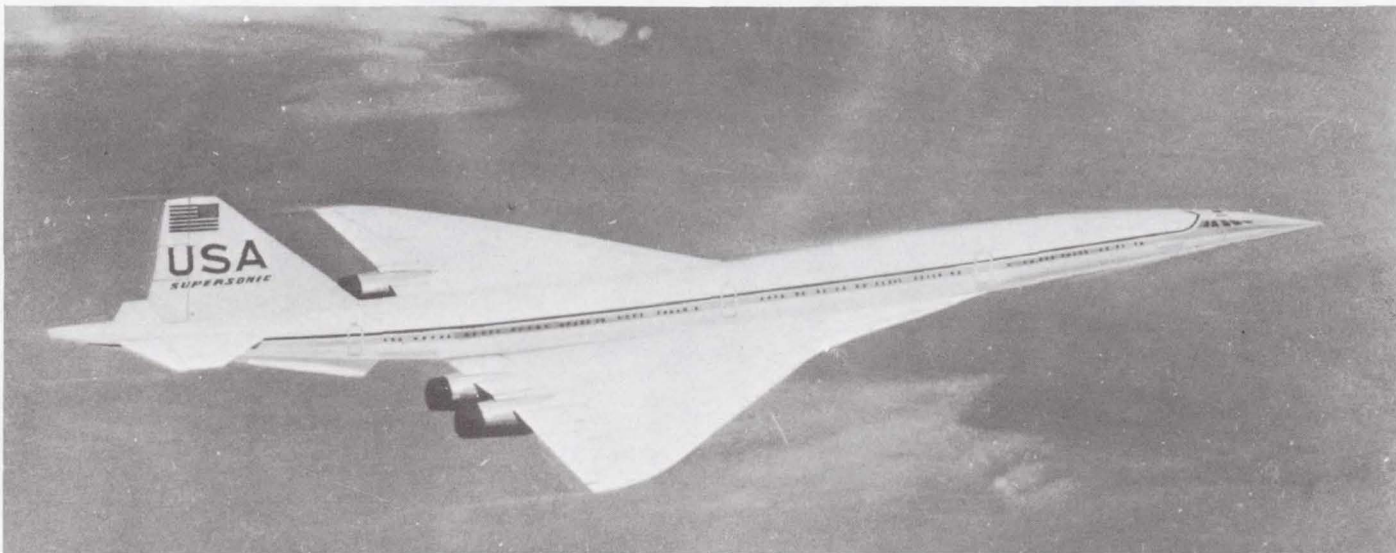
As compared with subsonic transports the primary new environment variable influencing fatigue design on the American SST is the thermal cycle associated with a Mach 2.7 cruise speed. The effects of this thermal cycle can be included in fatigue-check procedures by accounting for real-time and short-time test correlation, long-time temperature exposure, and phase cycle relationship of temperature and stress. Because of the SST type of operation, relatively large parts of fatigue damage develop on wing and body primary structure from ground-air-ground (GAG) cycles. By determining the relationship of GAG damage to total fatigue damage on typical primary structures, fatigue-check procedures can be greatly simplified.

By using a detail fatigue rating (DFR) designated by a maximum cyclic stress instead of using the apparent stress concentration factor directly, a better communication term is available to evaluate relative fatigue quality of design details.





TAKE-OFF



CRUISE

Figure 1.- The American supersonic transport.

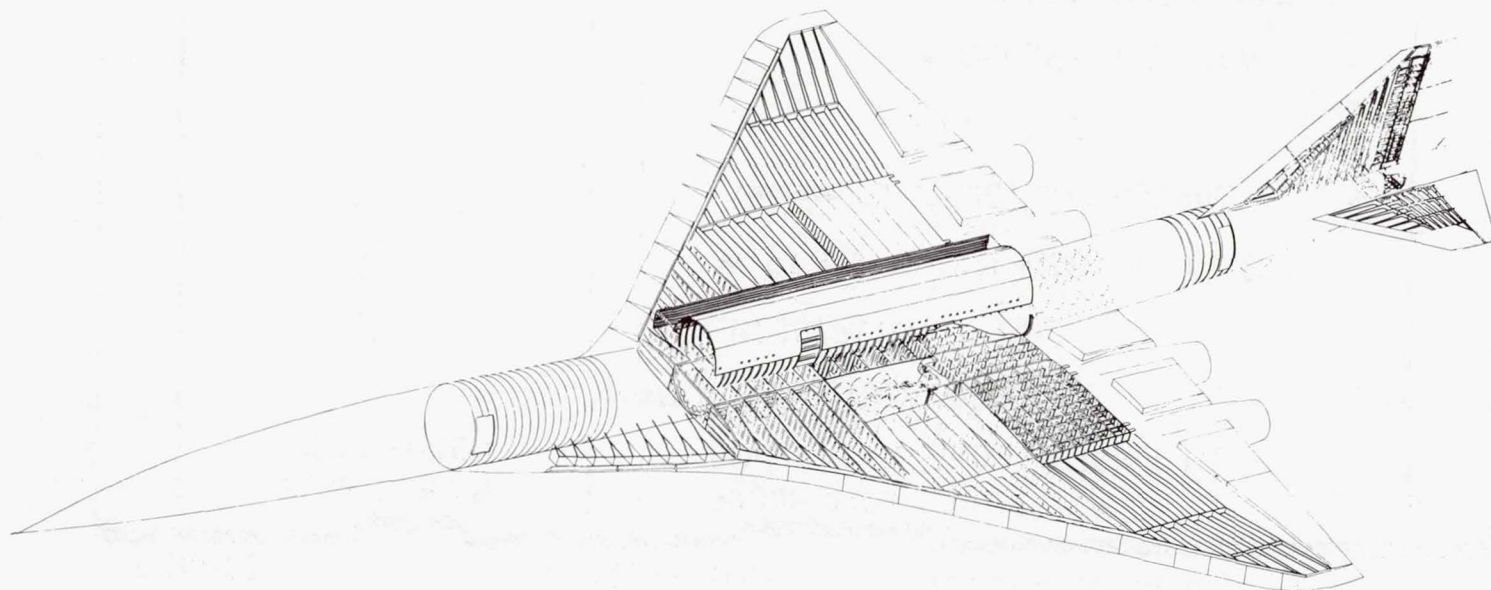


Figure 2.- Structural arrangement.



## SST PROGRAM SCHEDULE

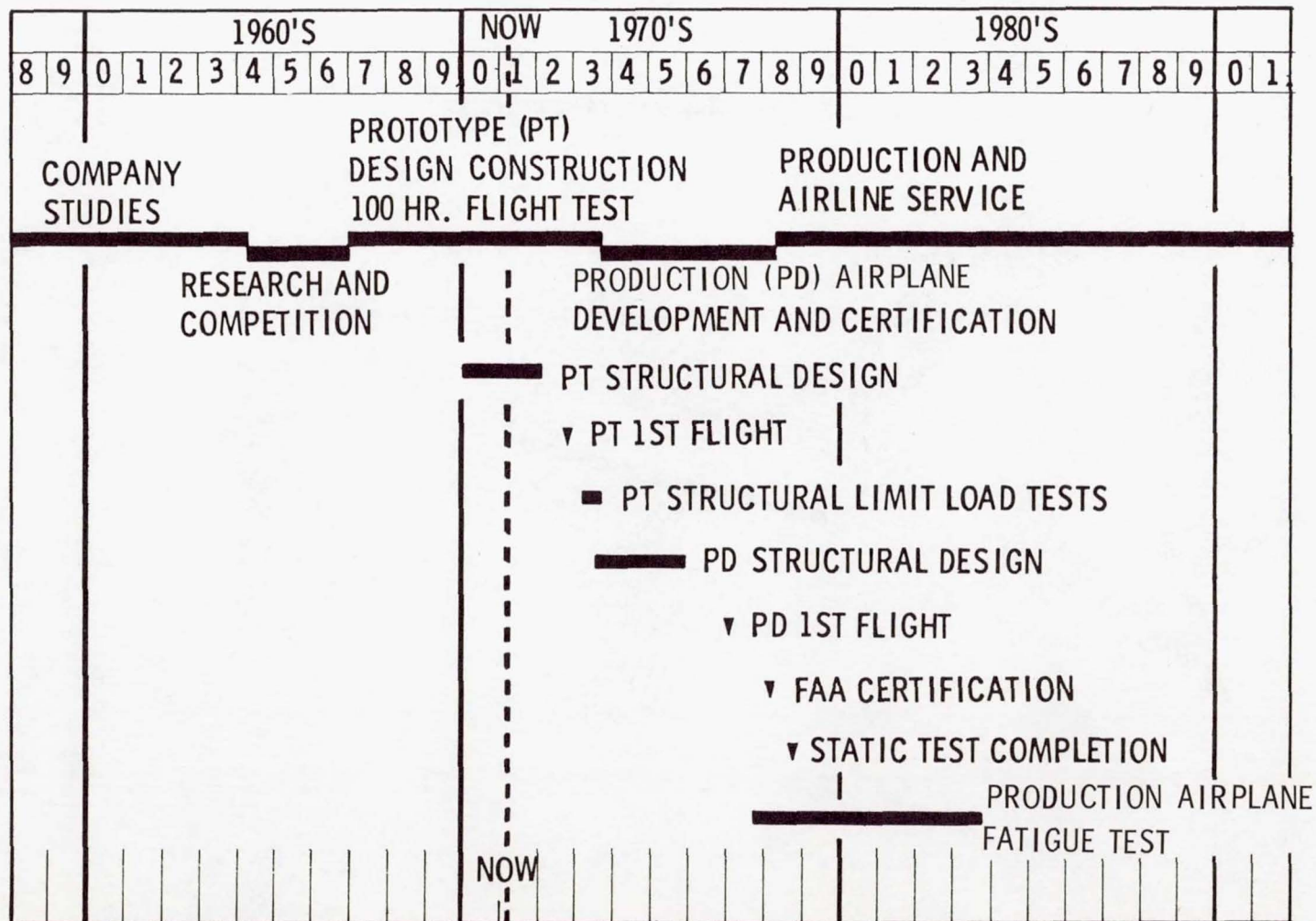


Figure 3.- SST program schedule.

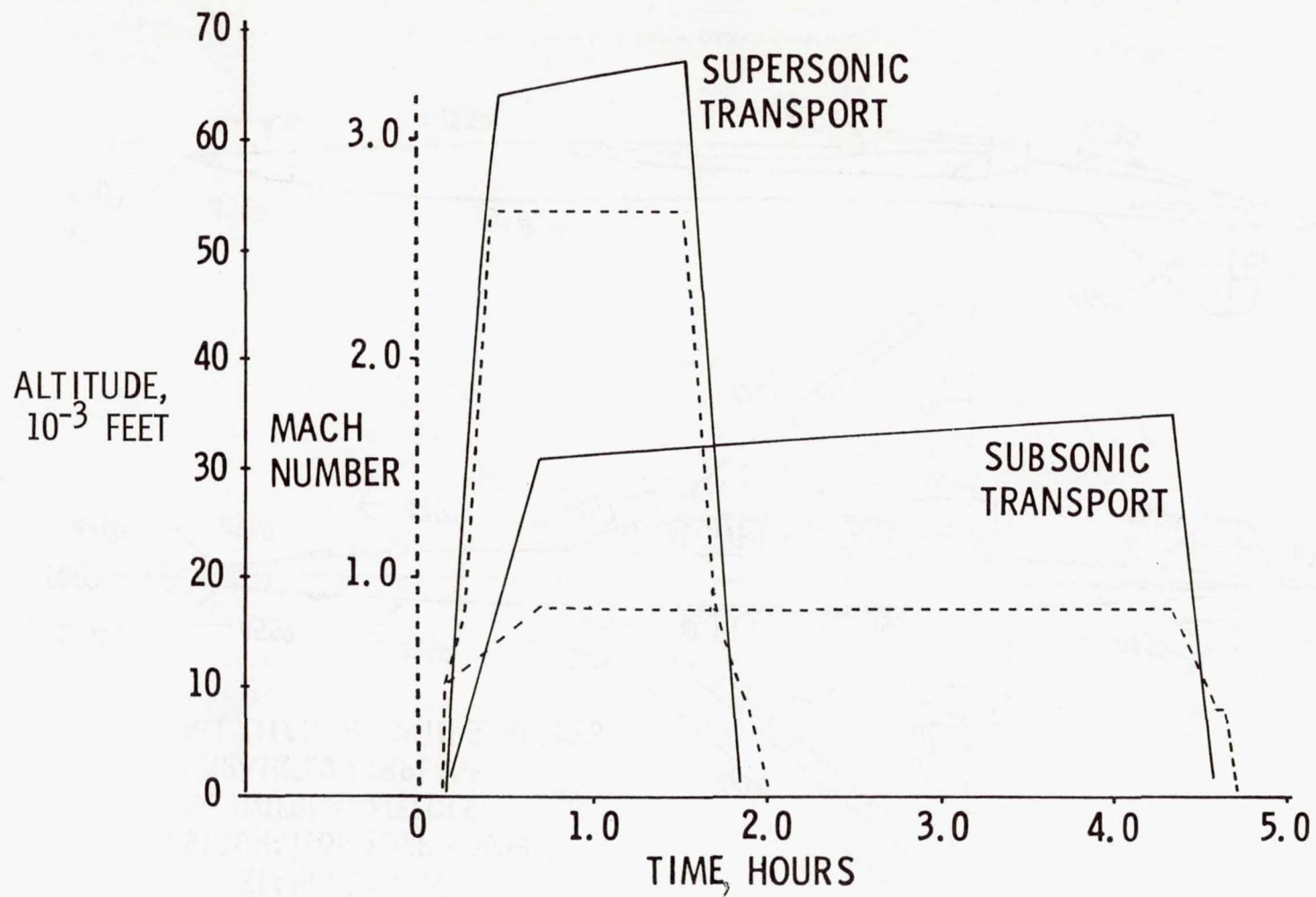


Figure 4.- Equidistant mission comparison.



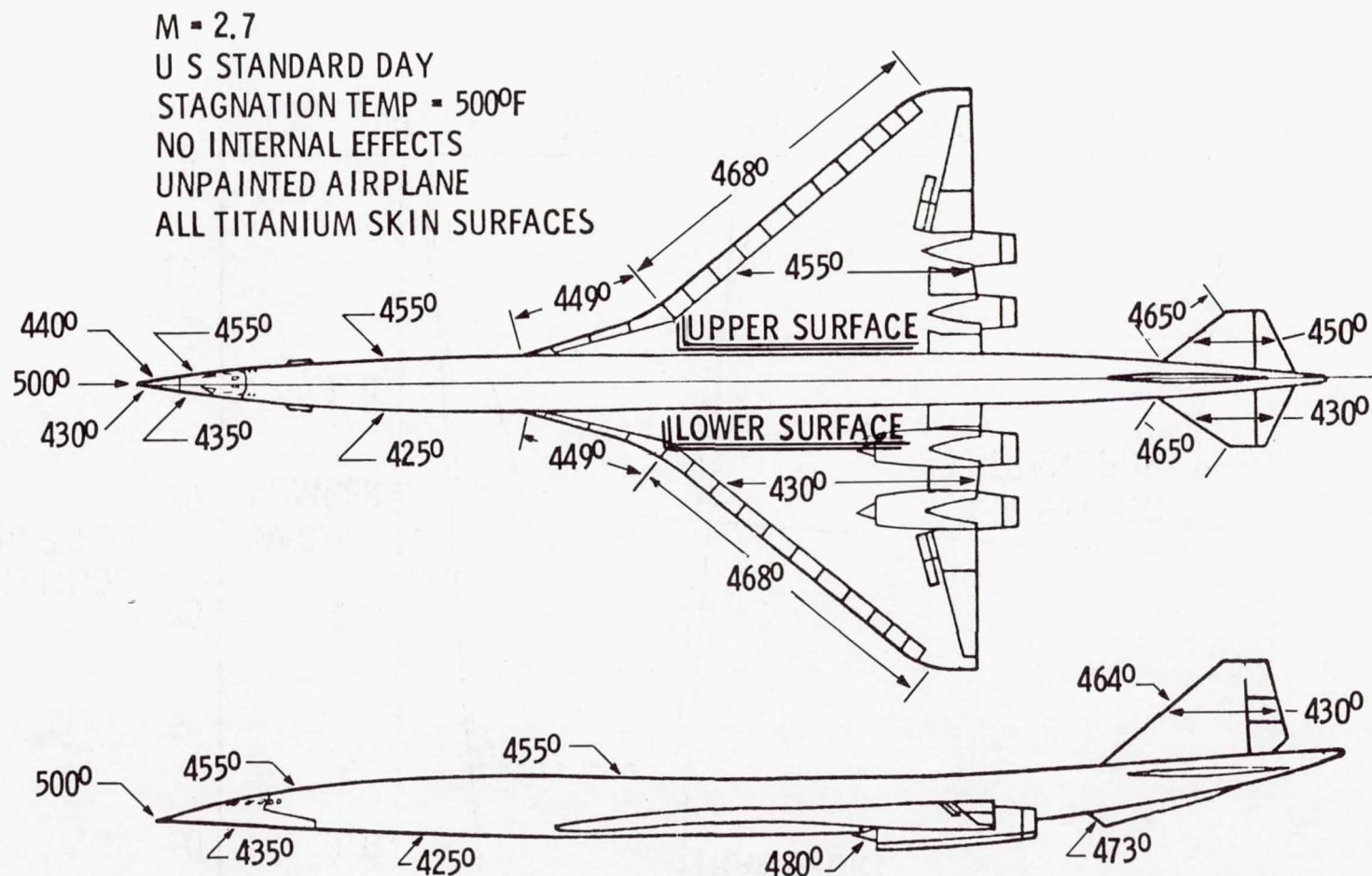


Figure 5.- Stabilized cruise temperatures.

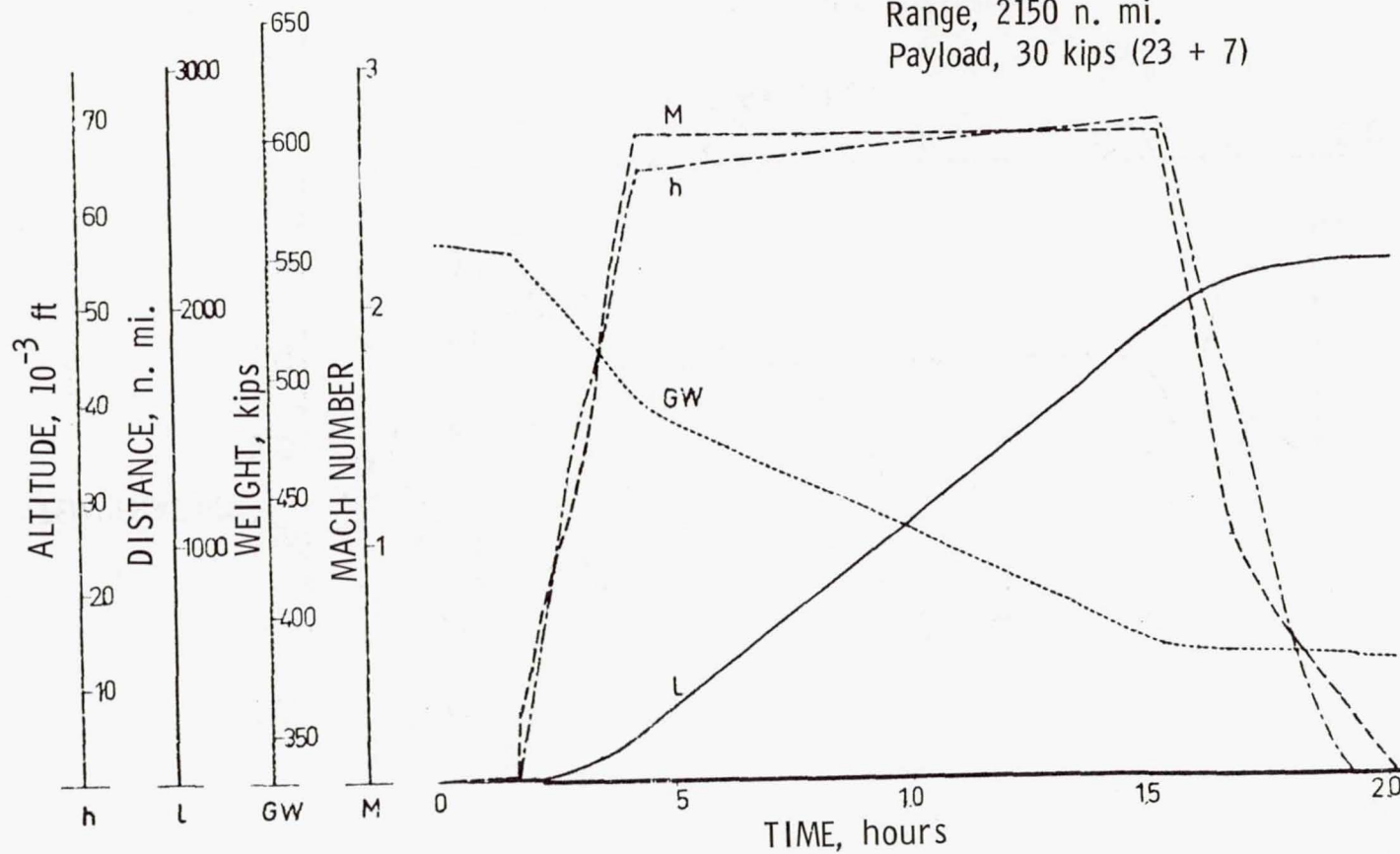


Figure 6.- Mean mission flight profile.



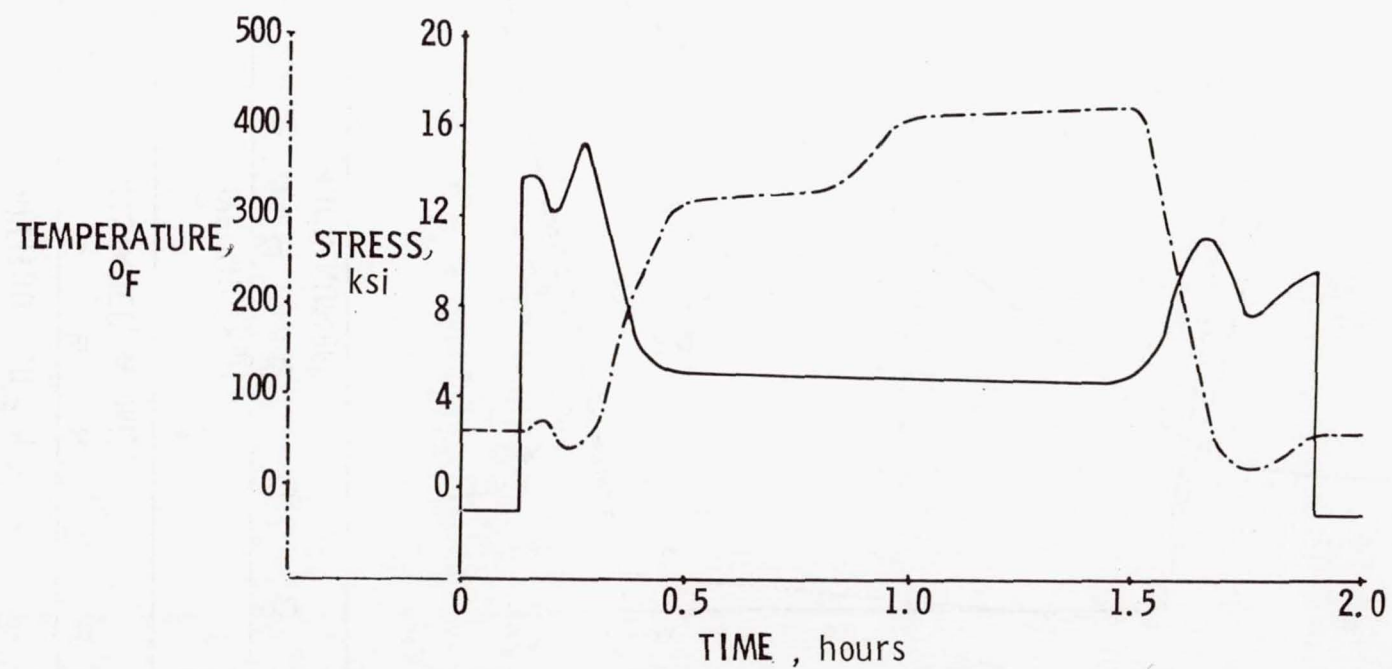


Figure 7.- Wing lower surface skin temperature and 1g stress.

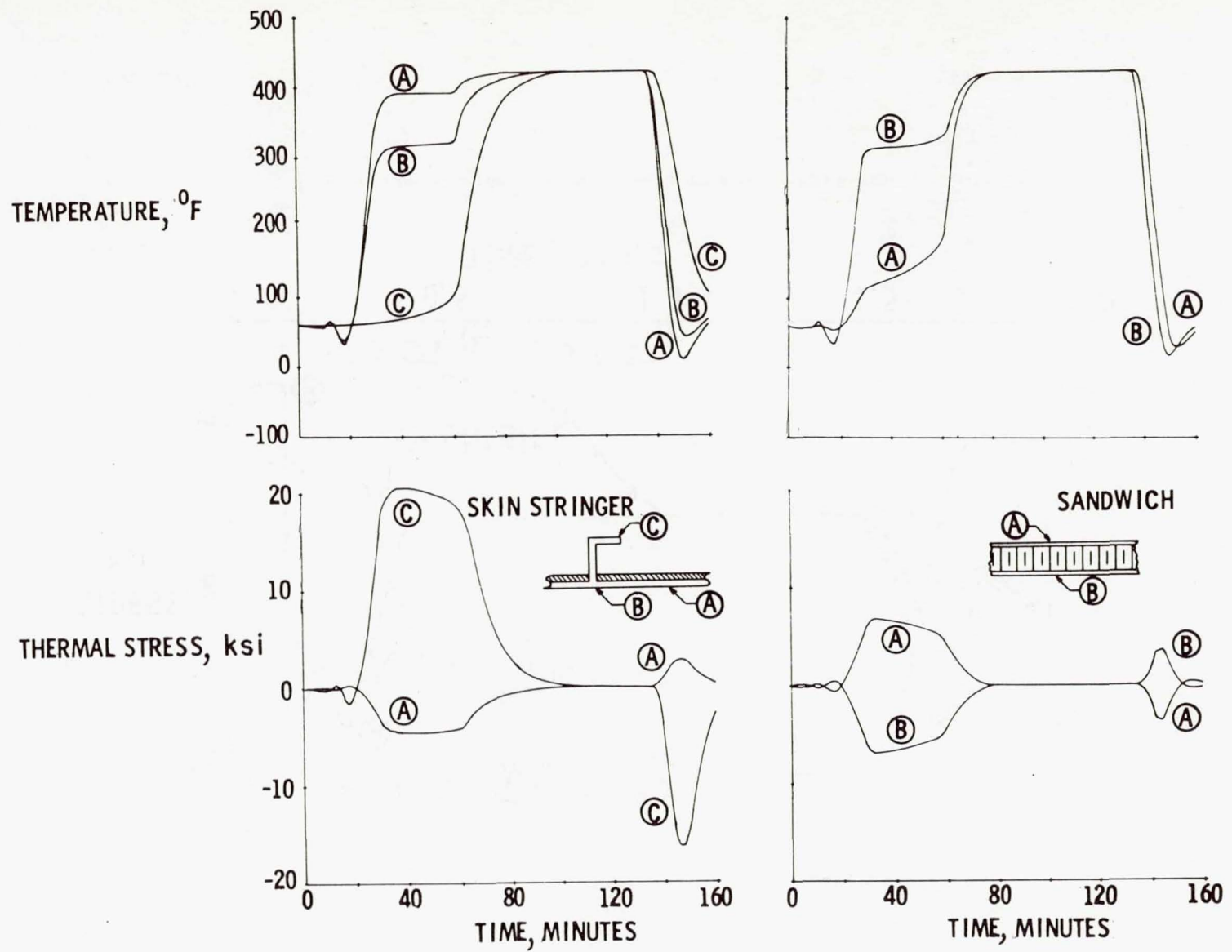


Figure 8.- Typical thermal gradient effects.



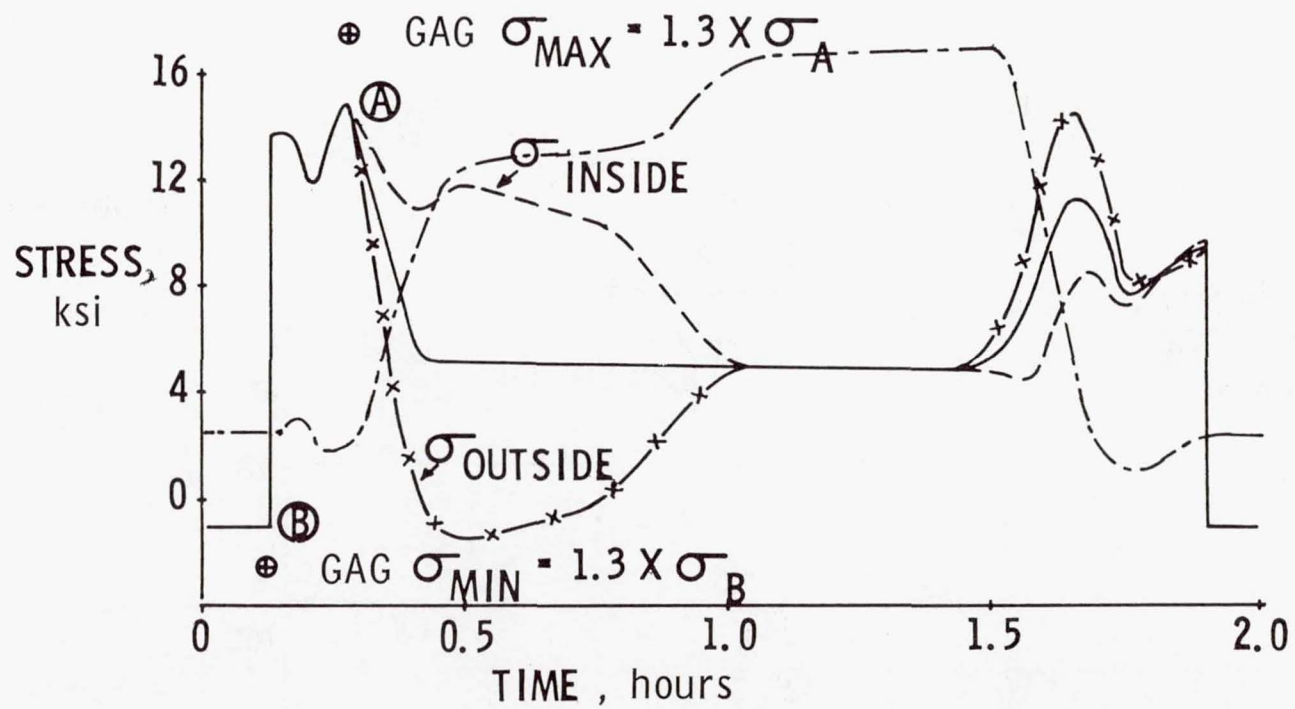
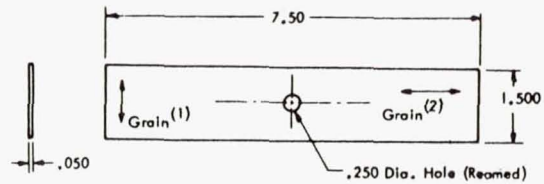
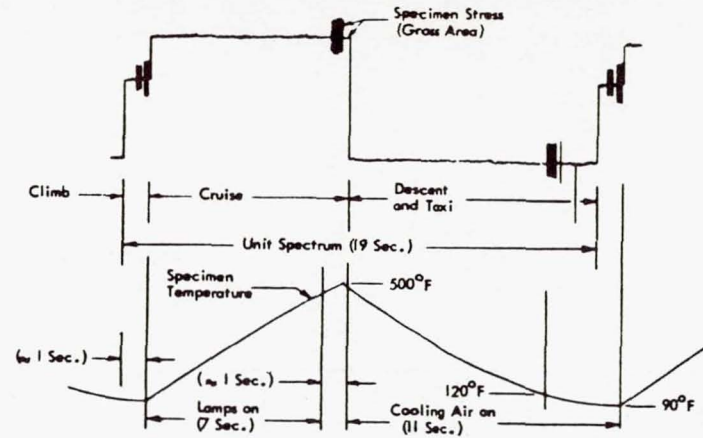


Figure 9.- Normal operation stress time history as influenced by thermal stress.

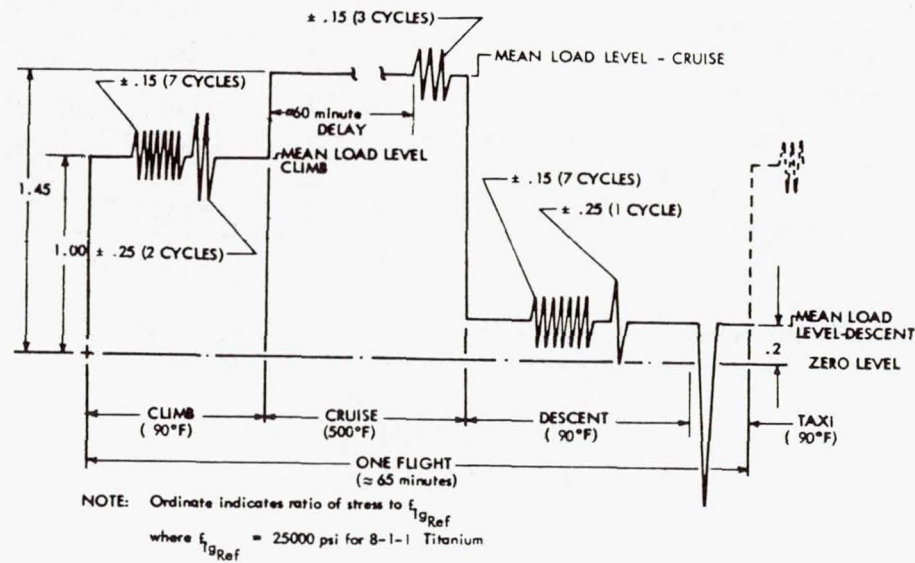


- (1) Sheet Specimens
- (2) Extrusion Specimens, Extruded Direction
- (3)  $K_t \approx 3$  (Gross Area)

(a) Center-notched fatigue specimen.



(b) Stress and temperature relationship for accelerated tests with cyclic temperature.



(c) Unit flight by flight loading sequences and magnitudes, real time.

Figure 10.- Real- and short-time correlation.



- o Mean value; number denotes number of tests  
 x Failure  
 | Current test status

MATERIAL DATA	SPECTRUM		NUMBER OF FLIGHTS UNTIL INITIAL CRACKING											
	TEMPERATURE	LENGTH	2 x 10 <sup>4</sup>			5 x 10 <sup>4</sup>			10 <sup>5</sup>					
6-4 SHEET .050" MILL- ANNEALED	90°F CONSTANT	19 SEC.												
	500°F CONSTANT	19 SEC.												
	90-500°F CYCLIC	19 SEC												
	90-500°F CYCLIC	1 HOUR												
6-4 EXTRUSION .050" S.T.A.	90°F CONSTANT	19 SEC												
	500°F CONSTANT	19 SEC												
	90-500°F CYCLIC	19 SEC												
	90-500°F CYCLIC	1 HOUR												

(d) Current status of real-time and accelerated testing.

Figure 10.- Concluded.

- RIVET, HI-SQUEEZE INSTALLATION
- BOLT, "HI-LOK"
- ▽ BOLT, "TAPER-LOK"

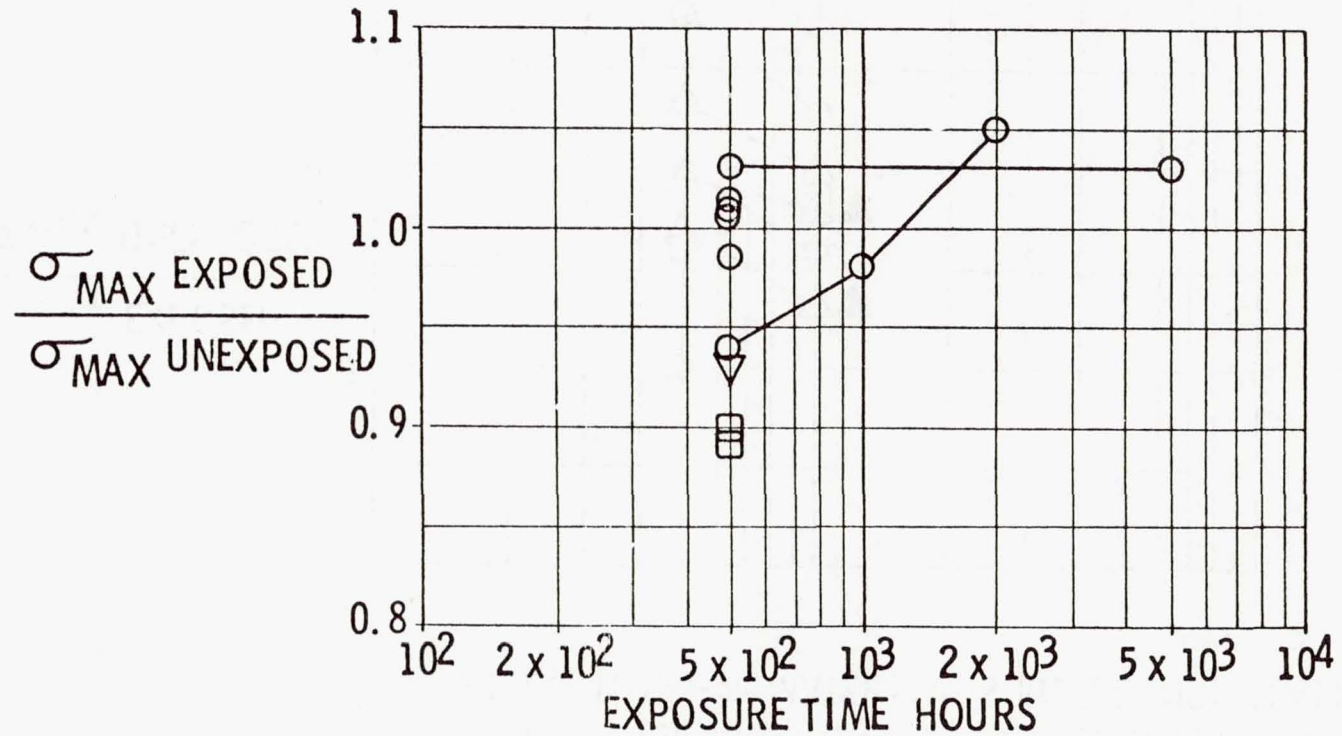


Figure 11.- Effect of temperature exposure.  $\sigma_{MAX}$  at  $R = 0.06$  for  $10^5$  cycles life. Ti-6Al-4V baseline specimens exposed to 500° F temperature.



- OPEN SYMBOLS INDICATE EXPOSURE AT 550°F  
 DARK SYMBOLS INDICATE EXPOSURE AT 450°F
- ▽ RIVET, A-286 MATERIAL, GUN DRIVEN INSTALLATION
  - RIVET, A-286 MATERIAL, SQUEEZE INSTALLATION
  - RIVET, Ti-6Al-4V MATERIAL, SQUEEZE INSTALLATION

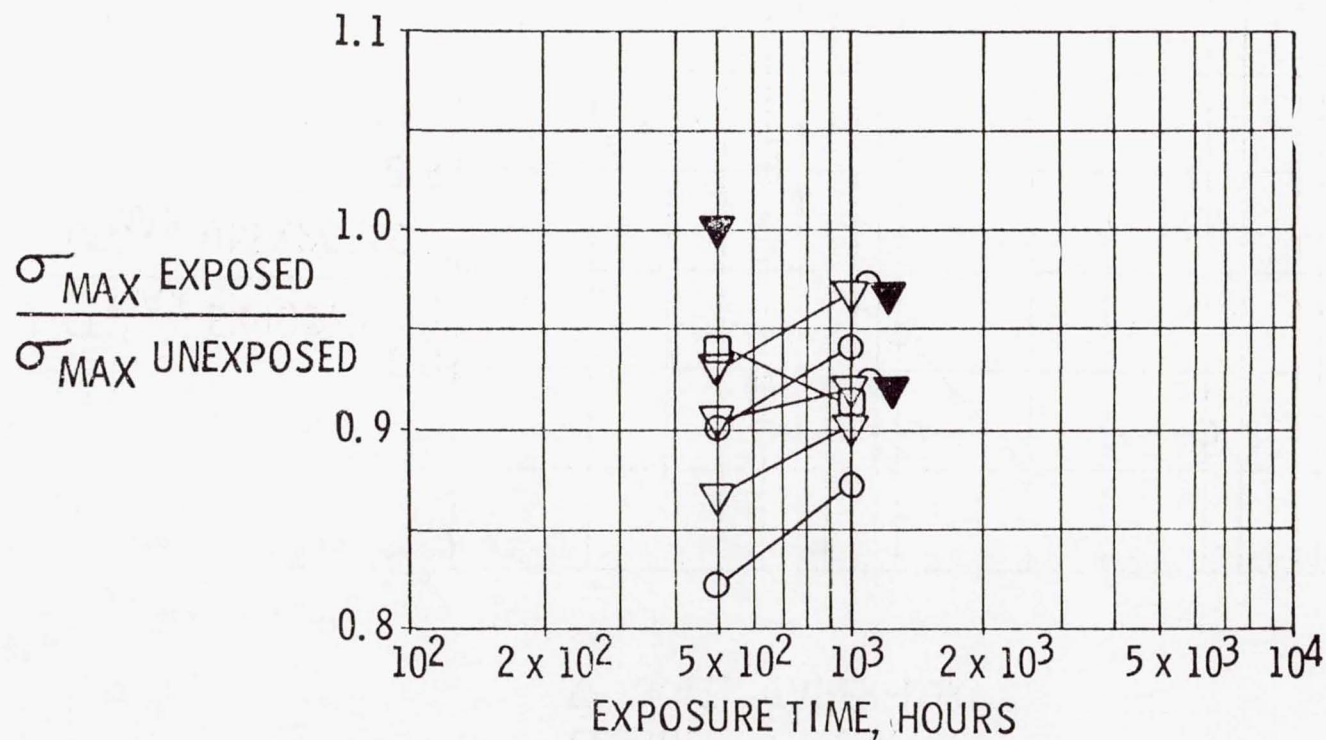


Figure 12.- Effect of load and temperature exposure lap shear joints.  $\sigma_{MAX}$  at  $R = 0.06$  for  $10^5$  cycles life. Ti-6Al-4V lap shear joint specimens exposed to temperature and 30 ksi stress.

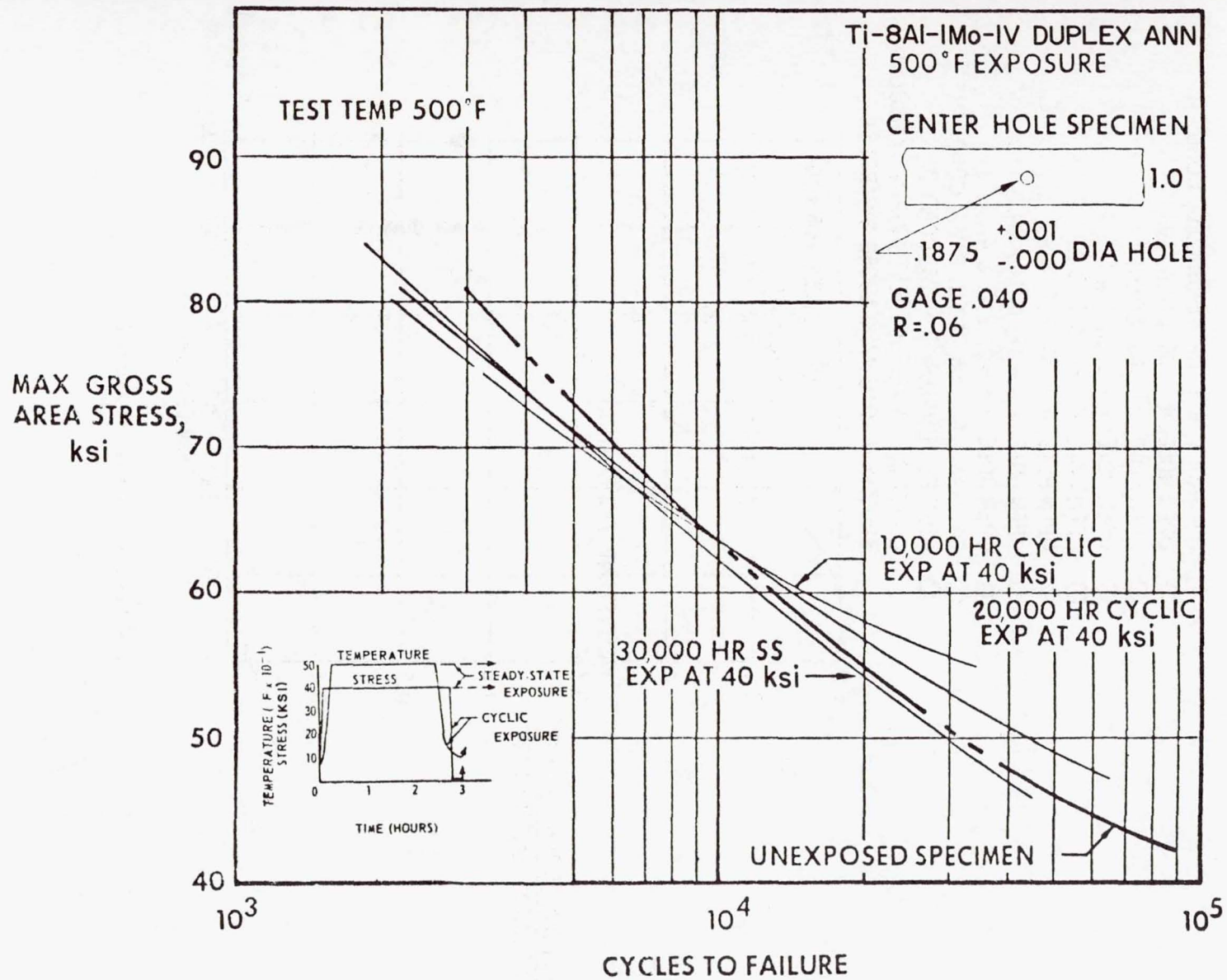


Figure 13.- Effect of load and temperature, steady-state and cyclic, on center-notched Ti-8Al-1Mo-1V duplex annelaed specimens.

- + H/C FACES, R = .06, AL-BRAZED, COND. IC.
  - ◇ OPEN HOLE, R = .06, COND. IV
  - OPEN HOLE, R = .06, COND. I
  - ◇ OPEN HOLE, R = 0, S.T. & A.
  - OPEN HOLE, R = -1, S.T. & A.
  - ◇ OPEN HOLE, R = .54, S.T. & A.
  - △ OPEN HOLE, R = -.47, MILL ANN.
  - OPEN HOLE, R = -.47, S.T. & A.
  - ◇ BASELINE, R = .06, H. SQ. RIV., COND. IV
  - ◇ RIVETED DOUBLER, R = .06, COND IV,
- CONSTANT AMPLITUDE TESTS (OPEN SYMBOLS)  
SPECTRUM LOADING (CLOSED SYMBOLS)

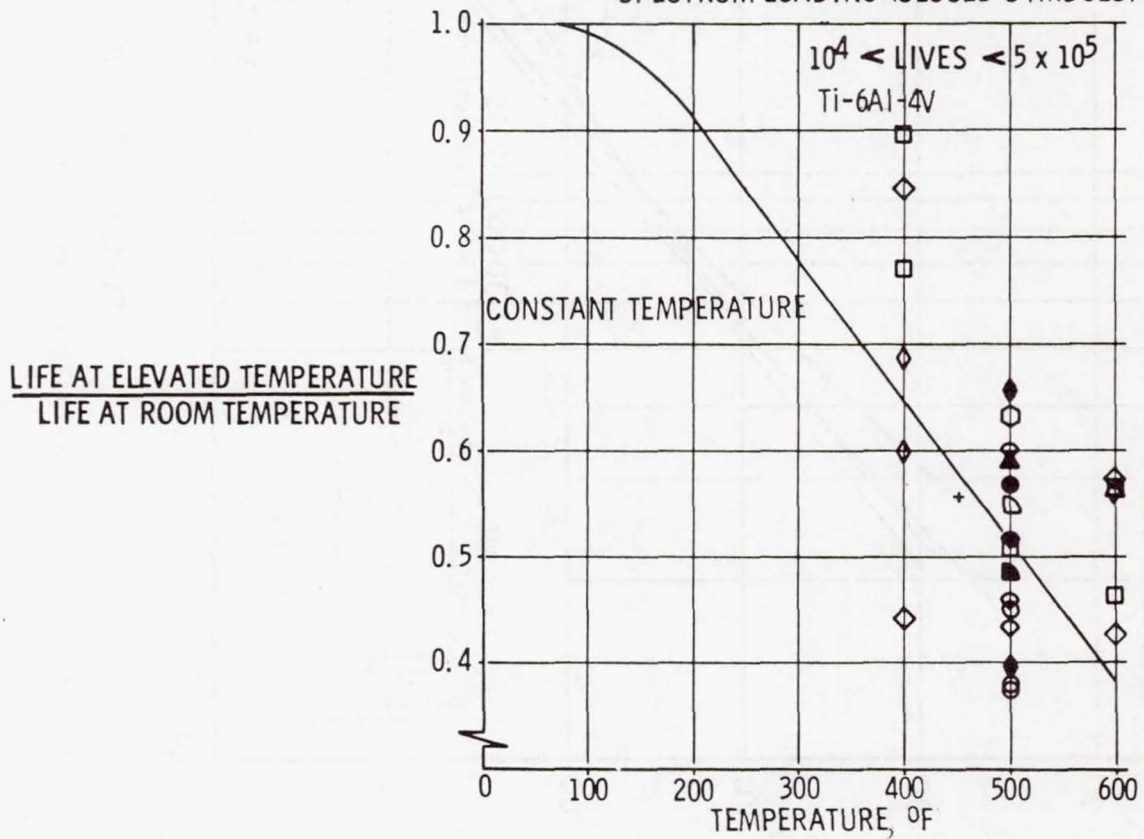


Figure 14.- Life at constant elevated temperature.



- $\triangle$  OPEN HOLE,  $R = -.47$ , MIL. ANN.  
 $\circ$  OPEN HOLE,  $R = -.47$ , S.T. & A.

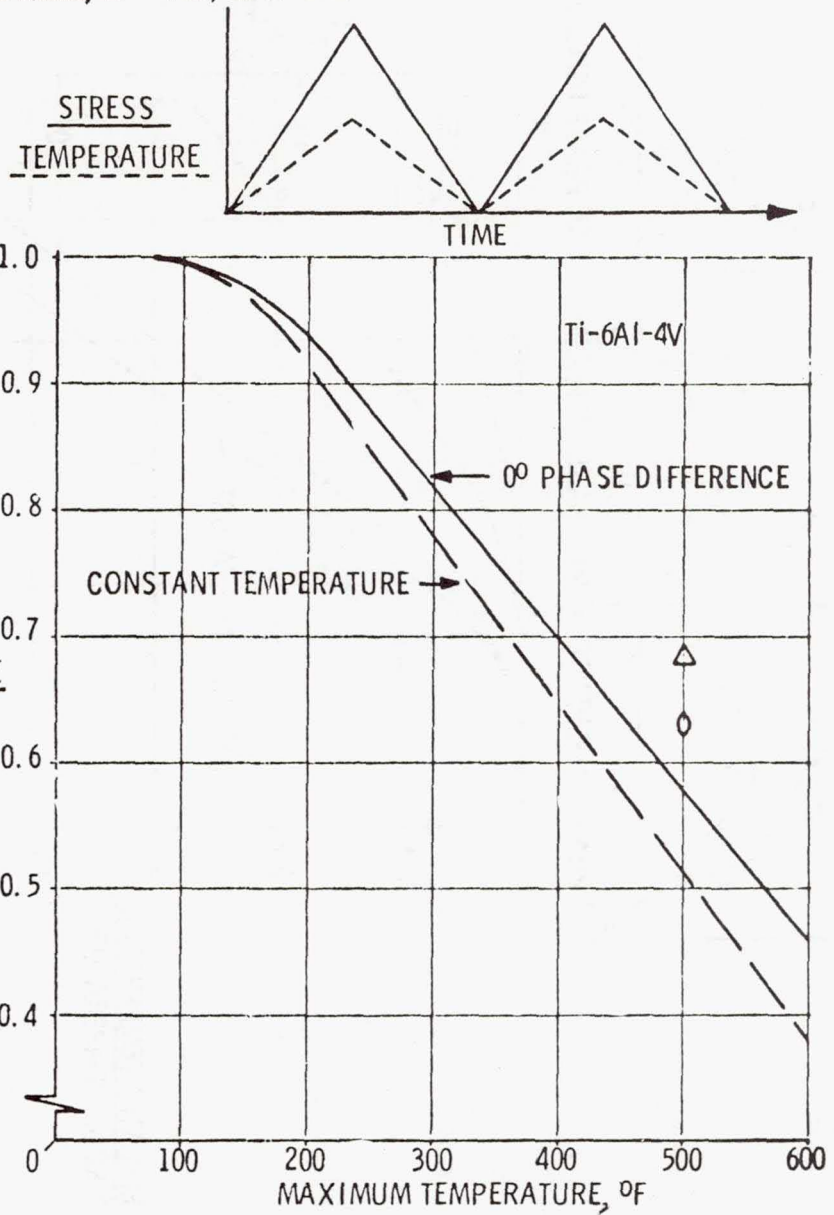
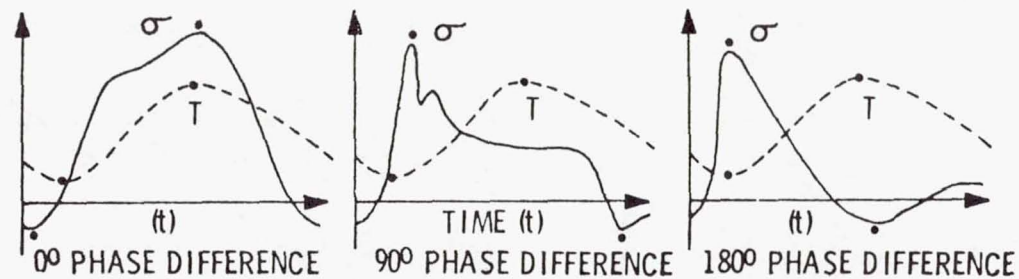


Figure 15.- Life at stress-temperature phase angle of 0°.



$$n = \frac{\text{LIFE AT ELEVATED TEMPERATURE}}{\text{LIFE AT ROOM TEMPERATURE}}$$

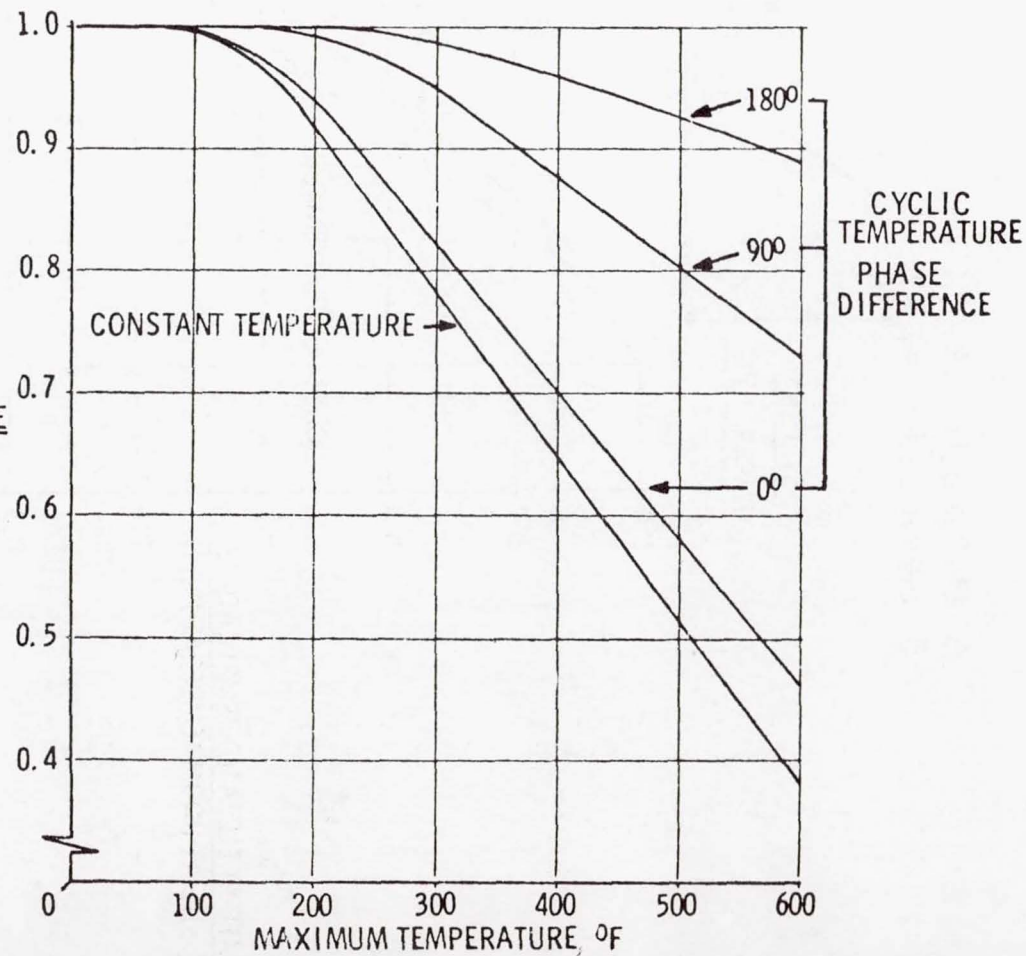


Figure 16.- Fatigue life ratio for the effect of stress-temperature cycle.  $\sigma$ , peak stress;  $T$ , peak temperature.

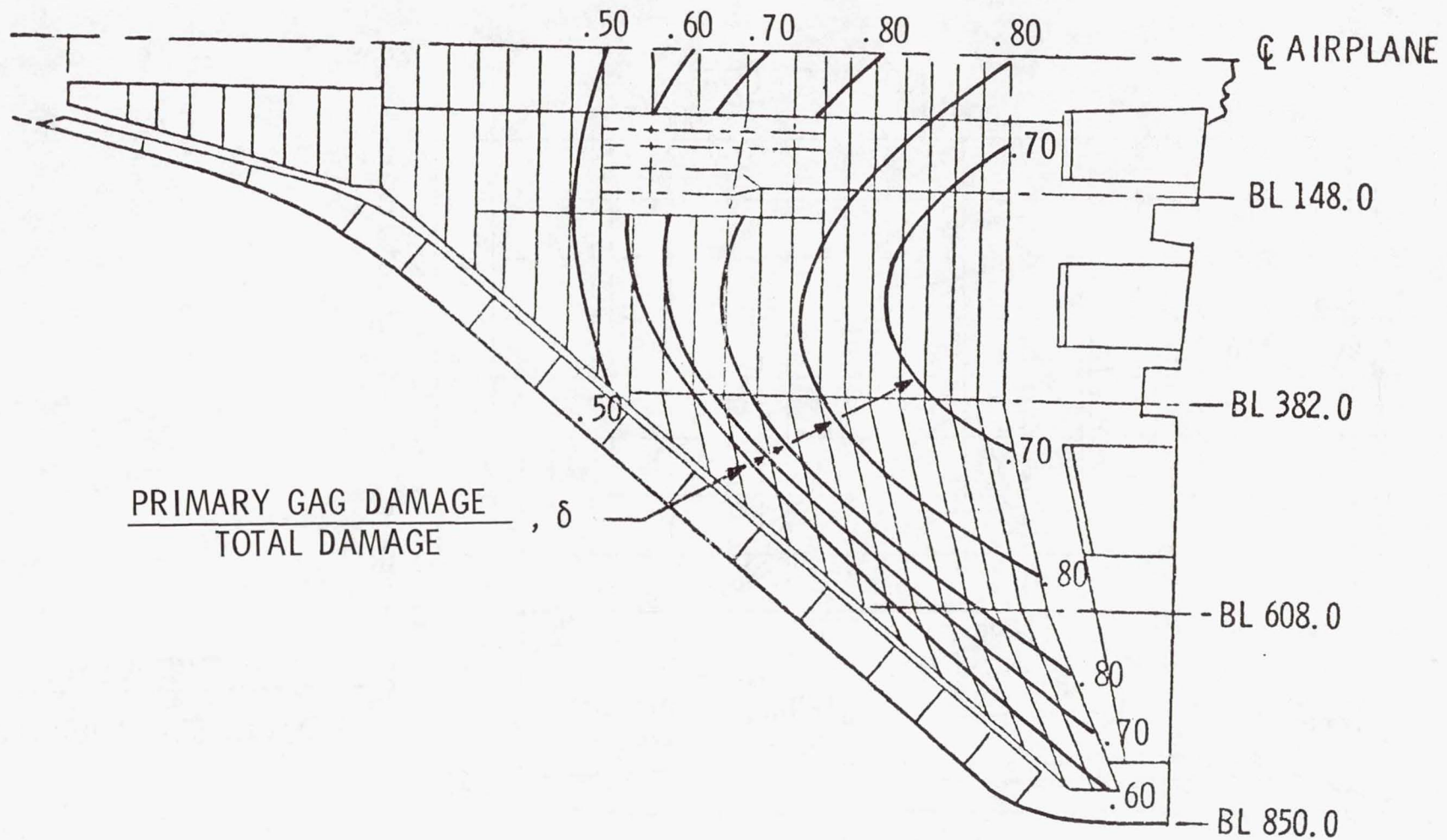


Figure 17.- Wing lower surface inner element primary GAG damage ratio.



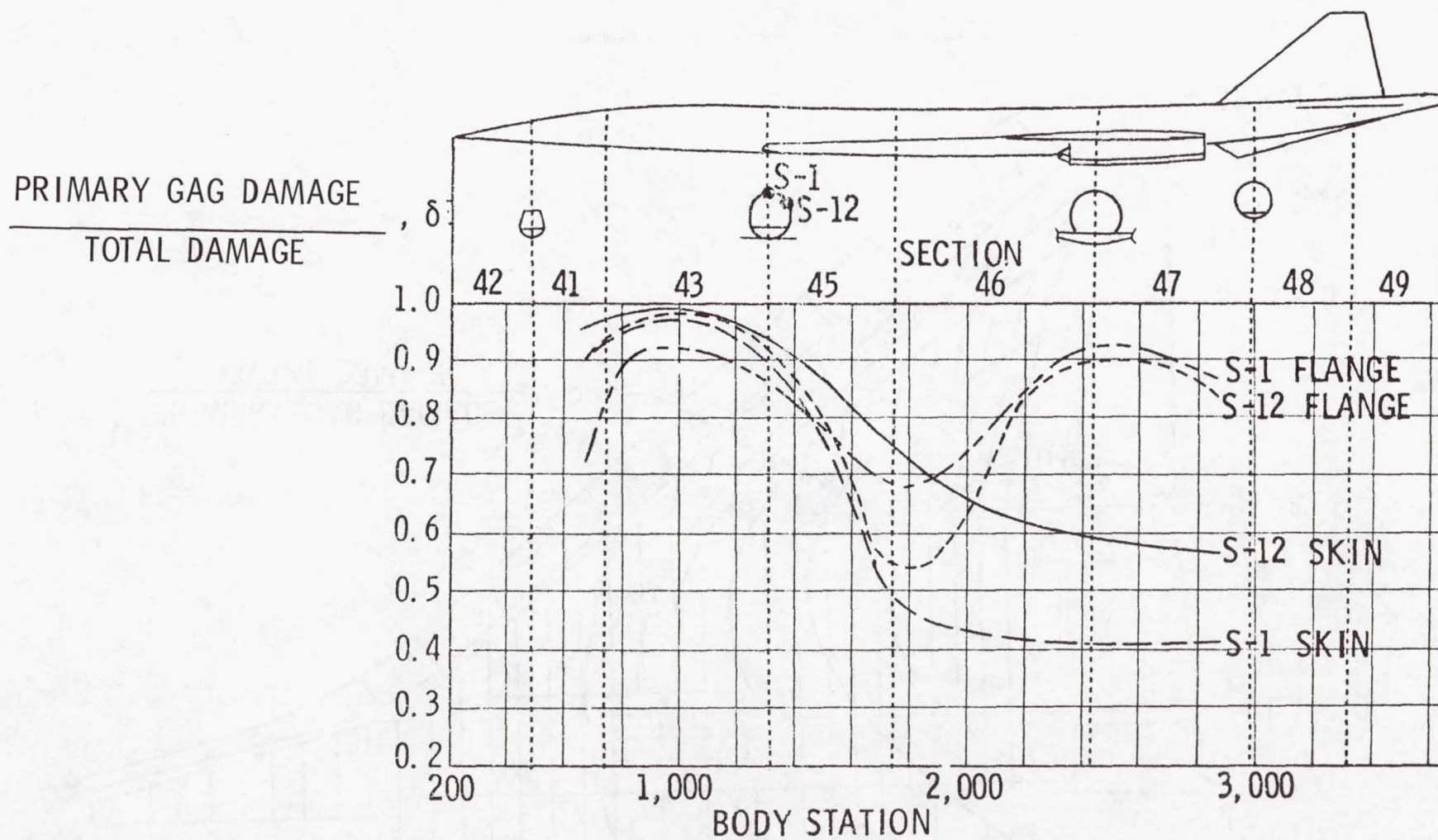


Figure 18.- Fuselage primary GAG fatigue damage ratio.

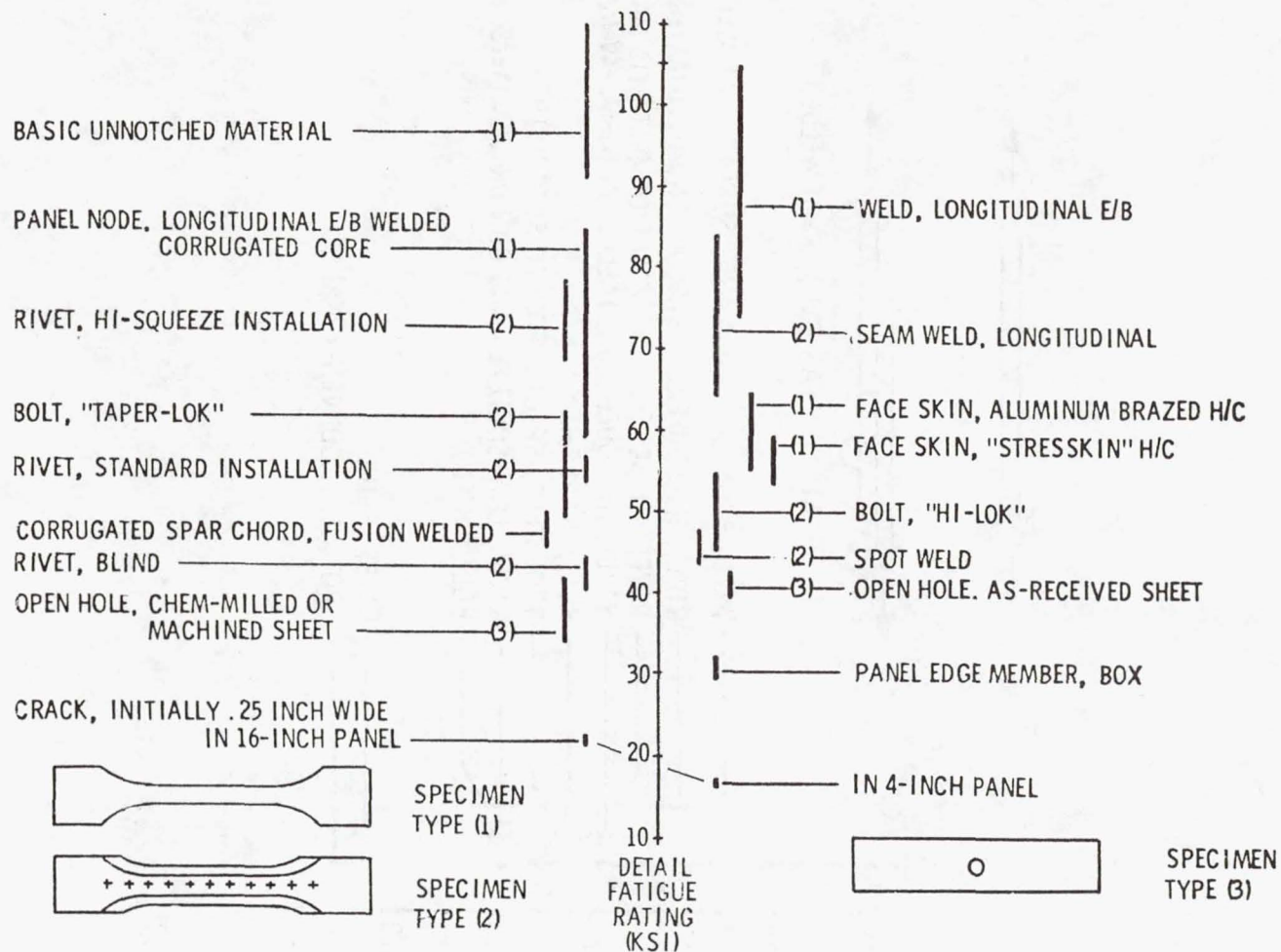


Figure 19.- Ti-6Al-4V basic structure detail fatigue rating.  $\sigma_{MAX}$  at  $R = 0.06$  at  $10^5$  cycles life.

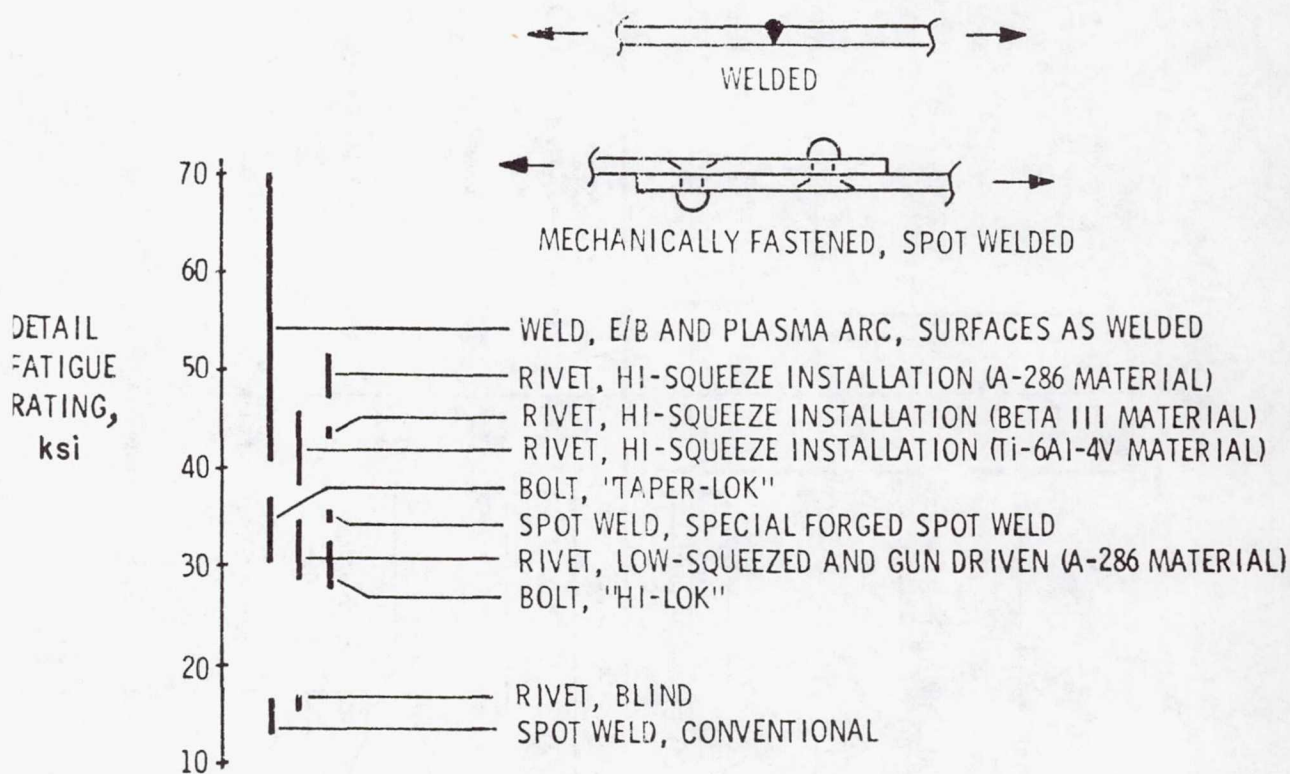


Figure 20.- Ti-6Al-4V joint detail fatigue rating.  $\sigma_{MAX}$  at  $R = 0.06$  at  $10^5$  cycles life.



$$DFR = \lambda L - \mu M \left( \frac{1}{K_{T,0}} - \frac{1}{K_T} \right)$$

WHERE: L & M ARE MATERIAL PARAMETERS

$\lambda, \mu$  AND  $K_{T,0}$  ARE DETAIL PARAMETERS

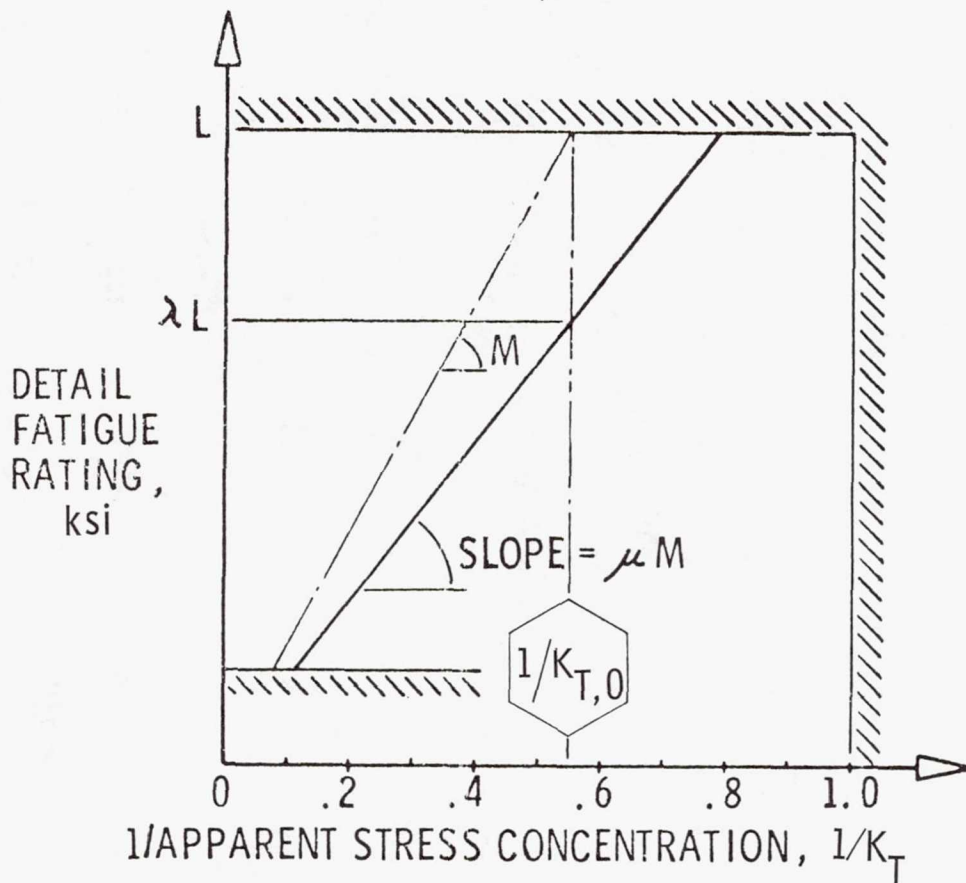
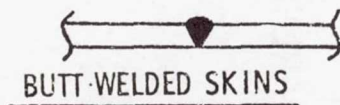
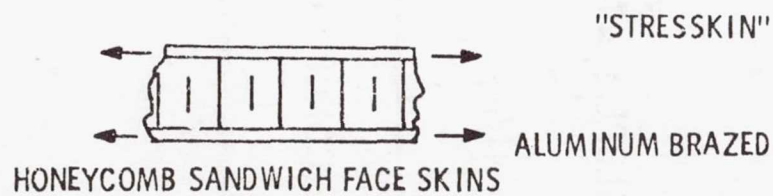
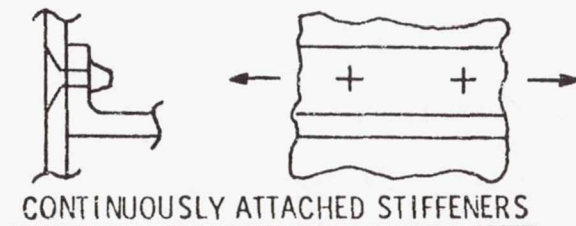


Figure 21.- Detail-fatigue-rating formulation.



SURFACES AS WELDED  
(UP TO .063 GAGE)

WELD AREA INCLUDING UNDERCUT  
MACHINED FLUSH  
(UP TO .125 GAGE)

"STRESSKIN"

DIFFUSION BONDED C. P. CORE  
DIFFUSION BONDED 3-2.5 CORE

ALUMINUM BRAZED  
.016 GAGE FACE SKIN  
OVER .040 GAGE FACE SKIN

DETAIL FATIGUE  
RATING,  
ksi

RIVET, HI-SQUEEZE INSTALLATION  
RIVET, STANDARD INSTALLATION  
BOLT, "HI-LOK";

CLASS I FIT  
TRANSITION FIT  
INTERFERENCE FIT

PROCESS  
ELECTRON BEAM  
PLASMA ARC

LOAD DIRECTION  
LONGITUDINAL  
TRANSVERSE

PLASMA ARC

ELECTRON BEAM

PLASMA ARC

LONGITUDINAL  
TRANSVERSE

LONGITUDINAL  
TRANSVERSE

LONGITUDINAL  
TRANSVERSE

65

56

46

50

54

53

53

55

65

65

55

65

55

65

65

65

65

Figure 22.- Typical detail fatigue ratings, basic structure.





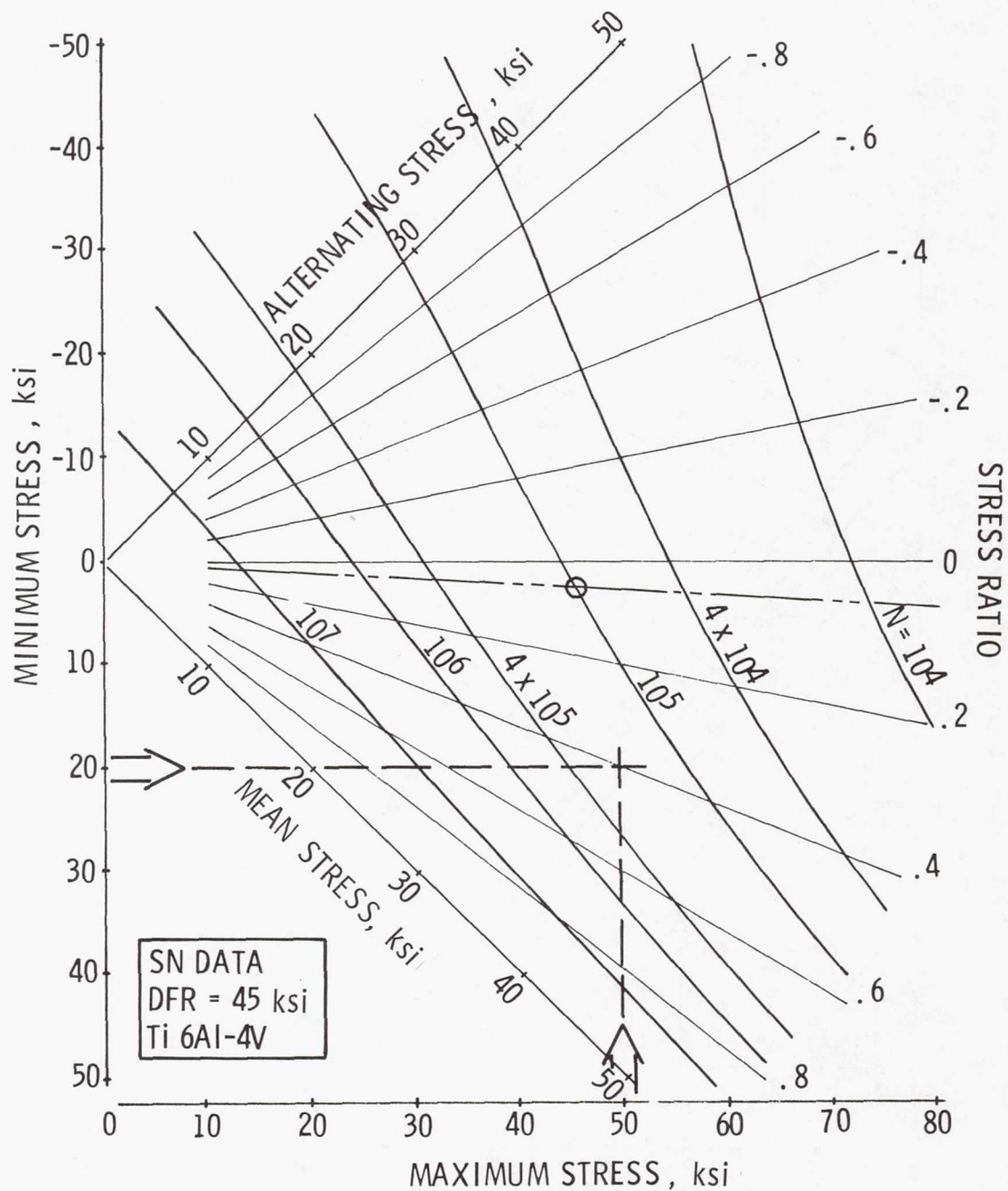


Figure 24.- Constant-life diagram for a component with DFR = 45 ksi.

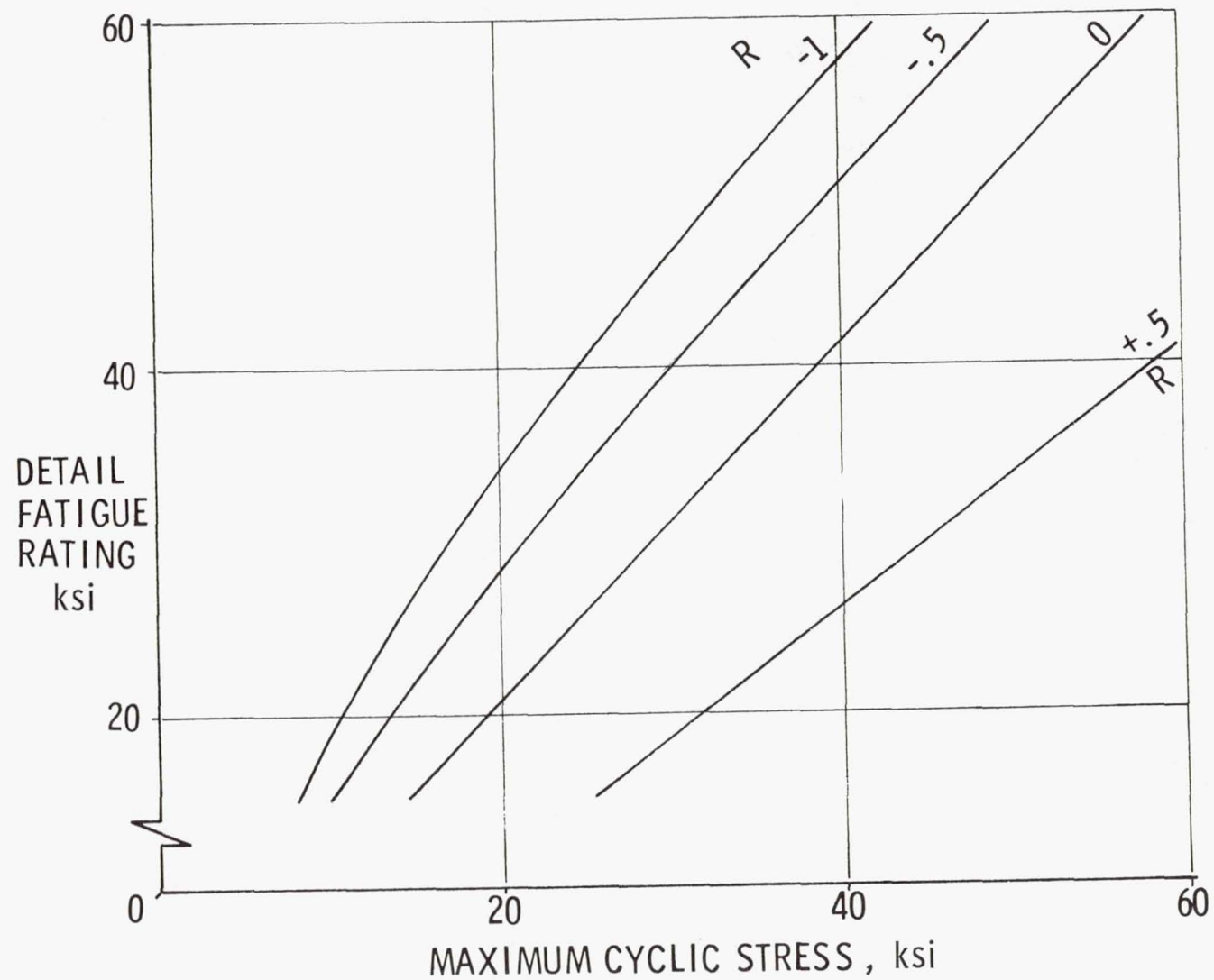


Figure 25.- Detail fatigue check at  $N = 100,000$  cycles.

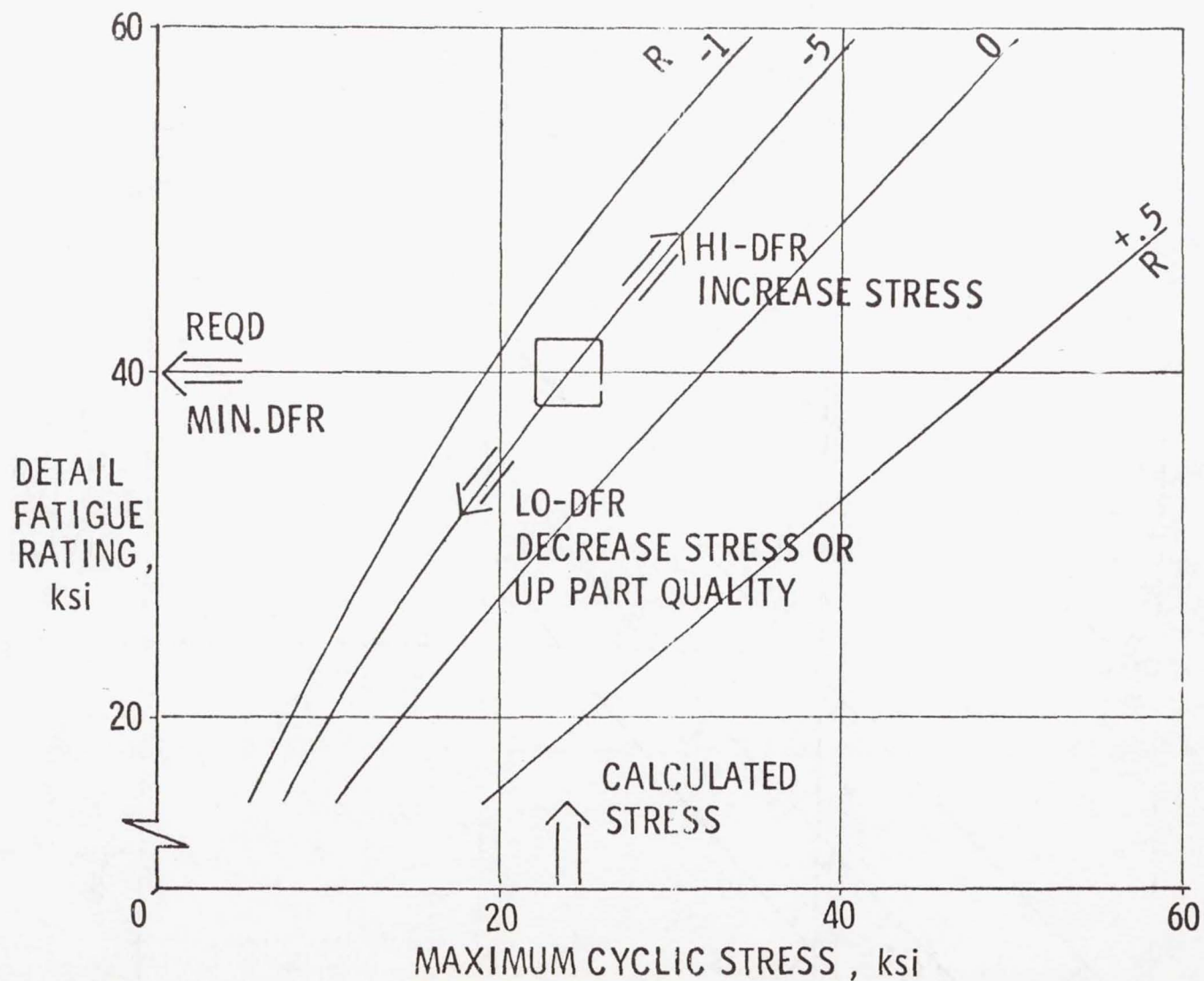


Figure 26.- Detail fatigue check at  $N = 200\,000$  cycles.



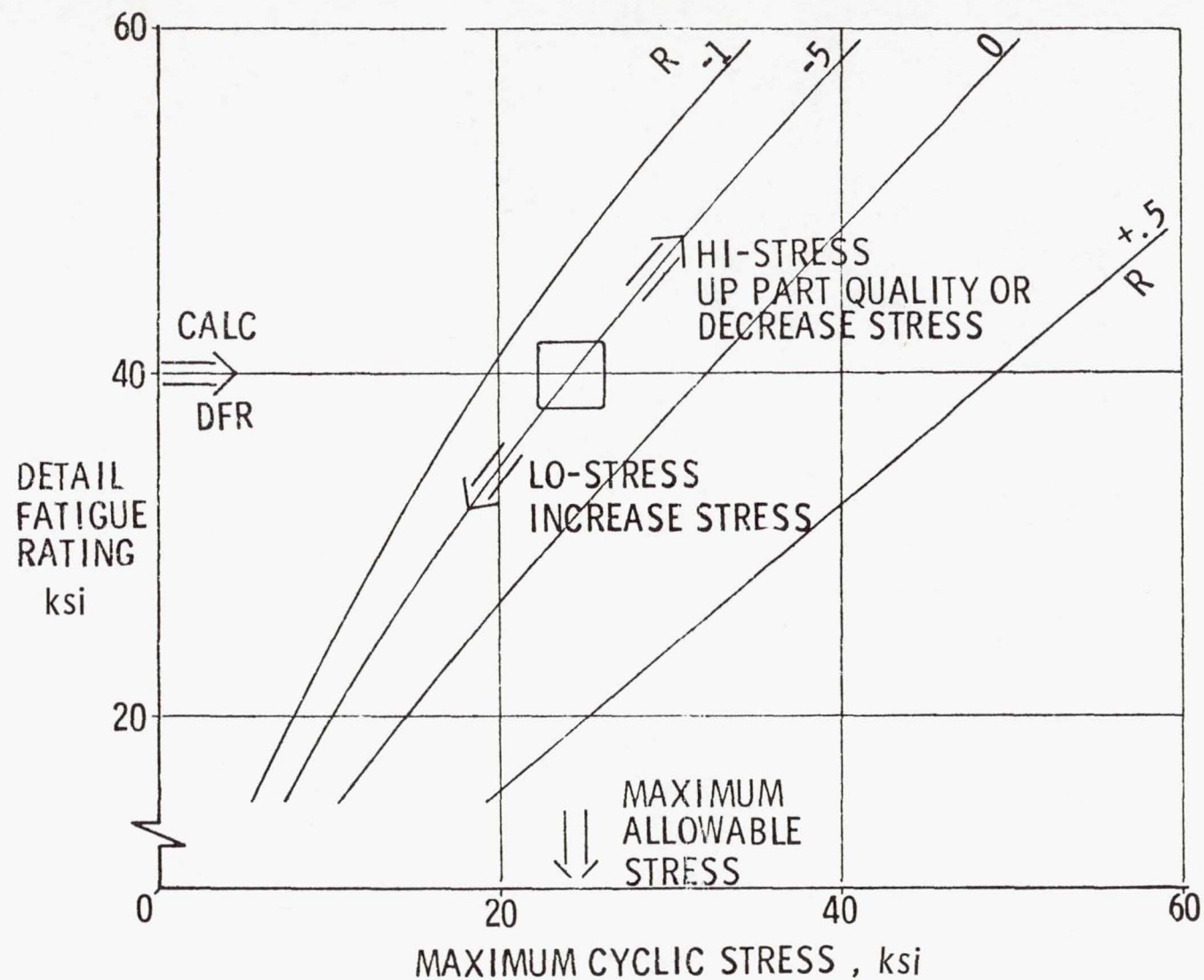


Figure 27.- Detail fatigue check at  $N = 200\,000$  cycles.

## PRACTICAL ASPECTS OF DESIGNING FOR AND EVALUATING STRUCTURAL INTEGRITY

By Marcel Peyrony and Daniel Chaumette  
Avions Marcel Dassault  
Saint-Cloud, France

### INTRODUCTION

The objective of this paper is not to show the results of very scientific studies, but only to put forward some points which can be of practical use to the designer. The following procedures apply generally in the tests discussed:

- (1) Skins are machined, either chemically or mechanically
- (2) Their surfaces are blasted with glass beads and wet sand
- (3) They are given a surface protection and painted
- (4) No bonding is used.

### FATIGUE PERFORMANCE IMPROVEMENT

It is well known that bolts with tight fit give a definite increase in fatigue life. However, this increase is guaranteed only if every bolt is mounted with the right fit and if no undetectable fault may change the assumed condition.

#### Conical Fasteners

For a long time we have been using bolts or fasteners with tight fits of 5 to 30 microns, with very satisfactory results. But it is quite a problem to achieve a guaranteed fatigue life of 40 000 hours while saving much weight, especially in the joints or in the lower skin of the wing. The search for a higher admissible stress is then a constant undertaking.

Conical bolts had at first sight appeared most interesting. There was indeed the danger of stress corrosion when a tight fit of 90 microns was used with alloys such as 2024-T3 and 2014-T6, but riveting on short transverse components is infrequent, and less sensitive alloys may be used. A test program was started with two types of test specimens, a "dog bone" type and a lap joint. (See fig. 1.)

The first test results (fig. 2) were most encouraging, until a test specimen broke after a disappointingly low number of cycles. A more thorough inspection of the test piece (which had been inspected prior to testing) showed a reaming fault as in figure 3. The bolt bears only on four regions.

It was necessary to determine why this fault existed and why it had escaped inspection. The first problem was easy to resolve. It took many years to learn how to drill a perfectly circular cylindrical hole. Conical holes, because of their high drilling torques, will surely require still more development and tooling for reliable results. With limited tooling, we succeeded in drilling correct holes up to 6 mm in diameter and 8 mm deep. But for larger diameters, very rigid jigs and expensive tooling were needed. Both the cost of tooling and the drilling time were found to be prohibitive for an extensive conical fastening.

Furthermore, inspection was most difficult, with the necessity of blueing checks at every hole, which increased the cost of the total operation. Finally, a subsequent test with holes purposely drilled incorrectly showed a dramatic decrease in fatigue life. (See fig. 4.) These results, added to the danger of stress corrosion, led to the decision not to use conical fasteners in the Mercure.

### Hole Preparation

In an attempt to increase the fatigue life of structures, the following processes were examined:

(1) The way in which the hole is made:

- (a) Normal reaming
- (b) Heli-Armor reaming
- (c) Broaching

(2) The finish given after reaming:

- (a) Deburring
- (b) Roll over

Significant differences were found between treated and untreated holes without rivets (fig. 5). On the other hand, once the bolt is set, these differences decrease and even disappear (fig. 6).

### Interference Fit

On one hand, interference fit has a positive influence on fatigue life, but on the other hand, beyond a certain level of interference (30 microns), fretting under the fastener becomes too important unless special care is taken. Figure 7 shows the type of failure in each case. With the free bolt, the crack started in the cylindrical part of the hole, but with the interference-fit bolts, the cracks started by fretting in the countersink.



## Antifretting Protection

In all previously described tests standard sealing and surface protection treatments were used; that is, rivets were wet mounted with PR 1422 or Blendexite and the test specimens were painted with PR 1460 or Cellolac 78-28. Figure 8 shows the effect on fatigue life when one of these two protections is omitted. The fatigue life was reduced by fretting underneath the fastener collar when the specimen was not painted, and in the countersink when the rivet was dry mounted.

## Selecting Parameters for Mounting a Fastener

The results of these experiments led to the selection of the following procedures:

- (1) Use of a moderate amount of interference (bearing in mind the problem of stress corrosion)
- (2) Painting and wet mounting

The influence of the way in which the hole is obtained is not so obvious. Broaching and Heli-Armor give comparable results, but broaching is an extremely reliable method of obtaining holes of a high standard, while Heli-Armor may be less reliable. The "miracle" alloy for the best life has appeared to be 2024-T3. (We have not tested 7075-T73.)

## FAIL-SAFE DESIGNS

### General Considerations

The greatest risk of crack initiation is surely incurred in joints. Multiplying stress concentrations by using, for example, riveted reinforcements around door openings should be avoided as much as possible. Integral structures mechanically or chemically milled might seem a good solution, but then the difficult problem of fail-safe design enters the picture.

We have already made some remarks about this problem at Melbourne, having been unfavorably impressed by some examples of so-called fail-safe design, the most classic being a structure cut in two pieces and bolted back together. Since then the situation has apparently worsened, judging by the design of some recent tail-unit hinges and control-surface bearings.

Are the regulations responsible? It is certain that FAR 25-573 encourages a designer who does not want to put questions to himself to demonstrate that a structure can sustain the required static load when one of the elements has failed. This test allows him to claim that his structure is fail-safe. Moreover, the same paragraph allows a failure to be considered only partial if it is obvious.

As far as fatigue is concerned, the basic idea, in itself quite legitimate, of assuring security by means of residual strength has been put in a wrong way.

### Fatigue and Fail-Safe

Of course a fatigue test is not a fail-safe demonstration by itself, but it is not negligible in assessing structural fail-safe designs. Also, fatigue testing is a good method for determining inspection schedules for the various parts of the airplane.

We do not believe that an element cut in two, but in which cracks appear and grow rapidly, is sufficiently fail-safe. What happens to the half of this element carrying the whole load when the other half has broken?

Some recent mishaps with elements working in parallel should prove of interest. One instance was the F-14 prototype, in which two hydraulic tubes used on separate circuits, but subjected to the same fatigue duty, gave up in a 5-minute interval.

Another example of a more structural nature was found during a fatigue test on a military aircraft. The main frame supporting the bending moment of the wing was made of two rings working in parallel. (See fig. 9.) Cracks appeared and grew almost identically in the two rings, and a rupture occurred in each, the load being then supported by the remaining structure outside.

Another example concerns a wing attachment (fig. 10). Cracks grew at the same time from five holes and, what is more, on both wings. To have separated the attachment into halves would only have given a formal fail-safe structure without increasing enough the safety of the design.

These problems occurred because the fatigue life was short enough for all the pieces involved to be damaged. A quite different case appeared in the test of the Mercure main frame. An artificial crack in the flange of the frame grew only on one half of the flange, not passing the "wall" of the web, and at a rate low enough to be found in inspections.

Here the stress was lower, and this explains most of the difference. Thus a fatigue test may give important indications for fail-safe designs.

There is a still worse method for obtaining fail-safe. Take a beam with an I-section, the tensioned flange of this beam being perfectly smooth, without any hole. Then replace the integral tension flange by riveted flanges, the tensioned area being the same. Fail-safe is not definitely guaranteed and fatigue life is severely decreased.

If you feel unable to insure safety with such a monopiece structure, you can design a double load path while avoiding putting rivets in the tensioned zone. You will keep good fatigue life and get a double load path at the same time, but perhaps you will have some trouble with fretting or corrosion.



## Fail-Safe and Unexpected Cracks

The double load path finds its soundest justification in unexpected cracks. However, this should not deter the designer from looking at the types of remaining risks and finding a solution to them. These risks can be defined as flaws in the material, fretting, and stress corrosion. With correct designs, care, and inspection these difficulties can be overcome, and we have to work for that in any possible way.

### Important Conclusions Regarding Fail-Safe

Certainly a low stress level is an important factor for fail-safe guarantee. For less important elements where weight loss is small, no regrets should be had in designing with important margins for a theoretically infinite life. But this is not enough. During the fatigue tests and after, it is necessary to monitor the crack propagation rates at every point which may be critical. The results should be linked with the inspection schedule of these particular points.

Double load path must not be neglected. But its reliability must be assured with regard to fatigue considerations as well as corrosion and fretting, and the structure must not be weakened by a bad design.

## OUR FAIL-SAFE APPROACH

It must be admitted that we have often used the classic fail-safe methods described here. However, even in these cases we applied the procedures described in the following paragraphs to investigate crack propagation.

### Photoelastic Tests

For the Mercure design, we had previously developed tests on photoelastic models and on metal parts coated with photostress material (figs. 11 to 13). Thus, we were able to study stress concentrations on a particular component, and even on an entire element of the fuselage. Also, we were able to determine critical areas where we could provoke cracks.

### Partial Fatigue Test

Usually the area where we want fail-safe capability of a one-piece structure is greatly overdimensioned for fatigue. So we perform tests with normal fatigue loads, followed by cycles at higher loads. During these tests, cracks must not originate.



## Crack Propagation

Next we artificially provoke cracks in critical areas – that is, areas where calculations and photostress investigations show stress concentrations. (See fig. 14.) The crack growth rate is plotted against time in order to define a schedule of inspections that will provide detection in service before the risk of dangerous failure is encountered. This implies that the tests are based on particular conditions.

It is best to have two types of cycles. The first, with only normal fatigue loads, is applied on specimens to monitor the crack growth rate. The second, including the same normal fatigue loads, also includes "fail-safe" loads, and is applied on other specimens to evaluate the critical length of crack beyond which a static failure may occur.

Another possible application for fail-safe design is found in secondary effects (fuel leakage, for instance).

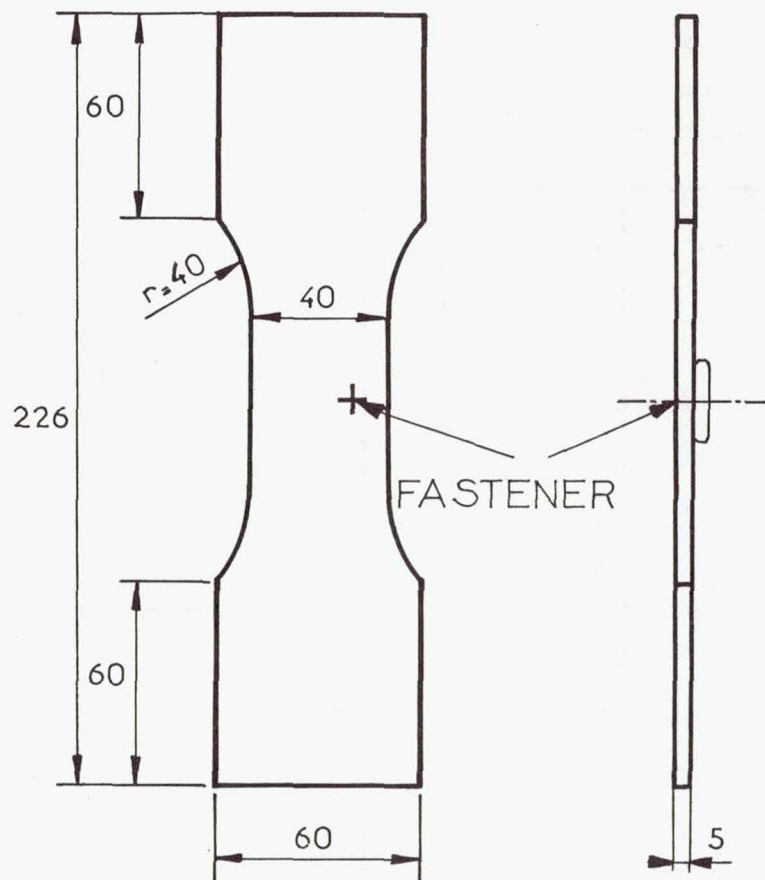
## CONCLUSIONS

The double load path, although a good fail-safe concept in many cases, is not entirely satisfactory. It may be insufficient when fatigue life is too short, and superfluous when the stress is low, detection is easy, or fail-safe capability is achieved by other means.

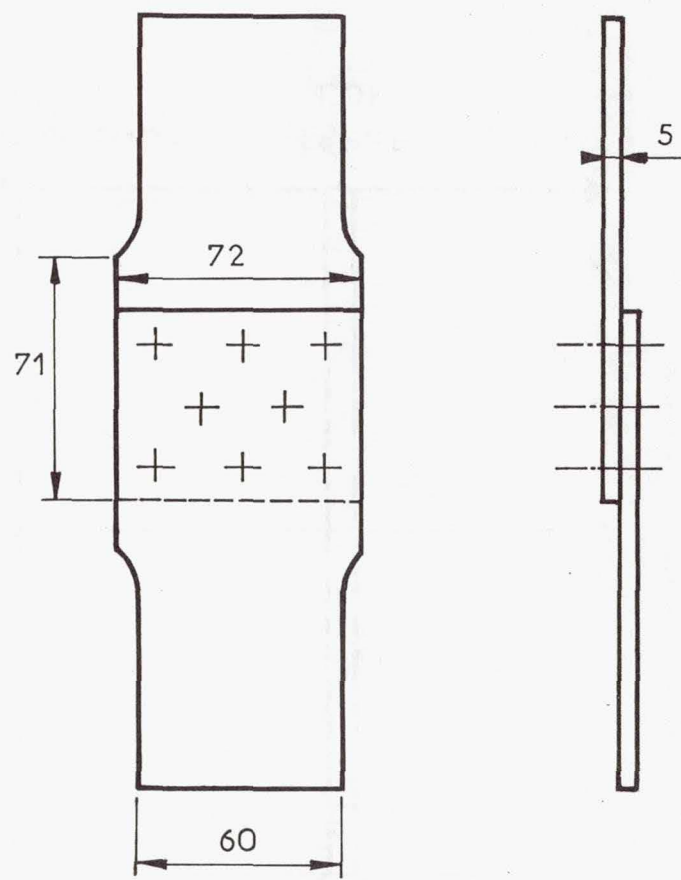
The best procedure is to rely on crack growth-rate studies and guaranteed crack detection by inspection in service.

The use of double load path to cope with unexpected phenomena such as stress corrosion or flaws seems rather makeshift, and it is better to seek specific action (improved forgings, inspection, protection) in each case.

The easier the inspection, the better for fail-safe.



"DOG BONE"



LAP JOINT

Figure 1.- Test specimens.

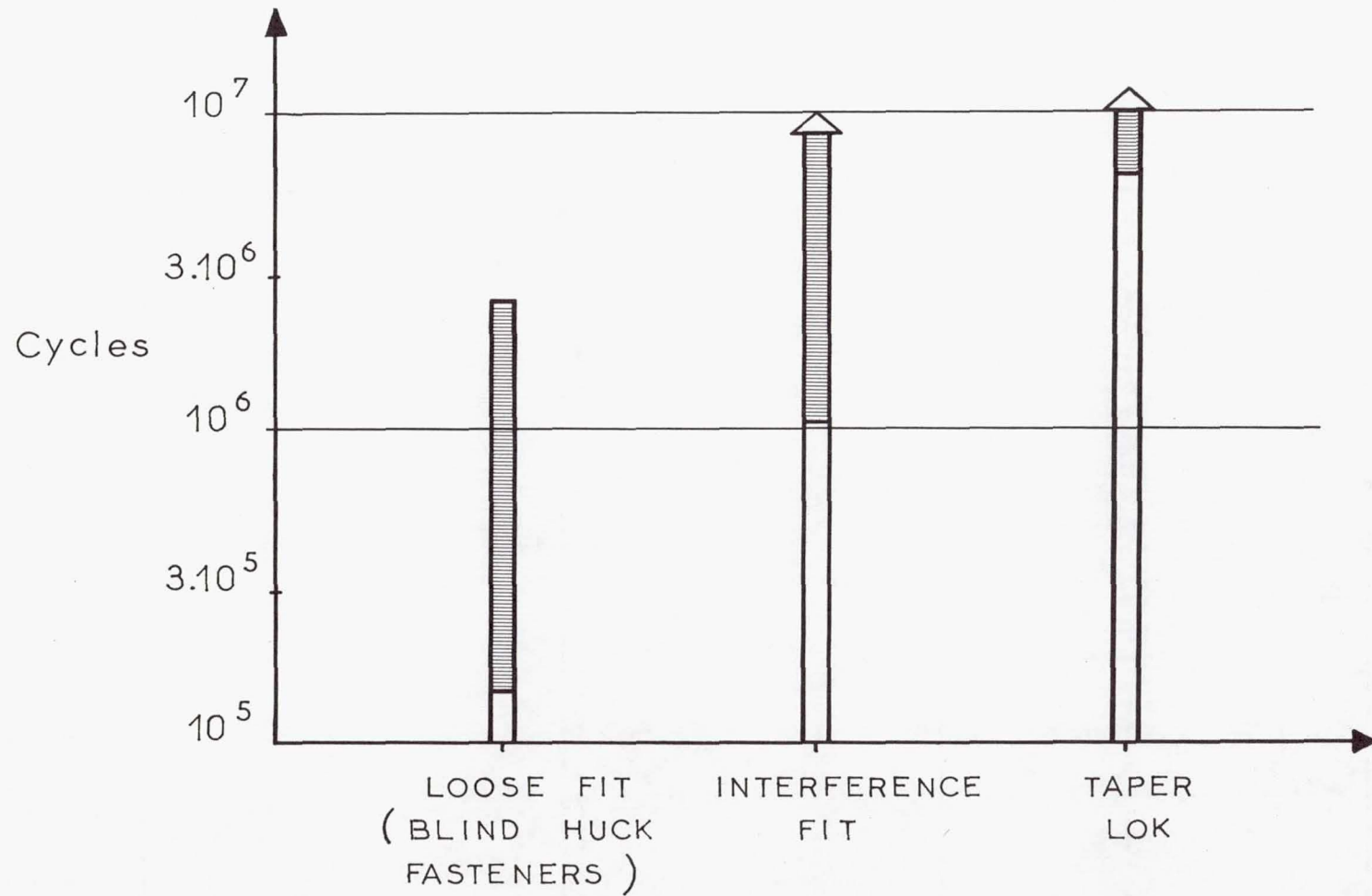


Figure 2.- Early results with Taper Lok and classic fasteners in "dog bone" sample of 2014 or 2024-T6 aluminum alloy. Test cycle  $\sigma = 10.8$  hectobars (15.7 ksi),  $R = 0.1$ .



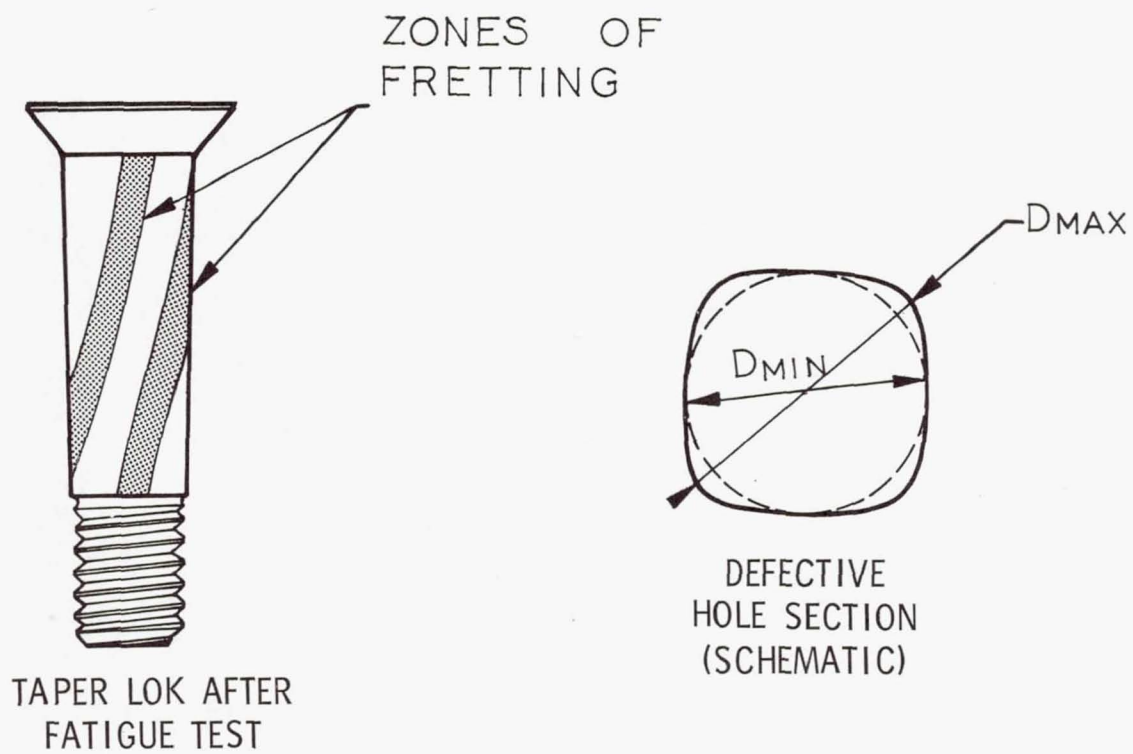


Figure 3.- Defective installation of Taper Lok.

C8

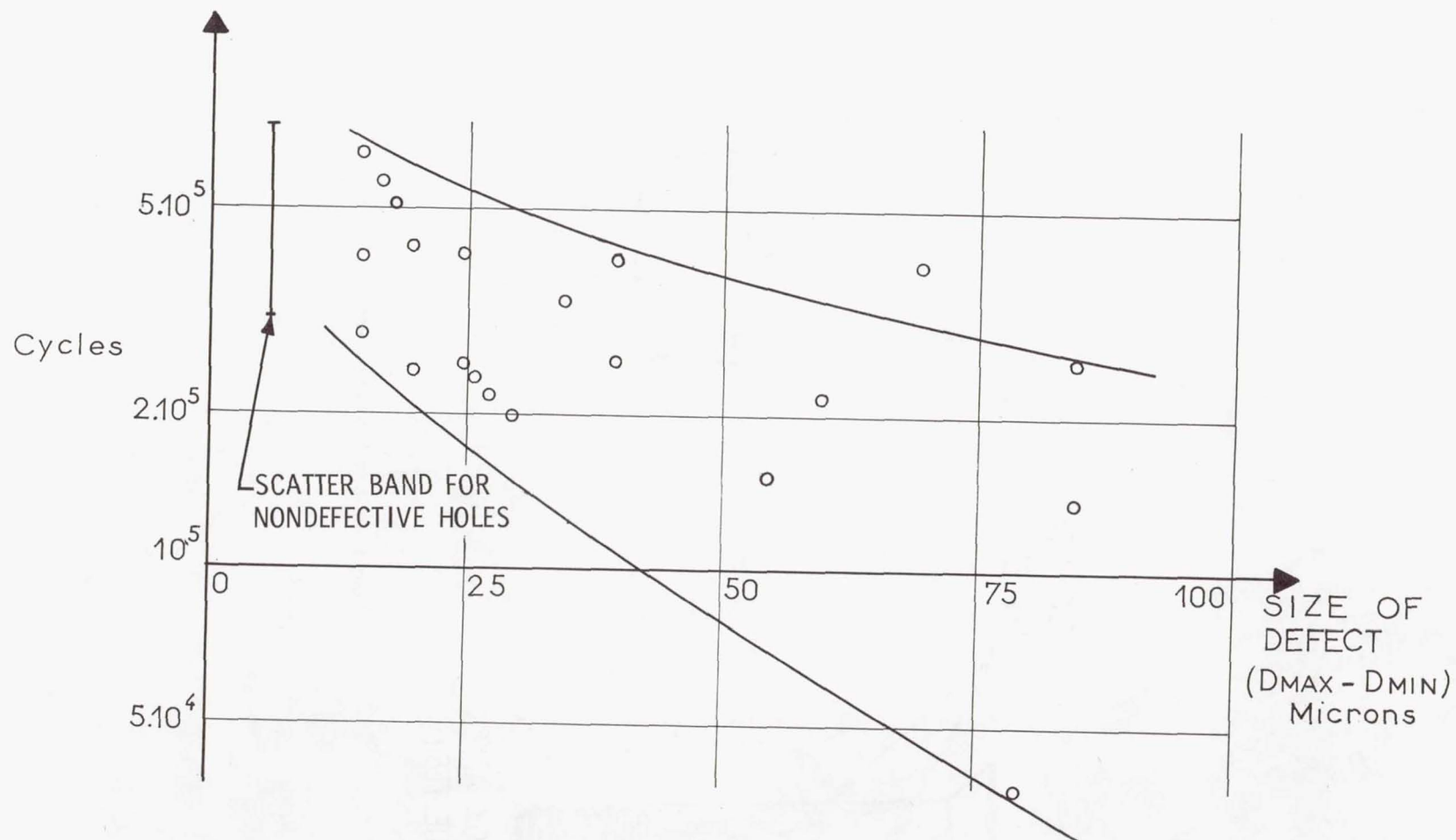


Figure 4.- Fatigue life as a function of size of defect in holes for Taper Lok. "Dog bone" sample of 2024-T6; test cycle  $\sigma = 17.2$  hectobars (25 ksi),  $R = 0.1$ ; fastener, 1/4-inch-diameter TL 100.

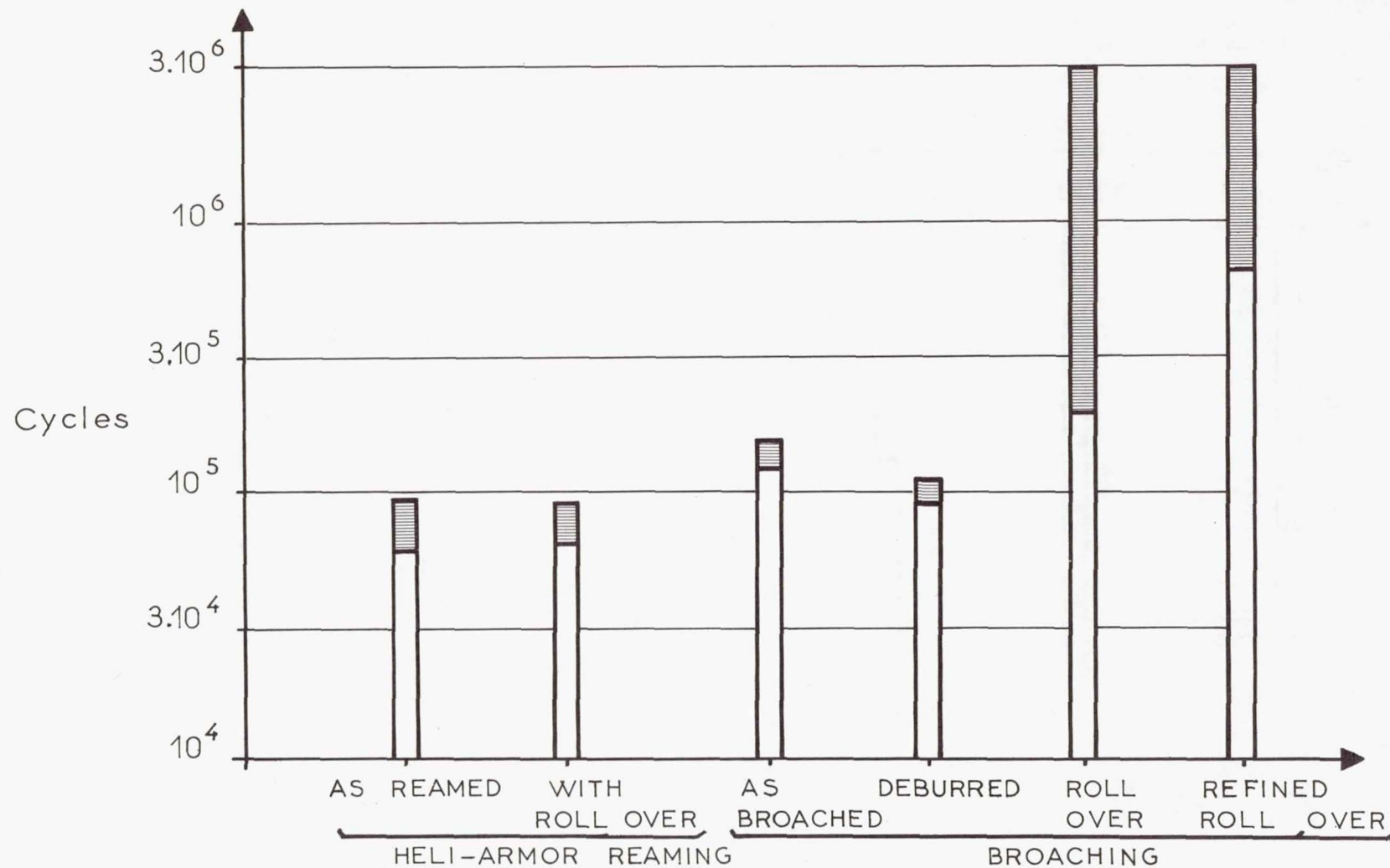


Figure 5.- Effect of finish of empty holes on fatigue life of 'dog bone' sample of 2014-T6. Test cycle  $\sigma = 13$  hectobars (18.8 ksi),  $R = 0.1$ .



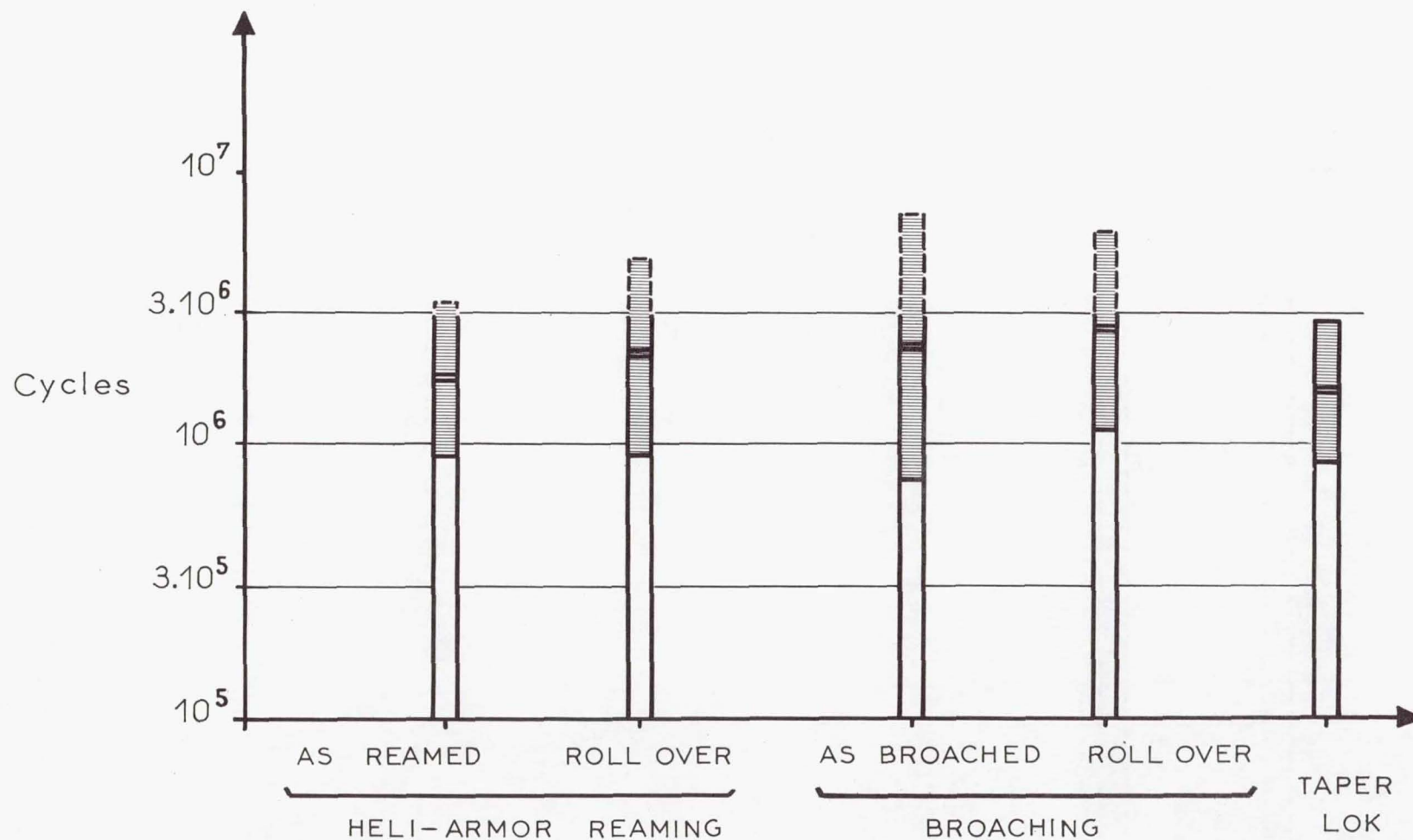


Figure 6.- Effect of finish of holes with fasteners on fatigue life of "dog bone" samples of 2014-T6. Fastener, 6-mm-diameter "SLF" titanium, interference approximately 30 microns; test cycle  $\sigma = 15$  hectobars (21.8 ksi),  $R = 0.1$ .

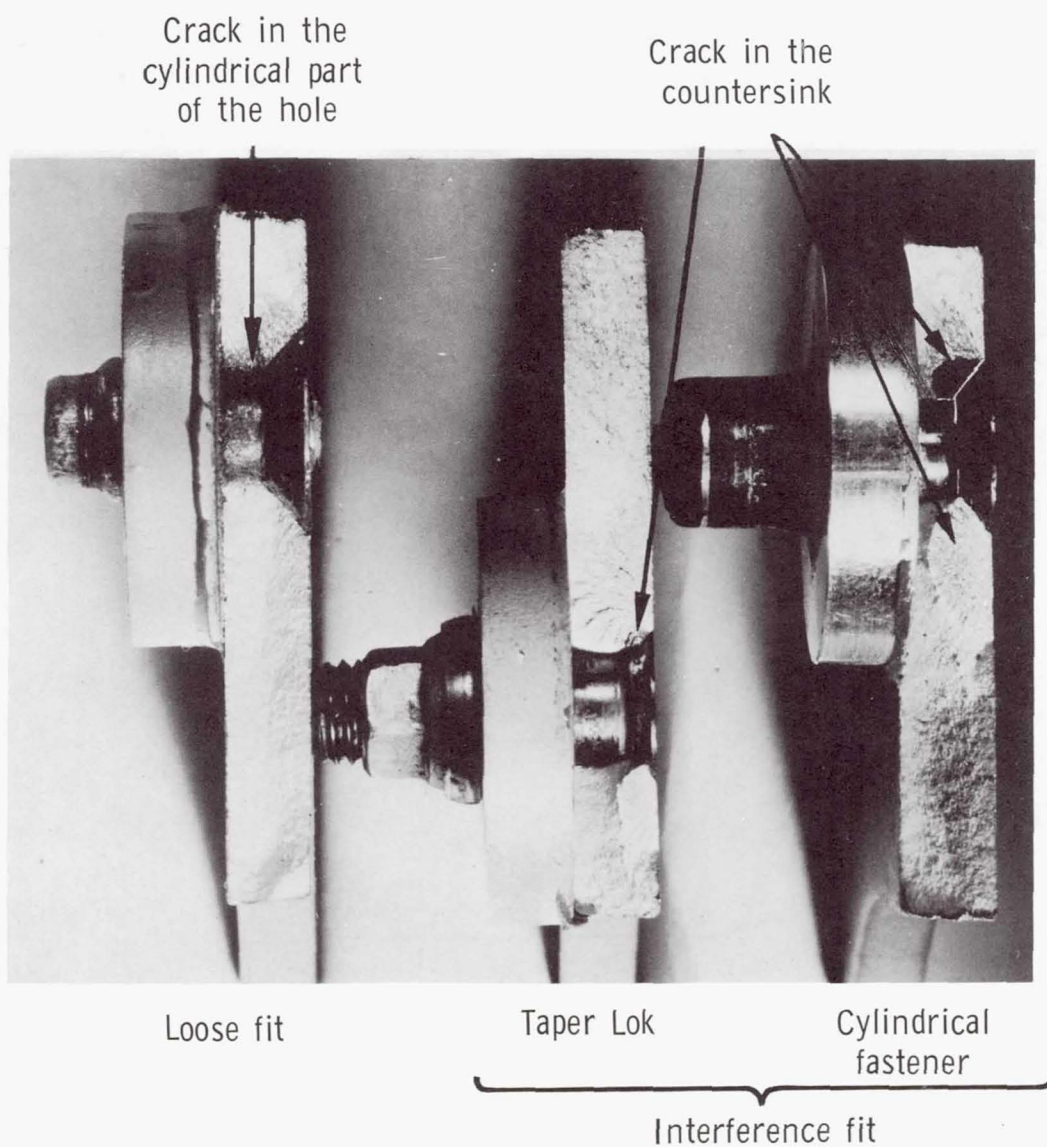


Figure 7.- Effect of interference on fracture mode.

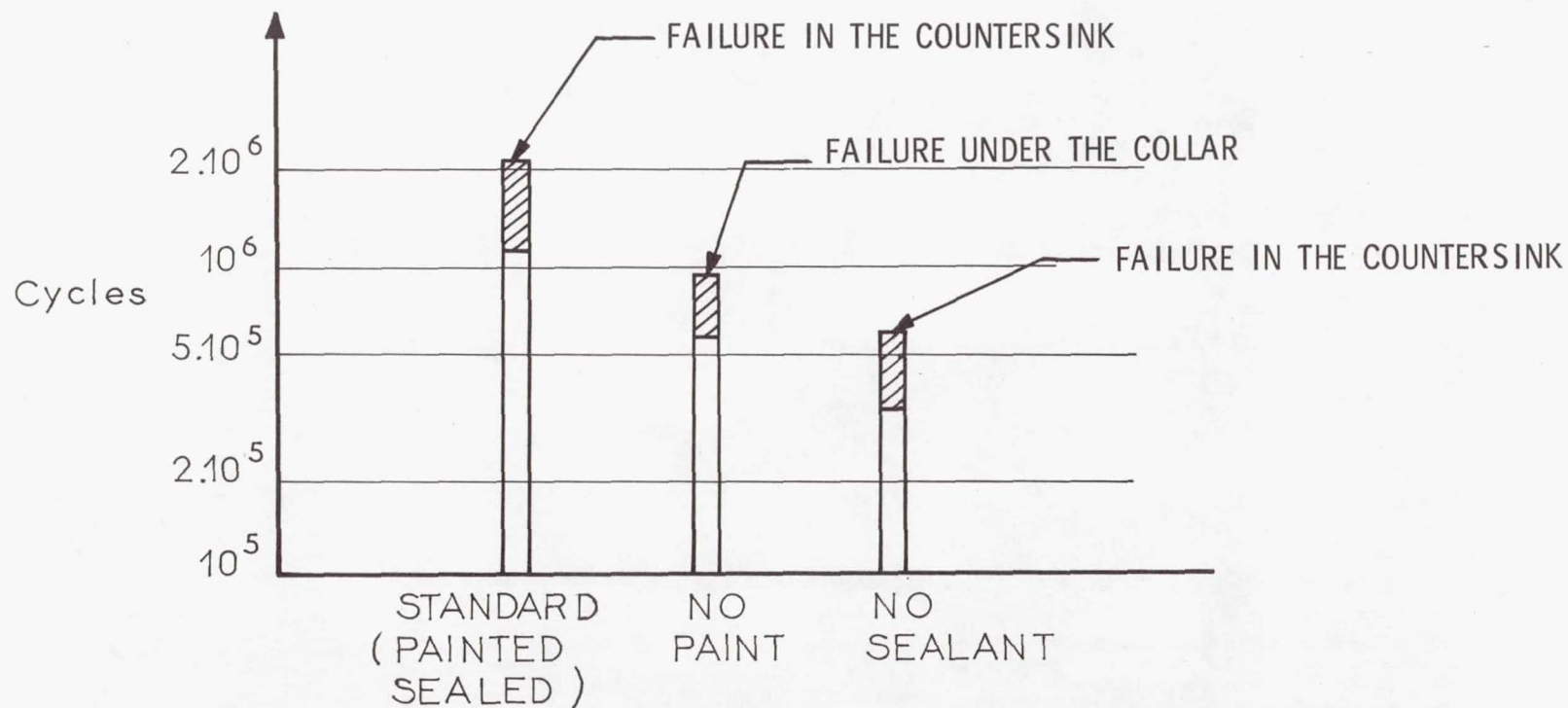


Figure 8.- Effect of paint and sealant on fatigue life of "dog bone" samples of 2024-T3. Fastener, 6-mm-diameter SL titanium, interference fit; test cycle  $\sigma = 17.2$  hectobars (25 ksi),  $R = 0.1$ .



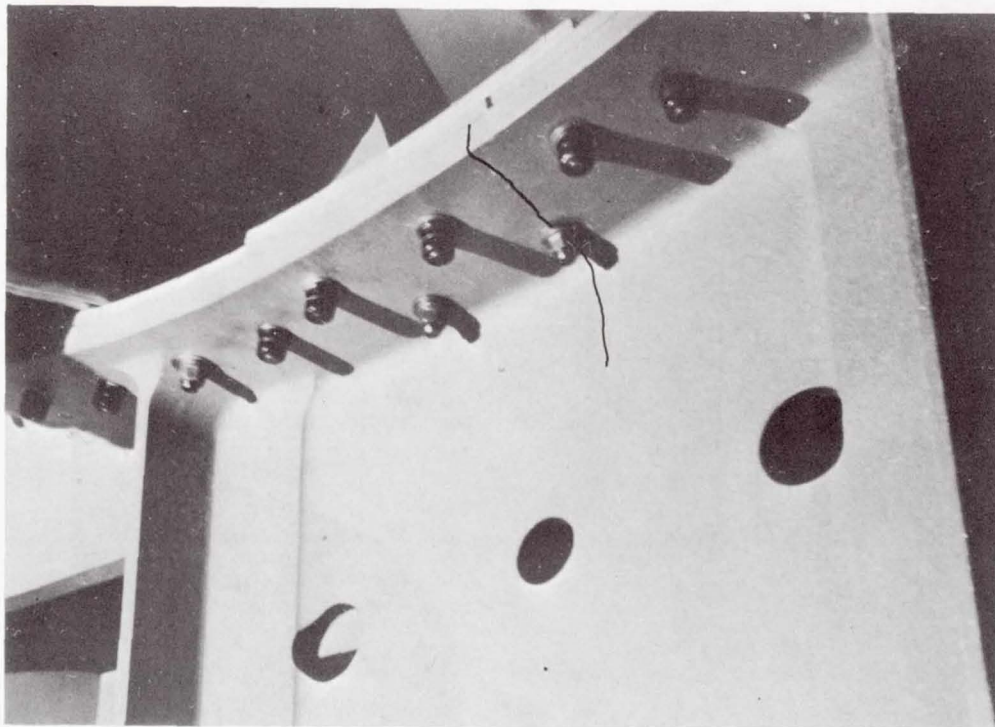
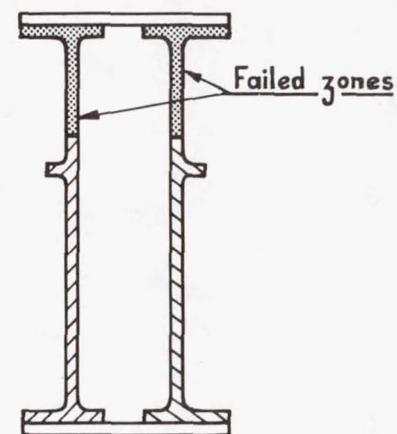


Figure 9.- Failure of a two-part main frame.



Section of the frame

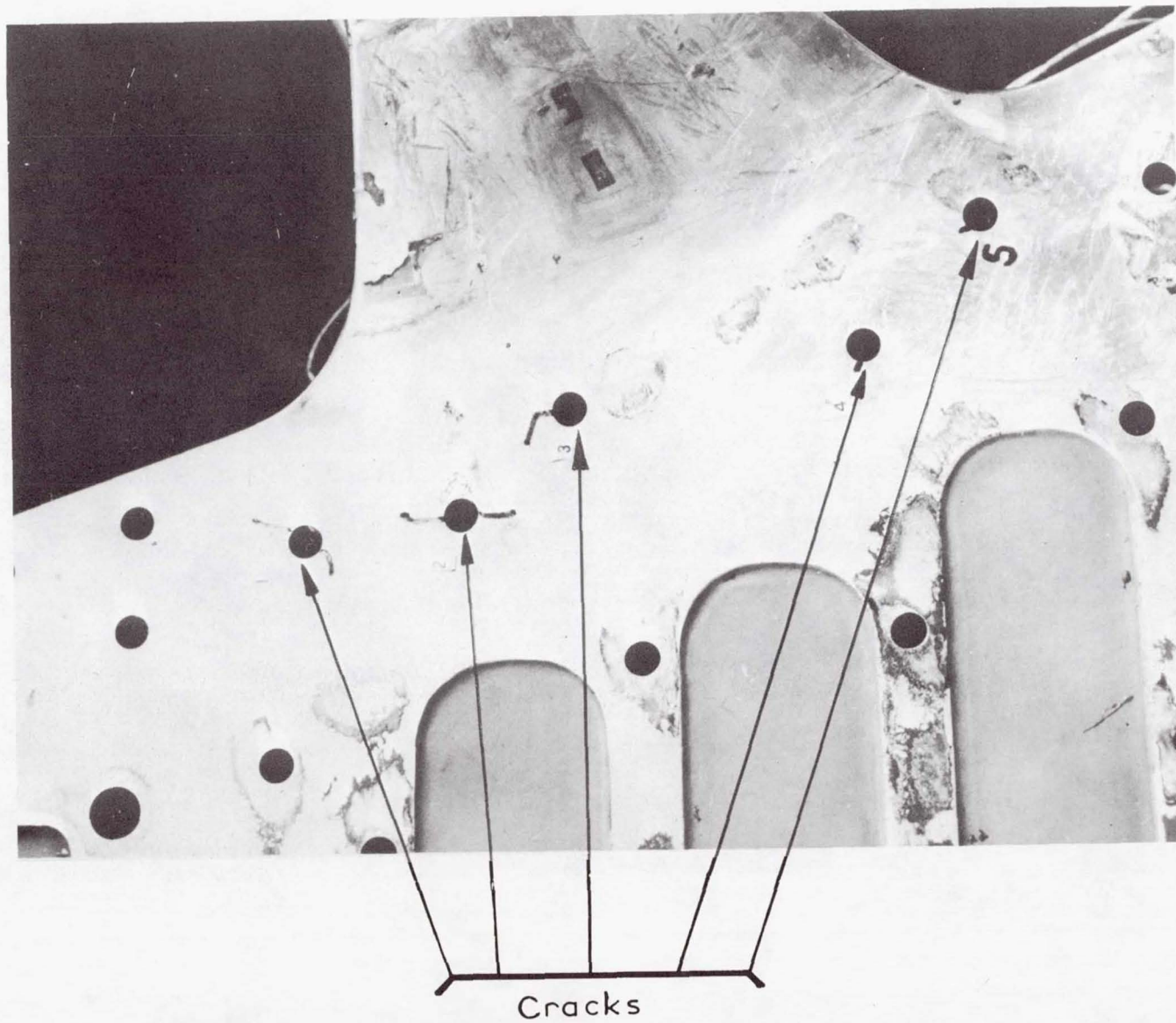
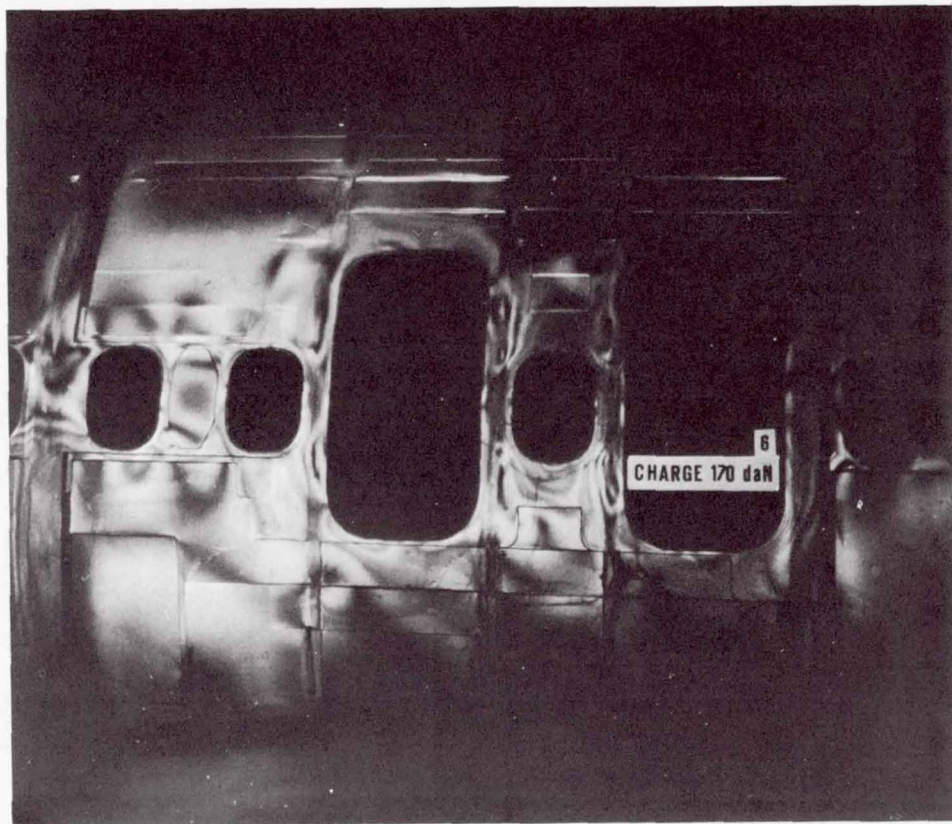
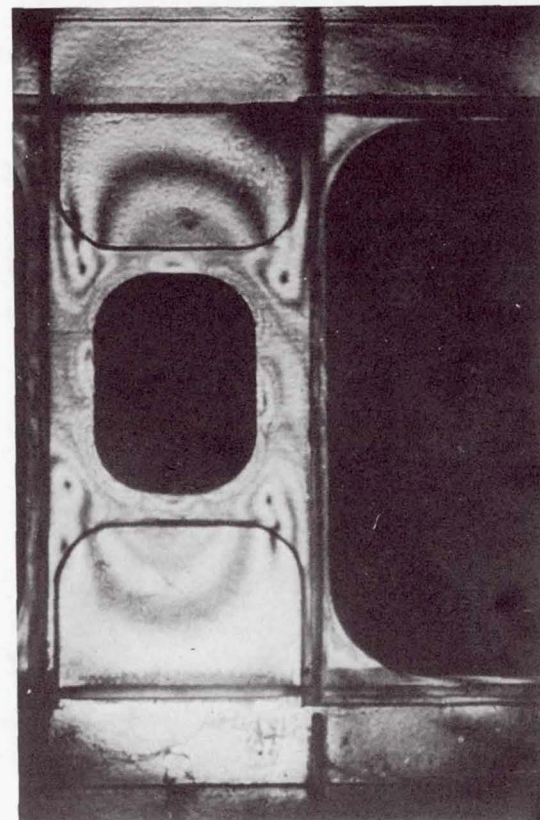


Figure 10.- Wing attachment fitting in which cracks grew at the same time from five holes.



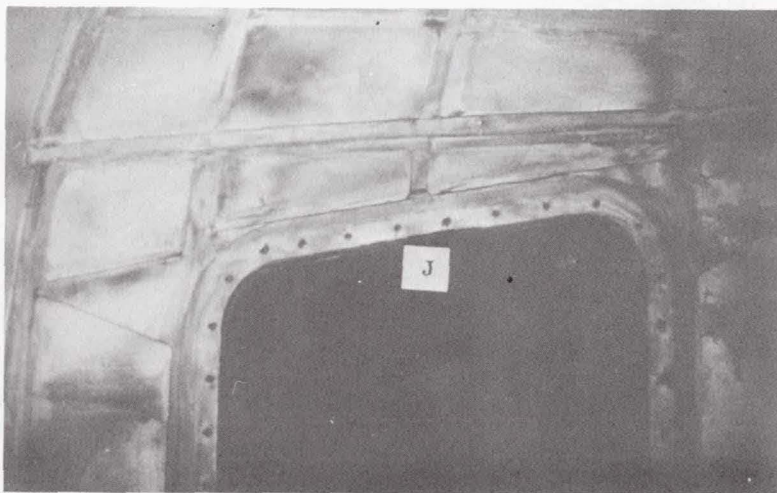
Overall view



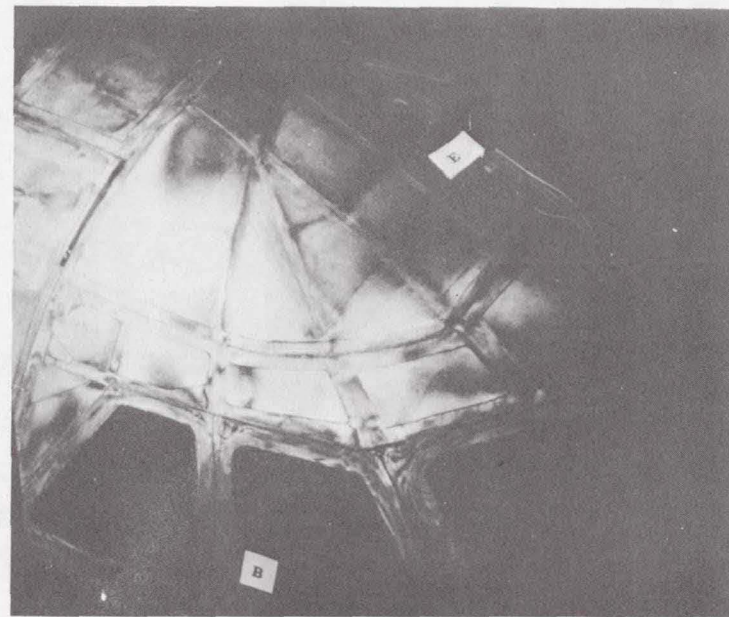
Emergency exit zone

Figure 11.- Study of photoelastic model of central part of fuselage.





Top part of passenger entrance



Cockpit

Figure 12.- Photoelastic model of front part of fuselage submitted to interior pressure.

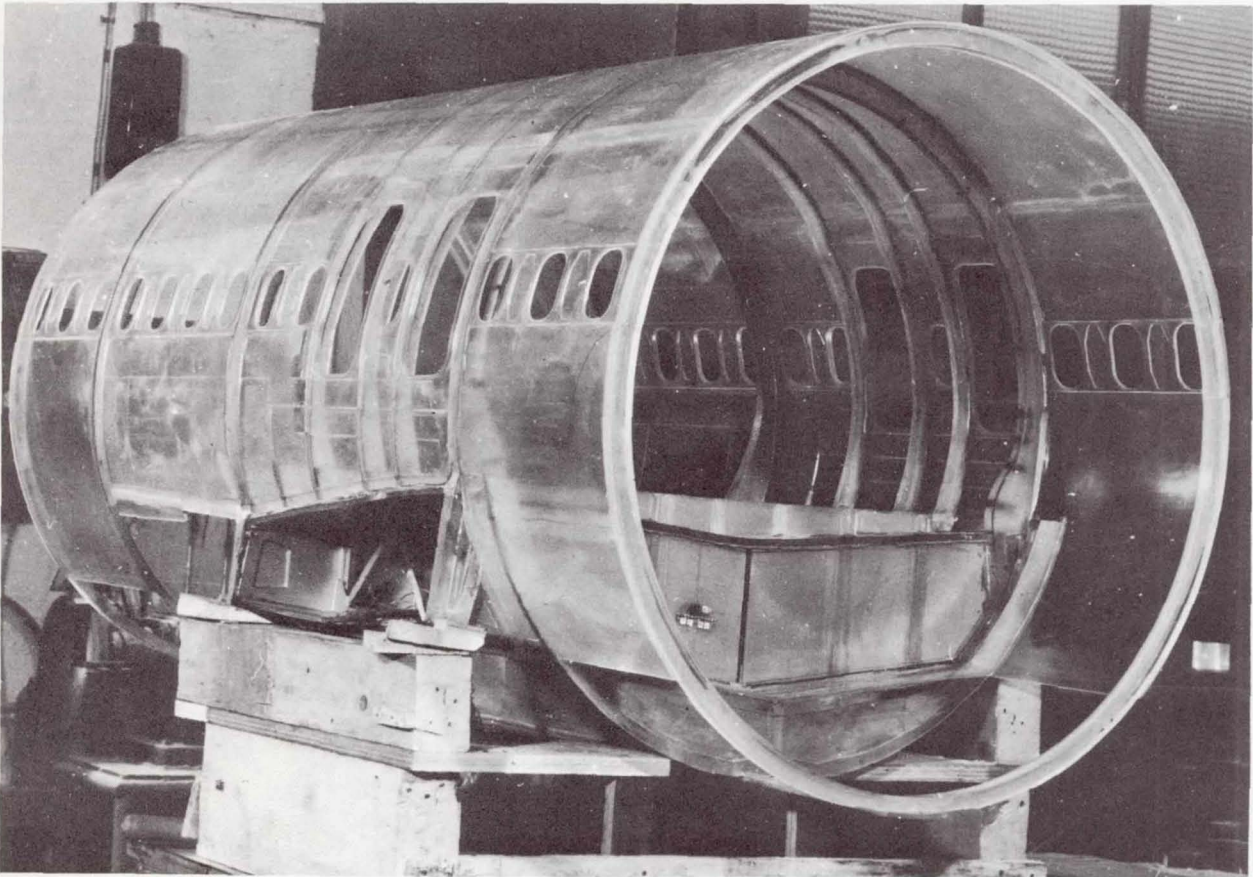
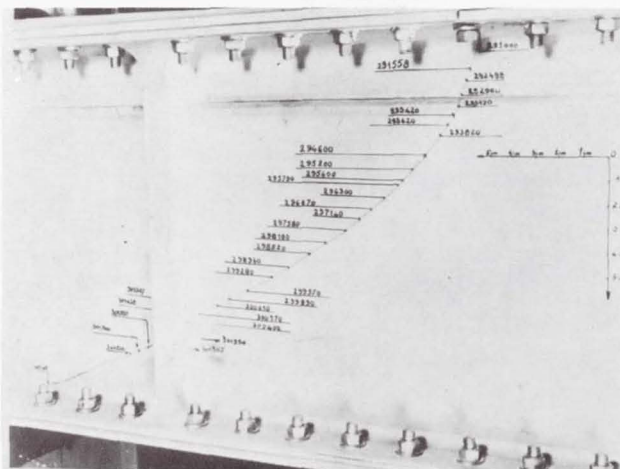
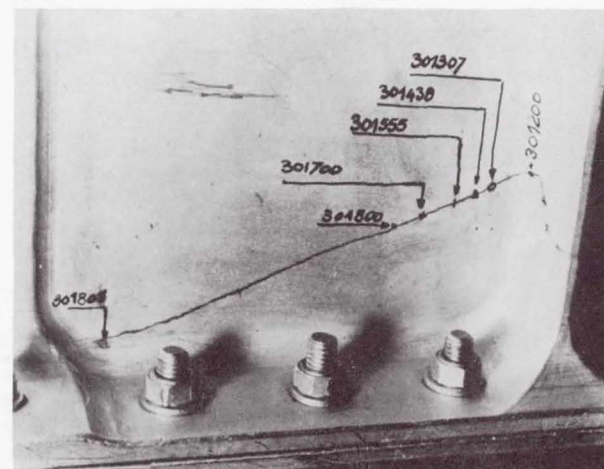


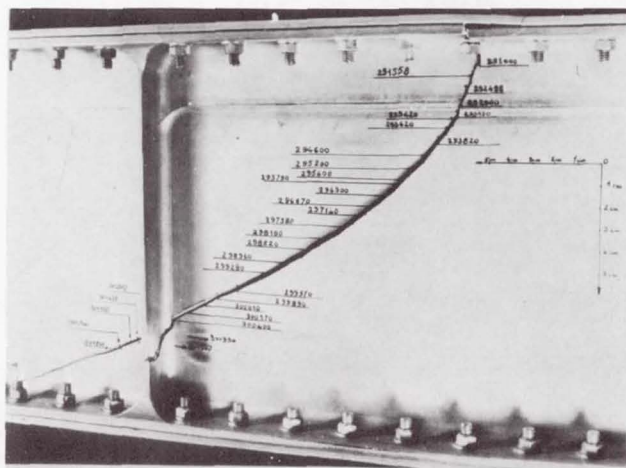
Figure 13.- Photoelastic model of central part of fuselage (1/5 scale).



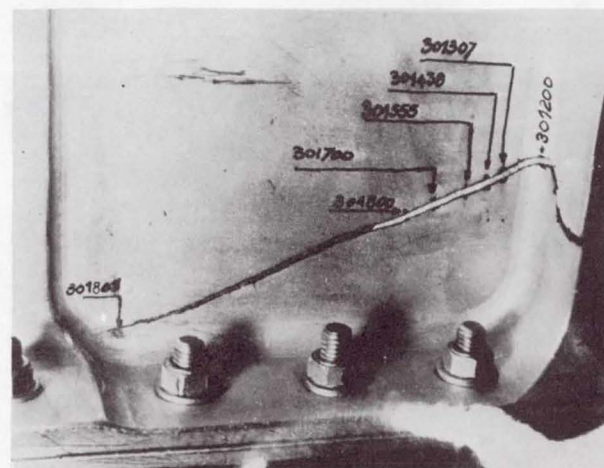
Overall view without load.



Closeup view without load.



Overall view under load.



Closeup view under load.

Figure 14.- Test of development of a crack in longeron no. 2.



# ON THE CYCLIC STRESS-STRAIN BEHAVIOR AND LOW-CYCLE FATIGUE OF AEROSPACE MATERIALS

By J. Burbach  
Krupp Forschungsinstitut, Germany

The elastic-plastic deformation behavior under cyclic stress of a number of different engineering materials was experimentally investigated with the aid of high-precision methods of measuring, some of which had been newly developed. (See refs. 1 to 4.) The report covers, in particular, experiments made with a variety of steels, the titanium alloy Ti-Al6-V4, a cobalt (tungsten) alloy, the high-temperature material Nimonic 90 and Dural (Al-Cu). The theory given – in an attempt to explain these experiments – is aimed at finding general formulas for the cyclic stress-strain behavior of engineering materials.

The experimental and theoretical investigations made can be summarily described as follows:

- (1) Geometric relationships of stable mechanical hystereses at a given variation of stress or strain and normal strain-rate dependence at cyclic deformation (plain and notched specimens) (refs. 5 and 6)
- (2) Accurate and direct measurement of the second-order elastic constants of polycrystals and their influence on the test result
- (3) Accurate balance of elastic and plastic energy in cyclic deformation, particularly in microscopic inhomogeneous plastic deformation
- (4) Spreading of Lüders bands in cyclic deformation; phenomena of strain hardening and removal of strain hardening
- (5) Inverse strain-rate dependence for aluminum-copper alloys
- (6) Investigations relating to cumulative damage at irregular cycling of stress.

The investigations, unfortunately, showed that cyclic stress-strain curves do not provide sufficient information for developing cumulative damage formulas that are sufficiently accurate from the physical aspect or suitable for engineering application. For this reason, it is not possible for the time being to give up practical simulation of actual material stresses with modern fatigue-testing machines.

The accuracy of the measurements made is exemplified by the cyclic stress-strain behavior of a round bar specimen with a sharp notch. (See figs. 1 and 2.) The stress – related to specimen cross-sectional area in the notch root – is plotted against the plastic deformation of the full-length specimen. It is clearly seen how the gradually

propagating crack causes a "nose" in the cyclic stress-strain curves; that is, the opening and closing of the crack becomes apparent.

In figure 1, the stress given is related to the notch-root cross section. The hysteresis curves shown were written with rising values of the plastic-strain amplitude. Strain measurement was made as usual at a distance between the edges of the inductive extensometer of 40 mm; thus, the mean value of the inhomogeneous extension was obtained.

The test represented by figure 1 was continued in such a way that with (approximately) constant amplitude of plastic strain, cyclic deformation proceeded. Continuation of the test eventually led to fracture of the specimen. See figure 2.

#### REFERENCES

1. Burbach, J.: A Tensile Machine With a Particularly High Spring Constant. Techn. Mitt. Krupp, Forsch.-Ber., Bd. 24, 1966, pp. 79-88.
2. Burbach, J.: The Static Tensile Test. Recent Methods of Metallurgical Investigation. Ver. Dt. Eisenhuttenleute (Dusseldorf), 1970, pp. 19-36.
3. Burbach, J.; and Vierling, P.: Experimental and Theoretical Studies of Strain Gauges, Particularly With Respect to Their Transverse Strain Sensitivity. Experimental Stress Analysis (Dusseldorf), VDI-Rep. 102, 1966, pp. 131-136.
4. Burbach, J.: Unavoidable Influences of the Loading Speed on the Indication of Load Cells. Precision Measurements With Strain Gauges for Force Measurement and Weighing (Dusseldorf), VID-Rep. 137, 1970, pp. 83-87.
5. Burbach, J.: Recent Investigations on the Plastic Behavior and Fracture Process of Hard Metals. Techn. Mitt. Krupp, Forsch.-Ber., Bd. 26, 1968, pp. 71-80.
6. Burbach, J.: Zum Zyklischen Verformungsverhalten Einiger Technischer Werkstoffe. Techn. Mitt. Krupp, Forsch.-Ber., Bd. 28, Heft 2, 1970.

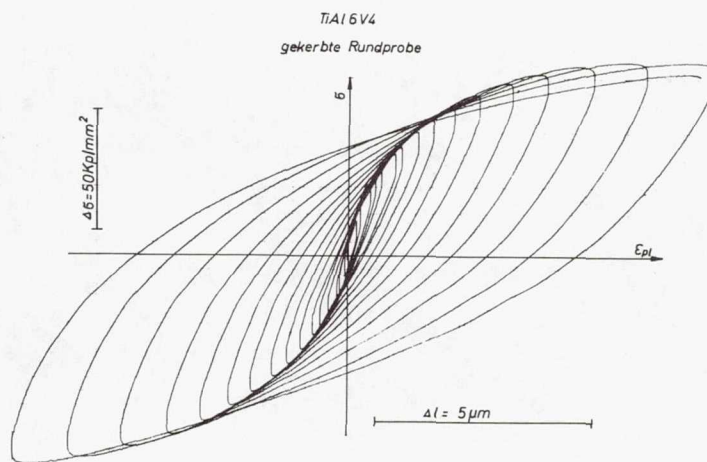


Figure 1.- Cyclic stress-strain behavior of a notched round bar specimen. Notch angle,  $60^\circ$ ; notch-root radius, 0.15 mm; notch-root cross-sectional diameter, 3 mm; Ti-Al6-V4.

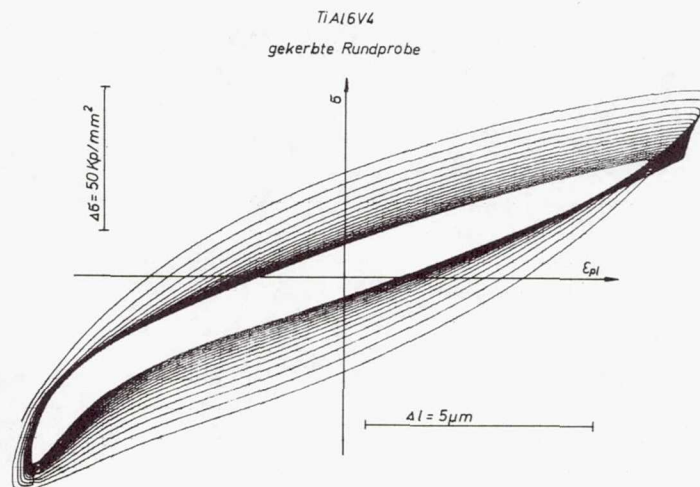


Figure 2.- Continuation of test measurements shown in figure 1 into the cracking stage. Ti-Al6-V4.



## A PARAMETRIC APPROACH TO IRREGULAR

## FATIGUE PREDICTION

By T. H. Erismann

Federal Laboratories for Testing Materials and Research

Dubendorf, Switzerland

## SUMMARY

The method proposed consists of two parts: empirical determination of certain characteristics of a material by means of a relatively small number of well-defined standard tests, and arithmetical application of the results obtained to arbitrary loading histories. The following groups of parameters are thus taken into account: the variations of the mean stress, the interaction of these variations and the superposed oscillating stresses, the spectrum of the oscillating-stress amplitudes, and the sequence of the oscillating-stress amplitudes. It is pointed out that only experimental verification can throw sufficient light upon possibilities and limitations of this (or any other) prediction method.

## FUNDAMENTALS OF PARAMETRIC APPROACH

The fundamental procedural scheme of the method evolved in this paper consists of the following phases:

- (1) Determination of a number of characteristics of the material by means of standard tests
- (2) Prediction of the fatigue life of the material on the basis of these characteristics and an analysis of the expected loading history.

The problem thus raised can, in principle, always be solved since for a specified accuracy there will always be a finite number of tests from which the necessary data for a satisfactory processing of the second phase can be drawn. There is, consequently, a problem of interpolation which can be solved with a finite number of base points. The question remains how to attain the goal economically. In view of the present state of development of servo-hydraulic testing equipment and digital computers, neither irregular stress sequences in the standard tests nor extensive algorithms in analysis and evaluation are prohibitive.

The progress of our knowledge of fatigue strength has in the last few decades become an alarming "parameter explosion." Thus, in order to avoid undue complications, no mention will be made of parameter groups connected with notch effect or environmental influences and nothing but the loading history will be considered.

Consequently, the following effects will be taken into account:

(1) Mean stress effect (index M), influence of the chronological curve of the mean stress

(2) Interaction effect (index J), influence of systematically occurring correlations between the effects of mean and oscillating stresses

(3) Spectral effect (index P), effect of the statistical distribution of the oscillating-stress variations

(4) Sequence effect (index Q), effect of the sequence in which the individual stress variations follow one another.

The parameters linked to these effects will be called in this paper "M.I.S.S. parameters" from their initial letters.

Owing to the inherent complexity of the problem, a certain number of simplifying assumptions must be made. In particular it is assumed that

(1) Miner's rule is applicable with sufficient accuracy to sufficiently narrow sections of a stress spectrum

(2) The influence of the mean-stress effect can be described with sufficient accuracy by the statistical amplitude distribution of the variations occurring in the mean stress

(3) Every increment of a loading history produces an incremental interaction effect approximately proportional to its mean stress level and to its "linear-damage increment" (according to Miner's rule)

(4) The effect of the sequence extends mainly to the "coarse sequence" (that is, to changes of the spectrum over longer periods of the loading history), whereas the "fine sequence" (that is, the individual sequence of the single-stress cycles) is of minor importance in practice, provided the process under consideration can be described with sufficient accuracy by stochastic characteristics

(5) The effects of the M.I.S.S. parameters allow with sufficient accuracy a linear (in one exceptional case, a quadratic) interpolation when the logarithm of the "Miner sum"

$$\sum = \sum_i \frac{n_i}{N_i} \cdot \dots \quad (1)$$

(which according to Miner's rule should always be equal to 1) is used as the interpolation value. In equation (1),  $n_i$  is the number of cycles applied at stress level whereas  $N_i$  is the total number of cycles to cause failure at stress level.

It is not possible here to justify these assumptions. A justification of these assumptions is given in reference 1.



## OUTLINE OF THE M.I.S.S. METHOD

The method outlined here starts from relation (1); it being clearly understood, however, that a sum not equal to 1 is permissible. In accordance with the assumptions made, the four M.I.S.S. parameters  $P_M$ ,  $P_J$ ,  $P_P$ , and  $P_Q$  are defined and

$$\sum = f(P_M, P_J, P_P, P_Q) \cdot \cdot \cdot \quad (2)$$

is postulated. This postulation means that the spectrum, as in Miner's rule, is still the most important group of parameters, but not the only decisive one.

Thus, the first phase of the method results in the performance of an unequivocally defined series of standard tests with well-defined M.I.S.S. parameters and the determination of the resulting standard Miner sums  $\sum_S$  which are to be considered as characteristics of the material.

The second phase, that is, the application to an expected loading history with a given nominal fatigue life, is divided into the following partial phases:

(1) Analysis of the loading history according to equation (1). The result is the Woehler-Miner sum  $\sum_W$ .

(2) Analysis of the loading history according to well-defined formulae for determining their M.I.S.S. parameters.

(3) Application of the M.I.S.S. parameters as a means of interpolation in the results field of the standard Miner sums. The result is the Effective Miner sum  $\sum_E$ .

(4) Formation of the quotient  $\sum_E / \sum_W$  which indicates the chances of survival of the specimen. For  $\sum_E / \sum_W > 1$ , survival of the loading history is to be expected.

The first and fourth phases are carried out according to the known algorithms of Miner's rule. The interpolation in the third phase must mainly be carried out linearly for  $\log \sum$ . Figure 1 shows the interpolation for  $P_M$  and  $P_J$ , with  $P_P$  and  $P_Q$  held constant. The heights of the column at its four edges represent the results of four standard tests. The result of the interpolation is the height (heavy dotted line) for  $P_M$  and  $P_J$ . Only the standard tests and the stress-history analysis need to be considered in more detail.



## MATHEMATICAL TREATMENT OF PARAMETER GROUPS

It would be impossible to give a complete review of the mathematical deductions applied to obtain appropriate equations for the calculation of the M.I.S.S. parameters. It must be referred, therefore, to more detailed works on the subject. (See refs. 1 and 2.) The following remarks are made in order to give a general idea of the logical structure of the method.

All the equations used in this connection are based solely on the simplifying assumptions made. For instance, the second assumption means only that the mean stress effect for given values of the other parameters is determined by the "spectrum of the mean stress" so that Miner's rule may be considered as applicable to the mean stress. Thus, an extremely simple definition of the mean-stress parameter is obtained; that is,

$$P_M = \sum \frac{m_\sigma}{N_\sigma \sum_W} \dots \quad (3)$$

where  $m_\sigma$  is the number of mean-stress variations of the value  $\sigma$ , and  $N_\sigma$  is the cycle number pertaining to  $\sigma$  according to the  $\sigma$ -N curve. The division by the Woehler-Miner sum  $\sum_W$  is used for normalizing purposes.

The spectrum of a loading history is represented in principle by a parabolic approximation so that theoretically, three parameters are needed for the mean value, the average slope, and the curvature of the parabola. The first of these parameters, however, is insignificant since in the chosen representation, the mean value of the parabola is given. It is a particular feature of the method that the ordinal numbers  $i$  of certain well-defined stresses  $\sigma_i$  are used as values of the independent variable of the approximation so that the respective numbers  $n_i$  are expressed by

$$\frac{n_i}{N_i \sum_W} = c_0 + c_1 \cdot i + c_2 \cdot i^2 \dots \quad (4)$$

where  $c_0$ ,  $c_1$ , and  $c_2$  are the spectral parameters  $P_P$ .

In a more or less analogous way, the parameters for interaction and sequence,  $P_J$  and  $P_Q$ , are deduced from the assumptions made. Both are connected with variations of the spectral parameter  $c_1$ ; thus, predominance of high- or low-stress amplitudes under particular conditions is indicated. Although  $P_J$  establishes a correlation with the mean stress  $\sigma_m$  (taking into account such phenomena as the increased dynamic forces due to increased payload of a vehicle),  $P_Q$  accounts for variations undergone in

the course of the loading history as a whole (as encountered owing to more frequent overload when an aircraft is transformed from passenger to cargo transport); thus, it serves as a safeguard against unpleasant surprises, because many materials have a shorter fatigue life when first subjected to low- and then to high-stress amplitudes.

The influence of parameter variations upon loading histories is illustrated in figures 2, 3, and 4. In figure 2, the oscillating stresses are not present for negative mean stresses because of the choice of constants in the equations. In figure 3 the stress amplitudes are higher in section II than section I; thus, a higher value of  $c_1$  is indicated. In figure 4, the variation of  $c_2$  results in predominance either of extreme (high and low) or of medium amplitudes. It will be observed that in figure 3, section II shows higher stress amplitudes than section I; thus, a higher value of  $c_1$  is indicated. Variation of  $c_2$  results in predominance either of extreme (high and low) or of medium amplitudes (fig. 4).

## STANDARD TESTS AND PRACTICAL APPLICATION

Since linear interpolation of  $\log \sum$  has been accepted for all parameters (excluding  $c_1$ ), variations through all possible combinations other than the meaningless ones ( $P_M = 0_i$ ;  $P_J + 0$ ) would give 36 base points which can be found from 36 tests (plus repetitions). The cost is considerable but is certainly justified for important materials.

Experience will show whether all 36 standard tests are really required. The number depends on how far the multidimensional functions of figure 1 can be approximated by plane surfaces. If, for example, it should be found that, apart from  $P_P$ , the function surface can be considered as sufficiently plane, then only the inclinations of this plane would have to be known; that is, for every additional parameter only one single base point would have to be determined and nine tests would suffice. Probably the truth lies between these two extremes.

An actual "cooking recipe" for the details of the method is found in reference 1. There the individual steps are not only commented on but are also compiled in tabular form so that the economic establishment of suitable computer programs is possible.

## POSSIBILITIES AND LIMITATIONS

By the method described, it is possible to determine the probable fatigue life of a given material under a given loading history without having to carry out a large number of loading tests. As a matter of fact, the standard Miner sums as characteristics of a material, together with the  $\sigma$ -N curve, should contain enough data to predict the fatigue



life of a material with sufficient accuracy even in irregular stress sequences. The main point obviously is 'What is meant by "sufficient accuracy"?' Of course, the M.I.S.S. method is more expensive than the determination of a number of  $\sigma$ -N curves, although not impossibly so. In return, it refines the results obtained from Miner's rule (which are derived only from  $\sigma$ -N curves). Only systematic tests with different materials can give a definite answer. Such tests should prove worthwhile, for even Miner's rule in its present form is better than it is usually believed to be. Thus, it should usually be possible to supplement it by introducing additional parameters (mean stress, interaction, and sequence) so that the result can satisfy the demands of practice.

It must be stressed in this connection that the testing equipment available should be improved in the sense of cheaper and faster execution of large numbers of irregular fatigue tests. Only such a development will guarantee in reasonable time the acquisition of the information necessary for an efficient verification of the methods proposed here or elsewhere.

#### REFERENCES

1. Erismann, T. H.: Ein Verfahren zur Abschätzung der Lebensdauer von Materialien bei unregelmässigen Belastungsfolgen. Schweizer Arch. angew. Wiss. Tech. 36, 1970, pp. 57, 103.
2. Erismann, T. H.: Fatigue-Life Prediction Under Irregular Stress Conditions. J. Strain Analysis, vol. 5, 1970, p. 207.

#### BIBLIOGRAPHY

1. Miner, M. A.: Cumulative Damage in Fatigue. Trans. ASME, Ser. A, J. Appl. Mech., vol. 67, 1945, p. 159.
2. Palmgren, A.: Die Lebensdauer von Kugellagern. ZVDI, Bd. 68, 1924, p. 339.



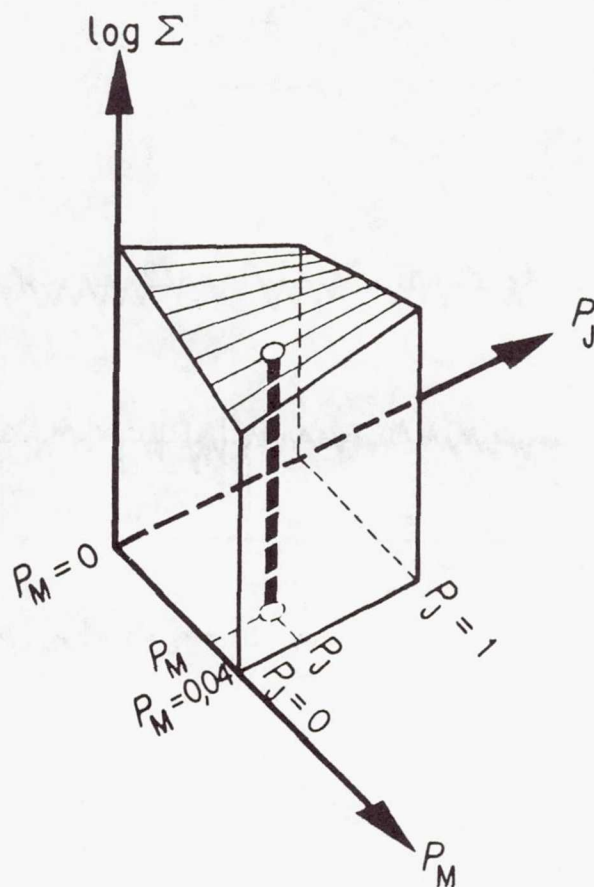


Figure 1.- Interpolation for  $P_M$  and  $P_J$ .

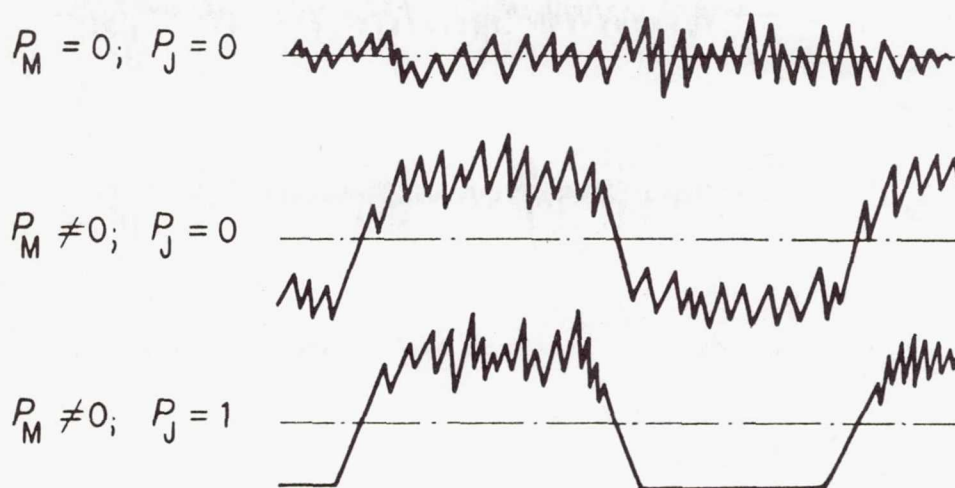


Figure 2.- Characteristic stress curves for various values of  $P_M$  and  $P_J$ .

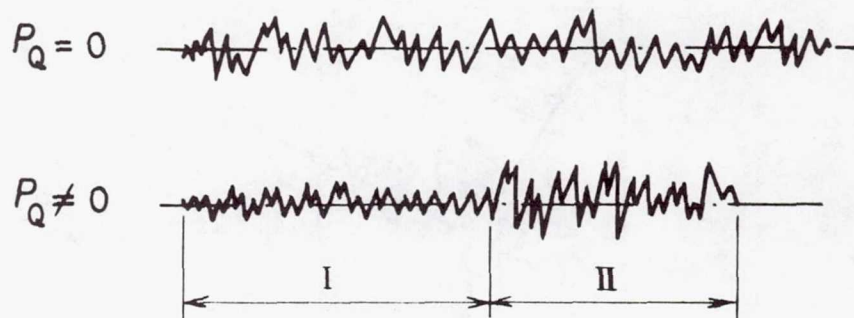


Figure 3.- Characteristic loading histories for  $P_Q = 0$  and  $P_Q \neq 0$  and  $P_M = P_J = 0$ .



Figure 4.- Characteristic stress curves for various values of the spectrum curvature parameter  $c_2$ .

## FRACTURE CONTROL PROCEDURES FOR AIRCRAFT STRUCTURAL INTEGRITY

By Howard A. Wood

Air Force Flight Dynamics Laboratory, U.S. Air Force  
United States

### SUMMARY

This report reviews the application of applied fracture mechanics in the design, analysis, and qualification of aircraft structural systems. Recent service experiences are cited.

Current trends in high-strength materials application are reviewed with particular emphasis on the manner in which fracture toughness and structural efficiency may affect the material selection process.

General fracture control procedures are reviewed in depth with specific reference to the impact of inspectability, structural arrangement, and material on proposed analysis requirements for safe crack growth. The relative impact on allowable design stress is indicated by example.

Design criteria, material, and analysis requirements for implementation of fracture control procedures are reviewed together with limitations in current available data techniques. A summary of items which require further study and attention is presented.

"Fracture Mechanics has, in fact, been a boon to the metal producing industry; it has made the finite crack in a structure reputable and even fashionable." (Quoted from A. M. Freudenthal, Miami Beach, Florida, December 1969.)

### INTRODUCTION

Primary aircraft structural components generally contain flaws or defects of variable shape, orientation, and criticality which are either inherent in the basic material or are introduced during the fabrication or assembly processes.

From an industry survey (ref. 1) it was concluded that the majority of cracks found in aircraft structures were initiated from tool marks, manufacturing defects, and the like. When not detected, these flaws experience the combined driving forces of environment and service loading and may grow to serious proportions resulting in



reduction of service life or complete loss of the aircraft. The final fracture process is most often sudden, unexpected, and almost totally devoid of gross plastic deformation or yielding. While this "brittlelike" behavior is most spectacular in the so-called high-strength alloys, it is seen to occur to some degree in most of the commonly used aircraft structural materials.

Recent cases of catastrophic failure in primary structure of first-line aircraft have emphasized the need for a "fresh" new look at the structural integrity process currently used to design and qualify structural systems. Under such an improved process, fracture control would insure the reduction in the probability of catastrophic failure due to the presence of undetected flaws and cracks. This assurance can best be achieved by the intelligent material selection based on fracture as well as common strength considerations and by assuming the existence of flaws in "new" structures and accounting for their probable growth during service.

Linear elastic fracture mechanics analysis and testing techniques have reached the state of development where they may be used with a moderate level of confidence to assess the degree of flaw criticality, to predict the extent of subcritical flaw growth prior to fracture, and to determine the resultant failure modes (ref. 2). Much of the basic groundwork for the current application of linear elastic fracture mechanics to "real" structures can be attributed to the investigation associated with fracture control of metallic pressure vessels for space applications (refs. 3 and 4). While attempts to translate this technology to aircraft usage have been moderately successful, limitations must be recognized which are due to the complex spectrum of loads, temperatures, and chemically aggressive agents that comprise the aircraft environment.

Fail-safe procedures in aircraft have resulted from civil requirements and from independent regulation within the particular airframe company. These efforts have been beneficial on many Air Force aircraft.

Application of fracture mechanics within the Air Force has been almost exclusively "after the fact" to determine remaining safe life with cracks, residual strength, and safe inspection intervals for older systems in which flaws have developed and progressed to near-critical dimensions. Some examples of service application in which the Air Force Flight Dynamics Laboratory (AFFDL) actively participated are summarized in table I (see refs. 5, 6, 7, 8, 9, and 10). In practically all cases, however, attempts to formulate reliable solutions were hampered by the lack of an adequate material-environmental data base and deficiencies in analysis techniques, particularly those techniques which must account for load interaction and environmental effects. One purpose of this paper is to review those areas of application where deficiencies in the technology exist and to offer suggestions for alleviating these deficiencies.

Under the F-111 Recovery Program (ref. 9), basic fracture mechanics data are currently being amassed for D6ac steel by the contractor and several laboratories. (See refs. 8, 11, and 12.)

Specific criteria, guidelines, or requirements for considering fracture mechanics principles in the design and procurement cycle for Air Force aircraft have not existed in the past. Only recently have requirements been levied for new systems. It is too early to assess their impact. In the proposed revisions to the Air Force Airplane Structural Integrity Program (ASIP) which is given in reference 13, damage tolerance considerations are outlined. These changes are currently being reviewed prior to being formally incorporated.

There exists a natural unwillingness amongst many to accept the "preexistent flaw" concept in aircraft design because of the weight penalties normally associated with damage-resistant structures. There are those who cite system performance degradation and the time and cost of implementing fracture requirements as deterrents. The imposition of arbitrary fracture requirements should be done cautiously under current state-of-the-art limitations in analysis methods and testing techniques are resolved and material-environmental behavior is better understood.

In this paper, recent structural material utilization cases are summarized to indicate those problems associated with the use of high-strength material. General fracture control procedures are reviewed with specific reference to the impact of safe crack growth and remaining strength requirements on system design. Examples are cited, including recent laboratory efforts in the analysis of crack growth under variable-amplitude spectrum loading. Limitations in basic design criteria, material data, and analysis are reviewed.

## SYMBOLS

$a$	crack size, length or depth, inches
$a_{cr}$	critical crack size, inches
$a_p$	proof-test crack size, inches
$\Delta a$	change in crack size, inches
$B, t$	thickness, inches
$c$	one-half surface crack length, inches



E	modulus of elasticity, ksi
f	frequency of test load application, cycle/minute
K	stress intensity factor, ksi- $\sqrt{\text{in.}}$
K <sub>c</sub>	critical stress intensity factor, ksi- $\sqrt{\text{in.}}$
K <sub>Ic</sub>	plane strain fracture toughness, ksi- $\sqrt{\text{in.}}$
K <sub>ISCC</sub>	critical stress intensity factor for stress corrosion cracking, ksi- $\sqrt{\text{in.}}$
K <sub>max</sub>	maximum stress intensity factor, ksi- $\sqrt{\text{in.}}$
K <sub>min</sub>	minimum stress intensity factor, ksi- $\sqrt{\text{in.}}$
$\Delta K = K_{\text{max}} - K_{\text{min}}$	ksi- $\sqrt{\text{in.}}$
M,N	number of load cycles
$\rho$	material density, lb/in <sup>3</sup>
$R = \frac{K_{\text{min}}}{K_{\text{max}}}$	
r <sub>y</sub> ,R <sub>y</sub>	radius of crack tip yield zone, inches
$\sigma$	stress, ksi
$\Delta\sigma$	change in stress, ksi
$\sigma_L$	limit stress, ksi
$\sigma_{ys}$	yield strength, ksi
da/dN	fatigue crack growth
da/dt	environmental crack growth



Subscripts:

0,1,2,3,... reference values

A,B,C,D,E,F,G requirements

c critical

i initial

f final

max maximum

min minimum

## MATERIALS UTILIZATION IN STRUCTURAL DESIGN - RESISTANCE TO FRACTURE

With the advent of higher performance air vehicles, weight minimization has necessitated optimum design and construction techniques and greater utilization of the high-strength, high-efficiency, and limited-ductility materials. The process also has evolved increased operating stresses and, thus, lower tolerance to flaws and cracks.

These applications have resulted in critical flaw dimensions of the order of the material thickness which make positive detection by current nondestructive inspection (NDI) practice questionable. Current trends in the structural design utilization of high-strength alloys for resistance to catastrophic fracture can be evaluated by examining trends in two basic material parameters, the plane strain fracture toughness index  $K_{Ic}$  and the conventional yield strength  $\sigma_{ys}$ .

For a specific application, the designer must select a material of reasonably high strength in order to meet static strength requirements and still achieve minimum weight. A parameter for evaluating structural efficiency ( $\sigma_{ys}/\rho$ ) is mentioned later. In the selection process, however, fracture toughness must be a consideration. The achievement of maximum yield strength and maximum fracture toughness is often difficult as is illustrated in figure 1. It is generally recognized that within certain material groups, toughness decreases with increasing yield strength. This trend is illustrated in figure 1 for aluminum, titanium, and several selected steels where material data from table II have been plotted. Variations in  $K_{Ic}$  can be expected for any given alloy and strength

level, and these variations are generally due to metallurgical aspects, impurities, or manufacturing processing. This variability makes the selection of a "design allowable" extremely difficult.

In specifying a particular material and strength level (minimum acceptable  $\sigma_{ys}$ ), the designer usually would not be concerned about those quantities of material which possessed strength levels on the upper end of the normal range. However, because of the dramatic decrease in  $K_{Ic}$ , he must in many cases limit the upper bound of acceptable range of yield strength. This is current practice in specifying titanium alloys. In figure 1,  $K_{Ic}$  ranges for two common titanium alloys are noted. These data are shown at one yield strength value to illustrate the fallacy in specifying only  $\sigma_{ys}$  minimum. Recent F-111 experience with D6ac steel has indicated a similar phenomenon; however, the variation of  $K_{Ic}$  is dependent upon the heat treatment procedure (ref. 9). In this case, two specimens of material from different lots might possess the same measured  $\sigma_{ys}$  and yet have a two-to-one range in  $K_{Ic}$ .

The material selection process is therefore a trade-off procedure wherein many concurrent requirements must be satisfied. For the case in point, the designer must establish criteria for accepting either a reduced toughness or a reduced strength level. The choice might be dictated by overall flaw tolerance. This is illustrated in figure 2 where the ordinate  $(K_{Ic}/\sigma_{ys})^2$ , a parameter indicative of crack size, is used. Since structures are designed to withstand (statically) a percentage of the yield strength, this parameter may be conveniently used to illustrate flaw tolerance sensitivity. Examination of figure 2 indicates a more dramatic reduction in the crack length parameter with increased yield strength.

The same trend is repeated in figure 3; however, the yield strength has been normalized with respect to the material density  $\rho$ . The parameter  $\sigma_{ys}/\rho$  is one form of structural efficiency used to select materials. Note that material ranking has changed, with titanium being superior to steel. One exception illustrated is that 18Ni-Co-Mo maraging steel and 9Ni-4Co-2C fall beyond the bounds illustrated. There are recognizable limits on the values of both  $(K_{Ic}/\sigma_{ys})^2$  and  $\sigma_{ys}/\rho$  for materials in use today. The bounds are illustrated in figure 3.

The data presented in figure 3 clearly illustrate the relationship of nondestructive inspection (NDI) capability and material selection to resist brittle fracture. For example, a through-the-thickness crack will experience plane strain fracture when  $K = K_{Ic} = \sigma \sqrt{\pi a_{cr}}$ . If fracture is assumed to occur at the design limit stress, the value of critical crack length  $a_{cr}$  can be computed. For many aircraft structures, design limit stress is of the order of  $\sigma_L = 0.6\sigma_{ys}$  and  $a_{cr} = \left( \frac{K_{Ic}}{0.6\sigma_{ys}} \right)^2 \frac{1}{\pi} \approx \left( \frac{K_{Ic}}{\sigma_{ys}} \right)^2$ . Thus each point in figure 3 might be considered the critical characteristic flaw dimension for plane



strain fracture and thus would describe the sensitivity level required for fleet inspection. For this type of selection criterion, many materials may be prohibited because of the extremely small flaws which must be detected. Limits of NDI practice are not well defined.

With the technological trend in material utilization growing toward greater strength-density ratios, it seems logical also to define more realistic limits on the material selection based on uncontrollable "human element" defects. Thus, the crack size definition of figure 3 might indicate limits produced by normal tool marks, scratches, or gouges produced during manufacture or maintenance. If these limits are recognized as sound, then more effective means of inspection may be required, such as proof testing, if use is to be made of these alloys (fig. 4).

All the data from table II has been plotted in figure 5 with both  $K_{IC}$  and  $\sigma_{ys}$  normalized with respect to density  $\rho$ . This plot indicates an apparent technological limit which material producers might find difficult to exceed (ref. 2).

In the previous discussion it was assumed that plane strain fracture is dominant. Fortunately, this is not always the case because of the effect of thickness, plasticity, and geometry (figs. 6 and 7). The question does remain, however, as to what role  $K_{IC}$  has in the material selection and analysis process.

It is perhaps safe to conclude that the selection of candidate materials for fracture considerations can be made on the basis of superior  $K_{IC}$ , as long as the materials are similar. The decision, however, rests upon the thickness required to fulfill the task. In figure 7, the variation of critical stress intensity factor with thickness is illustrated for several alloys (ref. 2).

## MATERIAL SELECTION – RESISTANCE TO FLAW GROWTH UNDER REPEATED LOADS

In the preceding discussion,  $K_{IC}$  and  $\sigma_{ys}$  were shown to be effective parameters in selecting a material class and alloy to resist brittle fracture under plane strain conditions. Wide variations in strength and toughness were indicated within a given material. Toughness was also seen to vary within a given alloy group.

Material selection based on cyclic growth considerations is not as clearly defined, since observed trends in rate data for a nonaggressive environment indicate that materials within a group or class generally fall within a narrow scatterband, with little, if any, dependence on toughness. Average growth-rate curves have been included in figure 8 to illustrate the relative relationship between materials. Hahn (ref. 6) has observed that the rate  $da/dN$  can be approximated for many materials as



$$\frac{da}{dN} = 8 \left( \frac{\Delta K}{E} \right)^2$$

in the central or log linear portion of the growth-rate curve. Several points are shown in figure 8 which were obtained by using the Hahn expression. Because of the relationship of growth rate to modulus  $E$ , the data can be normalized with respect to the material density  $\rho$  as indicated in figure 9 where rate curves are seen to converge. It is apparent, then, that a material's advantage can only be assessed on an individual application basis. Growth under variable-amplitude spectrum loading, for example, may produce different trends in growth retardation due to the interaction of loads. Generally speaking, however, the time to failure from an initial flaw is dependent primarily upon the toughness  $K_{Ic}$ . This is illustrated in figure 10, with cutoffs for several levels of toughness. The relative effect, however, may be dependent upon the shape and severity of the spectrum.

While the preceding discussion has been concerned with the cyclic flaw growth behavior, the selection of materials for repeated load application in the presence of flaws may be seriously influenced by the chemical and thermal environments in which the structure must operate. No attempt is made in this paper to cover these trends. The reader is referred to several excellent publications (refs. 6, 11, 14, and 15).

#### FRACTURE CONTROL – BASIC CONSIDERATIONS

The traditional Air Force approach to structural integrity (ref. 13) requires that "safe life" be evaluated through the cyclic test program. The success of this approach in determining the overall fatigue resistance of full-scale structures has been well documented (refs. 6 and 16). The achievement of "fatigue quality" through careful workmanship, surface finishes, and detailed design (local stress levels) and the demonstration of resistance to crack initiation are basic and reasonable goals. Therefore, before presenting suggested procedures for fracture control, it is important that two basic tenets be stated:

(1) Damage tolerant design and fracture control philosophy should not be considered as substitutes for adequate fatigue considerations.

(2) Consideration must be given to the probable existence of flaws within all basic primary structures.

Crack initiation resistance and fracture resistance should be considered as complementary objectives.

By virtue of its complex nature and varied operational regimes, an airframe encounters a wide variety of natural and induced environments. While this makes the application of fracture theory a rather difficult task, the general overall goals which must be achieved are rather simply stated, as follows:

- (1) Encourage the intelligent selection of fracture-resistant materials, manufacturing processes, and so forth
- (2) Provide an incentive to design for inspectability with damage-resistant structural configurations (i.e., multiple load paths)
- (3) Aid in establishing effective and realistic inspection procedures
- (4) Assist in selecting and controlling safe operating stresses

In the Materials Utilization section, materials data were presented to illustrate how strength-density ratio (efficiency) could result in the selection of material with an undesirable level of toughness. Likewise, the choice based on fatigue alone might lead to serious difficulty since many high-strength materials (steels, for example) may have acceptable fatigue resistance but possess low resistance to brittle fracture and subcritical flaw growth (stress corrosion cracking, for example).

Structural configurations which possess multiple load paths, crack stoppers, and so forth, are necessary and desirable; however, their ability to function and meet specific preassigned goals must be demonstrated early in design.

Controlling design stress levels for common structural materials can have untold benefits from both the strength and fatigue points of view and can prevent costly field maintenance problems. For example, multiple load path, redundant, and fail-safe arrangements may effectively prevent the loss of aircraft, so long as adequate and frequent inspections are planned. The sole dependence on the fail-safe approach to achieving fracture control without regard to limiting design stresses may result in frequent member failures, costly unscheduled maintenance, and aircraft downtime. This situation can be alleviated by requiring each member in the multiple or redundant set to be inherently resistant to flaw growth within prescribed bounds (i.e., it must have a safe life with cracks).

The ability to detect and quantify flaws and cracks, both in the raw product form and the final assembled structural article, remains as the most significant measure in deterring catastrophic fracture. Instituting fracture control procedures is, in fact, a frank admittance that serious flaws can and often do go undetected. This fact was dramatically pointed out by Packman, Pearson, Owens, and Young (ref. 17) in a study for the Air Force Materials Laboratory. The data in figure 11 have been obtained from that report and depict the sensitivity and reliability of common NDI methods in controlled laboratory experiments. The results are quite surprising because relatively large flaws were not detected. This does not mean that all hope is lost of improving present methods and procedures. On the contrary, continued development of improved NDI techniques is mandatory.



Fracture control procedures are most beneficial if effectively implemented and managed. Implementation consists of satisfying specific requirements for analysis and test based on established ground rules and definitions of required strength, assumed damage, service life, and inspection intervals. A balanced design within the goals of damage tolerance is thus insured. It is important that the basic definitions, goals, and fracture requirements be established early in the design phase in order to impact trade studies. Implementation requires a firm material data base, knowledge of operational environments, design criteria, and an analytical capacity to perform complex flaw-growth and strength analyses.

If fracture control procedures are instituted early, they form a portion of the basic design criteria and no weight penalties can then be attributed to their existence. Weight penalties are only recognized if the requirements are levied after the design is frozen.

### FRACTURE CONTROL - REQUIREMENTS

It should be acknowledged that the preparation of detailed step-by-step requirements for fracture control is a difficult task because of the numerous classes of aircraft (i.e., fighter bombers, trainers, etc.) in use today by the Air Force and because of the various types of structural arrangements which comprise these airframes. With regard to the structural aspects, the term "Damage Tolerant" is perhaps most common and is used within the Air Force (ref. 13) to describe those configurations "which will minimize the loss of aircraft due to the propagation of undetected flaws, cracks, or other damage."

Supplemental requirements for the ASIP (ref. 13) and various military specifications (ref. 18) are currently being formulated to insure the achievement of damage-tolerant design. Such requirements will be applicable to all primary structures, the failure of which would reduce the strength level below specified limits and endanger the safe operational flight characteristics of the aircraft.

In general, requirements to insure adequate fracture control take on the form of specific directives in the areas of (1) design, (2) analysis, and (3) test.

In the following discussion, a representative set of specifications for fracture control is described to indicate the relative levels of importance placed on structural arrangements, inspections, and so forth.

It is generally recognized that there are two major design steps which are required to produce a damage-tolerant structure:

- (1) Controlled safe flaw growth (safe life with cracks)
- (2) Positive damage containment (remaining or residual strength)



Neither of these should be considered separate and distinct, however, since it is the judicious combination of both that is required for effective fracture control.

Since the assumption is made that flaws do exist in new structures and can go undetected, full compliance with this philosophy requires that consideration be given to the probability that flaws will exist in any and/or all members, including each element of a redundant or multiple load path group. This is important because it is easy to rationalize that each member of the multiple set could be flawed. For example, if stress corrosion is responsible for the existence of subsurface cracks in one member, there is no assurance that each adjoining member does not contain cracks of a similar character. The first major requirement for fracture resistance must, therefore, dictate that any member must have a safe life with assumed cracks present.

For any given application, the overriding factors which govern the details and complexity of the fracture requirements and demonstrations are (fig. 12)

- (1) The class or type of structure
- (2) The quality of production and assembly NDI
- (3) The accessibility of the structure
- (4) The assurance that the member will be inspected in service
- (5) The probability that a flaw of subcritical size would go undetected even though periodic inspections are made

Most structural members can be classified by load path (fig. 13):

- (1) Single load path
- (2) Single primary load path with auxiliary crack arrest features
- (3) Multiple and redundant load path

Class 2 includes such items as pressure cabins and pressure vessels, where relatively large amounts of damage may be contained by providing tear straps, stiffeners, and the like. While some load shedding does take place, the primary load path is singular. Detection of damage for such cases is likely, because of fuel or pressure leakage.

Class 3 structures are generally designed so that some percentage of original strength is retained during and subsequent to the failure of one element (often called fail safe). Assurance of this capability should be mandatory by analysis and tests. The containment of damage is often produced by natural barriers such as production splices and so forth.

Accessibility and inspectability were indicated in the section on Basic Considerations for Fracture Control as major items in fracture control. This point cannot be

overemphasized. Not only should the structure be inspectable, but assurance must be given that it will be inspected periodically after assembly. Because of recent experiences with high-strength materials, speculation has arisen whether or not subsurface cracks of near-critical size can be found in service by use of routine inspection procedures and equipment. A positive criterion such as "leak before break" may have to be levied in order to assure their detection. Otherwise, an inspectable structure would have to be classified as noninspectable. (See fig. 14.)

### Engineering Criteria – Definitions

Before specific fracture requirements for design, analysis, and test can be levied, certain aspects of loading and service must be defined for each type of aircraft. In most cases, these items will be unique for each particular system and will be specified in the basic design criteria.

Strength limits.– The percentage of unflawed static strength which is to be maintained with prescribed amounts of damage must be established. This load is generally the limit load but may vary with aircraft types.

Dynamic factors.– The effect of dynamic load amplification due to the release of energy as the damage is introduced must be included.

Inspection intervals.– Inspection intervals shall be consistent with required safe crack growth intervals and the requirements for residual strength.

Damage limits.– The size of initial flaws which may be expected to slip by inspection must be established from NDI capability studies. Final damage limits will be based on fracture and inspection requirements. In addition, the number and locations of members which are to be considered failed for residual strength purposes must be identified. Damage limits should be established for each system based on individual requirements, materials applications, and so forth.

### Design Trade Study Analyses

A primary function of the fracture control requirements during early design stages is to assist in the selection of damage-resistant materials and structures, with some incentive offered to those that are easily inspectable and those that include multiple or redundant load paths. In figure 15, key factors which influence these trade studies are summarized. Each member is first classified as to structural type, inspectability, and so forth, and a candidate material is selected. Limits of assumed initial damage size are assigned together with the engineering criteria for life, strength, and final damage size. The analysis is then performed by utilizing the appropriate cyclic and sustained loads and environments. The process is then iterated until a satisfactory combination



of material and stress level is selected which fulfills the strength and life requirements. The resultant information is then incorporated with other design considerations until a satisfactory design is achieved.

### Analysis – Detailed Requirements

The analysis consists of determining the growth rates of initial flaws under cyclic loading and environment and insuring that these flaws remain subcritical for the specified time period. Initial flaw sizes generally reflect the NDI capability but may be influenced by such criteria as proof tests and manufacturing processes. The flaws are generally assumed to be normal to the maximum principal stress field. The character and shape of the flaws are usually influenced by such aspects as

- (1) Materials and processing
- (2) Manufacturing and assembly
- (3) Handling and service conditions

Experience has indicated that the flaw types shown in figure 16 are most representative in aircraft.

In table III, a set of hypothetical analysis requirements have been tabulated for the three classes of structures, based upon whether or not the assemblies will be inspected in service.<sup>1</sup> The information from table III has been translated into figures 17, 18, and 19 for clarity. As is indicated, each class is designed for a safe crack growth period from an initial flaw. The final fracture dimensions are governed by plane strain fracture at limit load unless conditions indicate that this mode of fracture is unlikely. Some motivation to design with inspectability and with high-toughness materials (and thus higher stresses) is offered for ( $a_3 > a_5$ ) and ( $a_4 > a_5$ ). The final crack dimensions  $a_3$  and  $a_4$  must truly be detectable however; otherwise, the structure should be reclassified as noninspectable. It was previously stated that subsurface flaws most likely should be put in the noninspectable class (for service inspections). However, in most cases, it is possible to achieve through-the-thickness cracks and thus "positive detection" with proper selection of materials and stresses.

A safe life period of two inspection intervals has been indicated for the class 1 and class 3 inspectable cases. This will result in a slight reduction in allowable design stresses but will offer more chance to detect the subcritical crack.

For the class 1, single load path, structure the requirement to satisfy a safe life with cracks is easily accepted because of the consequence of losing the member.

---

<sup>1</sup> These requirements are presented for purpose of illustration only and do not represent USAF policy.



However, as previously stated, the preexistent flaw concept requires that all members, including each member of a multiple load set, be assumed flawed. It is not sufficient simply to design the multiple load path structure to a remaining strength criterion with one principal member failed. This does not insure that initial flaws in a member will not grow to critical size in a relatively short period of time and result in broken members and unscheduled, costly maintenance. Therefore, the safe life requirements C and E as listed in table III and indicated in figure 18 are applicable to every member of the structure. However, since there should be some incentive to design class 3 structures, the size of the initial assumed flaws in the class 3 structure is reduced from that in the class 1 structure for the noninspectable case ( $a_1 < a_2$ ). By doing this, the designer is admitting that the design is more comfortable and that he is willing to take a larger risk of operating with cracks.

Supplemental safe life (with cracks) requirements (F and G) for the class 3 structure are listed in table III and are applicable to the remaining structure after the one principal member has failed. In these requirements, the assumption is made that the element could fail at any time during the life (or inspection period) and go undetected. The remaining structure (assumed to be flawed) would then be required to carry the maximum load for the duration of the remaining specified time period. The stresses which result from requirements F and G most likely will dominate the design. In actual practice, studies would have to be conducted to determine the most appropriate time to assume the member failure. In requirement F, the remaining growth period would be one inspection interval regardless of when the member was assumed to have failed. As is indicated in figure 19, the total growth in any one member is equal to the amount which occurs prior to the failure of the principal element plus the amount which occurs subsequent to the failure at an increased stress level.

#### Alternate Scheme to Assess Remaining Life

In the previous section, requirements F and G (table III) were presented to satisfy the requirement for some remaining life in the multiple load structure after the failure of any principal member. An alternate scheme, and one which may be less restrictive, has recently been prepared for use in the Air Force. The principal difference is that the remaining structure is considered to be intact (unflawed) subsequent to the failure of the principal element. The requirement is stated as follows in reference 18:

"Fail Safe. Primary structure that is designed fail safe shall be readily inspectable and meet the following requirements after failure of a principal structural element: (1) the remaining structure shall sustain without failure, the maximum expected load or limit load, whichever is greater, (2) the airplane shall be controllable within the design speed limits, and (3) catastrophic

failure of the remaining structure will not occur under repeated load conditions during the time period to the next opportunity to detect the failure. Verification of the ability of the remaining structure to withstand the repeated loads shall be accomplished by determining the crack growth period from an initial flaw to failure of the principal element, and then insuring that the life (including a factor of four) of the remaining structure will equal or exceed the time interval established for the next inspection. Inspection intervals shall be as agreed to by the procuring agency . . ."

#### Fracture Control – Verification and Demonstration

In the preceding discussion, requirements for analysis were presented. In certain instances, experimental verification or demonstration of compliance should be required.

Safe crack growth tests (class 1 and class 3).— Although basic growth-rate data will be generated to support analysis techniques, it is desirable to augment the constant-amplitude tests with spectrum crack growth tests conducted on a meaningful flight-by-flight basis. This is particularly true where reliance has been placed upon positive detection by surface flaws penetrating the member thickness. In most cases, these experiments can be conducted on representative coupons, or small specimens if stresses are well known. If the geometry is complex, it is more desirable to utilize prototype component structure and run the growth tests in conjunction with the static or cyclic preproduction tests.

Demonstration tests utilizing full-scale structures (i.e., complete aircraft) should not be necessary since it is generally quite easy to duplicate localized conditions surrounding the crack tip.

Damage arrest (class 2).— Demonstration of crack arrest capability and subsequent cyclic life should be required. These tests may be conducted on representative specimens or on the full-scale aircraft at the conclusion of the static or fatigue test. In most cases, critical damage is introduced mechanically to simulate service condition (battle damage, etc.).

#### Establishment of Inspection Procedures

An additional function served by the safe crack growth analysis is the establishment of inspection procedures for an individual structure or for all members in the aircraft which are manufactured from the same material. The use of fracture analysis procedures allows inspection or rejection with more confidence by classifying parts and regions within a part according to the required NDI sensitivity.



The development of such an inspection procedure for a typical application is illustrated as follows. Spectrum crack growth information is plotted in figure 20(a) as a function of the initial crack size (only  $a_0$  is shown) for various degrees of spectrum severity (maximum stress). In this example, the required safe growth period is  $N$  hours, and  $a_0$  is the largest crack size that can be tolerated for this material application. The maximum expected spectrum stress is  $\sigma_4$ . NDI procedures must insure the reliable detection of  $a_0$  during fabrication and assembly.

This spectrum growth information is translated into more meaningful form in figure 20(b) where, for any level of design stress, the largest tolerable flaw which would grow to failure in  $N$  hours is plotted. Rather than using fracture at  $N$  hours, a criterion based on positive detection could be substituted and produce a similar diagram.

### Application of Requirements

While the full impact of the proposed fracture requirements can only be assessed through an extensive design application study on an existing system, the relative severity can be assessed by studying typical examples. The following example illustrates the values of design stress for a single material which would result under each requirement listed in table III:

#### Example: Tension cover; aircraft type, fighter

Material, 7075-T6

$$K_{Ic} = 30 \text{ ksi} \cdot \sqrt{\text{in.}}$$

Thickness = 0.375 in.

Initial flaw assumptions (surface flaw) ( $a/2c = 0.5$ ):

$$a_1 = 0.050 \text{ in. (for all inspectable cases)}$$

$$a_2 = 0.150 \text{ in. (for all noninspectable cases)}$$

Final flaw size:

$$a_4 = \text{Minimum detectable size} = 0.375 \text{ in.}$$

$$a_3 = \text{Minimum acceptable equivalent} = 0.500 \text{ in. for single load path structure}$$

Stress information:

The fighter spectrum information is contained in table IV in terms of a unit of maximum stress value  $\sigma = 37 \text{ ksi}$ . These occurrences in table IV are the equivalent of 40 hours of flight. The maximum limit stress for design purposes is:

$$\sigma_L = 1.5\sigma = 55.5 \text{ ksi}$$



Spectrum growth-rate data:

By utilizing constant-amplitude growth-rate data (ref. 19), the CRACKS computer routine (ref. 20), and the AFFDL crack growth retardation model (ref. 10), the stress spectrum (table IV) was translated into plots of crack depth  $a$  as a function of number of flights starting with an initial crack length  $a_1 = 0.050$  in. (fig. 21) and  $a_2 = 0.150$  in. (fig. 22). All levels of stress from table IV were increased or decreased proportionally to achieve the variation in growth due to spectrum severity.

Material toughness:

The cutoff line for  $K_{IC} = 30 \text{ ksi} \cdot \sqrt{\text{in.}}$  is indicated in figures 21 and 22. The effect of varying this parameter was not investigated in this example.

Life requirement:

Service life = 160 blocks =  $160 \times 40 = 6400$  hours. Inspection intervals are planned each  $1/4$  lifetime of 40 blocks = 1600 hours.

#### Requirement A:

Initial crack depth:

$$a_1 = 0.050 \text{ in.}$$

Final crack depth:

$$a_3 = 0.500 \text{ in. (based on positive detection)}$$

Life requirement:

$$N_A = 80 \text{ blocks} = \text{Two inspection intervals}$$

Design stress  $\sigma_A$ :

This goal cannot be achieved with this material since  $K_{IC}$  is limited to  $30 \text{ ksi} \cdot \sqrt{\text{in.}}$  and the inspection requirement of 0.500 in. is not possible. A material change would most likely be required.

#### Requirement C:

Initial crack depth:

$$a_1 = 0.050 \text{ in.}$$

Final crack depth:

$$a_4 = 0.375 \text{ in. (based on positive detection)}$$

Life requirement:

$$N_C = 80 \text{ blocks}$$

Design stress, maximum:

$$\sigma_C (\text{allowable}) = 1.27\sigma = 47 \text{ ksi}$$

Requirement D:

Initial crack depth:

$$a_2 = 0.150 \text{ in.}$$

Life requirement:

$$N_D = 160 \text{ blocks} = \text{One lifetime}$$

Final crack depth:

$$a_5 = \text{Plane strain fracture} > 1.0 \text{ in.}$$

Design stress, maximum:

$$\sigma_D (\text{allowable}) = 0.81\sigma = 31 \text{ ksi}$$

Requirement E:

Initial crack depth:

$$a_1 = 0.050 \text{ in.}$$

Final crack depth:

$$a_5 = \text{Plane strain fracture} = 0.58 \text{ in.}$$

Life requirement:

$$N_E = 160 \text{ blocks}$$

Design stress, maximum:

$$\sigma_E (\text{allowable}) = 1.08\sigma = 40 \text{ ksi}$$

Requirement F:

Coupled with requirement C is the additional requirement that the structure remaining after failure of the principal member will be capable of carrying limit load for one additional inspection period, or 1/4 lifetime. The lower portion of the growth data from figure 21 has been replotted in figure 23.

(a) Assume that the member breaks accidentally after the first flight and remains undetected until the next inspection interval. The stress is assumed to increase by 20 percent, with the requirement being no failure at limit load in 1/4 lifetime or 40 blocks. From figure 23, it can be seen that a stress level

of approximately  $1.6\sigma = 60$  ksi would grow to failure in 40 blocks.  
Therefore

$$\sigma_{Fa}(\text{allowable}) = \frac{60}{1.20} = 50 \text{ ksi}$$

(b) Assume the member failure to be at  $1/4$  lifetime (just subsequent to inspection). The crack in the remaining structure has grown an amount  $\Delta a$  during the first inspection period. Thus,

$$\text{New initial } a = a_1 + \Delta a = 0.050 + \Delta a$$

This condition can be satisfied by trial and error by using figure 23. The result indicates that  $\sigma_{Fb} \approx 1.2\sigma = 44.4$  is appropriate for this condition. Failure at any other time could be checked to see whether a lower stress would result. Note that no criterion for positive detection was required since at the next inspection the broken member would be found.

#### Requirement G:

In a similar manner, requirement E should be checked for life after member failure.

(a) Assume failure on first flight (from fig. 21)

$$\sigma_E = 1.08\sigma = 40 \text{ ksi}$$

$$\therefore \sigma_{Ga} = \frac{\sigma_E}{1.2} = 33.3 \text{ ksi}$$

(b) Assume failure at  $1/2$  lifetime. The incremental growth during the first  $1/2$  lifetime must be added to  $a_1$ . The requirement for  $1/2$  remaining life shall then be determined. From figure 21, by trial and error, a stress level of  $\sigma_{Gb} = 1.0\sigma = 37.0$  ksi is seen to satisfy the requirements.

#### Summary:

The following table is a summary of the previous example:

Requirement	Design stress, $\sigma$ , ksi	Condition
A	Not satisfied	Inspectable class 1
C	47	Inspectable class 3
D	31	Noninspectable class 1
E	40	Noninspectable class 3
F <sub>a</sub>	50	Inspectable class 1
F <sub>b</sub>	44.4	
G <sub>a</sub>	33.3	Noninspectable class 3
G <sub>b</sub>	37.0	



The results clearly indicate the advantages offered by designing for inspectability since the allowable stresses for requirements C and F are greater than for requirement G. The incentive for multiple, in lieu of single, load path design is seen in the resultant allowable design stresses for requirements E and G being greater than for requirement D.

## ANALYSIS AND DATA REQUIREMENTS FOR IMPLEMENTATION

The successful implementation of the fracture control analysis requires the analytical capability for cyclic and environmental flaw growth, aircraft usage information, and basic strength and fracture data for proposed candidate materials.

### Criteria Requirements

Initial considerations for fracture resistance and control of subcritical flaw growth must be established during the criteria development stage and must reflect appropriate chemical, thermal, and operational loads environments. For example, recent materials usage has necessitated the generation of data on sustained-load flaw growth in aggressive environments such as fuel and water (fig. 24(a)). Because loading rate and dwell times are important in the assessment of environmental effects, it has become important also to generate load-time spectra of the type indicated in figure 24(b).

### Material Data Requirements

The major material strength and fracture properties required to perform the analyses and trade studies for fracture considerations are illustrated in figure 25. In all cases (except  $K_{IC}$ ) no approved standard test methods exist to determine these properties. Through experience, however, various test techniques and specimens have evolved. (See fig. 25.) As is often the case, a specimen developed for one function or application is used to generate a multitude of data. Testing techniques and data interpretation may mask important material responses or indicate false reaction to stress and environment. For example, in a recent comparison of cyclic growth-rate behavior in D6ac steel (refs. 9, 11, and 12) comparative growth rates obtained from compact tension and surface-flawed specimens indicated a predominant stress-level effect for the surface-flawed specimen, whereas no clear dependency was observed for the compact tension case (fig. 26). These effects are currently being investigated.

### Fracture Analysis Methods

Prediction of fracture and growth behavior requires a means of translating external applied loads into stresses in the region of the crack tip. Finite-element techniques

offer a vast potential in the area, particularly in complex structural arrangements (refs. 21 and 22). A rather broad collection of stress intensity solutions exists (ref. 4); however, their use is limited in many cases and extrapolation is often required to provide the best estimate of  $K$ .

Considerable effort is being expended in the development of computer routines to "integrate" growth-rate ( $da/dN$ ) data (ref. 20), for example, and to account for the retardation effect of overloads in variable-amplitude spectra. As an example of this type of activity, the AFFDL has recently developed a mathematical model for predicting the growth delay effect (ref. 10). The basic model is concerned with the effect of the overload plastic zone on the subsequent rate of growth as indicated in figure 27. A hypothetical residual or reduction stress is then computed which suppresses the subsequent cyclic loads. Retardation is accomplished in three modes, depending on the relative size of the overload in relation to the subsequent cyclic level (fig. 28). Effective  $\Delta K$  and  $R$  values are computed and reduced rates obtained from normal  $da/dN$  and  $\Delta K$  relationships. Note that growth can be completely stopped (fig. 28). An extensive testing program is being completed at AFFDL to evaluate the merit of the model. In figure 29 are some early correlations with single overloads in aluminum (ref. 6). Fairly good correlation is noted also with randomized block spectrum data for D6ac steel (fig. 30).

Growth analysis schemes need to be extended to include the effects of loading rate and delay time (sustained load growth). Free surface effects and flaw shape changes, including the transition of a surface flaw to a through crack, must be included.

#### SUGGESTED AREAS OF STUDY

The suggested areas of study for the application of fracture mechanics in structural integrity have been summarized and are presented as table V. This table is obtained from reference 23.

#### CONCLUDING REMARKS AND RECOMMENDED TOPICS FOR STUDY

The author has attempted to present the significant impact of fracture mechanics and fracture control in the overall program of airframe structural integrity. The true weight, cost, and performance trade-offs associated with the implementation of these or any requirement can best be judged by experience and application to existing systems. A fair assessment can only occur, however, if continued materials and structures development efforts are directed toward upgrading existing fracture mechanics and fracture analysis technology.

The author has summarized in tabular form a rather extensive "shopping list" of items which require attention. In many cases, a relatively high degree of proficiency exists and application experience is all that is necessary while others require new thought and new direction.



## REFERENCES

1. Donaldson, D. R.; and Anderson, W. E.: Crack Propagation Behavior of Some Airframe Materials. Proceedings of the Crack Propagation Symposium, Vol. II, Sept. 1961.
2. Wilhem, D. P.: Fracture Mechanics Guidelines for Aircraft Structural Applications. AFFDL-TR-69-111, U.S. Air Force, Dec. 1969.
3. Anon.: Fracture Control of Metallic Pressure Vessels, NASA Space Vehicle Design Criteria (Structures). NASA SP-8049, 1970.
4. Anon.: Fracture Toughness Testing and Application. ASTM STP 381, June 1964.
5. Wood, H. A.: A Study of the Residual Strength of Damaged Heavily Stiffened Sheet Structure. AFFDL-TR-(to be published).
6. Anon.: Proceedings of the Air Force Conference on Fatigue and Fracture of Aircraft Structures and Materials. AFFDL-TR-70-144, U.S. Air Force, Dec. 1969.
7. Gran, R. J.; Orasio, F. D., Jr.; Paris, P. C.; Hertzberg, R.; and Irwin, G. R.: Investigation and Analysis Development of Early Life Aircraft Structural Failures. AFFDL-TR-70-149, U.S. Air Force, Nov. 1970.
8. Wood, H. A.; and Haglage, T. L.: Crack Propagation Test Results for Variable Amplitude Spectrum Loading in Surface Flawed D6ac Steel. Tech. Memo FBR-71-2, U.S. Air Force, Feb. 1971.
9. Hinders, U. A.: F-111 Design Experience - Use of High Strength Steel. AIAA Paper 70-884, July 1970.
10. Willenborg, J. D.; Engle, R. M.; and Wood, H. A.: A Crack Growth Retardation Model Using an Effective Stress Concept. TM-FBR-71-1, U.S. Air Force, Jan. 1971.
11. Masters, J. N.; and White, J. L.: Development of Fracture Toughness Properties of D6ac Steel for F-111 Application. AFFDL-TR-70-310, U.S. Air Force, Nov. 1970.
12. Harmsworth, C. L.; and Cervay, R. R.: Fracture Toughness Evaluation of D6ac Steel in Support of the F-111 Aircraft Recovery Program. AFML/LAE 71-2, U.S. Air Force.
13. Anon.: The Air Force Airplane Structural Integrity Program (ASIP) Program Requirements. ASD-TR-66-57, U.S. Air Force, May 1970.
14. Wei, R. P.: Some Aspects of Environment Enhanced Fatigue Crack Growth. Paper presented at ASTM Fall Meeting (Atlanta, Ga.), 1968.

15. Hartman, A.; and Schijve, J.: The Effect of Environment and Load Frequency on the Crack Propagation Law for Macro Fatigue Crack Growth in Aluminum Alloys. NLR MP 68001U, 1968.
16. Lowndes, H. B., Jr.: Air Force Flight Dynamics Laboratory, Correlation Between Full Scale Fatigue Test and Service Experience. Paper presented at the Eleventh Conference of the International Committee on Aeronautical Fatigue (ICAF) (Stockholm), May 1969.
17. Packman, P. F.; Pearson, H. S.; Owens, J. S.; and Young, G.: The Applicability of a Fracture Mechanics - NDT Design Criterion for Aerospace Structures. WESTEC Conference (Los Angeles, Calif.), March 10, 1969.
18. Anon.: Airplane Strength and Rigidity - Reliability Requirements, Repeated Loads, and Fatigue. Mil. Specif. MIL-A-008866 A, Mar. 31, 1971.
19. Hudson, C. Michael: Effect of Stress Ratio on Fatigue-Crack Growth in 7075-T6 and 2024-T3 Aluminum-Alloy Specimens. NASA TN D-5390, 1969.
20. Engle, R. M., Jr.: CRACKS: A FORTRAN IV Digital Computer Program for Crack Propagation Analysis. AFFDL-TR-70-107, U.S. Air Force, Oct. 1970.
21. Chan, S. K.; Tuba, I. S.; and Wilson, W. K.: On the Finite Element Method in Linear Fracture Mechanics. Eng. Fracture Mech., July 1970, vol. 2, no. 1, Pergamon Press, pp. 1-17.
22. Byskov, E.: The Calculation of Stress Intensity Factors Using the Finite Element Methods With Cracked Elements. Int. J. Fracture Mech., vol. 6, no. 2, June 1970, pp. 159-167.
23. Wood, H. A.: The Role of Fracture Mechanics in the Air Force Airplane Structural Integrity Program. AFFDL-TM-70-5-FDTR, U.S. Air Force, June 1970.

TABLE I.- TYPICAL SERVICE APPLICATIONS OF FRACTURE MECHANICS

System	Problem	Material	Type of structure	Solution	Reference
C-130	Appearance of in-service cracks in center wing area. Extremely heavy usage of aircraft due to mission change. Structure readily inspectable. Plane stress case.	Aluminum sheet	Multiple load path, heavily stiffened "planks"	Analytical estimate of remaining strength with relatively large cracks. Stiffened case.  In-house experimental verification of K solution for stiffened structure. Simulated and actual panels.	5
F-100	"Thunderbird" accident. Discovery of small cracks in fastener holes during inspection. Structure not readily inspectable.	Aluminum plate	Single load path skin	Inspection program to determine maximum probable flaw sizes.  Analysis of spectrum growth (no retardation assumed). Estimate of residual strength.  Laboratory tests of spectrum growth with actual flaws from service and manufactured cracks.	6
T-37	Main spar failure, plane strain, crack originated in fastener hole. Structure moderately inspectable.	Aluminum "TEE" extrusion	Single load path	Estimate of stress intensity factor for complex geometry. Growth estimate for safe inspection interval.	7
F-111	Fatigue test failures. Plane strain cases.  Service failure (A/C) # 94). Surface flaw during manufacture, loss of aircraft. Structure not readily inspectable.	Steel plate and forging	Single load path cases	Test failure analysis.  Spectrum growth tests and analysis techniques for determination of inspection intervals following proof test.	8, 9, and 10



TABLE II.- TYPICAL MATERIAL PROPERTIES

[Source: Air Force Materials Laboratory]

Material	Yield strength, $\sigma_{ys}$ (typical), ksi	Plane strain toughness, $K_{Ic}$ , ksi- $\sqrt{\text{in.}}$	$2 \left( \frac{K_{Ic}}{\sigma_{ys}} \right)^2$ (a)	$\left( \frac{K_{Ic}}{\sigma_{ys}} \right)^2$ (b)	$\frac{\sigma_{ys}}{\rho}$	$\frac{K_{Ic}}{\rho}$
Steel						
D6ac	205	50 to 90	0.120 to 0.38	0.06 to 0.19	724	177 (318)
4340	220	53	.12	.06	777	187
300M	247	69	.16	.08	872	244
18Ni-Co-Mo	285	89	.20	.100	1007	314
H-11	294	40	.04	.02	1039	141
9Ni-4Co-2C	180 to 190	110 to 170	1.22	.61	600	467
Aluminum						
7075-T73 (forging)	66	31	0.44	0.22	660	310
2024-T851 (plate)	58	23	.32	.16	580	230
2024-T851 (extruded)	58	28	.46	.23	580	280
2014-T6	66	35	.56	.28	660	350
7075-T651 (plate)	78	26	.22	.11	780	260
7175-T73 (forging)	75	35	.44	.22	750	350
7075-T6 (plate)	76	27	.26	.13	760	270
7075-T6 (forging)	75	27	.26	.13	750	270
7079-T6	69	30	.38	.19	690	300
Titanium						
Ti-6Al-4V (ann)	137	50 to 60	0.26 (0.38)	0.13 (0.19)	856	312 (375)
Ti-6Al-4V (STA)	158	41	.14	.07	988	256
Ti-6Al-6V-2Sn (ann)	150	35 to 50	.10 (.22)	.05 (.11)	937	219 (312)
Ti-6Al-6V-2Sn (STA)	163	34	.08	.04	1018	212
Ti-13V-11Cr-3Al (STA)	168	25	.04	.02	1050	156

<sup>a</sup> ASTM thickness required for plane strain fracture.<sup>b</sup> Equivalent to  $a_{cr}$  for  $\sigma_L = 0.6\sigma_{ys}$ .

TABLE III.- FRACTURE CONTROL ANALYSIS REQUIREMENTS

Safe crack growth	Inspectable class (a)			Noninspectable class (a)	
	1	2	3	1	3
	Requirement A (fig. 17)	Requirement B	Requirement C <sup>b</sup> (fig. 18)	Requirement D (fig. 17)	Requirement E <sup>b</sup> (fig. 18)
Initial flaw . . . . .	a <sub>1</sub>		<sup>b</sup> a <sub>1</sub>	a <sub>2</sub>	<sup>b</sup> a <sub>1</sub>
Shall not grow to critical size . . .	<sup>c</sup> a <sub>3</sub>	<sup>d</sup> a <sub>6</sub>	<sup>c</sup> a <sub>4</sub>	a <sub>5</sub>	a <sub>5</sub>
In the specified time of . . . . .	Inspection period	One flight	Inspection period	One lifetime	One lifetime
Critical stress <sup>e</sup> . . . . .	Limit load stress	Limit load stress	Limit load stress	Limit load stress	Limit load stress

Remaining strength additional safe life. Class 3	Inspectable class 3	Noninspectable class 3
	Requirement F <sup>b</sup> (fig. 19(a))	Requirement G <sup>b</sup> (fig. 19(b))
Subsequent to failure <sup>f</sup> of one principal member, the remain- ing structure shall be capable of carrying. . . . .	Limit <sup>e</sup> load stress	Limit <sup>e</sup> load stress
At the end of . . . . .	One inspection period	One service lifetime

<sup>a</sup> Class 1 = Single load path.

Class 2 = Single load path (crack arrest features).

Class 3 = Multiple load path.

<sup>b</sup> Each member of class 3 structure shall be assumed to be flawed. The safe crack growth requirements shall be continuous throughout the specified time periods prior to and subsequent to the failure of the element.

<sup>c</sup> a<sub>3</sub> and a<sub>4</sub> are determined by fracture considerations but must be large and detectable (i.e., through-the-thickness cracks). Otherwise, classify as uninspectable. (Note: a<sub>3</sub> >> a<sub>4</sub>.)

<sup>d</sup> a<sub>6</sub> must be readily inspectable (i.e., pressure loss). Otherwise, classify as noninspectable class 3 structure.

<sup>e</sup> Will vary with aircraft type.

<sup>f</sup> Member can fail at any time during specified period.

TABLE IV.- STRESS SPECTRUM FOR FIGHTER AIRCRAFT EXAMPLE <sup>a</sup>

Layer	$\sigma_{\min}$ , ksi	$\sigma_{\max}$ , ksi	Cycles	Layer	$\sigma_{\min}$ , ksi	$\sigma_{\max}$ , ksi	Cycles
1	0.06	16.6	63	30	7.94	34.9	2
2	7.04	27.0	76	31	3.64	16.1	37
3	.45	13.7	371	32	7.57	16.8	367
4	5.90	26.4	37	33	7.15	25.6	109
5	.79	17.5	111	34	7.91	37.0	1
6	10.60	25.4	2	35	1.63	6.3	265
7	.76	14.2	363	36	.79	20.8	34
8	4.02	28.7	5	37	7.81	20.2	318
9	3.64	10.7	1280	38	3.68	11.8	6
10	6.77	22.9	62	39	0.0	11.3	21
11	3.64	16.6	1	40	7.18	17.9	374
12	6.07	17.5	89	41	2.01	13.9	478
13	8.64	21.8	41	42	1.59	8.8	46
14	9.51	19.1	57	43	.06	11.9	300
15	3.78	14.0	491	44	1.59	11.3	10
16	0.0	13.9	6	45	7.91	31.7	4
17	3.81	17.5	74	46	0.0	16.4	4
18	7.88	13.4	682	47	7.57	14.5	306
19	.72	10.4	1376	48	8.26	24.9	15
20	9.37	16.0	66	49	7.98	26.1	5
21	.52	17.2	34	50	8.19	12.9	230
22	6.76	8.6	1621	51	7.98	10.7	1338
23	7.98	11.8	1589	52	.06	19.8	19
24	.45	10.6	1374	53	3.85	10.4	1546
25	0.0	8.8	67	54	0.0	6.4	238
26	7.08	28.5	1	55	.48	16.1	114
27	7.39	22.8	250	56	7.08	14.9	370
28	.06	22.1	8	57	3.85	20.8	7
29	1.63	13.9	2	58	2.01	13.9	478

<sup>a</sup> Single block is equivalent of 40 flight hours.



TABLE V.- SUGGESTED AREAS OF STUDY FOR THE APPLICATION OF FRACTURE MECHANICS IN STRUCTURAL INTEGRITY

PROGRAM:	Implement rational fracture mechanics theory into the design criteria, material selection, analysis, qualification, and utilization of aircraft structural systems.	
TOPIC AREAS:	I	Criteria
	II	Data requirements and applications
	III	Fracture analysis methodology
	IV	Qualification for fracture resistance
	V	Utilization - structural concepts
SUBJECT BREAKDOWN:	I	Criteria
		a. Definition chemical and thermal environment for fracture requirements
		b. Review past experience, structural failure, and so forth
		c. Catalog critical structural materials arrangements and previous design considerations in order to establish which areas require extensive investigation
		d. Establish fracture criteria for material selection and trade-off studies
		e. Establish analogous "leak before break" criteria for aircraft application
		f. Assemble design data and criteria for fracture applications
		g. Definition of mission and analysis, including estimates of time at load factor
		h. Incorporate criteria in basic specifications including ASIP modification
	II	Data requirements and applications
		a. Establishment of measurable parameters $K_C$ , $K_{IC}$ , $K_{ISCC}$ , $da/dt$ , $da/dN$ , and others, including testing standards
		b. Application of $K_C$ and $K_{IC}$ in design
		c. Fatigue crack growth data
		d. Subcritical crack growth rate, environment, and temperature
		e. Effect of loading sequence on cyclic growth or growth retardation
		f. Nonpropagating crack study, threshold of $\Delta K$
		g. Parametric growth data, mission segments
		h. Extension of fracture mechanics testing standards to new classes of materials
		i. Study of statistically derived crack sizes and shapes based on nondestructive inspection (NDI) and nondestructive testing (NDT)
		j. Effect of stress state of fracture
		k. Mixed mode fracture study

TABLE V.- SUGGESTED AREAS OF STUDY FOR THE APPLICATION OF FRACTURE MECHANICS IN STRUCTURAL INTEGRITY - Concluded

- SUBJECT BREAKDOWN: III Fracture analysis methodology
- a. Assemblage of currently applicable  $K$  factor relationships including application
  - b. Guidelines for estimating  $K$  or approximate  $K$  for complex cases (including superposition)
  - c. Development of  $K$  for complex cases, elastic solutions
  - d. Finite-element studies, crack growth, subcritical growth development of  $K$ , model crack element for finite-element technique
  - e. Plasticity and free surface effects
  - f. Tabulation of equivalent cracks in complex flaw geometries
  - g. Analytical crack model for growth under variable loading
  - h. Routine for crack growth and life estimates including environment, rates, and load sequence effects
  - i. Analytical study of variation of flaw shape and surface flaws
  - j. Statistical analysis to establish confidence levels for toughness and life estimates, scatter factor for application to analysis results
  - k. Residual strength and static considerations
    - l. Handbook preparation and design guidelines
  - m. Development of semiempirical methods for estimating  $K$
  - n. Fracture arrest, damage-tolerant analysis methods
  - o. Study of the effect of crack bluntness on fracture behavior
- IV Qualification for fracture resistance
- a. Real-time flaw growth testing including temperature and environment (specimens)
  - b. Real-time flaw growth (structures)
  - c. Crack growth resistance and crack arrest testing
  - d. Damage tolerance or fail-safe testing
  - e. Test time reduction for (a) and (b) above
  - f. Proof testing:
    - Repeat work of Tiffany (Boeing) for typical aircraft structures
    - Extend knowledge and techniques to satisfy environment and requirements
    - Statistical assessment of the risks and merits of proof testing
- V Utilization - structural concepts
- a. Concepts for flaw and crack arrest
  - b. New material utilization
  - c. Performance and weight trade-off studies
  - d. Fabrication of structural concepts and full-scale testing
  - e. Inspection, fracture mechanics interface, and flaw classification
  - f. Proof testing, full scale

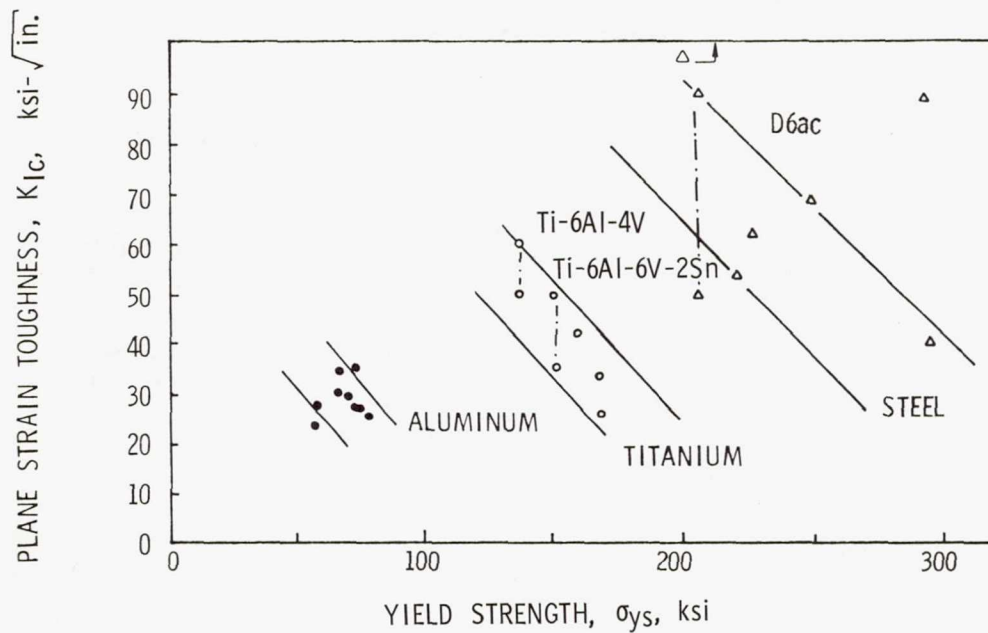


Figure 1.- Trends in toughness variation.

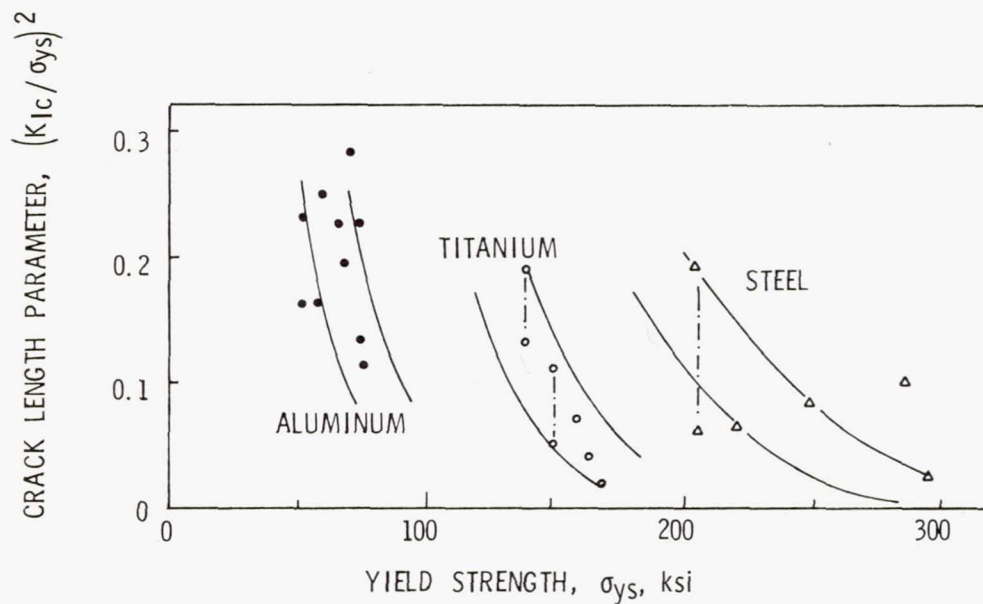


Figure 2.- Variation of crack length parameter with yield strength.



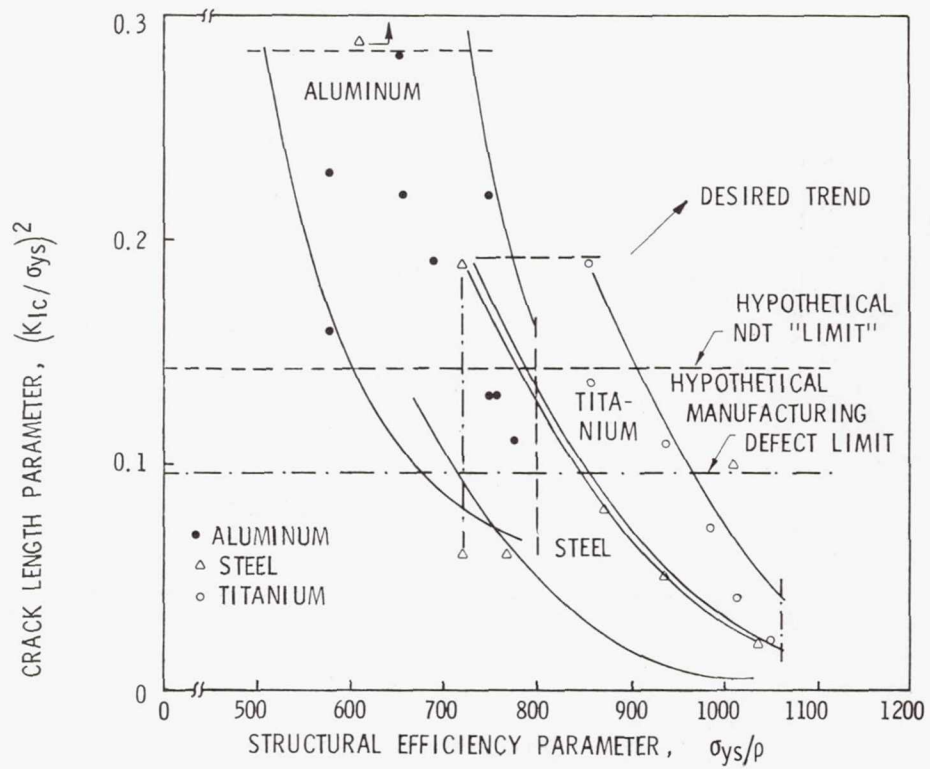


Figure 3.- Variation of crack length parameter with structural efficiency parameter.

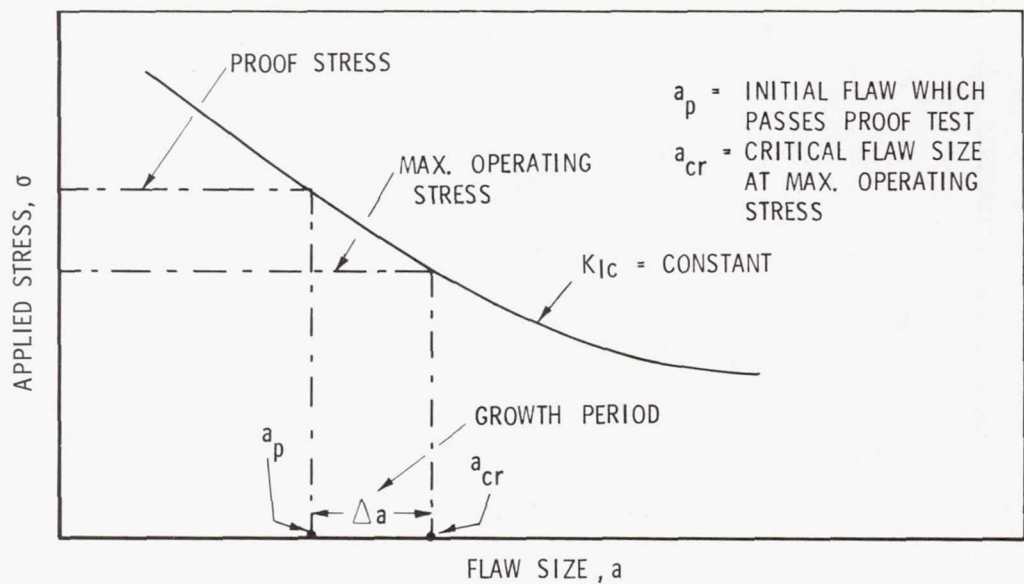


Figure 4.- Proof-test concept.

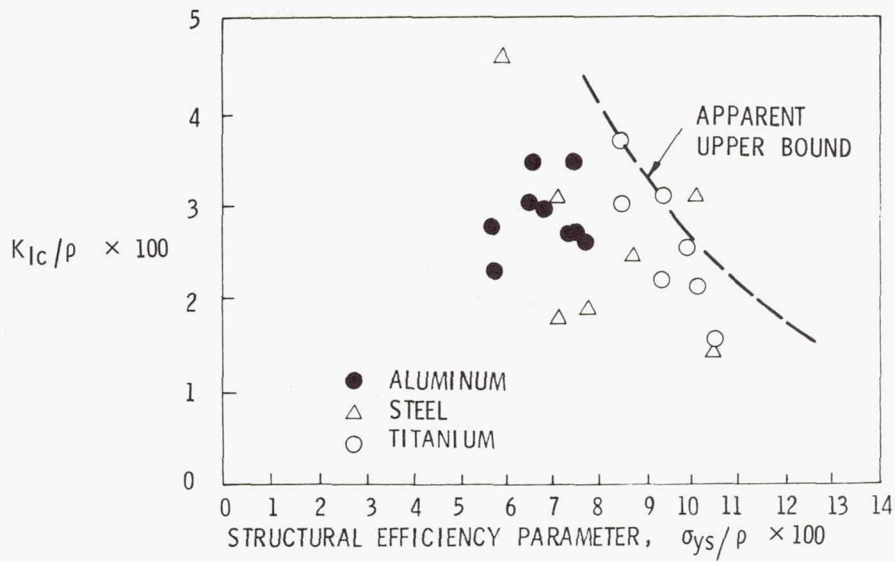


Figure 5.- Density-normalized variation of yield strength with fracture toughness.

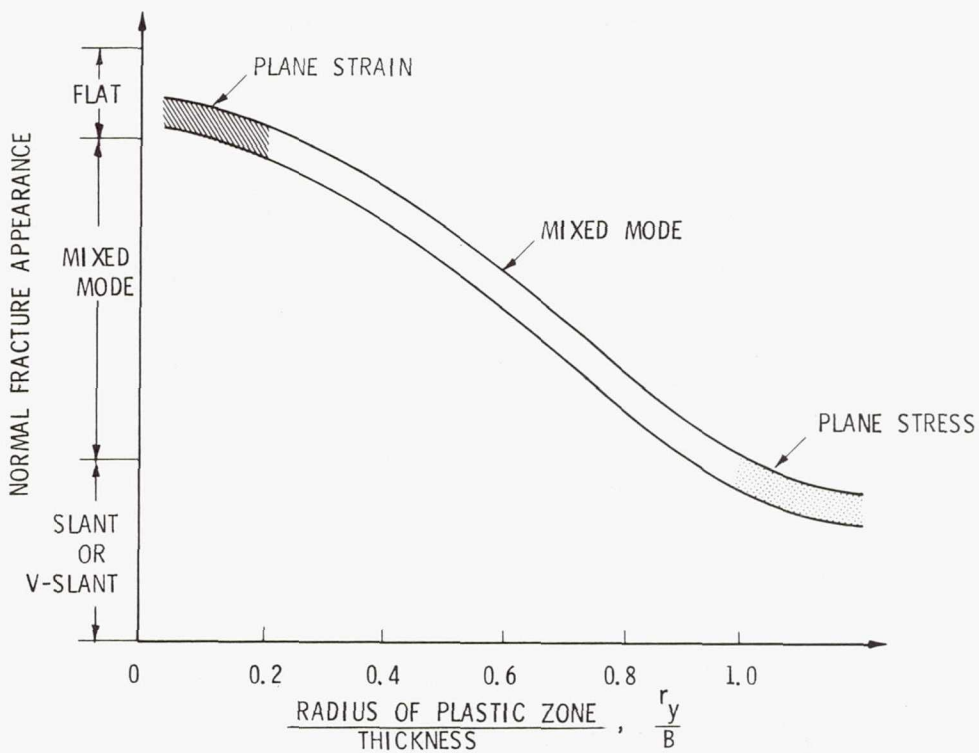


Figure 6.- Trend in fracture mode appearance as a function of crack tip plastic zone parameter (ref. 2).

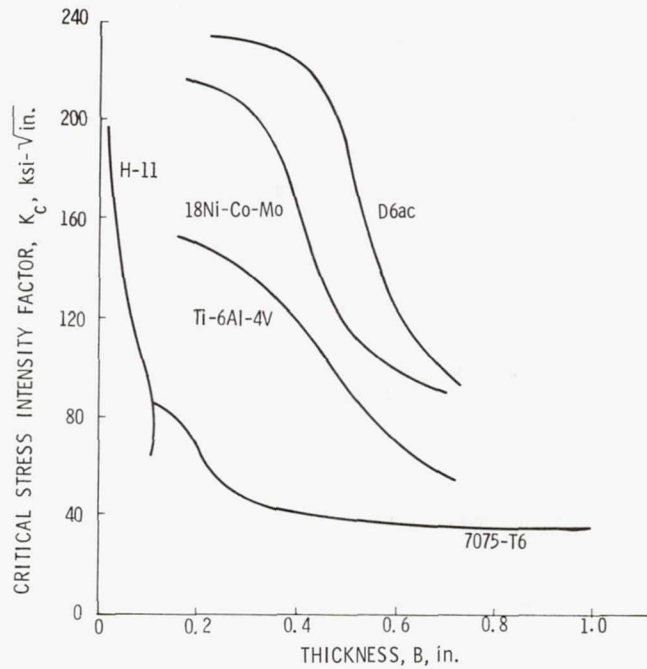


Figure 7.- Nominal critical stress intensities for several materials as a function of thickness (ref. 2).

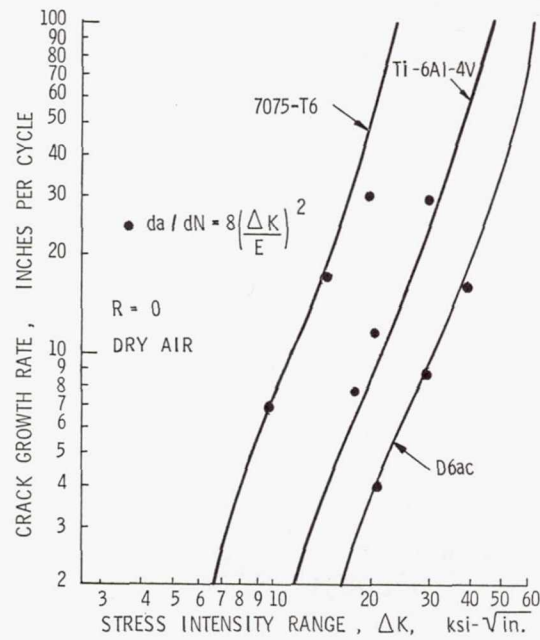


Figure 8.- Fatigue-crack-growth data for typical aircraft structural materials.



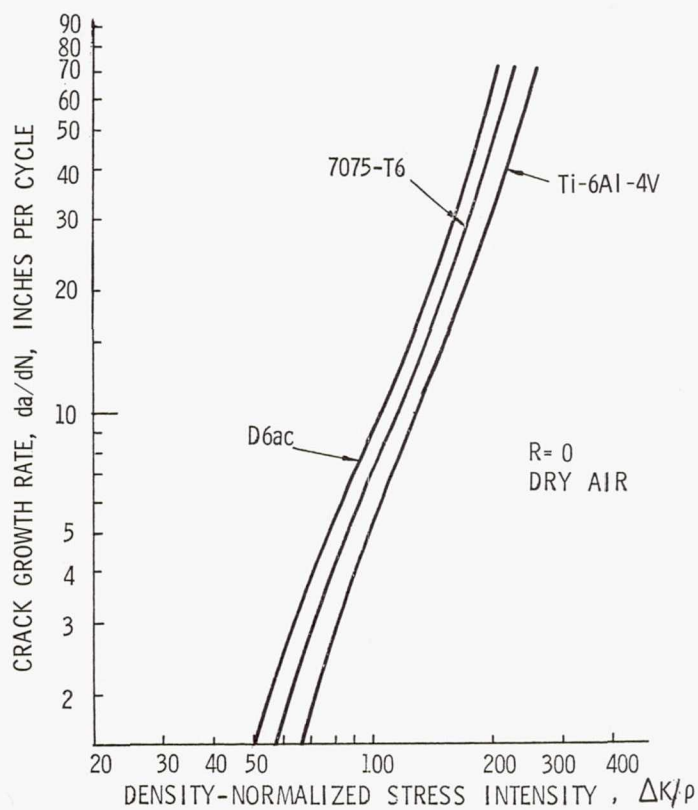


Figure 9.- Comparative crack growth data.

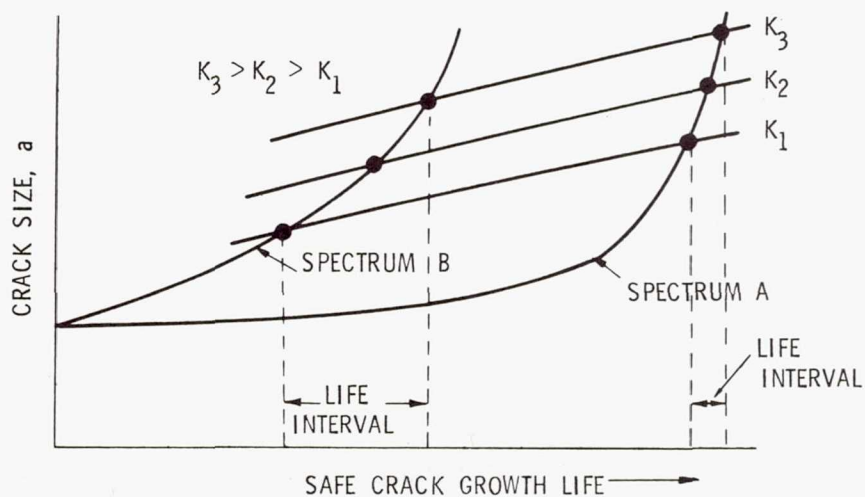


Figure 10.- Effect of fracture toughness life for various shape spectra.

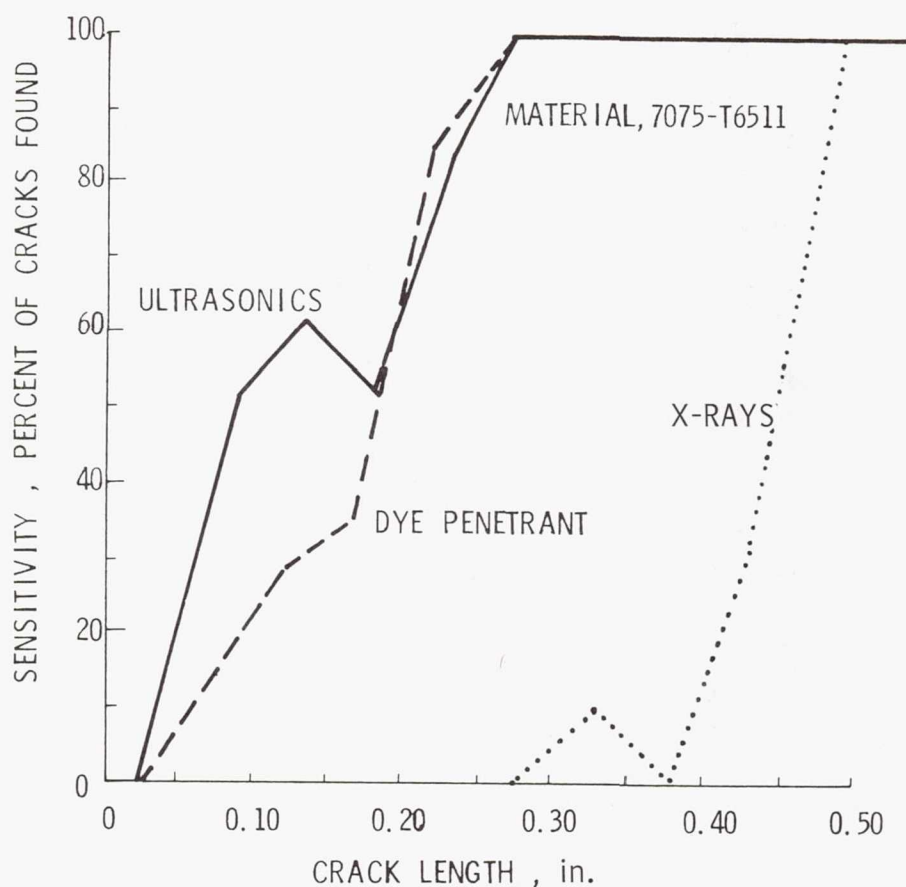


Figure 11.- Demonstration of flaw detection capability. (Data from ref. 17.)

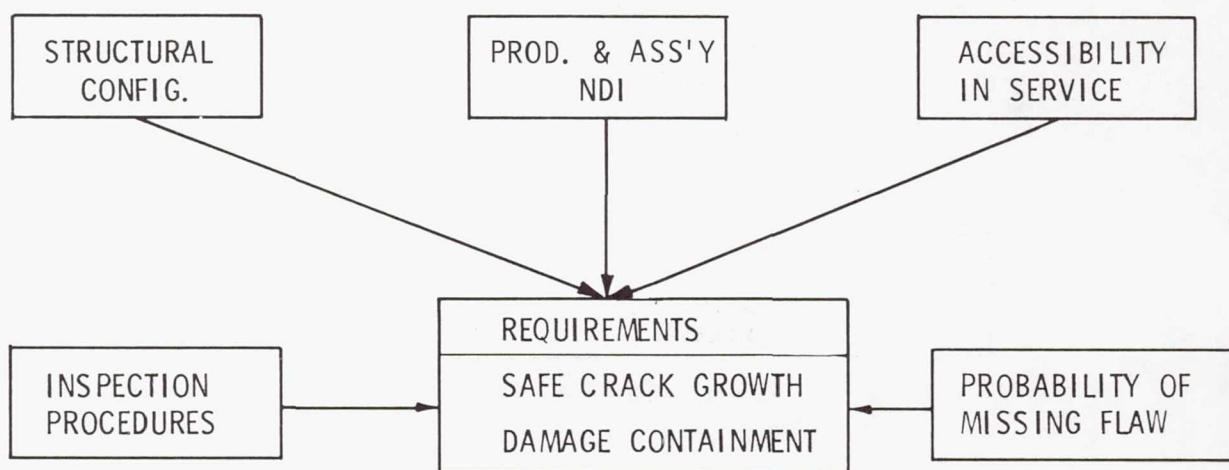


Figure 12.- Factors which affect requirements for fracture control.

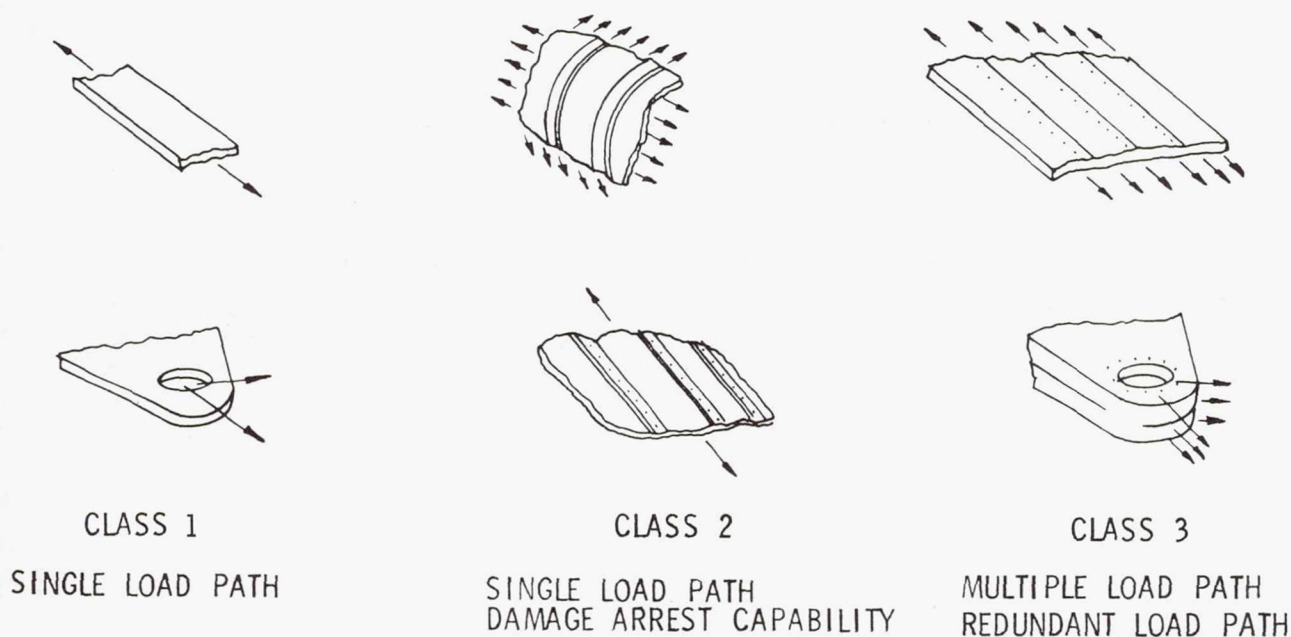
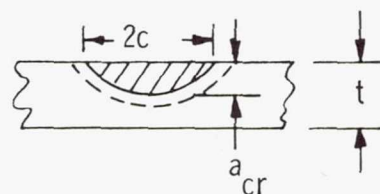
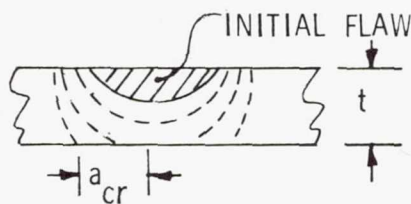


Figure 13.- Structural arrangements.

- POSITIVE CRACK GROWTH THROUGH THICKNESS INSURES DETECTION PRIOR TO CATASTROPHIC FAILURE
- MAY BE ACHIEVED BY SELECTING MATERIAL TOUGHNESS AND/OR GEOMETRY TO PRODUCE TRANSITIONAL GROWTH BEHAVIOR



(a) UNDETECTED



(b) DETECTED

Figure 14.- "Leak before break" criteria for positive detection.



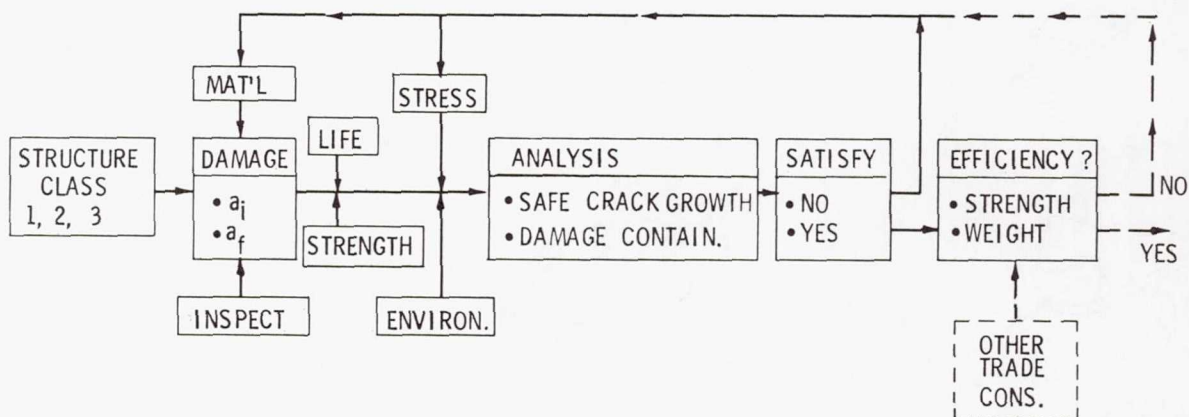


Figure 15.- Fracture control analyses for design trade studies.

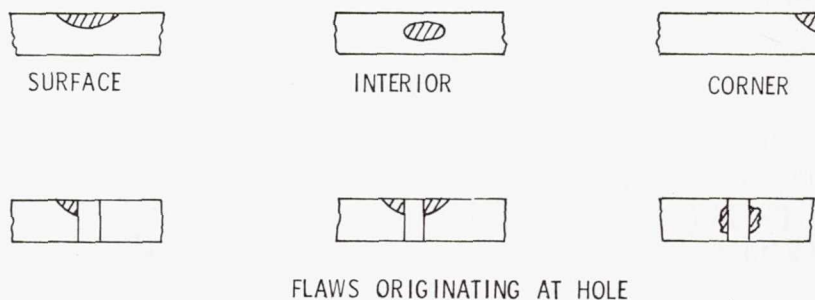


Figure 16.- Representative flaw shapes found in service.

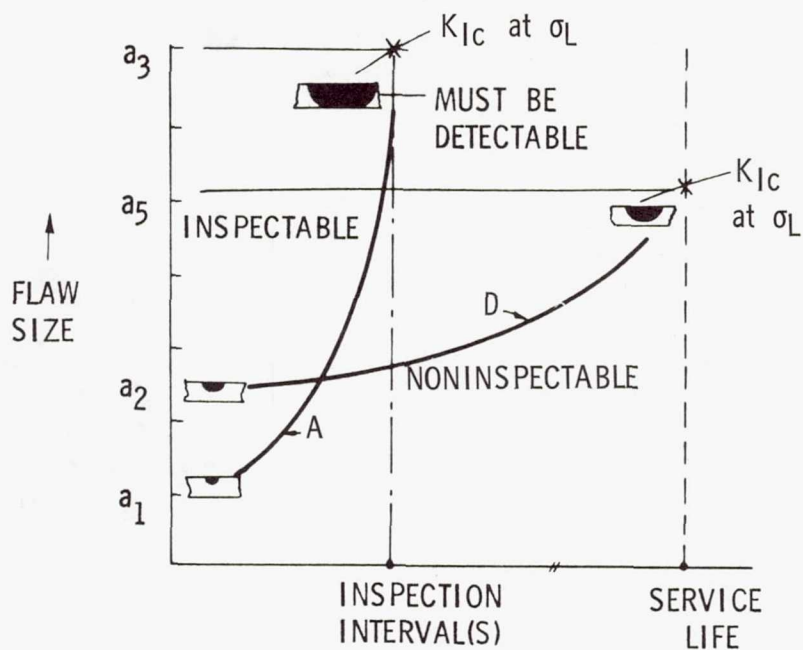


Figure 17.- Safe crack growth life requirements for class 1 structure.

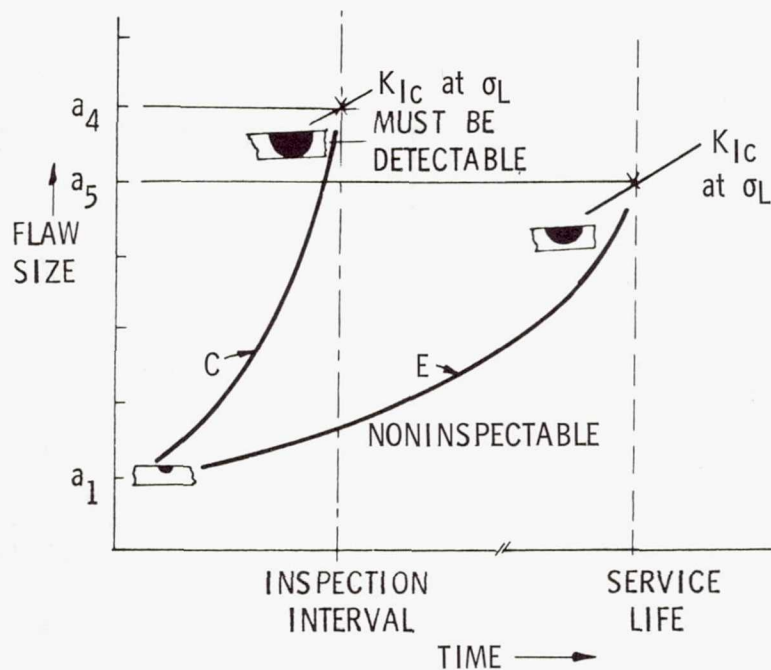
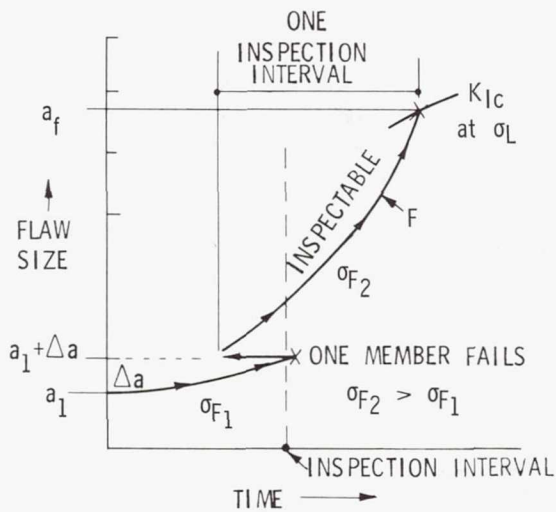
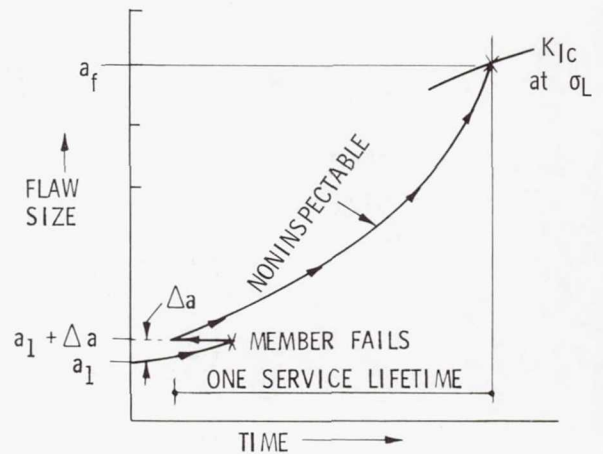


Figure 18.- Safe crack growth life requirements for class 3 structure (any member).

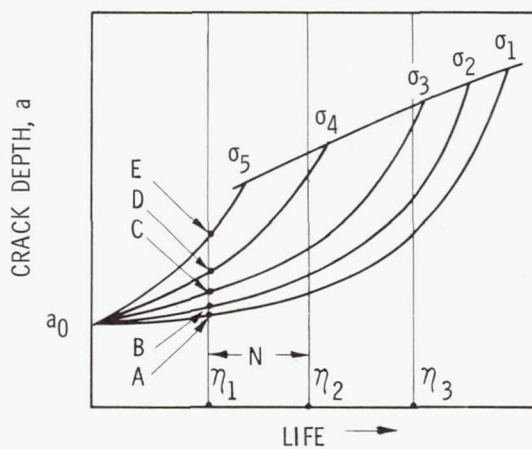


(a) Requirement F. Class 3 inspectable.

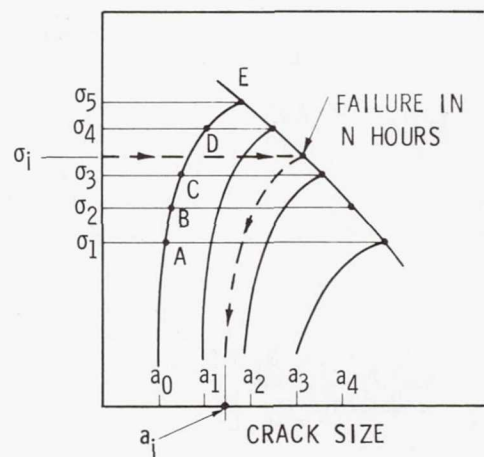


(b) Requirement G. Class 3 noninspectable.

Figure 19.- Safe life requirement for remaining structure after failure of single principal element.



(a)



(b)

Figure 20.- Illustration of inspection procedure based on safe crack growth analysis.



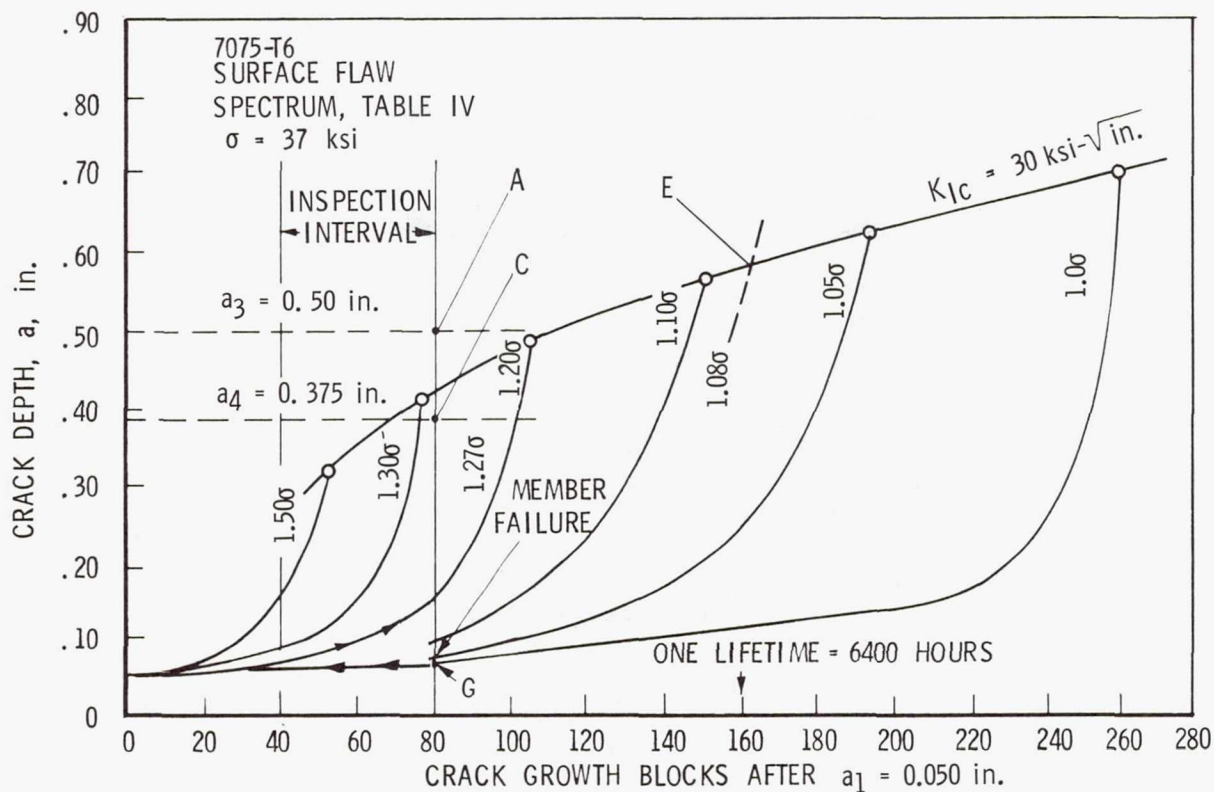


Figure 21.- Spectrum growth data. Fighter example.  $a_1 = 0.050$  in.

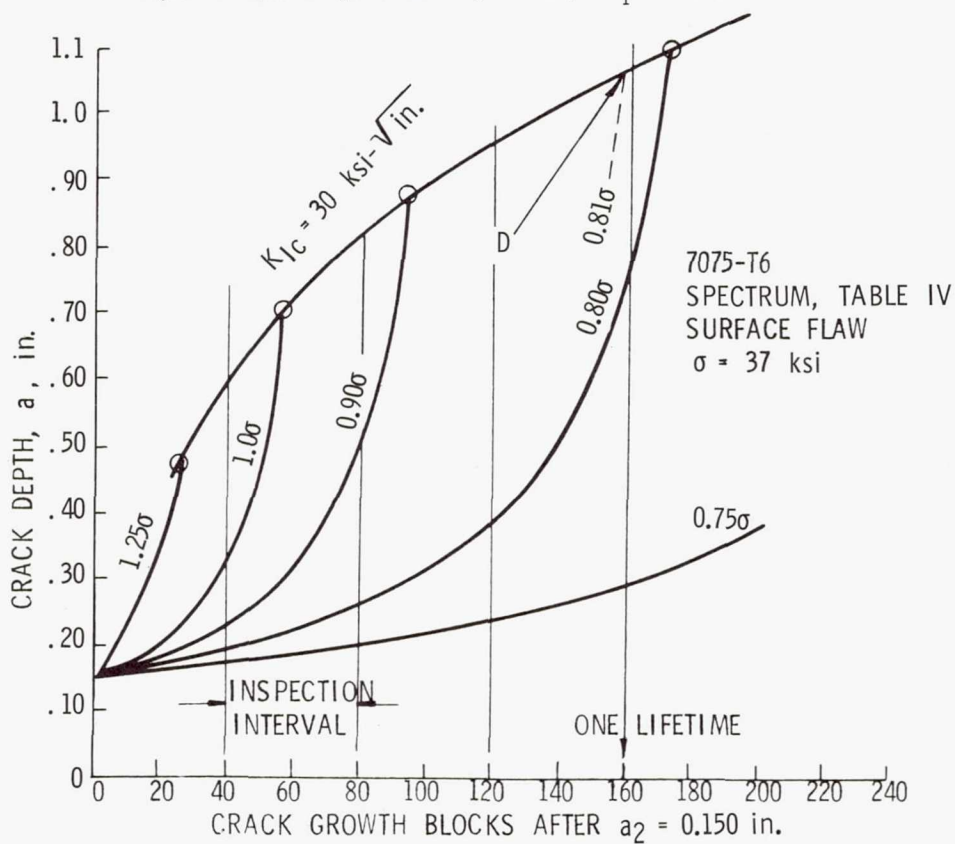


Figure 22.- Spectrum growth data. Fighter example.  $a_2 = 0.150$  in.

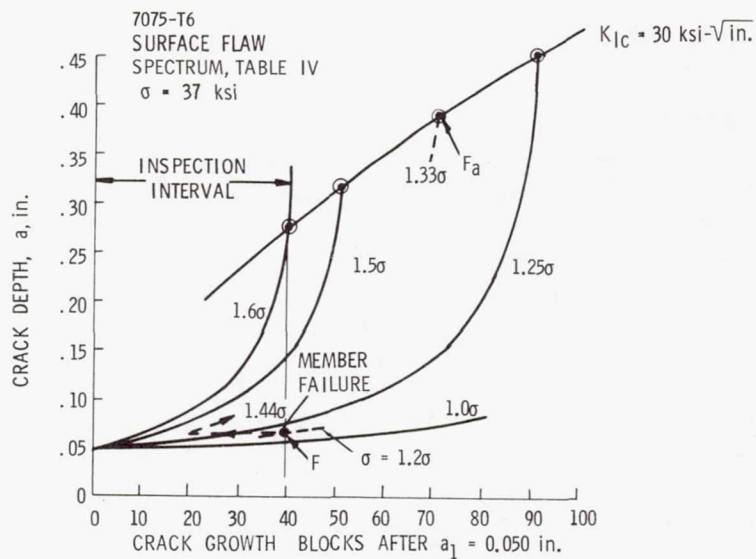
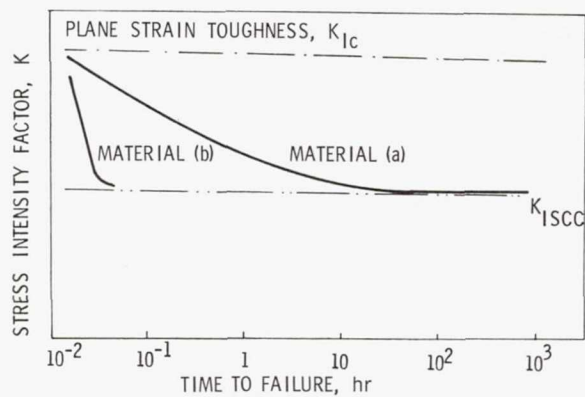
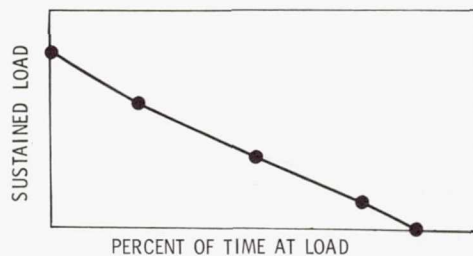


Figure 23.- Spectrum growth data. Fighter example. Data from figure 21.

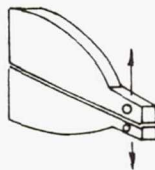
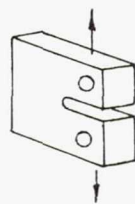


(a) Schematic of sustained load flaw growth.



(b) Schematic of sustained load spectrum.

Figure 24.- Sustained load growth and spectrum information requirements.



COMPACT  
TENSION

DOUBLE  
CANT. BEAM

SURFACE  
FLAW

CENTER CRACKED  
SHEET

FATIGUE CRACK GROWTH, $da/dN$	•	•	•	•
PLANE STRAIN TOUGHNESS, $K_{Ic}$	•	•	•	
PLANE STRESS TOUGHNESS, $K_{Ic}$				•
ENVIRONMENTAL CRACK GROWTH, $da/dt$	•	•	•	
FATIGUE GROWTH SPECTRUM EFFECTS			•	•

Figure 25.- Material fracture properties required for analyses and trade studies.



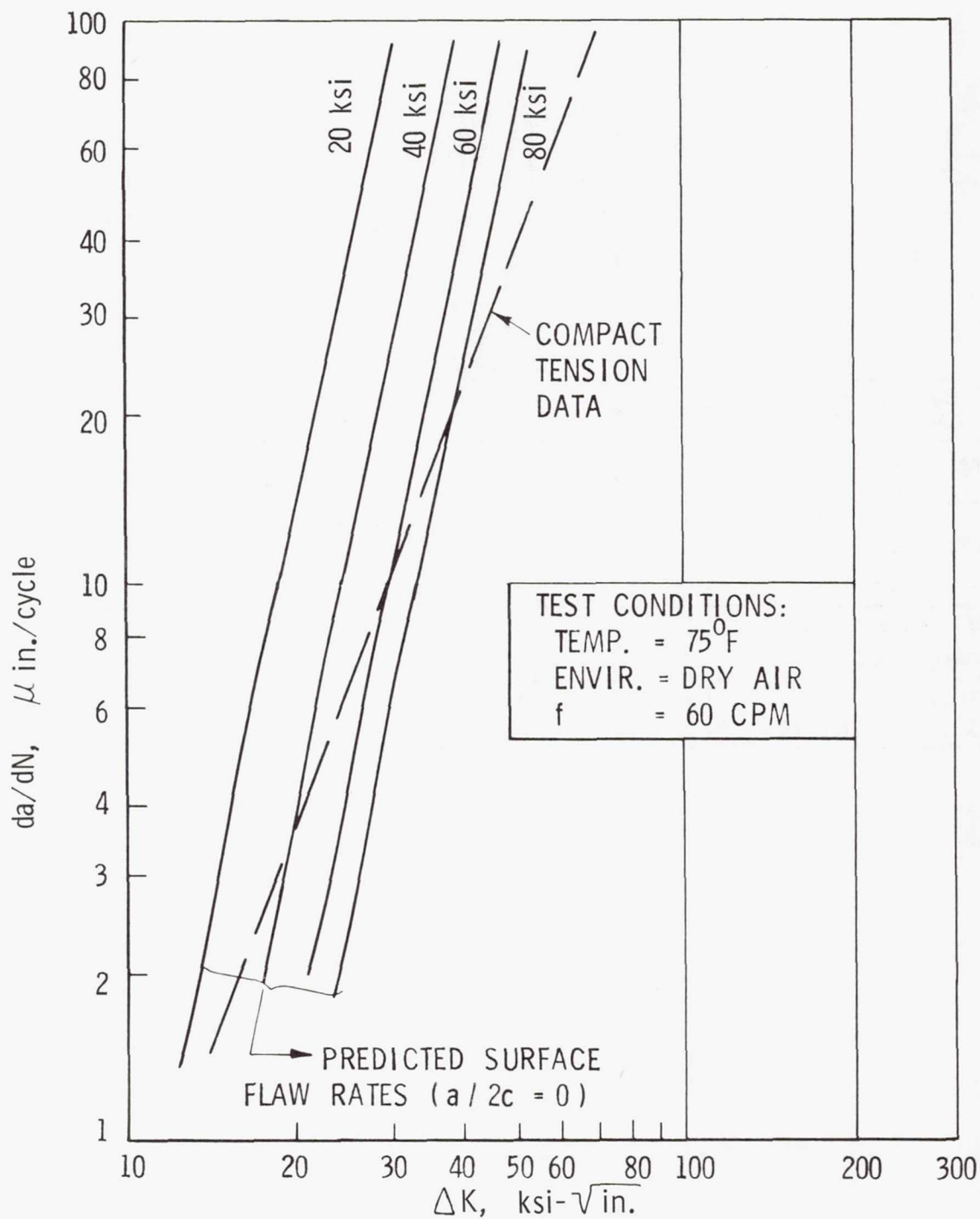
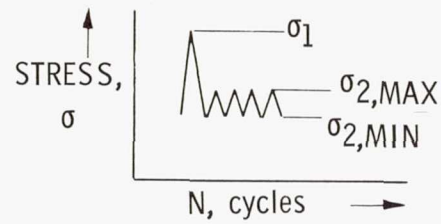
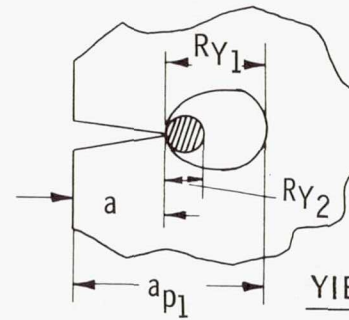


Figure 26.- Surface flaw data adjusted to  $a/2c = 0$  and compared with compact tension data from reference 11.



### LOADING



### YIELD ZONE SCHEMATIC

### SUMMARY OF AFFDL MODEL (REF. 10):

OVERLOAD  $\sigma_1$  RETARDS  $da/dN$  for  $\Delta\sigma_2$

$R_Y$  = SIZE OF YIELD ZONE

$a$  = INITIAL CRACK SIZE

$a_c$  = CRACK SIZE AT ANY TIME AFTER THE OVERLOAD

$a_{p1}$  = EXTENT OF THE PLASTIC ZONE  $R_{Y1}$  DUE TO OVERLOAD  $\sigma_1$

$$= \frac{K_1^2}{2\pi(\sigma_{YIELD})^2} + a \quad (\text{PLANE STRESS})$$

$\sigma_{ap}$  = STRESS REQUIRED TO PRODUCE A PLASTIC ZONE OF EXTENT  $a_{p1}$   
FOR ANY CRACK SIZE  $a_c + R_{Yc} < a_{p1}$

$$= \sigma_{YIELD} \sqrt{\frac{2(a_{p1} - a_c)}{a_c}}$$

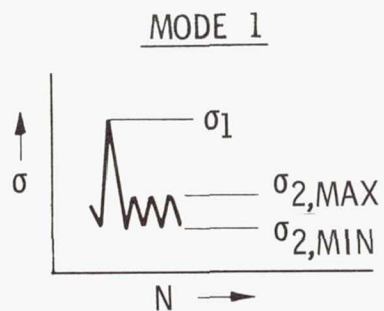
$\sigma_{red}$  = EFFECTIVE RESIDUAL STRESS CAUSED BY OVERLOAD - VARIABLE WITH  $a_c$

$$= \sigma_{ap} - \sigma_{2,MAX}$$

EFFECTIVE MAXIMUM AND MINIMUM STRESSES AND LOAD RATIO  $R$  COMPUTED FROM

$$\sigma_{2,MAX,EFF} = \sigma_{2,MAX} - \sigma_{red}; \quad \sigma_{2,MIN,EFF} = \sigma_{2,MIN} - \sigma_{red}$$

Figure 27.- Yield zone concept for retardation.



$$\sigma_1 > \sigma_2$$

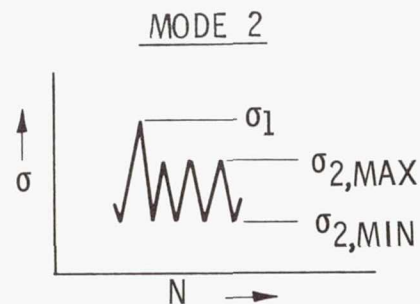
$$\sigma_{2,MIN,EFF} = \sigma_{2,MIN} - \sigma_{red} < 0$$

$$\therefore \sigma_{MIN,EFF} = 0$$

$$\Delta K_{2,EFF} = K_{2,MAX,EFF}$$

$$R_{2,EFF} = 0$$

RETARDATION DUE TO  
REDUCED  $\Delta K$ , R



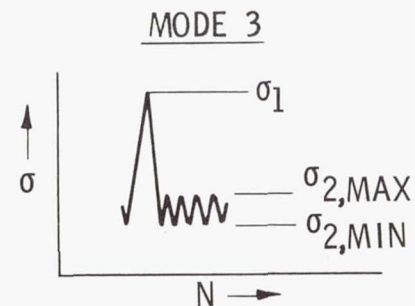
$$\sigma_1 \approx \sigma_2$$

$$\sigma_{2,MAX,EFF} \neq \sigma_{2,MIN,EFF} \neq 0$$

$$\therefore \Delta K_{2,EFF} = \Delta K_2$$

$$R_{2,EFF} = \frac{K_{MIN,EFF}}{K_{MAX,EFF}}$$

RETARDATION DUE ONLY  
TO REDUCED R



$$\sigma_1 \gg \sigma_2$$

$$\sigma_{2,MAX,EFF} \text{ AND } \sigma_{2,MIN,EFF} < 0$$

$$\therefore \sigma_{2,MAX,EFF} = \sigma_{2,MIN,EFF} = 0$$

$$\Delta K_{2,EFF} = R_{2,EFF} = 0$$

RETARDATION MAXIMUM -  
GROWTH STOPPED

Figure 28.- Modes of retardation - AFFDL model (ref. 10).



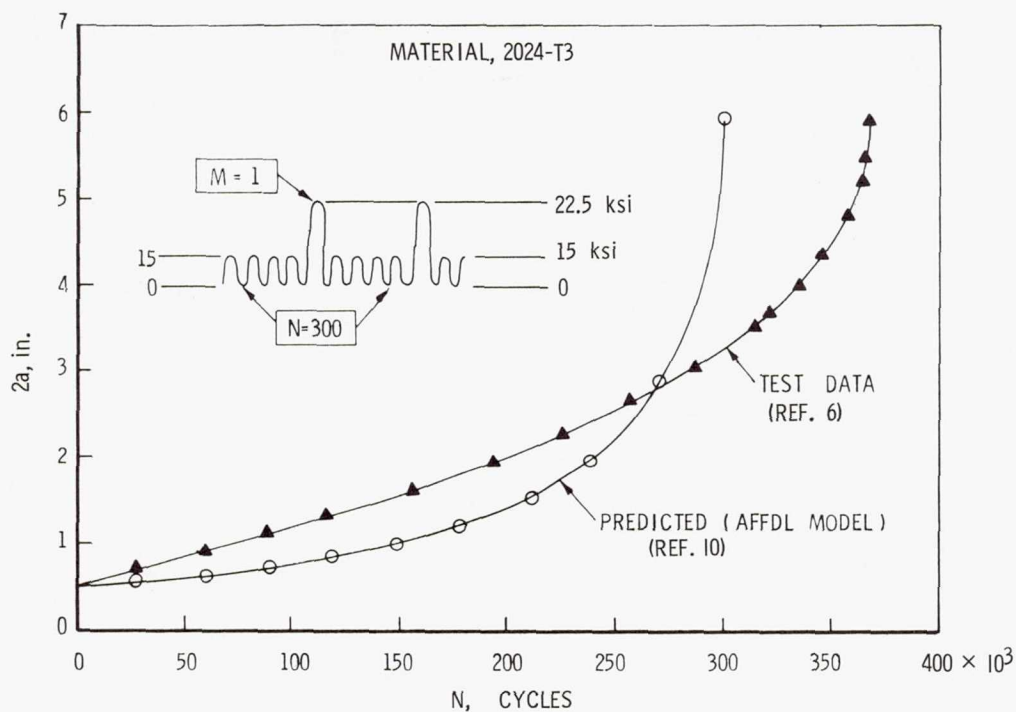


Figure 29.- Comparison of test and predicted crack growth. Single overload.

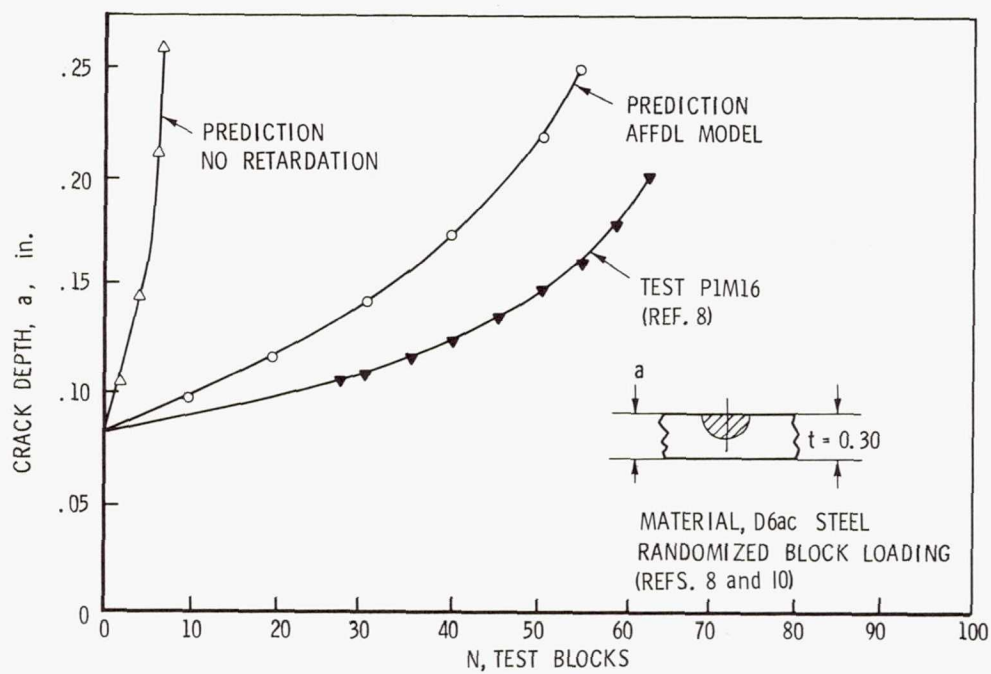


Figure 30.- Comparison of test and predicted crack growth. Randomized block spectrum loading.

## THE INFLUENCE OF MODIFICATIONS OF A FATIGUE LOADING HISTORY PROGRAM ON FATIGUE LIFETIME

By J. Branger  
Eidgenössisches Flugzeugwerk  
Emmen, Switzerland

### SUMMARY

Rectangular specimens of 7075 and 2014 aluminum alloys with two holes (stress concentration factor of 3.24) have been tested under axial fatigue loading on a six-rod test bed with modifications of the loading program, the surface particulars, and the frequency. The length of the precrack stage was investigated by use of a new crack detector.

In most cases the two alloys behaved similarly, with similar life to crack start under the same loading. Some overloads lengthened the life. Truncation by omission of the lowest peak loads should be limited to about 20 percent of the ultimate load. Simplifying counting methods gave misleading results. Very thin surface layers of anodizing, protection by vinyl, dry nitrogen atmosphere, as well as stepwise reaming or grinding the surface of the holes, lengthened the life; thick anodized layers shortened the life. Compressing the hole surface by rolling had no influence. Frequencies at about 210 to 240 cpm produced shorter lives than those at 40 cpm. At 5.4 cpm the life was considerably longer. A model to better understand the precrack-stage fatigue mechanism is discussed.

### INTRODUCTION

Fatigue test programs are usually designed to fit available test installations. Since the capability of most test facilities is limited, such test programs have to be simplified. The genuine sequence of the loading occurring in real flight usually has to be neglected. The influence of this neglect and also the influence of blocking cycles on the result of a fatigue test cannot be calculated by present methods nor can it be estimated because of many gaps in the knowledge of the fatigue mechanism. The need to remove these restrictions by appropriate tests is obvious. Test series considering the effect of variation of one or two parameters can help to find explanations of the fatigue mechanism or can at least prove whether proposed theories are possible or not.

Figure 1 represents a survey of the investigation of the influence of program modifications on the fatigue life of light alloy specimens. This paper is especially

dealing with the precrack stage of a specimen representing safe-life aircraft elements machined from bars and plates. Also, the crack-propagation life is considered to some extent.

Loading history which does not neglect the genuine sequence of the loads seems to be the only test approach to solve the problem. Moreover, since full loading history programs take a long time to run, means to shorten them without influencing the life to failure should be evaluated.

## SYMBOLS

A	chemical affinity
a	index for arithmetical
b	index for probable, or for bending ( $\sigma_b$ )
C	crack-stage length, $C = F - P$
$a_1, b_1, c_2, c_3$	material, surroundings, and loading parameters
c'	quasi-cycle (asymmetric)
D	damage
D'	amount of damage produced by $R'$ , that is, by the effective amount of reaction per cycle
D''	amount of damage produced by $R''$ , that is, by the reaction of one half-cycle
e	eccentricity
F	life to failure (number of cycles, flights or periods)
f	function
fi	flight number
f <sub>q</sub>	flight number per period



fs	scatter factor, $\frac{\overline{F}_{50}}{P_{99.9}}$
Hq	number of quasi-cycles of one period
I	intensity of incitation of chemical activity, $I = f(v) \cdot f(s)$
i	index for number of cycle, flight or period
$\left. \begin{matrix} K_1 \\ K_2 \end{matrix} \right\}$	stress concentration factors, calculated by RAS Data Sheets
L	load
Lq	highest peak load in one period
N	number (of cycles, flights or periods)
n	number of specimen; index for nominal
P	life to the end of the precrack stage, that is, to crack start (number of cycles, flights or periods)
p	duration of reaction = persistence (time)
q	period, index for period
R	reaction (chemical)
R'	effective amount of reaction per cycle
R''	amount of reaction in one half-cycle
S	strain, range of strain
s	empirical standard deviation $s = \left[ \frac{1}{n-1} \sum_{i=1}^n (\log N_i - \log \overline{N})^2 \right]^{1/2}$
s <sub>F</sub>	s for the number of periods up to failure

$s_p$	s for the number of periods up to the end of the precrack stage, that is, up to crack start
t	time
u	index for ultimate
v	rate of straining, $dS/dt$
y	probability of survival
z	electrical resistance
$\Delta$	lowest considered load step
$\nu$	rate of reaction (chemical), $f \left( I \cdot \frac{A}{\Omega} \right)$
$\sigma$	stress, load per unit of area
$\varphi$	function of
$\left. \begin{matrix} \psi_x \\ P \end{matrix} \right\}$	ordinate values for the third asymptotic extremal distribution (Smirnow)
$\Omega$	chemical resistance
$\omega$	frequency of cycles

A bar over a symbol denotes a mean value.

## MEANS AND METHODS

The means and methods used by the Swiss Federal Aircraft Establishment (called F + W) for the investigation and evaluation of the influence of program modifications involve a six-rod test bed, a crack detector, test rods, fatigue loading history, and probable mean and scatter. For test specimens which are not too large, this problem can be investigated on the six-rod fatigue test bed (fig. 2), developed and built by F + W (ref. 1), because this facility is capable of simulating the genuine sequence of loads up to 8 tons for each specimen. A structural component of a shape commonly used in aircraft, already mentioned in reference 2, was chosen as the test specimen (fig. 3). It is a slightly eccentric, axially loaded, notched specimen of rectangular cross section. A

better insight into the behaviour of fatigue is due to the crack detector (figs. 4 and 5), also developed by F + W and operational since 1969 (ref. 3).

Figure 6 defines fatigue loading history, that is, a loading in which all actual service loads essential for fatigue are applied in their genuine sequence, magnitude, and frequency, and only rest times and steady loads are omitted. Figure 7 presents the symbols and also explains how the results of the tests are evaluated. Since six test specimens, each with two identical notches, are run simultaneously, each run is giving the scatter of 12 precrack stages and the scatter of the crack-propagation life of the faster growing crack in each specimen. As Freudenthal (ref. 4) explained, it is the time to the first failure which is important, especially for safe-life elements. Therefore, all the tests are evaluated in the manner presented in figure 7. The log-extremal paper was devised by Smirnow (ref. 5). Moreover, figure 7 defines the scatter factor.

The properties of the investigated 7075 and 2014 light alloys are presented in figure 8. The 2014 alloy plate was delivered in the prestretched (2 percent) condition. The test specimens machined from this plate were fully heat treated after they were machined.

The main data of the loading programs are listed in table I.

The investigation has four main considerations: influence of omission of low loads and addition of overloads (group A), influence of different counting methods (group B), influence of surface particulars (group C), and influence of frequency (group D). A survey of the test-run numbers is given in figure 9.

## INVESTIGATIONS

### Group A

The aim of group A (fig. 10) is to disclose the influence of omitting the lowest load steps, as well as the influence of adding some overloads (fig. 11). The history program applied is the VENOM Program (ref. 6) consisting of 350 flights; the full program is called VENOM Program II. By omitting the smallest air and ground loads, program XIV was deduced from program II. In similar manner, programs XV (only the smallest air loads omitted) and XVI (only the smallest ground loads omitted) were deduced from program II. On the proposal of Hooke of ARL in Melbourne, program XVII was deduced from program XIV by omitting the next smallest air and ground loads, whereas program XVIII was deduced from program II by addition of some high peak loads exceeding the design limit load. At each fifth period an overload of 107.5 percent and at the tenth period one of 115 percent were applied. All these programs strictly observe the genuine load sequence in all 350 flights.



Figure 12 presents the results of the investigations of group A. The data are listed in tables II and III.

### Group B

There is still much speculation about the influence of different counting methods of the occurring fatigue loads on the fatigue life. Group B (fig. 13) is aiming to clear this. Although programs V' and VI' are deduced directly from program II by counting the peaks between the mean level crossings (these are the +1g level for V' and the zero-g level for VI'), LBF at Darmstadt composed two new programs: program XX by counting program II with the "level crossing" method and program XXI with the "range pair" method defined by Schijve (ref. 7), both furthermore pooling positive and negative peak loads and grouping the same cycles within each flight into blocks. This is represented on the right side of figure 13 by the hatching. The ground loads had to be presented separately.

More of the character of these program modifications is visible in figure 14. The differences from the basic program are evident.

Figure 15 and table IV present the results of group B, in which some comparative tests for specimens which were taken transversely from the plate were also included.

### Group C

On the basis of a hypothesis proposed by Schaub (ref. 8) in 1955, the investigation project was completed by considering the influence of surface particulars. Figure 16 and table V give a survey of this test series and the results. Anodic surface treatments are very widely applied where cladding is not possible. Their influence on fatigue is not sufficiently known. It was decided to test surface-layer thicknesses of about 20  $\mu$  and 6  $\mu$  for anodic oxidation in sulfuric acid and 3 to 4  $\mu$  for the anodic oxidation in chromic acid, known as the BF 4 procedure (a better defined version of Bengough). In most cases these treatments are applied before the holes are reamed; the same procedure was followed for these test specimens. It is of rather academic interest to hinder the chemical activity by a thin protective layer of vinyl as it is used to protect transistors or to lower the chemical affinity by an artificial atmosphere of commercially available dry nitrogen.

Similar to the tests of Schaub, test runs 69 and 71 were performed in such a manner that from time to time the holes 6.0 mm in diameter of the test rod were reamed or ground in steps of 0.1-mm diameter, up to five times, to a final diameter of 6.5 mm. Although by this procedure the net area was reduced by 2.5 percent and the stress concentration factor was increased from 3.24 to 3.30, the last crack started only at 115.2 periods on the reamed specimen and at 195.8 periods on the ground specimen (compared with 40.1 periods for the last crack start of those specimens which were reamed only once to a diameter of 6.0 mm). Therefore, to find the reason for the end of the precrack stage,

one needs to look only in the surface layer. This result confirms the findings of many authors. The very long life of the last three specimens after the last grinding is difficult to explain. Perhaps the workman did his job with extraordinary care because he knew what was expected and then produced a surface of higher quality than before.

No gain resulted from rolling the hole, notwithstanding the fact that it was made by a specialist.

#### Group D

The frequency effect on the fatigue life is still debated. It is therefore necessary to investigate its influence. Figure 17 and table VI present the results.

On a chain test bed 36 test rods of the same design were fatigue loaded parallel and simultaneously with the full-scale fatigue tests of three VENOM aircraft. The loading program I differs from program II only by those orders which were needed for the full-scale test; the loads, their sequence, and their number were exactly the same as with program II on the six-rod test bed. Both test beds are in the same room. The only differences were the frequency, 5.4 cpm (this test lasted  $6\frac{1}{2}$  years!), and the shape of the cycles (fig. 18). As an intermediate frequency to 210 or 240 cpm, 40 cpm was selected because it can be run on the six-rod test bed and at the same strain rate as for 210 or 240 cpm.

For program II the increasing (56 and 340 percent) life with decreasing frequency from 240 cpm to 40 cpm and 5.4 cpm is remarkable. Another comparison test was run with program XX, once with 96 cpm and once with 173 cpm. The opposite behavior is noteworthy.

#### PRECRACK STAGE

Student's test was used to determine the significance of the difference indicated in the tables by the ratio of the precrack-stage lives  $\bar{P}_{50}$ . The probability levels for the differences considered are listed in table VII. Levels of about 90 percent or higher indicate a significant difference; lower ones may indicate a trend, whereas very low levels indicate that the modification had no influence on the life. In some cases the actual thickness of the anodized layer must be taken into account and in some cases also the fact that the specimens were manufactured from different bars (as indicated by the test number). Generally, table VII hints that the significance is higher for 2014 alloy. The reason is the higher loading relative to the ultimate load.

#### Influence of Alloy

The test specimens of 7075 alloy, as well as those of 2014 alloy, were loaded to exactly the same absolute load values. Relative to the ultimate strength, the 2014 speci-



mens were thus loaded about 33 percent higher than the 7075 specimens. Nevertheless, the fatigue life of 2014 is only 19 percent shorter than that of 7075 (table VIII). This result confirms the well-known fact that the fatigue strength of the different aluminum alloys is nearly independent of their static strength. By the way, a part of the difference may be contributed to the 7075 specimens being machined from bars 15 by 60 mm, whereas the 2014 specimens were cut in the longitudinal direction from plates 32 by 1220 by 2290 mm. This also explains the slightly higher scatter for 2014.

#### Influence of Overloads

As expected and as reported and explained by many authors for program loading, the overloads lengthened both stages (table II) but much more so with 2014. For this alloy the relative overload (relative to the ultimate strength) was much higher: The highest peak load applied (+6075 kp) is 53 percent of the nominal ultimate load for 7075 but 71 percent of that for 2014. Nevertheless, overloads should not be taken into account because not all service aircraft experience them.

#### Influence of Omitting Cycles With the Lowest Peak Loads

For 7075 anodized to 20  $\mu$  the omission of the lowest and the next lowest peak loads (table III) has no significant influence on the life although the number of cycles is reduced by 81 percent. It seems that a favourable effect is abolished by another, unfavourable effect. In contrast, 2014 suffers a decrease in lifetime of 45 percent when the lowest peaks are truncated but has an increase of 63 percent when the next lowest peaks are also truncated. Relating programs XVII to XIV, this increase is as much as 195 percent. This increase of life may be explained by the truncation of the positive peaks at a relative level of 27.5 percent (relative to the ultimate load), whereas truncation at a level of 20.5 percent with 7075 has a slightly unfavourable effect. Taking into account the stress concentration factor of 3.24, the level of 27.5 percent is just at the nominal 0.2 yield strength of 2014, whereas the level of 20.5 percent is only at 77 percent of the nominal 0.2 yield strength of 7075. That is about the same for the lowest peak level omitted (program XIV) with 2014 (75 percent of 0.2 yield strength) where the effect is on the same side but faster. For these alloys, axial tension and compression, and a stress concentration factor of 3.24, the critical limit thus lies between 20.5 and 27.5 percent. Omitting loads smaller than this limit shortens the life, which seems to be very astonishing; whereas the omission of loads greater than this limit lengthens the life, as is expected. The strange shortening effect may be due to a recovery or a re-creation during the application of these lowest loads. This very interesting effect will be discussed further, in connection with surface influences and frequency.

Before the crack detector type 02 was developed, tests were performed with the same specimen and 7075 anodized to only 6  $\mu$ . For the arithmetical mean of six specimens, the



ratio of program XIV to II was 0.89 at failure. Later tests on 2014 at a higher relative load level had a similar, more pronounced trend. The influence of omitting some of the ground load cycles will be discussed subsequently.

### Influence of Counting Methods

The important decrease in the life by counting by the level-crossing method (program XX) has to be attributed mainly to the pooling of positive and negative peak loads into combined cycles. In the Swiss Review 1967 (ref. 1) a simplified test with the same 7075 specimen for the investigation of the pooling effect was reported. The pooled program (VIII) had a life ratio of 0.43 to that of the nonpooled program (XI), which is very near the ratios 0.34 for 7075 and 0.38 for 2014, when  $\overline{F}_{50}$  of program XX is compared with  $\overline{F}_{50}$  of program II.

The order-of-magnitude longer life with the program designed by the range-pair method (program XX) has to be attributed to the diminution of all positive peak loads, although such a big difference was not expected. It is noteworthy that both alloys behave nearly identically. Therefore, both counting methods have to be rejected. The same has to be said of the mean-crossing-peak counting method if this mean is zero (program VI') because this crude method omits too many cycles (fig. 14). The resulting increase of life was expected but perhaps not by this amount. About the same increase is valuable for the transversely machined 2014 specimens, as may be seen by comparing runs 100 and 97 in table IX. By putting the mean mainly at +1 of the air loads, only the ground loads are concerned. This will be discussed subsequently.

### Influence of Surface Particulars

The unfavourable effect of a thick 20- $\mu$  anodized surface layer, which is hard and cracks easily, thus forming stress raisers, is well known. The decrease of only 30 per cent is even less than expected by many people. In contrast, the important favourable effect of a thin anodized layer was not expected, certainly not by this amount. It may be that these thin layers are so elastic that they do not crack and hence fulfill their protective task. The influence of the thickness of the anodized layers was more important than had been expected. Therefore, measurements of the layer thickness of all test specimens were made after the tests. These measurements disclosed considerable differences in the nominal thickness. By this way, a part of the scatter was better explained. The only procedure which regularly gives the same thickness with a high reliability seems to be the BF 4 process.

The smaller favourable effect of the vinyl protection may be due to low porosity, which also explains the greater scatter. The fact that the life in a nitrogen atmosphere was only doubled (other authors reported much higher ratios) may be explained by the test

conditions: Commercially available dry nitrogen was used, the specimen was not cooled down, and testing was at room temperature. But a very important fact has to be noted: By simple chemical means the crack stage, as well as the precrack stage, can be lengthened considerably although the mechanical fatigue strengthening of the specimen is strictly the same.

Removing about 0.05 mm of the surface layer, by reaming or grinding, confirms the work of Schaub and his collaborators. The removal was accomplished by the same manner in which the hole was machined at the beginning. To avoid the effect of a further factor, the specimens were not electropolished. Although the crack detector was working perfectly, the removal procedure was made too late in some cases. Nevertheless, the increase of the life of the last four ground specimens is extraordinary.

In contrast, the test with the surface compressive treatment by a rolling procedure was disappointing. The main reason may be that the crack always starts at the edge of the hole because the special shape of the test rod has a slight eccentricity. This reveals the doubtful effect of treatments like this – doubtful because eccentricities are not completely avoidable in actual designs.

#### Influence of Frequency

Up to now there have been only a few reports on tests with increasing life at decreasing frequency. A note from Schütz related Weller's (Dresden) work, who reports (ref. 9) on both trends and who advocated in 1966 (ref. 10) that there must exist a frequency-dependent minimum of life with increasing life in both directions, that is, by decreasing the frequency and by increasing it from that minimum. Weller's assumption is obviously right, as will be discussed later.

There are three factors contributing to the frequency-dependent effect:

1. The genuine corrosion of unstrengthened aluminum alloys (in the present test series this influence may be neglected).
2. The strain rate, which in most cases increases with increasing frequency. Test runs 67/68/73 and 64, 57, and 55 (table VI and fig. 18) eliminate this factor because the strain rate is the same in all cases.
3. The proper frequency effect. This one is of special interest and must be discussed in connection with other influences, for example, the influence of omitting cycles, counting methods, and surface particulars.

For test run A (program I, fig. 18) the strain rate was greatly reduced. This test reflects the influence of two factors, which may explain the very long life.



The opposite trend of test runs 57 and 55 is remarkable and may be attributed at first to the very different program and cycle shape. This difference seems to move the frequency of the minimum of life to about 100 cpm, whereas for the loading history program shape this minimum lies at about 200 to 250 cpm.

In 1956 Wade and Grootenhuis (ref. 11) found that the life still increases if the frequency is increasing from 24 Hz to 3835 Hz (1440 to 230 000 cpm). But Wood and Mason (ref. 12) reported in 1968 and 1969 that by increasing the frequency from 1700 cpm to the ultrasonic range of 17 000 Hz (1 million cpm), the life decreased considerably. Two new factors (resonance and concentration in a few localities) are responsible for this result.

Thus, after the minimum proposed by Weller, there is a maximum, detected by Wood and Mason, at about 5000 times higher frequencies, as presented in figure 19. This down-up-down configuration comes about by the effects of different factors which predominate in turn. This will be discussed by means of a model.

### Influence of Compressive Loads

In these tests compressive loads are applied by ground loads and negative air loads. As the latter are very few compared with the ground loads, the findings reflect the importance of the ground loads.

Table X reveals opposite behaviour of 2014 and 7075 alloys. Program XVI, which omits all small ground load alterations (5 percent of ultimate load for 7075, 7 percent for 2014), gives shorter lives than program II in all three 7075 comparison tests (21 to 16, 76 to 67/68, and 104 to 92). This result is in accordance with the similar findings for program XIV for 7075. But in the 2014 comparison test the life with program XVI was longer than that with program II (test runs 88 to 91), which is not in accordance with the result of program XIV but with the result of program XVII. From this it may be deduced that the limit for ground loads, the omission of which has a life-lengthening effect, lies between 5 and 7 percent of the ultimate load, whereas the same limit for tension loads lies between 20 and 27 percent (as discussed in the section on omitting cycles). This result underscores the importance of compressive loads. The same trend of different behaviour appears in program V'.

### Material Flow

Because of the integral design of modern wing skins, thick plates are needed which are machined as a whole. These plates are stretched to about 2 percent before machining. This procedure outweighs the effect of rolling the plates in respect to fatigue loading history, as can be seen in table IX. The time to failure is shorter only for the transverse-directed material with program V'. This result indicates a ground-load effect.



## MODEL OF THE PRECRACK STAGE

In 1955 Schaub (ref. 13) put forward the following hypothesis: There must be two conditions for the start of a fatigue crack. One consists of the well-known physical-mechanical alterations due to fatigue loading; the other consists of a chemical reaction with the surrounding medium, which is derived from observations made by Kramer, Pepperhoff, and Churchill (ref. 13). On the same occasion it was mentioned that Gough and Sopwith, Weibull, Freudenthal, and others had found an important influence of the surrounding medium in classical constant-amplitude tests. Therefore, the inclusion of a chemical reaction for the explanation of the fatigue mechanism seems to be a more promising approach to clear the mystery of the precrack-stage fatigue mechanism than the physical-mechanical aspect alone. With the results of the tests on two aluminum alloys, this hypothesis may be refined by analysing a corresponding model of the first phase of fatigue damage, a scheme of which is presented in figure 20, and which may be called the "chemical phase."

1. Stress is inflicting strain (with all the well-known rules, especially important are those on the stress concentration factor and the residual stress originating from previous loadings (ref. 14)).

2. Strain, that is, the strain rate and the range of uninterrupted application of the variation of strain, is inciting chemical activity (apart from the well-known rules on the physical effects) between both mediums. By the way, steady strain is often the reason for stress corrosion, which should not be confused with the following description.

3. The intensity of incitation of this chemical activity, that is, the rate of reaction, is increasing with increasing strain rate and with increasing range.

4. This rate of reaction is more lively the better the affinity of these two mediums is and the lower the chemical resistance is.

5. The reaction may begin with a very short time delay after the inciting event but continues some time after it with decreasing intensity, like the persistence of a television screen.

6. The effect of this reaction is a new chemical product, most probably some composition between the two mediums concerned, that is, in most cases an oxide of the metal, in other words, damage.

7. The very thin layer of the genuine product of their affinity, for example 4 to 9 angstroms ( $10^{-10}$  m) of oxidation of aluminum alloys, does not hinder this activity if the inciting strain rate and range exceed a certain limit.

8. The (genuine) product produced at rest and the (artificial) product produced by strain rate and range are probably of the same nature, but the quantity of the latter is by far more rapidly increasing with continuing strain rate and range (called fatigue loading) than the former at rest.

9. Therefore, this accelerating (if not inciting at all) effect of the fatigue loading may be compared with the catalysis. Fatigue loading is, so to say, a dynamic catalyst.

10. This catalysis is producing an increasing thickness of the layer of the composition, for example, of the oxide, as long as fatigue loading continues.

11. There is no reason for a decomposition at rest.

12. The rate of increase in thickness will decrease with increasing thickness, as this effect begins to hinder the activity because of its chemical resistance. The rate of damage increase is thus decreasing. This is very important because a slowly increasing amount of damage explains the big scatter in the precrack stage of fatigue life, as will be seen later.

After this first phase of fatigue damage, a second phase, still in the precrack stage probably follows, which may be imagined as follows:

13. The layer of the new composition, for example this oxide layer has a Young's modulus different from that of the underlying metal, also a different yield strength. It is probably more brittle.

14. If the thickness of the layer exceeds a certain limit (which itself depends on the three-axial stress state), this layer may crack under a tension strain or form flakes under a compressive strain.

15. Those parts of the underlying metal, which are set free by these incidents and which get direct contact with the other medium, for example, with the atmosphere, will again be chemically activated, and so on.

16. Finally, the surface may get an aspect like the one which Wood (refs. 15 and 16) saw by scanning electron microscopy and on which a fatigue crack is starting.

The second part of the precrack stage may therefore be called the flake phase and is schematically presented by figure 21. Both these phases, that is, the whole process, is in fact a corrosion by fatigue and may be called fatigue corrosion, in contrast to corrosion fatigue, where a relatively quick genuine corrosion exists (and thus facilitates the fatigue corrosion). This definition differs somewhat from that given by McAdam (ref. 17), whose process "differs only in degree from stressless corrosion, but does not imply ordinary fatigue."

Most of these explaining steps are more or less evident. Step 2 was supposed by Schaub (ref. 8) 16 years ago and then supported by others. Step 15 was mentioned in 1960



by Broom and Nicholson (ref. 18). They also assumed a relation between fatigue deformation and hydrogen diffusion. Step 16 was detected only one and a half years ago by Wood (refs. 15 and 16). The increased oxide layer thickness (step 10) remains to be shown.

The most important supposition is step 5, the time-delaying activity, because by this persistence of a chemical process, the frequency influence may be explained as displayed in figure 20(g): By increasing the frequency, the reaction initially increases because of the not-yet-settled reaction of the preceding cycle; however, further increases in frequency decrease the relative damage per cycle. Obviously, together with step 3, the shape of the cycles (fig. 18) and their sequence are influencing the frequency at which the minimum life (fig. 19) is found; thus the seemingly opposite behaviour of programs II and XX is explained. Similar to figure 20(g) the omission of less effective, very low peaks (step 3) increases the value of the effective amount of reaction per cycle (and thus shortens the precrack life), whereas the crack-stage length increases by this same omission as expected (in table III compare test runs 74 with 73 and 86 with 91), thus supporting the hypothesis that the reason that the omission of the lowest peaks has a life-shortening effect originates entirely in the first damage phase.

Step 7 may explain the endurance limit to some extent. Finally, the larger scatter of the precrack stage may be explained by figure 20(h), as outlined in step 12.

The ultrasonic frequency range is not mentioned in this model because other factors are predominant and because frequencies higher than about 300 cpm do not occur in primary aircraft structures. But the model should still be valuable for acoustic fatigue (most at about 200 000 cpm).

### CRACK-PROPAGATION STAGE

Because the crack-propagation stage is not the topic of this paper, only some unusual observations are mentioned.

1. The type F + W crack detectors can detect the crack depth as well as the fatigue crack surface before final failure. Figure 22 presents a fatigue failure surface and the corresponding record from the detector. The record is not a linear, but an exponential, function. Its character also depends on the shape of the specimen.

2. The crack stage is short, much shorter than often reported or assumed, when differentiated from the precrack stage.

3. The crack stage is, on the whole, of an astonishingly constant length (fig. 23), which was computed as outlined in the appendix by P. Gschwind.

4. Crack-stage lives decrease with decreasing probability of survival (i.e., longer life), for example, by some hardening effect. (See test runs presented in fig. 23(a).) A



low frequency combined with a small strain rate showed a remarkably large effect (run A, fig. 18). Nitrogen atmosphere (72), high overloads (90), and low frequency (64) also had an effect.

5. Crack-stage lives increase with increasing precrack-stage lives, for example, by some weakening effect. (See test runs in fig. 23(c).) This result was most pronounced for run 100 (transverse, most simplified program).

6. Very short crack-stage lives were experienced with program XX.

7. The computation of the relative crack-stage life, that is,  $\frac{\bar{C}_{50}}{\bar{F}_{50}} \cdot 100$ , reveals astonishingly high and consistent values of 10 to 30 percent.

8. As was shown in Stockholm (ref. 19), the fatigue-cracked surface, as recorded by the crack detectors, is increasing by a simple law and with a very low scatter, which can be seen in figure 24.

## CUMULATIVE DAMAGE

The different character of the damage cumulation of the three phases of the model is presented in figure 25. The poor correlation of actual life until crack start with simple linear cumulative damage hypothesis originates mainly from the first phase, which reveals the influence of load sequence, cycle shape, and frequency. The proposed model is still a simplification and needs many tests to find quantitative coefficients, but it is hoped that the model helps for a better approach to the problem.

## CONCLUSIONS

Up to now results from the test project permit the following conclusions:

1. There is no important difference in time to crack start between these two alloys (2014 and 7075) if loaded to identical values. This result confirms earlier findings.

2. Overloads have a favourable effect. This result is also in agreement with findings of earlier and less sophisticated tests. This should, nevertheless, not be considered for calculations of time to failure.

3. Omission of low peaks does not affect the time to failure of tests if this omission concerns peaks lower than about 20 percent of the ultimate load at tension and 5 percent at compression.

4. Counting load occurrences by the so-called peak between +1g mean-crossing method, peak between zero-g mean-crossing method, level-crossing and range-pair

methods (both combined with pooling and blocking) is giving misleading results and must be rejected.

5. While thick ( $\sim 20 \mu$ ) sulfuric anodized surface layers have an unfavourable effect on the lifetime, the contrary is true for thin ( $\sim 6 \mu$ ) layers or BF 4 treated elements, which lengthen the life.

6. Stepwise reaming or grinding of holes can lengthen the life considerably, which may be useful for maintenance people; whereas rolling of hole surfaces alone has no effect.

7. There is a definite frequency effect with a minimum and a maximum.

8. There is a strain-rate effect — decreasing rate giving increasing life.

9. A model, assuming a catalytic effect of fatigue loading on the chemical activity of the surface, with a persistence of this activity, is presented, which could explain the influences of frequency, strain rate, and load sequence, as well as the trend of decreasing life by omission of the lowest (and most numerous) peaks. The model also reveals an important reason for the scatter in the precrack stage.

10. The crack stage, now easier to observe by a new crack detector, is (for machined specimens) short — much shorter than often reported. It is, on the whole, of an astonishingly constant length, with a lower scatter than the precrack stage, which also diminishes the scatter of the life to final fatigue failure.

#### ACKNOWLEDGMENTS

Many thanks are extended to the collaborators for their help: Mr. P. Gschwind for the mathematical part, Mr. E. Eberle for evaluation and figures, Miss L. Meierhans for typewriting, Mr. L. Richiger for tables, and Mr. K. Steiner and his team for the editing of this report, also many thanks to Mr. E. Kindlimann (hydraulics) and Mr. H. Widmer (electronics) and their teams for keeping the test beds and recorders running day and night.

This paper is published with the permission of G.R.D. (Armament, Technology and Procurement Group of E.M.D.), Berne, Switzerland.

## APPENDIX

### COMPUTATION OF THE MEAN CRACK-STAGE LIFE

By P. Gschwind

Let  $P(y)$  be the most probable line of precrack-stage life on log-extremal paper and  $F(y)$  be the most probable line of fatigue failure, both functions of life expectancy  $y$ . The mean crack-stage life must be computed,

$$C(y) = F(y) - P(y) \quad (1)$$

On log-extremal paper  $(u, Y)$  a straight line is defined by two constants

$$Y = a_2 u + a_1$$

and

$$u = \frac{1}{a_2} (Y - a_1)$$

For  $F$  and  $P$ , then

$$u_F = \frac{1}{a_2 F} (Y - a_1 F)$$

and

$$u_P = \frac{1}{a_2 P} (Y - a_1 P)$$

Because  $u$  is the common logarithm of  $F$  and  $P$ ,

$$\left. \begin{aligned} F &= 10^{\frac{1}{a_2 F} (Y - a_1 F)} \\ P &= 10^{\frac{1}{a_2 P} (Y - a_1 P)} \end{aligned} \right\} \quad (2)$$



# APPENDIX – Concluded

Otherwise on log-extremal paper,

$$y = e^{-e^Y}$$

or

$$Y = \log(-\log y) \tag{3}$$

Introducing equation (3) into equations (2) and (1) yields

$$C(y) = 10^{\frac{1}{a_2^F} \left[ \log(-\log y) - a_1^F \right]} - 10^{\frac{1}{a_2^P} \left[ \log(-\log y) - a_1^P \right]}$$

The constants  $a_1^F$ ,  $a_2^F$ ,  $a_1^P$ , and  $a_2^P$  are to be calculated with the least-square method from experimental data.

## REFERENCES

1. Branger, J.: Swiss Review 1965 – 1967. ICAF Doc. 412, Minutes of the Tenth ICAF Conference, J. Y. Mann, ed., 1967.
2. Branger, J.: Swiss Review 1961 – 1963. ICAF Doc. 271, Minutes of the Eighth ICAF Conference, V. Villa, ed., 1963.
3. Branger, J.: Life Estimation and Predicting of Fighter Aircraft. Proc. Int. Conf. on Structural Safety and Reliability, A. M. Freudenthal, ed., 1969.
4. Freudenthal, A. M.: Reliability Analysis Based on Time to the First Failure. Proc. of Fifth ICAF Symposium, J. Y. Mann and I. S. Milligan, eds., Pergamon, 1967.
5. Smirnow, N. W.; et al.: Mathematische Statistik in der Technik. VEB Deutscher Verlag der Wissenschaften, 1963.
6. Branger, J.: The VENOM Program, F + W S-197 (not yet published).
7. Schijve, J.: The Analysis of Random Load-Time Histories With Relation to Fatigue Tests and Life Calculations. Fatigue of Aircraft Structures, W. Barrois and E. L. Ripley, eds., Macmillan Co., 1963, pp. 115-149.
8. Schaub, C.; and Liedtke, W.: Der Mechanismus des Dauerbruchs metallischer Werkstoffe. Colloquium on Fatigue, W. Weibull and F. K. G. Odquist, eds., Springer, 1956.
9. Weller, J.: Die Bedeutung der Lastspielfrequenz beim Dauerschwingversuch metallischer Proben a.s.o. in Neue Hütte, 6. Jg., Dez. 1961.
10. Weller, J.: Kritischer Vergleich einer Auswahl von Aluminium-Konstruktionswerkstoffen a.s.o. in IfL-Mitt. 5, Heft 12, 1966.
11. Wade, A. R.; and Grootenhuis, P.: Very High-Speed Fatigue Testing. International Conference on Fatigue of Metals, I. Mech. Eng., 1956.
12. Wood, W. A.; and Mason, W. P.: Fatigue Mechanism in Iron at Ultrasonic Frequency. J. Appl. Phys., Oct. 1969.
13. Lissner, O.: Einige Versuche über die Vorgänge in der Oberflächenschicht von Ermüdungsproben. Colloquium on Fatigue, W. Weibull and F. K. G. Odquist, eds., Springer, 1956.
14. Haibach, E.; Schütz, D.; and Svenson, O.: Forschungsbericht FB 78/68 des LBF. ICAF Doc. 508, 1969.
15. Wood, W. A.: Fatigue Crack Initiation as Viewed by Scanning Electron Microscopy. Technical Report No. 1, George Washington Univ., Jan. 1970.

16. Wood, W. A.: Elastic Fatigue in Titanium Studied by Scanning Electron Microscopy. Technical Report No. 2, George Washington Univ., Apr. 1970.
17. McAdam, D. J.: The Influence of Stress Range and Cycle Frequency on Corrosion. Proc. ASTM 30 (1930), Part 2, pp. 411-447.
18. Broom, T.; and Nicholson, A.: Atmospheric Corrosion-Fatigue of Age-Hardened Aluminium Alloys. Journal of the Institute of Metals, vol. 89, 1960.
19. Branger, J.; and Ronay, M.: High Strength Steels Under Fatigue History Loading. ICAF Doc. No. 499, Proc. of the Technical Session of the 11th ICAF Meeting, G. Wallgren and S. Eggwertz, eds., 1969.



TABLE I.- DATA OF LOADING PROGRAMS

Program	Cycles $H_q$ in one period $q$ of 350 flights			Highest peak loads $L_q$ in one period $q$ , kp	
	Air	Ground	Total	Positive	Negative
II	20033	18515	38548	5265	-1600
V'	19553	350	19903	5265	-1600
VI'	638	350	988	5265	-1600
XIV	9180	3405	12585	5265	-1600
XV	9180	18515	27695	5265	-1600
XVI	20033	3405	23438	5265	-1600
XVII	6499	835	7334	5265	-1600
XVIII	20033	18515	38548	6075	-1600
XX			10150	5010	-1580
XXI			10150	4800	-1580

These data are valuable for both alloys investigated, also for all surface particulars and for all frequencies. All tests were run with the test rod (fig. 4) and all in the same test room at a room temperature of  $15^{\circ}$  to  $20^{\circ}$  C.

TABLE II. - OVERLOAD

Alloy 7075; 240 cpm								Alloy 2014; no anodic treatment; 210 cpm					
Test run	$s_F$	$s_P$	$\bar{C}_{50}$	$\bar{F}_{50}$	$\bar{P}_{50}$	Anodic treat., $\mu$	Program	$\bar{P}_{50}$	$\bar{F}_{50}$	$\bar{C}_{50}$	$s_P$	$s_F$	Test run
77	0.0699	0.0939	6.3	37.1	30.8	16.5	XVIII	41.6	53.1	11.5	0.1015	0.0673	90
73	.0408	.0550	4.9	32.8	27.9	20.3	II	30.4	38.3	7.9	.0774	.0576	91
	1.71	1.71	1.28	1.13	1.10		<u>XVIII</u> II	1.37	1.38	1.46	1.31	1.17	

TABLE III.- TRUNCATION

Alloy 7075; 240 cpm							Program	Alloy 2014; no anodic treatment; 210 cpm					
Test run	$s_F$	$s_P$	$\bar{C}_{50}$	$F_{50}$	$\bar{P}_{50}$	Anodic treat., $\mu$		$\bar{P}_{50}$	$F_{50}$	$\bar{C}_{50}$	$s_P$	$s_F$	Test run
67/68	0.0630	0.0882	6.7	32.9	26.2	23.7	II	30.4	38.3	7.9	0.0774	0.0576	91
73	.0408	.0939	4.9	32.8	27.9	20.3	II						
74	.0999	.1249	8.2	34.3	26.1	20.5	XIV	16.8	25.9	9.1	.1448	.1107	86
75	.1103	.1362	9.3	32.2	22.9	19.7	XV	23.8	35.1	11.4	.0753	.0900	87
79	.0628	.1020	7.0	31.3	24.3	24	XVII	49.7	61.8	12.1	.0823	.0606	89
							Ratios:						
							74/73	86/91	0.55	0.68	1.15	1.87	1.92
							79/67	89/68	1.63	1.61	1.53	1.06	1.05
							.63	.82	.85	.91	.93		
							2.70	1.45	1.90	.98	.82		
							1.10	1.09	1.13	.94	.88		
							79/74	89/86	2.95	2.38	1.33	.57	.55
							75/73	87/91	.78	.92	1.45	.97	1.56
							75/74	87/86	1.42	1.35	1.25	.52	.81
16	0.0452		$\bar{F}_a =$	86.2		5.2	II						
20	.0602			76.8		7.7	XIV						
19	.1064			97.3		7.9	XV						
							Ratios:						
							1.77						
							1.33						
							19/20						
							20/16						



TABLE IV.- COUNTING METHODS

Alloy 7075									Alloy 2014; no anodic treatment; 210 cpm					
Test run	$s_F$	$s_P$	$\bar{C}_{50}$	$\bar{F}_{50}$	$\bar{P}_{50}$	Freq., cpm	Anodic treat., $\mu$	Program	$\bar{P}_{50}$	$\bar{F}_{50}$	$\bar{C}_{50}$	$s_P$	$s_F$	Test run
67/68	0.0630	0.0882	6.7	32.9	26.2	240	23.7	II	30.4	38.3	7.9	0.0774	0.0576	91
96	.0629	.0880	6.8	35.9	29.1	210	22.8	V'	54.4	64.7	10.3	.1347	.1265	101
	1.00	1.00	1.02	1.09	1.11			V'/II	1.79	1.69	1.30	1.74	2.20	
92	0.0825	0.0688	13.8	81.9	68.1	210	5.5	II						
102	.0561	.0716	19.2	122.0	102.8	210	3.3	VI'	74.8	93.4	18.6	0.1208	0.1078	99
103	.0952	.0965	12.3	83.0	70.7	210	5	V'						
	0.68	1.04	1.39	1.49	1.51			VI'/II	2.46	2.44	2.35	1.56	1.87	
	.59	.74	1.56	1.47	1.45			VI'/V'	1.37	1.44	1.81	.90	.85	
Alloy 7075									Alloy 2014; no anodic treatment; 96 cpm					
54/56	0.0478	0.0547	7.9	46.5	38.7	240	21.6	II	see above					
55	.0445	.0893	3.5	15.8	12.3	96	21.2	XX	10.2	14.5	4.3	0.1102	0.1034	93
84	.0709	.0813	12.0	121.0	109.0	96	25.5	XXI	25.5	143.0	17.5	.1490	.1303	94
	0.93	1.63	0.44	0.34	0.32			XX/II	0.34	0.38	0.54	1.42	1.80	
	1.46	1.12	2.18	3.70	4.0			XXI/II	4.15	3.73	2.19	1.93	2.26	
	1.57	.69	5.0	10.9	12.5			XXI/XX	12.2	9.8	4.1	1.36	1.26	

TABLE V.- SURFACE

Alloy 7075; program II; 210 to 240 cpm						Surface particulars	Alloy 2014; program II; 210 cpm						
Test run	s <sub>F</sub>	s <sub>P</sub>	$\bar{C}_{50}$	$\bar{F}_{50}$	$\bar{P}_{50}$		$\bar{P}_{50}$	$\bar{F}_{50}$	$\bar{C}_{50}$	s <sub>P</sub>	s <sub>F</sub>	Test run	
67/68	0.0478	0.0737	8.0	45.6	37.6	No treatment ① Std. atm.	30.4	38.3	7.9	0.0774	0.0576	91	
73	0.0408	0.0939	4.9	32.8	27.9	②a 20.3 $\mu$							
67/68	.0630	.0882	6.7	32.9	26.2	②b 23.7 $\mu$							
92	0.0825	0.0688	13.8	81.9	68.1	③ Anodic BF4 5.5 $\mu$ 3.0 $\mu$	35.3	44.7	9.4	0.1513	0.1201	98	
70	0.0779	0.1023	10.6	64.1	53.4	④ Vinyl						106	
72	0.0516	0.0716	15.3	92.7	77.4	No treatment ⑤ Nitrogen						105	
	0.85	1.27	0.61	0.72	0.74	Ratios: ②a / ①	1.16	1.17	1.19	1.95	2.08		
	1.32	1.20	.84	.72	.70	②b / ①							
	1.73	.94	1.73	1.80	1.81	③ / ①							
	1.63	1.39	1.33	1.41	1.42	④ / ①							
	1.08	.97	1.91	2.03	2.06	⑤ / ①							
						No anodic ⑥							
80	0.0760	0.0641	7.5	44.5	37.0	Rolled surface							
	1.59	0.87	0.94	0.96	0.98	⑥ / ①							

TABLE VI.- FREQUENCY

Alloy 7075							Program		Alloy 2014; no anodic treatment					
Test run	Anodic treat., $\mu$	$s_F$	$s_P$	$\bar{C}_{50}$	$\bar{F}_{50}$	$\bar{P}_{50}$	Frequency, cpm		$\bar{P}_{50}$	$\bar{F}_{50}$	$\bar{C}_{50}$	$s_P$	$s_F$	Test run
67/							II	II						
68/	22.0	0.0487	0.0728	5.5	32.7	27.2	240	210	30.4	38.3	7.9	0.0774	0.0576	91
73														
64	21.2	0.0484	0.0724	8.0	50.5	42.4	II	II						107 (3 rods)
							40	40						
A	19.7	0.0286	0.0630	30.0	150.0	120.0	I	II						Nitrogen atm
							5.4	40						(107.3 r)
		1.00	1.00	1.46	1.55	1.56	40/	40/						
		.59	.86	5.5	4.6	4.4	240	210						
							5.4/	40N/						
							240	40						
							Program XX							
							Freq., cpm							
57	21.7	0.0693	0.0671	3.7	18.2	14.5	173							
55	21.2	.0445	.0893	3.5	15.8	12.3	96							
		0.64	1.33	0.95	0.87	0.85	96/							
							173							



TABLE VII.- STUDENT'S SIGNIFICANCE TEST

- ① Test run considered } Actual thickness of anodized layer in  $\mu$   
 ② Test run compared with }  
 ③ Probability level for the difference
- ◆ Analogous relation for 2014 and 7075 alloy and same trend  
 ✕ Analogous relation for 2014 and 7075 and opposite trend

①		②		③ %	①		②		③ %
No.	$\mu$	No.	$\mu$		No.	$\mu$	No.	$\mu$	
67/68	no	91	no	89	67/68	no	67/68	23.7	99
86	no	91	no	99	◆ 74	20.5	73	20.3	26
87	no	91	no	99	◆ 75	19.7	73	20.3	92
88	no	91	no	98	✕ 76	22.5	67/68	23.7	60
					◆ 104	7.5	92	5.5	>99
89	no	91	no	99	✕ 79	24.0	67/68	23.7	75
90	no	91	no	99	◆ 77	16.5	73	20.3	51
93	no	91	no	◆ 99	◆ 55	21.2	54/56	21.6	◆ 99
94	no	91	no	◆ 99	◆ 84	25.5	67/68	23.7	◆ 99
97	no	91	no	96					
98	BF4	91	no	85	◆ 67/68	no	92	5.5	99
99	no	91	no	99	◆ 102	3.3	92	5.5	>99
100	no	97	no	>99	◆				
101	no	91	no	>99	◆ 103	5.0	92	5.5	40
					◆ 96	22.8	67/68	23.7	49
105	N2	91	no		◆ 72	N2	67/68	no	99
106	Vinyl	91	no		◆ 70	Vinyl	67/68	no	97
107	no	91	no		◆ 64	21.2	73	20.3	99
95	no	101	no	>99	55	21.2	57	21.7	65
100	no	99	no	20	80	roll.	67/68	no	10
99	no	101	no	92	◆ 102	3.3	103	5.0	>99
100	no	95	no	>99	◆				
87	no	86	no	98	✕ 75	19.7	74	20.5	85
89	no	86	no	◆ 99	✕ 79	24.0	74	20.5	90.5

TABLE VIII.- ALLOY

Test run	Alloy	Surface treatment	Program	Frequency, cpm	$\bar{P}_{50}$	$\bar{F}_{50}$	$\bar{C}_{50}$	$s_P$	$s_F$
67/ 68	7075	None	II	240	37.6	45.6	8.0	0.0737	0.0478
91	2014	None	II	210	30.4	38.3	7.9	.0774	.0576
Ratio $\frac{2014}{7075}$ . . . . .					0.81	0.84	0.99	1.05	1.20

TABLE IX.- MATERIAL FLOW

Test run	Alloy	Flow direction	Program	Surface treatment	Frequency, cpm	$\bar{P}_{50}$	$\bar{F}_{50}$	$\bar{C}_{50}$	$s_P$	$s_F$	
91	2014	Long.	II	None	210	30.4	38.3	7.9	0.0774	0.0576	
97	2014	Trans.	II	None	210	36.7	42.5	5.8	.0705	.0514	
Transverse/Longitudinal . . . . .						1.20	1.11	0.73	0.91	0.89	
101	2014	Long.	V'	None	210	54.4	64.7	10.3	1.347	0.1265	
95	2014	Trans.	V'	None	210	35.0	38.1	3.1	.1473	.1283	
Transverse/Longitudinal . . . . .						0.64	0.59	0.30	1.09	1.01	
99	2014	Long.	VI'	None	210	74.8	93.4	18.6	0.1208	0.1078	
100	2014	Trans.	VI'	None	210	72.1	87.4	15.3	.0729	.0869	
Transverse/Longitudinal . . . . .						0.96	0.94	0.82	0.60	0.81	
Ratio 100/97 . . . . .						1.97	2.06	2.64	1.03	1.69	
100/95 . . . . .						2.06	2.30	4.94	.50	.68	



TABLE X.- GROUND LOADS

Alloy 7075							Program	Alloy 2014; no anodic treatment					
Test run	Anodic treat., $\mu$	$s_F$	$s_P$	$\bar{C}_{50}$	$\bar{F}_{50}$	$\bar{P}_{50}$		$\bar{P}_{50}$	$\bar{F}_{50}$	$\bar{C}_{50}$	$s_P$	$s_F$	Test run
67/68	23.7	0.0630	0.0882	6.7	32.9	26.2	II	30.4	38.3	7.9	0.0774	0.0576	91
76	22.5	.0407	.0729	6.2	27.0	20.7	XVI	43.6	52.2	8.6	.1367	.1085	88
96	22.8	.0629	.0880	6.8	35.9	29.1	V'	54.4	64.7	10.3	.1347	.1265	101
		0.79	0.83	0.93	0.82	0.79	XVI/II	1.43	1.36	1.09	1.77	1.88	
		1.00	1.01	1.02	1.09	1.11	V'/II	1.79	1.69	1.30	1.74	2.20	
Alloy 7075								7075:	$F_a$		$s_F$	Anodic treat., $\mu$	Test run
92	5.5	0.0825	0.0688	13.8	81.9	68.1	II		86.2		0.0452	5.2	16
104	7.5	.0902	.114	8.0	56.6	48.6	XVI		66.5		.0780	5.3	21
103	5.0	.0952	.0965	12.3	83.0	70.7	V'						
		1.09	1.62	0.58	0.69	0.71	XVI/II		0.77		1.73		
		1.15	1.40	.89	1.01	1.04	V'/II						

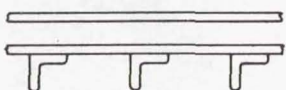
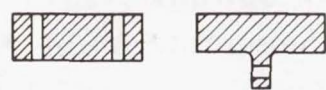

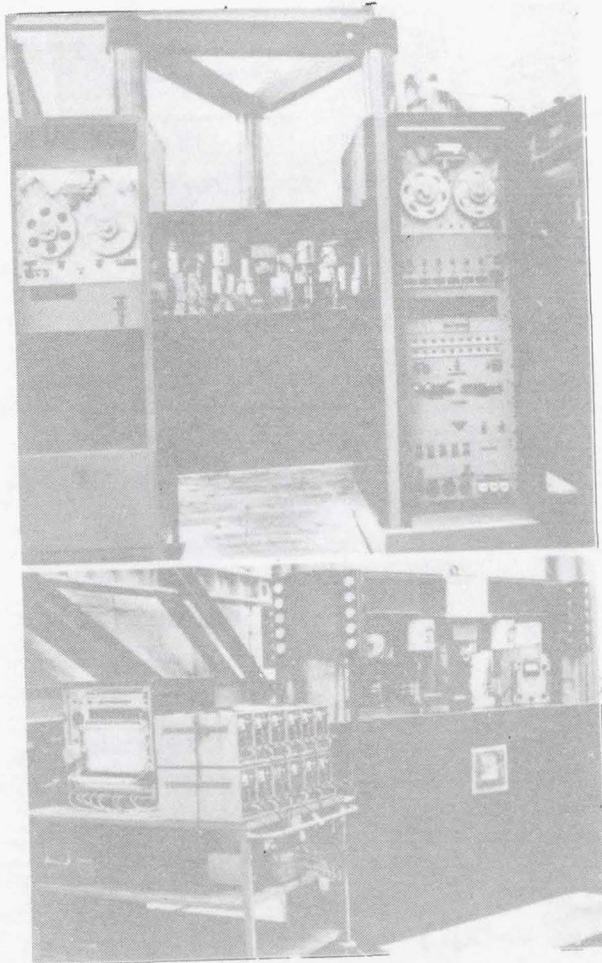
Survey of the Investigation of the Influence of Program Modifications on the Fatigue Life of Light Alloy Specimens			
Light Alloy Element or Component	Sheet 	Rod, Boom 	Plate 
Crack Propagation	slow	fast	very fast
Fatigue Behaviour	Fail safe	safe Life	safe Life
Precrack Stage		Field of this Report	
Crack Propagation Life			
Life to Failure			

Figure 1



### Six-Rod Fatigue Test Bed (F+W)

- For axial loads on 6 rods, tension and compression, up to 8 tons for each rod.
- Frequency 1 to 240 cpm
- Genuine sequence of loads
- 127 Load levels available
- Fully automatic electronic control, up to 120 000 orders in a unique and uninterrupted sequence.

Figure 2



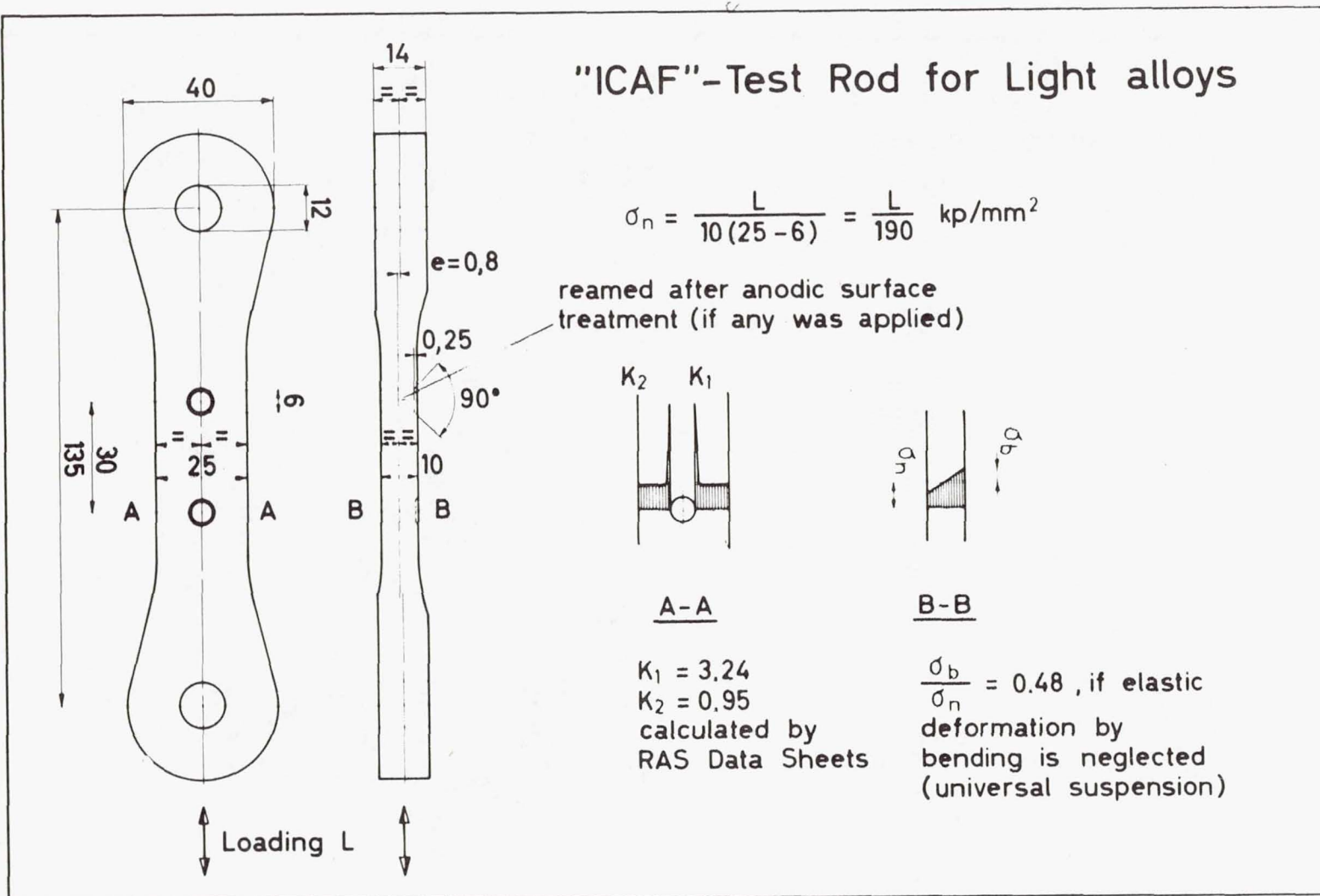
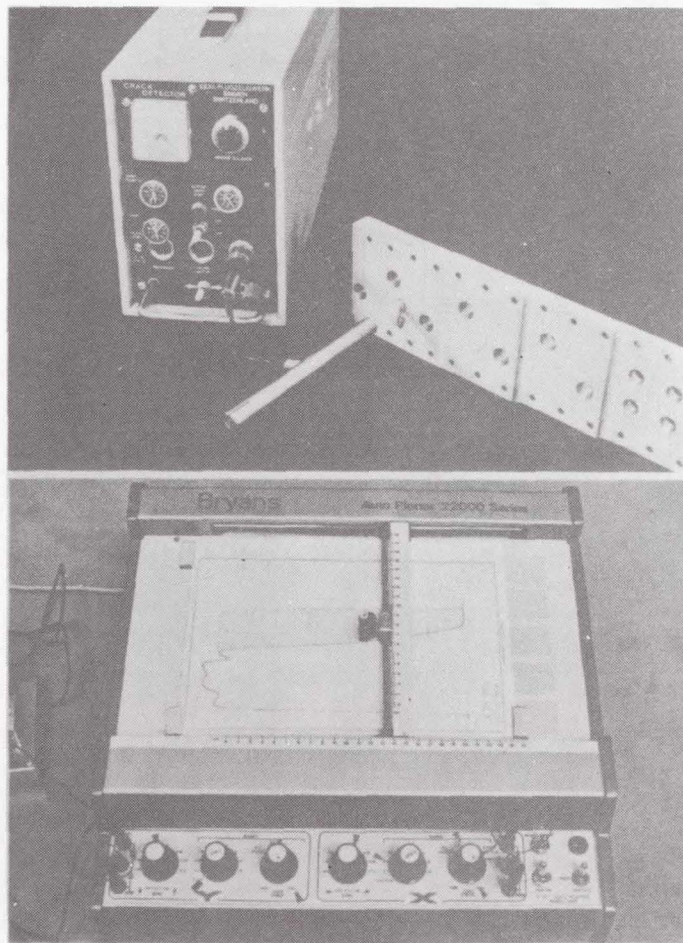


Figure 3



## Eddycurrent

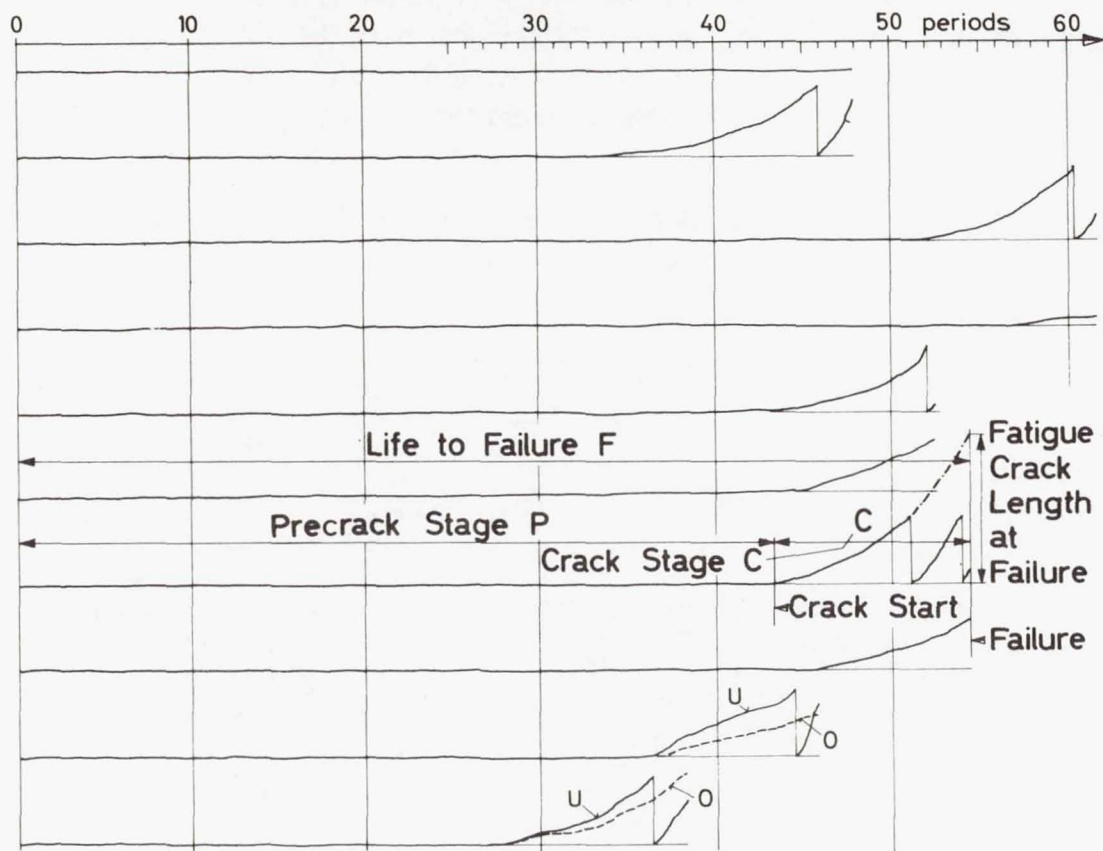
### Crack Detector Type 02 (F+W)

- For non-ferromagnetic alloys
- For holes 4 to 50 mm diameter and flat surfaces
- 5 to 1 Volt output per 0.1 mm crack depth
- Range up to 50 Volts
- Indication independent of scratches or undulations up to 0.5 mm or of conical holes up to 5°

Figure 4

# Crack Story of 12 Holes in 6 Rods

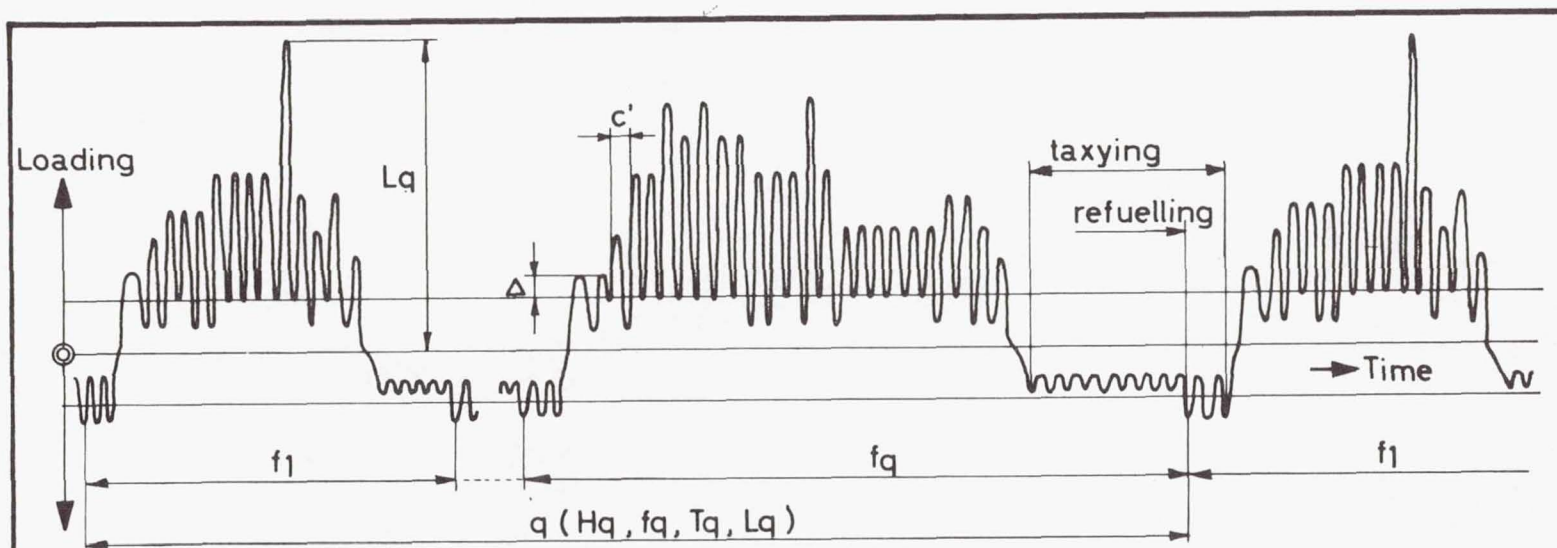
automatically recorded by the Crack Detector Type 02



test run No.90 program XVIII/100/5265			
rod No.	hole	crack start No. of periods	failure
E-144	o	—	—
E-144	u	34,4	47,821
E-143	o	51,4	61,406
E-143	u	56,4	—
E-142	o	43,4	52,406
E-142	u	44,4	—
E-141	o	43,4	54,406
E-141	u	45,8	—
E-140	o	37,4	45,839
E-140	u	36,4	
E-139	o	27,4	—
E-139	u	27,4	38,406

Figure 5



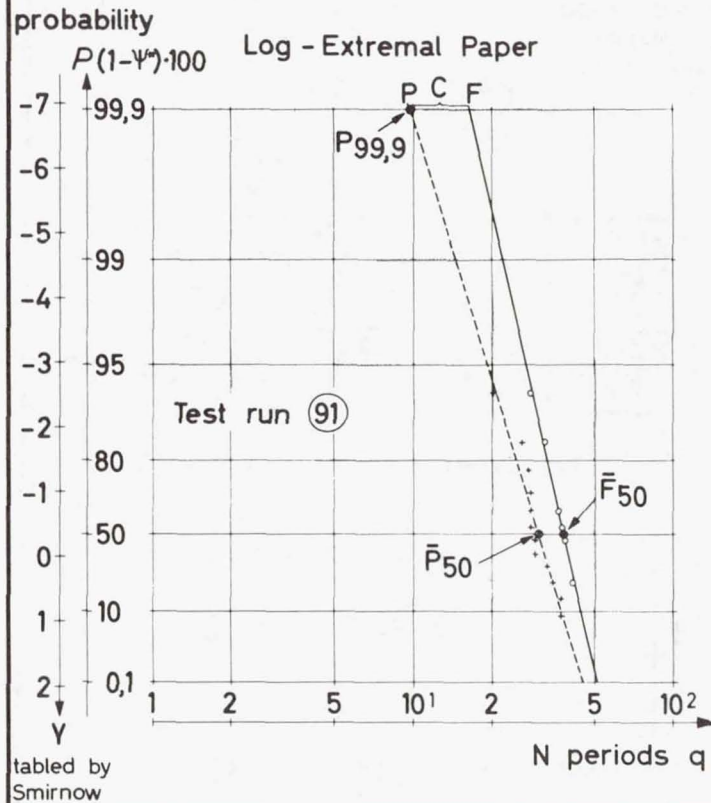


## Fatigue Loading History

- $c'$  quasi-cycle
- $\Delta$  lowest considered load step
- $f$  flight type
- $q$  period, consisting of the unique sequence of all flights
- $Hq$  Number of quasi-cycles of a period
- $f_q$  Number of flight types of a period (different or uniform)
- $T_q$  Number of the simulated service flight hours in one period
- $L_q$  highest peak load in one period

Figure 6

## Symbols s and $\bar{N}$



$n$  = number of holes (two per specimen)

$N$  = Number of periods  $q$  (350 flights per period)

$s$  = empirical standard deviation =

$$\left[ \frac{1}{n-1} \sum_{i=1}^n (\log N_i - \log \bar{N}_b)^2 \right]^{1/2}$$

$\bar{N}_a$  = arithmetical mean =

$$\frac{1}{n} \left( \sum_{i=1}^n N_i \right)$$

$\bar{N}_b = \phi$  = probable mean =

line of least squares at 50% probability of survival

$P$  = crack start ( $N$ )

$F$  = Failure ( $N$ )

$C = F - P$  = Crack stage

$\bar{P}_{50}$  = probable mean of crack start

$\bar{F}_{50}$  = probable mean of failure

$$\bar{C}_{50} = \bar{F}_{50} - \bar{P}_{50}$$

$$fs = \text{scatter factor} = \frac{\bar{F}_{50}}{P_{99.9}}$$

Figure 7

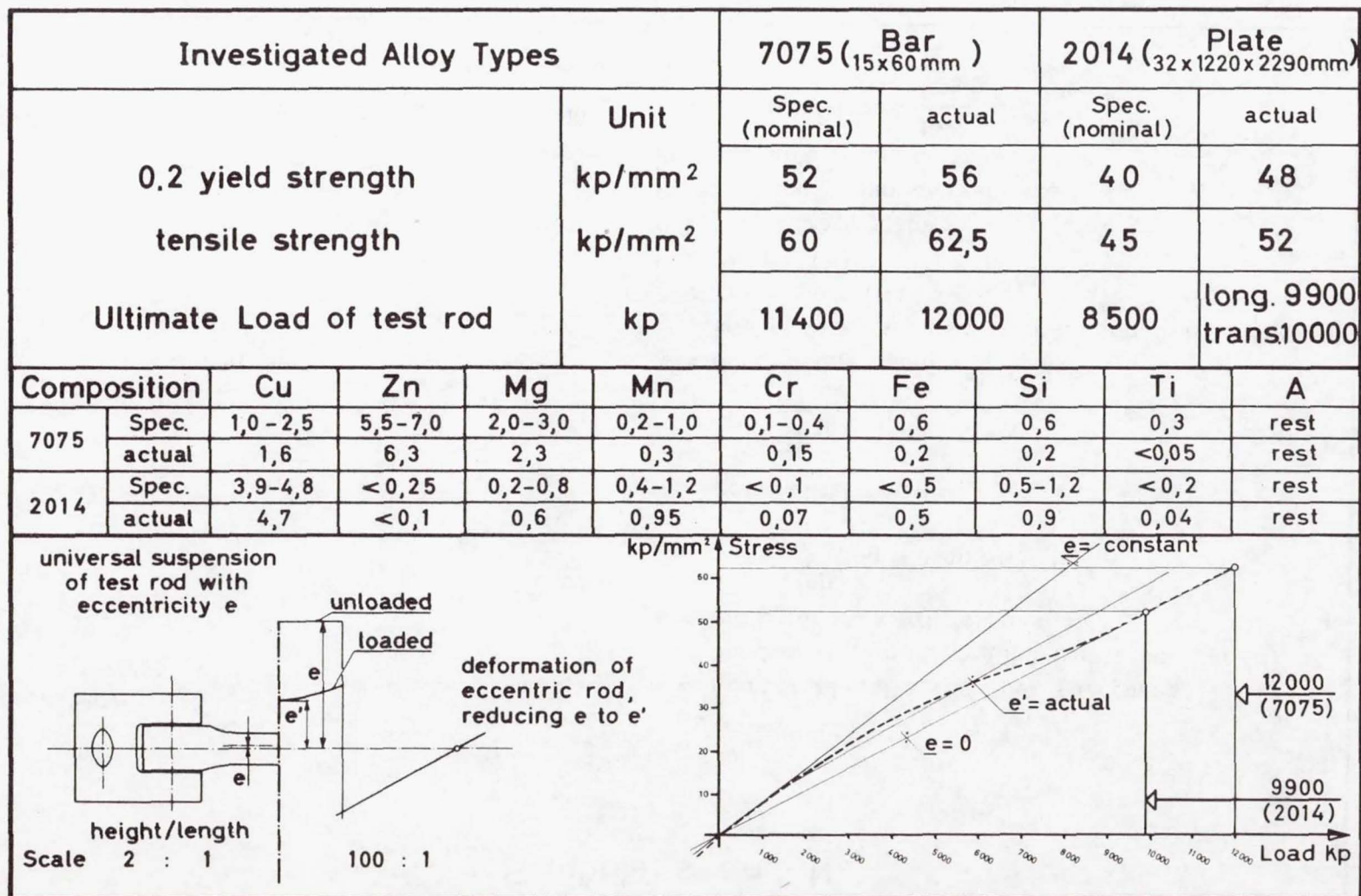


Figure 8



# Survey of the Investigation-Project : Test run No.

Fre- quen- cy cpm	alloy	7075								2014				
	flow	longitudinal								longitudinal				trans.
	surf. progr.	20 μ	6 μ	no	N2	Vinyl	reamed	ground	rolled	BF4	no	N2	Vinyl	no
210  to  240	XVIII	77									90			
	II	73*	92	67/68	72	70	69	71	80	98	91	105	106	97
	XIV	74									86			
	XV	75									87			
	XVI	76	104								88			
	XVII	79									89			
	V'	96	103								101			95
	VI'		102								99			100
173	XX	57												
96	XX	55								93				
96	XXI	84								94				
40	II	64								107				
5,4	I	A												

*	20.5	22.7	23.7	20.3
II	54	56	67/68	73

Figure 9

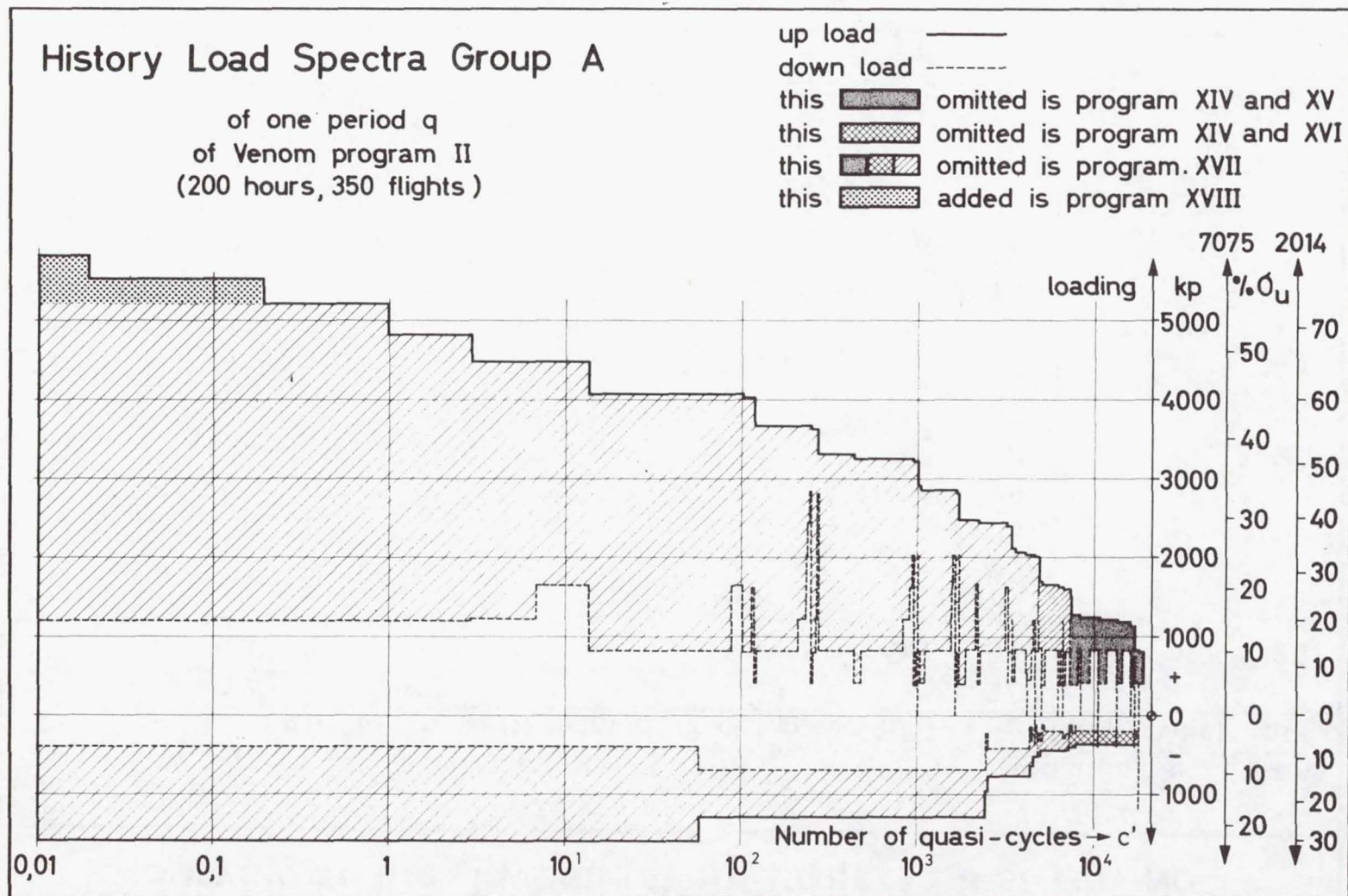


Figure 10

Program-Modification Group A				
Program No.	No. of cycles per q in air      on ground		Schematic presentation	actual flight No. 9
XVIII	20033	18515		
II	20033	18515		
XIV	9180	3405		
XVII	6499	835		
XVI	20033	3405		
XV	9180	18515		

Figure 11



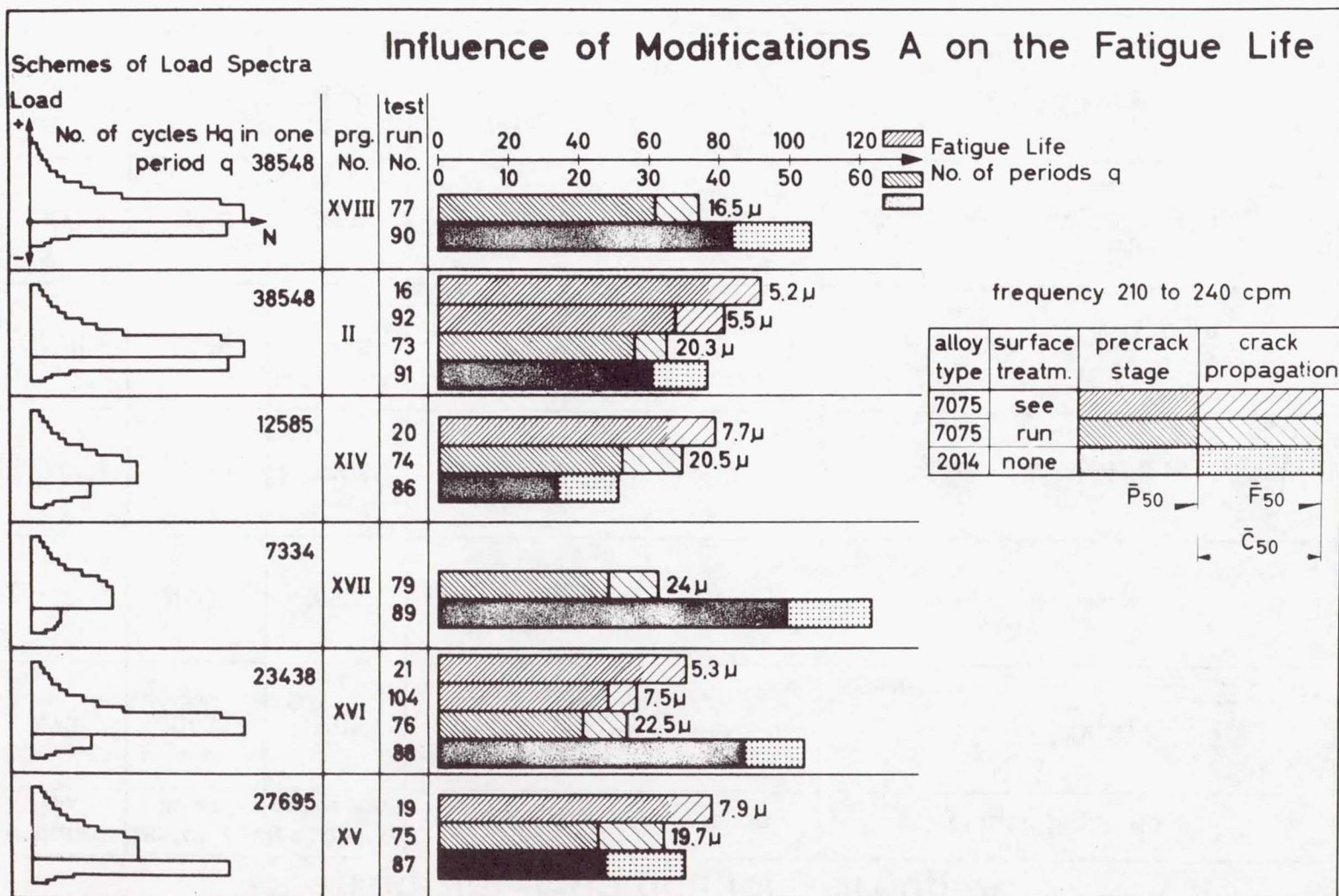


Figure 12

# Load Spectra Group B

for one period  $q$

basic Venom program II — up load  
----- down load

this omitted is program V'  
only peaks between  $+1g$  -crossings counted

this omitted is program VI'  
only peaks between zero-crossings counted

derivations from Venom program II:

program XX: level crossing method  
positive and negative peaks pooled

program XXI: range pair method  
positive and negative peaks pooled

ground loads in program XX and XXI

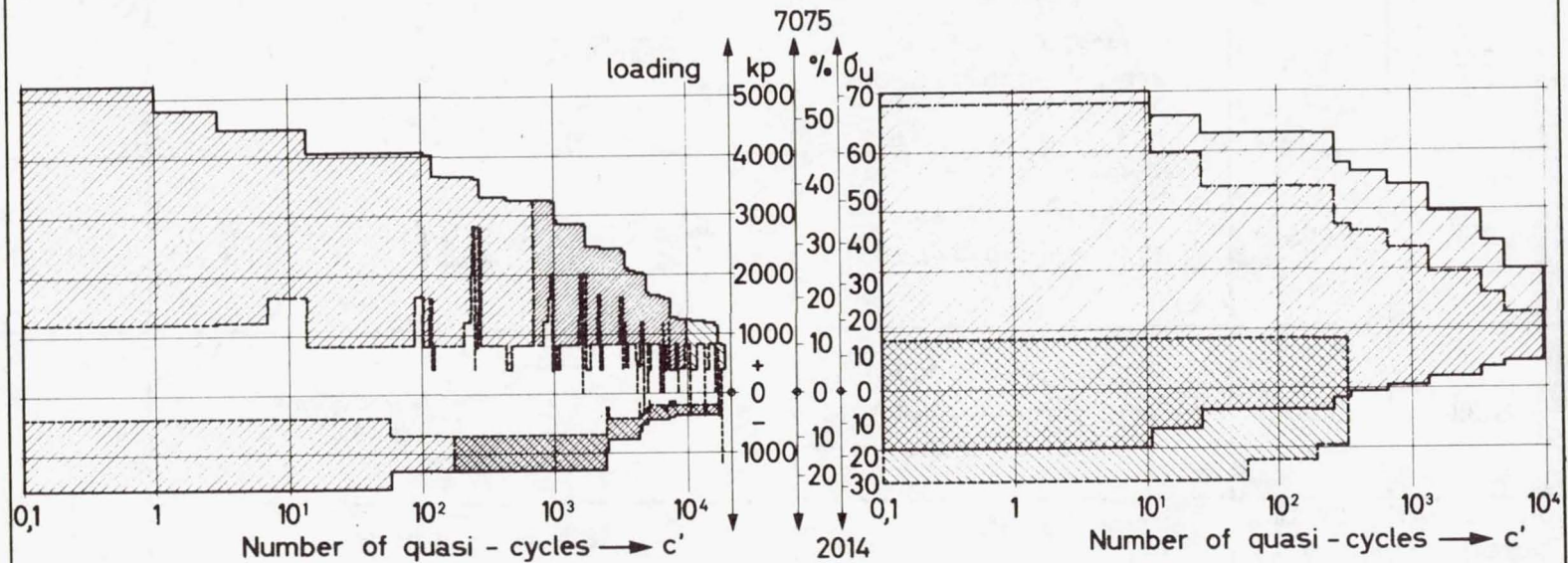


Figure 13

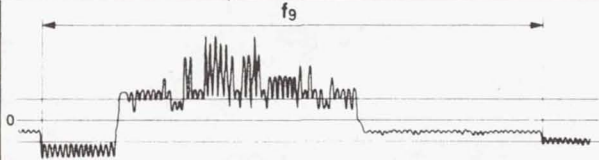
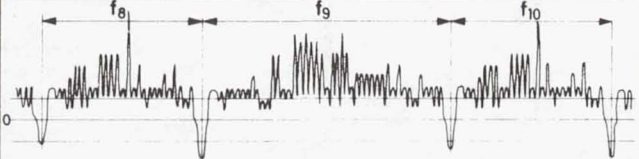
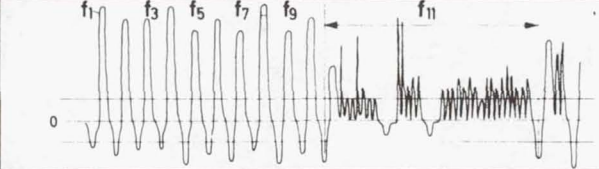
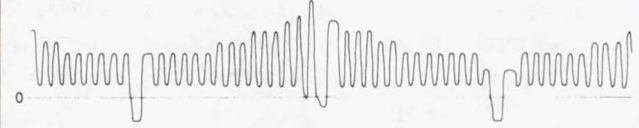

Program - Modification Group B				
Program No.	Actual program		No of cycles per q	
			in air	on ground
II		basic program reduced to the following count methods=	20033	18515
V'		mean-crossing peak, mean = +1g air	19553	350
VI'		mean-crossing peak, mean = 0g level	638	350
XX		level crossing (pooled blocks per flight)	10150	
XXI		range pair (pooled blocks per flight)	10150	

Figure 14



# Influence of Modifications B on the Fatigue Life

## Schemes of Load Spectra

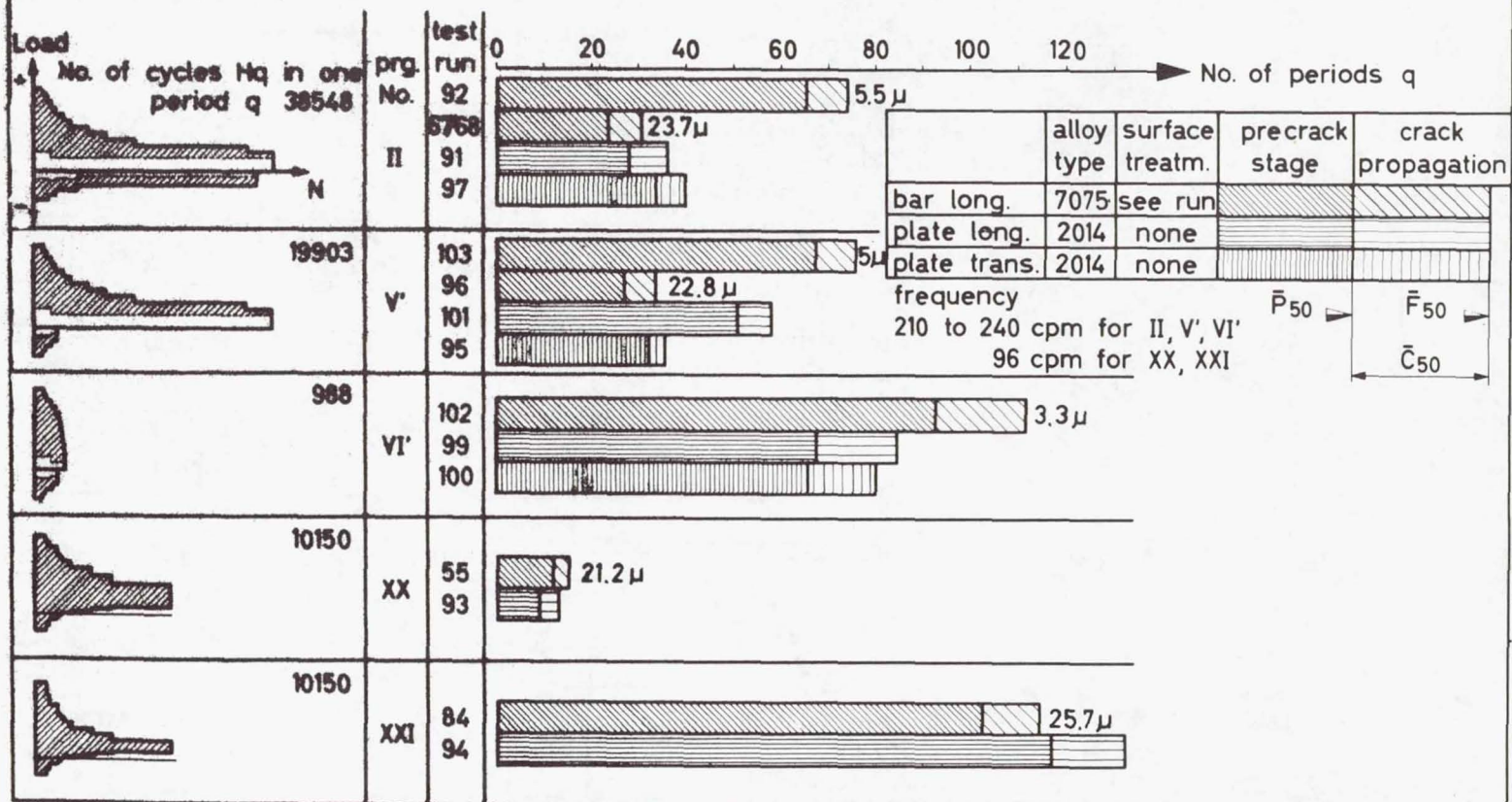


Figure 15

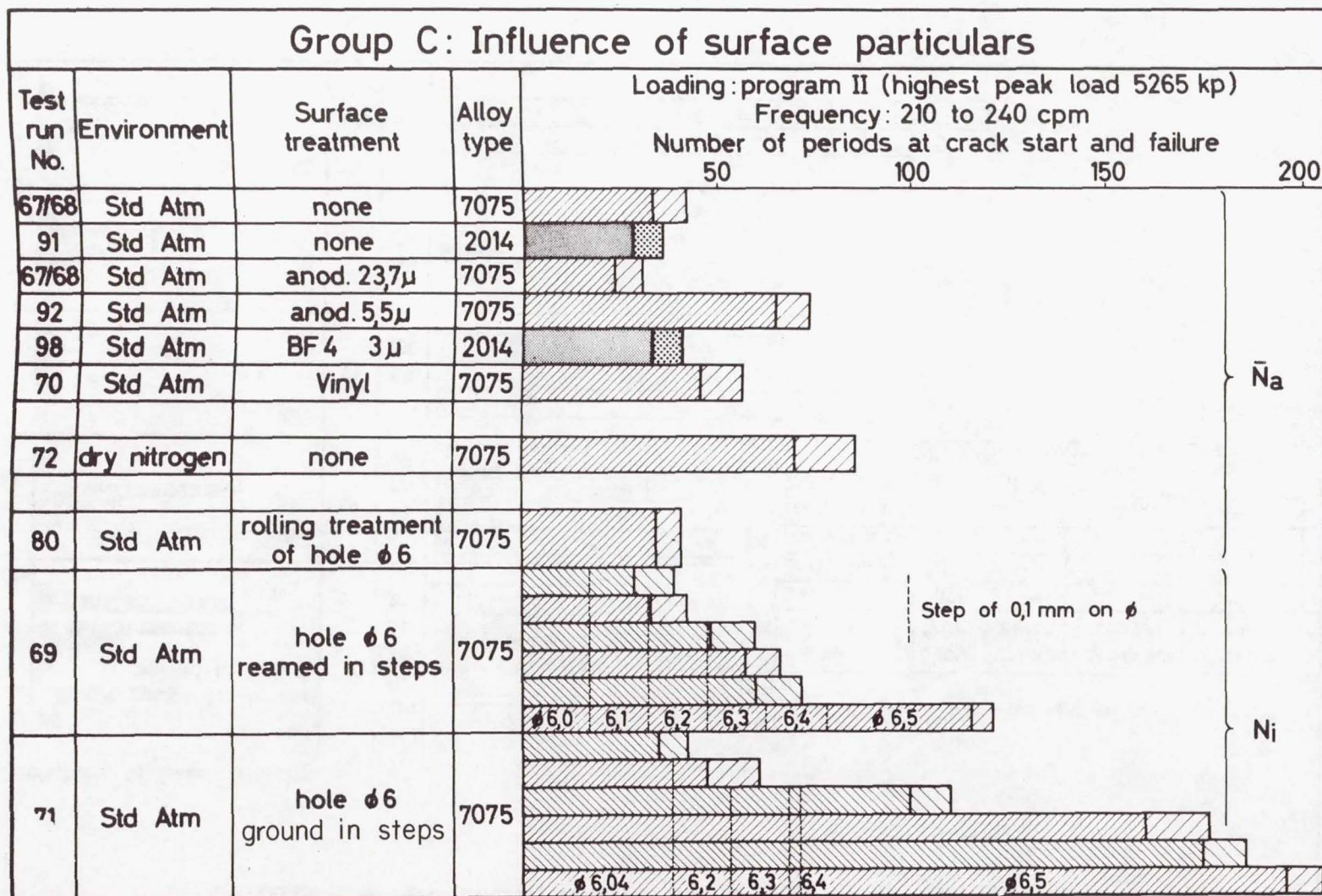


Figure 16



## Group D: Influence of the Load Frequency on the Fatigue Life

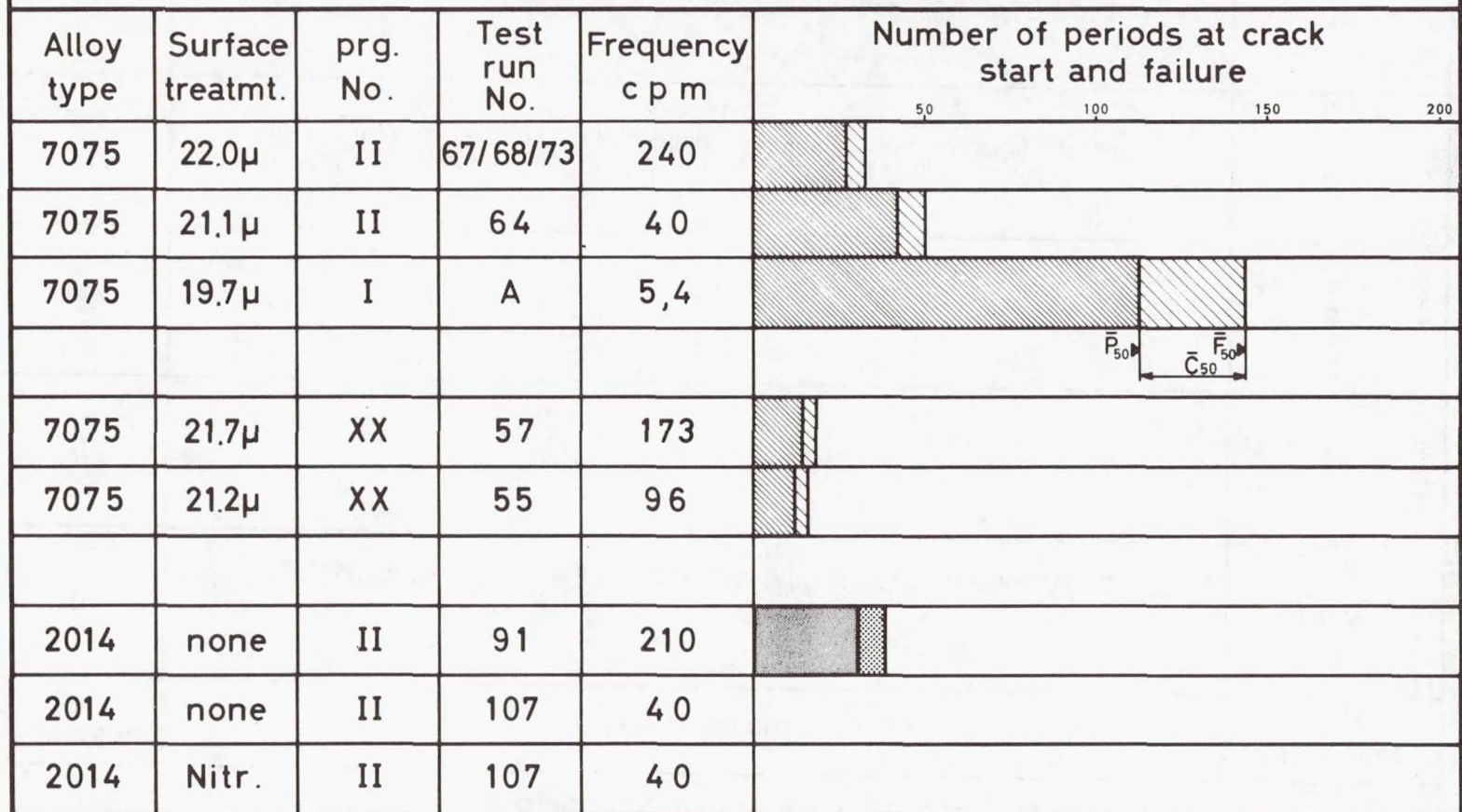


Figure 17



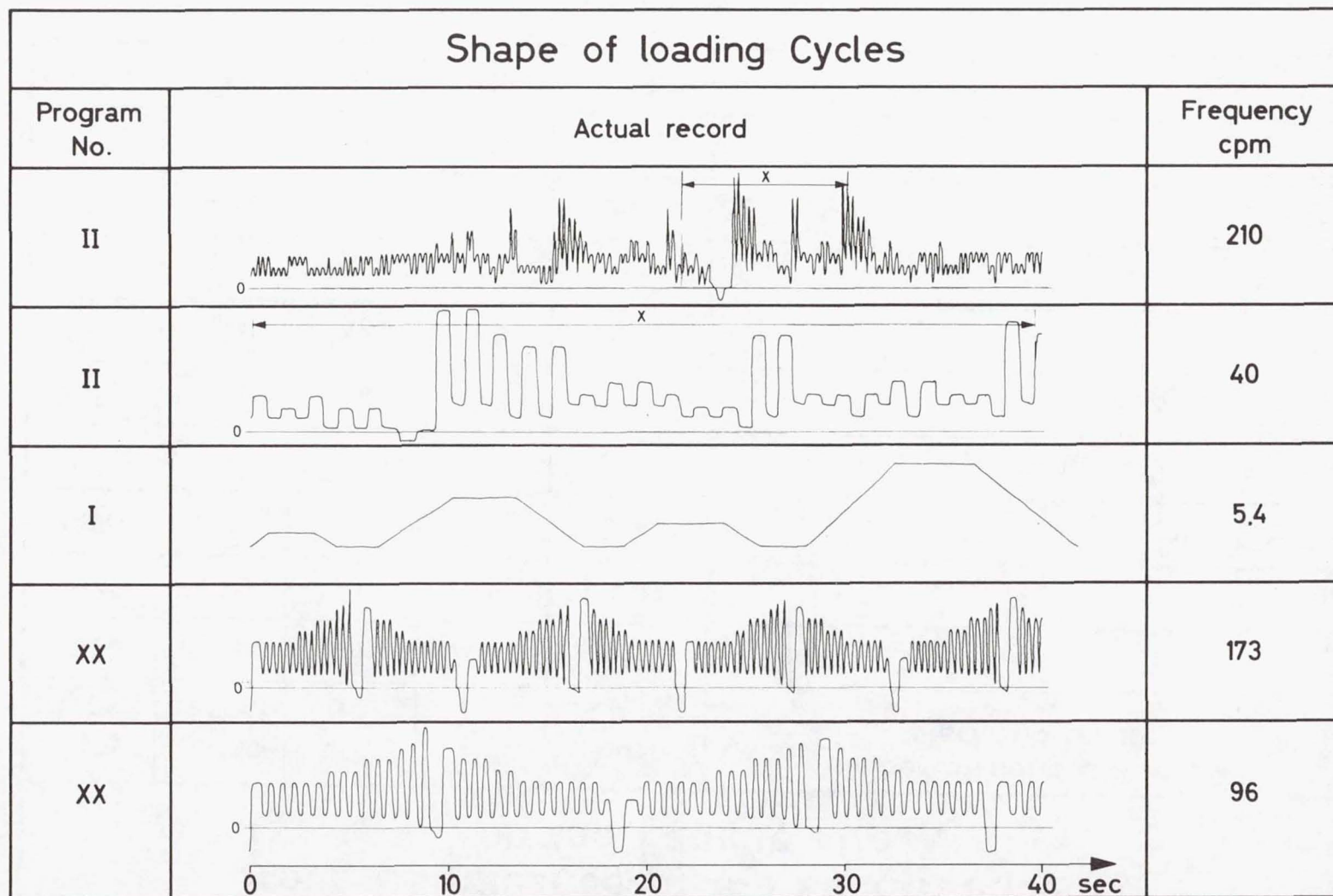


Figure 18

G.10

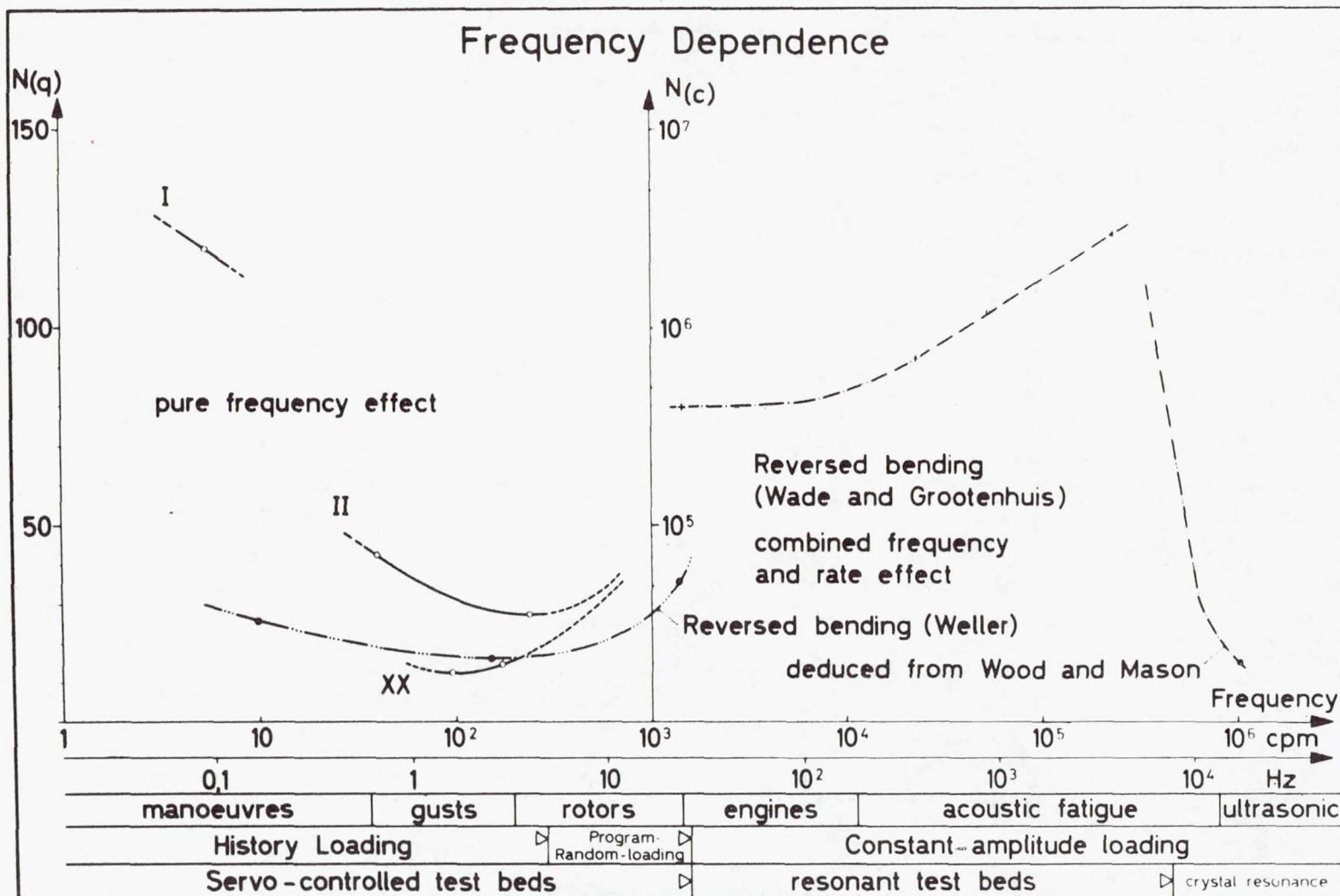


Figure 19

### Scheme of the Influence of the chemical Activity

$S$  = Range of strain in one half-cycle

$v$  = Rate of straining =  $\frac{dS}{dt}$

$I$  = Intensity of incitation of chemical activity =  $f(v) \cdot f(S)$

$\nu$  = Rate of reaction =  $f(I \cdot \frac{A}{\lambda})$

$A$  = chemical Affinity between the contacting mediums

$\lambda$  = chemical Resistance (e.g. oxide-layer) =  $f(N, I, A)$

$p$  = Duration of reaction = persistence =  $f(v)$

$R''$  = amount of reaction in one half-cycle =  $f(p, v, \omega)$

$D''$  = Damage produced by  $R''$  (e.g. oxide) =  $f(R'')$

$\omega$  = frequency of cycles

$R'$  = effective amount of reaction per cycle =  $f(R'', \omega)$

$N$  = Number of cycles, periods

$D'$  = amount of damage produced in one cycle =  $f(N, R')$

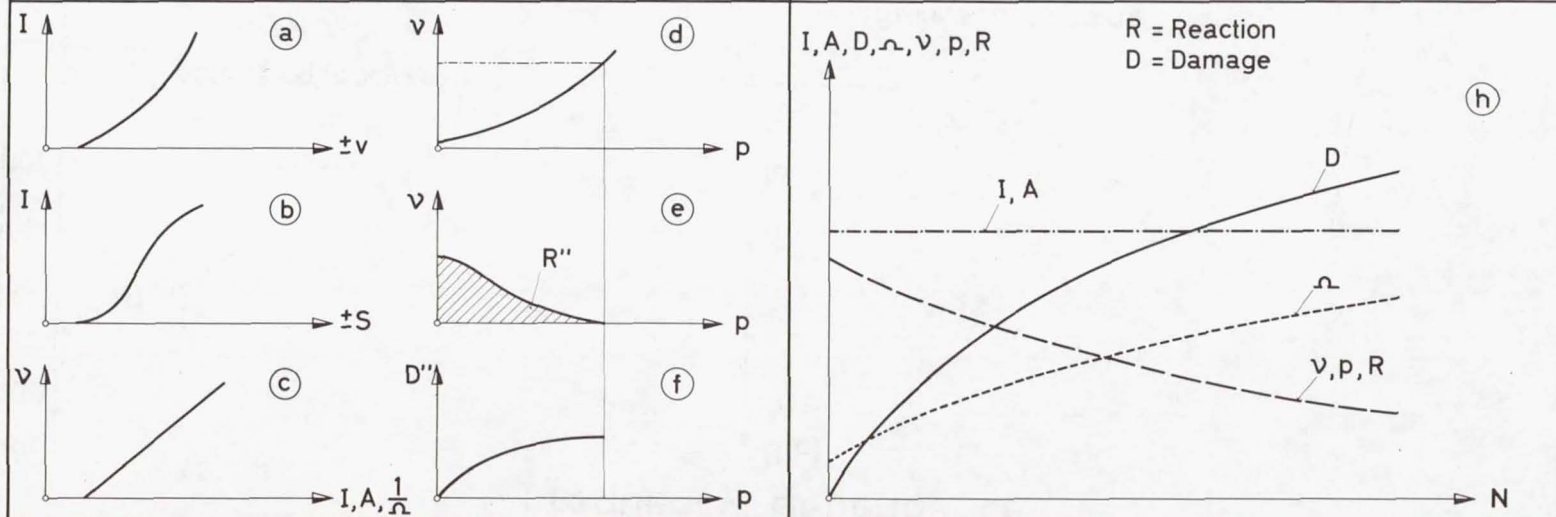


Figure 20



## Scheme of the flake phase

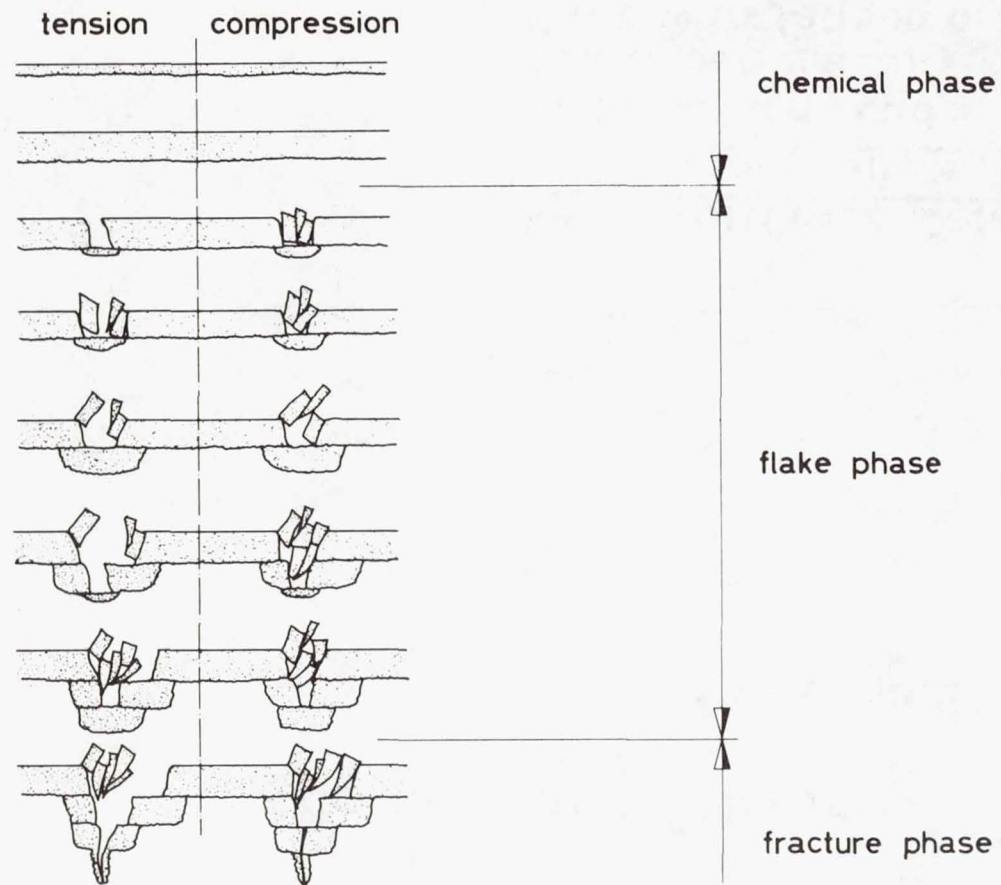
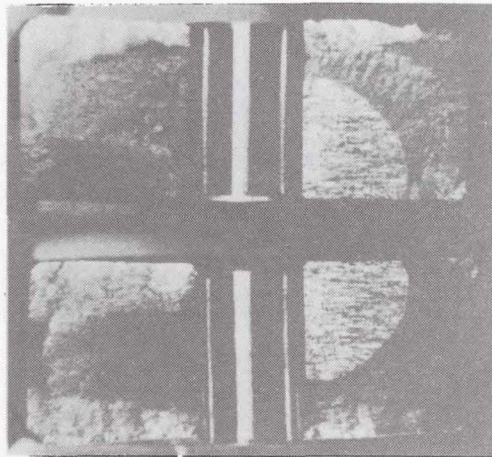


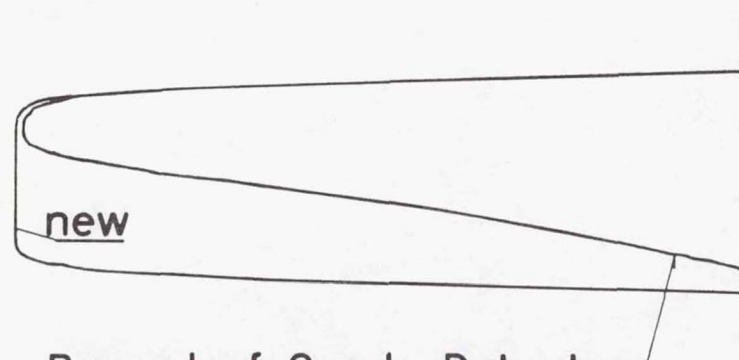
Figure 21

# Fatigue Crack Surface

of test rod E102



Failure surface



Record of Crack Detector  
before failure

Static failure Load :

new (mean value) 9900 kp

E 102 with fatigue crack 5890 kp

# Probable Crack - Stage Life as a function of the probability of survival

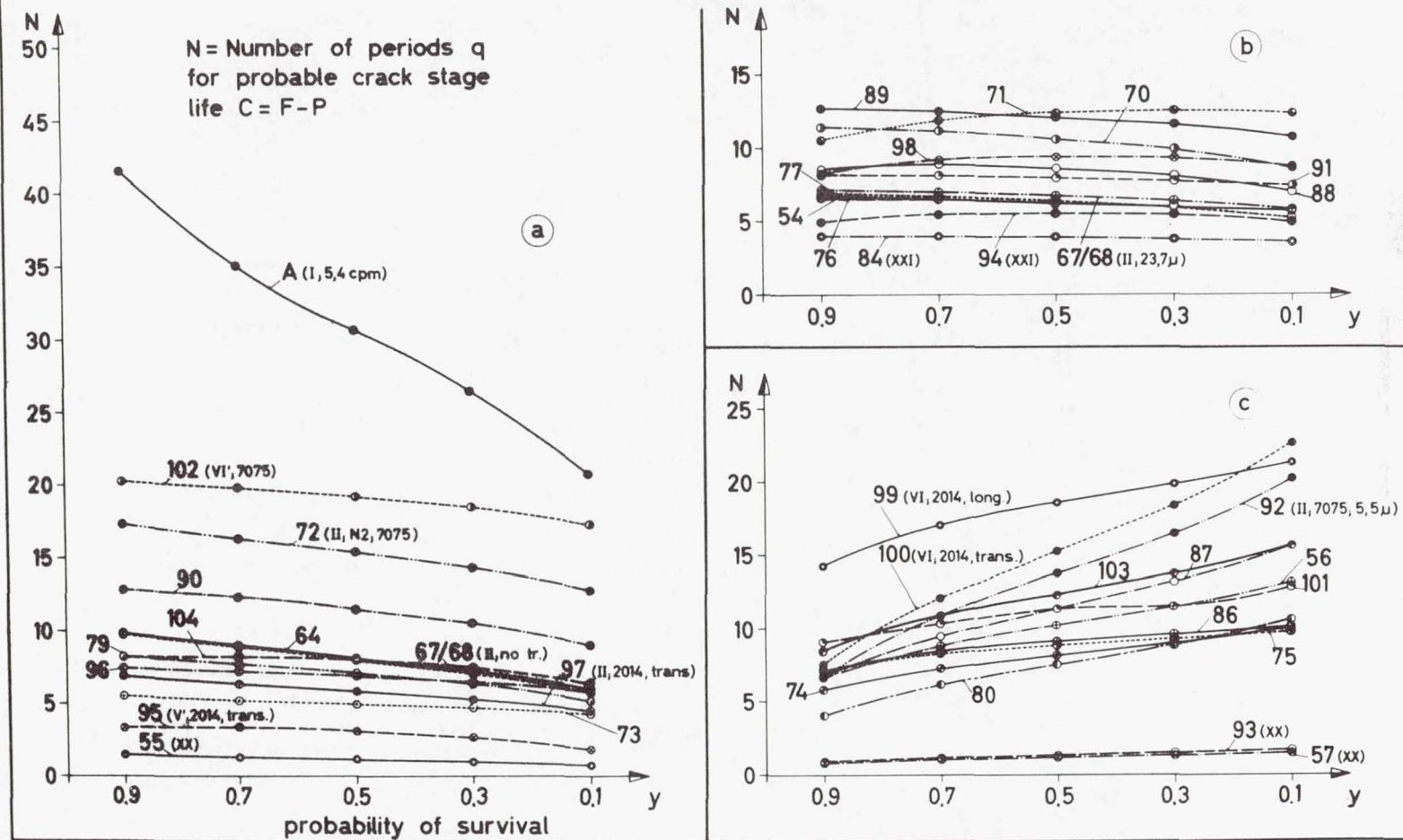


Figure 23



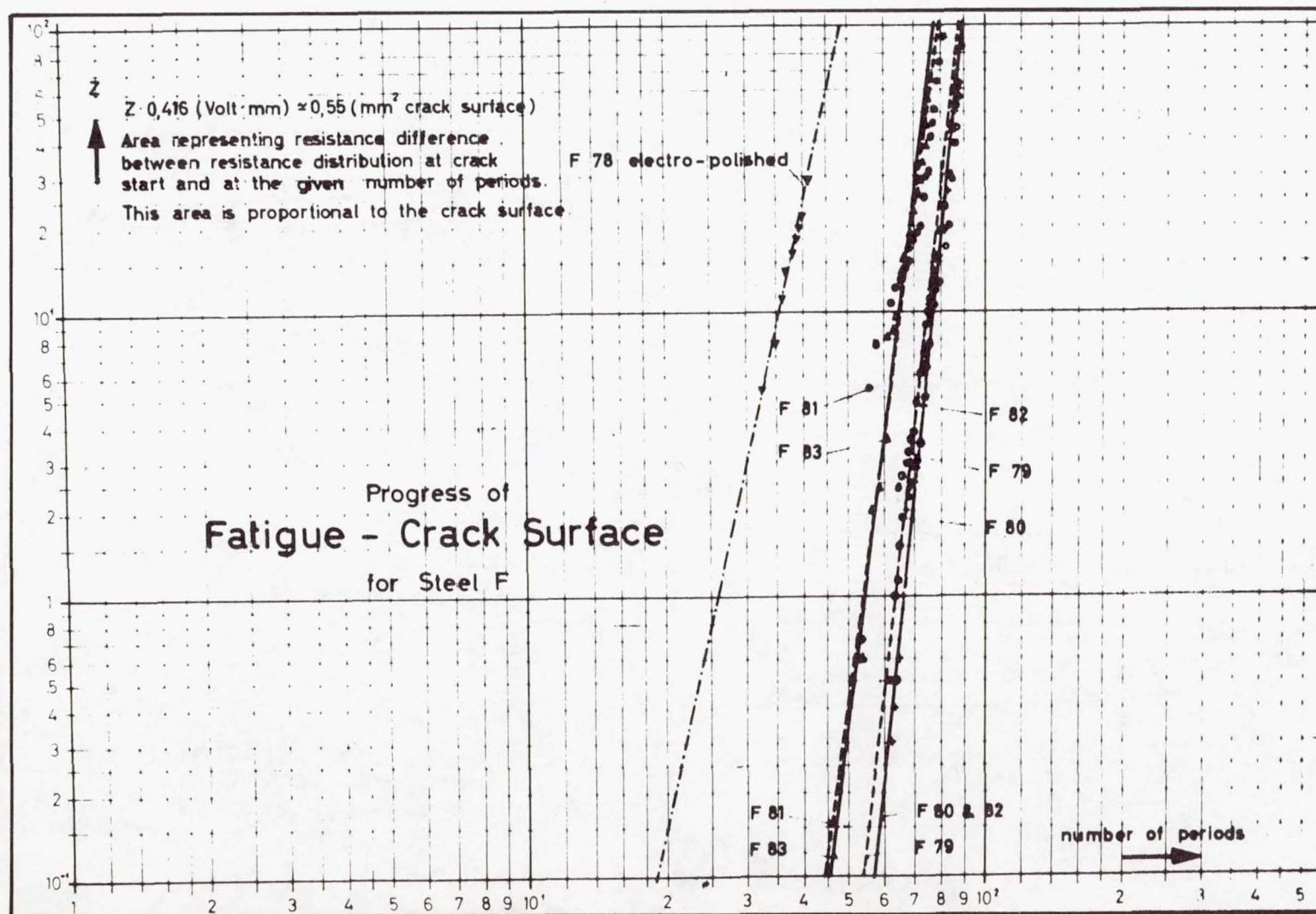


Figure 24

## Scheme of the three damage phases

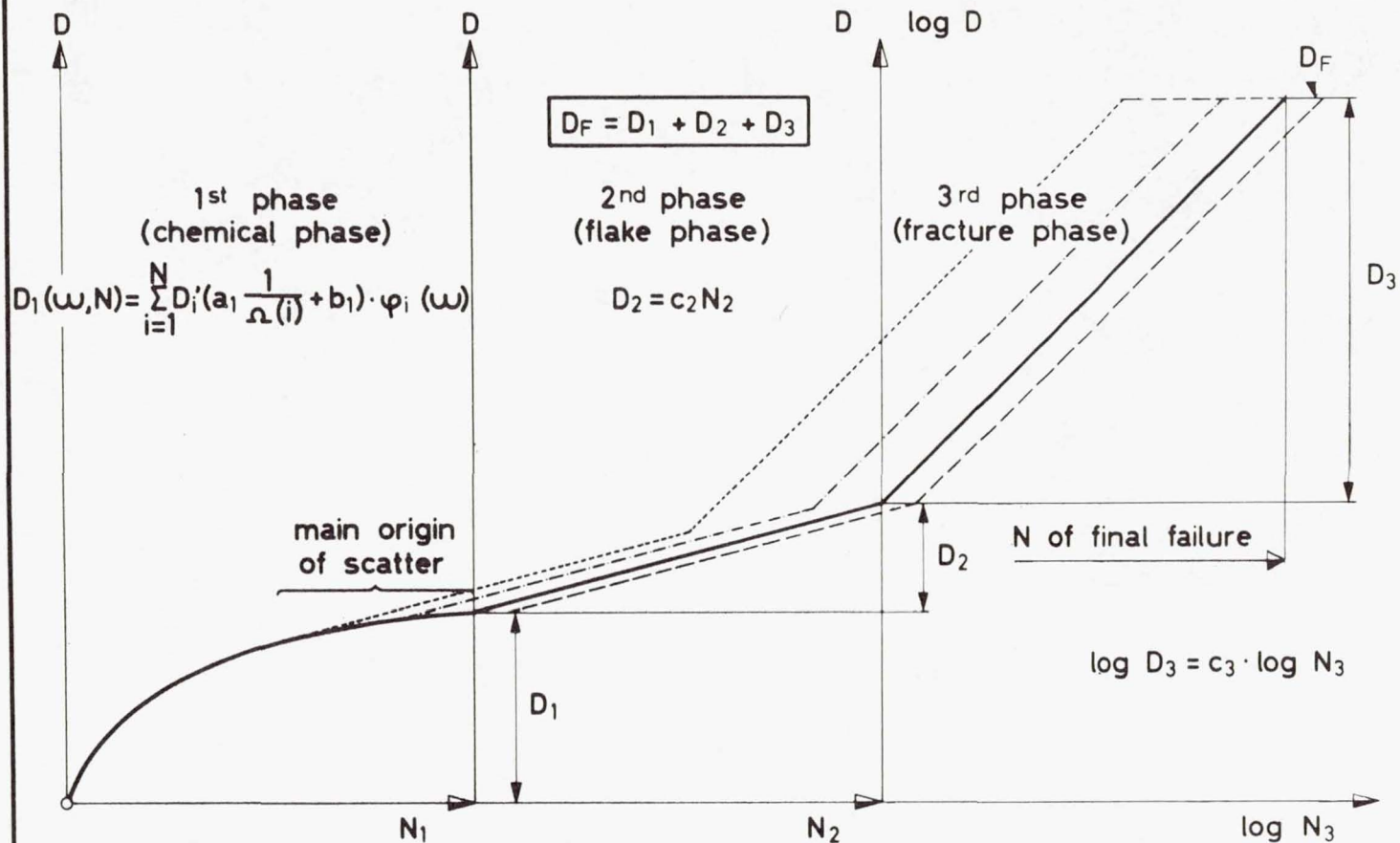


Figure 25

# STATISTICAL ANALYSIS OF MISSION PROFILE PARAMETERS OF CIVIL TRANSPORT AIRPLANES

By Otto Buxbaum  
Laboratorium für Betriebsfestigkeit  
Darmstadt-Eberstadt, Germany

## SUMMARY

To evaluate fatigue life, manufacturers must define and use typical mission profiles. The probability with which a mission profile (or one of its parameters) occurs can be used to quantitatively describe the term "typical." The airplane weight at any point in the mission is, of course, a very important parameter; the present paper presents some weight data and analyses from several types of airplanes. Several long-, medium-, and short-range airplanes, flown either in passenger or in cargo service of Lufthansa German Airlines, were observed between January and April 1969.

The statistical analysis of flight times as well as airplane gross weights and fuel weights of jet-powered civil transport airplanes has shown that the distributions of their frequency of occurrence per flight can be presented approximately in general form. Before, however, these results may be used during the project stage of an airplane for defining a typical mission profile (the parameters of which are assumed to occur, for example, with a probability of 50 percent), the following points have to be taken into account.

Because the individual airplanes were rotated during service, the scatter between the distributions of mission profile parameters for airplanes of the same type, which were flown with similar payload, has proven to be very small. Significant deviations from the generalized distributions may occur if an operator uses one airplane preferably on one or two specific routes.

Another reason for larger deviations could be that the maintenance services of the operators of the observed airplanes are not representative of other airlines. Although there are indications that this is unlikely, similar information should be obtained from other operators. Such information would improve the reliability of the data of the present report.

## INTRODUCTION

The airworthiness standards for transport category airplanes require that the fatigue strength evaluation include the typical loading spectrum expected in service. (See ref. 1.) The loading spectrum, however, depends on the mission profile, which has



been chosen in agreement with the requirements of the customers. Since the operational conditions will vary from flight to flight and probably different customers may operate the same type of airplane differently, several mission profiles will always be discussed for an airplane that is in the project stage. (See ref. 2.) The manufacturer then has to combine the various mission profiles into one or two so-called representative or typical ones on which to base the fatigue-life evaluation.

A quantitative description of the term "typical" may be obtained by defining the probability with which a mission profile or one of its parameters will occur. This definition can be achieved possibly for parameters like flight altitude and airspeed by means of results from measurements which have been carried out on airplanes of similar design features, for example, from VGH recordings. There is, however, still a lack of information insofar as parameters such as flight-time airplane weight and weight distribution are concerned.

In order to investigate the variation of mission-profile parameters and to gather information which could be used for the design of similar airplanes, the following analysis has been performed.

The author is indebted to the German Government, Ministry of Defense, for financial support and to the departments of structural engineering and performance and operation engineering of Lufthansa for their assistance and collaboration.

#### AIRPLANE TYPES, ANALYZED PARAMETERS, AND PERIODS OF OBSERVATION

Several long-, medium-, and short-range airplanes flown either in passenger or in cargo service of Lufthansa German Airlines have been observed during a period lasting from January to April 1969. As far as it was possible, the following parameters have been taken for each flight from flight and fuel logs as well as from the so-called "load sheets:" airborne time, take-off gross weight, landing gross weight, fuel take-off weight, and fuel landing weight. Information about the individual airplanes and their characteristics is presented in table 1. In addition to the analysis performed for the airplanes and the period of observation as mentioned, results from earlier similar investigations have been included for information.

#### PRESENTATION AND DISCUSSION OF RESULTS

The results are presented for each of the mission-profile parameters in form of cumulative frequency distributions, from which the number of occurrences per flight and the respective magnitude can be read, and in form of cross plots for any two parameters,

which have occurred during the same flight. In order to achieve the intended generalization, the airplane and fuel weights have been related to the maximum allowable weights as specified in table 1.

### Airborne Time

The cumulative frequency distributions of airborne times for the different types of airplanes are presented in figure 1. The longest flight time has been observed for a 707C airplane in cargo service; its flight time was 9.75 hours. Also a difference in flight times between cargo and passenger airplanes of the same type can be noted.

If the cumulative frequency distributions of airborne times are plotted on Gaussian probability paper with a logarithmic grid for the variate, then the distributions for the individual airplanes may be approximated by one or by a combination of several straight lines (fig. 2); that is, they correspond to logarithmic normal distributions, as it was demonstrated in reference 2. Only those data have been included in figure 2, which were obtained during the same period of observation. The following conclusions can be drawn:

- (a) The scatter between airplanes of the same type which were flown with similar payload is very low.
- (b) The distributions can be separated into three groups which actually correspond to short-range, medium-range, and long-range airplanes.
- (c) The difference between passenger and cargo airplanes increases with the range.
- (d) All long-range airplanes show the same asymptotic behaviour, which has been observed in a previous investigation. That behaviour could be caused either by the specific station-to-station distances as flown in service by the operator concerned, or by the limitation of fuel capacity, or – and that seems to be very likely – by a combination of the two reasons.

If it is assumed that other airlines operate similarly and the scatter for very short flights (which occur with probabilities above 99.5 percent) is neglected, then the following generalized information may be derived for the airborne times of jet-powered civil transport airplanes. The logarithmic mean value of the airborne time amounts for short-range airplanes to 37 minutes and for medium-range airplanes to 60 minutes. (See fig. 3.) The corresponding standard deviations, by which the slope in the probability paper is defined, are 0.155 and 0.215. The two logarithmic normal distributions intersect at a flight time of 11 minutes and are assumed to occur with a probability of 99.5 percent. At the same point also, the distributions for the long-range airplanes are assumed to have their origin. As has been mentioned before, the long-range airplanes show an asymptotic behaviour, which may be expressed by a mean value of 440 minutes and a standard deviation of 0.040; they do not, however, follow this distribution completely but only to a certain percentage,



which is about 25 for the passenger and 70 for the cargo airplanes. As the distribution for the long-range passenger airplanes leaves the asymptote already at a probability of 25 percent, its mean value is about 245 minutes instead of 440 minutes for the cargo version.

Two distributions for short- and medium-range airplanes can be used directly for an estimation of an airborne time belonging to a typical mission profile; in the case of the long-range airplanes a distinction has to be made between cargo and passenger service, and prior to the estimation, an assumption has to be made about the percentage of flights which will follow the asymptote, that is, which actually can be called long-range flights.

### Take-Off Weight

A similar analysis has been made for the take-off gross weights. As it has been said before, the results are presented in relation to the corresponding maximum allowable take-off weight. (See the cumulative frequency distributions in fig. 4.) It has to be noted here that for the 737 type airplanes only those take-off weights which have occurred at flights departing from and arriving at Frankfurt airport could be obtained. The data for the other airplanes resulted from succeeding flights in the periods of observation as given in table 1.

The scatter between the cumulative frequency distributions for the individual airplanes of the same type, which flew with the same payload, was very small. (See, as an example, that of passenger and cargo long-range airplanes in fig. 5.) This graph shows also that the cargo airplanes are generally flown with a much higher take-off weight than the passenger airplanes. An indication that this happens not only with the long-range airplanes as investigated for one operator but also with the whole fleet of all airplanes from all operators may be derived from the fact that a certain type of fatigue failure in the wing structure has occurred at a significantly shorter service life for cargo airplanes than for passenger airplanes. A careful fatigue-life evaluation has demonstrated that the reason why cargo airplanes have the shorter life must result from generally higher airplane gross weights. The data as presented in figure 5 confirm that prediction.

In order to obtain the intended generalization, the data as observed during the same period of time for jet-powered short-, medium-, and long-range airplanes have been plotted on probability paper. (See fig. 6.) The distributions for the short- and medium-range airplanes can be approximated by a rather small scatter band of two straight lines with a standard deviation of 0.03. It says that 99.95 percent of all flights were made with a take-off weight exceeding 70 to 75 percent of the maximum allowable one, and that in about 5 percent of all flights, 100 percent of the maximum take-off weight was reached. The variation of the relative take-off weight of long-range airplanes is larger than that of short- and medium-range types. But also the difference between



passenger and cargo service is larger for the long-range airplanes, because only 0.5 per cent of all flights of passenger airplanes took place with the maximum allowable take-off weight, whereas in the case of cargo airplanes it was almost every second flight.

As supplementary information, a cross plot of the variation of take-off weight with airborne time as observed on three long-range passenger airplanes is shown. (See fig. 7.) This example has been selected because it was the best correlation which has been obtained. For the other types of airplanes, the trend was not as clear. More details about this subject are given in reference 3.

### Landing Weight

If the cumulative frequency distributions of relative airplane landing gross weight (fig. 8) are compared with those of the take-off weight as shown in figure 4, it is evident that the curves for the landing weight of the individual types of airplanes are much more consistent and conformable. When plotting these distributions on logarithmic probability paper and approximating them by straight lines (fig. 9), it becomes apparent that for all types of airplanes, between 2 and 15 percent of all landings occurred with the maximum allowable landing weight. The distributions have almost the same slope with one exception, which is again the long-range cargo-type airplane. It has to be mentioned further that the scatter between the distributions for the individual airplanes of the same type was similar to that of the take-off weight and was very small. Unfortunately, for the short-range airplanes, only the landing weights for flights from and to Frankfurt airport could be obtained because of matters of organisation. This fact seems, however, to be of secondary importance with regard to the result.

In order to investigate the relation between airborne time and the respective landing weight, cross plots have been made which showed that the landing weight is more or less independent of the flight time. An example of this type of plotting is shown for three long-range passenger airplanes in figure 10.

### Take-Off Fuel Weight

The definition of a mission profile to be used for fatigue analysis has to include not only the airplane gross weight but also the appropriate weight distribution. Since the weight of the fuel, which the airplane is carrying, allows information to be derived about the weight distribution, an analysis similar to that for the airplane weights has been performed also for the fuel weights.

Figure 11 shows the cumulative frequency distributions of take-off fuel weights for the different types of airplanes in relation to the respective maximum fuel weights. This form of presentation is not very suitable for deducing a general trend, because the individual curves intersect at several points. Therefore an attempt was made to plot the ratio

between take-off fuel weights and the respective allowable airplane take-off weights on logarithmic probability paper. (See fig. 12.) The distributions appear as a family of curves with increasing standard deviation for increasing airplane size. They are clipped at the respective value of the ratio of maximum fuel to maximum allowable airplane take-off weight. Only the distributions for the long-range cargo airplanes behave as exceptions because they consist of two parts, each of which can be described by a logarithmic normal distribution. It has been demonstrated that almost every second flight of long-range cargo airplanes is made with the maximum allowable take-off weight. (See fig. 6.) If the maximum allowable payload was reached, the fuel weight had to be restricted in order not to exceed the maximum allowable airplane gross weight. That may have led to this combination of two logarithmic normal distributions. Furthermore, it can be seen in figure 12 that the variation between the cumulative frequency distributions as observed for airplanes of the same type which flew with similar payload is very small.

A generalized presentation and a good approximation to the results is obtained when the scatter as occurring in the range of probabilities between 90 and 99.5 percent is ignored and is replaced by a fictitious point at 95 percent, where all distributions are assumed to intersect at a weight ratio of 13 percent. (See fig. 13.)

#### Landing Fuel Weight

In opposition to the fuel weights as observed during take-off, it is not necessary to relate those occurring during landing to the respective airplane gross weight, it is sufficient for obtaining general information to relate them to the maximum fuel capacity of the airplane type. The results of the analysis are presented again in form of cumulative frequency distributions for the different types of airplanes. (See fig. 14.) From this graph, a further confirmation can be derived for the assumption which was made when explaining the fuel take-off weights of long-range cargo airplanes because it shows that these airplanes have generally the lowest percentage of maximum fuel weight during landing. From the presentation of the distributions in a probability paper (fig. 15), the percentages of maximum fuel weight as occurring during every second landing can be defined as 14.5 for the cargo and 20 for the passenger long-range airplanes. The corresponding figures for medium- and short-range airplanes are 38 and 49 percent, respectively. The latter value seems to be very high; it can, however, be explained by the fact that in short-range service, up to three flights were flown without refueling. It is interesting to note that the distributions for the individual airplane types are almost parallel to each other, a tendency which already has been observed for the airplane landing weights. (See fig. 9.)



## CONCLUDING REMARKS

The statistical analysis of flight times as well as airplane gross weights and fuel weights of jet-powered civil transport airplanes has shown that the distributions of their frequency of occurrence per flight can be presented approximatively in general form. Before, however, these results may be used during the project stage of an airplane for defining a typical mission profile (the parameters of which are assumed to occur, for example, with a probability of 50 percent), the following points have to be taken into account.

Because the individual airplanes were rotated during service, the scatter between the distributions of mission profile parameters for airplanes of the same type, which were flown with similar payload, has proven to be very small. Significant deviations from the generalized distributions may occur if an operator uses one airplane preferably on one or two specific routes.

Another reason for larger deviations could be that the maintenance services of the operators of the observed airplanes are not representative of other airlines. Although there are indications that this is unlikely, similar information should be obtained from other operators. Such information would improve the reliability of the data of the present report.

## REFERENCES

1. Anon.: Airworthiness Standards: Transport Category Airplanes. Federal Aviation Regulations, Pts. 25 and 25.571, FAA, May 8, 1970.
2. Buxbaum, O.; and Gassner, E.: Häufigkeitsverteilungen als Bestandteil der Lastannahmen für Verkehrsflugzeuge Zeitschr. Luftfahrttechnik-Raumfahrttechnik, Bd. 13, Nr. 4, 1967, pp. 78-84. (Also available as Library Translation No. 1303, Brit. R.A.E., June 1968.)
3. Buxbaum, O.; and Reinhold, P.: Statistische Auswertung der das Einsatzprofil von Transportflugzeugen kennzeichnenden Parameter. Tech. Rep. TB-88, Laboratorium für Betriebsfestigkeit, 1971. (To be distributed as ICAF-Document.)



TABLE 1  
AIRPLANE CHARACTERISTICS AND PERIODS OF OBSERVATION

Type of airplane	Payload	Period of observation	Number of airplanes observed	Maximum allowable weights, thousand lb		
				Take-off	Landing	Fuel (a)
Boeing 707 B	Passengers	} Jan. 1969 to Apr. 1969	2	150.9	97.5	72.2
Boeing 707 C	Cargo		2	150.9	112.0	72.2
Boeing 727 A	Passengers		2	69.2	61.2	21.7
Boeing 727 C	Cargo		1	72.8	64.6	21.7
Boeing 737 A	Passengers		3	44.2	40.7	10.7
Boeing 737 C	QC (Passenger/Cargo)		1	50.2	46.7	10.7
Boeing 707 B	Passengers	Apr. 1968 to July 1968	1	150.9	97.5	72.2
Boeing 720 B	Passengers	Jan. 1964 to Dec. 1964	1	106.1	79.4	
Bickers Viscount	Passengers	Apr. 1959 to Jan. 1961	1	32.8	29.0	

<sup>a</sup>Assumed fuel density: 0.8 kp/dm<sup>3</sup>.

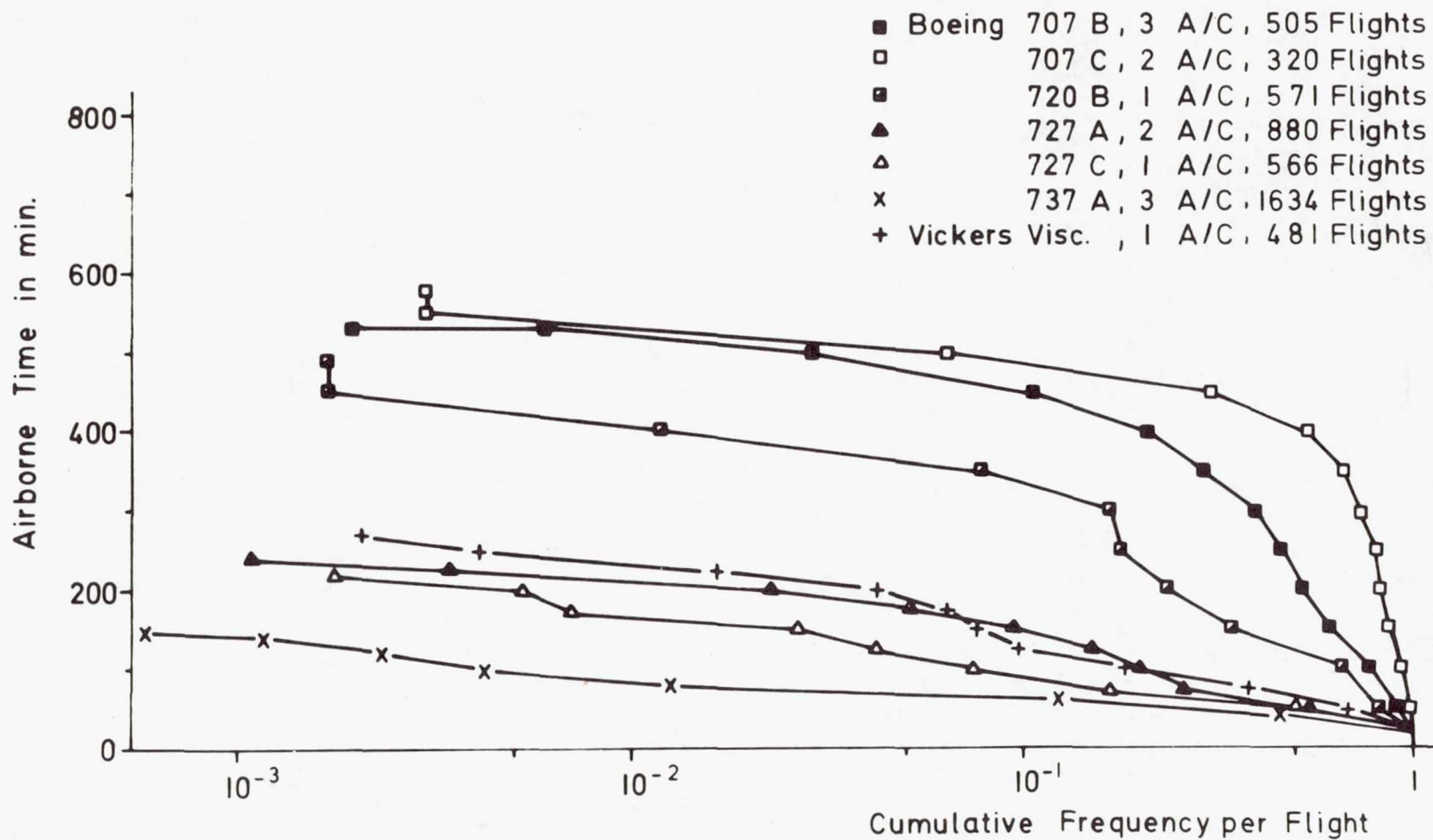


Figure 1.- Cumulative frequency distributions of airborne time for different types of transport airplanes.

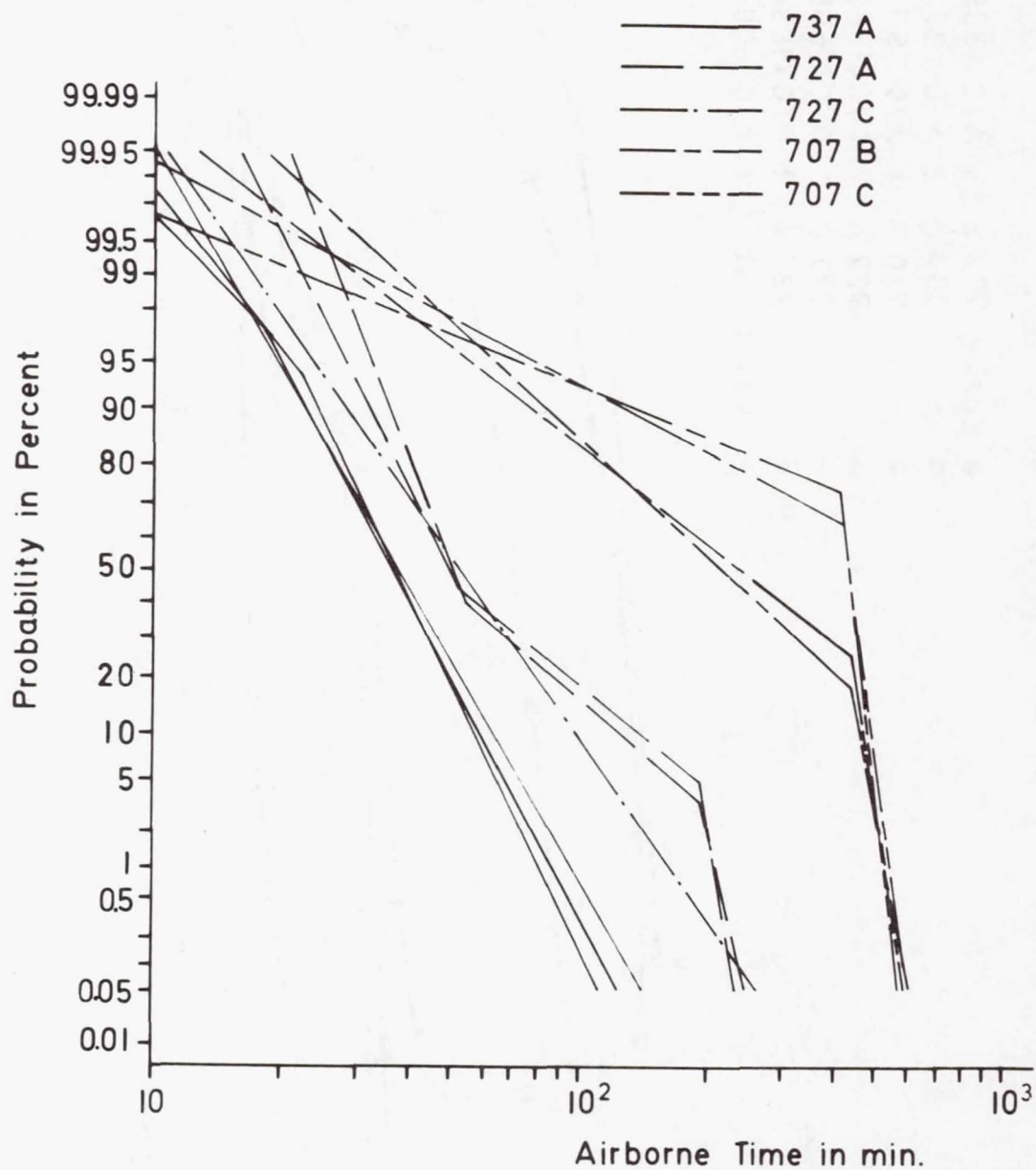


Figure 2.- Cumulative frequency distributions of airborne time for 10 airplanes during the same period of observation.



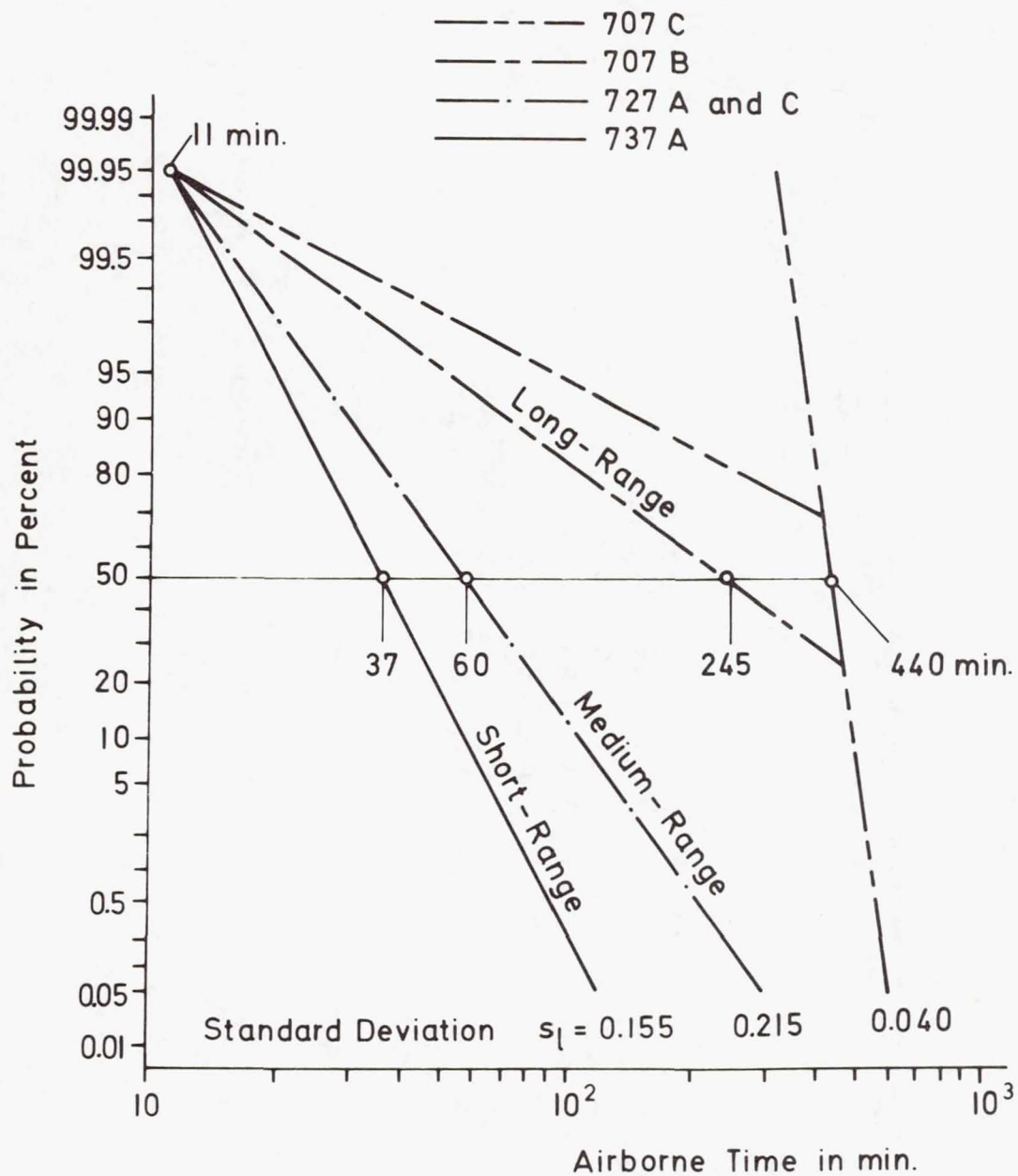


Figure 3.- Flight times of jet-powered short-, medium-, and long-range airplanes.

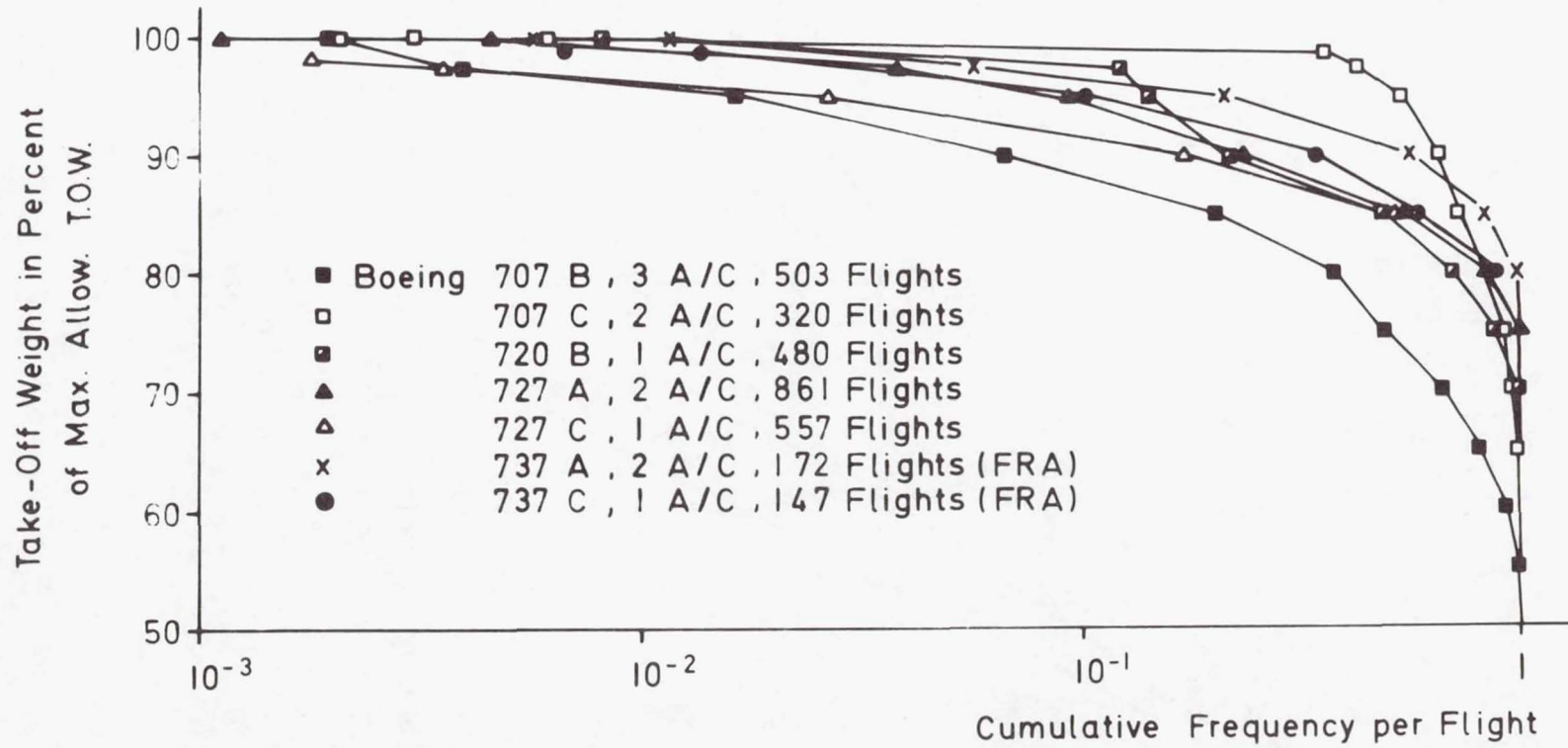


Figure 4.- Take-off gross weights of different types of transport airplanes in percentage of maximum allowable take-off weight.

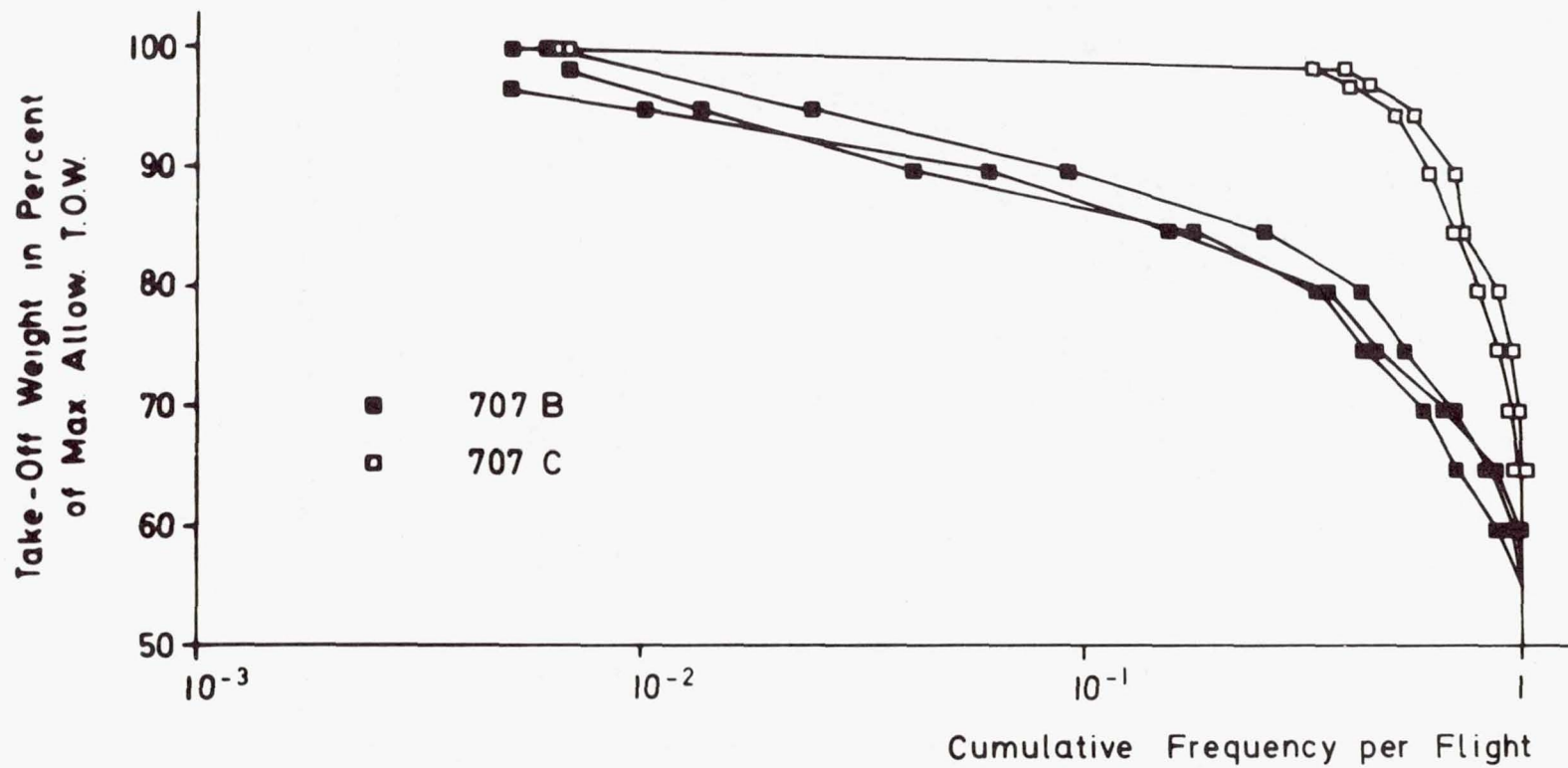


Figure 5.- Variation of cumulative frequency distributions of take-off gross weight for individual long-range airplanes.



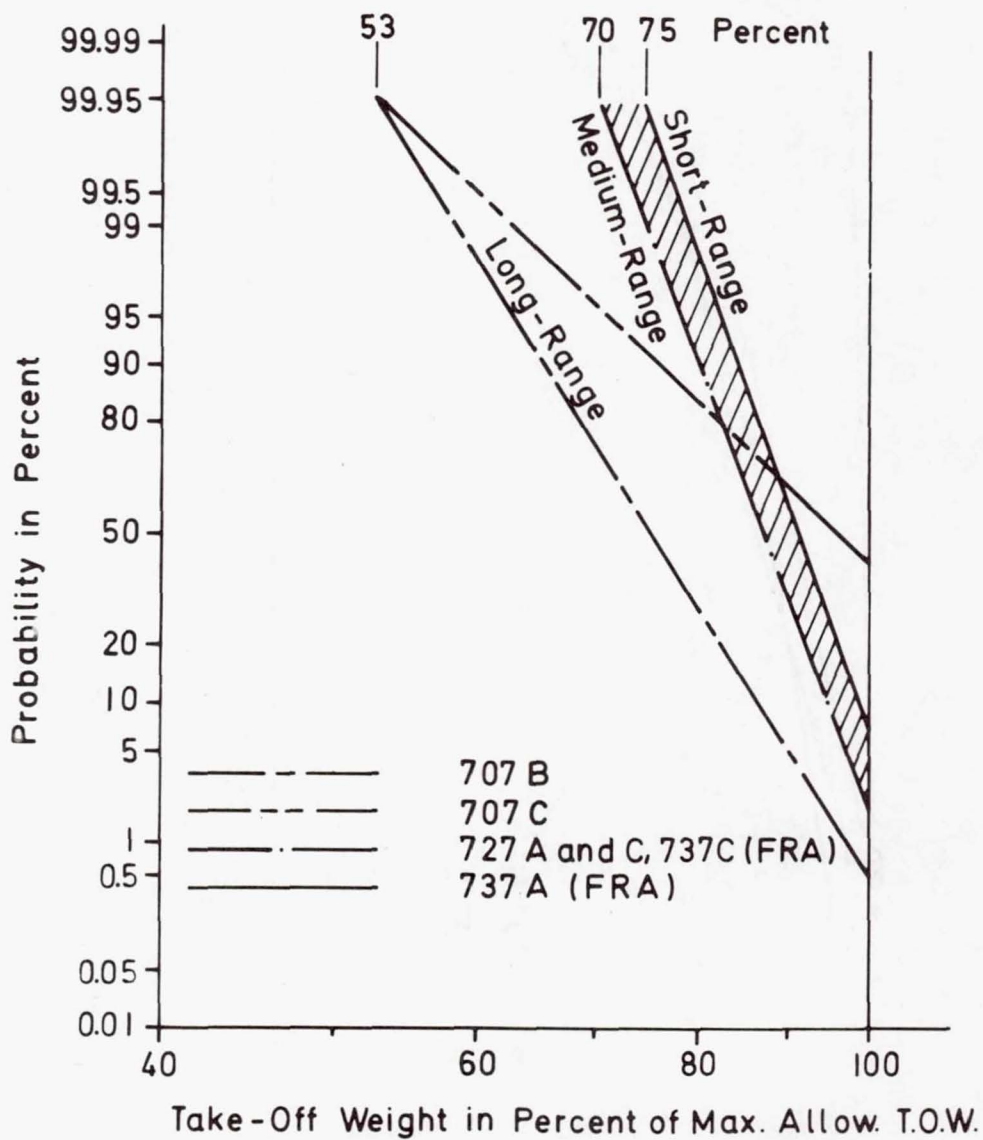


Figure 6.- Take-off weights of jet-powered short-, medium-, and long-range airplanes.

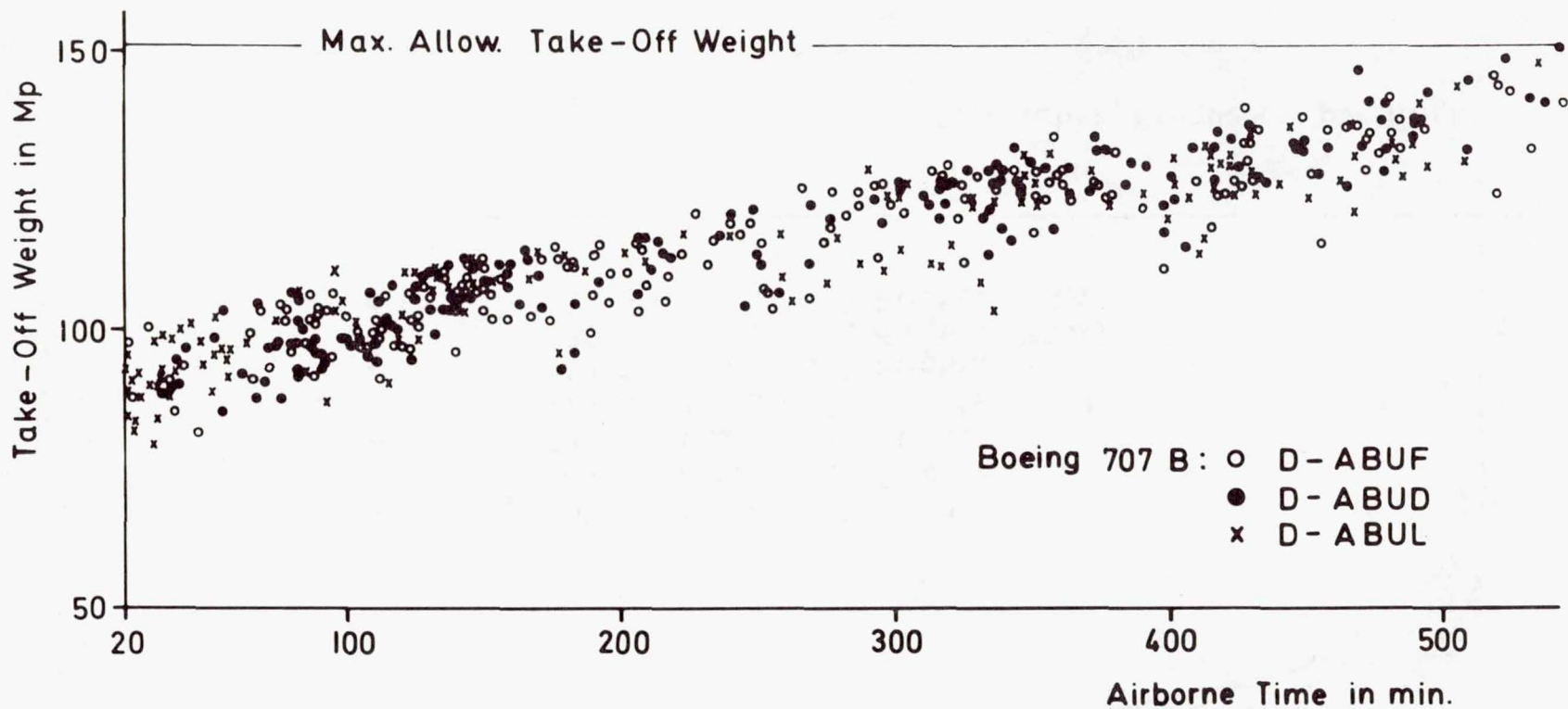


Figure 7.- Relation between take-off weight in megaponds and flight time as observed for three long-range airplanes in passenger service.

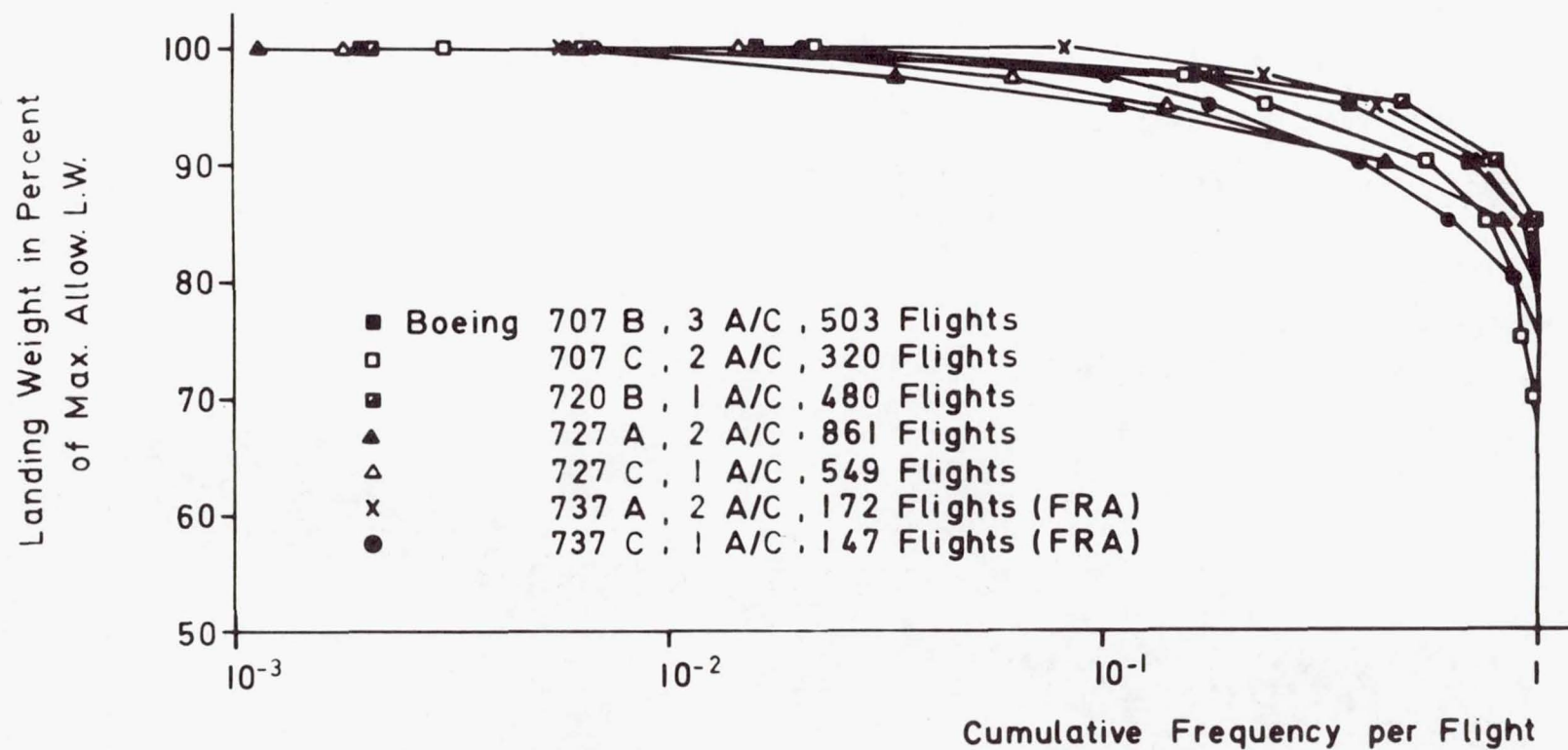


Figure 8.- Cumulative frequency distributions of landing weight in percent of maximum allowable landing weight for different types of transport airplanes.



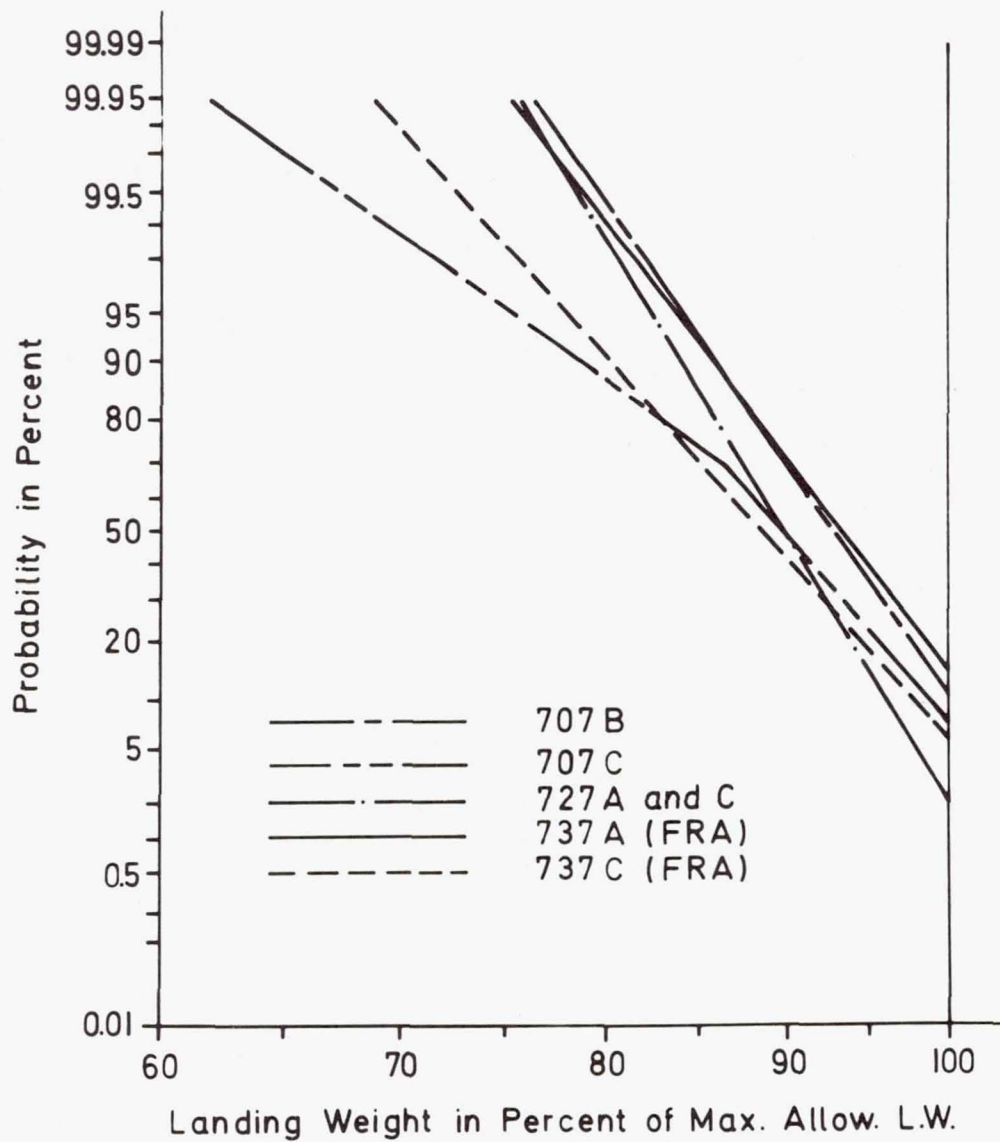


Figure 9.- Landing weights of jet-powered short-, medium-, and long-range airplanes.

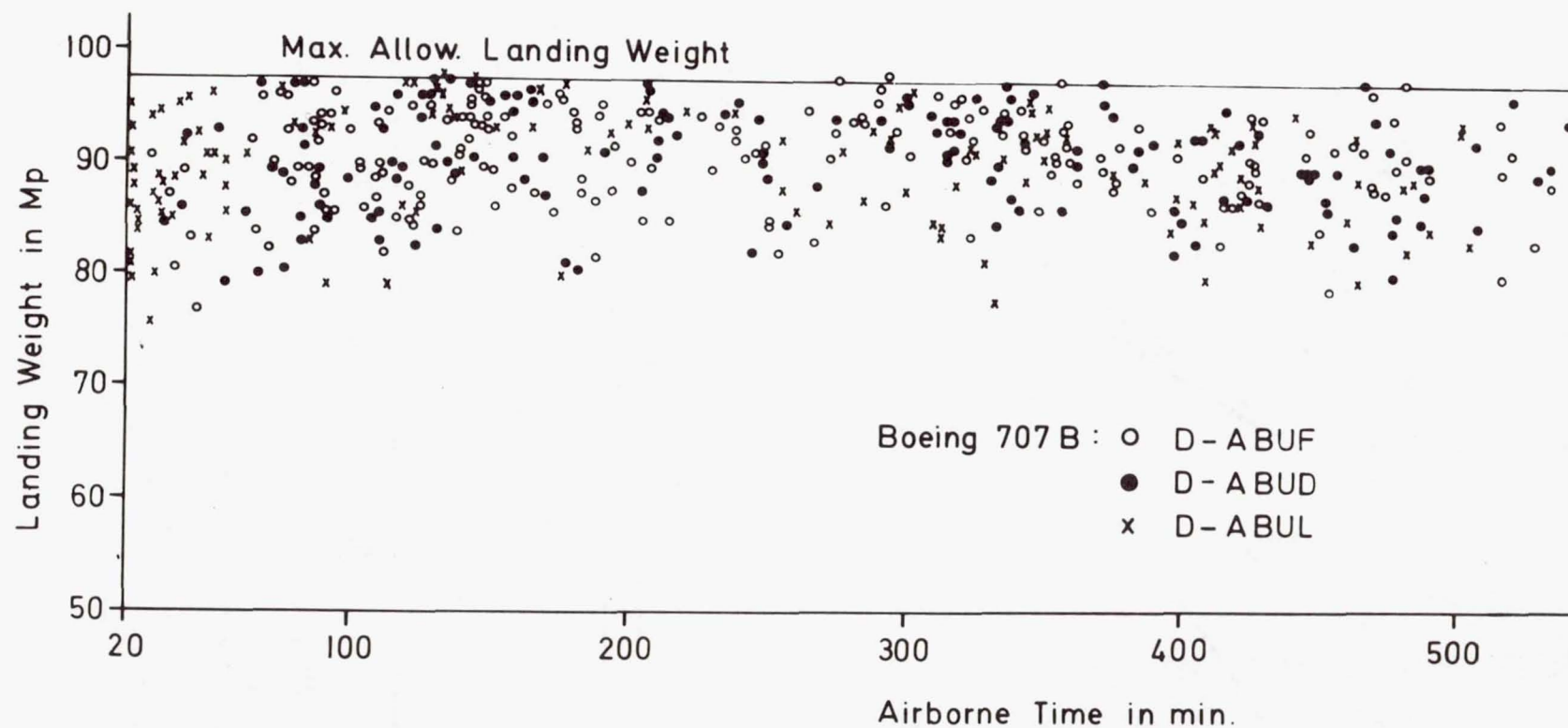


Figure 10.- Relation between landing weight in megaponds and flight time as observed for three long-range airplanes in passenger service.

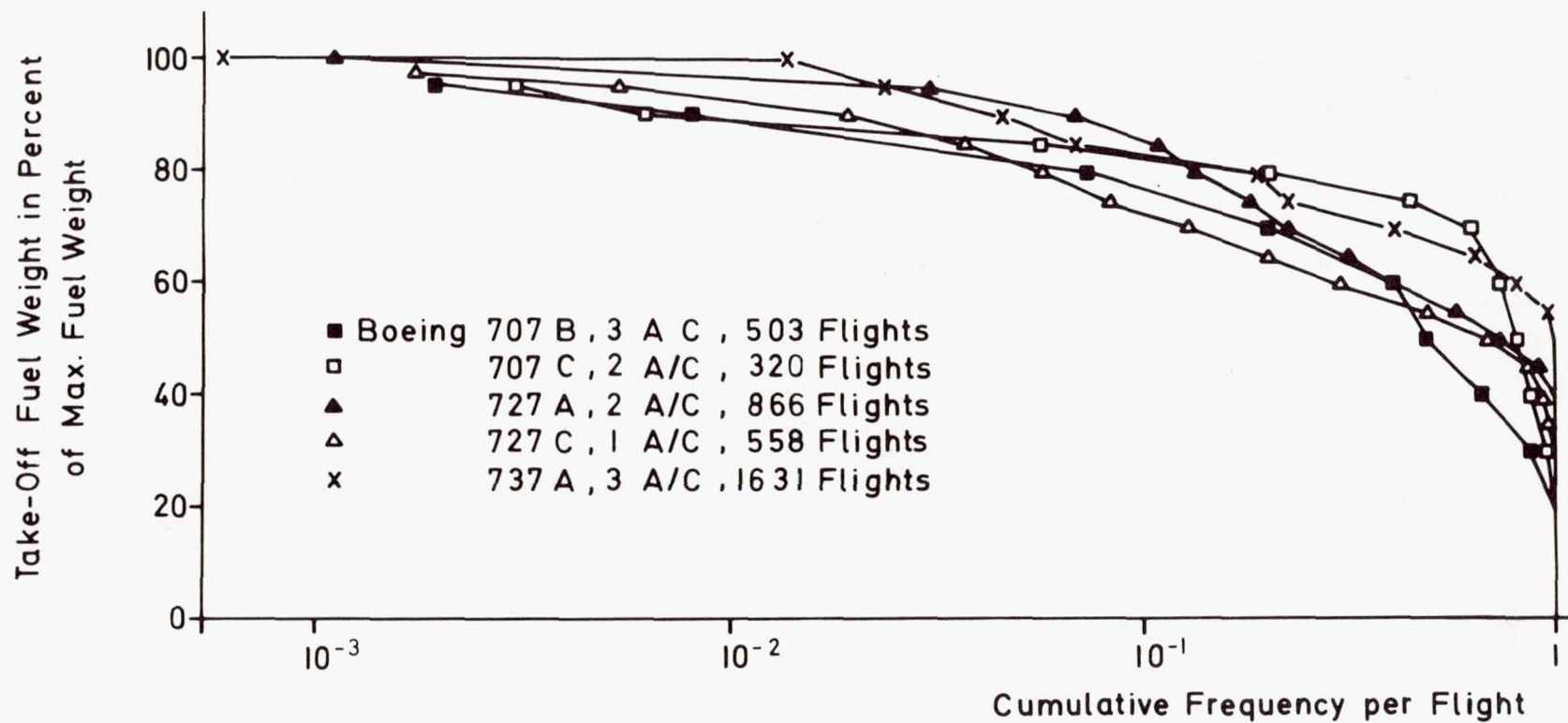


Figure 11.- Cumulative frequency distributions of take-off fuel weight for different types of transport airplanes.



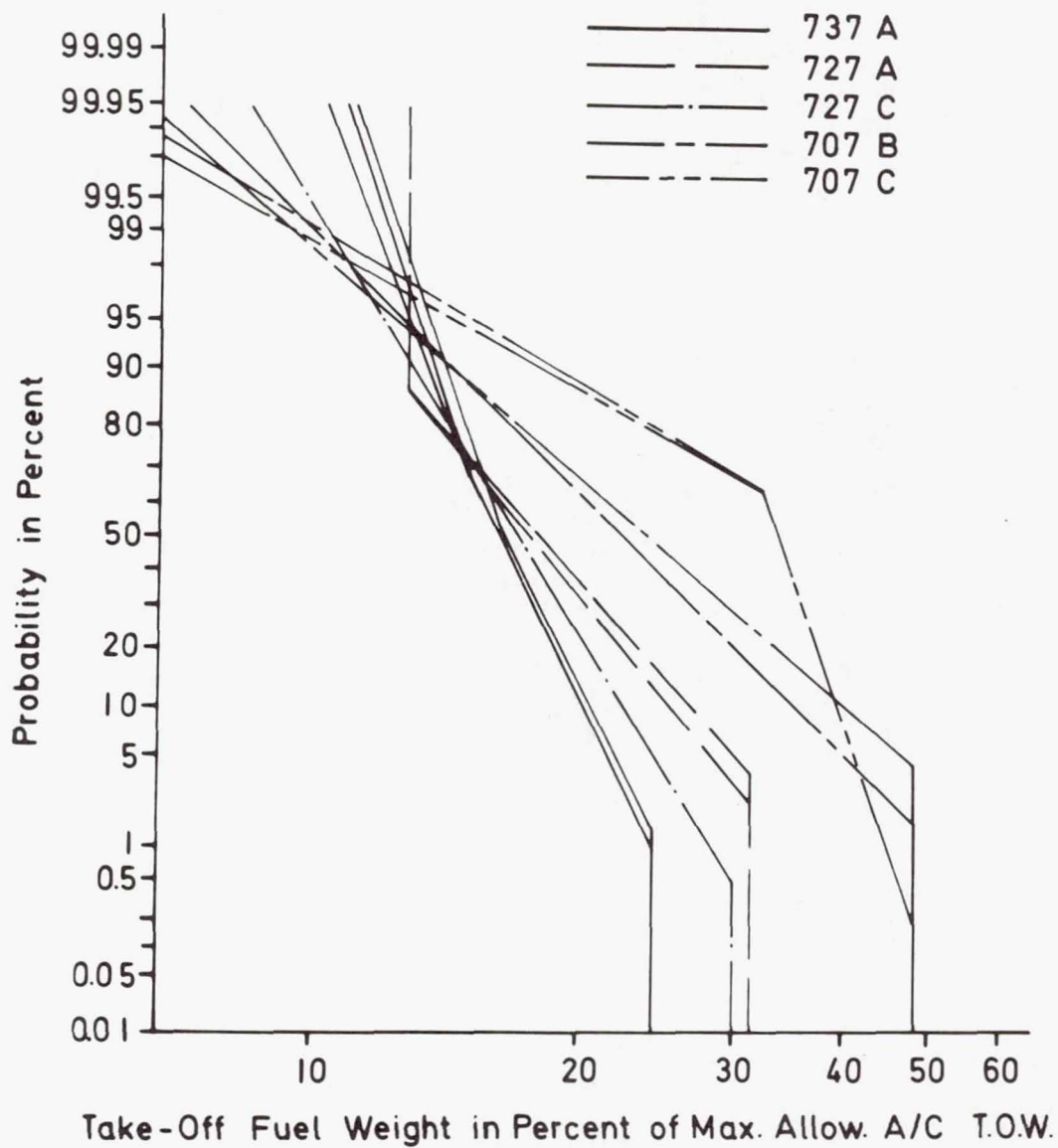


Figure 12.- Ratio of take-off fuel weights to airplane take-off weights for 10 airplanes during the same period of observation. Each line indicates a different airplane.

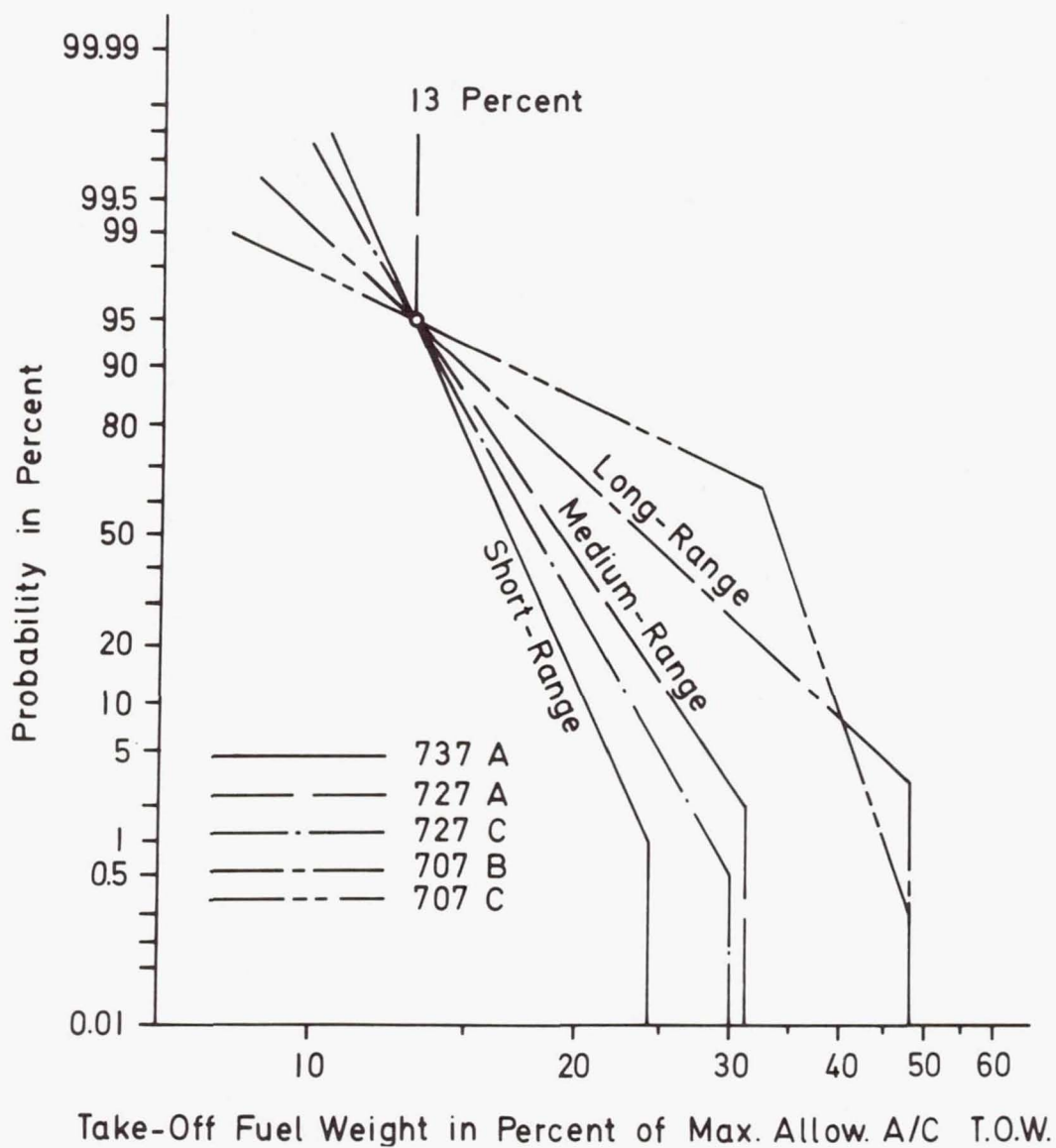


Figure 13.- Take-off fuel weights of jet-powered short-, medium-, and long-range airplanes.

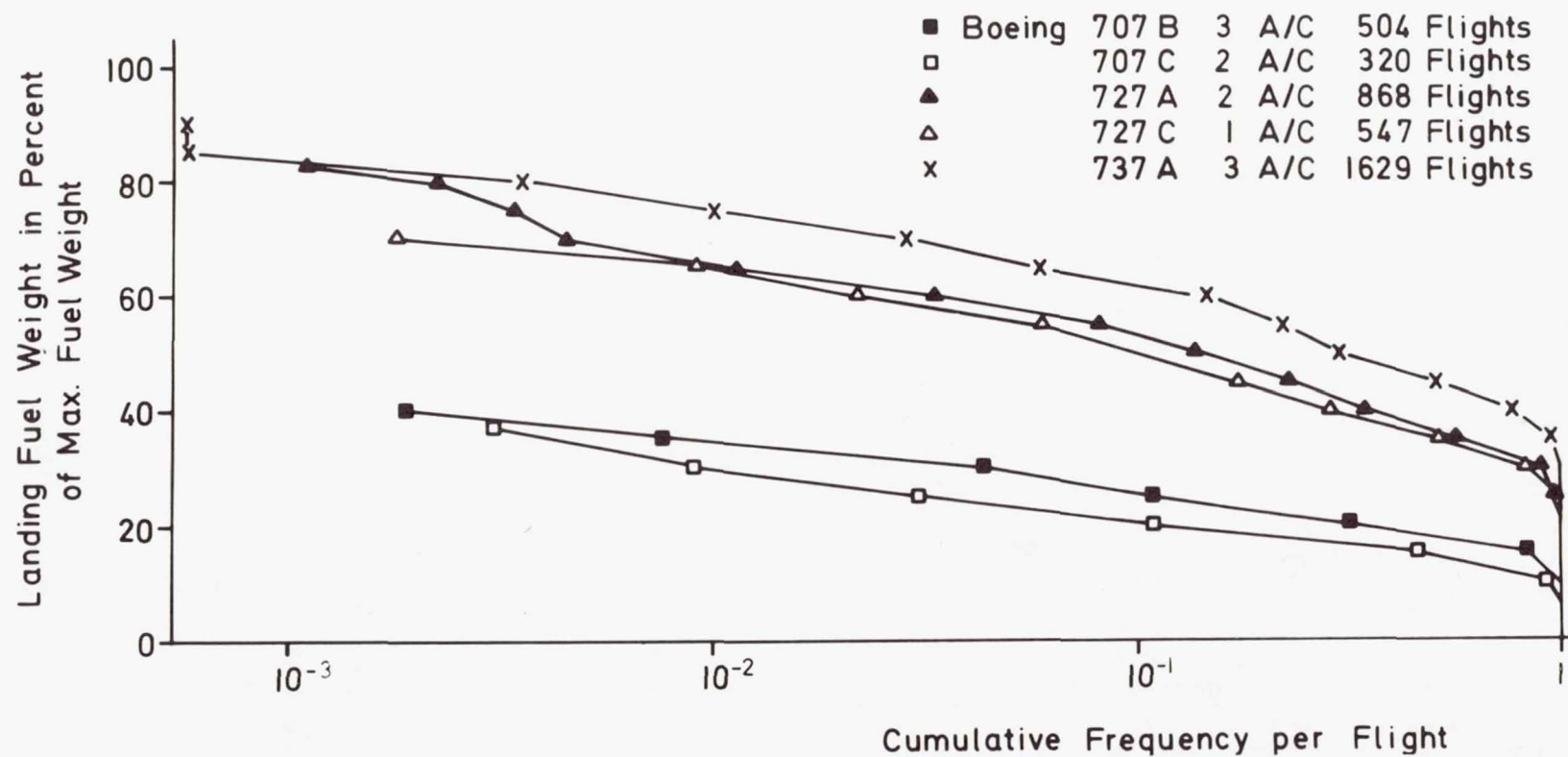


Figure 14.- Cumulative frequency distributions of landing fuel weight for different types of transport airplanes.



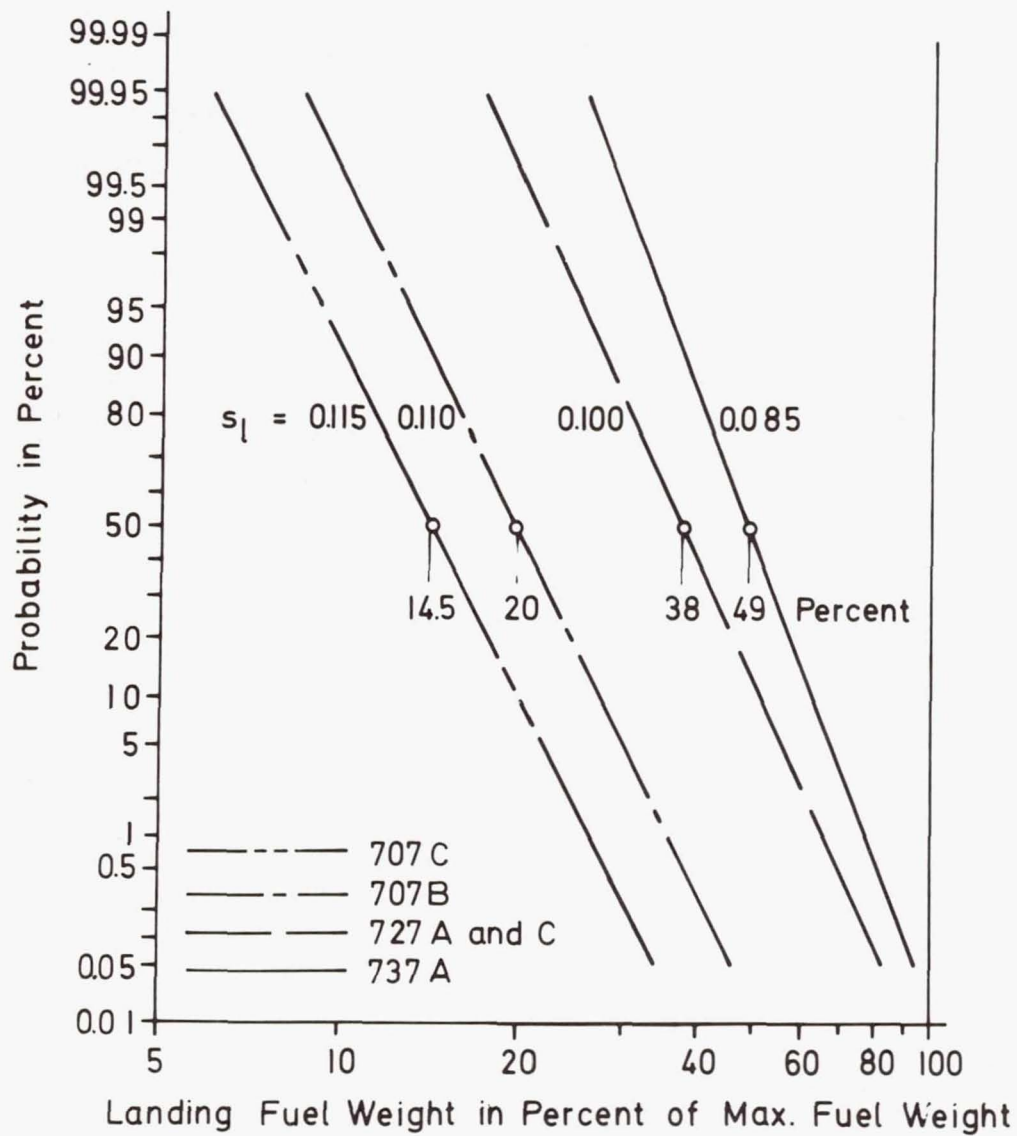


Figure 15.- Landing fuel weights of jet-powered short-, medium-, and long-range airplanes.

N72-29912

PRECEDING PAGE BLANK NOT FILMED

## STATISTICAL LOAD DATA PROCESSING

By G. M. van Dijk

National Aerospace Laboratory NLR, The Netherlands

### SUMMARY

In designing against fatigue the assessment of the loading environment still is a major problem. Especially with military trainer and fighter aircraft which may be used for a variety of duties, regular or continuous load recording programs have to be considered mandatory. Such load recording programs may serve either to assess the consumed fatigue life of operating aircraft or to select design spectra for future aircraft designs and a fatigue-test setup. Within this scope the National Aerospace Laboratory has carried out a tentative load monitoring program.

A recorder system has been installed on two operational fighter aircraft. Signal values from a c.g.-acceleration transducer and a strain-gage installation at the wing root were sampled and recorded in digital format on the recorder system. To analyse such load-time histories for fatigue evaluation purposes, a number of counting methods are available in which level crossings, peaks, or ranges are counted. Ten different existing counting principles are defined. The load-time histories are analysed to evaluate these counting methods.

For some of the described counting methods, the counting results might be affected by arbitrarily chosen parameters such as the magnitude of load ranges that will be neglected and other secondary counting restrictions. Such influences might invalidate the final counting results entirely. The evaluation shows that for the type of load-time histories associated with most counting methods, a sensible value of the parameters involved can be found at which the counting results are rather unique.

Besides assessing the influences of secondary parameter values, the different counting methods are compared with each other. The analysis shows that the counting results obtained by level-crossing count methods and peak count methods compare rather well. For most of these counting methods the differences actually turned out to be surprisingly small, especially for the c.g.-acceleration load-time history. The results of the range count methods exhibit larger differences. Also, with the range counting methods the differences appear to be larger for the strain-gage history. The comparison of the different counting methods with each other is concluded by comparing the level-crossing and peak count methods with the range count methods. Three different ways are used to convert level-crossing and peak countings into range countings. The results show that level-crossing and peak count methods do not compare well with range count methods.



Finally, the described counting methods are evaluated from the fatigue point of view while bearing in mind the purposes they will have to serve. It is concluded that in assessing the life consumed by individual aircraft, a sophisticated range count method applied to strain-gage histories should be preferred. For the selection of design spectra of future aircraft or a fatigue-test setup, level-crossing and peak count methods may be suitable; in fact, they may even be preferred.

## INTRODUCTION

A major question in designing against fatigue concerns the assessment of the loading environment to which the aircraft will be subjected during their service life. Civil and military transport aircraft generally appear to be fatigue sensitive with respect to gust loads. This gust loading environment is substantially independent of the aircraft itself. In the past, extensive measurement programs have been carried out which enabled the assessment of the quantitative rules determining this loading environment.

High-performance aircraft appear to be relatively insensitive to gust loads with respect to fatigue. With this type of aircraft, fatigue damage will be primarily due to maneuver loading. However, in contrast with gust loads the maneuver loading depends greatly on both the tasks to be carried out and the maneuverability of the aircraft and is substantially independent of external conditions. On the one hand, the maneuvering capabilities of the aircraft as well as the intended usage differ enormously from aircraft to aircraft. On the other hand, the way in which the intended composite tasks are carried out will be highly dependent on training philosophy, pilot experience, and such. Therefore, the resulting loading severity will be somewhat unknown and, in addition, will exhibit important differences from aircraft to aircraft. Consequently, to assure adequate structural integrity (especially with fighters and military trainer aircraft), load monitoring – either individual monitoring or sample monitoring – has to be considered mandatory. Such load monitoring will provide the means to assess the life consumed by the individual aircraft and will also provide information regarding load spectra to be used in future aircraft designs and fatigue testing. Within this scope the National Aerospace Laboratory has carried out a tentative load monitoring program under contract for the Royal Netherlands Air Force. Continuous load-time histories became available from both the c.g. acceleration and a wing-root-bending-moment strain-gage installation.

To analyse such load-time histories for fatigue evaluation purposes, a number of counting methods are available in which the number of certain load occurrences is counted. In the past, these counting methods were compared to each other with respect



to gust loads. Bearing in mind the nature of a gust loading environment, the results of that evaluation are not self-evidently applicable to maneuver-induced load-time histories.

The main theme of the present paper is to evaluate the basic counting methods with respect to maneuver-type loading. The results will be discussed from the fatigue point of view while taking into account the purposes they might serve.

## PRINCIPLES OF DATA ANALYSIS

Actual load-time histories will consist of a number of load excursions with an irregular pattern and in irregular random sequence. The analysis of load-time histories has to be such that the amount of damage caused by these load excursions is somehow quantitatively reflected in the final results. With all analysis procedures of present interest, the actual time scale is irrelevant. Actually, the assumption is made that for fatigue evaluation purposes load-time histories are fully characterized by all peak values in their actual sequence irrespective of the time elapsed between successive peaks.

A number of different counting methods do exist in which specific occurrences within such simplified load histories are counted. The occurrences of interest are the following:

- (1) Crossings of fixed levels with either a positive or a negative slope
- (2) Peak values (either maxima or minima)
- (3) Load variations (either load increments or decrements)

With counting procedures of type (1) and type (2), the counting results usually do not provide any direct information about those load variations known to influence the fatigue process. Additional information about the load patterns that do occur will generally be needed. Thus, secondary counting principles should be applied to account for sequence effects.

The different counting methods will be described in the next section. The discussion of each method will comprise these two distinct elements:

- (1) Uniqueness of the counting method
- (2) Usefulness of the counting results

The aspect of uniqueness will be discussed in connection with the secondary counting principles. In applying these secondary counting principles arbitrary parameter values may have to be adopted which may influence the final counting results.

Self-evidently, such influence (if considerable) would reduce the validity of the counting method, and the results would no longer be unique.

The usefulness of a counting method is influenced by its application; this relationship forms the basis for the discussion of the counting methods. The basic purposes are as follows:

- (1) Estimating the life consumed by individual aircraft
- (2) Estimating load spectra for future aircraft designs
- (3) Selecting the loads for fatigue testing

The discussion will take into account the state-of-the-art in realising these three purposes.

## DEFINITION OF COUNTING PROCEDURES

Ten different counting procedures are considered in the present evaluation, enumeration of which can be found in table I. It should be noted that although all methods are derived from the literature (refs. 1 to 7), slightly different names have been adopted for some of the methods to emphasize the characteristic differences between them.

### Simple Level-Crossing Count Method

The simple level-crossing count method is the simplest way of analysing load histories. A number of preset levels are chosen. Each time the load crosses one of these levels with positive (or negative) slope, a count is made. Obviously, it does not matter whether level crossings are counted with positive or negative slope. Both procedures will provide almost exactly the same results (maximum difference will be 1 count at each level for each load history analysed). With this method only momentary load values are of interest. Information regarding the actual load patterns is fully lost. In order to interpret the counting results for fatigue evaluation purposes, additional information will be needed regarding the expected load patterns. The insufficiency of this counting method is clearly demonstrated by figure 1. Although the load patterns shown on the left-hand and right-hand sides of this figure are highly different, the same counting results will be obtained. Small intermediate load variations, which virtually are of minor importance in the fatigue process, will give rise to additional countings. Generally, interpretation of the counting results will be such that the number of crossings of a level is assumed to equal the number of maxima above (or minima below) that level. Figure 1 also clearly demonstrates the incorrectness of this assumption. Obviously, small intermediate load variations seriously hamper the validity of this counting method. In practical applications a secondary restriction may be applied to



compensate to some extent for this setback. It may be decided to neglect level crossings which are associated with load variations smaller than a certain range value. This decision would actually mean skipping all load variations which do not exceed that assumed range value. This range filtering may be carried out by means of a logical system or may be due to the type of load transducer used, as for example with scratch gages (ref. 8).

#### Restricted Level-Crossing Count Method

The restricted level-crossing count method applies the same primary counting principles as the simple level-crossing count method. Different secondary counting principles are applied, however. A crossing of a level with positive (or negative) slope is not made until the load also has crossed a second lower (or higher) preset level in opposite direction. This counting method is associated with the so-called "Fatiguemeter" developed at the British Royal Aircraft Establishment (RAE) and is normally referred to in the literature as the Fatiguemeter count method. Although the Fatiguemeter was developed to count acceleration occurrences, the method may also be used to monitor other parameters such as strains. The adjustment of the secondary counting levels generally is of arbitrary nature. The drop or rise required to satisfy the secondary counting condition may be the same for all counting levels or may be chosen in a progressive way. With the progressive adjustment, the higher (or lower) the primary counting level concerned, the larger is the drop (or rise) required to satisfy the secondary counting condition. Still, however, interpretation is hampered by intermediate load cycles as is clearly demonstrated by figure 2. Rather different load patterns are depicted on the left-hand and right-hand sides of this figure but, as in the simple level-crossing count method, they will produce equal counting results.

#### Simple Peak Count Method

With the simple peak count method all peak values are counted. The counting results are presented separately for the maxima and the minima. From the definition it is understood that with this counting method, as well as with all other peak count methods, the load patterns that actually occur are taken into account to some extent since application of this method implies a peak detection. However, the counting results will not provide any information regarding the sequence of the maxima and the minima themselves. It is not possible to tell whether a counted peak was actually associated with small or large load variations. Again interpretation is seriously hampered by the smaller intermediate load variations. Much the same as with the simple level-crossing count method, a secondary counting condition may be introduced to more or less compensate for this setback by disregarding peaks which are not associated with at least a



certain load range. It sometimes is decided to count only maxima above a specified mean level and minima below that level. This simplification does not improve the validity of the counting results at all. For example, minima associated with minor load ranges are sometimes neglected whereas the adjacent maxima would still be counted.

#### Level-Restricted Peak Count Method

The principles of the level-restricted peak count method are very much the same as those of the restricted level-crossing count method (Fatiguemeter counting). In contrast, however, with the restricted level-crossing count method, only a count is made pertaining to the highest primary counting level that has been crossed before the secondary counting condition was met, after which all other previous crossings of primary counting levels are disregarded. Actually, the crossings of primary and secondary counting levels are considered merely to detect a peak associated with at least a certain load range. Figure 3 shows a comparison of this method (see fig. 3(b)) with the restricted level-crossing count method (see fig. 3(a)). The final counting results do not provide definite information regarding the actual sequence of the maxima and the minima. The method has been widely used in association with VGH recording programs (ref. 3).

#### Range-Restricted Peak Count Method

With the range-restricted peak count method, the intention is to count merely the more significant peaks. The method will merely count peaks that are associated with major load variations. The counting is restricted to peaks beyond mean threshold levels (e.g., minima below 0-g and maxima above 2-g). The peaks to be counted are those which are both preceded and followed by drops (or rises) of at least a certain magnitude (e.g., 1-g increment) or exceeding a fixed percentage of the incremental peak value (e.g., 50 percent), whichever is the greater. Here the incremental peak value is defined as the difference between the peak value itself and the mean load level. The counting conditions for a maximum count are illustrated in figure 4. From the definition it is understood that intermediate load fluctuations are disregarded rather rigorously by this method. The method also neglects some load fluctuations which are not truly insignificant. However, counts pertaining to the higher maxima and the lower minima have become more relevant. The method has been used extensively with VGH recording programs (ref. 6).

#### Peak-Between-Mean-Crossings Count Method

The peak-between-mean-crossings count method is also intended to count only the more significant peaks. Only the highest maximum or the lowest minimum between two successive crossings of a specified mean level is counted. With this method intermediate

load fluctuations are disregarded most rigorously. However, all counts are now known to be associated with major deviations from the steady-flight level. A further refinement of the counting procedure may be obtained by applying two mean threshold levels as references. The highest maximum will be counted between any two successive crossings of the upper threshold level, as well as the lowest minimum between any two successive crossings of the lower threshold level. The method is illustrated in figure 5. With this refinement, peaks associated with minor deviations from the steady-flight pattern will also be neglected. On the other hand, less high maxima and lower minima will be disregarded in applying this counting procedure. The method has been used extensively in evaluating VGH records (ref. 9).

#### Simple Range Count Method

With the simple range count method as well as with all other range count methods, the load fluctuations are of direct interest. The fluctuations are known to be a primary influence in the fatigue process. A range is defined as the difference between two successive peak values. With the simple range count method all ranges are counted. It should be noted here that counting ranges essentially implies a peak detection procedure. With this simple range count method the loading sequence is taken into account to some extent; that is, with each count two succeeding characteristic values of the load history are considered. However, information regarding the peak values themselves is completely lost.

In practical applications it may be decided to neglect small load fluctuations which are not of much importance for the fatigue process. As is illustrated in figure 6, disregarding such small load fluctuations does affect the final counting results seriously. Apparently, the final counting results will depend on the magnitude of the smallest load range that will be counted.

It may also be decided to count only ranges pertaining to load increments or load decrements. One should bear in mind, however, that the counting results for the positive ranges might differ appreciably from the counting results for the negative ranges. Consequently, such a simplification might yield less relevant results.

#### Range-Mean Count Method

The principles of the range-mean count method are very much the same as with the simple range count method. However, this counting method does provide additional information. Not merely the load ranges are counted. With each count the corresponding mean value of the load range counted will also be taken into account. So each count is now associated with two values which completely describe the load variation concerned.



As is clear from the definition, the counting results will again be sensitive to the smallest load range regarded.

### Range-Pair Exceedance Count Method

The range-pair exceedance count method is intended to analyse load histories in terms of load cycles rather than load ranges (half cycles). Since fatigue properties are generally presented in terms of load cycles, this is of course a favourable property.

To accomplish a count two conditions must be met. Each count of a range-pair exceedance of a certain specified magnitude, say  $R$ , will have to be associated with a load increment (positive range) of at least  $R$  succeeded by a load decrement (negative range) of at least  $R$ . By proceeding as such and consecutively considering a number of different range values, the counting result will finally give the number of range pairs (load cycles) exceeding a certain range value  $R$ . The counting procedure is illustrated in figure 7. The Vickers-Armstrongs strain range counter (ref. 10) is an example of a counting device operating according to this counting method. In considering figure 7, it becomes clear that the method will primarily count the major load fluctuations. Small intermediate load fluctuations will be regarded as superpositions on the major load patterns. Obviously, this counting method does take into account the loading sequence. Fatigue test experience indicates that this characteristic feature is desirable. The counting procedure also has the advantage of being insensitive to the magnitude of the smallest load range regarded.

Another interesting feature of this counting method will become clear by considering the largest range-pair value that will be present in the final counting results. By nature, the range-pair exceedance count method will combine the largest load increment and load decrement that both occur in the load history concerned and will count them as one load cycle of that specific magnitude. Likewise, the counting procedure will also combine the next largest load increment with the next largest load decrement, and so on. From fatigue experience it is known that extreme negative load excursions do actually influence the damage caused by a succeeding extreme positive load excursion. So it may be stated that fatigue experience is indeed reflected in the counting principles. Nevertheless, this feature does imply a complication. It certainly is not relevant to combine a very low minimum with a very high maximum which occur at instances very much apart. In practical applications the method should be carried out separately on segments of the load history to avoid irrelevant countings. Treating each flight as such, a separate load-history segment seems to be a both obvious and rather practical approach.

Another example of a counting device operating according to this counting procedure is the Schenck range-pair counter (ref. 5). With this counting device, however, the



starting procedure is not altogether in accordance with the basic counting principles. In starting the counting process the device will analyse the load history as if the starting point of the load history were an extreme minimum. This actually means that for the first count to be made, merely the second condition of the basic counting principles will have to be met. The effect is illustrated in figure 8 and demonstrates that the Schenck procedure will produce higher counting results than the basic procedure. In applying the counting procedure on a flight-by-flight basis, the effect on the final counting results might be significant.

Although the range-pair exceedance count method does apply rather sophisticated counting principles, the method is still hindered by two shortcomings:

(1) No information will be provided regarding the mean values of the load cycles counted.

(2) Not all load excursions will be fully counted (see fig. 9).

Both shortcomings are offset by the next counting method.

#### Range-Pair-Range Count Method

The range-pair-range count method is also intended to count load cycles. The counting procedure operates in two phases. In the first phase all intermediate load cycles are detected and counted in connection with the associated mean values. Each intermediate load cycle will be eliminated from the load history after being counted. The procedure is continued until the load history does not present any more intermediate load cycles. As may be easily verified, the residual load history will necessarily have a divergent-convergent envelope such as depicted in figure 9. In the second phase of the counting procedure, this residual load history is analysed according to the range-mean count method. These counting principles are illustrated in figure 10. The range-pair-range counting procedure is referred to in the literature as the NLR counting method (ref. 2) and the rain-flow counting method (ref. 4).

This range-pair-range counting method generally has the same advantages as the range-pair exceedance count method without being hindered by its previously mentioned shortcomings. It should be noted that this counting method also is intended to analyse load histories on a flight-by-flight basis.

#### NUMERICAL EVALUATION DATA

Under contract for the Royal Netherlands Air Force a tentative load monitoring program has been carried out. This load monitoring program was intended to serve the following primary purposes:

- (1) To demonstrate the feasibility of a digital load recording system
- (2) To demonstrate the feasibility of a strain gage as a load transducer in operational conditions for long-term load monitoring
- (3) To emphasize the desirability of recording strain histories instead of acceleration histories
- (4) To evaluate different counting methods

Two operational fighter aircraft have been equipped with both an accelerometer transducer at the aircraft c.g. and a bending-moment strain-gage installation in the wing root section. Signal values from both transducers were sampled at a scanning rate of 24/sec. After being digitised, the data were stored on a magnetic recorder medium with a 15-hour recording capacity. The beginning of each flight could be recognized by a series of marking numbers which were automatically entered on the recorder medium at the activation of the aircraft electrical power. Every 15 flight hours the recorder medium was removed for further processing on ground-based facilities. By means of a digital computer the data were checked for spurious readings after which a data compression was carried out.

The data compression reduced the enormous amount of data to a relatively small number of characteristic data resembling the peak values that did occur. The compressed load-time history still comprises all significant information for fatigue evaluation purposes. During the data compression phase more than just peak values are detected. Peaks which are not associated with at least a certain relatively small variation are disregarded to reduce the number of data and to remove data that are of less importance for the purposes concerned. The minimum load range thus left in the compressed load-time history amounted to approximately 7 percent of the aircraft limit load level. When applying the counting procedures just described, such a range filtering is either obligatory or does not significantly affect the counting results since other more stringent restrictions are applied. Consequently, the load histories resulting from the final data compression phase are still suited to evaluate the different statistical load counting procedures. A plot of such a compressed load-time history for a typical fighter mission is shown in figure 11. Such load histories – covering some 75 flight hours – were used to evaluate the different counting methods. The results of this numerical evaluation are presented in the next section.



## NUMERICAL RESULTS

### General Comments

The counting procedures which have been described herein were simulated by means of a digital computer to analyse the available load-time histories. The results obtained with the c.g.-acceleration history and the wing-root-bending-moment strain-gage history are presented separately. It should be noted that this paper is not intended to present a quantitative comparison of the counting results obtained for the acceleration history with those obtained for the strain-gage history.

The load data are presented in arbitrary units as a result of the digitisation process. In general, the counting results were calculated with an interval width of 8 units. The results have been plotted without any fairing.

Application of some counting methods did imply the definition of a mean level. For the c.g.-acceleration data the 1-g steady-flight level has been defined as such, although in terms of mathematical statistics this level is not actually the mean value but rather the most probable value. An "equivalent" 1-g level has been assessed to be used as mean reference level in the strain-gage data analysis. Actually, the equivalent 1-g strain-gage value is not a constant value. Nevertheless, the definition remains relevant since, on the one hand, merely a reference level has to be chosen while, on the other hand, with high-performance aircraft the variations in this 1-g strain-gage value are relatively small in comparison with the load fluctuations of general interest.

Before discussing the numerical results, it should be mentioned that the counting results obtained with different counting procedures are not all fully independent of each other. The following relations do exist which will all be easily understood by considering the definitions given for the various methods:

(1) Simple level-crossing counting results may be derived from the counting results obtained with the simple peak count method.

(2) Simple peak counting results may be derived from both the counting results obtained with the range-mean count method and those obtained with the range-pair-range count method.

(3) Simple range counting results may be derived from the range-mean counting results.

(4) The results obtained with the simple peak count method and the peak-between-mean-crossings count method will be the upper and lower limits of the counting results obtained with all other level-crossing and peak count methods described.



(5) Peak-between-mean-crossings counting results may be derived from the range-pair-range counting results.

### Results From Level-Crossing and Peak Count Methods

The results obtained with the level-crossing and peak count methods are presented in figures 12 to 15 and table II.

As previously stated, parameter values associated with secondary counting principles may influence the final counting results. The effect is illustrated in figure 12, figure 13, figure 14, and table II for the counting results obtained with the simple level-crossing count method, simple peak count method, peak-between-mean-crossings count method, and restricted level-crossing count method, respectively.

In figures 12 and 13 it is shown that the value of the smallest load range regarded does indeed affect the counting results obtained with the simple level-crossing and simple peak count method. The effect of doubling the basic range-filter value ( $R_0$ ) from 13 to 26 units does not seriously affect the counting results for the higher load values. Apparently the countings which were additionally disregarded were mainly associated with load cycles near the steady-flight level. Further increasing the range-filter value hardly changed the counting results for the higher load values. However, applying a smaller range-filter value yielded highly different counting results. The main conclusion to be drawn is that if a sensible range-filter value is adopted, the counting results for the higher load values are rather unique. It is nevertheless interesting to note that the counting results obtained by analysing the strain-gage history appear to be more sensitive to the adopted range-filter value than the results obtained by analysing the acceleration history. In considering both load histories in more detail, the major load excursions from the strain-gage history presented small intermediate load fluctuations more frequently than did the major load excursions from the acceleration history. This effect is most probably due to dynamic effects (dynamic overshoot and buffeting).

By definition it is clear that the restricted level-crossing count method, the level-restricted peak count method, and the range-restricted peak count method are intended to apply secondary counting principles which at least override the applied basic range filtering. From the preceding results the effect of the applied secondary parameter values may be expected to be rather limited. This limited effect is indeed confirmed by the data from table II, in which the restricted level-crossing counting results are tabulated by applying two different adjustments of the secondary counting levels. The counting results came out to be only slightly different. Similar results were obtained with the level-restricted and range-restricted count methods. Also with the peak-between-mean-crossings count method (fig. 14), the influence of the secondary parameter

values (e.g., mean threshold levels) was rather limited. From these findings it may be concluded that the majority of the load fluctuations of interest were separate excursions from the steady-flight level.

All the level-crossing and peak count methods described are compared in figure 15. As might be expected from the aforementioned findings, the differences are not large, although they are more pronounced with the strain-gage data than with the acceleration data. Nevertheless, when accurate data are required, the results obtained with different counting methods are not fully compatible (number of counts may differ by a factor of 2).

#### Results From Range Count Methods

The results obtained with the range count methods are depicted in figures 16 to 18. It should be noted that these results have been plotted without distinguishing between positive and negative ranges. This effect has been studied in connection with the simple range count method. Comparative results showed that when applying the basic range-filter value of 13 units, the number of positive and negative ranges counted did not differ very much. However, when applying a smaller range-filter value, the differences appeared to be much more pronounced. The counting results pertaining to the negative ranges appeared to be far more sensitive to the applied range-filter value than the counting results pertaining to the positive ranges. Apparently, small intermediate load fluctuations more frequently occurred after the load had reached a maximum. The overall effect of the applied range-filter value on the results obtained with the simple range count method is illustrated in figure 16. Doubling the basic range-filter value from 13 to 26 units does appreciably affect the counting results, especially the results obtained by analysing the strain-gage history. When applying a smaller range-filter value than the basic one, the differences were even more pronounced. It should be noted that further increasing the applied range-filter value (>26 units) still yielded appreciably different counting results. Consequently, it is stated that the results obtained by the simple range count method are not unique even when intermediate load fluctuations are disregarded.

The counting results from the various range count methods are compared in figure 17. The curves presented illustrate that the range-pair-range count method and both variants of the range-pair exceedance count method do not produce very different results. The simple range counting results, however, appear to be very different. It is interesting to note that with the strain-gage data, both variants of the range-pair exceedance count method coincide completely because of the presence of the Ground-Air-Ground (G-A-G) cycle (with every flight the strain-gage history will exhibit a relatively low starting value).

In comparing the mean countings as obtained by the range-mean count method and range-pair-range count method, the results have been averaged – that is, all mean



countings pertaining to a specified range interval have been averaged while a corresponding standard-deviation value has been calculated. The averaged means thus derived are represented in figure 18. With the c.g.-acceleration data as well as with the strain-gage data, the range-pair-range count method yielded lower averaged mean values than did the range-mean count method. However, the differences are much more pronounced with the strain-gage data. This fact may be easily understood by considering the counting principles of the range-pair-range count method and bearing in mind that in every flight the strain-gage history will both start and end with a low minimum due to the G-A-G cycle. These results clearly demonstrate that with the range-pair-range count method the G-A-G cycle is certainly accounted for.

The calculated standard-deviation values corresponding to the averaged means are not plotted in figure 18. It is interesting to note, however, that these standard-deviation values were approximately equal for all range intervals considered and, besides, appeared to be relatively small (order of magnitude of 10 units). From this finding it may be concluded that most load fluctuations of equal magnitude apparently occurred between approximately the same levels.

#### Comparison of Range Count Methods With Peak Count Methods

By nature the results obtained by the range count methods are not directly comparable with the countings resulting from the level-crossing and peak count methods since different types of occurrences are counted. To enable a comparison the counting results have to be converted. The present comparison will be accomplished by applying different ways of converting simple peak countings into range countings. Reference will be made especially to the range-pair-range counting results since this method is believed to represent best the amount of fatigue damage caused by the load history concerned. The following three conversion procedures are considered (see fig. 19):

(A) Maxima and minima are supposed to occur in random sequence.

(B) Maxima and minima are supposed to occur in random sequence; however, maxima below a certain level (e.g., 115 units) and minima above a certain level (e.g., 95 units) are neglected. Although the additional assumption seems a curious one, the case is relevant since actually the data disregarded generally are not available.

(C) Maxima are to be combined with minima having the same probability of exceedance (equal cumulative frequency).

The results of these converted simple peak countings as well as the range-pair-range countings and simple range countings are plotted in figure 19. As is illustrated, the applied conversion procedures do produce highly different results. Again the strain-gage data reveal the largest differences. However, none of the applied conversion



procedures produce counting results which approximately coincide with the range-pair-range countings. From these findings, it is concluded that a quantitative comparison of range countings with simple peak countings as well as with all other types of peak and level-crossing countings is hardly feasible for the type of load histories concerned.

## DISCUSSION

Basically the counting methods as described herein are intended to interpret irregular load-time histories by counting the number of specific types of load occurrences. In the preceding sections the uniqueness of the information has already been discussed and illustrated. In discussing the usefulness of the counting results, one should primarily take into account the purposes these results are meant to serve – that is, the type of information required.

In assessing the life consumed by individual aircraft, reference has to be made to experimental fatigue data, either simple S-N data or full-scale fatigue test data. Accomplishing such life calculations, however, will be useful only if the final counting results are sufficiently accurate. Thus, in assessing the life consumed by individual aircraft, a counting method should be used which fully takes into account the actual load-time history and which does not need the application of additional assumptions to be interpreted. Besides, the fatigue damage caused by the actual load-time history should be reflected in the counting results (interaction effects). By considering its definition and bearing in mind the aforementioned requirements, it is felt that the range-pair-range count method is best suited for assessing the individual aircraft fatigue damage. Also, the range-pair exceedance count method may be rather useful; however, with this method the counting results are not definite since no information is provided about the means of the range pairs counted. Consequently, less accurate results are to be expected. It should be noted that the same remarks hold when the counting methods are meant to compare with any degree of accuracy the life consumed by individual aircraft of the same type. Here, however, the requirements perhaps could be less stringent since it may be known that the aircraft are operating according to the same type of load patterns. In this case, restricted level-crossing or restricted peak count methods may be suited as well.

In estimating load spectra for future aircraft designs or selecting the loads for fatigue testing of an aircraft type that possibly has not even been in service operation, the requirements are somewhat different. Here, great accuracy would be more apparent than real. The load patterns as well as the sequence in which they occur may be entirely different with different types of aircraft. In particular, the number of intermediate load fluctuations at the higher load levels may be expected to be strongly related to the

aerodynamic performance capabilities, which may be highly different for different aircraft types. Estimating loading spectra as well as selecting loads for fatigue testing usually implies a mission analysis procedure. The number of exercises (during a mission) that will be carried out has to be estimated. The assumption made is that each separate exercise is associated with major load excursions from the steady-flight level ("characteristic events"). Small intermediate load fluctuations are considered of less or even irrelevant importance. A counting method should be chosen which will provide the number of such major load excursions and the peak levels they are associated with. As will be understood, the peak-between-mean-crossings count method is very well in accordance with these requirements. However, a restricted level-crossing or peak count method may be suited as well. To obtain a loading program for fatigue testing, the number of "events" counted may be arranged in a realistic sequence. Interaction effects will then be accounted for to some extent.

It can be concluded that the range-pair-range count method apparently has the best general validity. On the one hand, the method embodies some of the characteristics of the other counting methods mentioned (simple level-crossing countings, simple peak countings, and peak-between-mean-crossings countings may all be derived from the results of this range-pair-range count method). On the other hand, the load histories are taken into account by this method as much as possible from the fatigue point of view. Consequently, general application is recommended.

## CONCLUSIONS

(1) Some counting methods require secondary counting restrictions involving the choice of an arbitrary parameter value which may influence the final counting results. With the exception of the simple range count method and the range-mean count method, a sensible parameter value can be found which will yield rather unique counting results for maneuver-type load histories.

(2) The restricted level-crossing and restricted peak count methods will yield approximately equal counting results, especially at the higher load levels. The simple level-crossing and simple peak count methods, however, will yield conservative counting results.

(3) Level-crossing and peak countings virtually do not compare very well with range countings.

(4) The range-pair-range count method and the range-pair exceedance count method will produce approximately equal range counting results.



(5) Both the simple range count method and the range-mean count method will provide irrelevant information since the counting results are very sensitive to the magnitude of the smallest load ranges regarded.

(6) Both the range-pair exceedance count method and the range-pair-range count method provide relevant information in assessing the life consumed by individual aircraft. However, the range-pair-range count method is to be preferred since this method provides additional information about mean values of the ranges.

(7) In comparing individual lives of aircraft that are of the same type and that operate according to the same kind of duties, a restricted level-crossing or restricted peak count method may be sufficiently relevant.

(8) In estimating spectra for future aircraft designs or in selecting load events for fatigue testing, the peak-between-mean-crossings peak count method will provide relevant data.

(9) The range-pair-range count method will have the best general validity. The results obtained by this method are unique as well as definite and do suit all purposes.



## REFERENCES

1. Schijve, J.: The Analysis of Random Load-Time Histories With Relation to Fatigue Tests and Life Calculations. *Fatigue of Aircraft Structures*, W. Barrois and E. L. Ripley, eds., Macmillan Co., 1963, pp. 115-149.
2. De Jonge, J. B.: The Monitoring of Fatigue Loads. ICAS Paper No. 70-31, 1970.
3. Wells, Harold M., Jr.: Flight Load Recording for Aircraft Structural Integrity. AGARD Symposium on Flight Instrumentation, Paris, Sept. 1965.
4. Tucker, Lee E.: A Procedure for Designing Against Fatigue Failure of Notched Parts. Thesis, State University of Iowa, 1970.
5. Anon.: Instrument Combination for Counting According to the Range-Pair Method. Schenck Pamphlet Nr. P2047e.
6. Morton, W. Wallace, Jr.; and Peckham, Cyril G.: Structural Flight Loads Data From F-5A Aircraft. Technical Report SEG-TR-66-51, 1967.
7. Pitts, Felix L.; and Spencer, J. Larry: An Electronic Strain-Level Counter for Aircraft Structural Members. NASA TN D-5944, 1970.
8. Tipps, Daniel O.: F-5 Scratch Gage Correlation Data Report. Technology Incorporated, Report No. TI-375-71-1, 1971.
9. Donely, Philip; Jewel, Joseph W., Jr.; and Hunter, Paul A.: An Assessment of Repeated Loads on General Aviation and Transport Aircraft. Paper presented at 5th I.C.A.F. Symposium "Aircraft Fatigue - Design, Operational and Economic Aspects" (Melbourne, Australia), May 1967.
10. Teichmann, A.: The Strain Range Counter. Vickers-Armstrongs Ltd., Technical Office VTO/M/416.

## BIBLIOGRAPHY

- Incarbone, G.; and Padovano, E.: Methods of Evaluation of Extensiometric and Accelerometric Data To Determine Load Spectra on Aircraft. Paper presented at the First National Congress on Aeronautical Fatigue, Rome, May 16-19, 1960.
- Jost, G. S.: The Fatigue of 24-ST Aluminium Alloy Wings Under Asymmetric Spectrum Loading. ARL/SM 295, 1964.
- Ravishankar, T. J.: Simulation of Random Load Fatigue in Laboratory Testing. UTIAS Review No. 29, 1970.
- Roth, George J.; and West, Blaine S.: Parametric Fatigue Analysis of USAF Fighter Aircraft. Technical Report AFFDL-TR-69-85, U.S. Air Force, 1970.
- Schijve, J.: Cumulative Damage Problems in Aircraft Structures and Materials. NLR MP 69005 U, 1969. Aeronaut. J. Roy. Aeronaut. Soc., vol. 74, no. 714, June 1970, pp. 517-532.
- Schijve, J.; Broek, D.; et al.: Fatigue Tests With Random and Programmed Load Sequences With and Without Ground-to-Air Cycles. A Comparative Study on Full-Scale Wing Center Sections. NLR-TR S.613, 1965.

TABLE I: COUNTING PROCEDURES

SIMPLE LEVEL-CROSSING COUNT METHOD
RESTRICTED LEVEL-CROSSING COUNT METHOD
SIMPLE PEAK COUNT METHOD
LEVEL-RESTRICTED PEAK COUNT METHOD
RANGE-RESTRICTED     "     "     "
PEAK-BETWEEN-MEAN-CROSSINGS COUNT METHOD
SIMPLE RANGE COUNT METHOD
RANGE-MEAN     "     "
RANGE-PAIR EXCEEDANCE COUNT METHOD
RANGE-PAIR-RANGE COUNT METHOD

TABLE II: RESULTS OF RESTRICTED LEVEL-CROSSING COUNT METHOD FOR C.G.-ACCELERATION HISTORY

PRIMARY COUNTING LEVEL (G)	SECOND. COUNTING LEVEL (G)		NUMBER OF COUNTS	
	EQUIDISTANT ADJUSTMENT	PROGRESSIVE ADJUSTMENT	EQUIDISTANT ADJUSTMENT	PROGRESSIVE ADJUSTMENT
-1.0	-0.5	0	-	-
0	0.5	0.5	17	17
2.0	1.5	1.5	1019	1019
3.0	2.5	1.5	402	343
3.5	3.0	2.0	194	180
4.0	3.5	2.0	76	70
4.5	4.0	2.5	29	27
5.0	4.5	3.0	10	9



○ LEVEL CROSSINGS COUNTED

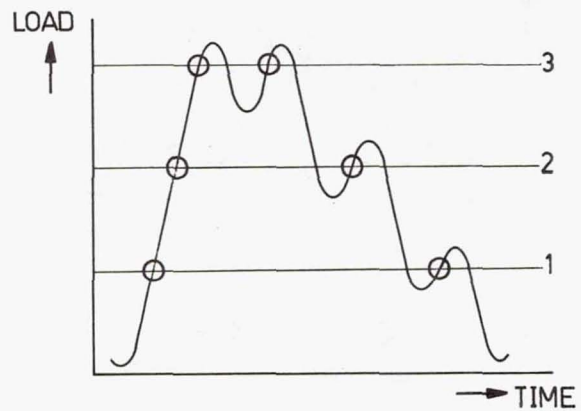
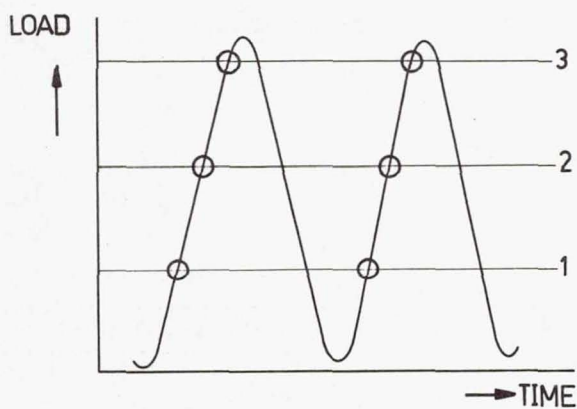


Figure 1.- Simple level-crossing count method.

○ FIRST COUNTING CONDITION SATISFIED  
● SECOND " " "

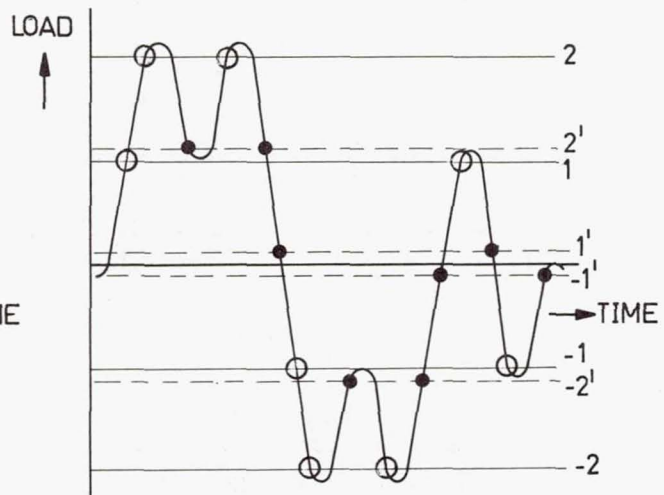
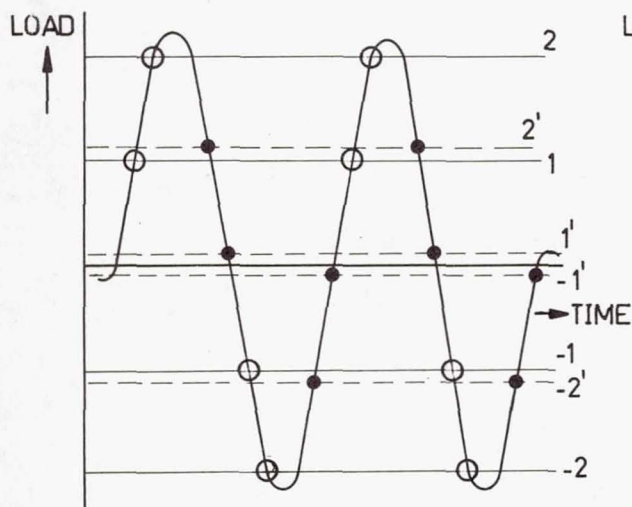


Figure 2.- Restricted level-crossing count method.

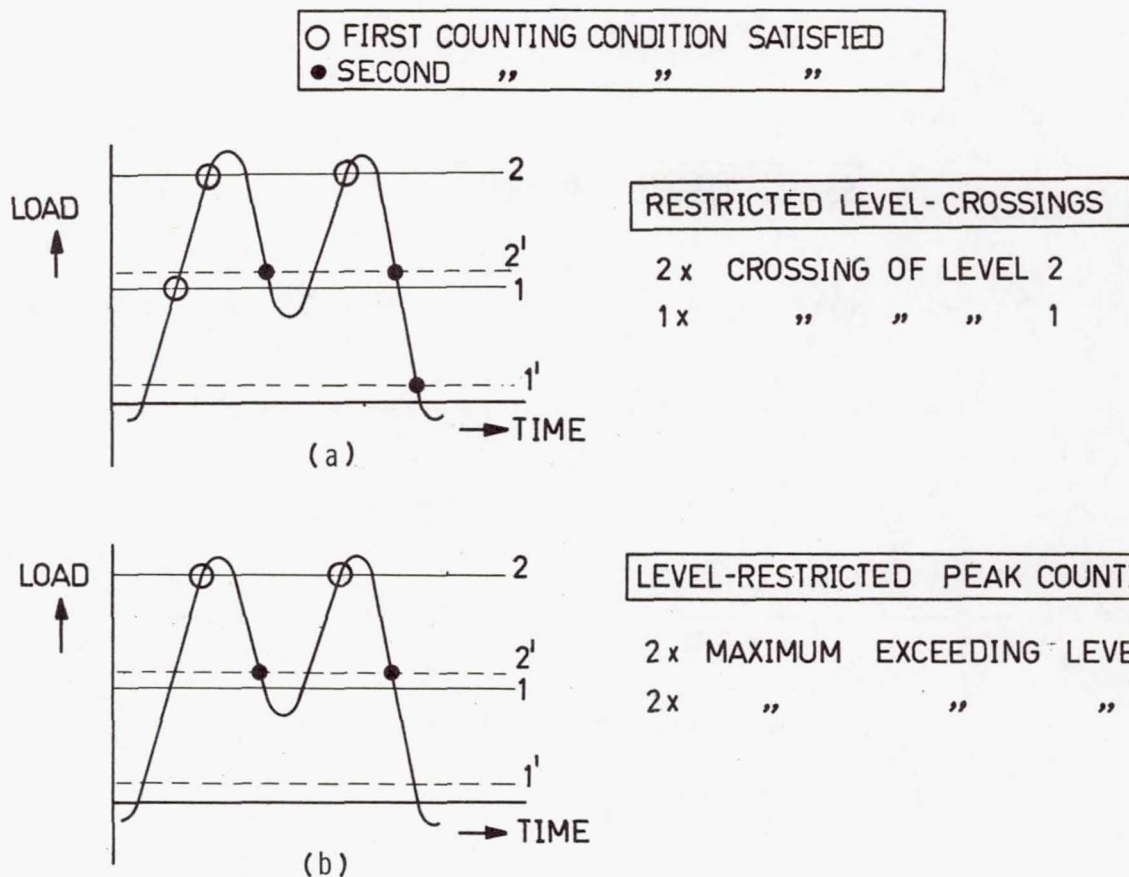
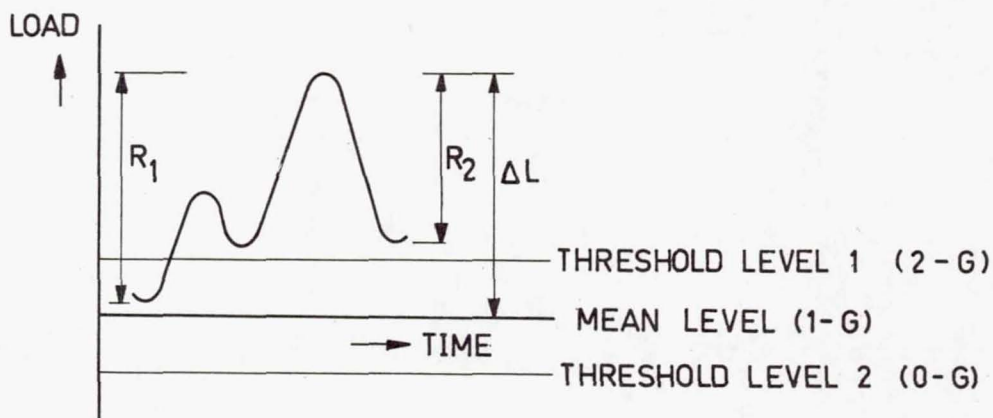


Figure 3.- Comparison of level-restricted peak count method with restricted level-crossing count method.



#### CONDITIONS FOR A MAXIMUM COUNT

- PEAK LOAD EXCEEDING LEVEL 1
- $R_1$  AND  $R_2$  ARE AT LEAST A FIXED VALUE (1-G)
- $R_1$  AND  $R_2$  " " " " " PERCENTAGE OF  $\Delta L$   
(50 PERCENT)

Figure 4.- Range-restricted peak count method.

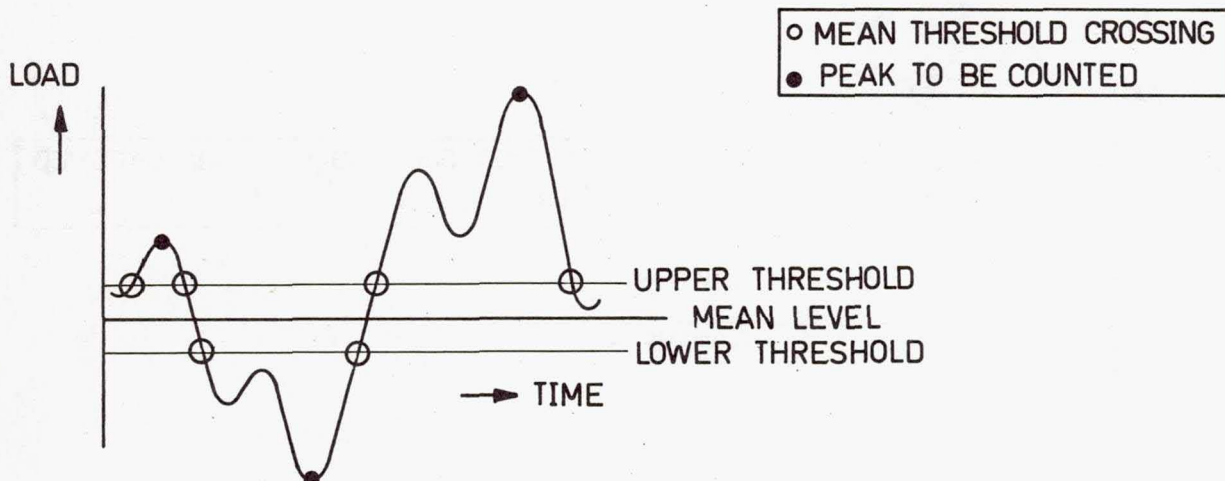
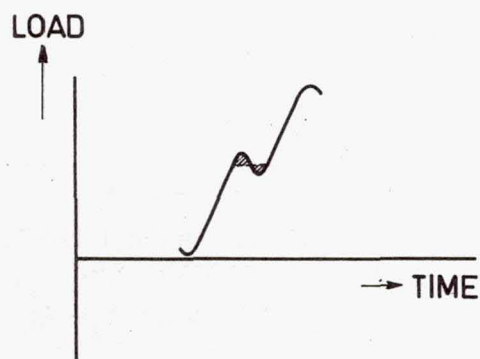
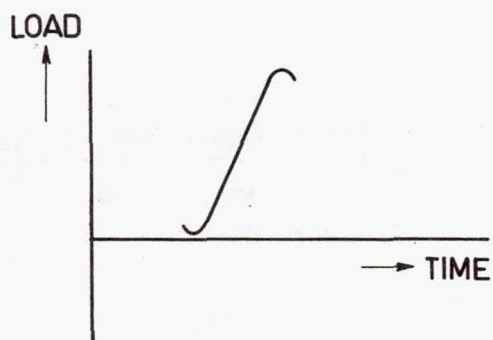


Figure 5.- Peak-between-mean-crossings count method.



WITH SMALL RANGE :  
SMALL AND INTERMEDIATE  
RANGES COUNTED



DISREGARDING SMALL RANGE :  
LARGE RANGE COUNTED

Figure 6.- Effect of disregarding small ranges with the simple range count method.





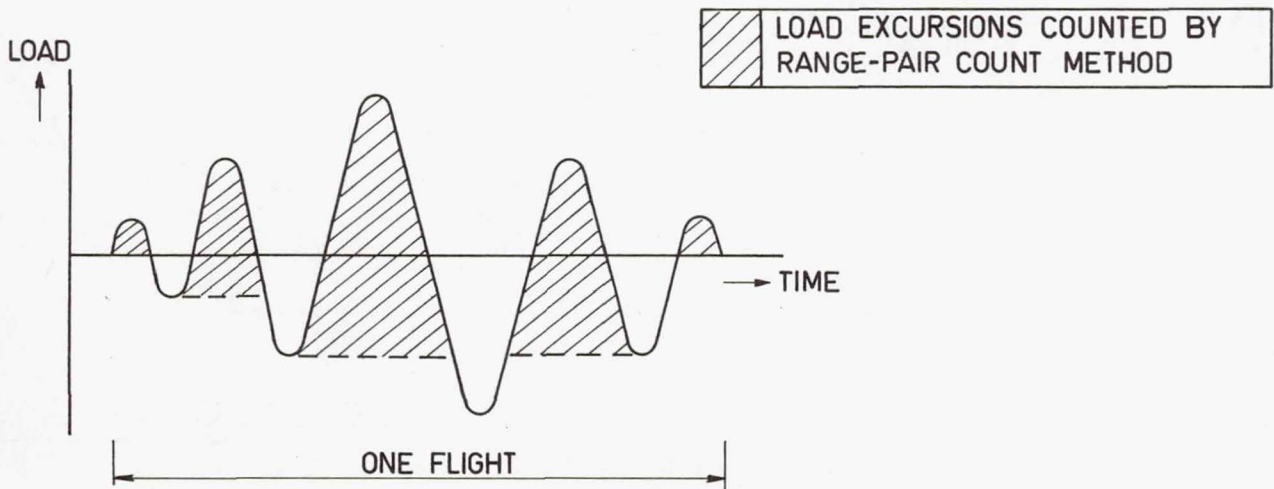


Figure 9.- Flight record with omission of intermediate load cycles.

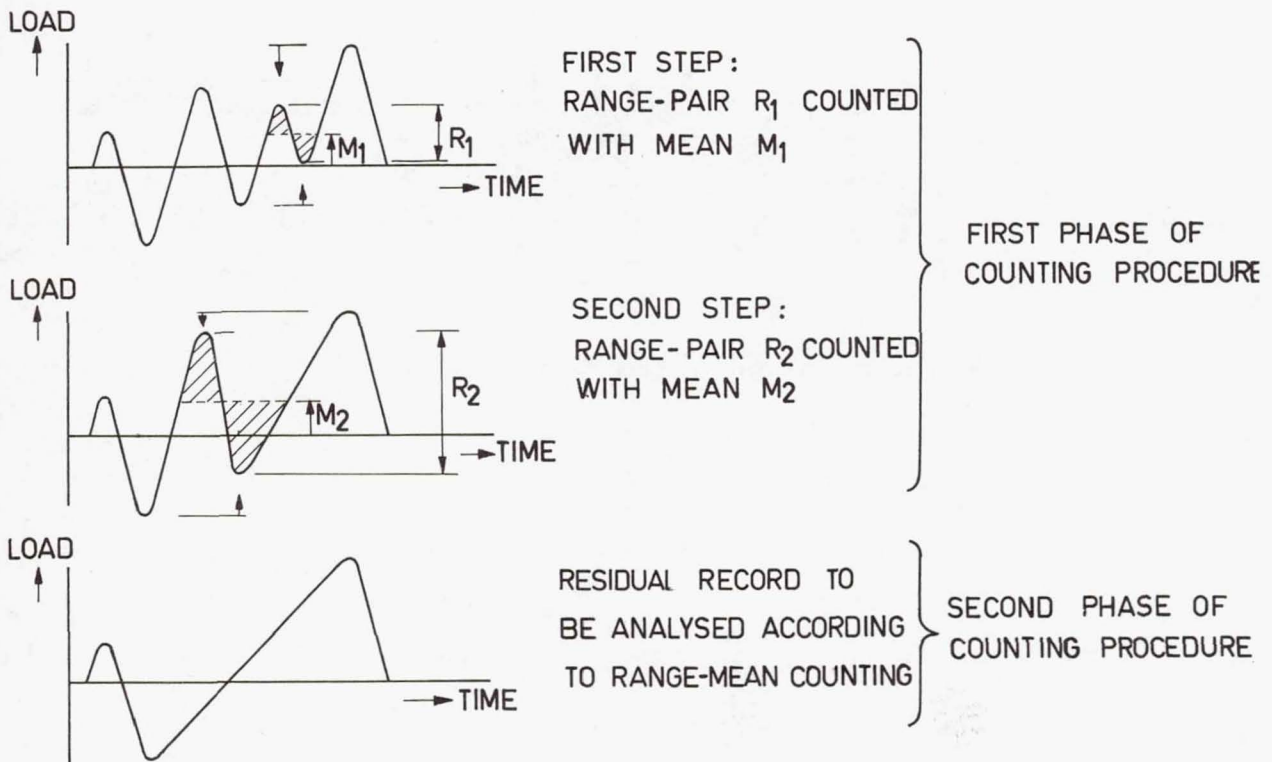


Figure 10.- Illustration of range-pair-range count method.

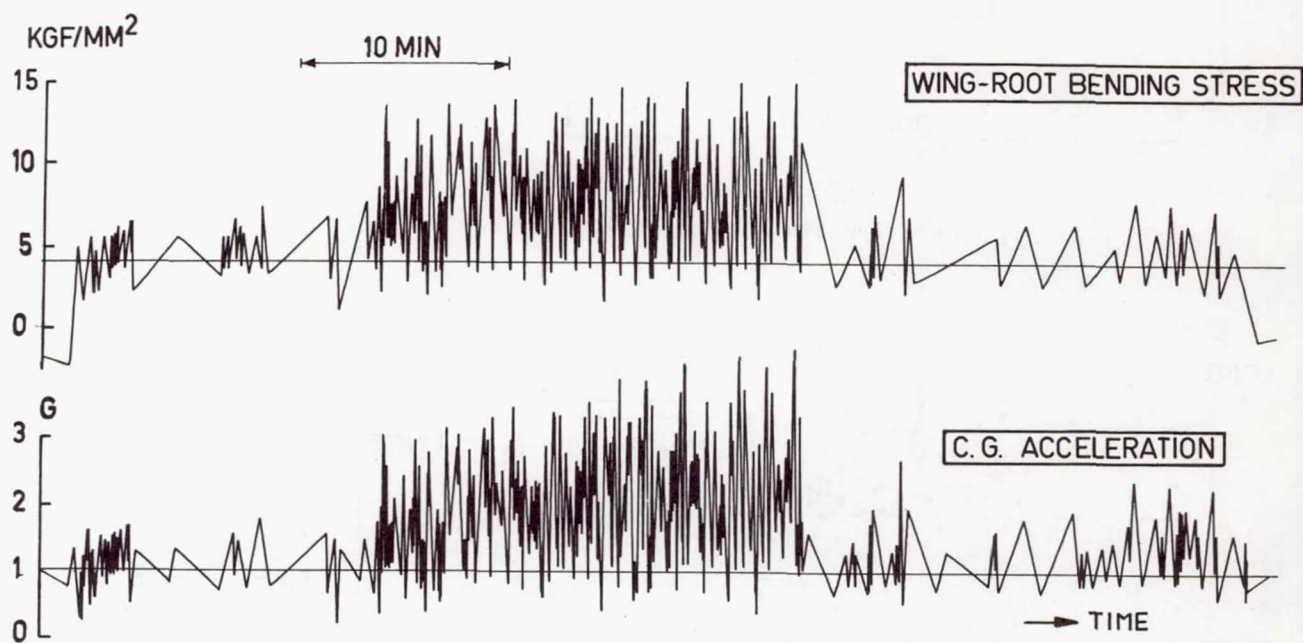
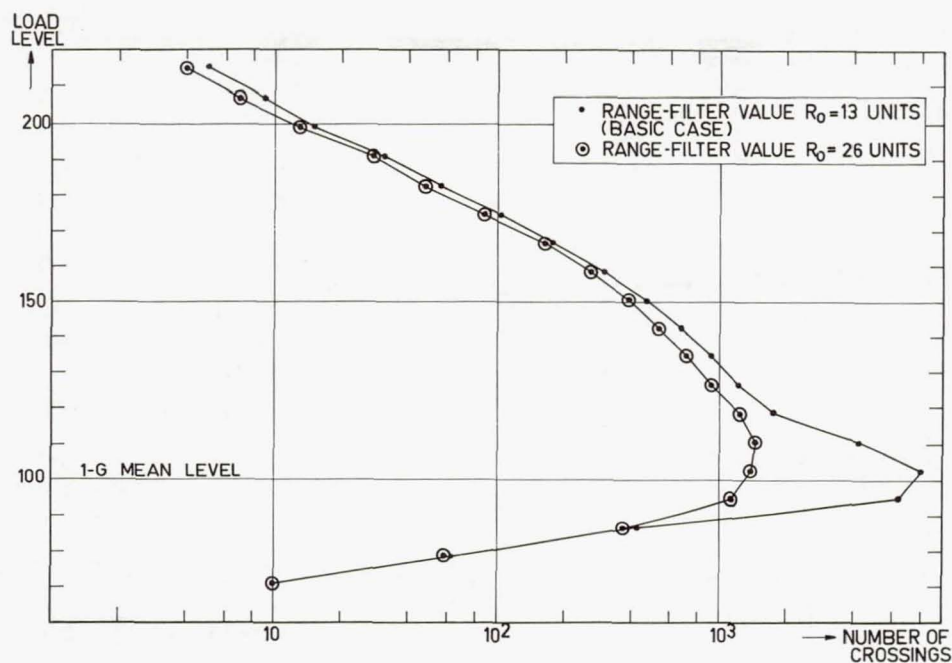


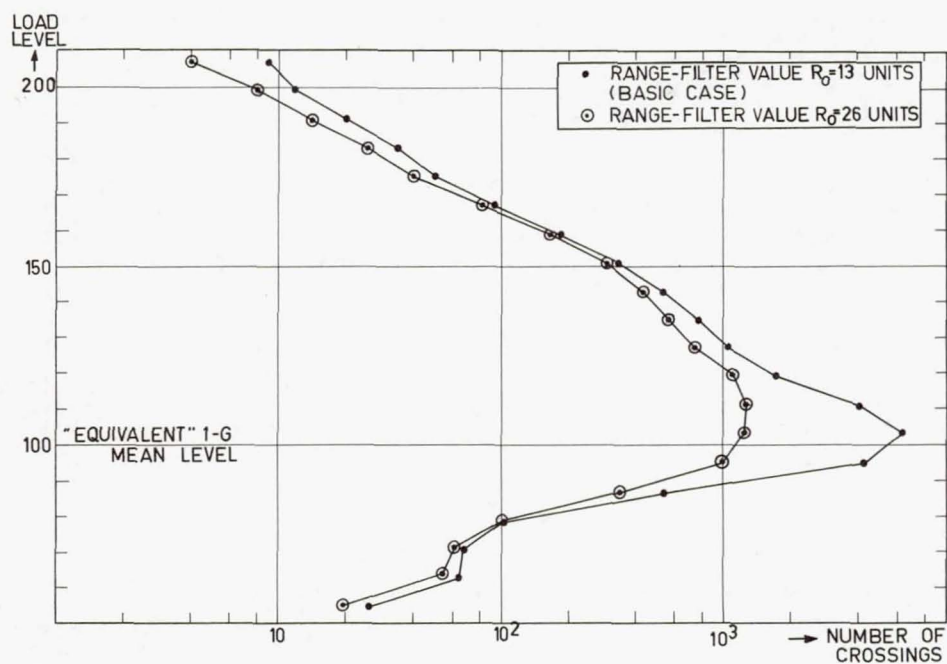
Figure 11.- Compressed load-time history of a typical fighter mission.





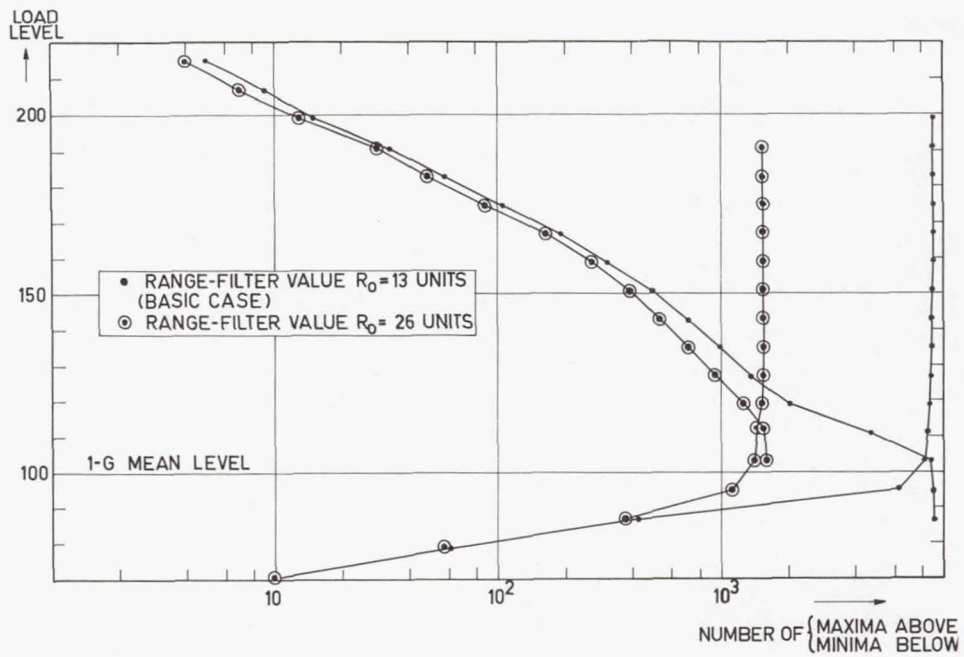
(a) Results for c.g. acceleration.

Figure 12.- Simple level-crossing counting results.



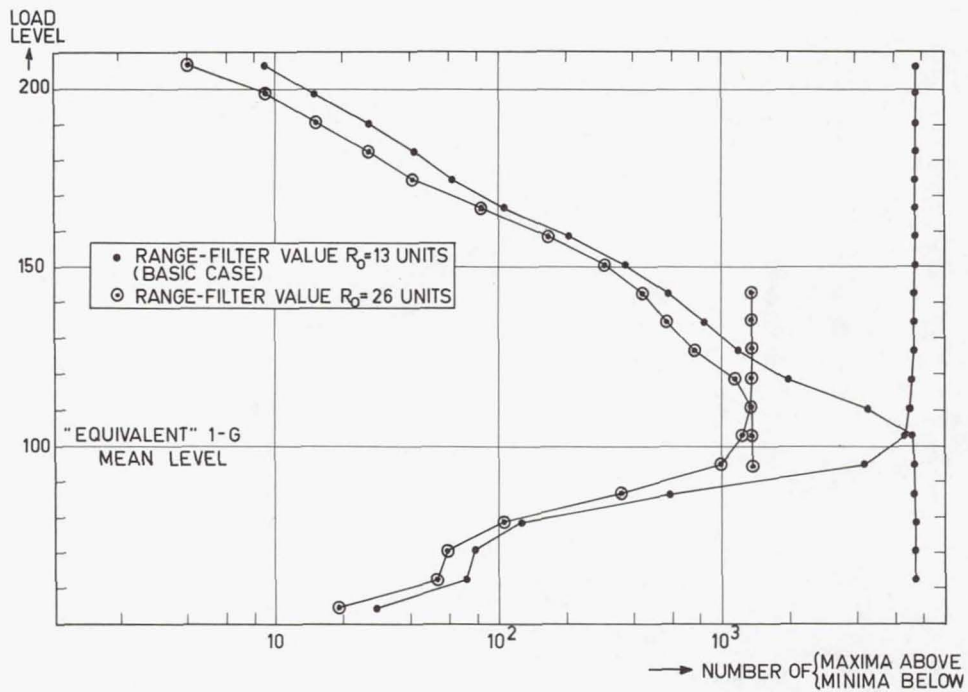
(b) Results for wing-root bending stress.

Figure 12.- Concluded.



(a) Results for c.g. acceleration.

Figure 13.- Simple peak counting results.



(b) Results for wing-root bending stress.

Figure 13.- Concluded.

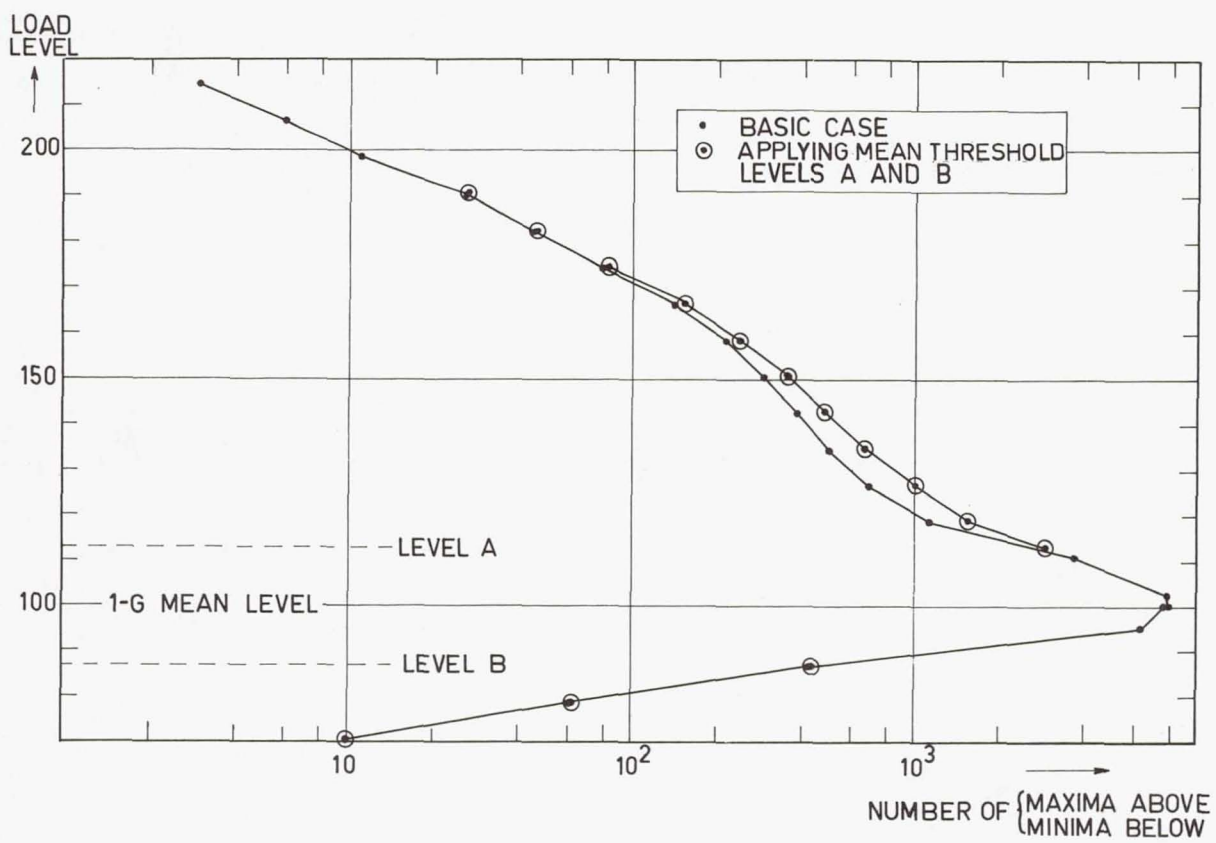
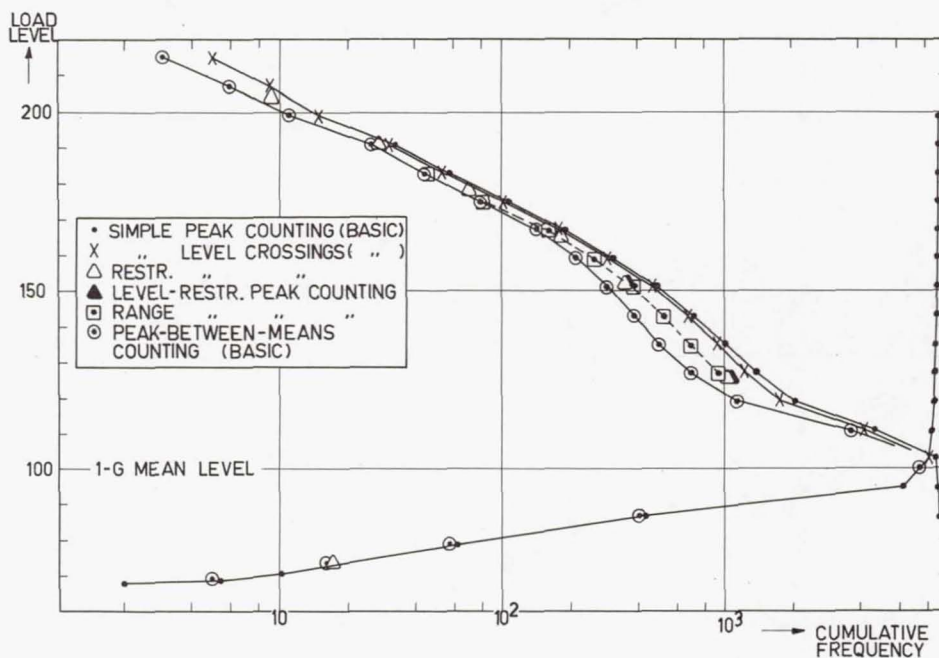


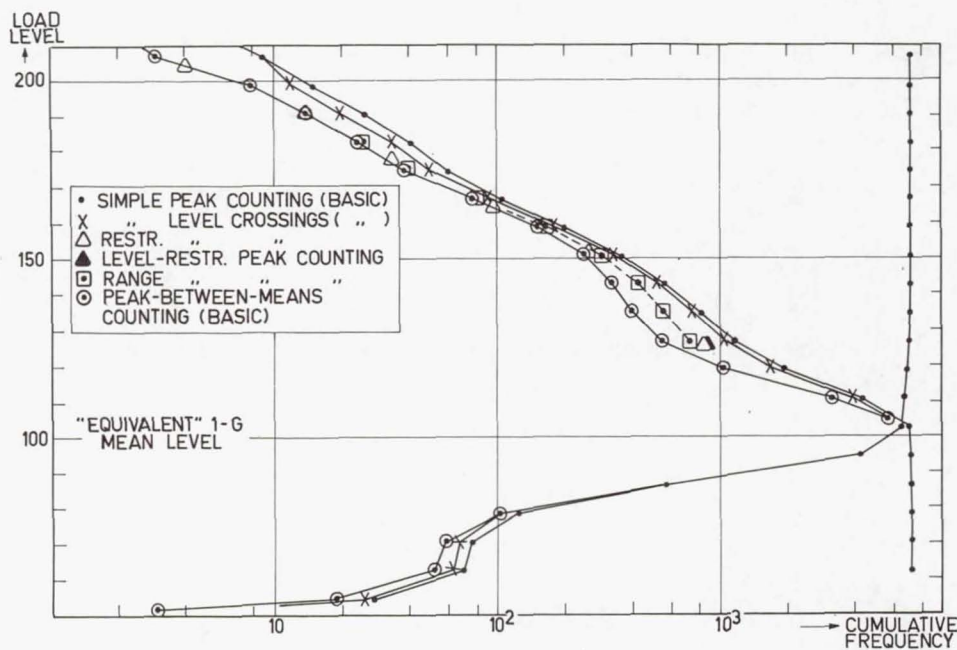
Figure 14.- Peak-between-mean-crossings counting results for c.g. acceleration.





(a) Results for c.g. acceleration.

Figure 15.- Comparison of level-crossing and peak count methods.



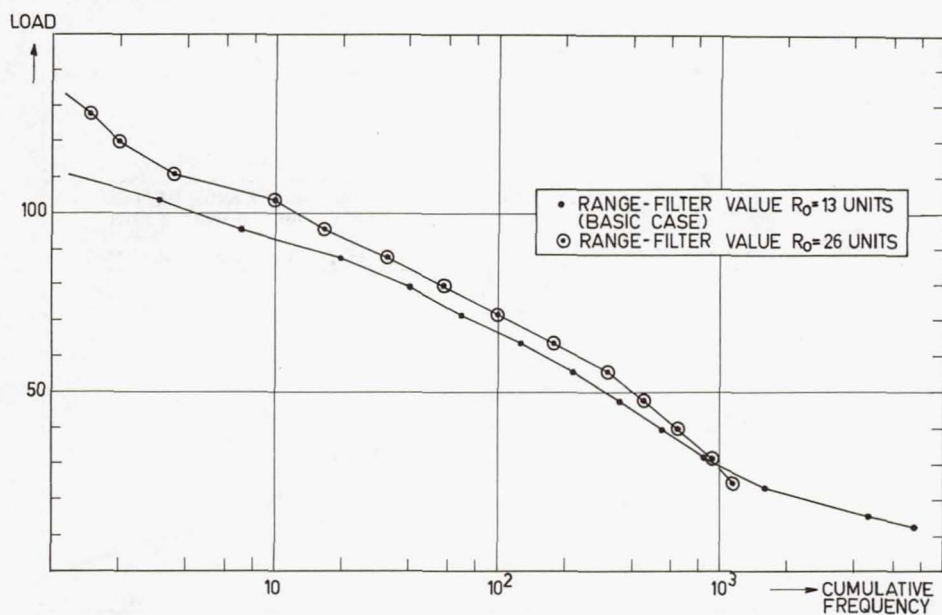
(b) Results for wing-root bending moment.

Figure 15.- Concluded.



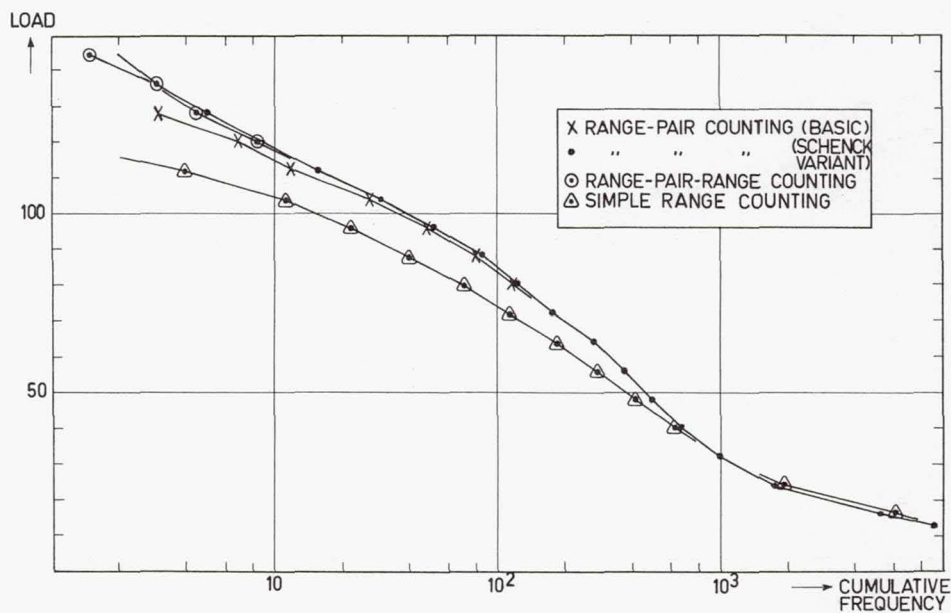
(a) Results for c.g. acceleration.

Figure 16.- Results of simple range counting.



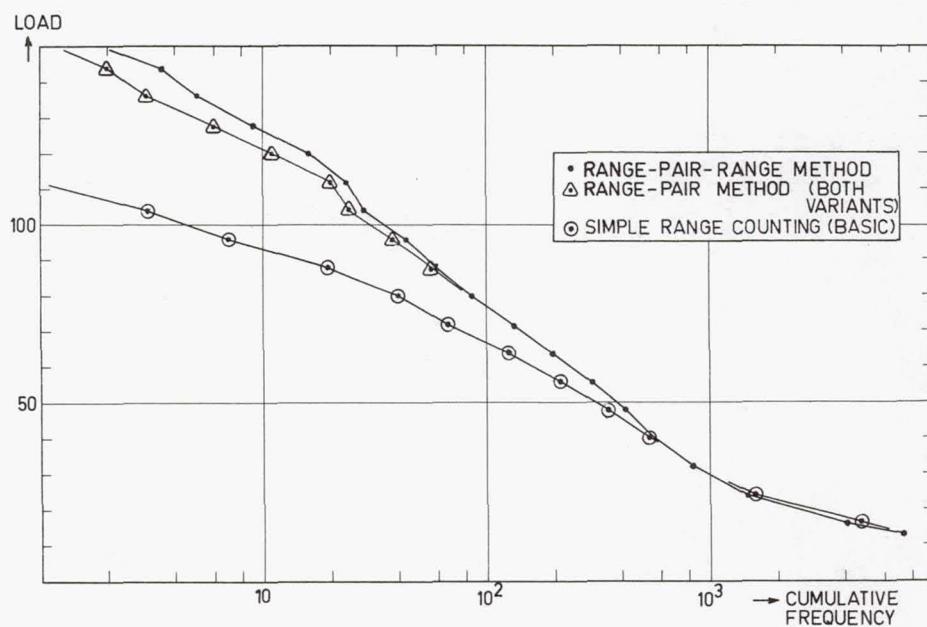
(b) Results for wing-root bending stress.

Figure 16.- Concluded.



(a) Results for c.g. acceleration.

Figure 17.- Range countings.



(b) Results for wing-root bending stress.

Figure 17.- Concluded.



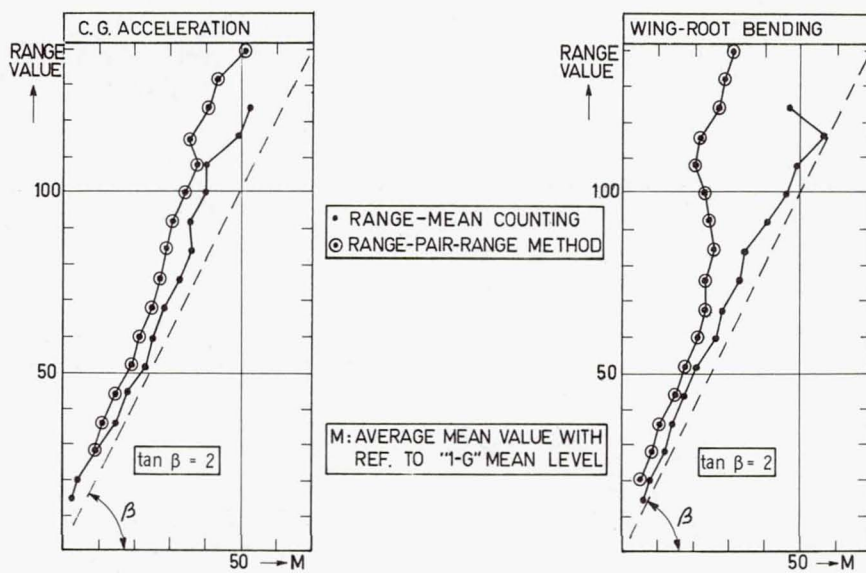
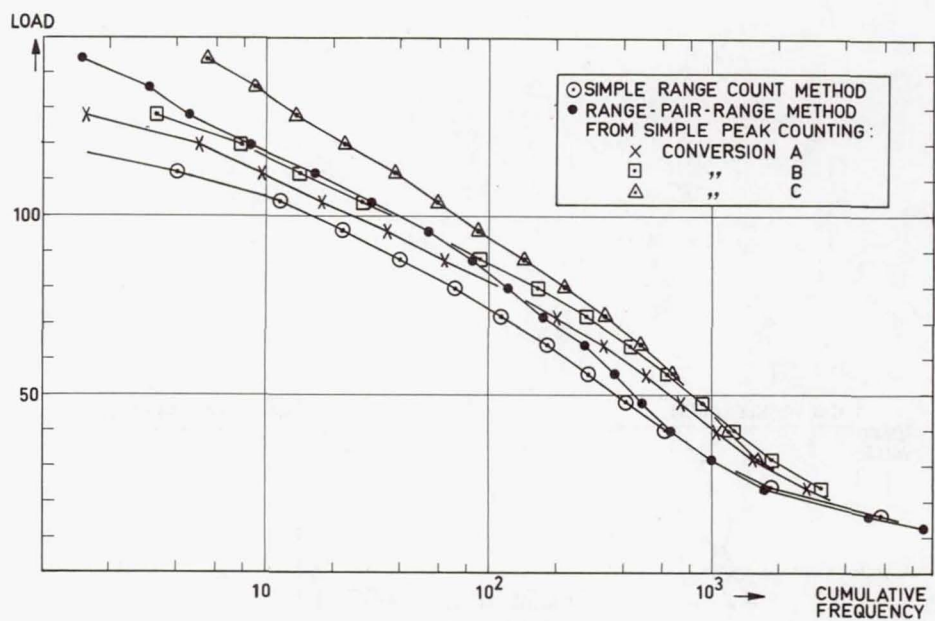
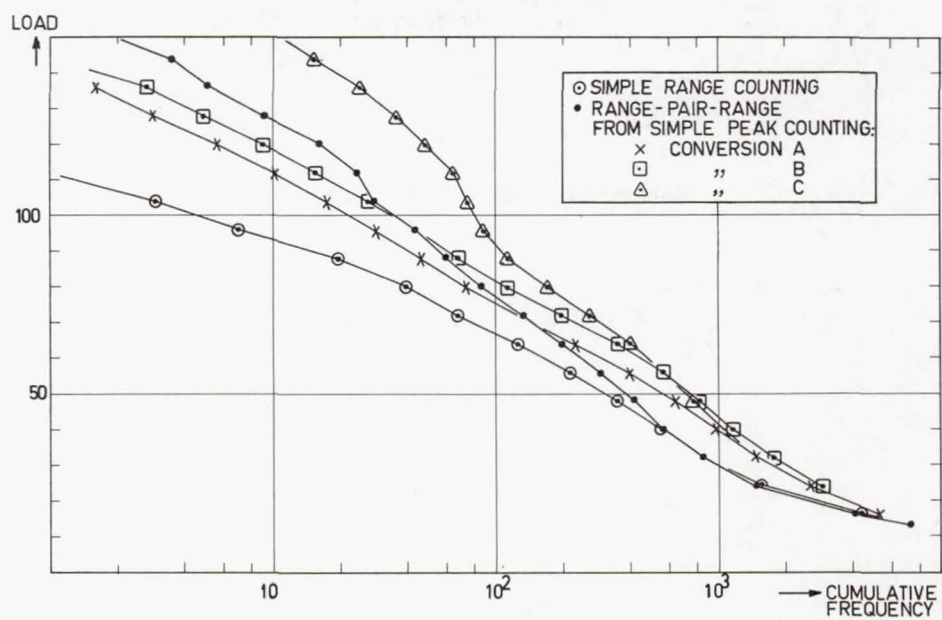


Figure 18.- Comparison of averaged means.



(a) Results for c.g. acceleration.

Figure 19.- Peak countings compared with range countings.



(b) Results for wing-root bending stress.

Figure 19.- Concluded.

## DETECTION OF STRUCTURAL DETERIORATION AND ASSOCIATED AIRLINE MAINTENANCE PROBLEMS

By H. D. Henniker  
British European Airways  
United Kingdom

and

R. G. Mitchell  
British Overseas Airways Corporation  
United Kingdom

### STRUCTURE INSPECTION

The requirement to operate a civil transport aircraft on scheduled operations for a period of perhaps 15 to 20 years, with a constant level of safety, creates a need for a system of continuous monitoring of the structure. At the same time it is implicit that no unnecessary work should be done and that the time out of service should be minimal.

It is perhaps necessary first to outline the approach to the maintenance and inspection of the components and systems of the aircraft. It has become apparent that most components, and therefore systems, suffer primarily from random effects. In a relatively few cases a life can also be dictated by a wear-out rate, but random defects predominate and have to be dealt with by inspections and functional checks so that the defect is detected at the earliest opportunity.

By duplication, or triplication, the integrity of the aircraft can be maintained, and the study of reliability levels can set the periods for inspection or checks which limit the period of dormant failure. Since a large number of components are functioned on each flight, the number of additional checks required to reveal a dormant fault is reduced.

It can be seen that for systems and components, the optimum periods for inspection, maintenance, and overhaul can be safely developed in respect of a particular aircraft type and a particular operation by a process of recording and analysing data on failures and strip reports and by general experience gained in service. The aircraft itself determines its own maintenance schedule.

In respect of structures, a different approach has to be adopted. With the advent of fail-safe structures, the duplication of load path which provides failure survivability has been achieved. Unfortunately, no ready indication of failure is available. The purpose of inspection is therefore to detect failures before they become catastrophic,



and to detect such deterioration with time and use which, in itself, will lead to failure. The object of maintenance is to restore the structure to its original condition and to maintain the failure survivability originally built into it.

It is natural that there should be a desire to use the same downtime of the aircraft to deal both with structure and systems. Improved component life and improved reliability lead to longer intervals between major maintenance inputs. There is therefore an inevitable clash of requirements because the structure tends to deteriorate with age and demands increased vigilance.

The structure inspection that emerges is therefore a compromise influenced by opportunity, and it changes with time. In deciding initially on the nature and extent of inspection, the design philosophy and the background of fatigue and fail-safe substantiation tests are of paramount importance. A structure inspection schedule for the lead fleet of a new type of aircraft is arrived at by extracting the structure content from the total schedule. A typical structure schedule is outlined as follows (in this schedule flight-hours and flights are approximately the same):

At each departure and at each 72 hours elapsed time: A general walk-around check which would detect gross damage, due to either serious structural failure or damage inflicted on the ground.

At each 300 hours or flights: A general visual inspection of the complete exterior, supplemented by opportunity inspection of such areas where access is required for maintenance and servicing. This check is also used to monitor any item on special surveillance.

At 2000 hours (12 to 15 months): A more detailed visual inspection of the lower fuselage, externally and internally, including pressure bulkheads, and door-surround structure. This is aimed primarily at detecting corrosion. Ultrasonic checks are also made at this interval on bonded stringers in the lower fuselage, and radiographic inspection is made in those areas of the lower fuselage not accessible for visual inspection.

At 5000 to 6000 hours or flights (2 to  $2\frac{1}{2}$  years): The major maintenance check in which all access panels are removed and all structure inspected visually. This represents the most detailed routine visual inspection of the structure possible by normal access, that is, without stripping out interior trim and lagging. At the same intervals – but not necessarily at the same time – radiographic inspections are made of closed structures such as

Horizontal stabilizer

Fin

Primary control surfaces

Slats, flaps, airbrakes, and so forth

All these inspections are carried out on all aircraft in the fleet. The extensive areas of the internal structure of the upper fuselage (above floor level) are the subject of a sampling procedure. This approach is made because of the extensive downtime involved if all trim, soundproofing, thermal lagging, air ducts, and so forth are removed. Experience has shown that the area below floor level is that most prone to corrosion. This can occur early in the aircraft life and can progress relatively rapidly. Experience also suggests that the upper areas dry out more rapidly, and corrosion is only likely at a later stage and will develop less rapidly.

The sampling programme is therefore started in about the 5th year of operation (10 000 to 12 000 hours). Because of the large work load and downtime involved, radiographic inspection is used extensively but is supported by visual inspection as follows: In each of the 5th, 6th, 7th, and 8th years of operation, one composite aircraft is examined, 25 percent by visual means and 75 percent by radiographic means. The samples involve not less than 60 percent of the fleet, and at the end of this period one complete composite fuselage will have been examined visually; and three, radiographically. It is planned that after the 9th year the sampling will be extended so that by the 20th year all aircraft in the fleet will have been examined completely both visually and radiographically.

The choice of inspection method is basically economic. Where visual inspection is viable, it is preferred. Radiography is an adequate tool to detect the significant cracking of internal structure such as frames, stringers, and cleats. It can also indicate corrosion and paint flaking – but requires considerable skill in interpretation. A 10-percent reduction in material thickness can be reliably detected, provided the corrosion deposits are not retained. The critical corrosion along the heel line of a stringer or lap joint is detected mainly by evidence on the adjoining surface.

In a particular case where this inspection schedule has been applied up to an average aircraft life of 12 000 flights or 6 years, 38 defects have been identified. Of these, 16 involved fatigue cracks, in secondary structure, and two involved corrosion in primary structure. Most of these defects were detected on the major check. In the period concerned, the major check period has been progressively increased from 3000 to 5000 hours, or flights, on the basis that those items which have shown up and are not subject to modification action are retained as specific items on the annual or 300-hour inspection.

For detection of deterioration that could be the cause of fatigue, this increase in the major check period is feasible. If, however, the major check is to form the basis for detection of fatigue cracks concerned with the fail-safe design concept, then the period between inspections must have some finite limit. This should be the interval assumed in the design concept from first detectable crack to the point at which crack propagation reduces the static strength to proof load. Ideally, this should be demonstrated by a full-scale test for all fatigue-critical regions of the structure. For the aircraft concerned



the period is not less than 5000 flights, with proof load applied each 2500 flights. On this basis each aircraft structure must be examined in detail at maximum intervals of 5000 flights. It might well be argued, however, that when the aircraft life is relatively low, so that this interval represents a significant part of the probable scatter between identical failures on aircraft of the same fleet, then staggered inspection over a longer period is perhaps justified on the basis that no cracked aircraft will fly more than 5000 flights before the defect is detected in another of them. It is implicit that all aircraft will be checked within a short period from the discovery of the first defect.

As the aircraft life increases, so that the safe period of crack propagation becomes small in relation to the probable scatter in failure, the inspection would have to be increased to cover each aircraft in 5000 flights. As the aircraft life increases still further so that the probability of failure is high and simultaneous failures become probable, it would be prudent to reduce the inspection interval.

Finally, it would seem logical that whilst the ratio of test life to aircraft life is 5 or more, inspection can be done on a sampling basis only, to assess the general deterioration, such as corrosion. Thus, an ideal structure inspection schedule would result and would be based on aircraft life and test life. (See fig. 1.) The practical problem would then be to integrate this schedule with the remainder of the maintenance requirements and the seasonal demands on aircraft.

If there are several operators involved in making up a significant fleet of "lead" aircraft, there is a case for spreading the initial sampling across all the aircraft to thus reduce the requirement on the individual operator. This involves a reporting system so that the manufacturer can coordinate results. There are possibly limitations to this approach, since each operator tends to operate on a different route structure and in a different environment.

Most aircraft types operated by British European Airways (B.E.A.) have carried some form of in-flight recording equipment, either fleetwise or on selected aircraft. In some cases this has been a condition in the terms of the warranty on the fatigue life of the primary structure. The recording equipment has fallen into two categories:

- (1) Continuous recording of acceleration thresholds or strain-range thresholds on entire fleets
- (2) Continuous recording of acceleration thresholds together with other flight data on a limited number of aircraft

In the first category, counting accelerometers mounted at the center of gravity record threshold counts at increments of 0.2g between 0 and 2g. Total counts in each level are read and recorded at each 300-hour check.



Fatigue-meter data are fed back to the respective manufacturers at intervals, together with operational data from which a typical flight plan, representative of the route network, can be deduced. This is done by taking significant samples of summer and winter operations and includes take-off weight, fuel state at take-off, cruise altitude, and flight duration. Fuel burn-off is computed and thus actual weight and fuel state at each phase of flight are deduced. The aircraft manufacturer then computes fatigue damage rate and compares this with the damage rate used in the fatigue test or calculated fatigue life.

Similar procedures are adopted in the case of strain-range counters, except that these give a more direct indication of damage rate and require less operational data.

In both cases the manufacturers concerned have stated that an increase in service life of up to 30 percent has been possible compared with the service life that would otherwise be imposed. So far, this has all been in respect of those parts of the structure which are on a "safe life" basis.

Both these types of recording instrument are such that they are quite practical for an airline to carry on all aircraft. They need little attention and are reasonably reliable. As long as there are safe-life items in the primary structure, the improvement in life that has been possible would appear to be adequate return.

The more comprehensive type of observer unit is more questionable. Attempts have been made on two types of aircraft to get a simultaneous record of acceleration counts, speed, height, time of flight, and so forth by use of film recorders, switched on at take-off and off on landing by an airspeed switch. They have been installed in perhaps two aircraft of a new fleet with the object of obtaining more complete data for an initial period. The problems with film recorders have been

- (1) Short duration of film leading to either much lost recording time, or very frequent film changes
- (2) Unserviceability revealed only after film development
- (3) Reference still required to flight documents to obtain aircraft weight and other data
- (4) Low order of reliability

The authors have found from experience that only about 10 percent of the total hours flown by the aircraft equipped with the film recorders were satisfactorily recorded. It does not seem practical to use this type of equipment in the environment of day-to-day airline operation.

It has been B.E.A. policy to record manually maximum cabin differential pressures for each flight on all aircraft. The pilot records this in an appropriate box in the techni-

cal log. This information is extracted and the total flights in each band of pressure, in increments of 1/2 psi, are computed. Where there are maximum lives prescribed for modification or replacement of structure, this information is forwarded to the manufacturers and to the airworthiness authorities at six monthly intervals. All unrecorded flights are assumed to be at maximum differential pressure, and a factor of 10 percent is added to the recorded pressures to allow for inaccuracies of recording. At the same time, the equivalent flights at maximum differential pressure are computed and forwarded to the inspection department to allow mandatory life requirements to be monitored.

This policy has yielded significant benefits where safe-life situations have existed. It allows advantage to be taken of all flights where only low pressures are needed, yet retains the advantage of operational flexibility, such as cruise altitude on longer flight sections and occasional high rates of descent. This flexibility is otherwise lost if pressure is permanently reduced. On one type of aircraft it has allowed an extension from 12 500 to 30 000 flights before a major modification, with its accompanying weight penalty, was required and from 17 000 to 50 000 flights before wholesale replacement of fuselage skins.

It is true to say that the advantages so far gained by continuous recording in airline operation have all been associated with safe-life structure situations. It is questionable whether real advantages can accrue in the case of a truly fail-safe structure. One of the advantages, to the manufacturer, of a fail-safe philosophy is that the duration of the full-scale test can be reduced. If the structure is designed for a long fatigue life, it is probable that natural failures will not be produced on test. Provided adequate fail-safe tests are carried out, this may be satisfactory from an airworthiness point of view, but it would seem pointless, in this case, to try and correlate test and actual aircraft usage in order to try and predict the operator's long-term planning requirements.

Only if full-scale testing is extended until fatigue failures occur – and perhaps only if these then indicate the need to impose a finite life when action must be taken – can better data on actual aircraft usage yield some dividends.

## MAINTENANCE ASPECTS

It will be appreciated that although the modern public transport aircraft is a highly complex and sophisticated engineering product, it is also the means by which the airlines earn their revenue. The aircraft utilisation rate, which varies during the year and reaches its peak during the summer months, is laid upon a foundation of known work programmes which stipulate that various aircraft will be undergoing maintenance for block periods of time during the year. It will be seen, therefore, that in order to support the commercial plans, an extremely well-devised maintenance programme is required. For



an airline to operate at optimum efficiency, the maintenance programmes are planned to ensure that the work requirement is matched by the necessary spares, materials, tools, equipment, and labour at the commencement of the hangar check.

The unexpected and nonscheduled problem is, therefore, strictly an economic embarrassment. The discovery of a fatigue crack, corrosion, or any of the other mechanical faults which beset airline operators from time to time and which must be repaired on an urgent basis are the ones which really cause the headaches.

Ideally, the airline engineering base should be a facility carrying out planned maintenance and changing or repairing wornout components. This is, of course, an ideal situation which never exists in practice. For instance, a piece of ground-support equipment could be run into the side of an aeroplane and thus cause a delay to the service. Similarly, the work necessary to repair the unexpected crack in a major piece of structure can soon seriously upset the best planned engineering commitment and rapidly lead to nonavailability of aircraft.

It must also be remembered that there will be an internal conflict of interests within the airline. The production and maintenance departments are charged with producing aeroplanes for service to meet the commercial demands, and an engineering requirement which may extend the hangar check times or takes aircraft out of service is resisted, unless vital to continued safe operation. Also, since modern aircraft construction is making ever-increasing use of integrally machined components, which in themselves are much more difficult to repair in terms of time and complexity than the riveted skin-stringer combination, it also follows that the flow of spare parts from the manufacturer in the event of a rash of fatigue problems across the fleet could be inadequate to meet the demand.

All aircraft exhibit cracks in various structural components. Many of these, having relieved a local stress condition, will then remain static in length for a considerable period of time, and the aircraft will continue in service with these known defects. Normally such defects are examined for signs of propagation at each scheduled inspection until the part can be replaced or repaired, ideally at a convenient hangar check. This applies mainly to multi-load-path and secondary structure, but of course all cracks and defects are evaluated and a course of action decided upon which is dependent upon the significance of the defect. In the case of more serious defects the normal procedure is to raise a special check on the remainder of the fleet to determine the extent of the problem fleetwise. The speed at which the fleet examination takes place, of course, depends upon the severity of the initial defect. In this way the extent of the problem is assessed and the final action will take the form of a modification or repair, which can be raised either by the airline or manufacturer, or by replacement on a life basis. In many cases the defect is subsequently monitored by the addition of a specific item to the approved



maintenance schedule for inspection at appropriate intervals, or included in the reportable structural inspection programme.

In the case of a repair, the structure is usually returned to the "as new" condition, but when this is impractical or economically not justified, the fatigue life of the repair must at least match the residual life of the aircraft. In many cases when extensive testing or investigation of a fatigue problem is required, it may be necessary to incorporate a temporary repair which satisfies limit loads and thus keeps the aircraft flying. The long-term action which may require a slightly more extensive repair can then be carried out at a later stage, usually at a major overhaul. It has been found from experience that the manufacturer's solution to most light-alloy fatigue failures invariably results in a steel replacement.

Once a defect is found, a repeat inspection of the area is established, which can be extremely frequent in serious cases. The general accessibility and nature of the defect will determine the method of inspection, that is, visual or nondestructive testing techniques. In any event the general aim is to implement modification-campaign action to eliminate the defect and its associated inspection.

When a new defect is found, the airline informs the manufacturer, who then advises all operators of similar equipment to inspect for that particular defect. The manufacturer's notification usually ranges from a newsletter covering general advice, the service bulletin which forms the usual channel of communication, to the service cable for serious problems which require rapid investigation.

Since fatigue failures are generally related to total flying hours or landings, it follows that an airline operating "young" aircraft is less likely to be hit by the nonscheduled problem than an operator with older aircraft of the same type, and has a better chance of carrying out the rectification on a planned basis.

A large number of fatigue problems encountered can be traced to detail design faults, and occasionally the classic "don'ts," such as sharp section changes and stress raisers, still seem to be perpetuated.

It has been found from experience that unnecessary disturbance of an area during maintenance can in fact be detrimental in the long run. For example, abrasion of surfaces can break down sealants, particularly in integral fuel tanks, and minute scratches are then susceptible to corrosion or crack initiation.

The Corporation is an approved design organisation and designs and incorporates a great deal of repair work, particularly to components. For example, the Corporation has a great deal of experience on the repair of honeycomb structures. Any repair work must maintain the aircraft to airworthiness requirements. This, of course, includes correct heat-treatment techniques, particularly with the high-strength steels, and maintenance



of adequate strength reserves after such rework. A copy of the repairs is automatically sent to the manufacturer for his information, but naturally in the event of serious problems the manufacturer is consulted prior to making the repair.

Although the primary airframe structure, critical joints, representative panels, and the like are subjected to extensive fatigue testing at the design and construction stage to prove the integrity of the basic airframe, secondary structure does not receive the same consideration. Experience shows that defects in secondary structure tend to be repetitive and are both costly and time consuming to repair or replace. For example, certain areas of most aircraft floors require frequent replacement because of corrosion under and adjacent to galley and toilet areas and for damage due to cargo loading and repeated walking traffic. It would seem that the original floor is largely designed by static load requirements on the grounds that a stronger and longer lasting floor, because of the weight penalty incurred, is not justifiable on economic grounds. This, of course, is all good theory, but replacement floor costs are extremely high. Because of the absence of reliable fatigue data on floor materials, various sandwich floor-panel materials were investigated on a cost-effective basis which involved static testing and fatigue testing a large number of samples. In fact, representative panels of various materials have been installed for service evaluation. The airline is, of course, ideally suited to perform actual in-service tests, and new ideas are often subjected to field tests in a true operational environment. Although in the manufacturer's initial fatigue test every attempt is made to represent a true operational condition, it sometimes happens that despite the best efforts of the designer, a part will fail prematurely because of the influence of a secondary unknown or neglected loading system. A case in point recently occurred when a fairly substantial shear angle hidden from immediate view was found to have cracks of considerable length along the bend radius. On investigation the fracture face showed that the angle, which had been designed to carry shear loads, was in fact also being subjected to secondary bending loads which tended to open and close the angle. Fortunately, in this case, the cracks were found before a failure occurred.

Another example in which the initial design failed to take complete account of the full loading cycle is the fatigue cracks experienced in top wing skins of some aluminium alloys containing a high percentage of zinc. The alloy is chosen in the first instance because of its mechanical properties and because the normal flight loads give a compressive loading. It has been established, however, that the ground loads, which reverse the wing bending system, cause tensile loads of sufficient magnitude to cause fatigue cracks around stress concentrations, fastener holes, for example, in this material.

One interesting case of structural failure occurred when the designer had assumed a certain airspeed for flaps extended for his fatigue analysis within the flaps-out speed range. The pilots, however, were in fact flying the aircraft right up to the flap limit speed, and premature failures occurred. Another problem which occurred was that in

the original design certain assumptions were made with respect to ground turns based upon airports known at that time. Subsequently the Commercial Department decided that a great deal of revenue was forthcoming from lesser known airports, and ground manoeuvres in excess of the assumptions were made. Airports are very congested places on the ground as well as in the air, and ground turns can be dictated by available ground space.

An aspect of airline usage which is outside the normal operating pattern is crew training. It is quite normal for one aeroplane to spend a considerable time on a training detail, and this operation sometimes results in flying techniques which are not up to normal standards. The number of landings are very considerable over a short period of time and since one of the objects of the exercise is to acquaint flying crews with aircraft-handling characteristics which are seldom met in practice, the airframe is subjected to a great number of loads which are not normally met in passenger service. These facts must be recognized at the design stage. Airframe damage has, in fact, resulted from training details.

Civil aircraft are in service for a considerable period of time, some 15 years or more typically. Airframe lives on the order of 60 000 flying hours are commonplace with the current generation of aircraft, and of course the fatigue problem intensifies as the aircraft get older. The economics of airline operation is such that operators are carrying out life-extension programmes in order to achieve these lives by replacing and/or reworking critical areas at some stage during the service life of the aircraft. It is vital, therefore, that the initial assumptions, analysis, and testing faithfully represent as far as possible the complete loading programme and its environment, and that the effect of new materials is fully examined, particularly where no previous experience is available.

Each new generation of aircraft brings a new challenge both to the operator and manufacturer, and the SST will be no exception. The operator must rely on the manufacturer to provide a trouble-free product, and to this end, practical airline experience of day-to-day operational problems and practices is freely available. Operational experience should be fed back into new designs to ensure long, trouble-free lives, particularly at the detail design stage.

The addition of speed and temperature will bring new complications to the SST. It is to be hoped that the racehorse will not exhibit the temperament of a thoroughbred but will retain the cart-horse stamina for everyday reliability.



# SUGGESTED BASIS OF MAJOR STRUCTURE INSPECTION

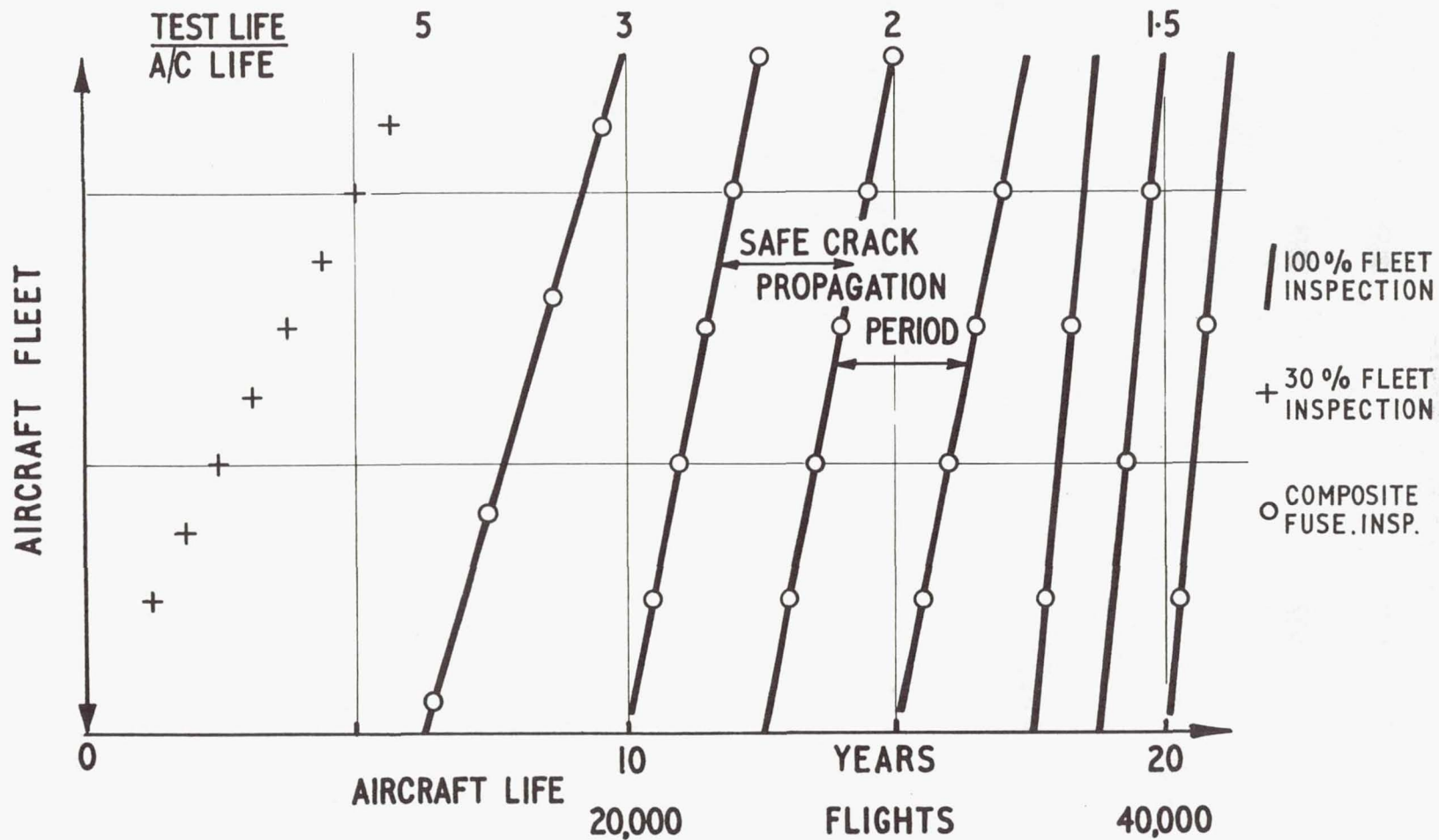


Figure 1.

N72-29914

FATIGUE FAILURE OF METAL COMPONENTS AS A FACTOR  
IN CIVIL AIRCRAFT ACCIDENTS

By William L. Holshouser and Ruth D. Mayner  
National Transportation Safety Board  
Washington, D.C., U.S.A.

SUMMARY

A review of records maintained by the National Transportation Safety Board showed that 16 054 civil aviation accidents occurred in the United States during the 3-year period ending December 31, 1969. Material failure was an important factor in the cause of 942 of these accidents. Fatigue was identified as the mode of the material failures associated with the cause of 155 accidents and in many other accidents the records indicated that fatigue failures might have been involved. There were 27 fatal accidents and 157 fatalities in accidents in which fatigue failures of metal components were definitely identified.

Fatigue failures associated with accidents occurred most frequently in landing-gear components, followed in order by powerplant, propeller, and structural components in fixed-wing aircraft and tail-rotor and main-rotor components in rotorcraft.

In a study of 230 laboratory reports on failed components associated with the cause of accidents, fatigue was identified as the mode of failure in more than 60 percent of the failed components. The most frequently identified cause of fatigue, as well as most other types of material failures, was improper maintenance (including inadequate inspection). Fabrication defects, design deficiencies, defective material, and abnormal service damage also caused many fatigue failures.

Four case histories of major accidents are included in the paper as illustrations of some of the factors involved in fatigue failures of aircraft components.

INTRODUCTION

Civil aviation accidents in the United States were investigated by the Civil Aeronautics Board from 1940 until 1967, when the National Transportation Safety Board was established as an independent agency within the Department of Transportation. On April 1, 1967, the safety functions of the Civil Aeronautics Board, including the responsibility for investigating and determining the cause of civil aviation accidents, were transferred to the new Safety Board. Hence, the information on accidents used in the preparation of this paper was taken from records and files accumulated partly by the



Civil Aeronautics Board (CAB) but now maintained by the National Transportation Safety Board (NTSB).

An aircraft accident is defined in NTSB Regulations as "an occurrence associated with the operation of an aircraft which takes place between the time any persons board the aircraft with the intention of flight until such time as all such persons have disembarked, in which any person suffers death or serious injury as a result of being in or upon the aircraft or by direct contact with the aircraft or anything attached thereto, or the aircraft receives substantial damage." The Board regulations also contain definitions of terms, such as "serious injury" and "substantial damage," that form a part of the definition of an accident. During the last 10 years (1960-1970) the number of civil aircraft accidents per year meeting this definition has ranged from 4709 in 1961 to 6185 in 1967. More than 98 percent of these accidents were in general aviation, which, of course, means that, in general, they involved relatively small aircraft engaged in private flying, business trips, and small commercial operations.

Information on the extent to which fatigue failures in metal components are involved in the cause of accidents was obtained by reviewing accident records and laboratory reports that are available in Safety Board files. The accident records provided considerable data on material failures but did not provide statistically reliable information regarding either the mechanism or cause of failure. Hence, the data presented under the heading of "Accident Records" is included primarily as background information for the results of the study of laboratory reports. Four case histories of major accidents are presented as illustrations of some of the factors that are involved in fatigue failures of aircraft components.

### ACCIDENT RECORDS

There were 16 054 civil aviation accidents in the United States during the 3-year period between January 1, 1967, and December 31, 1969. NTSB records show that material failure caused, or was a factor in the cause of, 942 of these accidents. Thus, material failure was involved in the cause of slightly less than 6 percent of the total number of accidents during this period. Only 20 of the 942 material failure accidents occurred in air carrier operations.

Fatigue was identified as the mode of material failure in 155 accidents. There were many other accidents in which fatigue failures might have been involved but the fractures were not identified as fatigue in the record. For example, there were a number of in-flight failures of propeller blades and many cases of connecting rods, connecting rod caps, or connecting rod cap bolts failing in reciprocating engines in which the mode of failure was not identified. It seemed likely that in many cases the investigator may



have been unable to recognize evidence of fatigue or that such evidence might have been destroyed by subsequent damage to the fracture surfaces.

Information obtained from the accident records is summarized in tables 1 and 2. The serious nature of fatigue failure accidents is shown by the fact that the 16.4 percent of the material failure accidents in which fatigue failures were identified accounted for 31 percent of the aircraft that were completely destroyed, 46 percent of the fatal accidents, and 63 percent of the fatalities.

There may be some inaccuracies in the classification of components in table 2 because the specific part that failed was not always adequately identified in the record. For example, a few parts listed as landing-gear components might actually be parts of the hydraulic system or some parts listed under powerplants might be more properly identified as electrical system components. However, the general trend of component failures shown in the table indicates that landing gears and powerplants are major problem areas.

The records from which the data in tables 1 and 2 were obtained did not provide any significant amount of information regarding the basic cause of failure except in one category. Definite evidence of improper maintenance or inadequate inspection was found in 130 accidents, whereas there were indications that many other accidents might have been prevented by better inspection and maintenance procedures.

The number of accidents listed in the tables, of course, represent only a small percentage of the total number of material failures in civil aircraft. Most of such failures do not result in accidents and the failed components are replaced or repaired on a more or less routine basis.

## LABORATORY REPORTS

Additional information regarding the mechanisms and causes of aircraft material failures was obtained from a study of 230 laboratory reports on the examination of failed components. These were reports on work done in the Safety Board's laboratory, work done for the CAB and the Safety Board at the National Bureau of Standards, and a few reports from industry laboratories. All the reports were on components from aircraft that had been involved in accidents between 1962 and 1970. Reports on failed components that were not pertinent to the cause of an accident were eliminated from the study insofar as possible.

A summary of the results of the study is given in table 3. In classifying the causes of failure, fabrication defects were listed as such only when they appeared to have been caused by a manufacturing operation. When this kind of deficiency occurred during maintenance, the cause of the resulting failure was classified as "improper maintenance."

The "abnormal service damage" category includes only failures caused by service damage that probably would not have been detected by normal inspection procedures. The cause of failure was listed as improper maintenance if it appeared that the service damage could have been found and repaired prior to failure by ordinary good maintenance practice. As anyone who has been involved in the investigation of service failures will realize, the evidence regarding the cause of failure was not always conclusive. In many of the cases studied, some element of judgment entered into the classification. Stress corrosion and hydrogen embrittlement failures were grouped together in the table because, in some cases, reports of studies of the fracture surfaces with an electron microscope identified the fractures as "stress corrosion or hydrogen embrittlement" but did not attempt to distinguish between the two failure mechanisms.

Fatigue failures accounted for more than 60 percent of the failed components on which laboratory reports were available in NTSB accident files. The distribution of fatigue failures among the causes listed in table 3 illustrates one of the major difficulties of preventing such failures in aircraft. So many different kinds of material defects, design errors, mechanical damage, and corrosive attack can contribute to the cause of fatigue failures that it is extremely difficult to guard against all of the possibilities. As in the review of accident records, the results of the study of laboratory reports indicated that improper maintenance is the most frequent cause of fatigue and other types of material failures that contribute to the cause of aircraft accidents.

Specific causes of failure included in each category in table 3 are as follows. (No attempt was made to list these causes in order of frequency of occurrence. The exact number of failures due to each specific cause could not be determined because in many cases the failure could be placed in one of the broad categories but the cause could not be more specifically defined, mainly because of discrepancies in maintenance records, inconclusive results of laboratory work, and more than one factor being involved in the cause of failure.)

Improper maintenance:

- Inadequate inspection

- Failure to replace damaged parts

- Failure to comply with manufacturer's service bulletins or FAA Airworthiness Directives

- Inadequate lubrication

- Failure to service air drying system

- Unsatisfactory welding

- Inadequate shot peening

- Failure to repair damaged protective coating

- Inadequate or excessive torque applied to fasteners

- Failure to install fasteners



- Use of unsatisfactory replacement parts
- Inadequate cleanup after repairs
- Foreign material left in gear housing
- Improper alteration of components
- Surface damage due to misuse of tools
- Inadequate control of plating operations
- Grinding cracks
- Application of excessive force to press fits not adequately prepared for assembly
- Improper adjustment of gear engagement
- Insufficient thread engagement
- Damage from misuse of inspection equipment

Design deficiencies:

- Inaccurate stress analysis (mainly due to insufficient consideration of sources of stress concentration)
- Inadequate specification of dimensional tolerances
- Failure to allow for fabrication and assembly variables
- Selection of unsuitable material or incompatible combinations of material
- Insufficient consideration of the effect of possible bending loads on parts designed to resist tension or compression loads
- Insufficient consideration of the direction of grain flow in forgings and extrusions
- Insufficient consideration of maintenance problems
- Failure to specify adequate decarburization limits

Fabrication defects:

- Machining errors
- Unsatisfactory welding or brazing
- Unsatisfactory plating
- Improper drilling of rivet holes
- Surface damage by defective tools
- Damage by careless use of tools
- Failure to remove cleaning solution from a closed cavity
- Inadequate cleaning after an internal machining operation
- Inadequate control of bonding operation

Defective material:

- Surface decarburization
- Heat treating cracks
- Omitting heat treatment or surface hardening operation
- Forging flaws
- Defective extrusion bonding
- Overheating during heat treatment



- Casting porosity or cracks
- Excessive nonmetallic inclusions
- Gas contamination
- Failure to use specified material

Abnormal service damage:

- Engine overspeed
- Excessive vibration
- Failure of pilot to follow operating instructions
- Inadequate securing of cargo
- Unauthorized towing procedures
- Excessive maneuvering loads
- Deformation from undetermined source
- Bird strike
- Excessive loads resulting from damage to an associated component

## DISCUSSION

The results of the studies summarized in this paper emphasize the importance of fatigue and maintenance problems in the operation of aircraft equipment. By far the most common type of material failure encountered in aircraft accident investigation is in landing-gear and powerplant components of small fixed-wing aircraft. Material failures most frequently cause accidents when they occur while the aircraft is airborne or during landing, although serious accidents may result from failures during any phase of operation.

Opportunities to reduce the number of accidents caused by fatigue failures and other types of material problems exist in almost all phases of aircraft construction, maintenance, and operation. The greatest potential for reduction in the number of accidents is in improving the maintenance of general aviation aircraft. However, numerous accidents in both general aviation and air carrier operations could be prevented by improvements in design; better quality control during material processing, fabrication, and assembly; improved inspection and maintenance programs; and more careful handling of aircraft, particularly on the ground during taxiing and towing operations.

Although the air carriers have had relatively few accidents caused by material failure, in the 3-year period included in the review of accident records, 6 of the 20 air carrier accidents in which material failure contributed to the cause resulted in 138 fatal injuries. Accidents involving fatigue failure accounted for 103 of these air-carrier fatalities. In several failures of landing-gear components and jet engine compressor and turbine disks, major disasters were avoided only by fortunate circumstances. Thus, this study indicates that air carrier, as well as general aviation, aircraft have serious material failure problems.

## CASE HISTORIES

Four case histories of accidents due to fatigue failures of components are presented.

### I. Los Angeles Airways, Sikorsky S-61L Helicopter; Compton, California; August 14, 1968

This helicopter crashed when a fatigue failure of one of the main rotor blade spindles caused the blade to separate from the rotor hub. The drawing of the failed spindle in figure 1 shows the location of the fracture. A fatigue crack had propagated from a single origin (fig. 2) in the journal-bearing fillet through approximately 70 percent of the cross section of the spindle shank prior to complete failure. The spindle was made of quenched and tempered 4340 steel, with a specified hardness of 34 to 38 Rockwell C and a specified minimum ultimate tensile strength of 150 000 pounds per square inch. This spindle had been reworked in 1966, 2 years before the accident, according to a procedure recommended by the manufacturer. The rework included regrinding, shot peening, and nickel plating the journal bearing surface and fillet where the fatigue crack originated. In June 1968, approximately 2 months before the accident, during a regular periodic inspection, the spindle was inspected for cracks by a fluorescent magnetic particle method. No cracks were detected.

A laboratory study after the accident revealed the following factors that were probably involved in the cause of the spindle failure:

1. The fatigue crack was a high cycle, low stress, slowly propagating crack that probably had been present when the spindle was inspected for cracks 2 months before the accident.

2. The fatigue nucleus was in the steel, under the nickel plating, in an area where very small, shallow pits were found in the surface of the fillet.

3. In the area where the fatigue crack originated the steel had a banded microstructure. The overall hardness in this area was 28 Rockwell C, below the specified minimum of 34 Rockwell C, and the fatigue nucleus was in one of the softer bands where the local hardness was well below 28 Rockwell C.

4. Residual tensile stress in the fillet surface as a result of nickel plating might have contributed to the initiation of the fatigue crack although the plating process specified by the manufacturer was selected to minimize residual stresses.

5. The fillet where the fatigue crack originated had not been properly shot peened. This fact is considered to be an important contributing factor as adequate shot peening would probably have eliminated the effect of the shallow pits and would have reduced the effect of the banded microstructure and low hardness.



II. Lake Central Airlines, Allison Prop-Jet Convair 340; Marseilles, Ohio;  
March 5, 1967

A fatigue failure of a propeller torque cylinder (fig. 3) precipitated the crash of this two-engine, turboprop aircraft. The fatigue failure, however, was caused by a prior failure in another component of the propeller pitch control system. The initial failure was excessive wear in the splines of the torque piston.

Propeller blade pitch in this aircraft is controlled through torque units (one unit for each of the four propeller blades) operated by hydraulic oil pressure. Through a system of splines, linear movement of the torque piston in the torque cylinder produces changes in propeller pitch. An increase in hydraulic pressure moves the piston outward to increase blade angle and a decrease in pressure permits the normal aerodynamic loads on the propeller to decrease blade angle. The piston has both internal and external splines and after the accident both sets of splines in one piston were found to be severely worn. These splines had not been nitrided as required by the manufacturer's specification for the piston. The excessive wear in the splines allowed the piston to float free in the cylinder without engaging the splines of the mating parts. This condition did not immediately cause any detectable change in the operation of the propeller because of the redundancy built into the pitch control system. However, each time the oil pressure in the system was increased the free piston was forced hard against the cylinder cap. This force resulted in stresses exceeding the fatigue strength of the cylinder wall and eventually caused a complete fatigue failure of the cylinder.

Examination of the fracture (fig. 4) showed that small fatigue cracks had propagated from the inner surface of the cylinder wall and combined to form a continuous crack completely around the inner circumference of the cylinder. This fatigue crack did not penetrate completely through the wall so that hydraulic pressure was maintained until the cylinder failed completely. When the cylinder failed, loss of hydraulic pressure occurred so suddenly that the propeller pitch lock failed and resulted in a severe propeller overspeed. All four propeller blades were thrown off the propeller hub; and one of them went through the fuselage and caused the airplane to break up in the air and crash.

The series of events that led to this accident started with the omission of the nitriding of the torque piston splines. As a result of investigations associated with the accident, changes were made in the quality control system of the propeller manufacturer and several design modifications were made in the propeller pitch control system. These changes appear to be adequate to prevent a similar set of circumstances causing another accident.



III. Wein Consolidated Airlines, Fairchild F-27B; Pedro Bay, Alaska;  
December 2, 1968

This aircraft encountered severe to extreme clear-air turbulence and crashed during a flight from Anchorage to Iliamna in Alaska. Investigation of the accident showed that an in-flight structural failure of the right wing had occurred through an area where fatigue cracks had weakened the structure on both sides of an access door in the bottom surface of the wing.

The piece of wreckage in which the fatigue fractures were found is shown in figure 5. Fatigue cracks had originated at four fastener holes, two on each side of the access door, that were alined in a chordwise direction. These initial cracks had propagated and joined to form a crack about  $3\frac{1}{4}$  inches long on the aft side of the access opening and about  $2\frac{1}{2}$  inches long on the forward side. No evidence of fatigue cracking was found in the access door cover. Adjacent to the fastener holes, the fracture surfaces were flat and smooth, as shown in figure 6, but as the cracks progressed away from the holes, they showed an increasing tendency to propagate as slant fractures. Numerous crack jump marks (small regions of ductile rupture) were found in both the flat and slant fracture areas. An example of the appearance of these jump marks is shown in figure 7.

Fatigue and fail-safe tests of an F-27 wing made several years before the accident gave some indication that a load equal to about 77 percent of limit load might have been required to break the wing with cracks about 3 inches long on both sides of the No. 1 access door. However, the numerous indications of high stress intensity found on the fatigue fracture surfaces suggested the possibility that high gust loads might have caused a rapid tearing extension of the cracks shortly before the wing failed completely. Such a rapid crack extension would not have left any visible evidence on the fracture surface. If it included rupture of the access door cover, it would have connected the two fatigue cracks; thus the crack length was increased to more than 17 inches and the load required for final failure was reduced.

A Federal Aviation Administration (FAA) Airworthiness Directive requires U.S. operators to make periodic inspections for cracks at many locations in the F-27 wings. For several years before the accident, X-ray inspections at 1200-hour service time intervals had been made in the area of the No. 1 access door in both wings of the plane that crashed. There was nothing in the aircraft maintenance records to indicate that cracks had been detected. Reexamination of the inspection radiographs after the accident, however, revealed evidence that cracks had been present in the vicinity of the access doors in both wings for more than a year before the accident. Crack indications were found in three sets of radiographs made during this period. If the cracks had been detected and

reported, the operator would have been required by the Airworthiness Directive to make an approved modification of the wing structure which would have increased the strength of the access door area where the wing failed.

As soon as the crack indications were found in the radiographs, the FAA was notified and a special inspection was recommended by the Safety Board. The FAA issued a telegraphic Airworthiness Directive requiring an immediate inspection for cracks in the wings of all F-27 aircraft with 5000 hours or more time in service. Sixty-seven aircraft were inspected in compliance with the Airworthiness Directive and 13 cracks were found in eight aircraft.

IV. TAG Airlines DeHavilland Dove; Lake Erie near Cleveland, Ohio;  
January 28, 1970

A TAG Airlines DeHavilland Dove crashed through the ice into Lake Erie in January 1970, after a fatigue failure of a wing attachment fitting. The appearance of the failed fitting is shown in figure 8 and the surfaces of the fatigue fracture in figure 9. Fatigue cracks had originated at the edge of the hole for the main wing-to-fuselage attachment bolt and had propagated through approximately 75 percent of the cross-sectional area at that point before the fitting failed completely.

The fitting was made of steel that had been heat treated to an ultimate tensile strength of approximately 175 000 pounds per square inch, and the bore of the hole where the failure occurred had been chromium plated. No chromium plating had been used in the original design, but some fittings with chromium plating in the attachment bolt hole were installed prior to 1961. The National Transportation Safety Board report on this accident stated:

"The manufacturer had long been aware of the problem caused by the chromium plating process and had reduced the 'safe life' of this fitting to 10 000 flying hours in July 1961 (Technical News Sheet 178). At this time, it was recommended that an inspection for the chromium plating of the root-joint attach fitting be carried out at the next convenient opportunity and, in any case, prior to the accumulation of 10 000 flying hours. It was recommended that any fitting found to have the chromium plating be changed at the next removal of the wing or before 10 000 hours, whichever came first. This recommendation had the approval and concurrence of the United Kingdom's Air Registration Board. These requirements became mandatory for aircraft registered in the United Kingdom but not for those registered in the United States.

"Based upon this recommendation by the manufacturer, the Federal Aviation Administration issued Airworthiness Directive 61-18-3, effective September 1, 1961. This directive repeated the opening preamble of the Technical News Sheet 178 but adopted only the requirement to inspect the fitting for chromium plating and to



replace it, if so plated, prior to the accumulation of 10 000 flying hours. The recommendation to replace any chromium plated fittings at the next wing removal was not made a part of the requirement by the FAA on the U.S. registered aircraft."

In November 1965 the wings of the aircraft had been removed for certain required modifications. At that time, the fitting that eventually failed had been in service for 4998 hours. It was inspected for cracks, but was not replaced, and failed after 9383 hours of service time. A factor in the failure of the fitting before it reached the 10 000-hour mandatory removal time was the severe operating conditions at TAG Airlines. TAG flights were considerably shorter and were flown at higher speeds and lower altitudes than the standard flight profile for Dove aircraft.



TABLE 1.- U.S. CIVIL AVIATION ACCIDENTS INVOLVING MATERIAL FAILURE  
AS A CAUSE OR CONTRIBUTING FACTOR  
[January 1, 1967 to December 31, 1969]

	Air carrier	General aviation	Total
All material failure accidents:			
Number of accidents . . . . .	20	922	942
Number of fatal accidents . . . . .	6	53	59
Number of fatalities . . . . .	138	110	248
Material failure accidents involving fatigue failure:			
Number of accidents . . . . .	12	143	155
Number of fatal accidents . . . . .	4	23	27
Number of fatalities . . . . .	103	54	157

TABLE 2.- U.S. CIVIL AVIATION ACCIDENTS INVOLVING MATERIAL FAILURE  
AS A CAUSE OR CONTRIBUTING FACTOR  
[January 1, 1967 to December 31, 1969]

	Number of accidents	Number of accidents in which fatigue failures were identified
Type of aircraft:		
Small fixed wing . . . . .	814	107
Large fixed wing		
Turboprop . . . . .	16	7
Reciprocating engine . . . . .	11	5
Turbojet and turbofan . . . . .	5	2
Helicopters . . . . .	96	34
Phase of operation:		
In-flight . . . . .	416	76
Landing . . . . .	352	45
Take-off . . . . .	145	28
Taxiing or towing . . . . .	28	6
Parked . . . . .	1	---
Extent of damage to aircraft:		
Substantial . . . . .	818	117
Destroyed . . . . .	122	38
Minor or none . . . . .	2	---
Type of component that failed:		
Landing gear . . . . .	371	58
Powerplant . . . . .	333	23
Propeller assembly . . . . .	76	35
Flight controls . . . . .	25	5
Structural . . . . .	24	10
Fuel system . . . . .	24	1
Hydraulic system . . . . .	17	1
Electrical system . . . . .	14	---
Tail rotor assembly . . . . .	25	14
Main rotor assembly . . . . .	23	8
Instruments . . . . .	5	---
Auxiliary components . . . . .	5	---

TABLE 3.- SUMMARY OF DATA FROM 230 LABORATORY REPORTS ON FAILED COMPONENTS

Classification of causes	Number of failures due to --							Totals
	Fatigue	Overload	Stress corrosion or hydrogen embrittlement	Excessive wear or deformation	Corrosion	Stress rupture	High temperature oxidation	
Improper maintenance	52	18	11	15	4		2	102
Fabrication defects	31	6			1		1	39
Design deficiencies	24	5	4	1	1	1	1	37
Defective material	10	3	1	1				15
Abnormal service damage	13	7	1			2		23
Undetermined	11	2	1					14
Totals	141	41	18	17	6	3	4	230



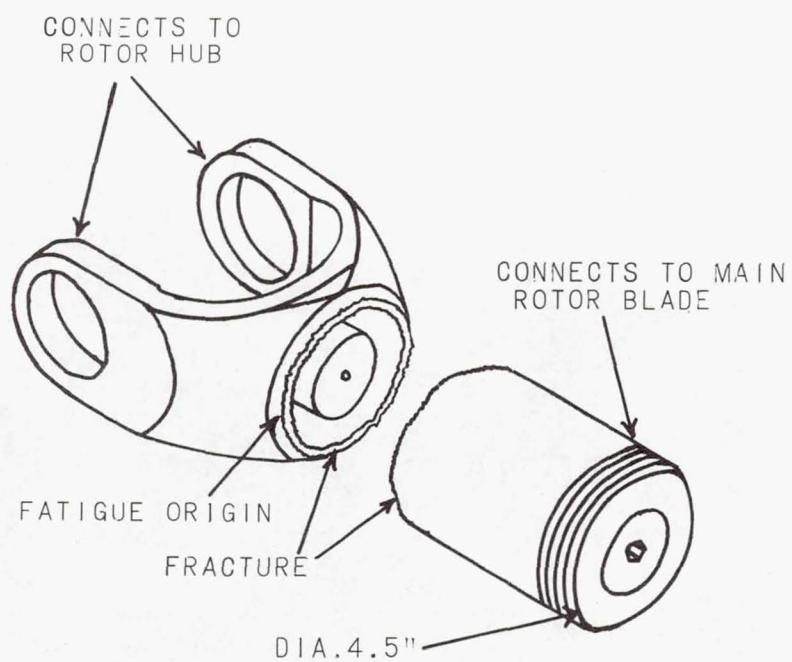


Figure 1.- Drawing of the failed main rotor spindle, showing the location of the fracture.

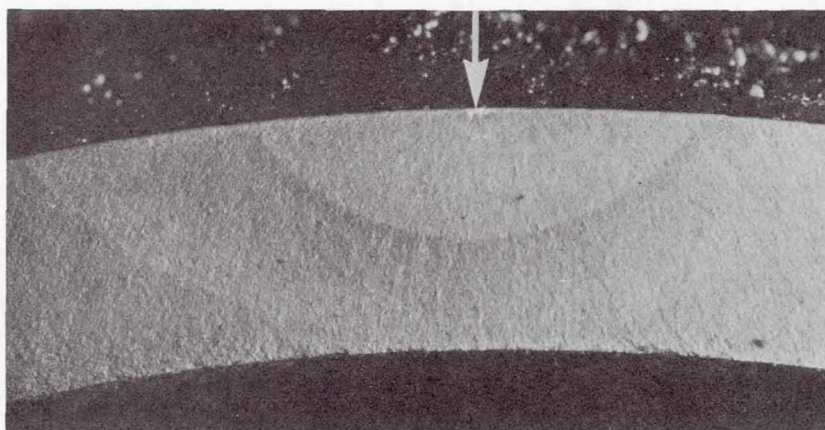


Figure 2.- Appearance of the spindle fracture in the vicinity of the fatigue origin (arrow). X 6.



Figure 3.- Failed torque cylinder. Arrows indicate the mating surfaces of the fracture in the two pieces. Approximately X 1/2.

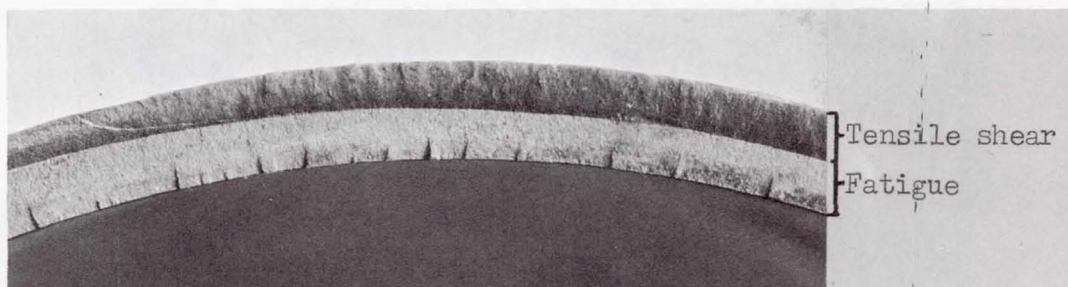


Figure 4.- A portion of the fracture in the torque cylinder shown in figure 3. The remainder of the fracture was similar in appearance. X 3.

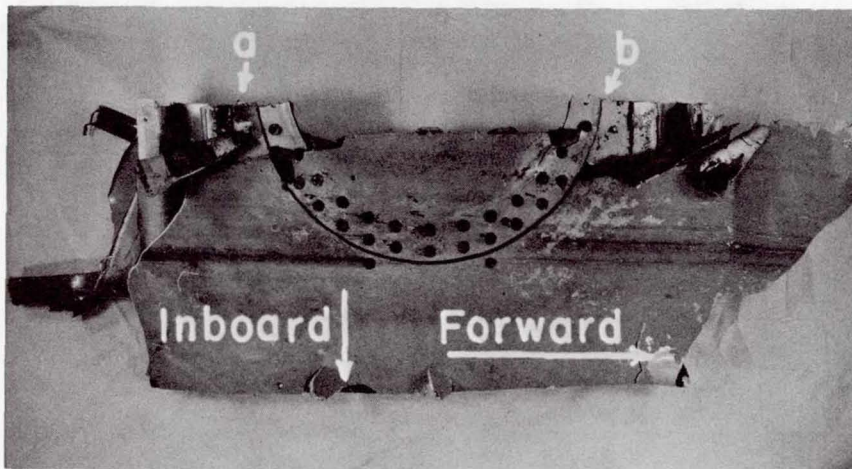


Figure 5.- Piece of the lower surface of the right wing, including the inboard end of the No. 1 access door. Arrows "a" and "b" indicate the location of fatigue fractures. X 1/8.



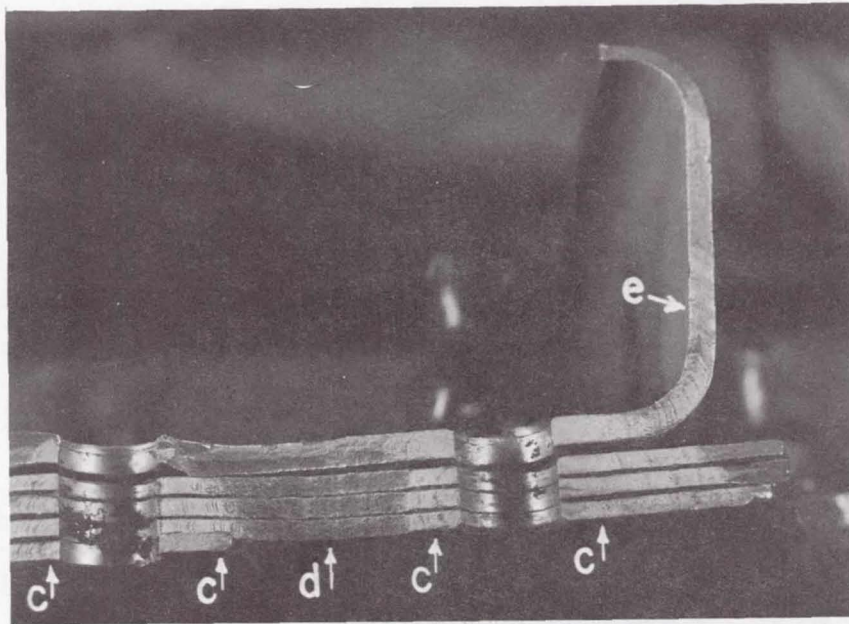


Figure 6.- A portion of the fatigue fracture indicated by arrow "a", figure 5. Arrows "c" indicate flat fracture areas; arrows "d" and "e," slant fractures. X 2.

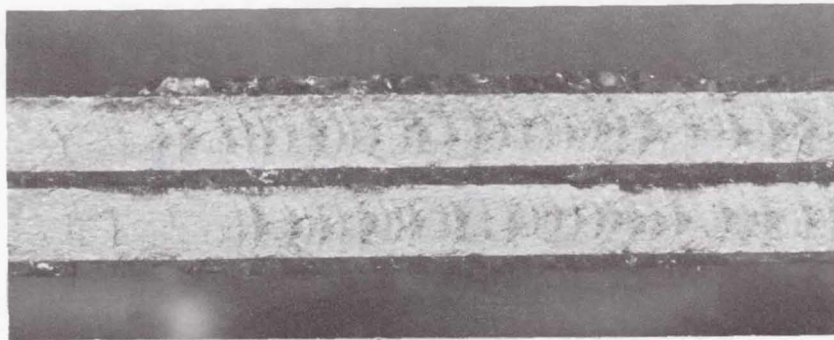


Figure 7.- Appearance of one of the fatigue fracture areas that showed numerous small regions of ductile rupture between fatigue striations. X 8.

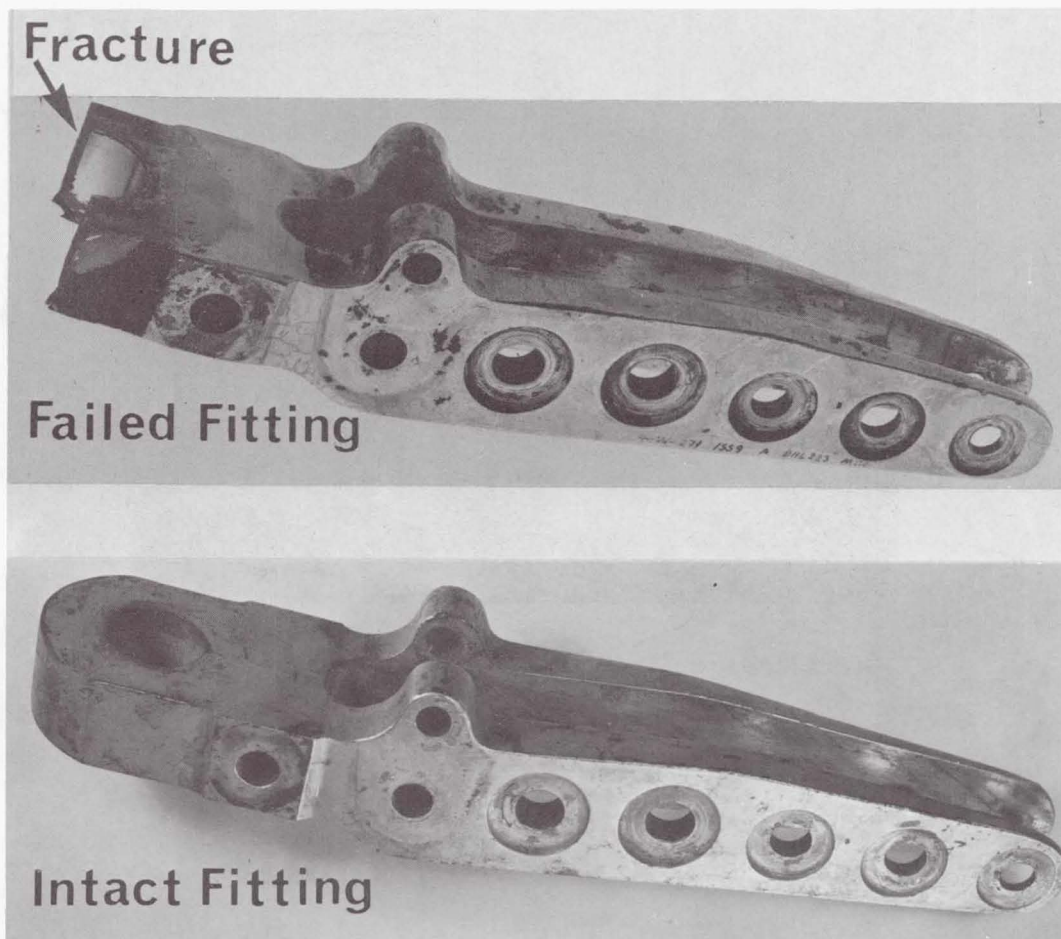


Figure 8.- Failed wing attachment fitting with an intact fitting to show the shape of the end where the fracture occurred. X 2/3.

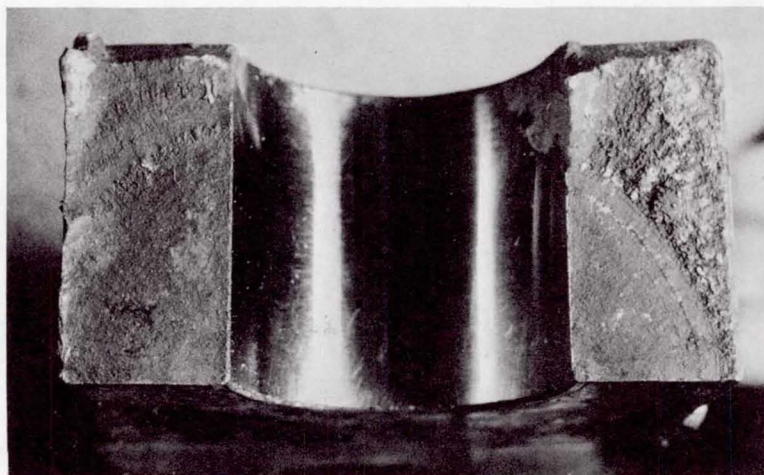


Figure 9.- Appearance of the fracture in the failed fitting shown in figure 8. X 2.



# FATIGUE TESTS ON BIG STRUCTURE ASSEMBLIES OF CONCORDE AIRCRAFT

By V. P. N'Guyen

Société Nationale Industrielle Aérospatiale  
Toulouse, France

and

J. P. Perrais

Centre d'Essais Aéronautiques  
Toulouse, France

## INTRODUCTION

The Concorde, a delta-shaped-wing aircraft, has been submitted to numerous material, attachment and protection tests since, with its structural design, it is capable of reaching supersonic speeds (Mach number, 2.05). In addition, this aircraft has been tested in the scope of structural engineering tests performed on substructures. In this paper, only development tests on large structure assemblies and airworthiness substantiation full-scale tests are considered.

This paper is limited to the tests performed at the Centre d'Essais Aéronautiques of Toulouse (C.E.A.T.), France. The tests carried out in the United Kingdom are to be presented by the Royal Aircraft Establishment (R.A.E.). As a rule, the development tests achieved both in France and in the United Kingdom are usually performed on structures for which Aérospatiale and British Aircraft Corporation are responsible. All certification static tests are to be carried out in France and all certification fatigue tests are to be performed in the United Kingdom.

## EXPERIENCE FROM STATIC TESTS

Two main sections have been submitted to pressure, mechanical load, and thermal static tests and are shown in figure 1.

### Fuselage Section 1 bis.

The structure, named fuselage section 1 bis. or 1(a), consisted of a 4.68-meter-long twin-looped cylindrical fuselage section including six standard frames and two main frames. On both sides of the lower part of the fuselage, rectangular structural boxes represented the wing assembly and its fuselage junction section. The purpose of this operation was to create the same thermal stresses over this area as those encountered

in flight. The skin panels (A-U2GN sheet) were attached in a classical way to the stringers and frames.

The aim of the tests was to observe the structural behaviour under the most severe flight conditions such as combined pressurization, fuselage torsion and loads on floor, and thermal stresses. Test measurements of temperatures and mechanical strains were also compared with calculated values of thermal stresses in order to (1) justify design methods, (2) make an analysis of the role played by thermal stresses among total stresses (to manage a test program of structures which will be tested in the future), and (3) perfect new test methods, especially in the scope of infrared heating and air-cooling units injecting liquid nitrogen. The tests started at the end of 1964 and ended in the spring of 1966.

This testing enabled the manufacturer to check for the thermal stress level in the fuselage areas hidden by the wing assembly and in the longitudinal stringers located at the bottom of the fuselage. (Fig. 2 shows the results of comparative tests on the heated lower part and the unheated lower part to simulate the presence of a fuel tank.) It was necessary to carry out tests, especially fatigue tests, by representing in a most accurate way thermal stresses where they are significant.

#### Section 2.8.b

The test structure, section 2.8.b, was composed of a fuselage section (first definition of the aircraft, 10 m  $\approx$  35 ft long) and of main adjacent wing elements having an overall span of 44 ft. (Refer to fig. 1.) This structure is a genuine aircraft element. The purpose of the test was

(1) To check in a more exact way the aircraft design methods. Therefore, the test structure itself with its proposed end effects has been calculated by means of the same network as an aircraft (analog electrical network for internal load computation).

(2) To compare thermal stress distributions obtained from different aircraft missions. These distributions are not easily obtained by computation.

(3) To evaluate fuel influence in the tanks on these thermal stresses.

(4) To study the superimposition of cabin and tank pressure, of air and inertia loads, and thermal effects.

(5) To prove the "fail-safe" characteristics of this structure by making some cuts to simulate cracks in the main spars, ribs, and frames, and then performing residual-strength tests.



(6) To familiarize test laboratories with exceedingly complex installations in order to proceed with the certification static tests on a full-scale aircraft structure (fig. 3) under satisfactory conditions.

These tests commenced in the autumn of 1966 and ended in the summer of 1969. Results are too extensive to be presented in this paper. Therefore, only tests which made it possible to perfect the fatigue test programs are presented.

It was shown by the design calculations that the maximum thermal stress values highly depended upon the aircraft acceleration laws. This dependence was verified when a few wing panels buckled locally during tests simulating missions with high acceleration and low take-off weight. (See fig. 4.) (It was a case of a flight corresponding to a previous definition of the aircraft.) The purely thermal stresses remain moderate in absolute value but are reversed, and their peak-to-peak values are significant. The presence of fuel causes the stresses in heavy parts of spars and ribs to be reduced. On the other hand, the internal skin surface is subjected to tensile thermal stresses when the fuel tank is empty. These tensile stresses add to the internal tensile stresses due to flight loads. The following conclusion may be drawn from this program. For tests on partial structures, great care should be exercised in simulating the temperature distributions over the fuselage internal areas (especially those areas hidden by wing assemblies). (The parasite end effects are very strong.)

Because of the high strength of the fuselage in the presence of large cuts (as required in the FAA fail-safe tests), fatigue tests can be safely conducted by using air to cyclically pressurize the fuselage.

A few "dynamic-cut" tests which were performed on the fuselage throughout frames ended the fail-safe tests; the data from these tests will be used for certification substantiation.

#### STATIC TESTS FOR AIRWORTHINESS SUBSTANTIATION

The test structure is a full-scale aircraft. The test program consists of a sequence of tests to be performed under room-temperature conditions and including five different tests with loads on a part of the aircraft. All tests were conducted at least up to ultimate design load of the structure and some of them even beyond. The latter sequence of tests will be made under thermal conditions about July 1971 and will start with thermal tests only, during which several aircraft missions will be achieved under realistic conditions. In a first stage, to investigate ovens and cooling problems, C.E.A.T. will use calculated temperatures which are being verified by means of flight measurements on the prototype. The test temperatures will be submitted to the Airworthiness Authorities for approval. Figures 5 and 6 illustrate different static-test sequences.



## FATIGUE TESTS

These tests have been performed on many structural components, but the test programs achieved by use of big substructures 2.3.2 and 2.6/2.7 (fig. 1) are by far the most significant.

Preliminary static tests showed that it was necessary to reproduce the temperature distributions during acceleration and deceleration sequences. When the fatigue test programs were initiated, it was found that this operation would require a test of long duration; the time cycle in the laboratory was almost equal to the time required for an actual flight. It was absolutely necessary to compromise some part of the test program in order to obtain some desired results for the structural behaviour within a reasonable period of time.

Two changes were made in the test program to compensate for accelerating the thermal tests: (1) To compensate for creep, normal structural temperature has been increased by  $20^{\circ}\text{C}$  (from  $100^{\circ}\text{C}$  to  $120^{\circ}\text{C}$ ), (2) To compensate for deteriorations due to thermal stresses, the heating rate  $d\theta/dt$  has been increased during acceleration and deceleration sequences in order to increase the stresses by 15 to 20 percent, depending upon particular components.

In order to accelerate testing, the time during which the external wall temperatures were constant was decreased. Figure 7 shows that this decrease was feasible since (a) the same maximum temperatures were achieved as in actual flight for both external wall and internal structure, (b) the wall and structure returned to room temperature at the end of the programmed time cycle, and (c) the heating sequence during the time of constant temperature produced satisfactory thermal gradients during the deceleration sequence.

On the test section 2.3.2, this requirement was met by blowing hot or cold air onto fuselage areas hidden by the wing assembly. On test section 2.6/2.7, the same result was obtained by injecting hot and cold liquid into the fuel tanks, as required. These procedures are called "complementary means."

### Determination of Cycle

Random maneuver and gust loads were applied by lever jigs. For these development tests to be performed, it was preferable to reduce the typical loading spectrum to its simplest terms to investigate more easily the possible crack propagation rates. Pressure loads, since they are actually known, have been used at their flight true values; that is,  $p = 736\text{ mb}$  inside the cabin compartment, and  $p = 250\text{ mb}$  inside the fuel tanks. Thermal stresses were increased 10 to 20 percent, depending upon the area, to accelerate

the observance of the deteriorations due to thermal stresses. By using this increase, an attempt was made to double the damage value due to thermal stresses.

Three mechanical and three pressure cycles were superposed on each thermal stress cycle. In one instance (A), the mechanical and the pressure cycles were applied simultaneously while the thermal stresses were high. In two other instances (2B), the mechanical and pressure cycles were applied simultaneously while the thermal stresses were small or nil (corresponding to a slow return to room temperature). This sequence of loading produced a threefold increase in damage due to the usual loads. Cycles  $C = A + 2B$  are performed one after the other.

### Final Test Conditions

Final test conditions were based on and perfected from typical tests. During these typical tests, the actual flight real time requirements were met in order to accurately determine the required heating rates and thermal stresses during a flight. Based on the results of these typical tests, several short time cycles were tested and complementary means were used to obtain the desired temperature and stress evolution (especially peak-to-peak) at all significant measurement points. The complete time cycle of test 2.3.2 is shown in figure 8; whereas the complete time cycle of test 2.6/2.7 is shown in figure 9. It is easily noticed that with 1 hour's cycle (of which 40 minutes is thermal) for 2.6/2.7 tests and that with a 34 minutes' cycle (of which 26 minutes is thermal) twice the thermal damage and three times the mechanical damage of a 3 hr 15 min flight is produced.

### Results Obtained on Test Structure 2.6/2.7

By March 10, 1971, 9900 cycles ( $A + 2B$ ) and 10 900 additional B cycles (representing purely subsonic flights) were applied. This stress history corresponds to the damage caused by 40 600 flights under mechanical fatigue conditions and about 19 800 flights under thermal fatigue conditions. The deteriorations that were noticed occurred on the (current) fuselage frames at the level of the cabin floor. They were due to a combination of pressurization and thermal cycles. As a result of these deteriorations, design improvements were made on partial assemblies representing the damaged area (fig. 10). In tests on these partial assemblies, a special fixture was used to simulate the frame warping due to thermal stresses. The results of these tests were very satisfactory, and enabled an excellent behaviour of the frames to be foreseen on series aircraft.



### Results Obtained on Test Structure 2.3.2

By March 1, 1971, 14 000 complete cycles (A + 2B) and 4000 purely subsonic flights were applied. This stress history corresponds to the damage caused by 46 000 flights under mechanical fatigue conditions and about 28 000 flights under thermal fatigue conditions. The deteriorations that were noticed confirm those which were obtained with the substructure 2.6/2.7, and indicated that the same design improvements were required. Some minor deteriorations were found in the door and emergency exit locking devices. These deteriorations very likely come from local bending effects due to thermal stresses, and to defects in the door. A few cracks on metal sheets were detected and the investigation of the crack propagation rate is being made. Inside the wing fuel tanks, the original rods fitted with clevis welded by an electron bombardment process did not have a suitable fatigue life and have been replaced by conventional design rods.

### Residual Strength After Deteriorations

Deteriorations, especially those concerning fuselage frames, were always found during the systematic inspection of the structures, that is, following completion of a program block including 1000 cycles (A + 2B). The damaged structure exhibited satisfactory residual strength during the last cycles of the program block.

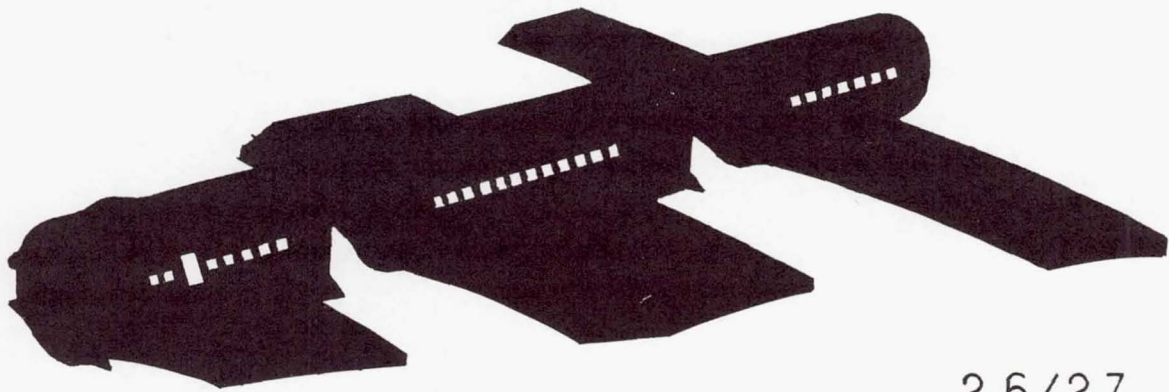
A flight limit load test upon occurrence of deteriorations has just been made on structure 2.6/2.7; this test will be used for certification purposes. Figures 11 and 12 illustrate the test rigs 2.3.2 and 2.6/2.7.

### CONCLUSIONS FROM DEVELOPMENT TESTS

The main conclusions are as follows:

1. On a supersonic aircraft whose structure weight is a significant part of the weight analysis, many fatigue and static strength development tests should be made.
2. Fatigue thermal tests are absolutely necessary. Temperature and thermal stress calculations, although they are very developed, cannot foresee any fatigue failures caused by distortion incompatibilities which are not easily evaluated.





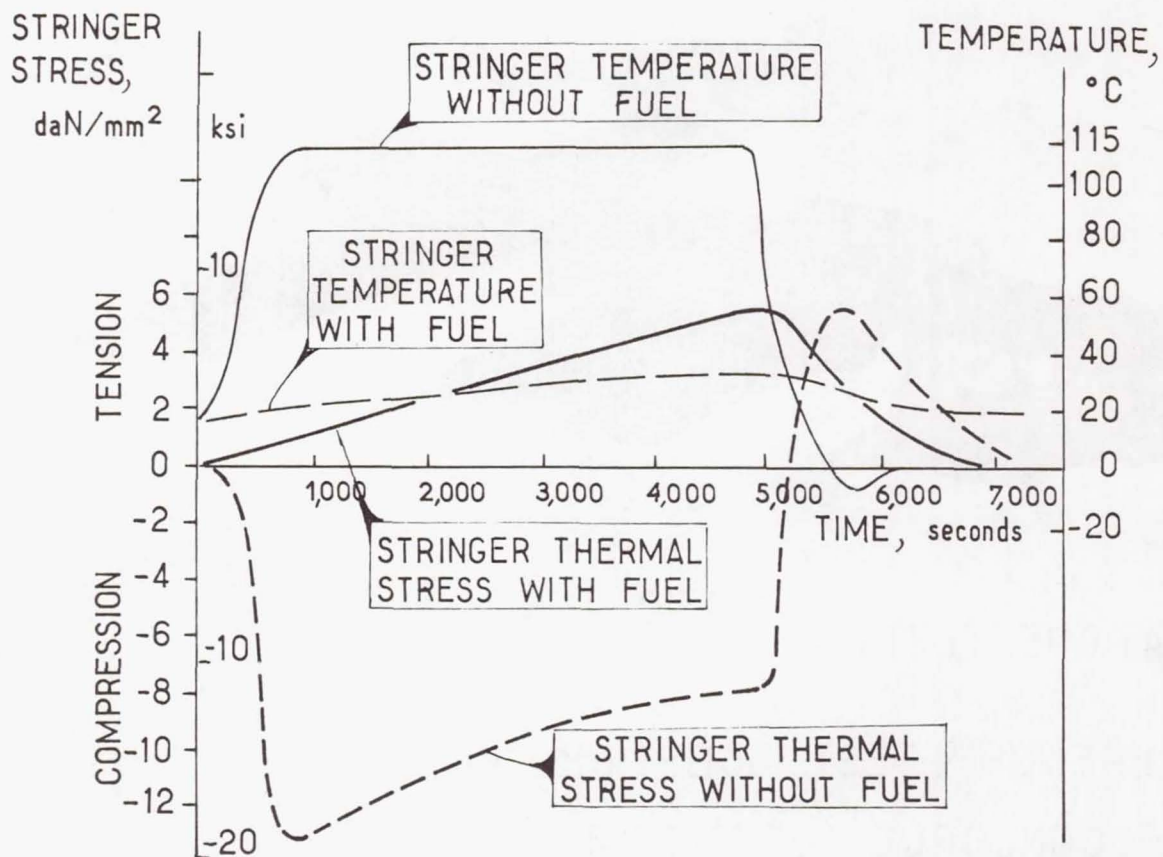
2.3.2  
FATIGUE TEST

2.8. b  
STATIC TEST

2.6/2.7  
FATIGUE TEST

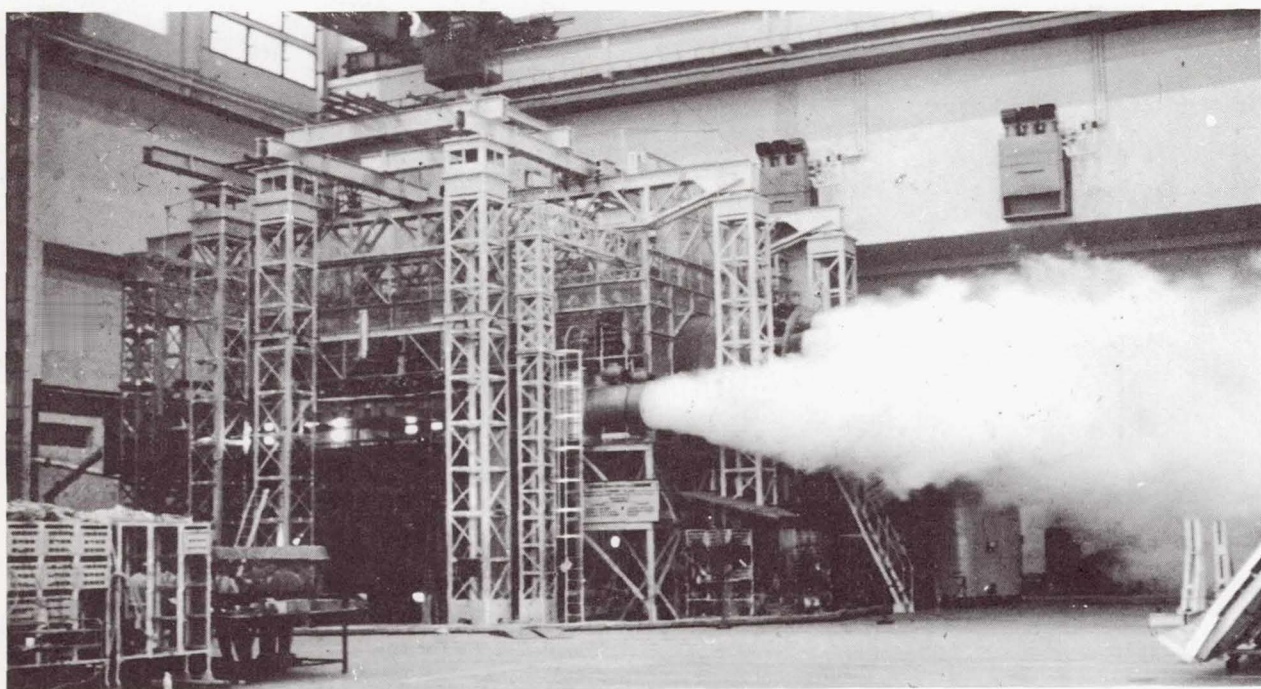
FRENCH TEST SUBSTRUCTURES FOR  
CONCORDE DEVELOPMENT TESTS

Figure 1.

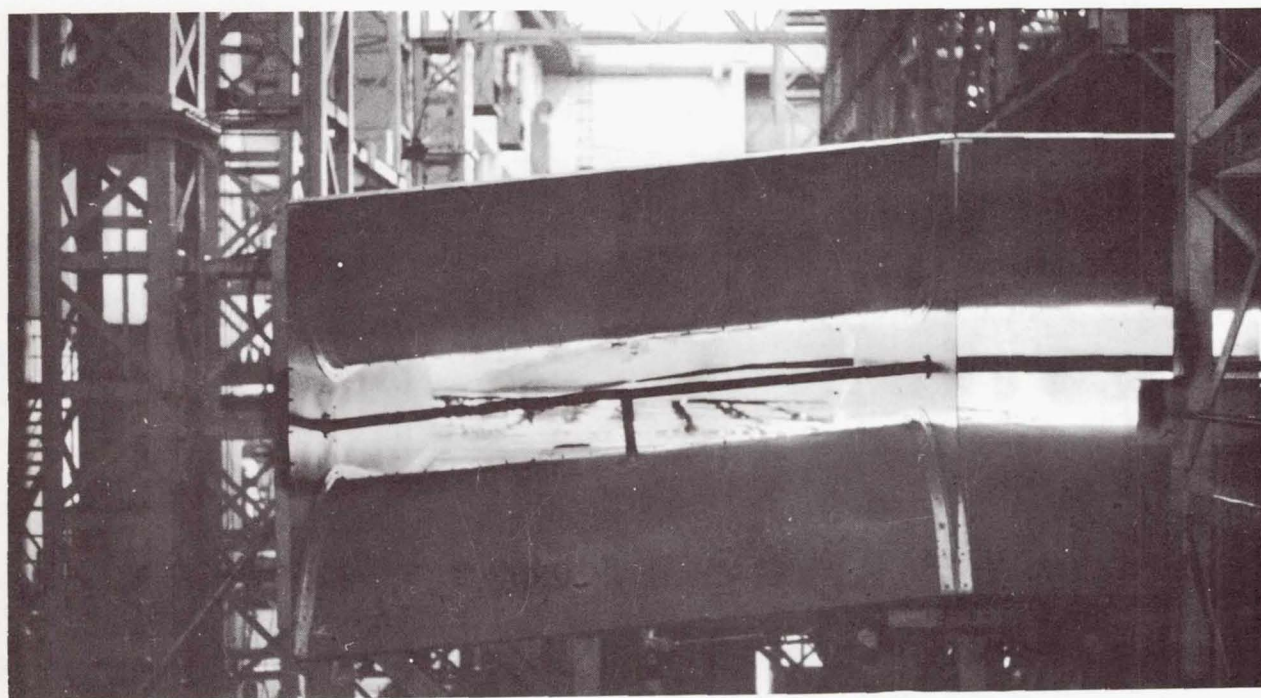


STRUCTURE 1 bis -EFFECT OF THE FUEL ON LONGITUDINAL THERMAL STRESSES ON A BOTTOM STRINGER OF A FUSELAGE FUEL TANK

Figure 2.



2.8.b THERMAL TEST - COOLING BY LIQUID NITROGEN

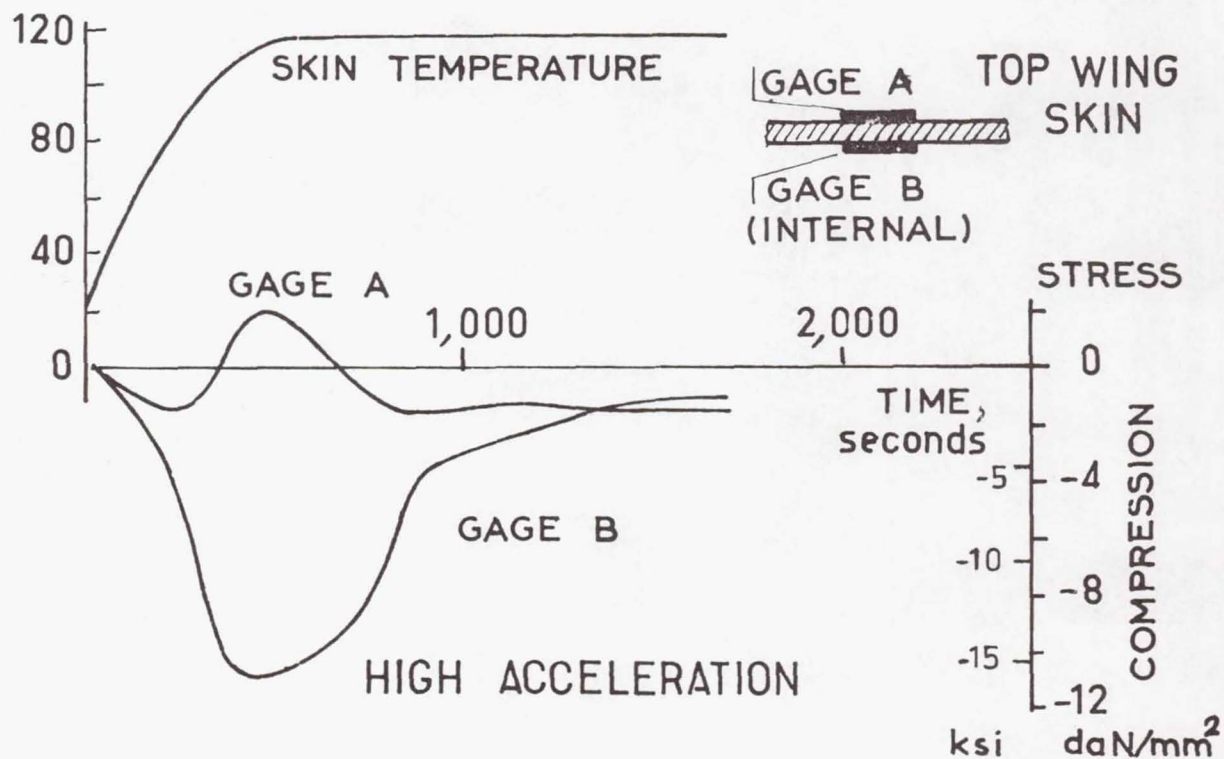


2.8.b THERMAL TEST - WING OVENS

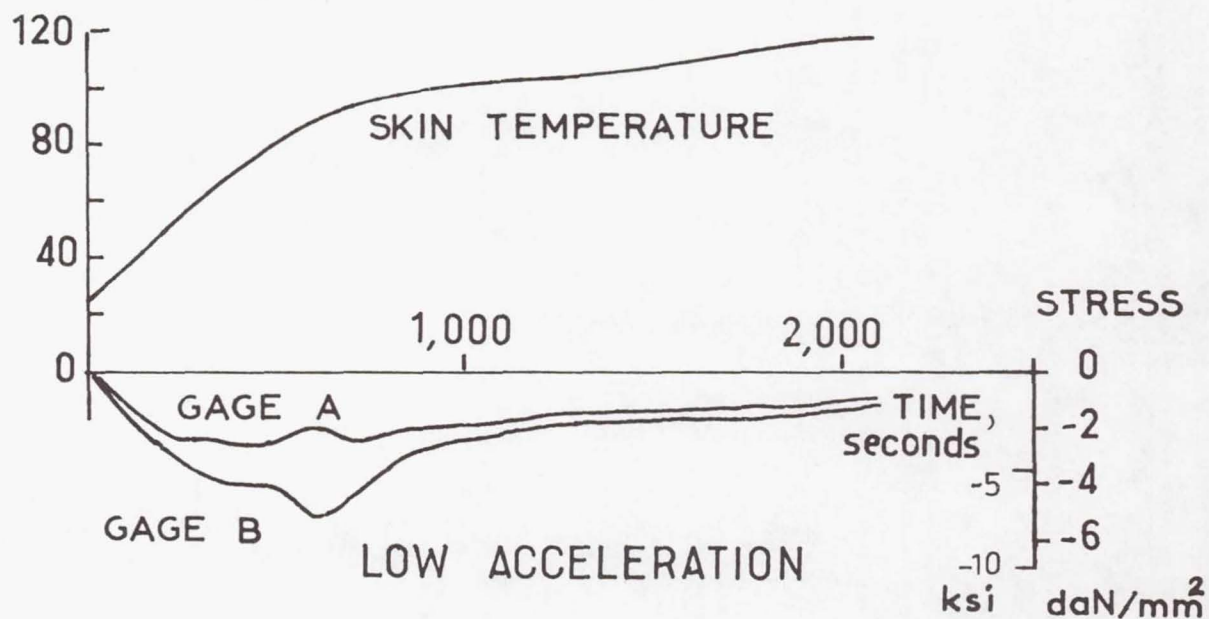
Figure 3.



TEMPERATURE,  $\theta$ , °C

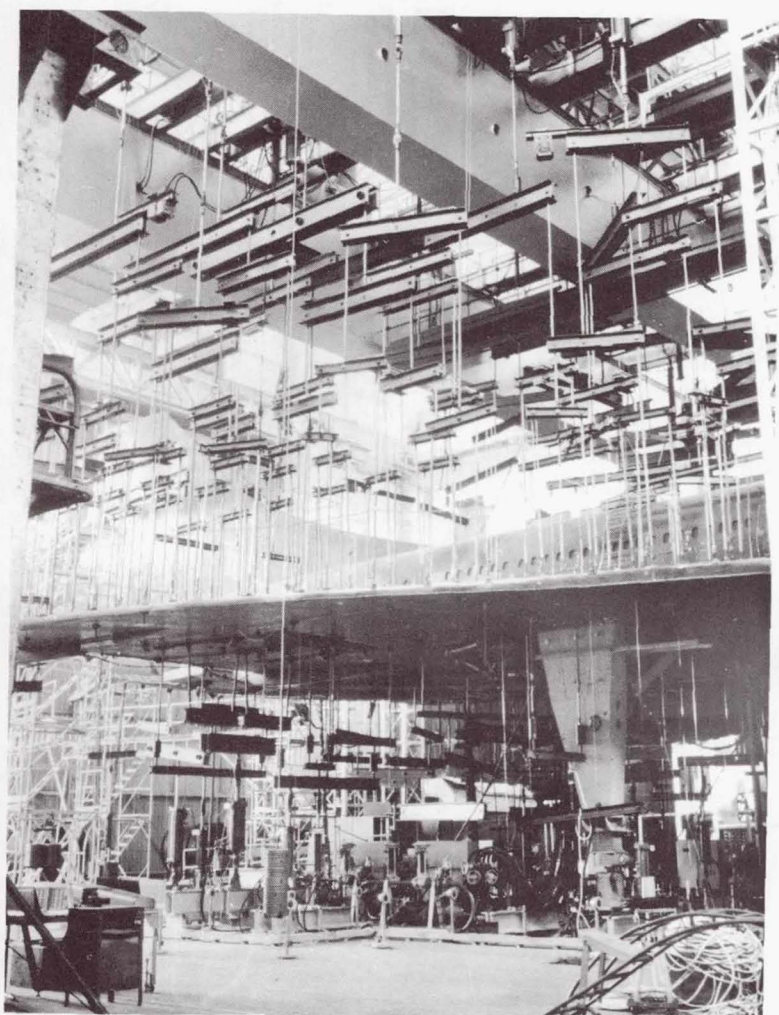
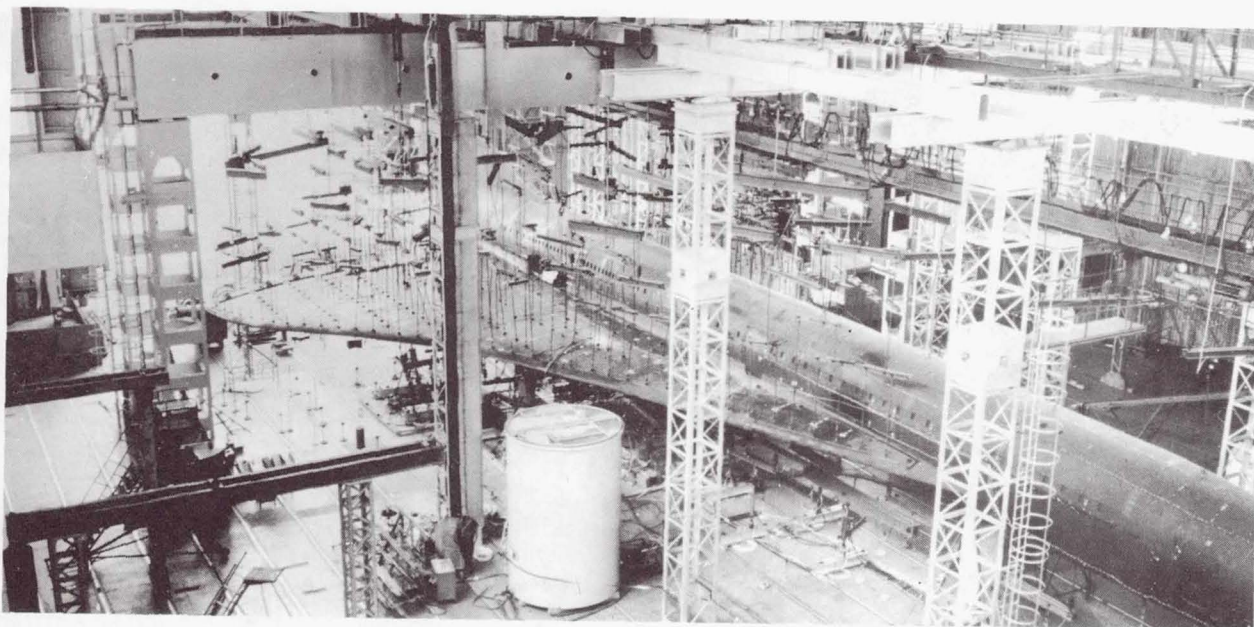


TEMPERATURE,  $\theta$ , °C



## 2.8.b STRUCTURE - THERMAL TESTS.

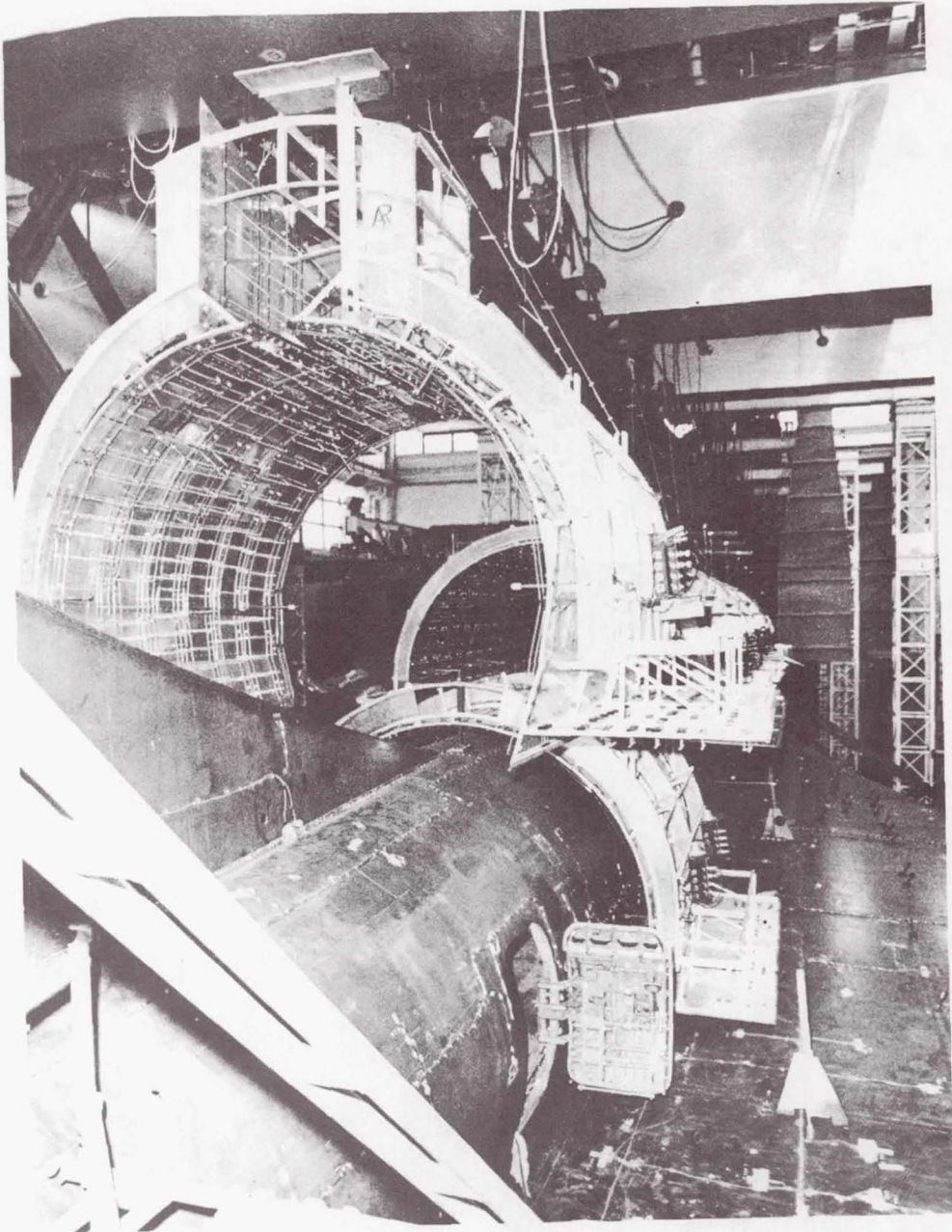
Figure 4.



MAJOR STATIC TEST-  
GENERAL VIEWS.

Figure 5.



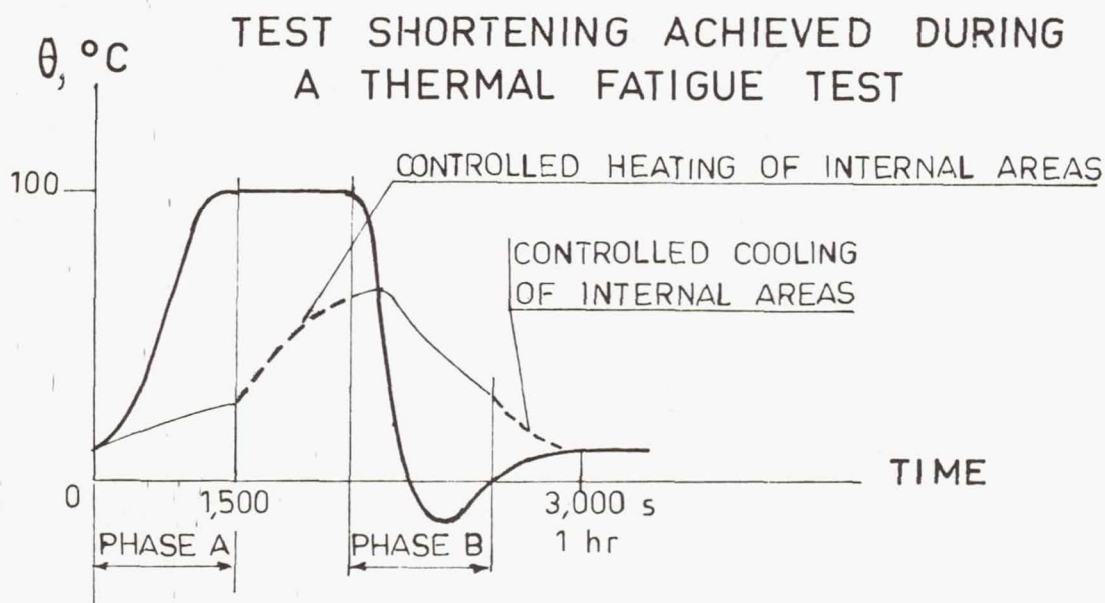
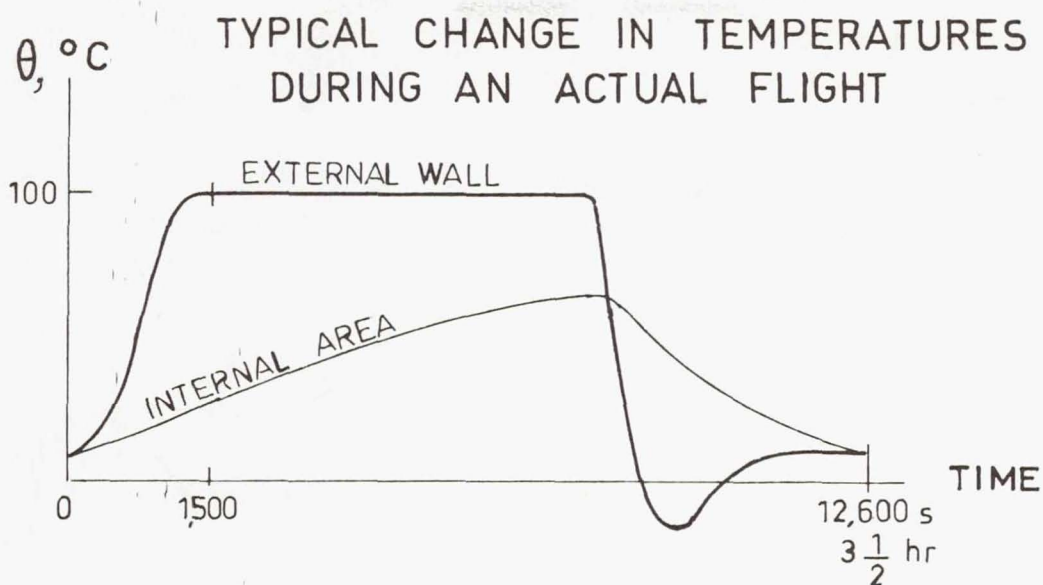


## THERMAL STATIC TEST.

INFRA-RED OVENS ARE BEING INSTALLED AROUND  
THE FUSELAGE.

Figure 6.

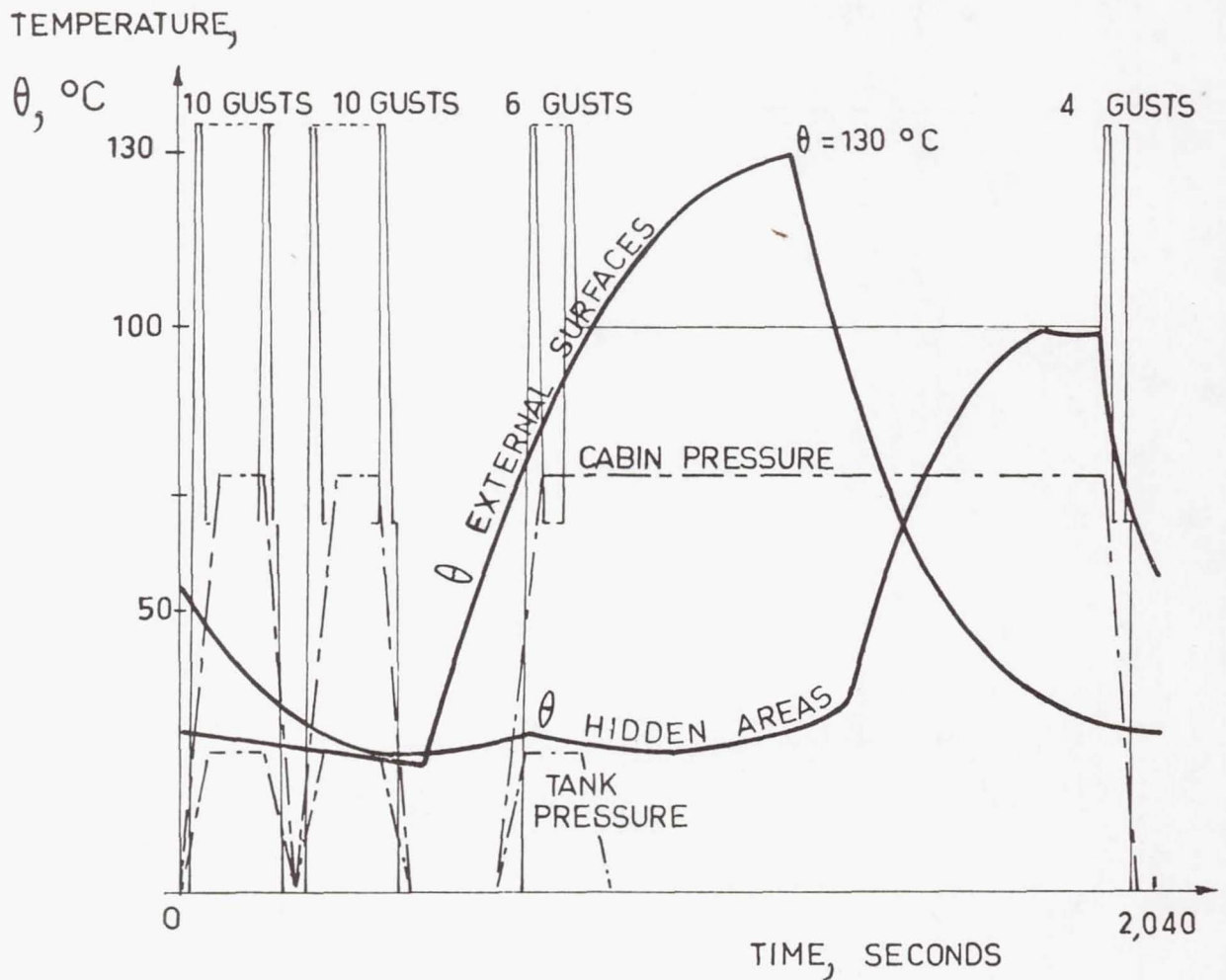




FOR A AND B PHASES THE TEMPERATURES  
CHANGE AS IN THE ACTUAL FLIGHT.

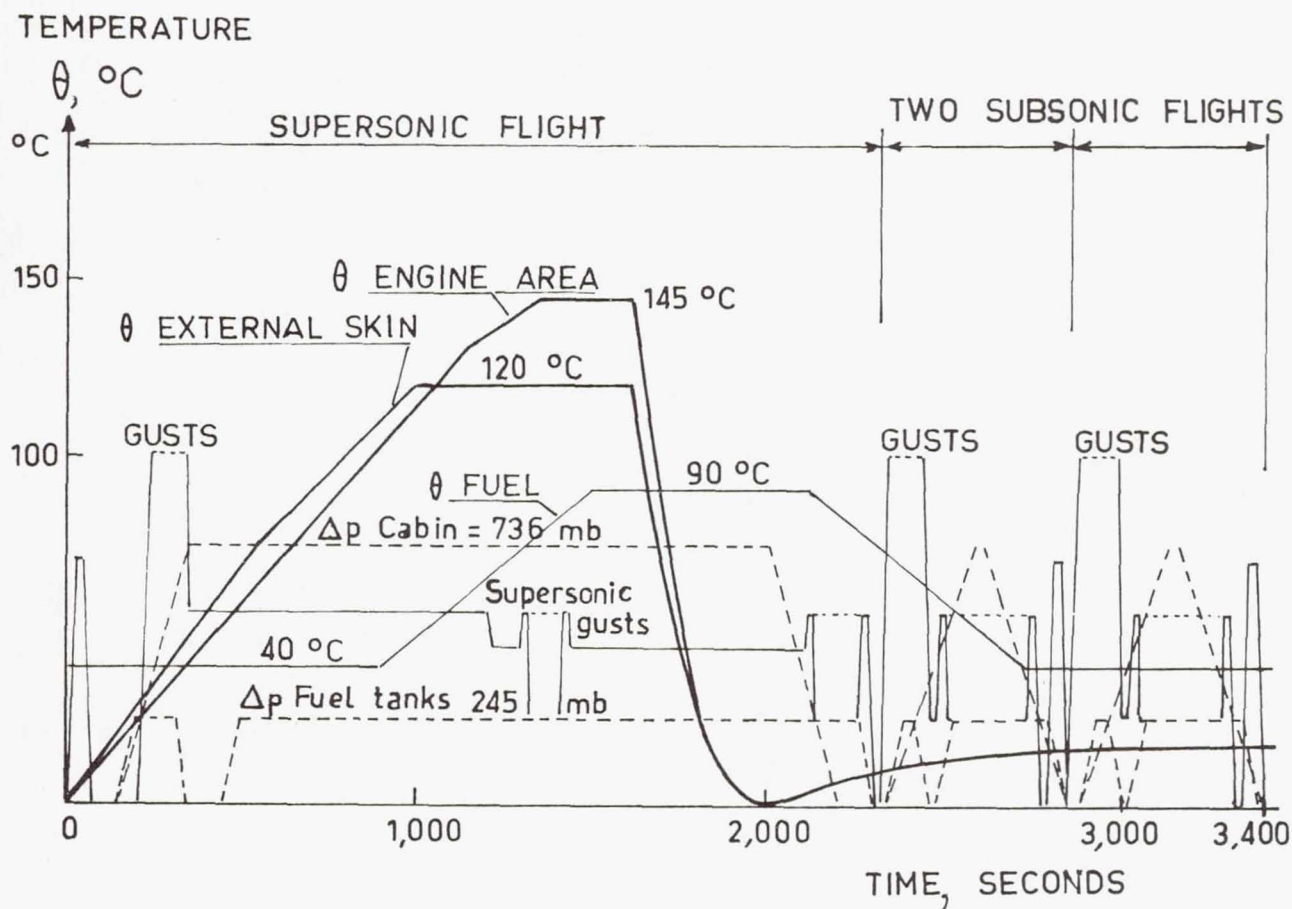
THE PRINCIPLE USED TO SHORTEN  
THE THERMAL CYCLE DURATION

Figure 7.



TEMPERATURE AND FATIGUE CYCLE OF THE  
CONCORDE 2.3.2 DEVELOPMENT FATIGUE TEST.

Figure 8.

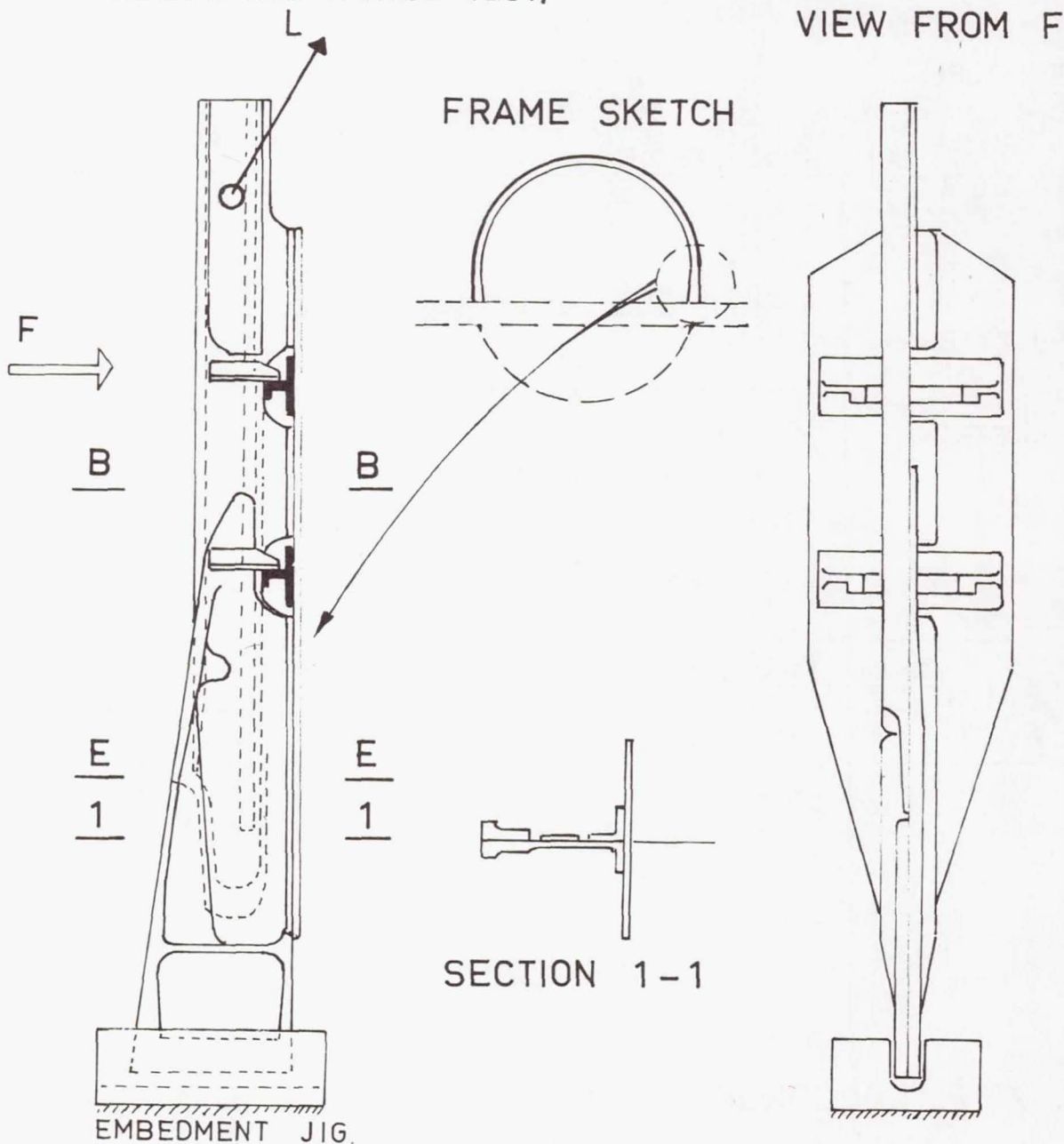


## 2.6/2.7 CONCORDE TEST STRUCTURE - TEMPERATURE AND FATIGUE CYCLE.

Figure 9.

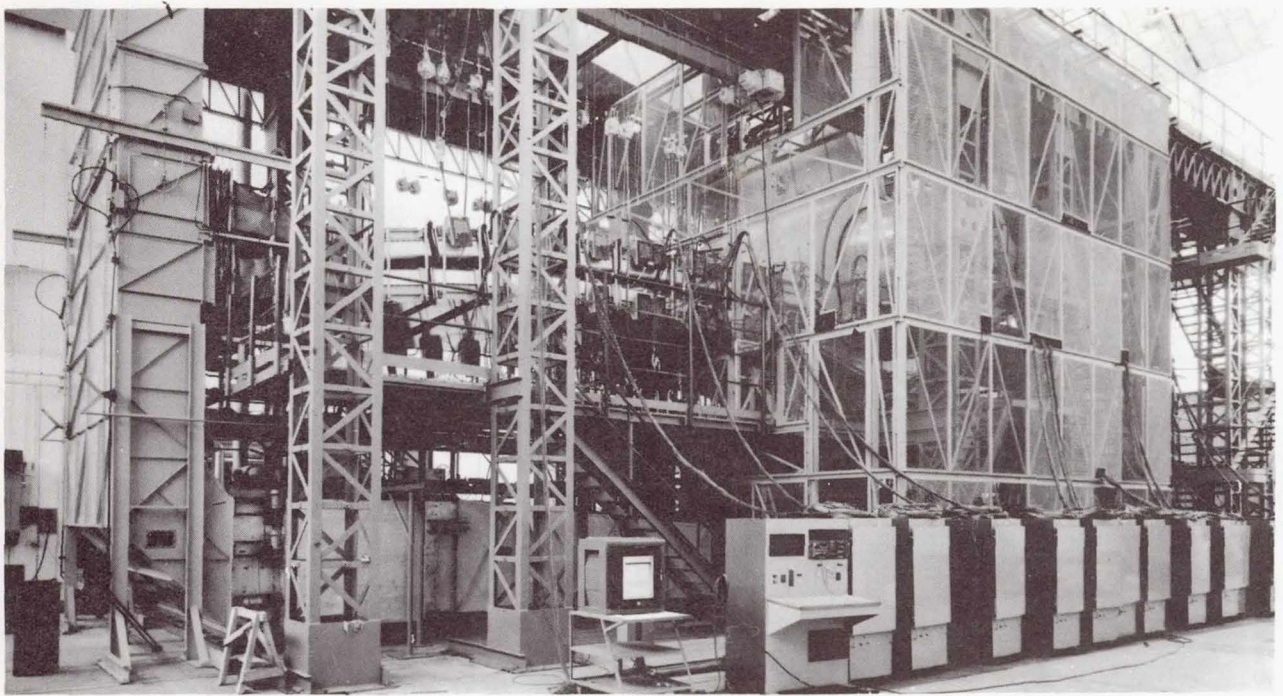


NOTE: THE LOAD L WAS DETERMINED TO OBTAIN BETWEEN B- AND E- SECTIONS THE STRESS DISTRIBUTIONS THAT WERE MEASURED ON FRAMES OF THE 2.6/ 2.7 STRUCTURE DURING THERMAL AND MECHANICAL FATIGUE TEST.

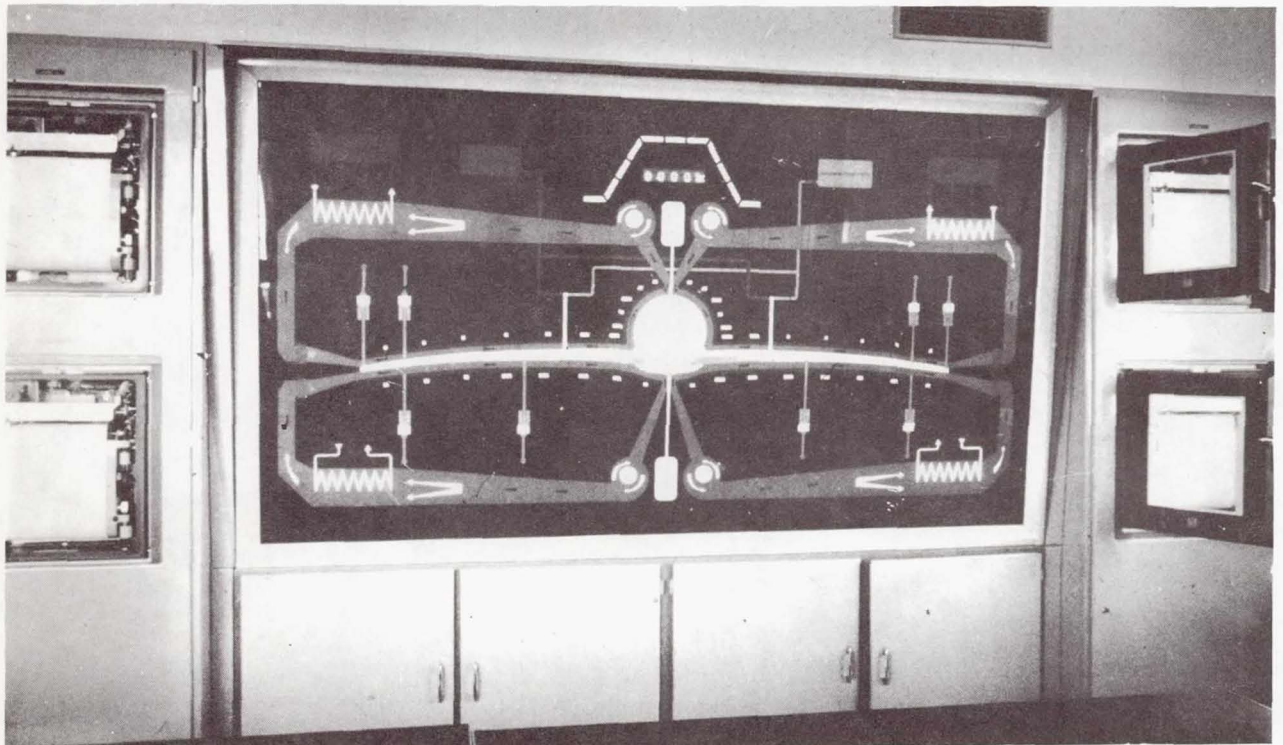


DEVELOPMENT SPECIMEN TO APPRAISE IN A SHORT TIME IMPROVEMENTS OF THE FUSELAGE FRAME DESIGN.

Figure 10.



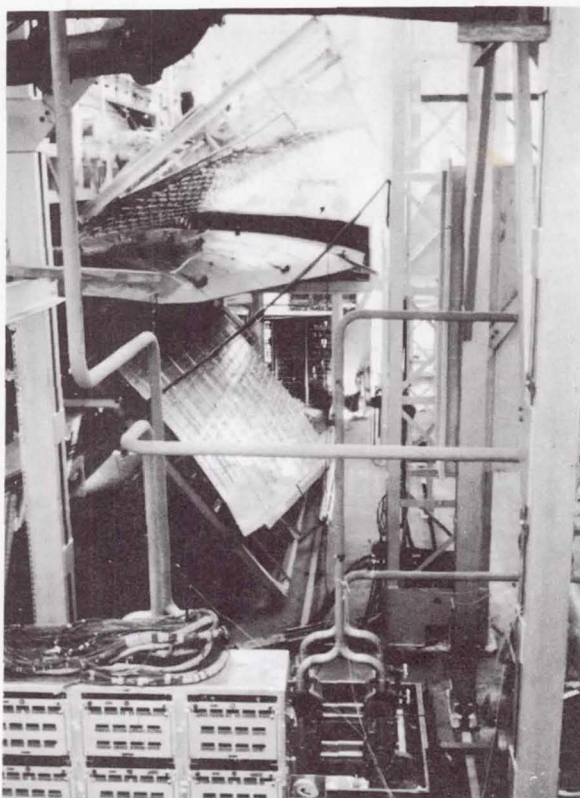
GENERAL VIEW OF THE 2.6/2.7 TEST RIG.



CONTROL ROOM OF THE 2.6/2.7 FATIGUE TEST.

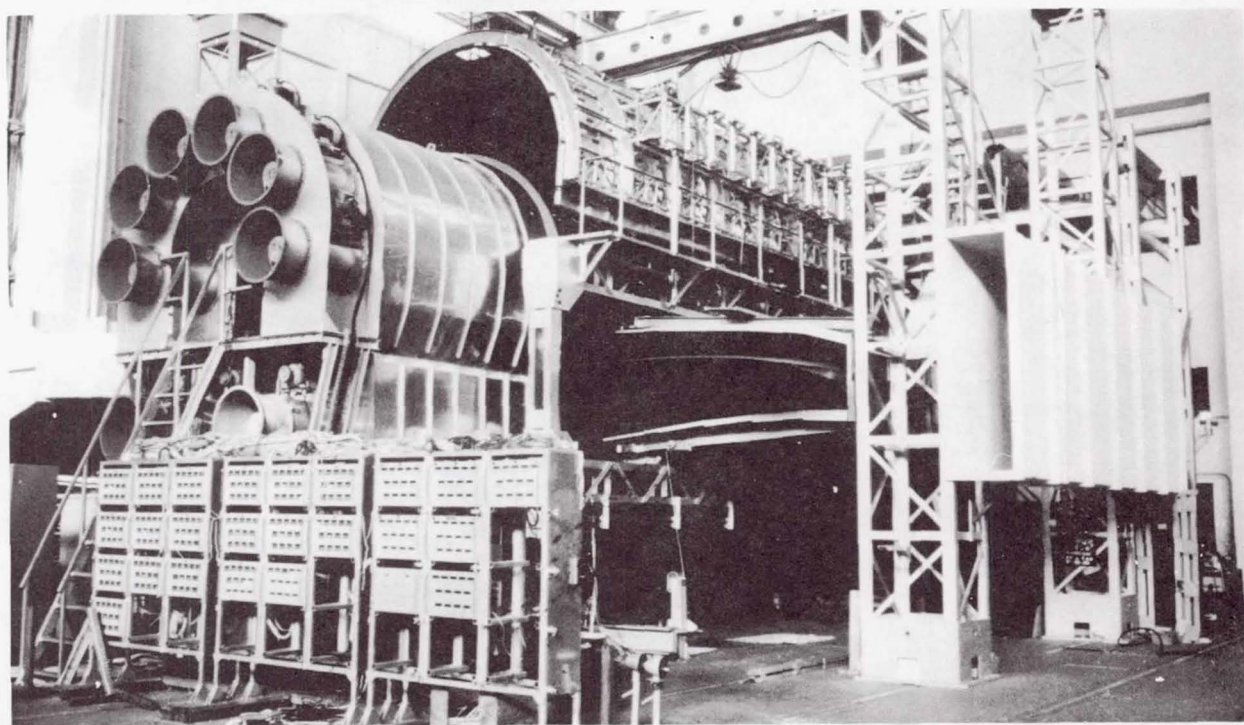
Figure 11.





### 2.3.2 FATIGUE TEST RIG.

THE WING PART IS VISIBLE  
BETWEEN TOP AND BOTTOM  
WALLS OF THE OPEN OVEN.



GENERAL VIEW OF THE 2.3.2 FATIGUE TEST RIG.

Figure 12.



# STRUCTURAL TESTING OF CONCORDE AIRCRAFT – FURTHER REPORT ON UNITED KINGDOM TESTS

By Norman Harpur  
British Aircraft Corporation Limited  
Filton, United Kingdom

## SUMMARY

This section of the United Kingdom review of structural testing for the period 1969 to 1971 gives a summary of the tests being carried out on Concorde nacelle structure as part of the structural development and certification programme. It attempts to complete the overall picture provided by other papers which primarily deal with testing of the remainder of the Concorde airframe.

## INTRODUCTION

During this symposium, much information has been presented on the structural testing of Concorde. In particular, paper no. 1 by E. L. Ripley, given as the Third Frederick J. Plantema Memorial Lecture, deals extensively with the Concorde airframe major fatigue test and similar development tests on fuselage components. Paper no. 20 by V. P. N'Guyen and J. P. Perrais gives a summary of the Concorde major airframe static test and other large fuselage-wing component tests at the Centre d'Essais Aéronautiques de Toulouse (C.E.A.T.) in France.

To complete the picture, the present paper gives an account in general terms of a series of tests being carried out in the United Kingdom (U.K.) on Concorde nacelle components. These components are relatively large structural elements (e.g., the intake is 3.5 by 7 by 17 feet) subject to unique types of loading and involving novel forms of design and construction. They are designed to meet the full static strength, fail-safe, and fatigue requirements of the basic airframe and, thus, have to be the subject of a complete certification test programme. In this sense, they must be considered as a complementary part of the major static and major fatigue test programmes.

## SYMBOLS

M	Mach number
n	manoeuvring load factor

$V_C$  design cruising speed

$V_D$  design diving speed

## DESCRIPTION OF NACELLE STRUCTURAL SPECIMENS

A supersonic aircraft, such as Concorde, requires a sophisticated power-plant installation, including a variable-geometry intake with its own automatic-control system, an engine bay providing full accessibility, and a variable-geometry nozzle incorporating thrust reversers. A general view of the complete Concorde nacelle is shown in figure 1, and a more detailed description of the specimens is given in the appendix.

Part of the basic philosophy for the production nacelle structure has been to design the three main components – intake, engine bay, and nozzle – as separate units linked together in a statically determinate manner to minimise redundant interaction forces arising because of wing distortions. For the same reason, the engine bay itself has been designed in two halves – a forward bay and a rear bay – simply spigoted together at the joint.

Advantage has been taken of this design philosophy to reduce the complexity of testing; thus, the air intake was tested separately from the engine bay and nozzle, and the forward engine bay was tested independently of the rear engine bay.

A summary of the nacelle structural test specimens either tested or to be tested as part of the Concorde development and certification programme is given in table 1 for the intake and in table 2 for the engine bay and nozzle.

An additional production nozzle specimen is also being provided, and will be tested under operating environmental conditions behind a pair of Olympus engines installed in a test bed at Société Nationale d'Etude et de Construction de Moteur d'Aviation (SNECMA) in France.

## PROBLEMS ASSOCIATED WITH INTAKE TESTING

### Summary of Loading Actions

The primary loading action on the intake results from internal pressures due to the airflow through the ducts. The internal pressures due to two typical operating conditions are shown in figure 2. Since part of the top of the intake is closed by the lower surface of the wing, these pressures produce significant loads in the wing-nacelle attachment links, as well as designing the intake shell. Additional loading in intake and links is due to the interaction forces at the links due to wing distortions.



During supersonic cruise conditions, the intake is also subjected to elevated temperatures with the internal temperature reaching a maximum of  $125^{\circ}$  to  $130^{\circ}$  C and the external temperature a value of  $100^{\circ}$  C. Because both inside and outside surfaces are subjected to similar forcing conditions, thermal stresses during acceleration and deceleration are, in general, less than those produced by the cruise temperature gradients quoted previously.

### Test Realisation

For all three intake test specimens, the approach to the problem of simulating wing interaction loads and pressure loads is the same. To represent wing-nacelle interaction loads, the specimens are mounted from a rigid test frame by links at the points A, C, E, and G shown in figure 1. Each link is then calibrated to enable the link-reaction load to be measured. Three remaining links (points B, D, and F) are attached to hydraulic jacks which are controlled to apply specified displacements.

The representation of the varying pressure distributions within the ducts has been a major difficulty. The interior of the specimen was divided into four main zones, with a fifth zone representing the boundary-layer bleed between the wing and the forward part of the intake. (See fig. 2.). Between adjacent zones a pressure seal has had to be developed in such a way that while maintaining the interzone pressure differentials, local loading and restraint to specimen movement have been avoided. The final solution, following extensive development, has led to the design of flexible suction seals mounted off a central core rigidly supported by the test frame. The assembly of one such core for the room-temperature tests on specimen 2.9B is shown in figure 3.

For the thermal testing on specimen 2.9.4, the specimen has to be heated cyclically inside and outside. Each internal zone is thus supplied with pressurized air through a separate closed-circuit system of ducts with outlets into the specimen through the central core. The heating of this air is controlled through a heat exchanger. For cooling, the circuit is depressurized and switched to open circuit; ambient air is then blown through the specimen. The exterior of the specimen is surrounded by a duct through which unpressurized air is blown at the requisite temperatures. This system, which is duplicated for each intake duct, results in an extremely complex facility. A scale model of this facility is shown in figure 4.

With this facility it is possible to simulate adequately the major loading actions. In the fatigue test, advantage is taken of the absence of significant climb and descent thermal stresses by shortening the thermal cycle to simulate only cruise gradients and imposing a test cruise time of 12 minutes compared with an average aircraft cruise time of 75 minutes. To compensate for this shorter test time at temperature, creep rate is increased by a factor of approximately 5 by increasing maximum test temperatures  $15^{\circ}$  C. The



proposed test cycle is shown in figure 5. The aim is to achieve a rate of testing comparable with the major airframe fatigue test (where each 1-hour test cycle simulates the damage done in two typical aircraft supersonic flights).

## PROBLEMS ASSOCIATED WITH ENGINE-BAY AND NOZZLE TESTING

### Summary of Loading Actions

The loading actions on the engine bay and nozzle are similar to those on the intake, but there are some significant differences which are summarized below:

(1) The distribution of pressure in the engine bay and nozzle is essentially constant; thus, only one internal-pressure zone is required in each duct.

(2) The concentrated system of hydraulic jacks required to represent reverse-thrust bucket loads, bucket operating jack loads, and engine jet pipes leads to local complications in the heating, cooling, and pressurisation system.

(3) The maximum operating temperatures in the rear engine bay and nozzle are high, reaching about  $240^{\circ}\text{C}$  in the engine bay and between  $320^{\circ}\text{C}$  and  $410^{\circ}\text{C}$  in the nozzle; as in the intake, a steady gradient is present during cruise causing significant thermal stresses. In addition, large transient thermal gradients arise in the nozzle centre-wall structure during descent and due to reheat in the climb and result in another thermal-stress cycle. These temperatures are shown diagrammatically in figure 6.

### Test Realisation

Two of the engine-bay specimens (specimen 1.11.2.2 and specimen 2.9.4.2) are relatively simple; tests on these specimens involve static pressure and mechanical loading at room temperature. Specimen 2.9.4.3 is subjected to a pressure fatigue test at elevated temperature. This test poses no serious problems apart from the control and monitoring of temperature and the timing of the pressure cycle to ensure a consistent accumulation of creep and fatigue damage.

The fourth specimen, specimen 2.9.6, is subjected to both static and fatigue testing with representation of thermal conditions. This testing requires a complex test facility similar to that for the intake shown in figure 4. The simulation of wing distortions and bay pressures is done in a similar manner to that for the intake; the number of pressure zones is less, but seal design is complicated by the higher temperatures required.

In order to limit the test temperatures, advantage is taken of the fact that thermal stress due to temperature gradient is the most significant requirement since creep and material degradation at the aircraft temperature levels are unimportant for the stainless steel materials of the nozzle bay and the titanium and inconel alloys of the engine bay.

The required temperature gradients of about  $250^{\circ}\text{C}$  maximum through the nozzle side-walls are therefore obtained by blowing air at room temperature over the outside of the specimen and blowing hot air from the rear to the front through the inside. A special problem arises in simulating the temperature gradients through the centre wall of the nozzle during descent and due to reheat in the climb.

To achieve these in as short a time as possible, a special system is provided to blow alternately hot and cold air into the centre wall void. This system is switched on at appropriate times in the cycle, thus enabling the required cruise and recovery equilibrium conditions to be rapidly achieved. (See fig. 7.) A diagram of the fatigue cycle achieved with this forcing system is shown in figure 8; the target, as in the case of the intake, is to achieve a rate of testing comparable with the major airframe fatigue test.

### TEST CONTROL

Both the intake (specimen 2.9.4) fatigue test and the engine-bay and nozzle (specimen 2.9.6) fatigue test are to be controlled and monitored by a single IBM 1800 computer, which will also provide data logging and both on-line and off-line data analysis and display.

The monitoring facility checks the applied values of all control variables with the required values against a set of inner and outer limits; the inner limit exceedances are printed-out and the outer limit exceedances cause shutdown of the test.

A general view of this installation is shown in figure 9, and a flow diagram illustrating the control logic of the test facility is shown in figure 10.



## APPENDIX

### DESCRIPTION OF PRODUCTION NACELLE STRUCTURE

#### Air-Intake Structure

A structural breakdown of the intake is shown in figure 11. The operating temperature during Mach 2.0 cruise is approximately  $120^{\circ}\text{C}$ , and aluminium alloy is used for all the structure with the exception of the rear frame (frame 204), which is made from titanium alloy to provide a fireproof bulkhead. The forward lip, the forward- and centre-duct skins, and the intake frames are mostly machined from thick plate. The moveable ramps are made from aluminium alloy honeycomb.

The intake is suspended from the wing at six points, with a forward and rear attachment on each of the three walls. Five of the attachments are simple links taking vertical loads only; the sixth, at the centre of the rear frame, is a fixed-point attachment taking loads in all planes. A secondary horizontal link is also provided on the forward centre wall to provide yawing restraints.

#### Engine-Bay Structure

The general arrangement of the engine bay can be seen from figure 1. Since the engines are mounted directly from the wing, engine-bay loads derive predominantly from internal pressures. The bay consists of a forward and rear section, simply spigotted together; each section consists of a fixed centre wall with an L-shaped door forming the side and bottom walls of each bay. The front and rear bulkheads of the bay are formed by the rear frame of the intake and the front frame of the nozzle-fixed structure, respectively.

The centre wall (see fig. 12) has a maximum operating temperature of  $250^{\circ}\text{C}$  and must resist flame temperatures of up to  $1100^{\circ}\text{C}$  for 5 minutes. Thus, both front and rear sections are made from a nickel alloy (Inconel 718) honeycomb-sandwich panel.

The forward doors (see fig. 13) have a maximum operating temperature of  $150^{\circ}\text{C}$  and are made from aluminium alloy. Inner and outer skins are riveted and spot-welded, respectively, to close-pitched frames of the extruded I-section. The rear doors (shown in fig. 14), where maximum operating temperatures are about  $200^{\circ}\text{C}$ , are of similar construction but made of titanium alloy with the frames either machined from bar or fabricated from welded plate. Both sets of doors are provided with fore and aft sliding freedom of about 30 mm along a line near the door corner. This freedom has been provided to eliminate large interaction forces between the wing and door which would otherwise arise because of wing distortions in flight. The slide also incorporates a hinge, so that



## APPENDIX

it is possible to open the bottom part of the door independently for simple servicing. Also to avoid interaction forces due to distortion, the doors are supported from two hinges, at the front and rear of the top edge only. Intermediate hinges are provided but are designed to only restrain the door against lateral pressure forces.

### Nozzle Structure

The general arrangement of the nozzle fixed structure is shown in figure 15. The maximum operating temperature of the structure is in the region of  $450^{\circ}\text{C}$ , and for this region stainless steel is the basic structural material.

The basic structure is made up of a pair of barrels forming the main ducts, supported by spectacle frames and enclosed by an outer fairing. These components are mainly fabricated from stainless steel stressskin honeycomb. Upper and lower fore and aft longerons run between the inner barrels and outer fairings in the sidewalls and centre walls. These form the primary load path for the reverser bucket loads; these buckets are attached to hinge fittings which connect with the aft end of these longerons.

This fixed structure is attached to the engine-bay—wing interface at three non-redundant fittings, one on each sidewall and one on the centre wall. A fourth attachment at the centre wall is provided as a fail-safe standby. The main centre-wall attachment connects with the engine-bay centre wall, the two sidewall attachments connecting with a pair of triangulated frames attached to the wing undersurface.

Provision in the fixed structure is made for attaching the engine primary nozzle by means of three spigot fittings projecting into the main ducts. Additional attachments are provided for the reverser-bucket operating jacks, four in each duct.

TABLE 1.- INTAKE MAJOR STRUCTURAL TEST SPECIMENS

Description	Remarks	Summary of test requirements		
		Static	Fail-safe	Fatigue
Specimen 2.9B (prototype air intake)	A twin left-hand intake to prototype standard.  Rig applies internal pressure in four zones per duct with wing distortions.	Static design cases at room temperature up to 85% ultimate load to clear prototype flying.  Test cases include (1) Symmetric and asymmetric surge cases (2) Ground running manoeuvre cases at $V_D$ .		
Specimen 2.9.4 (production air-intake fatigue specimen)	A twin right-hand intake to preproduction standard.  Rig applies internal and external heating in association with internal pressure in four internal zones. Wing distortion can be simulated.  Static-strength certification of the intake is based on hot tests to limited loads	Static design cases for certification at elevated temperature as appropriate up to 50% ultimate load in order not to invalidate fatigue test.  Test cases include (1) Ground running single engine surge (2) Single engine surges at $V_C$ , $M = 0.66$ (3) Double engine surges at $V_C$ , $M = 2.0$ (4) Supersonic wing distortion, $M = 2.13$ at $V_D$ , $n = 2.5$ .		Certification fatigue test. Cyclic temperature, pressures, and wing distortions.  Temperatures increased by $15^\circ\text{C}$ to give a factor of 5 on creep, resulting in a shorter test cycle.
Specimen 2.9.5 (production air-intake fail-safe and static-strength specimen)	Basically a twin right-hand intake to production standard.  Rig similar to that for specimen 2.9.4 but at room temperature only.  Static-strength certification of the intake is based on cold tests to 100% ultimate load.	Static design cases for certification up to 100% ultimate load. All tests were at room temperature; for hot cases, loads and pressures are adjusted to allow for thermal stresses, adjustment based on results from specimen 2.9.4.  Test cases were the same as those for specimen 2.9.4.	Crack propagation and residual tests to meet FAA fail-safe requirements for intake structure.  All tests will be done at room temperature.	

TABLE 2.- ENGINE-BAY AND NOZZLE MAJOR STRUCTURAL TEST SPECIMENS

Description	Remarks	Summary of test requirements		
		Static	Fail-safe	Fatigue
Specimen 1.11.2.2 (prototype engine-bay centre-wall specimen)	Rig applies lateral pressures, engine mounting loads, and nozzle loads.	Static design cases at room temperature to clear prototype flying.  Design cases include (1) Ground running (2) Symmetric reverse thrust (3) One engine windmilling (4) Manoeuvre at $V_D$ (with and without nacelle twist)		
Specimen 2.9.4.2 (preproduction engine-bay centre-wall specimen)	Test to provide Mach 2.0 flight clearance for 01 aircraft flying.  Test at room temperature since temperature not critical for this component.	A single design case to 100% ultimate load. Outboard engine, windmilling at $V_C$ , $M = 2.0$ (inboard engine, normal running).		
Specimen 2.9.4.3 (forward engine-bay door)	Fatigue and creep test for certification.  Static certification of this component is being based on calculation plus detail tests.			Certification fatigue test: cyclic pressure and wing distortion, at constant elevated temperature.  A temperature gradient is maintained through the door, temperature levels being increased to accelerate creep.
Specimen 2.9.6 (rear engine bay and type 28 nozzle)	A twin left-hand rear engine bay and type 28 nozzle to production standard.  Rig applies internal heating and pressurisation in association with primary nozzle and reverser bucket loads.  Heating represents internal to external temperature gradients only; absolute temperature judged to be not critical.	Static design cases for certification with thermal stresses. Where appropriate, loads and pressures are limited in the right-hand duct in order not to invalidate fatigue test; thus, symmetric cases are taken to 50% ultimate load; asymmetric cases to 85% ultimate load in the left-hand duct.  Design cases include (1) Reverse thrust on ground (2) Ground running, maximum take-off power (3) Manoeuvre at $V_D$ , $M = 2.2$ (4) One engine windmilling, $V_C$ , $M = 2.0$ (5) Single-engine surge, $V_C$ , $M = 2.0$	Nozzle loads only applied with various members disconnected in turn.  Redistribution of stresses measured.  Load levels limited to avoid invalidation of fatigue test.	Certification fatigue test: cyclic temperatures and pressures with distortions and nozzle loads.



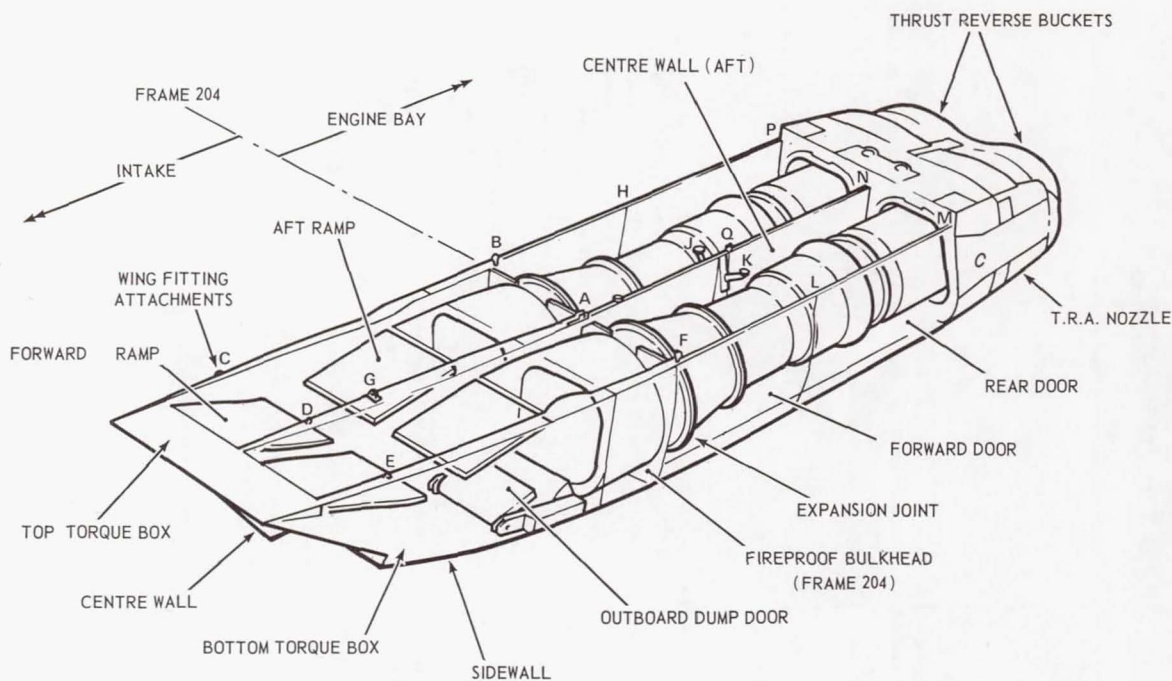


Figure 1.- General view of complete nacelle.

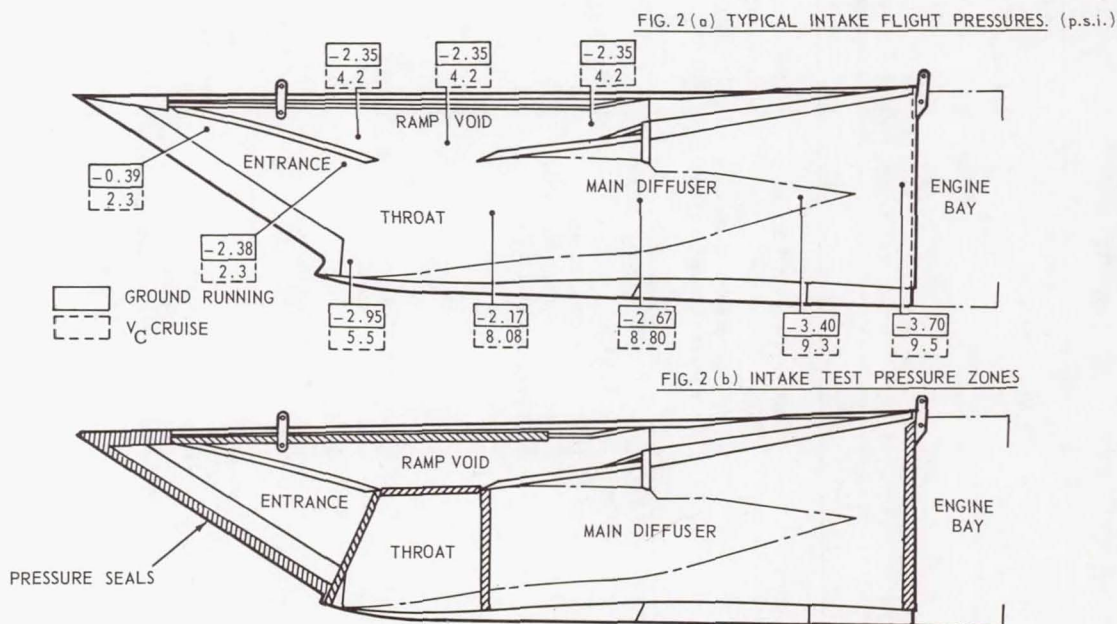


Figure 2.- Intake pressures and pressure test zones.

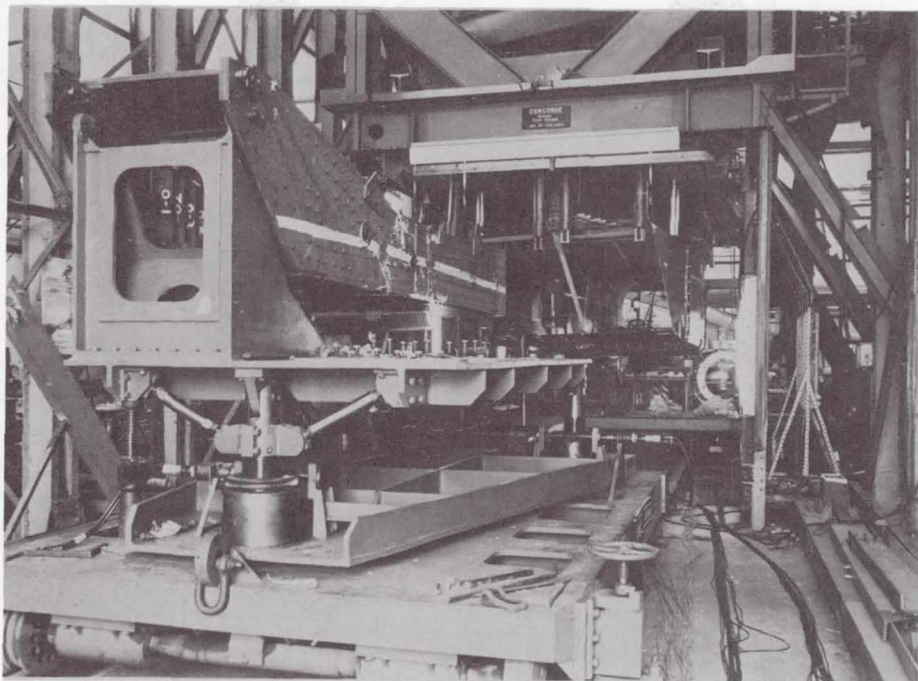


Figure 3.- Internal core for one intake duct (specimen 2.9B).

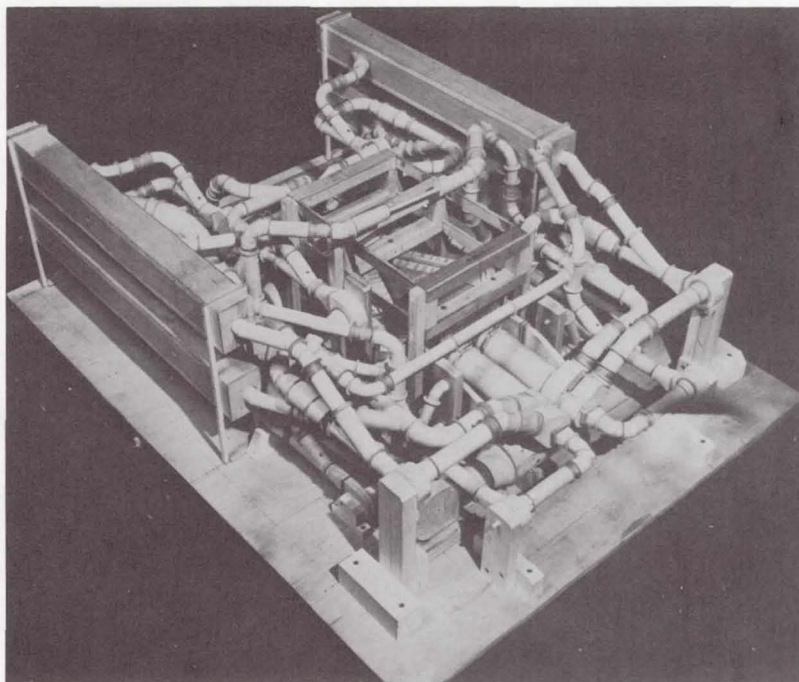


Figure 4.- Model of intake test rig.

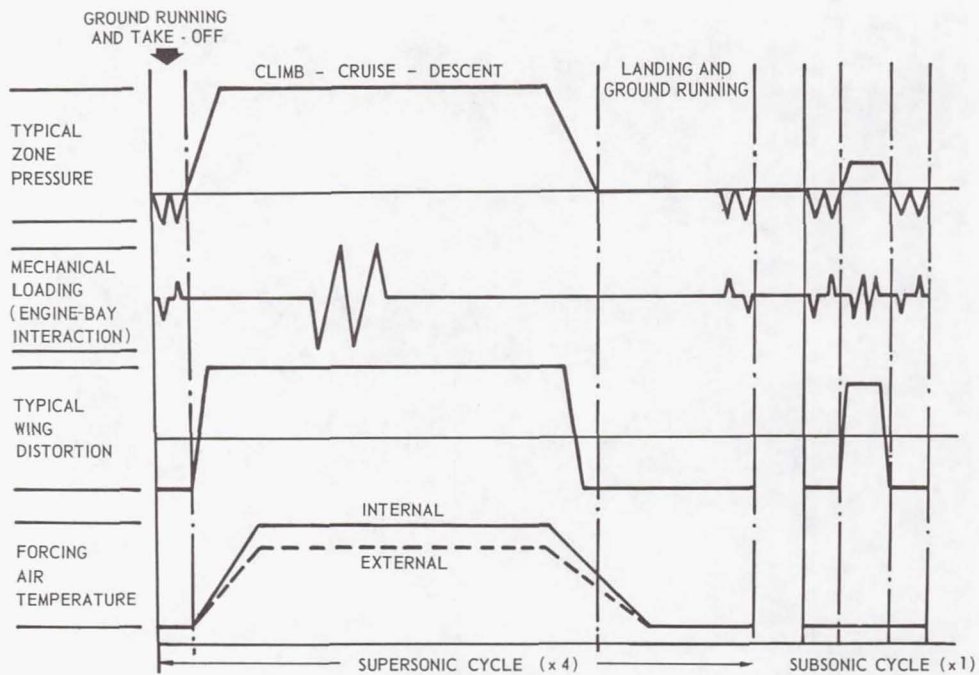


Figure 5.- Diagrammatic representation of intake fatigue cycle.

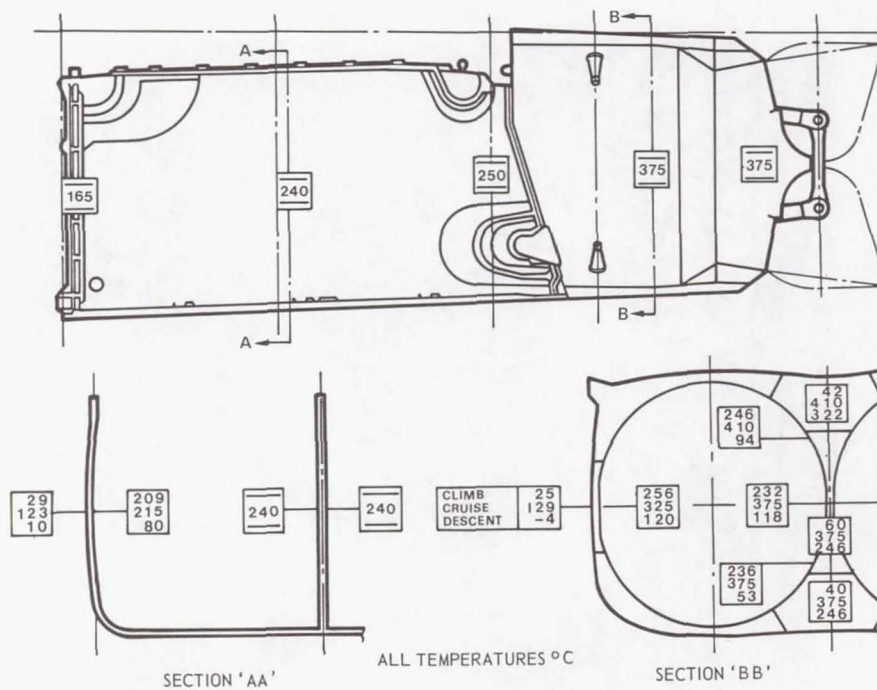


Figure 6.- Engine-bay and nozzle temperature distribution.



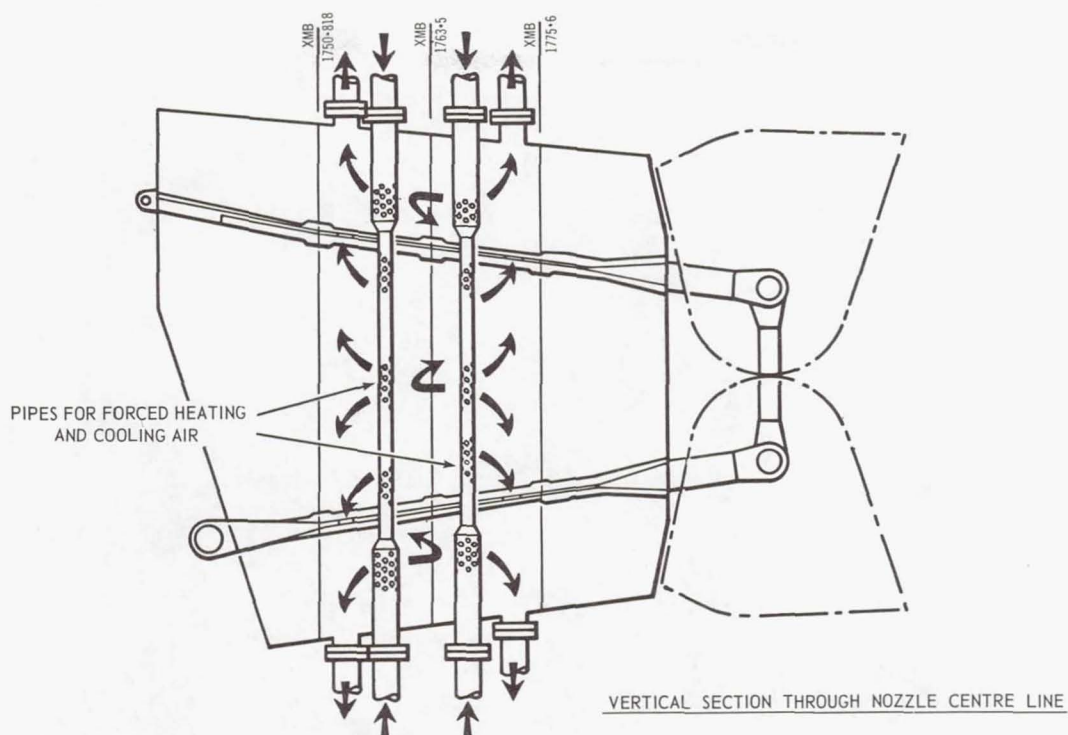


Figure 7.- Internal forced heating and cooling of nozzle centre wall.

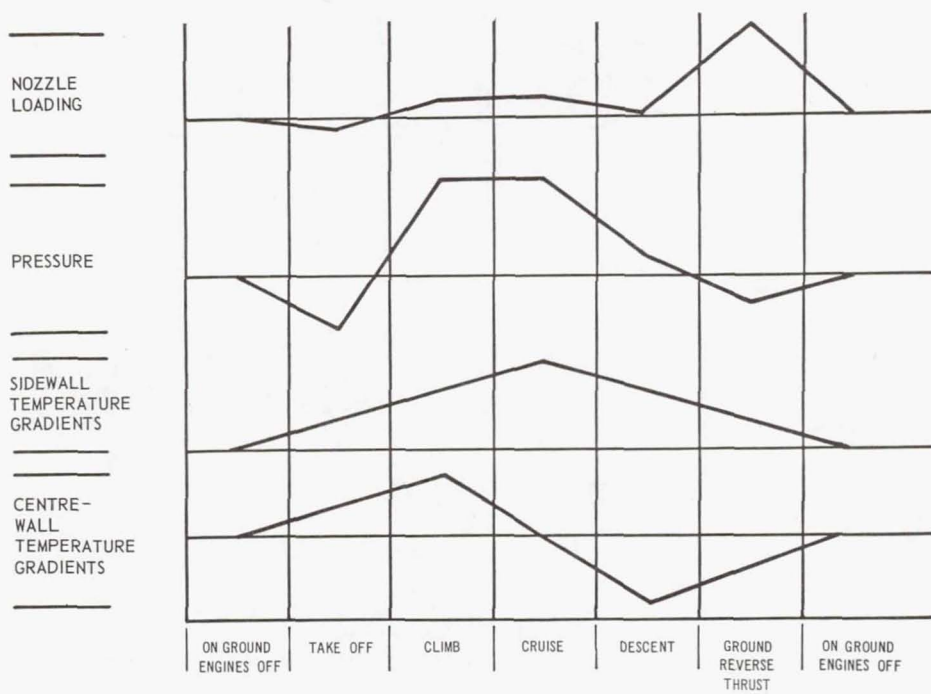


Figure 8.- Diagrammatic representation of engine-bay and nozzle fatigue cycle.

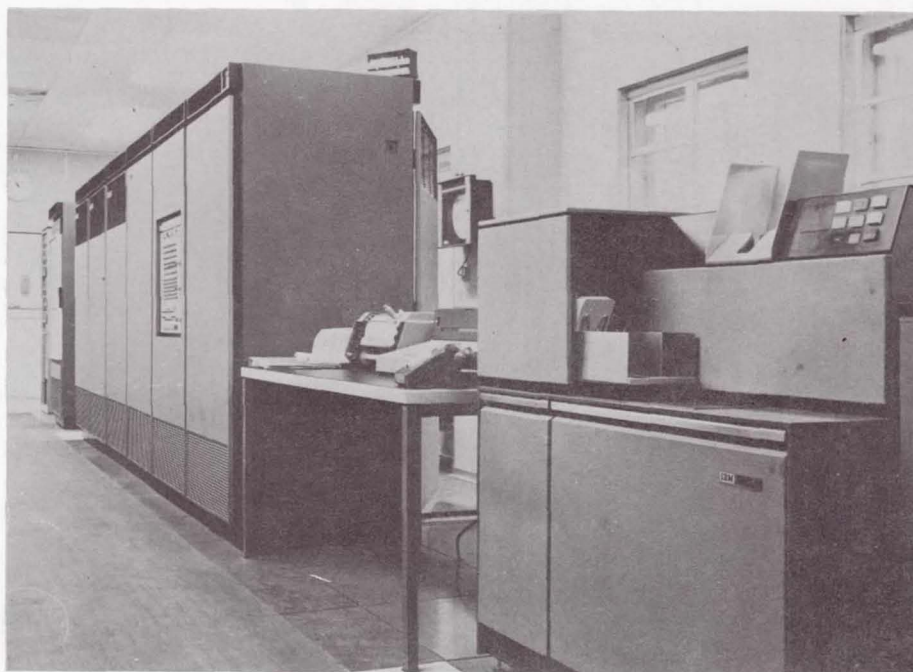


Figure 9.- IBM 1800 computer installation.

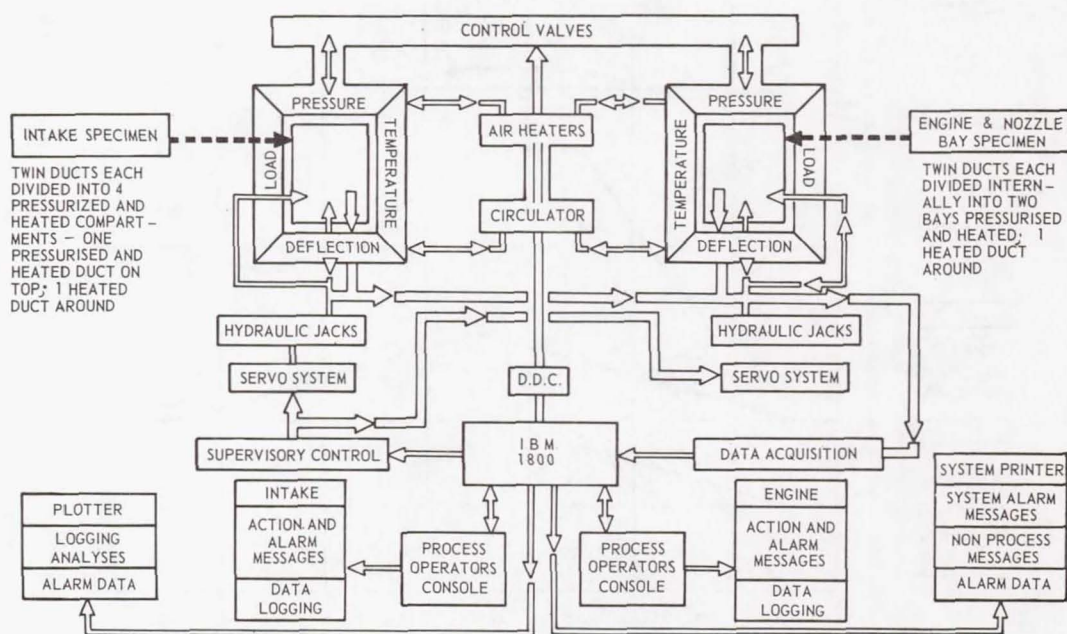


Figure 10.- Nacelle test-control flow diagram.

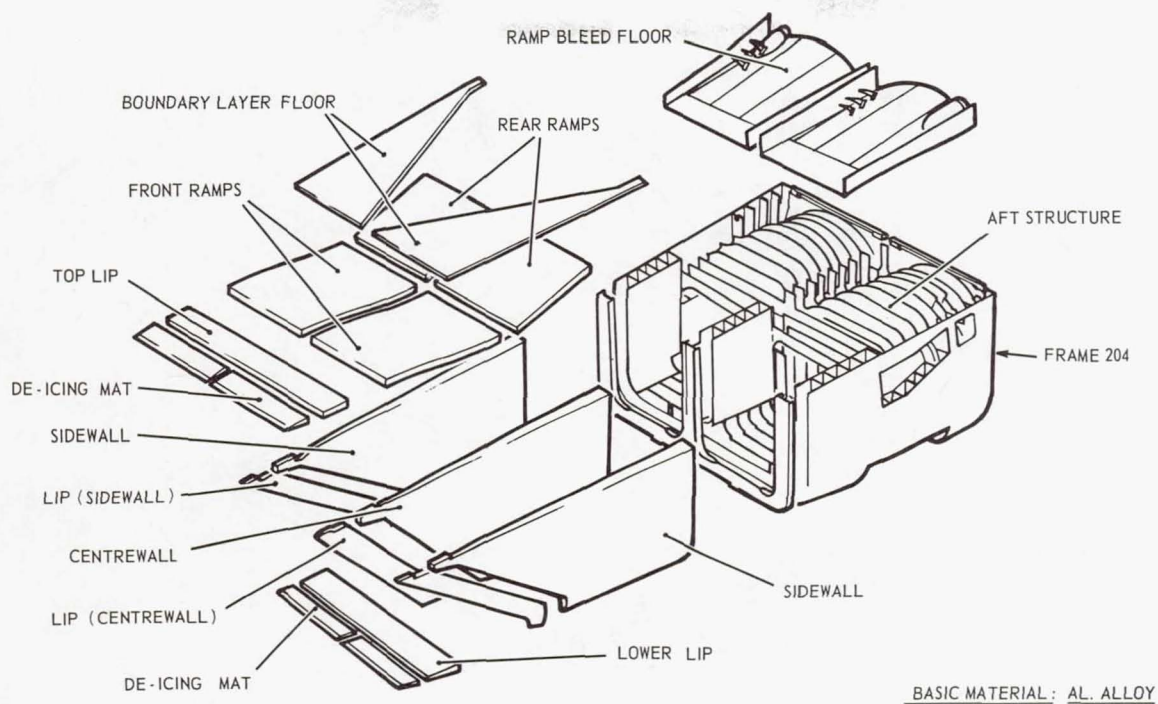


Figure 11.- Structural breakdown of the intake.

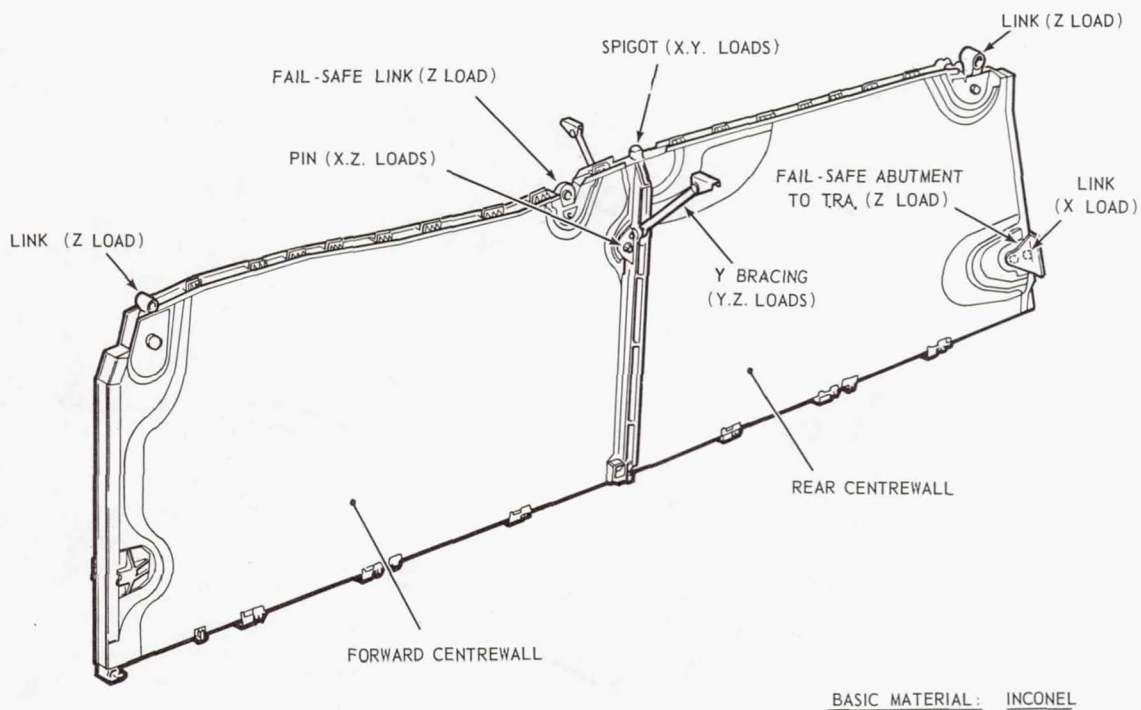
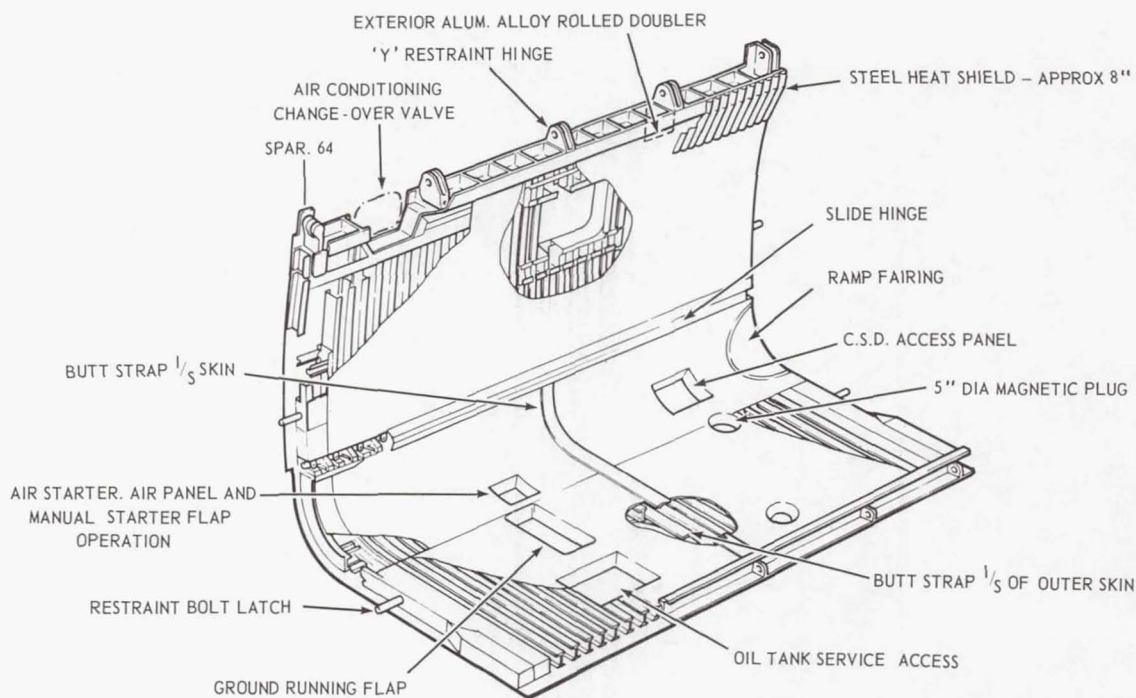


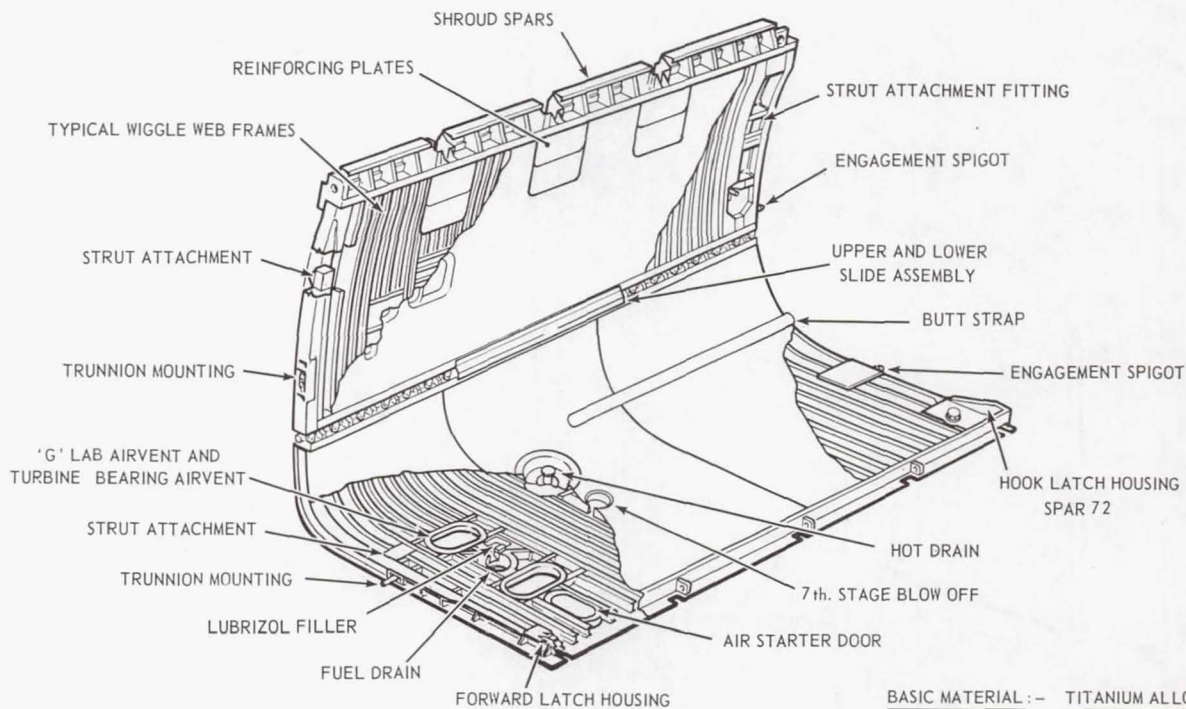
Figure 12.- Engine-bay centre wall.





BASIC MATERIAL: AL. ALLOY

Figure 13.- Engine-bay forward door(s).



BASIC MATERIAL: - TITANIUM ALLOY

Figure 14.- Engine-bay rear door(s).

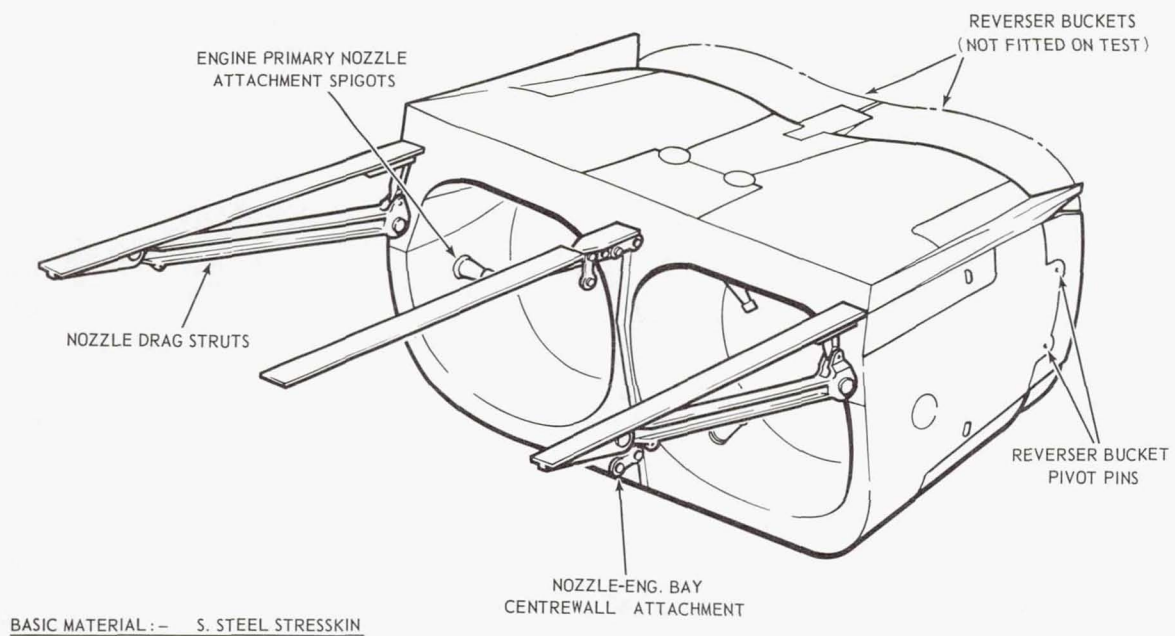


Figure 15.- General arrangement of nozzle structure.

## A COMPARISON OF RELIABILITY AND CONVENTIONAL ESTIMATION OF SAFE FATIGUE LIFE AND SAFE INSPECTION INTERVALS

By F. H. Hooke

Aeronautical Research Laboratories

Department of Supply

Commonwealth of Australia

22

### SUMMARY

Both the conventional and reliability analyses for determining safe fatigue life are predicated on a population having a specified (usually log normal) distribution of life to collapse under a fatigue test load.

Under a random service load spectrum, random occurrences of load larger than the fatigue test load may confront and cause collapse of structures which are weakened, though not yet to the fatigue test load. These collapses are included in reliability but excluded in conventional analysis.

The theory of risk determination by each method is given, and several reasonably typical examples have been worked out, in which it transpires that if one excludes collapse through exceedance of the uncracked strength, the reliability and conventional analyses gave virtually identical probabilities of failure or survival.

### INTRODUCTION

The conventional approach to safe-life estimation envisages a fatigue test which imposes on at least one full-scale structure the equivalent fatigue damaging effect of service loading, according to some regular pattern which restricts, however, the largest load, regularly applied, to some fraction of the virgin strength. Life to collapse is regarded as a statistical variable, of whose population mean the test failure is treated as an estimator. Variability is estimated from other representative experiments in which each member's strength falls to a single lower value (in different life-times), which is accounted failure, and the probability density function of life to failure is usually assumed log normal.

Determination of the safe life as a function of desired or acceptable probability of failure requires merely the estimation of the desired percentile of the population, that is, the desired percentile of the distribution of fatigue lives, measured to the point at which each member's strength has fallen to the largest applied load in the test sequence.



Reliability theory, applied to this problem attributes the same strength properties to the population as before, including the decay of strength as fatigue crack growth occurs, but does not assume that collapse occurs when each member's strength has fallen to a common value. Collapse occurs rather when a member of the population meets a load larger than its current strength, and this event would correspond to a conventionally assessed life for that member if the service spectrum were modified or truncated so that all load peaks larger than the fatigue test load were reduced to that value.

The purpose of this study was to present the theory of risk determination for each method and to ascertain by the working of several reasonably typical examples whether the conventional method significantly underestimated the failure risk through ignoring service loads higher than the fatigue test load.

### SYMBOLS

$b$	ratio of maximum fatigue test load to virgin strength or strength at critical crack length
$g$	ratio of crack propagation time (from detectable to critical size) to total life $H$
$H$	population life in hours; a log normal random variable
$\tilde{H}$	population geometric mean life in hours
$l$	crack length
$l_{cr}$	"critical" crack length at which strength $U$ has fallen to $bU_0$
$l_d$	crack length detectable with certainty
$\tilde{m}(V)$	frequency of occurrence, per hour, of applied load $>V$
$n$	number of load cycles applied
$p(U)$	probability density function of strength for population
$p(V)$	probability density function for applied load $V$ for some arbitrary time interval

$P(t)$	probability of collapse before time $t$
$P(n)$	probability of collapse before $n$ th applied load
$P_c$	probability of collapse in arbitrary time interval
$\delta P_c$	probability of collapse in arbitrary time interval of small element of population characterised by its value of $H$
$r(t)$	risk or risk rate or risk of failure at time $t$ of survivors at time $t$
$r(n)$	risk or rate of failure at the $n$ th applied load of survivors of $(n-1)$ th load
$R(t)$	reliability at time $t$ or probability of survival to time $t$
$R(n)$	reliability at $n$ th applied load or probability of survival from first to $(n-1)$ th load
$t$	time, hours
$T_b$	safe inspection period for probability of failure $p = p$ percent of $gH$
$U$	strength
$U_0$	virgin strength
$V$	applied load
$\sigma$	standard deviation of $\log H$
$\phi$	strength decay function of crack size
$\psi$	crack propagation (time function)

#### STATISTICAL MODEL AND SAFE-LIFE ANALYSES

The statistical model used herein is the one used in references 1 and 2, as shown in figure 1 in both normal and logarithmic coordinates, and has the following features:

(1) The population life  $H$  is log normally distributed with geometric mean  $\tilde{H}$  and variance  $\sigma^2$ ,  $H$  being the hours in which the strength  $U$  is reduced from  $U_0$  to  $bU_0$  which corresponds to the largest load in the test spectrum.

(2) Crack propagation in each member is scaled to the member's potential life to failure  $H$  under the specified test history and follows the expression

$$\frac{l}{l_{cr}} = \psi\left(\frac{t}{H}\right)$$

(3) Strength is related to crack size; thus,

$$\frac{U}{U_0} = \phi\left(\frac{l}{l_{cr}}\right)$$

and the condition (1) gives  $\phi(1) = b$ .

(4) Whereas crack propagation is governed by condition (2), failure is governed by the frequency of occurrence  $\tilde{m}(V)$  per hour, of service loads exceeding  $V$ , or in non-dimensional terms, the frequency  $\tilde{m}(V/U_0)$  of service loads greater than  $V/U_0$ .

In conventional analysis, a safe life for a probability of failure  $p$  is merely the  $p$  percentile of the variable  $H$ . Insofar as  $H$  is the time at which  $U$  falls to  $U_0$ , it is independent of the shape of the crack propagation curve and is only dependent on the time  $H$  at which  $l = l_{cr}$ .

The calculation of failure by the reliability approach requires the following definitions (refs. 4 and 5):

$P(t)$  probability of fracture before time  $t$

$R(t)$  reliability at time  $t$  or probability of survival to time  $t$

$r(t)$  risk or rate of failure at time  $t$  of survivors to time  $t$ ,  $\frac{1}{R(t)} \frac{dP(t)}{dt}$

and the expression

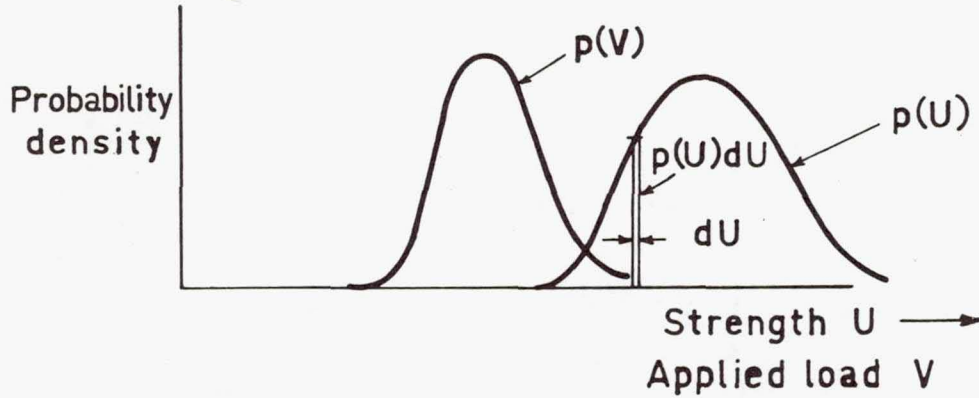
$$R(t) = e^{-\int_0^t r(t) dt} \quad (1)$$

Or, alternatively, the probability of failure before a given time, the reliability and the risk (hazard rate or force of mortality) may be expressed as a function of number of cycles  $n$ , as  $P(n)$ ,  $R(n)$ , and  $r(n)$ . In this case  $r(n) dn$  is the probability of failure



in  $dn$  cycles of members surviving at  $n$  cycles, so that (with  $dn = 1$ ),  $r(n)$  is the probability of failure per cycle of members which survive to the  $n$ th cycle.

If the probability density functions of strength and of load occurring in some arbitrary time are  $p(U)$  and  $p(V)$ , respectively, as shown in the following diagram,



then the probability of collapse in this arbitrary time is the probability that a load  $V$  falls on a structure of strength  $U$  less than  $V$ . For a load lying between  $V$  and  $V + dV$ , occurring with probability  $p(V) dV$ , its contribution to the probability of collapse is

$$p(V) dV \int_{U=0}^{U=V} p(U) dU \quad (2)$$

and the total probability of collapse is

$$P_c = \int_{V=0}^{V=\infty} p(V) \int_{U=0}^{U=V} p(U) dU dV \quad (3)$$

Or, alternately, if there is considered an element of the population of structures lying between  $U$  and  $U + dU$ , the probability of a structure having a strength in this interval being  $p(U) dU$ , its contribution to the probability of collapse is

$$p(U) dU \int_{V=U}^{V=\infty} p(V) dV \quad (4)$$

so that the total probability of collapse is also

$$P_c = \int_{U=0}^{U=\infty} p(U) \int_{V=U}^{V=\infty} p(V) dV dU \quad (5)$$

In the example of concern, in which strength  $U$  is distributed as a function of  $H$  and also decreases with time, the calculation is most readily made by taking small elements  $p(H) dH$  of the population characterised by their values of  $H$  and using equation (4) to find the contribution to the probability of failure by each element; that is,

$$\begin{aligned}\delta P_c &= p(H) dH \int_{V=U}^{V=\infty} p(V) dV \\ &= p(H) dH [\Pr(V > U)]\end{aligned}\quad (6)$$

It will be noted that  $U$  is a function of time  $U(t) = U_0 \phi \{\psi(t/H)\}$  so that

$$\begin{aligned}\delta P_c &= p(H) dH [\Pr(V > U(t))]\end{aligned}$$

$$= p(H) dH \left\{ 1 - e^{-\int_0^t r(t) dt} \right\}$$

from equation (1),  $r(t)$  being the risk function for this element,

$$\delta P_c = p(H) dH \left\{ 1 - e^{-\int_0^t \tilde{m}(V > U(t)) dt} \right\} \quad (7)$$

where  $\tilde{m}(V > U(t))$  is the frequency per hour with which the applied load exceeds the element's strength  $U(t)$ .

The total probability of collapse is

$$P_c = \int_{H=0}^{H=\infty} p(H) \left\{ 1 - e^{-\int_0^t m(V > U(t)) dt} \right\} dH \quad (8)$$

which is identical, allowing for a difference in notation, with the expression

$$P(t) = \int_{F(U)=0}^{F(U)=1} \left\{ 1 - e^{-\int_0^t n(U) dt} \right\} dF(U)$$

of reference 2 (p. 29).

## INSPECTION INTERVAL ANALYSIS

Safety may be achieved in an inspectable structure if the critical crack length  $l_{cr}$ , at which strength falls to a selected unsafe value, is larger than the crack length detectable with certainty  $l_d$ . The time remaining in which a crack propagates from  $l_d$  to  $l_{cr}$  (and strength to  $U = bU_0$ ) is some fraction of the life  $H$ , say  $gH$ , and with this model  $g$  is a constant for all members of the population. Thus  $gH$  is log normally distributed with median  $g\tilde{H}$  and variance  $\sigma^2$ .

In conventional analysis, the critical length  $l_{cr}$  is the same for all members of the population, and the unsafe value of strength is equated to  $bU_0$ , the highest load in the fatigue test programme. A safe operating period after inspection  $T_b$  for a probability of failure  $p$  in the interval is the  $p$  percentile of the variable crack propagation time  $gH$ , since it can readily be seen that only  $p$  percent of cracks can propagate from  $l_d$  to  $l_{cr}$  in a time less than  $T_b$ . This result assumes that all structures are cracked to just below  $l_d$  at the inspection date, and it is seen to be independent of the shape of the crack propagation curve for cracks smaller than  $l_d$ .

In reliability analysis, structures may be considered to be cracked to just below  $l_d$  at the beginning of the propagation time but to reach a failure state governed by load exceeding strength. Where the safe lives, as calculated by reliability and conventional methods, coincide it is concluded that this will imply a coincidence of the values of safe inspection intervals.

## APPLICATION OF THE THEORY TO TYPICAL EXAMPLES

Example A(1) represents a military aircraft situation where the structures are subjected to the manoeuvre load spectrum (curve A of fig. 2) in which limit load is exceeded once per 100 hours, crack size  $l/l_{cr}$  is a power function of  $t/H$ , the decay of strength with crack size conforms to the laws of fracture mechanics, and the standard deviation  $\sigma$  is 0.167.

Example A(2) represents the same situation as example A(1) except that the standard deviation  $\sigma$  is  $0.167\sqrt{2}$ .

Example B(1) represents a civil aircraft situation where the structures are subjected to the gust spectrum (curve B of fig. 2) in which three-fourths of limit load is exceeded once in 5000 hours, crack propagation follows figure 28 of reference 3, the decay of strength is a linear function of crack length, and the standard deviation is 0.17.

Example B(2) represents the same situation as example B(1) except that (perhaps unrealistically) crack growth is assumed linear from zero time up to failure.



Constants used in the various calculations are listed in table I, and the results of the calculations are shown in figure 3 where probability of failure or survival is plotted against life in hours. Calculations for the conventional analysis have been made with the same computer programme by truncating the load spectra at  $bU_0$ .

## DISCUSSION OF RESULTS OF THE ANALYSIS

Examination of figure 3 shows that for the Civil example B(1) both methods of analysis gave virtually identical results within the computed range from  $p = 0.001$  to  $p = 0.999$ . In the computations the distribution of  $H$  was divided into its 0.1 percentile. If results are desired for  $p < 0.001$  these can readily be obtained by computing with smaller elements of the distribution of  $H$ . For example A(1), both methods gave virtually identical probabilities of failure for lifetimes longer than 3000 hours, but for shorter lifetimes the reliability method gave higher probabilities than the conventional method. It is appreciated that the reliability method of analysis included, whereas the conventional method excluded, the risk of failure from loads exceeding the virgin strength (whether of uncracked structure or of cracked but yet unweakened structure).

The probability of such overload failures can readily be derived from the frequency of exceedance of  $U_0$  for example A, namely once per million hours. This probability of overload failures is plotted as a dashed line in figure 3; the reliability calculation closely approximates this curve at low probabilities of failure.

The result for example A(2) is similar to that for example A(1), except that, because of the larger scatter, the reliability calculation assessed a given probability to have been reached in a slightly shorter lifetime; for example, a probability of failure of 0.002 was reached in 1500 hours by reliability analysis and in 1750 hours by conventional analysis with the corresponding scatter factors being  $5\frac{1}{3}$  and  $4\frac{4}{7}$ , respectively. Again, at a probability of failure of 0.001, the major contribution was overload failure through loads greater than the virgin strength.

Reliability analysis provides a rigorous method for validating the conventional methods of safe life and inspection interval analyses which are based upon a seemingly arbitrary choice of the value of unsafe strength, this choice having been made by choosing what is to be the highest load in the fatigue test programme on the representative structure to estimate mean life. The conventional analysis is vastly less time consuming than the reliability analysis, since it involves a simple slide-rule calculation rather than a complex digital computer programme run.

Examples A(1), A(2), and B(1) were constructed to represent closely conditions existing in military and civil aircraft situations. For the most part the reliability analysis validates the simpler conventional analysis. For the military type of spectrum and at

short lives, the probability of failure is dominated by loads exceeding the uncracked strength; when these are added to the conventional analysis, the result agrees closely with the reliability methods.

Example B(2) represents an artificial extreme example of a structure assumed to have linearly decaying strength from zero time up to failure. Nevertheless, here again, at probabilities of failure less than 20 percent, the corresponding lifetimes were virtually identical with those for a more usual strength-decay curve, or, indeed, for the step-function strength decay curve which is implicit in the conventional analysis.

The examples that have been discussed have not considered the case of a long period of detectable crack propagation during which the strength does not decay below virgin strength. Here inspection will not prevent failures from exceedance of the virgin strength, but will weed out cracked structures before they become weakened.

### CONCLUSIONS

For a range of conditions which are typical of military and civil aircraft structures and load histories, reliability analysis validates the much simpler conventional methods of safe life and inspection interval analysis.

The reliability method, ipso facto, includes the probability of failure through loads exceeding the virgin strength — a factor which is inevitable by any fatigue analysis, inspection schedule, or safe-life determination.

Where there is a long detectable crack propagation time without diminution of the structural strength, inspection will weed out cracked structures before they become weakened but will not prevent failures from loads exceeding the virgin strength.

### ACKNOWLEDGEMENT

The author desires to gratefully acknowledge the assistance of Mr. M. R. Thomson in performing the computations.

## REFERENCES

1. Hooke, F. H.: Consideration of the Rationale of the Use of Half Critical Crack Length as a Failure Criterion. A.R.L. Internal Paper, Oct. 1969.
2. Hooke, F. H.: The Fatigue Life of Safe-Life Structures - An Australian Approach. Report from Laboratorium für Betriebsfestigkeit (Darmstadt), Apr. 1970.
3. Payne, A. O.: Determination of the Fatigue Resistance of Aircraft Wings by Full Scale Testing. Proceedings of Symposium on Full-Scale Fatigue Testing of Aircraft Structures, F. J. Plantema and J. Schijve, eds., Pergamon Press, 1961, pp. 76-132.
4. Myers, R. H.; Wong, K. L.; and Gordy, H. M.: Reliability Engineering in Electronic Systems. John Wiley & Sons, Inc., 1964.
5. Bazovsky, I.: Reliability Theory and Practice. Prentice-Hall, Inc., 1962.



TABLE I  
CONSTANTS USED IN EXAMPLES A(1) AND A(2) (MILITARY) AND  
EXAMPLES B(1) AND B(2) (CIVIL) SAFE-LIFE ANALYSIS

Constant in calculation	Example A (military aircraft)	Example B (civil aircraft)
$\tilde{H}$ = Median population life	8000 hours	25 000 hours
$\sigma$ = Standard deviation	0.167 for A(1) 0.167 $\sqrt{2}$ for A(2)	0.17
$bU_0$ = Highest test load	0.67 $U_0$	0.5 $U_0$
$l/l_{cr} = \psi(h/H)$	$(t/H)^{9.0}$	B(1): 0 for $t/H < 0.6$ $t/H - 0.6$ for $0.6 < t/H < 0.97$ $-20 + 21t/H$ for $t/H > 0.97$ B(2): $l/l_{cr} = t/H$
$U/U_0 = \phi(l/l_{cr})$	1 for $l/l_{cr} < 0.44$ $0.67\sqrt{l_{cr}/l}$ for $l/l_{cr} > 0.44$	$1 - l/2l_{cr}$
$U/U_0 = \phi\{\psi(t/H)\}$	1 for $t/H < 0.91$ $0.67(H/t)^{4.5}$ for $t/H > 0.91$	B(1): 0 for $t/H < 0.6$ $1.3 - 0.5t/H$ for $0.6 < t/H < 0.97$ $11 - 10.5t/H$ for $t/H > 0.97$ B(2): $1 - 0.5t/H$
$\tilde{m}(V/U_0)$	$10^6 - 12V/U_0$	$10^{4.3} - 15V/U_0$

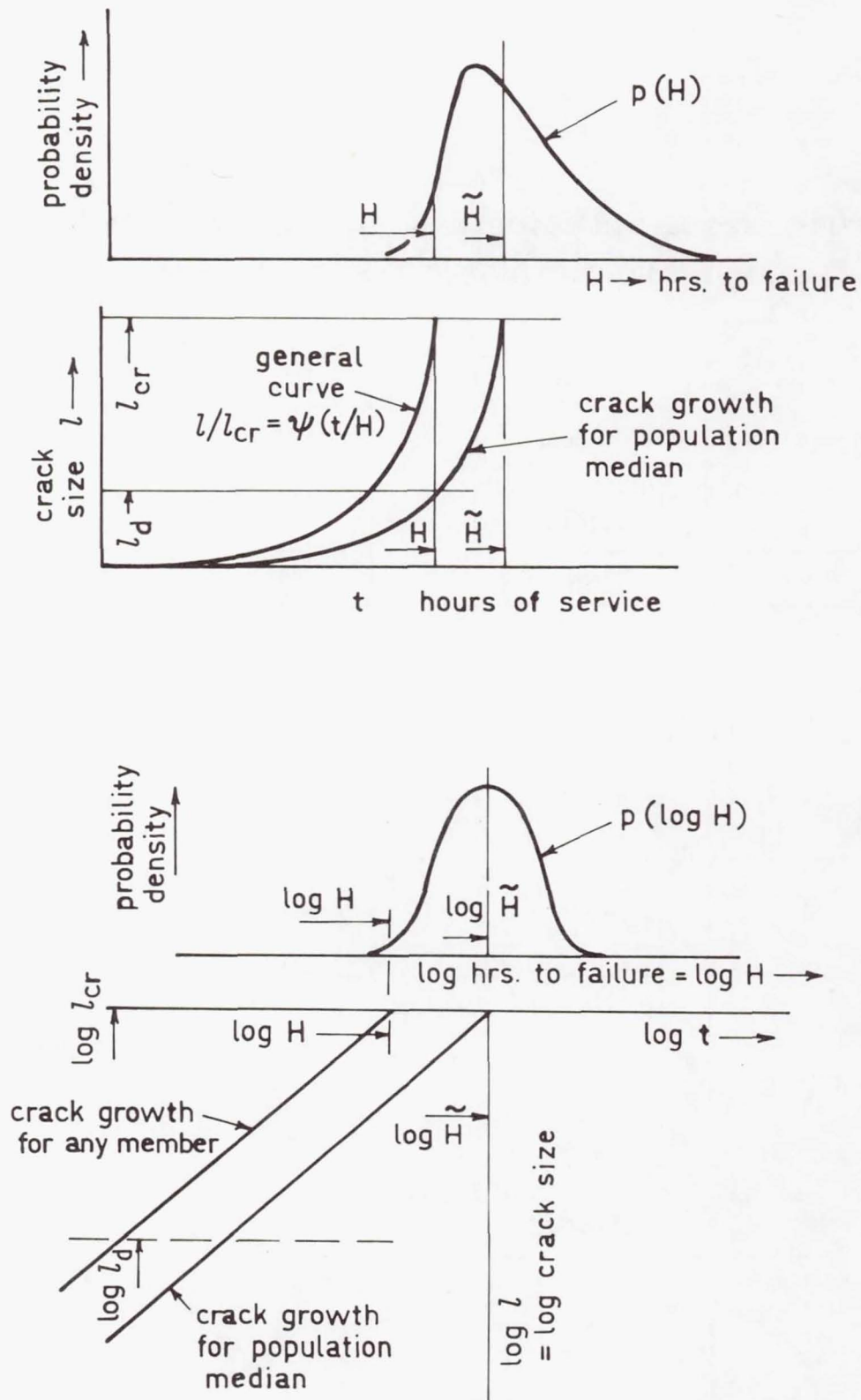


Figure 1.- Crack growth and failure distribution model.

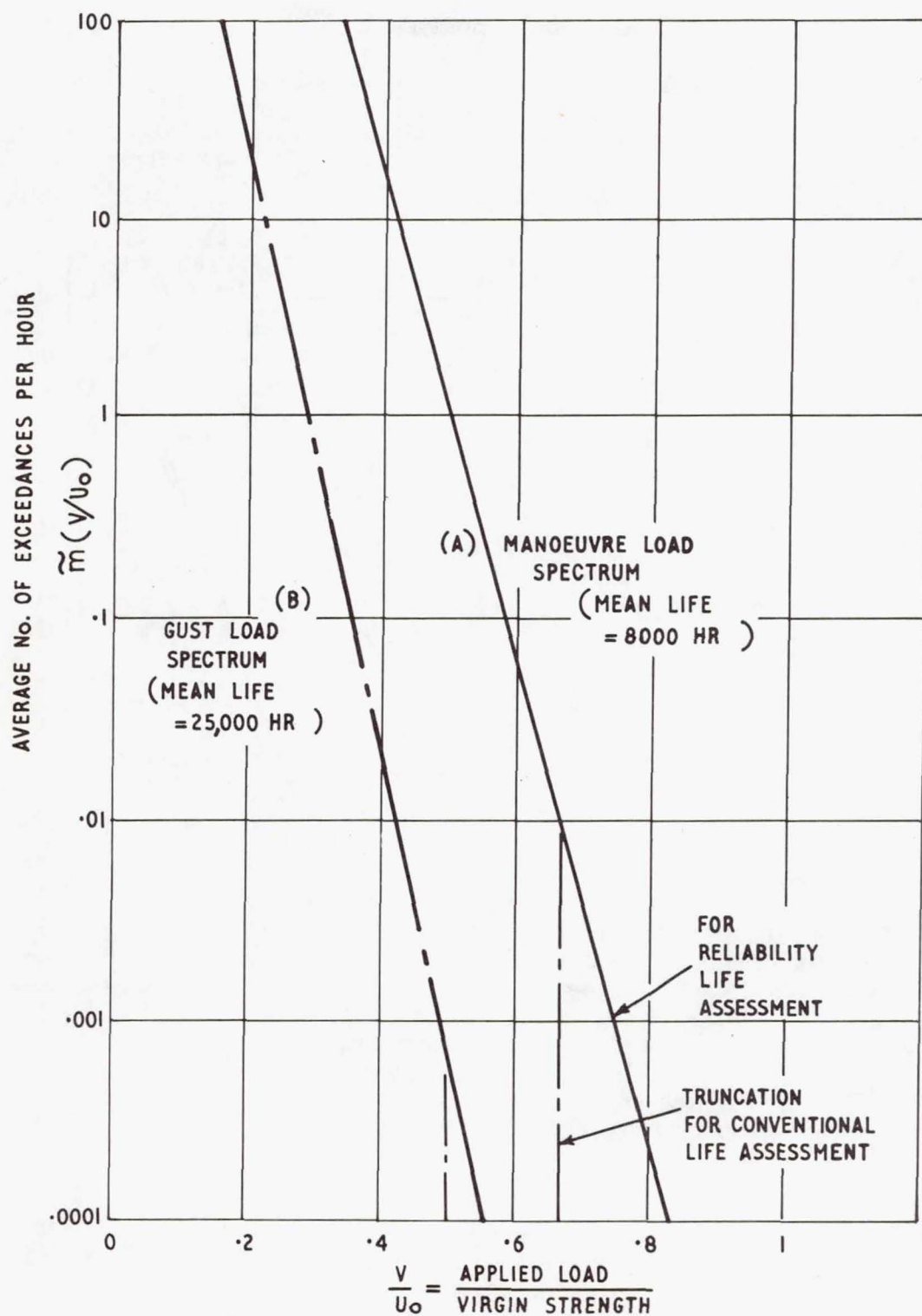


Figure 2.- Typical load exceedance curves.



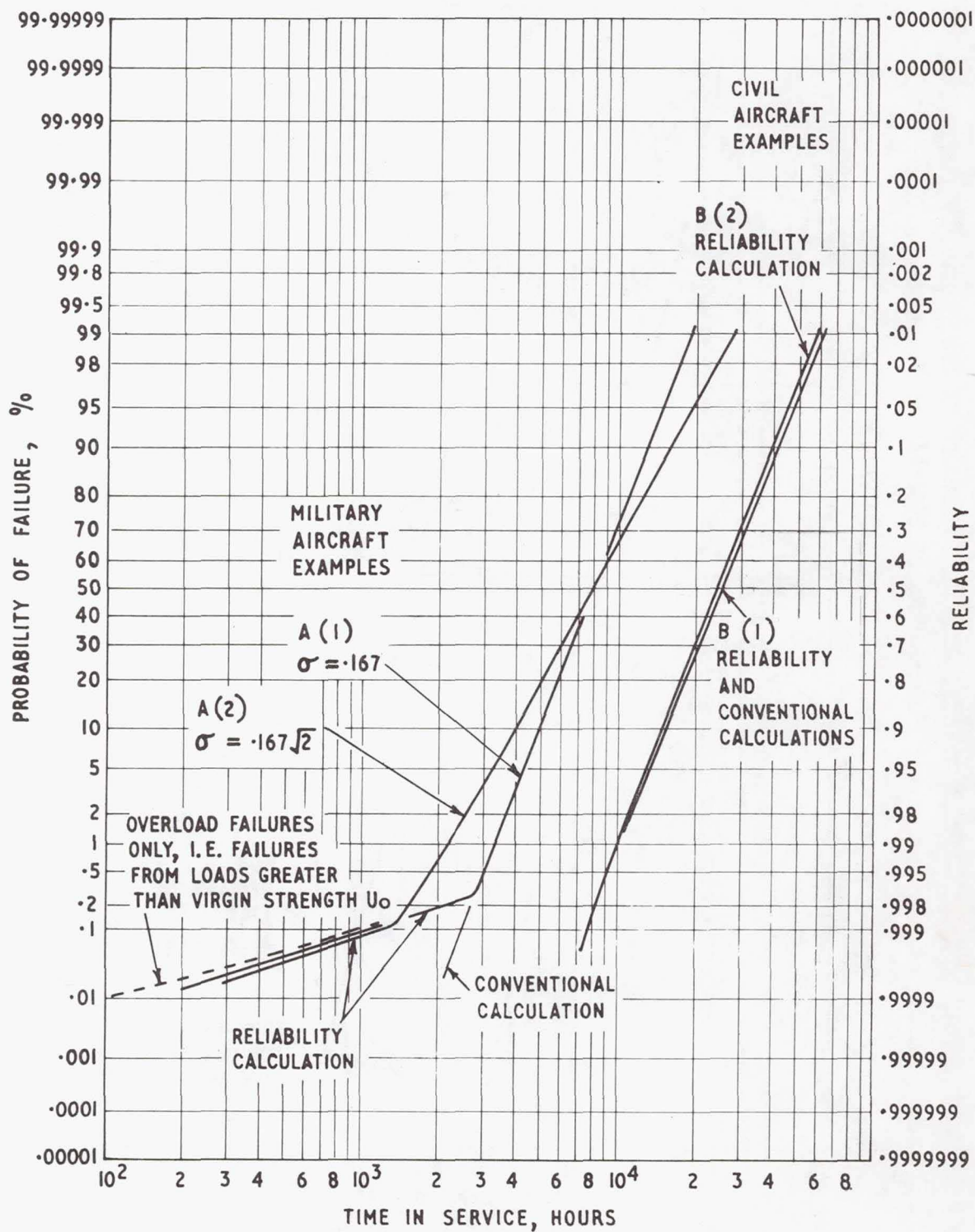


Figure 3.- Probabilities of failure and survival calculated by reliability and conventional analyses.